On demand

[J] Poster | U (Union)：Union

[U-12] Future of Earth and Planetary Science (10): Big Data and Open Science

convener:Ryoichi Fujii(Research Organization of Information and Systems), Hodaka Kawahata(Atmosphere Ocean Research Institute, the University of Tokyo), Eiichi Tajika(Department of Earth and Planetary Science, Graduate School of Science, The University of Tokyo), Gaku Kimura(Tokyo University of Marine Science and Technology)

[U12-P01] Algorithm construction test for interdisciplinary science

*Norio Umemura[1], Shuji Abe[2], Yoshimasa Tanaka[3,4], Shin ya Nakano[5], Atsuki Shinbori[1], Yasuo Saito[3], Yasuyuki Minamiyama[6] (1.Institute for Space-Earth Environmental Research, Nagoya University, 2.International Center for Space Weather Science and Education, Kyushu University, 3.National Institute of Polar Research, 4.Joint Support-Center for Data Science Research, Research Organization of Information and Systems, 5.The Institute of Statistical Mathematics, 6.National Institute of Informatics)

[J] Poster | U (Union)：Union

[U-24] COVID-19, the Earth's Environment and Disaster

convener:Jun Matsumoto(Deaprtment of Geography, Tokyo Metropolitan University), Yukihiro Takahashi(Department of Cosmosciences, Graduate School of Science, Hokkaido University), Akira Wada(Tokyo Institute of Technology), Manabu D. Yamanaka(Research Institute for Humanity and Nature / Professor Emeritus of Kobe University)

[U24-P01] Seismic noise reduction in Tokyo urban area due to social activity reduction for COVID-19

*Suguru Yabe[1], Kazutoshi Imanishi[1], Kiwamu Nishida[2] (1.National Institute of Advanced Industrial Science and Technology, 2.ERI, UTokyo)

[U24-P02] Ensemble Data Assimilation of COVID-19 Epidemic Model: Relationships between Infectivity and Earth Environments

*Shunji Kotsuki[1], Atsushi Okazaki[2] (1.Center for Environmental Remote Sensing, Chiba University, 2.Department of Meteorology & Atmospheric Science, Penssylvania State University)

[U24-P03] Air pollution status over China during lockdown caused by COVID-19

*Pradeep Khatri[1], Tadahiro Hayasaka[1] (1.Center for Atmospheric and Oceanic Studies,Tohoku University)

[U24-P04] Study on the Status of Website Information Dissemination by Japan’s Prefectural and Municipal Governments about "Evacuation and Sheltering during Natural Disasters" under Coronavirus Infection (Preliminary Report)

*SANO Hiroaki[1], Yohei CHIBA[1], Shinya MIURA[1], Yuichiro Usuda[1] (1.National Research Institute for Earth Science and Disaster Resilience)

[U24-P05] Impact of air quality caused by the COVID-19 lockdown in China, observed at downwind of Japan’s mountainous area.

*Osamu Nagafuchi[1], Koyomi Nakazawa[1], Ken'ichi Shinozuka[1] (1.Fukuoka Institute of Techology)

[J] Poster | O (Public)：Public

[O-04] Poster presentations by senior high school students

convener:Tatsuhiko Hara(International Institute of Seismology and Earthquake Engineering, Building Research Institute), Katsuyoshi Michibayashi(Department of Earth and Planetary Sciences, Nagoya University), Miwa Kuri(Japan Meteorological Agency), Keiko Konya(Japan Agency for Marine-Earth Science and Technology)

[O04-P01] Weather in Ishikawa Prefecture in the Edo Period from the Kakuson diary

*Terumasa Hashino[1], *Sumire Tanaka[1], *Aten Noguchi[1], *Ai Minemoto[1], *Tomoki Sononaka[1], *Kaho Tokuda[1], *Masaaki Yamahata[1], *Kaisei Uchida[1], *Shinsyu Ohshiro[1], *Yasuhumi Hatashima[1], *Takuto Yoshimori[1], *Waka Sonoda[1], *Daisuke Taniguchi[1], *Eitaro Tozawa[1] (1.Ikeda Gakuen Ikeda Senior High School)

[O04-P02] The Project of digitizing seismometer records

*Masaki Yashiro[1], *Akira Taguchi[1], *Eishi Chihara[1], *Katsuaki Miyazawa[1], *Asumi Yamada[1] (1.Yashiro High School)

[O04-P03] Predict future tyhoons with statistics

*Atsushi Kobayashi[1] (1.Yashiro High School)

[O04-P05] Simplified observation of the bright meteor using web-camera images exposed for two seconds

*Takaaki TSUJI[1], *Naomasa OKADA[1], *Kouki YAMADA[1] (1.Nagoya High School)

[O04-P06] Production of improved Rain-go-round

*yuga morita[1] (1.Taki High School)

[O04-P07] the current situation and improvement plans of light pollution around Ichikawa city

*Mutsumi Goto[1] (1.Ichikawagakuen Ichikawa high school)

[O04-P08] Relations of the size of tsunami and the destruction rate of the house

*Keita Ichikawa[1] (1.Ichikawagakuen Ichikawa high school)

[O04-P09] What does annual drainage have an effect on phosphorus cycle of irrigation ponds?

*Hiiro TABATA[1], Yuki TAKAHASHI[1], Ayane INOUE[1], Haruto TAKEYAMA[1], Kousuke MANO[1], Rio YAMANO[1] (1.Hyogo Prefectural Kakogawahigashi High School)

[O04-P10] Reviewing Muroto High School Evacuation Management Manual –Investigation on Natural Environment around the Evacuation Site-

*Misaki WATANABE[1], *Kurumi HASHIMOTO[1] (1.Kochi Prefectural Muroto High School)

[O04-P11] What Affects the View of Mirage

*# [1] (1.Yokohama Science Frontier High School)

[O04-P12] An ancient large earthquake revealed from the trace of the earthquake, and possibility of existence of “Unknown Fault” in Tama Hills

*Takuma FUKUNAGA[1] (1.Yokohama Science Frontier High School)

[O04-P13] Estimating of paleoenvironment using fossils of shells produced in the Kanzawa Formation, Nakatsu Group

*Hotaka OGURA[1] (1.Yokohama Science Frontier High School)

[O04-P14] Evaluating the Effect of Global Warming on Yokohama Using Nightlight Satellite Data and Large Point Sources Data

*Sota Komiya[1] (1.Yokohama Science Frontier High School)

[O04-P15] Comparison of Fluid Resistance and Experience for Calculation of Resistance Coefficient according to Object Shape

*Senri Shimamura[1] (1.Sakaehigashi Senior High School)

[O04-P17] Examination of evacuation routes considering damage caused by liquefaction

*KOYA TAKAHASHI[1] (1.tosa high school)

[O04-P18] Relationship between four giant jets in the past and meteorological phenomena in the troposphere

*Yuya Okubo[1], Huga Suzuki[1], Yuya Takahashi[1] (1.Shizuoka Prefectural Iwata Minami High School)

[O04-P19] Spectroscopy of plasma generated in a microwave using a newly developed simple spectrometer with high resolution

*Ayaka Akase[1], *Kento Takase[1], *Reiji Iwamoto[1], *Keishi Okumi[1], *Mayu Naito[1], *Hiromu Fujimoto[1], *Yamato Yasuhara[1], *Natsuki Yamamoto[1] (1.Hyogo Prefectural Himeji Higashi Senior High School Science Club (Plasma team))

[O04-P20] Circulation of residual magma during consolidation of granitoid magma

*Kento Takase[1], *Ayaka Akase[1], *Reiji Iwamoto[1], *Keishi Okumi[1] (1.Hyogo Prefectural Himeji Higashi Senior High School Science Club (Magma team))

[O04-P21] Indicate the intensity of ultraviolet rays using the degree of fading of cotton yarn dyed with reactive dye

*Natsuki Yamamoto[1], *Ayaka Akase[1], *Kento Takase[1], *Reiji Iwamoto[1], *Keisi Okumi[1], *Mayu Naito[1], *Hiromu Fujimoto[1], *Yamato Yasuhara[1], *Nanami Kishimoto[2], *Sayuki Fujii[2], *Nagisa Yokoyama[2], *Soya Obata[2], *Hinako Kobayashi[2], *Haruki Murakami[2], *Reo Yamada[2], *Syo Yoshida[2] (1.Hyogo Prefectural Himeji Higashi Senior High School Science Club (Ultraviolet rays team), 2.Hyogo Prefectural Nishiwaki Senior High School Earth Science Club)

[O04-P22] Seasonal alterations in carbon assimilation of marine organisms

*Hiroto ICHIKAWA[1], Hayato Kurosawa[1], Ryushi Abe[1] (1.Miyagi Rifu high school)

[O04-P23] The relationship between Intensity of radiation energy and soils variety

*Ryushi Abe[1], Hiroto Ichikawa[1] (1.Miyagi Rifu high school)

[O04-P24] Specific heat of various soils measured by radiation thermometer

*Hayato Kurosawa[1], Hiroto Ichikawa[1] (1.Miyagi Rifu high school)

[O04-P25] Relationship between astronomical observation and water vapor in weather forecast

*Aoi Takamori[1] (1.Suwa Seiryo Senior High School)

[O04-P26] Research about Moriya Formation

*Yusuke Morozumi[1] (1.Suwa seiryo senior high school)

[O04-P27] Making solid version chromatography ~Separation and identification of solid particles by magnetic field gradient using microgravity~

*Satoru Kitada[1], Takuya Hanasaki[1], Yuichiro Okuno[1], Ryota Iwamoto[2], Keita Maishi[3], Kyoya Okada[3] (1.Imamiya Technology Senior High School of Osaka Prefecture The evening course, 2.Otemae Senior High School of Osaka Prefecture The evening course, 3.Kasugaoka Senior High School of Osaka Prefecture The evening course)

[O04-P29] Earthquake prediction by an electromagnetic wave

*Ousuke Yagasaki[1], Mizuho Fujiwara[1], Maika Yashima[1], Shougo Takeda[1], Aiku Tanaka[1] (1. Tokyo Metropolitan Tama High School of Science and Technology)

[O04-P30] Classification of Herbig Ae/Be Stars by Spectroscopic Observations

*Aika Koyama[1], *Riko Iida[1], *Hazuki Ueyama[1] (1.Nara Prefectural Seisho High School)

[O04-P31] The Research for Asteroid's Surface Color ~ Difference of BVR magnitude ~

*Asahi Tajima[1], *Mirei Matoba[1] (1.Nara Prefectural Seisho High School)

[O04-P32] The igneous rocks which is distributed around The Kabutoyama mountain, the northern part of Kofu Basin

*Masahiro Okuyama[1], Dai Iijima[1], Haruta Moriya[1], Ayato Watanabe[1] (1.Yamanashi Prefectural Hikawa Highschool)

[O04-P33] Studies on the Urban Heat Islands and Measures against Heat

*Mio Takakura[1] (1.Tokyo Metropolitan Toyama High School)

[O04-P34] **Geological Survey by Boring a Core from Toyama's Schoolgrounds**

*Ryotaro Terabe[1] (1.Tokyo Metropolitan Toyama High School)

[O04-P35] Long-term Fluctuation of Snowfall/Precipitation Ratio and Global Warming

*Yukihiro Takaki[1] (1.Tokyo Metropolitan Toyama High School)

[O04-P36] Factors for variations in bombcyclones

*Minori Iida[1] (1.Tokyo Metropolitan Toyama High School)

[O04-P38] Spectroscopic observation of sprite

*Kotone Asano[1], *Ayaka Okumura[1], Ryuya Nagao[1], Keisuke Nobutoki[1], Momoo Hayashi[1] (1.Ichinomiya High School)

[O04-P39] The relationship between the shape of columnar jointing and the viscosity of lava flow

*Kanta Takakura[1] (1.Kaijo high school)

[O04-P40] How ripples formation dependence on the size of sand grains and the amplitude of vibration cycle

*Tsuyoshi Enta[1], *Ryutaro Mitsui[1] (1.Kaijo Junior and Senior High School)

[O04-P41] Development of the Portable Equatorial Mount with high operability and applicability

*Jun Ikeda[1] (1.Kaijo high school)

[O04-P42] Proposal of GEO-KAMISHIBAI that enhances the appeal of SANRIKU GEOPARK-3 the Taneichi Layer

*Hitomi Kimura[1], *Rio Yaguchi[1], *Kyougo Sakashita[1], *Asahi Sekibata[1] (1.MARIENT CHIKYU TANKEN CLUB SENIOR)

[O04-P43] Proposal of GEO-KAMISHIBAI that enhances the appeal of SANRIKU GEOPARK-4 the Hachinohe Canyon

*Mai Kawabata[1], *Haruto Kawasaki[1], *Sarina Shinohe[1] (1.MARIENT CHIKYU TANKEN CLUB SENIOR)

[O04-P44] **Spectroscopic Observation of Meteors**

*Shotaro Mino[1], *Yui Satou[1] (1.Furukawa Reimei Junior High School / High School)

[O04-P45] Comparison of frequency (HRO/VOR-RO) and detection number in meteor radio wave observation

*Sora Endo[1], *Rio Saito[1], *Aki Sato[1], *Sachi Sato[1], *Sakura Yuki[1] (1.Furukawareimei Junior High School / High School)

[O04-P47] Research about Greenhouse effect of water vapor~Can we control the temperature of the earth with water vapor!?~

*Hikaru Abe[1], *Michiru Suzuki[1], *Ruka Suzuki[1], Furi Seino[1] (1.Sakata Minami High School)

[O04-P48] **A study of the fluctuations in the water level of Kohama pond**

*Akari Nakata[1], *Kira Yamamoto[1], Koharu Fukusi[1], *Hinata Muto[1] (1.Nirayama High School)

[O04-P49] **Research on statistical observation of columnar joint form and its origin by high precision 3D model by drone and potato starch experiment**

*Makoto Iida[1], *Ryo Aoki[1], *Ryuki Mochizuki[1], *Takato Okumura[1] (1.Nirayama High School)

[O04-P50] Marine pollution by Microplastics

*Nanako Aono[1], *Kaito Isoya[1], *Kouki Sugiyama[1], *Yuki Nakata[1], *Genki Yano[1] (1.Nirayama High School)

[O04-P51] Invisible ability of soil –Soil evaluation by zero point of charge-

*Ayano Hayashi[1], *Ayano Soga[1] (1.Kyoto Prefectural Sagano High School)

[O04-P52] Multivariate analysis of data of forest soil by using "Face Chart"

*Fujimoto Takeshi[1], *Hina Nakatani[1], *Hokuto Nakatsu[1] (1.Kyoto Prefectural Sagano High School)

[O04-P53] Manufacture of Azumaya in WFS -Examination of the method of drying the trees-

*Kanako Inoda[1] (1.Kyoto Prefectural Sagano High School)

[O04-P54] Project Regeneration of Gensei's Bamboo Volume 1

*Takeshi Fujimoto[1], *Yosuke Yukawa[1], *Nanami Aoki[1], *Yusuke Yamazaki[1] (1.Kyoto Prefectural Sagano High School)

[O04-P55] To develop an efficient geological survey method and its effectiveness by using natural radiation

*Taisei Takagi[1], *Momoka Tanaka[1], *Ayane Matsuoka[1], *Kosei Yoshimura[1], *Chiharu Yamaguchi[1] (1.FUKUI PREFECTURAL WAKASA SENIOR HIGH SCHOOL)

[O04-P56] Kantemboki ~To research the accuracy of Japanese old sayings about weather~

*Yuki Takemura[1], *Toro Higashino[1], *Haruki Fukuda[1] (1.FUKUI PREFECTURAL WAKASA SENIOR HIGH SCHOOL)

[O04-P57] Proposal of new embankment ~Proposal of prevention method of piping phenomenon

*Daiki Tanabe[1], *Soshi Hirata[1] (1.FUKUI PREFECTURAL WAKASA SENIOR HIGH SCHOOL)

[O04-P58] Protect the traditional shrimp fishing in Obama Bay

*Taisei Hayashi[1], *Masakazu Muramatsu[1], *Chiaki Ose[1], *Kanta Nakai[1] (1.FUKUI PREFECTURAL WAKASA SENIOR HIGH SCHOOL)

[O04-P59] Correlation between liquefaction and grainsize distribution of ground

*Ryo Beppu[1] (1.Saitama prefectural Kasukabe High School)

[O04-P60] Fine laminated structure of stromatolite suggests summer and winter in cretaceous period?

*Taiga Tsujimoto[1] (1.Saitama prefectural Kasukabe High School)

[O04-P61] How long did it take to form the Pothole in Joga-Shima Island?

*Yusuke Izumi[1] (1.Saitama prefectural Kasukabe High School)

[O04-P62] Clothing change from meteorological data

*Hinane Chiba[1], *Misaki Ishii[1], *Kaho Kubota[1], *Nanami Nakao[1] (1.Chiba Prefectural Funabashishibayama High School)

[O04-P63] Analog modeling of dust devil -Study of its growth and dissipation-

*Daisuke Suzuki[1], Yuto Akaike[2] (1.Shizuoka Senior High School, 2.Fuji Senior High School)

[O04-P64] Automatic observation of Visibility

*HARUTO TANAKA[1], *MITSUKI BABA[1], *YUYA HAMASHIMA[1] (1.Tokyo Metropolitan Tachikawa High School)

[O04-P65] Analysis of sunspot observation data over 70 years and future prospects

*HAMASHIMA YUYA[1] (1.Tokyo Metropolitan Tachikawa High School)

[O04-P67] Development of an automatic observation and notification system for the meteor shower ~A signal detection and data output using Arduino~

*Koichi Sato[1], *Junsei Okuma[1] (1.Chuo University Junior and Senior High School)

[J] Poster | O (Public)：Public

[O-05] Understanding of formation process of Japanese archipelago from Japanese Geoparks

convener:Noritaka Matsubara(Graduate School of Regional Resource Management, University of Hyogo), Yayoi ICHIHASHI(Sado Island Geopark Promotion Office), HIROKO IMAI(Com Support Office /Wakayama University Center for Tourism Research), Hokuto Obara(Mine-Akiyoshidai Karst Plateau Geopark Promotion Council)

[O05-P01] Learning about and Protecting Stones in the Itoigawa UNESCO Global Geopark: Stone Guide System

*Takahiko Ogawara[1], Ko Takenouchi[1], Yosuke Ibaraki[1], Takeo Kobayashi[2] (1.Fossa Magna Museum, 2.Itoigawa City Hall Geopark Promotion Office)

[O05-P02] Creating walking map for visitors in winter season in Minami-Alps Geopark.

Yuko Miyazaki[1], *Eri Ozawa[2] (1.Oshika museum of Japan Median Tectonic Line, 2.Minami-Alps MTL Area Geopark Council)

[O05-P03] Sustainable dissemination activities realized through the partnership "Making the stone specimen in Hakusan Tedorigawa Japanese Geopark"

*Yuya Kitoh[1], Satoshi Hirai[1], Kiyofumi Tamamura[1], Tsuyoshi Hibino[2], Kaori Nakano[2], Tomoaki Morishita[3], Yoshihiro Hiramatsu[3], Maki Hamada[3] (1.Ishikawa Geological Survey Association, 2.Hakusan Tedorigawa Geopark Promotion Council, 3.Kanazawa University)

[O05-P04] A case study of geo-education at an geo/ecological site in the Dinosaur Valley Fukui Katsuyama National Geopark

*Yoshihiro Moriishi[1], Sumiaki Machi[1], Eiichi saito[2], Kensuke Hirose[2], Yukie Yasui[1,3], Msahiro Amadate[1] (1.Dinosaur Valley Fukui Katsuyama Geopark Promotion Council , 2.Heisenji Elementary School, 3.Katsuyama City Education Board)

[O05-P05] The support systems and practice examples of geopark education at elementary and junior high schools in the Dinosaur Valley Fukui Katsuyama National Geopark

*Sumiaki Machi[1], Masahiro Amadate[1], Yukie Yasui[1,2], Yoshihiro Moriishi[1], Keisuke Nunome[3], Kazutaka Izukura[4], Naoya Doseki[3], Hiroyuki Ito[4] (1.Dinosaur Valley Fukui Katsuyama Geopark Promotion Council, 2.Katsuyama City Education Board, 3.Arado Elementary School, 4.Katsuyama Nanbu Junior High School)

[O05-P06] Creating regional brands using geoparks

*Kei SHIMOMURA[1,2], Ken'ichi KURIHARA[3,4] (1.Mikasa Geopark Promotion Counsil, 2.Regional Development and Geopark Promotion Council, 3.Geo.Labo.corporation, 4.Hokkai Gakuen University)

[O05-P07] The first geotour consisted of activity programs for overseas student in Shikoku Seiyo Geopark.

Yuto Kamei[2], Keita Murakami[2], Yuichi Murakami[2], *Takumi Sakakiyama[1], Fumito Doi[1], Tsukasa Takahashi[1], Masayuki Sakakibara[2,3] (1.Seiyo City, 2.Faculty of Collaborative Regional Innovation, Ehime University, 3.Research Institute for Humanity and Nature)

[O05-P08] Making learning handbook for Nanki Kumano Geopark from the viewpoint of teachers

*YUMINE Toshiki[1], SUZUKI Toshikazu[2], TABUCHI Yu[3], NAKANISHI Dai[4], NOGAMI Seiji [5], MATUSHITA Hutoshi[6], YOKOYAMA Kazuya[5] (1.Chiben Gakuen Wakayama elementary school, 2.Susami Elementary School in Susami town, 3.Shinjo Junior high School in Tanabe city, 4.Wakayama University Elementary school, 5.Wakayama city science museun for children, 6.Wakayama Biological Club)

[O05-P09] Making Use of Mining Heritage in Mine-Akiyoshidai Karst Plateau Geopark

*Hokuto Obara[1], Tomoyuki Narasaki[1], Tomoko Muratani[1], Tristan Gray[1], Yutaka Kuramasu[1], Tatsuo Sueoka[1], Kazuhiro Yuhora[2], Koji Wakita[3] (1.Mine-Akiyoshidai Karst Plateau Geopark Promotion Council, 2.Tottori University of Environmental Studies, 3.Yamaguchi University)

[O05-P10] Four geological body constructing Shimokita Geopark

*Satoshi Ishikawa[1] (1.Shimokita geopark promotion council)

[O05-P11] Shimonita Geopark-Town planning utilized local resorce-

*Hara Hideo[1] (1.Geopark Shimonita Council)

[O05-P12] Plate Collision and Life of people at Mt. Apoi UNESCO Global Geopark

*Kato Satomi[1] (1.Mt. Apoi Geopark promotion council)

[O05-P14] Connecting Local governments with Geopark activities

*Suzuka Koriyama[1], Sanin Kaigan Geopark Promotion Council (1.Sanin Kaigan Geopark Promotion Council)

[O05-P15] Revised action plan for the first time in four years, created through direct dialogue with local residents

*Hidetaka Akiyoshi[1], Harumi Koumura[1] (1.San'in Kaigan Geopark Promotion Council)

[O05-P16] Reconstruction of two types of Miocene volcanoes in the northern part of hyogo, San’in Kaigan Geopark, based on facies analysis.

*Noritaka Matsubara[1], Suzuka Koriyama[2] (1.Graduate School of Regional Resource Management, University of Hyogo, 2.San'in Kaigan Geopark Promotion Council)

[O05-P17] **Practical use of geosites in Sado Island Geopark and the issues related to their use**

*Takeyoshi SADAKANE[1] (1.Sado Geopark Promotion Office)

[O05-P18] Process of Making a Field Trip Route in Sado Island Geopark

*Yayoi ICHIHASHI[1] (1.Sado Island Geopark Promotion Office)

[O05-P19] Activities to protect the formation locality of quartz twins on the Japanese law in the Goto Islands Geopark concept.

*Mana Yasui[1], Koichi Iwata[2], Hirotaka Karatsu[2], Ichiro Hosoda[2] (1.Waseda research institute for science and engineering, 2.Goto municipal office Geopark promotion group.)

[O05-P20] Mystery solving event using geosites at Shirataki Geopark

*Yoshihumi Matsumura[1], Makoto Kumagai[1] (1.Shirataki Geopark Promotion Council)

[O05-P21] The Land Formed by severe crustal movement and the Lives of its People
–case study of the Misaki Group in Tosashimzu Geopark Plan–

*Satoru Imai[1], Michiru Sakai[1], Aika Sakuda[1], Natsuki Moriguchi[1] (1.Tosashimizu Geopark Promotion Council)

[O05-P22] Geology, topography and life of the people in Oita Himeshima Geopark

*Yu Horiuchi[1], Takeaki Suga[1], Norimitsu Suka[1] (1.Oita Himeshima Geopark Promotion Office)

[O05-P23] Educational Program on spring water of Aso UNESCO Global Geopark related with electrical conductivity

*Tsuneomi Kagiyama[1], Shuhei Takamori[1], Natsuko Kodama[1], Shinichiro Ikebe[1], Akinobu Ishimatsu[1] (1.Aso Geopark Promotion Council)

[O05-P24] Sharing volcano experiments conducting at some UGGp in Japan

*Hikaru Yokoyama[1,2], Taku Morimoto[3], Kenji Kato[4], Dong-Won Choi[5], Naoko Imabeppu[5] (1.Hokusho University, 2.Toya-Usu Unesco Global Geopark, 3.Unzen Volcanic Area Unesco Global Geopark, 4.Izu Peninsula Geo Guide Association, 5.Hantangang River Geopark)

[O05-P25] A geo-tour for disaster prevention in the Bandaisan Geopark -relation between the Nagase River flood and the Bandai Volcano eruption-

*Yojiro Taketani[1], Hiroshi Sato[1,2], Makoto Hasuoka[1] (1.Bandaisan Geopark Council, 2.Mt. Bandai Museum)

[O05-P26] Revalidation mission of Toya-Usu UNESCO Global Geopark in 2019
-Strategy of the mission for green card-

*Yuki Nishi[1], Masato Takekawa[1], Nire Kagaya[1], Asami Nakaya[1], Yoshiaki Hata[1] (1.Toya-Usu UNESCO Global Geopark Council)

[O05-P27] Review of actions in Mishima Village Kikai Caldera Geopark, and agenda for revalidation of Japanese Geopark Network

*Geopark Council Mishima Village[1], Mahito Watanabe[2], Kei SHIMOMURA[3] (1.Mishima Village office, Kagoshima Prefecture, 2.Institute of Geology and Geoinformation, National Institute of Advanced Industrial Science and Technology, 3.Mikasa Geopark Promotion Counsil)

[O05-P28] Activities to promote the local sustainable development - Report on recertification review of “Kurikomasanroku no Megumi” special products from Mt.kurikoma Area geopark -

Kobayashi Mizuki[1], *Tanaka Seiya[1], Nakagawa Rie[1] (1.Mt. Kurikoma Area Geopark Promotion Committee)

[O05-P29] Disaster Prevention practice at Naeba-Sanroku Geopark ~Typhoon No.19(Hogibis) disaster and response in 2019~

*Kouhei Nakano[1] (1.Naeba-Sanroku Geopark Promotion Council)

[O05-P30] Did the Chinda Falls recede? – Evolution of river topography in the Oita Bungoono Geopark, Japan

*Toshikazu Yoshioka[1] (1.Oita Bungoono Geopark Promotion Council)

[O05-P31] Globally Important Agricultural Heritage System "Minabe-Tanabe Ume System" viewing from geomorphological aspects of three small catchment area, central part of Wakayama Prefecture

*Yoshinori Kodama[1], Kazuki Taira[2] (1.Faculty of Agriculture, 2.Wakayama Prefecture)

[O05-P32] Systemization of the Certified Tourism Guide Program and its Significance – An Example by the Hakusan Tedorigawa Geopark

*Tsuyoshi Hibino[1], Ryoichi Onishi[1], Yoshiko Funatsu[2] (1.Hakusan Tedorigawa Geopark Promotion Council, 2.Hakusan City Tourism League)

[O05-P33] Evaluation of explanation panels setting at Geopark’s site 2 - case study of the explanation panel at Obama Hot springs in Unzen Volcanic Area UNESCO Global Geopark, Japan -

Kenshin OSHIMA[1], Yui KURITA[1], Miyu KAWAZOE[1], Rinna TAKEICHI[1], Ayaka OHIRA[1], Ayuka BABA[1], Ayuko SAGARA[1], Nagisa NAKAMURA[1], Takuji MURAOKA[2], Toshiki HIGASHIUCHI[2], *Marekazu OHNO[3] (1.Glocal Course, Nagasaki Prefectual Koka High School, 2.Nagasaki Prefectual Koka High School, 3.Unzen Volcanic Area Geopark Promotion Office)

[O05-P35] Meteorological landscape over the geopark: A lined-up cumulus row generated by the mountains in the western part of Oga Peninsula, Akita Prefecture, Japan

*Norihito Kawamura[1], Seiji Yamashita[2] (1.School of Regional Resource Management, Graduate School, University of Hyogo, 2.Faculty of Education ans Human Studies)

[O05-P36] Inform of weather disasters in geoparks

*Hiroshi Sato[1,2], shinichi Sugimoto[3], Makoto Aoi[4], Shinya Miura[4] (1.Mt.Bandai Museum, 2.Bandaisan Geopark Council, 3.Sanriku Geopark, 4.National Research Institute for Earth Science and Disaster Resilience)

[O05-P37] Foreign Tourist Survey: Places of Interest, Transportation, etc.

*Susan May[1] (1.Hakusan Tedorigawa Geopark Promotion Council)

[O05-P38] Education activities of museum encouraged establishing of graduate school in geopark - Museum of Nature and Human Activities and San’in Kaigan UNESCO Global Geopark

*Tohru Sakiyama[1] (1.Institute of Geo History, Japan Geochronology Network)

[O05-P39] Trends on and assessments of "ecological resources" in the Evaluation Mission Reports for Japanese Geoparks

*Kazuhiko HIRATA[1,2], Yuya Kato[1,3], Shinsuke Nakamura[1], Rieko Fujii[1], Natsuki Moriguchi[1,4] (1.Ecological Working Group for Japan Geopark Network, 2.Natural History Museum and Institute, Chiba, 3.Noyama Company, 4.Tosashimizu Geopark Promotion Council)

[O05-P40] Case study of Children’s Summer School on Earthquakes and Volcanoes in Tango area of San-’in Kaigan UNESCO Global Geopark

*Tomoya Hiiro, Satoko Murotani[1], Ai Toma[2], Children’s summer school on Earthquakes and Volcanoes Committee for[3,4,5] (1.National Museum of Nature and Science,Tokyo, 2.Keio University, 3.Seismological Society on Japan, 4.Volcanological Society of Japan, 5.Geological Society of Japan)

[O05-P41] Educational Effects of Screening a Geopark Film at a Local Science Museum

*Rin Nodera[1,2] (1.Kurobe Yoshida Science Museum, 2.Tateyama Kurobe Geopark Society)

[O05-P42] Examples of activities in collaboration with Tateyama Kurobe Geopark and University of Toyama

*Takuya Harada[1], Yuta Yamaoka[2], Kiichi Yamahori[2], Kiyoshi Nakagawa[2], Koji Ohnishi[1], Ken-ichi Yasue[1] (1.University of Toyama, 2.Tateyama Kurobe Geopark Society)

[O05-P43] Approach of Health Promotion with Geotourism in Central area of Toyama City

*Ken-ichi Yasue[1], Yuta Yamaoka[2], Tomoya Tanabe[3], Takuya Harada[1], Utako Uchikoshiyama[2], Toshimi Tajima[3], Kiyoshi Nakagawa[2], Koji Ohnishi[1], Kiichi Imahori[2] (1.University of Toyama, 2.Tateyama Kurobe Geopark Society, 3.Approved Specified Nonprofit Corporation Machizukuri Spot)

[O05-P44] Creating relationship between University of Toyama higher education and Tateyanakurobe Geopark activity

*Koji Ohnishi[1], Ken-ichi Yasue[1], Yuta Yamaoka[2], Takuya Harada[1], Kiichi Imahori[2] (1.University of Toyama, 2.TateyamaKurobe Geopark Society)

[O05-P46] 30 years since the eruption of Teishi Knoll in 1989

*Yusuke Suzuki[1] (1.Izu Peninsula Geopark Promotion Concil)

[J] Poster | O (Public)：Public

[O-06] Kitchen Earth Science: Let's stimulate your brain by hands-on experiments!

convener:Ichiro Kumagai(School of Science and Engineering, Meisei University), Miwa Kuri(Japan Meteorological Agency), Mie Ichihara(Earthquake Research Institute, University of Tokyo), Kei Kurita

[O06-P01] Observation of phase transitions for ammonium nitrate using hot plate and polarizing sheets

*Masami Kanzaki[1] (1.Institute for Planetary Matereials, Okayama University)

[O06-P02] What is “fluid”?, a brain-stimulative experimental subject based on soft-gel suspension dynamics

*Kei Kurita[1], Ichiro Kumagai[2], Anne Davaille[3], Nicolo Sgreva[3] (1.ERI,The University of Tokyo, 2.Meisei University, 3.Universite Pari-Saclay)

[O06-P03] Activity report on Kitchen Earth Science: Workshops supported by Earthquake Research Institute from 2017 to 2019

*Ichiro Kumagai[1], Mie Ichihara[2], Miwa Kuri[3], Kei Kurita[4] (1.School of Science and Engineering, Meisei University, 2.Earthquake Research Institute, University of Tokyo, 3.Fukuoka Regional Headquarters, Japan Meteorological Agency, 4.University of Tokyo)

[J] Poster | P (Space and Planetary Sciences)：P-PS Planetary Sciences

[P-PS09] Planetary Sciences

convener:Yusuke Nakauchi(Japan Aerospace Exploration Agency), Yuko Daket(University of Aizu)

[PPS09-P01] Cratering experiments on snow at very low temperature: Scaling law of crater size in gravity regime

*Minami Yasui[1], Suzuno Oyama[2], Mare Takagi[2], Masahiko Arakawa[1] (1.Department of Planetology, Graduate School of Science, Kobe University, 2.Department of Planetology, Faculty of Science, Kobe University)

[PPS09-P02] Laboratory collisional disruption experiments of D-type asteroids analogue targets

*Shiomoto Jyunpei[1], Akiko Nakamura[1], Sunao Hasegawa[2], Hideaki Miyamoto[3], Takafumi Niihara[3] (1.Kobe University, 2.ISAS/JAXA, 3.Department of Systems Innovation, Graduate school of Engineering, University of Tokyo)

[PPS09-P03] Experimental study on impact disruption for low strength target and implication for effect of tensile strength on impact strength

*Kazuhiro Horikawa[1], Masahiko Arakawa[1], Minami Yasui[1], Ryo Sugimura[1] (1.Graduate School of Science , Kobe University)

[PPS09-P04] Effect of porosity on restitution coefficients of snowball simulating Saturn's ring: implication for inelastic collision

*Yukari Toyoda[1], Minami Yasui[1], Masahiko Arakawa[1] (1.Graduate School of Science, Kobe University)

[PPS09-P05] Crater scaling laws of ejecta velocity distribution and crater size constructed for very low strength target

Ryo Sugimura[1], *Masahiko Arakawa[1], Minami Yasui[1], Hiroki Senshu[2], Sunao Hasegawa[3] (1.Graduate School of Science, Kobe University, 2.Planetary Exploration Research Center, Chiba Institute of Technology, 3.Japan Aerospace Exploration Agency)

[PPS09-P06] Accretion of gas and solid materials into the circumplanetary disk of a growing giant planet: Dependence on planetary mass

*Natsuho Maeda[1], Keiji Ohtsuki[1], Ryo Suetsugu[2], Masahiro N Machida[3] (1.Graduate school of science, Kobe University , 2.University of Occupational and Hnvironmental Health, 3.Graduate school of science, Kyushu University)

[PPS09-P07] Parameter Study of Satellite Formation via Giant Impact by N-body Simulation

*Yuichi Hasegawa[1], Ishizawa Yuya[1], Natsuki Hosono[2], Takanori Sasaki[1] (1.Department of Astronomy, Kyoto University, 2.Japan Agency for Marine-Earth Science and Technology)

[PPS09-P08] Numerical Analysis of Penetration Dynamics into Regolith using Compressible and Non-Expanding Plastic Gas Model

*Kojiro Suzuki[1] (1.Graduate School of Frontier Sciences, The University of Tokyo)

[PPS09-P09] Test of a model for the gas accretion onto giant planets by two-dimensional hydrodynamical simulations

*saho nakazawa[1], Yuki Tanaka[1], Hidekazu Tanaka[1] (1.Tohoku University)

[PPS09-P10] An Explanation for Physical Mechanism of the Streaming Instability in Dust Dominant Regime

*Hiroaki Kaneko[1], Taishi Nakamoto[1] (1.Tokyo Institude of Technology)

[PPS09-P11] The influence of dust evolution on the vertical shear instability in protoplanetary disks

*Yuya Fukuhara[1], Satoshi Okuzumi[1] (1.Department of Earth and Planetary Sciences, Tokyo Institute of Technology)

[PPS09-P12] Collisional Growth and Fragmentation of Dust Aggregates with Low to Very High Mass Ratios

*Yukihiko Hasegawa[1], Takeru Suzuki[1], Hidekazu Tanaka[2], Hiroshi Kobayashi[3], Koji Wada[4] (1.The University of Tokyo, 2.Tohoku University, 3.Nagoya University, 4.Chiba Institute of Technology)

[PPS09-P13] Partitioning of H, C, N and S on a growing Earth estimated by empirical thermodynamic modelling

MURASE YUTARO[1], Hiroaki Saito[1], *Kiyoshi Kuramoto[1] (1.Department of Cosmosciences, Graduate School of Sciences, Hokkaido University)

[PPS09-P14] Automatic segmentation of rayed craters on the Moon by applying deep learning technique

*Yuko Daket[1], Chikatoshi Honda[1], Takashi Sonoke[1], Hirohide Demura[1] (1.University of Aizu)

[PPS09-P15] Simulation of space weathering with mixture lunar-like composition

*Ryota Shimana[1], Sho Sasaki[1], Takahiro Hiroi[2] (1.Departure Earth and Space Science, Osaka University, 2.Department of Earth, Environmental and Planetary Sciences, Brown University)

[PPS09-P16] The 1300 km diameters ring fault around Orientale basin from gravity data

*Qingyun Deng[1], Fei Li[1,2], Jianguo Yan[1], Zhiyong Xiao[3], CHONG ZHENG[1], Chi Xiao[1], Jean-Pierre Barriot[1,4], Mao Ye[1] (1.The State Key Laboratory of Information Engineering in Surveying, Mapping and Remote Sensing, Wuhan University, 2.Chinese Antarctic Center of Surveying and Mapping, Wuhan University, 3.School of Atmospheric Scienses, Sun Yat-sen University, 4.Université de la Polynésie Française)

[PPS09-P17] The thermal history of comets derived from the EUV spectra data observed by HISAKI

*Kanae Nomura[1], Kazuo Yoshioka[1], Kei Masunaga[2] (1.University of Tokyo, 2.University of Colorado Boulder)

[PPS09-P18] A search for the non-water ices on the icy Galilean moons of Jupiter with ground-based telescope

*Seiko Takagi[1], Taro Matsuo[2], Jun Kimura[3] (1.Hokkaido University, Graduate School of Science, 2.Nagoya University, 3.Osaka University)

[PPS09-P19] Simulation study to detect Mars atmosphere by satellite gravimetry

*Keiko Yamamoto[1] (1.National Astronomical Observatory of Japan)

[PPS09-P20] Effects of the haze layer on Titan's atmospheric dynamics

*Motoki Sumi[1], Shin-ichi Takehiro[2], Wataru Ohfuchi[3], Hideko Nomura[4], Yuka Fujii[5] (1.Department of Earth & Planetary Sciences, Tokyo Institute of Technology, 2.Research Institute for Mathematical Sciences, Kyoto University, 3.Department of Planetology/CPS, Graduate School of Science, Kobe University, 4.Division of Science, National Astronomical Observatory of Japan, 5.Earth-Life Science Institute, Tokyo Institute of Technology)

[PPS09-P21] Participation of Japanese planetary science community to the Mercury exploration mission BepiColombo

*Shunichi Kamata[1], Ryuki Hyodo[2], Futoshi Takahashi[3], Takashi Yoshizaki[4], Yota Ishigaki[2], Kiyoshi Kuramoto[1], Go Murakami[2], Masaki Fujimoto[2] (1.Hokkaido Univ., 2.ISAS/JAXA, 3.Kyusyu Univ., 4.Tohoku Univ.)

[PPS09-P22] **Mercury Trek: A New Online NASA Visualization and Analysis Portal**

*Brian Hamilton Day[1], Emily Law[2], NASA Solar System Treks Team -[2] (1.NASA Ames Research Center, 2.NASA Jet Propulsion Laboratory)

[PPS09-P23] Proposed comet impacts forming Lake Michigan as an explanation of the formation of the Carolina bays.

*John Anthony Burgener[1] (1.Telegistics Inc.)

[J] Poster | P (Space and Planetary Sciences)：P-PS Planetary Sciences

[P-PS10] Formation and evolution of planetary materials in the Solar System

convener:Wataru Fujiya(Ibaraki University, College of Science), Megumi Matsumoto(Graduate School of Science, Tohoku University), Shin Ozawa(Department of Earth Science, Graduate School of Science, Tohoku University), Yuki Hibiya(Submarine Resources Research Center, Japan Agency for Marine-Earth Science and Technology)

[PPS10-P01] Quantitative shock stage evaluation of chondrites from X-ray diffraction: A new method

*Naoya Imae[1,2], Makoto Kimura[1] (1.Antarctic Meteorite Research Center, National Institute of Polar Research, 2.SOKENDAI)

[PPS10-P02] Synthesis of Mn-, Cr-bearing calcite, dolomite, and magnesite for Mn-Cr dating of carbonates

*Shingo Sugawara[1], Wataru Fujiya[1] (1.Ibaraki University)

[PPS10-P04] Aqueous interaction between olivine and organic compounds to imply spatial distribution of organics in meteorites

*Keisuke Muneishi[1], Hiroshi Naraoka[1] (1.Kyushu University)

[PPS10-P05] Formation process of a unique hydrous micrometeorite with abundant Fe-rich saponite and Fe sulfide

Shota Shimizu[1], Sakiko Kikuchi[2], *Tomoki Nakamura[1], Megumi Matsumoto[1], Takazo Shibuya[2], Cecile Engrand[3], Jean Duprat[3] (1.Department of Earth and Planetary Materials Sciences, Faculty of Science, Tohoku University, 2.JAMSTEC, 3.CSNSM, Université Paris-Sud)

[PPS10-P06] Microtexutural observations of TCIs in five CM carbonaceous chondrites and implications to aqueous environments on CM parent bodies.

Akane Iemoto[1], *Yusuke Seto[1], Akira Miyake[2] (1.Graduate School of Science, Kobe University, 2.Graduate School of Science, Kyoto University)

[PPS10-P07] Spectral measurements of carbonaceous chondrite in the extreme ultraviolet range

*Hiromasa Akadama[1], Kazuo Yoshioka[1], Takashi Mikouchi[1] (1.University of Tokyo)

[PPS10-P08] Elemental, isotopic, and structural analyses of insoluble organic matter from in Jbilet Winselwan carbonaceous chondrite

*Kanami Kamide[1], Hikaru Yabuta[1], Minoru Ikehara[2] (1.Hiroshima University, 2.Kochi University)

[PPS10-P09] **Synchrotron radiation-based X-ray computed nanotomography of unheated and experimentally heated Murchison CM chondrite**

*Megumi Matsumoto[1], Akira Tsuchiyama[2,3], Masahiro Yasutake[4], Akira Miyake[5], Kentaro Uesugi[4], Akihisa Takeuchi[4], Tsukasa Nakano[6], Tomoki Nakamura[1] (1.Graduate School of Science, Tohoku University, 2.Research Organization of Science and Technology, Ritsumeikan University, 3.Guangzhou Institute of Geochemistry, Chinese Academy of Sciences, 4.Japan Synchrotron Radiation Research Institute, 5.Graduate School of Science, Kyoto University, 6.Geological Survey of Japan, National Institute of Advanced Industrial Science and Technology)

[PPS10-P10] Fine-grained dark inclusion with very small chondrules in the NWA 1723 L chondrite

*Miki Takahashi[1], Tomoki Nakamura[1], Michael Zolensky[2] (1.Tohoku University, 2.NASA/JSC)

[PPS10-P11] Phosphate and phosphide in mesosiderites

*naoji sugiura[1], tomoko Arai[1], Matsui Takanori[1] (1.Chiba Institute of Technology)

[PPS10-P12] Multiple sulfur isotopic composition of mesosiderite meteorites: Implication for formation processes

*Shun Mihira[1], Akira Yamaguchi[2], Madhusoodhan Satish-Kumar[1] (1.Niigata University, 2.National Institute of Polar Research)

[PPS10-P13] Aqueous alteration in the nakhlites Y 000802

Ayaka Nakamura[1], *Masaaki Miyahara[1], Hiroki Suga[2], Akira Yamaguchi[3], Daisuke Wakabayashi[4], Shohei Yamashita[4], Yasuo Takeichi[4], Yoshio Takahashi[2], Eiji Ohtani[5] (1.Department of Earth and Planetary Systems Science, Graduate School of Science, Hiroshima University, 2.Department of Earth and Planetary, Graduate School of Science, The

University of Tokyo, 3.National Institute of Polar Research, 4.Institute of Materials Structure Science, High-Energy Accelerator Research Organization, 5.Department of Earth Sciences, Graduate School of Science, Tohoku University)

[J] Poster | P (Space and Planetary Sciences)：P-CG Complex & General

[P-CG26] New Developments of Planetary Sciences with ALMA

convener:Tetsuo Hasegawa(National Astronomical Observatory of Japan, National Institutes of Natural Sciences), Takayuki Muto(Division of Liberal Arts, Kogakuin University), Takahiro IINO(Information Technology Center, the University of Tokyo), Masumi Shimojo(National Astronomical Observatory of Japan)

[PCG26-P01] Difficulties in planetary formation theories revisited in light of ALMA observations

*Tetsuo Hasegawa[1] (1.National Astronomical Observatory of Japan, National Institutes of Natural Sciences)

[PCG26-P02] Recent progresses of the observational study on planet formation with ALMA and the future prospects including the connection with ngVLA

*Munetake Momose[1] (1.The College of Science, Ibaraki University)

[PCG26-P03] Three-dimensionl Simulations of Head-on/Oblique Collisions of Sintered Dust Aggregates

*Hidekazu Tanaka[1], Satoshi Okuzumi[2], Koji Wada[3] (1.Tohoku University, 2.Tokyo Institute of Technology, 3.Chiba Institute of Technology)

[PCG26-P04] Collisional Growth from dust to Planets and Protoplanetary Disks Observed by ALMA

*Hiroshi Kobayashi[1], Satoshi Ohashi[2] (1.Department of Physics, Nagoya University, 2.RIKEN)

[PCG26-P05] ALMA High Resolution Observations of GW Ori

Jiaqing Bi[2], Ruobing Dong[2], *Takayuki Muto[1] (1.Division of Liberal Arts, Kogakuin University, 2.University of Victoria)

[PCG26-P06] Dust grain growth in asymmetrical protoplanetary disk of V1247 Ori

*Kohki Gotoh[1], Misato Fukagawa[2], Takayuki Muto[3] (1.The university of Tokyo, 2.NAOJ, 3.Kogakuin University)

[PCG26-P07] Structure of Protoplanetary disk around WW Chameleon

*Kazuhiro Kanagawa[1], Jun Hashimoto[2], Takayuki Muto[3] (1.The University of Tokyo, 2.National Astronomical Observatory of Japan, 3.Kogakuin University)

[PCG26-P08] High-resolution ALMA and NIR Imaging of Protoplanetary Disk around T Tauri star

*Mihoko Konishi[1], Jun Hashimoto[2], Takayuki Muto[3] (1.Oita University, 2.Astrobiology Center, 3.Kogakuin University)

[PCG26-P09] Recent advances in the solar system science brought by ALMA observations

*Hideo Sagawa[1], Takahiro IINO[2] (1.Kyoto Sangyo University, 2.The University of Tokyo)

[PCG26-P10] Current status and prospects of solar observations with ALMA

*Masumi Shimojo[1] (1.National Astronomical Observatory of Japan)

[J] Poster | P (Space and Planetary Sciences)：P-CG Complex & General

[P-CG27] Origin and evolution of materials in space

convener:Hideko Nomura(Division of Science, National Astronomical Observatory of Japan), Takafumi Ootsubo(Institute of Space and Astronautical Science, Japan Aerospace Exploration Agency), Hitoshi Miura(Graduate School of Natural Sciences, Department of Information and Basic Science, Nagoya City University), Aki Takigawa(Department of Earth and Planetary Science, The University of Tokyo)

[PCG27-P01] Diffusion mechanisms of H^+ in interface between forsterite glass and amorphous ice

*Ayane Kubo[1], Junya Nishizawa[1], Tomoko Ikeda-Fukazawa[1] (1.Department of Applied Chemistry, Meiji University, Japan)

[PCG27-P02] Effects of deposition temperature on structure of amorphous ice

*Yui Ono[1], Kengo Oki, Tomoko Fukazawa[1,2] (1.Meiji University, 2.The Japanese Society of Snow and ice)

[PCG27-P03] Study of formation processes of $C_2H_2N_2$ by quantum chemical calculation

*Teppei Yonetsu[1], Hiroyuki Maezawa[1] (1.Osaka Prefecture University)

[PCG27-P04] Formation of Complex Organic Molecules via Ice Mantle Reactions in Protoplanetary Disks

Chen-En Wei[1], *Hideko Nomura[2], Catherine Walsh[3], Patrice Theule[4] (1.Department of Earth and Planetary Sciences, Tokyo Institute of Technology, 2.Division of Science, National Astronomical Observatory of Japan, 3.University of Leeds, 4.Aix-Marseille Universite)

[PCG27-P05] Complex organic molecules in comet 21P/Giacobini-Zinner

*Takafumi Ootsubo[1], Hideyo Kawakita[2], Shinnaka Yoshiharu[2], Jun-ichi Watanabe[3], Mitsuhiko Honda[4] (1.Institute of Space and Astronautical Science, Japan Aerospace Exploration Agency, 2.Kyoto Sangyo University, 3.National Astronomical Observatory of Japan, 4.Okayama University of Science)

[J] Poster | A (Atmospheric and Hydrospheric Sciences)：A-AS Atmospheric Sciences, Meteorology & Atmospheric Environment

[A-AS15] Progress in dense observation and numerical modeling of micro-scale meteorology

convener:Junshi Ito(Atmosphere and Ocean Research Institute, The University of Tokyo), Kentaro Araki(Meteorological Research Institute), Nobumitsu Tsunematsu(Tokyo Metropolitan Research Institute for Environmental Protection), Keigo Matsuda(Japan Agency for Marine-Earth Science and Technology)

[AAS15-P01] Preliminary consideration of the wind and pressure balance in multigrid assimilation scheme

*weiyu ding[1] (1.Institute of Tropical and Marine Meteorology, CMA, Guangzhou, China)

[AAS15-P02] Micro-Scale Atmospheric Pressure Measurement on the Campus of J. F. Oberlin University

*Atsushi Mori[1] (1.J. F. Oberlin University)

[AAS15-P03] **Statistical reconstruction of the heterogeneity of a dense urban wind field using a sparse network of weather stations**

*Ziv Klausner[1], Eyal Fattal[1] (1.Israel Institute for Biological Research)

[AAS15-P04] **Polarimetric Observations of Precipitating and Non-precipitating Stratiform Clouds**

*Kenneth Allan Sinclair[1] (1.NASA Goddard Institute for Space Studies)

[AAS15-P05] Numerical simlation of tornado occured at Nobeoka accompanied by TC1917

*Junshi Ito[1], Hiroshi Niino[1] (1.Atmosphere and Ocean Research Institute, The University of Tokyo)

[AAS15-P06] Quantifying the Impact of Future Urbanization on Urban Microclimate Over Mumbai Metropolitan Region, India.

*Vinayak Nitin Bhanage[1], Han Soo Lee[1], Shirishkumar Gedam[2] (1.CSRE,Indian Institute of Technology,Bombay,India. and Graduate School for International Development and cooperation,Hiroshima University,Japan, 2.CSRE,Indian Institute of Technology,Bombay,India)

[AAS15-P07] Characteristics of Variation of the Atmospheric Boundary Layer Affected by the Gust Fronts

*jie lan Xie[1,2,3], Shao jia Fan[1,2,3] (1.School of Atmospheric Sciences, Sun-Yatsen University, 2.Observation and Research Station for Climate Environment and Air Quality Change in the Pearl River Estuary, 3.Southern Marine Science and Engineering Guangdong Laboratory(Zhuhai))

[AAS15-P08] Development process of convective boundary layer and turbulence characteristic above urban canopy with heterogeneous heating at building and street surface

*Yasuo Hattori[1], Shuji Ishihara[2], Hitoshi Suto[1], Keisuke Nakao[1], Yuma Hasebe[2], Hiromaru Hirakuchi[1] (1.Central Research Institute of Electric Power Industry, 2.Denryoku Computing Center)

[J] Poster | A (Atmospheric and Hydrospheric Sciences)：A-OS Ocean Sciences & Ocean Environment

[A-OS18] Coastal circulation and material cycle and freshwater discharge through rivers

convener:Shinichiro Kida(Research Institute for Applied Mechanics, Kyushu University), Kiyoshi Tanaka(University of Tokyo), Dai Yamazaki(Institute of Industrial Sciences, The University of Tokyo), Yuichi Hayami(Saga University)

[AOS18-P01] A regional river-ocean seamless model for Kyushu

*Shinichiro Kida[1], Takahiro Tsutsumi[2], Yosuke Alexandre Yamashiki[3], Ryusuke Kuroki[3] (1.Research Institute for Applied Mechanics, Kyushu University, 2.Interdisciplinary Graduate School of Engineering Science, Kyushu University, 3.Graduate School of Advanced Integrated Studies in Human Survivability, Kyoto University)

[AOS18-P02] Relationship between environment and macrobenthos distribution in the coastal area of Kashima city in Ariake Sea

*Yuichi Hayami[1], Naoki Fujii[1] (1.Saga University)

[AOS18-P03] SST variability in Suruga Bay and its surrounding area due to Kuroshio path variability

*Yuya Hirano[1], Kazuyuki Uehara[1] (1.The Graduate School of Geo-environmental Science, Tokai University)

[AOS18-P04] The seasonal cycle of phytoplankton biomass concentration along the coast of Japan

*Shimada Hiroaki[1], Shinichiro Kida[2] (1.Interdisciplinary Graduate School of Engineering Sciences , Kyushu University, 2.Research Institute for Applied Mechanics , Kyushu University)

[AOS18-P05] **Modelling Study of the Zhe-Min Coastal current**

*yang zhang[1], min bao[1] (1.Second Institute of Oceanography, MNR)

[AOS18-P06] Sea surface temperature and chlorophyll *a* variations in the Sanriku Coastal area and their influence on the environment of Otsuchi Bay

*XUANYU LIU[1], Sachihiko Itoh[1], Eisuke Tsutsumi[1], Kiyoshi Tanaka[1] (1.University of Tokyo)

[AOS18-P07] Multi-layer temperature variability at Kurasawa on the back of Suruga Bay.

*Mito Nakamura[1], Kazuyuki Uehara[1] (1.tokai university the graduate school of marine science and technology)

[J] Poster | A (Atmospheric and Hydrospheric Sciences)：A-OS Ocean Sciences & Ocean Environment

[A-OS26] Global ocean observing systems, their recent status, research results and future directions

convener:Shigeki Hosoda(Japan Marine-Earth Science and Technology), Shuhei Masuda(Japan Agency for Marine-Earth Science and Technology), Yosuke Fujii(Meteorological Research Institute, Japan Meteorological Agency), Fujiki Tetsuichi(Japan Agency for Marine-Earth Science and Technology)

[AOS26-P02] **Introduction of bio-chemilcal observation data on GCM assimilation with a lower ecosystem model**

*Takashi SETOU[1], Takeshi OKUNISHI[1], Hiroshi Kuroda[1], Naoki Yoshie[3], Shin-ichi Ito[2], Kiyotaka Hidaka[1], Taketoshi Kodama[1], Yugo SHIMIZU[1], Daiki Ito[1] (1.Fisheries Research and Education Agency, 2.University of Tokyou, 3.Ehime University)

[AOS26-P03] Progress of the decadal scale anthropogenic CO_2 in the Southern Ocean

*BOFENG LI[1], Xianliang Pan[1], Shun Yunoki[1], Yutaka Watanabe[1] (1.Hokkaido University)

[AOS26-P04] Spatiotemporal distribution of anthropogenic nitrogen and internal nitrogen dynamics in the Southern Ocean

*Xianliang Pan[1], Bofeng Li[1], Zhigang Chen[1], Yutaka Watanabe[1] (1.Hokkaido University)

[AOS26-P05] Initiation of biogeochemical float observations in the western North Pacific

*Fujiki Tetsuichi[1], Shigeki Hosoda[1] (1.Japan Agency for Marine-Earth Science and Technology)

[AOS26-P06] Small water mass transport across the Kuroshio Extension region in the thermocline by Seaglider and BGC Argo floats: Hints of integrated ocean observations

*Shigeki Hosoda[1], Ryu Inoue[1], Masami Nonaka[1], Hideharu Sasaki[1], Yoshikazu Sasai[1], Mizue Hirano[1] (1.Japan Marine-Earth Science and Technology)

[AOS26-P07] Halocline Structures in the Subarctic North Pacific Detected by Argo Data

*Shota Katsura[1], Ueno Hiromichi[2], Humio Mitsudera[3], Shinya Kouketsu[4] (1.Scripps Institution of Oceanography, University of California, San Diego, 2.Faculty of Fisheries Science, Hokkaido University, 3.Institute of Low Temperature Science, Hokkaido University, 4.Japan Agency for Marine-Earth Science and Technology)

[AOS26-P08] **The propagation of spiciness anomalies in the upper North Pacific**

*Tong Wang[1], Toshio Suga[1,2], Shinya Kouketsu[2] (1.Graduate School of Science, Tohoku University, 2. Japan Agency for Marine-Earth Science and Technology)

[AOS26-P09] Release of Deep Argo floats' salinity correction dataset

*Kanako Sato[1], Taiyo Kobayashi[1], Shigeki Hosoda[1], Shuhei Masuda[1] (1.Japan Agency for Marine-Earth Science and Technology)

[AOS26-P10] Boundaries of Physical Structures in the Mid-latitude Northwest Pacific Ocean Identified based on Unsupervised Clustering

*Fumika Sambe[1], Toshio Suga[1,2] (1.Graduate School of Science, Tohoku University, 2.JAMSTEC)

[J] Poster | A (Atmospheric and Hydrospheric Sciences)：A-OS Ocean Sciences & Ocean Environment

[A-OS27] Chemical and Biological Oceanography

convener:Kazuhiro Misumi(Environmental Science Research Laboratory, Central Research Institute of Electric Power Industry), Sayaka Yasunaka(Japan Agency for Marine-Earth Science and Technology)

[AOS27-P01] Evaluation of uncertainty of nutrient measurements

*Daisuke Sasano[1], Michio Aoyama[2,3], Toshiya Nakano[4], Naoki Nagai[1] (1.Japan Meteorological Agency, 2.University of Tsukuba, 3.JAMSTEC, 4.Nagasaki Meteorological Office)

[AOS27-P02] Effect of ocean acidification on bioavailability of iron bound to natural iron-complexing ligands

*Shigenobu Takeda[1], Koichi Hideshima[1], Yoshiko Kondo[1], Mitsuhide Sato[1] (1.Nagasaki University)

[AOS27-P03] Radiocesium in the Kuroshio region and the Taiwan Strait from 2017 to 2018

*Wei-Jen Huang[1], Chen-Tung Arthur Chen[1], Ming-An Lee[2], Sen Jan[3], Yiing-Jang Yang[3] (1.National Sun Yat-sen University, 2.National Taiwan Ocean University, 3.National Taiwan University)

[AOS27-P05] pH measurement of transparent exoplymeric particles secreted by oceanic diatoms

*Tasuku Akagi[1], Rin Ito[2], Takeshi Ishihara[3] (1.Department of Earth and Planetary Sciences, Kyushu University, 2.Department of Earth and Planetary Sciences, Faculty of Sciences, Kyushu University, 3.Department of Biology, Kyushu University)

[J] Poster | A (Atmospheric and Hydrospheric Sciences)：A-OS Ocean Sciences & Ocean Environment

[A-OS28] Physical Oceanography (General)

convener:Yoshimi Kawai(Research Institute for Global Change, Japan Agency for Marine-Earth Science and Technology), Kitade Yujiro(Tokyo University of Marine Science and Technology)

[AOS28-P01] Upper-Ocean Circulation Anomalies of the Western Equatorial Pacific Observed in 2016 Summer

★Invited Papers

*Yilong Lyu[1] (1.Institute of Oceanology, Chinese Academy of Sciences)

[AOS28-P02] **Seasonal variability of the Upper Mixed Layer Temperature in Sulawesi Sea**

*Xiaofang Wan[1], Aijun Pan[1] (1.Third Institute of Oceanography, Ministry of Natural Resources,China)

[AOS28-P04] **Response of Near-Inertial Shear to Wind Stress Curl and Sea Level**

*Jing Gao[1,2], Jianing Wang[1,3], Fan Wang[1,2,3] (1.Institute of Oceanology, Chinese Academy of Sciences, 2.University of Chinese Academy of Sciences, 3. Laboratory for Ocean and Climate Dynamics, Qingdao National Laboratory for Marine Science and Technology)

[AOS28-P05] **The ocean-atmosphere interaction over a summer upwelling system in the South China Sea**

*Yi Yu[1], Yuntao Wang[1] (1.State Key Laboratory of Satellite Ocean Environment Dynamics, Second Institute of Oceanography, Ministry of Natural Resources)

[AOS28-P06] Tracking Experiment of adrift object using Surface Drifter in Southeast coast 2019

*SeungYun HA[1], YoungTaeg Kim[1], SeokJae Kwon[1], JaeMin Kim[1], JooEun KIM[1], Ho-Kyun Kim[1] (1.Korea Hydrographic and Oceanographic Agency, Busan, Republic of Korea)

[AOS28-P07] Prediction of Storm Surge due to Typhoon passing Korea using by Machine Learning

*Boonsoon Kang[1], Jongjib Park[2], Wanhee Cho[3], Jongyoon Mun[3], Seokjae Kwon[1], Eunil Lee[1] (1.Ocean Research Division, Korea Hydrographic and Oceanographic Agency(KHOA), 2.Department of Coastal Management, Geosystem Research Corporatio, 3.Oceanographic Division, Marine information Technology Corporation)

[AOS28-P08] Impact of applying tidal correction to marginal-sea bathymetry dataset

*Katsuto Uehara[1] (1.Kyushu University)

[AOS28-P09] Changes of the obduction and subduction rates accompanied by anomalous winters

*Yoshimi Kawai[1], Kazuyuki Uehara[2], Shigeki Hosoda[1] (1.Research Institute for Global Change, Japan Agency for Marine-Earth Science and Technology, 2.School of Marine Science and Technology, Tokai University)

[AOS28-P12] Estimation of duration for 2017 Kuroshio large meander

*Takashi SETOU[1], Yugo SHIMIZU[1], Akira KUSAKA[1], Daisuke AMBE[1], Daiki Ito[1], Takuhiko KAMEDA[1] (1.Fisheries Research and Education Agency)

[AOS28-P13] **Baroclinic vertical modes around the East Asian seas**

*You-Soon Chang[1], Byeong-Jun Lim[1], Do-Youn Kim[2] (1.Kongju National University, 2.Ara Consulting & Technology)

[J] Poster | A (Atmospheric and Hydrospheric Sciences)：A-OS Ocean Sciences & Ocean Environment

[A-OS29] Ocean Research Planning for UN Decade of Ocean Science for Sustainable Developments (2021-2030)

convener:Kentaro Ando(Japan Agency for Marine and Earth Science and Technology), Yoshiko Kondo(Nagasaki University), Eitarou Oka(Atmosphere and Ocean Research Institute, The University of Tokyo), Sanae Chiba(JAMSTEC)

[AOS29-P01] Reports on the UN Ocean Science Decade Regional Planning Workshop for the North Pacific and Western Pacific Marginal Seas in the last August and recent activities for the UN Decade in the IOC/WESTPAC region

*Kentaro Ando[1], Wenxi Zhu[2] (1.Japan Agency for Marine and Earth Science and Technology, 2.IOC/WESTPAC secretariat)

[AOS29-P03] Toward an attractive “UN Decade of Ocean Science”

*Sayaka Yasunaka[1], Kaoru Kubokawa[2], Naomi Harada[1] (1.Japan Agency for Marine-Earth Science and Technology, 2.Teikyo University)

[J] Poster | A (Atmospheric and Hydrospheric Sciences)：A-HW Hydrology & Water Environment

[A-HW34] Isotope Hydrology 2020

convener:Masaya Yasuhara(Rissho Univ.), Kohei Kazahaya(Geological Survey of Japan, AIST), Shinji Ohsawa(Institute for Geothermal Sciences, Graduate School of Science, Kyoto University), Kazuyoshi Asai(Geo Science Laboratory)

[AHW34-P01] Establishment of accurate estimation method of heavy metal loads in an agricultural river and origins of heavy metals in Fuku River, Saitama, Japan

*Manatsu Kimura[1], Masaya Yasuhara[2], Seongwon Lee[2] (1.Graduate Cource in Environment Systems of Geo-Environmental Science RISSHO University, 2.Environment Systems of Geo-Environmental Science RISSHO University)

[AHW34-P02] The influence of geology on river water quality and chemical loads in Oshika Village, Nagano, Japan

Miyuki Mori[1], *Masaya Yasuhara[1], Seongwon Lee[1], Yuri Hirano[1], Fumitake Kusuhara[2], Noritoshi Morikawa[3], Kohei Kazahaya[3] (1.Rissho Univ., 2.Central Research Institute of Electric Power Industry, 3.Geological Survey of Japan, AIST)

[AHW34-P03] A study on life cycle of freshwater copepod in Chino-ike(Bloody lake), an ephemeral lake on the top of Mt.Akagi, central Japan

*Yuri Hirano[1], Masaya Yasuhara[2], Seongwon Lee[2], Nozomu Iwasaki[2], Yasuhiro Funyu[3], Natumi Simota[4] (1.Rissho University(undergraduate student), 2.Rissho University, 3.Graduate School of Geo-environmental Science, Rissho University, 4.Corporation Belc)

[AHW34-P04] Estimation of Excess Air in groundwater using dissolved Nitrogen and Argon

Kazuyoshi Asai[1], *Kazumi Asai[1] (1.Chikyukagakukenkyusho inc)

[AHW34-P05] Vertical distribution of stable isotopes in deep groundwater of Kofu basin

*Ruri Isobe[1], Takashi Nakamura[1] (1.International Research Center for River Basin Environment, University of YAMANASHI)

[AHW34-P06] On balance of chloride ion in Kanna river aroud Wataruse area, Kamikawa, Saitama, Japan

*Taketoshi Hasegawa[1], Masaya Yasuhara[2], Seongwon Lee[2], Noritoshi Morikawa[3], Tsukamoto Hitoshi[3] (1.KYODO ENGINEERING Corp., 2.Rissho University of Geo-environmental science, 3.Geological Survey of Japan, AIST)

[AHW34-P07] Estimation of groundwater residence time in Mt. Iwaki

Kazumi Asai[1], Seiichiro Ioka[2], *Kazuyoshi Asai[1] (1.Geo Science Laboratory, 2.Hirosaki University)

[AHW34-P08] Isotope tracing for mountain groundwater recharges in volcanic and non-volcanic mountains

*Takashi Nakamura[1], sano anna[1], Kei Nishida[1] (1.International Research Center for River Basin Environment, University of YAMANASHI)

[AHW34-P09] Water chemistry of shallow groundwater and its evolution processes in southern parts of Okinawa island, Japan

Kaede Shimoji[1], *Masaya Yasuhara[1], Seongwon Lee[1], Takashi Nakamura[2], Kazuyoshi Asai[3] (1.Rissho Univ., 2.Yamanishi Univ., 3.Geoscience Laboratory)

[AHW34-P10] Depleting trend of deuterium excess in precipitation observed from 1998 to 2018 at Tiksi, Russia

*Kimpei Ichiyanagi[1], Hotaek Park[2], Masahiro Tanoue[3], Takayuki Uesugi[1] (1.Kumamoto University, 2.JAMSTEC, 3.National Institute for Environmental Studies)

[AHW34-P11] Groundwater recharge in the Kurobe River Alluvial Fan and the nutrient dynamics using chemical compositions, oxygen and hydrogen isotopes: influence by land-use and climate changes over the past 30 years

*YUNYE LIU[1], JING ZHANG[2], Saki KATAZAKAI[1], Yuhei Nakayasu[1], Rezedan Aray[1] (1.Graduate School of Science and Engineering, University of Toyama, 2.Faculty of Science, Academic Assembly, University of Toyama)

[J] Poster | A (Atmospheric and Hydrospheric Sciences)：A-HW Hydrology & Water Environment

[A-HW35] Perspectives on Surface- and subsurface-water resources, society, and the environment

convener: Abhishek(Tokyo Institute of Technology), Tsuyoshi Kinouchi(Tokyo Institute of Technology), Brijesh K yadav(Indian Institute of Technology Roorkee)

[AHW35-P01] **Why full overturning in Lake Biwa was incomplete in spring 2019? : Simulation study**

*Satoshi Nakada[1], Kenta Yamada[2], Takahiro Okamoto[2], Haruki Yamamoto[2], Koichi Shimotori[1], Akio Imai[1] (1.National Institute for Environmental Studies, 2.Lake Biwa Environmental Research Institute)

[AHW35-P02] Groundwater Resource Assessment using Geophysical Investigation and Hydrological Modelling in Vindhyan-Ganga Sedimentary Formations

*Manik Goel[1], Pankaj Kumar Gupta[2], Brijesh K yadav[1] (1.Indian Institute of Technology Roorkee, Roorkee, India, 2.University of Waterloo, Waterloo, ON, Canada)

[AHW35-P03] **Data Selection for Parameter Estimation Robust to Changing Climatic Conditions**

*Avantika Rathore[1], Joseph H. A. Guillaume[2], Anthony J. Jakeman[2] (1.Indian Institute of Technology Roorkee, 2. Australian National University, Australia)

[AHW35-P04] Impact of mining on water quality and heavy metal dynamics in southern Lao PDR : A brief report

Nanthana Boungnaphalom[1], JING ZHANG[1], *Saki KATAZAKAI[1] (1.Graduate school of science and endneering, University of Toyama)

[AHW35-P05] **GIS-based spring potential mapping in Beijing using machine learning methods**

*Huixiang Li[1], Yun Pan[1], Ying Sun[2] (1.Capital Normal University, 2.Beijing Institute of Hydrogeology and Engineering Geology)

[AHW35-P06] **Greening and browning analysis in Peninsular India detected by change in Leaf Area Index and its relation to the climatic conditions**

*Bageshree K[1], Tsuyoshi Kinouchi[1] (1.Tokyo Institute of Technology)

[AHW35-P07] **Hydrochemical characteristics and sources of brines in the Sua Pans, Botswana.**

*Fiona Segolame Motswaiso[1], Kengo Nakamura[1], Noriaki Watanabe[1], Takeshi Komai[1] (1.Tohoku Univeristy Graduate School of Environmental Studies)

[J] Poster | A (Atmospheric and Hydrospheric Sciences)：A-HW Hydrology & Water Environment

[A-HW36] Water Environment and Geology in Urban Areas

convener:Takeshi Hayashi(Faculty of Education and Human Studies, Akita University)

[AHW36-P01] Evaluation of subsurface warming in the Tokyo metropolitan area: characteristics of long-term change in subsurface temperature beneath Yokohama and Kawasaki areas

*Akinobu Miyakoshi[1], Takeshi Hayashi[2] (1.Geological Survey of Japan, AIST, 2.Faculty of Education and Human Studies, Akita University)

[AHW36-P02] Development of multi-tracer method for evaluation of water cycle process in urban area

*Takeshi Hayashi[1], Masaya Yasuhara[2], Takashi Nakamura[3] (1.Faculty of Education and Human Studies, Akita University, 2.Faculty of Geo-environmental science, Rissho University, 3.Graduate Faculty of Interdisciplinary Research Faculty of Engineering, University of Yamanashi)

[AHW36-P03] Water supply system and environmental impacts of chemical release accidents caused by the major earthquake

*Lisa Ito[1], Akihiro Tokai[1], Toyohiko Nakakubo[2] (1.Graduate School of Engineering, Osaka University, 2.Natural Science Division, Fuculty of Core Reserch, Ochanomizu University)

[AHW36-P04] **Exploring the linkage between urban flood risk and spatial characteristics in small urbanized catchments of Beijing, China**

*Lei Yao[1] (1.Shandong Normal University)

[AHW36-P05] Flood disasters and river management in the downstream of Tama River following 2019 Typhoon Hagibis (JMA Typhoon No. 19)

*Jiro Komori[1] (1.Teikyo Heisei University)

[AHW36-P06] Development of a detailed land surface state estimation method toward usage in weather prediction

*Yuuki Myo[1], Kazuyoshi Souma[1] (1.University of Yamanashi)

[J] Poster | A (Atmospheric and Hydrospheric Sciences)：A-CC Cryospheric Sciences & Cold District Environment

[A-CC39] Glaciology

convener:Takayuki Nuimura(Tokyo Denki University), Ishikawa Mamoru(Hokkaido University), Kzutaka Tateyama(National University Corporation Kitami Institute of Technology), Hiroto Nagai(Waseda Univ., School of Education)

[ACC39-P01] Estimation of mass balance of glaciers in the Northern Japanese Alps using SfM-MVS

*Kenshiro Arie[1], Chiyuki Narama[1], Kotaro FUKUI[2], Hajime IIDA[2] (1.Niigata University, 2.Tateyama Caldera Sabo Museum)

[ACC39-P02] Glacier flow velocity changes near the border of Alaska-Yukon detected by the Sentinel-1B SAR images

*Natsuki Muto[1] (1.Department of Natural History Sciences, Hokkaido University)

[ACC39-P03] Drainage from short-lived glacial lake in the Tien Shan, Central Asia.

Mirlan Daiyrov[1], *Chiyuki Narama[2], Tsutomu Yamanokuchi[3] (1.Central-Asian Institute for Applied Geosciences (CAIAG), 2.Niigata University, Department of Science, 3.RESTEC)

[ACC39-P04] Ice cliff dynamics in Trakarding Glacier, Nepal Himalaya

*Yota Sato[1], Koji Fujita[1], Hiroshi Inoue[2], Sojiro Sunako[2], Akiko Sakai[1], Akane Tsushima[3], Evgeny A. Podolskiy[4,5], Berthier Etienne[6], Kayastha Rijan[7] (1.Graduate School of Environmental Studies, Nagoya University, 2.National Research Institute for Earth Science and Disaster Resilience, 3.Meteorological Research Institute, 4. Arctic Research Center, Hokkaido University, 5.Global Station for Arctic Research, Global Institution for Collaborative Research and Education, Hokkaido University, 6.Université de Toulouse, 7. School of Science, Kathmandu University)

[ACC39-P05] Normally collapse of hanging glaciers at Mt. Langtang Lirung in Nepal

*Kosuke Matsumoto[2], Chiyuki Narama[1], Honami Watanabe[3], Katsuhisa Kawashima[1], Hiroshi YAGI[4], Daisuke Higaki[5], Akihiko Wakai[6] (1.Niigata University, 2.Graduate school of Niigata University, 3.RESTEC, 4.Yamagata University, 5.Hirosaki University, 6.Gunma University)

[ACC39-P06] The surface change of glacier-derived rock glacier in the northern Tien Shan

*Shun Okuyama[1], Chiyuki Narama[1], Hideyuki Takadama[2] (1.Niigata University, 2.PASCO Co.)

[ACC39-P07] Estimation of snow surface patterns between Showa Station and Dome-Fuji Station of Antarctica using camera images

*Konosuke Sugiura[1], Hirotaka Tomita[1], Kengo Watanabe[1], Naohiko Hirasawa[2], Kenji Kawamura[2], Fumio Nakazawa[2], Hiroshi Ohno[3], Shuji Fujita[2], Ikumi Oyabu[2], Takashi Yamanouchi[2], Hideaki Motoyama[2] (1.University of Toyama, 2.National Institute of Polar Research, 3.Kitami Institute of Technology)

[ACC39-P08] **Temporal and spatial variations of melting and Rain-On-Snow event on the sheets detected by Microwave observation**

Nuerasimuguli Alimasi[1], *Hiroyuki Enomoto[1], Naohiko Hirasawa[1] (1.National Institute of Polar Research)

[ACC39-P09] Monitoring Snow Avalanches by Infrasonic and Seismic Sensors on Mt.Fuji in 2018-2019 Winter Season

*Wataru Ikeda[1], Mie Ichihara[1], Ryo Honda[2], Hiroshi Aoyama[3], Shin'ichi Sakai[1] (1.Earthquake Research Institute, University of Tokyo, 2.Mount Fuji Research Institute, Yamanashi Perfectual Government, 3.Institute of Seismology and Volcanology, Faculty of Science, Hokkaido University)

[ACC39-P10] Application of SGLI and MSI sensor to estimate ice breakup dates on Lake Suwa

*Takashi Nonaka[1], Tomohiro Nakazawa[1] (1.College of Industrial Technology, Nihon University)

[ACC39-P11] Microplastics in rime-ice observed in Kyushu Mountain area, Japan

*Osamu Nagafuchi[1], Koyomi Nakazawa[1], kenichi Shinozuka[1], Koji KaneFuji[2] (1.Fukuoka Institute of Technology , 2.The Institute of Statistical Mathematics)

[ACC39-P12] The relationship between distribution of snow algae and vegetation: Mt. Naeba, Japan.

*Tsubasa Takahashi[1], Suzuki Takumi[1], Nozomu Takeuchi[1] (1.Chiba University)

[J] Poster | A (Atmospheric and Hydrospheric Sciences)：A-CG Complex & General

[A-CG54] Biogeochemical cycles in Land Ecosystem

convener:Tomomichi Kato(Research Faculty of Agriculture, Hokkaido University), Kazuhito Ichii(Chiba University), Takeshi Ise(FSERC, Kyoto University), Munemasa Teramoto(Arid Land Research Center, Tottori University)

[ACG54-P01] Long-term observations of plant phenology, and land cover and land use change by satellite remote-sensing in Asia

*Shin Nagai[1], Taku M Saitoh[2] (1.Earth Surface System Research Center, Research Institute for Global Change, Japan Agency for Marine-Earth Science and Technology, 2.River Basin Research Center, Gifu University)

[ACG54-P02] Carbon emission estimation through tropical peatland subsidence using interferometric synthetic aperture radar analysis

*Tomohiro Shiraishi[1], Ryuichi Hirata[1], Masato Hayashi[2], Takashi Hirano[3] (1.National Institute for Environmental Studies, 2.Japan Aerospace Exploration Agency, 3.Research Faculty of Agriculture, Hokkaido University)

[ACG54-P03] Effect of global warming on forest ecosystem in Japan: Data analysis using tree-rings, satellite images and earth system model

*Shunsuke Tei[1] (1.Arctic Research Center, Hokkaido University)

[ACG54-P04] A large-scale evaluation of bamboo stand expansion using deep learning and its effect on ecosystem carbon storage

*Yurika Oba[1], Takeshi Ise[2] (1.Center for the Promotion of Interdisciplinary Education and Research, Kyoto University, 2.Field Science Education and Research Center, kyoto University)

[ACG54-P05] Subdaily natural CO_2 flux simulation in Kantō area to support inversion analysis of Tokyo's anthropogenic CO_2 emission

*Qiao Wang[1], Ryoichi Imasu[1], Yutaka Arai[1], Satoshi Ito[1], Takahiro Sasai[2], Hiroaki Kondo[3] (1.AORI, The University of Tokyo, 2.Department of Geophysics, Tohoku University, 3.National Institute of Advanced Industrial Science and Technology)

[ACG54-P06] A long term evaluation of carbon balance in a managed urban forest in central Japan using a Forest Biogeochemical Model (BGC-ES)

Guochao Wang[4], *Tomotsugu Yazaki[1], Makoto Ooba[2], Toshio Kume[4], Takamitsu Kai[3] (1.School of Agriculture, Meiji University, 2.National Institute for Environmental Studies, 3.Kurokawa Field Science Center, Meiji University, 4.Graduate School of Agriculture, Meiji University)

[ACG54-P07] **The long-term observation of PRI and LUE and phenology changes in a temperate Japanese cypress forest at Kiryu Japan.**

*CHEN SIYU[1], Yoshiko Kosugi[1], Tatsuro Nakaji[2], Hibiki M Noda[3], Kenlo Nishida Nasahara[4], Kouki Hikosaka[5] (1.Graduate school of agriculture,Kyoto University, 2.Hokkaido University, 3.National Institute for Environmental Studie, 4.University of Tsukuba, 5.Tohoku University)

[ACG54-P08] **Challenging the detection of solar-induced fluorescence from lower resolution field-measured spectrum in Japan**

*Naohisa Nakashima[1], Tomoki Morozumi[1], KANOKRAT BUAREAL[3], Tomomichi Kato[1], Katsuto Tsujimoto[2], Tomoko Akitsu[4], Kenlo Nasahara[4], Keisuke Ono[5], Hiroyuki Muraoka[6] (1.Research Faculty of Agriculture, Hokkaido University, 2.Graduate School of Life Sciences, Tohoku University, 3.Graduate School of Global Food Resources, Hokkaido University, 4.Faculty of Life and Environmental Sciences, University of Tsukuba, 5.National Institute for Agro-Environmental Sciences, 6.River Basin Research Center, Gifu University)

[ACG54-P09] Influence of climatic fluctuations on crop production for 135 years in Japan

*Tomomichi Kato[1], Moeka Ono[1], Daiki Watanabe[1] (1.Research Faculty of Agriculture, Hokkaido University)

[ACG54-P10] Long-term warming effect on soil carbon fluxes in a red pine forest in Tsukuba

*Munemasa Teramoto[1], Naishen Liang[1], Jiye Zeng[1], Jun Koarashi[2], Toshiaki Kondo[3], Mariko Atarashi-Andoh[2], Takafumi Aramaki[1], Xin Zhao [1] (1.National Institute for Environmental Studies, 2.Japan Atomic Energy Agency, 3.Japan International Research Center for Agricultural Sciences)

[J] Poster | A (Atmospheric and Hydrospheric Sciences)：A-CG Complex & General

[A-CG55] Coastal Ecosystems - 1. Water Cycle and Land-Ocean Interactions

convener:Makoto Yamada(Faculty of Economics, Ryukoku University), Ryo Sugimoto(Faculty of Marine Biosciences, Fukui Prefectural University), Masahiko Fujii(Faculty of Environmental Earth Science)

[ACG55-P01] Reconstitution of the environment of Submarine Groundwater Discharge (SGD) in the near past by using carbon and oxygen stable isotope ratio in the shell of bivalve

*Osamu Tominaga[1], Seira Tobe[1], Tatsuhiro Ishida[1] (1.Fukui Prefectural University)

[ACG55-P02] Effects of the inflow of hot spring drainage into rivers in Beppu City, Oita Prefecture on benthos in the estuary area.

*Kazuya Shimizu[1], Makoto Yamada[1], Makoto Uenishi[1], Shinji Ohsawa[2] (1.Ryukoku University, 2.Institute for Geothermal Sciences, Kyoto University)

[ACG55-P03] Spatial and seasonal variation of water quality in Batan Bay, Philippines

*Toshihiro Miyajima[1], Ryan Basina[2], Charissa M. Ferrera[3], Naoko Morimoto[1], Yasmin H. Primavera Tirol[2], Maria Lourdes San Diego-McGlone[3], Masami Hamaguchi[4] (1.Marine Biogeochemistry Group, Division of Ocean-Earth System Science, Atmosphere and Ocean Research Institute, The University of Tokyo, 2.Aklan State University New Washington, 3.Marine Science Institute, University of the Philippines Diliman, 4.National Research Institute of Fisheries and Environment of Inland Sea, Japan Fisheries Research and Education Agency)

[ACG55-P04] Influence of River Discharge on the Spatial and Temporal Variability of Chlorophyll-a in the Toyama Bay

*Eligio de Raus Maure[1], Genki Terauchi[1], Yasuyuki Harada[1] (1.Northwest Pacific Region Environmental Cooperation Center)

[J] Poster | A (Atmospheric and Hydrospheric Sciences)：A-CG Complex & General

[A-CG56] Coastal Ecosystems-2. Coral reefs, seagrass and macroalgal beds, and mangroves

convener:Yu Umezawa(Tokyo University of Agriculture and Technology), Toshihiro Miyajima(Marine Biogeochemistry Group, Division of Ocean-Earth System Science, Atmosphere and Ocean Research Institute, The University of Tokyo), Atsushi Watanabe(The ocean policy research institute, The Sasakawa peace foundation), Tomihiko Higuchi(Atmosphere and Ocean Research Institute, The University of Tokyo)

[ACG56-P01] Nano-SIMS analysis can highlight the effect of symbiotic zooxanthellae on sulfur utilization of corals

*Tomihiko Higuchi[1], Kentaro Tanaka[1], Kotaro Shirai[1], Ikuko Yuyama[2], Takuma Mezaki[3], Naoto Takahata[1], Yuji Sano[1] (1.Atmosphere and Ocean Research Institute, The University of Tokyo, 2.University of Tsukuba, 3.Kuroshio Biological Research Foundation)

[ACG56-P02] Compound specific stable nitrogen isotope analysis of amino acids and sulfur-containing component analysis of reef corals: Toward method development for the prevention of coral bleaching and for recovering from damaged status.

*Yohei Matsui[1,2], Toshihiro Miyajima[1], Tomihiko Higuchi[1], Kentaro Tanaka[1], Naoko Morimoto[1], Yanhui Yang[1], Hiroyuki Fujimura[3], Naoko Yasuda[3], Sylvain Agostini[4], Ikuko Yuyama[4], Takashi Nakamura[5], Masahiro Yuki[6], Shingo Kato[6], Wataru Fujisaki[2] (1.Atmosphere and Ocean Research Institute (AORI), The University of Tokyo, 2.Japan Agency for Marine-Earth Science and Techonology (JAMSTEC), 3.University of the Ryukyus, 4.University of Tsukuba, 5.Tokyo Institute of Technology, 6.RIKEN)

[ACG56-P03] Examination of potential effects of nitrogen supply on nitrogen content and decomposition characteristics of eelgrass (*Zostera marina*)

*Toru Miyata[1], Yu Umezawa[1], Makoto Watanabe[1], Yoshiki Horikawa[1], Masahiro Nakaoka[2] (1.Tokyo University of Agriculture and Technology, 2.Hokkaido University)

[ACG56-P04] Macroalgal metabolism and carbon budgets affect atmospheric CO_2 uptake in a temperate *Sargassum* bed

*Kenta Watanabe[1], Goro Yoshida[2], Masakazu Hori[2], Yu Umezawa[3], Hirotada Moki[1], Tomohiro Kuwae[1] (1.Port and Airport Research Institute, 2.National Research Institute of Fisheries and Environment of Inland Sea, 3.Tokyo University of Agriculture and Technology)

[ACG56-P05] Degradation characteristics of large brown algae *Ecklonia cava* according to environmental conditions

*Takunari Ida[1], Yu Umezawa[1], Shigeki Wada[2], Horikawa Yoshiki[1] (1.Tokyo University of Agriculture and Technology, 2.University of Tsukuba)

[J] Poster | A (Atmospheric and Hydrospheric Sciences)：A-CG Complex & General

[A-CG57] Science in the Arctic Region

convener:Masashi Niwano(Meteorological Research Institute), Shunsuke Tei(Arctic Research Center, Hokkaido University), Tetsu Nakamura(Faculty of Environmental Earth Science, Hokkaido University), Jun Ono(Atmosphere and Ocean Research Institude, The University of Tokyo)

[ACG57-P01] A hemispheric extreme cold winter in 2017/18 controlled by the lowest extent of Chukchi sea-ice

*Keisuke Ota[1], Yoshihiro Tachibana[1], Yuta Ando[1] (1.Graduate School of Bioresources, Mie University)

[ACG57-P02] Detection of a weakening of the polar night jet in early winter and its relation to cooling over Siberia

*Yuta Ando[1], Koji Yamazaki[2], Yoshihiro Tachibana[1], Masayo Ogi[3], Jinro Ukita[4] (1.Graduate School of Bioresources, Mie University, 2.Hokkaido University, 3.Centre for Earth Observation Science, University of Manitoba, 4.Faculty of Science, Niigata University)

[ACG57-P03] Trends of summer precipitation over northern Eurasia in historical simulations with MIROC6

*Manabu Abe[1], Hironari Kanamori[2], Hatsuki Fujinami[2], Tetsuya Hiyama[2], Hiroaki Tatebe[1] (1.Japan Agency for Marine-Earth Science and Technology, 2.Institute for Space-Earth Environmental Research)

[ACG57-P04] External drivers on the Arctic warming and associated sea ice reduction in the early 20th century in a new climate model MRI-ESM2.0

*Takuro Aizawa[1,2], Masayoshi Ishii[2], Naga Oshima[2], Seiji Yukimoto[2], Hiroyasu Hasumi[1] (1.Atmosphere and Ocean Research Institute, University of Tokyo, 2.Meteorological Research Institute)

[ACG57-P05] Meteorological and snow/ice data around the Greenland ice sheet (1980-2019) calculated by the high-resolution polar regional climate model NHM-SMAP

*Masashi Niwano[1], Akihiro Hashimoto[1] (1.Meteorological Research Institute)

[ACG57-P06] **Surface elevation changes of glaciers along the coast of Prudhoe Land, northwestern Greenland, from 1985 to 2018**

*YEFAN WANG[1,2], Shin Sugiyama[1], Daiki Sakakibara[3] (1.Institute of Low Temperature Science, Hokkaido University, 2.Graduate School of Environmental science, Hokkaido University, 3.Arctic Research Center, Hokkaido University)

[ACG57-P07] **Quantifying Chukchi Polynya Occurrence Using Passive Microwave and Local Indigenous Observational Data**

*Pacifica Kitrea Mai Takata-Glushkoff[1,2], Angela C. Bliss[2] (1.Bowdoin College Earth and Oceanographic Science, 2.Oregon State University College of Earth, Ocean, and Atmospheric Sciences)

[ACG57-P08] Increasing Zooplankton Biomass Associated with Sea Ice Loss in the Western Arctic Ocean

*Motoyo Itoh[1], Minoru Kitamura[1], Amane Fujiwara[1], Eddy Carmack[2], Kazuo Amakasu[3], Koichi Ara[4], Mario Uchimiya[5], Toru Hirawake[6], Jonaotaro Onodera[1], Shigeto Nishino[1], Takashi Kikuchi[1] (1.Japan Agency for Marine-Earth Science and Technology, 2.Fisheries and Ocean Canada, Institute of Ocean Science, 3.Tokyo University of Marine Science and Technology, 4.Nihon University, 5.Riken, 6.Hokkaido University)

[ACG57-P09] Influence of physical oceanographic condition to transportation of biosiliceous particles in the Pacific side of the Arctic Ocean

*Jonaotaro Onodera[1], Eiji Watanabe[1], Satoshi Kimura[1], Kohei Mizobata[2], Yuichiro Tanaka[3], Naomi Harada[1] (1.Research and Development Center for Global Change, JAMSTEC, 2.Dept. Ocean Sciences, School of Marine Life Science, TUMSAT, 3.Geological Survey of Japan, AIST)

[ACG57-P10] Surface Waves Under the Arctic Sea Ice Observed by Drifting Wave Buoys

*Tsubasa Kodaira[1], Takuji Waseda[1], Takehiko Nose[1], Kazutoshi Sato[2], Jun Inoue[3] (1.The University of Tokyo, 2.KITAMI INSTITUTE OF TECHNOLOGY, 3.National Institute of Polar Research)

[ACG57-P11] Covariability between Atmospheric Teleconnections and GDP Growth Rates

*Akane Kato[1], Yoshihiro Tachibana[1], Kensuke K. Komatsu[1], Yuta Ando[1] (1.Faculty of Bioresources, Mie University)

[ACG57-P12] Remote influence on extreme weather in mid and high latitudes over the Northern Hemisphere driven by deep convection over Sahel

*Tomoe Nakanishi[1], Yoshihiro Tachibana[1], Yuta Ando[1] (1.Graduate School of Bioresources, Mie University)

[ACG57-P13] Recent Increase of Extreming Snowfall events in Kanto and its Relation to the Shift of Large-scale Atmospheric Circulations.

*Yuki Nakamura[1], Yoshihiro Tachibana[1] (1.Fac. of Bioresources, Mie Univ)

[J] Poster | A (Atmospheric and Hydrospheric Sciences)：A-CG Complex & General

[A-CG58] Aircraft and UAV Observations for Earth-planetary sciences

convener:Nobuhiro Takahashi(Institute for Space-Earth Environmental Research, Nagoya University), Makoto Koike(Department of Earth and Planetary Science, Graduate School of Science, The University of Tokyo), Toshinobu Machida(National Institute for Environmental Studies), Taro Shinoda(Institute for Space-Earth Environmental Research, Nagoya University)

[ACG58-P01] **Estimation of Turbulence Kinetic Energy dissipation rate (ε) using High-Resolution Pitot differential pressure sensor onboard a Small Unmanned Aircraft System (sUAS)**

*Abhiram Doddi[1], Dale Lawrence[1], Lakshmi Kantha[1], Hubert Luce[2] (1.University of Colorado Boulder, USA, 2.Université de Toulon, France)

[ACG58-P02] Development of Method for Turbulence Simulation using Onboard LIDAR Data Assimilation

*Ryoichi Yoshimura[1], Aiko Yakeno[1], Ryota Kikuchi[3], Takashi Misaka[2], Shigeru Obayashi[1] (1.Institute of Fluid Science, Tohoku University, 2.National Institute of Advanced Industrial Science and Technology , 3.DoerResearch, Inc.)

[ACG58-P04] Characteristic analysis of measurement error in GNSS-R UAV Altimeter

*wang chuanbing[1], Kaoru Ichikawa[1] (1.Kyushu University)

[ACG58-P05] NICT third generation airborne SAR system

*Shoichiro Kojima[1], Junpei Uemoto[1], Yuya Arima[1], Masanori Gocho[1] (1.National Institute of Information and Communications Technology)

[ACG58-P06] Variation of ultra fine particle concentrations within the winter boundary layer observed by a Multicopter UAV

*Masahiko Hayashi[1], Akihiro Yasunaga[1], Ryohei Haraguchi[2] (1.Faculty of Science, Fukuoka University, 2.Graduate school of Fukuoka University)

[ACG58-P07] Proposal to the master plan 2020: Promotion of Scientific Research on Climate and Earth System Sciences Using Aircrafts

*Nobuhiro Takahashi[1], Makoto Koike[2] (1.Institute for Space-Earth Environmental Research, Nagoya University, 2.School of Science, The University of Tokyo)

[J] Poster | A (Atmospheric and Hydrospheric Sciences)：A-CG Complex & General

[A-CG59] Biogeochemical linkages between the surface ocean and atmosphere

convener:Sohiko Kameyama(Hokkaido University), Yoko Iwamoto(Graduate School of Integrated Sciences for Life, Hiroshima University), Maki Aita Noguchi(Japan Agency for Marine-Earth Science and Technology), Daisuke Sasano(Japan Meteorological Agency)

[ACG59-P01] Model analysis of atmospheric concentrations and depositions on the Eastern Indian Ocean observed by R/V Hakuho Maru

*Kazuyo Yamaji[1], Katsuhiro Kawamoto[1], Moe Tauchi[1], Yoko Iwamoto[2], Kazuhiko Matsumoto[3], Makio Honda[3], Yugo Kanaya[3], Takashi Sekiya[3], Maki Noguchi Aita[3], Tomoki Nakayama[4], Satoru Chatani[5], Fumikazu Taketani[3] (1.Kobe University, 2.Hiroshima University, 3.Japan Agency for Marine-Earth Science and Technology, 4.Nagasaki University, 5.National Institute for Environmental Studies)

[ACG59-P02] Influence of deposition of atmospheric nitrogen compounds on the surface marine ecosystem at the Japan Sea

*Fumikazu Taketani[1], Maki Noguchi Aita[1], Takashi Sekiya[1], Kazuyo Yamaji[1,2], Kohei Ikeda[3], Makio Honda[1], Kazuhiko Matsumoto[1], Kosei Sasaoka[1], Yugo Kanaya[1] (1.Japan Agency for Marine-Earth Science and Technology, 2.Kobe University, 3.National Institute for Environmental Studies)

[ACG59-P03] Estimation of atmospheric nitrogen deposition over the Kuroshio region in the Autumn of 2015

*Yoko Iwamoto[1,3], Kazuki Kamezaki[2], Shohei Hattori[2], Mako Hirota[1], Shuei Kaizuka[1], Kazuhiko Takeda[1], Kazuhiko Miura[3], Mitsuo Uematsu[4,5] (1.Hiroshima University, 2.Tokyo Institute of Technology, 3.Tokyo University of Science, 4.Atmosphere and Ocean Research Institute, the University of Tokyo, 5.Center of Environment Science in Saitama)

[J] Poster | A (Atmospheric and Hydrospheric Sciences)：A-CG Complex & General

[A-CG60] Adaptation for climate change and social implementation

convener:Yoichi Ishikawa(JAPAN Agency for Marine-Earth Science and Technology), Hiroya Yamano(National Institute for Environmental Studies), KOJI DAIRAKU(University of Tsukuba), Shingo Watanabe(Japan Agency for Marine-Earth Science and Technology)

[ACG60-P01] Possible historical impact of urbanization on the surface air temperature in Sofia, Bulgaria

*Lidia Lazarova Vitanova[1,2], Hiroyuki Kusaka[1] (1.Center for Computational Sciences, University of Tsukuba, 2.Nikken Sekkei Research Institute)

[ACG60-P02] High school Investigation activities for the Carbonates quantities interaction between the ocean lives' shells and atmosphere-ocean.

*Ryo S Nakamura[1] (1.Miyagi Rifu high school)

[ACG60-P03] Prediction of future soil erosion risk in Japan considering climate change

*Gen Machida[1], Kazutoshi Osawa[2], Taku Nishimura[3] (1.Graduate School of Regional Development and Creativity, Utsunomiya University, 2.School of Agriculture, Utsunomiya University, 3.School of Agriculture, Tokyo University)

[J] Poster | H (Human Geosciences)：H-GG Geography

[H-GG01] Use, change, management of natural resources and environment: Interdisciplinary perspectives

convener:Toru Sasaki(Miyagi University of Education), Gen Ueda(Graduate School of Social Sciences, Hitotsubashi University), Takahisa Furuichi(Miyagi University of Education), Yoshinori OTSUKI(Institute of Geography, Graduate School of Science, Tohoku University)

[HGG01-P01] Climatological study of the wind hole in Shodoshima Island

*Masaki HORIUCHI[1], Takako YAMAGUCHI[2] (1.Hosei University, Graduate School of Humanities, 2.Hosei University)

[HGG01-P02] Evaluation of geoheritage for protection

*Kuniyasu Mokudai[1] (1.Tohoku Gakuin University)

[HGG01-P03] Vegetation changes in under semi-arid climate, central Kenya, using opal phytolith analysis

*Asaka Konno[1], Yoshinori OTSUKI[2] (1.Tokoha University, 2.Tohoku University)

[HGG01-P04] Sand harvesting in soil-eroded area under semi-arid climate, central Kenya

*Yoshinori OTSUKI[1], Matheaus Kioko KAUTI[2], Asaka KONNO[3], Miharu TANAKA[4] (1.Institute of Geography, Graduate School of Science, Tohoku University, 2.Southeast Kenya University, 3.Tokoha University, 4.Kanto Regional Development Bureau, Ministry of Land, Infrastructure, Transport and Tourism)

[HGG01-P05] Exploring the Spatial-temporal Coupling Pattern of Grain Yield and Fertilization from Historical Practice for Better Future Application: A Case in the North China Plain

Wenjia Yu[2], *Yaojie Yue[1,2] (1.Key Laboratory of Environmental Change and Natural Disaster of Ministry of Education of China, 2.Faculty of Geographical Science, Beijing Normal University, China)

[HGG01-P06] Land use patterns optimization research under climate change adaptation and mitigation strategies—A case study in China

*Ying Xu[1] (1.Shandong Jiaotong University)

[HGG01-P07] A STUDY ON SAND INDUSTRY IN THE MU US SAND LAND

*Yue Wang[1], Xuemin Liu[1], Shushan Du[1], Ruiyin Dou[1] (1.Beijing Normal University)

[J] Poster | H (Human Geosciences)：H-GM Geomorphology

[H-GM03] Geomorphology

convener:Tsuyoshi Hattanji(Faculty of Life and Environmental Sciences, University of Tsukuba), Masayuki Seto(Fukushima Future Center for Regional Revitalization, Fukushima University)

[HGM03-P03] Chemical and physical weathering processes of hydrothermally-altered sandstone: changes of hydraulic and mechanical properties

*Miho Kikuchi[1], Yuki Matsushi[1] (1.Disaster Prevention Research Institute, Kyoto University)

[HGM03-P04] Behavior of the sediments and detritus transported by floodwater on the embanked riverside land and its depositional record in the lower reaches of the Natori River

*Hiroshi Shimazu[1], Takako UTSUGAWA[1] (1.Department of Geography, Faculty of Geo-Environmental Science, Rissho University)

[HGM03-P05] Channel migration in the middle Tama River, central Japan, affected by Typhoon 1919 estimated from the sedimentological characteristics

*Takako UTSUGAWA[1], Masaaki Shirai[2] (1.Department of Geography, Faculty of Geo-Environmental Sciences, Rissho University, 2.Department of Geography, Tokyo Metropolitan University)

[HGM03-P06] Elevation change in a river park flooded by the typhoon Hagibis in 2019

*Keisuke Taniguchi[1], Hirotsugu Arai[1], Hirofumi Yoshita[1], Kazuki Fujita[1], Takuhei Yamasaki[1], Akihiro Maekawa[1], Noritaka Endo[2] (1.Centre for Environmental Creation Fukushima Prefecture, 2.Kanazawa University)

[HGM03-P07] Terrain analysis of terrace spread in Shinano River basin, Niigata Prefecture using detailed DEM data

*Toshifumi Koseki[1], Mamoru Koarai[2] (1.Graduate school of Science and Technology, Ibaraki University, 2.earth science course, college of sciense, Ibaraki University)

[HGM03-P08] Distribution map of subsurface Late Pleistocene fluvial terraces in the lower Sagami Plain, central Japan

*Yoshiki Sato[1], Sumiko KUBO[2] (1.Geological Survey of Japan, Advanced Industrial Science and Technology, 2.School of Education, Waseda University)

[HGM03-P09] **GPR survey for estimating the internal structure of the beach levee formed in the coastal lowland of Enshunada Sea**

*Takayuki Nakano[1], Nobuhisa Matsuta[2], Kazuaki Hori[3], Daisuke Hirouchi[4], Nobuhiko Sugito[5], Yoshiki Sato[6], Tatsuya Ishiyama[7] (1.GSI of Japan, 2.Okayama Univ., 3.Nagoya Univ., 4.Shinshu Univ., 5.Hosei Univ., 6.AIST, 7.ERI, Univ. of Tokyo)

[HGM03-P10] Geomorphic analysis of the active fault in volcanic area based on GIS

*Daisaku Kawabata[1], Haruo Kimura[2], Yasuhira Aoyagi[2] (1.Institute of Geology and Geoinformation, Geological Survey of Japan, AIST, 2.Central Research Institute of Electric Power Industry)

[HGM03-P11] Acquisition of detailed topographic data for active volcano using UAV LiDAR

*Takayama Toko[1], Takayuki Hashimoto[1], Naijia Zhang[1], Yuto Nomura[1] (1.Asia Air Survey Co.,Ltd.)

[HGM03-P12] Effect of past human activities on the 2009 shallow landslide hazard in the Houfu District, western Japan

*Hiromu Daimaru[1] (1.Forestry and Forest Products Research Institute)

[J] Poster | H (Human Geosciences)：H-QR Quaternary research

[H-QR05] Natural hazard and human activity recorded in underwater geoarchaeological structure

convener:Wataru Tanikawa(Japan Agency for Marine-Earth Science and Technology, Kochi Instutute for Core Sample Research), Tokuyama Hidekazu(Center for advanced marine core research, Kochi University), Shintaro Yamasaki(Disaster Prevention Research Institute, Kyoto University)

[HQR05-P01] Underwater geoarchaeological research at the coastal area of Kochi prefecture to reveal the traditional tale of “Kurodagori”

*Wataru Tanikawa[1], Tokuyama Hidekazu[2], Yuhji Yamamoto[2], Masafumi MURAYAMA[2], Kouki Tanaka[2], Akira Ijiri[1], Tatsuhiko Hoshino[1] (1.Japan Agency for Marine-Earth Science and Technology, Kochi Instutute for Core Sample Research, 2.Kochi University)

[HQR05-P02] Characteristics and its significance of marine cores collected from inner Uranouchi Bay, Kochi Prefecture

*Masafumi MURAYAMA[1], Wataru Tanikawa[2], Akira Ijiri[2], Tatsuhiko Hoshino[2], Takehiro Hirose[2], Toshiya Fujiwara[2], Kazuya Kitada[2], Kastuya Nejigaki[3], Tokuyama Hidekazu[4], Go-Ichiro Uramoto[4], Kazuno Arai[4], Kondo Yasuo[3], Yuhji Yamamoto[4], Research Member Kurodagoori[4] (1.Faculty of Agriculture and Marine Science, Kochi University, 2.JAMSTEC, 3.Graduate School of Integrated Arts and Sciences, Kochi University, 4.Center for Advanced Marine Core Research, Kochi University)

[HQR05-P03] A case study on 3D measurement of underwater structure by using digital image data taken with a digital camera

*Akira Ijiri[1], Wataru Tanikawa[1], Masafumi MURAYAMA[2], Tokuyama Hidekazu[2] (1.Japan Agency for Marine-Earth Science and Technology, 2.Kochi University)

[HQR05-P04] Environmental change over the past 2000 years in Lake Kawahara and Ryuuoo in southern Japan

*Cho Ara[1], Kota Katsuki[2], Jonathan D Woodruff[3], Kaoru Kashima[1], Hannah Elizabeth Baranes[3], Caroline Ladlow[3] (1.Kyushu University, 2.Shimane University, 3.University of Massachusetts)

[HQR05-P05] Application of Boxfish ROV and Boxfish 360 camera to Underwater Archaeological Survey

*Yuka Masaki[1], Hideki Sezoko[2], Masayuki Nagayama[3], Wataru Tanikawa[4], Yuhji Yamamoto[5], Shinichiro Ito[1] (1.COSMOS SHOJI Co., Ltd., 2.Nippon Marine Enterprises, Ltd., 3.360 Planet, 4.Japan Agency for Marine-Earth Science and Technology, 5.Kochi University)

[J] Poster | H (Human Geosciences)：H-QR Quaternary research

[H-QR06] Quaternary, Diachronic dynamics of human-environment interactions

convener:Mamoru Koarai(Earth Science course, College of Science, Ibaraki University), Yusuke Yokoyama(Atmosphere and Ocean Research Institute, University of Tokyo), Koji Okumura(Graduate School of Letters, Hiroshima University), Yasufumi Satoguchi(Lake Biwa Museum)

[HQR06-P01] **Radiocarbon ages of tsunami deposits from the Lake Harutori in Kushiro City along the Pacific coast of eastern Hokkaido, northeastern Japan**

*Kiyoyuki Shigeno[1], Toshimichi Nakanishi[2], Wan Hong[3], Futoshi Nanayama[4,5] (1.Meiji consultant co.,Ltd., 2.Tono Geoscience Center, Japan Atomic Energy Agency, 3.Geochemical Analysis Center, Korea Institute of Geoscience & Mineral Resources, 4.Geological Survey of Japan,AIST, 5.CWMD, Kumamoto University)

[HQR06-P03] Characteristics of gradient of valley plaine in Ibaraki Prefecture

*Mamoru Koarai[1], Tomoya Sekine[1], Takayuki Nakano[2] (1.Earth Science course, College of Science, Ibaraki University, 2.Geospatial Information Authority of Japan)

[HQR06-P04] Grain Size Composition of Crevasse Spray Sediments in the middle part of Kinu River

*Yoshiki Sato[1], Atsushi Urabe[2] (1.Geological Survey of Japan, Advanced Industrial Science and Technology, 2.Research Institute for Natural Hazards and Disaster Recovery, Niigata University)

[HQR06-P05] Geomorphic development of the Takaragi terrace since the Last Interglacial Period in the North Central Part of Kanto Plain, Japan

*Taiga Kimori[1], Toshihiko Sugai[1], Tatsuki Miyamoto[1], Tetsuya Komatsu[2], Nakanishi Toshimichi[2] (1.The University of Tokyo,Graduate School of Frontier Sciences, 2.Japan Atomic Energy Agency)

[HQR06-P06] Characteristics of the Fuji-Sagamigawa Lahar deposit at the upper reaches of Sagami River, central Japan

*Masaaki Shirai[1], Makoto Kobayashi[2], Takako UTSUGAWA[3], Kiyokazu Kawajiri[4], Takayuki Takahashi[1] (1.Tokyo Metropolitan University, 2.Mt. Fuji World Heritage Centre, Shizuoka, 3.Rissho University, 4.Sagamihara Cuty Museum)

[HQR06-P07] Landform Evolution of Budokubo Area, Niigata Prefecture, Japan

*Kosuke Sasamori[1], Mamoru Koarai[1] (1.Department of Earth Sciences, College of Science, Ibaraki University)

[HQR06-P08] Middle Holocene changes in relative sea-level on western Shikoku Island, Japan

*Tatsuhiko Yamaguchi[1], Tomohiro Tsuji[2], Futoshi Nanayama[3,4], Toshimichi Nakanishi[9], Michiharu Ikeda[8], Yasuo Kondo[5], Michiko Miwa[6], Yohei Hamada[7] (1.Nation. Mus. Nat. Sci., 2.Yamaguchi Univ., 3.AIST, 4.Kumamoto Univ., 5.Kochi Univ., 6.JAPEX, 7.JAMSTEC, 8.Shikoku Research Institute Inc, 9.Japan Atomic Energy Agency)

[HQR06-P09] Depositional sequence of the Post-LGM incised-valley fill controlled by seismic crustal deformation and large-scale lahars: An example of SKM core obtained from the Sukumo coastal lowland along the Nankai Trough, Japan

*Futoshi Nanayama[1,2], Tatsuhiko Yamaguchi[3], Nakanishi Toshimichi[4], Tomohiro Tsuji[5], Michiharu Ikeda[5], Kondo Yasuo[6], Michiko Miwa[7], Shinji Sugiyama[8], Kazunari Kimura[9] (1.Geological Survey of Japan, AIST, 2.CWMD, Kumamoto University, 3.National Museum of Nature and Science, 4.Japan Atomic Energy Agency, 5.Shikoku Research Institute Inc., 6.Kochi University, 7.JAPEX Research Center, 8.Paleo Environment Research Center, 9.Naiba Ehime Branch)

[J] Poster | H (Human Geosciences)：H-SC Social Earth Sciences & Civil/Urban System Sciences

[H-SC07] CCUS (Carbon Dioxide Capture, Utilization, and Storage) for Climate Mitigation

convener:Masao Sorai(Institute for Geo-Resources and Environment, National Institute of Advanced Industrial Science and Technology), Ziqiu Xue(Research Institute of Innovative Tech for the Earth), Masaatsu Aichi(Graduate School of Frontier Sciences, University of Tokyo), Yoshihiro Konno(The University of Tokyo)

[HSC07-P01] On the relationship between Vp and CO_2 saturation in the logging data at the Nagaoka site

*Takahiro Nakajima[1,2], Ziqiu Xue[1,2] (1.Research Institute of Innovative Technology for the Earth, 2.Geological Carbon Dioxide Storage Technology Research Association)

[HSC07-P02] Changes in hydraulic properties associated with fault development in sedimentary rocks from the Otway Basin using true triaxial testing techniques

*Takato Takemura[1], Eric Tenthorey[2,3], Hinako Hosono[1], Minoru Sato[4,5], Daisuke Asahina[4] (1.Nihon University, 2.Geoscience Australia, 3.CO2CRC, 4.Geological Survey of Japan, AIST, 5.Central Research Institute of Electric Power Industry)

[HSC07-P04] Fiber-optic sensing for CO_2-induced strain detection

*Hyuck Park[1], Yankun Sun[1], Yi Zhang[1], Ziqiu Xue[1] (1.Research Institute of Innovative Technology for the Earth)

[HSC07-P05] Feasibility of Distributed Fiber Optic Vibration Sensing for seismicity monitoring

*Takayuki Miyoshi[1], Takahiro Nakajima[1], Ziqiu Xue[1] (1.Research Institute of Innovative Technology for the Earth)

[HSC07-P06] **Derivation of contact angle for evaluation of caprock's sealing performance**

*Masao Sorai[1,2], Katsuya Honda[3] (1.Geological Carbon Dioxide Storage Technology Research Association, 2.Institute for Geo-Resources and Environment, National Institute of Advanced Industrial Science and Technology, 3.VALUENEX Japan Inc.)

[HSC07-P07] Molecular Dynamics Study on the Dynamic Contact Angle of CO_2/H_2O/Mineral System in Nano Pore Throat

*Masashige Shiga[1,2], Masao Sorai[1], Masaatsu Aichi[2], Hiromi Honda[2] (1.The National Institute of Advanced Industrial Science and Technology, 2.The University of Tokyo)

[HSC07-P08] Numerical study on leakage suppression of CO_2 stored in sub-seabed strata by gas hydrate formation

*TAKUYA WAKO[1], Toru Sato[1], Yousuke Sawano[1] (1.The University of Tokyo Graduate School of Frontier Sciences Department of Ocean Technology, Policy, and Environment)

[HSC07-P09] Access to Chinese rural landscapes from the perspective of Satoyama environmental education - a case study of Japanese undergraduate students

*XIANG QIONGYING[1], SHIXIAN LUO[1], Katsunori Furuya[1] (1.Chiba University)

[HSC07-P10] **Relationship between the impact of flower viewing tourism and residents' attitude**

*SHIXIAN LUO[1], JING XIE[2], Katsunori Furuya[1] (1.Chiba Univ., 2.Sichuan Agricultural Univ.)

[HSC07-P11] Analyze the impact of the climate change and human activity to the Ulz river basin and compare the protection methods

*Bayanjargal Darkhijav[1], Khulan Myagmar[1], Tsolmon Renchin[1], Bayanmunkh Norovsuren[1], Tsolmon Altanchimeg[1] (1.National University of Mongolia, Mongolia)

[J] Poster | H (Human Geosciences)：H-DS Disaster geosciences

[H-DS12] Geohazards in humid, tectonically active countries and their precursors

convener:Satoru Kojima(Department of Civil Engineering, Gifu University), Hiroshi YAGI(Faculty of Art, Science and Education, Yamagata University), Taro Uchida(University of Tsukuba), Yoshihiko Kariya(Department of Environmental Geography, Senshu University)

[HDS12-P01] Geomorphological and geological details of the Mizore large-scale landslide and its causal link to AD1586 Tensho Earthquake in Gifu Prefecture, central Japan

★Invited Papers

*Takahiro Kurimoto[1], Yoshihiko Kariya[2], Kuniyasu Mokudai[3], Ryuji Yamada[4], Takashi Kimura[5], Masaki Sano[6], Akane Tsushima[7], Zhen Li[8], Takeshi Nakatsuka[8] (1.Graduate student , Senshu Univ., 2.Senshu Univ., 3.Tohoku Gakuin Univ., 4.NIED, 5.Ehime Univ., 6.Waseda Univ., 7.MRI, 8.Nagoya Univ.)

[HDS12-P02] Deep-seated gravitational slope deformation process deduced from composition and age of sediments accumulated in a linear depression of Nishifuruike on the ridge near Kamikochi, Northern Japan Alps

*Satoru Kojima[1], Hidehisa Nagata[2] (1.Department of Civil Engineering, Gifu University, 2.Fu-Sui-Do Company Limited)

[HDS12-P03] Gravitational deformation on mountain slope to the northeast of Tokugotoge Pass, Nagano Prefecture, Japan

*Hidehisa Nagata[1], Satoru Kojima[2] (1.Fu-Sui-Do Company Limited, 2.Department od Civil Engineering, Gifu University)

[HDS12-P04] Holocene gravitational rock slope deformation and large-scale landslide features in the western Kamikochi Valley, northern Japanese Alps

*Yoshihiko Kariya[1], Sadao Takaoka[1] (1.Department of Environmental Geography, Senshu University)

[HDS12-P05] **Surface changes of rock slopes in the Shirouma-Daisekkei Valley, the Northern Japanese Alps**

*Hirotaka Sugiyama[1], Chiyuki Narama[1], Hiroshi Inoue[2] (1.Niigata University, 2.National Research Institute for Earth Science and Disaster Resilience)

[HDS12-P06] Surface changes of Ganpei landslide in Joetsu region

*Yutaka Inoue[3], Chiyuki Narama[1], Chunxiang Wang[2], Eiji Takita[2] (1.Niigata University, 2.KITAK Corporation, 3.Graduate Student,Niigata University)

[HDS12-P07] The characteristic of ground motion amplification based on the Fourier spectrum ratio between surface and underground of the KiK-net seismic observation points - Basic study of landslides caused by earthquakes -

*Tomoyuki Iida[1], Chi-Wen Chen[1], Masato SATO[1], Hidemitsu Tokui[2], Tetsuya Onodera[2], Hiroshi Kawabe, Ryuji Yamada[1] (1.National Research Institute for Earth Science and Disaster Prevention, 2.Technicallinc Kabushiki kaisya)

[HDS12-P08] Gigantic landslides distributed in the upper course of Marsyandhi river in Nepal Great Himalaya

*Hiroshi YAGI[1], Yuki Matsushi[2], Hiroshi P Sato[3], Akihiko Wakai[4] (1.Faculty of Art, Science and Education, Yamagata University, 2.DPRI, Kyoto University, 3.College of Humanities and Sciences, Nihon University, 4.Faculty of Technology, Gunma University)

[J] Poster | H (Human Geosciences)：H-RE Resource and Engineering Geology

[H-RE13] Resource Geology

convener:Tsubasa Otake(Division of Sustainable Resources Engineering, Faculty of Engineering, Hokkaido University), Ryohei Takahashi(Graduate School of International Resource Sciences, Akita University), Tatsuo Nozaki(Submarine Resources Research Center, Research Institute for Marine Resources Utilization, Japan Agency for Marine-Earth Science and Technology), Kenzo Sanematsu(Mineral Resource Research Group, Institute for Geo-Resources and Environment, Geological Survey of Japan, National Institute of Advanced Industrial Science and Technology)

[HRE13-P01] Brecciation event elucidate the high energy processes involved in porphyry copper deposit

*Geri Agroli[1], Atsushi Okamoto[1], Masaoki Uno[1], Noriyoshi Tsuchiya[1] (1.Tohoku University)

[HRE13-P02] **Geology and geochemistry of the Chifumbazi and Mugomo gold prospects, Tete province, Mozambique**

*Euclesia Paulina Francisco Cossa[1], Ryohei Takahashi[1], Andrea Agangi[1], Pearlyn Manalo[1], Hinako Sato[1], Akira Imai[2] (1.Akita Univ. , 2.Kyushu Univ.)

[HRE13-P03] **High Temperature Silicified Zone as a Potential Caprocks for Supercritical Geothermal Reservoir**

*Fajar Febiani Amanda[1], Ryoichi Yamada[1], Masaoki Uno[1], Noriyoshi Tsuchiya[1] (1.Graduate School of Environmental Studies, Tohoku University)

[HRE13-P04] **The zircon Hf-isotope constraints on the distribution of mineral deposits in the Sukhothai Fold Belt, Thailand**

*Apivut Veeravinantanakul[1], Ryohei Takahashi[1], Andrea Agangi[1], Tsukasa Ohba[1], Yasushi Watanabe[1], Marlina Elburg[2], Henriette Ueckermann[2], Punya Charusiri[3,4] (1.Akita Univ., 2.Univ. of Johannesburg, 3.Chulalongkorn Univ., 4.DMR)

[HRE13-P05] Subseafloor mineralization in the Shimokawa Cu-Zn ore deposits in Hokkaido

*Masahito Ikeda[1], Tsubasa Otake[2], Nakayama Ken[3], Tsutomu Sato[2] (1.Division of Sustainable Resource Engineering, Graduate School of Engineering, Hokkaido University, 2.Division of Sustainable Resource Engineering, Faculty of Engineering, Hokkaido University, 3.Center for Advanced Marine Core Research, Kochi University)

[HRE13-P06] Contemporaneous occurrence of spheroidal dolomites and framboidal pyrites in the Shimokawa deposit, Hokkaido, Japan

*Ken Nakayama[1], Masafumi MURAYAMA[2] (1.Center for Advanced Marine Research, Kochi Univ., 2.Faculty of Agriculture and Marine Sciences, Kochi Univ.)

[HRE13-P07] Magnetite Ore Deposit of the Naka-Osaka Mine (Shimonita, Gunma Pref.) is probably IOA (Kiruna) type

*Atsushi MIYASHITA[1], Hiroyasu MURAKAMI[2], Wataru FUJITA[1], Masakazu RIKITA[3], Takashi ICHIKAWA[4], Tomohiko SEKIYA[5] (1.Seikei University, 2.Waseda University, 3.Shimonita Nature School, 4.Keyaki Special Support School, 5.Shimonita Geopark)

[J] Poster | H (Human Geosciences)：H-TT Technology & Techniques

[H-TT16] Development and application of environmental traceability methods

convener:Ichiro Tayasu(Research Institute for Humanity and Nature), Ki-Cheol Shin(Research Institute for Humanity and Nature), Katsuyuki Yamashita(Graduate School of Natural Science and Technology, Okayama University)

[HTT16-P01] Comparative study of elementary runoff in the Tohoku basin and watershed based on numerical geographic information

*Yusuke Hataya[1] (1.Fukushima university)

[HTT16-P02] Neutralization of acid discharged water from the Kusatsu hot spring area of Japan utilizing industrial by-products

*Takeshi Saito[1], Naoki Watanabe[2] (1.Graduate School of Science and Engineering, Saitama University, 2.Research Institute for Natural Hazards and Disaster Recovery, Niigata University)

[HTT16-P03] Experimental and Simulation Study on the Migration Rule of Arsenic in the Soil of Surface Karst Zone in Southwest China

*bin zeng[1] (1.China University of Geosciences)

[HTT16-P04] Effects of natural and anthropogenic substances on atmospheric deposition in the Kyoto-Osaka-Kobe area using strontium and lead isotope ratios

Ryota Ando[1], *Yoriko Yokoo[1], Naoto Ishikawa[2], Ki-Cheol SHIN[3] (1.Faculty of Science and Engineering, Doshisha University, 2.Faculty of Sustainable Design, Toyama University, 3.RIHN)

[HTT16-P05] Analysis of nitrogen and phosphorus loading in Saijo Plain using trace elements as tracer

*Minoru TOKUMASU[1], Ki-Cheol SHIN[2], Yoshihiro YAMADA[3] (1.The United Graduate School of Agricultural Sciences, Ehime University, 2.The Research Institute for Humanity and Nature, 3.The Faculty of Agriculture of Kagawa University)

[HTT16-P06] Sulfur and Oxygen Isotopic Ratios of Rain Water Sulfate at Tottori-Okayama and Water-soluble Sulfate Ion in Suspended Particulate Matter at Okayama City

*Hitoshi CHIBA[1], Tatsuya Fujiike[1], Tsubasa Yamamoto[1] (1.Department of Earth Sciences, Okayama University)

[HTT16-P08] Characteristics of stable isotopes in monthly precipitation at Oshino village and northern slope of Mt. Fuji from Dec. 2016 to Mar. 2020

*Shiho Yabusaki[1], Makoto Taniguchi[1], Ichiro Tayasu[1], Tomoya Akimichi[1], Noboru Ohomori[2], Souichirou Watanabe[2], Hisamaru Osada[2], Ken Goto[2] (1. Research Institute for Humanity and Nature, 2.Oshino Village office)

[J] Poster | H (Human Geosciences)：H-TT Technology & Techniques

[H-TT17] Environmental Remote Sensing

convener:Hiroto Shimazaki(National Institute of Technology, Kisarazu College), Akihiko Kondoh(Center for Environmental Remote Sensing, Chiba University), HASEGAWA Hitoshi(Kokushikan University), Teppei Ishiuchi(Miyagi University)

[HTT17-P01] Application of the Gaussian fitting for mineral composition mapping using airborne hyperspectral sensor data

*Yoshitoshi Tochikura[1], Yasushi Yamaguchi[1], Yukie Asano[2], Shuho Noda[2], Yuu Kawakami[2], Kazuo Masuda[2] (1.Nagoya Univ., 2.JOGMEC)

[HTT17-P02] **Analysis of vegetation recovery after shallow landslides: a comparative study between the Toyota City and the Shōbara City, Japan**

*CHENXI ZHONG[1], Wei Yang[2], Akihiko Kondoh[2] (1.Graduate School of Science and Engineering, Chiba University, 2.Center for Environment Remote Sensing, Chiba University)

[HTT17-P03] **Land Use and Land Cover Change and Its Factor Analysis in Dakhla Oasis and Kharga Oasis in New Valley Province, Egypt**

*Xuechen Wang[1], Akihiko Kondoh[2] (1.Graduate School of Science and Engineering, Chiba University, 2.Center for Environmental Remote Sensing, Chiba University)

[HTT17-P04] High-Resolution Irrigated Area Mapping in Dakhla and Kharga Oasis, Egypt, from 2015 to 2019 Using Sentinel-2 Data

*AYIHUMAIER HALIPU[1], Akihiko Kondoh[2] (1.Graduate School of Science and Engineering, 2.Center for Environmental Remote Sensing Chiba University)

[J] Poster | H (Human Geosciences)：H-TT Technology & Techniques

[H-TT18] New Developments in Shallow Geophysics

convener:Kyosuke Onishi(Public Works Research Institute), Kunio Aoike(Oyo corporation), Tishiyuki Yokota(National Institute of Advanced Industrial Science and Technology), KEISUKE INOUE(National Agriculture and Food Research Organization)

[HTT18-P01] **An integrated GIS and Geophysical-based approach for geohazards risk assessment in coastal region: a Case study in Suez city, Egypt**

*Youssef Mohammed Youssef[1,2], Michiaki - Sugita[2], Khaled Sayed Gemail [3], Saada Ahmed Saada[4], Mostafa - Teama[1], Mohammed ElBarqawy [5] (1.Department of Science and Mathematical Engineering, Faculty of Petroleum and Mining Engineering, Suez University, Suez 43518, Egypt, 2.Faculty of Life and Environmental Sciences, University of Tsukuba, Tsukuba 305-8572, Japan, 3.Environmental Geophysics Lab (ZEGL) Department of Geology, Faculty of Science, Zagazig University, Zagazig 44519, Egypt, 4.Department of Geology, Faculty of Science, Suez University, Suez 43518, Egypt, 5.Department of Geological Engineering, Faculty of Petroleum and Mining Engineering, Suez University, Suez 43518, Egypt)

[HTT18-P02] Shallow seismic imaging of the active fault integrated with other geophysical methods

*Nomin-Erdene Erdenetsogt[1], Tseedulam Khuut[2], Batsaikhan Tserenpil[1], Nyambayar Tsend-Ayush[1], Bayarsaikhan Enkhee[1] (1.Institute of Astronomy and Geophysics, Mongolian Academy of Sciences, 2.Mongolian University of Science and Technology)

[HTT18-P03] Shallow geophysical survey in Goshougake geothermal area.

*Yuya Tada[1], Shin'ya Sakanaka[1], Ryuichi Takei[1], Tomoya Moriwaki[1], Shogo Uechi[1], Shinpei Suzuki[1], Shinzi Ikuta[1] (1.Akita university)

[HTT18-P04] Seismic response characteristics in Fukuyama plain estimated by using the microtremor measurements

*Atsushi Mukai[1], Yukihiko Tsutsumi[1], Hiromu Ishio[1], Yuki Sawada[1] (1.Faculty of Urban Management, Fukuyama City University)

[HTT18-P05] Effects of Surface Geology on Seismic Motion of The 2011 Tohoku Earthquake in Monou-Cho, Ishinomaki

*Keisuke Mizutani[1], Yoshiya Oda[1] (1.Tokyo Metropolitan University)

[HTT18-P06] Data acquisition and analysis of three-dimensional resistivity survey by means of a distributed resistivity measurement system

*Hiroshi Kisanuki[1], Ken Sakurai[1] (1.OYO corporation)

[HTT18-P07] **An attempt to estimate the water level change of undamaged groundwater by earth resistance (II) - Preliminary observations at the PTU borehole in Musashino Upland -**

*Kunihiro Ryoki[1] (1.Polytechnic University)

[HTT18-P08] Development of 3D self-potential tomography for visualization of groundwater condition

*ayaka ishikawa[1], Katsumi Hattori[1] (1.chiba university)

[HTT18-P09] Development of nuclear magnetic resonance scanners for the nondestructive measurement of water fractions in boring cores

*Yoshito Nakashima[1] (1.National Institute of Advanced Industrial Science and Technology)

[HTT18-P10] A case study of 3-D GPR survey and the ground truth at test sites for detection of buried objects

*Takanori Ogahara[1], Kunio Aoike[1] (1.OYO Corporation)

[HTT18-P11] Identifying wetting areas of a concrete deck slab by time-lapse surveys using ground-penetrating radar

*Kyosuke Onishi[1], Takayuki Kobayashi[1], Tadashi Matsumoto[1], Tsubasa Noda[1] (1.Public Works Research Institute)

[HTT18-P12] Conjecture of sourcing wavelet conditions suitable for the simultaneous sourcing 3D seismic survey with the underwater speakers

*Mayu Ogawa[1], Seishiro Furuyama[1], Tetsuro Tsuru[1] (1.Tokyo University of Marine Science and Technology)

[J] Poster | H (Human Geosciences)：H-TT Technology & Techniques

[H-TT19] Geographic Information System and Cartography

convener:Mamoru Koarai(Earth Science course, College of Science, Ibaraki University), Kazunari Tanka(Department of Civil Engineering and Urban Design, Faculty of Engineering, Osaka Institute of Technology), Kazuhiko W. Nakamura(The University of Tokyo)

[HTT19-P01] Consideration of essential information and understandable representation method for liquefaction hazard map: Opinions from local government staffs and residents

*Ryo Endo[1], Takayuki Nakano[1], Takashi Ishii[2], Takashi Hoshikawa[2], Seina Yamanaka[3], Yukiko Takeuchi[3], Shingo Watanabe[4], Keita Takada[4], Takuma Fujita[4] (1.GSI of Japan, 2.City Bureau, Ministry of Land, Infrastructure and Tourism, 3.Kumamoto University, 4.Fukken Co., Ltd.)

[HTT19-P02] Introductions of Evaluation method of chart adequacy using satellite derived bathymetry "Nautical Chart Adequacy Evaluation Procedure" and a trial case study in the waters around Japan

*Haruka Ogawa[1], Takahumi Hashimoto[1], MASANAO SUMIYOSHI[1], Hirokazu Mori[2] (1.Technology Planing and International Affairs Divixion Hydrographic and Oceanographic Department Japan Coast Guard , 2.Hydrograhpic Surveys Division Hydrographic and Oceanographic Department Japan Coast Guard)

[HTT19-P03] **Applications of Stereoscopic viewer for the Seamless Geographical Information System and its Prospect**

*Kunihiro Ryoki[1] (1.Polytechnic University)

[HTT19-P04] Green structural analysis by hierarchical cluster analysis and linear model regression analysis
and evaluation of green environment for continuous cityscape using green visibility and green coverage

*Taiichiro Watanabe[1], Tatsuto Aoki[2] (1.Kanazawa University , 2.Kanazawa University)

[HTT19-P05] Initiatives for an initial disaster response by townspeople using a drone: "Chisan chibou project", a locally operated countermeasure for natural hazards in Jinsekikogen Town, Japan

*Shoichiro Uchiyama[1] (1.National Research Institute for Earth Science and Disaster Resilience)

[HTT19-P06] Effect of topographic expression in Geopark Map

*Mamoru Koarai[1], Naoki Takeda[2], Kazuki Kidoguchi[1], Taiga Suzuki[1], Miteki Sato[1], Kasumi Kobayashi[1], Yuusuke Yokoro[1], Takumi Sekiya[1], Shiori Sugitake[1], Naoki Yamada[1], Misaki Kawamata[1], Shiori Watanabe[1], Miu Ogawa[1], yoshihiro Kurihara[1], Misa Tanaka[1] (1.Earth Science course, College of Science, Ibaraki University, 2.Geopark promotion office, Ibaraki University)

[HTT19-P07] Changes in movements of people to prevent the spread of COVID-19 in Japan since January 2020 based on geotagged Twitter data

*Takashi Kirimura[1] (1.Kogakkan University)

[J] Poster | H (Human Geosciences)：H-CG Complex & General

[H-CG28] Nuclear Energy and Geoscience

convener:Eiji Sasao(Tono Geoscience Center, Japan Atomic Energy Agency), Ryuta Hataya(Central Research Institute of Electric Power Industry), Shinji Takeuchi(Department of Earth and Environmental Sciences, College of Humanities & Sciences, Nihon University)

[HCG28-P01] Collection and Organization of Geoscientific Information for Improvement of Impacts Assessment Model of Seismic and Fault Activities for HLW Geological Disposal

*Makoto Kawamura[1] (1.Japan Atomic Energy Agency)

[HCG28-P02] Systematization from Case Studies of Natural Phenomena to Impacts Assessment on a HLW Geological Disposal

*Makoto Kawamura[1], Tsuneari Ishimaru[1], Masakazu Niwa[1], Tetsuya Komatsu[1] (1.Japan Atomic Energy Agency)

[HCG28-P03] Advanced examination technique for crustal deformation in stable area: a case study of the Kanto Plain, Japan

*Nakanishi Toshimichi[1], Tetsuya Komatsu[1], Misao Hongo[2], Marie Noguchi[3], Tatsuki Miyamoto[4], Taiga Kimori[4], Toshihiko Sugai[4] (1.Japan Atomic Energy Agency, 2.Alps Technical Research Lab. Co. Ltd., 3.Paleo Labo Co. Ltd., 4.Univ. Tokyo)

[HCG28-P04] Distribution map of erosion rates on timescales of 10^2–10^4 years in the Japanese Islands

*Yuki Hiura[1], Tetsuya Komatsu[1], Shigeru Sueoka[1], You Kitamura[2], Tomoji Sanga[2] (1.Japan Atomic Energy Agency, 2.JX Nippon Exploration and Development co. Ltd.)

[HCG28-P05] Machine learning for activity evaluation of crush zones using chemical composition: introduction of examples

*Koji Shimada[1], Ryo Tateishi[2] (1.Japan Atomic Energy Agency, 2.University of Toyama)

[HCG28-P06] Trial of domain segmentation of granite based on fracture orientations using Dip Azimuth Vector plot

*Shuji Terusawa[1], Koji Shimada[2] (1.OYO CORPORATION, 2.Japan Atomic Energy Agency)

[HCG28-P07] Hydrothermal alteration in the Toki granitic body, central Japan
-Mass transfer associated with precipitation of carbonate minerals-

*Hatsukawa Haruka[1], Nakashima Kazuo[2], Yuguchi Takashi[1] (1.Yamagata University Graduate School, 2.ASN Co., Ltd.)

[HCG28-P08] Hydrogeological structures of hydraulic conductive fractures at a depth of 300 m

*Ai Hamada[1] (1.Central Research Institute of Electric Power Industry)

[HCG28-P09] Properties of precipitates in alkaline Fe^{2+}-SiO_2-H_2O systems

*Yuki Sakuma[1], Yuto Nishiki[1], Ryosuke Kikuchi[2], Tsubasa Otake[2], Tsutomu Sato[2] (1.Graduate school of Engineering, Hokkaido university, 2.Faculty of Engineering, Hokkaido University)

[J] Poster | H (Human Geosciences)：H-CG Complex & General

[H-CG29] Role of scientists in rehabilitation of nuclear disaster areas

convener:Taku Nishimura(Deptartment of Biological and Environmental Engineering, Graduate School of Agricultural and Life Sciences, University of Tokyo), Masaru Mizoguchi(Graduate school of Agricultural and Life Sciences, The University of Tokyo), Kosuke Noborio(Meiji University)

[HCG29-P01] Evaluation of water erosion of Andisol under climate chage

*Sotaro Makino[1], Shoichiro Hamamoto[1], Kazutoshi Osawa[2], Onishi Taisuke[3], Taku Nishimura[1] (1.The University of Tokyo, 2.Utsunomiya University, 3.NTC International Inc.)

[HCG29-P02] **Analysis of radiocesium discharge distribution using GeoWEPP in Iitate village, Fukushima**

*Seigo Fujiwara[1], Mari Saito[2], Kazutoshi Osawa[2], Hiroyuki Matsui[2] (1.Center for Research in Isotopes and Environmental Dynamics, University of Tsukuba, 2.School of Agriculture, Utsunomiya University)

[HCG29-P03] Temporal and Spatial Transport of Radiocesium on a Slope after Scraping Surface Soil Off

*Yuki Sunakawa[1], Yuki Ito[2], Yuki Takagi[1], Ryuta Honda[3], Taku Nishimura[4], Masaru Mizoguchi[4], Kosuke Noborio[3] (1.Graduate School of Agriculture, Meiji University , 2.Gilat Research Center, Agricultural Research Organization, Israel, 3.School of Agriculture, Meiji University, 4.Graduate School of Agriculture and Life Sciences, The University of Tokyo)

[HCG29-P04] A study on the run-off of dissolved ^{137}Cs from contaminated slopes to an irrigation canal after the Fukushima Dai-ichi Nuclear Power Plant accident

*Satoshi Tajima[1], Shuichiro Yoshida[1], Taku Fukui[1], Naoto Nihei[2] (1.The Univ. of Tokyo, 2.Fukushima Univ.)

[HCG29-P05] Radioactive cesium binding to dissolved organic matter extracted from litter collected at forest in Fukushima prefecture

*Takahiro Tatsuno[1], Shoichiro Hamamoto[1], Naoto Nihei[2], Taku Nishimura[1] (1.Deptartment of Biological and Environmental Engineering, Graduate School of Agricultural and Life Sciences, University of Tokyo, 2.The Faculty of Food and Agricultural Sciences, Fukushima University)

[HCG29-P06] **Overview of Academic Studies on Iitate Village and its Revival Knowledge**

Hiroaki Sugino[1], *Masaru Mizoguchi[1] (1.Graduate school of Agricultural and Life Sciences, The University of Tokyo)

[J] Poster | H (Human Geosciences)：H-CG Complex & General

[H-CG30] Archeological Science: Earth Sciences and Archaeology

convener:Yorinao Shitaoka(Department of Environment System, Faculty of Geo-environmental Science, Rissho University), Tadahiro Hatakeyama(Information Processing Center, Okayama University of Science), Masataka Hakozaki(National Museum of Japanese History)

[HCG30-P01] Significance of detection of ancent city of Phasis with Earth Sciences and Archaeology

*Satoru Oishi[1], Vakhtang Licheli[2] (1.Research Center for Urban Safety and Security Kobe University, 2.Iv. Javakhishvili Tbilisi State University)

[HCG30-P02] High-precision chronology of paleoenvironmental changes by utilizing Jomon pottery types

*Koji Umeda[1], Masatoshi Shiba[1], Misaki Kondo[1], Tatsuhito Sekine[2], Kodai Igarashi[3], Mizuki Takeuchi[3] (1.Graduate School of Science and Technology, Hirosaki University, 2.Faculty of Humanities and Social Sciences, Hirosaki University, 3.Faculty of Science and Technology, Hirosaki University)

[HCG30-P05] Development of the ultra-high resolution photography for detecting the abnormal tree-rings

*Masataka Hakozaki[1] (1.National Museum of Japanese History)

[HCG30-P06] **Middle Paleolithic records of control fire events in north-central India**

*Deepak Kumar Jha[1], Rahul Samrat[1], Prasanta Sanyal[1] (1.Department of Earth Sciences, Indian Institute of Science Education and Research Kolkata, India)

[HCG30-P07] Magnetic surveys for archaeology

*Tadahiro Hatakeyama[1,2], Yu Kitahara[3], Nobutatsu Mochizuki[4] (1.Information Processing Center, Okayama University of Science, 2.Graduate School of Biosphere-Geosphere Science, Okayama University of Science, 3.Graduate School of Social and Cultural Studies, Kyushu University, 4.Faculty of Advanced Science and Technology, Kumamoto University)

[HCG30-P08] Analyzing the early 19th century's local geographical points in latitude and longitude of 0.2 second level and geomagnetic declination through Japan from Tadataka Inoh's magnetic survey azimuth ledger simultaneously.

*Motohiro Tsujimoto[1], Akitoshi - Omotani[2] (1.none, 2.San-in.System Consultant Co.Ltd)

[HCG30-P09] What can archaeomagnetism contribute for Southeast Asian archeology?

*Yu Kitahara[1], Mariko Yamagata[2], Masao Ohno[1], Yuhji Yamamoto[3], Tadahiro Hatakeyama[4] (1.Faculty of Social and Cultural Studies, Kyushu University, 2.Faculty of Management, Okayama University of Science, 3.Center for Advanced Marine Core Research, Kochi University, 4.Information Processing Center, Okayama University of Science)

[HCG30-P10] Archeological material and archeo-sediment analysis using luminescence method

*Yorinao Shitaoka[1] (1.Department of Environment System, Faculty of Geo-environmental Science, Rissho University)

[HCG30-P11] Interpreting the Ancient Legend “Descent of Ganga” of India as a Historical Record of a Comet Impact 6000 years ago.

*Mahesh Uday Patil

[HCG30-P12] A human exploitation of obsidian in Pre-Hispanic Tenerife, Canary Islands, Spain: A preliminary result of obsidian sourcing based on pedestrian survey and geochemical analysis

*Yuichi Nakazawa[1], Cristina Vega Maeso[2], Mari Sumita[3], Eduardo Carmona-Ballestero[4], John Rissetto[5], Alberto Berzosa Ordaz[4], Yasuo Naoe[6], Kensho Dohi[7], Mina Araya[7], Mercedes del Arco-Aguilar[8], Hans-Ulrich Schmincke[3] (1.Faculty of Medicine / Hokkaido University, Japan, 2.University of Cantabria, Spain, 3.GEOMAR Helmholtz Centre for Ocean Research Kiel, Germany, 4.University of Burgos, Spain, 5.Nebraska State Historical Society, USA, 6.Chitose Board of Education, Japan, 7.Hokkaido Archaeological Operations Center, Japan, 8.Tenerife Archaeological Museum, Spain)

[J] Poster | H (Human Geosciences)：H-CG Complex & General

[H-CG31] Coastal wetlands: geomorphologic, biologic and anthropogenic processes

convener:Kiyoshi Fujimoto(Nanzan University), Toyohiko Miyagi(Advantechnology Co., Ltd.)

[HCG31-P01] Emerging influences of rapid sea-level rise on Micronesian mangrove forests: Ground level dynamics in the main communities and prop roots dynamics of a *Rhizophora stylosa* community

*Kiyoshi Fujimoto[1], Kenji Ono[2], Shin Watanabe[3], Shingo Taniguchi[3], Keita Furukawa[4], Yasumasa Hirata[5], Kodai Hasada[6], Renpei Suwa[7], Saimon Lihpai[8] (1.Nanzan University, 2.Tohoku Research Center, FFPRI, 3.The University of Ryukyus, 4.Association for Shore Environment Creation, 5.FFPRI, 6.Hosei University, 7.JIRCAS, 8.Pohnpei State Government)

[HCG31-P02] Consideration of sea level rise effect on sediment transport process in mangrove forest

*Keita Furukawa[1], Kiyoshi Fujimoto[2], ONO Kenji[3], Shin Watanabe[4], Shingo Taniguchi[4], Yasumasa Hirata[3], Kodai Hasada[5], Renpei Suwa[7], Saimon Lihpai[6] (1.Association for Shore Environemt Createion, 2.Nanzan University, 3.Forestry and Forest Productis Research Institute, 4.Universtiy of the Ryukyu, 5.Hosei University, 6.Pohnpei State Government, 7.Japan International Research Center for Agricultural Sciences)

[HCG31-P03] Comparison of belowground root production of the mangrove forests in the Western Pacific Ocean islands among tropical and subtropical regions and mangrove species.

*Kenji ONO[1], Kiyoshi FUJIMOTO[2], Rempei SUWA[3], Rene ROLLON[4], Ariel C. BLANCO[4], Giannina MARIE G. ALBANO[4], Green ANN A. CRUZ[4], Yasmin H. PRIMAVERA-TIROL[5], Ronald J. MALIO,[5], Ryan M. BASINA[5], Shingo TANIGUCHI[7], Shin WATANABE[7], Yasumasa HIRATA[1], Saimon LIHPAI[6,8], Kazuo NADAOKA[6] (1.Forestry and Forest Products Research Insititute, 2.Nanzan University, 3.Japan International Research Center of Agricultural Science, 4.University of the Philippines, 5.Aklan State University, 6.Tokyo Institute of Technology, 7.University of the Rhyukyu, 8.Pohnpei State Government, FSM)

[HCG31-P04] Mangrove swamp distribution mapping by the whole earth directsensing approach

*Toyohiko Miyagi[1], Shigeyuki Baba[2], Tomomi Inoue[3], Yasuo Akaji[3], Gakugun Chou[3], Keita Furukawa[4], Hideaki Yanagisawa[5] (1.NIES・Tohoku-Gakuin Univ., 2.ISME, 3.NIES, 4.PEMSEA, 5.Tohoku-Gakuin University)

[J] Poster | H (Human Geosciences)：H-CG Complex & General

[H-CG32] Risk of Nuclear Technology and Geoscience: Dialogue with Engineers

convener:Kohta Juraku(Department of Humanities, Social and Health Sciences, School of Engineering, Tokyo Denki University), Satoshi Kaneshima(Department of Earth and Planetary Sciences, Kyushu University), Takeshi Sagiya(Disaster Mitigation Research Center, Nagoya University), Daisuke Suetsugu(institute for Marine Geodynamics, Japan Agency for Marine-Earth Science and Technology)

[HCG32-P01] Communication gap between scientists and the society associated with uncertain risk information

*Takeshi Sagiya[1] (1.Disaster Mitigation Research Center, Nagoya University)

[HCG32-P02] Summary of 2019 JPGU session about strong ground motions anticipated at nuclear power plants in Japan

*Satoshi Kaneshima[1] (1.Department of Earth and Planetary Sciences, Kyushu University)

[HCG32-P03] A review: Earthquake activity of the Median Tectonic Line, Japan

*Daisuke Suetsugu[1] (1.institute for Marine Geodynamics, Japan Agency for Marine-Earth Science and Technology)

[HCG32-P04] Does Science Give Us THE Answer?
Issues Centering on Risk and Social Decision-Making

*Kohta Juraku[1] (1.Department of Humanities, Social and Health Sciences, School of Engineering, Tokyo Denki University)

[J] Poster | H (Human Geosciences)：H-CG Complex & General

[H-CG33] Improvement of Integrated Research on Disaster Risk

convener:Keiji Kimura(Department of Geography, Nara University)

[HCG33-P01] Risk Assessment of Tropical Cyclone Disaster over the Seas around China under Climate Change

*Xin Li[1,2], Ren Zhang[1], Ju Wang[1], Mei Hong[1], Xueliang Zhou[1] (1. College of Meteorology and Oceanography, National University of Defense Technology, China, 2.State Key Laboratory of Numerical Modeling for Atmospheric Sciences and Geophysical Fluid Dynamics (LASG), Institute of Atmospheric Physics, Chinese Academy of Sciences)

[HCG33-P02] Wildfire risk prediction in Indonesia with the soil water by the numerical meteorological simulation WRF

*Keiji Kimura[1], Natsuki Takano[4], Mitsuru Osaki[2], Albertus Sulaiman[3], Pribadi Awal[3] (1.Department of Geography, Nara University, 2.Faculty of Agriculture, Hokkaido University, 3.Agency for the Assessment and Application of Technology, Indonesia, 4.Riso Kagaku Co.Ltd.(Graduated student, Nara University))

[HCG33-P03] Evaluation framework of health impacts caused by massive earthquakes in Osaka

*Koki Adachi[1], Lisa Ito[1], Akihiro Tokai[1] (1.Graduate School of Engineering, Osaka University)

[HCG33-P04] Promoting pre-disaster prevention actions in cooperation with school, boards of education, and researchers Part 2: Proposal of procedure manual to read hazard map

*Tatsuto Aoki[1], Kiyomi Hayashi[1] (1.School of Regional Development Studies, Kanazawa University)

[J] Poster | H (Human Geosciences)：H-CG Complex & General

[H-CG34] Human social activities and earth and planetary sciences

convener:Kazuo Amano(Center for Spatial Information Science, The University of Tokyo), Takashi Oguchi(Center for Spatial Information Science, The University of Tokyo), Masaki Ito(Institute of Industrial Science, the University of Tokyo), Kayoko Yamamoto(University of Elctro-Communications)

[HCG34-P01] Tourism and education utilizing local resources in the sand dunes and lagoon area of the San'in Kaigan UNESCO Global Geopark

*Kyoko Kanayama[1], Akira Kaigo[2], Yuki Iwamoto[3], Noritaka Matsubara[4], Aya Genseki[5], Emiko Sawa[5], Juna Nakagawa[6], Kitamura Sayaka[7], Kagari Ikezoe[7] (1.San'in Kaigan Geopark Museum of the Earth and Sea, Tottori Prefectural Government, 2.Hamayuyama and Tanegaike Vitalization Committee, 3.Secretariat of San'in Kaigan Geopark Promotion Council, 4.Graduate School of Regional Resource Management, University of Hyogo, 5.Uradome Ranger Office, Kinki Regional Environment Office, Ministry of the Environment Government of Japan, 6.Tottori Sand Dunes Visitor Center, San'in Kaigan National Park, 7.Tourism and Geopark Promotion Division, Tottori City Hall)

[HCG34-P02] Balloon Bomb Tour in the North Ibaraki Geopark Plan

*Kazuo Amano[1,2], North Ibaraki Geopark Plan Geonet Kitaibaraki (1.Center for Spatial Information Science, The University of Tokyo , 2.Amano Geological Laboratory, Japan)

[HCG34-P03] Identification of historical building stones and their distribution on the basis of magnetic susceptibility of granites

*Tohru Sakiyama[1] (1.Institute of Geo History, Japan Geochronology Network)

[HCG34-P04] Geology, soils, and wine

*Takashi Oguchi[1] (1.Center for Spatial Information Science, The University of Tokyo)

[HCG34-P05] Social Media Mapping for Disaster Prevention and Reduction

*Kayoko Yamamoto[1] (1.University of Elctro-Communications)

[HCG34-P06] Vulnerable people and hazard map

*SATOSHI KANAGURI[1], Kazuo Amano[2] (1.Amano Geological Laboratory, JAPAN, 2.Center for Spatial Information Science, The University of Tokyo)

[HCG34-P07] Development of Web Portal to Support for Remote Island

*Kayoko Yamamoto[1] (1.University of Elctro-Communications)

[HCG34-P08] The latest state of community formation through online/offline interaction

*Masaki Ito[1] (1.Institute of Industrial Science, the University of Tokyo)

[J] Poster | H (Human Geosciences)：H-CG Complex & General

[H-CG35] Advanced life support systems with closed bio-ecosystems and thier applications

convener:Masanori Shinohara(Teikyo University of Science), Kaori Tomita-Yokotani(Faculty of Life and Environmental Sciences University of Tsukuba), Hiroshi Katoh(Division of Plant Functional Genomics, Advanced Science Research Promotion Center, Organization for the Promotion of Regional Innovation, Mie University)

[HCG35-P03] Identification of proteins found in the process of slow dehydration in a terrestrial cyanobacterium, *Nostoc* sp. HK-01

*Hiroko Tanaka[1], Nagamine Myu[1], Tomoko Abe[1], Shunta Kimura[2], Hiroshi Katoh[3], Kaori Tomita-Yokotani[4] (1.School of Science and Engineering, Tokyo Denki University, 2.Graduate School of Agricultural and Life Sciences, The University of Tokyo, 3.Organization for the Promotion of Regional Innovation, Mie University, 4.Faculty of Life and Environmental Sciences, University of Tsukuba)

[HCG35-P04] Usefulness of an organic wastewater treatment focused on bacteria of the genus *Bacillus*

Chika Watanabe[1], Toshiharu Takayama[2], Tomoyuki Kuribayashi[2], *Tomoko Abe[1] (1.School of Science and Engineering, Tokyo Denki University, 2.KPS-3IV New Applications Research Center, KOA Corporation)

[HCG35-P05] What's life? Wandering about life from the viewpoint of "transition" of evolutions.

*Masanori Shinohara[1] (1.Teikyo University of Science)

[J] Poster | S (Solid Earth Sciences)：S-GD Geodesy

[S-GD02] Geodesy

convener:Koji Matsuo(Geospatial Information Authority of Japan), Yusuke Yokota(Institute of Industrial Science, The University of Tokyo), Daisuke Oka(Geological Survey of Hokkaido, Environmental and Geological Research Department, Local Independent Administrative Agency, Hokkaido Research Organization)

[SGD02-P01] Projected Barzilai-Borwein method for the acceleration of gravity field data inversion

*wei li[1,2,3,4], zhao hai meng[5,6], hao wen yan[1,2,3] (1.Faculty of Geomatics, Lanzhou Jiaotong University, Lanzhou 730070, China, 2.National-Local Joint Engineering Research Center of Technologies and Applications for National Geographic State Monitoring, Lanzhou 730070, China, 3.Gansu Provincial Engineering Laboratory for National Geographic State Monitoring, Lanzhou 730070, China, 4.School of Civil Engineering, Lanzhou Jiaotong University, Lanzhou 730070, China, 5.Tianjin Navigation Instrument Research Institute, Tianjin 300131,China, 6.Institute of Geology and Geophysics, Chinese Academy of Sciences, Beijing 100083, China)

[SGD02-P02] **Post-seismic gravity change modelling based on spectral finite element method**

*Changda Yan[1], SHINICHI MIYAZAKI[1] (1.Graduate School of Science, Kyoto University)

[SGD02-P03] Preliminary result of gravimetric geoid computation using airborne gravity data over the Boso peninsula

*Koji Matsuo[1] (1.GSI of Japan)

[SGD02-P04] Mesurement for vertical gravity gradient by CG-5 Autograv Gravimeter

*Masami Handa[1], Akira Tomiyama[1], Tokuro Kodama[1], Shinobu Kurihara[1], Kumikazu Ochi[1], Shuichi Omori[1] (1.GSI of Japan)

[SGD02-P05] An attempt to detect the variation of attractive forces from deep belowground using the Vertical Gravimeter Array.

*Toshiyuki Tanaka[1] (1.Tono Research Institute of Earthquake Science, Association for the Development of Earthquake Prediction)

[SGD02-P06] An attempt to observe gravity fluctuations caused by groundwater table response to tidal fluctuations by continuous gravity measurement near the coast

*Hiroki Goto[1,2], Mituhiko Sugihara[1,2], Yuji Nishi[1,2], Hiroshi Ikeda[2] (1.Geological Carbon Dioxide Storage Technology Research Association, 2.National Institute of Advanced Industrial Science and Technology)

[SGD02-P07] Effect of seasonal snow-mass change on geodetic solutions at Syowa Station: elastic deformation and gravitational attraction

*Akihisa Hattori[1], Yuichi Aoyama[2,1], Koichiro Doi[2,1], Jun'ichi Okuno[2,1] (1.The Graduate University for Advanced Studies (SOKENDAI), 2.The National Institute of Polar Research)

[SGD02-P08] Calculation method of the compliance parameters of the Earth's rotation: Influence of the fluid core and the solid inner core

*Yuji Harada[1,2], Shuhei Okubo[3,4] (1.State Key Laboratory of Lunar and Planetary Science, Space Science Institute, Macau University of Science and Technology, 2.Ocean Hemisphere Research Center, Earthquake Research Institute, University of Tokyo, 3.Department of Surveying and Geoinformatics, Faculty of Geosciences and Environmental Engineering, Southwest Jiaotong University, 4.University of Tokyo)

[SGD02-P09] Utilization of Interferometric Synthetic Aperture Radar Technology for Disaster Prevention

*Takako Nakamura[1], Shuichi Rokugawa[1] (1.The University of Tokyo)

[SGD02-P10] **Postseismic crustal deformation of the 2011 Tohoku earthquake, obtained from tidal data analysis**

*Kei Ishikawa[1], Takahito Kazama[1] (1.Graduate School of Science, Kyoto University)

[SGD02-P11] Performance assessment of the GNSS carrier phase to fault slip approach and its feasibility for seismic monitoring

*Yusuke Tanaka[1], Yusaku Ohta[1] (1.Tohoku University)

[SGD02-P12] Consideration of antenna phase calibration for new GEONET analysis

*Kazuyuki OHASHI[1], Hiroki MURAMATSU[1], Tomoaki FURUYA[1], Yasuaki KAKIAGE[1] (1.GSI of Japan)

[SGD02-P13] Research on the development of rapid and accurate GNSS routine analysis system (3)

*Hiroyuki Nakagawa[1] (1.GSI of Japan)

[SGD02-P14] Proposal to avoid inserting leap seconds

*Kozo Takahashi

[J] Poster | S (Solid Earth Sciences)：S-SS Seismology

[S-SS11] Crustal Structure

convener:Kazuo Nakahigashi(Tokyo University of Marine Science and Technology)

[SSS11-P01] Measurement of seismic velocity anisotropy in the Tohoku region, NE Japan by shear wave splitting analysis

*Tatsuya Mizuta[1], Tomomi Okada[1], Martha K Savage[2], Ryota Takagi[1], Keisuke Yoshida[1], Hiroshi Yakiwara[3], Takeshi Matsushima[4], Hiroshi Katao[5], Yoshiko Yamanaka[6], Masahiro Kosuga[7], Kei Katsumata[8], Mako Ohzono[8], Takashi NAKAYAMA[1], Satoshi Hirahara[1], Toshio Kono[1], Toru Matsuzawa[1], Group for the aftershock observations of the 2011 off the Pacific coast of Tohoku Earthquake (1.Tohoku University , 2.Victoria University of Wellington, 3.Kagoshima University, 4.kyushu University, 5.Kyoto University, 6.Nagoya University, 7.Hirosaki University, 8.Hokkaido University)

[SSS11-P02] An attempt to estimate the migration pathway of slab-derived fluid using shear wave splitting analysis

*Shinya Hiratsuka[1], Koichi Asamori[1], Atsushi Saiga[1] (1.Japan Atomic Energy Agency)

[SSS11-P03] **Estimation of crust and upper mantle velocity structure of the Himalayas and North-Eastern part of India using surface wave data**

*Mradula Vashishtha[1], Sagarika Mukhopadhyay[1] (1.Department of Earth Sciences, Indian Institute of Technology Roorkee, Roorkee- 247667, India)

[SSS11-P04] 1-D layered crustal and uppermost mantle structure beneath Botswana

*Admore Phindani Mpuang[1], Takuo Shibutani[2] (1.Graduate School of Science, Kyoto University, 2.Research Center for Earthquake Prediction, Disaster Prevention Research Institute, Kyoto University)

[SSS11-P05] Receiver function imaging of the Philippine Sea plate subducting beneath Shikoku (2)

*Takuo Shibutani[1], Nakagawa Jun[1], Nagaoka Airi[1], Tsutomu Miura[1], Yusuke Yamashita[1], Ken'ichi Yamazaki[1], Shintaro Komatsu[1] (1.Kyoto University)

[SSS11-P06] 3D Seismic Reflection Imaging with Microearthquake Sources recorded by Dense Nodal Arrays

*Larry D Brown[1], Doyeon Kim[2], Diego Quiros[3] (1.Cornell Univ, 2.Univ Maryland, 3.Capetown Univ)

[SSS11-P07] Imaging of S wave reflector in the crust obtained from a dense seismic array at the southern part of Abukuma Plateau

*Yuta Usuda[1], Takashi Iidaka[2], Toshihiro Igarashi[2], Kazushige Obara[2], Shin'ichi Sakai[2], Shigeki Nakagawa[2], Tetsuya Takeda[3] (1.UNIC Corporation, 2.Earthquake Research Institute, University of Tokyo, 3.National Research Institute for Earth Science and Disaster Resilience)

[SSS11-P08] Stability of H/V spectra of ambient noise from ocean bottom seismometers (OBS) near the Japan Trench

*Atikul Haque Farazi[1], Yoshihiro Ito, Emmanuel Soliman M Garcia (1.Disaster Prevention Research Institute, Kyoto University)

[SSS11-P09] Moho depth of the Korean Peninsula via P-coda autocorrelation analysis

*Hyejeong Cho[1], Sang-Jun Lee[1], Junkee Rhie[1], Seongryong Kim[2] (1.Seoul National Univ., 2.Chungnam National Univ.)

[SSS11-P10] The gravity anomaly of western offshore of Noto peninsula and the estimation of basement structure

*Akihiro Sawada[1], Yoshihiro Hiramatsu[1] (1.Geosciences and Civil Engineering, College of Science and Engineering, Kanazawa University)

[SSS11-P11] Study of subsurface and geological structure around the Togi–gawa Nangan Fault based on integrated analysis of seismic reflection method and gravity exploration

*Wataru Kobayashi[1], Masaaki Hamada[1], Yasuhisa Tanaka[2], Shinji Kawasaki[2], Takuya Murakami[3], Manabu Sakashita[3], Akihiro Sawada[4], Yoshihiro Hiramatsu[4] (1.Hokuriku Electric Power Company, 2.JGI, Inc., 3.DIA Consultants, 4.Kanazawa Univ.)

[J] Poster | S (Solid Earth Sciences)：S-SS Seismology

[S-SS12] Seismic wave propagation: Theory and Application

convener:Kiwamu Nishida(Earthquake Research Institute, University of Tokyo), Kazuya Shiraishi(Japan Agency for Marine-Earth Science and Technology), Takao Nibe(JAPEX), Kaoru Sawazaki(National Research Institute for Earth Science and Disaster Resilience)

[SSS12-P01] **Oscillations and traveling perturbations observed from ground to the ionosphere after the 2011 Mw9.0 Tohoku earthquake**

*Xiangxiang Yan[1], Yang-Yi Sun[1] (1.Institute of Geophysics and Geomatics, China University of Geosciences)

[SSS12-P02] Waveform feature extraction and similar waveform detection by Locality Sensitive Hashing

*KOMAGATA Ryota[1], Shiro Hirano[1], Hironori Kawakata[1], Makoto Naoi[2] (1.Ritsumeikan University, 2.Kyoto University)

[SSS12-P03] Separation of the temporal variation of the ACROSS signal using independent component analysis

*rina suzuki[1], Koshun Yamaoka[2] (1.Graduate School of Environmental Studies, Nagoya University, 2.Earthquake and Volcano Research Center, Graduate School of Environmental Studies, Nagoya University)

[SSS12-P04] Performance evaluation of methods to estimate temporal changes in attenuation property using active sources

*Shuhei Tsuji[1], Koshun Yamaoka[1], Ryoya Ikuta[2] (1.Graduate School of Environmental Studies, Nagoya University, 2.Faculty of Science, Shizuoka University)

[SSS12-P05] Review and preview of artificial seismic sources of ACROSS

*Koshun Yamaoka[1] (1.Earthquake and Volcano Research Center, Graduate School of Environmental Studies, Nagoya University)

[SSS12-P06] Repeated noises of 7-15 second interval in the seismograms recorded at the seashore landslide

*Issei Doi[1], Sumio Matsuura[1], Hikaru Osawa[3], Tatsuya Shibasaki[2], Shinichi Tosa[2] (1.Disaster Prevention Research Institute, Kyoto University, Japan, 2.Japan Conservation Co. Ltd., 3.Mountain Science Center, University of Tsukuba, Japan)

[SSS12-P07] Towards the detection of the mantle-reflected P wave

*Shota Kato[1], Kiwamu Nishida[1] (1.ERI, University of Tokyo)

[SSS12-P08] Retrieving reflection waves from the Philippine Sea plate boundary using seismic interferometry with the PKIKP phases

*Toshiki Watanabe[1], Naoki Sogawa[1] (1.Graduate School of Environmental Studies, Nagoya University)

[SSS12-P10] **Site classification of recording stations of EEW System for Garhwal region of Uttarakhand, India**

*Pankaj Kumar[1], Ashok Kumar[1], Ajay Gairola[1], Kamal .[1] (1.Indian Institute of Technology Roorkee, India)

[SSS12-P12] Passive seismic imaging of crustal structures: numerical study on acoustic and elastic reverse time migration

*Kazuya Shiraishi[1], Toshiki Watanabe[2] (1.Japan Agency for Marine-Earth Science and Technology, 2.Nagoya University)

[SSS12-P13] Analytical solution of near-field term, intermediate term, far-filed term, and quasi-static displacement due to rectangular fault in a homogeneous whole space

*Kotaro Tarumi[1], Hiroshi Takenaka[1] (1.Okayama University)

[SSS12-P14] Characteristics of teleseismic S-wave response of the Kanto sedimentary basin inferred from dense seismic observation and numerical simulation

*Yue Nakagawa[1], Kazuo Yoshimoto[1], Shunsuke Takemura[2] (1.Yokohama City University, 2.Earthquake Research Institute, the University of Tokyo)

[SSS12-P15] A numerical study on P-wave travel time fluctuation and amplitude fluctuation in the short-wavelength inhomogeneous crustal structure

*Kazuo Yoshimoto[1], Shunsuke Takemura[2] (1.Graduate School of Nanobioscience, Yokohama City University, 2.Earthquake Research Institute, the University of Tokyo)

[SSS12-P16] **Seismic body wave attenuation characteristics within the heterogeneous crust of Northeast India**

*Rabin Das[1], Sagarika Mukhopadhyay[1] (1.Department of Earth Sciences, Indian Institute of Technology Roorkee, Roorkee- 247667, India)

[SSS12-P17] Trans-dimensional imaging or random inhomogeneities at northern Ryukyu arc with a non-diagonal covariance matrix

*Tsutomu Takahashi[1], Yojiro Yamamoto[1], Yasushi Ishihara[1], Koichiro Obana[1], Seiichi Miura[1], Shuichi Kodaira[1], Yoshiyuki Kaneda[2] (1.Japan Agency for Marine-Earth Science and Technology, 2.Kagawa Univ.)

[SSS12-P18] Propagation characteristics of two-dimensional scalar waves in alternating layered structures

*Kazuki Kidoguchi[1], Jun Kawahara[1] (1.Graduate School of Science and Engineering, Ibaraki University)

[SSS12-P19] Angular distribution of energy fluxes of seismic waves in two-dimensional random heterogeneous media

*Kentaro Emoto[1] (1.Graduate School of Science, Tohokuk University)

[J] Poster | S (Solid Earth Sciences)：S-SS Seismology

[S-SS13] Seismicity

convener:Yasuhiro Yoshida(Meteorological College, Japan Meteorological Agency)

[SSS13-P01] Visualization of spatial and temporal change in b values and survey for the relationship between b value and the size of next earthquake

*Toshiki Shimbaru[1] (1.Fukuoka Regional Headquarters, JMA)

[SSS13-P02] Spatial and temporal change in b values on the fault plane of the 2016 Kumamoto earthquakes.

*Toshiki Shimbaru[1] (1.Fukuoka Regional Headquarters, JMA)

[SSS13-P03] A discussion of causes of succeeding small and moderate-sized earthquake in a short time - A case study of earthquakes east off the Osumi Peninsula-

*Yuko Yamada[1], Nobuyuki Hirota[2], Toshiki Shimbaru[1] (1.Fukuoka Regional Headquarters Japan Meteorological Agency, 2.Japan Meteorological Agency)

[SSS13-P04] Case study of succeeding earthquakes in the Hyuga-nada Sea, Japan

*Nobuyuki Hirota[1], Yuko Yamada[2], Toshiki Shimbaru[2] (1.Japan Meteorological Agency, 2.Fukuoka Regional Headquarters, JMA)

[SSS13-P05] **Relevalence of seismic activity between the inland crustal earthquakes in Hidaka district, Hokkaido and the great interplate earthquakes along the southern Kuril Trench**

*Tetsuo Takanami[1,2] (1.Hokkaido Research Center of Geology, 2.Carnegie Institution for Science)

[SSS13-P06] Seismic observation for an anomalous activity of shallow low frequency events mixed with normal earthquakes at Hakodate

*Shinako Noguchi[1], Keiji Kasahara[1], Masahiro Kosuga[2], Takuto Maeda[2], Yuta Amezawa[2], Taichi Haruyama[2], Sayumi Ishida[2], Yuki Matsuno[2], Itsuki Orui[3] (1.Association for the Development of Earthquake Prediction, 2.Graduate School of Science and Technology, Hirosaki University , 3.Faculty of Science and Technology, Hirosaki University)

[SSS13-P07] Continuous observation of ocean bottom earthquakes in Suruga Bay. - Hypocenter redetermination using velocity structure model obtained by Air-gun OBS refraction seismic survey.-

*Nakao Nagisa[1], Hisatoshi Baba[1], Takahito Nishimiya[2], Kayoko Tsuruga[3] (1.Graduate School of Oceanography, Tokai University, 2.Meteorological Research Institute,Japan Meteorological Agency, 3.Tokyo University of Marine Science and Technology)

[SSS13-P08] Swarm Activity in the Hida Mountain Range, Central Japan, Started in April 2020.; Comparison with Past Activity

*Shiro Ohmi[1] (1.Earthquake Hazards Division, Disaster Prevention Research Institute, Kyoto University)

[J] Poster | S (Solid Earth Sciences)：S-SS Seismology

[S-SS14] Crustal Deformation

convener:Tadafumi Ochi(Institute of Earthquake and Volcano Geology, Geological Survey of Japan, The National Institute of Advanced Industrial Science and Technology), Masayuki Kano(Graduate school of science, Tohoku University)

[SSS14-P01] The Influence on the Regional Crustal Deformation and Stress Field of the Wenchuan M_S 8.0 Earthquake

*Qi Liu[1], Xueze Wen[2], Zhigang Shao[1] (1.Institute of Earthquake Forecasting, China Earthquake Administration, 2.Institute of Geology, China Earthquake Administration)

[SSS14-P02] **Co-Seismic deformation of the 2017 *Ms*6.6 JingHe, China earthquake derived from Sentinel-1 data and speculate seismogenic fault**

*Wei Feng[1], Ze chao Bai[2], Zhi gang Shao[1], Jian bo Chen[3] (1.Institute of Earthquake Forecasting, China Earthquake Administration, 2.North China University of Technology, 3.Earthquake Administration of Xinjiang Uygur Autonomous Region)

[SSS14-P03] Application of a slow slip objective detection method

*Akio Kobayashi[1] (1.Meteorological Research Institute, Japan Meteorological Agency)

[SSS14-P04] The 2018 Hyuga-nada and Bungo channel long-term SSE detected by GEONET

*Shinzaburo Ozawa[1], Ryoji Kawabata[1], Kensuke Kokado[1], Hiroshi Yarai[1] (1.Geographical Survey Institute of Japan)

[SSS14-P05] Inversion analyses of long-term slow slip events using GNSS and strain data

*Takahiro Tsuyuki[1], Akio Kobayashi[1], Kana Akiyama[2], Reiko Kai[2], Kazuki Miyaoka[2] (1.Meteorological Research Institute, 2.Japan Meteorological Agency)

[SSS14-P06] Spatiotemporal evolution of Slow Slip Events along the southern Ryukyu subduction zone, using GNSS data collected by new stations

*Kazuki Komano[1], Shin'ichi Miyazaki[1], Masayuki Kano[2], Takeshi Matsushima[3], Takuya Nishimura[4] (1.Earth and Planetary Science, School of Science, Kyoto university, 2.Geophysics, School of Science, Tohoku university, 3.Earthquake and Volcano observation center, Kyushu University, 4.DPRI, Kyoto University)

[SSS14-P07] Long-term postseismic deformation at the eastern margin of the Japan Sea implied by temporal changes in areal strain rates and background seismicity rates

*Issei Kosugi[1], Yuta Mitsui[2] (1.Graduate School Of Science and Technology, Shizuoka University , 2.Faculty of Science, Shizuoka University)

[SSS14-P08] Temporal changes of areal strains estimated from three continuous GNSS stations in the vicinity of faults before the 2011 Tohoku and the 2016 Kumamoto earthquake

*Daisuke Sato[1], Masayuki Murase[2] (1.NIHON University Graduate School of Integrated Basic Sciences, 2. Department of Earth and Environmental Sciences, College of Humanities and Sciences, NIHON University)

[SSS14-P09] Seasonal adjustment for tidal data (3)

*Tadafumi Ochi[1] (1.Institute of Earthquake and Volcano Geology, Geological Survey of Japan, The National Institute of Advanced Industrial Science and Technology)

[SSS14-P10] **Vertical annual cyclic movement model of Mainland China and its analysis based on GPS observations**

*Hongbao Liang[1], Wei Zhan[1], Jinwu Li[1,2] (1.First Crust Monitoring and Application Center, CEA, Tianjin 300180, China., 2.School of Geodesy and Geomatics, Wuhan University, Wuhan 430079, China.)

[SSS14-P11] Strain changes due to the co-seismic fault slips observed in Kobe

*Atsushi Mukai[1], Shigeaki Otsuka[2], Yoichi Fukuda[3] (1.Faculty of Urban Management, Fukuyama City University, 2.Former Professor at Kobe Gakuin University, 3.Graduate School of Science, Kyoto Univ.)

[SSS14-P12] Development of the New GEONET Analysis Strategy

*Yasuaki Kakiage[1], Hiroki MURAMATSU[1], Kazuyuki OHASHI[1], Satoshi Abe[1], Tomoaki Furuya[1], Yuki Hatanaka[1] (1.Geospatial Information Authority of Japan)

[SSS14-P13] Estimation of fault models by MCMC method

*Ryoji Kawabata[1] (1.GSI of Japan)

[SSS14-P14] Estimation on fault-slip distributions without smoothing constraints by Reversible-jump MCMC

*Fumiaki Tomita[1], Takeshi Iinuma[1], Ryoichiro Agata[1], Takane Hori[1] (1.Japan Agency for Marine-Earth Science and Technology)

[SSS14-P15] Analysis of ocean bottom pressure gauge data by a hybrid method of MSSA and fitting of a parametric function

*Koichi Murata[1], Toshinori Sato[2], Hajime Shiobara[3], Masanao Shinohara[3], Tomoaki Yamada[4] (1.Graduate School of Science and Engineering, Chiba University, 2.Graduate School of Science, Chiba University, 3. Earthquake Research Institute, University of Tokyo, 4.Japan Meteorological Agency)

[SSS14-P16] **Earthquake potential in Costa Rica estimated by the integration of the interseismic geodetic data with seismicity records and inland faulting traces**

*Luis Alejandro Carvajal Soto[1,2], Takeo Ito[2], Marino Protti[3], Hiroshi Kimura[2] (1.Universidad Latina de Costa Rica, 2.Nagoya University, 3.Universidad Nacional de Costa Rica)

[SSS14-P17] The Fault model of the 2017 M5.6 earthquake estimated from precise leveling survey data in the Eastern flank of the Ontake volcano 2

*Masayuki Murase[1], Fumiaki Kimata[2], Yoshiko Yamanaka[3], Takeshi Matsushima[4], Hitoshi Yamashita Mori[1], Daisuke Sato[1], Takahiro Kunitomo[3], Yuta Maeda[3], Shinichiro Horikawa[3], Takashi OKUDA[3], Kenjoro Matsuhiro[3], Kazushi Tanoue[3], Kazunari Uchida[4], Shin Yoshikawa[5], Hiroyuki Inoue[5], Takahiro Yanada[6], Takahiro Kako[1,6], Hiroyuki Ishimori[6] (1.Department of Earth and Environmental Sciences, College of Humanities and Sciences, NIHON University, 2.Tono Research Institute of Earthquake Science, 3.Earthquake and Volcano Research Center, Graduate School of Environmental Studies, Nagoya University, 4.Institute of Seismology and Volcanology, Kyushu University. , 5.Aso Volcanological Laboratory , Kyoto University, 6.Japan meteorological agency)

[SSS14-P18] Change in area strain around Toyama prefecture during the period of 2005–2018

*Kohei Hotta[1] (1.University of Toyama)

[SSS14-P19] **Estimation of Deformation Fields from GNSS Data Using Basis Function Expansion: Comparison with the Method by Shen et al. (1996)**

*Tomohisa Okazaki[1], Yukitoshi Fukahata[2], Takuya Nishimura[2] (1.Center for Advanced Intelligence Project, RIKEN, 2.Disaster Prevention Research Institute, Kyoto University)

[SSS14-P20] Reconsidered source model of short-term slow slip event by using spatial distribution of strain change

*Noa Mitsui[1], Yasuhiro Asai[1], Satoshi Itaba[2] (1.Tono Research Institute of Earthquake Science, 2.National Institute of Advanced Industrial Science and Technology)

[SSS14-P21] Bayesian l_1 trend filtering for slow slip detection

*Keisuke Yano[1], Masayuki Kano[2] (1.The University of Tokyo, Graduate School of Information Science and Technology, 2.Tohoku university, Graduate School of Science)

[SSS14-P22] Detection of multiple inflection points in time-series of GNSS-acoustic data for a shallow part of the Nankai Trough based on a MCMC method

*Ryoya Igashima[1], Yuta Mitsui[2] (1.Nagoya University, 2.Shizuoka University)

[SSS14-P23] GNSS observation around a shear zone in southern Kyushu, southwest Japan (The fourth report)

*Tsuyoshi Watanabe[1], Koichi Asamori[1], Akiomi Shimada[1], Hiroki Ogawa[1], Atsushi Saiga[1], Koji Umeda[2] (1.Japan Atomic Energy Agency, 2.Hirosaki University)

[SSS14-P24] **Seismic Risk on the Northern Xiaojiang Fault Implied by the Latest and Nearest GPS Observations**

*Zhen Fu[1], Lisheng Xu[1] (1.Institute of Geophysics, China Earthquake Administration)

[SSS14-P26] An Analysis for the Shape of Subducting Oceanic Plate using Shortest-Path Algorithm in GIS

Yuki tsukamoto[1], *Shinsuke Okada[2], Tatsuya Sumita[3], Daisaku Kawabata[3] (1.Graduate School of Science, Tohoku University, 2.International Research Institute of Disaster Science, Tohoku University, 3.Geological Survey of Japan, National Institute of Advanced Industrial Science and Technology)

[SSS14-P27] Toward the development of a kinematic block motion model in Indonesia based on GNSS observation

*Rio Raharja[1], Takeo Ito[1], Hiroshi Kimura[1], Irwan Meilano[2] (1.Graduate School of Environmental Studies, Nagoya University, Japan, 2.Faculty of Earth Sciences and Technology, Bandung Institute of Technology, Indonesia)

[SSS14-P28] Def3D, a three-dimensional FEM tool for modeling deformation near active faults and volcanic centers

*luyuan Huang[1] (1.institute of crustal dynamics,CEA)

[SSS14-P29] The changes of interplate coupling area and the vertical changes at Shikoku before the 1946 Nankai earthquake.

*Yasuhiro Umeda[1] (1.former DPRI Kyoto Univ., former AIST)

[J] Poster | S (Solid Earth Sciences)：S-SS Seismology

[S-SS15] Fault Rheology and Earthquake Physics

convener:Keisuke Yoshida(Tohoku University), Keishi Okazaki(Japan Agency for Marine-Earth Science and Technology), Shunya Kaneki(Disaster Prevention Research Institute, Kyoto University), Hiroyuki Noda(Kyoto University, Disaster Prevention Research Institute)

[SSS15-P01] Estimation of thermal structure around the Median Tectonic Line in Shikoku, SW Japan

*Hideto Uchida[1], Michiharu Ikeda[1], Takeshi Tsuji[2], Kozo Onishi[3], Naoki Nishizaka[3] (1.Shikoku Research Institute inc., 2.Department of Earth Resources Engineering, Kyushu University, 3.Shikoku Electronic Power)

[SSS15-P02] Pore geometry and elastic moduli of fault rocks accompanied by the Median Tectonic Line in Shikoku, southwestern Japan

*Michiharu Ikeda[1], Kakda Kret[2], Takeshi Tsuji[3], Tatsunori Ikeda[3], Tomohiro Tsuji[4], Kozo Onishi[5], Naoki Nishizaka[5] (1.Department of Civil Engineering, Shikoku Research Institute Incorporated, 2.Institute of Technology of Cambodia, 3.Kyushu University, 4.Yamaguchi University, 5.Shikoku Electoric Power Co. Inc.)

[SSS15-P04] Development of composite-planer fabrics and its physical aspect

Akari Fuke[1], *Tetsuro Hirono[1], Satoshi Yukawa[1] (1.Department of Earth and Space Science, Graduate School of Science, Osaka University)

[SSS15-P05] Evaluation of reactivity under hydrous condition on thermal maturity of carbonaceous materials as a proxy of seismic slip

*Keita Iwagaki[1], Tetsuro Hirono[1] (1.Department of Earth and Space Science, Graduate School of Science, Osaka University)

[SSS15-P06] Experimental investigation of cumulative effect on thermal maturation of carbonaceous material by repeated earthquakes

*Yutaro Shimamura[1], Tetsuro Hirono[1], Hideki Mukoyoshi[2] (1.Department of Earth and Space Science, Graduate School of Science, Osaka University, 2.Department of Geoscience Interdisciplinary Graduate School of Science and Engineering, Shimane University)

[SSS15-P07] Thermal maturation of carbonaceous material as a proxy for earthquake slip: Evaluation of effects by initial maturity, heating rate, and mechanochemical activation

*Shuhei Yamashita[1], Tetsuro Hirono[1] (1.Department of Earth and Space Science, Graduate School of Science, Osaka University)

[SSS15-P08] Effects of initial crack distribution on inner-structures and flow properties of shear deformed rocks

*Yuka Kikuchi[1], Shin-ichi Uehara[1] (1.Toho University)

[SSS15-P09] Frequency characteristics of acoustic emission in granite during triaxial compression tests

*Sueyoshi Kazumasa[1], Manami Kitamura[2], Xinglin Lei[2], Ikuo Katayama[1] (1.Department of Earth and Planetary Systems Science, Hiroshima University, 2.National Institute of Advanced Industrial Science and Technology)

[SSS15-P10] Measurement of shear-wave polarization anisotropy in water-saturated Aji granite during shear experiment

*Jinki Tanaka[1], Ikuo Katayama[1] (1.Hiroshima University)

[SSS15-P11] Relationship between elastic wave velocity and attenuation ; An example of water-saturated granite

*Keiya Yamada[1], Kazuki Sawayama[2], Ikuo Katayama[1] (1.Hiroshima University, 2.Kyushu University)

[SSS15-P12] Development of new rock deformation apparatus with solid confining medium designed to reproduce the Pc-Pp-T condition of the base of the seismogenic zone

*Keishi Okazaki[1], Jun Muto[2], Yohei Hamada[1], Wataru Tanikawa[1], Takehiro Hirose[1] (1.Kochi Institute for Core Sample Research, Japan Agency for Marine-Earth Science and Technology, 2.Department of Earth Sciences, Tohoku University)

[SSS15-P13] Generation mechanism of slow stick slip verified from friction properties of mixed quartz/talc gouges

*Ryota Hibi[1], Risako Shirahige[1], Ken-ichi Hirauchi[1], Takato Takemura[2] (1.Department go Geoscience, Faculty of Science, Shizuoka University, 2.Nihon University)

[SSS15-P14] Effects of ambient temperature on the frictional strength and frictional heating of dolerite

*Michiyo Sawai[1], Yuuki Yokoyama[1], Manami Kitamura[2], Kyuichi Kanagawa[1] (1.Chiba University, 2.Geological Survey of Japan, AIST)

[SSS15-P16] Receiver Function Analysis of Laboratory Frictional Experiments

*Yasunori Sawaki[1], Miyuu Uemura[1], Ikuo Katayama[2], Yoshihiro Ito[3] (1.Graduate School of Science, Kyoto University , 2.Graduate School of Science, Hiroshima University , 3.Disaster Prevention Research Institute, Kyoto University)

[SSS15-P17] Statistical analysis for stick-slip experiments: Effects of inertial term and granular gouge

*Shinichi Oba[1], Yuta Mitsui[2] (1.Graduate School of Science and Tecnology, Shizuoka University, 2.Faculty of Science, Shizuoka University)

[SSS15-P18] System stiffness and unstable slip in the lab and in nature

*Akihiro Shimoda[1], Eiichi Fukuyama[1,2], Futoshi Yamashita[2], Shiqing Xu[2,3] (1.Kyoto Univ., 2.National Research Institute for Earth Science and Disaster Resilience, 3.Southern University of Science and Technology)

[SSS15-P19] Determination of frictional characteristics and evaluation of strong motion by dynamic rupture simulations of the Kamishiro fault at the 2014 Northern Nagano earthquake

*Takeshi Miyamoto[1], Kenichi Tsuda[2], Tetsuro Hirono[1] (1.Department of Earth and Space Science, Graduate School of Science, Osaka University, 2.Institute of Technology, Shimizu Corporation)

[SSS15-P20] Evaluation of ground motions generated from the splay fault of 1896 Rikuu earthquake - Preliminary study by dynamic rupture simulation

*Shuji Kumagai[1], Kiyoshi Hirotani[1], Yuta Mitsuhashi[2], Yusuke Saijo[2] (1.Tohoku Electric Power Co.,Inc., 2.KOZO KEIKAKU ENGINEERING Inc.)

[SSS15-P21] A Study on Dynamic of Strike-slip and Reverse Faults Based on Numerical Simulation

*Arzpeima Samaneh[1], Kenichi Tsuda[2], Sachio Ogawa[1] (1.Ohsaki Research Institute, 2.Shimizu corporation)

[SSS15-P22] Estimation of parameter values for a slip-dependent friction law using slip-stress relations of the Boso slow slips

*Reo Uchida[1], Toshinori Sato[1], Takuma Kobayashi[1,2] (1.Chiba University , 2.Asia Air Survey Co.,Ltd.)

[SSS15-P23] Relationship between the spatiotemporal change of the inelastic strain rate and the state of stress in the aftershock area of the 2016 Kumamoto earthquake sequence

*Ayaho Mitsuoka[1], Satoshi Matsumoto[2], Azusa Shito[2], Hiroshi Shimizu[2], Group for urgent joint seismic observation of the 2016 Kumamoto earthquake (1.Department of Earth and Planetary Sciences, Graduate School of Science, Kyushu University, 2.Institute of Seismology and Volcanology, Faculty of Science, Kyushu University)

[SSS15-P24] Stress tensor inversion in the focal area of the 2016 M_w7.8 Kaikoura earthquake, New Zealand (4)

*Miu Matsuno[1], Tomomi Okada[1], Satoshi Matsumoto[2], Yuta Kawamura[2], Yoshihisa Iio[3], Tadashi Sato[1], Takashi NAKAYAMA[1], Satoshi Hirahara[1], Stephen C Bannister[4], John Ristau[4], Martha K Savage[5], Clifford Thurber[6], Rick Sibson[7] (1.Research Center for Prediction of Earthquakes and Volcanic Eruptions Graduate School of Science, Tohoku University, 2.Institute of Seismology and Volcanology, Faculty of Sciences, Kyushu University, 3.Disater Prevention Research Institute, Kyoto University, 4.GNS Science, Lower Hutt, New Zealand, 5.Victoria University of Wellington, Wellington, New Zealand, 6.University of Wisconsin, Madison, 7.University of Otago, Dunedin, New Zealand)

[SSS15-P25] Stress field in the eastern margin of the Japan Sea and its relationship with faults of recent earthquakes

*Ayaka Tagami[1], Tomomi Okada[1], Shin'ichi Sakai[2], Mako Ohzono[3], Kei Katsumata[3], Masahiro Kosuga[4], Yoshiko Yamanaka[5], Hiroshi Katao[6], Takeshi Matsushima[7], Hiroshi Yakiwara[8], Takashi NAKAYAMA[1], Satoshi Hirahara[1], Toshio Kono[1], Shu'ichiro Hori[1], Toru Matsuzawa[1], Group for the aftershock observations of the 2011 off the Pacific coast of Tohoku Earthquake (1.Research Center for Prediction of Earthquakes and Volcanic Eruptions, Graduate School of Science, Tohoku University., 2.Earthquake Research Institute, University of Tokyo, 3.Institute of Seismology and Volcanology, Graduate School of Science, Hokkaido University, 4.Graduate School of Science and Technology,

Hirosaki University, 5.Graduate School of Encironmental Studies, University of NAGOYA, 6.Research Center for Earthquake Prediction, Disaster Prevention Research Institute, Kyoto University, 7.Institute of Seismology and Volcanology, Faculty of Sciences, Kyushu University, 8.Nansei-toko Observatory for Earthquakes and Volcanoes, Kagoshima University)

[SSS15-P26] Stress field estimated from microseismicity in the northeastern edge of the Honshu around the junction between the northeastern Japan arc and the Kurile arc

*Sumire Maeda[1], Toru Matsuzawa[2], Tomomi Okada[2], Takeyoshi Yoshida[2], Masahiro Kosuga[3], Hiroshi Katao[4], Makoto Otsubo[1] (1.Research Institute of Earthquake and Volcano Geology, Geological Survey of Japan/AIST, 2.Graduate School of Science, Tohoku University, 3.Graduate School of Science and Technology, Hirosaki University, 4.Research Center for Earthquake Prediction, Disaster Prevention Research Institute, Kyoto University)

[SSS15-P27] **Monitoring of temporal change in the interseismic plate coupling using misfit angles of focal mechanisms relative to the slip-deficit induced stress field: The Nankai trough case**

*Kazutoshi Imanishi[1], Akemi Noda[2] (1.Geological Survey of Japan, AIST, 2.National Research Institute for Earth Science and Disaster Resilience)

[SSS15-P28] Early rupture process of the 2019 Off Yamagata earthquake

*Ryo Fujimoto[1], Hirofumi Kowari[1], Masanao Komatsu[1], Hiroshi Takenaka[1] (1.Department of Earth Sciences, Graduate School of Natural Science and Technology, Okayama University)

[SSS15-P29] Development of a non-linear inversion method to estimate fault geometry from teleseismic data

*Kousuke Shimizu[1], Yuji Yagi[2], Ryo Okuwaki[2], Yukitoshi Fukahata[3] (1.Graduate School of Life and Environmental Sciences, University of Tsukuba, 2.Faculty of Life and Environmental Sciences, University of Tsukuba, 3.Disaster Prevention Research Institute, Kyoto University)

[SSS15-P31] Determination of pre-earthquake megathrust strength and frictional properties on seismogenic faults from near-field data

*Hongfeng Yang[1], Suli Yao[1] (1.The Chinese University of Hong Kong)

[SSS15-P32] Comparison of the rupture processes of the repeating earthquake sequences off-Iwate that occurred after the 2011 Tohoku oki earthquake

*Ahyi KIM[1], Naoki UCHIDA[2] (1.Yokohama City University, 2.Tohoku University)

[SSS15-P33] Spatiotemporal change in source parameters of repeating earthquakes due to the 2011 Tohoku-oki earthquake

*Kazuya Tateiwa[1], Tomomi Okada[1], Naoki Uchida[1], Toshio Kono[1] (1.Research Center for Prediction of Earthquakes and Volcanic Eruptions, Graduate School of Science, Tohoku University)

[SSS15-P34] Characteristics of Source Parameter for Aftershocks of the 2016 Kumamoto Earthquake Estimated by the Coda Spectral Ratio Method

*Naoto Maesako[1], Satoshi Matsumoto[2], Ayaho Mitsuoka[1], Group for Urgent Joint Seismic Observation of the 2016 Kumamoto Earthquake (1.Department of Earth and Planetary Sciences, Graduate School of Science, Kyushu University, 2.Institute of Seismology and Volcanology, Faculty of Science, Kyushu University)

[SSS15-P35] Simultaneous estimation of stress drop and rupture directivity of small to medium earthquakes around the Fukushima-Ibaraki border

*Rina Ikeda[1], Keisuke Yoshida[1], Ryo Takahashi[2,1], Toru Matsuzawa[1], Akira Hasegawa[1] (1.Tohoku University, 2.Japan Meteorological Agency)

[SSS15-P36] Estimating and considering the finiteness of small and moderate earthquakes in Iwaki area

*Naoto Yokotani[1], Aitaro Kato[1], Kazushige Obara[1], Shin'ichi Sakai[1], Takashi Iidaka[1], Tetsuya Takeda[2] (1.Earthquake Research Institute, the University of Tokyo, 2.National Research Institute for Earth Science and Disaster Resilience)

[SSS15-P37] Estimation of near-source Q and its temporal varaiation associated with pore pressure change: a case study of the Yamagata-Fukushima border swarm

*Keisuke Yoshida[1] (1.Tohoku University)

[SSS15-P38] Foreshocks immediately before the starting of earthquakes

*Masaki Yamana[1], Aitaro Kato[1] (1.Earthquake Research Institute, the University of Tokyo)

[SSS15-P39] Estimation of P-wave arrival time differences using P-wave first motion similarity with sampling frequency of 10 kHz

*Yuki Noda[1], Yoshihisa Iio[2] (1.Kyoto University Graduate School of Science, 2.Kyoto University Disaster Prevention Research Institute)

[J] Poster | S (Solid Earth Sciences)：S-SS Seismology

[S-SS16] Active faults and paleoseismology

convener:Mamoru Koarai(Earth Science course, College of Science, Ibaraki University), Hisao Kondo(Geological Survey of Japan, National Institute of Advanced Industrial Science and Technology), Takashi OGAMI(National Institute of Advanced Industrial Science and Technology), Yoshiki Sato(Advanced Industrial Science and Technology, Geological Survey of Japan)

[SSS16-P02] Discovery of active faults in the Abukuma Mountains, northeast Japan

*Masayoshi Tajikara[1], Takashi Nakata[2], Hideaki Goto[3] (1.Association for the Development of Earthquake Prediction, 2.Hiroshima Univ. Emeritus Prof., 3.Hiroshima Univ.)

[SSS16-P04] Paleoseismology of the northren part of Kamishiro fault, ISTL active fault zone, central Japan

*Daisuke Hirouchi[1], Nobuhisa Matsuta[2], Tatsuya Ishiyama[3], Kenichi Yasue[4], Nobuhiko Sugito[5], Yoshihiro Takeshita[1], Natsuko Fujita[7], Hiroshi Sawa[6], Kotaro Mizutani[8], Kaoru Taniguchi[9] (1.Faculty of Education, Shinshu University, 2.Okayama Univ., 3.Univof Tokyo, 4.Toyama Univ., 5.Hosei Univ., 6.Tsuruoka , 7.JAEA, 8.GRI, 9.Pasco)

[SSS16-P05] Characteristics of the latest slip zone in the near-surface fault zone of the Neodani Fault

Aiki Tsuru[1], *Tomoyuki Ohtani[1], Kazuma Yatabe[1] (1.Department of Civil Engineering, Gifu University)

[SSS16-P06] Holocene tectonic landform of the eastern marginal fault of the Nara basin

*Hiroyuki Tsutsumi[1], Nobuhiko Sugito[2], Noriyoshi Yoshida[1], Haruo Kimura[3] (1.Department of Environmental Systems Science, Faculty of Science and Engineering, Doshisha University, 2.Faculty of Sustainability Studies, Hosei University, 3.Central Research Institute of Electric Power Industry)

[SSS16-P07] Drifted huge boulders by storm surges since 1976 derived from the dike of quartz porphyry in Hashigui-iwa facing the Nankai Trough, Pacific side of central Japan

*Hideaki Maemoku[1], Yuichi Namegaya[2], Masanobu Shishikura[2], Tomoo Echigo[3], Kanae Suzuki[4] (1.Department of Geography, Hosei University, Japan, 2.AIST, Geological Survey of Japan, 3.Geo-Research Institute, Japan, 4.A Graduate of Hosei University)

[SSS16-P08] Densely microtremor observation to estimation of subsurface structure at Shikano fault due to the 1943 Tottori earthquake, Japan

*Tatsuya Noguchi[1], Kasuki Kobayashi[2], Sanri Okano[1], Isamu Nishimura[3], Takao Kagawa[1] (1.Faculty of Engineering, Tottori University, 2.Graduate School of Sustainability Science, Tottori University, 3.Graduate School of Engineering, Tottori University)

[SSS16-P09] Fault history and Trench survey of separated area from surface ruptures in Futagawa fault zone, Kumamoto Prefecture

*Noriyuki Shibuya[1], Masashi Omata[1], Yoshiki Mori[1], Naoto Inoue[2], Naoko Kitada[2], Tonagi Masao[3], Tsutomu Takahama[3] (1.PASCO CORPORATION, 2.Geo-research Institute, 3.KOZO KEIKAKU ENGINEERING Inc.)

[SSS16-P10] Paleoseismic history and horizontal slip of the Futagawa–Hinagu fault zone based on paleoseismological and tectonic geomorphological survey at Hirata, Mashiki Town, Kumamoto Prefecture

*Yoshiya Iwasa[1], Yasuhiro Kumahara[2], Hideaki Goto[3], Masayuki Torii[4] (1.Student of Graduate School of Education, Hiroshima University, 2.Graduate School of Education, Hiroshima University, 3.Graduate School of Letters, Hiroshima University, 4.Center for Water Cycle, Marine Environment and Disaster Management, Kumamoto University)

[SSS16-P11] Compiling descriptions on tsunami accompanied with the 1914 Sakurajima earthquake and inferred causes

*Reiji Kobayashi[1], Kazutoshi Kawano[2], Atsushi Kuroda[2], Keigo Haruta[2], Shunichiro Fujii[2] (1.Graduate School of Science and Engineering, Kagoshima University, 2.Faculty of Science, Kagoshima University)

[SSS16-P12] Tectonic landform and rock-controlled landform along fault trace of the Aceh segment, the northernmost Sumatran Fault

*Yoshio Soeda[1], Hiroyuki Tsutsumi[2], Nobuhisa Matsuta[3], Nazli Ismail[4], Bukhari Ali[4] (1.West Japan Engineering Consultants,Inc., 2.Doshisha University, 3.Okayama University, 4.Syiah Kuala Univ.)

[SSS16-P13] Triggered Surface Faults Associated with Large Earthquakes Detected by L-band SAR Interferometry

*Satoshi Fujiwara[1], Takayuki Nakano[1], Yu Morishita[1] (1.GSI of Japan)

[SSS16-P14] Estimation of fault activity by linear discriminant analysis using chemical composition of fault gouge

*Ryo Tateishi[1], Koji Shimada[2], Mayuko Shimizu[2], Shigeru Sueoka[2], Masakazu Niwa[2], Tsuneari Ishimaru[2] (1.University of Toyama, 2.Japan Atomic Energy Agency)

[SSS16-P16] Study on the structure of sediment covering basement rock in trench survey

*Shiro Tanaka[1], Shingo Kimura[2], Norihiko Sakakura[3] (1.Central Research Institute of Electric Power Industry, 2.Hokuriku Electric Power Company, 3.Dia Consultants Co., Ltd)

[SSS16-P17] Some outcrops along the Ide Fault, a part of the eastern margin fault zone of the Nara basin, central Hoshu.

*Taku Komatsubara[1] (1.Institute of Geology and Geoinformation, Advanced Industrial Science and Technology)

[J] Poster | S (Solid Earth Sciences)：S-SS Seismology

[S-SS17] Seismology General

convener:Masayuki Obayashi(Japan Agency for Marine-Earth Science and Technology), Kazuo Nakahigashi(Tokyo University of Marine Science and Technology), Tadafumi Ochi(Institute of Earthquake and Volcano Geology, Geological Survey of Japan, The National Institute of Advanced Industrial Science and Technology)

[SSS17-P01] Using a Structure Correction Method to Improve the Location Accuracy of the Hotan Seismic
Array

*Chunyue Hao[1] (1.Institute of Geophysics, China Earthquake Administration)

[SSS17-P02] Accuracy improvement of DONET seismometer orientations estimated from seismic waveforms

*Takehiro Nishiyama[1], Shuichiro Yada[1], Masaru Nakano[1], Keisuke Ariyoshi[1], Kentaro Sueki[1], Takane Hori[1], Narumi Takahashi[1,2] (1.Japan Agency for Marine-Earth Science and Technology, 2.National Research Institute for Earth Science and Disaster Resilience)

[SSS17-P03] **Determination of Current Seismotectonic Properties of Denizli and Its Region**

*Dogan Kalafat[1], Yavuz Gunes[1], Mehmet Kara[1], Kivanc Kekovali[1] (1.Bogazici University Kandilli Observatory and Earthquake Research Institute Cengelkoy, Istanbul Turkey)

[SSS17-P04] Analysis of stress drop ratio of slow tsunami earthquake to usual earthquake

*Takahito Nishimiya[1], Akio Katsumata[1] (1.Meteorological Research Institute, Japan Meteorological Agency)

[SSS17-P06] Source process of the 14 April 2016 earthquake (M6.5) in Kumamoto area estimated by back-projection analysis

*Mitsutaka Oshima[1], Hiroshi Takenaka[2], Makoto MATSUBARA[3] (1.Shimizu corporation, 2.Okayama university, 3.Makoto Matsubara)

[SSS17-P07] Analysis on the role of branching angles in dynamic rupture processes on 3-D branching fault system

*Haiming Zhang[1], Jingxing Fang[1], Feng Qian[1] (1.School of Earth and Space Sciences, Peking University)

[SSS17-P08] Estimation of seismic motion at depth from records at a ground surface station without assumption of plane wave incidence

*Tomotsugu Watanabe[1], Hiroshi Takenaka[1], Masanao Komatsu[1], Mitsutaka Oshima[2], Takeshi Nakamura[3] (1.Okayama University , 2.Shimizu Corporation, 3.National Research Institute for Earth Science and Disaster Resilience)

[SSS17-P09] Implosion earthquakes at very shallow level beneath lava dome, Unzen Volcano, Japan

*Tasuku Hashimoto[1], Koki Aizawa[2], Takeshi Matsushima[2], Yuto Hayashida[1], Kaori Tsukamoto[3], Yuto Yamamoto[1], Yuhei Yuasa[1], Kanta Miyano[1], Naoto Maesako[1], Yuta Kawamura[1], Hiroshi Shimizu[2], Satoshi Matsumoto[2], Megumi Kamizono[4], Ayaho Mitsuoka[1] (1.Department of Earth and Planetary Sciences, Graduate School of Science, Kyushu University, 2.Institute of Seismology and Volcanology, Faculty of Science, Kyushu University, 3.Fukuoka Regional Headquarters, JMA, 4.DIA CONSULTANTS CO., LSD.)

[SSS17-P10] Spatial-temporal and Seismogram Characteristics of Foreshock and Aftershock Activities for Tsunami Earthquakes

*Liu Yifeng[1], Yoshihiro Ito[2], Kazuaki Ohta[3], Satoshi Katakami[1] (1.Kyoto University, 2.Disaster Prevention Research Institude, Kyoto University, 3.NIED)

[SSS17-P11] Screening for elastic multipathing effects on teleseismic body waves

*Melissa J Bernardino[1], Craig H Jones[1] (1.University of Colorado at Boulder)

[SSS17-P12] Signal detection by amplitude distribution and Kullback-Leibler divergence

*Mitsutaka Oshima[1], Hiroshi Takenaka[2] (1.Shimizu corporation, 2.Okayama university)

[SSS17-P13] Re-evaluation of the relation between various magnitude scales

*Nobuo HAMADA[1] (1.none)

[SSS17-P14] The 3-stage earthquake generation process observed during 3 months before the 2011 Tohoku earthquake (4)

*Yoshiki SUE[1] (1.none)

[J] Poster | S (Solid Earth Sciences)：S-EM Earth's Electromagnetism

[S-EM21] Electromagnetic Induction in the Earth and Planetary Interiors, and Tectono-Electromagnetism

convener:Tetsuo Matsuno(Kobe Ocean Bottom Exploration Center, Kobe University), Maki Hata(Earthquake Research Institute, the University of Tokyo)

[SEM21-P01] 3-D resistivity models beneath two active volcano groups in a graben by Network-MT data of reticular arrangements (2)

*Maki Hata[1], Makoto Uyeshima[1], Yoshikazu Tanaka[2], Takeshi Hashimoto[3], Ryokei Yoshimura[4], Naoto Oshiman[4] (1.Earthquake Research Institute, the University of Tokyo , 2.Kyoto University, 3.Institute of Seismology and Volcanology, Graduate School of Science, Hokkaido University, 4.Disaster Prevention Research Institute, Kyoto University)

[SEM21-P02] A preliminary resistivity model in the south part of Mt. Ontake volcano

*Shuhei Nishijima[1], Hiroshi Ichihara[1], Shinichiro Horikawa[1], Yuta Maeda[1], Kenjiro Matsuhiro[1], Kazushi Tanoue[1], Takahiro Kunitomo[1] (1.Graduate School of Environmental Studies, Nagoya University)

[SEM21-P03] **A research report on the fundamental investigations of an electrical resistivity structure beneath Chugoku and Shikoku regions, southwestern Japan(2019)**

*Ichiro Shiozaki[1], Tomofumi Uto[1], Makoto Uyeshima[2], hiroshi hataoka[3], Hideki Murakami[4], Naoto Oshiman[5], Yoshihisa Iio[5], Kazuya Ando[6] (1.Graduate School of Engineering, Tottori University, 2.Earthquake Research Institute, University of Tokyo , 3.Technical Department, Tottori University, 4.Research and Education Faculty , Kochi University, 5.Disaster Prevention Research Institute, Kyoto University, 6.San'in Kaigan Geopark Museum of the Earth and Sea)

[SEM21-P04] Estimation of MT response function to reveal resistivity structure around the Hyuganada area

*Hayato Nakamura[1], Hiroshi Ichihara[1], Tada-nori Goto[2], Tetsuo Matsuno[3], Noriko Tada[4], Shinya Sato[5] (1.Graduate school of environmental studies, Nagoya University, 2.Graduate School of Life Science, University of Hyogo, 3.Kobe Ocean Bottom Exploration Center, Kobe University, 4.Japan Agency for Marine-Earth Science and Technology, 5.Kyoto Univesity, Graduate School of Engineering)

[SEM21-P05] 3D resistivity structure of the Matsukawa geothermal area using magnetotelluric data

*KENTARO AOYAMA[1], Toru Mogi[2], Junna Kanehiro[1], Koichi Suzuki[1] (1.Hokkaido University, 2.Tokyo Institute of Technology)

[SEM21-P06] MT data analysis with Multi-channel Spectrum Analysis (MSSA)

*Shu Kaneko[1], Katsumi Hattori[2], Toru Mogi[2], Chie Yoshino[2] (1.Chiba University Graduate School of Science and Engineering, 2.Chiba University Graduate School of Science)

[SEM21-P07] Effects of source field on MT responses of the flat Earth and the spherical Earth

*Shinya Sato[1] (1.Kyoto Univesity, Graduate School of Engineering)

[SEM21-P08] Electromagnetic field fluctuations recorded in MT data during the eruption of Kirishima Shinmoe-dake in 2018

*Satoru ANIYA[1], Koki Aizawa[2], Takeshi Matsushima[2] (1.Department of Earth and Planetary Sciences,Graduate School of Sciences,Kyushu University, 2.Institute of Seismology and Volcanology, Facurity of Sciences, Kyushu University)

[J] Poster | S (Solid Earth Sciences)：S-EM Earth's Electromagnetism

[S-EM22] Geomagnetism, paleomagnetism and rock magnetism

convener:Masahiko Sato(Department of Earth and Planetary Science, The University of Tokyo), Chie Kato(Faculty of Social and Cultural Studies, Kyushu University)

[SEM22-P01] The geomagnetic field modeling of different areas of China based on the Three-dimensional Surface Spline model

*yan feng[1,2], Yi Jiang[1], Shuang Liu[1] (1.The College of Mathematics and Statistics, Nanjing University of Information Science & Technology, Nanjing 210044, China., 2.State Key Laboratory of Space Weather, Chinese Academy of Sciences, Beijing 100190, China.)

[SEM22-P02] Forecasts of geomagnetic secular variation using core surface flow models (2)

*Masaki Matsushima[1], Hisayoshi Shimizu[2], Futoshi Takahashi[3], Takuto Minami[4], Shin ya Nakano[5], Ryosuke Nakashima[3], Hinami Taniguchi[3], Hiroaki TOH[6] (1.Department of Earth and Planetary Sciences, School of Science, Tokyo Institute of Technology, 2.Earthquake Research Institute, University of Tokyo, 3.Department of Earth and Planetary Sciences, Graduate School of Science, Kyushu University, 4.Department of Planetology, Graduate School of Science, Kobe University, 5.Institute of Statistical Mathematics, 6.Data Analysis Center for Geomagnetism and Space Magnetism, Kyoto University)

[SEM22-P03] Statistical property of the polarity reversals in numerical dynamo models with implications for the geomagnetic field reversals

*Futoshi Takahashi[1], Yuhji Yamamoto[2] (1.Faculty of Sciences, Kyushu University, 2.Center for Advanced Marine Core Research, Kochi University)

[SEM22-P04] Investigation of equatorial symmetry of the flow and magnetic fields in numerical dynamos with dipolar reversal

*takumi kera[1], Yuto Katoh[1], Yuki Nishida[1], Hiroaki Matsui[2] (1.tohoku university, 2.Dept. of Earth and Planetary Sciences, University of California, Davis Dept. of Earth and Planetary Sciences, University of California, Davis)

[SEM22-P06] Magnetic minerals in a speleothem from Tonga, the southern Pacific: Observation from scanning SQUID microscopy and rock magnetism

*Naoto Fukuyo[1,3], Hirokuni Oda[2], Geoffrey Clark[4], Yusuke Yokoyama[1,3] (1.Atmosphere and Ocean Research Institute, The University of Tokyo, 2.Institute of Geology and Geoinformation, Geological Survey of Japan, AIST, 3. Department of Earth and Planetary Science, The University of Tokyo, 4.College of Asia and the Pacific,The Australian National University)

[SEM22-P07] Paleomagnetic direction of the Paleogene Kobe Group ; the constraints on the paleoposition of Southwest Japan

*Hiroki Senda[1], Akira Hayashida[1] (1.Doshisha Univ.)

[SEM22-P08] A paleomagnetic record of the upper Olduvai polarity transition from the Hata Formation, Chikura Group, in the southernmost part of the Boso Peninsula

*Takahiro Kitamura[1], Makoto Okada[2] (1.Graduate School of Science and Engineering, Ibaraki University, 2.Department of Earth Sciences, Faculty of Science, Ibaraki University)

[SEM22-P09] Paleomagnetic secular variation and rock magnetic characteristics for the last 30 kyrs from the Nankai Trough sediments, Japan

*Ryoya Goto[1], Toshitsugu Yamazaki[1], Natsumi Okutsu[1,2], Juichiro Ashi[1] (1.Atmosphere and Ocean Research Institute, The University of Tokyo, 2.Japan Agency for Marine-Earth Science and Technology)

[SEM22-P10] Paleo-stress analysis of fault gouges using Raman spectroscopy and rock magnetic methods

Yuki Nose[2], *Norihiro Nakamura[1,2], Hiroyuki Nagahama[2] (1.Institute for Excellence in Higher Education, Tohoku University, 2.Department of Earth Science, Tohoku University)

[SEM22-P12] Coercivity- and blocking temperature-dependent remanence properties of single plagioclase crystals with exsolved magnetite

*Yoichi Usui[1], Chie Kato[2] (1.Japan Agency for Marine-Earth Science and Technology, 2.Earth-Life Science Institute, Tokyo Institute of Technology)

[SEM22-P13] Preliminary paleomagnetic study on single plagioclase crystals separated from the anorthositic dike in the Doshi gabbroic body

*Haruka Nagai[1], Masahiko Sato[1], Chie Kato[2], Kazuhito Ozawa[1] (1.The University of Tokyo, 2.Tokyo Institute of Technology)

[SEM22-P14] “On-land investigation of a sea-floor spreading in Ethiopia”
Geo-electromagnetic research at the center of a divergent plate boundary in Afar depression, Ethiopia

*Naoto Ishikawa[1], Ryokei Yoshimura[2], Tesfaye Kidane Birke[3], Shin-ichiro Higashino[4], Shin-ichi Kagashima[5], Ameha A. Mulneh[6], Kirika Kitagawa[5], Nobutatsu Mochizuki[12], Masakazu Fujii[7], Mamoru Kadoya[11], Mitsuhiro Iwamoto[11], Noriaki Obara[9], Yo-ichiro Otofuji[8], Minoru Funaki, Tetsu Kogiso[10] (1.Faculty of Sustainable Design, Toyama University, 2.Disaster Prevention Research Institute, Kyoto University., 3.University of KwaZulu Natal, 4.Graduate School of Engineering, Kyushu University, 5.Yamagata University, 6.Addis Ababa University, 7.National Institute of Polar Research, 8.Japan Geochronology Network, 9.Robotista, 10.Graduate School of Human and Environmental Studies, Kyoto University, 11.X-treme Composite Japan, 12.Kumamoto University)

[SEM22-P15] Periodic change of magnetic susceptibility observed in the dolerite

*Masaru Nakamura[1], Kohei Oda[1], Masaaki Tanaka[1], Daisuke Kashima[1], Yuichi Shimizu[1], Koki Takuwa[2], Shimpei Miyamoto[2] (1.The Chugoku Electric Power Co., Inc., 2.Chuden Engineering Consultants Co., Ltd.)

[SEM22-P16] **Shock remanence structure of natural basalt and granite samples**

*Masahiko Sato[1], Kosuke Kurosawa[2], Shota Kato[1], Masashi Ushioda[3], Sunao Hasegawa[4] (1.The University of Tokyo, 2.Chiba Institute of Technology, 3.National Institute of Advanced Industrial Science and Technology, 4.Japan Aerospace Exploration Agency)

[J] Poster | S (Solid Earth Sciences)：S-GL Geology

[S-GL34] Geochronology and Isotope Geology

convener:Takahiro Tagami(Graduate School of Science, Kyoto University), Yuji Sano(Division of Ocean and Earth Systems, Atmosphere and Ocean Research Institute, University of Tokyo)

[SGL34-P01] Cellulose oxygen isotopic time series of teak disks collected from Java, Indonesia

★Invited Papers

*Yumiko Watanabe[1], Ryo Hisamochi[1], Masaki Sano[2], Takeshi Nakatsuka[3], Takahiro Tagami[1] (1.Department of Earth and Planetary Scineces, Kyoto University, 2.Faculty of Human Sciences, Waseda University, 3.Nagoya University)

[SGL34-P02] Cellulose oxygen isotopic time series of teak disks collected from Bago Mountains, Myanmar

Wataru Ohmuro[1], *Yumiko Watanabe[1], Zhen Li[2], Takeshi Nakatsuka[2] (1.Department of Earth and Planetary Scineces, Kyoto University, 2.Nagoya University)

[SGL34-P03] Stable Sr isotopes of saline water from non-volcanic Arima-type spring in Japan: Sr isotope fractionation during fluid generation from subducting carbonate?

*Tomomi Kani[1], Keiji Misawa[2], Noritoshi Morikawa[3], Kohei Kazahaya[3], Fumitake Kusuhara[4], Yasutaka Terakado[5] (1.Department of Earth and Environmental Sciences, Kumamoto University, 2.National Institute of Polar Research , 3.Geological Survey of Japan, National Institute of Advanced Industrial Science and Technology (AIST) , 4.Central Research Institute of Electric Power Industry , 5.Graduate School of Human Development and Environment, Kobe University)

[SGL34-P05] Zircon U-Pb age and stratigraphy of some Quaternary tephras around Kagoshima Bay

*Hisatoshi Ito[1], Shimpei Uesawa[1], Futoshi Nanayama[2], Hiroomi Nakazato[3] (1.Central Research Institute of Electric Power Industry, 2.National Institute of Advanced Industrial Science and Technology, 3.National Agriculture and Food Research Organization)

[SGL34-P07] Formation ages of the Konosuyama Formation and the Shinobu Diorite and the provenance of the Douge Formation in the Noto Peninsula, central Japan

*Xianyu Chen[1], Hiroto Ota[1], Koh Kubomi[1], Mitsuhiro Nagata[1], Koshi Yamamoto[2], Shigeru Otoh[3] (1.Graduate School of Science and Engineering, University of Toyama, 2.Graduate School of Department of Earth and Environmental Studies,Nagoya Unversity, 3.Academic Assembly, Faculty of Sutainable Design, University of Toyama)

[SGL34-P08] Late Mesozoic magmatism and associated porphyry Mo mineralization in the the Xiong'ershan area, East Qinling Orogen, China

*Xinkai Hu[1,2], Toshiaki Tsunogae[1] (1.Graduate School of Life and Environmental Sciences, University of Tsukuba, 2.School of Earth Sciences and Resources, China University of Geosciences Beijing)

[SGL34-P09] **Paleozoic magmatism in the Alxa Block and its geological implication: constraints from geochronology and geochemistry of the Devonian plutons in the Bayanwulashan area**

*Kaiyuan Xu[1,2], Changqing Yin[1,2], Jian Zhang[1,2], Jiahui Qian[1,2], JIngna Liu[1,2] (1.School of Earth Sciences and Engineering, Sun Yat-sen University, Guangzhou 510275, P.R. China, 2.Southern Marine Science and Engineering Guangdong Laboratory (Zhuhai), Zhuhai 519082, P.R. China)

[SGL34-P10] Constraining timing of thrust activity within the Nobeoka Thrust, SW Japan

*Horst Zwingmann[1], Masakazu Niwa[2], Asuka Yamaguchi[3], Koichiro Fujimoto[4] (1.Kyoto University, 2.Tono Geoscience Center, JAEA, 3.Atmosphere and Ocean Research Institute, Tokyo University, 4.Faculty of Education, Tokyo Gakugei University)

[SGL34-P11] Observation result of 3.1Ga Cleaverville Banded Iron Formation in the Coastal Pilbara Craton, Western Australia.

*Kohei Ishikawa[1], Shoichi Kiyokawa[1] (1.Kyushu Univ.)

[J] Poster | S (Solid Earth Sciences)：S-VC Volcanology

[S-VC44] Hydrothermal systems of volcanoes

convener:Yasuhiro Fujimitsu(Department of Earth Resources Engineering, Faculty of Engineering, Kyushu University), Wataru Kanda(Volcanic Fluid Research Center, School of Science, Tokyo Institute of Technology), Takeshi Ohba(Department of chemistry, School of Science, Tokia University)

[SVC44-P01] Geochemical study of High-T hydrothermal fluid and chimney obtained from Tarama Hydrothermal Vent Field in southern Okinawa Trough

*Toshiro Yamanaka[1], Eri Yokota[1], Kei Okamura[2], Takuro Noguchi[2], Tomohiro Toki[3], Urumu Tsunogai[4], Yuji Onishi[5], Hiroko Makita[1] (1.Tokyo University of Marine Science and Technology, 2.Kochi University, 3.University of Ryukyus, 4.Nagoya University, 5.Kyoto University)

[SVC44-P02] Water chemistry of fluid supplied from subaqueous fumaroles of Yugama crater lake, Kusatsu-Shirane volcano, inferred from geochemical heterogeneities of lake water

*Leona Suzuki[1], Akihiko Terada[1], Muga Yaguchi[2], Masanori Takahashi[1], Takeshi Ohba[3] (1.Tokyo Institute of Technology, 2.Meteorological Research Institute,JMA, 3.Department of chemistry,School of Science,Tokai University)

[SVC44-P03] Preliminary resistivity structure model around Kusatsu-Shirane Volcano revealed by broadband Magnetotellurics

*Yasuo Matsunaga[1], Wataru Kanda[2], Shinichi Takakura[3], Takao Koyama[4], Tatsuji Nishizawa[2] (1.Department of Earth and Planetary Sciences, School of Science, Tokyo Institute of Technology, 2.Volcanic Fluid Research Center, School of Science, Tokyo Institute of Technology, 3.National Institute of Advanced Industrial Science and Technology, 4.Earthquake Research Institute, University of Tokyo)

[SVC44-P04] Geophysical implication of the high Vp/Vs zone at depth of approximately 3.6 km obtained by the DAS measurements at the Medipolis geothermal filed

*Junzo Kasahara[1,2], Yoko Hasada[1,3], Haruyasu Kuzume[1] (1.ENAA, 2.Shizuoka University, 3.Daiwa Exploration and Consulting Co. Ltd.)

[SVC44-P05] Estimation of Temperature and Permeability Distribution in Kakkonda Geothemal Field, Iwate Prefecture, Japan, Using Neural Network

*Ugo Tsubasa[1], Kazuya Ishitsuka[2], Toru Mogi[4], Koichi Suzuki[4], Yosuke Kobayashi[3] (1.Department of Environmental Circulation Systems, Hokkaido University, 2.Kyoto University, 3.Muroran Institute of Technology, 4.Hokkaido University)

[SVC44-P06] Extraction of features of strata using borehole data of geothermal area by multivariate analysisExtraction of features of strata using borehole data of geothermal area by multivariate analysis

*Ojima Hiroki[1], Kazuya Ishitsuka[2], Toru Mogi[1], Kajiwara Tatsuya[3], Takeshi Sugimoto[3], Hiroshi Asanuma[4] (1.Hokkaido University, 2.Kyoto University, 3.Geothermal Engineering Co., Ltd., 4. Fukushima Renewable Energy Institute, AIST)

[SVC44-P07] Geochemical characteristics of silica scales precipitated from the geothermal water at the Onuma geothermal power plant.

*CHEN FEIYANG[1], Mayuko Fukuyama[1] (1.Akita University)

[SVC44-P08] Hydrothermal system around the Iwo-yama fumarolic field in Kuju volcano (Japan) inferred from a 3-D resistivity structure model

*Wataru Kanda[1], Mitsuru Utsugi[2], Hiroyuki Inoue[2], Shogo Komori[3], Tsuneomi Kagiyama[4] (1.Volcanic Fluid Research Center, School of Science, Tokyo Institute of Technology, 2.Aso Volcanological Laboratory, Graduate School of Science, Kyoto University, 3.National Institute of Advanced Industrial Science and Technology (AIST), 4.Aso Geopark Promotion Council)

[SVC44-P09] Gravity changes inferred from hydrothermal simulation before and after the 1995 eruption in Kuju volcano, Oita prefecture

*Jun Nishijima[1], Yoshiyuki Mizusawa[2], Yasuhiro Fujimitsu[1] (1.Department of Earth Resources Engineering, Faculty of Engineering, Kyushu University, 2.Department of Earth Resources Engineering, Graduate School of Engineering, Kyushu University)

[SVC44-P10] Updating the conceptual model of Tendaho geothermal field, Afar Region, Ethiopia

*belete ashenafi fekadu, Yasuhiro Fujimitsu, Jun Nishijima, Mitsuo Matsumoto

[J] Poster | S (Solid Earth Sciences)：S-VC Volcanology

[S-VC45] Active Volcanism

convener:Yuta Maeda(Nagoya University), Takahiro Miwa(National research institute for earth science and disaster prevention), Takeshi Nishimura(Department of Geophysics, Graduate School of Science, Tohoku University)

[SVC45-P01] Unrest event at Nakamachinesiri crater of Meakandake in 2019; insight from total magnetic field observations

*Ryo Tanaka[1] (1.Hokkaido University,Institute of Seismology and Volcanology)

[SVC45-P02] Possible very micro low-frequency earthquakes in the Showa-Shinzan lava dome in the Usu volcanic region captured by dense seismic campaign

*Akiko Takeo[1], Motoko Ishise[1], Kiwamu Nishida[1], Hiroshi Aoyama[2], Yosuke Aoki[1] (1.Earthquake Research Institutute, the University of Tokyo, 2.Institute of Seismology and Volcanology, Faculty of Science, Hokkaido University)

[SVC45-P03] Detection of long-period volcanic earthquakes using continuous wavefield processing system

*Mare Yamamoto[1] (1.Research Center for Prediction of Earthquakes and Volcanic Eruptions, Graduate School of Science, Tohoku University)

[SVC45-P04] Geothermal Activity by Observation using Infrared Thermal Camera during the 2018-19 Volcanic Activity at Azumayama

*Susumu Seki[1], Masayuki Oishi[1], Tomoyuki Matsumura[1] (1.Japan Meteorological Agency)

[SVC45-P05] Reactivation of volcanic activity on May 2019 at Azumayama – Importance of precise ground deformation monitoring near the crater

*Jun Okada[1], Yu Nihara[2], Shin Chikasawa[3], Takuya Yamamura[3], Susumu Seki[3], Koki Sasaki[2], Akimichi Takagi[4], Keiichi Fukui[4] (1.Volcanology Research Department, Meteorological Research Institute, JMA, 2.Regional Volcanic Observation and Warning Center, Sendai Regional Headquarters, JMA, 3.Seismology and Volcanology Division, Sendai Regional Headquarters, JMA, 4.Volcanology Division, Seismology and Volcanology Department, JMA)

[SVC45-P06] Detection of crustal deformation owing to volcanic activity of the Oana crater in the Mt. Azuma area using interferometric synthetic aperture radar and pressure source estimation

*Sota Nagagata[1], Koichi Suzuki[1], Toru Mogi[2] (1.Hokkaido University, 2.Tokyo Institute of Technology)

[SVC45-P07] Consideration of JMA tilt meter data around volcano using boundary element method (2)

*Ryohei Kawaguchi[1] (1.Meteorological Research Institute)

[SVC45-P08] Imaging of the volcanic activity process beneath the Yugama crater at Kusatsu-Shiranesan volcano

*Akimichi Takagi[1], Tsukasa Kobayashi[1], Takahiro Kitagawa[1], Kousuke Takahashi[1], Koji Kato[1], Jun'ichi Miyamura[1] (1.Seismology and Volcanology Department, Japan Meteorological Agency)

[SVC45-P09] Self-potential and geomagnetic total intensity observations at Motoshirane volcano after the 2018 eruption (2)

*Akira Yamazaki[1], Hideki Iino[1], Shin Akira[1], Jun Shimokawa[1] (1.Kakioka Magnetic Observatory)

[SVC45-P10] Crack resonances at an LP source beneath Kusatsu-Shirane volcano triggered by volume changes with vapor condensation

*Kimiko Taguchi[1], Hiroyuki Kumagai[1], Yuta Maeda[1] (1.Nagoya University Environmental Studies)

[SVC45-P11] Forward analysis of seismic waves accompanied by tilt ground motion during the eruption of Mt. Motoshirane, Japan, on January 23, 2018

*Ryohei Takahashi[1], Yuta Maeda[1], Toshiki Watanabe[1] (1.Graduate School of Environmental Studies, Nagoya University)

[SVC45-P12] Real time monitoring of underground temperature in Jigokudani, Midagahara volcano using LPWA devices

*Tohru Watanabe[1] (1.University of Toyama)

[SVC45-P13] Development of a system for FEM-based crustal deformation analysis

*Tomokazu Kobayashi[1], Shinya Yamada[1] (1.GSI of Japan)

[SVC45-P14] Silisic magma reservoirs beneath Fuji Volcano, Japan, constrained from interstitial melt in gabbroic xenoliths

*Megu Otsuka[1], Hidemi Ishibashi[2], Natsumi Hokanishi[3], ATSUSHI YASUDA[3] (1.Graduate School of Integrated Science and Technology, Shizuoka University, 2.Shizuoka University, 3.Earthquake Research Institute,The University of Tokyo)

[SVC45-P15] Corrections of individual properties of relative gravimeters by using cooperative precise gravity measurement data in Izu-Oshima volcano

*Shin'ya Onizawa[1], Ryuichi Nishiyama[2], Shuhei Okubo[2,3], Yutaka Nagaoka[1], Yasuo Hirayama[4], Takanori Ishihara[4], Kensuke Matsuda[4], Yuya Kaneko[4], Yoshihiro Ueda[4], Yuichi Imanishi[2], Atsushi Watanabe[2], Miwako Ando[2], Shikou Sakashita[2] (1.Meteorological Research Institute, JMA, 2.Earthquake Research Institute, The University of Tokyo, 3.Southwest Jiaotong University, 4.Seismological and Volcanological Department, JMA)

[SVC45-P16] Temporal gravity change observed on Izu-Oshima Island in 2010's

*Ryuichi Nishiyama[1], Yuichi Imanishi[1], Shin'ya Onizawa[2], Shuhei Okubo[1,3], Miwako Ando[1], Atsushi Watanabe[1], Shikou Sakashita[1], Yutaka Nagaoka[2], Yoshiyuki Tanaka[4], Hidefumi Watanabe[1,5] (1.Earthquake Research Institute, The University of Tokyo, 2.Volcanology Research Department, Meteorological Research Institute, JMA, 3.Southwest Jiaotong University, 4.Graduate School of Science, The University of Tokyo, 5.Disaster Prevention Division, Tokyo Metropolitan Government)

[SVC45-P18] Vesiculation texture and change in the amount of phenocrysts of the summit eruption of the Izu-Oshima volcano - Comparison between the An'ei and the 1986 eruption -

*Yuya Ikenaga[1], Fukashi Maeno[1], ATSUSHI YASUDA[1] (1.Earthquake Research Institute, The University of Tokyo)

[SVC45-P19] A study on surface displacement and pressure source of Kozushima Island based on InSAR analysis

*Wataru Uehara[1], Yoshiya Oda[1] (1.Tokyo Metropolitan University)

[SVC45-P20] Automatic Seismic Wave Detection with Deep Learning
- Application to temporary observation data at Hachijojima Island -

*Ryohei Tottori[1], Hiroyuki Azuma[1], Yoshiya Oda[1], Toshifumi Matsuoka[2] (1.Tokyo Metropolitan University, 2.Fukada Geological Institute)

[SVC45-P21] Temporary dense seismic observation in Hachijojima Island

*Ryotaro Kanemaru[1], Yoshiya Oda[1], Hiroyuki Azuma[1], Kentaro Omori[1], Syotaro Kanke[1], Toshiki Watanabe[2] (1.Tokyo Metropolitan University, 2.Earthquake and Volcano Research Center Graduate School of Environmental Studies, Nagoya University)

[SVC45-P22] Lava discharge rate in Nishinoshima volcano, Ogasawara Islands revealed using ALOS-2/PALSAR-2

*Shinobu Ando[1], Satoshi Okuyama[2], Shinichi Matsusue[3] (1.Seismology and Tsunami Research Department, Meteorological Research Institute, 2.Volcanology Research Department, Meteorological Research Institute, 3.Volcanology Division, Japan Meteorological Agency)

[SVC45-P23] Spatial variation of magma compositions at the Abu Monogenetic Volcano Group, SW Japan

*Kenyo U[1], Koji Kiyosugi[1], Yasuko Itoh[2], Yoshiyuki Tatsumi[1] (1.Kobe University, 2.Hagi Geopark Promotion Division)

[SVC45-P24] Repeated aeromagnetic survey on Kuju Volcano using drone, unmanned multicopter.

*Mitsuru Utsugi[1], Takeshi Hashimoto[2], Akinori Satoh[2], Noriko Tada[3], Toyonobu Ota[4], Shin Yoshikawa[1], Hiroyuki Inoue[1] (1.Kyoto University, 2.Hokkaido University, 3.JAMSTEC, 4.Tierra Tecnica)

[SVC45-P26] Seismo-acoustic signals before ash emissions at Aso volcano, Japan

*Akihiko Yokoo[1] (1.Graduate School of Science, Kyoto University)

[SVC45-P27] Waveform analysis of infrasound pulses observed before the phreatomagmatic explosion on October 23, 2015

*Yuto Kozawa[1], Akihiko Yokoo[1] (1.Graduate School of Science, Kyoto University)

[SVC45-P28] Melt inclusion constraints on the pre-eruptive process of Kirishima-Ohachi 1235 subplinian eruption

*Yoshiharu Iwaki[1], Hidemi Ishibashi[2], Natsumi Hokanishi[3], ATSUSHI YASUDA[3], Toru Ishikawa[4] (1.Shizuoka University Graduate School of Integrated Science and Technology, 2.Shizuoka University, 3.Earthquake Research Institute,The University of Tokyo, 4.Kirishima Geopark Council)

[SVC45-P29] Temporal and spatial variations of helium isotope ratios in volcanic gases at Kirishima volcanic group

*Hirochika Sumino[1], Kotaro Toyama[1], Takeshi Ohba[2], Muga Yaguchi[3] (1.Department of Basic Science, Graduate School of Arts and Sciences, The University of Tokyo, 2.Department of Chemistry, Tokai University, 3.Meteorological Research Institute)

[SVC45-P30] Vertical ground deformation in Sakurajima volcano measured by precise leveling survey (during Nov. 2018 - Nov. 2019)

*Keigo Yamamoto[1], Takeshi Matsushima[2], Shin Yoshikawa[3], Hiroyuki Inoue[3], Tadaomi Sonoda[1], Taishi Yamada[1], Yichen Tang[2], Koki Yoshinaga[2], Takamitsu Ikegame[4], Hiroshi Kishimoto[4], Takahiro Ohkura[3] (1.Disaster Prevention Research Institute, Kyoto University, 2.Faculty of Sciences, Kyushu University, 3.Graduate School of Science, Kyoto University, 4.Japan Meteorological Agency)

[SVC45-P31] Changes in carrier phase residuals of GPS satellite radio waves following the eruptions of Sakurajima
-Data analysis from 2013 to 2019-

*Yukako Asakura[1], Takeshi Nishimura[1], Yusaku Ohta[1], Masayuki Kano[1] (1.Graduate school of science, Tohoku University)

[SVC45-P32] Detection of volcanic earthquakes and estimation of internal attenuation structure beneath the Kikai submarine caldera

Yasutomo Seto[1], *Hiroko Sugioka[1], Tsutomu Takahashi[2], Yojiro Yamamoto[2] (1.Kobe University, 2.JAMSTEC)

[SVC45-P33] Occurrence and distribution of pyroclastic fall deposits of Kuchinoerabujima volcano 2020 eruption

*Masashi NAGAI[1], Shojiro Nakagawa[2], Yu Iriyama[3], Takahiro Miwa[1], Setsuya Nakada[1] (1. Volcano Research Department, National Research Institute for Earth Science and Disaster Resilience, 2.Yakushima Chigaku Club, 3.Research and Industrial Collaboration Department, Kyushu University)

[SVC45-P34] Three-dimensional resistivity imaging of Taal Volcano, Philippines

*Yusuke Yamaya[1], Paul Alanis[2] (1.National Institute of Advanced Industrial Science and Technology, 2.Philippine Institute of Volcanology and Seismology)

[SVC45-P35] Detection of the volcanic plume by 19 February 2018 eruption of Mount Sinabung deduced from GNSS post-fit phase residual analysis

*Yusaku Ohta[1], Masato Iguchi[2], Gunawan Hendra[3], Umar Rosadi[3], Estu Kriswati[3] (1.Research Center for Prediction of Earthquakes and Volcanic Eruptions, Graduate School of Science, Tohoku University, 2.Sakurajima Volcano Research Center, Disaster Prevention Research Institute, Kyoto University, 3.Center for Volcanology and Geological Hazard Mitigation)

[SVC45-P36] The performance of the back elevation angle estimation of 3-dimensional infrasonic small array observation

*Kazuya Yamakawa[1], Mie Ichihara[1], Claudia Sánchez[2], Wataru Ikeda[1], Giorgio Lacanna[2], Maurizio Ripepe[2] (1.Earthquake Research Institute, University of Tokyo, Japan, 2.Department of Earth Sciences, University of Florence, Italy)

[SVC45-P37] A trial to quantify volcanic activities using the JMA unified earthquake catalog and the ETAS model

*Yuta Maeda[1] (1.Nagoya University)

[SVC45-P38] Temporal relationship between seismic activity and ground deformation by GNSS data with applying the stacking method

*Yo Kanno[1], Akimichi Takagi[1], Takashi YOKOTA[2], Kazuki Miyaoka[1] (1.Seismology and Volcanology Department, Japan meteorological agency, 2.Aichi Institute of Technology)

[SVC45-P39] Multi-sensor system with air blowers for airborne volcanic gas survey using drones: an improvement of a sensor response time

*Kohki Matsuura[1], Akihiko Terada[1], Toshiya Mori[2], Takato Ono[2] (1.Volcanic Fluid Research Center, Tokyo Institute of Technology, 2.Chemical Research Center, Graduate School of Science, The Univercity of Tokyo)

[SVC45-P40] Tephra segregation profiles from Vulcanian eruptions on Sakurajima volcano, Japan, based on settling velocity observations

*Kosei Takishita[1], Masato Iguchi[2], Alexandros Panagiotis Poulidis[2], Tadaomi Sonoda[2] (1.Division of Earth and Planetary Sciences, Graduate School of Science, Kyoto University, 2.Sakurajima Volcano Research Center, DPRI, Kyoto Univ.)

[J] Poster | S (Solid Earth Sciences)：S-VC Volcanology

[S-VC46] Mitigation of volcanic disasters - basic and applied researches

convener:Shinji Takarada(Geological Survey of Japan, National Institute of Advanced Industrial Science and Technology), Mitsuhiro Yoshimoto(Mount Fuji Research Institute, Yamanashi Prefectural Government), Tatsuro Chiba(Asia Air Survey Co., Ltd.), Tomohiro Kubo(Mount Fuji Research Institute)

[SVC46-P01] Research on observation method of volcanic ash accumulation using spaceborne SAR: Quantitative extraction of decorrelation by volcanic ash-fall

*Taku Ozawa[1], Eisuke Fujita[1] (1.National Research Institute for Earth Science and Disaster Resilience)

[SVC46-P02] How to set wind condition data for stochastic ashfall risk assessment?

*Yoshinori TOKIZANE[1], Masatsugu Wakaura[1], Himeka Kikuchi[1] (1.OYO RMS Corporation)

[SVC46-P03] Validity of thickness of Aso-4 tephra fall deposit of the Uwa Basin, western Shikoku

*Chisato Nakamura[1], Tomohiro Tsuji[2], Michiharu Ikeda[3], Naoki Nishizaka[4], Kozo Ohnishi[4], Masayuki Sakakibara[5,6] (1.NAIBA Co. Ltd., 2.Graduate School of Science and Technology for Innovation, Yamaguchi University, 3.Shikoku Research Institute INC., 4.Shikoku Electric Power Co. Ltd., 5.Faculty of Collaborative Regional Innovation, Ehime University, 6.Research Institute for Humanity and Nature)

[SVC46-P04] Improvement of accuracy of DEM generated using UAV -a case study of the central crater of Izu-Oshima volcano, Japan-

*mori takaaki[1], Shunsuke Miura[1], Takumi Mochizuki[1], Shino Naruke[1], Hideki Nonaka[1], Hisashi Sasaki[1], Kenichi Arai[1], Koji Fujita[1], Toshihiro Urayama[1], Tatsuro Chiba[1] (1.ASIA AIR SURVEY CO.,LTD.)

[SVC46-P05] Types and characteristics of evacuation shelters for volcanic eruption in Japan

*Hisashi Sasaki[1], Shino Naruke[1], Hiroyuki Yamada[2] (1.Asia Air Survey Co., Ltd., 2.National Defense Academy)

[SVC46-P06] Disaster prevention using data of climber’s movement and tendency in active volcanoes

*Yosuke Miyagi[1], Setsuya Nakada[1], Mitsuhiro Yoshimoto[2], Tomohiro Kubo[2], Ryo Honda[2] (1.National Research Institute for Earth Science and Disaster Resilience, 2.Mount Fuji Research Institute)

[SVC46-P07] Development of Proto-type Educational Web Contents for the Municipalities’ Disaster Response Staff

*Tomohiro Kubo[1], Mitsuhiro Yoshimoto[1], Yuki Horiuchi[1], Ryo Honda[1], Yasuhiro Ishimine[1], Yosuke Miyagi[2] (1. Mount Fuji Research Institute, 2.National Research Institute for Earth Science and Disaster Resilience)

[J] Poster | S (Solid Earth Sciences)：S-VC Volcanology

[S-VC47] Volcanic and igneous activities, and these long-term forecasting

convener:Teruki Oikawa(GSJ, National Institute of Advanced Industrial Science and Technology), Takeshi Hasegawa(Department of Earth Sciences, College of Science, Ibaraki University), Daisuke MIURA(Department of Physical Science, Graduate School of Science, Osaka Prefecture University), Nobuo Geshi(Geological Survey of Japan, The National Institute of Advanced Industrial Science and Technology)

[SVC47-P01] Yield strength obtained from tree molds and lava tube caves of Medicine Lake Volcano

*Tsutomu Honda[1] (1.Vulcano-speleological Society)

[SVC47-P02] Phase separation in mushy magma reservoirs

*Christian Huber[1], Matej Pec[2], Olivier Bachmann[3] (1.Brown University, 2.MIT, 3.ETH Zurich)

[SVC47-P03] **Age of the Toya caldera eruption**

*Akihiko Tomiya[1], Isoji Miyagi[1] (1.Geological Survey of Japan, National Institute of Advanced Industrial Science and Technology)

[SVC47-P04] Stratigraphy and eruption styles of 40 ka Kp I eruption, Kutcharo Volcano, Eastern Hokkaido, Japan

*Shibata Shohei[1], Takeshi Hasegawa[2] (1.Graduate school of Science and Engineering, Ibaraki University, 2.Depeartment of Earth Sciences, College of Science, Ibaraki University)

[SVC47-P05] Volcanic structure and tephrostratigraphy of the Iwate volcano clarified by the determination of collapse source of debris avalanches

*Nobuo Doi[1] (1.Research Center for Regional Disaster Management, Iwate University)

[SVC47-P06] Experimental constraints on magma storage conditions for caldera-forming eruptions of Towada volcano, Japan: a preliminary report

*Takayuki Nakatani[1], Toshihiro Suzuki[1], Takashi Kudo[1], Masashi Ushioda[1], Akihiko Tomiya[1], Akiko Tanaka[1] (1.Geological Survey of Japan, AIST)

[SVC47-P07] Transition sequence of the Y4 Eruption, Izu-Oshima volcano, Japan.

*Yoshihisa Kawanabe[1] (1.Geological Survey of Japan, AIST)

[SVC47-P08] Eruptive stratigraphy and magma compositions of the Tsubota stage (4.0-2.5 ka) in the southern part of the Miyakejima Volcano, Japan

*Shota Watanabe[1], Takeshi Hasegawa[1], Teruki Oikawa[2], Nobuo Geshi[2] (1.Graduate School of Science and Engineering, Ibaraki University, 2.Geological Survey of Japan, The National Institute of Advanced Industrial Science and Technology)

[SVC47-P09] Reconsideration of Late Quaternary tephrostratigraphy on Mikurajima Volcanic Island, Izu Islands.

*Tomohiro Tano[1], Takehiko Suzuki[1,2], Daisuke Ishimura[1,2], Satoshi Terayama[1], Tatsuki Watanabe[1] (1.Department of Geography, Tokyo Metropolitan University , 2.Research Center for Volcanic Hazards and Their Mitigation,Tokyo Metropolitan University)

[SVC47-P10] Holocene volcano of Kazafuki Volcano, Shirouma-Oike volcanoes, central Japan.

*Teruki Oikawa[1], Shun Nakano[1] (1.GSJ, National Institute of Advanced Industrial Science and Technology)

[SVC47-P11] The Omine Tuffite Dike and its Accompanied Andesite Fragments, Central Kii Peninsula, SW Japan

*Yutaka WADA[1], Kohnosuke NISHIMOTO[2] (1.Department of Earth Sciences, Nara University of Education, 2.Heguri Junior High School)

[SVC47-P12] Volcanic activity of the Miocene Basalts in Yatakayama Area, Kibi Plateau, Takahashi City, Okayama Prefecture, SW Japan

*Takumi Nagato[1], Shigeyuki Suzuki[1], Haruo Koami[2], Kotaro Nakai[1], Toru Tachibana[3] (1.Okayama University, 2.Okayama Prefectual Okayama Asahi Senior High School, 3.Soil Engineering Corporation)

[SVC47-P13] Textural observation and chemical analyses of 1716-1717 Kyoho eruption pumice at Shinmoedake, Kirishima volcano group

*Akari Kagawa[1], Atsushi Toramaru[1] (1.Kyushu university)

[SVC47-P14] **Identification of lava flow temperature by lava tube cave structure of Mt.Etna**

*Tsutomu Honda[1] (1.Vulcano-speleological Society)

[J] Poster | S (Solid Earth Sciences)：S-GC Geochemistry

[S-GC49] Solid Earth Geochemistry, Cosmochemistry

convener:Gen Shimoda(Geological Survey of Japan, AIST), Katsuhiko Suzuki(Submarine Resources Research Center, Japan Agency for Marine-Earth Science and Technology), Katsuyuki Yamashita(Graduate School of Natural Science and Technology, Okayama University), Akira Ishikawa(Department of Earth and Planetary Sciences, Tokyo Institute of Technology)

[SGC49-P01] **Particle size control of olivine alteration pathway and rate for simultaneous H_2 generation and CO_2 storage**

*Jiajie Wang[1], Noriaki Watanabe[1], Atsushi Okamoto[1], Kengo Nakamura[1], Takeshi Komai[1] (1.Tohoku University)

[SGC49-P02] Chemical composition of river sediments around Lake Biwa area, southwestern Japan

*Masako Kato[1], Motohiro Tsuboi[1] (1.Kwansei Gakuin University)

[SGC49-P03] Highly siderophile element geochemistry of komatiites from Pilbara Craton, Western Australia

*Shun Nakano[1], Akira Ishikawa[1], Yuichiro Ueno[1], Tetsuya Yokoyama[1] (1.Tokyo Institute of Technology)

[SGC49-P04] Time scale of the separation of molten metal droplets in the magma ocean: implications to metal-metal differentiation during core-mantle segregation

HIrotaro Sagi[1], *Tetsu Kogiso[1] (1.Kyoto Univ.)

[SGC49-P05] Geochemical investigations for magma genesis of Pre-Unzen volcano, Shimabara Peninsula, Kyushu, Japan

*Tomoyuki Shibata[1], Takuma Yoshida[1], Takeshi Sugimoto[2] (1.Graduate School of Science, Hiroshima University, 2.Geothermal Engineering Co., Ltd.)

[SGC49-P08] **Ship Detection Using Synthetic Aperture Radar**

*Kengo Iwata[1] (1.Tokyo Denki University)

[J] Poster | S (Solid Earth Sciences)：S-CG Complex & General

[S-CG66] Ocean Floor Geoscience

convener:Kyoko Okino(Atmosphere and Ocean Research Institute, The University of Tokyo)

[SCG66-P01] Relationship between the oblique opening system in the back-arc basin and Hamilton's principle

*Takao Eguchi

[SCG66-P02] A sand-box experiment for understanding marine self-potential anomalies

*Yoshifumi Kawada[1,2], Takafumi Kasaya[2] (1.International Research Institute of Disaster Science, Tohoku University, 2.Japan Agency for Marine-Earth Science and Technology)

[SCG66-P03] Sandbox analogue experiments to examine how syntectonic sedimentation influence on forearc basin stratigraphy and accretionary wedge growth

*Atsushi Noda[1], Hiroaki Koge[1], Yasuhiro Yamada[2,3,4], Ayumu Miyakawa[1], Juichiro Ashi[5] (1.National Institute of Advanced Industrial Science and Technology, 2.Japan Agency for Marine-Earth Science and Technology, 3.Faculty of Science and Technology, Kochi University, 4.Department of Earth Sciences, Royal Holloway University of London, 5.Atmosphere and Ocean Research Institute, The University of Tokyo)

[SCG66-P04] Geophysics in the R/V Hakuho-maru 2019-2020 expeditions around the world, 30th anniversary

*Masakazu Fujii[1,2], Hiroaki Koge[3], Hiroshi Sato[4], Kyoko Okino[5], Chiori Tamura[5], ZHOU JINYU[5], Kosuke Inoue[5] (1.National Institute of Polar Research, 2.The Graduate University for Advanced Studies, SOKENDAI , 3.AIST, 4.Senshu University, 5.Atmosphere and Ocean Research Institute, UTokyo)

[SCG66-P05] **How fracture zones work on subducting lithosphere?**

*Nobukazu Seama[1,2], Tomoeki Nakakuki[3] (1.Department of Planetology, Graduate School of Science, Kobe University, 2.Kobe Ocean Bottom Exploration Center, Kobe University, 3.Department of Earth and Planetary Systems Science, Graduate School of Science, Hiroshima University)

[SCG66-P06] Topographic features of rift zones of the seamounts on the Pacific Plate

*Megumi Fujimoto[1], Masao Nakanishi[2] (1.Graduate School of Science and Engineering, Chiba University , 2.Department of Earth Sciences Graduate School of Science, Chiba University)

[SCG66-P07] Dredge cruise on petit-spot volcanoes and IODP drilling earth science -Great discovery : explosion crater (Maar) in the abyssal plane, off Tohoku-

*Teruaki Ishii[1], Makoto Kaneko[2], Naoto Hirano[3], Shiki Machida[4], Asako Matsumoto[4], Norikatsu Akizawa[5], Yuki Sato[3], Taku Yutani[6], Keishiro Azami[5], Yuki Katsuragi[3], Shunta Sakai [3], Yukihiko Nakano[7], Takuya Matsuzaki[8] (1.Center for Integrated Research and Education of Natural Hazards, Sizuoka University, 2.Fukada Geological Institute, 3.Tohoku University, 4.Chiba Institute of Technology, 5.The University of Tokyo, 6.Tohoku University,University of Bayreuth (Germany), 7.Nippon Marine Enterprises, LTD, 8.Kochi University)

[SCG66-P09] Geophysical analysis of the Yonaguni, Irabu and Tarama knolls

*ZHOU JINYU[1], Kyoko Okino[1], Masakazu Fujii[2] (1. Atmosphere and Ocean Research Institute, The University of Tokyo, 2.National Institute of Polar Research)

[SCG66-P10] **Reflection seismic survey data around ring structures of the submarine Kikai Caldera, south offshore Kyushu, Japan**

*Jih-Hsin Chang[1], Takahiko Inoue[1], Ayanori Misawa[1], Kohsaku Arai[1] (1.Geological Survey of Japan, National Institute of Advanced Industrial and Science Technology.)

[SCG66-P11] Pore fluid chemistry at a small pockmark with liquid CO_2 venting within an active hydrothermal field in the Okinawa Trough

Shunta Ueno[1], Akihi Tsutsumi[1], Akiko Makabe[2], Shinsuke Kawagucci[2], Masahiro Yamamoto[2], *Jun-ichiro Ishibashi[1] (1.Department of Earth and Planetary Sciences, School of Science, Kyushu University, 2.Japan Agency for Marine-Earth Science and Technology)

[SCG66-P12] Precipitation environment and preservation mechanism in formation of iron hydroxide in Satsuma Iwo-jima, Kagoshima, Japan.

*Koki Hori[1], Shoichi Kiyokawa[2] (1.Department of Earth and Planetary Sciences, Graduate School of Sciences, Kyushu University, 2.Kyushu University Earth and Planetary Science)

[SCG66-P14] **Developing efficient methods to collect and observe microfossils of fish teeth (ichthyoliths) from pelagic clay for determining depositional ages of pelagic clay**

*Kazuhide Mimura[1], Shugo Minabe[1], Junichiro Ohta[1,2,3], Kentaro Nakamura[1], Kazutaka Yasukawa[1,2], Koichiro Fujinaga[2,1], Kazuhiro Takao[1], Yasuhiro Kato[1,2] (1.Department of Systems Innovation, School of Engineering, the University of Tokyo, 2.ORCeNG, Chiba Institute of Technology, 3.JAMSTEC)

[SCG66-P15] Chemostratigraphy of ferromanganese crusts based on Independent Component Analysis

*Keishiro Azami[1], Qing Chang[2], Jun-Ichi Kimura[2], Kazutaka Yasukawa[1,3], Kentaro Nakamura[1], Yasuhiro Kato[1,3] (1.Department of System Innovation, Graduate School of Engineering, The University of Tokyo, 2.Japan Agency for Marine-Earth Science and Technology, 3.Chiba Institute of Technology)

[SCG66-P16] Buoy-mounted system for continuous and real-time seafloor crustal deformation measurements

*Keiichi Tadokoro[1], Natsuki Kinugasa[1], Teruyuki Kato[2], Yukihiro Terada[3], Kenjiro Matsuhiro[4] (1.Research Center for Seismology, Volcanology and Earthquake and Volcano Research Center, Nagoya University, 2.Hot Springs Research Institute of Kanagawa Prefectural Government, 3.National Institute of Technology, Kochi College, 4.Technical Center, Nagoya University)

[SCG66-P17] Evaluation of the effects of seafloor station array size on the accuracy of GNSS-A observation using synthetic data

*Yuto Nakamura[1], Yusuke Yokota[2], Tadashi Ishikawa[1], Shun-ichi Watanabe[1] (1.Hydrographic and Oceanographic Department, Japan Coast Guard, 2.Institute of Industrial Science, University of Tokyo)

[SCG66-P18] High-resolution bathymetry and efficient geological survey using submersible SHINKAI 6500 equipped with MBES and SBP in the petit-spot volcanic fields around Minamitorishima Island.

*Junji Kaneko[1], Shiki Machida[2] (1.Japan Agency for Marine-Earth Science and Technology, 2.Chiba Institute of Technology)

[SCG66-P19] An efficient method for high-res deep ocean mapping newly developed in the international unmanned survey competition

*MASANAO SUMIYOSHI[1] (1.Hydrographic and Oceanographic Department, Japan Coast Guard)

[SCG66-P20] Recovery operation of "anchor-recovery type OBSs" – KR19-06C cruise of R/V Kairei, off Yamagata, Japan Sea

*Ryo Miura[1], Tetsuo No[1], Shuichi Kodaira[1], Takuya Maekawa[2], Ikumasa Terada[2], Hidenori Shibata[2], Keiji Okabe[3] (1.Japan Agency for Marine-Earth Science and Technology, 2.Nippon Marine Enterprises, Ltd., 3.Mitsuya, Ltd.)

[J] Poster | S (Solid Earth Sciences)：S-CG Complex & General

[S-CG67] Crustal fluids and deformation

convener:Yuichi Kitagawa(Tectono-Hydrology Research Group, Geological Survey of Japan, National Institute of Advanced Industrial Science and Technology), Naoji Koizumi(School of Environmental Science,the University of Shiga Prefecture), Koji Umeda(Hirosaki University), Fumiaki Tsunomori(Geochemical Research Center, Graduate School of Science, University of Tokyo)

[SCG67-P01] **Changes in stream water and spring water after the 2016 Kumamoto earthquake, Japan**

*Naoji Koizumi[1], Shinsuke Minote[2], Tatsuya Tanaka[3], Azumi Mori[4], Takumi Ajiki[5], Tsutomu Sato[6], Hiroshi A Takahashi[6], Norio Matsumoto[6] (1.School of Environmental Science,the University of Shiga Prefecture, 2.Taneya Co.Ltd., 3.JA Lake Otsu, 4.Yodogawa Hu-Tech Co., Ltd., 5.Kinki Eco Science Inc., 6.Geological Survey of Japan, AIST)

[SCG67-P02] Post-seismic slow strain changes and groundwater level changes in the case of the KST observation site of AIST

*Yuichi Kitagawa[1], Satoshi Itaba[1], Norio Matsumoto[1] (1.Tectono-Hydrology Research Group, Geological Survey of Japan, National Institute of Advanced Industrial Science and Technology)

[SCG67-P04] Experimental study on the effect of the oscillating confining pressure on permeability of fractured rock

*Yang Li[1,3], Shogo Kawakita[2], Daisuke Asahina[3], Takato Takemura[4] (1.Integrated Basic Sciences, Nihon Univ., 2.Graduate School of Science & Technology, Nihon Univ., 3.Geological Survey of Japan AIST, 4.Nihon Univ.)

[SCG67-P06] Relationship between geology and ^{222}Rn concentration in hot springs and groundwater around Kagoshima city, Japan

*Kuniyo Kawabata[1], Mai Watanabe[2,3], Ryosuke Nakano[2], Yujin Kitamura[4], Takashi Tomiyasu[4] (1.Institute for Comprehensive Education, KAGOSHIMA UNIVERSITY, 2.Faculty of Science, Kagoshima University, 3.Konica Minolta Planetarium Co., Ltd., 4.Graduate School of Science Engineering, Kagoshima University)

[J] Poster | S (Solid Earth Sciences)：S-CG Complex & General

[S-CG68] Environment formed and maintained by active faults

convener:Naoji Koizumi(School of Environmental Science,the University of Shiga Prefecture), Makoto Yamano(Earthquake Research Institute, the University of Tokyo), Takafumi Kasaya(Japan Agency for Marine-Earth Science and Technology), Hideki Hamamoto(Center for Environmental Science in Saitama)

[SCG68-P01] Three-dimensional distinct element (DEM) simulation of shear bands formation and their time development for strike-slip faults

*Satoru Yamaguchi[1], Daigo Furukawa[1], Tada-nori Goto[2] (1.Graduate School of Science, Osaka City University, 2.Graduate school of Life Science, University of Hyogo)

[SCG68-P02] Profiles of magnetic susceptibility and resistivity along an "outcrop" of the Atera fault

Shuhei Sogi[1], *Tada-nori Goto[1] (1.Graduate School of Life Science, University of Hyogo)

[SCG68-P03] **Effect of active faults on the water quality of the Ado river and neighboring spring waters in Shiga Prefecture**

*Naoji Koizumi[1], Keisuke Ishida[1], Natsuko Oshida[1], Masahiro Maruo[1] (1.School of Environmental Science,the University of Shiga Prefecture)

[SCG68-P04] Discussion on the environment formed and maintained by active faults

*Naoji Koizumi[1] (1.School of Environmental Science,the University of Shiga Prefecture)

[J] Poster | S (Solid Earth Sciences)：S-CG Complex & General

[S-CG69] Rheology, fracture and friction in Earth and planetary sciences

convener:Miki Tasaka(Shizuoka University), Osamu Kuwano(Japan Agency for Marine-Earth Science and Technology), Ichiko Shimizu(Division of Earth and Planetary Sciences, Graduate School of Science, Kyoto University), Shintaro Azuma(Department of Earth and Planetary Sciences, School of Science, Tokyo Institute of Technology)

[SCG69-P01] Deformation of dry orthoenstatite under high *P-T* conditions and its implication for the variation in strength of oceanic plates

*Yumiko Tsubokawa[1], Tomohiro Ohuchi[1], Yuji Higo[2], Yoshinori Tange[2], Tetsuo Irifune[1] (1.Ehime University Geodynamics Research Center, 2.Japan Synchrotron Radiation Research Institute)

[SCG69-P02] **Influence of hydration products on brittle deformation of olivine gabbro**

*Yuya Akamatsu[1], Ikuo Katayama[1] (1.Hiroshima University)

[SCG69-P03] Deformation experiments of chlorite at high pressures and temperatures: A preliminary study

*Sachiko Yamauchi[1], Tomoaki Kubo[2], Mori Yuichiro[2], Rei Shiraishi[3], Yuji Higo[4], Yoshinori Tange[4] (1.Department of Earth and Planetary Sciences, Graduate School of Sciences, Kyushu University, 2.Kyushu Univ., 3.Tohoku Univ., 4.JASRI)

[SCG69-P04] Dependency of crack distributions in granite on elastic velocities

Kanami Iwazaki[1], *Shinichi Uehara[1], Miki Takahashi[2], Manami Kitamura[2] (1.Faculty of Science, Toho University, 2.National Institute of Advanced Industrial Science and Technology)

[SCG69-P05] Image analysis on experimentally sheared granitic rocks: Shear zone development at brittle-ductile transition zone

*Shun Arai[1], Jun Muto[1], Takamoto Okudaira[2], Daichi Iwata[1] (1.Department of earth science, Tohoku University, 2.Department of Geosciences, Graduate School of Science, Osaka City University)

[SCG69-P06] Experimental study and numerical simulation of failure of feldspathic-mafic rocks by phase change of fluid

*Katsuya Mizuno[1], Nobuo Hirano[1], Noriyoshi Tsuchiya[1], Atsushi Okamoto[1] (1.Tohoku university)

[SCG69-P07] Continuously sheared granular matter reproduces in detail seismicity laws

*Victor Simon Levy dit Vehel[1], Sebastien Lherminier, Ramon Planet[3], Gilles Simon[1], Knut Jørgen Måløy[2], Loic Vanel[1], Osvanny Ramos[1] (1.Institut Lumiere Matiere Lyon 1, 2.University of Oslo, 3.University of Barcelona)

[SCG69-P08] Response and fracture of a viscoelastic fluid under unsteady shear rate

*Osamu Kuwano[1], Mie Ichihara[2] (1.Japan Agency for Marine-Earth Science and Technology, 2.Earthquake Research Institute, University of Tokyo)

[SCG69-P09] Evolution of size and shape distributions of comminuted particles under shear deformation

*Osamu Kuwano[1], Daisuke Sasakura[2] (1.Japan Agency for Marine-Earth Science and Technology, 2.Malvern Panalytical Japan, Div of Spectris Co., Ltd.)

[SCG69-P10] Microstructural analyses of peridotite xenoliths in Shimane prefecture ~ implications for plastic deformation during Japan Sea opening

*Miki Tasaka[1], Hiroyuki Oma[2], Shunsuke Inagawa[2] (1.Shizuoka University, 2.Shimane University)

[SCG69-P11] Structural and petrological analyses of blocky serpentinite in the Sanbagawa belt, central Shikoku, Japan: Implications for deep slow earthquakes

*Yurina Nagata[1], Kengo Kataoka[1], Ken-ichi Hirauchi[1], Katsuyoshi Michibayashi[2] (1.Department of Geosciences, Faculty of Science, Shizuoka University, 2.Department of Earth and Planetary Sciences, Graduate School of Environmental Studies, Nagoya University)

[SCG69-P12] **Relationship between stylolite and faults in chert**

*Kota Kojima[1], Jun-ichi Ando[1], Kaushik Das[1], Naotaka Tomioka[2] (1.Department of Earth and Planetary Systems Science, Hiroshima University, 2.Kochi Institute for Core Sample Research, Japan Agency for Marine-Earth Science

and Technology)

[SCG69-P13] **Textural analyses for K-feldspar inclusions within a micro-shear zone developed in Teshima granite, the Ryoke metamorphic belt**

*Tae-Hoon Uhmb[1], Katsuyoshi Michibayashi[1] (1.Department of Earth and Planetary Sciences, Research group of Petrology and Mineralogy, Nagoya University)

[J] Poster | S (Solid Earth Sciences)：S-CG Complex & General

[S-CG70] Reducing risks from earthquakes, tsunamis & volcanoes: new applications of realtime geophysical data

convener:Masashi Ogiso(Meteorological Research Institute, Japan Meteorological Agency), Masumi Yamada(Disaster Prevention Research Institute, Kyoto University), Naotaka YAMAMOTO CHIKASADA(National Research Institute for Earth Science and Disaster Resilience), Yusaku Ohta(Research Center for Prediction of Earthquakes and Volcanic Eruptions, Graduate School of Science, Tohoku University)

[SCG70-P01] Estimation of seismic energy sources inferred from Source-Scanning-Algorithm method: Case of the 2018 M6.6 Hokkaido Eastern Iburi Earthquake and the 2019 M6.7 Yamagata-Oki Earthquake

*Mugi Yamamoto[1], Ken Moriwaki[1] (1.Japan Meteorological Agency)

[SCG70-P02] Development of the parallelized code of the numerical shake prediction scheme

*Masashi Ogiso[1] (1.Meteorological Research Institute, Japan Meteorological Agency)

[SCG70-P03] Development of the spatial information data base using building damage of the 2019 Yamagata offshore earthquake

*Shohei Naito[1], Hiromitsu Nakamura[1], Hiroyuki Fujiwara[1], naokazu momma[2], Tetsuya Yamada[2] (1.National Research Institute for Earth Science and Disaster Resilience, 2.PASCO Corporation)

[SCG70-P04] Cluster analysis of tsunami inundation distribution for improvement of tsunami early prediction

*Masato Kamiya[1], Toshitaka Baba[1] (1.Tokushima University)

[SCG70-P05] Long-term evaluation of S-net pressure data for real-time tsunami forecasting

*Naotaka YAMAMOTO CHIKASADA[1], Tatsuya Kubota[1] (1.National Research Institute for Earth Science and Disaster Resilience)

[SCG70-P06] Real–time uncertainties evaluation of coseismic fault models and Tsunami inundation deduced from GNSS observations

Keitaro Ohno[1], *Yusaku Ohta[1] (1.Research Center for Prediction of Earthquakes and Volcanic Eruptions, Graduate School of Science, Tohoku University)

[J] Poster | S (Solid Earth Sciences)：S-CG Complex & General

[S-CG71] Volcanic roots

convener:Naofumi Aso(Tokyo Institute of Technology), Tsuyoshi Iizuka(University of Tokyo), Shuhei Sakata(Earthquake Research Institute, The University of Tokyo), Yohei Yukutake(Hot Springs Research Institute of Kanagawa Prefecture)

[SCG71-P01] Focal Mechanisms of Volcanic Deep Low Frequency Earthquakes in Northeast Japan

*Genki Oikawa[1], Naofumi Aso[1], Junichi Nakajima[1] (1.Tokyo Institute of Technology)

[SCG71-P02] Deep Long-Period Earthquakes in Eastern Shimane

*Naofumi Aso[1] (1.Tokyo Institute of Technology)

[SCG71-P03] S-wave reflectors below the earthquake swarm in the Yonezawa-Kitakata area, NE Japan

*Manami Suzuki [1], Tomomi Okada[1], Akiko Hasemi[1], Toru Matsuzawa[1], Norihito Umino[1], Takashi NAKAYAMA[1], Noriko Tsumura[2], Tadashi Yamashina[3], Group for the aftershock observations of the 2011 off the Pacific of Tohoku Earthquake (1.Research Center for Prediction of Earthquakes and Volcanic Eruptions, Graduate School of Science, Tohoku University, 2.Graduate School of Science, Chiba University, 3.Faculty of Science and Technology, Kochi University)

[SCG71-P04] V_{SV} and V_{SH} structures beneath Asama volcano

*Yutaka Nagaoka[1], Kiwamu Nishida[2], Yosuke Aoki[2], Minoru Takeo[2] (1.Volcanology Research Department, Meteorological Research Institute, 2.Earthquake Research Institute, The University of Tokyo)

[SCG71-P05] Simultaneously determination of U-Pb age and titanium concentration: A case study of the Kurobegawa granite.

*Kozue Ishibashi[1], Shuhei Sakata[2], Hayato Yamazaki[1], Takashi Yuguchi[1] (1.Yamagata University, 2.The University of Tokyo)

[SCG71-P06] Unraveling the generation process of granitoid magmas in the Hidaka Metamorphic Belt by in situ geochemical and Sr isotopic analyses of plagioclase

*Tokiyuki Morohoshi[1], Otaro Kobayashi[1], Tsuyoshi Iizuka[1] (1.University of Tokyo)

[J] Poster | B (Biogeosciences)：B-BG Biogeosciences & Geosphere-Biosphere Interactions

[B-BG02] Interaction between Life, Water, Mineral, and Atmosphere

convener:Yuichiro Ueno(Department of Earth and Planetary Sciences, Tokyo Institute of Technology), Takeshi Kakegawa(Graduate School of Science, Tohoku University), Ken Takai(Extremobiosphere Research Center, Japan Agency for Marine-Earth Science & Technology), Yohey Suzuki(Graduate School of Science, The University of Tokyo)

[BBG02-P01] Analysis of 13C-13C isotopologue of ethane and ethanol by a fluorination method

*Taguchi Koudai [1], Tomonari Yamamoto[1], Mayuko Nakagawa[1,2], Alexis Gilbert[1,2], Yuichiro Ueno[1,2,3] (1.Department of Earth and Planetary Sciences, Tokyo Institute of Technology, 2.Earth-Life Science Institute (WPI-ELSI), Tokyo Institute of Technology, 3.Department of Subsurface Geobiological Analysis and Research (D-SUGAR), Japan Agency for Marine-Earth Science and Technology (JAMSTEC))

[BBG02-P02] Iron isotope fractionation in the 3.2Ga Moodies Banded Iron Formations, Barberton Greenstone Belt, South Africa

*RYOHEI SUGIURA[1], Tsubasa Otake[2], Daizo Yamauchi[1], Yoko Ohtomo[2], Tsutomu Sato[2] (1.Graduate school of Engineering, Hokkaido University, 2.Facility of Engineering, Hokkaido University)

[BBG02-P03] Geochemical studies on the mobilization of phosphorus during seawater/rock interaction of Miocene lava flows in the *Hokuroku* district in Akita, Japan

*Tsukasa Sai[1], Takeshi Kakegawa[1] (1.Graduate School of Science, Tohoku University)

[BBG02-P04] Passive treatment of acid mine drainages containing dissolved iron

*Tatsuya Matsui[1], Sereyroith Tum[1], Frances Chikanda [1], Yoko Ohtomo[2], Tsubasa Otake[2], Ryosuke Kikuchi[2], Tsutomu Sato[2] (1.Graduate School of Engineering, Hokkaido University, 2.Faculty of Engineering, Hokkaido University)

[BBG02-P05] Textual characteristics of laminated silica hot spring deposits in Kagoshima Prefecture

*Chizuru Takashima[1], Tomoyo Okumura[2], Akihiro Kano[3], Susumu Kakubuchi[1] (1.Faculty of Education, Saga University, 2.Center for Advanced Marine Core Research, Kochi University, 3.Department of Earth and Planetary Science The University of Tokyo)

[BBG02-P06] Formation mechanism of halloysite-rich layer by differential weathering of tephra under a reduced condition

*Hirokazu Fukui[1], Yuki Matsushi[2], Tetsuhiro Watanabe[3] (1.Graduate school of Science, Kyoto University, 2.Disaster prrevention research institute, Kyoto university, 3.Graduate School of Agriculture, Kyoto university)

[BBG02-P07] Aquifer Nitrate Concentration and Associated Human Health Risk Assessment of Haridwar District of Uttarakhand, India

*AHTESHYAM AHTESHYAM[1], Shaveta Sawhney[1], Jahangeer -[2] (1.Patanjali Medical College, Haridwar, India, 2.Nebraska Water Center, University of Nebraska Lincoln USA)

[BBG02-P08] Global ocean pigments transport by mesoscale eddies

*xiangguang zhang[1,2,3], yongsheng Xu[1,2,3] (1.Key Laboratory of Ocean Circulation and Waves, Institute of Oceanology, Chinese Academy of Sciences, 2.Center for Ocean Mega-Science, Chinese Academy of Sciences, 3.Laboratory for Ocean and Climate Dynamics, Qingdao National Laboratory for Marine Science and Technology)

[BBG02-P09] Screening of Genes from Subseafloor Sediments and Co-Rich Ferromanganese crust Using Substrate-induced Gene Expression (SIGEX) Method.

*Aki Yoshida[1], Taisuke Wakamatsu[1], Takashi Morisawa[1], Takeshi Terada[3], Shunichi Ishii[2], Yuki Morono[2] (1.Kochi university, 2.Kochi Institute for Core Sample Research, JAMSTEC, 3.Marine Works Japan Ltd.)

[BBG02-P10] Spatial analysis of water quality data to prioritize sites for oyster reef restoration

*Cameron Chase Atkinson[1], James Deemy[1] (1.College of Coastal Georgia)

[J] Poster | G (General)：General

[G-02] Comprehensive disaster prevention education

convener:Hitoshi Nakai(Kobuchisawa Research Institute for Nature and Education), Jiro Komori(Teikyo Heisei University), Shintaro Hayashi(Akita University Graduate School of Education)

[G02-P01] Thinking about Needs for minority victims in Multicultural Collaboration society

*ITOYA NATSUMI[1], MICHITAKA TAHARA[1], SHUNSUKE HAMADA[1] (1.oyo corporation)

[G02-P02] A Proposal of Universal Design Teaching Material for Education of Disaster Risk Reduction

*Haruka Matsuoka[1], Kei Takashima[1], Tsukasa Sano[1], Asako Nakagawa[2], Seiji Hori[1], Minako Noda[1] (1.Faculty of Business and Informatics, Tsukuba Gakuin University, 2.Faculty of Home Economics, Otsuma Women's University)

[G02-P03] Reconsideration of the Cause of the Accident Given in the Tsunami Judgment of Okawa Elementary School

*Mamoru Hayashi[1] (1.University of TOYAMA)

[G02-P04] Case report of education about earthquakes and faults in elementary schools

*Noa Mitsui[1], Kumi Yoshitake[2], Kazuyuki Nakagawa[3] (1.Tono Research Institute of Earthquake Science, 2.University of human environments, 3.Jiji Press)

[G02-P05] Consideration on Education of Disaster Prevention Jointly Practiced with the Field

*Erina Hyuga[1], Ami Pareek[1], Hikari Tanaka[1], Mirei Toba[1], Chisa Funada[1], Satoko Oki[1] (1.Keio University)

[G02-P06] Junior high school students experienced the "Shelter Management Game"

*Takeshi Matsumoto[1] (1.Faculty of Science, University of the Ryukyus)

[G02-P07] What is the "comprehensive" in disaster prevention education?

*Hitoshi Nakai[1] (1.Kobuchisawa Research Institute for Nature and Education)

[J] Poster | G (General)：General

[G-03] Geoscience education from elementary school to university students

convener:Masatsune Hatakeyama(Seiko Gakuin High School), Yoshihiro Niwa(Center for Ocean Literacy and Education, Graduate School of Education, The University of Tokyo)

[G03-P01] Recipe 2.0 for rock thin-section study in a classroom. Part 1. Observation

*Yoshio Okamoto[1] (1.Kamnoetvidya Science Academy, PCSHS Mukdahan, Thailand)

[G03-P02] Recipe 2.0 for rock thin-section study in a classroom. Part 2. Making

*Yoshio Okamoto[1] (1.Kamnoetvidya Science Academy, PCSHS Mukdahan, Thailand)

[G03-P03] Implementing Concept Mapping to Evaluate College Students' Ocean Literacy

*ChengChieh Chang[1], YaHsin Lu[2], LiangTing Tsai[2], KuoChen Chang[2], ChunChieh Hsu[1], MeiChun Lin[2], TingKuang Yeh [3] (1.National Taiwan Ocean University, 2.Taiwan Marine Education Center, 3.National Taiwan Normal University)

[G03-P04] The Oceanographic Society of Japan (JOS) School Visit Program

*Yushi Morioka[1], Naoki Fujii[2], Ueno Hiromichi[3], Akihiro Senda[4], Hideki Kaeriyama[5], Sayaka Yasunaka[1] (1.Japan Agency for Marine-Earth Science and Technology, 2.Saga University, 3.Hokkaido University, 4.The Japan Science Society, 5.Japan Fisheries Research and Education Agency)

[G03-P05] Using a borehole for groundwater observation in junior high school

*takashi morie[1] (1.Faculty of Risk and Crisis Management, Chiba Institute of Science)

[G03-P06] Hands-on learning of science for elementary school students in Kyotango-city,Kyoto Prefecture.

*Makoto Obase[1] (1.kyoto Prefectural Mineyama High School)

[G03-P07] The Logical Thinking Ability that High School Students want to acquire through Inquiry Learning

*Kazuya Kawakatsu[1] (1.Hyogo Prefectural Himeji Higashi senior high school)

[G03-P08] Future Geospatial Information Authority of Japan Geography Education Support Based on Questionnaire Results to High School Geoscience Teachers

*Hiroaki Tanaka[1], Ryouichi Kojiroi[1] (1.Geospatial Infomation Authority of Japan)

[G03-P09] Learning ambient noise analysis with Raspberry Pi and accelerometers

*Naofumi Aso[1], Ritsuya Shibata[1], Junichi Nakajima[1] (1.Tokyo Institute of Technology)

[J] Poster | G (General)：General

[G-04] Geoscinece Outreach

convener:Jiro Komori(Teikyo Heisei University), Takeyuki Ueki(Faculty of Risk and Crisis Management, Chiba Institute of Science), Naoko HASEGAWA(Ochanomizu University), Satoko Oki(Faculty of Environment and information Studies)

[G04-P01] Diversity concept of the new curriculum "Inquiry learning"-To increase the number of student's presentations-

Masao Mukoh[2], *Tomoko Goto[1], Kazuyo Nagahama[3], Hideki Ishida[4] (1.Earthquake Research Institute, the University of Tokyo, 2.Tokyo Metropolitan Institute Fuji Senior High School・Junior High School, 3.Mejiro University, 4.Tohoku University)

[G04-P02] Kochi Core School for Asian Young Scientists at Kochi Core Center: new international outreach activity in marine sediment core and related sciences

*Go-Ichiro Uramoto[1], Hiroki Matsui[1], Kazuno Arai[1], Naohisa Nishida[2], Hirofumi Asahi[1], Yusuke Kubo[3], Satoshi Tonai[1], Wataru Tanikawa[3], Yurika Ujiie[1], Yuhji Yamamoto[1], Minoru Ikehara[1] (1.Kochi University, 2.Tokyo Gakugei University, 3.Japan Agency for Marine-Earth Scienct and Technology (JAMSTEC))

[G04-P03] A Pilot Study of an Active Learning Program for the General Public using Radiological Monitors

*Haruka Matsuoka[1] (1.Department of Business and Informatics, Tsukuba Gakuin University)

[G04-P04] Spread of hemispherical multi-touch panel for rear projection type digital globe "Dagik Earth"

*Yukinobu Koyama[1], Akinori Saito[2] (1.KINDAI University Technical College, 2.Graduate School of Science, Kyoto University)

[G04-P05] Practice report of geological excursion for elementary school students using terrain model made by 3-D printer

*Iida Kazuya[1] (1.Komaba-Toho Junior and Senior High School)

[G04-P06] A support activity for field excursion by a voluntary organization “Geo-Education”

*Jiro Komori[1], Tomoaki Kitayama[2], Iida Kazuya[3] (1.Teikyo Heisei University, 2.JAMSTEC, 3.Komaba Toho Junior & Senior High School)

[G04-P07] The report of the International Earth Science Olympiad (IESO) 2020

*Norihito Kawamura[1], Yutaka Takigami (1.School of Regional Resource Management, Graduate School, University of Hyogo)

[G04-P08] Standing on an asteroid: using virtual reality for outreach and education

*Elizabeth Tasker[1], Alexander Kaurov[2,3] (1.Institute of Space and Astronautical Science (ISAS), JAXA, 2.Institute for Advanced Study, 3.OmniScope)

[J] Poster | M (Multidisciplinary and Interdisciplinary)：M-IS Intersection

[M-IS20] Atmospheric Electricity: Lightning discharges and related physical phenomena

convener:Yasuhide Hobara(Graduate School of Information and Engineering Department of Communication Engineering and Informatics, The University of Electro-Communications)

[MIS20-P02] **Characteristics of Medium-low Frequency Magnetic Fields of Initial Continuous Current in Triggered Lightning**

*Yanfeng Fan[1], Yang Zhang[1], Weitao Lyu[1], Dong Zheng[1], Xiangpeng Fan[1] (1.State Key Laboratory of Severe Weather, Chinese Academy of Meteorological Sciences)

[MIS20-P03] Study on the time development of lightning and precipitation activities by LLS and radar observations

*Takeshi Morimoto[1], Keichiro Boda[1], Yoshitaka Nakamura[2], Hideo Sakai[3], Masahito Shimizu[4] (1.Kindai University, 2.Kobe City College of Technology, 3.University of Toyama, 4.Chubu Electric Power Co. Inc.)

[J] Poster | M (Multidisciplinary and Interdisciplinary)：M-IS Intersection

[M-IS21] Geopark

convener:Keiichi Tadokoro(Research Center for Seismology, Volcanology and Earthquake and Volcano Research Center, Nagoya University), Takayuki Ogata(Disaster Prevention Research Center for Island Regions, University of the Ryukyus), Marekazu OHNO(Unzen Volcanic Area Geopark Promotion Office), Takayuki Arima(Yokohama City University)

[MIS21-P01] **Educational application of Geopark in order to better understanding the regional resource management**

*Kyohei Sano[1] (1.Graduate School of Regional Resource Management, University of Hyogo)

[MIS21-P02] Thinking Geopark and Geo-story through an active Learing methode Mystery

*Ryuta YAMAMOTO[1] (1.Center for professional development of teachers Shizuoka University)

[MIS21-P03] Efforts to improve the quality of the sea activity guide through collaboration between the private sector, the government, and experts: San’in Kaigan UNESCO Global Geopark GEO×Activity Project

*Kyoko Kanayama[1], Yuzo Ota[1], Yuki Iwamoto[2], Suzuka Koriyama[2], Akio Yamashita[3], Yoshinori Kodama[4], Yoshiaki SUGAMORI[4], Kyohei Sano[5] (1.San'in Kaigan Geopark Museum of the Earth and Sea, Tottori Prefectural Government, 2.Secretariat of San'in Kaigan Geopark Promotion Council, 3.Develop Surf & Sea, 4.Faculty of Agriculture, Tottori University, 5.Graduate School of Regional Resource Management, University of Hyogo)

[MIS21-P04] Approach of Nanki Kumano Geopark Guided tours add value to tourist destinations Guide to hotel-hosted bus tours

*TAKAMARU NAKAE[1] (1.Japanese Geoparks Network)

[MIS21-P05] Reorganization of “sites” in Unzen Volcanic Area UNESCO Global Geopark ver.2020

*Taku MORIMOTO[1] (1. Unzen Volcanic Area Geopark Promotion Office)

[MIS21-P06] **The Permian–Triassic granitoid and gneiss in the Dinosaur Valley Fukui Katsuyama Geopark and other areas, Fukui Prefecture, Central Japan**

*Sachiho Koizumi[1], Shigeru Otoh[1] (1.Graduate School of Science and Engineering, University of Toyama)

[MIS21-P07] Re-discovering the Lake Towada area as a geological heritage: A key to the revitalization of the local community

*Yusuke Kuwahara[1], Mizuki Ishida[1], Mio Kobayashi[2], Katsuya Ohnuma[3], Yasuhiro Kato[4,1,5] (1.Department of Systems Innovation, School of Engineering, The University of Tokyo, 2.Department of Eco System Studies, School of Agricultural and Life sciences, The University of Tokyo, 3.Department of Physics, School of Science, The University of Tokyo, 4.Frontier Research Center for Energy and Resources, School of Engineering, The University of Tokyo, 5.Ocean Resources Research Center for Next Generation, Chiba Institute of Technology)

[MIS21-P08] 10 years cooperation history of geopark activity between Fossa Magna Museum and Niigata University in Itoigawa geopark.

*Yousuke Ibaraki[1], Ko Takenouchi[1], Takahiko Ogawara[1], Takeo Kobayashi[2], Atsushi Matsuoka[3] (1.Fossa Magna Museum, 2.Itoigawa Geopark Council, 3.Niigata University)

[MIS21-P09] Japan-China Comparison of the Role of Museums in Lifelong Education——To consider the role of education in geoparks

*Qikun Zhou[1] (1.Graduate School of Tourism, Wakayama University)

[J] Poster | M (Multidisciplinary and Interdisciplinary)：M-IS Intersection

[M-IS22] Exploring the origin of space, solar system, earth, moon, plate tectonics, life, etc.

convener:Akira Taneko(SEED SCIENCE Lab.)

[MIS22-P01] Moon, Earth (ocean floor, plate boundary, plate tectonics, driving force), asteroid belt and differentiated meteorites, origin of Jupiter's Great Red Spot, all sources verified by Abduction

★Invited Papers

*Akira Taneko[1] (1.SEED SCIENCE Lab.)

[MIS22-P02] No mechanism to expand Space! Big Bang hypothesis has 't been proven!
Red-shift can be explained by New stationary space theory based on Quantum Red-Shift. Neither black holes nor Dark matter are required. Validated by Abuduction

★Invited Papers

*Akira Taneko[1] (1.SEED SCIENCE Lab.)

[J] Poster | M (Multidisciplinary and Interdisciplinary)：M-IS Intersection

[M-IS23] Interface- and nano-phenomena on crystal growth and dissolution

convener:Yuki Kimura(Institute of Low Temperature Science, Hokkaido University), Hitoshi Miura(Graduate School of Natural Sciences, Department of Information and Basic Science, Nagoya City University), Hisao Satoh(Low-Level Radioactive Waste Disposal Center, Japan Nuclear Fuel Limited)

[MIS23-P01] A new theory of impurity incorporation into a growing crystal

*Hitoshi Miura[1] (1.Graduate School of Natural Sciences, Department of Information and Basic Science, Nagoya City University)

[MIS23-P02] Homogeneous nucleation of iron from saturated vapor by molecular dynamics simulation

*Kyoko Kitakami Tanaka[1,2] (1.Tohoku University, 2.Nihon University)

[MIS23-P03] Homogeneous nucleation of silicate nanoparticles in a microgravity environment using a sounding rocket

*Yuki Kimura[1], Joseph A Nuth[3], Frank Ferguson[4], Yuko Inatomi[2] (1.Institute of Low Temperature Science, Hokkaido University, 2.JAXA/ISAS, 3.NASA's Goddard Space Flight Center, 4.Catholic Univ. America at NASA's Solar System Exploration Division)

[MIS23-P04] Preparation for nucleation experiment of ice nanoparticles by the low-temperature gas evaporation method

*Yuki Kimura[1], Akira Kouchi[1] (1.Institute of Low Temperature Science, Hokkaido University)

[MIS23-P05] Growth of ice crystals via quasi-liquid layers: Effect of nitric acid gas

*Ken Nagashima[1], Josée Maurais[2], Ken-ichiro Murata[1], Yoshinori Furukawa[1], Patrick Ayotte[2], Gen Sazaki[1] (1.The Institute of Low Temperature Science, Hokkaido University, 2.Université de Sherbrooke, Québec, Canada)

[MIS23-P06] Radiolysis-induced crystallization process of salt in liquid cell transmission electron microscopy

*Tomoya Yamazaki[1], Yuki Kimura[1] (1.Institute of Low Temperature Science Hokkkaido University)

[MIS23-P07] Pore space property of clay in the forms of gelled and compacted

*Hisao Satoh[1], Yuki Araki[2], Ken Nagashima[3] (1.Naka Energy Research Laboratory, Mitsubishi Materials Corporation, 2.Department of Physical Sciences, College of Science and Engineering, Ritsumeikan University, 3.The Institute of Low Temperature Science, Hokkaido University)

[MIS23-P08] **Growth of SrB_4O_7 crystal fibers with near stoichiometric composition by the micro-pulling-down method**

*Harutoshi Asakawa[1], Takaaki Machida[1], Sho Inaba[1], Yu-ki Hamada[1], Hiroshi Uneda[1], Ryuichi Komatsu[1], Arashi Kitakaze[1] (1.Graduate School of Sciences and Technology for Innovation Yamaguchi University)

[MIS23-P09] Thermodynamic stability of norsethite $BaMg(CO_3)_2$ under hydrothermal conditions

*Koki Suga[1], Harutoshi Asakawa[1], Hiroshi Uneda[1], Itaru Echigo[1], Kaoru Isobe[1], Ryuichi Komatsu[1] (1.Graduate School of Sciences and Technology for Innovation Yamaguchi University)

[J] Poster | M (Multidisciplinary and Interdisciplinary)：M-IS Intersection

[M-IS24] Mountain Science

convener:Keisuke Suzuki(Research Center for Mountain Environment, Shinshu University), Yoshihiko Kariya(Department of Environmental Geography, Senshu University), Akihiko SASAKI(Department of Geography and Environmental Studies, Kokushikan University), Chiyuki Narama(Niigata University, Department of Science)

[MIS24-P01] Large-scale landslide immediately occurred at the fallout of Aira-Tn tephra (31 cal ka BP) in the northern Tenshu Mountains, central Japan

*Keiju Kimura[1], Yoshihiko Kariya[2] (1.Undergraduate Senshu University, 2.Senshu University)

[MIS24-P02] The effects of temporal continuity of grasslands on plant- and butterfly- communities

*Taiki INOUE[1], Yuki Yaida[2], Yuki Yaida[2], Koki Katsuhara[2], Keiko Takashima[2], Takeharu Seki[1], Yuka Yamamoto[1], Atsushi Ushimaru[2], Tanaka Kenta[1] (1.University of Tsukuba, 2.Kobe University)

[MIS24-P05] Clarification of cause of temporal tracer variations in spring water, Kamikochi, Shinshu

*Yoshitake Nagahata[1], Koichi Sakakibara[1], Keisuke Suzuki[1] (1.Shinshu University)

[MIS24-P06] Hydraulic connectivity between groundwater and surface water in Suwa region, Japan

*Mizuki Hori[1], Koichi Sakakibara[1], Yuichi Miyabara[1], Keisuke Suzuki[1] (1.Shinshu University)

[MIS24-P07] Development of a high-resolution prediction model for spatio-temporal dynamics of snowmelt using time-lapse camera images at west side of Mt. Tateyama

*Reiko Ide[1], Ryotaro Okamoto[2], Hiroyuki Oguma[1], Wataru Shimada[3], Kazuma Aoki[3] (1.National Institute for Environmental Studies, 2.University of Tsukuba , 3.University of Toyama)

[MIS24-P08] Factor that results in a decrease in snow surface albedo that promotes snow melting in the Kamikochi, Taisyoike

*Miu Otsuka[1], Keisuke Suzuki[1], Motoshi NISHIMURA[2] (1.Faculty of Science, SHINSHU UNIVERSITY, 2. Interdisciplinary Graduate School of Science and Technology ,SHINSHU UNIVERSITY)

[MIS24-P09] Spatiotemporal variations in stable isotope ratios of precipitation in the Japanese Alps Region

*Tsukasa Katsuragawa[1], Tsutomu Yamanaka[2], Akihiko SASAKI[3], Yuki Kurokumo[1], Motoshi NISHIMURA[1], Shimizu Hironori[1], Keisuke Suzuki[4] (1.Graduate School of Science and Technology,Shinshu University, 2.Faculty of Life and Environmental Sciences, University of Tsukuba, 3.Kokushikan University, 4.Shinshu University)

[MIS24-P11] Variation of snow in the Japanese Alps

*Keisuke Suzuki[1] (1.Research Center for Mountain Environment, Shinshu University)

[J] Poster | M (Multidisciplinary and Interdisciplinary)：M-IS Intersection

[M-IS25] Biogeochemistry

convener:Keisuke Koba(Center for Ecological Research, Kyoto University), Hideaki Shibata(Field Science Center fot Northern Biosphere, Hokkaido University), Naohiko Ohkouchi(Japan Agency for Marine-Earth Science and Technology), Youhei Yamashita(Faculty of Environmental Earth Science, Hokkaido University)

[MIS25-P01] Model estimation of natural terrestrial methane emission and their stable carbon isotope ratio at broad scale

*Akihiko Ito[1] (1.National Institute for Environmental Studies)

[MIS25-P02] In-situ determination of denitrification, assimilation, and nitrification rates in urban streams

*Fumiko Nakagawa[1], Kensuke Suzuki[1], Masanori Ito[1], Urumu Tsunogai[1] (1.Graduate School of Environmental Studies, Nagoya University)

[MIS25-P03] Are sediment-derived long-chain *n*-alkanes a reliable paleoenvironmental indicator?

*Vijayananda Sarangi[1], Prasanta Sanyal[1] (1.Indian Institute of Science Education and Research Kolkata)

[MIS25-P04] Nitrate contamination of mountainous headwater streams from adjacent agricultural and pasture lands beyond the watershed boundary in eastern Hokkaido, Japan

*Keitaro Fukushima[1], Kenta Iwasaki[2], Yoshiya Oda[3], Masaru Sakai[4], Yuji Onishi[1], Keisuke Koba[1], Genki Katata[5], Takashi Yamaguchi[2], Tomohiro Kubota[5], Hirohiko Nagano[6], Makoto Watanabe[7], Jun Koarashi[6] (1.Kyoto University, 2.Hokkaido Research Organization, 3.Tokyo Metropolitan University, 4.Chuo University, 5.Ibaraki University, 6.Japan Atomic Energy Agency, 7.Tokyo University of Agriculture and Technology)

[MIS25-P05] Stable carbon and nitrogen isotope analysis of bacterial nucleic acid

*Yuji Onishi[1], Keitaro Fukushima[1], Keisuke Koba[1] (1.Center for Ecological Research, Kyoto University)

[MIS25-P06] Individual specificity of feeding habit analyzed by stable isotope in a group of Japanese macaque.

*Kazuho Funakawa[1], Keisuke Koba[1] (1.Kyoto University)

[MIS25-P07] Geological, anthropogenic and tidal effects for stream water chemistry of the Yoshinogawa river systems in the Shikoku region

*Yoriko Yokoo[1], Saki Nagayama[1], Tomohiro Yoshida[1], Ryo Anma[2] (1.Faculty of Science and Engineering, Doshisha University, 2.Graduate School of Technology, Industrial and Social Sciences, Tokushima University)

[MIS25-P08] Biogeochemistry and benthic community structure of volcanic stream ecosystems in northern Japan

*Kazuki Marumo[1], Tomoya Iwata[1], Kokichi Aoya, Kazumi Tanida[2], Satoko Noda[1], Nozomi Kasai[1], Masahiro Yuki[3] (1.University of Yamanashi, 2.Osaka Museum of Natural History, 3.RIKEN)

[MIS25-P09] Determine of host-parasitic relationship of freshwater parasites using stable isotope analysis

*Kei Kinoshita[1], Keitaro Fukushima[1], Yuji Onishi[1], Keisuke Koba[1] (1.Department of biology, Graduate School of Science, Kyoto University)

[MIS25-P10] **Variation among carbon isotopes of plants growing in mixed evergreen-deciduous ecosystem.**

*AKANKSHA RAI[1], Biswajit Roy[1], Padmasini Behera[1], Prasanta Sanyal[1] (1.INDIAN INSTITUTE OF SCIENCE EDUCATION AND RESEARCH KOLKATA)

[MIS25-P11] Effect of watershed-scale practical forest management on nitrogen leaching in a cool-temperate natural forest in northern Japan

*Karibu Fukuzawa[1] (1.Field Science Center for Northern Biosphere, Hokkaido University)

[MIS25-P12] Interaction between marine bacterial community and dissolved organic matter released by pelagic phytoplankton

*Yuya Tada[1], Koji Suzuki[2], Youhei Yamashita[2] (1. National Institute For Minamata Disease, 2.Hokkaido Univ.)

[MIS25-P13] Relationship of N_2O emission and environmental factor between different vegetation in a cool temperature

*Miwako Nagane[1], Hideaki Shibata[2], Yoshitaka Uchida[3], Ryunosuke Tateno[4], Atsuko Sugimoto[5] (1.Graduate school if Environmental Science, Hokkaido University, 2.Field Science Center for Northern Biosphere, Hokkaido University, 3.Faculty of Agriculture, Hokkaido University, 4.Field Science Education and Research Center, Kyoto University, 5.Arctic Research Center, Hokkaido University)

[J] Poster | M (Multidisciplinary and Interdisciplinary)：M-IS Intersection

[M-IS26] Electromagnetic phenomena associated with seismic and volcanic activities

convener:Tetsuya Kodama(Research Unit I, Research and Development Directorate, Japan Space Exploration Agency), Toshiyasu Nagao(Institute of Oceanic Research and development, Tokai University)

[MIS26-P01] An internal/external separation of Sq geomagnetic daily variation on quiet days in January 2011 around Japan

*Tsutomu Ogawa[1] (1.Earthquake Research Institute, the University of Tokyo)

[MIS26-P03] **3D-Tomography of the Ionospheric Anomalies Immediately Before and After the 2011 Tohoku-oki (M_W9.0) Earthquake**

*Ihsan Naufal Muafiry[1,2], Kosuke Heki[1] (1.Hokkaido University, Japan, 2.Universitas Esa Unggul, Indonesia)

[J] Poster | M (Multidisciplinary and Interdisciplinary)：M-IS Intersection

[M-IS27] Geophysical fluid dynamics-Transfield approach to geoscience

convener:Keita Iga(Atmosphere and Ocean Research Institute, The University of Tokyo), Shigeo Yoshida(Department of Earth and Planetary Sciences, Faculty of Sciences, Kyushu University), Takatoshi Yanagisawa(Research Institute for Marine Geodynamics, Japan Agency for Marine-Earth Science and Technology), Hidenori AIKI(Nagoya University)

[MIS27-P01] Transient flow states during convective spin-up

*Daisuke Noto[1], Yuji Tasaka[2], Takatoshi Yanagisawa[3,2], Takehiro Miyagoshi[3], Yuichi Murai[2] (1.Graduate School of Engineering, Hokkaido University, 2.Faculty of Engineering, Hokkaido University, 3.Japan Agency for Marine-Earth Science and Technology (JAMSTEC))

[MIS27-P02] Axial flow characteristics of a liquid metal roll convection under a horizontal magnetic field

Koki Sawada[1], *Yuji Tasaka[1], Takatoshi Yanagisawa[2,1], Yuichi Murai[1], Ataru Sakuraba[3] (1.Faculty of Engineering, Hokkaido University, 2.Japan Agency for Marine-Earth Science and Technology, 3.Department of Earth and Planetary Science, University of Tokyo)

[MIS27-P03] Influence of side-wall Hartmann braking in a liquid metal convection under a horizontal magnetic field

*Takatoshi Yanagisawa[1], Koki Sawada[2], Yuji Tasaka[2], Takehiro Miyagoshi[3], Ataru Sakuraba[4] (1.Research Institute for Marine Geodynamics, Japan Agency for Marine-Earth Science and Technology, 2.Faculty of Engineering, Hokkaido University, 3.Research Institute for Value-Added-Information Generation, Japan Agency for Marine-Earth Science and Technology, 4.Faculty of Science, University of Tokyo)

[MIS27-P04] Shallow water MHD waves trapped in the polar regions on a rotating sphere with an imposed azimuthal magnetic field

*Ryosuke Nakashima[1], Shigeo Yoshida[2] (1.Faculty of Sciences, Kyushu University, 2.Department of Earth and Planetary Sciences, Faculty of Science, Kyushu University)

[MIS27-P05] Sporadic low salinity signals in the oceanic mixed layer observed by the Kuroshio Extension Observatory buoy

Kohei Kameyama[1], *Hidenori AIKI[1], Yuki Kanno[1], Shun Ohishi[2], Hiroyuki Tomita[1], Fukutomi Yoshiki[1] (1.Nagoya University, 2.RIKEN)

[MIS27-P06] Laboratory experiments of vortices and internal waves around oscillating rectangular cylinder in a stratified viscous fluid

*Tatsuo Motoi[1], Shigenori Murakami [1], Nobuyuki Kinoshita[1], Mitsuo Ohizumi[1], Teruyuki Kato[1] (1.Meteorological College)

[MIS27-P07] Resonance between waves propagating on the flow in a cylindrical tank with a rotating bottom

*Keita Iga[1] (1.Atmosphere and Ocean Research Institute, The University of Tokyo)

[MIS27-P08] About the collapse of a huge ice sheet lake on the Laurentide ice sheet.

*SHOUJI Yoshinori

[J] Poster | M (Multidisciplinary and Interdisciplinary)：M-IS Intersection

[M-IS28] History X Earth and Planetary Science

convener:Yasuyuki Kano(Earthquake Research Institute, The University of Tokyo), Hiroaki Isobe(Faculty of Fine Arts, Kyoto City University of Arts), Kei Yoshimura(Institute of Industrial Science, The University of Tokyo), kiyomi iwahashi(National Institute of Japanese Literature)

[MIS28-P01] Recompilation of online data for historical earthquake studies

*Yasuyuki Kano[1] (1.Earthquake Research Institute, The University of Tokyo)

[MIS28-P02] Estimation of the rice production in the early 20th century of China: its explanation and impact in both hydrological and historical ways

★Invited Papers

*CHANG LIU[1], Akiyuki KAWASAKI[1], Tomoko SHIROYAMA[2] (1.Department of Civil Engineering, The University of Tokyo, 2.Graduate School of Economics, The University of Tokyo)

[MIS28-P03] Historical flood disaster in the southern area of Gunma Prefecture infered from the memorial monuments of flood

*Masafumi Aoyama[1] (1.Faculty of Education, Gunma University)

[MIS28-P04] Consideration on problems and classification methods of "Disaster Monument"

*Junzo Ohmura[1] (1.Earthquake Research Institute,The University of Tokyo)

[MIS28-P05] Atmospheric data assimilation which accomodates weather descriptions as observations of solar radiation: Evaluation of performance with a modern one-year case

*Kooiti Masuda[1], Panduka Neluwala[2], Kinya Toride[4,3], Kei Yoshimura[3], Hidenori Tanaka[5], Sho Miyazaki[5], Satoshi Nozawa[5], Mika Ichino[6], Yu Okubo[7,8], Junpei Hirano[7] (1.Department of Geography, Tokyo Metropolitan University, 2.Department of Civil Engineering, University of Peradeniya, 3.Institue of Industrial Science, University of Tokyo, 4.Department of Atmospheric Sciences, University of Washington, 5.Department of Earth Science, College of Science, Ibaraki University, 6.ROIS-DS Center for Open Data in the Humanities, 7.Department of History, Teikyo University, 8.Department of Geography, Senshu University)

[MIS28-P06] Application of Observational Seismology to Historical Seismology (1) A pilot seismic observations in the suburbs to investigate regional variations in seismic intensity from the 1855 Ansei Edo-Earthquake

*Motoko Ishise[1], Ryoichi Nakamura[1], Tomoya Harada[1], Takashi Iidaka[1], Shigeki Nakagawa[1], Ayakia Saiki[1], Kazuhito Hikima[2], Shin'ichi Sakai[1] (1.Earthquake Reseach Institute, University of Tokyo, 2.Tokyo Electric Power Company Holdings, Inc.)

[MIS28-P07] Sunspot Observation before 1945 in Nagashima Aiseien

*Harufumi Tamazawa[1], Hiroaki Isobe[1] (1.Kyoto City University of Arts)

[MIS28-P08] A Linkage between climatic condition and market economy in the 19th century Japan - Analysis of solar radiation from historical documents and rice price -

*Mika Ichino[1], Kooiti Masuda[2], Takehiko Mikami[2], Yasuo Takatsuki[3] (1.Center for Open Data in the Humanities, Joint Support-Center for Data Science Research, Research Organization of Information and Systems , 2.Tokyo Metropolitan University, 3.Research Institute for Economics and Business Administration, Kobe University)

[MIS28-P09] Discovery of Original Material of Nakamura Nakazo's Account on the 1855 Ansei Edo Earthquake

*Ryoichi Nakamura[1], Motoko Ishise[1], Reiko Sugimori[2,3], Kenji Satake[1,3] (1.Earthquake Research Institute, The University of Tokyo, 2.Historiographical Institute, The University of Tokyo, 3.Collaborative Research Organization for Historical Materials on Earthquakes and Volcanoes)

[MIS28-P10] Comparison between interannual variation of snowfall frequency in Nagasaki and 20th century reanalysis data from 1836 to 1868

*Junpei Hirano[1], Takehiko Mikami[2], Masumi Zaiki[3], Mika Ichino[4] (1.Teikyo University, 2.Tokyo Metropolitan University, 3.Seikei University, 4.Center for Open Data in the Humanities)

[MIS28-P11] Attempt to restore the forest cover in China's planned economic period using declassified American and Soviet reconnaissance information: A case of Northern Shaanxi Loess Plateau
★Invited Papers

*Yuta Hara[1] (1.Komaba Organization for Educational Excellence, College of Arts and Sciences, The University of Tokyo)

[MIS28-P12] Philological and scientific assessment of aurora records in historical documents

*Hiroaki Isobe[1], kiyomi iwahashi[2], Harufumi Tamazawa[1] (1.Faculty of Fine Arts, Kyoto City University of Arts, 2.National Institute of Japanese Literature)

[J] Poster | M (Multidisciplinary and Interdisciplinary) : M-IS Intersection

[M-IS29] Mud volcano x Chemosynthetic communities

convener:Yusuke Miyajima(Geomicrobiology Research Group, Research Institute for Geo-Resources and Environment, Geological Survey of Japan, National Institute of Advanced Industrial Science and Technology), Tomohiro Toki(Faculty of Science, University of the Ryukyus), Robert Jenkins(School of Geosciences and Civil Engineering, College of Science and Engineering, Kanazawa University), Akira Ijiri(Japan Agency for Marine-Earth Science and Technology)

[MIS29-P01] Characteristics and origin of sediments collected from mud volcanos off Tanegashima

Ryoma Setoguchi[1], *Masafumi MURAYAMA[1], Akira Ijiri[2], Juichiro Ashi[3], Takeyasu Yamagata[4], Hiroyuki Matsuzaki[4] (1.Faculty of Agriculture and Marine Science, Kochi University, 2.Kochi Institute for Core Sample Research, JAMSTEC, 3.The Atmosphere and Ocean Research Institute, The University of Tokyo , 4.The University Museum,The University of Tokyo)

[MIS29-P02] An *in situ* rapid burial experiment of "*Calyptogena*" clams for decoding history of submarine mud volcano activities

*Takami Nobuhara[1] (1.Shizuoka Univ. (Fac. Educ.))

[MIS29-P03] Community compositions in Late Cretaceous methane-seeps in the Nakagawa area, Hokkaido

So Watanabe[2], *Robert Jenkins[1] (1.School of Geosciences and Civil Engineering, College of Science and Engineering, Kanazawa University, 2.Graduate School of Natural Science and Technology, Kanazawa University)

[MIS29-P04] Estimated and realized dispersal potentials in deep-sea chemosynthesis-based communities: the case of a Pacific galatheid crab

*Hiromi Kayama WATANABE[1], Satoshi Mitarai[2], Chen Chong[1], Hiroyuki Yamamoto[1] (1.Japan Agency for Marine-Earth Science and Technology (JAMSTEC), 2.Okinawa Institute of Science and Technology (OIST))

[J] Poster | M (Multidisciplinary and Interdisciplinary)：M-IS Intersection

[M-IS30] Ocean Plastics, an earth science perspective

convener:Atsuhiko Isobe(Research Institute for Applied Mechanics, Kyushu University), Kiichiro Kawamura(Yamaguchi University), Yusuke Okazaki(Department of Earth and Planetary Sciences, Graduate School of Science, Kyushu University), Masashi Tsuchiya(Research Institute for Global Change, Japan Agency for Marine-Earth Science and Technology)

[MIS30-P01] A numerical approach to determining the behavior of microplastics and mesoplastics from the Changjiang River in the East Asian marginal seas

*Iwasaki Shinsuke[1] (1.Civil Engineering Research Institute for Cold Region of Public Works Research Institute)

[MIS30-P02] The horizontal distribution of pelagic microplastics around Japan

*Daisuke Ito[1], Atsuhiko Isobe[2] (1.Kyushu University, 2.Research Institute for Applied Mechanics, Kyushu University)

[MIS30-P03] Foraminiferal thamatocoenosis as a tracer of the sorting process in the coastal surf zone

*Hiroki Hayashi[1], Masashi Tsuchiya[2] (1.Interdisciplinary Faculty of Science and Engineering, Shimane University, 2.Japan Agency For Marine-Earth Science and Technology)

[MIS30-P04] Microplastics in the river bottom sediment in the urban river of Mongolia

*Masayuki Kawahigashi[1], Batdulam Battulga[1] (1.Tokyo Metropolitan University)

[MIS30-P05] Detection of microplastics less than 330 μm using μFTIR

*HARUKA NAKANO[1], Ridvan Kaan Gürses[1], Yuji Tanaka[1], Hisayuki Arakawa[1], Mao Kuroda[1], Keiichi Uchida[1], Tetsutaro Aikawa[1], Toshifumi Hayashi[1], Tadashi Tokai[1] (1.Tokyo University of Marine Science and Technology)

[MIS30-P06] Fundanmental parameters for detection of Microplastics based on hyperspectral imaging

*Chunmao Zhu[1], Yugo Kanaya[1], Ryota Nakajima[1], Masashi Tsuchiya[1], Hidetaka Nomaki[1], Tomo Kitahashi[1], Katsunori Fujikura[1] (1.Japan Agency for Marine-Earth Science and Technology)

[MIS30-P07] Time-course analysis of gene expression of a benthic protist during exposure to titanium dioxide nanoscale particles.

*Yoshiyuki Ishitani[1], Yurika Ujiie[2], Caterina Ciacci[3], Frontalini Fabrizio[3], Yuji Inagaki[1] (1.University of Tsukuba, 2.Center for Advanced Marine Core Research, Kochi University, 3.Urbino University)

[MIS30-P08] Spatial distribution of microplastics in Shimane Peninsula, Japan

*Akira Tsujimoto[1], Kana Yamaguchi[1] (1.Faculty of Education, Shimane University)

[J] Poster | M (Multidisciplinary and Interdisciplinary)：M-IS Intersection

[M-IS31] Planetary Volcanology

convener:Rina Noguchi(Institute of Space and Astronautical Science, Japan Aerospace Exploration Agency), Tomokatsu Morota(Department of Earth and Planetary Science, The University of Tokyo), Nobuo Geshi(Geological Survey of Japan, The National Institute of Advanced Industrial Science and Technology)

[MIS31-P01] Study of the lava flow under the Marius Hills Hole on the Moon by analogy on the Earth

*Tsutomu Honda[1] (1.Vulcano-speleological Society)

[MIS31-P02] Machine learning for grain images of volcanic ash based on grain shape and transparency

*Rina Noguchi[1], Takuya Itaki[2], Daigo Shoji[3], Shizuka Otsuki[4] (1.Institute of Space and Astronautical Science, Japan Aerospace Exploration Agency, 2.Geological Survey of Japan, AIST, 3.Earth-Life Science Institute, Tokyo Institute of Technology, 4.Nippon Steel Technology Co., Ltd.)

[MIS31-P03] Relation between volcanism on Jupiter moon Io and the atmosphere and plasma torus observed by ALMA and Hisaki

*Ryoichi Koga[1], Yasuhiro Hirahara[2], Tatsuya Suzuki[2], Fuminori Tsuchiya[1], Masato Kagitani[1], Takeshi Sakanoi[1], Tomoki Kimura[1], Ichiro Yoshikawa[3], Kazuo Yoshioka[3], Go Murakami[4], Atsushi Yamazaki[4] (1.Tohoku University, 2.Nagoya University, 3.The University of Tokyo, 4.ISAS/JAXA)

[J] Poster | M (Multidisciplinary and Interdisciplinary)：M-IS Intersection

[M-IS32] Gas hydrate in environmental-resource sciences

convener:Hitoshi Tomaru(Department of Earth Sciences, Chiba University), Akihiro Hachikubo(Kitami Institute of Technology), Shusaku Goto(Institute for Geo-Resources and Environment National Institute of Advanced Industrial Science and Technology), Atsushi Tani(Department of Human Environmental Science, Graduate School of Human Development and Environment, Kobe University)

[MIS32-P01] Bacterial Clathrate-Binding Proteins Alter Gas Clathrate Morphology

*Jennifer B Glass[1], Abigail M. Johnson[1], Dustin J.E. Huard[1], Jongchan Kim[1], Priyam Raut[1], Anton S. Petrov[1], Loren Dean Williams[1], Sheng Dai[1], Raquel L. Lieberman[1] (1.Georgia Institute of Technology Main Campus)

[MIS32-P02] Gas hydrate survey at the gas seepage area off Rebun Island, Japan Sea

*Yunosuke Hase[1], Akihiro Hachikubo[1], Satoshi Yamashita[1], Hirotoshi Sakagami[1], Masaaki Konishi[1], Hirotsugu Minami[1], Kenji Nishina[2], Tadashi Misaka[3] (1.Kitami Institute of Technology, 2.Geological Survey of Hokkaido, Hokkaido Research Organization, 3.Wakkanai Fisheries Research Institute, Hokkaido Research Organization)

[MIS32-P03] Total organic carbon in subsurface sediment off Abashiri, the Sea of Okhotsk

*daisuke yahagi[1], Akihiro Hachikubo[1], Masaaki Konishi[1], Hirotoshi Sakagami[1], Hirotsugu Minami[1], Satoshi Yamashita[1], Kenji Nishina[2], Yasuhito Uchida[2], Kenji Sakaguchi[3] (1.kitami institute of technology, 2.Geological Survey of Hokkaido, Hokkaido Research Organization, 3.Kushiro Fisheries Research Institute, Hokkaido Research Organization)

[MIS32-P04] Characteristics of gas in shallow sediments from seepage field off Tokachi (the Pacific Ocean)

*Hiromi Kimura[1], Yunosuke Hase[1], Yuki Ikeura[1], Ryoya Kamata[1], Akihiro Hachikubo[1], Masaaki Konishi[1], Hirotoshi Sakagami[1], Hirotsugu Minami[1], Satoshi Yamashita[1] (1.Kitami Institute of Technology)

[MIS32-P05] Geochemistry of pore water and headspace gas in the Tatar Trough

*Musashi Yokoyama[1], Hitoshi Tomaru[1], Ryo Matsumoto[2], Glen Snyder[2], A.V. Yatsuk[3], Shvalov D.A.[3] (1.Chiba University, 2.Meiji University, 3.Gas Geochemistry Laboratory, V.I.Ilichev Pacific Oceanological Institude)

[MIS32-P06] Characteristics of methane hydrate fields in the southwestern margin of the Yamato Basin, southern Japan Sea

*Naoto Ishida[1], Hidefumi Fujioka[2], Hitoshi Tomaru[3], Takao Ebinuma[1], Ryo Matsumoto[4] (1.Social Systems and Civil Engineering, Graduate School of Engineering, Tottori University, 2.Tottori Prefectural Fisheries Experiment Station, 3.Department of Sciences, Chiba University, 4.Gas hydrate Labratory, Meiji University)

[MIS32-P07] Origin of methane in gas hydrate field, Hikurangi Subduction Margin: application of geochronological method using a long-lived radioisotope of iodine

*Satoko Owari[1], Hitoshi Tomaru[2] (1.Tokyo University of Marine Science and Technology, 2.Chiba University)

[MIS32-P08] Observation of hydrogen transfer reactions via radical species in chibaite

*Yuka Yokoyama[1], Shusuke Isogai[1], Kenta Kusuki[1], Hirotsugu Nishido[2], Atsushi Tani[1] (1.Graduate School of Human Development and Environment, Kobe University, 2.Faculty of Biosphere-Geosphere Science, Okayama University of Science)

[MIS32-P09] Investigation on thermal stability of radical species in chibaite

*Shusuke Isogai[1], Yuka Yokoyama[1], Kenta Kusuki[1], Hirotsugu Nishido[2], Atsushi Tani[1] (1.Graduate School of Human Development and Environment, Kobe University, 2.Faculty of Biosphere-Geosphere Science, Okayama University of Science)

[MIS32-P10] Experimental study on the phase equilibrium condition of carbon dioxide hydrate with sediments

*Tatsuki Iwamoto[1] (1.Chiba University)

[MIS32-P11] Formation of gas hydrates composed of methane and helium

*Hiromi Kimura[1], Shota Shirakura[1], Akihiro Hachikubo[1], Satoshi Takeya[2] (1.Kitami Institute of Technology, 2.National Institute of Advanced Industrial Science and Technology (AIST))

[MIS32-P12] Direct measurement of hydration number of gas hydrates

*RYOYA KAMATA[1], Hiromi Kimura[1], Emi Sugimori[1], Akihiro Hachikubo[1], Satoshi Takeya[2] (1.Kitami Institute Of Technology, 2.National Institute of Advanced Industrial Science and Technology (AIST))

[MIS32-P13] Effect of salinity on self-preservation effect of mixed gas hydrate

*Yunosuke Hase[1], Hiromi Kimura[1], Akihiro Hachikubo[1], Satoshi Takeya[2] (1.Kitami Institute of Technology, 2.National Institute of Advanced Industrial Science and Technology (AIST))

[MIS32-P14] Making of large scale ice block simulating shallow type methane hydrate for performance confirmation of submarine drilling rig

*yuya ono[1], Satoshi Yamashita[2], shunsuke Iwamoto[3], kouzi Mochiduki[3] (1.KITAMI Institute of Teclhnology, graduate school, 2.KITAMI Institute of Technology, 3.Mitsui E&S Shipbuilding Co., Ltd)

[J] Poster | M (Multidisciplinary and Interdisciplinary)：M-GI General Geosciences, Information Geosciences & Simulations

[M-GI39] Data-driven geosciences

convener:Tatsu Kuwatani(Japan Agency for Marine-Earth Science and Technology), Hiromichi Nagao(Earthquake Research Institute, The University of Tokyo), Kenta Ueki(Japan Agency for Marine-Earth Science and Technology), Shin-ichi Ito(The University of Tokyo)

[MGI39-P01] Global Seismicity Dynamics – Synchronicity in Correlated Seismicity of Global Subduction and Ridge Zone

*mitsuhiro toriumi[1] (1.Japan agency of marine science and technology)

[MGI39-P02] Forward modeling and inversion analysis for geochemical-process extraction: an application to chemical compositions of surface soils in Ibaraki Prefecture, Japan

*Tatsu Kuwatani[1], Kengo Nakamura[2], Shotaro Akaho[3], Takeshi Komai[2] (1.Japan Agency for Marine-Earth Science and Technology (JAMSTEC), 2.Tohoku University, 3.National Institute of Advanced Industrial Science and Technology (AIST),)

[MGI39-P03] Geochemical characteristics of Japan Arc basements from the geochemical database, and origin of these characteristics

*Satoru Haraguchi[1], Kenta Ueki[2], Hikaru Iwamori[1] (1.Earthquake Research Institute, University of Tokyo, 2.Japan Agency for Marine-Earth Science and Technology)

[MGI39-P04] **Estimation of mass transfer and protolith composition for mafic metamorphic rocks using machine learning**

*Matsuno Satoshi[1], Masaoki Uno[1], Atsushi Okamoto[1], Noriyoshi Tsuchiya[1] (1.Tohoku University)

[MGI39-P05] Numerical Evaluation of geochemical discrimination of tsunami deposits by HCA(Hierarchical Clustering Analysis)

*Satoh Kenta[1], Noriyoshi Tsuchiya[1] (1.Graduate school of environmental studies)

[MGI39-P06] **Characterization of permeability based on topological data of fracture network**

*Anna Suzuki[1], Miyuki Miyazawa[1], James Minto[2], Takeshi Tsuji[3], Takatoshi Ito[1] (1.Tohoku Univ., 2.Univ. of Strathclyde, 3.Kyushu Univ.)

[MGI39-P07] Bayesian Data-driven Approach for Extracting Nonlinear Dynamics of Heterogeneous Reactions

*MASAKI ITO[1], Tatsu Kuwatani[2], Ryosuke Oyanagi[2], Toshiaki Omori[1] (1.Kobe University, 2.JAMSTEC)

[MGI39-P08] Super-resolution for seafloor topography using deep convolutoinal neural networks

*Mitsuko Hidaka[1], Daisuke Matsuoka[1], Tatsu Kuwatani[1], Yukari Kido[1], Junji Kaneko[1], Takafumi Kasaya[1], Eiichi Kikawa[1] (1.Japan Agency for Marine-Earth Science and Technology)

[MGI39-P09] Detection of hydrothermal alteration zones distribution by applying linear unmixing method to hyperspectral satellite imagery for densely vegetated geothermal area

*Hiroaki Gonnokami[1], Taiki Kubo[1], Arie Naftali Hawu Hede[2], Asep Saepuloh[2], Katsuaki Koike[1] (1.Laboratory of Environmental Geosphere Engineering, Department of Urban Management, Graduate School of Engineering, Kyoto University, 2.Bandung Institute of Technology)

[J] Poster | M (Multidisciplinary and Interdisciplinary)：M-GI General Geosciences, Information Geosciences & Simulations

[M-GI40] Development of computational sciences on planetary formation, evolution and surface environment

convener:Yoshi-Yuki Hayashi(Department of Planetology/CPS, Graduate School of Science, Kobe University), Masaki Ogawa(Division of General Systems Studies, Graduate School of Arts and Sciences, University of Tokyo), Shigeru Ida(Earth-Life Science Institute, Tokyo Institute of Technology), Kanya Kusano(Institute for Space-Earth Environmental Research, Nagoya University)

[MGI40-P01] A study on numerical accuracy of atmospheric dynamical cores necessary for large eddy simulations

*Yuta Kawai[1], Hirofumi Tomita[1] (1.RIKEN Center for Computational Science)

[MGI40-P02] Surface zonal flows induced by anelastic thermal convection in a rapidly rotating spherical shell

*Youhei SASAKI[1], Shin-ichi Takehiro[2], Keiichi Ishioka[3], Takeshi Enomoto[4] (1.Institute of Fundamental Sciences, Faculity of Science and Engineering, Setsunan University, 2.Research Institute for Mathematical Sciences, Kyoto University, 3.Department of Earth and Planetary Sciences, Kyoto University, 4.Disaster Prevention Research Institute, Kyoto University)

[MGI40-P03] Local node refinement using the Schmidt transform for RBF advection models

*Koji Ogasawara[1], Takeshi Enomoto[2] (1.Graduate School of Science, Kyoto University, 2.Disaster Prevention Research Institute, Kyoto University)

[MGI40-P04] Evolution of orbits of Trans Neptunian Objects in the Galactic Potential

*Yoko Funato[1] (1.University of Tokyo)

[J] Poster | M (Multidisciplinary and Interdisciplinary)：M-GI General Geosciences, Information Geosciences & Simulations

[M-GI41] Earth and planetary informatics with huge data management

convener:Ken T. Murata(National Institute of Information and Communications Technology), Rie Honda(Department of Science and Technology, System of Natual Science, Kochi University), Susumu Nonogaki(Geological Survey of Japan, National Institute of Advanced Industrial Science and Technology), Takeshi Horinouchi(Faculty of Environmental Earth Science, Hokkaido University)

[MGI41-P01] Himawari Data Transfer to Asian Countries

*Praphan Pavarangkoon[1], Ken T. Murata[1], Kazunori Yamamoto[1], Atsushi Higuchi[2], Takamichi Mizuhara[3], Yuya Kagebayashi[3], Ayahiro Takaki[3], Kazuya Muranaga[4], Chalermpol Charnsripinyo[5], Bayani Benjamin R. Lara[6], Joel Joseph S. Marciano, Jr.[6], Eric Yen[7], Simon C. Lin[7], Keiichiro Fukazawa[8] (1.National Institute of Information and Communications Technology, Japan, 2.Center for Environmental Remote Sensing, Chiba University, Japan, 3.CLEALINK TECHNOLOGY Co., Ltd., Japan, 4.Systems Engineering Consultants Co., Ltd., Japan, 5.National Electronic and Computer Technology Center, Thailand, 6.Advanced Science and Technology Institute, Department of Science and Technology, Philippines, 7.Academia Sinica Grid Computing Centre, Taiwan, 8.Academic Center for Computing and Media Studies, Kyoto University, Japan)

[MGI41-P02] An Initial Report of StarBED for HpFP Development

*Praphan Pavarangkoon[1], Ken T. Murata[1], Tsubasa Yumura[1], Kazunori Yamamoto[1], Takamichi Mizuhara[2], Yuya Kagebayashi[2], Yasunori Kakizawa[2], Kazuya Muranaga[3] (1.National Institute of Information and Communications Technology, Tokyo, Japan, 2.CLEALINK TECHNOLOGY Co., Ltd., Kyoto, Japan, 3.Systems Engineering Consultants Co., Ltd., Tokyo, Japan)

[MGI41-P03] HpFP: development of high-speed data transfer applications (1)

Yasunori Kakizawa[1], Ayahiro Takaki[1], *Takamichi Mizuhara[1], Yuya Kagebayashi[1], Praphan Pavarangkoon[3], Kazuya Muranaga[2], Kazunori Yamamoto[3], Ken T. Murata[3] (1.CLEALINK TECHNOLOGY CO., LTD., 2.SEC CO., LTD., 3. National Institute of Information and Communications Technology)

[MGI41-P04] Programming Environment of Visual IoT Tools Working on Single-Board Computer (Raspberry Pi) (3)

Toshiki Aoki[1], *Takamichi Mizuhara[1], Ken T. Murata[2], Kazunori Yamamoto[2], Yakanari Yamasaki[2], Praphan Pavarangkoon[2], Kazuya Muranaga[3] (1.CLEALINK TECHNOLOGY CO., LTD., 2.National Institute of Information and Communications Technology, 3.SEC CO., LTD.)

[MGI41-P05] Investigation of Raspberry Pi and development of intelligent watch-dog

Mehdad Shirazi[1], *Takamichi Mizuhara[1], Toshiki Aoki[1], Ken T. Murata[2], Kazunori Yamamoto[2], Kazuya Muranaga[3], Praphan Pavarangkoon[2] (1.CLEALINK TECHNOLOGY CO., LTD., 2.National Institute of Information and Communications Technology, 3.SEC CO., LTD.)

[MGI41-P07] Communication Experiment of the Sensor Network in Chikuma City

*Kohei Mizuani[1], Takeshi Ken Murata[1], Kazunori Yamamoto[1], Praphan Pavarangkoon[1], Kazuya Muranaga[2], Takamichi Mizuhara[3] (1.National Institute of Information and Communications Technology, 2.Systems Engineering Consultants Co., LTD, 3.CLEALINKTECHNOLOGY Co.,Ltd.)

[MGI41-P08] A Trial to Identify Problems in Multi-disciplinary Data Usage: Study of Environmental Influences on Economic Activities in 18th-19th Centuries including the Sunspot Dalton Minimum

*Takashi Watanabe[1] (1.ICSU World Data System International Programme Office)

[MGI41-P09] Large-scale 4-D WebGIS applications to synchronize space and time (1)

Kazuya Muranaga[2], *Ken T. Murata[1], Kazunori Yamamoto[1], Praphan Pavarangkoon[1] (1.National Institute of Information and Communications Technology, 2.Systems Engineering Consultants Co., LTD.)

[MGI41-P10] Improvement of database system of research vessel operation information and causal analysis of past cruise downtime

*Yasuko Yamagishi[1], Ken Yatsu[1], Kazuhiko Kashiwase[1], Tetsuji Maki[1], Hide Sakaguchi[1] (1.Japan Agency for Marine-Earth Science and Technology)

[J] Poster | M (Multidisciplinary and Interdisciplinary)：M-AG Applied Geosciences

[M-AG44] Dynamics of radionuclides emitted from Fukushima Dai-ichi Nuclear Power Plant in the environment

convener:Daisuke Tsumune(Central Research Institute of Electric Power Industry), Yoshio Takahashi(Department of Earth and Planetary Science, Graduate School of Science, The University of Tokyo), Yuichi Onda(Center for Research on Isotopes and Environmental Dynamics, University of Tsukuba), Kazuyuki Kita(Faculty of Science, Ibaraki University)

[MAG44-P01] The time-fractional diffusion equation as the governing equation of the concentraiton of Cs-137 in the environment

★Invited Papers

*Yuko Hatano[1], Eiichi Suetomi[1], Yukiko Okada[2], Naoto Hagura[2], Takafumi Uchiyama[2] (1.Graduate School of Systems and Information Engineering, University of Tsukuba, 2.Atomic Energy Research Laboratory, Tokyo City University)

[MAG44-P02] Atmospheric resuspension of insoluble Cs radioactive particles found in polluted area in Fukushima

Peng Tang[1], Kohtaro Hatanaka[1], *Kazuyuki Kita[1], Yukihiko Satou[2], Takeshi Kinase[3], Kouji Adachi[3], Yuji Zaizen[3], Kazuhiko Ninomiya[4], SHINOHARA ATSUSHI[4], Yasuhito Igarashi[5] (1.Faculty of Science, Ibaraki University, 2.JAEA, 3.MRI, 4.Osaka University, 5.Institute for Integrated Radiation and Nuclear Science, Kyoto University)

[MAG44-P03] Contribition of bioaerosols to the atmospheric resuspension of radioactive cesium in summer and autumn

*Kazuyuki Kita[1], Naho Hayashi[1], Koutaro Minami[1], Teruya Maki[2], Kentaro Hosaka[3], Yasuhito Igarashi[4] (1.Faculty of Science, Ibaraki University, 2.Kanazawa university, 3.National musium of nature and science, 4.Institute for Integrated Radiation and Nuclear Science, Kyoto University)

[MAG44-P04] Preferential infiltration of the Fukushima accident-derived radiocesium into soil in the vicinity of Japanese cedar trunk

*Hikaru Iida[1], Hiroaki Kato[1], Tomoki Shinozuka[1], Satoru Akaiwa[1], Tatsuya Yokoyama[1], Sean Hudson[1], Janice Hudson[1], Yuichi Onda[1] (1.Center for Research in Isotopes and Environmental Dynamics, University of Tsukuba)

[MAG44-P05] Variation of soil water content in litter and soil layer impacts radiocesium air dose in the forests of Yamakiya District, Fukushima Prefecture

*Janice Elaine Hudson[1], Momo Kurihara[2], Sean Andrew Hudson[1], Kato Hiroaki[1], Yuichi Onda[1] (1.University of Tsukuba, 2.National Institutes for Quantum and Radiological Science and Technology)

[MAG44-P06] Difference of ^{137}Cs concentration between Preferential flow and Matrix in forest soil in Fukushima Prefecture

*Ono Tetsuya[1], Junko Takahashi[2], Tetsuya Sasaki[2], Yuichi Onda[2] (1.Doctoral program in integrative environment and biomass science, Graduate school of life and environmental science, University of Tsukuba, 2.Center for reserch in isotopes and environmental dynamics, University of Tsukuba)

[MAG44-P07] Formation mechanism of radiocesium concentration in throughfall in a cedar forest

*Tomoki Shinozuka[1], Hiroaki Kato[2], Yuichi Onda[2], Satoru Akaiwa[1] (1.Doctoral Program in Integrative Environment and Biomass Sciences, Graduate School of Life and Environmental Sciences, University of Tsukuba, 2.Center for Research on Isotope and Environmental Dynamics, University of Tsukuba)

[MAG44-P08] Change in the elution behavior of dissolved radiocesium and physical property in the decay degree of litter of deciduous broad-leaved trees

*Yoshito Sasaki[1], Tadafumi Niizato[1], Satomi Ito[1], Takayoshi Watanabe[1] (1.Japan Atomic Energy Agency)

[MAG44-P09] Dynamics of radioactive cesium in forest-stream ecosystem in a mountainous watershed

*Yuiko Chino[1], Takashi Gomi[1], Yoshito Oyama[1] (1.Department of Agriculture, Tokyo University of Agriculture and Technology)

[MAG44-P10] Seasonal change and formation factors of dissolved radiocesium concentration in a headwater catchment after the Fukushima Dai-ichi Nuclear Power Plant accident

*Satoru Akaiwa[1], Hiroaki Kato[2], Yuichi Onda[2], Tomoki Shinozuka[1] (1.Doctoral Program in Integrative Environment and Biomass Sciences, University of Tsukuba, 2.Center for Research in Isotopes and Environmental Dynamics,

University of Tsukuba)

[MAG44-P11] Change in the spatial distribution of the air dose rate in the riverside park affected by decontamination and floods

*Takuhei Yamasaki[1], Satoshi Suzuki[1] (1.Fukushima Prefectural Centre for environmental Creation)

[MAG44-P12] Accumulation and redistribution of ^{137}Cs on floodplains along the Abukuma River

★Invited Papers

*Yoshifumi Wakiyama[1], Alexei Konoplev[1], Valentin Golosov[2], Maxim Ivanov[2], Mikhail Komissarov[3] (1.Institute of Environmental Radioacitivity, Fukushima Universiy, 2.Faculty of Geography, M.V. Lomonosov Moscow State University, 3.Ufa Institute of Biology UFRC, Russian Academy of Science)

[MAG44-P13] Re-circulation of ^{137}Cs concentrations in surface seawater in the western North Pacific Ocean

★Invited Papers

*Yayoi Inomata[1], Michio Aoyama[2] (1.Kanazawa University, Institute of Nature and Environmental Technology, 2.Tsukuba University, Center for Research in isotopes and Environmental Dynamics)

[MAG44-P15] Distribution of dissolved and particulate radiocesium from the downstream of rivers to the costal waters off Fukushima.

*Hyoe Takata[1], Tatsuo Aono[2], Michio Aoyama[3], Hideki Kaeriyama[4], Mutsuo Inoue[5] (1.Fukushima Univ., 2.QST, 3.Tsukuba Univ., 4.FRA, 5.Kanazawa Univ.)

[J] Poster | M (Multidisciplinary and Interdisciplinary)：M-SD Space Development & Earth Observation from Space

[M-SD47] Future Missions of Satellite Earth Observation

convener:Yoshiaki HONDA(Center for Environmental Remote Sensing, Chiba University), Yukari Takayabu(Atmosphere and Ocean Research Institute, the University of Tokyo), Shinichi Sobue(Japan Aerospace Exploration Agency), Yuki Kaneko(Japan Aerospace Exploration Agency)

[MSD47-P01] Realization of pseudo high-frequency high-resolution observation by combined observation of geostationary satellite and orbiting satellite

*Yoshiaki HONDA[1], Koji KAJIWARA[1], Ryota ISHIBASHI[1] (1.Center for Environmental Remote Sensing, Chiba University)

[MSD47-P02] Mission on monitoring and elucidating global environmental changes (global radiative forcing and ecosystem changes that affect global warming) (successor to GCOM-C)

*Yoshiaki HONDA[1], Teruo Aoki[2], Takashi Nakajima[3], Mitsuhiro Toratani[4], Koji KAJIWARA[1], Ryota Ishibashi[1] (1.Center for Environmental Remote Sensing, Chiba University, 2.Research Organization of Information and Systems, National Institute of Polar Research, 3.Tokai University Research & Information Center, 4.Tokai University Department of Optical and Imaging Science and Technology)

[MSD47-P03] Geostationary Satellite Ocean Color Mission

*Joji Ishizaka[1], Mitsuhiro Toratani[2], Toru Hirawake[3], Takafumi Hirata[4], Hiroshi Kobayashi[5], Yuji Sakuno[6], Hiroto Higa[7] (1.Institute for Space-Earth Environmental Research, Nagoya University, 2.School of Engineering, Tokai University, 3.Faculty of Fisheries Sciences, Hokkaido University, 4.Arctic Research Center, Hokkaido University, 5.Graduate School of Interdisciplinary Research, University of Yamanashi, 6.Graduate School of Engineering, Hiroshima University, 7.Faculty of Urban Innovation, Yokohama National University)

[MSD47-P04] Satellite Observation of the Whole Atmosphere - Superconducting Submillimeter-Wave Limb-Emission Sounder (SMILES-2)

*Masato Shiotani[1], Akinori Saito[1], Takatoshi Sakazaki[1], Satoshi Ochiai[2], Philippe Baron[2], Toshiyuki Nishibori[3], Makoto Suzuki[3], Takumi Abe[3], Hiroyuki Maezawa[4], Shin-ichiro Oyama[5,6] (1.Kyoto University, 2.National Institute of Information and Communications Technology, 3.Japan Aerospace Exploration Agency, 4.Osaka Prefecture University, 5.Nagoya University, 6.University of Oulu)

[MSD47-P05] FTS satellite observation mission for understanding chemical and dynamical processes in the upper atmosphere

*Nawo Eguchi[1], Kaley A. Walker[2], Naoko Saitoh[3], Yukio Yoshida[4], Kei Yoshimura[5], Kinya Toride[5], Masatomo Fujiwara[6], Yoshio Kawatani[7], Yousuke Eguchi Yamashita[7], Ray Nassar[8], Dylan Jones[2], David Plummer[8], Kimberly Strong[2] (1.Kyushu University, 2.University of Toronto, 3.Chiba University, 4.National Institute for Environmental Studies, 5.University of Tokyo, 6.Hokkaido University, 7.JAMSTEC, 8.Environment and Climate Change Canada)

[MSD47-P06] Imaging spectrometer for km-class observation of SLCP

*YASUKO KASAI[1], Hiroshi Tanimoto[3], Yugo Kanaya[2], JPSAC Satellite group (1.NICT, 2.JAMSTEC, 3.NIES)

[MSD47-P07] Global measurement system of wind using LIDAR and Imaging FTS

*Okamoto Hajime[1], Toshiyoshi Kimura[2], Daisuke Sakaizawa[2], Shoken Ishii[3], Tomoaki Nishizawa[4] (1.Kyushu University, 2.Japan Aerospace Exploration Agency, 3.National Institute of Information and Communications Technology, 4.National Institute for Environmental Studies)

[MSD47-P08] Precipitation observation by small precipitation radar satellites

*Nobuhiro Takahashi[1], Kinji Furukawa[2], Takuji Kubota[2], Yamaji Moeka[2], Riko Oki[2] (1.Institute for Space-Earth Environmental Research, Nagoya University, 2.Japan Aerospace Exploration Agency)

[MSD47-P09] Technology demonstration mission for next generation precipitation observation radars

*Daisuke Jodoi[1], Kinji Furukawa[1], Riko Oki[1], Tomoo Ushio[2], Kenji Nakamura[3] (1.Japan Aerospace Exploration Agency, 2.Osaka University, 3.Dokkyo University)

[MSD47-P10] Monitoring and evaluation of near real-time water cycle fluctuations by microwave remote sensing

*Kazuyoshi Suzuki[1], Misako Kachi[2], Kazuyuki Saito[1], Hideki Kobayashi[1], Tetsuya Hiyama[3], Milija Zupanski[4] (1.Japan Agency for Marine-Earth Science and Technology, 2.JAXA, 3.ISEE, Nagoya University, 4.CIRA, Colorado State University)

[MSD47-P11] Development of new satellite to monitor SIF and PRI of terrestrial vegetation

*Hibiki M Noda[1], Kenji Omasa[2], Kouki Hikosaka[3], Kazuhito Ichii[4], Hideki Kobayashi[5], Tomomichi Kato[6], Hiroyuki Muraoka[7] (1.NIES National Institute of Environmental Studies, 2.Takasaki University of Health and Welfare, 3.Tohoku University, 4.Chiba University, 5.JAMSTEC, 6.Hokkaido University, 7.Gifu University)

[J] Poster | M (Multidisciplinary and Interdisciplinary)：M-TT Technology & Techniques

[M-TT51] Frontiers in Geochemistry

convener:Shogo Tachibana(UTokyo Organization for Planetary and Space Science, University of Tokyo), Yusuke Yokoyama(Atmosphere and Ocean Research Institute, University of Tokyo), Hiroyuki Kagi(Geochemical Research Center, Graduate School of Science, University of Tokyo)

[MTT51-P01] Measurement of helium isotope ratio using multi-turn time-of-flight mass spectrometer

*Yuki Hattori[1], Yoshihide Akiyama[1], Hirochika Sumino[1] (1.Department of Basic Science, Graduate School of Arts and Sciences, The University of Tokyo)

[MTT51-P02] **Ba stable isotopes in the East China Sea, Japan Sea, Gulf of Alaska, and the South Pacific**

*Keiji Horikawa[1], Yuuki Tezuka[2], Takashi Miyazaki[3], Shigeyuki Wakaki[4] (1.Graduate School of Engineer and Science for Research, University of Toyama, 2.Graduate School of Engineer and Science for Education, University of Toyama, 3.Department of Solid Earth Geochemistry, JAMSTEC, 4.Kochi Institute for Core Sample Research, JAMSTEC)

[MTT51-P03] Boron isotope as tracer for seawater pH reconstruction and submarine hydrothermal circulation

*Ryuichi Shinjo[1] (1.Department of Physics and Earth Sciences, University of the Ryukyus)

[MTT51-P04] **Effect of experimental, optical, and geometrical variables on the laser heating of inclusions during Raman spectroscopic analysis**

*Yuuki Hagiwara[1], Kenta Yoshida[2], Akira Yoneda[3], Junji Torimoto[2], Junji Yamamoto[1] (1.Hokkaido University, 2.Japan Agency for Marine-earth Science and Technology, 3.Osaka University)

[MTT51-P05] Pressure dependence of micro-Raman mass spectrometry for carbon isotopic composition of carbon dioxide fluid

*Lena Yokokura[1], Yuuki Hagiwara[1], Junji Yamamoto[2] (1.Hokkaido University, 2.Hokkaido University Museum)

[J] Poster | M (Multidisciplinary and Interdisciplinary)：M-TT Technology & Techniques

[M-TT52] Brand-new scope of coupling geophysics being established by infrasound and associated waves

convener:Masa-yuki Yamamoto(Department of systems engineering, Kochi University of Technology), Nobuo Arai(Disaster Mitigation Research Center, Nagoya University), Mie Ichihara(Earthquake Research Institute, University of Tokyo), Takayuki Otsu(Japan Weather Association)

[MTT52-P01] Establishment of Nationwide Infrasound Observation Consortium and Future Plan for Disaster Mitigation Application

*Masa-yuki Yamamoto[1,2], Nobuo Arai[2,3], Takayuki Otsu[2,4] (1.Department of systems engineering, Kochi University of Technology, 2.Nationwide Infrasound Observation Consortium, 3.Disaster Mitigation Research Center, Nagoya University, 4.Japan Weather Association)

[MTT52-P02] Infrasound signals propagated from volcanic eruption detected at long distances

*Makiko Iwakuni[1], Takayuki Otsu[1], Nobuo Arai[2], Mami Nogami[1], Masashi Motohashi[1], Takanari Fujii[1], RYOHEI EMURA[1], Takahiko Murayama[1] (1.JAPAN WEATHER ASSOCIATION, 2.Disaster Mitigation Research Center, Nagoya University)

[MTT52-P03] Volcanic atmospheric perturbation detected with barometer, broadband seismometer, and GNSS-TEC: comparison with ray-tracing calculation

*Yuki Nakashima[1], Kiwamu Nishida[1], Yosuke Aoki[1], Kosuke Heki[2] (1.ERI, Univ. Tokyo, 2.Space Geodesy Lab., Hokkaido Univ.)

[MTT52-P04] The 3 types of infrasound generated by "The 2018 Hokkaido Eastern Iburi Earthquake"

★Invited Papers

*Mami Nogami[1], Takahiko Murayama[1], Takayuki Otsu[1], Makiko Iwakuni[1] (1.Japan Weather Association)

[MTT52-P05] Development and test operation of small infrasound data loggers

*Yuichiro Inoue[1], Masa-yuki Yamamoto[1] (1.Kochi University of Technology)

[MTT52-P06] Infrasound measurement with MEMS sensors

★Invited Papers

*Ryouichi Nishimura[1] (1.National Institute of Information and Communications Technology)

[J] Poster | M (Multidisciplinary and Interdisciplinary)：M-ZZ Others

[M-ZZ55] Culture geology

convener:Hisashi Suzuki(Otani University), Tohru Sakiyama(Institute of Geo History, Japan Geochronology Network), Naoki Takahashi(Natural History Museum and Institute, Chiba)

[MZZ55-P01] Did Mitsuhide AKECHI change the channel of the River Yura?

★Invited Papers

*Kotaki Atsuo[1] (1.Kyoto Prefectural University)

[MZZ55-P02] Consideration on quarrying history of Rokko Granites on the basis of historical booklets “Meisho-zue” .

*Tohru Sakiyama[1] (1.Institute of Geo History, Japan Geochronology Network)

[MZZ55-P03] Transition of the use of building stones through the age in Chiba Prefecture

*Naoki Takahashi[1], Takuya Akashi[2] (1.Natural History Museum and Institute, Chiba, 2.Hisui-no-kai)

[MZZ55-P04] Finding the context of culture geology by utilizing local stone: A case study of the "Shindosaki stone" of Oiso town, Kanagawa prefecture

*Kiminori Taguchi [1] (1.Kanagawa Prefectural Museum of Natural History)

[MZZ55-P05] **Geomorphology and geology of pilgrimage grottoes in mountain region, northern part of Oita Prefecture, Japan**

*Norihito Kawamura[1] (1.School of Regional Resource Management, Graduate School, University of Hyogo)

[MZZ55-P06] Progress of culture geology in Japan and other countries

*Hisashi Suzuki[1] (1.Otani University)

[J] Poster | M (Multidisciplinary and Interdisciplinary)：M-ZZ Others

[M-ZZ56] Studies of Geoscience : historical, philosophical and STS studies

convener:Michiko Yajima(College of Humanity and Science, Nihon University), Toshihiro Yamada(Taisho University), Shigeyuki Aoki(Faculty of Letters, Chuo University), Shigeo Yoshida(Department of Earth and Planetary Sciences, Faculty of Sciences, Kyushu University)

[MZZ56-P01] **Inquiry of Origin**,
All Inquiries can not be achieved by **Induction** and **Deduction** alone;
Creative Inference using **Results (characteristics) of Evolution**,
called **Abduction** is a **Method of Evaluation** that transcends **Time** and **Space.**

*Akira Taneko[1] (1.SEED SCIENCE Lab.)

[MZZ56-P02] A study on recognition of indigenous knowledge in college students

*LU KE[1], CHENWEI CAI[1], HANQIU ZHANG[1], SHIXIAN LUO[1], JIAYING SHI[1], Damayanti Rosyi[1], Azuki Kiriyama[1], Mai Uemura[1], Katsunori Furuya[1] (1.Chiba University)

[MZZ56-P03] Harnessing the power of geoscience as a vehicle for interdisciplinary collaboration across borders

*Felix Kwabena Donkor[1] (1.University of South Africa)

[MZZ56-P04] An Archaeological Investigation inti the Use of Landscape for the Irrigation of Ancient Sri Lanka

*Chandana Rohana Withanachchi[1,2] (1.Sri Lanka Council of Archaeologists, 2.Rajarata University of Sri Lanka)

[MZZ56-P05] “The life and achievement of Sugi, Kenichi” Chikukagaku, 56, 35-39, by Miyashiro, Akiho, 1961

*Hidehisa Mashima[1] (1.Center for Obsidian and Lithic Studies, Meiji University)

[J] Poster | M (Multidisciplinary and Interdisciplinary)：M-ZZ Others

[M-ZZ57] Marine Manganese Minerals: Science, Engineering and Application

convener:Akira Usui(Marine Core Research Center, Kochi University), Yoshio Takahashi(Department of Earth and Planetary Science, Graduate School of Science, The University of Tokyo), Katsuhiko Suzuki(Submarine Resources Research Center, Japan Agency for Marine-Earth Science and Technology), Takashi Ito(Faculty of Education, Ibaraki University)

[MZZ57-P01] Sediment property in the exploration area for cobalt-rich crusts

*Kyoko Yamaoka[1], Atsushi Suzuki[1], Yuki Ota[1], Yuichiro Tanaka[1], Akifumi Shimamoto[2], Tatsuo Fukuhara[2], Junpei Minatoya[3], Shogo Kato[3], Yoshiaki Igarashi[3], Nobuyuki Okamoto[3] (1.Geological Survey of Japan, National Institute of Advanced Industrial Science and Technology, 2.KANSO Co.,Ltd., 3.Japan Oil, Gas and Metals National Corporation (JOGMEC))

[MZZ57-P02] GEOCHEMICAL AND MINERALOGICAL CHARACTERIZATION OF THE MOLANGO MN DEPOSITS: CONSTRAITS ON GENESIS

*Joseph Madondo[1], Carles Canet[2,1], Eduardo Gonzalez-Partida[4], Augusto Antonio Rodriguez-Diaz[1], Fernando Nuñez-Useche[3] (1.Institute of Geophysiscs (UNAM) , 2.Centre for Atmospheric Sciences (UNAM), 3.Institute of Geology (UNAM), 4.Centre for Geosciences (UNAM))

[MZZ57-P03] **Relationship between isotope fractionation and valence of tellurium adsorbed on the Fe-Mn oxides from seawater**

*Yusuke Fukami[1], Teruhiko Kashiwabara[2], Hiroshi Amakawa[3], Takazo Shibuya[2], Akira Usui[4], Katsuhiko Suzuki[2] (1.Gakushuin University, 2.Japan Agency for Marine-Earth Science and Technology, 3.Atmosphere and Ocean Research Institute The University of Tokyo, 4.Marine Core Research Center, Kochi University)

[MZZ57-P04] **Formation process of different types of manganese nodules collected on seamounts in the Northeast Pacific**

Wataru Katanoda[1], *Masafumi MURAYAMA[1], Akira Usui[2], Takeyasu Yamagata[3], Hiroyuki Matsuzaki[3] (1.Faculty of Agriculture and Marine Science, Kochi University, 2.Center for advanced Marine Core Research, Kochi University, 3.The University Museum,The University of Tokyo)

[J] Poster | U (Union)：Union

[U-12] Future of Earth and Planetary Science (10): Big Data and Open Science

convener:Ryoichi Fujii(Research Organization of Information and Systems), Hodaka Kawahata(Atmosphere Ocean Research Institute, the University of Tokyo), Eiichi Tajika(Department of Earth and Planetary Science, Graduate School of Science, The University of Tokyo), Gaku Kimura(Tokyo University of Marine Science and Technology)

Rapid growth of Science produces big data sets. A broad discussion is to a consensus that scientific outcomes should be recorded with primary data set and accessible samples. Such strict but reasonable criteria affect repository system of research institution and science society. In this union session, we examine the present status of the openness of Earth & Planetary Science and discuss its future development.

[U12-P01] Algorithm construction test for interdisciplinary science

*Norio Umemura[1], Shuji Abe[2], Yoshimasa Tanaka[3,4], Shin ya Nakano[5], Atsuki Shinbori[1], Yasuo Saito[3], Yasuyuki Minamiyama[6] (1.Institute for Space-Earth Environmental Research, Nagoya University, 2.International Center for Space Weather Science and Education, Kyushu University, 3.National Institute of Polar Research, 4.Joint Support-Center for Data Science Research, Research Organization of Information and Systems, 5.The Institute of Statistical Mathematics, 6.National Institute of Informatics)

Algorithm construction test for interdisciplinary science

*Norio Umemura[1], Shuji Abe[2], Yoshimasa Tanaka[3,4], Shin ya Nakano[5], Atsuki Shinbori[1], Yasuo Saito[3], Yasuyuki Minamiyama[6]

1. Institute for Space-Earth Environmental Research, Nagoya University, 2. International Center for Space Weather Science and Education, Kyushu University, 3. National Institute of Polar Research, 4. Joint Support-Center for Data Science Research, Research Organization of Information and Systems, 5. The Institute of Statistical Mathematics, 6. National Institute of Informatics

The preliminary project in ROIS (Research Organization of Information and Systems), which consists of several researchers in ISM (The institute of Statistical Mathematics), NIPR (National Institute of Polar Research), Nagoya University and Kyushu University, has developed the data-driven method to calculate the relationship among various events indicated by several scientific data, and has confirmed whether the output results are scientifically valid or not. First of all, we have applied NIPR data (time-series data: climatology data, environmental data, magnetic field data and so on, spatial distribution data: sea water temperature data and so on by multi-site collection, and frequency distribution data: mineral composition analysis and so on) as a sample case, and obtained the following results.
In the case of time-series data on 22 Dec. 2014, through correlation analysis, we confirmed that the correlation value between the variations of radiation obtained at Skarvsnes on Soya Coast, East Antarctica and the variation of UV (ultraviolet) obtained at Skallen on Soya Coast, East Antarctica was 0.4040, and the correlation value between the variations of solar radiation and geomagnetic field was -0.0024. This result suggests scientifically that the amount of heat flowing into the earth’ s surface from the sun has a high interaction with that of UV radiation, but has a low relationship with temperature and/or geomagnetic variations. In the case of frequency distribution data on 1986, with Earth Mover’ s Distance (EMD), we confirmed the similarity value EMD(P, Q) between the distributions of the meteorite component collected at Asuka Observational Base in Antarctica and Yamato Mountains in Antarctica was 2.23, but the EMD(P, Q) of each meteorite collected at the same Asuka Observational Base was 1028.05. In this meteorite case, we have not found the spatial deviation of meteorites with similar components. However, if there is a spatial deviation, it is also possible to extract whether a peculiar phenomenon, such as temperature fluctuation, has occurred or not at that particular point. That is, this result of data-comparison, data-relation, and data-segmentation can work as an interdisciplinary system for the investigation of scientific relationships even though data format and/or science field are different, as well as a conventional comparison system.
Actually, we are able to confirm the similarity with the matrix-like combinational calculations. These results has been already registered into database, and the preparation for storing hundreds of million results is in progress. Further, this calculation refers the actual data through metadata to work across several research institutions and universities. In 2020, we will build a comprehensive virtual network of data knowledge from the same and neighboring fields to completely different fields by increasing the number of data and algorithms and expanding to distribution data such as literature data and pharmaceutical analysis data, and public this system. Then, we will contribute to the realization of an interdisciplinary science society while fulfilling the mission of providing the research infrastructure to research institutions and universities.

Keywords: Data Science, Interdisciplinary Science, Data-Driven Science

©2020. Japan Geoscience Union. All Right Reserved.

[J] Poster | U (Union)：Union

[U-24] COVID-19, the Earth's Environment and Disaster

convener:Jun Matsumoto(Deaprtment of Geography, Tokyo Metropolitan University), Yukihiro Takahashi(Department of Cosmosciences, Graduate School of Science, Hokkaido University), Akira Wada(Tokyo Institute of Technology), Manabu D. Yamanaka(Research Institute for Humanity and Nature / Professor Emeritus of Kobe University)

[U24-P01] Seismic noise reduction in Tokyo urban area due to social activity reduction for COVID-19

*Suguru Yabe[1], Kazutoshi Imanishi[1], Kiwamu Nishida[2] (1.National Institute of Advanced Industrial Science and Technology, 2.ERI, UTokyo)

[U24-P02] Ensemble Data Assimilation of COVID-19 Epidemic Model: Relationships between Infectivity and Earth Environments

*Shunji Kotsuki[1], Atsushi Okazaki[2] (1.Center for Environmental Remote Sensing, Chiba University, 2.Department of Meteorology & Atmospheric Science, Penssylvania State University)

[U24-P03] Air pollution status over China during lockdown caused by COVID-19

*Pradeep Khatri[1], Tadahiro Hayasaka[1] (1.Center for Atmospheric and Oceanic Studies,Tohoku University)

[U24-P04] Study on the Status of Website Information Dissemination by Japan’s Prefectural and Municipal Governments about "Evacuation and Sheltering during Natural Disasters" under Coronavirus Infection (Preliminary Report)

*SANO Hiroaki[1], Yohei CHIBA[1], Shinya MIURA[1], Yuichiro Usuda[1] (1.National Research Institute for Earth Science and Disaster Resilience)

[U24-P05] Impact of air quality caused by the COVID-19 lockdown in China, observed at downwind of Japan’s mountainous area.

*Osamu Nagafuchi[1], Koyomi Nakazawa[1], Ken'ichi Shinozuka[1] (1.Fukuoka Institute of Techology)

Seismic noise reduction in Tokyo urban area due to social activity reduction for COVID-19

*Suguru Yabe[1], Kazutoshi Imanishi[1], Kiwamu Nishida[2]

1. National Institute of Advanced Industrial Science and Technology, 2. ERI, UTokyo

In order to deal with COVID-19 pandemic, social activities have been reduced around the world. Tokyo metropolitan area is no exception, where more than 30 million people live. Self-restraint was requested in various situations by local and Japanese governments, which drastically changed our life. Working from home or layoff was introduced in many companies. Shopping malls were closed. The movement of people was reduced, and economic activities stagnated.

A part of noise observed by seismometers is due to human activities including transportations and machine vibrations. It is well known that seismic noise level in the daytime is higher than in the nighttime. The social activity reduction for COVID-19 is expected to decrease seismic noise in a different way from regular pattern, which would provide us a good opportunity to improve our understanding of seismic noise. Better understanding of seismic noise may also provide us a new way to monitor human activities using seismic observations. This study investigated continuous record of seismic stations in Metropolitan Seismic Observation network (MeSO-net) maintained by National Research Institute for Earth Science and Disaster Resilience (NIED). Seismic stations of MeSO-net are settled at the bottom of shallow borehole (~20 m) in the Tokyo metropolitan area. We measured hourly seismic noise level and compared its temporal changes with a timeline of COVID-19 in Tokyo metropolitan area.
We observe two types of seismic noise reduction associated with different causes in MeSO-net stations. The first one is often observed in frequency bands higher than 20 Hz. This seismic noise reduction started at the beginning of March 2020. This timing corresponds to when Japanese government closed schools. As many MeSO-net stations are settled in school property, human activities there are considered to influence seismic records of MeSO-net stations strongly in a high frequency band. The second seismic noise reduction is often observed in lower frequency band between 1-20 Hz. This seismic noise reduction started on April 13th 2020. This timing corresponds to the first beginning of week after the Japanese government declared a state of emergency in Tokyo metropolitan area on April 8th 2020. Seismic noise reduction in lower frequency band is expected to be related with stagnated economic activities, such as decreasing transportations and closing buildings or factories.

Keywords: COVID-19, Seismic noise, MeSO-net, Tokyo metropolitan area

©2020. Japan Geoscience Union. All Right Reserved.

Ensemble Data Assimilation of COVID-19 Epidemic Model: Relationships between Infectivity and Earth Environments

*Shunji Kotsuki[1], Atsushi Okazaki[2]

1. Center for Environmental Remote Sensing, Chiba University, 2. Department of Meteorology & Atmospheric Science, Penssylvania State University

The worldwide epidemic of COVID-19 has required more understandings of its infectivity and impacts on Earth environments. This study proposes a method enabling such assessments by integrating mathematical approaches and Earth environments. We first developed a modified epidemiological model based on a commonly used compartment model. The model assigns population into five compartments, Susceptible, Exposed, Infectious, Recovered, and Death; hereafter SEIRD model). In this outbreak, there are daily reports of COVID-19-induced deaths, as opposed to influenza epidemics. Hence we updated the commonly used SEIR model to additionally consider deaths. We conducted ensemble data assimilation of the SERID model for individual countries using daily reports of new cases and deaths as observation data. The data assimilation revealed that time series of infectivity of COVID-19 clearly corresponded with political decisions such as the rock-downs and economic activity resume in the U.S., and economic restraint in Japan. Additionally, satellite observations of NO2 also supported the economic restraints. Based on worldwide data assimilation experiments and atmospheric data, we are now investigating the relationships between COVID-19 infectivity and environments, which is one of COVID-19's uncertainty. This presentation will include the most recent progress up to the time of the conference.

Keywords: COVID-19, Epidemiological Model, Data Assimilation, Infectivity, Satellite Observations, Atmospheric Reanalysis Data

©2020. Japan Geoscience Union. All Right Reserved.

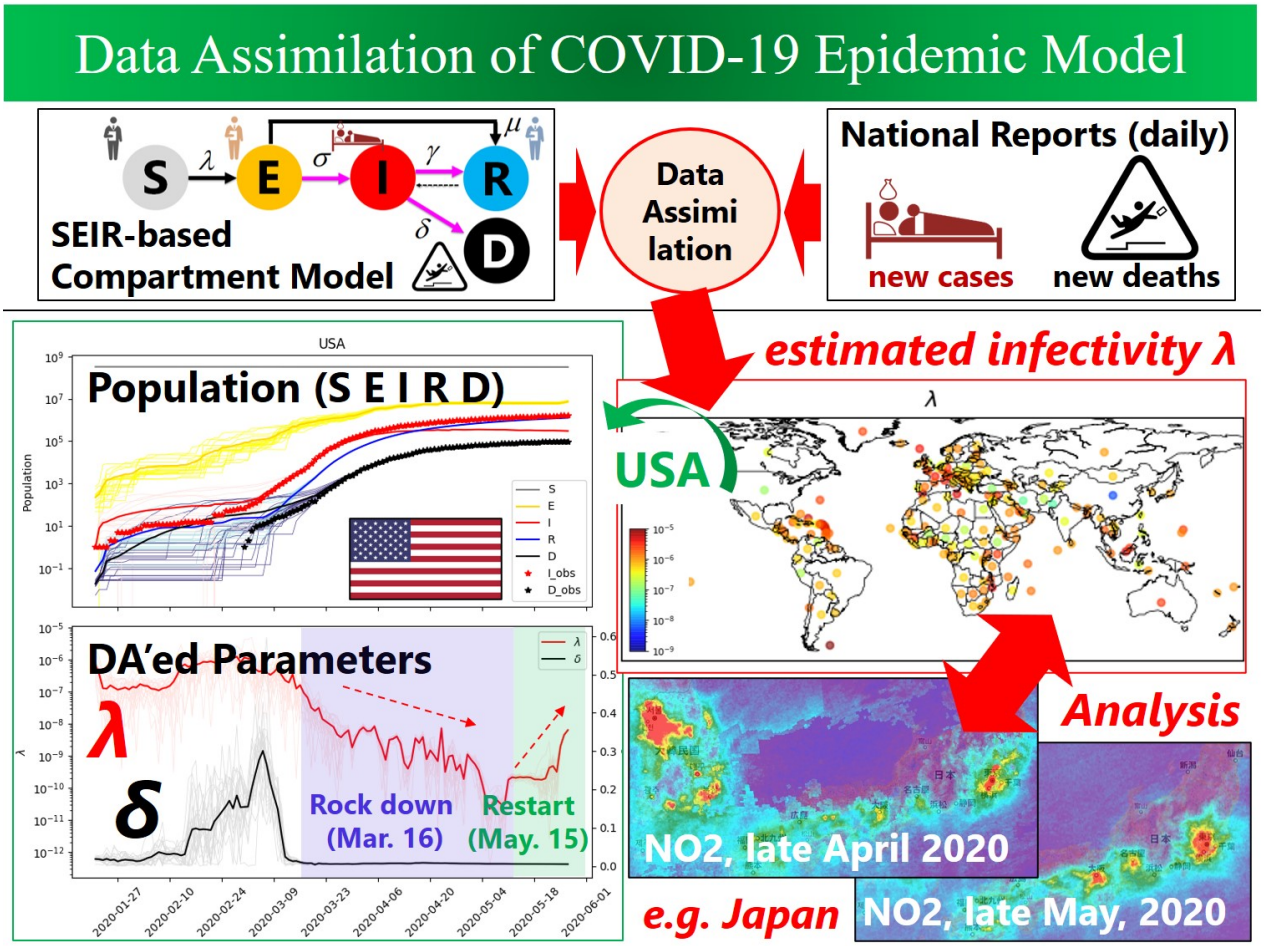

©2020. Japan Geoscience Union. All Right Reserved.

Air pollution status over China during lockdown caused by COVID-19

*Pradeep Khatri[1], Tadahiro Hayasaka[1]

1. Center for Atmospheric and Oceanic Studies,Tohoku University

In response of COVID-19 outbreak, China imposed lockdown in Wuhan from 23 January, 2020. Within days of "Wuhan lockdown" , restrictions on travel and social and economic activities were imposed on other Chinese cities as well, which inevitably altered the proportion of human-made air pollution than previous years. This lockdown provided an important opportunity for atmospheric scientists to unravel several uncertainties related to the impacts of man-made air pollutants on climate change, water cycle, human health, agriculture and so on. Grabbing this opportunity, we attempted to understand the change in air pollution over China during lockdown period and its possible link with energy consumption pattern. Aerosol, trace gases, energy consumption, and night light intensity for January - April of 2016 - 2020 available from satellite and surface observation, reanalysis, and government bodies are used. Our preliminary analyses indicate substantial reduction in energy consumption and air pollutions in industry and possibly transportation sector, but not significant change in residential sector during lockdown period. This resulted to reduce light-scattering aerosols in higher proportion than light-absorbing aerosols, and comparatively southern part sees more reduction than northern part.

Keywords: Aerosols, Trace graces, Lockdown, Energy

©2020. Japan Geoscience Union. All Right Reserved.

Study on the Status of Website Information Dissemination by Japan’s Prefectural and Municipal Governments about "Evacuation and Sheltering during Natural Disasters" under Coronavirus Infection (Preliminary Report)

*SANO Hiroaki[1], Yohei CHIBA[1], Shinya MIURA[1], Yuichiro Usuda[1]

1. National Research Institute for Earth Science and Disaster Resilience

Due to the spread of coronavirus infection (COVID-19) in Japan, the Ministry of Health, Labour and Welfare (MHLW) and other ministries and agencies propose a "new way of life". This has led to changes in daily life and lifestyle in Japan. The proposal describes that particularly in the expansion phase of COVID-19, avoiding the three densities of enclosed spaces, congested areas, and close scenes is recommended. It then mentions that by keeping from these three conditions, the risk of cluster development, which is a factor in the spread of infectious diseases, can be avoided.
In recent years, earthquake disasters such as the 2016 Kumamoto Earthquake and the 2018 Hokkaido Eastern Iburi Earthquake, and heavy rainfall and typhoons such as the heavy rainfall event of July 2018, Typhoon Faxai and Typhoon Hagibis of 2019, caused extensive damages in Japan. In order to protect ourselves from such natural disasters, we need to avoid these risks appropriately. Especially during the upcoming rainy season and typhoon
season, we need to make sure that we do not suffer any damages. It is important to "avoid" the three conditions. However, it is difficult to avoid them under COVID-19 when evacuating from a disaster.

Therefore, the Cabinet Office's Disaster Prevention and Management Agency and other ministries and agencies are prepared for upcoming natural disasters with the Notification of Response to Novel Coronavirus Infections in Evacuation Centers (April 1st and April 7th, 2020). This notification states that "when a disaster occurs and an evacuation center is set up, it is important to take all possible measures against infectious diseases based on the status of COVID-19" (from the April 1 notice), and presents nine concerns as "reference for preparation in advance and response to disasters" (from the April 7 notice).

Keeping these in mind, the presenters aim to comprehensively understand the preparedness of prefectural and municipal governments for natural disasters under COVID-19, based on the directives issued by the Cabinet Office for disaster prevention and others. First of all, we searched official websites of prefectural and municipal governments all over Japan to collect information on "evacuation" or "shelters" under COVID-19. In addition, a map-based visualization application was released to enable these governments to holistically understand the status of information dissemination. We then discussed the establishment of a system to enable the national, prefectural and municipal governments to refer to each other's efforts and to obtain necessary and useful information for evacuation under COVID-19 conditions through the publication of the application.

Comprehensive collection of information regarding COVID-19×Disaster Evacuation and Sheltering was conducted in 37 prefectures and 666 municipalities (as of June 12th, 2020). We organized and mapped the collected information at the prefectural and municipal levels and published an application (https://dil.bosai.go.jp/disaster/covid19/index.html). This application aims to enable the national government, prefectural and municipal governments to mutually refer to each other's efforts to obtain and utilize necessary and useful information. In addition, based on the nine concerns from the April 7 notice,

©2020. Japan Geoscience Union. All Right Reserved.

we prepared a summary report of the efforts undertaken by municipalities and other organizations. This application was released on May 25th, 2020 and was viewed by 5,056 as of June 10th, 2020.
The goal of this application is still in progress. Through the collection and accumulation of such case studies, we would like to extract cases and essences that can be applied to other regions. We also hope that this application will provide information that can lead to implementation of evacuation and sheltering in natural disasters, and countermeasures under COVID-19 in Japan as a whole.

Keywords: Evacuation, Sheltering, Web information, COVID-19, Natural Disasters

©2020. Japan Geoscience Union. All Right Reserved.

Impact of air quality caused by the COVID-19 lockdown in China, observed at downwind of Japan’ s mountainous area.

*Osamu Nagafuchi[1], Koyomi Nakazawa[1], Ken'ichi Shinozuka[1]

1. Fukuoka Institute of Techology

Covid-19 lockdown have led to a drastic improvements of air quality in many cities all over the world. The Himalayas were visible from the city areas in India, which have not been seen for 30 years due to the air pollution. In China, during the Olympic period in 2008, temporal improvement of air quality was recognized in Beijing. However, this is the first time since improvements of air quality in many cities in China. In this research, in order to clarify whether the improvement of air quality was observed or not caused by COVID-19 lockdown in Kyushu mountainous region, Japan, where the downwind of these are highly are polluted cities in main land China, we observed the NO3-, nssSO_4^{2-}, T-Hg, and microplastics in the rime ice. We collected rime ice from 1,500 to 1,700 m a.s.l.

NO_3^-, nssSO_4^{2-} Hg concentration and number of microplastics in rime ice sampled in mountainous area of Kyushu in Japan, are drastically decreased after lockdown which were conducted in January 23 and 24 in Hubei region, China. NO_3^-, nssSO_4^{2-} and T-Hg in rime ice collected on the 18th January, which is before lockdown, were 12.3 mg/L 6.02 mg/L, and 27.7 ng/L, respectively. Number of microplastics was 56 $\times 10^3$ N/L. On the other hand, the rime ice collected on 18 February after lockdown of Hubei region, China, NO_3^-, nssSO_4^{2-} and T-Hg concentration were 1.61 mg/L, 5.54 mg/L and 5.71 ng/L, respectively. Also, the number of microplastics were 22 $\times 10^3$ N/L.
Authors have been collected rime ice since 1990s and these NO_3^- and nssSO_4^{2-} concentrations observed in 18 February were lower than 1990s level.

Keywords: COVID-19, Lockdown, Air pollution, Long-range transport, Rime ice, Free trophosphere

©2020. Japan Geoscience Union. All Right Reserved.

[J] Poster | O (Public)：Public

[O-04] Poster presentations by senior high school students

convener:Tatsuhiko Hara(International Institute of Seismology and Earthquake Engineering, Building Research Institute), Katsuyoshi Michibayashi(Department of Earth and Planetary Sciences, Nagoya University), Miwa Kuri(Japan Meteorological Agency), Keiko Konya(Japan Agency for Marine-Earth Science and Technology)

Senior high school students provide poster presentations on subjects in fields of earth and planetary sciences. This session provides an opportunity for senior high school students to give their presentations in the JpGU meeting and to have discussions with researchers. This session has been conducted as a public outreach session since 2006.

[O04-P01] Weather in Ishikawa Prefecture in the Edo Period from the Kakuson diary

*Terumasa Hashino[1], *Sumire Tanaka[1], *Aten Noguchi[1], *Ai Minemoto[1], *Tomoki Sononaka[1], *Kaho Tokuda[1], *Masaaki Yamahata[1], *Kaisei Uchida[1], *Shinsyu Ohshiro[1], *Yasuhumi Hatashima[1], *Takuto Yoshimori[1], *Waka Sonoda[1], *Daisuke Taniguchi[1], *Eitaro Tozawa[1] (1.Ikeda Gakuen Ikeda Senior High School)

[O04-P02] The Project of digitizing seismometer records

*Masaki Yashiro[1], *Akira Taguchi[1], *Eishi Chihara[1], *Katsuaki Miyazawa[1], *Asumi Yamada[1] (1.Yashiro High School)

[O04-P03] Predict future tyhoons with statistics

*Atsushi Kobayashi[1] (1.Yashiro High School)

[O04-P05] Simplified observation of the bright meteor using web-camera images exposed for two seconds

*Takaaki TSUJI[1], *Naomasa OKADA[1], *Kouki YAMADA[1] (1.Nagoya High School)

[O04-P06] Production of improved Rain-go-round

*yuga morita[1] (1.Taki High School)

[O04-P07] the current situation and improvement plans of light pollution around Ichikawa city

*Mutsumi Goto[1] (1.Ichikawagakuen Ichikawa high school)

[O04-P08] Relations of the size of tsunami and the destruction rate of the house

*Keita Ichikawa[1] (1.Ichikawagakuen Ichikawa high school)

[O04-P09] What does annual drainage have an effect on phosphorus cycle of irrigation ponds?

*Hiiro TABATA[1], Yuki TAKAHASHI[1], Ayane INOUE[1], Haruto TAKEYAMA[1], Kousuke MANO[1], Rio YAMANO[1] (1.Hyogo Prefectural Kakogawahigashi High School)

[O04-P10] Reviewing Muroto High School Evacuation Management Manual –Investigation on Natural Environment around the Evacuation Site-

*Misaki WATANABE[1], *Kurumi HASHIMOTO[1] (1.Kochi Prefectural Muroto High School)

[O04-P11] What Affects the View of Mirage

*# [1] (1.Yokohama Science Frontier High School)

[O04-P12] An ancient large earthquake revealed from the trace of the earthquake, and possibility of existence of “Unknown Fault” in Tama Hills

*Takuma FUKUNAGA[1] (1.Yokohama Science Frontier High School)

[O04-P13] Estimating of paleoenvironment using fossils of shells produced in the Kanzawa Formation, Nakatsu Group

*Hotaka OGURA[1] (1.Yokohama Science Frontier High School)

[O04-P14] Evaluating the Effect of Global Warming on Yokohama Using Nightlight Satellite Data and Large Point Sources Data

*Sota Komiya[1] (1.Yokohama Science Frontier High School)

[O04-P15] Comparison of Fluid Resistance and Experience for Calculation of Resistance Coefficient according to Object Shape

*Senri Shimamura[1] (1.Sakaehigashi Senior High School)

[O04-P17] Examination of evacuation routes considering damage caused by liquefaction

*KOYA TAKAHASHI[1] (1.tosa high school)

[O04-P18] Relationship between four giant jets in the past and meteorological phenomena in the troposphere

*Yuya Okubo[1], Huga Suzuki[1], Yuya Takahashi[1] (1.Shizuoka Prefectural Iwata Minami High School)

[O04-P19] Spectroscopy of plasma generated in a microwave using a newly developed simple spectrometer with high resolution

*Ayaka Akase[1], *Kento Takase[1], *Reiji Iwamoto[1], *Keishi Okumi[1], *Mayu Naito[1], *Hiromu Fujimoto[1], *Yamato Yasuhara[1], *Natsuki Yamamoto[1] (1.Hyogo Prefectural Himeji Higashi Senior High School Science Club (Plasma team))

[O04-P20] Circulation of residual magma during consolidation of granitoid magma

*Kento Takase[1], *Ayaka Akase[1], *Reiji Iwamoto[1], *Keishi Okumi[1] (1.Hyogo Prefectural Himeji Higashi Senior High School Science Club (Magma team))

[O04-P21] Indicate the intensity of ultraviolet rays using the degree of fading of cotton yarn dyed with reactive dye

*Natsuki Yamamoto[1], *Ayaka Akase[1], *Kento Takase[1], *Reiji Iwamoto[1], *Keisi Okumi[1], *Mayu Naito[1], *Hiromu Fujimoto[1], *Yamato Yasuhara[1], *Nanami Kishimoto[2], *Sayuki Fujii[2], *Nagisa Yokoyama[2], *Soya Obata[2], *Hinako Kobayashi[2], *Haruki Murakami[2], *Reo Yamada[2], *Syo Yoshida[2] (1.Hyogo Prefectural Himeji Higashi Senior High School Science Club (Ultraviolet rays team), 2.Hyogo Prefectural Nishiwaki Senior High School Earth Science Club)

[O04-P22] Seasonal alterations in carbon assimilation of marine organisms

*Hiroto ICHIKAWA[1], Hayato Kurosawa[1], Ryushi Abe[1] (1.Miyagi Rifu high school)

[O04-P23] The relationship between Intensity of radiation energy and soils variety

*Ryushi Abe[1], Hiroto Ichikawa[1] (1.Miyagi Rifu high school)

[O04-P24] Specific heat of various soils measured by radiation thermometer

*Hayato Kurosawa[1], Hiroto Ichikawa[1] (1.Miyagi Rifu high school)

[O04-P25] Relationship between astronomical observation and water vapor in weather forecast

*Aoi Takamori[1] (1.Suwa Seiryo Senior High School)

[O04-P26] Research about Moriya Formation

*Yusuke Morozumi[1] (1.Suwa seiryo senior high school)

[O04-P27] Making solid version chromatography ~Separation and identification of solid particles by magnetic field gradient using microgravity~

*Satoru Kitada[1], Takuya Hanasaki[1], Yuichiro Okuno[1], Ryota Iwamoto[2], Keita Maishi[3], Kyoya Okada[3] (1.Imamiya Technology Senior High School of Osaka Prefecture The evening course, 2.Otemae Senior High School of Osaka Prefecture The evening course, 3.Kasugaoka Senior High School of Osaka Prefecture The evening course)

[O04-P29] Earthquake prediction by an electromagnetic wave

*Ousuke Yagasaki[1], Mizuho Fujiwara[1], Maika Yashima[1], Shougo Takeda[1], Aiku Tanaka[1] (1. Tokyo Metropolitan Tama High School of Science and Technology)

[O04-P30] Classification of Herbig Ae/Be Stars by Spectroscopic Observations

*Aika Koyama[1], *Riko Iida[1], *Hazuki Ueyama[1] (1.Nara Prefectural Seisho High School)

[O04-P31] The Research for Asteroid's Surface Color ~ Difference of BVR magnitude ~

*Asahi Tajima[1], *Mirei Matoba[1] (1.Nara Prefectural Seisho High School)

[O04-P32] The igneous rocks which is distributed around The Kabutoyama mountain, the northern part of Kofu Basin

*Masahiro Okuyama[1], Dai Iijima[1], Haruta Moriya[1], Ayato Watanabe[1] (1.Yamanashi Prefectural Hikawa Highschool)

[O04-P33] Studies on the Urban Heat Islands and Measures against Heat

*Mio Takakura[1] (1.Tokyo Metropolitan Toyama High School)

[O04-P34] **Geological Survey by Boring a Core from Toyama's Schoolgrounds**

*Ryotaro Terabe[1] (1.Tokyo Metropolitan Toyama High School)

[O04-P35] Long-term Fluctuation of Snowfall/Precipitation Ratio and Global Warming

*Yukihiro Takaki[1] (1.Tokyo Metropolitan Toyama High School)

[O04-P36] Factors for variations in bombcyclones

*Minori Iida[1] (1.Tokyo Metropolitan Toyama High School)

[O04-P38] Spectroscopic observation of sprite

*Kotone Asano[1], *Ayaka Okumura[1], Ryuya Nagao[1], Keisuke Nobutoki[1], Momoo Hayashi[1] (1.Ichinomiya High School)

[O04-P39] The relationship between the shape of columnar jointing and the viscosity of lava flow

*Kanta Takakura[1] (1.Kaijo high school)

[O04-P40] How ripples formation dependence on the size of sand grains and the amplitude of vibration cycle

*Tsuyoshi Enta[1], *Ryutaro Mitsui[1] (1.Kaijo Junior and Senior High School)

[O04-P41] Development of the Portable Equatorial Mount with high operability and applicability

*Jun Ikeda[1] (1.Kaijo high school)

[O04-P42] Proposal of GEO-KAMISHIBAI that enhances the appeal of SANRIKU GEOPARK-3 the Taneichi Layer

*Hitomi Kimura[1], *Rio Yaguchi[1], *Kyougo Sakashita[1], *Asahi Sekibata[1] (1.MARIENT CHIKYU TANKEN CLUB SENIOR)

[O04-P43] Proposal of GEO-KAMISHIBAI that enhances the appeal of SANRIKU GEOPARK-4 the Hachinohe Canyon

*Mai Kawabata[1], *Haruto Kawasaki[1], *Sarina Shinohe[1] (1.MARIENT CHIKYU TANKEN CLUB SENIOR)

[O04-P44] **Spectroscopic Observation of Meteors**

*Shotaro Mino[1], *Yui Satou[1] (1.Furukawa Reimei Junior High School / High School)

[O04-P45] Comparison of frequency (HRO/VOR-RO) and detection number in meteor radio wave observation

*Sora Endo[1], *Rio Saito[1], *Aki Sato[1], *Sachi Sato[1], *Sakura Yuki[1] (1.Furukawareimei Junior High School / High School)

[O04-P47] Research about Greenhouse effect of water vapor~Can we control the temperature of the earth with water vapor!?~

*Hikaru Abe[1], *Michiru Suzuki[1], *Ruka Suzuki[1], Furi Seino[1] (1.Sakata Minami High School)

[O04-P48] **A study of the fluctuations in the water level of Kohama pond**

*Akari Nakata[1], *Kira Yamamoto[1], Koharu Fukusi[1], *Hinata Muto[1] (1.Nirayama High School)

[O04-P49] **Research on statistical observation of columnar joint form and its origin by high precision 3D model by drone and potato starch experiment**

*Makoto Iida[1], *Ryo Aoki[1], *Ryuki Mochizuki[1], *Takato Okumura[1] (1.Nirayama High School)

[O04-P50] Marine pollution by Microplastics

*Nanako Aono[1], *Kaito Isoya[1], *Kouki Sugiyama[1], *Yuki Nakata[1], *Genki Yano[1] (1.Nirayama High School)

[O04-P51] Invisible ability of soil –Soil evaluation by zero point of charge-

*Ayano Hayashi[1], *Ayano Soga[1] (1.Kyoto Prefectural Sagano High School)

[O04-P52] Multivariate analysis of data of forest soil by using “Face Chart”

*Fujimoto Takeshi[1], *Hina Nakatani[1], *Hokuto Nakatsu[1] (1.Kyoto Prefectural Sagano High School)

[O04-P53] Manufacture of Azumaya in WFS -Examination of the method of drying the trees-

*Kanako Inoda[1] (1.Kyoto Prefectural Sagano High School)

[O04-P54] Project Regeneration of Gensei’s Bamboo Volume 1

*Takeshi Fujimoto[1], *Yosuke Yukawa[1], *Nanami Aoki[1], *Yusuke Yamazaki[1] (1.Kyoto Prefectural Sagano High School)

[O04-P55] To develop an efficient geological survey method and its effectiveness by using natural radiation

*Taisei Takagi[1], *Momoka Tanaka[1], *Ayane Matsuoka[1], *Kosei Yoshimura[1], *Chiharu Yamaguchi[1] (1.FUKUI PREFECTURAL WAKASA SENIOR HIGH SCHOOL)

[O04-P56] Kantemboki ~To research the accuracy of Japanese old sayings about weather~

*Yuki Takemura[1], *Toro Higashino[1], *Haruki Fukuda[1] (1.FUKUI PREFECTURAL WAKASA SENIOR HIGH SCHOOL)

[O04-P57] Proposal of new embankment ~Proposal of prevention method of piping phenomenon

*Daiki Tanabe[1], *Soshi Hirata[1] (1.FUKUI PREFECTURAL WAKASA SENIOR HIGH SCHOOL)

[O04-P58] Protect the traditional shrimp fishing in Obama Bay

*Taisei Hayashi[1], *Masakazu Muramatsu[1], *Chiaki Ose[1], *Kanta Nakai[1] (1.FUKUI PREFECTURAL WAKASA SENIOR HIGH SCHOOL)

[O04-P59] Correlation between liquefaction and grainsize distribution of ground

*Ryo Beppu[1] (1.Saitama prefectural Kasukabe High School)

[O04-P60] Fine laminated structure of stromatolite suggests summer and winter in cretaceous period?

*Taiga Tsujimoto[1] (1.Saitama prefectural Kasukabe High School)

[O04-P61] How long did it take to form the Pothole in Joga-Shima Island?

*Yusuke Izumi[1] (1.Saitama prefectural Kasukabe High School)

[O04-P62] Clothing change from meteorological data

*Hinane Chiba[1], *Misaki Ishii[1], *Kaho Kubota[1], *Nanami Nakao[1] (1.Chiba Prefectural Funabashishibayama High School)

[O04-P63] Analog modeling of dust devil -Study of its growth and dissipation-

*Daisuke Suzuki[1], Yuto Akaike[2] (1.Shizuoka Senior High School, 2.Fuji Senior High School)

[O04-P64] Automatic observation of Visibility

*HARUTO TANAKA[1], *MITSUKI BABA[1], *YUYA HAMASHIMA[1] (1.Tokyo Metropolitan Tachikawa High School)

[O04-P65] Analysis of sunspot observation data over 70 years and future prospects

*HAMASHIMA YUYA[1] (1.Tokyo Metropolitan Tachikawa High School)

[O04-P67] Development of an automatic observation and notification system for the meteor shower
~A signal detection and data output using Arduino~

*Koichi Sato[1], *Junsei Okuma[1] (1.Chuo University Junior and Senior High School)

Weather in Ishikawa Prefecture in the Edo Period from the Kakuson diary

*Terumasa Hashino[1], *Sumire Tanaka[1], *Aten Noguchi[1], *Ai Minemoto[1], *Tomoki Sononaka[1], *Kaho Tokuda[1], *Masaaki Yamahata[1], *Kaisei Uchida[1], *Shinsyu Ohshiro[1], *Yasuhumi Hatashima[1], *Takuto Yoshimori[1], *Waka Sonoda[1], *Daisuke Taniguchi[1], *Eitaro Tozawa[1]

1. Ikeda Gakuen Ikeda Senior High School

Motivation for research
In the past four years, we have analyzed the weather of Sekiguchi diary, Nijo family diary,Myohoin diary, Moriyatoneri diary and Hirosaki domain diary.
This year, we analyzed the Kakuson diary. The purpose of the research
(1) Create a database in conjunction with these old documents examined in the past year.
(2) The 1816, which was said to be the "year without summer" due to the eruption of the Tambora volcano in Indonesia, and 1836, which was the most severe in Tenpoh famine, were compared. The research method
We classified the weather recorded in the historical diaries to make them closer to the definitions used by the Modern Meteorological Agency.
The data about the weather for 21 years: 7, 148 days has been gathered. Data1
The Kakuson diary calculated the rate of appearance for the entire period of weather and the period of the eruption of theTambora volcano from 1812 to 1816.
During the eruption period of the volcano, it was found that the rate of appearance of sunny weather decreased, and the rate of occurrence of rain increased.
It can also be seen that the incidence of sunny weather decreased further in the Great Tenpoh famine in1836, and the rate of occurrence of rain increased significantly. Data2
Compared to the weather in May and September of 1816 and 1836 in four ancient documents, it is common that the incidence of cloudy in July is high. The difference between 1816 and 1836 is a marked pick-up in the appearance rate of sunny weather in August 1816. Data3
Compared to the weather in May and September of 1816 and 1836 in four ancient documents, it is common that the incidence of cloudy in July is high. The difference between 1816 and 1836 is a marked pick-up in the appearance rate of sunny weather in August 1816. Data4
Looking at the rate of lightning in the four seasons, the rate of lightning in the summer of 1816 has decreased compared to the previous and previous years. On the other hand, autumn was the highest in 1816. Data5
Here, We decided to compare it with Ms. Mika Ichino`s paper by calculating the weather class and the global solar radiation by referring to the paper of her of the National Institute of Informatics. Since the description of the weather of the old document is various, the diary weather class is classified into three categories: sunny, cloudy, rainy weather and snow. This graph is converted from weather information in ancient documents to total solar radiation each year and compared over multiple years.
From this data, both 1816 and 1836 are lower than the average between 1821 and 1850. In other words, throughout two years, the total solar radiation is low, the cold season continues, and there is an impact on crops, etc., and it can be seen that famine has occurred. Discussion
First,as shown in the data 1 and, the appearance rate of sunny weather in 1812-1816 during the eruption activity period of the Tambora volcano was 36.12%, and it was 1.88% lower than the entire period, so daylight hours may have decreased and temperatures were low.
In addition, rom the data 2, in 1816, from summer to winter of Kakuson diary, the appearance rate of rainy

©2020. Japan Geoscience Union. All Right Reserved.

exceeds the one of sunny weather. It is thought that it was a year when the temperature of summer and autumn did not rise. Second, from data3 ,in the Kakuson diary, Hirosaki diary, Sekiguchi diary and Nijou family diary, the appearance rate of sunny in 1816 and 1836 has decreased.
The Tenpoh famine was to have been particularly severe lying in the Tohoku region, but as the latitude rises, the difference in the appearance rate of sunny between 1816 and 1836 is large. Third, comparing the average of 30 years from 1821 to 1850 and the total solar radiation in the summer of 1816 and 1836, the total solar radiation in both years are low.
Therefore, we think that the temperature also decreased. Summary of the study
(1)The appearance rate of sunny during the eruption activity period of Tambora volcano in the Kakuson diary was 36.31%, 1.71% lower than all periods, and the daylight hours may have decreased and the temperature may have decreased.
(2)It is said that the Tenpoh famine was particularly severe in the cold damage in the Tohoku region, but as the latitude rises, the difference in the appearance of sunny in 1816 and 1836 increases.
(3)The total solar radiation volume was lower than the average from 1821 to 1850 in 1816 and 1836. In other words, for the past two years, we can see that the total solar radiation has been low throughout the year, and the cold season has continued. Challenges for the Future
We will make data of the Sabae domain diarty and restore the weather information by using it. After that , we will analyze it in the wider period.

Keywords: Kakuson diary, Tenpoh famine, ancient document, total solar radiation volume

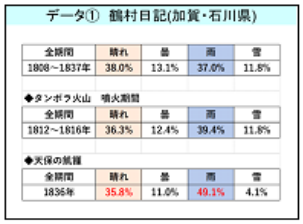

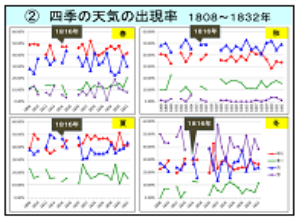

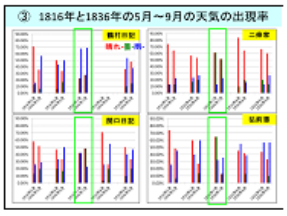

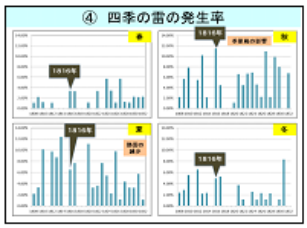

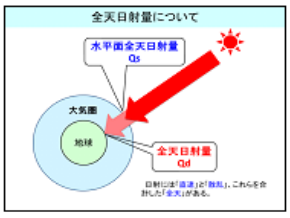

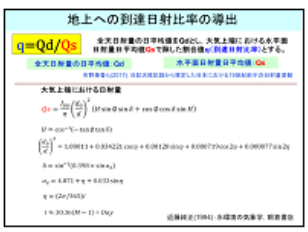

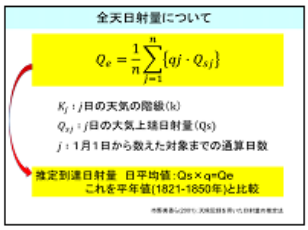

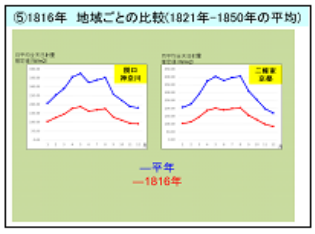

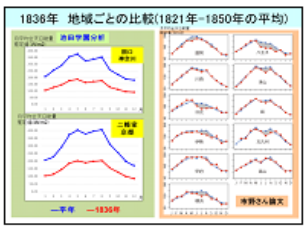

©2020. Japan Geoscience Union. All Right Reserved.

The Project of digitizing seismometer records

*Masaki Yashiro[1], *Akira Taguchi[1], *Eishi Chihara[1], *Katsuaki Miyazawa[1], *Asumi Yamada[1]

1. Yashiro High School

This project is a request from Harvard University professor Ishii Miaki for cooperation from Japanese high school students. We are digitizing seismometer records recorded on paper in the past by using a computer software called DigitSeis. Digitized seismograph records contribute to research in seismology and natural sciences. And it will play an active part in various scenes. We participated in this project because we wanted to help in future research.

©2020. Japan Geoscience Union. All Right Reserved.

Predict future tyhoons with statistics

*Atsushi Kobayashi[1]

1. Yashiro High School

In recent years , I feel that typhoons have caused enormous damage in Japan.I was wondering how the typhoons have changed.So, I created statistical data such as the number of typhoons and their power from some typhoon data.As a result, it was found that the number of typhoons was decreasing and their power was increasing little by little.Convection, which is one of the factors that causes typhoon, is less likely to occur, and the amount of water vapor above the sea has increased. I think that global warming caused these, which affected the results.Global warming is now considered ongoing.Therefore, the number of future typhoons may decrease and their power may increase.

©2020. Japan Geoscience Union. All Right Reserved.

Simplified observation of the bright meteor using web-camera images exposed for two seconds

*Takaaki TSUJI[1], *Naomasa OKADA[1], *Kouki YAMADA[1]

1. Nagoya High School

From August 2019 to December 2019, we conducted photographic observations of meteors by using a web-camera attaching a standard lens towards the night sky and acquiring continuously 2-second exposures.
We collected data of Geminids meteors and identified the radiant hour by hour.
Since this method can set data volume to 1/60 of the usual video observationans of the same time and also can compress it, handling of data is easy.
Therefore, it is possible to record the whole observational data of one evening on a personal computer also in the crowded sky of a city area with many streaks (airplanes and artificial satellites) other than heavenly bodys.
This technique can contribute to the spread of meteor observations.

Keywords: radiant, Geminids, meteor observations, web-camera

©2020. Japan Geoscience Union. All Right Reserved.

Webカメラの2秒露出画像を使った明るい流星の簡易観測

辻 孝明　岡田 直征　山田 紘暉
(名古屋高校地球科学部，指導教員　岡田　素彦・市川　圭太)

＜要旨＞Webカメラの2秒露出静止画連続取得の手法で流星観測を試み，輻射点の決定につながるデータを取得することに成功した。この手法は流星観測の普及に貢献できる。

＜序論＞惑星観測用に購入したWebカメラ(ZWOASI385MC)に標準レンズを取り付けて空に向けたところ，恒星が確認できた。流星観測に使えるのではないかと考え，2秒静止画連続取得による流星観測法を編み出した。近年，流星のビデオ観測が盛んであるが，高感度カメラが必要で，かつ，長時間撮影すると，データが大きくなるためデジタルデータとして扱いにくくなる。今回試みた方法を使えば，比較的安価なWebカメラとパソコンを一晩置きっぱなしにして撮影でき，デジタルデータの取扱も元データ量が同じ時間の動画の60分の1のデータ量になり，さらに圧縮が可能なので，データの取扱が容易である。流星観測の普及につながる内容であると思われるので，報告する。

名古屋高校屋上(5階)にWebカメラを設置

Webカメラ(ZWOASI385MC)

＜研究対象と方法＞　ふたご座流星群の極大日を含む，2019年12月13日～16日にかけての夜間，Webカメラ(ZWOASI385MC)に標準レンズを取り付け，名古屋市の名古屋高校屋上(5階)に設置し，天頂に向け，2秒露出の静止画像を連続取得した。画像解析を行い，毎時の流星数を調べた。流星の多い時間帯について，比較明合成により，合成画像を作成した。

観測方法はURL1に準じ，10分ごとの雲量，最微光星も調べた。最微光星はURL2の表を使用して求めた。
＜使用機材＞
・ZWOASI385MC･･･非冷却 カラーCMOSカメラUSB接続 解像度1936×1096
・ノートパソコン(Dell Vostro3580 Windows10,intel Core i5-8265U,RAM8GB,SDD225GB)
・カメラ用三脚　　・電源ドラム（30m）
＜Webカメラ制御ソフトウェア＞SharpCap3.2.6117
撮影設定は　Colour Space：RGB24，Output Format:PNG Files(*.png)，Exposure:2.0s，Gain:300,Brightness:100とし，「Capture」で「Time Limit」を（12時間の場合）「12：00：00」に設定し，「Start」を押して撮影を開始した。

＜結果・考察＞

- 流星と飛行機，人工衛星を見分けることができた。
- 群流星と散在流星を見分けることができた。
- 輻射点のおおよその位置を示すことができた。
- 流星群の極大の頃流星数が多くなることを示せた。
- 流星の等級は，発光継続時間が2秒であれば,同じ明るさの恒星と同等の明るさで写り,0.8秒であれば、同じ明るさの恒星よりも1等級暗く写るはず。

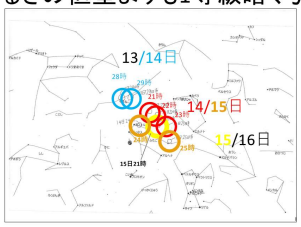

ふたご座流星群
輻射点の移動
2019年12月

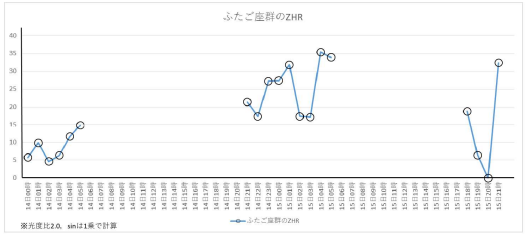

2019年12月ふたご群のZHR〔個/時間〕推移

＜結論・展望＞
2秒静止画連続取得による流星観測は，簡易に流星の個数と軌跡を記録することのできる手段として優れている。
使用する機材が，多目的に使用でき，かつ，比較的安価に備えられるため，高校の部活動で同様の観測に取り組める可能性が高い。複数の地点での同時観測が実現すれば，流星や火球の軌道を特定できるはずである。

＜引用文献･使用ソフトウエア＞
- 〔URL1〕流星の眼視観測をしよう http://s-uchiyama.na.coocan.jp/meteor/visualobs.html (2020年1月6日確認)
- 〔URL2〕International Meteor Organization Determination of the limiting magnitude
  https://www.imo.net/observations/methods/visual-observation/major/observation/(2020年1月30日確認)
- 天体画像処理ソフトウェア　　ステライメージ8（8.0h　アップデータ)
- 天文シュミレーションソフト　　ステラナビゲーター11

©2020. Japan Geoscience Union. All Right Reserved.

Production of improved Rain-go-round

*yuga morita[1]

1. Taki High School

Our club activities have been conducting experiments on acid rain for several years.At that time, we were using a device named Rain-go-round for collecting rain samples.However, as the research progressed, the shortcomings of this device became apparent.I made a device that overcomes the drawbacks.

Keywords: Rain-go-round

©2020. Japan Geoscience Union. All Right Reserved.

the current situation and improvement plans of light pollution around Ichikawa city

*Mutsumi Goto[1]

1. Ichikawagakuen Ichikawa high school

We measured the brightness of the night sky by using SQM(Sky Quality Meter). Based on the measurement results in June and October, we made comparisons under different conditions, such as the season, weather, and surrounding environment, and the current state of light pollution was considered. The results showed that the amount of pollutants in the air, as well as the number of surrounding populations and lighting, was related to light pollution. Removing unnecessary lighting, avoiding cars to reduce emissions, and reducing the amount of garbage in our lives could be a countermeasure for light pollution.

Keywords: light pollution, SQM; Sky Quality Meter, Ichikawa city

©2020. Japan Geoscience Union. All Right Reserved.

Relations of the size of tsunami and the destruction rate of the house

*Keita Ichikawa[1]

1. Ichikawagakuen Ichikawa high school

Hatori (1984) discusses the tsunami damage caused by the Chilean earthquake and the 1933 Sanriku-oki Earthquake in three points: the relationship between destruction rate and tsunami height, water pressure and the location of houses, and water pressure and destruction rate. Therefore, I demonstrated in terms of destruction rate and tsunami height in the tsunami caused by the Great East Japan Earthquake which was not revealed by Hatori (1984) or other previous studies. Graphing the relationship between tsunami height and destruction rate in the 20 areas affected by the main tsunami revealed a positive correlation coefficient. It turns out that the height of the tsunami and destruction rate are related.

Keywords: Tsunami, Tohoku Earthquake, destruction rate

©2020. Japan Geoscience Union. All Right Reserved.

What does annual drainage have an effect on phosphorus cycle of irrigation ponds?

*Hiiro TABATA[1], Yuki TAKAHASHI[1], Ayane INOUE[1], Haruto TAKEYAMA[1], Kousuke MANO[1], Rio YAMANO[1]

1. Hyogo Prefectural Kakogawahigashi High School

Harima, Hyogo prefecture is one of the regions which have the greatest concentration of irrigation ponds in Japan. The goal of this study was to explore the effects involved in “Ikeboshi”, which means draining and drying up ponds for a certain period of time.

Our research was performed to examine whether “Ikeboshi” was effective in improving and maintaining water quality. To prove causal relations, we determined the amount of phosphorous contained in water of two irrigation ponds: Genta-Ike, which had never been drained for decades and Shinkawa-Ike, which is drained once a year.

First, we collected mud from pond bottom, determined its organic matter content and analyzed the elution rate of phosphorous. Then, we have clarified the patterns of annual mutation which phosphorus circulation went through in the drained pond, considering whether the pond is anaerobic or aerobic, and it is drained or not.

Keywords: irrigation ponds, annual drainage, phosphorus cycle, elution, organic matter decomposition

©2020. Japan Geoscience Union. All Right Reserved.

図１　兵庫県加古川市の地図

図２　源太池の池底断面図　出典：現地調査により作成

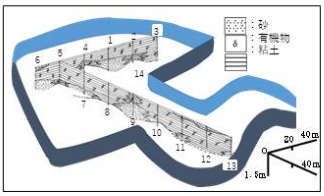

図３　新川池の底泥の堆積構造

図４　底泥の有機物含有率

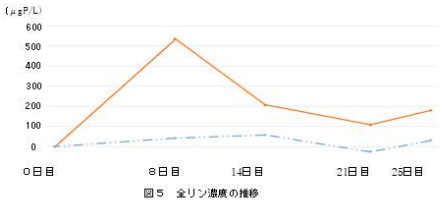

図５　全リン濃度の推移

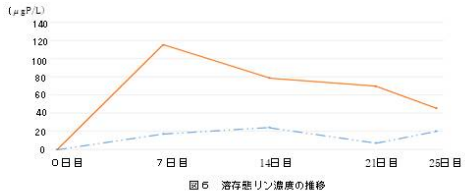

図６　溶存態リン濃度の推移

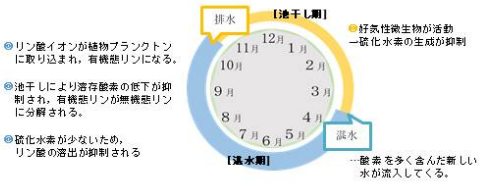

図７　池干しをおこなっている新川池のリン循環モデル

©2020. Japan Geoscience Union. All Right Reserved.

Reviewing Muroto High School Evacuation Management Manual –Investigation on Natural Environment around the Evacuation Site-

*Misaki WATANABE[1], *Kurumi HASHIMOTO[1]

1. Kochi Prefectural Muroto High School

This research examines whether school facilities can work appropriately as an evacuation shelter expected by the “Evacuation Management Manual” developed by Kochi Prefectural Muroto High School.

Muroto High School has a North Building with mainly regular classrooms, South Building with specific classrooms, and the gym/field on its campus. According to the Manual, when an earthquake occurs, most of the classrooms and school facilities will be open for evacuees and a headquarter for disaster control. However, several cracks on the wall have been already found in some classrooms. The area would experience several aftershocks even after the main earthquake. It is not sure whether the school building can survive the shakes.

The Manual decides on an expected capacity for each classroom but it does not include desks and chairs in the class. It moreover does not say that those classroom items can be stored or not.

Geological and geographical environment surrounding the school would be a problem. A hazard map made by Kochi Prefecture says that the location of the school is labeled as a “liquefiable site.” The hazard map also published by the prefecture warns of landslide disasters behind the gym which was appointed as the first evacuation place for school students. We should also consider the river flooding affecting the school evacuation management.

It is not realistic for this research to conclude that “Muroto High School is not suitable for the evacuation shelter” because of the above geological/geographical environment. Kochi prefecture, Muroto City, and Muroto High School have worked together to make an evacuation management. This research, therefore, investigates which school facilities can be used as evacuation shelter safely, and what measures should be taken for safety evacuation management cooperated with Muroto City Disaster Reduction Division and Muroto Geopark Promotion Committee.

Keywords: Evacuation Shelter Management, Evacuation shelter and its surroundings, Earthquake Disaster Risk Management

©2020. Japan Geoscience Union. All Right Reserved.

What Affects the View of Mirage

*#[1]

1. Yokohama Science Frontier High School

Through observations and laboratory experiments, the conditions which mirage is likely to occur were investigated. It was found that some of the mirage was affected by recesses in the observation area and some of them were not. As a result, it was found that the sunshine is the most important factor, and that it is wrong to say that it is easier to see the difference between the temperature on the ground and the temperature in the air. In the experiment, the goal was to generate mirage on a hot plate, but it was not possible to do so. However, when the experiment was photographed through a thermographic camera, it was confirmed that a layer of air had been formed.

Keywords: Meteorology

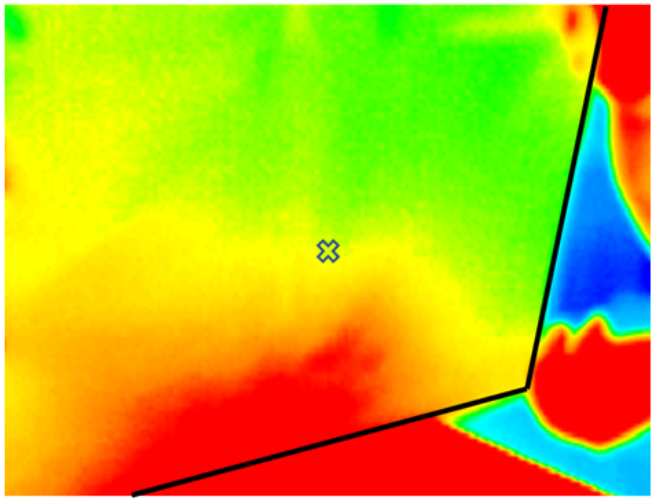

©2020. Japan Geoscience Union. All Right Reserved.

An ancient large earthquake revealed from the trace of the earthquake, and possibility of existence of “Unknown Fault” in Tama Hills

*Takuma FUKUNAGA[1]

1. Yokohama Science Frontier High School

In my research, I speculated two things about “sand boils” and “clastic dikes” found in Kanagawa prefecture and Tama area (suburb of Tokyo) by the field survey. Sand boils and clastic dikes are known as traces of liquefaction phenomenon and they are mainly found in sedimentary rock layers. Due to the decrease in outcrops because of the construction of residential land in recent years, confirmation of the traces was only five places. An earthquake was estimated by the trace’s condition, the positional relationship of traces, and the sedimentary environment of the layers which contain the traces. The first estimation is the reality of the earthquake that triggered them, and the location and scale were estimated using the formula of the distance relation between epicenter and the point which the traces occur. As a result, it was revealed that there was a possibility that an earthquake of magnitude 5.5 or more occurred after 1.43 million years ago near the Tama hills, and an earthquake of magnitude 6.0 or more occurred after 7.00 million years ago in the Shonan area(coast area of sagami bay). The second estimation is about the strange traces that were confirmed in the field survey. Multiple clastic dikes (consist of silt) have been confirmed on the riverbed of the Tamagawa River in Komae City, suburb of Tokyo. As a result of measuring the direction of the dike using a clinometer and examining the distribution of the dikes from GPS position data, it was found that they were in approximately parallel. They seemed Riedel shear as a trace of the strike-slip fault, and it can be seen from the Mi (one of Japanese Katakana characters)-type arrangement that it was caused by the left-slip fault. As a result of checking the relationship between the direction of Riedel shear and the motion direction of the strike-slip fault, and the distribution and direction of the strike-slip faults in the surrounding area, the faults that correspond to the surroundings were not confirmed well, and this trace shows the unknown strike-slip near the Tama hills. Or it was revealed that it may have been caused by the fault or some activity of the Shiozawa fault zone in Shizuoka prefecture (next to Kanagawa prefecture). However, if there is an unknown fault, where is it and how large the earthquake is? Or if it is due to the activity of the Shiozawa Fault zone, how much a fault moves to occur dikes? I have not yet guessed that. These speculations are my future challenges.

Keywords: sand boil, clastic dike, riedel shear

©2020. Japan Geoscience Union. All Right Reserved.

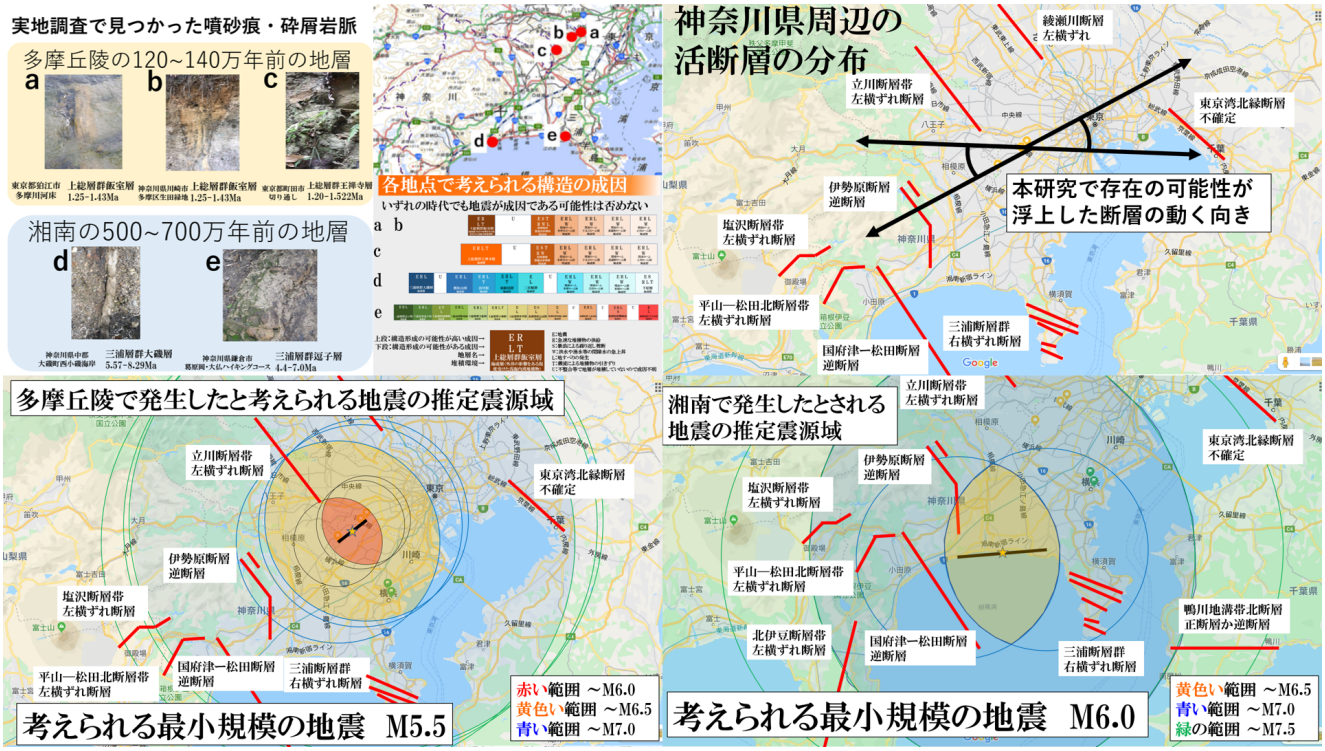

©2020. Japan Geoscience Union. All Right Reserved.

Estimating of paleoenvironment using fossils of shells produced in the Kanzawa Formation, Nakatsu Group

*Hotaka OGURA[1]

1. Yokohama Science Frontier High School

In this study, I collected fossils of shells from an outcrop of Kanzawa Formation, Nakatsu Group, which is distributed in Midori Ward, Sagamihara City, Kanagawa Prefecture and analyzed it and estimated environment of when Kanzawa Formation was piled up.

Kanzawa Formation is a marine sediment which is piled up about 2.5 million years ago and wide variety of fossils are produced in Kanzawa Formation. A lot of studies about Kanzawa Formation have been conducted, but air temperature, sea water temperature, influence of sea current, bottom sediment of sea floor which Kanzawa Formation was piled up, sea area which Kanzawa Formation was piled up and so on are not clarified in detail. So, in this study, I estimated these paleoenvironments in detail.

As a result, I estimated that air temperature and sea water temperature of those days was similar to those of the present coast of Kanagawa prefecture and Shizuoka prefecture and the vicinity of where I collected fossils was influenced by both a warm sea current and a cold sea current

Also, I estimated that a basin or a shallow sea whose most of sea floor was covered with sand spread there. From these, I estimated the environment of the vicinity of where I collected fossils was similar to those of the present coast of Sagami Bay or Suruga Bay.

In the future, I think that I will compare fossils of shells using in this study with fossils of pollen and foraminifera produced in Kanzawa Formation and fossils of Kazusa Group and Miura Group, which was piled up in the same period of Kanzawa Formation. Also, I think I will estimate environment of each period and estimate climate change.

Keywords: Kanzawa Formation, Nakatsu Group, fossil of shells, paleoenvironmennt, Sagamihara

©2020. Japan Geoscience Union. All Right Reserved.

Evaluating the Effect of Global Warming on Yokohama Using Nightlight Satellite Data and Large Point Sources Data

*Sota Komiya[1]

1. Yokohama Science Frontier High School

Global warming refers to the increase in the earth's average temperature that occurs naturally or, as theorized in recent years, is induced by human activity. It was alarming for many people in Japan that so many factors affected our planet. This investigation uses two kinds of data: D1-Nightlight Satellite Data from NASA and D2- Large Point Source from the Japanese Ministry of the Environment in order to analyze greenhouse gas emissions using the Nightlight and Large Point Source data. This work introduces a new way to investigate the greenhouse gases emissions in Yokohama using kernel density estimations and makes some grids to identify key areas to observe for consumption of greenhouse gases. In this investigation, there were two major methods of observation (1) requesting disclosure of data regarding greenhouse emissions and (2) making a coordinates table from the data. This helped in identifying the greenhouse gas situation in Yokohama. This research is now undergoing its final stage in gathering more data and analyzing the greenhouse effect in Yokohama.

Keywords: Environment, Global Warming, Greenhouse Gas

©2020. Japan Geoscience Union. All Right Reserved.

Comparison of Fluid Resistance and Experience for Calculation of Resistance Coefficient according to Object Shape

*Senri Shimamura[1]

1. Sakaehigashi Senior High School

At first, we measured air resistance with variation of shape by dropping physical objects from a height of 15.75 meters, the fifth floor of our school building. As Experiment 1, we prepared four kinds of wooden objects such as cube, quadrangular pyramid, cone and sphere with similar volume (Table 1). The result of the experiment includes errors caused by deficiencies of shape varieties and data, being inhomogeneous of density of wood, inaccuracy of shape, and by rotation of falling object around its horizontal axis. For the purpose of improving these problems we used the same settings as Experiment 2. We prepared six kinds of objects adding column and rectangular parallelepiped made by a 3D printer with a filament of PLA resin (Table 1). The problem of rotation of the falling object was solved by passing a nylon thread through the center of each object. According to the above two experiments, the resistance depends on the front shape of the object. A globe has the smallest value of resistance, followed by pyramidal or conic shape and a flat shape has the largest value. The order corresponds to the tendencies in textbooks for senior high school students and college students.

Next, we focused on the cones in the above six kinds of shapes. Cones are one of the most useful shapes in daily life. We can easily reproduce several patterns of apex angles. Therefore, we attempted to estimate the values of the fluid resistance coefficient in conjunction with the apex angles using two methods. One method is hitting the object with fluid and the other is calculating the coefficient from the terminal velocity of the falling object. We called these Experiment 3 and 4, respectively.

In Experiment 3, eight types of objects (Table 2) with different central angles were made with the 3D printer. The cones were suspended by spring scales, and we poured water fallen freely on them from a position a certain distance away from the objects. When water is allowed to fall freely on the top of an object, the pressure applied to the object is measured in gram weight units, and the pressure can be calculated. The resistance coefficient was calculated from the experimental results, and a graph corresponding to the change in the central angle was created (Fig 1). Fig 1 shows a curve in which the resistance coefficient increases exponentially with the increase in the central angle. Also, the resistance coefficient obtained in the experiment was displayed using function display software (FunctionView Ver 6.02), and the approximate function was predicted to obtain the equation to calculate resistance coefficient. Exponential function expressions are cumbersome and the accuracy of the approximate expression is not known. To simplify the calculation and use the standard deviation to estimate the expression more accurately, a first-order approximation using logarithms is used. An approximation using logarithms to make calculations is easier and to use the standard deviation estimates a more accurate expression. Further, the value of the resistance coefficient obtained in Experiment 3 was lower than the value described in the above reference book or the like. As the reason, we thought to be that the area that the dropped water hits is smaller than the projected area of the object, and that there is a diffrence in the force between "the object moving in the fluid" and "the fluid hitting the stopped object".

In Experiment 4, we prepared cones with no bottoms (hollow cones) with different apex angles made of copy paper (PPC paper) of uniform thickness. And we experimented in the same place in the author's house for the whole experiment (no wind, indoors). After dropping the object from a height of 2.5 meters

©2020. Japan Geoscience Union. All Right Reserved.

above the floor, the speed reached terminal velocity at 2.0 meters above the floor. We measured the time taken from 2.0 meters above the floor to the landing. The terminal velocity is calculated from the measured time, and the resistance coefficient is obtained. In Experiment 4, as in Experiment 3, we will create a graph which shows relationship between central angle and resistance coefficient, and predict approximated equation using the function software.

Keywords: Fluid dynamics, Air resistance, Resistance coefficient, Cone

©2020. Japan Geoscience Union. All Right Reserved.

表 1　実験 1・2 で用いた各物体の概形及び体積（実験 1(Experiment 1)：1～4　実験 2(Experiment 2)：1～6）

Table 1　Rough shapes, its vertical sections and volumes of each object used in the Experiments 1 and 2.

番号(No.)	1	2	3	4	5	6
形状名 (shape name)	球 (sphere)	円錐 (cone)	四角錐 (quadrangular pyramid)	立方体 (cube)	円柱 (column)	直方体 (※1)
概形※2 (rough shape)	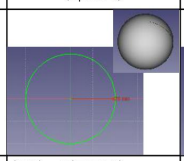	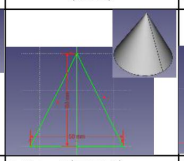	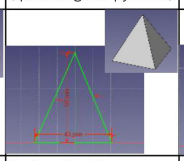	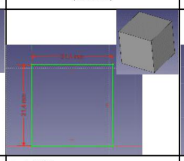	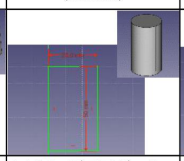	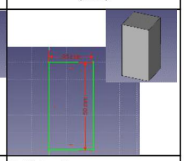
体積 (volume)	(4/3)×3(円周率) ×2^3 =32.00〔cm³〕	2.5^2×3(円周率) ×5×1/3 =31.25〔cm³〕	4.3^2×5×1/3 =30.82〔cm³〕	3.14^3 =30.96〔cm³〕	1.44^2×3(円周率)×5 =31.10〔cm³〕	2.5^2×5 =31.25〔cm³〕

※1　rectangular parallelepiped

※2　概形(右上)・鉛直断面図(左下) / rough shape and its vertical cross section

表 2　実験 3 で用いた円錐の中心角及び概形

Table 2　Central angles and rough shapes of the cones used in the Experiment 3.

中心角 (central angle)	30°（A）	40°（B）	45°（C）	50°（D）
概形 (rough shape)	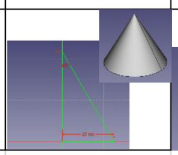	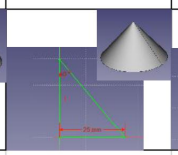	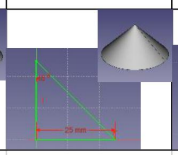	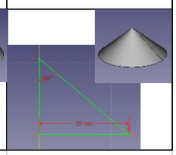
中心角 (central angle)	60°（E）	65°（F）	70°（G）	75°（H）
概形 (rough shape)	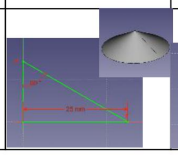	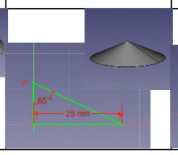	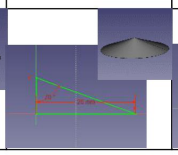	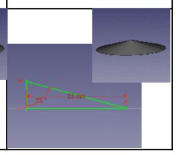

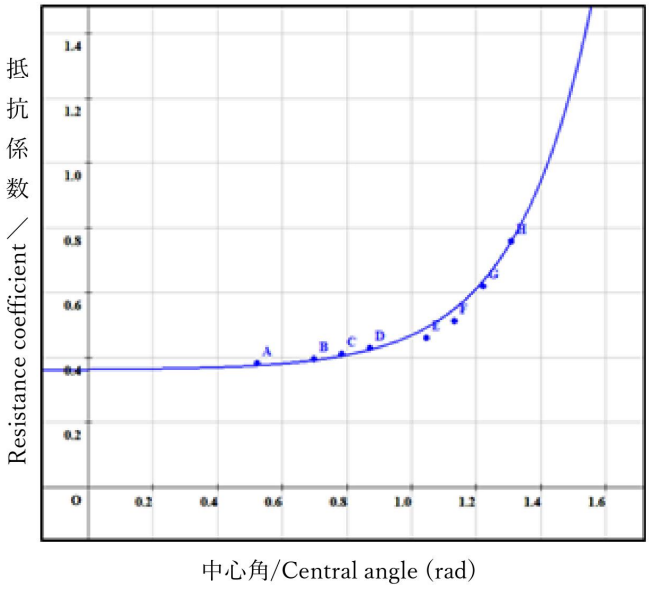

・A~H support the points plotted in the Figure 1, respectively.

・The real line shows the estimated function in this study.

$$C_d=0.36+1.2\exp[4.2\{\theta-(\pi/2)\}]$$

(Therefore, C_d and θ are resistance coefficient and central angle, respectively.)

図 1　実験 3 によって得られた円錐の中心角と抵抗係数の関係(実線は本研究で推定した関数)

Fig 1　Relationship between central angle and resistance coefficient by the Experiment 3.

©2020. Japan Geoscience Union. All Right Reserved.

Examination of evacuation routes considering damage caused by liquefaction

*KOYA TAKAHASHI[1]

1. tosa high school

Currently, evacuation drills for the Nankai Trough Earthquake are carried out in Kochi City. However, I realized that the damage predicted after the earthquake is not taken into account. Therefore I wonder if we can evacuate safely in the same way as the evacuation drills when the earthquake occurs. Then, I studied the influence of ground liquefaction on evacuation in order to propose more realistic procedure for evacuation.

In this study, I targeted Ushioe area in Kochi City. When the earthquake occurs in the assumed maximum scale, it is predicted that a more than 30cm–high tsunami, which makes our evacuation difficult, will reach 30 minutes after the earthquake occurs. Also, it is predicted that ground subsidence will happen due to liquefaction, so a hazard map was created by earthquake specialists. At first, I thought to use this hazard map in this study, but I recognized that this hazard map was not detailed and I couldn’t consider narrow areas because it adopted 250m mesh. For this reason, I decided to create my own hazard map. I obtained some documents of the boring survey in this area and read the information such as “Fine particle content”, “N value” and so on in the data. And, I calculated "the earthquake shear stress ratio", "the dynamic shear stress ratio" and "a liquefaction index" (PL level). Then I calculated the liquefaction index at the point, and I made a hazard map of the 125m mesh based on the value.

I actually superimposed the evacuation routes used in the evacuation drills on my hazard map. Then I found that some liquefaction would occur over a wide area. And, in this area, about three-minute shaking is predicted. Therefore, we can’t start to evacuate within four minutes after the earthquake occurs. Also, we need two minutes for vertical evacuation. It means that we can have only 24 minutes to evacuate. That is why I decided to compare the evacuation considering damages caused by liquefaction with that not considering them. I focused on an area which will have a big damage caused by liquefaction. I selected 18 places randomly, and simulated two evacuation patterns.

First I considered the evacuation not considering the damage caused by liquefaction. In this case, I found that people in the 18 places can evacuate in 24 minutes, and more than half of them can in 15 minutes. From these things, I found that administrative agencies had established evacuation shelters in consideration of evacuation time and the number of people.

Next, I considered the evacuation considering the damage caused by liquefaction. In this case, I found that there are some evacuation routes which we won’t be able to use because of liquefaction. For this reason, we need to go a long way round and it takes long time to go to shelter. Also I found that it takes 1.5 times as long as the first research, and some people can’t evacuate within 24 minutes. For these reasons, we must regard these areas as vulnerable to damage by liquefaction. That is why I feel that not only the number of the evacuation routes but also the shelters should increase even more.

In this study, I only studied an evacuation when the routes are damaged by liquefaction of the ground because now we don’t know where liquefaction will occur. So now, we will have to evacuate looking for a safe evacuation route. As a result, we will actually spend more time to evacuate than this prediction.

©2020. Japan Geoscience Union. All Right Reserved.

Because of these, it is necessary to inform people more about the danger of the damage caused by liquefaction. And, local governments need to examine evacuation drills considering damage by liquefaction.

In this study, I considered only evacuation routes considering damage caused by liquefaction. But, actually there will be various factors which will make our evacuation difficult, for example, collapse of block walls and wooden buildings. For this reason, I think that it is necessary to consider more factors in order to make realistic procedure for evacuation.

Keywords: earthquake, liquefaction

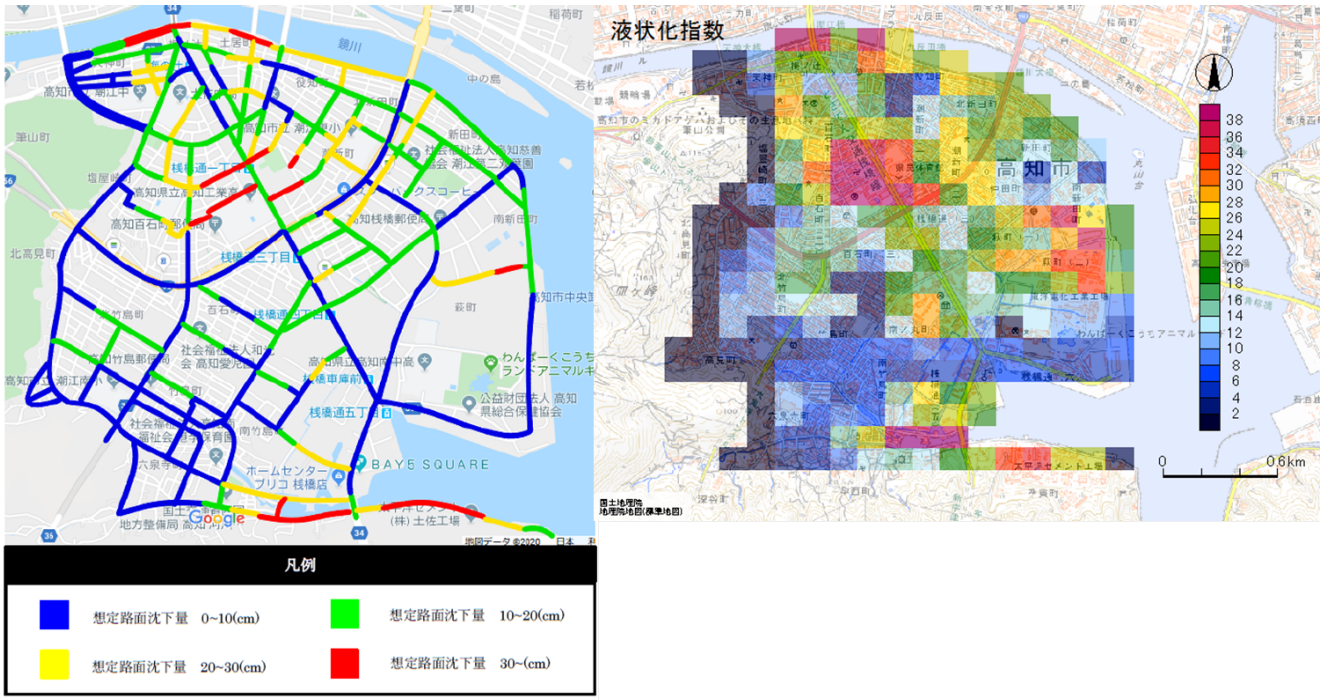

避難路用の道路での地盤の液状化による想定路面沈下量

©2020. Japan Geoscience Union. All Right Reserved.

Relationship between four giant jets in the past and meteorological phenomena in the troposphere

*Yuya Okubo[1], Huga Suzuki[1], Yuya Takahashi[1]

1. Shizuoka Prefectural Iwata Minami High School

“Transient Luminous Events” is a discharge light emission phenomenon that occurs from the stratosphere to the lower thermosphere at about 20km to 100km above the sky. Giant jets are also a kind of this type. It is inverted cone-shaped luminous phenomenon .its lower end is at about 20km above the sky and upper end is at about 70km to 90km above the sky. Our school has been observing high-altitude luminous phenomena using three high-sensitivity CCD cameras every night since 2007. There are few observation examples, and the unexplained portion occupies most of the occurrence mechanism.

In past studies, there were some problems in its process. One is that although there were four observation records, only one giant jet was investigated. The other is that the cause of the rise in seawater temperature and the decrease in temperature above the sky has not been verified other than those mentioned above.

In this study, a total of five giant jets were studied, all four giant jets observed at our school and those that occurred off southern Kanto in September 2019 and we did a survey on them in the way we did in the past. Then, we found that the value of direct solar radiation energy and downward infrared radiation was not so large at the observation points nearest the points which giant jets occurred in the day which giant jets occurred compared with other days in the same month. In addition, only two out of five cases the cold front passed , which was attributed to a decrease in the temperature above the sky. From these results, it was verified using the seawater temperature map and radiosonde upper temperature data to confirm whether the seawater temperature rise and the temperature decrease in the sky actually occurred. Then, the seawater temperature was higher than the average value during the days around the giant jet occurred, and when the temperature of the sky was compared with the average of the week before and after the day when the giant jet occurred, there were places in the troposphere where the day when the giant jet occurred was lower. From the above, it was found that the situation described in the previous research was correct. From the fact that seawater was not warmed by solar radiation, we first expected the warm seawater flowed in from other waters. Therefore, we used the figure showing the velocity of the ocean current. Then, it was found that the two giant jets for which data were obtained were near the end of the area where the current of the Japan Current, which is a warm current, was fast. This suggests that warm seawater from the tropics was rapidly transported and reached the vicinity of the giant jet occurrence site at a high temperature, where it stayed there. Next, the cause of the lowering of the temperature in the sky could be read again from the weather map. We found that of the five days which giant jet occurred, on all three days when the cold front did not pass, there was a low pressure near the point where the giant jet occurred, a high pressure on the east coast of mainland China, and a north-south high-low pressure arrangement. This suggests that cold air was flowing from Siberia.

Based on the above, the occurrence mechanism common to these five giant jets was considered. As a result, the giant jets were caused by a rise in seawater temperature due to warm currents, and a strong ascending current caused by the temperature difference caused by the passage of the cold front or the inflow of cold air into the sky due to the north-south high-low pressure arrangement. The ice crystals intensely collided with each other, resulting in the separation of enormous amounts of charge, which led

©2020. Japan Geoscience Union. All Right Reserved.

to the conclusion that a discharge occurred from a cumulonimbus cloud containing a large amount of charge, resulting in a giant jet. In addition, the giant jets are considered to occur easily sea areas where the seawater temperature tends to be high like off Shikoku and south of Kanto and off Chiba and Ibaraki Prefecture.

Keywords: Transient Luminous Events, Giant jets

©2020. Japan Geoscience Union. All Right Reserved.

Spectroscopy of plasma generated in a microwave using a newly developed simple spectrometer with high resolution

*Ayaka Akase[1], *Kento Takase[1], *Reiji Iwamoto[1], *Keishi Okumi[1], *Mayu Naito[1], *Hiromu Fujimoto[1], *Yamato Yasuhara[1], *Natsuki Yamamoto[1]

1. Hyogo Prefectural Himeji Higashi Senior High School Science Club (Plasma team)

We conducted the following basic research on plasma. When a mechanical pencil’ s core is heated in a microwave oven, yellow plasma is emitted. High resolution spectrometers are expensive and we cannot buy them. In order to confirm the identity of this light, we developed the simple spectroscope that has the resolution to split the D line of a sodium lamp into two lines, and that can obtain a stable and clear image with a digital camera. We used this spectrometer to split the plasma light emitted from the mechanical pencil’ s core in a microwave oven. As a result, the light was found to be a strong emission line of sodium. The plasma is generated by exciting the sodium of the ceramic table by the mechanical pencil's core acting as an antenna.

Keywords: plasma in a microwave oven, developed of the simple spectroscope, exciting of the sodium

©2020. Japan Geoscience Union. All Right Reserved.

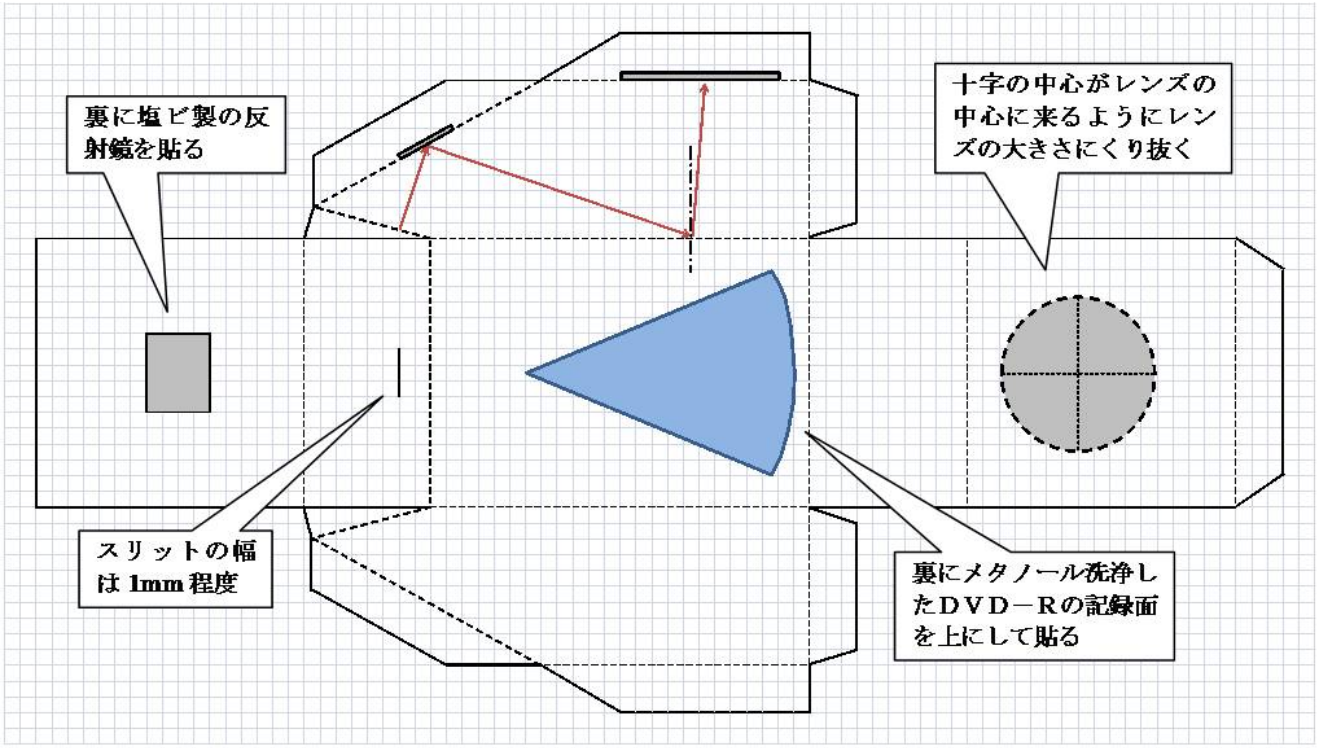

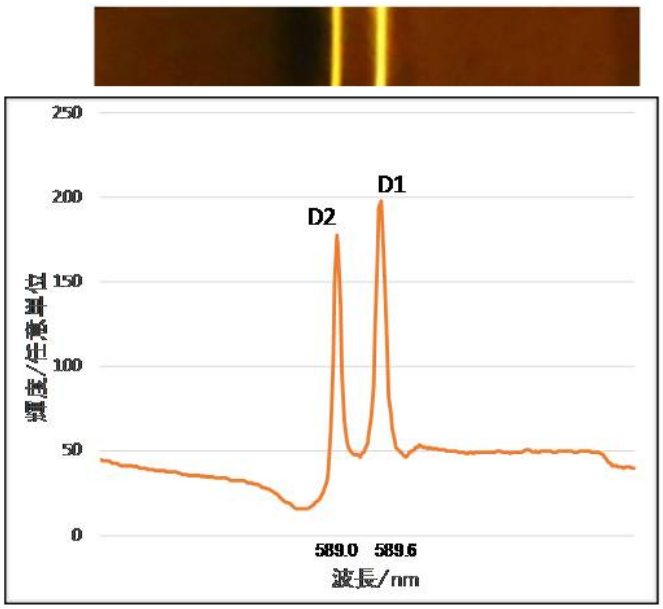

上：製作した簡易分光器の型紙とその精度（ナトリウムのＤ線が２本に分光されている）

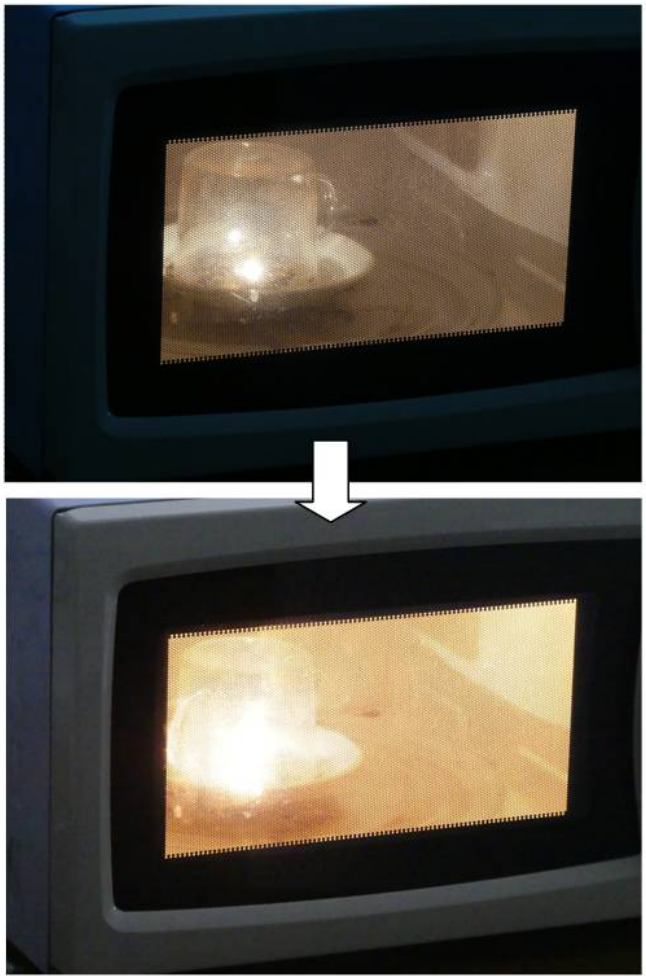

右：電子レンジ内でシャープペンシルの芯の両端から周期的にプラズマが発生し、ガラスのコップ内上方で一体となるようす

©2020. Japan Geoscience Union. All Right Reserved.

Circulation of residual magma during consolidation of granitoid magma

*Kento Takase[1], *Ayaka Akase[1], *Reiji Iwamoto[1], *Keishi Okumi[1]

1. Hyogo Prefectural Himeji Higashi Senior High School Science Club (Magma team)

The Harima granites which are spotted between Himeji and Kakogawa city, and the Rokko granites which are widely distributed in Kobe city, intruded rhyolite tuff in the late Cretaceous. We have found that the amphiboles of the Harima granites has an oscillatory zonal structure with a width of several micrometers. We estimated the environments at the latest magma differentiation process based on the features of this structure. This structure is not found in Rokko granite amphiboles. The Harima granites are considered to be the periphery of the rock body because the surrounding tuff is thermally metamorphosed. The oscillatory zonal structure of amphibole was formed by secondary ion replacement by circulation of the residual magma. On the other hand, this structure was not found in the Rokko granites, indicating that the circulation of magma residue does not occur in the center of the huge rock body.

Keywords: Harima granites, oscillatory zonal structure, circulation of the residual magma

©2020. Japan Geoscience Union. All Right Reserved.

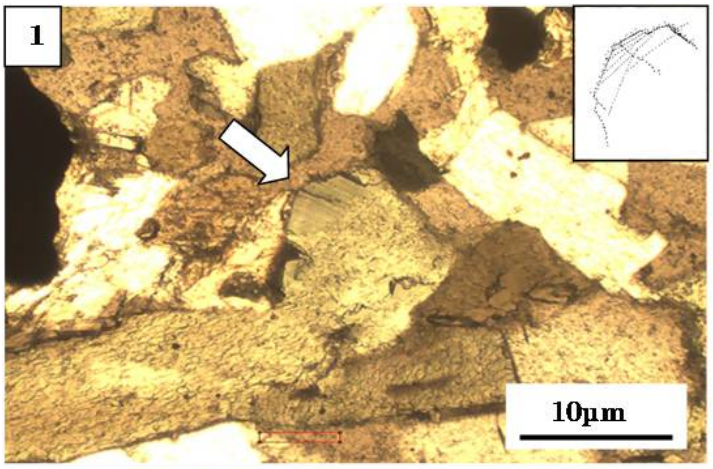

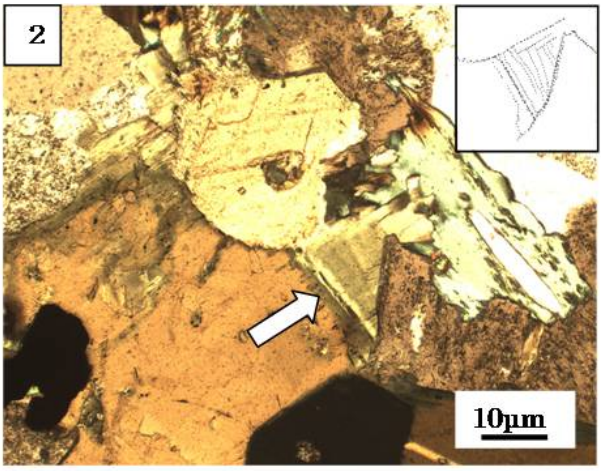

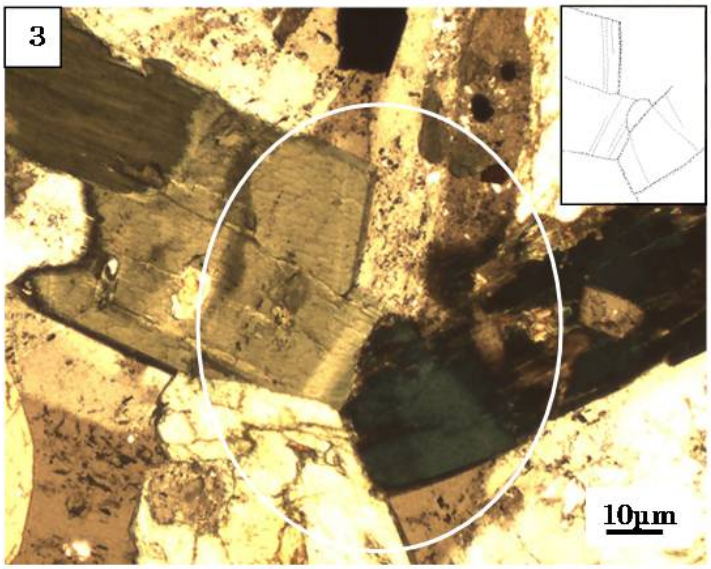

（1）姫路市の花崗閃緑岩の角閃石の波状累帯構造（オープンニコル×100）
（2）加古川市の花崗閃緑岩の角閃石の波状累帯構造（オープンニコル×100）
（3）加古川市の花崗閃緑岩の角閃石の波状累帯構造（オープンニコル×100）

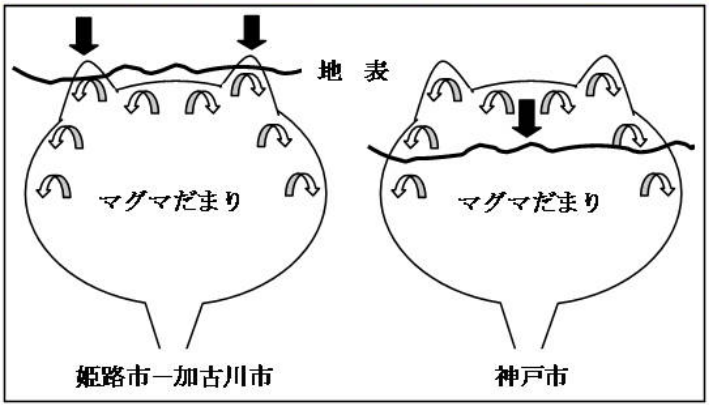

マグマ残液の循環の仮想モデル図
（矢印は熱水の循環を表わす）

©2020. Japan Geoscience Union. All Right Reserved.

Indicate the intensity of ultraviolet rays using the degree of fading of cotton yarn dyed with reactive dye

*Natsuki Yamamoto[1], *Ayaka Akase[1], *Kento Takase[1], *Reiji Iwamoto[1], *Keisi Okumi[1], *Mayu Naito[1], *Hiromu Fujimoto[1], *Yamato Yasuhara[1], *Nanami Kishimoto[2], *Sayuki Fujii[2], *Nagisa Yokoyama[2], *Soya Obata[2], *Hinako Kobayashi[2], *Haruki Murakami[2], *Reo Yamada[2], *Syo Yoshida[2]

1. Hyogo Prefectural Himeji Higashi Senior High School Science Club (Ultraviolet rays team), 2. Hyogo Prefectural Nishiwaki Senior High School Earth Science Club

Ultraviolet rays fade the color of clothing. We thought that the intensity of ultraviolet rays could be indicated using the degree of fading of cotton yarn dyed with a reactive dye. The following three points became clear as a result of irradiating the cotton yarn of three colors of blue, yellow and red with ultraviolet rays. (1) Ultraviolet rays damage fibers, and the strength of fibers becomes extremely low after the sixth day of irradiation. (2) The ratio of magenta to cyan decreases until the sixth day of irradiation, and the blue and red yarns fade. This indicates that magenta has been destroyed by ultraviolet rays. (3) This tendency is not seen in the yellow yarn. The yellow yarn is less likely to fade than the blue and the red yarn. The intensity of ultraviolet rays can be indexed by the ratio of magenta dye to cyan.

Keywords: reactive dye, intensity of ultraviolet rays, fading

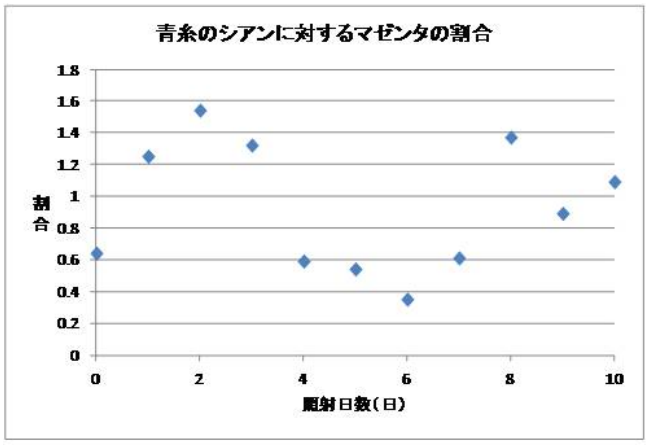

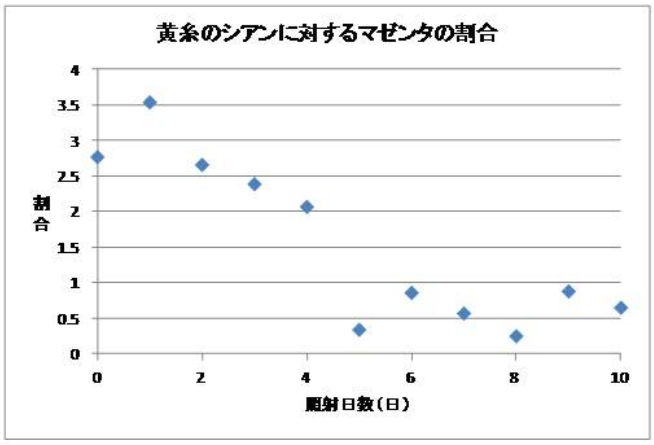

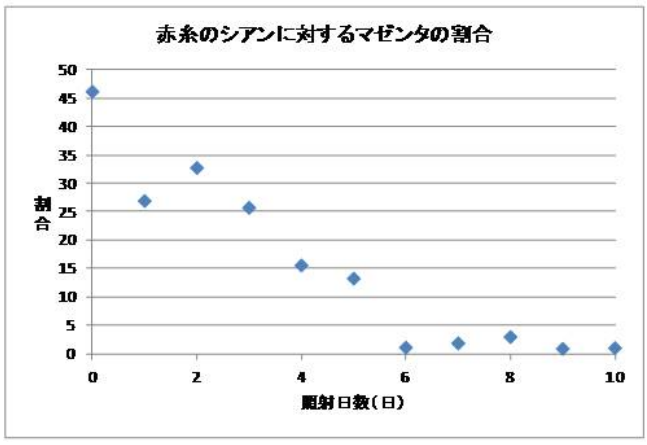

©2020. Japan Geoscience Union. All Right Reserved.

Seasonal alterations in carbon assimilation of marine organisms

*Hiroto ICHIKAWA[1], Hayato Kurosawa[1], Ryushi Abe[1]

1. Miyagi Rifu high school

We have conducted the ocean water salinity and ion measurements in Matsushima Bay, we have found that salinity and Ca caions are seasonally varying. It is easy to imagine that the fluctuations will be influenced by the inflowing freshwater and the living organisms in the ocean.
We will mention about the relationships between carbonate quantity which composed in the calcareous organisms incorporated and sea water Ca cation as which has a loose relationship.

Keywords: Ocean salinity and biosphere, carbon dioxide in the shell

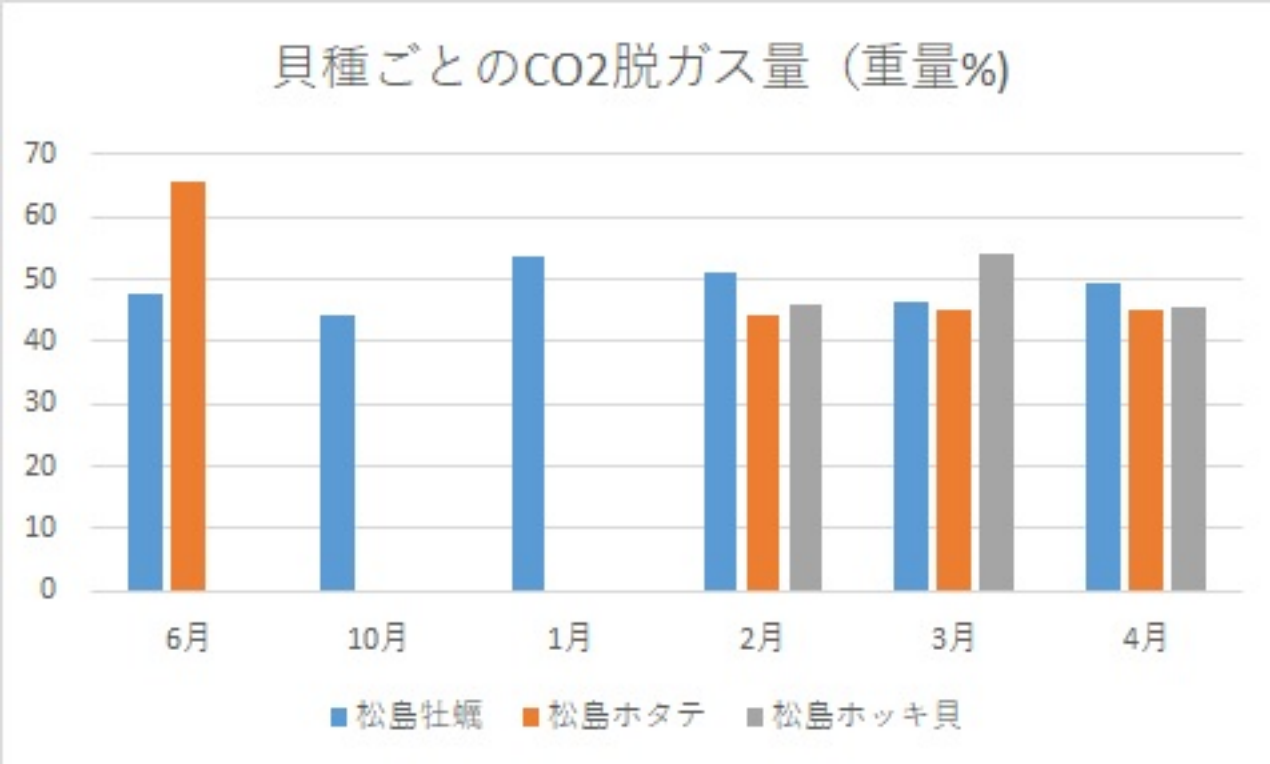

©2020. Japan Geoscience Union. All Right Reserved.

The relationship between Intensity of radiation energy and soils variety

*Ryushi Abe[1], Hiroto Ichikawa[1]

1. Miyagi Rifu high school

We have been monitored changes in environmental radiation quantity over the past three years. We also found that the influence of the measured ground (weather, water content) is strongly affected. In our previous study have shown that the difference in the soil of the ground tends to lower the dose due to the difference in volcanic soil, mulch, and sand, and the large amount of water.

This time, we made a device that puts soil in a plastic container and puts a space where a Geiger counter can be put in the soil, put Kanuma soil, Akatama soil, zeolite, river sand in it and see the difference in dose. Whether the test was conducted 20 times, it was observed that there was a significant decrease in the dose in Kanuma soil, etc., although it depended on the weather conditions such as humidity.

It is a content that we realize that there are very many errors as the experiment continues, but we will have a presentation together with the evaluation of the error of the experiment how the soil brings about the high or low radiation doses.

Keywords: Natural radiation energy monitoring

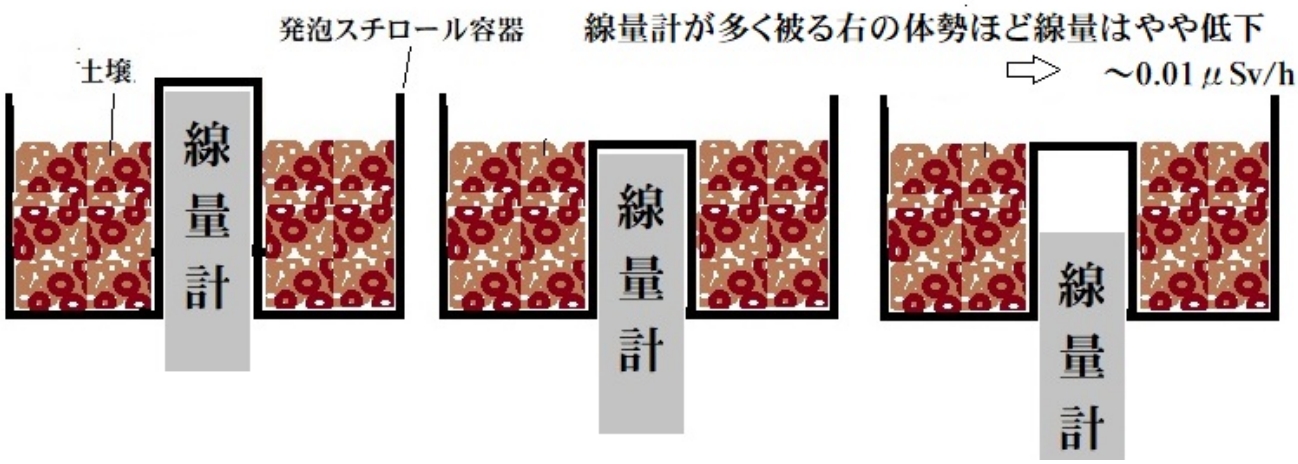

©2020. Japan Geoscience Union. All Right Reserved.

Specific heat of various soils measured by radiation thermometer

*Hayato Kurosawa[1], Hiroto Ichikawa[1]

1. Miyagi Rifu high school

The ground is composed of various substances. When the same amount of heat is applied, the temperature rises and falls differently. In order to mention the homeostacy of the environment or investigate the greenhouse effects, it is useful to compare the thermos-tendency, . When measuring the temperature, we measured the temperatures for several times under similar conditions using a infrared radiation thermometer.
When the sun is strong, the temperature changes greatly on asphalt and soil. Therefore, even if the same heat is applied, the way the temperature rises greatly differs depending on the soil and ground components. From this fact, it is considered that the various materials that make up the ground have different specific heats, so an investigation was conducted using a radiation thermometer (SK-8940, SATO).
The difference in heat capacity between asphalt and brick was small and the influence of external factors was small, but the difference in heat capacity between grassland, sand and soil was large. I thought that this might be influenced by external factors such as wind. To obtain the heat capacity of vegetated soil, and thus the specific heat, it will be necessary to measure under more stable conditions.

Keywords: Soil components, Heat capacity of the soils

赤外放射温度計で計測

measured by infrared radiation thermometer

計測場所　1～7：植生込み　A～D：舗装部

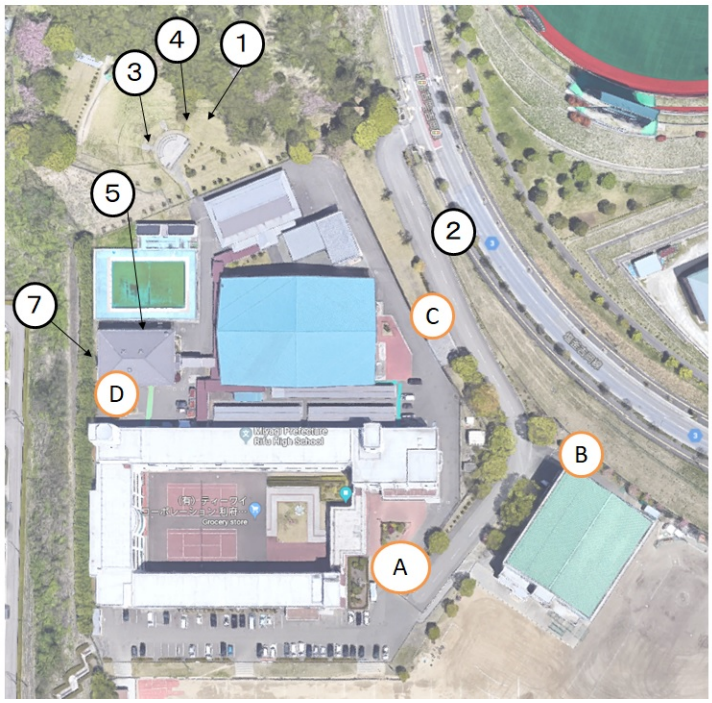

©2020. Japan Geoscience Union. All Right Reserved.

Relationship between astronomical observation and water vapor in weather forecast

*Aoi Takamori[1]

1. Suwa Seiryo Senior High School

1.Motivation and purpose

The purpose of this study was to estimate the amount of water vapor from the visibility of stars and to predict the weather.

2.Research Methods

2-1 Observations

The weather conditions in the upper reaches of the sky were analyzed by the upper-height weather map (850 hPa).

2-2 observation base

In order to verify the accuracy of the data obtained by the wind thermometer and hygrometer, three observation sites were set up in the vicinity of our house (Fig. 3).

2-3 Exposure time

In order to quantify the way stars are seen, the degree of exposure (in seconds) in which the target star no longer appears in the photograph is called the exposure time.

3. observation results

3-1 Purpose.

The purpose of this study was to determine the amount of water vapor from the visibility of stars, and to explore the relationship between the amount of water vapor and humidity observed by the wind speed

©2020. Japan Geoscience Union. All Right Reserved.

thermometer and hygrometer and the exposure time observed by the camera application.

3-2 Results.

2 It was found that the exposure time of the plots surrounded by orange circles in Fig. 5 was significantly different even though there was almost no difference in humidity.

3-3 verification

Based on the above, I hypothesized that the difference in the visibility of the stars was caused not only by the ground but also by the sky above.

Difference of humidity on the ground 1%...(1)

The difference in humidity in the sky is 17%...(2)

From (1) and (2), it was found that the visibility of the stars is significantly different depending on the high humidity in the sky, even if the humidity on the ground is the same. In addition, in order to investigate the cause of the results in *1 and *3, we analyzed the upper-tier weather map.

The difference between the dew point and the temperature at 9:00 a.m. on the day of the observation is less than 9.78 degrees Celsius...(3)

The difference between the dew point and the temperature at 9:00 a.m. on the day of the observation was more than 22.25 degrees...(4)

From (3) and (4), it was found that it rained when the difference between the temperature and the dew point (humidity) at 9:00 a.m. on the day of the observation exceeded 22.25˚C in winter and summer.

3-4 Considerations.

When it rained the next day, the day of the observation was covered by a high pressure system with dry air (Fig. 7), but a low pressure system with moist air that generated precipitation on the day after the observation was advancing from the west (Fig. 8).

4. Weather forecasting

4-1 Purpose.

©2020. Japan Geoscience Union. All Right Reserved.

The time of exposure was substituted for the straight line of graphs in Figs. 4 and 5 to find out the relationship between the amount of water vapor and the amount of precipitation on the next day.

4-2 ways

Amount of precipitation on the next day ÷Amount of water vapor derived by substituting a straight line...(5)

Equation (5) compares the values derived from the equation (what percentage of the water vapor on the day of observation will be the precipitation of the next day).

4-3 Results.

Thirty percent of the values obtained in (5) were approximated in the 10% range.

4-4 Considerations.

On a day when the values were in the teens, the high-rise weather map seemed to show warm, moist air entering the area where the contour line rises from the south to the north.

5.Conclusion.

It was also found that depending on the weather conditions in the sky above, a percentage of the amount of water vapor observed on a given day would change to the amount of precipitation on the following day.

6. Issues and suggestions for improvement
In the future, I would like to estimate the tendency of the amount of water vapor only by the way the stars look based on the relationship with the method that can be observed every day, and finally, I would like to be able to predict the weather only by the way the stars look.

Keywords: Weather forecasting, Astronomical observation, Water vapor

©2020. Japan Geoscience Union. All Right Reserved.

観測時期	対象とした星	等級
2019年2月～3月	オリオン座のA星	情報なし
2019年4月～7月	北斗七星	３等星
2019年8月～10月	白鳥座	３等星
2019年11月～2020年1月	オリオン座のA星	情報なし

図1 対象とした星

図2 ★対象としている星

図3 観測拠点

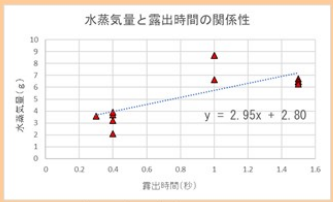

図4 オリオン座(2019.11～2020.2)を対象とした

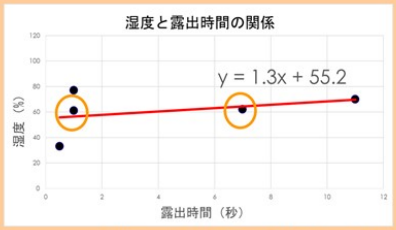

図5 北斗七星(2019.4～7)を対象とした

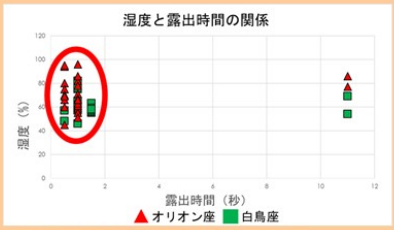

図6 オリオン座(2019.2～3)と白鳥座(2019.8～10)を対象とした

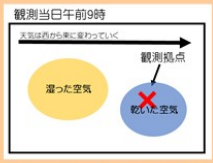

図7 観測当日の午前9時の気象状態

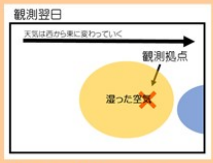

図8 観測翌日の気象状態

©2020. Japan Geoscience Union. All Right Reserved.

Research about Moriya Formation

*Yusuke Morozumi[1]

1. Suwa seiryo senior high school

I checked the fossils from Moriya formation to identify the geological time and the depositional environment of it.

I discovered some fossils of *Mizuhopecten kimurai* that is the index fossils of Langhian. So,the geological time is Langhian. Many people told that it was Aquitanian or Burdigalian. It’ s wrong.

However,I collected many fossils of *Anadara* and *Macoma* from old formations. They lived in the shallow sea. So,there was the shallow sea. But I collected many fossils of *Mizuhopecten kimurai* and *Cyclocardia siogamensis* from new formations. They lived in the deep sea. So,there was the deep sea. These results told that the sea got deep. I checked the formations in detail, I discovered some traces of transgression and regression.
In addition, I compared the fossils from Moriya formation with the fossils from other formations. I discover some common points and differences. If I check these discoveries in detail, I can identify the sea connection in Fossa Magna area.

Keywords: Moriya Foration, Geological time, Depositional Environment

図：調査地点の位置

図：露頭Aの様子

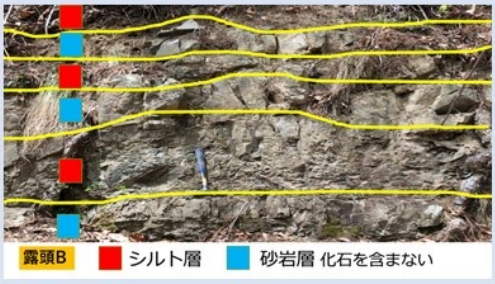

図：露頭Bの様子

図：露頭Cの様子
最上位の砂岩層のみ

図：露頭Aから産出した
キムラホタテ

©2020. Japan Geoscience Union. All Right Reserved.

Making solid version chromatography ~Separation and identification of solid particles by magnetic field gradient using microgravity~

*Satoru Kitada[1], Takuya Hanasaki[1], Yuichiro Okuno[1], Ryota Iwamoto[2], Keita Maishi[3], Kyoya Okada[3]

1. Imamiya Technology Senior High School of Osaka Prefecture The evening course, 2. Otemae Senior High School of Osaka Prefecture The evening course, 3. Kasugaoka Senior High School of Osaka Prefecture The evening course

Solid particles released in a monotonically decreasing magnetic field under microgravity move translational motion caused by field gradient force. The acceleration of a particle is independent of the mass of the particle and depends only on the magnetic susceptibility of the material. Therefore, it is expected that particles will be separated and translated into different groups for each type of material. Using this principle, we have demonstrated that a small neodymium magnet and a self-made microgravity generator can separate and collect a mixture of solid particles for each type of material. The microgravity required for the experiment was generated in a small drop capsule (30 ×30 ×20 cm). The fall distance is 1.8 m, and the microgravity duration time is about 0.5 seconds. A neodymium magnetic circuit, a high-speed camera, a sample collection plate, and a lighting equipment were placed in the drop capsule. The diamagnetic material particles of 6 kinds of inorganic materials and 6 kinds of organic materials could be collected on the collecting plate as a particle group for each different material. The magnetic susceptibility χ of the sample can be obtained by analyzing the recorded particle motion. Therefore, the correlation between the position of the separated particles on the collecting plate and the magnetic susceptibility χ is obtained. The material can be estimated from the position on the collection plate. It can be applied as a "solid chromatography" technique for separating a solid mixture into individual materials prior to precision analysis.

Keywords: microgravity, diamagnetic material, magnetic separation, solid version chromatography

©2020. Japan Geoscience Union. All Right Reserved.

Earthquake prediction by an electromagnetic wave

*Ousuke Yagasaki[1], Mizuho Fujiwara[1], Maika Yashima[1], Shougo Takeda[1], Aiku Tanaka[1]

1. Tokyo Metropolitan Tama High School of Science and Technology

A presage phenomenon by an earthquake and done radio wave radiation are caught and earthquake prediction is enabled. Radio wave radiation observation by an earthquake presage is caught and the magnitude of the earthquake and an area in the epicenter are predicted the signal strength from a relation of duration and data in the radiation direction.
The radio wave radiation which occurs between the ionosphere from a ground level, by 2 receivers, the signal strength, every 1 second, it's being recorded continuously. An antenna is installed in 17 m more and omni-directional and a directivity antenna are used.
An observation of the electromagnetic phenomenon which occurs before an earthquake at my school will be the 8th year. The observation is continued along the preceding study.

Keywords: Earthquake, Electromagnetic wave noise

©2020. Japan Geoscience Union. All Right Reserved.

Classification of Herbig Ae/Be Stars by Spectroscopic Observations

*Aika Koyama[1], *Riko Iida[1], *Hazuki Ueyama[1]

1. Nara Prefectural Seisho High School

Both T Tauri Stars and Herbig Ae/Be Stars are pre-main-sequence stars and it is known that T Tauri Stars are classified into two types based on their 10 Å equivalent width of Hα emission lines. However, there has been no classification of Herbig Ae/Be Stars based on their emission line. We set our goal to determine the standard value and classify Herbig Ae/Be Stars according to their equivalent width of Hα emission lines.
First, the spectrum chart of Herbig Ae/Be Stars were collected from observations at Bisei Astronomical Observatory and from the European Southern Observatory website. After that, the stars' equivalent width of the Hα emission line were calculated using "Microsoft Excel".
We discussed about the standard value which classify the HerbigAe/Be Stars from three different viewpoints. As a result, the standard was concluded to be 25 Å equivalent width.
This work may prove useful for future research into pre-main-sequence stars.

Keywords: Pre-main-sequence Star, T Tauri Star, Equivalent Width

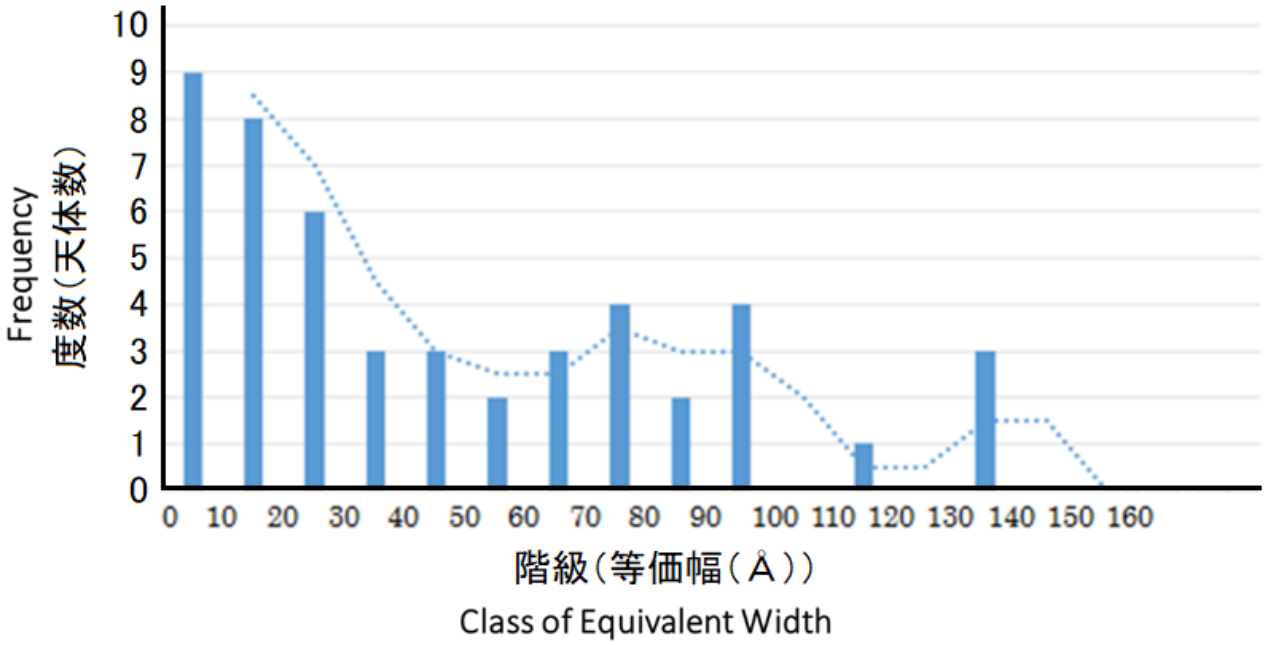

図　ハービッグAe/Be型星のHα輝線の等価幅の分布

Fig. Histogram about Equivalent width of HerbigAe/Be Stars

©2020. Japan Geoscience Union. All Right Reserved.

The Research for Asteroid's Surface Color ~ Difference of BVR magnitude ~

*Asahi Tajima[1], *Mirei Matoba[1]

1. Nara Prefectural Seisho High School

There are around 400,000 asteroids in the space between Mars and Jupiter. There is currently no to way an Asteroid’s composition using only its surface color. The current research investigate the relationship between an asteroid’s surface color and its composition. First, we observed eleven target asteroids using photometric observation. Second, we measured the brightness of target asteroids and compared these using “Makali’i” software. Third, we determined an asteroid’s class and observed B(Blue),V(Visual),R(Red) magnitude. Results showed the presence of three distinct spectral emission groups which were strongly correlated to the three composition groups investigated. In conclusion, there is a relationship between an asteroid’s composition and the asteroid’s surface color.

Keywords: Photometric Observation, BVR Magnitude, Physical Quantity

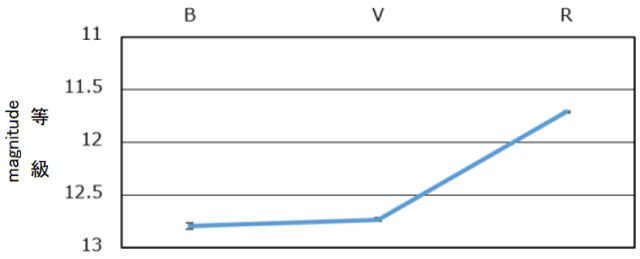

図１　AbundantiaのBVR等級
Fig.1. BVR magnitude of Abundantia

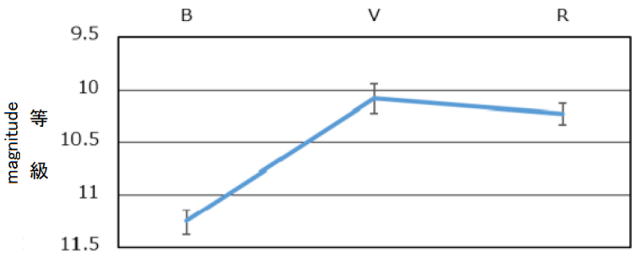

図２　VictoriaのBVR等級
Fig.2. BVR magnitude of Victoria

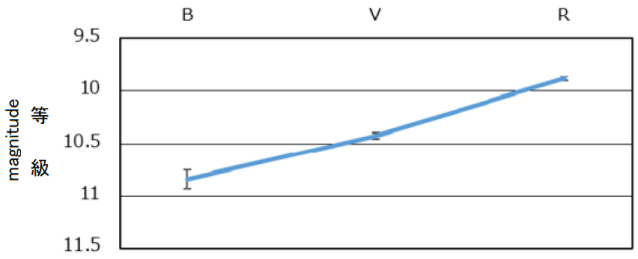

図３　AriadneのBVR等級
Fig.3. BVR magnitude of Ariadne

©2020. Japan Geoscience Union. All Right Reserved.

The igneous rocks which is distributed around The Kabutoyama mountain, the northern part of Kofu Basin

*Masahiro Okuyama[1], Dai Iijima[1], Haruta Moriya[1], Ayato Watanabe[1]

1. Yamanashi Prefectural Hikawa Highschool

The Kabutoyama mountain located in the northern part of Kofu Basin, distributed in the volcanic rock area including the dacite called the Konarayama volcanic rocks. We were interested in the shape of the Kabutoyama mountain and investigated The Kabutoyama mountain and the neighboring rocks. The rock is andesity tuff. Pyroclastic flow takes in in a part of Kofu granite body, and deposit to layer.

©2020. Japan Geoscience Union. All Right Reserved.

Studies on the Urban Heat Islands and Measures against Heat

*Mio Takakura[1]

1. Tokyo Metropolitan Toyama High School

In the urban area, the heat island effect is caused now. The main factors of the heat island include an ground surface state and artificial exhaust heat. Therefore I actually measured it after having checked how temperature went up and down by the ground surface state and the quantity of artificial exhaust heat from past temperature and infrared radiant quantities, data of the artificial exhaust heat. Furthermore, I attached an awning to the outdoor unit of the air conditioner and checked whether cooling efficiency rose on seeing a change of the power consumption. As a result, the surface temperature of the asphalt pavement reaching a factor of the heat island highly, the surface temperature of grassland, waterside, heat insulation paving were low, and it became clear that it was for heat measures. In addition, it became clear that the temperature went up so that there was much quantity of exhaust heat. And it becomes some energy saving by the outdoor unit experiment, and it is thought that some cooling efficiency rose.

Keywords: heat island effect, ground surface state, artificial exhaust heat

©2020. Japan Geoscience Union. All Right Reserved.

Geological Survey by Boring a Core from Toyama’s Schoolgrounds

*Ryotaro Terabe[1]

1. Tokyo Metropolitan Toyama High School

In the summer of 2018, I went to near Mt.Aso to visit my grandmother. At that time I found an outcrop on the roadside. I haven't decided what kind of theme I'm going to research. So, I just took some soils and bring them to school. After I washed them and found they contained volcanic ash. I observed those, then, from the percentage of minerals contained and their shape I thought that volcanic ash is the ash called AT(Aira-Tanzawa tephra) which has produced from Aira Tanzawa Caldera.
Also, on December 27th in 2018, we surveyed the soil at Toyama High School. The cores were collected from the surface of the earth to a depth of 12 meters underground. The school is at an altitude of about 28 meters and its soil layers are categorized into a topographic surface called the "Musashino surface." Then, I wash the soils the same as Aso’s soil, made samples, and I found volcanic ash from the core. I was interested in those, and I wanted to know where they come from. Because one of it was looks like the ash I found in Mt.Aso called AT.
As studying the refractive index of volcanic glass, However, the ash I took from Mt.Aso was not AT. It was K-Tz(Kikai-Tozurahara tephra). And Toyama boring core's volcanic ash, I found the core contained volcanic ash called AT around 1.3m from the surface.
Furthermore, I conjectured the depth of Hk-TP and On-Pm using the depth of AT. Comparing with the data of the observation result using a microscope, I found that the depth of Hk-TP and On-Pm was a high possibility of correctness.
In the future, I want to research the depth of Hk-TP and On-Pm estimated from the observation and analysis results are truly correct. And I would like to find out the layer containing much gravel and sand was originated from the Ko-Tama River, which was said to have flowed near Toyama High School.

Keywords: volcanic ash, volcanic glass, reflective index, AT(Aira-Tanzawa tephra)

©2020. Japan Geoscience Union. All Right Reserved.

Long-term Fluctuation of Snowfall/Precipitation Ratio and Global Warming

*Yukihiro Takaki[1]

1. Tokyo Metropolitan Toyama High School

In this study, I focused on long-term fluctuation of snow quality. I used data for half a century, which is from japan meteorological agency. Using snowfall/precipitation ratio (S/R, a barometer of snow quality), I researched on long-term changing of S/R and a relationship between snow quality and temperature. There was a correlation between them and S/R was decreasing in half a century. I concluded that the decreasing of S/R was a result of influenced by global warming.

Keywords: global warming, climate changing, snowfall/precipitation ratio

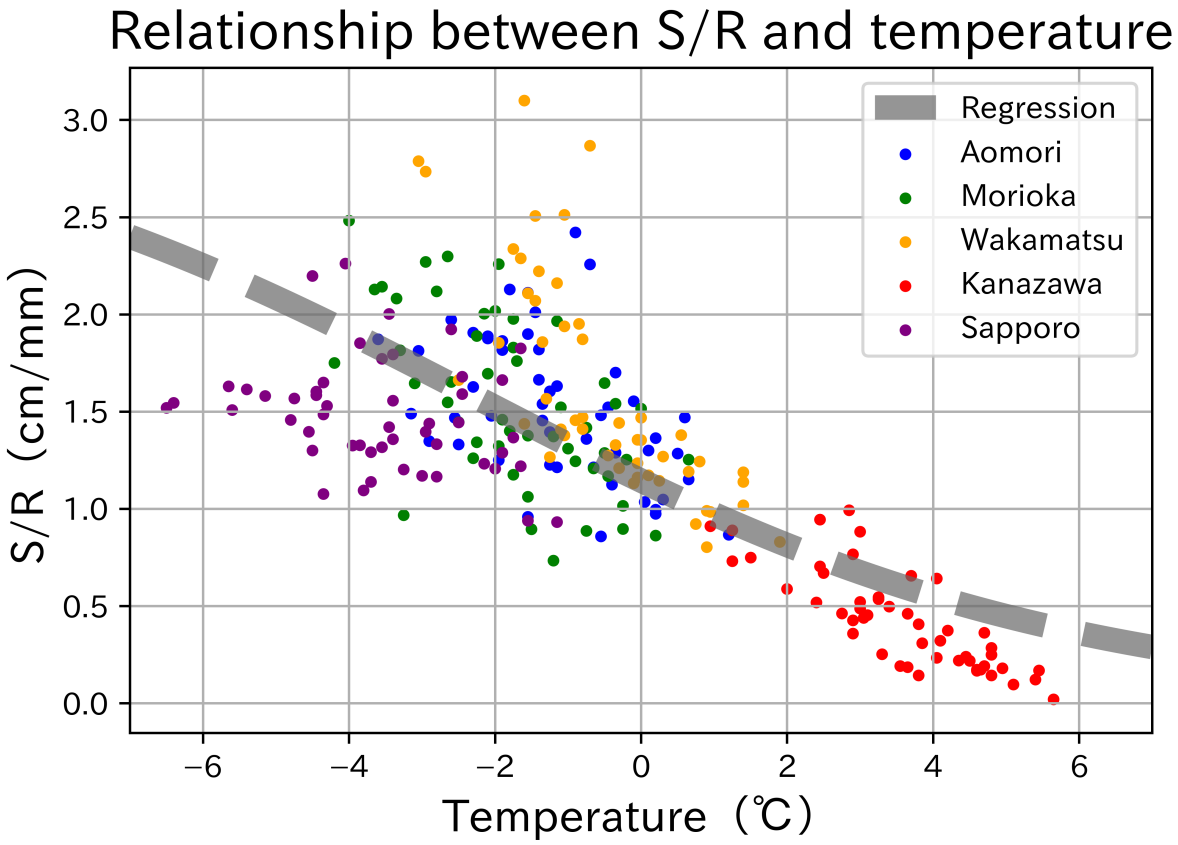

©2020. Japan Geoscience Union. All Right Reserved.

Factors for variations in bombcyclones

*Minori Iida[1]

1. Tokyo Metropolitan Toyama High School

In this study, I researched about the case that some bomb cyclones show really strong development to know what the factor that makes bomb cyclones' development stronger is, because I was interested in the fact that there are some kinds of bomb cyclones; firstly, which shows really strong development, secondary, which shows just a standard of development rate to say to be a bomb cyclones, and the middle of them. To know how some bomb cyclones develop so strong, and what makes the bomb cyclones' development stronger, I started this research.
Firstly, following the result of study by JMASTEC which shows that Kuroshio current helps the develop of bomb cyclones, I checked that the temperature difference between the warmth brought by Kuroshio current and cold air came from north makes bomb cyclones' development stronger, and in the El Nino phenomenon, the tend of the bomb cyclones' development becomes weak because the sea surface temperature rises in winter in El Nino phenomenon.
Secondary, remarking the data which shows the amount of energy which is conducted to atmosphere from sea surface named sea surface flux, that bomb cyclones makes the sea surface flux bigger with the high wind speed of own and to use the energy, bomb cyclones develop more and more became clear.

Keywords: Kuroshio current, temperature difference, sea surface flux

©2020. Japan Geoscience Union. All Right Reserved.

Spectroscopic observation of sprite

*Kotone Asano[1], *Ayaka Okumura[1], Ryuya Nagao[1], Keisuke Nobutoki[1], Momoo Hayashi[1]

1. Ichinomiya High School

Our Earth Science Club has been observing sprite since 2005, when we set two video cameras(Watec 100N,12mm F1.2, 8mm F0.8) on the roof of our school building. We have been analyzing bright line spectrum of meteor, using diffraction gratings(Edmund Optics 600 grooves/mm). On December 12, 2019, we succeeded in getting bright line spectrum of sprite. Using Hg lump and Na lump, we made a conversion formula that shows relation between the pixel distance from light source to the bright line and the wavelength of the lumps. We were able to get N2 near 750nm on the wavelength of the bright line of spite.

Keywords: sprite, Spectroscopic observation, diffraction gratings

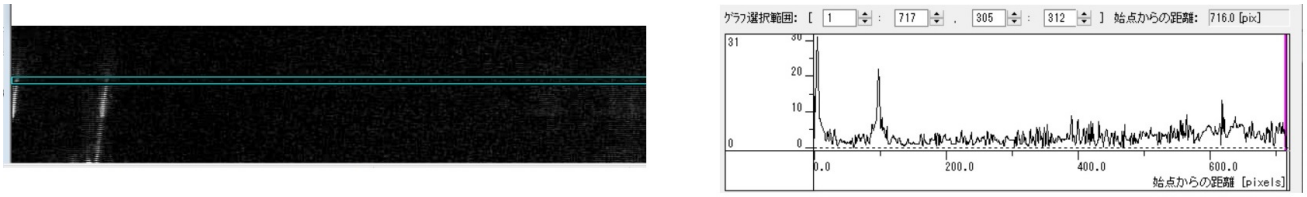

図1

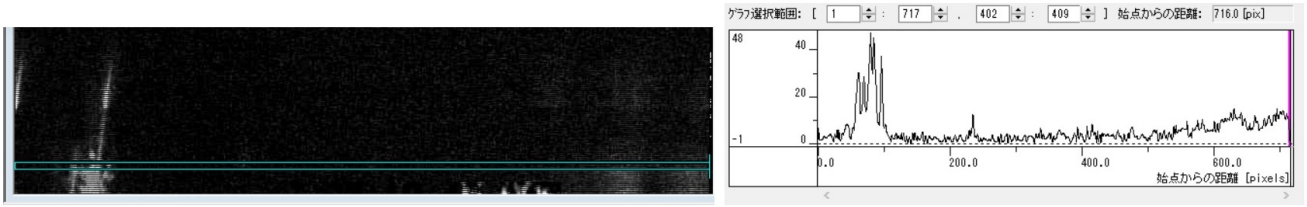

図2

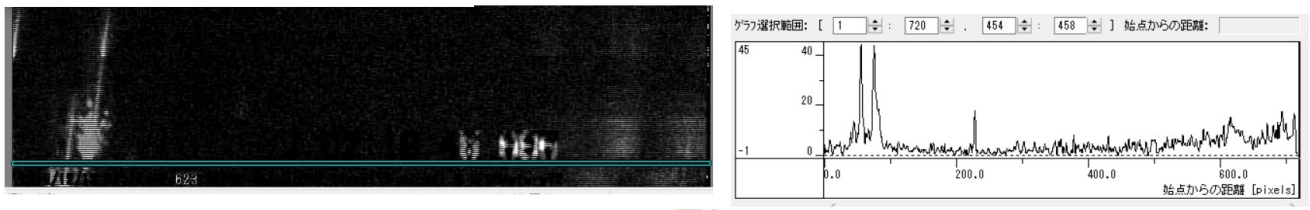

図3

©2020. Japan Geoscience Union. All Right Reserved.

The relationship between the shape of columnar jointing and the viscosity of lava flow

*Kanta Takakura[1]

1. Kaijo high school

Columnar joints are columnar volcanic landforms that consist of cracks in the direction perpendicular to the cooling surface, which can be formed by the lava flow cooling in the cold atmosphere and solidifying while causing volume contraction. Generally, the cross section of columnar joints is said to be regular hexagons, and theoretically all should be regular hexagons. However, when observing the actual columnar joints, I realized that not all the cross sections were regular hexagons, but many were distorted shapes such as pentagons. Therefore, I wondered why there are shapes other than the regular hexagon that should not theoretically exist, and whether there are features such as figures that frequently appear for each columnar joint, and I began this research. It was First, as a hypothesis that answers the above questions,
I thought that the viscosity of the lava flow that created columnar joints might affect the shape of the cross section. Then, in order to prove this hypothesis, the following verifications were conducted and research was advanced.
First, an experiment was conducted in which the starch starch was dissolved in water, and then the water was evaporated to cause volume contraction to reproduce the "columnar joint" 1). Also, the difference in viscosity was reproduced by changing the amount of water dissolved in the same amount of potato starch. Then, we considered how many polygons are included in the created one by comparing the appearance frequency for each "pillar" while counting and comparing with other conditions. Although detailed data is not mentioned in the preliminary paper, lava flow with low viscosity was found to increase the proportion of figures with a larger number of angles in the case of mixing more water with the same amount of starch starch powder than in other cases. It was found that the number consisting of consists of more figures with more angles.
Next, we paid attention to the figure called Voronoi figure, and made it possible to create a Voronoi figure on a PC and perform more diverse and repeated experiments. Voronoi figure is a figure made from a perpendicular bisector that connects an arbitrary point and its adjacent point, and is said to be able to reproduce the shape of columnar joints 2). Moreover, Python and its module OpenCV were used for the creation on the PC. Further, the number of points plotted per same area was changed, and this was set as a condition corresponding to "viscosity". Although detailed results are not described here, the polygon shape increases when the viscosity is low because the proportion of pentagons increased when the plot points were increased (= increasing cooling nuclei = reproducing viscous lava flow). Then, the result was consistent with the result of the potato starch experiment.
Then, in order to confirm whether the same can be said for the actual columnar joints as well as the results obtained in the experiment of Katakuri powder and Voronoi figure, the columnar joints were aerial photographed with a drone to create an ortho image and analyzed with GIS. .
Currently, we are conducting GIS analysis, and I would like to introduce the results on the day of JpGU. Also, I will introduce the consideration based on everything I did on the day.

1) Noritaka Endo et al., Modeling of topographical phenomena (2017)
2) Akihito Ota et al. Statistical analysis of columnar joint morphology using high-precision 3D model by drone and its origin (2019)

©2020. Japan Geoscience Union. All Right Reserved.

Keywords: Columnar joint, Volcano, Lava flow, Earth science, Geology

©2020. Japan Geoscience Union. All Right Reserved.

How ripples formation dependence on the size of sand grains and the amplitude of vibration cycle

*Tsuyoshi Enta[1], *Ryutaro Mitsui[1]

1. Kaijo Junior and Senior High School

We researched on how ripples formation dependence on the size of sand grains and the amplitude of vibration cycle by using a plastic bottle containing water and sand. We also pursued more precise conclusions by changing many parameters such as the size of the sand grains and the amplitude of vibration cycle. A total of eight mechanically controlled vibrations were applied using the LEGO BLOCK Mindstorm motor and programming. The particle size of the sand was also divided into many patterns. By using a color sand having a different color for each particle size, it became possible to record the state when a ripple mark is made of sand mixed with different particle sizes.The effect of each parameter on the pattern was discussed from the observation of the number of wave ripple peaks made of each pattern and the features of the pattern. We also studied of ripple mark through the computer simulation. By examining both from experiments and simulations, we consider the effect of changes in particle size and waves on ripple marks. In this research, I was instructed by the assistant professor Naofumi Yamaguchi of the University of Tsukuba.

Keywords: Ripple mark, Sedimentology

©2020. Japan Geoscience Union. All Right Reserved.

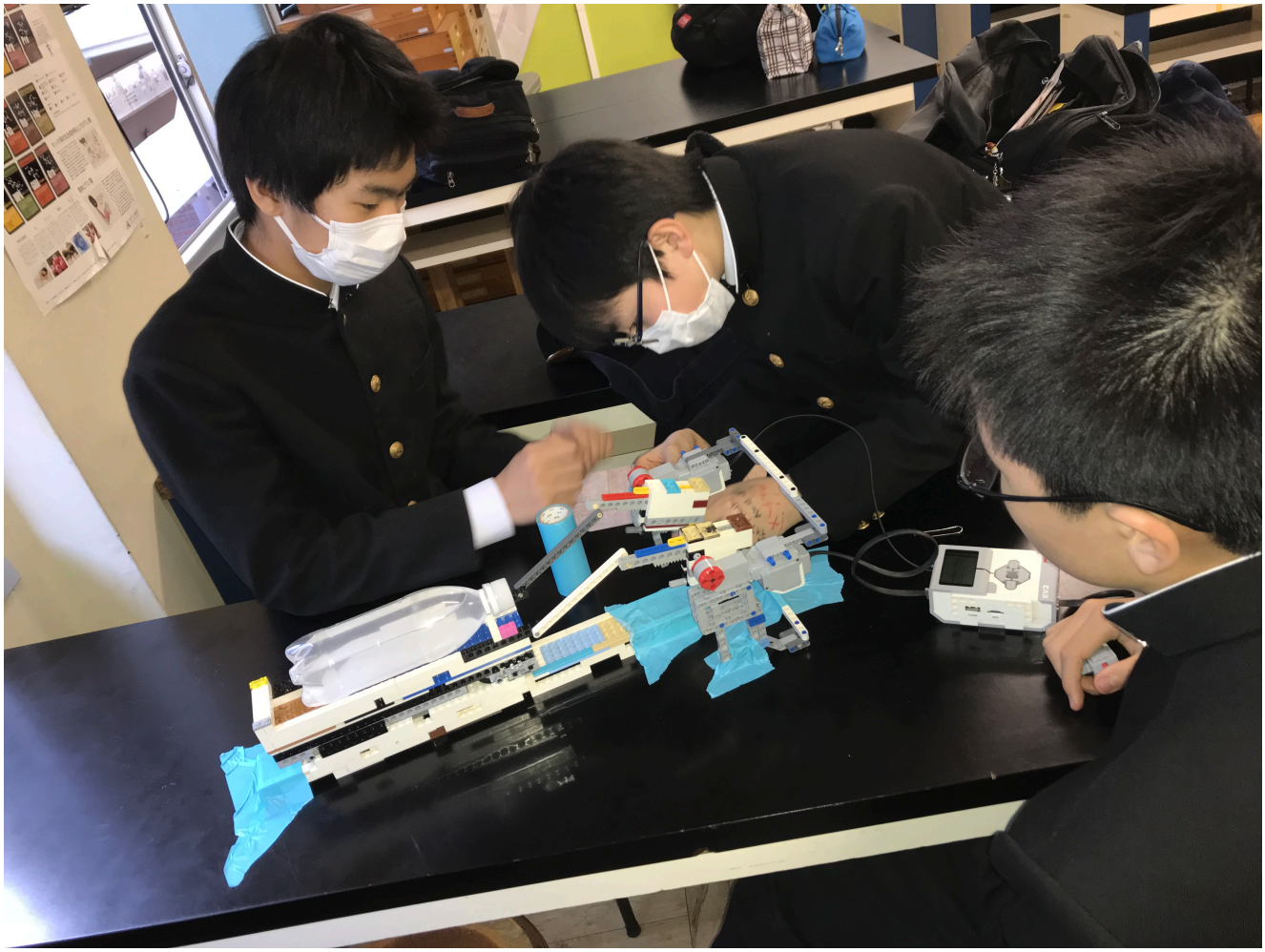

©2020. Japan Geoscience Union. All Right Reserved.

Development of the Portable Equatorial Mount with high operability and applicability

*Jun Ikeda[1]

1. Kaijo high school

I'm developing a portable equatorial mount that has high operability and applicability. An equatorial mount is a device that rotates observation tools such as a telescope and a camera according to the diurnal motion of the celestial body to enable more detailed observation. A highly accurate tracking function has been realized through the first and second machines.
After that, I started the third machine development aiming to differentiate it from the commercially available equatorial mount. In equatorial mounts, the axis of rotation must first be aligned with the celestial north pole, but since the this accuracy has a large effect on tracking performance, I aim to automate axis alignment. Further, as a weak point of the portable equatorial mount, when the direction of the telescope is changed to taget another celestial body, the entire mount may be slipped off, and in that case, it is necessary to re-align the axis again. In order to solve this problem, the declination rotation can be controlled by a motor. Next, with the aim of messuring the accuracy, in addition to the existing index, periodic motion, a unique index for directly obtaining the tracking speed is being able to be mesured. The final goal is to publish the assembly guide on the Internet.

First, in order to realize special rotations of ultra-low speed and high torque in fine steps (smoothly), I used a stepping motor, subdivided voltage changes, and a worm gear with a high reduction ratio. As a result, I achieved a high torque of approximately 56kgf * cm even in the declination rotating part, lightest Unit in the third machine, and the step angle was in increments of 0.00018 ˚.
Next, regarding the operation of the motor, I decided to link with a smartphone. By using the Arduino-compatible ESP32 microcomputer for the program processing, I succeeded in communicating with an Android smartphone via Bluetooth and changing the motor speed with low cost. On the other hand, it has not been confirmed yet on iOS smartphones, so I am considering switching to WiFi communication.
Also, if the shaft of the gear does not mesh correctly, the accuracy will be greatly affected. Therefore, I devised a method of fixing the shaft. Instead of tightening the motor with screws to fix it, the motor is sandwiched with screws so that fine adjustments can be made even after fixing. In addition, the bearing uses commercially available L-shaped metal fittings, and this can also be finely adjusted and fixed to achieve a certain degree of accuracy.

With the first and second equatorial mounts, I was able to confirm a certain degree of tracking accuracy, but I could not show an objective value. For that reason, I'm writing a program that uses Python to determine the angle of view and declination of the observation target.

Presently, in version 3 machine, only declination rotating unit is assembled. However, there are still unsoleved issues. Being heavier by devised method of fixing and ext. make the lower units require more torque, and brought about necessity to re-design these units considering it. Moreover, the Python program for messuring the tracking accuracy is not completed yet, and it is required to adjust thresholds more.

©2020. Japan Geoscience Union. All Right Reserved.

Keywords: astronomy, engineering, astronomical observation

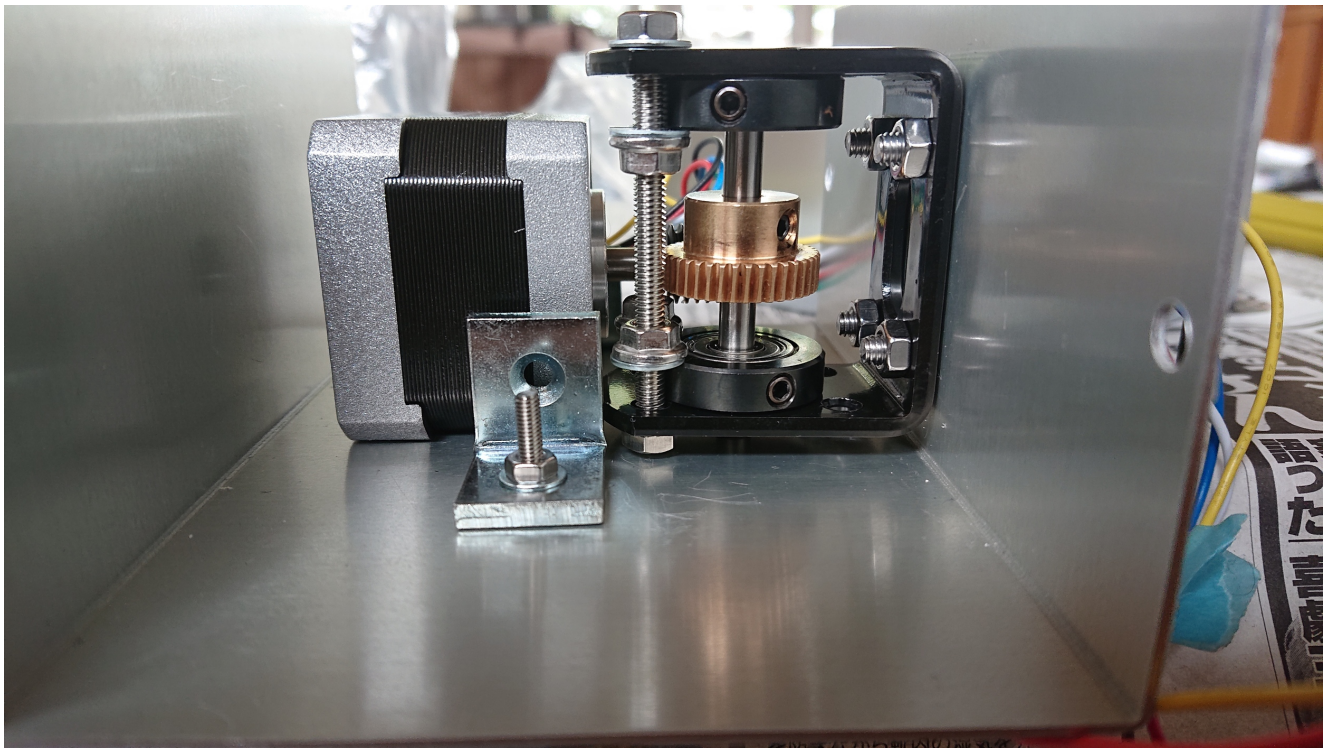

©2020. Japan Geoscience Union. All Right Reserved.

Proposal of GEO-KAMISHIBAI that enhances the appeal of SANRIKU GEOPARK-3 the Taneichi Layer

*Hitomi Kimura[1], *Rio Yaguchi[1], *Kyougo Sakashita[1], *Asahi Sekibata[1]

1. MARIENT CHIKYU TANKEN CLUB SENIOR

The Sanriku Geopark covers the area from Aomori Prefecture through the coast of Iwate Prefecture and down to Miyagi Prefecture. Hachinohe City Marine Science Museum is located on the northern edge of that and to that belongs to the Mariento Chikyu Tanken club. We learned about Sanriku Geopark from 2019. And we announced this activity at the jpGU2019 and the Japanese Geoparks Network Meeting at Ohoita.

There is 2 Geosites in Hirono town by the sea. One is the Taneichi beach park. Sea cliffs of Hirono town, for example Mado-Iwa and nearby, you can observe oyster fossils located around the rocky areas. Other fossils such as the amount and mosasaurus fossils were also discovered from the same area. And can enjoy the scenery of the herringbone cross-stratification sequence and the sand nodules. They are shown in Figures 1 and Picture 1.

Another one is the sea urchin farming beds was a characteristic of the fishing industry in Hirono town and is a feature of Taneichi Layer.

We had the field trips to Hirono town and some lectures by Sanriku Geopark authorized guide. Then we thought that this geosite focused on the Taneichi Layer and needed a storyline description.
So, we wrote GEO-KAMISHIBAI to easy to understand the history of the earth and people's lives.
Unfortunately, we can't exhibit GEO-KAMISHIBAI because of an Corona-Virus(COVID-19) problem. We'd like to postpone it after opening to the public about the value of the GEO-KAMISHIBAI.

Keywords: Geopark, Sanriku Geopark, Taneichi Layer, Regional activity, Club activities

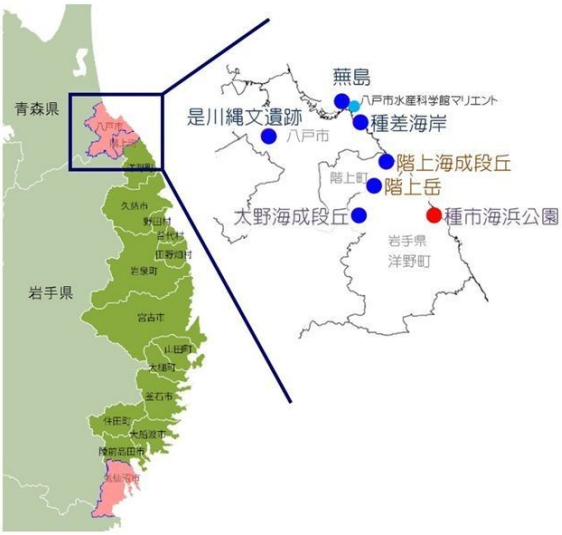

図１　三陸北部エリアのジオサイト

写真１　種市層のノジュール塊

©2020. Japan Geoscience Union. All Right Reserved.

Proposal of GEO-KAMISHIBAI that enhances the appeal of SANRIKU GEOPARK-4 the Hachinohe Canyon

*Mai Kawabata[1], *Haruto Kawasaki[1], *Sarina Shinohe[1]

1. MARIENT CHIKYU TANKEN CLUB SENIOR

The Sanriku Geopark covers the area from Aomori Prefecture through the coast of Iwate Prefecture and down to Miyagi Prefecture. Hachinohe City Marine Science Museum is located on the northern edge of that and to that belongs to the Mariento Chikyu Tanken club. We learned about Sanriku Geopark from 2019. And We announced this activity at the jpGU2019 and the Japanese Geoparks Network Meeting at Ohoita.

Hachinohe Canyon is an open-pit limestone mine. Its official name is The Hachinohe Limestone Mine. The quarry is 1,000 meters from east to west and 1800 meters from north to south. The mine’ s lowest point is currently 170 meters below sea level. It is said to be the furthest place from the sky in Japan. They are shown in Figures 1 and Picture 1. This mine contributed to a Hachinohe city's becoming an industrial city. And it's wonderful view is also a tourist attraction. But this isn't authorized by Geosite category in Sanriku Geopark.

We had the field trips to Hachinohe Canyon and some lectures by Sanriku Geopark authorized guide. After we made "GEO-KAMISHIBAI" to propose approving Hachinohe Canyon a Geosite category in Sanriku Geopark. Unfortunately, we can't exhibit GEO-KAMISHIBAI because of an Corona-Virus(COVID-19) problem. We'd like to postpone it after opening to the public about the value of the GEO-KAMISHIBAI.

Keywords: Geopark, Sanriku Geopark, Limestone, Regional activity, Club activities

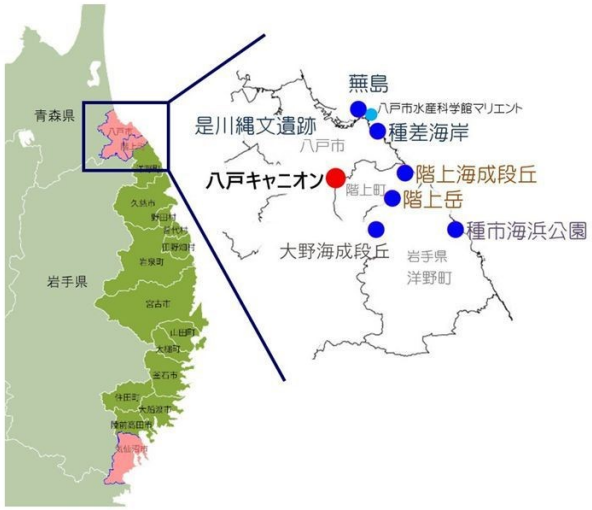

図1 三陸北部エリアのジオサイトと八戸キャニオン

写真1 空から見た八戸キャニオン

©2020. Japan Geoscience Union. All Right Reserved.

Spectroscopic Observation of Meteors

*Shotaro Mino[1], *Yui Satou[1]

1. Furukawa Reimei Junior High School / High School

This study is to make spectroscopic observations of meteors from the ground and infer the elements contained in their luminescence by shooting with a digital single-lens reflex camera having diffraction grating. We have spent five years shooting and analyzing 49 meteors. As a result, we discovered some characteristics of each meteor shower. We confirmed the Gemini meteor shower contains less sodium than other meteor showers. It means the parent meteor body also contains less sodium and the longer time has passed since its formation. We found luminescence that contained oxygen atom (557.73 nm) at the Perseus and the Orion meteor showers. It is called “oxygen forbidden line” and the light is emitted only under limited conditions. We think that we could confirm many oxygen forbidden lines because the ground speed of those meteor showers was higher than the ground speed of other meteor showers.

Keywords: meteor, spectroscopic observation, diffraction grating

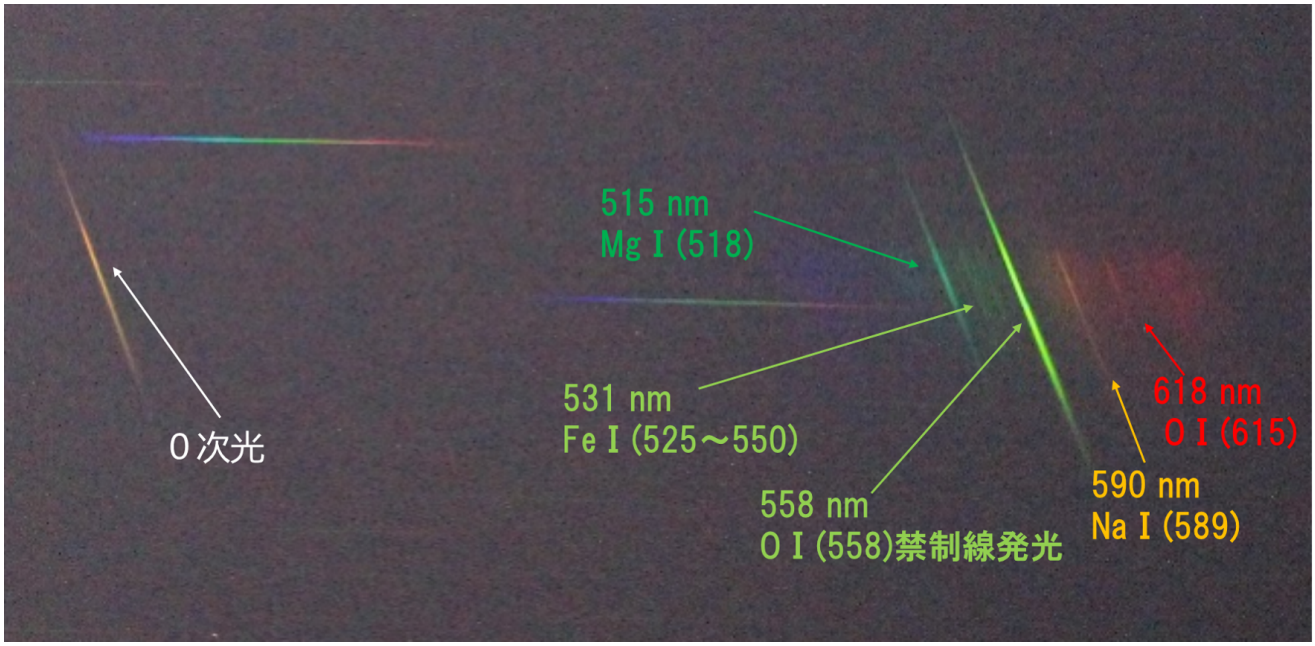

©2020. Japan Geoscience Union. All Right Reserved.

Comparison of frequency (HRO/VOR-RO) and detection number in meteor radio wave observation

*Sora Endo[1], *Rio Saito[1], *Aki Sato[1], *Sachi Sato[1], *Sakura Yuki[1]

1. Furukawareimei Junior High School / High School

We, Miyagi Furukawa Reimei Junior and Senior High School Astronomical Group, have been conducting research on astronomy, but "astronomical observation" is an absolutely essential activity in astronomy research. However, they usually use large telescopes or CCD cameras for such observations, requiring them to move to specialized facilities. Also, it is mainly a nighttime activity and cannot be done during school club activities. Furthermore, even if these problems can be solved, the effects of the weather are large and it is not possible to observe them reliably. Here, we tried radio wave observation of meteors using amateur radio waves that can be observed and analyzed in rainy or cloudy weather, indoors, day or night.

When a meteor appears, ionized gas (plasma) is generated along the path of the meteor. This gas becomes a reflector of the radio wave, and usually receives the radio wave from the transmitting station temporarily in an observation place where the radio wave from the transmitting station does not reach. This is a meteor observation method using this principle. HRO (Ham-band Radio Observation) is a method of observing meteor radio waves, and is currently widely practiced in Japan from high school students to professionals. Mr. Kimio Maekawa is transmitting radio waves around the clock. The place of origin is Fukui Prefectural University. An ultra-high frequency omnidirectional radio beacon is an aircraft radio beacon that uses VOF band (ultra-high frequency band) radio waves. It knows the direction of an aircraft around a beacon. Can be. The origins are almost all airports throughout Japan. This time, we compared the difference in the number of meteor detections by frequency using two types of radio waves with different frequencies of Fukui HRO (53.755MHz) and Komatsu Airport VOR-RO (112.00MHz). Note that the geographical conditions of the transmitting station and the conditions such as directions from the Reimei Furukawa Junior High School and High School in Miyagi Prefecture, which are the receiving places of radio waves, are almost the same.

Next, the observation results. Even if meteors were detected on the VOR-RO observation screen, only the noise, which is not necessary for observation, was observed on the HRO observation screen, and meteors could not be detected. In addition, lightning noise was observed in the HRO, and meteors were sometimes not detected. When the Taurus meteor shower, which reached its maximum in November 2019, was counted, VOR-RO detected more meteors than HRO near the maximum day. In addition, when the data was collected from March 10 to March 20 in 2020, VOR-RO detected more meteors than HRO. Comparing from May to December 2019 by month, VOR-RO detected more meteors than HRO from May to June. However, from August to December, HRO detected more meteors than VOR-RO.
Finally, considerations and future issues. From May to July, the number of detected HROs less than the number of VOR-ROs may be due to the influence of noise such as the Sporadic E layer. It is considered that the number of HRO detections decreased due to the influence, and VOR-RO is less likely to be affected by noise. Especially in June, we were able to reduce the effect of noise by about 45% compared to HRO. From the above, it was found that the detection accuracy differs depending on the season. Observations will continue in the future, and from the observation results throughout the year, there will be a difference in the maximum detection accuracy as to how much the VOR-RO (112.00MHz) and HRO (57.755MHz) will be affected by noise in each season. I would like to investigate further.

©2020. Japan Geoscience Union. All Right Reserved.

Keywords: meteor

流星電波観測における周波数（HRO・VOR-RO）と検知数の比較

宮城県古川黎明中学校　自然科学部　天文班

3年　遠藤空　2年　齊藤りお，佐藤阿希，佐藤幸，結城さくら

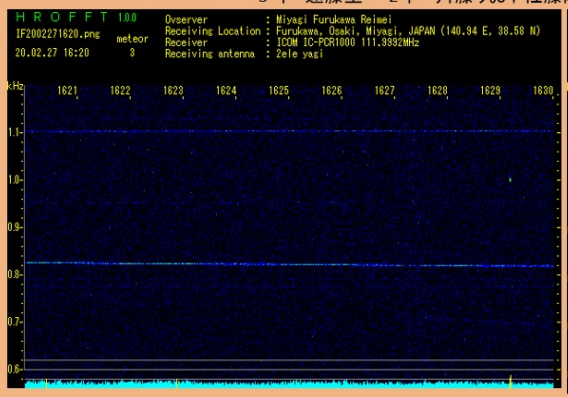

2020年2月27日16:20の観測画面(VOR-RO)

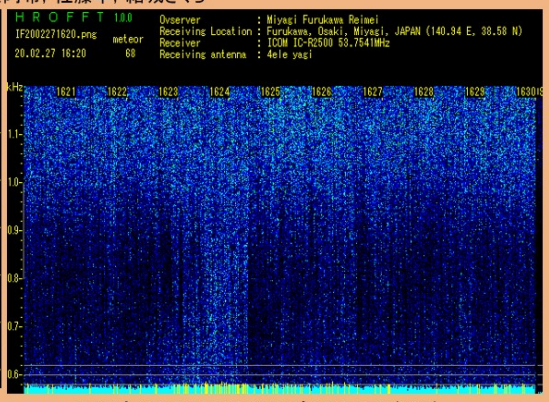

2020年2月27日16:20の観測画面(HRO)

観測画面

©2020. Japan Geoscience Union. All Right Reserved.

Research about Greenhouse effect of water vapor~Can we control the temperature of the earth with water vapor!?~

*Hikaru Abe[1], *Michiru Suzuki[1], *Ruka Suzuki[1], Furi Seino[1]

1. Sakata Minami High School

Recently, Global Warming is drawing attention as a global issue from all over the world.We turn our attention to the reason why Global Warming is caused.Above all,it’ s interesting that water vapor occupies about 80% of Greenhouse gas functions.So,we are going to explore how to control the temperature of the earth and the possibility,using Greenhouse effect.

Hypothesis

"Changes in water vapor and interrelates with changes in temperature."

Means

・water vapor

・elevation

・sunlight injection

・ultraviolet rays

First,we verify whether the temperature changes from the above.

Second,we consider which circumstance is easy to change temperature through experiments.

< Literature survey>

Reading the paper

Prospects

We would like to make an environment whose temperature is changed artificially,and reconfirm our experiments,from No.1 to No.4 .

Keywords: Global warming, Meteorology, Water vapor, Greenhouse effect

©2020. Japan Geoscience Union. All Right Reserved.

A study of the fluctuations in the water level of Kohama pond

*Akari Nakata[1], *Kira Yamamoto[1], Koharu Fukusi[1], *Hinata Muto[1]

1. Nirayama High School

Kohama pond in Rakujuen in Mishima city is a pond where spring water collects, and it has had a close relationship with people living near it for a long time.

At present, however, there are lots of questions that are yet to be defined, such as the full-water period and seasonal water level changes.

In this study we surveyed and considered its fluctuations in the water level in terms of weather, water veins, and water quality.

We made a graph focused to the term after typhoon 19 hit to reveal the relation between precipitation and the fluctuations. As a result, we concluded that Gotenba city’ s precipitation does not have any direct relation with it for the reason that there is no correlation between them from Nov. 17 to Nov. 18, and the distance from Gotenba city to Mishima city is about 32.9 km.

We then considered whether the Great East Japan earthquake made its average water level rise.

We found the importance of caution in using the data of Kohama pond because the spring water spreads when the water level is over 0m.

The differences of Electric Conductivity (EC) is due to the time when lava was made. In general, the flow velocity of the new lava groundwater is faster than the old one, and the amount of ions dissolved from lava is in proportion to the flow of time.

Because of these, the Hakone and Ashitaka lava water veins, which are known to be old-class water veins, both showed high EC.

Therefore, we inferred that the water vein of the water purifying plant in Izushimada whose EC was as low as 146, is the same as that of Kohama pond whose EC was about 159.

Acknowledgment:

Yusuke Suzuki (Izu Peninsula Geopark Promotion Council)

References:

©2020. Japan Geoscience Union. All Right Reserved.

Open data of Mishima city, https://www.city.mishima.shizuoka.jp/ipn017227.html;

Japan Meteorological Agency, http://www.jma.go.jp/jma/menu/menureport.html;

The data of water purifying plant in Izushimada

Keywords: fluctuations, pond, Electric Conductivity

©2020. Japan Geoscience Union. All Right Reserved.

Research on statistical observation of columnar joint form and its origin by high precision 3D model by drone and potato starch experiment

*Makoto Iida[1], *Ryo Aoki[1], *Ryuki Mochizuki[1], *Takato Okumura[1]

1. Nirayama High School

Many columnar joints which were formed by volcanic activity. can be seen on the Izu Peninsula. Therefore, we conducted research to statistically clarify the characteristics of the cross-sectional shape of columnar joints formed by geometric patterns, and to clarify the relationship between statistics and a mass of igneous rock formation conditions.

We did our research in three ways. First, we took an aerial photograph using a drone at Hutou coast in Nishiizu, Shizuoka Prefecture. From that, we created orthographic images, created polygon data using QGIS, and collected the number of corners and area fom the data. Graphing the data and comparing it with last year's data, it was shown that the columnar joints surveyed last year had the most hexagons, but the columnar joints at Hutou coast mainly formed pentagons, and the number of corners was widely dispersed. From this, we thought that the columnar joints on the Hutou coast were formed of thin dikes, and that the cooling condition was poor, which could cause variations in the angular distribution.

Second, we collected data on the angular distribution of various columnar joints around the world from foreign literature, and examined their correlation with the Hutou coast and the columnar joints examined last year. The literature shows that a burnt island dyke is a columnar joint formed of thin dikes, while others are columnar joints formed of thicker rocks. Also, the columnar joint in foreign countries have more hexagons, and the Hutou coast's kurtosis has lower levels than domestic and foreign columnar joint's kurtosis. From these, we can see that columnar joints made in relatively thick lava or magma have more hexagons and a higher kurtosis, but the columnar joints of thin dikes have a variable number of corners and a lower kurtosis.

Finally, we tried to make columnar joint made of potato starch by drying the mixture of water and potato starch in a container. In addition, when drying, a non-uniform cooling condition was reproduced by applying a temperature gradient using an incandescent lamp. As a result of graphing the data obtained by dividing the resulting columnar joint by voronoi division, the ratio of the hexagons to the total ratio under all conditions was the largest. Therefore, focusing on the portion with a large temperature gradient, the unevenly heated samples has a larger area as it is closer to the heat source, and is not affected by heat when it is separated to a certain point. Furthermore, when comparing the portions close to the heat source, the unevenly heated samples showed a larger variation in the number of corners than the uniformly heated sample. From these, we thought that the uniformity of heating was related to the distribution of the number of squares.

©2020. Japan Geoscience Union. All Right Reserved.

From these experiments, we found that the columnar joints had more hexagonal distributions in thicker rocks, and a greater variation in the number of corners in thinner rocks and dikes. We also found that the cooling temperature becomes uneven due to the rock and dike, and the area also varies. In addition, the same could be reproduced with potato starch.

Keywords: columnar joint, high precision 3D model

Ⅰ、浮島海岸の柱状節理を昨年の柱状節理のデータと比較

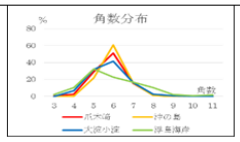

Ⅱ、海外の柱状節理のデータを日本の柱状節理のデータと比較

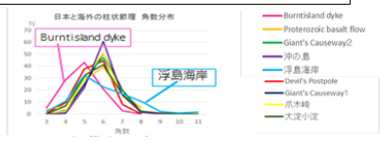

Ⅲ、片栗粉実験で白熱電球の位置条件をまとめた表

	1－1	2－2	3－2
片栗粉	300g	300g	300g
白熱球の位置	熱源を端に置いた場合	熱源を中央に置いた場合	インキュベータで均一に40度で加熱した場合

Ⅲ、片栗粉実験で使用したサーモグラフィーカメラの写真（熱源を中央に置いた場合）横から撮影

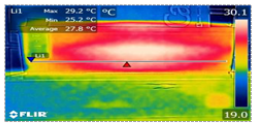

Ⅲ、片栗粉実験で得たデータを、縦軸を面積、横軸を熱源からの距離としてグラフ化した
左側　（熱源を端にした場合）　右側　（熱源を中央とした場合）

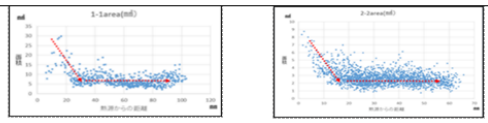

Ⅲ、片栗粉実験で得たデータを、縦軸を全体の個数に対する割合、横軸を熱源からの距離としてグラフ化した

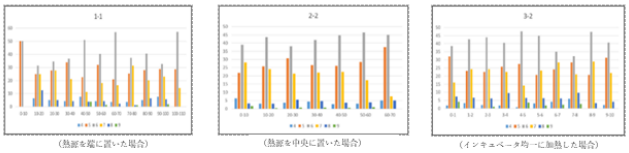

（熱源を端に置いた場合）　（熱源を中央に置いた場合）　（インキュベータ均一に加熱した場合）

©2020. Japan Geoscience Union. All Right Reserved.

Marine pollution by Microplastics

*Nanako Aono[1], *Kaito Isoya[1], *Kouki Sugiyama[1], *Yuki Nakata[1], *Genki Yano[1]

1. Nirayama High School

1, Research Background

Today, marine pollution by microplastics (hereinafter: MPs) is in progress. When marine organisms take MPs themselves and harmful substances attached to them, bioaccumulation affect seabirds and human health. To determine the degree of contamination, it is necessary to know the amount of MP, but there are few measured data in Shizuoka Prefecture. Therefore, we established a method for detecting MPs that even high school students can use, and examined how many MPs are in the sea and river around Izu Peninsula.

2. Our achievement to date

Since school equipment can not detect the substances which plankton net with too narrow mesh gather, the mesh of the plankton net was set to 315 μm ,and MP was successfully collected. We removed organic matter from the collected river and sea water, and succeeded in making a sample that can easily detect MP. MP was successfully detected from the sample. When the sample was exposed to blue light, we found that some plastics emit light.

3. Discussion

It has been found that even high school students can detect MPs on the Izu Peninsula and Kano River with equipment in the high school. Judging from the research results, the number of MPs detected in rivers tends to be higher than in the oceans other than Numazu Port, so the cause of marine pollution in this area is likely to be MP outflow from rivers. Therefore, it is important not to dump waste into rivers in order to prevent marine pollution. Numazu Port, which is a fishing port, is likely to have a high number of detections due to the high frequency of plastic use. The amount of MP is thought to be deeply linked to human life.

4. Future prospective

Examine the type of plastic detected at each point. Since the mesh of the plankton net used is 315 μm, the target is spread to MPs with a size of 315 μm or less. In this measurement, since the values measured after Typhoon No. 19 are also included, the amount of MP and the location of outflow in the coastal area of the Izu Peninsula are estimated by performing sample collection over a wider area and performing fixed point observation. In addition to establishing a method for detecting MP using blue light, a method for detecting MP that does not react with blue light needs to be found.

5.References

Establishment of survey method for microplastics in coastal areas
http://www.pref.shizuoka.jp/kousei/ko-510/documents/412slide.pdf

6. Acknowledgments

Yuji Hiramatsu, Shizuoka Prefectural Institute of Environmental Health Sciences
Toshihiko Sato, Shimoda Rinkai Center, University of Tsukuba

Keywords: Microplastics, Izu Peninsula

©2020. Japan Geoscience Union. All Right Reserved.

Invisible ability of soil –Soil evaluation by zero point of charge-

*Ayano Hayashi[1], *Ayano Soga[1]

1. Kyoto Prefectural Sagano High School

Soil, which has a central role in the forest ecosystem, has charge. These soils and their charges are very different depending on the state of the organic terminal groups. Therefore, in this study, the purpose was to evaluate the Zero Point of Charge (ZPC) of the soil and learn what soil nutrients were in the soil in the Woods for Field Practice Owned by Sagano High School. The field is located in the Satoyama area, a buffer zone between Kyoto city's forests and urban area. And it is a mixed needleleaf and broadleaf forest that is about 70 years old. The result we learned was that the $pH_{(H2O)}$ was a low value of 3.7 and the $pH_{(KCl)}$ was about 1 lower than it. We will try to measure the ZPC by STPT-ZPC method (Sakurai et al., 1988).

Keywords: Forest soil, Experiment forest, Satoyama, Zero Point of charge, pH

©2020. Japan Geoscience Union. All Right Reserved.

Multivariate analysis of data of forest soil by using “Face Chart”

*Fujimoto Takeshi[1], *Hina Nakatani[1], *Hokuto Nakatsu[1]

1. Kyoto Prefectural Sagano High School

The data of the soil profile survey is difficult for non-experts to understand what the soil is like. Therefore, the purpose of this study was to make the soil survey results visually easy to understand by performing a multivariate analysis (principal component analysis, cluster analysis (Ward method)) on the soil data and showing it on a face chart which would be easy for the layman to understand. We did soil profile surveys at the Woods for Field Practice Owned by Sagano H.S. (a mixed forest) located in the Satoyama woods area in Kyoto city. We analyzed these results. We used “R” to analyze. As a result, we could visualize the main data of soil profiles by using these face charts. The soil is so complex that we have to consider multicollinearity in future.

Keywords: Forest, Soil profile, Face chart, Multivariate analysis, Multicollinearity

©2020. Japan Geoscience Union. All Right Reserved.

Manufacture of Azumaya in WFS -Examination of the method of drying the trees-

*Kanako Inoda[1]

1. Kyoto Prefectural Sagano High School

Building materials are classified into artificial drying types and natural drying types. Artificially dried wood is less glossy and less durable than naturally dried wood. Also, artificial drying needs many initial costs and a limit should be set in place. The purpose of this study is to examine the method of natural drying of trees in the field and to make buildings using these wood. In the Woods for Field Practice Owned by Sagano High School located in the Satoyama area of the Kyoto city area, cedar and cypress with a breast height of about 20 cm were cut down, the bark was immediately peeled off, and dried in the air. As a result, dependent on the weather, in September, it was found that it took about two weeks to reach the desired final moisture content. From November to February, the water content declined slowly.

Keywords: Forest, Satoyama, Thinned wood, Drying method, Experiment forest

©2020. Japan Geoscience Union. All Right Reserved.

Project Regeneration of Gensei’ s Bamboo Volume 1

*Takeshi Fujimoto[1], *Yosuke Yukawa[1], *Nanami Aoki[1], *Yusuke Yamazaki[1]

1. Kyoto Prefectural Sagano High School

Before the renovation of Sagano High School's buildings, there were three points related to the founder of the school, Chashitsu-rijinken (tea ceremony room), a stone monument, and Gensei's bamboo. But now, that bamboo has been lost. The purpose of this study was to research the physical properties of the soil needed to be transplanted in order to regenerate Gensei's bamboo. The survey items are the confirmation of the soil layers by using a soil sampler, the measurement of the soil hardness by using a Yamanaka-type Soil Hardness Scale and the measurement of soil crackle strength by using a Hasegawa-type Soil Penetrometer (H-60). The on-site soil was composed of heterogeneous soil due to development and was classified as man-made soil. Also, we found many breccia of about 3 cm in size. Since there was no layer that inhibited root elongation and the proportion of gas phase was high, it was considered that bamboo transplantation was possible without any particular problems. From now on, we plan to do a similar survey and compare where the bamboo is growing.

Keywords: Bamboo, Soil Profile, Soil Physical Property, Soil Classification

©2020. Japan Geoscience Union. All Right Reserved.

To develop an efficient geological survey method and its effectiveness by using natural radiation

*Taisei Takagi[1], *Momoka Tanaka[1], *Ayane Matsuoka[1], *Kosei Yoshimura[1], *Chiharu Yamaguchi[1]

1. FUKUI PREFECTURAL WAKASA SENIOR HIGH SCHOOL

Natural radiation which exists naturally around us is emitted from rocks and varies with the type of rocks. We assumed that we could use its property for geological surveys and geological mapping. With support from the Kyoto Municipal Science Center For Youth, we measured the radiation dose of rocks sampled around the west of Reinan area in Fukui prefecture. As a result, the indicated amount of radiation varied even the same type of rocks, so that radiation dose was probably affected by the size of rocks and the distance from other samples. In this experiment, we measured each sample without considering external factors caused by other samples. We need to eliminate the external factors to improve our methods, so that we will surround the measuring device for radiation with a lead pipe. We also consider other factors (size, surface area, density, etc.) might cause different outcomes in radiation emission in spite of the same type of rock. However, the viewpoint may or may not be accurate because it is under survey.

Keywords: radiation, rocks, geology,, mineral, geological survey

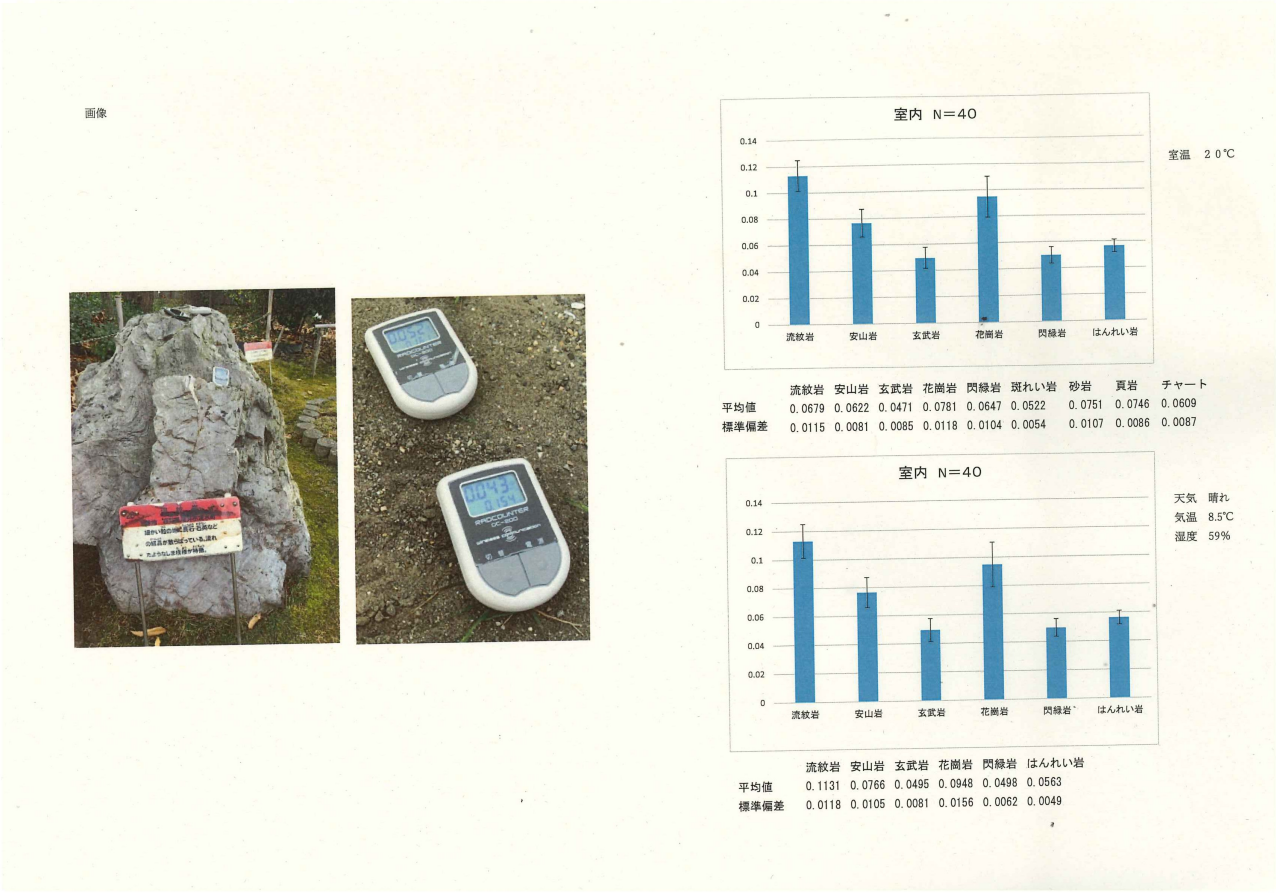

©2020. Japan Geoscience Union. All Right Reserved.

Kantemboki ~To research the accuracy of Japanese old sayings about weather~

*Yuki Takemura[1], *Toro Higashino[1], *Haruki Fukuda[1]

1. FUKUI PREFECTURAL WAKASA SENIOR HIGH SCHOOL

“Kantemboki” is Japanese old sayings about weather. People used to look up the sky and observe the color of sky, the shapes and the movements of clouds, the direction and strength of wind blows, visibility of the Sun and the moon, change in animal activities. Then people empirically predicted the weather using those natural phenomena.

Those sayings range from major ones widely spread throughout Japan to minor ones vary by local areas. However, some of them have not been scientifically proven whether or not they work. We aim to verify the accuracy of weather lore by observational data collection.

We selected the following three “Kantemboki”s to verify. “The one relates to Mt.Aoba in Takahama town”, “The one relates to the direction of wind blows”,” “The one relates to the Sun”.

Keywords: weather, statistics, old sayings, weather forecast, prediction

©2020. Japan Geoscience Union. All Right Reserved.

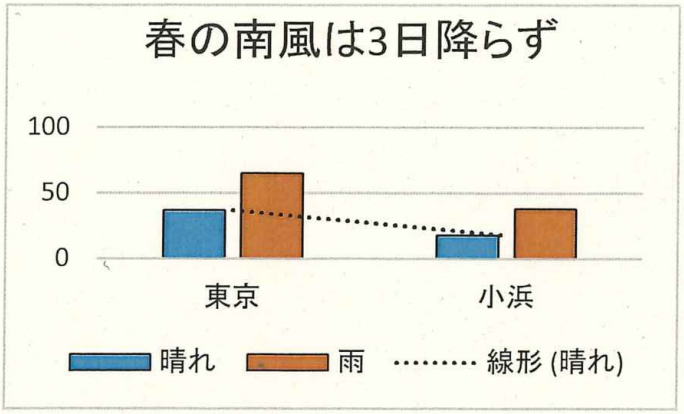

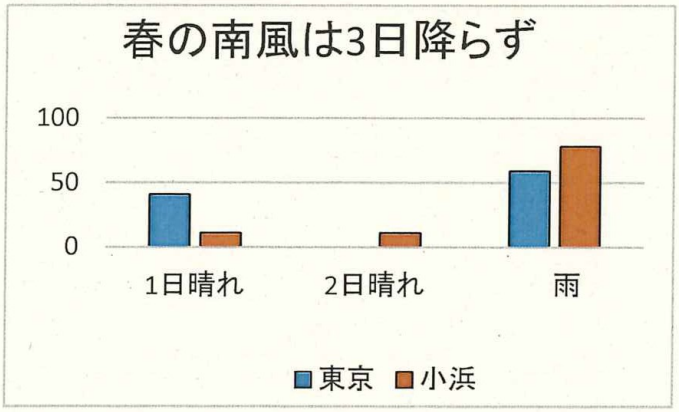

©2020. Japan Geoscience Union. All Right Reserved.

Proposal of new embankment ~Proposal of prevention method of piping phenomenon

*Daiki Tanabe[1], *Soshi Hirata[1]

1. FUKUI PREFECTURAL WAKASA SENIOR HIGH SCHOOL

Nowadays, lots of water damages caused by piping phenomenon have reported throughout Japan. As the water levels of the river increase, river bottom receives stronger pressure from water. If water penetrability of river bottom is higher, water penetrates into soil and build water path and flood hits the cities. It is called piping phenomenon.

There is no preventive measure against piping phenomenon, so that we aim to research river bottom structure which is supposed to be one of the causes of piping phenomenon. Piping phenomenon occurs when river bottom receives strong water pressure, therefore we focus on river bottom structure in order to reduce water pressure. We made a following hypothesis about prevention against piping phenomenon, If bottom space of river is wider, piping phenomenon will be prevented. We will build a miniature model of river as an experimental equipment to verify our hypothesis.

Keywords: prevention of disaster, banks, form or shape, natural disaster, overflown river

©2020. Japan Geoscience Union. All Right Reserved.

Protect the traditional shrimp fishing in Obama Bay

*Taisei Hayashi[1], *Masakazu Muramatsu[1], *Chiaki Ose[1], *Kanta Nakai[1]

1. FUKUI PREFECTURAL WAKASA SENIOR HIGH SCHOOL

The traditional shrimp fishing is operated from June to August at around Obama Bay in Obama-city, Fukui Prefecture. However Shirasa shrimp (Scientific name: Metapenaeus ensis) is a target for this fishing, catch of shrimp (Metapenaeus ensis) has dropped drastically. It is not known exactly why it is happening. Around Obama Bay, in the past, there were 30 fisherpersons to operate this fishing at its peak, but only one fisherperson lasts now. We went on the field survey in order to find out a cause of fall of catch and to protect this traditional fishing. We assumed from the results that decrease of seagrass meadow and landfill might be the cause of dropping. We will continue to research.

©2020. Japan Geoscience Union. All Right Reserved.

Correlation between liquefaction and grainsize distribution of ground

*Ryo Beppu[1]

1. Saitama prefectural Kasukabe High School

It is known that the ground where liquefaction occurs has many voids and the groundwater level is high. And the particle size of the ground is related to the amount of voids. Therefore, in order to verify the relationship between the porosity of the ground and the particle size, a ground model was created for each particle size using four types of alumina spheres, and the porosity was calculated from the model volume and the total volume of the spheres. Compared with particle size. In addition, in order to verify the relationship between the porosity of the ground and the likelihood of liquefaction, I created six types of ground models with different porosities by mixing spheres with different particle sizes, and started liquefaction after starting vibration. The number of vibrations until the occurrence of was recorded. Then, the vibration frequency and the porosity of each model were compared. As a result, it was confirmed that the porosity is related to the average particle size of the ground and the uniformity of the particle size, and that liquefaction is more likely to occur in the ground with a higher porosity.

Keywords: earthquake, liquefaction, grain size, particle size composition

©2020. Japan Geoscience Union. All Right Reserved.

Fine laminated structure of stromatolite suggests summer and winter in cretaceous period?

*Taiga Tsujimoto[1]

1. Saitama prefectural Kasukabe High School

I studied formation processes of fine laminated structures of three types with different lithology stromatolites in the El Morino formation (latter term of cretaceous period) in the Andes, Bolivia in South America. According to observation of thin sections, fine laminated structures consist of the thin layers of light layers and dark layers less than 2mm thickness, made from calcium carbonate($CaCO_3$). Light layers and dark layers are acknowledged the differences of variation width of layer thickness and particle sizes and shapes of $CaCO_3$. Especially, difference in size of thickness is remarkable. That`s because there is a difference in crystallization amount of $CaCO_3$ with variation of carbon dioxide concentration in sea water. And I considered variation of carbon dioxide concentration by relating the amount of photosynthesis of cyanobacteria and carbon dioxide solubility. As a result, I concluded that fine laminated structures are corresponded seasonal seasonal changes.

Keywords: stromatolite, cyanobacteria

©2020. Japan Geoscience Union. All Right Reserved.

How long did it take to form the Pothole in Joga-Shima Island?

*Yusuke Izumi[1]

1. Saitama prefectural Kasukabe High School

Joga-shima Island is located at the southernmost tip of the Miura Peninsula. This island has been raised by the earthquakes that occurred in the past, and forms a coastal terrace. There are some potholes on the terrace. For one of them, I considered the formation period of the pothole from two records. One is the record of crustal movement during the 1703 Genroku Kanto earthquake and the 1923 Taisho Kanto earthquake. And another is the record of the trace fossils made by boring shells in my field survey. As a result, it became clear that the target Pothole had been formed for about 220 years from the 1703 Genroku Kanto earthquake to the 1923 Taisho Kanto earthquake.

Keywords: Joga-shima , Pothole, Earthquake, Trace fossils, Coastal terrace

©2020. Japan Geoscience Union. All Right Reserved.

Clothing change from meteorological data

*Hinane Chiba[1], *Misaki Ishii[1], *Kaho Kubota[1], *Nanami Nakao[1]

1. Chiba Prefectural Funabashishibayama High School

According to our school regulation, we need to change into winter uniforms on the beginning of October. However, we felt very hot so as not to be able to spend time with summer uniforms last October. On that day, we had a question that our clothing change may not suit the actual situation of climate change. Using AMeDAS in Funabashi city, we examine the temperature in 40 years, and clarified a rise in temperature. In addition, we compared Funabashi, Sakura, and Ryugasaki city. As Funabashi city had a big rise in temperature, we considered it is “heat island effect”. We suggested two ideas to change our regulations; “Clothing change in summer makes 2 weeks earlier and it in winter makes 2 weeks later” and “We can choose summer uniforms and winter uniforms”. We have begun to move to improve our school regulation that suits the real situation.

Keywords: Meteorological data, Clothing change, Temperature, Heat island effect, School regulation, Global warming

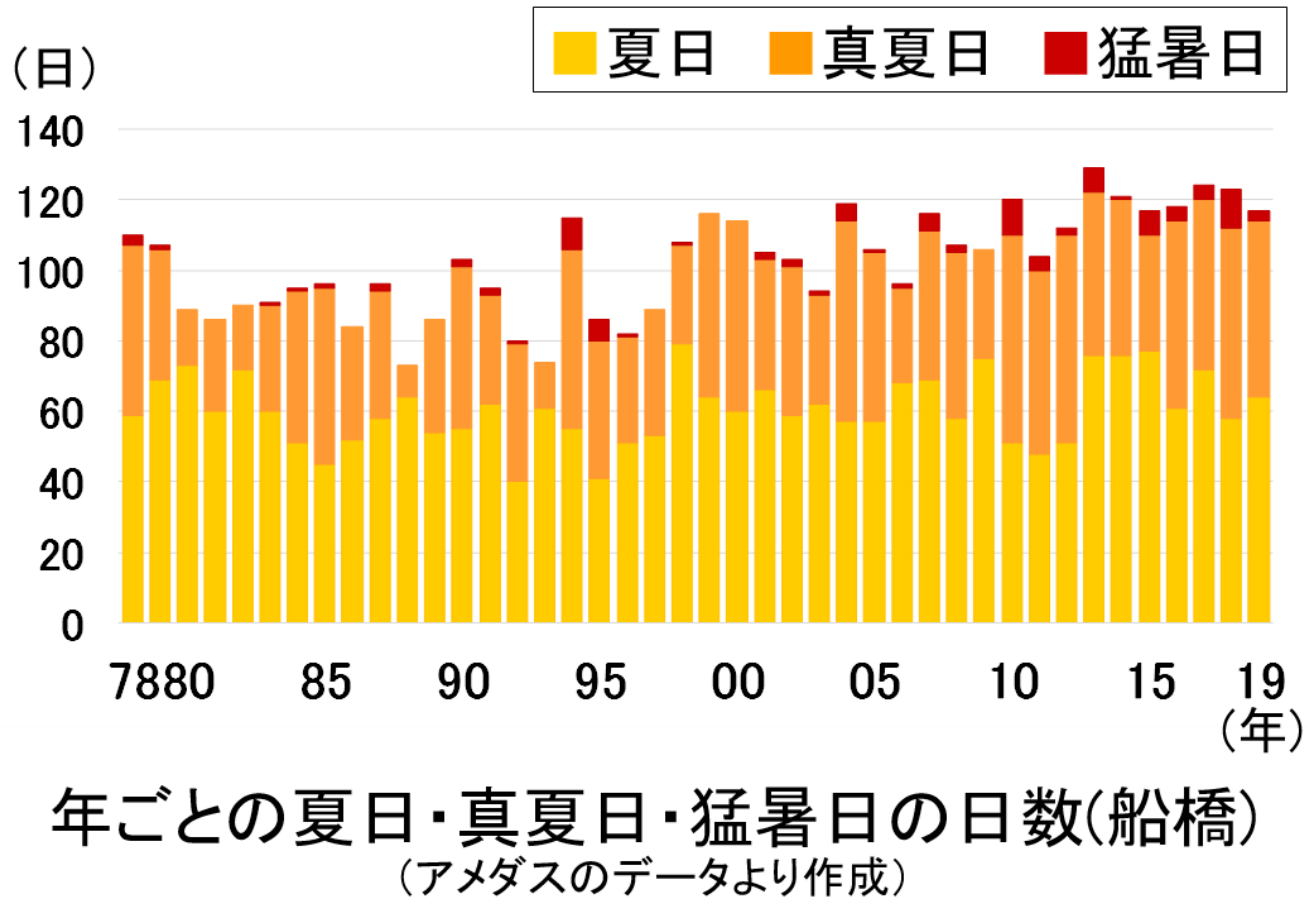

年ごとの夏日・真夏日・猛暑日の日数(船橋)
(アメダスのデータより作成)

©2020. Japan Geoscience Union. All Right Reserved.

Analog modeling of dust devil -Study of its growth and dissipation-

*Daisuke Suzuki[1], Yuto Akaike[2]

1. Shizuoka Senior High School, 2. Fuji Senior High School

1. The background of this research

The purpose of this research is to search the conditions of the growth and dissipation of the dust devil by analog experiments. For this purpose, we developed an analog model that generates a vertical vortex like dust devil.

Dust devil is a strong vertical vortex that suddenly occurs in the middle of the sunny day. We wondered why such a strong vortex grow up and dissipates suddenly. In the resent years, many numerical studies related to dust devils have been reported. However, while numerical simulation is good at studying the impact of the control parameters to the phenomena, it should approximate fine vortex structure and cannot incorporate fine surface geometries due to the limit of discretization. Therefore, we decided to develop an analog experiment system to generate dust devil in laboratory. We started this research with the hope that we could discover detailed properties of the dust devil that could not be found in the numerical simulations by quantifying the parameters of the dust devil observed under controlled environmental conditions by the analog experiment.

2. Method

By referring to the previous research on the generation mechanism of the dust devil, we created a device that reproduces the environment which generates dust devils.

We made a device that heats the ground surface (water) with a hot plate to generate an ascending air current and rotates a cylindrical wire mesh to give an angular momentum to the inflowing air current. The purpose of heating the water is to generate steam and visualize the dust devil. Furthermore, by applying a sheet-shaped laser beam to this steam, we developed a system to measure the cross section of an vortex quantitatively. Using this system, we measured the diameter of the vortex which was visualized by the sheet-shaped laser in the video image. We measured the change in diameter of the vortex and the temperature distribution inside the vortex with various given angular momentum.

3. Result and discussion

As the ground surface temperature was kept constant and the given angular velocity of the cylinder was increased, the vortex diameter increased. The temperature inside of the vortex was higher than the surrounding, and the temperature difference between them was more significant with smaller vortex diameter was small.

The vertical temperature gradient of the central part was larger when the vortex diameter was large, that is, when the angular momentum was large.

It is suggested that the dust devil plays a certain role in heat transportation and the given angular

©2020. Japan Geoscience Union. All Right Reserved.

momentum should control its efficiency. The reason why the center of the vortex shows higher temperature than the surrounding area is that the hot air near the ground surface is collected by the pressure gradient force in the direction of the center of the vortex, which is the result of the high temperature near the center. However, we have not reached to a clear answer as to why a large centrally oriented pressure gradient force is generated in the early stages of the formation of the vortex.

By conducting quantitative evaluations in the future, we will clarify the mechanism by which the given angular momentum and ground surface temperature affect the scale and structure of the vortex.

By applying the scaling of real whirlwind and experimental equipment using eddy viscosity, we want to find out the conditions critical to the growth and dissipation of the dust devil.

4. Acknowledgement

I would like to thank Dr. Ryoya Ikuta, associate professor of the Department of Earth Science, Faculty of Science, Shizuoka University, and the Shizuoka University FSS Secretariat for their support.

5. References

・Ito, J., (2017), Formation, Intensification, and Gusty Winds of Dust Devils (Japanese), Wind Engineers, JAWE Vol.42, No.1(No.150)

・Niino, H., (2009), Tornadoes and Dust devils: Current Understandings and Future Subjects (Japanese), 58th National Congress of Theoretical and Applied Mechanics

Keywords: meteorology

©2020. Japan Geoscience Union. All Right Reserved.

©2020. Japan Geoscience Union. All Right Reserved.

Automatic observation of Visibility

*HARUTO TANAKA[1], *MITSUKI BABA[1], *YUYA HAMASHIMA[1]

1. Tokyo Metropolitan Tachikawa High School

Research background and purpose:
Since about 70 years ago, meteorological observation (temperature, atmospheric pressure, humidity, wind speed, rainfall, visibility observation, etc.) has been continued twice a day. Since 1995, the number of missing measurements has increased, but in 2007, automatic observation equipment was introduced to resume non-visibility observations. In 2018, we resumed visual visibility observation, but it was difficult to observe at the same time every day, and the number of missing measurements increased significantly compared to the past. In this study, in order to solve this problem, we have developed a new method of observation by taking a picture of the subject on time with a computer-controlled camera. By using a camera, it is also possible to eliminate the influence of the observer's eyesight.

Manufacture and installation of automatic observation equipment:
Five rooftops were selected as places with more target scan in the city center, and the foundation was attached to the railing to secure the observation device. The container made a sealed case covered with aluminum sheet to protect the equipment from dust and wind and rain, and worked to connect outdoor power cords and LAN cables from the room to supply the power supply. The observation device consisted of an SLR camera and a Raspberry Pi to control the camera. The program wrote an instruction in Python to take a picture on time and automatically upload the captured image to Google Drive. In addition, we have also created a program to control the observation device through Slack so that it can be photographed by operation by Smartphone, so that you can check the state of the sky at that time and the condition of visibility.

Observation methods and results:
In order to make automatic observations, it is necessary to determine in advance the settings for shooting, such as the proper exposure and sensitivity of the camera. I took several photos with different shooting settings at the same time, and repeatedly selected a photo with the right exposure, and decided on the setting. The focal length was fixed to 150mm, and three different shooting settings were set for a single observation. For the building group of the sky tree of 36km ahead and Shinjuku 25km ahead, when the result of the visual observation of the same time and the result of the photographed image of the camera were compared, the one that was able to be seen by visual observation can be confirmed in three photographed images, it was found that there is no difference in the observation results visually and the camera.It is necessary to further consider the difference between the identification in the visual and the image by increasing the observation.

Considerations:
Comparing the data obtained from this automatic observation with the data from the same period (winter) in the 1950s and 60s of the previous study, the visibility is much better now. In the past, there were many days with visibility of less than 4km, and previous studies mentioned that winter mornings and air pollution were a factor in visibility, but now the weather has made visibility worse, and there are few occurrences in the morning. In the future, we will investigate the relationship between visibility and

©2020. Japan Geoscience Union. All Right Reserved.

weather, and seasons, yellow sand and air pollution.

Keywords: Meteorology, Visibility, Visibility observations

©2020. Japan Geoscience Union. All Right Reserved.

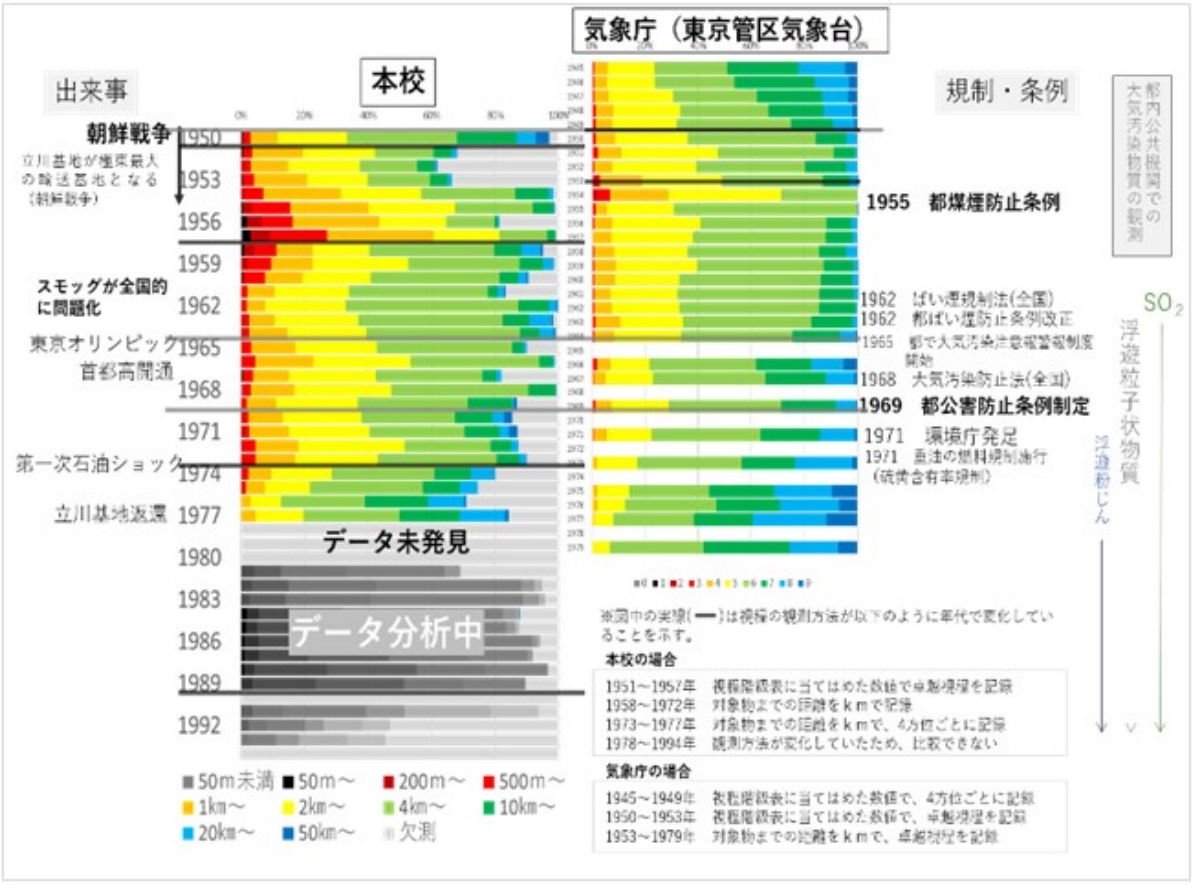

図1: 本校と気象庁の過去の視程

©2020. Japan Geoscience Union. All Right Reserved.

Analysis of sunspot observation data over 70 years and future prospects

*HAMASHIMA YUYA[1]

1. Tokyo Metropolitan Tachikawa High School

Background:
Tachikawa High School's Astronomy and Meteorology Club have been observing sunspots for more than 70 years since 1947. Five years ago, seniors created a continuous graph of relative sunspot number from a record of about 5,500 days. Three years ago, we measured the rotation period of the sun point from an observational sketch and stuied on the differential rotation of the sun. In this study, we added new data to the prior research, and measurement scan was reviewed for differential rotation, and detailed analysis was performed.
Objective:
We analyze the sunspot observation data over 70 years and analyze the three points between the increase or decrease in , the tendency of differential rotation, and the relationship between the sunspot area and the relative sunspot number.
Meth
1)About the relative sunspot number
We added the observation data about 500 days' worth of observation data to create a continuous graph of relative numbers. In addition, compared the cycle 19, which was observed the highest sun score in the maximum period in the school data, cycle 24.
2)About differential rotation
25 data was added to the 53 sunserp of the maximum period, select the sunspot group capable of calculating the rotation period, read longitude and latitudeof the sunspot group and the moved angle with a dedicated tracing paper. Next, we get a revolution period, taking into account the rotation angle of the earth.Next, we reviewed measurement data ,and was graphed the relationship between thie average latitude of the sun point and the rotation period . The theoretical value was determined by the formula of the rotation period of the earth according to the chronological sycientific tables , considering the revolution period of the earth.
3)About area of sun spot and relative sunspot number
For the white full light image of the sun observed by the National Astronomical Observatory (1997-2019), the area of the sunspot was calculated by the program (Python) using openCV, and the relationship between this value (number of pixels) and the relative sunspot number of our school was chronology.
Results and Considerations:
1)About the relative sunspot number
The change in the number of relative number over the 70 years, which added recent observationdata, was roughly consistent with the public observation agencies. The relative sunspot number of in cycle 24 is very small compared to cycle 19, and in view of the large flow of the greatest period, the next cycle 25 may be even smaller than this time.
2)About differential rotation
The regression curve of the estimate sedate from the measurement of our school showed the tendency of differential rotation, and it was almost consistent with the theoretical value in the low latitude. In addition, in the high latitude showed a larger value, but a long sunspot of the rotation cycle was measured many, there was a considerable width to the variation of the data.
3)About the sunspot area and the relative sunspot number

©2020. Japan Geoscience Union. All Right Reserved.

The area of the sunspot (number of pixels) calculated from the data of the National Astronomical Observatory and the relative sunspot number of our school showed a tendency of the same increase or decrease, and a positive strong correlation was observed. It is thought that the area of the sunspot becomes large as the activity of the sun is active.
Issues on future observations:
In the future, the appearance of sun scores will decrease, and as a part of the department, there is a concern that the number of opportunities for observation will decrease. Since there are complex procedures for sunspot observation and it is not easy to learn, we have prepared a manual that explains the observation methods in an easy-to-understand way of using illustrations and photographs. We have also attempted observations using theHα Solar Telescope, but it is difficult to use them, and we are considering whether there are any new observation methods. Public observers have changed from sketch observationto CCD image observations, and although web data can be obtained every day, we would like to continue sketching observations and conduct research.

Keywords: sun, sunspot, differential rotation, area of sunspots

©2020. Japan Geoscience Union. All Right Reserved.

図１　15cm屈折望遠鏡

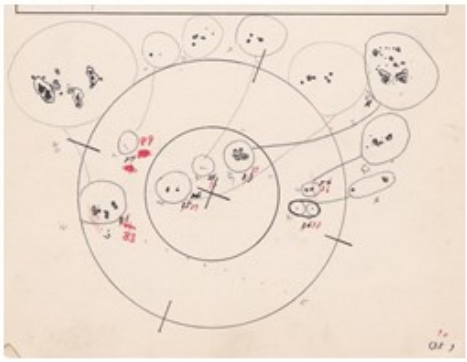

図２　実際のスケッチ

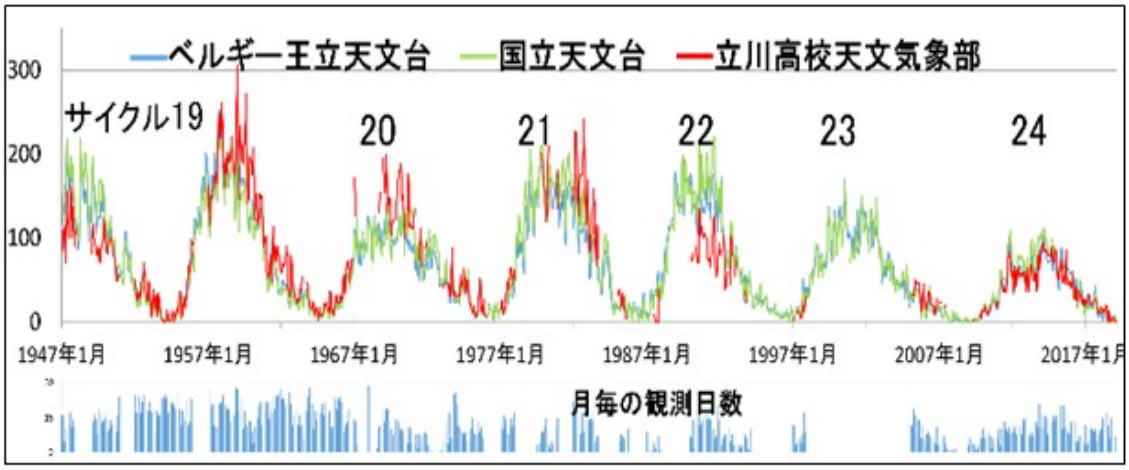

図３　1947～2018年黒点相対数（月平均）

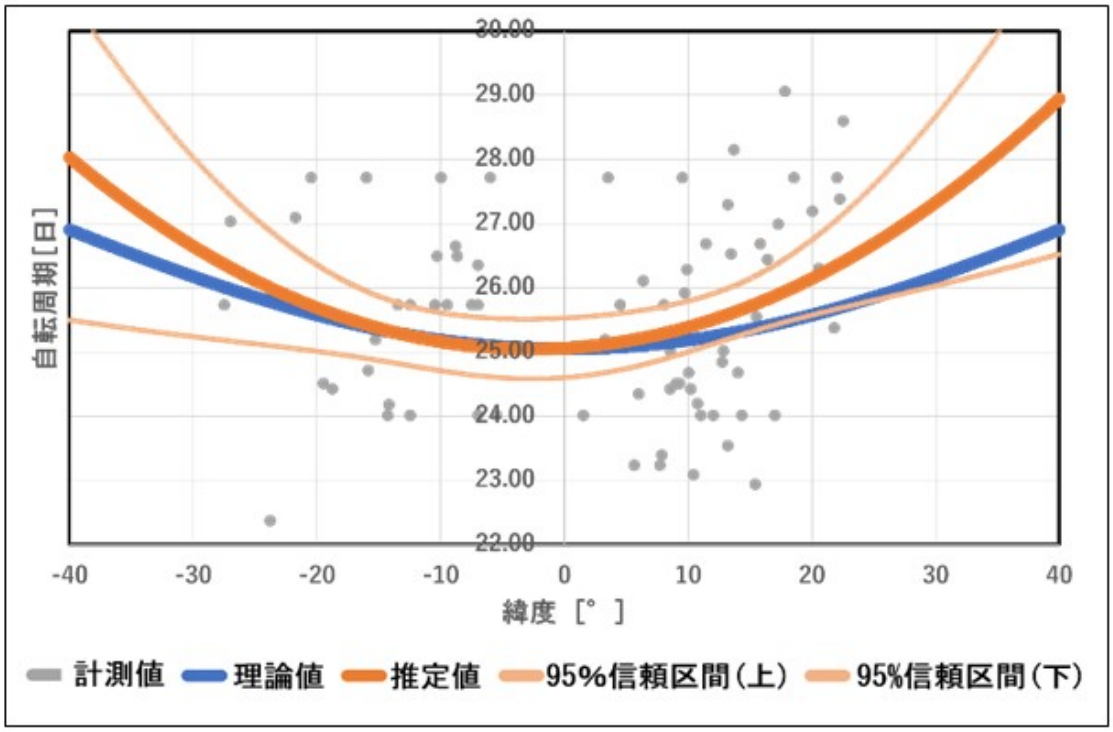

図４　平均緯度と自転周期の関係

©2020. Japan Geoscience Union. All Right Reserved.

Development of an automatic observation and notification system for the meteor shower
~A signal detection and data output using Arduino~

*Koichi Sato[1], *Junsei Okuma[1]

1. Chuo University Junior and Senior High School

Introduction:

In general, radio meteor observation is conducted using a receiver with an antenna, which receives a specific radio wave frequency. Passing a meteor through the upper atmosphere causes ionization on the ionosphere. The ionized meteor trail reflects radio waves from the transmitters on the ground, and we observe the reflected radio waves as a meteor signal (HRO or FRO method). The observed data is obtained as a figure file by HROFFT software. The number of the meteor is counted by the meteor echo or Activity Level (the difference between the number of measured echoes and the mean value of echoes for the past two weeks). However, there are some issues in this method, for example, the huge uncertainties for measurement and the high expense for radio meteor observation (e.g., radio wave receiver and antenna). The objective of this study is to develop an automatic observation and notification system for the meteor shower in order to observe the meteors more readily.

Method:

Our developed system was organized by two sections: 1) radio meteor observation section using a radio wave receiver and a 2-element antenna, and 2) analysis section using a PC with Arduino. We focused on audio data (frequency and volume data, i.e., meteor audio data), which was collected during the radio meteor observation. The meteor audio data was analyzed by WaveSpectra software and Fast Fourier Transform (FFT) library in Arduino. Moreover, we developed a notification system of meteor signals.

Results and Discussions:

We compared the meteor audio data with published observation data (The International Project for Radio Meteor Observation). As a result, we found the meteor signal with a peak of 495 Hz. For detecting the meteor signals, the required sound volume was five times larger than the mean value of the obtained data. Besides, we developed a program that automatically detects the meteor signals and notifies them on a PC screen. Moreover, it was successful in transforming quantitative data of the meteor signal into numerical data, and then it compiled as a text file. Thus, the procedure through the observation, analyzing, and data output of radio meteor signals became automatic. This system allowed the quantitative and stable data collection.

Conclusion:

Our developed system succeeded in providing the new automatic method for radio meteor observation and meteor signal data output. It is necessary to develop the application for the public, which notifies the measured and analyzed meteor signals detected by our system. It will promote the opportunity of observing the meteor shower.

©2020. Japan Geoscience Union. All Right Reserved.

Keywords: radio meteor observation, automatic observation system, Arduino

©2020. Japan Geoscience Union. All Right Reserved.

[J] Poster | O (Public)：Public

[O-05] Understanding of formation process of Japanese archipelago from Japanese Geoparks

convener:Noritaka Matsubara(Graduate School of Regional Resource Management, University of Hyogo), Yayoi ICHIHASHI(Sado Island Geopark Promotion Office), HIROKO IMAI(Com Support Office /Wakayama University Center for Tourism Research), Hokuto Obara(Mine-Akiyoshidai Karst Plateau Geopark Promotion Council)

As of October 2019, there are 9 UNESCO Global Geoparks and 35 Japanese National Geoparks in Japan. Each geopark records the formation process of the Japanese archipelago, and we can know the formation of the Japanese archipelago by connecting all the geoparks. In this session, we discuss about formation process of Japanese archipelago and relationship between Geology and people's lives through the Japanese Geoparks.

[O05-P01] Learning about and Protecting Stones in the Itoigawa UNESCO Global Geopark: Stone Guide System

*Takahiko Ogawara[1], Ko Takenouchi[1], Yosuke Ibaraki[1], Takeo Kobayashi[2] (1.Fossa Magna Museum, 2.Itoigawa City Hall Geopark Promotion Office)

[O05-P02] Creating walking map for visitors in winter season in Minami-Alps Geopark.

Yuko Miyazaki[1], *Eri Ozawa[2] (1.Oshika museum of Japan Median Tectonic Line, 2.Minami-Alps MTL Area Geopark Council)

[O05-P03] Sustainable dissemination activities realized through the partnership "Making the stone specimen in Hakusan Tedorigawa Japanese Geopark"

*Yuya Kitoh[1], Satoshi Hirai[1], Kiyofumi Tamamura[1], Tsuyoshi Hibino[2], Kaori Nakano[2], Tomoaki Morishita[3], Yoshihiro Hiramatsu[3], Maki Hamada[3] (1.Ishikawa Geological Survey Association, 2.Hakusan Tedorigawa Geopark Promotion Council, 3.Kanazawa University)

[O05-P04] A case study of geo-education at an geo/ecological site in the Dinosaur Valley Fukui Katsuyama National Geopark

*Yoshihiro Moriishi[1], Sumiaki Machi[1], Eiichi saito[2], Kensuke Hirose[2], Yukie Yasui[1,3], Msahiro Amadate[1] (1.Dinosaur Valley Fukui Katsuyama Geopark Promotion Council , 2.Heisenji Elementary School, 3.Katsuyama City Education Board)

[O05-P05] The support systems and practice examples of geopark education at elementary and junior high schools in the Dinosaur Valley Fukui Katsuyama National Geopark

*Sumiaki Machi[1], Masahiro Amadate[1], Yukie Yasui[1,2], Yoshihiro Moriishi[1], Keisuke Nunome[3], Kazutaka Izukura[4], Naoya Doseki[3], Hiroyuki Ito[4] (1.Dinosaur Valley Fukui Katsuyama Geopark Promotion Council, 2.Katsuyama City Education Board, 3.Arado Elementary School, 4.Katsuyama Nanbu Junior High School)

[O05-P06] Creating regional brands using geoparks

*Kei SHIMOMURA[1,2], Ken'ichi KURIHARA[3,4] (1.Mikasa Geopark Promotion Counsil, 2.Regional Development and Geopark Promotion Council, 3.Geo.Labo.corporation, 4.Hokkai Gakuen University)

[O05-P07] The first geotour consisted of activity programs for overseas student in Shikoku Seiyo Geopark.

Yuto Kamei[2], Keita Murakami[2], Yuichi Murakami[2], *Takumi Sakakiyama[1], Fumito Doi[1], Tsukasa Takahashi[1], Masayuki Sakakibara[2,3] (1.Seiyo City, 2.Faculty of Collaborative Regional Innovation, Ehime University, 3.Research Institute for Humanity and Nature)

[O05-P08] Making learning handbook for Nanki Kumano Geopark from the viewpoint of teachers

*YUMINE Toshiki[1], SUZUKI Toshikazu[2], TABUCHI Yu[3], NAKANISHI Dai[4], NOGAMI Seiji [5], MATUSHITA Hutoshi[6], YOKOYAMA Kazuya[5] (1.Chiben Gakuen Wakayama elementary school, 2.Susami Elementary School in Susami town, 3.Shinjo Junior high School in Tanabe city, 4.Wakayama University Elementary school, 5.Wakayama city science museun for children, 6.Wakayama Biological Club)

[O05-P09] Making Use of Mining Heritage in Mine-Akiyoshidai Karst Plateau Geopark

*Hokuto Obara[1], Tomoyuki Narasaki[1], Tomoko Muratani[1], Tristan Gray[1], Yutaka Kuramasu[1], Tatsuo Sueoka[1], Kazuhiro Yuhora[2], Koji Wakita[3] (1.Mine-Akiyoshidai Karst Plateau Geopark Promotion Council, 2.Tottori University of Environmental Studies, 3.Yamaguchi University)

[O05-P10] Four geological body constructing Shimokita Geopark

*Satoshi Ishikawa[1] (1.Shimokita geopark promotion council)

[O05-P11] Shimonita Geopark-Town planning utilized local resorce-

*Hara Hideo[1] (1.Geopark Shimonita Council)

[O05-P12] Plate Collision and Life of people at Mt. Apoi UNESCO Global Geopark

*Kato Satomi[1] (1.Mt. Apoi Geopark promotion council)

[O05-P14] Connecting Local governments with Geopark activities

*Suzuka Koriyama[1], Sanin Kaigan Geopark Promotion Council (1.Sanin Kaigan Geopark Promotion Council)

[O05-P15] Revised action plan for the first time in four years, created through direct dialogue with local residents

*Hidetaka Akiyoshi[1], Harumi Koumura[1] (1.San'in Kaigan Geopark Promotion Council)

[O05-P16] Reconstruction of two types of Miocene volcanoes in the northern part of hyogo, San’in Kaigan Geopark, based on facies analysis.

*Noritaka Matsubara[1], Suzuka Koriyama[2] (1.Graduate School of Regional Resource Management, University of Hyogo, 2.San'in Kaigan Geopark Promotion Council)

[O05-P17] **Practical use of geosites in Sado Island Geopark and the issues related to their use**

*Takeyoshi SADAKANE[1] (1.Sado Geopark Promotion Office)

[O05-P18] Process of Making a Field Trip Route in Sado Island Geopark

*Yayoi ICHIHASHI[1] (1.Sado Island Geopark Promotion Office)

[O05-P19] Activities to protect the formation locality of quartz twins on the Japanese law in the Goto Islands Geopark concept.

*Mana Yasui[1], Koichi Iwata[2], Hirotaka Karatsu[2], Ichiro Hosoda[2] (1.Waseda research institute for science and engineering, 2.Goto municipal office Geopark promotion group.)

[O05-P20] Mystery solving event using geosites at Shirataki Geopark

*Yoshihumi Matsumura[1], Makoto Kumagai[1] (1.Shirataki Geopark Promotion Council)

[O05-P21] The Land Formed by severe crustal movement and the Lives of its People
–case study of the Misaki Group in Tosashimzu Geopark Plan–

*Satoru Imai[1], Michiru Sakai[1], Aika Sakuda[1], Natsuki Moriguchi[1] (1.Tosashimizu Geopark Promotion Council)

[O05-P22] Geology, topography and life of the people in Oita Himeshima Geopark

*Yu Horiuchi[1], Takeaki Suga[1], Norimitsu Suka[1] (1.Oita Himeshima Geopark Promotion Office)

[O05-P23] Educational Program on spring water of Aso UNESCO Global Geopark related with electrical conductivity

*Tsuneomi Kagiyama[1], Shuhei Takamori[1], Natsuko Kodama[1], Shinichiro Ikebe[1], Akinobu Ishimatsu[1] (1.Aso Geopark Promotion Council)

[O05-P24] Sharing volcano experiments conducting at some UGGp in Japan

*Hikaru Yokoyama[1,2], Taku Morimoto[3], Kenji Kato[4], Dong-Won Choi[5], Naoko Imabeppu[5] (1.Hokusho University, 2.Toya-Usu Unesco Global Geopark, 3.Unzen Volcanic Area Unesco Global Geopark, 4.Izu Peninsula Geo Guide Association, 5.Hantangang River Geopark)

[O05-P25] A geo-tour for disaster prevention in the Bandaisan Geopark -relation between the Nagase River flood and the Bandai Volcano eruption-

*Yojiro Taketani[1], Hiroshi Sato[1,2], Makoto Hasuoka[1] (1.Bandaisan Geopark Council, 2.Mt. Bandai Museum)

[O05-P26] Revalidation mission of Toya-Usu UNESCO Global Geopark in 2019
-Strategy of the mission for green card-

*Yuki Nishi[1], Masato Takekawa[1], Nire Kagaya[1], Asami Nakaya[1], Yoshiaki Hata[1] (1.Toya-Usu UNESCO Global Geopark Council)

[O05-P27] Review of actions in Mishima Village Kikai Caldera Geopark, and agenda for revalidation of Japanese Geopark Network

*Geopark Council Mishima Village[1], Mahito Watanabe[2], Kei SHIMOMURA[3] (1.Mishima Village office, Kagoshima Prefecture, 2.Institute of Geology and Geoinformation, National Institute of Advanced Industrial Science and Technology, 3.Mikasa Geopark Promotion Counsil)

[O05-P28] Activities to promote the local sustainable development - Report on recertification review of “Kurikomasanroku no Megumi” special products from Mt.kurikoma Area geopark -

Kobayashi Mizuki[1], *Tanaka Seiya[1], Nakagawa Rie[1] (1.Mt. Kurikoma Area Geopark Promotion Committee)

[O05-P29] Disaster Prevention practice at Naeba-Sanroku Geopark ~Typhoon No.19(Hogibis) disaster and response in 2019~

*Kouhei Nakano[1] (1.Naeba-Sanroku Geopark Promotion Council)

[O05-P30] Did the Chinda Falls recede? – Evolution of river topography in the Oita Bungoono Geopark, Japan

*Toshikazu Yoshioka[1] (1.Oita Bungoono Geopark Promotion Council)

[O05-P31] Globally Important Agricultural Heritage System "Minabe-Tanabe Ume System" viewing from geomorphological aspects of three small catchment area, central part of Wakayama Prefecture

*Yoshinori Kodama[1], Kazuki Taira[2] (1.Faculty of Agriculture, 2.Wakayama Prefecture)

[O05-P32] Systemization of the Certified Tourism Guide Program and its Significance – An Example by the Hakusan Tedorigawa Geopark

*Tsuyoshi Hibino[1], Ryoichi Onishi[1], Yoshiko Funatsu[2] (1.Hakusan Tedorigawa Geopark Promotion Council, 2.Hakusan City Tourism League)

[O05-P33] Evaluation of explanation panels setting at Geopark’s site 2 - case study of the explanation panel at Obama Hot springs in Unzen Volcanic Area UNESCO Global Geopark, Japan -

Kenshin OSHIMA[1], Yui KURITA[1], Miyu KAWAZOE[1], Rinna TAKEICHI[1], Ayaka OHIRA[1], Ayuka BABA[1], Ayuko SAGARA[1], Nagisa NAKAMURA[1], Takuji MURAOKA[2], Toshiki HIGASHIUCHI[2], *Marekazu OHNO[3] (1.Glocal Course, Nagasaki Prefectual Koka High School, 2.Nagasaki Prefectual Koka High School, 3.Unzen Volcanic Area Geopark Promotion Office)

[O05-P35] Meteorological landscape over the geopark: A lined-up cumulus row generated by the mountains in the western part of Oga Peninsula, Akita Prefecture, Japan

*Norihito Kawamura[1], Seiji Yamashita[2] (1.School of Regional Resource Management, Graduate School, University of Hyogo, 2.Faculty of Education ans Human Studies)

[O05-P36] Inform of weather disasters in geoparks

*Hiroshi Sato[1,2], shinichi Sugimoto[3], Makoto Aoi[4], Shinya Miura[4] (1.Mt.Bandai Museum, 2.Bandaisan Geopark Council, 3.Sanriku Geopark, 4.National Research Institute for Earth Science and Disaster Resilience)

[O05-P37] Foreign Tourist Survey: Places of Interest, Transportation, etc.

*Susan May[1] (1.Hakusan Tedorigawa Geopark Promotion Council)

[O05-P38] Education activities of museum encouraged establishing of graduate school in geopark -Museum of Nature and Human Activities and San'in Kaigan UNESCO Global Geopark

*Tohru Sakiyama[1] (1.Institute of Geo History, Japan Geochronology Network)

[O05-P39] Trends on and assessments of "ecological resources" in the Evaluation Mission Reports for Japanese Geoparks

*Kazuhiko HIRATA[1,2], Yuya Kato[1,3], Shinsuke Nakamura[1], Rieko Fujii[1], Natsuki Moriguchi[1,4] (1.Ecological Working Group for Japan Geopark Network, 2.Natural History Museum and Institute, Chiba, 3.Noyama Company, 4.Tosashimizu Geopark Promotion Council)

[O05-P40] Case study of Children's Summer School on Earthquakes and Volcanoes in Tango area of San-'in Kaigan UNESCO Global Geopark

*Tomoya Hiiro, Satoko Murotani[1], Ai Toma[2], Children's summer school on Earthquakes and Volcanoes Committee for[3,4,5] (1.National Museum of Nature and Science,Tokyo, 2.Keio University, 3.Seismological Society on Japan, 4.Volcanological Society of Japan, 5.Geological Society of Japan)

[O05-P41] Educational Effects of Screening a Geopark Film at a Local Science Museum

*Rin Nodera[1,2] (1.Kurobe Yoshida Science Museum, 2.Tateyama Kurobe Geopark Society)

[O05-P42] Examples of activities in collaboration with Tateyama Kurobe Geopark and University of Toyama

*Takuya Harada[1], Yuta Yamaoka[2], Kiichi Yamahori[2], Kiyoshi Nakagawa[2], Koji Ohnishi[1], Ken-ichi Yasue[1] (1.University of Toyama, 2.Tateyama Kurobe Geopark Society)

[O05-P43] Approach of Health Promotion with Geotourism in Central area of Toyama City

*Ken-ichi Yasue[1], Yuta Yamaoka[2], Tomoya Tanabe[3], Takuya Harada[1], Utako Uchikoshiyama[2], Toshimi Tajima[3], Kiyoshi Nakagawa[2], Koji Ohnishi[1], Kiichi Imahori[2] (1.University of Toyama, 2.Tateyama Kurobe Geopark Society, 3.Approved Specified Nonprofit Corporation Machizukuri Spot)

[O05-P44] Creating relationship between University of Toyama higher education and Tateyanakurobe Geopark activity

*Koji Ohnishi[1], Ken-ichi Yasue[1], Yuta Yamaoka[2], Takuya Harada[1], Kiichi Imahori[2] (1.University of Toyama, 2.TateyamaKurobe Geopark Society)

[O05-P46] 30 years since the eruption of Teishi Knoll in 1989

*Yusuke Suzuki[1] (1.Izu Peninsula Geopark Promotion Concil)

Learning about and Protecting Stones in the Itoigawa UNESCO Global Geopark: Stone Guide System

*Takahiko Ogawara[1], Ko Takenouchi[1], Yosuke Ibaraki[1], Takeo Kobayashi[2]

1. Fossa Magna Museum, 2. Itoigawa City Hall Geopark Promotion Office

Itoigawa City is the first region in Japan to be certified a UNESCO Global Geopark and promotes a variety of activities which make use of its natural resources. The Itoigawa-Shizuoka Tectonic Line is a massive fault which runs through the center of Itoigawa, splitting it between east and west. This fault line is responsible for Itoigawa’s great diversity of rock types, including jade.

As part of a new city promotion campaign as “Stone Town Itoigawa” in 2019, a new Stone Guide System was established with the goal of promoting Itoigawa’s many fascinating stones, including jade. The Stone Guides System was founded with a goal of promoting to local people and visitors not only the appeal of Itoigawa’s many stones, but also the importance of conserving them for future generations, in accordance with the objectives of the Itoigawa UNESCO Global Geopark and the Sustainable Development Goals. The courses undertaken by these Stone Guides include both foundational and practical courses. Individuals who have passed both of these courses in addition to the Beginner Level of the Itoigawa Geopark Certification Exam are eligible to take the Stone Guide Certification Exam.

In the first year of the program (2019), 172 individuals participated in the foundational and practical courses and 42 individuals have signed up for the certification exam.

Keywords: Itoigawa UNESCO Global Geopark, Stone guide system

©2020. Japan Geoscience Union. All Right Reserved.

Creating walking map for visitors in winter season in Minami-Alps Geopark.

Yuko Miyazaki[1], *Eri Ozawa[2]

1. Oshika museum of Japan Median Tectonic Line, 2. Minami-Alps MTL Area Geopark Council

In winter, there are few visitors to Minami-Alps MTL area Geopark because of little snow and severe cold. However, in warm winters, it is warm enough to enjoy walking during the daytime on a sunny day.
So, we created the walking map to observe the topography and the geology along the Median Tectonic Line.

Keywords: Geopark, Median Tectonic Line, walking map

©2020. Japan Geoscience Union. All Right Reserved.

Sustainable dissemination activities realized through the partnership "Making the stone specimen in Hakusan Tedorigawa Japanese Geopark"

*Yuya Kitoh[1], Satoshi Hirai[1], Kiyofumi Tamamura[1], Tsuyoshi Hibino[2], Kaori Nakano[2], Tomoaki Morishita[3], Yoshihiro Hiramatsu[3], Maki Hamada[3]

1. Ishikawa Geological Survey Association, 2. Hakusan Tedorigawa Geopark Promotion Council, 3. Kanazawa University

One of the real pleasures of the Geopark is that people from various perspectives collaborate, looking at the region from the viewpoint of Earth sciences. Our goal is to understand and share each goal and achieve them through the partnership in the field of the Geopark. We believe that active interest in the region, thinking together, and taking action are the steps we should take for sustainable development of the region.
We have held the event entitled “Making the stone specimen in Hakusan Tedorigawa Japanese Geopark" for elementary school students and their parents since 2017. This event utilizes a field of the Geopark, aiming to make children, as the next generation, have interests in nature and natural science.
On Saturday 5 October 2019, 28 pairs of children over the fourth grade in elementary schools and their guardians joined the event. After learning stones and how to distinguish them, they collected stones and made the stone specimens with students from various countries and others using hammers, loupes, and medicinal liquids. We hope that they know the origin of the Earth from the formation of the "familiar stones" under their foot, and have a chance to learn the grace and the disaster brought by the Earth and the relationship with people's lives.
We learn the curiosity of the children as well as guardians about the stone and nature. Besides, a questionnaire conducted after the event shows that children are strongly interested in “familiar natures” such as fossils and pieces of jewelry in addition to stones. We also explore the new activities on the theme of "familiar natures". We hope to continue with the Geopark activities that lead to the sustainable development of the region and the securing and training of new leaders.

Keywords: Geopark, Partnership, Region, Outreach, Sustainable development

©2020. Japan Geoscience Union. All Right Reserved.

A case study of geo-education at an geo/ecological site in the Dinosaur Valley Fukui Katsuyama National Geopark

*Yoshihiro Moriishi[1], Sumiaki Machi[1], Eiichi saito[2], Kensuke Hirose[2], Yukie Yasui[1,3], Msahiro Amadate[1]

1. Dinosaur Valley Fukui Katsuyama Geopark Promotion Council , 2. Heisenji Elementary School, 3. Katsuyama City Education Board

All of the elementary schools and junior high schools in the Dinosaur Valley Fukui Katsuyama Geopark are member of the UNESCO School and imprement ESD (education for sustainable development) on the fields of the geopark. Each school conducts community learning which the students can learn from their familiar nature so that to enhance their civic prides.
We will report a case study of geo-education that we conducted at the Heisenji elementary school in collaboration with some stakeholders and discuss about our challenges and prospects.

Keywords: Dinosaur Valley Fukui Katsuyama National Geopark, Geopark Education, School Educatiom, ESD

©2020. Japan Geoscience Union. All Right Reserved.

The support systems and practice examples of geopark education at elementary and junior high schools in the Dinosaur Valley Fukui Katsuyama National Geopark

*Sumiaki Machi[1], Masahiro Amadate[1], Yukie Yasui[1,2], Yoshihiro Moriishi[1], Keisuke Nunome[3], Kazutaka Izukura[4], Naoya Doseki[3], Hiroyuki Ito[4]

1. Dinosaur Valley Fukui Katsuyama Geopark Promotion Council, 2. Katsuyama City Education Board, 3. Arado Elementary School, 4. Katsuyama Nanbu Junior High School

The Dinosaur Valley Fukui Katsuyama National Geopark is a Japanese geopark covering whole territory of Katsuyama city, Fukui prefecture. There are 9 elementary schools and 3 junior high schools in the area and they are member of UNESCO Associated Schools, base for ESD (Education for Sustainable Development) promotion. We will report our support systems and practice examples, conducted at the Arado elementary school and Katsuyama Nanbu junior high school, of geopark education at the schools in our geopark and discuss about our challenges and prospects.

Keywords: Dinosaur Valley Fukui Katsuyama National Geopark, Geopark Education, School Education, ESD

©2020. Japan Geoscience Union. All Right Reserved.

Creating regional brands using geoparks

*Kei SHIMOMURA[1,2], Ken'ichi KURIHARA[3,4]

1. Mikasa Geopark Promotion Counsil, 2. Regional Development and Geopark Promotion Council, 3. Geo.Labo.corporation, 4. Hokkai Gakuen University

This year, we will explore the creation of a new system by linking to the national workshop "Thinking about" local brands that utilize Geoparks "held at Mikasa Geopark.

Keywords: geostory, Regional brand, SDGs, Geopark activities, Sustainable communities

©2020. Japan Geoscience Union. All Right Reserved.

The first geotour consisted of activity programs for overseas student in Shikoku Seiyo Geopark.

Yuto Kamei[2], Keita Murakami[2], Yuichi Murakami[2], *Takumi Sakakiyama[1], Fumito Doi[1], Tsukasa Takahashi[1], Masayuki Sakakibara[2,3]

1. Seiyo City, 2. Faculty of Collaborative Regional Innovation, Ehime University, 3. Research Institute for Humanity and Nature

In Geopark, the sights called “Geosite” designate high natural science, humanities and social science values among the certified areas. On the tourism of geopark in Japan, we have performed the sightseeing (Geotourism) with explanation of local geoguides. Concerning for the tours for foreigners, it was suggested that the issues: (1) there are few guides speaking English, (2) Guide’s telling tends to be one-sided information transmission from the guide to the participants, making it difficult to provide a place for interactive communication, and (3) they cannot enjoy the unique cultural experience in the locals that foreign tourists expected. In Shikoku Seiyo Geopark, we have never conduct the geotour about foreign tourists. There has been no improvement of facilities for foreigners visiting sightseeing, and no training of English speaking guides. On the other hand, the figure of domestic tourists has decreased to the half of 2017 affecting by the 2018 Japan Floods. Seiyo City need the recovery of tourists and the development tours.

In order to expand the range of target tourists and enhance sustainable development of tourism in Seiyo City, we planned the first geotour consisted of activity programs for overseas student in Shikoku Seiyo Geopark. The program was scheduled from December 22 to 23 (an overnight stay) to ten visitors, overseas students and the families. The planners considered that the tourists can enjoy even if Japanese guides who are not fluent in English, therefore the program was mainly consisted of experiential activities. The tour participants tried to harvest oranges in terraced farms made of stone walls and experienced Japanese traditional event in the historic street developed by rice cultivation in the vast basin. The guides told as little as possible about the sights by using the tour pamphlet distributed in advance or when we arrived at the sight.

We conducted the questionnaire after the tour was finished. As the result, six of the seven respondents said “I didn’t know the geopark” or “I heard it for the first time.” On the other hand, three answered "very well known" and four said "known" about the geopark after the tour. As for the degree of satisfaction, 5 participants were "very satisfied" and 2 persons were "satisfied". On the other hand, there was an opinion that tourists wanted the geological and geographical interpretation about the sights of Shikoku Seiyo Geopark because of the bias toward experiential activities. With this initiative alone, it is not possible to evaluate the satisfaction of the tour for all foreign tourists or to evaluate whether it has led to an increase in the profits of the accepting side. We would like to evaluate quantitatively whether the tour will result in sustainable development of the region by conducting tours in the future.

Keywords: Geopark, Seiyo City, tourism, foreign tourist, susutinable development

©2020. Japan Geoscience Union. All Right Reserved.

Making learning handbook for Nanki Kumano Geopark from the viewpoint of teachers

*YUMINE Toshiki[1], SUZUKI Toshikazu[2], TABUCHI Yu[3], NAKANISHI Dai[4], NOGAMI Seiji [5], MATUSHITA Hutoshi[6], YOKOYAMA Kazuya[5]

1. Chiben Gakuen Wakayama elementary school, 2. Susami Elementary School in Susami town, 3. Shinjo Junior high School in Tanabe city, 4. Wakayama University Elementary school, 5. Wakayama city science museun for children, 6. Wakayama Biological Club

As a teachers who made a learning handbook for Nanki Kumano Geopark, We will present the issues and ideas of making a learning handbook.Also, one of the things that I want to cherish in science learning is the attitude of questioning things.
Students need an attitude to think about why.

We feel that what the student learns has nothing to do with real events or phenomena.
Especially with regard to earth science, students know the name but have never seen it.
The handbook for learning was created to relate the contents of what you learn in school to the actual land of Nanki Kumano.
There were various challenges in creating a learning handbook, and we needed to study anew.
The original text of the learning handbook was written by university teachers and is difficult for junior high school students to understand.

The members of the editorial board are made up of science teachers, who specialize in various fields such as chemistry, biology and physics. Furthermore, even if they are specialized in geology, they are 40 years ago and do not fully understand the current theory of plate tectonics. It is also necessary to deal with geopark-specific themes such as culture and disaster.

We distributed the first edition of the learning handbook to about 9,000 first-year junior high school students in Wakayama Prefecture in March 2018. In order to further enhance the learning effects of the students, the content was reviewed and the second edition was distributed in March 2019. Currently working on the third edition.

Keywords: Education, Education for disaster prevention, Culture

©2020. Japan Geoscience Union. All Right Reserved.

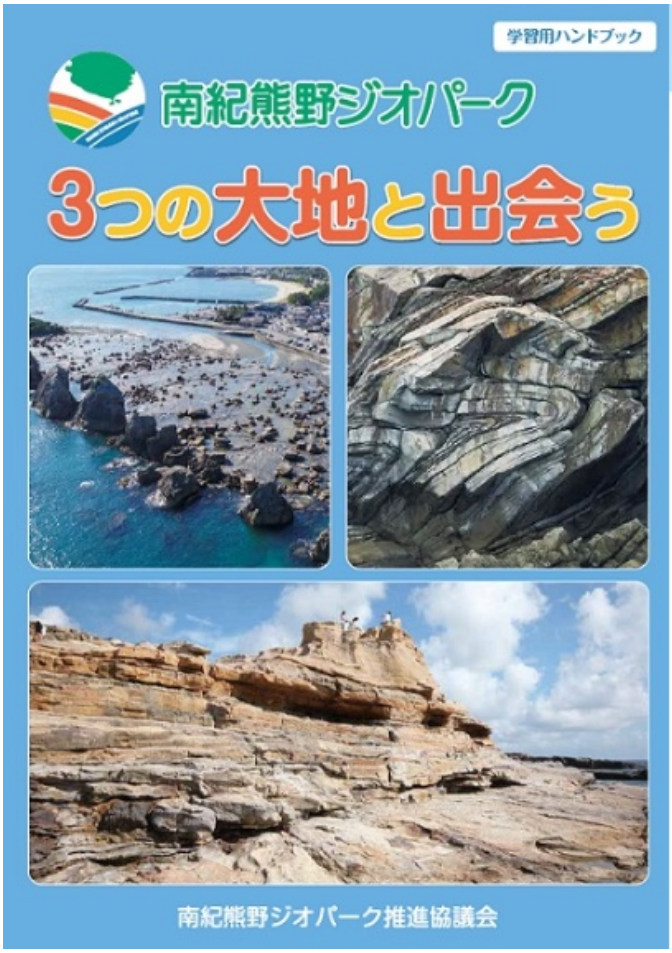

©2020. Japan Geoscience Union. All Right Reserved.

Making Use of Mining Heritage in Mine-Akiyoshidai Karst Plateau Geopark

*Hokuto Obara[1], Tomoyuki Narasaki[1], Tomoko Muratani[1], Tristan Gray[1], Yutaka Kuramasu[1], Tatsuo Sueoka[1], Kazuhiro Yuhora[2], Koji Wakita[3]

1. Mine-Akiyoshidai Karst Plateau Geopark Promotion Council, 2. Tottori University of Environmental Studies, 3. Yamaguchi University

In Mine-Akiyoshidai Karst Plateau Geopark, mining has been carried out since ancient times: from the Nara period, the mining of copper ore and the smelting of copper; from the Meiji period, the extraction of anthracite coal as well as the mining of limestone and marble, and the production of lime. Post-war, the large-scale mining of limestone began, supported by the demand for cement during the Economic Miracle period and which still continues today.
Within the geopark, the remains of mining activity can be seen all around, but several problems need to be solved before we can make use of this heritage. 1) Very few people who worked in the mines are still around today, and tales of what the mine was like have been lost. 2) Local mining companies do not allow the use of land they own on safety grounds. 3) Regular maintenance such as grass cutting is necessary. 4) Structures has become weakened by the inexorable ravages of time.
In order to overcome these challenges, particularly with regard to former coal mines and lime kilns, we have undertaken the following measures. 1) Conducting interviews with former miners. 2) The collection and digitisation of old photographs and other materials from the archives of local mining companies and libraries. 3) Negotiations with mining companies regarding the use of their land. 4) Collaboration with local groups.
We hope that by using this material as part of our geotours, the local people and tourists who take part in them will be encouraged to think about how they use and look after the earth’s materials. This, we hope, will contribute towards achieving SDGs number 7, ‘affordable and clean energy’, and number 12, ‘responsible consumption and production’.

Keywords: Mine-Akiyoshidai Karst Plateau Geopark, Japanese Geoparks, geopark activity, mining heritage, Sustainable Development Goals

©2020. Japan Geoscience Union. All Right Reserved.

Four geological body constructing Shimokita Geopark

*Satoshi Ishikawa[1]

1. Shimokita geopark promotion council

The land of Shimokita Geopark is constructed by the four geological bodies; Accretionary prism formed in Mesozoic, Submarine volcanic depositions formed in Paleogene, Volcanic depositions erupted in Quaternary and Depositional plains. In Shimokita Geopark, there are various stories including geological, ecological and anthropological fragments to know the interesting stories. These geological bodies indicate not only the history of formation of Shimokita area but also that of Japan.

Keywords: Shimokita Geopark, Accretionary prism, Submarine volcano, Quaternary volcano, Depositional plain, Northeast Japan arc

©2020. Japan Geoscience Union. All Right Reserved.

SHIMOKITA
GEOPARK

©2020. Japan Geoscience Union. All Right Reserved.

Shimonita Geopark-Town planning utilized local resorce-

*Hara Hideo[1]

1. Geopark Shimonita Council

The Shimonita Geopark is located in Southwest Gunma.
In this report, I report the activity of Shimonita Geopark ten years

Keywords: Geopark, Town planninig, Gunma Prefecture

©2020. Japan Geoscience Union. All Right Reserved.

Plate Collision and Life of people at Mt. Apoi UNESCO Global Geopark

*Kato Satomi[1]

1. Mt. Apoi Geopark promotion council

Mt. Apoi geopark

Keywords: Mt. Apoi, Horoman peridotite, plate

©2020. Japan Geoscience Union. All Right Reserved.

Connecting Local governments with Geopark activities

*Suzuka Koriyama[1], Sanin Kaigan Geopark Promotion Council

1. Sanin Kaigan Geopark Promotion Council

As of January 2020, there are 44 Japanese National Geoparks and 9 UNESCO Global Geoparks in Japan. In many Geoparks, the local governments play an important role in terms of budget and operation.

The San’in Kaigan UGGp consists of 6 municipalities from 3 prefectures. It declared a Japanese Geopark in 2008 and a UNESCO Global Geopark in 2010.

In the operation of the San’in Kaigan, main financial resources are contributed from local governments and most of Council staffs is assigned from local governments. It looks as if the local governments are taking the initiative in Geopark activities.

From the beginning, we faced various issues in coordination and stakeholder engagement arising from multi-municipality promotion and are currently working on solving them. Consequently we have taken various measures to solve these issues. In this presentation, we discuss about the difficulty of administer Geopark activities with multiple local governments.

©2020. Japan Geoscience Union. All Right Reserved.

Revised action plan for the first time in four years, created through direct dialogue with local residents

*Hidetaka Akiyoshi[1], Harumi Koumura[1]

1. San'in Kaigan Geopark Promotion Council

The San'in Kaigan Geopark is reviewing its action plan evert four years, and FY2019 was the year of revision. The revision work started in started in September and took five months to complete at the end of January. The reason we spent so long was to have a chance to talk with all the stakeholders.
Behind this is the Japan Geopark Commission's 2017 report. In other words, there is a lack of information sharing and discussion among stakeholders to determine the future direction of the Geopark. "Define future directions." The action plan is the foremost of this. The amendment has been discussed frankly with all stakeholders involved.
The San'in kaigan Geopark is 120 km east and west, and the municipalities consist of three prefectures, three cities and three towns, making it one of the most extensive geoparks in Japan. There are of course many stakeholders. Putting this together, we focused on two things in order to head for Geopark activities with the same vector.
One is that all stakeholders have the opportunity to participate and freely discuss. The other is to reflect as much as possible the opinions expressed in this discussion and make them effective. With the emphasis on these two, the action plan finally completed. The revised content is important, but I think the process has greater meaning. Here are some of them.

©2020. Japan Geoscience Union. All Right Reserved.

Reconstruction of two types of Miocene volcanoes in the northern part of hyogo, San’in Kaigan Geopark, based on facies analysis.

*Noritaka Matsubara[1], Suzuka Koriyama[2]

1. Graduate School of Regional Resource Management, University of Hyogo, 2. San'in Kaigan Geopark Promotion Council

The Japanese archipelago was previously part of the Asian Continent, and was separated from the continent by back-arc rifting that occurred on the eastern edge of the continent. Traces of various volcanic activities and sedimentation processes involved in this dynamic tectonic event were left across a wide area along the Sea of Japan coast of the Japanese archipelago. While many traces of activities in the sea are found in northeastern Japan, The San’in Kaigan UGGp has traces of the tectonic history of this area, changing from solid land through partial sea to shallow sea. Strata, fossils, volcanic rocks, and other features related to the traces are designated as geosites in the San’in Kaigan UGGp. Although ongoing rifting in various places on the earth is a tectonic event causing the formation of island arcs and epicontinental seas, its mechanism is still under discussion. We research evidence of rifting and the formation of the Sea of Japan in the San’in Kaigan UGGp area. In this session, we will discuss about reconstruction of two types of Miocene volcanoes in the northern part of hyogo, San’in Kaigan Geopark, based on facies analysis.

Keywords: formation of sea of japan, facies analysis, Miocene

©2020. Japan Geoscience Union. All Right Reserved.

Practical use of geosites in Sado Island Geopark and the issues related to their use

*Takeyoshi SADAKANE[1]

1. Sado Geopark Promotion Office

Some sites have been re-selected on Sado Island Geopark. The island is divided into 10 areas, and we started with selecting the geosites that are closely related to the Globally Important Agricultural Heritage Systems (GIAHS) sites, as well to the sites seeking inscription as a UNESCO world heritage on the island. When re-selecting geosites, those that have not only geological value but also practical facilities such as parking lots and toilets were particularly chosen as “geosites that can be utilized for educational activities and tourism”. These sites are the places where inhabitants and visitors can easily learn about the geo-story of Sado Island.
Over the past year, we have created some new geopark routes and told the public about these geosites at seminars and lectures.
Re-selecting the geosites which are aimed for educational use and tourism allows us to prioritize certain geosites.
I will describe some details about how these sites are being made more accessible, and some issues related to their use.

Keywords: Sado Island, geopark, geotourism, geosite, geological heritage

©2020. Japan Geoscience Union. All Right Reserved.

Process of Making a Field Trip Route in Sado Island Geopark

*Yayoi ICHIHASHI[1]

1. Sado Island Geopark Promotion Office

In 2019, we made several routes for a school trip. The participants were teachers, tourism operators and geopark guides.
The creation process for the routes as well as future prospects will be stated.

Keywords: Sado Island, Geopark

©2020. Japan Geoscience Union. All Right Reserved.

Activities to protect the formation locality of quartz twins on the Japanese law in the Goto Islands Geopark concept.

*Mana Yasui[1], Koichi Iwata[2], Hirotaka Karatsu[2], Ichiro Hosoda[2]

1. Waseda research institute for science and engineering, 2. Goto municipal office Geopark promotion group.

The Goto Islands have been engaged in various activities for Geopark certification. However, the Goto Islands Geopark was not certified by the Japan Geopark Committee in 2019. The Goto Islands Geopark Promotion Council has been conducting various activities with the aim of improving the understanding and awareness of Geopark activities more than ever, aiming to solve the issue indicated in the review result report presented by the Japan Geopark Committee. As part of this, we will report on the activities to protect the locality of quartz twins on the Japanese law from Narushima. Narushima is known to researchers and mineral collectors as a very famous locality of quartz twins on the Japanese law, and its detailed location has been featured in many books, guidebooks, and the Internet. In recent years, quartz twins on the Japanese law have been sold at high prices on the Internet, and illegal collections have continued despite collection bans. As the results, quartz twins on the Japanese law are more difficult to find as before, and protecting them with the island residents, seems urgent. The poster presentation will introduce the twins and explain their activities at the place of origin and possible actions to protect the place of production with the aim of understanding and cooperating with the Narushima residents.

Keywords: Goto Islands Geopark concept, protection method of mineral distribution area, quartz twins on the Japanese low

©2020. Japan Geoscience Union. All Right Reserved.

Mystery solving event using geosites at Shirataki Geopark

*Yoshihumi Matsumura[1], Makoto Kumagai[1]

1. Shirataki Geopark Promotion Council

Shirataki Geopark aims to achieve sustainable economic development using geosites.

Keywords: geopark, geotourism

©2020. Japan Geoscience Union. All Right Reserved.

The Land Formed by severe crustal movement and the Lives of its People
–case study of the Misaki Group in Tosashimzu Geopark Plan–

*Satoru Imai[1], Michiru Sakai[1], Aika Sakuda[1], Natsuki Moriguchi[1]

1. Tosashimizu Geopark Promotion Council

Tosashimizu Geopark Plan committee is located on the southwestern tip of Shikoku in Tosashimizu City, Kochi Prefecture. The geology of Tosashimizu consists of accretionary prism (28 to 16 Ma), the Misaki Group of forearc basin sediments (17 to 15 Ma), and Ashizuri granite (13 Ma). The Misaki Group and Ashizuri Granite are very important in understanding the origin of the Japan arc, because they are strongly related to severe crustal movement during the Japan Sea Opening. And these geological bodies not only have a value to the earth sciences but they also have a great influence on industry, culture and natural disasters.
In this presentation, we will introduce the history of the Japan arc, which can be understood from the Misaki Group, and the life on the Misaki Group, and how to understand and experience them.

Keywords: Tosashimizu Geopark Plan, Geopark, Japan Sea Opening

©2020. Japan Geoscience Union. All Right Reserved.

Geology, topography and life of the people in Oita Himeshima Geopark

*Yu Horiuchi[1], Takeaki Suga[1], Norimitsu Suka[1]

1. Oita Himeshima Geopark Promotion Office

Oita Himeshima Geopark is a certified Japanese Geopark as of 2013, known as "A mysterious island formed from volcanoes". Himeshima is an isolated island, which is located westernmost area of Seto Inland Sea, Southwest Japan. The island measures 2.6 km from the north to the south, and 6.6 km from the east to the west, and has a perimeter of 17 km.
Himeshima is located on the West Japan Volcanic Belt and characterized by the Quaternary monogenetic volcanoes. Coastal erosion and sedimentation of the Seto Inland Sea formed unique topography of Himeshima. Life, history, and culture of the people are also attractive aspects of the Oita Himeshima Geopark.
In this presentation, we discuss the formation process of the topography and geology found in Himeshima with the positioning in the Japanese archipelago, and the relationship with the life, history and culture of the people living there.

Keywords: Quaternary, monogenetic volcano, Seto Inland Sea, the West Japan Volcanic Belt, sand bar, coastal erosion

©2020. Japan Geoscience Union. All Right Reserved.

Educational Program on spring water of Aso UNESCO Global Geopark related with electrical conductivity

*Tsuneomi Kagiyama[1], Shuhei Takamori[1], Natsuko Kodama[1], Shinichiro Ikebe[1], Akinobu Ishimatsu[1]

1. Aso Geopark Promotion Council

Spring water is one of the important components of Aso UNESCO Global Geopark. We made an education program for local community to have more understandings on spring water of Aso Geopark.

Aso Geopark has 3 kinds of spring water depending on electrical conductivity; spring water around the caldera wall about 10 mS/m, spring water around the foot of central cones about 30 mS/m, and hot spring water more than 100 mS/m. These waters have different relation with Aso volcanic system.

We made educational programs how to understand the difference of electrical conductivity of spring waters; at first for high school students, and for kids and citizens later. We introduce our program briefly.
We have to express thanks to Kyushu Geopark Network.

Keywords: Aso UNESCO Global Geopark, Spring water, Electrical conductivity

©2020. Japan Geoscience Union. All Right Reserved.

Sharing volcano experiments conducting at some UGGp in Japan

*Hikaru Yokoyama[1,2], Taku Morimoto[3], Kenji Kato[4], Dong-Won Choi[5], Naoko Imabeppu[5]

1. Hokusho University, 2. Toya-Usu Unesco Global Geopark, 3. Unzen Volcanic Area Unesco Global Geopark, 4. Izu Peninsula Geo Guide Association, 5. Hantangang River Geopark

There are several geoparks in Japan that have active volcanoes as geosites. Each geopark have conducted volcanic experiments to spread volcanic phenomena and disasters to children and citizens. Each volcanoes in Japan have various characteristics, so various experiments have been developed and practiced.
On the other hand, there are many geosites due to volcano in areas without active volcanoes. However, in these areas, peaple are less interested in volcanoes and have less understanding about volcanoes.
As in Japan, Hantangang River Geopark in the northern part of Korea has many geosites composed of lava between 130 Ka and 500 Ka. However, people of the area do not understand much about volcanic eruptions, becouse this area don't have active volcanoes. Although many of the main geosites were provided by volcanoes, guide groups have not understanded much about volcanoes. So the guide groups wanted to increase the content of the volcano experiment to inflate the image of the volcanic phenomena that had not seen.
We Toya-Usu UGGp, Unzen Volcanic Area UGGp, and Izu Peninsula UGGp have active volcanoes. And we have conducted volcano experiments many times. So we carried out the volcano experiments lesson for the guide group in Hantangang River Geopark, and wanted to share our contents of volcano experiments.
The volcano experiment lesson was held on December 14, 2019 at Hantangang River Geopark Center in Pocheon City. Under the theme of volcanic activity learned through volcanic experiments, we conducted experiments on the mechanism of volcanic eruptions, the formation of volcanic plumes and pyroclastic flows, the collapse of mountains, and the experiments on lava flows.
We hope to promote activities to deepen the understanding of many citizens on the diversity of various geological phenomena including volcanoes by sharing contents of experiments among some geoparks.
Part of this work was supported by JSPS KAKENHI Grant Number JP17K01041.

Keywords: Volcano experiment, Network, Geo-Diversity

©2020. Japan Geoscience Union. All Right Reserved.

A geo-tour for disaster prevention in the Bandaisan Geopark -relation between the Nagase River flood and the Bandai Volcano eruption-

*Yojiro Taketani[1], Hiroshi Sato[1,2], Makoto Hasuoka[1]

1. Bandaisan Geopark Council, 2. Mt. Bandai Museum

The intense rain caused by the typhoon No.19 generated in October 2019 brought heavy flood damage in the East Japan. There was a heavy human damage that 32 people died in Fukushima Prefecture, too. Flood hazard map having high precision is maintained for the disaster in each place, but the spread is insufficient, and it is thought that delay of the evacuation order, delay of the refuge and belief of the security enlarged damage.
Not only merely fixing the system sheltering in emergency based on flood hazard map, but also local inhabitants knowing the history of the river and understanding the character of the water current and the flood mechanism are important in preparing for the disaster.
Because a lot of natural disasters such as eruption, earthquake and typhoon occur in Japan, the Japanese Geopark network puts effort into the disaster prevention. The Bandaisan Geopark also has poured power for the spread of the Bandai volcanic disaster prevention until now. Triggered by this flood disaster, we want to concentrate power on not only the volcanic disaster but also the flood disaster prevention.
The Nagase River, located in the Bandaisan Geopark, gathers many branches of the north side mountains of Mt. Bandai, flows south along the east foot of Mt. Bandai, and flows into Lake Inawashiro. It is the maximum river flowing into the lake. The river formed a large Inawashiro plain in the north side of the lake and has given great usefulness for life and industry of people in this area. On the other hand, it often overflowed and changed the channel, and damaged the villages of the river basin. It is handed down by tradition that the flow channel of the Nagase River was once greatly different from the present.
The volcanic activity of Mt. Bandai also had a great influence on the channel change of the Nagase River. Especially, by the Mt. Bandai eruption in 1888, a large quantity of gravel that occurred by a mountain body collapse drifted along the Nagase River and let the delta of the river mouth extend. In addition, the thick gravel that deposited along the river brought a rise of the riverbed surface and often caused floods. Above all, by the flood in 1913, five places of dikes of the basin collapsed, and 64 people died. After the dams for regulating water level were built beside the lakes of the upper Nagase River, the flood control advanced, but danger of the flooding is not gone afterwards.
We will attempt a tour around the Nagase River basin as the “Geology Day geo-tour" in May of 2020. By the geo-tour, the participants can see the old flow channel, the present channel and flood plain of the Nagase River, and the delta and terrace formed by the gravel that flowed down by the Mt. Bandai eruption, including the trace of the inhabitants’ effort who dealt with the floods.
We want to contribute to improvement of the disaster prevention consciousness by the local inhabitants and to deepen cooperation with the Japanese Geopark network in the disaster prevention field through this activity.

Keywords: Bandaisan Geopark, disaster prevention, Nagase River

©2020. Japan Geoscience Union. All Right Reserved.

Revalidation mission of Toya-Usu UNESCO Global Geopark in 2019 -Strategy of the mission for green card-

*Yuki Nishi[1], Masato Takekawa[1], Nire Kagaya[1], Asami Nakaya[1], Yoshiaki Hata[1]

1. Toya-Usu UNESCO Global Geopark Council

UNESCO obliges Global Geopark revalidation mission every 4 years. Subsequently, the Geopark was judged by UNESCO either green card (certification for 4 years), yellow card (certification for 2 years) or red card (revocation of certification). In 2017, Toya-Usu Global Geopark was given yellow card. 2 years later, the result of next revalidation mission was green card.
In the revalidation mission, UNESCO sends two evaluators to Geopark, and they inspect Geo-site and related facilities based on the UNESCO Geopark criteria.
In this time, we would like to describe about the revalidation mission in Toya-Usu UNESCO Global Geopark in 2019, provide useful information to UNESCO Global Geoparks in Japan or regions which aim to be Global Geopark.

Keywords: Geopark, Toya-Usu UNESCO Global Geopark, Global Geopark revalidation mission

©2020. Japan Geoscience Union. All Right Reserved.

Review of actions in Mishima Village Kikai Caldera Geopark, and agenda for revalidation of Japanese Geopark Network

*Geopark Council Mishima Village[1], Mahito Watanabe[2], Kei SHIMOMURA[3]

1. Mishima Village office, Kagoshima Prefecture, 2. Institute of Geology and Geoinformation, National Institute of Advanced Industrial Science and Technology, 3. Mikasa Geopark Promotion Counsil

The Mishima Village Kikai Caldera Geopark consists of three main islands and surrounding sea area. Residents in this geopark is only 369 people (Feb 2020), which is the smallest in Japan. This geopark is certified as a member of Japanese Geopaks Network in September 2015, and had revalidation in 2019. The geopark was certified with reservation, which means it will have revalidation in two years.

In this presentation, we review the process of our activity of this four years, and thinking about guideline for future activity. We also point out some agenda on revalidation process of Japanese Geoparks Network that we find out through this process, and discuss about them.

Keywords: Geopark, Kikai Caldera, Mishima village

©2020. Japan Geoscience Union. All Right Reserved.

Activities to promote the local sustainable development - Report on recertification review of “Kurikomasanroku no Megumi” special products from Mt.kurikoma Area geopark -

Kobayashi Mizuki[1], *Tanaka Seiya[1], Nakagawa Rie[1]

1. Mt. Kurikoma Area Geopark Promotion Committee

As one of the economic activities of Geoparks, many Geoparks have been developing "Geo-goods" and "Geo-Foods", but there were few products have taken advantage of their own location and locality.

At the Mt.Kurikoma Area Geopark, visitors and partners proposed to develop Geo-goods. Therefore, the “Geo-goods” development project was launched in 2015, mainly by the Development Working Group within the Tourism Division of the Mt. Kurikoma Area Geopark Promotion Committee. After a preparation period for program development, the program for “Kurikomasanroku no Megumi” was started in 2017, and certified 35 items from three categories: "Cuisine", "Souvenir", and "Recipe", through two reviews of stories and tasting. In 2019, the second recruitment was conducted and 6 new products were certified. Currently, the total number of certified products is 41 in total of the three categories.

In addition, this system conducts a recertification review once every two years to encourage sustainable activities in order to have certified stores use the Mt.Kurikoma Area Geopark. For stores subject to the recertification screening, a questionnaire survey will be conducted on the efforts for two years after the previous certification, such as changes in annual sales volume and sales promotion activities for certified products.

In this presentation, based on the results of the questionnaire survey on the first recertification audit conducted in 2019, we will discuss the local sustainable development.

Keywords: Mt.Kurikoma Area Geopark, Geopark, Geopark Product Certification Program, Sustainable Development, Local Participation, Empowerment

©2020. Japan Geoscience Union. All Right Reserved.

Disaster Prevention practice at Naeba-Sanroku Geopark ~Typhoon No.19(Hogibis) disaster and response in 2019~

*Kouhei Nakano[1]

1. Naeba-Sanroku Geopark Promotion Council

1. Purpose
In Naeba-Sanroku Geopark, disasters such as levee collapse and inundation related to Typhoon No. 19(Hogibis) in October 2019 occurred last year.

We would like to consider the outline of the damage and the response, and the resulting ongoing issues, disaster prevention measures, etc.

2. Contents
(1) Regional overview
(2) Damage of Typhoon No. 19 in Naeba-Sanroku Geopark from a geological viewpoint
(3) Correspondence of this Geopark and ongoing issues.
(4) Photos of the damage and brief explanation
(5) Summary (Proposals for disaster prevention measures and disaster prevention education as seen from the Geopark programs that we want to promote in the future.)

Keywords: Disaster prevention practice

©2020. Japan Geoscience Union. All Right Reserved.

Did the Chinda Falls recede? –Evolution of river topography in the Oita Bungoono Geopark, Japan

*Toshikazu Yoshioka[1]

1. Oita Bungoono Geopark Promotion Council

The Chinda Falls is one of the major sites of the Oita Bungoono Geopark, those are composed of O-daki (Male Falls) over the main stream of the Ono River and Me-daki (Female Falls) over the tributary Hirai River. These waterfalls were formed by the erosion of the columnar jointed welded tuff of the Aso-4 pyroclastic flow of about 90,000 years ago. The distance between these two waterfalls is about 300 meters, however the painting by Sesshu that is a famous painter in 15th Century show that the two waterfalls are close to each other. Some local people say the O-daki receded a few hundred meters after 15th Century.
The width of the Ono River is almost constant in the downstream of O-daki fall except for just below the fall. This means that the location of the fall is stable for a while and the lateral erosion is continuing at this point.
The rock wall in the south of the O-daki fall, where a tunnel of a channel for fishes was built in 1913, collapsed down in these tens of years. The columnar-jointed welded tuff of this wall overlies on the sedimentary rocks of Upper Cretaceous Onogawa Group, and the boundary between these two rocks is inclined to the river. This means that the wall of welded tuff is easy to collapse down. Collapsing of walls is a problem for the conservation of sites however the typical topography of the Oita Bungoono Geopark is formed by such collapsing. It is necessary to enhance the understanding of the people in local community for the conservation of sites and the disaster prevention.

Keywords: Chinda Falls, receding, Aso pyroclastic flow, conservation, disaster prevention, Oita Bungoono Geopark

©2020. Japan Geoscience Union. All Right Reserved.

Globally Important Agricultural Heritage System "Minabe-Tanabe Ume System" viewing from geomorphological aspects of three small catchment area, central part of Wakayama Prefecture

*Yoshinori Kodama[1], Kazuki Taira[2]

1. Faculty of Agriculture, 2. Wakayama Prefecture

We discussed relationship between globally Important Agricultural Heritage System "Minabe-Tanabe Ume System" in Central Wakayama and geomorphological features of the area, which situates adjacent to Nanki-Kumano Japan Geopark. Three small drainage areas: the Kirime River, the Minabe River and the Haya River were surveyed from fluvial geomorphological aspects. We found two characteristics: i) distribution differences in slightly elevated area, and ii) size differences in alluvial plain. Slightly elevated area connects to natural levee, which reflects river-bed material and to rolling hill area for supplying small particles to the Minabe and the Haya. According to analyses of bore-hole data, the deeper alluvial deposit basement is, the larger alluvial plain is. Minabe-Tanabe Ume System traces back to these geomorphological features.

Keywords: GIAHS ” Minabe-Tanabe Ume System”, slightly elevated area, basement of alluvial deposit, fluvial geomorphology, rolling hill

©2020. Japan Geoscience Union. All Right Reserved.

Systemization of the Certified Tourism Guide Program and its Significance –An Example by the Hakusan Tedorigawa Geopark

*Tsuyoshi Hibino[1], Ryoichi Onishi[1], Yoshiko Funatsu[2]

1. Hakusan Tedorigawa Geopark Promotion Council, 2. Hakusan City Tourism League

The Hakusan Tedorigawa Geopark, which began in 2010, and was certified nationally in 2011, has been running for close to ten years. Tourism has been one of the focal points of the Geopark, with related activities being started since early-on.
There are many challenges involved in promoting tourism, one of which is increasing the quality of Geopark guides. In 2011 when the Geopark was certified, there was already a large volunteer-guide presence within the area, so we were unable to start up a Geopark guide group. Furthermore, many of these guides were very passionate about volunteering. In 2015, during the Global Geopark Screening Process, it was suggested that we implement a training course and certification for guided tours.
As a result, from 2017 we started the Hakusan Tedorigawa Geopark Certified Guide Training Course, with the initial passing examinees being certified in 2018. In addition to the difficulty of the written test, we also held in-person interviews in the hopes that the examinees' nervousness throughout the exams further increased their confidence upon passing. While the number of people who pass the exam is quite low compared to the number of examinees, taking into account the current needs, we are approaching the Certified Guide Program with a "quality over quantity" approach.
While the results of this program will continue to compile from now, one of the challenges for the near future is the fact that there is currently no standard of quality, as the guide skill levels vary from person to person. Another problem faced is that the system for the training course and certification is not yet fixed.

Keywords: Tourist Guide, Certification System, Tourism, Geopark

©2020. Japan Geoscience Union. All Right Reserved.

Evaluation of explanation panels setting at Geopark’s site 2 - case study of the explanation panel at Obama Hot springs in Unzen Volcanic Area UNESCO Global Geopark, Japan -

Kenshin OSHIMA[1], Yui KURITA[1], Miyu KAWAZOE[1], Rinna TAKEICHI[1], Ayaka OHIRA[1], Ayuka BABA[1], Ayuko SAGARA[1], Nagisa NAKAMURA[1], Takuji MURAOKA[2], Toshiki HIGASHIUCHI[2], *Marekazu OHNO[3]

1. Glocal Course, Nagasaki Prefectual Koka High School, 2. Nagasaki Prefectual Koka High School, 3. Unzen Volcanic Area Geopark Promotion Office

Introduction

Explanation panels are essential for tourists who visit Geopark sites to understand the value of the site. However, since the present explanation panels were made by the experts of geography or geology, many tourists who don’t have such knowledge might not be able to understand them smoothly. Therefore, we did a survey about the panels set at “a memorial park of houses destroyed by debris flows“ in Unzen Volcanic Area UNESCO Global Geopark in 2018 (Ota *et al.*, 2019). Then we made a new draft of explanation panel based on the results of the survey and investigated visitor’s impressions on the panel at the Geopark’s site.

As a reflecting points of the investigation of last year, we changed the design of explanation panels without considering of tourists’ backgrounds and their needs. So this time, we took questionnaire in order to know the purpose of their visit first. And we chose “Hot Foot 105” in Unzen Volcanic Area UNESCO Geopark Site as a target of survey.

Methods

We picked up “Hot Foot 105” in Obama Hot spring district, which was a 105-meter-long footbath opened in February 2010, as a point of survey. On August 7th and October 5th, 2019, we looked into the visitor’s gender, age, hometown, and impression on the panel. The impressions are evaluated from 1 to 6 points on four different perspectives: total impression, pictures, content of explanation, the number of letters, and font size. 6 points is the highest score while 1 point is the lowest evaluation. As for font size, 1 means too small and 6 means too large. As for the number of letters, 1 means too small and 6 means too much.

Then, based on the results, we redesigned the panel and had the same investigation on November 16th and December 7th, then compared the results from both studies.

Results

[original panel]

The number of visitors who answered the questionnaire was 89. The average points were as follows;

content 4.1 / picture 4.2 / number of letters 4.2 / font size 2.8

Based on the opinions of visitors, we redesigned the panel. We decreased the number of letters, enlarge the font size and pictures. We thought the drawings on the right side of panel a little too complicated. So we simplified the drawings so that children could easily understand. As for the number of letters, we removed English explanation because there were no Westerners among the visitors. We added some quiz, pictures of local foods with hot spring water, process to become tourist site, and the effect of hot spring to

©2020. Japan Geoscience Union. All Right Reserved.

catch visitors' eyes.

[redesigned panel]
The number of visitors who answered our questionnaire was 44. The results are as follows;

content 5.1 / picture 5.0 / number of letters 5.0 / font size 4.8

The perspective "explanation" and "picture" were more highly evaluated than original panel. On the other hand, the evaluation on "number of letters" and "font size" became worse than original.

Future prospects
Geopark site is sure to have academic value. We define that good explanation panels enable us to know the value properly and easily. This time, we redesigned the panel taking only visitors' needs into consideration. From now on, we will keep improving the panel by changing the contents and design.

Keywords: Unzen Volocanic Area UNESCO Global Geopark, explanation panel, Nagasaki Prefectural Koka high school

©2020. Japan Geoscience Union. All Right Reserved.

Meteorological landscape over the geopark: A lined-up cumulus row generated by the mountains in the western part of Oga Peninsula, Akita Prefecture, Japan

*Norihito Kawamura[1], Seiji Yamashita[2]

1. School of Regional Resource Management, Graduate School, University of Hyogo, 2. Faculty of Education ans Human Studies

We show a case of meteorological landscape characterized by a row of cumulus over Oga-Peninsula Ogata geopark. A series of clouds caused by mountains in the western part of the peninsula. The clouds will appear under clear and westerly wind conditions in warm season.

Keywords: natural landscape, cumulus, geomorphology, Oga-Peninsula Ogata Geopark

©2020. Japan Geoscience Union. All Right Reserved.

Inform of weather disasters in geoparks

*Hiroshi Sato[1,2], shinichi Sugimoto[3], Makoto Aoi[4], Shinya Miura[4]

1. Mt.Bandai Museum, 2. Bandaisan Geopark Council, 3. Sanriku Geopark, 4. National Research Institute for Earth Science and Disaster Resilience

Japan has many natural disasters such as earthquakes and volcanic disasters, but weather disasters are the most common.
In recent years, large-scale weather disasters have been on the decline, but in 2018 and 2019, large-scale disasters occurred one after another. These disasters are not unique to others, but can also occur in geopark areas.
The Disaster Prevention WG of the Japan Geopark Network (hereinafter referred to as JGN) believes that these disasters should be reported in all geopark areas, and has held discussions with the National Research Institute for Earth Science and Disaster Resilience and concluded an agreement on a comprehensive partnership in 2018. As a concrete measure, a system called "Earthquake!" which informs the occurrence of an earthquake in real time, is being constructed and a new exhibition is being tried in the geopark.
In order to cope with last year's devastating typhoon damage, the two companies decided to work together to create an exhibition panel on the typhoon disaster. We would like to exhibit these panels in the Geopark area to help raise disaster literacy by taking typhoon disasters as our own.
JGN has been proposing to put more effort into disaster prevention in the UNESCO Geopark, and in the future, we would like to strengthen activities to communicate various disasters in geopark regions throughout Japan.

Keywords: weather disaster, typhoon disaster, disaster prevention, Geopark

©2020. Japan Geoscience Union. All Right Reserved.

Foreign Tourist Survey: Places of Interest, Transportation, etc.

*Susan May[1]

1. Hakusan Tedorigawa Geopark Promotion Council

Since the completion of the Hokuriku Shinkansen the number of tourists visiting Kanazawa, located near the Hakusan Tedorigawa Geopark, has greatly increased, such that Kanazawa is now a popular tourist destination. Although the Hakusan Tedorigawa Geopark can be accessed from Kanazawa within 10 to 30 minutes, the number of tourists is exceptionally low.
To find out why tourists aren’ t visiting, and how we can get them to visit, we conducted a survey in Kanazawa during October, 2019. Two staff members spent one day around Kanazawa Station, directly asking foreign tourists to complete the survey.
As a result of the survey, we were able to discover that very few people know about Geoparks. Not only did most people not know what a Geopark was, not one single person had heard of the Hakusan Tedorigawa Geopark.
In regards to whether people are travelling outside of Kanazawa, but within Ishikawa Prefecture, most people replied that they were not. The biggest reason provided was that there was not enough time. On the other hand, when shown photos of the Geopark, particularly photos of Hakusan’ s diverse nature, most people were extremely interested. Many people exclaimed that they wanted to visit the places shown in the photos.
However, there is very limited public transport within the Hakusan Tedorigawa Geopark. Unawares of this, most people believed that they could access the sites in the photos via public transport. There was a big impression that you can travel anywhere in Japan using just trains and buses.
Furthermore, when asked if they would consider renting a car, roughly half of participants said they wouldn’ t, and half said they would. Of the half who would not consider renting a car, the biggest reason provided was that they either did not have an international license, or getting an international license was too much of a hassle. Therefore, rather than promoting the use of rental cars, it may be more beneficial to provide and promote better and more accessible public transport.
From the results of this survey we were able to obtain a lot of information that is useful to Geoparks. However, the survey is limited in many ways. For example the number of participants in this survey was low, and the participants were limited to the quite niche Kanazawa area. Furthermore, the results discussed are just a selection of key results found throughout the survey. Therefore, we ask for your discretion when considering the results of this survey.

Keywords: Tourists, Foreigners, Travel, Transportation

©2020. Japan Geoscience Union. All Right Reserved.

Education activities of museum encouraged establishing of graduate school in geopark -Museum of Nature and Human Activities and San’in Kaigan UNESCO Global Geopark

*Tohru Sakiyama[1]

1. Institute of Geo History, Japan Geochronology Network

Museum of Nature and Human Activities was established as prefectural museum of Hyogo Prefecture in 1992. Some stuffs of the museum played important role as management stuffs of the geopark council at early stage of establishment of San’in Kaigan Geopark. It resulted in establishing of Graduate School of Regional Resource Management, University of Hyogo in the San’in Kaigan Geopark. It depends on management process of lifelong education activities of the museum that stuffs of the museum participated in activities of the geopark easily. This presentation shows evolution process of the museum and their interaction to the geopark.

Keywords: management, geopark, museum, lifelong education

©2020. Japan Geoscience Union. All Right Reserved.

Trends on and assessments of "ecological resources" in the Evaluation Mission Reports for Japanese Geoparks

*Kazuhiko HIRATA[1,2], Yuya Kato[1,3], Shinsuke Nakamura[1], Rieko Fujii[1], Natsuki Moriguchi[1,4]

1. Ecological Working Group for Japan Geopark Network, 2. Natural History Museum and Institute, Chiba, 3. Noyama Company, 4. Tosashimizu Geopark Promotion Council

It is important to focus on not only geological but also ecological and cultural resources in the geoparks. However, understanding and utilization of ecological resources are not sufficient in many geopark areas. To advance understanding and utilization of ecological resources in Japanese Geoparks, we picked out descriptions about “ecological resources” from Evaluation Mission Reports for Japanese Geoparks and reviewed those trends.

Keywords: Japanese geoparks, ecological resources, Evaluation Mission Report

©2020. Japan Geoscience Union. All Right Reserved.

Case study of Children’s Summer School on Earthquakes and Volcanoes in Tango area of San-’in Kaigan UNESCO Global Geopark

*Tomoya Hiiro, Satoko Murotani[1], Ai Toma[2], Children’s summer school on Earthquakes and Volcanoes Committee for[3,4,5]

1. National Museum of Nature and Science,Tokyo, 2. Keio University, 3. Seismological Society on Japan, 4. Volcanological Society of Japan, 5. Geological Society of Japan

Children’s summer school on Earthquakes and Volcanoes has been managed by the Seismological Society of Japan, the Volcanological Society of Japan, and the Geological Society of Japan since 1999. In 2019, this event was held in Kyotango City and Miyazu City in the northern part of Kyoto Prefecture for two days from August 10 to 11. The host organization was “Chikyu Design School”). The purpose of this event is to learn about a blessing of nature, the tourism, the natural disasters, the forming process of Tango Peninsula, and the past, present and future images of Tango area through field observations, experiments and research regarding the history from the expansion of the Sea of Japan to the present and its relationship with the local community.

The San’in Kaigan UNESCO Global Geopark, which was approved to join the Global Geopark Network in October 2010, spreads over 120km east to west, from Kyoto to Tottori Prefecture, and measures 2458.44 km^2. Tango area is located at the eastern end of the geopark. Based on geological view point, Tango area is mainly composed of basement rocks of Cretaceous-Paleogene Miyazu granite, Neogene Miocene Hokutan Group, intrusive rocks, and Ouaternary Middle Pleistocene. Furthermore, the Gomura and Yamada fault zones which caused the 1927 Kita-Tango earthquake are located in Tango area.

In 2019, twenty children were divided into four teams and toured Amanohashidate, Araizaki Shrine, Tango Umi-to-Hoshi Mieru-oka park, the Hi-net Amino station, the Gomura fault, and Kyotango City Folk Museum.

They study the fault shape from the topographical observation and experimental observations at Amanohashidate, Araizaki Shrine, Tango Umi-to-Hoshi Mieru-oka park. During the experiments using everyday things, they considered about the expansion of the Sea of Japan, the formation of hyaloclastite in Hokutan Group, the fault forming process, and the formation of Amanohashidate. In additions, they studied the damage and reconstruction related to the 1927 Kita-Tango earthquake at the the Gomura fault and Kyotango City Folk Museum.

At the end of the program, the participants summarized what they had learned for each team and made a presentation about "How was Tango Peninsula formed?" and "How to play and live in Tango Peninsula". They presented that the disasters by major earthquakes would trigger a development of a stronger and safer town. They also present their ideas that they want to prevent the erosion of Amanohashidate while maintaining the natural scenery and protect a good place in Tango area. Their presentations shows that children had deeply considered through the event.

After the event, we conducted a questionnaire for children who participated in the event. As a result of the questionnaire, more than 80% of the participants answered “good” for all of the four experiments. This indicates that children were highly interested in the experiment. In addition, nineteen participants out of 20 (95%) responded “good” for the observations of the Gomura fault, which indicates a high level of interest in various phenomena such as active faults and large earthquakes.

This event is a good opportunity for children to learn about the local environment and disasters by interacting with nature.

©2020. Japan Geoscience Union. All Right Reserved.

©2020. Japan Geoscience Union. All Right Reserved.

Educational Effects of Screening a Geopark Film at a Local Science Museum

*Rin Nodera[1,2]

1. Kurobe Yoshida Science Museum, 2. Tateyama Kurobe Geopark Society

1. Introduction

Kurobe Yoshida Science Museum is a science museum located in Kurobe City, Toyama Prefecture. The museum functions as one of the base facilities of Tateyama Kurobe Geopark and, as such, conducts various educational activities utilizing the Geopark. Additionally, a variety of programs are screened in the museum using its 20-meter-diameter planetarium dome. One such program is "Ken no Yama," a film which features Tateyama Kurobe Geopark. This publication provides an overview of the film and the results of a questionnaire survey conducted among viewers of the program.

2. Overview of "Ken no Yama"

“Ken no Yama” is a live-action science drama film produced by Kurobe City and LIVE Company Ltd. set in Tateyama Kurobe Geopark. The film was created to fit the specifications of a full-dome screen, and when projected, fills the entire planetarium dome. The story of “Ken no Yama” concerns the journey of a boy who lost his father in a mountain-related accident as a young child. Through climbing the mountain with his friends, the protagonist is able to connect with the nature of Tateyama and Kurobe and thus re-examine the relationship between himself and the mountain.

The film is screened once per day at the museum, excepting days on which the museum is closed. In addition, since October 2018, the museum has provided all sixth-grade elementary school students within Kurobe City the opportunity to view the film.

3. Questionnaire Results

At the museum, a questionnaire survey was given to all students who viewed “Ken no Yama”. The survey was conducted in two parts: students answered a pre-viewing questionnaire prior to watching the film, then a post-viewing questionnaire after seeing the film. The survey asked students about their level of interest in scientific fields as covered by the film on a scale of one to five: 1 (Very interested), 2 (Somewhat interested), 3 (Neutral), 4 (Not very interested), 5 (Not at all interested). The post-viewing questionnaire also included the one-to-five rating scale in addition to providing a free-response space in which viewers could write any additional thoughts they had.

The results of the survey were as follows: in the pre-viewing questionnaire, the average degree of interest in water, rocks, topography, Earth, space, and living things was 2.7, 2.9, 2.6, 2.2, 2.1, and 2.3., respectively. Conversely, the post-viewing questionnaire indicated averages of 2.3, 2.5, 2.3, 2.0, 2.0, and 2.2, respectively. In the free-response area, the answer, “I learned for the first time that mountains change,” was seen frequently.

4. Discussion

©2020. Japan Geoscience Union. All Right Reserved.

Based on the results of the pre- and post-viewing questionnaires, this program can be considered an appropriate teaching material for elementary school students to cultivate interest in geology and topography. It can also be said that, through this film, the imagery of how topography changes over time can be conveyed to elementary school students.
From the above, we may consider that educational activities carried out by the Geopark in cooperation with science museum facilities such as planetariums can provide even stronger educational effects.

Keywords: Tateyama Kurobe Geopark, Science museum, Planetarium dome, Education

©2020. Japan Geoscience Union. All Right Reserved.

Examples of activities in collaboration with Tateyama Kurobe Geopark and University of Toyama

*Takuya Harada[1], Yuta Yamaoka[2], Kiichi Yamahori[2], Kiyoshi Nakagawa[2], Koji Ohnishi[1], Ken-ichi Yasue[1]

1. University of Toyama, 2. Tateyama Kurobe Geopark Society

Introduction

Tateyama Kurobe Geopark is a Japanese National Geopark composed of 9 municipalities in eastern Toyama Prefecture and a part of Toyama Bay. This geopark is operated by a general incorporated association and is developing activities in collaboration with many companies and organizations. University of Toyama has been involved since the establishment of the geopark, and has collaborated in many situations, such as developing projects and requesting lecturers. In this report, we introduce examples of collaboration so far and discuss future prospects.

Examples

Collaboration cases can be roughly divided into the following 3: (1) dispatch of instructors to Tateyama Kurobe Geopark, (2) participation in university education, and (3) joint development of products and plans. In the first case, the teachers of the university participate in the educational activities conducted in the geopark, leading to science education, community learning and disaster prevention education. Also, he explained the knowledge and skills necessary for guide activities as a guide training lecturer. In the second case, geopark are involved in lecture and training at university, and cooperate with local education. In the third case, we are developing geotours and creating guidebooks with university teachers and students. In addition, we conduct collaborative research targeting the area of the geopark, and incorporate exercises on the subject of the geopark in lectures at University of Toyama.

Future outlook

Collaboration of geopark and university seems to have merits for both. As a geopark, (1) you can receive academic support, and (2) you can get opinions and approaches from various viewpoints about the project. Also, (3) the number of students who are interested in geoparks and want to work in the field may increase. On the university side, (a) it will be easier to engage in research targeting the geopark area, (b) it will be possible to return expertise and research results to the community, and (c) students will improve their skills and careers. By the way, in Japanese National Geoparks of today, the population of specialists is on the decline on the whole, and one of the issues at Tateyama Kurobe Geopark was that it was not possible to hire multiple specialists. Therefore, close collaboration with university can be expected to provide some follow-up, such as academic support to supplement the shortage of specialists and support for planning and operation. At present, Tateyama Kurobe Geopark and University of Toyama are conducting discussions with the aim of concluding an agreement to achieve stronger collaboration.

Keywords: Tateyama Kurobe Geopark, University of Toyama, collaboration, regional development

©2020. Japan Geoscience Union. All Right Reserved.

Approach of Health Promotion with Geotourism in Central area of Toyama City

*Ken-ichi Yasue[1], Yuta Yamaoka[2], Tomoya Tanabe[3], Takuya Harada[1], Utako Uchikoshiyama[2], Toshimi Tajima[3], Kiyoshi Nakagawa[2], Koji Ohnishi[1], Kiichi Imahori[2]

1. University of Toyama, 2. Tateyama Kurobe Geopark Society, 3. Approved Specified Nonprofit Corporation Machizukuri Spot

The Tateyama Kurobe Geopark consists of 9 municipalities of the eastern part of Toyama and part of Toyama Bay. Toyama city in the municipalities promotes the town which we want to walk. In addition, the Tateyama Kurobe Geopark Society has problem about the signature and spread of the Geopark in the town area. The society considers in the material of the Geotourism with University of Toyama. A member concerned with these shared information and problems, and planned the geotourism in the town area.
In 2019, participants walked the town area while learning the topography and so on. The participant shared information and the knowledge across the generations. This tour was held once a month from July to November.
One of the points of this town walk is finding of the questions by the participants. Furthermore, we expect the increase of the opportunity to walk in a town because a participant solves a question.
It is support of the inquisition, a viewpoint to notice strangely, a memory and an episode of each person, independent talks, story that we kept in mind in the case of a guide. In particular, the making of story is important so that a connection is felt.
In 2020, we will carry out two tours to feel nature and to hear memory in the same area. In addition, we will consider the mechanism which can participate positively to make an action sustainable.

Keywords: Tateyama Kurobe Geopark, University of Toyama, Machizukuri Spot, Health, Town areas

©2020. Japan Geoscience Union. All Right Reserved.

Creating relationship between University of Toyama higher education and Tateyanakurobe Geopark activity

*Koji Ohnishi[1], Ken-ichi Yasue[1], Yuta Yamaoka[2], Takuya Harada[1], Kiichi Imahori[2]

1. University of Toyama, 2. TateyamaKurobe Geopark Society

Tateyama Kurobe Geopark consists of 9 municipalities in eastern Toyama Prefecture and the part of Toyama Bay. University of Toyama consists of three campuses, two in Toyama city and one in Takaoka city. The Gofuku and Sugitani campuses in Toyama City are located in Toyama city so that these are in Geopark area. While the Takaoka campus is outside of the area, but overlooks the Tateyama Mountains, which form a symbolic landscape of the Geopark. Since University of Toyama is located in the geopark should be used for higher education contents not only earth science but also humanities and social science education.
There is a class in University of Toyama's liberal arts education course called "Local Development in Toyama". This class is for first-year students, with local government staff giving lectures on local government initiatives in Toyama Prefecture and Toyama City, It consists of a one-day workshop that considers the future regional development of Toyama City.
The Tateyama Kurobe Geopark Association explained about the geopark activities, explained the features of this geopark, the geosite seen from the university campus, and the significance of thinking about Toyama through the geopark. Based on this knowledge, we hold workshops to think about how to solve local issues. In 2018, we considered the local sustainability focus on resilience, and considered what kind of people from outside Toyama Prefecture could be brought in for tourism and migration. In 2019, a workshop was held to give Toyama a look at what it would like to be in 30 years from the perspective of the SDGs. Through these workshops, students were able to use the local government's efforts and geopark knowledge gained in previous classes so that they could be actively used when considering various local issues.
University of Toyama has several The teacher's license renewal courses. One course was titled "Tateyama Kurobe Geopark as Teaching Materials", with lecture and field trip. Participants realized the importance of using visible teaching materials in the Geopark area for their own classes. In addition, it was an opportunity to think about how to use the geopark's theme, the 4,000m elevation difference and the water circulation for school education contents.
In this way, geopark and geopark activities have useful contents for higher education. These education trials are gateway for citizens to understand the importance of the Geopark.

Keywords: Tateyama Kurobe Geopark, University of Toyama, Excursion, Workshop, Renewal of teaching license

©2020. Japan Geoscience Union. All Right Reserved.

30 years since the eruption of Teishi Knoll in 1989

*Yusuke Suzuki[1]

1. Izu Peninsula Geopark Promotion Concil

On July 13, 1989, a submarine eruption occurred off the coast of Ito city, Shizuoka pref. The Teishi Knoll was formed by this eruption at a depth of about 80m. This year, 2019, has been 30 years since the eruption. It is said that the mass memory of disasters will be lost in about 20 to 30 years. This eruption is a disaster in which it is difficult to maintain local memory because there are no deaths due to the disaster and no remains of the disaster are left.

Izu Tobu Volcano Group including the Teishi Knoll are important heritages in the Izu Peninsula Geopark, and it is necessary to bring the correct knowledge to the local people and use it appropriately. This presentation will report about the activities of the Izu Peninsula Geopark, such as symposiums and video recordings of the seabed, related to the seafloor eruption.

Keywords: Geopark, Volcanic disaster

©2020. Japan Geoscience Union. All Right Reserved.

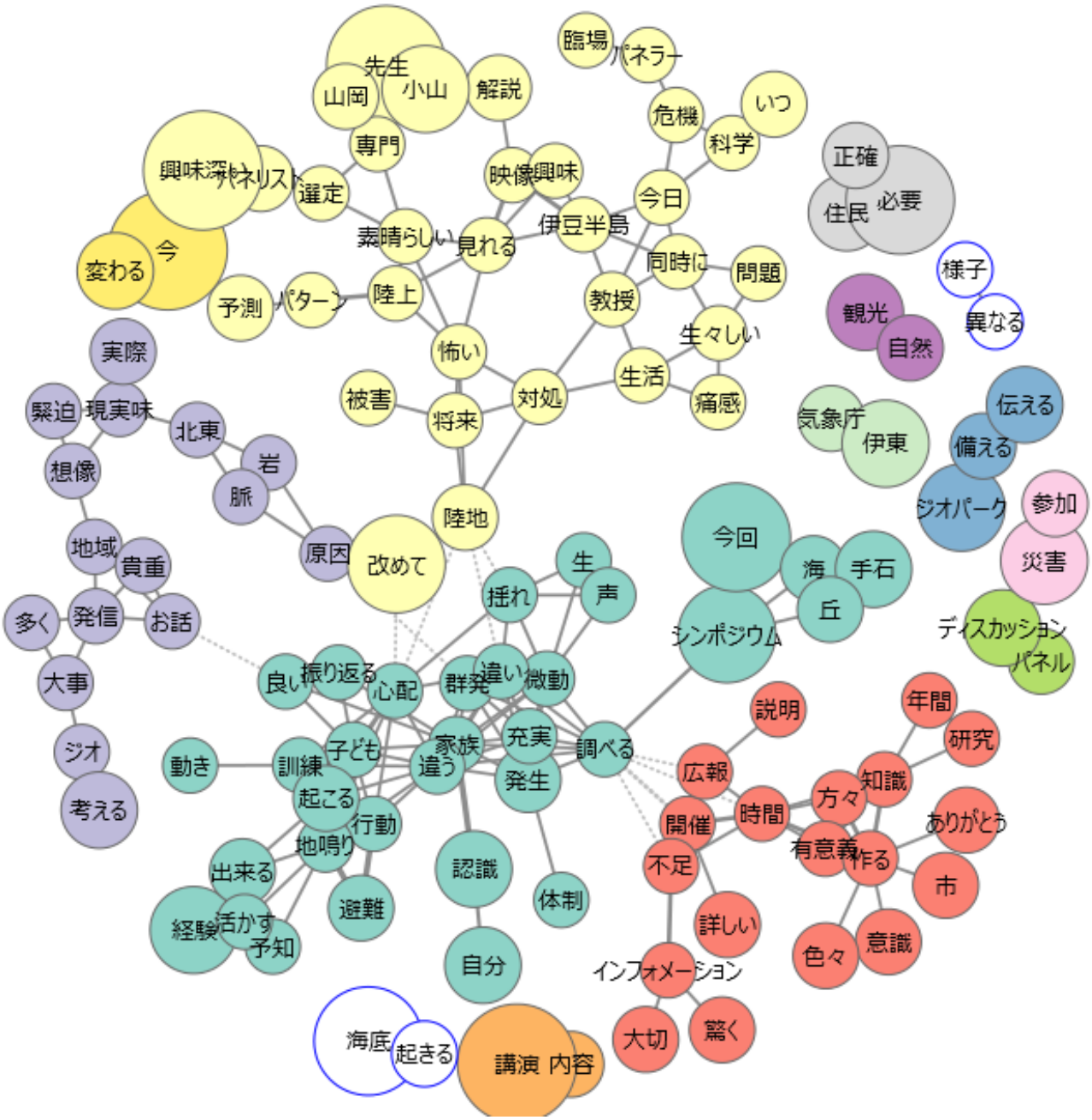

©2020. Japan Geoscience Union. All Right Reserved.

[J] Poster | O (Public)：Public

[O-06] Kitchen Earth Science: Let's stimulate your brain by hands-on experiments!

convener:Ichiro Kumagai(School of Science and Engineering, Meisei University), Miwa Kuri(Japan Meteorological Agency), Mie Ichihara(Earthquake Research Institute, University of Tokyo), Kei Kurita

"Kitchen Earth Science" aims at understanding a natural phenomenon in Earth and planetary sciences by analogue experiments using goods and tools in our daily life. Analogue experiments have a function to unveil the fundamental physics governing the phenomenon. At the same time, they essentially include uncertainties so that unexpected results are frequently obtained, which have a potential for surprising discoveries. These findings also provide a good opportunity for deeply thinking, and raise new questions to explore. Such experience is precious not only for young researchers in Earth and planetary sciences, but also non-expert people who need a scientific thinking to live wisely. In this session, we focus on "advantages of doing hands-on science experiments" and discuss the significance of analogue experiments with uncertainties, which cause unpredictable results: even if the experiment fails, we learn a lot of things from the failure which may lead to a great success. We are accepting a variety of experimental researches and case studies on scientific education such as introductory educational experiments for Earth and planetary sciences in elementally and junior/high schools, general science education and interdisciplinary researches in post-high schools, and new approaches to citizen science and outreach. We welcome all the participants who are interested in Kitchen Earth Science to stimulate your brain by hands-on science experiments. We also welcome speakers who report the hands-on experiments for scientific research and education from overseas.

[O06-P01] Observation of phase transitions for ammonium nitrate using hot plate and polarizing sheets

*Masami Kanzaki[1] (1.Institute for Planetary Matereials, Okayama University)

[O06-P02] What is “fluid”?, a brain-stimulative experimental subject based on soft-gel suspension dynamics

*Kei Kurita[1], Ichiro Kumagai[2], Anne Davaille[3], Nicolo Sgreva[3] (1.ERI,The University of Tokyo, 2.Meisei University, 3.Universite Pari-Saclay)

[O06-P03] Activity report on Kitchen Earth Science: Workshops supported by Earthquake Research Institute from 2017 to 2019

*Ichiro Kumagai[1], Mie Ichihara[2], Miwa Kuri[3], Kei Kurita[4] (1.School of Science and Engineering, Meisei University, 2.Earthquake Research Institute, University of Tokyo, 3.Fukuoka Regional Headquarters, Japan Meteorological Agency, 4.University of Tokyo)

Observation of phase transitions for ammonium nitrate using hot plate and polarizing sheets

*Masami Kanzaki[1]

1. Institute for Planetary Matereials, Okayama University

Experimental observation of phase transitions of minerals will generally need expensive instruments, and also care is needed for safety. However, for educational and demonstration purposes, much simpler and cheaper approaches are needed. Ammonium nitrate (NH_4NO_3) has low melting point of 175 °C, and can be melted using a hot plate for kitchen purpose. It has four phases (cubic, tetragonal, orthorhombic I, and orthorhombic II) between the melting point and room temperature, and impressive phase transitions can be easily observed using polarizing sheets. I have demonstrated those phase transitions to students and general public, and here I will present how to conduct this experiment.
Ammonium nitrate, polarizing sheets (at least two sheets), slide glass, cover glass, an hot plate are necessary for the demonstration. First, place the slide glass on the heated hot plate. Put some powder on the slide glass, and then put the cover glass over the powder. When the powder melted, thin sample section is automatically produced. For non-in-situ study, just remove the slide glass from the hot plate, and let it cool. You can observe the orthorhombic I (if it is still a bit warm) or orthorhomibic II (if it is cooled to room temperature). Both are very colorful when the slide glass is inserted between two polarizing sheets with Cross Nicol orientation. Occasionally, you may see orthorhombic I to II transition (Tc: about 32 °C). This section is a good teaching aid to learn polarization. It can be also used as an alternative to real thin section of rocks. To observe the sample, you may hold it in your hand and observe it through sunlight or ceiling light. Alternatively, you can observe using a light box for tracing purpose which is now very cheap. Put the slide glass and two polarizing sheets on the light box, then more than one person can see same time, and it is much easy to explain. If a binocular microscope with transmission illumination is available, the sample can be observed more closely. Since the grain size and the texture will change depending on the cooling rate of the sample and the water content, the heating and cooling may be repeated to see difference.
If you observe the cooling process starting from the melted state, you can see phase transitions. In order to avoid direct contact between the heated slide glass and the polarizing sheet, thick paper with a central hole may be used to separate them. The paper may be fixed to the polarizing sheet by adhesive tape. The melted sample on the hot plate should be quickly moved on the thick paper with the polarizing sheet underneath. Then, quickly cover the slide glass with the polarizing sheet with the thick paper. To observe crystallization from melt, you better avoid Cross Nicol position as first crystallizing phase is cubic. After that, further transitions to tetragonal, orthorhombic I, and orthorhombic II can be observed as the temperature drops. By observing cooling of the melted sample, you may see four phase transitions (including melt/cubic phase). If available, use a binocular microscope for close observation. The transitions at higher temperature occur quickly, so it is necessary to reduce the cooling rate. Ask participants to come up with ideas for how to realize slower cooling rate. In the case of high school / college students, it is advisable to ask them questions; how many phase transitions can be observed, what is the crystal system of each phase based on observations with polarized light, and observe textural changes at the time of transition. A video of ammonium nitrate during cooling using a polarizing microscope is available from here
(http://www.misasa.okayama-u.ac.jp/~masami/pukiwiki/index.php?%B6%B5%BA%E0).
It should be noted that ammonium nitrate absorbs moisture in the air, so that the current thin section state lasts only several hours to several days unless the sample is stored in a dry state, and the sample

©2020. Japan Geoscience Union. All Right Reserved.

becomes an aqueous solution. Also, be careful not to get burned by a hot plate or heated slide glass. Use tweezers and instruct them not to directly touch the high-temperature objects.

Keywords: phase transition, In-situ observation, ammonium nitrate, polarizing microscope

©2020. Japan Geoscience Union. All Right Reserved.

What is “fluid”?, a brain-stimulative experimental subject based on soft-gel suspension dynamics

*Kei Kurita[1], Ichiro Kumagai[2], Anne Davaille[3], Nicolo Sgreva[3]

1. ERI,The University of Tokyo, 2. Meisei University, 3. Universite Pari-Saclay

In the education of university freshman course reconsideration of the fundamental concepts is a good chance for a self-motivating start of learning. In the high school education the fundamental concepts such as in physics are usually given over head without enough attentions. A good example is the concept of mass. It is vaguely defined in high school level and the deep insight on the concept of mass leads to the modern physics. In the freshman course education we should provide a chance in the classroom for regarding the fundamental concepts with suspicions.
In this presentation we propose dynamics of soft gel suspension as a stimulative and intuitive experimental subject which can be used in the class room to reconsider the concept of fluid.
Let’s consider at first a simple case of a sphere falling through viscous fluid. By comparing force balance between viscous force and buoyancy the falling velocity is given as a function of viscosity and size of the sphere. This can be demonstrated easily by using a steel sphere and sugar syrup in a transparent acrylic tube. Measurement of the position of falling sphere easily leads to the Stokes’s formula.
After learning fluid dynamics of falling sphere through viscous fluid based on conventional textbooks we replace the fluid with soft-gel dense suspension. Soft gel is easily prepared by using SAP(Super Absorbent Polymer, which is available as “Mizu no Orusuban” at 100-yen shop). SAP absorbs water and expands by 100-200 times. By adding adequate amount of water dense suspension of soft gel is prepared. To control the grain size of the suspension SAP grains are selected from sieved fractions(for example, 90-100micron for the final gel size of less than1mm and 425 to 500 micron for several mm). By conducting similar falling sphere experiment three kinds of interesting behaviors can be identified in terms of changing the size of sphere(Sgreva et al, 2019,2020). When the size is larger enough than the size of gel the sphere falls as similar to viscous fluid. When it is smaller than the size of gel it never falls. The soft gel suspension behaves as a yield stress fluid depending on the scale. At the intermediate size breathtaking behavior can be observed. Falling speed is not homogenous and the sphere sometimes stops for a while, then moves again. Not only the stop & go behavior it sometimes sways away horizontally. We name this regime as a meditated fall. By inspection of the motion of the sphere closely through laser illumination it is shown the sphere explores available routes to move among the gels and gels slowly deform and migrate to give a way to the sphere. This process seems to be controlled by the permeability. Based on the observations about the behaviors of sphere in the classroom we can discuss what is fluid and what is solid and the nature of viscosity. Detailed syllabus will be shown in the presentation.
Reference:
N.Sgreva et al EGU 2019 #7870 Scale-dependent magma rheology: insights from laboratory experiments
N.Sgreva et al EGU 2020 #9113 Probing the characteristics of mush-magma transition: insights from laboratory experiments

Keywords: brain-stimulative experiment, soft gel suspension, yield stress fluid

©2020. Japan Geoscience Union. All Right Reserved.

Activity report on Kitchen Earth Science: Workshops supported by Earthquake Research Institute from 2017 to 2019

*Ichiro Kumagai[1], Mie Ichihara[2], Miwa Kuri[3], Kei Kurita[4]

1. School of Science and Engineering, Meisei University, 2. Earthquake Research Institute, University of Tokyo, 3. Fukuoka Regional Headquarters, Japan Meteorological Agency, 4. University of Tokyo

From 2017 to 2019, workshops entitled “Kitchen Earth Science” were held at the Earthquake Research Institute (ERI, the University Tokyo), which were supported by ERI Joint Usage. We invited more than 40 domestic and foreign speakers over a wide area (Science, Engineering, Scientific Education, etc.). The theme of the workshop was “brain stimulation by hands-on experiments”. Every year, there were attractive demonstrations of participant’s experiments as a live show of “Kitchen Earth Science”, which stimulated our brain and excited our discussion. We are now making a recipe book of Kitchen Earth Science. In this presentation, we will report our recent activity on Kitchen Earth Science.

Keywords: Education, Experiments, Hands on Experiments

©2020. Japan Geoscience Union. All Right Reserved.

[J] Poster | P (Space and Planetary Sciences)：P-PS Planetary Sciences

[P-PS09] Planetary Sciences

convener:Yusuke Nakauchi(Japan Aerospace Exploration Agency), Yuko Daket(University of Aizu)

We call for general interest papers for Planetary Sciences. Planetary Sciences consist o f a variety of studies on the past, present, and future of our solar system and exoplanatory systems, Discussions based on various backgrounds are encouraged.

[PPS09-P01] Cratering experiments on snow at very low temperature: Scaling law of crater size in gravity regime

*Minami Yasui[1], Suzuno Oyama[2], Mare Takagi[2], Masahiko Arakawa[1] (1.Department of Planetology, Graduate School of Science, Kobe University, 2.Department of Planetology, Faculty of Science, Kobe University)

[PPS09-P02] Laboratory collisional disruption experiments of D-type asteroids analogue targets

*Shiomoto Jyunpei[1], Akiko Nakamura[1], Sunao Hasegawa[2], Hideaki Miyamoto[3], Takafumi Niihara[3] (1.Kobe University, 2.ISAS/JAXA, 3.Department of Systems Innovation, Graduate school of Engineering, University of Tokyo)

[PPS09-P03] Experimental study on impact disruption for low strength target and implication for effect of tensile strength on impact strength

*Kazuhiro Horikawa[1], Masahiko Arakawa[1], Minami Yasui[1], Ryo Sugimura[1] (1.Graduate School of Science , Kobe University)

[PPS09-P04] Effect of porosity on restitution coefficients of snowball simulating Saturn's ring: implication for inelastic collision

*Yukari Toyoda[1], Minami Yasui[1], Masahiko Arakawa[1] (1.Graduate School of Science, Kobe University)

[PPS09-P05] Crater scaling laws of ejecta velocity distribution and crater size constructed for very low strength target

Ryo Sugimura[1], *Masahiko Arakawa[1], Minami Yasui[1], Hiroki Senshu[2], Sunao Hasegawa[3] (1.Graduate School of Science, Kobe University, 2.Planetary Exploration Research Center, Chiba Institute of Technology, 3.Japan Aerospace Exploration Agency)

[PPS09-P06] Accretion of gas and solid materials into the circumplanetary disk of a growing giant planet: Dependence on planetary mass

*Natsuho Maeda[1], Keiji Ohtsuki[1], Ryo Suetsugu[2], Masahiro N Machida[3] (1.Graduate school of science, Kobe University , 2.University of Occupational and Hnvironmental Health, 3.Graduate school of science, Kyushu University)

[PPS09-P07] Parameter Study of Satellite Formation via Giant Impact by N-body Simulation

*Yuichi Hasegawa[1], Ishizawa Yuya[1], Natsuki Hosono[2], Takanori Sasaki[1] (1.Department of Astronomy, Kyoto University, 2.Japan Agency for Marine-Earth Science and Technology)

[PPS09-P08] Numerical Analysis of Penetration Dynamics into Regolith using Compressible and Non-Expanding Plastic Gas Model

*Kojiro Suzuki[1] (1.Graduate School of Frontier Sciences, The University of Tokyo)

[PPS09-P09] Test of a model for the gas accretion onto giant planets by two-dimensional hydrodynamical simulations

*saho nakazawa[1], Yuki Tanaka[1], Hidekazu Tanaka[1] (1.Tohoku University)

[PPS09-P10] An Explanation for Physical Mechanism of the Streaming Instability in Dust Dominant Regime

*Hiroaki Kaneko[1], Taishi Nakamoto[1] (1.Tokyo Institude of Technology)

[PPS09-P11] The influence of dust evolution on the vertical shear instability in protoplanetary disks

*Yuya Fukuhara[1], Satoshi Okuzumi[1] (1.Department of Earth and Planetary Sciences, Tokyo Institute of Technology)

[PPS09-P12] Collisional Growth and Fragmentation of Dust Aggregates with Low to Very High Mass Ratios

*Yukihiko Hasegawa[1], Takeru Suzuki[1], Hidekazu Tanaka[2], Hiroshi Kobayashi[3], Koji Wada[4] (1.The University of Tokyo, 2.Tohoku University, 3.Nagoya University, 4.Chiba Institute of Technology)

[PPS09-P13] Partitioning of H, C, N and S on a growing Earth estimated by empirical thermodynamic modelling

MURASE YUTARO[1], Hiroaki Saito[1], *Kiyoshi Kuramoto[1] (1.Department of Cosmosciences, Graduate School of Sciences, Hokkaido University)

[PPS09-P14] Automatic segmentation of rayed craters on the Moon by applying deep learning technique

*Yuko Daket[1], Chikatoshi Honda[1], Takashi Sonoke[1], Hirohide Demura[1] (1.University of Aizu)

[PPS09-P15] Simulation of space weathering with mixture lunar-like composition

*Ryota Shimana[1], Sho Sasaki[1], Takahiro Hiroi[2] (1.Departure Earth and Space Science, Osaka University, 2.Department of Earth, Environmental and Planetary Sciences, Brown University)

[PPS09-P16] The 1300 km diameters ring fault around Orientale basin from gravity data

*Qingyun Deng[1], Fei Li[1,2], Jianguo Yan[1], Zhiyong Xiao[3], CHONG ZHENG[1], Chi Xiao[1], Jean-Pierre Barriot[1,4], Mao Ye[1] (1.The State Key Laboratory of Information Engineering in Surveying, Mapping and Remote Sensing, Wuhan University, 2.Chinese Antarctic Center of Surveying and Mapping, Wuhan University, 3.School of Atmospheric Scienses, Sun Yat-sen University, 4.Université de la Polynésie Française)

[PPS09-P17] The thermal history of comets derived from the EUV spectra data observed by HISAKI

*Kanae Nomura[1], Kazuo Yoshioka[1], Kei Masunaga[2] (1.University of Tokyo, 2.University of Colorado Boulder)

[PPS09-P18] A search for the non-water ices on the icy Galilean moons of Jupiter with ground-based telescope

*Seiko Takagi[1], Taro Matsuo[2], Jun Kimura[3] (1.Hokkaido University, Graduate School of Science, 2.Nagoya University, 3.Osaka University)

[PPS09-P19] Simulation study to detect Mars atmosphere by satellite gravimetry

*Keiko Yamamoto[1] (1.National Astronomical Observatory of Japan)

[PPS09-P20] Effects of the haze layer on Titan's atmospheric dynamics

*Motoki Sumi[1], Shin-ichi Takehiro[2], Wataru Ohfuchi[3], Hideko Nomura[4], Yuka Fujii[5] (1.Department of Earth & Planetary Sciences, Tokyo Institute of Technology, 2.Research Institute for Mathematical Sciences, Kyoto University, 3.Department of Planetology/CPS, Graduate School of Science, Kobe University, 4.Division of Science, National Astronomical Observatory of Japan, 5.Earth-Life Science Institute, Tokyo Institute of Technology)

[PPS09-P21] Participation of Japanese planetary science community to the Mercury exploration mission BepiColombo

*Shunichi Kamata[1], Ryuki Hyodo[2], Futoshi Takahashi[3], Takashi Yoshizaki[4], Yota Ishigaki[2], Kiyoshi Kuramoto[1], Go Murakami[2], Masaki Fujimoto[2] (1.Hokkaido Univ., 2.ISAS/JAXA, 3.Kyusyu Univ., 4.Tohoku Univ.)

[PPS09-P22] **Mercury Trek: A New Online NASA Visualization and Analysis Portal**

*Brian Hamilton Day[1], Emily Law[2], NASA Solar System Treks Team -[2] (1.NASA Ames Research Center, 2.NASA Jet Propulsion Laboratory)

[PPS09-P23] Proposed comet impacts forming Lake Michigan as an explanation of the formation of the Carolina bays.

*John Anthony Burgener[1] (1.Telegistics Inc.)

Cratering experiments on snow at very low temperature: Scaling law of crater size in gravity regime

*Minami Yasui[1], Suzuno Oyama[2], Mare Takagi[2], Masahiko Arakawa[1]

1. Department of Planetology, Graduate School of Science, Kobe University, 2. Department of Planetology, Faculty of Science, Kobe University

In order to estimate the surface age of solid bodies in the solar system except for the Moon, the crater size scaling law should be applied to the crater chronology. Icy satellites are expected to be covered with ice particles formed by the excavation of impact craters (We call this as regolith layer). Furthermore, the surface temperature of icy satellites is very low, so the ice particles constituting the regolith layer are expected not to be sintered like sand. In this case, it is necessary for the crater size scaling law in the gravity regime to apply the crater chronology of icy satellites. However, the crater size scaling law of ice in the gravity regime is not clarified because ice particles are sintered very quickly in the freezer so they have physical strength. Therefore, in this study, we established the method of impact experiments at very low temperature (<210 K). Then, we conducted impact cratering experiments on unsintered ice particles (snow) and study the crater size scaling law of ice in the gravity regime.

Ice particles with the diameter less than 710 μm were used as target. When ice particles were put into the target container, liquid nitrogen was also put in several times simultaneously, so the very low temperature could be kept. The porosity of snow target was 50%. The thermocouples were set on the bottom and the surface of the target, and the temperature during the evacuation and just before the shot was measured. The target bottom temperature just before the shot was 110–210 K. We used five kinds of spherical projectiles with the diameter of 2 mm, nylon, aluminum, titanium, stainless-steel, and brass. The impact velocity ranged from 77 to 168 m/s. The target container was set in the vacuum chamber at <100 Pa. The ejecta curtain growth was observed by using the high speed camera. The target was recovered after the shot to measure the crater diameter and depth. We determined the sintering degree of snow target at the crater formation by using the images of ejecta curtain growth and the crater morphology.

First, we examined the relationship between the target temperature and the crater diameter and found that the crater diameter was about 1.5 times larger at the temperature lower than 160 K when the kinetic energy of projectile was same. At the temperature higher than 160 K, the discontinuous ejecta curtain, typical one in the strength regime, was observed in the images of high speed camera, and the crater rim was unclear. Therefore, we expected that the temperature boundary between the gravity regime and the strength regime, T_b, was 160 K. Next, we examined the relationship between the crater diameter, D, and the kinetic energy of projectile, E_k, at low T_b. As a result, the relationship can be fitted by $D=aE_k^b$, and the parameters, a and b, were obtained to be 51.5 and 0.17. Furthermore, we compared our results with the previous results of 15-min sintered snow at 258K obtained by Arakawa & Yasui [1] and found that the data at low T_b was about 1.5 times larger than them at same kinetic energy of projectile.

We examined the crater size scaling law of ice by using the results at low T_b. The crater size scaling law is expressed as $\pi_R=K_1\pi_2^p\pi_4^q$, where π_R, π_2, and π_4 are the non-dimensional parameters: $\pi_R=R(\rho_t/m_p)^{1/3}$ (R is the crater radius and m_p is the projectile mass), $\pi_2=r_pg/v_i^2$ (r_p is the projectile radius, g is the gravitational acceleration, and v_i is the impact velocity), and $\pi_4=\rho_t/\rho_p$ (ρ_t and ρ_p are the density of target and projectile, respectively. As a result, the parameters, K_1, p, and q were obtained to be 0.55, -0.17, and 0.20. Our data was almost consistent with that of quartz sand obtained by Tsujido et al. [2].

©2020. Japan Geoscience Union. All Right Reserved.

Furthermore, the scaling parameter, *m*, was obtained to be 0.41 from the parameter, *q*, and it was same as that of sand (Housen & Holsapple [3]).

[1] Arakawa & Yasui (2011), Icarus 216, 1–9. [2] Tsujido et al. (2015), Icarus 262, 79–92. [3] Housen & Holsapple (2011), Icarus 211, 856-875.

Keywords: cratering experiments, porous ice, very low temperature, crater scaling law, gravity regime

©2020. Japan Geoscience Union. All Right Reserved.

Laboratory collisional disruption experiments of D-type asteroids analogue targets

*Shiomoto Jyunpei[1], Akiko Nakamura[1], Sunao Hasegawa[2], Hideaki Miyamoto[3], Takafumi Niihara[3]

1. Kobe University, 2. ISAS/JAXA, 3. Department of Systems Innovation, Graduate school of Engineering, University of Tokyo

Background

D-type asteroids are found outside the asteroid belt, in the Hilda group and the Trojans. The Mars moons Phobos and Deimos also have reflectance spectra close to those of D-type asteroids[*1]. Tagish Lake is a unique meteorite, which exhibits a reflectance spectrum similar to the spectra of the D-type asteroids. Tagish lake has a different chemical composition and oxygen isotope ratio from those of CM and CI chondrites, and it does not belong to any existing chemical groups[*2].

Collisional disruption threshold and re-accumulation conditions of the fragments have been studied for chondrites and chondrite analogue targets. The disruption threshold Q* of 3 ordinary chondrites (OCs) and 1 carbonaceous chondrite (CV) is approximately 1400 J/kg, which is nearly 2 times that of terrestrial rocks[*3]. Experiments using targets simulating internal structure of parent bodies of ordinary chondrites showed that fragments from catastrophic destruction of parent bodies of ordinary chondrites more easily re-accumulate regardless of the size of the chondrules than those without chondrules[*4]. The purpose of this study is to investigate the collisional disruption threshold of D-type asteroids and the re-accumulation conditions of the fragments by conducting collisional disruption experiments using a Phobos simulant (UTPS-TB)[*5].

Experiments

The density of the sample was 1.43 ±0.04 g/cm^3. If the composition of the simulant is the same as that of the Tagish Lake meteorite, the porosity of the simulant is 46%. Tensile strength and compressive strength were measured at a loading rate of 0.001 mm/s for a cylinder with a diameter of 20 mm and a height of 6 -21 mm. The results were 0.222 ±0.087 MPa and 1.11 ±0.31 MPa, respectively.

Laboratory collisional disruption experiments were conducted by using a horizontal two-stage light gas gun at Institute of Space and Astronautical Science, JAXA, with a 1/8 inch nylon spherical projectile at a velocity of 4.1-5.3 km/s. The target was prepared by cutting the sample into cubes about 5 cm in length. Three high-speed cameras were installed around the target to obtain images for analyzing the fragment velocity. One of the cameras observed the target from the top. The others observed from the side.

Results

Fragments were grouped into three. The largest fragment, several smaller fragments, and fine fragments. An empirical relationship between the largest fragment mass fraction, m_1/M_t, where m_1 is the mass of the largest fragment and M_t is the mass of the pre-impacted target, respectively, and the specific energy Q was given as: $m_1/M_t = 10^{3.05\pm1.44} \cdot Q^{-1.11\pm0.48}$. The disruption threshold Q*, that is the specific energy necessary for $m_1/M_t = 0.5$, is obtained Q*=1000 J/kg. This is comparable to OC and CV [*3] and smaller than the value of gypsum [*6,7] and larger than the value of glass[*8].

We measured the velocity of the fragments from the corners of the impacted surface of the targets in the center-of-mass system from the high speed images. The fragment velocity at catastrophic disruption, i.e., $m_1/M_t = 0.5$, is almost the same as that of gypsum (porosity 50%)[*4] and is about 4 -5 times faster than that of an ordinary chondrite analogue target (porosity 35%)[*4]. The result suggests that the re-accumulation of bodies composed of UTPS-TB is less likely to occur than those composed of the ordinary chondrite

©2020. Japan Geoscience Union. All Right Reserved.

analogues, but occur in the similar degree with those composed of gypsum.

References

1 Fraeman, A. A., et al. (2014), Icarus 229, 196-205.
2 Hiroi, T. et al. (2001), Science, 293, 2234-2236.
3 Flynn, G. J. and Durda, D, D. (2004), Planet. Space Sci., 52, 1129-1140.
4 Yasui, M. and Arakawa, M. (2011), Icarus, 214, 754-765.
5 Miyamoto, H. et al. (2018), LPSC 49th, Abstract #1882.
6 Kawakami, S., et al. (1991), A & A, 241, 233-242.
7 Okamoto, C. and Arakawa, M. (2009), Meteorit. & Planet. Sci., 44, 1947-1954.
8 Gault, D. E, and Wedekind, J. A. (1969), JGR , 74, 6780-6794.

Keywords: collisional disruption, D-type asteroid, Tagish Lake meteorite

©2020. Japan Geoscience Union. All Right Reserved.

Experimental study on impact disruption for low strength target and implication for effect of tensile strength on impact strength

*Kazuhiro Horikawa[1], Masahiko Arakawa[1], Minami Yasui[1], Ryo Sugimura[1]

1. Graduate School of Science , Kobe University

Asteroids could be composed of various materials based on the study of meteorite parent bodies. S-type and C-type asteroids are predicted to be composed of mm-sized chondrules and μm-sized matrix which are the constituents of chondrites. Some of C-type and S-type asteroids have been observed to have a large porosity inside. The impact strength is one of the most important physical properties of asteroids because it could determine the evolution of the size-frequency distribution of asteroid. The impact strength strongly depends on the asteroid size and it is dominated by the material strength of the bodies at the size smaller than 100m. In laboratory experiments, a lot of studies have been conducted for rock, ice, and their porous materials to investigate the effects of material strength on the impact strength. However, the impact experiments using the target with simulating asteroids with the strength continuously changed and with low tensile strength simulating asteroids have been hardly conducted so far.

In this study, we conducted impact experiments using the targets simulating asteroids composed of chondrules, matrix and pore and changed the internal structure of the target such as matrix contents and porosity; the tensile strength was changed about two orders of magnitude, then we studied the relationship between the internal structure and the impact strength(Q*).

Impact experiments were conducted by using two-stage light gas gun at Kobe University, and we used a polycarbonate projectile with the size of 4.7mm and a nylon projectile with the size of 2mm. They were lunched at the impact velocity from 0.9km/s to 5.7km/s, and impacted at a head-on collision. Spherical targets with the size of 40mm, 60mm and 80mm were prepared by using quartz sands with the size of 100μm and porous gypsum, and they were mixed with various mass ratio of quartz to gypsum at 2:1, 4:1, 8:1 and 20:1. The tensile strength of these materials (Y_t) was measured by using Brazilian test. The impact disruption was observed by a high-speed camera at 10^5 FPS.

Brazilian tests showed that tensile strength of the targets decreased from 800kPa to 10kPa with decreasing gypsum mass contents. The impact experiments gave the relationship between the specific energy (Q: kinetic energy of projectile / original target mass) and the normalized largest fragment mass (m_l/M_t), and this relationship is described by the equation: m_l/M_t=AQ^-b. The constant A changed from 10^3.6 to 10^1.2 and the constant b changed from 1.3 to 0.6 with the decrease of the gypsum mass contents. Therefore, the Q* was found to change from 1900J/kg to 100J/kg with the decrease of the gypsum mass contents. This means that the Q* is directly proportional to the tensile strength. On the other hand, the ejection velocity at the antipodal point of the target (V_a), which was measured by using high-speed images, had a power-law relationship (V_a=10^-2.0Q^0.7) with the specific energy, Q, and the V_a was found to be independent of tensile strength.

Finally,in order to discuss the scaling law for the catastrophic disruption of a targets mixed with quartz and gypsum, we investigated the relationship between A non-dimensional impact strength(P_I) and m_l/M_t. P_I is defined as the ratio of the target tensile strength to the antipodal pressure, and is expected to scale the difference of tensile strength. As a result, the relationship between P_I and the m_l/M_t was shown by P_I=C(m_l/M_t)^-d. However, we found two different relationships in this empirical

©2020. Japan Geoscience Union. All Right Reserved.

equation. When the mass ratios of quartz to gypsum are 2:1 and 4:1, the constants C and d are derived to be 10^0.3 and 1.2, respectively, and when the mass ratios of quartz to gypsum are 8:1 and 20:1, the constants C and d are derived to be 10^1.0 and 1.5, respectively.

Keywords: impact disruption, low strength target, impact strength

©2020. Japan Geoscience Union. All Right Reserved.

Effect of porosity on restitution coefficients of snowball simulating Saturn’s ring: implication for inelastic collision

*Yukari Toyoda[1], Minami Yasui[1], Masahiko Arakawa[1]

1. Graduate School of Science, Kobe University

Saturn's rings have a width of tens of thousands of kilometers and a thickness of hundreds of meters, and they are composed of water ice particles with a diameter of mm to meters. The average relative impact velocity among ring particles is estimated to be less than several cm/s. Numerical simulations indicate that the restitution coefficient of ring particles should be less than 0.6 to maintain thin annular rings. Higa et al. (Icarus, 1998) showed that the restitution coefficient of ice ball covered with a thin ice frost was <0.6 . However, Cassini's observations expected that ring particles might be aggregates of ice particles with high porosity while the porosity of their ice ball were almost zero so it is inappropriate for the candidate of ring particles. Therefore, it is necessary to examine whether the porous ice can maintain the thin annular Saturn’s rings or not.

The purpose of this study is to clarify the mechanism of energy dissipation for the inelastic collision of porous ice and to estimate the internal structure of ring particles for maintaining thin annular Saturn’s rings. Therefore, we conducted low-velocity impact experiments for porous ice balls in order to examine the effect of porosity on the relationship between the impact velocity and the restitution coefficient.

We did free-fall impact experiments for a porous ice ball on a plate. Porous ice sphere (radius of 1.5 cm, porosity Φof 47%, 53%, 60%) was made by compacting ice particles (average size of 20 μm) into spheres by using a spherical jig. The target plates were a granite plate, an ice plate, and a porous ice plate with a radius of 1.5 cm, a height of 2 cm, and a porosity of 43% to 62% which was made in the same way as the spheres. The restitution coefficient was determined by measuring the time interval between the collision using an AE sensor, a laser displacement meter, and a small high-speed camera. The impact velocity ranged from 0.78 to 265.8 cm/s.

The restitution coefficient of the porous ice ball, *e*, continued to decrease with increasing the impact velocity for all plates. At high impact velocity, the *e* decreased as the porosity increased, while it was almost consistent, irrespective of porosity at small impact velocity. This relationship can be expressed by the empirical equation, $e=e_0 \cdot v_i^{-b}$, and the *b* increased with increasing the porosity.

We calculated the collisional energy dissipation by using the obtained *e* and the compression volume by using the width of depression of sphere. The relationship could be expressed by the empirical equation, $V=V_0 \cdot E_{dis}^{n}$ and the *n* was determined as 0.75–1.53, that is, the compression volume was proportional to the energy dissipation. Therefore, we assumed the energy conservation in collision and obtained the equation, $E_{dis}=Y_{d_i} \cdot V$. From this equation, the compressive strength, Y_{d_i}, was estimated to be 5.25–7.97 MPa for Φ=47%, 3.46–5.19 MPa for 53%, and 0.27–0.50 MPa for 60%.

We also conducted compression deformation tests for a porous ice ball by using a small deformation tester. We calculated the compression volume by using the width of depression of ice ball and the compression energy by using the load to estimate the compressive strength by using the formula $E_{comp}=Y_{d_d} \cdot V$. As a result, the compressive strength, Y_{d_d}, was estimated to be 2.72 MPa for Φ=47%, 1.35 MPa for 53%, and 0.45 MPa for 60%. We found that the Y_{d_i} for Φ=60% was almost same with the Y_{d_d}, but the Y_{d_i}

©2020. Japan Geoscience Union. All Right Reserved.

was about 2–4 times largerthan the Y_{d_d} for 47 and 53%. Therefore, the reduction mechanism of the restitution coefficient of a porous ice with Φ=60% might be explained by the compression volume and the compressive strength. However, for Φ=47 and 53%, other energy dissipation mechanisms might affect.

We estimated the restitution coefficient, *e*, of Saturn’s ring particles by extrapolating our results to the range of their impact velocities and found that the *e* for a collision between porous ices was <0.6.

©2020. Japan Geoscience Union. All Right Reserved.

Crater scaling laws of ejecta velocity distribution and crater size constructed for very low strength target

Ryo Sugimura[1], *Masahiko Arakawa[1], Minami Yasui[1], Hiroki Senshu[2], Sunao Hasegawa[3]

1. Graduate School of Science, Kobe University, 2. Planetary Exploration Research Center, Chiba Institute of Technology, 3. Japan Aerospace Exploration Agency

Impact craters are very common geological feature on solid bodies, and the size-frequency distribution of these craters are used to determine the surface age of various solid bodies such as asteroids and satellites according to the crater chronology. The crater size scaling law, which can allow us to predict the crater size from the impact condition such as an impact velocity, an impactor size and density, a target density etc., is necessary to apply the crater chronology for each solid body. The crater size scaling law depends on the crater formation mechanisms; they are controlled by a surface gravity or a surface strength. Then, we need to use an appropriate crater size scaling law suitable for each solid body.
In general, the surface gravity of small bodies is too small to control the crater size so that the surface strength is a dominant mechanism to control the crater size. Although the surface strength of small rubble-pile bodies is estimated to be kPa order, the kPa order strength is enough large to control the crater size on small bodies. However, there are no systematic cratering experiments in low strength material to construct the crater scaling law applicable for small rubble-pile bodies. Thus, we made impact cratering experiments on very low strength targets changing from 400 Pa to 800 kPa to construct the crater scaling laws for the size and the ejecta velocity distribution.
Impact experiments were conducted by using a two-stage light gas-gun set at Kobe University and JAXA. A spherical Al-projectile with the diameter of 2mm was launched at 2, 4, 6 km/s. The targets were made of the mixture of quartz sand and porous gypsum changing the contents from 1 to 23 vol.%, and the target shape was cylinder with the dimeter of 25 cm and the height of 10 cm. The crater formation process was observed by a high-speed camera with the frame rate of 10^5FPS, and the slit with the width of 1 cm covered the target surface to observe the ejecta curtain in 2-dimension.
The crater spall radius, R, was found to increase with the decrease of the target tensile strength, Y, and the results are well described by the π-scaling theory in the strength regime as follows: $\pi_R=0.82\ \pi_Y^{-0.18}$. The ejecta curtain was observed to be a Y-shape at the initial stage of the ejecta curtain growth, then the curtain shape changed to the pillar-like shape at the later stage. The ejecta particles composed of the Y-shape curtain were measured in the high-speed images to determine each trajectory, and then each initial position and velocity was calculated to construct the eject velocity scaling law. The relationship between the initial position (x) and the ejection velocity was well scaled by the specific velocity (v^*) derived from the target density and strength, $v^*=(Y/\rho)^{1/2}$, and the crater spall radius as follow, $v^*/v=0.64(x/R)^{-4.0}$. We found that the ejection angle of impact fragments became higher with approaching the crater wall, and this ejection angle change with the distance from the impact point could originate the Y-shape ejecta curtain observed only in the strength regime. This characteristic feature of the Y-shape curtain cannot be explained by Maxwell Z-model applicable for sand-like incompressible material. Then, we proposed a modified Z-model considering a rigid boundary with the crater shape, and this model can reconstruct the Y-shape curtain.

Keywords: Impact crater, Crater scaling law, Ejecta curtain

©2020. Japan Geoscience Union. All Right Reserved.

Accretion of gas and solid materials into the circumplanetary disk of a growing giant planet: Dependence on planetary mass

*Natsuho Maeda[1], Keiji Ohtsuki[1], Ryo Suetsugu[2], Masahiro N Machida[3]

1. Graduate school of science, Kobe University , 2. University of Occupational and Hnvironmental Health, 3. Graduate school of science, Kyushu University

Regular satellites such as the Galilean satellites are likely formed by accumulation of solid particles supplied into the circumplanetary disks. Small particles so-called pebbles are considered to be important material of satellite formation (Shibaike et al. 2019). Since small particles are easily affected by gas flow around the planet, we have to take account of the gas flow around the planet obtained by hydrodynamic simulation to examine how they are delivered into the circumplanetary disk to form satellites. Tanigawa et al. (2014) examined accretion of solid particles initially confined within the midplane of the protoplanetary disk into the circumplanetary disk of a growing giant planet whose mass is 0.4 M_J (M_J being Jupiter's mass) using gas flow obtained by hydrodynamic simulation. Homma et al. (in revision) examined supply of vertically stirred solid particles into the circumplanetary disk using the same gas flow. However, current satellite systems were likely formed in the late stage of the formation of the host planet, and different behavior would be expected depending on planetary mass.

In this study, we focus on dependence of mass of the host planet. We examine gas flow in the cases of planetary mass of 1, 0.7, and 0.4 M_J obtained by isothermal, local hydrodynamic simulation, and investigate vertical accretion of pebbles by the circumplanetary disk under the influence of such a gas flow. We found that the width of the radial band for gas accretion into the circumplanetary disk becomes larger with increasing planetary mass. On the other hand, the gas gap formed in the vicinity of the planet's orbit becomes deeper and the surface densities of gas and dust becomes smaller with increasing planetary mass. Also, the size of the planet's Hill sphere becomes larger than the gas scale height of the protoplanetary disk for a sufficiently massive planet. Our result show that the rates of accretion of gas and dust onto the circumplanetary disk are determined by a balance among these effects.

Keywords: planets and satellites: formation –protoplanetary disks

©2020. Japan Geoscience Union. All Right Reserved.

Parameter Study of Satellite Formation via Giant Impact by N-body Simulation

*Yuichi Hasegawa[1], Ishizawa Yuya[1], Natsuki Hosono[2], Takanori Sasaki[1]

1. Department of Astronomy, Kyoto University, 2. Japan Agency for Marine-Earth Science and Technology

In the late stage of planet formation, there would be collisions between protoplanets. For example, the Moon is considered to be acreeted from a debris disk generated by the impact of Mars-sized protoplanet and the proto-Earth.While the moon formation process has been studied in detail, statistical study on satellite formation from impact-generated disks has not been done.

However, it is important to understand the general satellite formation process because satellites around exoplanets are expected to be a major observational targets. In this study, we modeled a variety of debris disk parametrized with initial disk mass and radius, and performed N-body simulations to investigate the position, number, and mass of formed satellites. We found that largest satellite formed just outside the Roche limit radius on almost all condition, and a few smaller satellites formed in outer regions.

Keywords: satellite formation, N-body simulation, giant impact

©2020. Japan Geoscience Union. All Right Reserved.

Numerical Analysis of Penetration Dynamics into Regolith using Compressible and Non-Expanding Plastic Gas Model

*Kojiro Suzuki[1]

1. Graduate School of Frontier Sciences, The University of Tokyo

To reveal the structure and properties under the surface of a celestial object, impact probes like an impactor, a penetrator and so on are expected to play an important role. For development of such impact probes, the numerical method to simulate the flow of the regolith around a body must be established as a convenient analysis tool. To reduce the computational cost, the fluid dynamics model, rather than the particle-based model, seems promising, because the properties of the regolith are defined using the equation of state with a small number of parameters. However, the flow of the regolith is essentially different from the flow of the conventional compressible fluid from a viewpoint of the irreversibility at compression. Once the regolith is compressed, its density remains higher than that in the initial uncompressed state even after the compression force is removed. As a result, no expansion waves are expected through the impact event in the regolith.

To describe such irreversible nature of the regolith flow, the "Compressible and Non-Expanding Fluid (CNEF)" model, which can be classified into the plastic gas model, has been proposed and its solution method has been developed by the author (Suzuki, K., AIAA Paper 2016-4107, 2016). In the CNEF model, the irreversible compression is described by assuming the different speed of sound in the unloading process from that in the compression process. For simplicity of analysis, the temperature effects are ignored and the pressure is defined as function of the density. By choosing a downward convex function for the irreversible compression process, the hardening effect, by which higher resistance force is generated against compression at higher density, is easily described. When the compression force disappears, the pressure is rapidly relaxed to zero with much higher speed of sound than in the compression process. To uniquely determine the state of the fluid, the internal energy, which is defined as the work done by the compression, was introduced. The numerical scheme to solve the Euler equations for the CNEF model was constructed in the framework of the finite volume method, Godunov method and the Riemann solver. A complete set of the fundamental solutions of the Riemann problem were analytically formulated for the CNE fluid (Suzuki, K., Aerospace Technology Japan, 16(3), 2018).

First, the two-dimensional crater formation problem was solved using the CNEF flow simulation code. The crater and the rim were successfully formed with the surface tracking technique by the VOF method. The compressed regolith with high density remained in the shallow zone under the bottom surface of the crater around the impact point (Suzuki, K., 32ISTS, 2019-k-24, 2019).

In the present study, the flow of the regolith around a flat-tipped cylindrical penetrator body was numerically analyzed at the impact velocity from 100 m/s to 300 m/s, solving the axi-symmetric Euler equations on the moving coordinates fixed at the penetrator. The highly compressed regolith was formed in front of the nose just after the impact. The density of the regolith in front of the nose remained high even after the penetrator was decelerated. The body had to push the high density regolith to continue to penetrate into the regolith. Consequently, the force acting on the penetrator nose became much higher than the impact pressure in the uncompressed regolith. The radius of the crater was larger than the penetrator radius. The cylindrical side wall of the penetrator was detached from the regolith and no force was acting there. The variation of the deceleration, which is in proportion to the pressure at the nose wall,

©2020. Japan Geoscience Union. All Right Reserved.

with the velocity was similar to the variation pattern observed at the experiment of the LUNAR-A penetrator (Suzuki, K. et al., 20ISTS, 96-i-02v, 1996).
This work is supported by Grant-in-Aid for Scientific Research (B) No. 19H02339 of Japan Society for the Promotion of Science.

Keywords: penetrator, compressible fluid, irreversibility, regolith, computational fluid dynamics

©2020. Japan Geoscience Union. All Right Reserved.

Test of a model for the gas accretion onto giant planets by two-dimensional hydrodynamical simulations

*saho nakazawa[1], Yuki Tanaka[1], Hidekazu Tanaka[1]

1. Tohoku University

Giant planets are generally considered to have formed by capturing disk gas in a protoplanetary disk. However, we do not have a reliable model which predicts an accurate gas accretion rate onto a planet for a given disk. Without such a model, we cannot fix the growth time and final mass of giant planets.

Because of its strong gravity, a giant planet excites density waves and creates a gap (i.e., a low-density annular region) along the planetary orbit. Tanigawa & Tanaka (2016) constructed a model of the gas accretion rate onto a planet, by assuming that the gas accretion rate is proportional to the gas surface density in the gap. Although their model is almost consistent with some three-dimensional hydrodynamic simulations, the accuracy of the model is still uncertain. In this study, we test their model in detail , by performing two-dimensional hydrodynamic simulations with FARGO code.

First, we perform test simulations of gap formation without gas accretion onto the plant for various planet masses and viscosities. Then, we confirm that our results are consistent with an empirical formula of gap depth derived by Kanagawa et al. (2015).

In the simulations with the gas accretion onto the planet, we model the gas accretion onto the planet, by reducing the gas surface density in the accretion region around the planet with a certain reduction timescale. Then, we have three parameters, i.e., the radius of the accretion region, the reduction timescale, and the smoothing length in the planetary gravitational potential. We perform simulations with various values of these parameters and find that the gas accretion rate is almost independent of the radius of accretion region and the smoothing length, if these are less than the disk scale height. Although the gas accretion rate depends on the reduction timescale, it converges for a short reduction timescale. Furthermore, we compare our converged accretion rate with the model by Tanigawa & Tanaka (2016) and find that our results are consistent with their model for various viscosities.

Keywords: planet formation, gas accretion, hydrodynamics

©2020. Japan Geoscience Union. All Right Reserved.

An Explanation for Physical Mechanism of the Streaming Instability in Dust Dominant Regime

*Hiroaki Kaneko[1], Taishi Nakamoto[1]

1. Tokyo Institude of Technology

Streaming Instability (SI) is one of the promising paths against difficulties in planetesimal formation. Recently, numerical simulations have confirmed that in the nonlinear stage, SI generates a local high solid concentration followed by a gravitational collapse that may lead to the planetesimal formation. Its physical mechanism in the linear stage has also been discussed in some papers. However, these previous works cannot fully capture the physical features of SI such as the vertical advection and the dependence on the density ratio between dust and gas. In this work, we show a new physical understanding of SI that explains them.

Based on the equilibrium drift speeds of dust particles given by Nakagawa *et al.* (1986), we derive the dust mass flux in *x*-*z*plane with only the density perturbation and show the interpretation of the phase speed in SI. We use the terminal velocity approximation and solve the dispersion relation to see the motion and the concentration of dust and gas in both dust-dominant and gas dominant regimes. It is revealed that in the gas dominant regime, the dust vertical advection enhances the density maxima, while the dust radial advection weakens it. In the dust dominant regime, these features are opposite. We show an explanation for the physical mechanism in both the regimes.

Keywords: protoplanetary disk, planetesimal formation, instability

©2020. Japan Geoscience Union. All Right Reserved.

The influence of dust evolution on the vertical shear instability in protoplanetary disks

*Yuya Fukuhara[1], Satoshi Okuzumi[1]

1. Department of Earth and Planetary Sciences, Tokyo Institute of Technology

Protoplanetary disks are places of planet formation. Gaps in disks revealed by recent high-resolution radio observations (e.g., Andrews et al. 2018) may indicate that planets form far away from the central stars (10–100 au). How dust in such distant regions grows into planetesimals and planets remains an open question.
To address this question, it is crucial to understand turbulence in the outer regions of protoplanetary disks. Turbulence in protoplanetary disks is known to induce collisional fragmentation and diffusion of dust particles (e.g., Ormel & Cuzzi 2007), both of which prevent planetesimal formation. Turbulence can also promote planetesimal formation by selectively collecting particles of a particular size (e.g., Pan et al. 2011). However, it is still unclear what mechanism mainly drives turbulence in outer disk regions.
In this study, we discuss the viability of the vertical shear instability (VSI) as a mechanism driving turbulence in outer disk regions. The VSI is a hydrodynamic instability of accretion disks with a vertical gradient in the rotation velocity and operates when the thermal relaxation time of the disk gas is much shorter than the orbital period. Previous studies (Pfeil & Klahr 2019) suggest that the VSI is apt to occur in outer disk regions. However, the calculation of the thermal relaxation time in the previous studies assumed micron-sized dust grains, which is inapplicable to circumstances where dust evolution has already proceeded.
The purpose of this study is to clarify the influences of dust evolution on the spatial extent of the VSI-unstable region. To this end, we use a model based on the local stability analysis of the VSI (Malygin et al. 2017; Pfeil & Klahr 2019) and study how the VSI-unstable region changes with the maximum size and total amount of dust particles. The vertical distribution of the particles is determined from the balance between sedimentation and turbulent diffusion, assuming a given strength of VSI-driven turbulence.
We find that the VSI-unstable region shrinks as the maximum particle size increases, and/or the total amount of dust decreases. This is because thermal relaxation becomes faster as small dust grains are removed. In the particular case where the total disk mass is 1% of the solar mass, the VSI-unstable region is confined within one gas scale height above and below the midplane if the maximum particle size is larger than 1 mm, or the dust-to-gas surface density ratio is below 0.1% .
Our results suggest that dust evolution suppresses VSI-driven turbulence. Given that turbulence generally prevents dust coagulation, the coevolution of dust and VSI may promote further dust growth. Our results also imply the presence of positive feedback between dust setting and VSI suppression, namely, dust settling makes VSI weaker and thereby further promotes the settling itself.

Keywords: Protoplanetary disk, vertical shear instability

©2020. Japan Geoscience Union. All Right Reserved.

Collisional Growth and Fragmentation of Dust Aggregates with Low to Very High Mass Ratios

*Yukihiko Hasegawa[1], Takeru Suzuki[1], Hidekazu Tanaka[2], Hiroshi Kobayashi[3], Koji Wada[4]

1. The University of Tokyo, 2. Tohoku University, 3. Nagoya University, 4. Chiba Institute of Technology

For the process in forming planetesimals in protoplanetary disks, growth of dust aggregates through collisions between aggregates is important. However, in this process, high-velocity collisions cause collisional fragmentation and prevent aggregates from growing further. The critical velocity of collisional fragmentation is investigated in many previous studies, but especially in numerical simulations, the critical velocity was investigated only for cases with the mass ratio of colliding aggregates lower than 100. We carry out numerical simulations of collisions between icy aggregates with various mass ratios from 1 to 1024 and present the critical velocity of collisional fragmentation for mass ratios not presented in previous studies. Our simulation results show that the critical velocity for very high mass ratios is much higher than ones shown by previous studies and 100 m per second. On the other hand, for low mass ratios, it is suggested that the critical velocity is lower than half of the typical maximum collision velocity in the typical model of the protoplanetary disk. This tendency was not shown in previous simulations.

©2020. Japan Geoscience Union. All Right Reserved.

Partitioning of H, C, N and S on a growing Earth estimated by empirical thermodynamic modelling

MURASE YUTARO[1], Hiroaki Saito[1], *Kiyoshi Kuramoto[1]

1. Department of Cosmosciences, Graduate School of Sciences, Hokkaido University

Partitioning of volatile elements on an accreting planet among vapor, silicate melt and molten iron is a key process that controls initial inventories of these elements among the planetary surface and interior. So far, most studies have evaluated it separately for each element by applying gas solubility data and/or element distribution coefficients among liquid phases. Actually, however, volatile elements do form various chemical compounds, which affects fugacities of chemical species that control their amounts in liquid phases. Here we have developed an empirical thermodynamic model solving equilibrium chemical speciation of major volatiles H, C, N and S and their partitioning among vapor, silicate melt and molten iron applying a Gibbs free energy minimization method. Chemical potentials of volatile solutes in liquid phases are modeled from experimental data of gas solubilities into silicate melt and molten iron. Given the bulk elemental composition of Earth’s building block by the two component model (Wanke and Dreibus, 1988) and conditions with high temperature (1500 K- 3000 K) and pressure (up to 1000 bar) on a terrestrial magma ocean, our model predicts 1) H_2-rich vapor containing H_2O, CO, CH_4 and SH as secondary species and 2) preferential partitioning of C, N and S into molten metal and significant H_2O partitioning into silicate melt at elevated pressures. These results imply selective removal of C and N from a thick proto atmosphere to the core, which is consistent with the observed strong depletion of C and N from the present Earth’s surface and depleted mantle compared to the chondritic proportion of volatile elements. N_2 is the dominant nitrogen species in vapor whereas NH_3/N_2 ratio reaches to order of 10^{-3} to 10^{-1}, which may be large enough to produce significant greenhouse effect and have impacts on prebiotic synthesis of amino acid after the cooling of proto-atmosphere.

Keywords: volatile elements, accretion, partitioning, magma ocean, proto atmosphere

©2020. Japan Geoscience Union. All Right Reserved.

Automatic segmentation of rayed craters on the Moon by applying deep learning technique

*Yuko Daket[1], Chikatoshi Honda[1], Takashi Sonoke[1], Hirohide Demura[1]

1. University of Aizu

Introduction: These days, numerous images of planetary surfaces have been taken. In order to process them efficiently, it is required to reduce human tasks to process those big data. Application of machine learning techniques will be one of the solutions. In this study, we focused on making a thematic map containing rayed craters and their ejecta. Geologic maps are integration of multiple thematic maps and are used to investigate scientific objects and mission planning. In this study, we made the thematic map by applying a machine learning technique, called Efficient Neutral Network (Enet).

Data: Visible and near-infrared images obtained by Terrain Camera (TC) and Multi-band Imagers (MI) were employed. TC and MI were onboard SELENE. Spatial resolution of TC and MI images are ~10 m/pix and ~60 m/pix, respectively. TC observed lunar surface with visible range. MI observed lunar surface in 9 different channels whose wavelength range from 415 to 1055 nm. These images are advantageous to perform global survey in same quality, because they cover the entire lunar surface in same resolution and same illumination condition.

Study area and Method: The region of south Sinus Medii (3x3 degrees in size) was chosen for the training, validating, and the testing fields. The area is located on the nearside mare. Several grabens, sinuous rilles, and remained old crater rims are observed in the region. In order to the automatic segmentation, we employed Enet, a supervised machine learning technique. It is a deep neural network architecture for semantic segmentation. It requires low real-time inference in comparison to other deep neutral networks. To train a model, Enet requires input images with labeled images.

The composite image of TC and MI images were used as the input image. The lunar surface spectral features vary due to the difference in composition and amount of space weathering. Ejecta exposed by rayed craters are not space weathered, therefore they show different spectral features from the surrounding area. Thus, using visible and near-infrared images makes it easier to recognize rayed craters and their ejecta. The composite image is made of TC image as red, MI band ratio image of 749 nm/1001 nm as green, MI band ratio image of 414 nm/749 nm as blue. In order to adjust the gap of spatial resolution between TC and MI images, MI images are artificially interpolated and set to the resolution of 10 m/pix by nearest neighbor.

We also manually prepared the labeled images that have three classes, “rayed craters”, “ejecta”, and “others”. The composite image and the labeled image divided into 576 pieces, 512x512 pixels size each. Among them 504 labeled images were used to train the model. 72 images were used to validate the model.

Results: The small craters (~70 m<D<~1 km) predicted by the trained model met good agreement with the manually extracted craters. Although the predicted ejecta extents were slightly different from expected ones, this difference is negligible. Even manual analyze, it is hard to tell clear end line of ejecta, because they gradually thinner and disappears as they get far from the crater. The predicted large craters (D>~1 km) and their ejecta were not well extracted. The lack of supervised images for the craters can explain the

©2020. Japan Geoscience Union. All Right Reserved.

disagreement. There were only ~10 rayed craters larger than 1 km. Referring to ambiguous small craters (D<~70 m), although craters themselves were not well extracted, their ejecta were mapped well. The reason why small craters were not extracted well is explained by the spatial resolution. Their dimeters are close to detection limit, because spatial resolution of MI is ~60 m/pix.

Keywords: Moon, Crater, Machine learning

©2020. Japan Geoscience Union. All Right Reserved.

Simulation of space weathering with mixture lunar-like composition

*Ryota Shimana[1], Sho Sasaki[1], Takahiro Hiroi[2]

1. Departure Earth and Space Science, Osaka University, 2. Department of Earth, Environmental and Planetary Sciences, Brown University

Space weathering is an effect that changes an optical property of mineral when surface of asteroids or airless-bodies are exposed to the space for long time. Space weathering makes reflectance spectra redder (steeper), darker and weaken absorption bands.
Such changes are caused by the production of nanometer-sized iron fine particles created by the reduction of iron ions containing in the mineral on airless body’ s surface. Due to the impact of micrometeoroids, irradiation of the solar wind, and irradiation of the cosmic ray iron ions are reduced and nanometer-sized iron fine particles are produced, then optical property changed.
The degree of space weathering varies depending on various factors such as the mineral composition, its particle size, a distance from the sun, and so on.
Plagioclase which is abundant on the lunar surface is little affected by space weathering. Plagioclase contains small amount of olivine, however lunar surface weathered much. In this study, mixtures of plagioclase and olivine is used as samples, and the space weathering of the lunar surface was simulated by irradiation with a nanosecond pulse laser, and the reflectance spectra was measured with a spectrometer(250-2500nm).
In data analysis such as remote sensing, it is important to consider the influence of its phase angle (observer-object-light source). The reflectance changes depending on the phase angle.
To assess the degree of the phase angle dependence, we measured the samples which are the mixtures of olivine and plagioclase and these irradiated by laser under the 12 different phase angle conditions. As a result, redness due to an increase of the phase angle was observed.
This effect also needs to be considered in the same way as reddening by simulation of space weathering.

Keywords: Space weathering, Reflectance spectra, lunar-like composition

©2020. Japan Geoscience Union. All Right Reserved.

The 1300 km diameters ring fault around Orientale basin from gravity data

*Qingyun Deng[1], Fei Li[1,2], Jianguo Yan[1], Zhiyong Xiao[3], CHONG ZHENG[1], Chi Xiao[1], Jean-Pierre Barriot[1,4], Mao Ye[1]

1. The State Key Laboratory of Information Engineering in Surveying, Mapping and Remote Sensing, Wuhan University, 2. Chinese Antarctic Center of Surveying and Mapping, Wuhan University, 3. School of Atmospheric Scienses, Sun Yat-sen University, 4. Université de la Polynésie Française

Orientale basin is the youngest and best preserved multi-ring basin on the Moon, featured with four concentric topography rings. Those inward-facing ring scarps are suggested to be correlated with normal faults induced by the collapse of impact transient crater. GRAIL gravity data further confirmed the existence of deep penetrated ring faults around Orientale basin, which well matching their surface scarps. Geometry of those large scale normal faults provide information about the physical properties of lunar crust, and shed light to impact cratering models. In this work, we proposed a novel gravity gradient eigenvalue to emphasize concentric signatures around Orientale basin in gravity data. The possible 1300 km diameters ring outside Cordillera main rim (D~937km) is reflected in our new eigenvalue map. Gravity inversion indicates its subsurface density structures, suggesting that the modification range of impact cratering is underestimated by previous researches. Implications for the crustal properties and modeling of impact process are also discussed.

Keywords: Gravity inversion, Multi-ring basin, Impact cratering

©2020. Japan Geoscience Union. All Right Reserved.

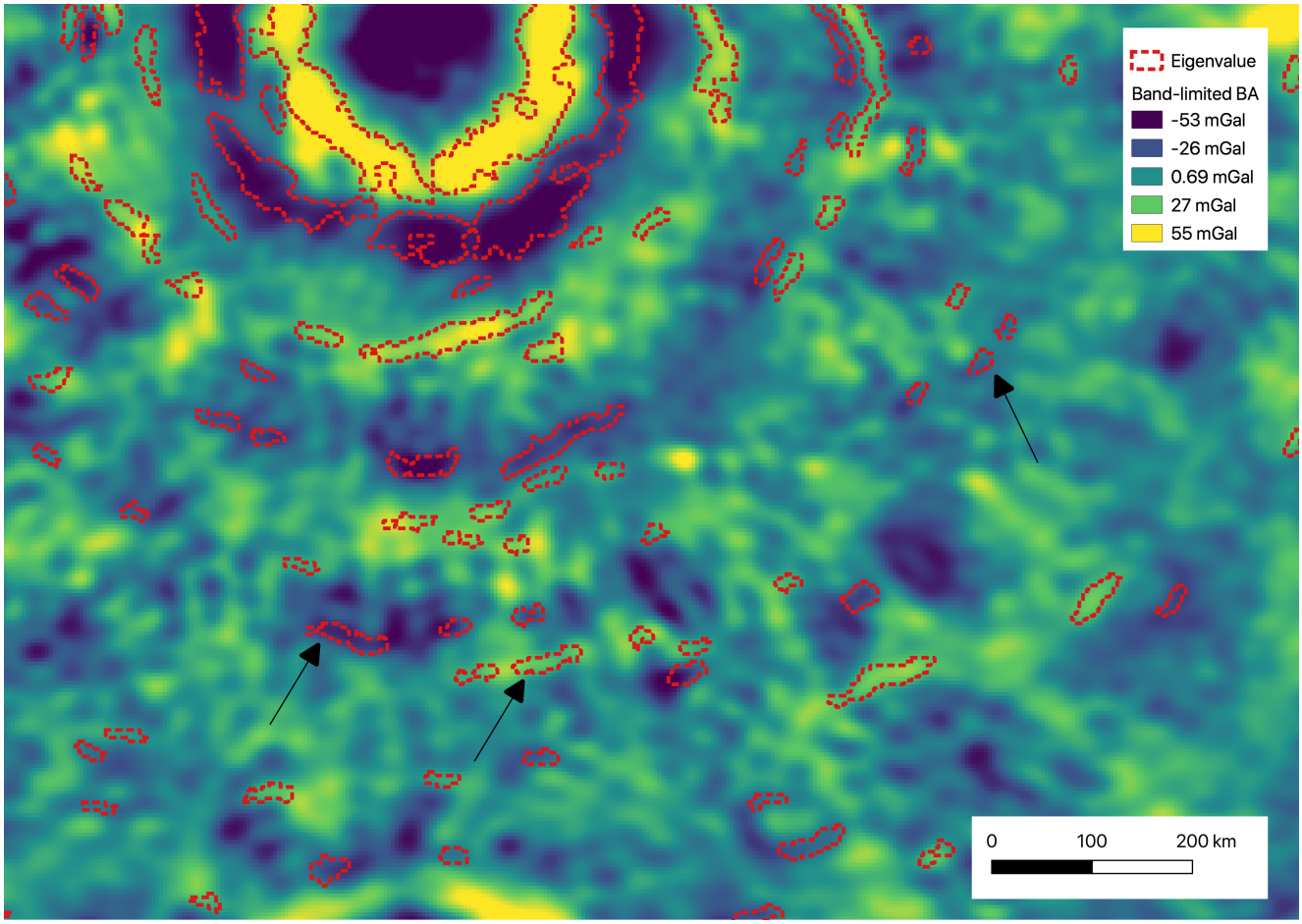

©2020. Japan Geoscience Union. All Right Reserved.

The thermal history of comets derived from the EUV spectra data observed by HISAKI

*Kanae Nomura[1], Kazuo Yoshioka[1], Kei Masunaga[2]

1. University of Tokyo, 2. University of Colorado Boulder

From 2015 to 2018, five comets (C/2013 X1 Panstarrs, C/2013 US10 Catalina, 46P/Wirtanen, 21P/Giacobini-Zinner, and 67P/Churyumov-Gerasimenko) had been observed by HISAKI that is the spectroscopic observatory of planets from the low earth orbit. By comparing with the background data, the spectra of two comets (Panstarrs and Catalina) could be revealed. We derived the extreme ultraviolet (EUV) lights spectra of various species of atomic and molecular in these comets by subtracting geocorona around the Earth from the observed data. It is thought that comets keep the information about the temperature environment and materials in the protoplanetary disk. Therefore, to study the chemical composition of the comets' comae and nuclei helps us to obtain information about the protoplanetary disk. Particularly, H_2O, CO_2 and CO, which are the main ingredients of comets, are the most important clues to know the evolution of comets. The difference in the sublimation temperature of H_2O, CO_2 and CO reflects the temperature environment at the formation stage of the protoplanetary disk. On the other hand, the ratio of CO_2/CO reflects the oxidation environment (Ootsubo et al., 2012). In this presentation, we will introduce the EUV spectra of comets obtained by HISAKI and physical processes about the emission of several atomic species (H, C, O). We will also show the ratio of H_2O, CO_2, CO that was derived from the emission of atomic species and discuss the scientific scenarios by comparing with the values of the other comets that have been observed in the past.

Keywords: Comets, HISAKI, Extreme Ultraviolet (EUV), Chemical composition

©2020. Japan Geoscience Union. All Right Reserved.

A search for the non-water ices on the icy Galilean moons of Jupiter with ground-based telescope

*Seiko Takagi[1], Taro Matsuo[2], Jun Kimura[3]

1. Hokkaido University, Graduate School of Science, 2. Nagoya University, 3. Osaka University

In the outer region of the Solar System, the Jovian system and beyond, most of solid bodies are generally covered with the solid water ice on their surfaces, and thus they are called as icy bodies. In addition, various non-water ice(s) can be found on the many objects, e.g., CH_4 and NH_3in the Saturn moons and N_2 and CO in the Neptunian moon Triton and the icy dwarf planet Pluto. As a first approximation, highly volatile ices exist in a farther region from the Sun, thus such distribution of non-water ices in the outer Solar System seem to reflect the temperature environment during the formation of the Solar System and the positional relationship between the snowline and the place where the planetary system formed.

In the Jovian system, the only non-water volatiles which have been inferred is CO_2, by the presence of an absorption band at ~4.26 microns in reflectance spectra returned by the Near Infrared Mapping Spectrometer (NIMS) aboard the Galileo spacecraft. On Callisto, trailing hemisphere and several fresh impact craters show enrichment in carbon dioxide. On the other hand, no such distributions of CO_2 can be seen on Ganymede. Thus the origin of CO_2 on their moons, whether these are primordial and degassed from the interior or are exogenic and delivered through the impact, is still controversial. Identifying the presence of non-water ices on the Jovian system could be an important key to know the formation environment of the outer Solar System, by comparing the material distribution on the other giant planet systems, Saturnian system and beyond.
We search the non-water ices, e.g., CH_4 and NH_3, on the icy Galilean moons of Jupiter; Europa, Ganymede and Callisto, using the ground-based telescope of Hokkaido University (Pirka telescope, the primary mirror is 1.6 m in diameter). The Pirka telescope and its on-board observation device has started full-scale operation in 2011 with priority to observe planetary bodies in the Solar System. The multi spectral imaging device has been installed at the Cassegrain focus of the telescope and it allow us to obtain surface spectral data with wavelength between 350 and 1050 nm. Here we will report the investigation.

Keywords: Galilean Satellite, ground-based observation

©2020. Japan Geoscience Union. All Right Reserved.

Simulation study to detect Mars atmosphere by satellite gravimetry

*Keiko Yamamoto[1]

1. National Astronomical Observatory of Japan

On many planets, like the Earth, the atmosphere plays an important role in regulating the surface environment of the planet. Atmospheric circulation accompanies the movement of mass on the planet's surface and therefore can be detected as a temporal variation of the gravity field. In this study, we focus on the circulation of the Martian atmosphere and discuss the possibility of detecting it by satellite gravimetry. To evaluate whether the magnitude of surface mass variations due to Martian atmosphere are detectable by satellite gravimetry, we investigated the magnitude and spatiotemporal properties of the mass variations caused by Martian atmosphere and other potentially detectable mass variable components (CO_2 ice, dust, H_2O ice), using Mars Climate Database (MCD) 5.3. Based on the obtained results, we discussed the required sensitivity, number, observation period, and orbit design of the spacecraft to detect each signal effectively. We also discussed the possibility to estimate the Mars' load Love numbers by detecting temporal mass and volume changes of the surface CO_2 ice, combining satellite gravimetry and altimetry.

Keywords: satellite gravimetry, Mars

©2020. Japan Geoscience Union. All Right Reserved.

Effects of the haze layer on Titan's atmospheric dynamics

*Motoki Sumi[1], Shin-ichi Takehiro[2], Wataru Ohfuchi[3], Hideko Nomura[4], Yuka Fujii[5]

1. Department of Earth & Planetary Sciences, Tokyo Institute of Technology, 2. Research Institute for Mathematical Sciences, Kyoto University, 3. Department of Planetology/CPS, Graduate School of Science, Kobe University, 4. Division of Science, National Astronomical Observatory of Japan, 5. Earth-Life Science Institute, Tokyo Institute of Technology

Titan’s stratosphere has been observed to be in a strong superrotation state, where the atmosphere rotates many times faster than the surface does. The Huygens Doppler Wind Experiment (DWE) probed Titan’s atmosphere near the equator and observed the eastward winds at all altitudes except near the surface. The zonal wind speed increases as the altitude increases aside from the dormant region at about 80 km, and reaches 100 m/s at about 120 km. In addition, the brightness temperature of the atmosphere above an altitude of 140 km observed by Cassini Composite Infrared Spectrometer (CIRS) has revealed that there is also in the strong superrotation state (Achterberg et al., 2008).

Another major feature of Titan’s atmosphere is the presence of a thick haze layer. Titan’s haze layer absorbs about 90% of solar radiative flux and increases the temperature of the upper atmosphere, significantly affecting the structure of the atmosphere (Mckay et al., 1991). However, the effect of haze layers on the atmospheric dynamics has not yet been well studied. Understanding such effects of the haze layers would provide the key insights into the atmospheric dynamics of terrestrial planets in general as well as Titan.

In this study, we performed numerical experiments using a General Circulation Model (GCM) with the purpose of elucidating the mechanism of superrotation in Titan and understanding the general circulation patterns associated with it. In the experiments, we used DCPAM, a general circulation model based on the primitive equation system for planetary atmospheres, developed by GFD Dennou Club. We newly employed the gray radiation model of McKay et al.(1999), where the greenhouse effects by the atmospheric gases and the absorption of the sunlight by the haze layer with several parameters are represented by several parameters. The phase change of Methane or the seasonal changes are not taken into account so as to focus on the effects of the radiation field structure. Our atmospheric grid consists of T10L55 (55 pressure levels and 32 longitude 16 latitude grids), and we began the experiments with the atmosphere at rest with respect to the surface of Titan, and with a radiative-equilibrium temperature profile. These models ran until the atmosphere is fully spun up, i.e., has reached steady state (approximately 100,000 Earth days).

We found that calculations with the radiation parameters that reproduced the actual temperature structure of Titan yielded the global eastward wind around the equator with a maximum speed of more than 100 m/s at an altitude of ~200 km. This is roughly consistent with the CIRS data (Achterberg et al., 2008). On the other hand, in the lower atmosphere, the mean value of the zonal winds is very small with no strong vertical gradient, in contrast to the observed substantial increase of the wind speed with the altitude. By changing the parameters of the radiation model, we found that the altitude at which the eastward wind reaches its maximum depended on the altitude of the haze layer. In addition, the intensity of the eastward wind increased as the solar flux absorption rate of the haze layer increased. We did not observe superrotation when the solar flux absorption in haze layer was eliminated. In this presentation, we will discuss these parameter dependencies and the differences from the observation.

©2020. Japan Geoscience Union. All Right Reserved.

Keywords: Titan, Atmospheric General Circulation Model, superrotation, haze layer

©2020. Japan Geoscience Union. All Right Reserved.

Participation of Japanese planetary science community to the Mercury exploration mission BepiColombo

*Shunichi Kamata[1], Ryuki Hyodo[2], Futoshi Takahashi[3], Takashi Yoshizaki[4], Yota Ishigaki[2], Kiyoshi Kuramoto[1], Go Murakami[2], Masaki Fujimoto[2]

1. Hokkaido Univ., 2. ISAS/JAXA, 3. Kyusyu Univ., 4. Tohoku Univ.

The BepiColombo mission to Mercury is a joint mission between Europe and Japan and is ongoing. It was launched on Oct. 20, 2018 from French Guiana and will be inserted to the orbit in Dec. 2025. This mission uses two satellites; "Mio" provided by JAXA will mainly investigate the magnetosphere and the exosphere, and "Mercury Planetary Orbiter" provided by ESA will investigate the surface and interior of Mercury. Because of this, Japanese planetary science community has a little involvement into the mission. However, an international call for Interdisciplinary Scientists (IDS) for the mission last year has changed this situation. We have started to model the multi-step formation and evolution theory of Mercury and to test it using various kinds of data sets. In this presentation we will report our activities and future plan.

Keywords: BepiColombo, Mercury, Planetary formation, Planetary evolution

©2020. Japan Geoscience Union. All Right Reserved.

Mercury Trek: A New Online NASA Visualization and Analysis Portal

*Brian Hamilton Day[1], Emily Law[2], NASA Solar System Treks Team -[2]

1. NASA Ames Research Center, 2. NASA Jet Propulsion Laboratory

In its investigations of the planet Mercury, NASA’s MESSENGER returned an immense amount of data detailing the dynamic surface of our solar system’s innermost planet. As the Japanese and European space agencies prepared for the launch of BepiColombo, the next mission to explore Mercury, BepiColombo’s project science team asked NASA to produce a new portal within the Solar System Treks suite (https://trek.nasa.gov) featuring data returned by MESSENGER from Mercury. This new portal would be used both for mission planning and for public outreach by the BepiColombo mission. While initially populated with Messenger data, the portal is also being designed to facilitate visualization, analysis, and dissemination of data from BepiColombo after it commences science operations in orbit around Mercury. The initial release of the Mercury Trek in 2019 shortly followed the launch of BepiColombo on its journey to Mercury.

The initial release of Mercury Trek features data products from the Mercury Dual Imaging System (MDIS) instrument that operated aboard NASA’s MErcury Surface, Space ENvironment, GEochemistry and Ranging (MESSENGER) mission while in orbit around Mercury from 2011 to 2015. These products include the MDIS Global Mosaic, MDIS BDR Global Mosaic, MDIS Color Global Mosaic, MDIS MD3 Color Global Mosaic, MDIS Enhanced Color Global Mosaic, MDIS LOI (low-incidence angle) Global Mosaic, MDIS Global Digital Elevation Model (DEM), and MDIS Color Hillshade Global map derived from the DEM. Mercury Trek’s data visualization capabilities make it easy to stack and blend different data layers in order to optimize depictions of a wide variety of surface features.

Data products can be viewed in equatorial, or polar projected views, or on an interactive 3D globe. The Trek interface allows the user to maneuver a first-person visualization of “flying” across the surface of the Mercury.

Analysis tools make it easy to measure distances (either straight-line or along a user-defined path) and to create elevation profiles for surface features. Users can draw user-defined bounding boxes across Mercury’s terrain to generate STL or OBJ files for 3D printing. They can also draw a freehand path anywhere across the surface and have Mercury Trek return a QR code that can be scanned into a smartphone (Android or iOS). The smartphone can then be placed into a pair of inexpensive cardboard-compatible goggles. The user will then be able to fly their defined path in virtual reality.

We intend to continue working with the Bepi-Colombo mission and the greater planetary science community to enhance the new Mercury Trek portal with additional data products, and solicit suggestions from the community.

Mercury Trek is the latest addition to the NASA Solar System Treks Project, available at https://trek.nasa.gov. NASA's Solar System Trek online portals for lunar and planetary mapping and modeling provide web-based suites of interactive data visualization and analysis tools to enable mission planners, planetary scientists, students, and the general public to access mapped data products from past and current missions for the Moon, Mars, Vesta, Ceres, Titan, seven of Saturn’s smaller icy moons (Dione, Enceladus, Iapetus Mimas, Phoebe, Rhea, and Tethys), and now Mercury. As web-based toolsets,

©2020. Japan Geoscience Union. All Right Reserved.

the portals do not require users to purchase or install any software beyond current web browsers. These portals are being used for site selection and analysis by NASA and a number of its international partners, supporting upcoming missions.

Keywords: Mercury, BepiColombo, MESSENGER, Solar System Treks, GIS, Data Visualization

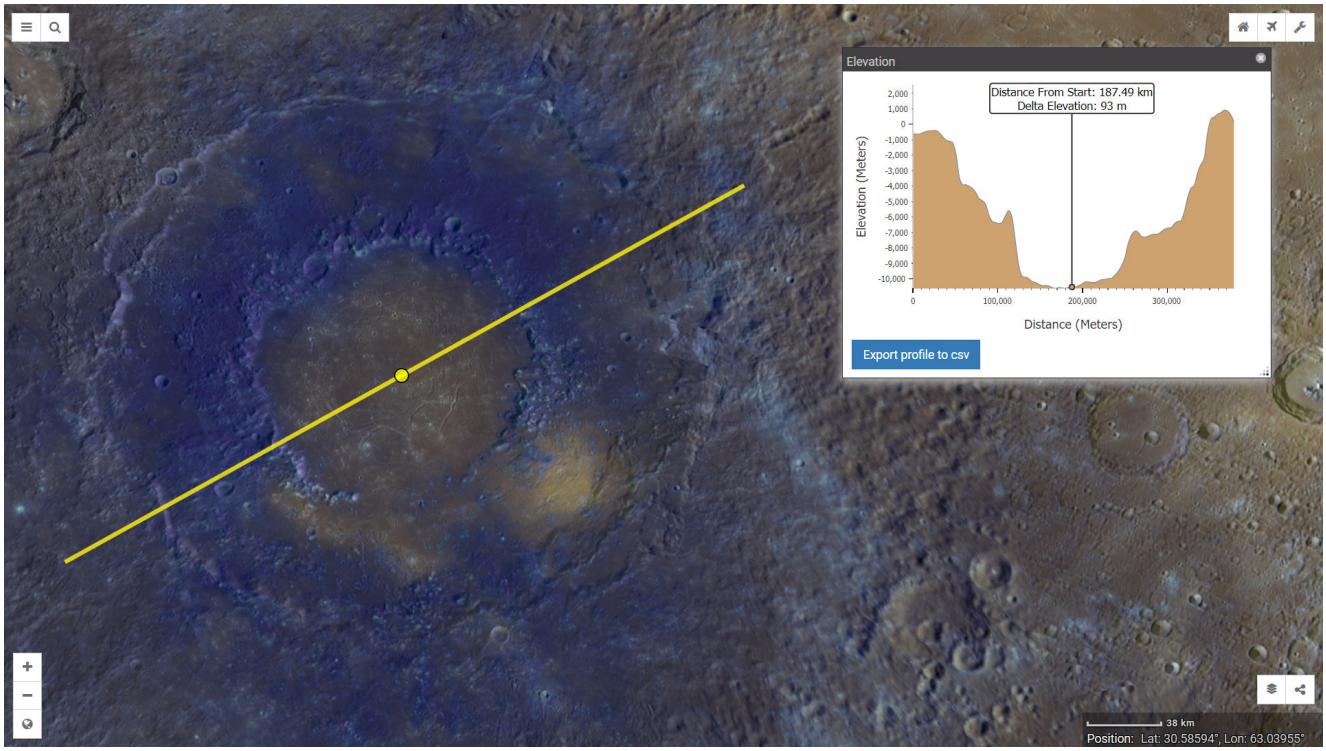

©2020. Japan Geoscience Union. All Right Reserved.

Proposed comet impacts forming Lake Michigan as an explanation of the formation of the Carolina bays.

*John Anthony Burgener[1]

1. Telegistics Inc.

The Carolina bays are a group of hundreds of thousands of elliptical, shallow depressions along the eastern coast of North America and in the middle of North America. Their origins have been discussed for many years as possible wind erosion events or possible splash formations due to ejecta from an asteroid or comet impact. Wind erosion is not a satisfactory explanation since the axis of the bays are not all aligned, and the axis are not aligned with the prevailing winds. Several attempts have been made to explain the bays as splash marks from an impact in the vicinity of Lake Michigan, but no one has considered the Lake itself as the crater related to the impact primarily due to it being considered much too large to be an impact event.

Burgener 2019 (1), demonstrated that Kuiper Belt object orbits are typically unstable and therefore comet impacts should be more frequent and larger than previously expected, with new 10+ km size comets in Earth Crossing Orbits every 130,000 years. While not all will impact Earth, some will, and the frequency should be high enough to find such craters at present.

It is recognized that the angle of impact of 45˚ has the highest probability of occurring and that low angle impacts are much less common. What is often overlooked, is that although 45˚ has the highest probability, it is not true that low angle impacts are rare. The probability of an impact between 40˚ and 50˚ is 17.4%, but the probability of an impact between 0 and 25˚ is 17.9%. The probability of an impact between 0 and 10˚ is 3%, which is still high enough that some such impacts will happen. The chance of such a low angle impact leaving a noticeable crater or scar is minimal on a hard rock surface such as the Moon, but in this case, Lake Michigan was covered with a layer of 2 to 3 km thick ice, and the ground under the ice was relatively soft sediments. So a very low angle of impact would leave a splash scar of shallow depth, and send most of the impacted ice and sediments far away as ejecta. The comet itself would most likely continue on into space, as comets travel at speeds well above Earth escape velocity and such a low angle of impact would lead to a skip instead of an explosion.

It is proposed that a comet in several pieces, impacted Earth at the end of the ice age, about 12,700 years ago, impacting the present location of Lake Michigan and with a portion hitting the middle of Lake Superior, and ejecting large quantities of ice and sediments south east and south west. These large pieces of ice and sediments landed along the east coast of North America and in the middle of North America at low velocity due to air resistance slowing them, and hitting at very low angles of incidence due to their original momentum being directed away from the comet splash location. As such, elliptical depressions would form, with shallow depth. As most were formed from ice, most would leave no remaining typical asteroid or comet debris in the depressions.

©2020. Japan Geoscience Union. All Right Reserved.

The remaining scar due to the comet impact / skip is a large portion of the present day Lake Michigan and a smaller depression in the middle of Lake Superior.

(1) Burgener, J., "The Influence of Dwarf Planets on the Stability of Objects in the Kuiper Belt", 50th Lunar and Planetary Science Conference, March 18-22, 2019, presentation #3163

Keywords: Comet, Impact, Carolina Bays

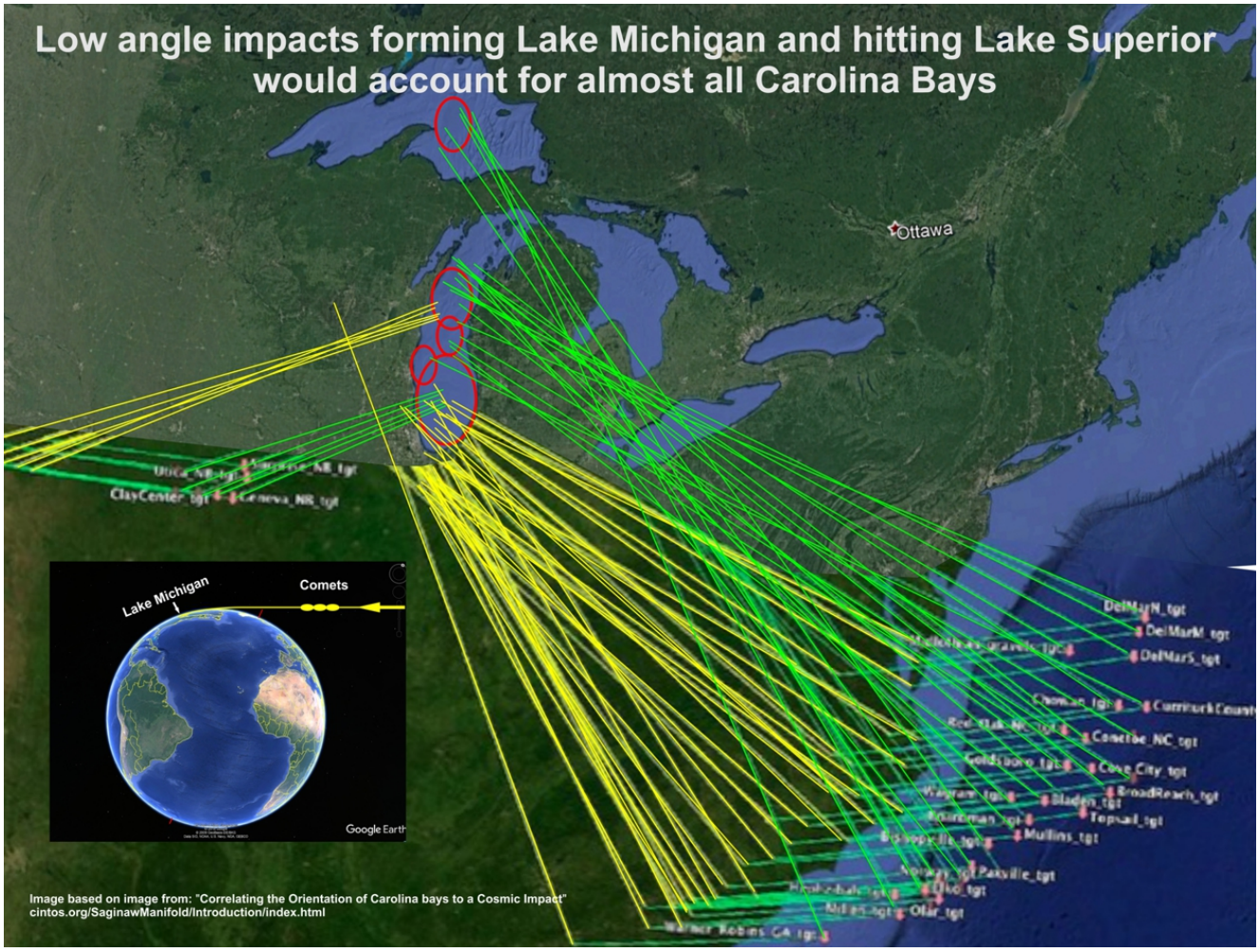

©2020. Japan Geoscience Union. All Right Reserved.

[J] Poster | P (Space and Planetary Sciences)：P-PS Planetary Sciences

[P-PS10] Formation and evolution of planetary materials in the Solar System

convener:Wataru Fujiya(Ibaraki University, College of Science), Megumi Matsumoto(Graduate School of Science, Tohoku University), Shin Ozawa(Department of Earth Science, Graduate School of Science, Tohoku University), Yuki Hibiya(Submarine Resources Research Center, Japan Agency for Marine-Earth Science and Technology)

In this session, we will discuss the material evolution in the Solar System based on extraterrestrial sample analyses and experimental works. We will look over recent knowledge from primitive materials such as chondrites, interplanetary dust particles, and returned samples by space missions. Research works on meteorite parent body processes such as aqueous alteration, thermal metamorphism, shock metamorphism, volcanic activity, and core-mantle-crust differentiation will also be discussed. The topics of this session include experimental studies which, together with meteorite studies, help us to understand the material formation/evolution in the Solar System as well as processes on meteorite parent bodies. Presentations on new innovative analytical and theoretical techniques in various research fields are highly welcome to submit for future studies of the Solar System evolution.

[PPS10-P01] Quantitative shock stage evaluation of chondrites from X-ray diffraction: A new method

*Naoya Imae[1,2], Makoto Kimura[1] (1.Antarctic Meteorite Research Center, National Institute of Polar Research, 2.SOKENDAI)

[PPS10-P02] Synthesis of Mn-, Cr-bearing calcite, dolomite, and magnesite for Mn-Cr dating of carbonates

*Shingo Sugawara[1], Wataru Fujiya[1] (1.Ibaraki University)

[PPS10-P04] Aqueous interaction between olivine and organic compounds to imply spatial distribution of organics in meteorites

*Keisuke Muneishi[1], Hiroshi Naraoka[1] (1.Kyushu University)

[PPS10-P05] Formation process of a unique hydrous micrometeorite with abundant Fe-rich saponite and Fe sulfide

Shota Shimizu[1], Sakiko Kikuchi[2], *Tomoki Nakamura[1], Megumi Matsumoto[1], Takazo Shibuya[2], Cecile Engrand[3], Jean Duprat[3] (1.Department of Earth and Planetary Materials Sciences, Faculty of Science, Tohoku University, 2.JAMSTEC, 3.CSNSM, Université Paris-Sud)

[PPS10-P06] Microtexutural observations of TCIs in five CM carbonaceous chondrites and implications to aqueous environments on CM parent bodies.

Akane Iemoto[1], *Yusuke Seto[1], Akira Miyake[2] (1.Graduate School of Science, Kobe University, 2.Graduate School of Science, Kyoto University)

[PPS10-P07] Spectral measurements of carbonaceous chondrite in the extreme ultraviolet range

*Hiromasa Akadama[1], Kazuo Yoshioka[1], Takashi Mikouchi[1] (1.University of Tokyo)

[PPS10-P08] Elemental, isotopic, and structural analyses of insoluble organic matter from in Jbilet Winselwan carbonaceous chondrite

*Kanami Kamide[1], Hikaru Yabuta[1], Minoru Ikehara[2] (1.Hiroshima University, 2.Kochi University)

[PPS10-P09] **Synchrotron radiation-based X-ray computed nanotomography of unheated and experimentally heated Murchison CM chondrite**

*Megumi Matsumoto[1], Akira Tsuchiyama[2,3], Masahiro Yasutake[4], Akira Miyake[5], Kentaro Uesugi[4], Akihisa Takeuchi[4], Tsukasa Nakano[6], Tomoki Nakamura[1] (1.Graduate School of Science, Tohoku University,

2.Research Organization of Science and Technology, Ritsumeikan University, 3.Guangzhou Institute of Geochemistry, Chinese Academy of Sciences, 4.Japan Synchrotron Radiation Research Institute, 5.Graduate School of Science, Kyoto University, 6.Geological Survey of Japan, National Institute of Advanced Industrial Science and Technology)

[PPS10-P10] Fine-grained dark inclusion with very small chondrules in the NWA 1723 L chondrite

*Miki Takahashi[1], Tomoki Nakamura[1], Michael Zolensky[2] (1.Tohoku University, 2.NASA/JSC)

[PPS10-P11] Phosphate and phosphide in mesosiderites

*naoji sugiura[1], tomoko Arai[1], Matsui Takanori[1] (1.Chiba Institute of Technology)

[PPS10-P12] Multiple sulfur isotopic composition of mesosiderite meteorites: Implication for formation processes

*Shun Mihira[1], Akira Yamaguchi[2], Madhusoodhan Satish-Kumar[1] (1.Niigata University, 2.National Institute of Polar Research)

[PPS10-P13] Aqueous alteration in the nakhlites Y 000802

Ayaka Nakamura[1], *Masaaki Miyahara[1], Hiroki Suga[2], Akira Yamaguchi[3], Daisuke Wakabayashi[4], Shohei Yamashita[4], Yasuo Takeichi[4], Yoshio Takahashi[2], Eiji Ohtani[5] (1.Department of Earth and Planetary Systems Science, Graduate School of Science, Hiroshima University, 2.Department of Earth and Planetary, Graduate School of Science, The University of Tokyo, 3.National Institute of Polar Research, 4.Institute of Materials Structure Science, High-Energy Accelerator Research Organization, 5.Department of Earth Sciences, Graduate School of Science, Tohoku University)

Quantitative shock stage evaluation of chondrites from X-ray diffraction: A new method

*Naoya Imae[1,2], Makoto Kimura[1]

1. Antarctic Meteorite Research Center, National Institute of Polar Research, 2. SOKENDAI

1. Introduction

Stöffler et al. (1991) have established the shock stage classification of ordinary chondrites by the global textural observations and the shock recovery experimental results, which is defined to be S1 to S6. A further consideration, a quantitative analytical technique of shock effects on ordinary chondrites, is still much in concern. The mean lattice strain in main constituent minerals (olivine and orthoenstatite) is one of the primary parameters quantitatively for evaluating the shock history of the stony meteorites (e.g., Uchizono et al., 1999; Imae 2019). However, this was not enough since the shock effect also appears as mechanical destruction of grains, and this may be reflected in the decrease of the crystallite sizes. In the present study, the X-ray diffraction of L6 ordinary chondrites with a single lithology (the shock stage = S1-S5) were obtained from the in-plane rotation method of the polished thin sections (PTSs). Then the obtained diffraction was successfully analyzed, focusing on the mean lattice strains and crystallite sizes of olivines and orthoenstatites. The new analytical technique would generally be suitable for the quantitative shock classification of stony meteorites.

2. Experiments

Using X-ray diffractometer (SmartLab, Rigaku), PTSs for 14 L6 chondrites (9 Antarctic and five non-Antarctic meteorites) were measured on the conditions of the scanned twofold Bragg angle in the range of 3-75º and the length limiting slit of 5 mm with the divergence angle of (1/6)º. The sample stage was rotated with a rate of 100 rpm during the measurements. Focused Bragg indices were 130, 211, 222, and 322 for olivines, and 610, 511, 421, 631, and 12 12 for orthoenstatites, since their indices are almost isolated peak.

3. Results and Discussion

The Williamson-Hall plot (Williamson and Hall, 1953) is given by tangent of the Bragg angle of the focused indices as the horizontal axis and the integral breadths (in the range of more than zero and much less than one degree) as the vertical axis. The plots for olivines and orthoenstatites of the measured samples showed good correlation factors >˜0.8-0.9 except for several. The mean lattice strain is obtained from the slope, and the crystallite size is from the reciprocal of the cross-section with the vertical axis. Then the mean lattice strains were in the range of 0.05 (S1) -0.25% (S6) for olivines, and those in 0.1 (S1) -0.4% (S5) for orthoenstatites. The crystallite sizes are sub-μm, decreasing from S1 to S6. Then the shock stage parameter is newly defined to be [strain /log (integral breadth at horizontal axis zero)]. The shock stage parameters for olivines and orthoenstatites are correlated with the shock stage by Stöffler et al. (1991).

4. Summary

The new shock stage parameter combing lattice strains with crystallite sizes is useful clearly for estimating the shock stage of stony meteorites.

5. References

Imae N. 2019. 10th Polar Science Symposium (abstract).
Stöffler D. et al. 1991. Geochim. Cosmochim. Acta 55, 3845.

©2020. Japan Geoscience Union. All Right Reserved.

Uchizono A. et al. 1999. Min. J. 21, 15.
Williamson G. K. and Hall W. H. 1953. Acta Metallurgica 1, 22.

Keywords: shock metamorphism of chondrites, mean lattice strains, crystallite size, olivine, orthoenstatite, X-ray diffraction

©2020. Japan Geoscience Union. All Right Reserved.

Synthesis of Mn-, Cr-bearing calcite, dolomite, and magnesite for Mn-Cr dating of carbonates

*Shingo Sugawara[1], Wataru Fujiya[1]

1. Ibaraki University

Carbonate minerals are often observed in CI, CM, and CR chondrites. Carbonate minerals formed by aqueous alteration on asteroids and are important materials because their formation ages can be measured by ^{53}Mn-^{53}Cr dating (half-life: 3.7 Ma) (e.g., Fujiya et al., 2012).
Secondary Ion Mass Spectrometry (SIMS) is normally used for Mn-Cr dating of carbonates. In SIMS analyses, measurements of a standard material with the same crystal structure and chemical composition as carbonates are necessary because of the matrix effect. Sugiura et al. (2010) synthesized Mn- and Cr-bearing calcite ($CaCO_3$) in aqueous solution because natural carbonate minerals do not incorporate Cr. However, quantitative analysis of Mn and Cr is difficult because precipitation in aqueous solution results in zoning of Mn and Cr concentrations during crystallization. In this study, we try to synthesize calcite, dolomite, and magnesite containing Mn and Cr homogeneously.

Incompatible elements for calcite may be incorporated into amorphous calcium carbonate (ACC). ACC crystalizes to calcite at high pressure or temperature, where large amounts of incompatible elements such as Sr, U, and Pb can homogeneously be distributed (Matsunuma et al., 2014; Miyajima et al., 2019). In this study, we applied this method to Mn and Cr. We mixed cold 0.1M Na_2CO_3 and 0.1M (Ca, Mn, Cr) Cl_2 aqueous solutions to produce ACC. The ACC was subsequently separated by vacuum-filtration, and was dried in a vacuum desiccator for one day. The ACC crystallized to calcite by heating under IW-buffer at 400 ℃ for two hours. The material before and after heating were confirmed as ACC and calcite, respectively, by using powder X-ray diffraction (XRD). Then, the calcite was embedded in resin and its surface was polished. We conducted semi-quantitative analysis of Mn and Cr by using SEM-EDS. Manganese and Cr were homogeneously incorporated into the calcite grains with Mn/Ca and Cr/Ca ratios of 1.47 ±0.09 and 0.96 ±0.07 (2 σ), respectively.
Next, we produced amorphous carbonates with Ca/Mg ratios of ~1 and 0 using the same method as the Mn-, Cr-bearing calcite. However, these did not crystallize to dolomite and magnesite by heating. Then, we tried to produce dolomite and magnesite via hydrothermal synthesis. We put an aqueous solution with amorphous carbonate in autoclave and heated it at 200℃ for three days. Dolomite and magnesite were successfully synthesized, and in the future, we will try to dope Mn and Cr into the synthesized dolomite and magnesite.

Keywords: amorphous calcium carbonate, standard, Mn-Cr dating

©2020. Japan Geoscience Union. All Right Reserved.

Aqueous interaction between olivine and organic compounds to imply spatial distribution of organics in meteorites

*Keisuke Muneishi[1], Hiroshi Naraoka[1]

1. Kyushu University

Introduction

Carbonaceous meteorite is relatively enriched in volatile materials including water and organic matter, recording the chemical evolution of organic compounds in the primordial solar system. The organic compounds could be absorbed on and/or intercalated in clay minerals formed from anhydrous silicates during aqueous alteration in a meteorite parent body. However, it is not well understood how organic compounds interacted with anhydrous silicates during the alteration. The spatial distribution of alkylimidazole ($C_nH_{2n-2}N_2$) and alkylpyridine ($C_nH_{2n-5}N$) was distinct in the Murray meteorite (CM2) depending on their species and homologues (Naraoka & Hashiguchi, 2018). The result may infer aqueous interaction between mineral and organic compounds in the meteorite parent body. In this study, we examined interactions between the CHN compounds and olivine, which is one of the major anhydrous silicates in chondritic meteorites.

Materials and Methods

The powder of San Carlos olivine (particle size; ~μm to ~hundred μm) was packed in a stainless-steel tube (1.7 mm i.d. ×5.0 cm in length) to prepare a column for liquid chromatography. A mixed standard solution of four CHN compounds; i) imidazole, ii) 2-methylimidazole, iii) 2-methylpyridine, and iv) 3-methylpyridine was injected into the column connected to a mass spectrometer. The interaction between the organic compounds and olivine was evaluated by comparing their retention times. The same chromatography without olivine powder was also examined as a reference. The following three experiments (Exp. 1 to 3) were performed depending on pH and temperature. Exp.1: Neutral eluent conditions (H_2O) at 40˚C. Exp. 2: Effect of eluent pH using CH_3COONH_4 buffer (pH 8.95), NH_3aq (pH 10.57), and formic acid solution (pH 2.57) at 40˚C. Exp. 3: Effect of temperatures; H_2O eluent at 20˚C and 30˚C, CH_3COONH_4 buffer (pH8.92) and NH_3aq (pH10.35) at 20˚C.

Results and Discussion

Exp. 1: The four compounds had an identical retention time in the absence of olivine powder. In contrast, the retention times by the olivine column ranged in the order; iii) 2-methylpyridine ~ iv) 3-methylpyridine < i) imidazole < ii) 2-methylimidazole. This order is correlated with the acid dissociation constant (p*K*a) of each compound, suggesting that the CHN compounds are present as cations (e.g. $C_3H_5N_2^+$ for imidazole) interacting more strongly with the oxyanions of silicic acid in olivine.

Exp. 2: Under alkaline conditions, the retention times of all compounds decreased with the increase of pH. This is probably because the cation strength of the CHN compounds became weaker by decreasing the amount of protons in the eluent. Under acidic conditions, the retention times of imidazoles were shorter and those of methylpyridines were longer. The mechanism of this phenomenon is under consideration.

Exp. 3: Under neutral conditions, the retention times of all compounds increased with the decrease of the temperature (i.e. 20˚C > 30˚C > 40˚C). The compounds retained longer in the column at 40˚C showed larger increase in retention times than those shorter retained at lower temperature. Under alkaline conditions, the retention times did not change significantly with the decrease of temperatures probably due to the weak strength of ionic bonds even at lower temperature. The results indicate that the CHN

©2020. Japan Geoscience Union. All Right Reserved.

compounds have a stronger ionic association with olivine under neutral conditions because it is difficult for the ions on the surface of olivine to transfer into the mobile phase at lower temperatures.
These observations suggest that olivine of the carbonaceous meteorites could affect the interaction between organic matter and water and might have influenced the spatial distribution of organic compounds on the meteorite parent bodies.

Keywords: Carbonaceous meteorite, Olivine, Organic compounds, Aqueous alteration, Ionic interactions

©2020. Japan Geoscience Union. All Right Reserved.

Formation process of a unique hydrous micrometeorite with abundant Fe-rich saponite and Fe sulfide

Shota Shimizu[1], Sakiko Kikuchi[2], *Tomoki Nakamura[1], Megumi Matsumoto[1], Takazo Shibuya[2], Cecile Engrand[3], Jean Duprat[3]

1. Department of Earth and Planetary Materials Sciences, Faculty of Science, Tohoku University, 2. JAMSTEC, 3. CSNSM, Université Paris-Sud

The Antarctic micrometeorites (AMMs) collected from recent snow are almost free of terrestrial alteration and heavy impacts upon collection and therefore are the best dust samples that coming from outer asteroids and comets [1]. We have collected AMMs from filters that gathered dust particles in the snow recovered by CSNSM with support from IPEV. Among the AMMs we identified, detailed analysis was done for one AMM SSP4E5 for its mineralogy and chemistry. SSP4E was first analyzed by synchrotron-XRD at KEK, Japan. Ultrathin sections were prepared by ultramicrotomy and the sections are observed by FE-TEM/EDS and the remaining putted butt was observed by FE-SEM/EDS and FE-EPMA.

SSP4E5 is a fine-grained, unmelted carbonaceous chondrite-like AMM with 80 μm in diameter. Synchrotron XRD analysis of SSP4E5 indicates that strong diffractions from pyrrhotite and saponite are detected and no other diffractions such as serpentine, carbonates, and anhydrous silicates are not detected, suggesting that pyrrhotite and saponite are dominant phases. Observation of the cross section showed that pyrrhotite abundantly occurs and distributes entirely in this sample as aggregates (grain size ~1 μm), isolated grains (~10 μm) and numerous submicron particles. Submicron particles are arranged along the outline edge of voids. Average composition of the entire cross section indicates that sulfur is enriched and concentration is 3 times higher than solar abundance.

Saponite in SSP4E5 has Fe-rich chemical composition and an average Fe:Mg ratio was estimated as 55:45, which is higher than saponite in any carbonaceous chondrites reported so far (e. g., 2 for Tagish Lake). The relative mineral abundance is 45wt% of pyrrhotite, 49wt% of saponite, and other ~5% amorphous phases of rich in SiO_2. The mineral assemblage and chemical composition imply that SSP4E5 has experienced aqueous alteration in the unique conditions. We explored thermodynamically the condition of the alteration that reproduces the relative mineral abundance and the saponite composition.

We examined aqueous alteration at various water/rock weight ratios (0.1-100) and temperatures (25, 100, 200, and 350℃). The fluid is supposed to be composed mainly of H_2O and small amounts of H_2S (0.5 and 1.5 mol %: 0.5 mol% of H_2S is comet value [3]). We assumed that half of S originally exists as FeS in the rock and the rest half is supplied by H_2S in the water. The results of the calculations indicate that the relative mineral abundance and the saponite composition of SSP4E5 are reproduced well by the alteration at temperatures higher than 200℃ with water/rock ratios higher than 7 (in case of 0.5 mol% of H_2S in the solution) and 2.5 (in case of 1.5 mol% of H_2S in the solution). Therefore, the calculation envisions that SSP4E5 was likely to have been produced by high temperature aqueous alteration at a location where water and FeS are abundant. This is consistent with observation. The absence of anhydrous minerals such as olivine in SSP4E5, which suggests pervasive aqueous alteration at high temperature. The presence of small pyrrhotite around rims of pore spaces, which suggests pyrrhotite precipitation from a fluid that filled pore spaces where local high water-rock ratios were attained. Our results imply that high-temperature aqueous alteration caused local concentrations of Fe-rich saponite and pyrrhotite in the primitive small body formed in the early solar system.

©2020. Japan Geoscience Union. All Right Reserved.

References [1] Duprat et al. (2007) Adv. Space Res. 39, 605-611. [2] Nakamura et al. (2003) EPSL 207, 83-101. [3] Mumma and Charnley (2011) Annu. Rev. Astron. Astrophys.49, 471–524.

Keywords: Micrometeorites, Aqueous alteration

©2020. Japan Geoscience Union. All Right Reserved.

Microtexutural observations of TCIs in five CM carbonaceous chondrites and implications to aqueous environments on CM parent bodies.

Akane Iemoto[1], *Yusuke Seto[1], Akira Miyake[2]

1. Graduate School of Science, Kobe University, 2. Graduate School of Science, Kyoto University

Introduction: CM chondrites are aqueously altered meteorites which contain around 10 wt% H2O in hydrous minerals. TCIs, fine intergrowths of tochilinite (6(Fe0.9S)・5[(Mg,Fe)(OH)2]) and cronstedtite (Fe-bearing serpentine), are one of the characteristic products of CM parent body aqueous alteration. TCIs are considered to be divided into two types based on the textural feature. Type I TCIs are generally found in the chondrules and believed to be altered from iron metal because they often contain kamacite inside [e.g., 1]. Type-II TCIs are found within the matrices. Although several formation processes of type-II have been proposed [e.g., 2,3], the argument has not yet been settled. TCIs potentially provide important information regarding aqueous environments on chondrite parent bodies. Here, we report microtextures of type-II TCIs in five CM chondrites and discuss the formation processes.

Materials and methods: We observed the following five CM chondrites; Cold Bokkeveld (2.2), Nogoya (2.2) , Murray (2.4-2.5), Murchison (2.5) , QUE 97990 (2.6). The numbers in parenthesis are the alteration index for CM chondrites proposed by Rubin et al. (2007) [4], in which the index is defined ranging from 2.6 (less altered) to 2.0 (highly altered). Textural observation and chemical analyses were performed using an SEM-EDS (JEOL, JSM-6480LAII), and nanometer-scale observations using an STEM-EDS (JEOL, JEM-2100F) after processing into thin films using an FIB (FEI, Quanta 3DS).

Results and discussion: In the less altered CM chondrites (QUE 97990 and Murchison), their type-II TCIs showed a similar texture. They are widely distributed in the matrices as compact aggregates of a few hundred nm-sized tochilinite and cronstedtite. From the TEM observations, thin veins of tochilinite were developed inside cracks or cleavages of cronstedtite, suggesting that tochilinite had been crystallized after the formation of cronstedtite. In contrast, the TCIs in Cold Bokkeveld (highly altered) showed core-rim structure. The core region is often rich in mixed layer phase (MLP; alternately stacked phase of tochilinite/cronstedtite layer in nanometer scale), and the rim mainly consists of coarse-grained tochilinite and cronstedtite, which resembles those of the less altered meteorites. Another highly altered meteorite Nogoya (2.2) also has TCIs with zonal texture, where very fine (several tens of nm) and fluffy serpentine rich material is located around core, and toward rim, gradually changed to fibrous cronstedtite and MLP. Murray, intermediately altered CM, has both type of TCIs seen in less and highly altered ones as noted above, indicating Murray was at an intermediate stage during the course of TCIs formation. All observed type-II TCIs in the present study do not include any precursor minerals such as anhydrous silicates or iron metal. TCIs of the two highly altered CM chondrites (Cold Bokkeveld and Nogoya) showed fluffy texture at their core region. These results probably suggest that fluffy type-II TCIs were not formed directly from solid material (like type-I), but crystallized under mobile environments such as water solution. In the case, changes of the fluid condition during the TCI formation resulted in the zonal texture as seen in the highly altered meteorites. The fact that the TCIs in QUE 97990 and Murchison resembles the coarse-grained rim of those in Cold Bokkeveld indicates the two less altered meteorites had experienced aqueous alteration similar to the last stage of aqueous alteration that Cold Bokkeveld had experienced.

©2020. Japan Geoscience Union. All Right Reserved.

References: [1] Tomeoka and Buseck. (1985) Geochimica et Cosmochimica Acta 49:2149–2163. [2] Pignatelli. et al. (2016) Meteoritics & Planetary Science 51:785-805. [3] Lee et al. (2013) Geochimica et Cosmochimica Acta 121:452-466. [4] Rubin et al. (2007) Geochimica et Cosmochimica Acta 71:2361-2382.

Keywords: Carbonaceous chondrite, Aqueous alteration, Tochilinite

©2020. Japan Geoscience Union. All Right Reserved.

Spectral measurements of carbonaceous chondrite in the extreme ultraviolet range

*Hiromasa Akadama[1], Kazuo Yoshioka[1], Takashi Mikouchi[1]

1. University of Tokyo

Spectroscopic observations have been done in many space exploration missions for the purpose of revealing physical quantities and material compositions of the objects. In particular, overviewing past missions focusing on the surface environment of solid planets, the infrared (IR) and visible have been commonly used. On the other hand, in recent years, there are some missions doing spectroscopic observations in the ultraviolet (UV) region, such as MESSENGER, MAVEN, and DAWN. One of the reasons that these missions select UV is that this band represents the features of the state of molecular electronic transition. These features are impossible to identify through IR or visible. The state of molecular electronic transition changes over time due to exposure to cosmic rays and solar radiation. This effect is called “space weathering” and its quantitative assessment links the current features obtained from observations with the past appearance of the substance. For example, it is known that spectra of hydrocarbons redden by the cutting of C-H bond due to space weathering.

To discuss the physical and chemical state of the celestial body from the spectra obtained from the spectroscopic observations, it is necessary to measure the spectra of the samples to be compared in the laboratory. The carbonaceous materials that we focused on in this study can be materials for life, and their state is of great scientific significance. As a general trend, these materials have a low reflectivity not only in the UV but also in a wide wavelength range, which makes it difficult to measure them. However, in the near ultraviolet (NUV) range (200nm$< \lambda <$380nm), the spectra of carbonaceous samples such as graphite and coal are already measured “Applin et al., (2018)”. On the other hand, in the extreme ultraviolet (EUV) range ($\lambda <$150nm), the reflectivity is even lower than that of NUV and the types of light sources that can be used are limited, so that a measurement method has not yet been established.

We established the method to measure the reflection spectrum of carbonaceous chondrite using a high-frequency excited gas flow lamp that can also give off EUV light, instead of a deuterium lamp that has been widely used as an UV light source. In this presentation, we will introduce the details of the reflectance measurement method and the spectrum of the Allende meteorite taken through the system.

Keywords: carbonaceous chondrite, extreme ultraviolet, space weathering

©2020. Japan Geoscience Union. All Right Reserved.

Elemental, isotopic, and structural analyses of insoluble organic matter from in Jbilet Winselwan carbonaceous chondrite

*Kanami Kamide[1], Hikaru Yabuta[1], Minoru Ikehara[2]

1. Hiroshima University, 2. Kochi University

Introduction: Complex organic macromolecules in meteorites were resulted from the chemical evolution of organic molecules from interstellar clouds to protoplanetary disks and planetesimals in the early Solar System (Ehrenfreund and Charnley‚ 2000). Insoluble organic macromolecule (IOM) accounts for a major portion of organic carbon in carbonaceous chondritic meteorites (Glavin et al. 2018). It has been known that IOM sensitively records chemical history of meteorite parent body processes (Alexander et al. 2007). To date‚ graphitization degrees of IOM have been often used to evaluate long duration heating events of petrologic type 3 chondrite parent bodies (e.g.‚ Busemann et al. 2007; Cody et al. 2008). However‚ relationship between chemical variations of IOM and short duration heating events of types 1 and 2 carbonaceous chondrites have not been systematically understood. Therefore‚ we investigated the elemental and isotopic compositions‚ and chemical structures of IOM from thermal metamorphosed CM chondrite‚ Jbilet Winselwan meteorite (King et al 2019). The chemical compositions of this meteorite were compared with those from primitive CM2 chondrites and thermal metamorphosed CV3 chondrite.

Samples and methods: Four kinds of carbonaceous chondrites‚ Jbilet Winselwan (CM2)‚ Murray (CM2)‚ Murchison (CM2)‚ Allende (CV3) meteorites‚ were used in this study. IOM were purified from each meteorite powder by HCl⁄HF and⁄or CsF⁄HF treatment. The IOM samples were analyzed by a Flash elemental analyzer (EA) 1112 (Thermo Fisher Scientific‚ The Center for Advance Marine Core Research)‚ a FlashEA 1112 linked to a Delta Plus Advantage mass spectrometer (Thermo Fisher Scientific‚ The Center for Advance Marine Core Research)‚ and a micro-Raman spectroscopy (T64000‚ Horiba-JY‚ Hiroshima University).

Results and discussion: Elemental and isotopic analyses of IOM from Jbilet Winselwan meteorite estimated H⁄C atomic ratio of 0.405±0.039‚ N⁄C atomic ratio of 0.0368± 0.0018‚ and δ^{13}C of -10.408±0.486‰. Comparing with the data by Alexander et al (2007)‚ Jbilet Winselwan meteorite showed clearly different compositions from those of primitive CM chondrites and thermally metamorphosed CV chondrites. On the other hand‚ the values were plotted in a similar range of those from some of the thermal metamorphosed CM chondrites (Yamato 793321‚PCA91008‚WIS91600) and ungrouped C2 Tagish Lake chondrite. In particular‚ the compositions of Jbilet Winselwan were comparable with those of WIS 91600 meteorite. Thus‚ it is likely that the two meteorite parent bodies experienced a similar thermal history. It has been discussed that WIS 91600 meteorite experienced a moderate heating at 400 - 500 ℃ after an episode of aqueous alteration under conditions that were similar to those experienced by Tagish Lake meteorite (Yabuta et al. 2010). Despite different H⁄C ratios‚ Raman spectra of IOM from the Jbilet Winselwan were similar to those from Murchison‚ and Murray meteorites but Allende meteorite‚ indicating that IOM of Jbilet Winselwan meteorite is as disordered as those of primitive chondrites. However‚ the values of Raman D- and G-band widths for Jbilet Winselwan IOM were deviated from a linear relationship of these parameters between Murchison and Murray IOMs and Allende IOM‚ which is reflected by graphitization of IOM during long duration heating (Busemann et al.

©2020. Japan Geoscience Union. All Right Reserved.

2007). Thus‚ aromatic condensation of IOM does not efficiently during the short duration heating.

Keywords: Carbonaceous chondrite, Insoluble organic matter

©2020. Japan Geoscience Union. All Right Reserved.

Synchrotron radiation-based X-ray computed nanotomography of unheated and experimentally heated Murchison CM chondrite

*Megumi Matsumoto[1], Akira Tsuchiyama[2,3], Masahiro Yasutake[4], Akira Miyake[5], Kentaro Uesugi[4], Akihisa Takeuchi[4], Tsukasa Nakano[6], Tomoki Nakamura[1]

1. Graduate School of Science, Tohoku University, 2. Research Organization of Science and Technology, Ritsumeikan University, 3. Guangzhou Institute of Geochemistry, Chinese Academy of Sciences, 4. Japan Synchrotron Radiation Research Institute, 5. Graduate School of Science, Kyoto University, 6. Geological Survey of Japan, National Institute of Advanced Industrial Science and Technology

Hayabusa2 mission succeeded to touchdown on the surface of C-type asteroid 162173 Ryugu and will bring Ryugu surface material to the earth. Spectroscopic observation shows that Ryugu surface is dark and exhibits a small 2.7 μm absorption band suggesting a presence of phyllosilicates [1-3]. The spectroscopic feature is similar to partially dehydrated carbonaceous chondrites. This means that heated hydrous carbonaceous chondrites are the closest analogues to Ryugu surface material. In this study, we obtained three-dimensional (3D) microstructures of unheated, 400℃-, and 600℃-experimentally heated Murchison CM chondrite matrix [4] using a synchrotron radiation-based X-ray computed nanotomography (SR-XCT) at SPring-8 BL47XU.

Two ~50 μm particles for each of the unheated, 400℃-, and 600℃-heated Murchison chondrite matrix were mounted on C-fibers or Ti-needles and analyzed by the SR-XCT using two methods: dual energy tomography (DET) and scanning imaging X-ray microtomography (SIXM) [5, 6]. In the DET, we obtained 3D images with X-ray linear attenuation coefficients (LACs) at 7 and 7.35 keV; one above and one below the K-absorption edge energy of iron. The images at 7 keV correspond closely to compositional (Z) contrast, and those at 7.35 keV strongly depend on Fe content and emphasize Fe-rich materials. In the SIXM, we obtained 3D images with X-ray phase contrast reflecting refractive index decrements (RIDs). RID is simply the difference between the refractive index and unity and is almost proportional to material density. We performed image matching at common voxel size (60.4 nm) and sample direction on the three kinds of CT images. The well-matched CT image sets give us both LAC and RID values for specific voxels. This enables us to obtain 3D distribution of specific phases in micro-samples. We also made 2D histogram plots of LAC and RID values for each sample to obtain bulk mineralogies. Besides the XCT, we performed X-ray diffraction (XRD) analysis on the particles mounted on C-fibers at KEK-PF BL3A.

The 3D imaging revealed that the unheated Murchison samples mainly consist of a few micron-sized forsterite, enstatite, and nano-sized Fe-Ni sulfides embedded in matrix. The matrix is divided into Fe-rich and Fe-poor regions. Considering the XRD results, the former and the latter consist mainly of tochilinite-cronstedtite intergrowth and Mg-rich serpentine, respectively. The volume proportion of the two components varies in samples. In 2D histogram plots of LAC and RID values, the two components form one broad sum peak around the serpentine-cronstedtite line. The peak top located in Mg-rich side (close to serpentine point). The 400℃ samples are texturally similar to the unheated ones. In 2D histogram plots, Fe-poor matrix forms a broad peak similar to that of the unheated samples while Fe-rich matrix forms another peak close to cronstedtite point. The difference should reflect mineralogical changes due to heating that were confirmed by XRD: decomposition of serpentine and tochilinite and formation of unknown phase(s). The 600℃ samples are texturally homogeneous compared to the unheated and the 400℃ samples and contain small amounts of nano-sized secondary Fe-rich metal grains. In 2D histogram plots, the homogenized matrix forms a broad peak at the intermediate point of the two peaks found for

©2020. Japan Geoscience Union. All Right Reserved.

the 400℃ samples. It is noted that the XRD results suggest the presence of secondary olivine that should be contained in the homogenized matrix.

These suggest that the SR-XCT technique is useful to estimate heating degrees of hydrous carbonaceous chondrites and Ryugu sample. We will perform further microscopic analysis to uncover microtextural changes due to heating.

[1] Watanabe et al. (2019) *Science* **364**. [2] Sugita et al. (2019) *Science* **364**. [3] Kitazato et al. (2019) *Science* **364**. [4] Mogi et al. (2017) *The 80th Annual Meeting of the Meteoritical Society*, Abstract #6225. [5] Tsuchiyama et al. (2013) *GCA* **116**. [6] Takeuchi et al. (2013) *JSR* **20**.

Keywords: CM carbonaceous chondrite, SR-XCT, SR-XRD, Hayabusa2

©2020. Japan Geoscience Union. All Right Reserved.

Fine-grained dark inclusion with very small chondrules in the NWA 1723 L chondrite

*Miki Takahashi[1], Tomoki Nakamura[1], Michael Zolensky[2]

1. Tohoku University, 2. NASA/JSC

Dark inclusions are rock fragments with low visible reflectance which have mineralogical and petrological features different from the host meteorites. Some dark inclusions show unique petrographic properties, and they may contain material information never found in meteorites. In this study, we conducted a petrographic study of a dark inclusion in the NWA 1723 L chondrite and found that the inclusion has petrological features that have never been found in any meteorite types.

The dark inclusion consists mainly of fine-grained (mostly < 5 μm) olivine ($Fa_{23.3\pm0.4}$), low-Ca pyroxene ($Fs_{2.6\text{-}22.2}$, $Wo_{0\text{-}49.4}$) and albite ($Ab_{81.8\text{-}99.9}$) with minor amounts of Fe sulfides and taenite. Olivine compositions are similar to the host rock ($Fa_{22.9\pm2.4}$). On the other hand, the pyroxene composition is different from the host rock ($Fs_{13.4\text{-}32.6}$, $Wo_{0.3\text{-}5.2}$). The relative abundance of olivine and low-Ca pyroxene is approximately 2:1. Taenite occurs as tetrataenite with high Al concentration (up to 20wt%): Al shows zoning where Al is concentrated at the center of crystals. Small amounts of phyllosilicates were detected from a part of the matrix by X-ray diffraction analysis, but were not detected from another location in matrix, suggesting that the abundance of phyllosilicates is low in the dark inclusion.

The dark inclusion shows a unique texture where small chondrules (mostly <100 μm) are scattered with a high matrix/chondrule volume ratio (~10). We identified 69 chondrules in the dark inclusion and 57 chondrules are smaller than 100 μm in size. The chondrules are classified to four types (Type A-D) according to mineralogical and petrological features. Type-A chondrules consists of fine-grained olivine (10-20 μm), poikilitic Ca-pyroxene (~200 μm), opaque minerals, and glass. Type-B consists of fine-grained olivine (<10 μm), opaque minerals, and glass. Most of the chondrules are type A and type B (47/69 chondrules). Type C has coarse-grained olivine and metal. Type D consists of coarse-grained opaque minerals and plagioclase. The Ca/Al ratios in the type A, B, and C chondrules are higher than solar abundance, but Na contents are lower. Al content in the glass of chondrules is low. Small opaque inclusions are dispersed in all chondrule types. It is likely that the precursor of type A and B, possibly type C, are common, because they show a similar mineralogy of silicates and opaque minerals, although the relative mineral abundances differ among them. In addition, they seem to have been reheated after formation, based on petrologic evidence.

The dark inclusion consists mainly of fine-grained matrix and contains small amounts and small sizes of chondrules. The petrology indicates that the origin of the dark inclusion is different from the host meteorite, suggesting that the inclusion came from a different parent body. The size of chondrules and the abundance of matrix are different from any hydrous carbonaceous chondrites such as CIs or CMs. The texture is dissimilar not only to host L chondrites, but also to any types of chondrite meteorites (e.g. Brearley and Jones, 1998; Jones 2012). The high matrix abundance suggests that the parent body of the dark inclusion was located far from the sun. The low abundance of phyllosilicates suggests that the parent body formed without water ice or formed late. Many features in the dark inclusion have never been reported in previous studies. Thus, learning the origin of the dark inclusion is important for understanding the evolution of the early solar system.

©2020. Japan Geoscience Union. All Right Reserved.

©2020. Japan Geoscience Union. All Right Reserved.

Phosphate and phosphide in mesosiderites

*naoji sugiura[1], tomoko Arai[1], Matsui Takanori[1]

1. Chiba Institute of Technology

Introduction: Abundant phosphate is a characteristic feature of mesosiderites. It formed by reheating after the mixing of metal with silicates. Hence it reflects the reheating process. Phosphide (schreibersite) is complementary to phosphate, forming from the remaining phosphorous in the metal during cooling from the peak temperature. Hence it also provides information on the reheating event(s). Here we describe phosphate and phosphide in 16 mesosiderites. Note that mineral identification is solely based on the compositions which were obtained by nominal EDS and hence not very accurate.

Observations and interpretation: The most abundant phosphate is merrillite. Stanfieldite (Ca4Mg5(PO4)6) and farringtonite (Mg3(PO4)2) are rather rare, found only in a few mesosiderites. Nearly pure Ca-phosphate (called Ca-merrillite following Xie X. +, 2015, Am. Min., 100, 2753-2756) was found in two type-C mesosiderites. Apatite is very rare; only one grain was found in a Bondoc metal nodule. As for the morphology, the Bondoc nodule contains idiomorphic merrillite which presumably formed from an immiscible melt. The Bondoc nodule also contains irregularly shaped merrillite in the peripheral part of globular inclusions, detached from metal, suggesting formation by partial melting of pre-existing merrillite. Otherwise, merrillite mostly occurs on the surface of metal, suggesting formation at lower temperatures. Two types of schreibersite morphology are observed. One is in direct contact with taenite and another is close to but not in contact with taenite. The latter formed by quick cooling and the former formed by slower cooling. This interpretation is supported by the Ni/Fe ratios. A distinct occurrence of schreibersite is observed in Dong Ujimquin Qi; schreibersite is associated with troilite and kamacite. This mineral assemblage suggests its formation from a eutectic Fe-Ni-S-P melt. The abundance ratios of phosphide to phosphate is controlled by the closure of the phosphate formation reaction and are related to the cooling rate. NWA 2924 and Estherville show high phosphide/phosphate abundance ratios, suggesting that they cooled quickly. Their schreibersite morphology also suggests quick cooling. Na/Ca atomic ratios in merrillite ranges from less than 0.02 to higher than 0.07. The lowest ratio is observed in Dong Ujimquin Qi, which is characterized by high Fe-Ni metal abundance, presence of cordierite and stanfieldite. The exact mechanism to make the low Na/Ca ratio is not clear but a relatively low abundance of plagioclase (hence Na), and a high metal abundance (which produces more merrillite) probably conduced to the low Na/Ca ratio. High Na/Ca ratios are observed in merrillite that formed from (or in contact with) a melt at high temperatures. The high ratios are probably due to Na/Ca partition between phosphate and silicate melt at high temperatures. The stanfieldite in Dong Ujimquin Qi was probably formed at low temperatures under a low Ca-activity. The low Ca-activity is suggested by the presence of cordierite. Farringtonite is always located at the silicate-metal interface, protruding into the metal. This suggests its formation at very low temperatures. Na-free Ca-merrillite in type-C mesosiderites coexists with merrillite with normal Na/Ca ratios. The coexistence of two Ca-bearing phosphates suggests disequilibrium caused by a quick reheating event. We suggest that initially apatite existed which disintegrated by the reheating, resulting in Ca-merrillite. Phosphate is supposed to disintegrate by reheating to high temperatures (Harlow G.E. +, 1982, GCA, 46, 339-348.). But in many mesosiderites that were heated to high temperatures, some phosphate remains without disintegration, suggesting that the reheating event was short. This allows us to recognize multiple reheating events that were experienced by mesosiderites.

©2020. Japan Geoscience Union. All Right Reserved.

Keywords: mesosiderites

©2020. Japan Geoscience Union. All Right Reserved.

Multiple sulfur isotopic composition of mesosiderite meteorites: Implication for formation processes

*Shun Mihira[1], Akira Yamaguchi[2], Madhusoodhan Satish-Kumar[1]

1. Niigata University, 2. National Institute of Polar Research

Mesosiderites and HED (howardite, eucrite, diogenite) meteorites are considered to have a common origin, from the asteroid Vesta. However, the information on processes that led to the origin of mesosiderites and their relation with HED's are not clear yet. In this respect, multiple sulfur isotopic composition may track their petrological relationships and suggest genetic links of mesosiderites with other meteorites. In this study, multiple sulfur isotopic compositions of two mesosiderites (Asuka-882023, Asuka-880154) and one diogenite (Yamato-74013) were obtained. The $d^{34}S$ and $D^{34}S$ relationships of the mesosiderites indicate that they are not match with those of HED meteorites reported in Rai et al. (2005), however, they have some similarities with main group pallasites, a group of stony-iron meteorites (Dottin et al., 2018). This suggests that the variations in sulfur isotopic compositions in mesosiderites might have resulted from metal-silicate fractionation and mixing process and not related to their predecessor. According to Clayton et al. (1996), the $D^{17}O$ value suggested the genetic links with pallasites, IIIAB iron meteorites, and HED. In this study, the values of sulfur isotopes of mesosiderites indicate similar value with IIIAB iron meteorites and pallasites but not similar to HED. This result suggest that the sulfur isotopic composition does not track their parent body but may relate to metal-silicate reaction.
The formation process of mesosiderites is explained by hit-and-run model (Haba et al. 2019). In this study, comparing $D^{33}S$ value of mesosiderites and HED. Mesosiderites and diogenites had experienced similar environment of formation. Also, including to consider about offset of the value of stony-iron meteorites by their metal phase and silicate phase, the material of mesosiderite can be diogenitic silicate and origin of ⅠC, ⅡAB, ⅢAB, and ⅣA iron meteorites or howarditic silicate and origin of IAB or IVB iron meteorites.

Keywords: Mesosiderites, Sulfur isotopes, Meteorite

©2020. Japan Geoscience Union. All Right Reserved.

Aqueous alteration in the nakhlites Y 000802

Ayaka Nakamura[1], *Masaaki Miyahara[1], Hiroki Suga[2], Akira Yamaguchi[3], Daisuke Wakabayashi[4], Shohei Yamashita[4], Yasuo Takeichi[4], Yoshio Takahashi[2], Eiji Ohtani[5]

1. Department of Earth and Planetary Systems Science, Graduate School of Science, Hiroshima University, 2. Department of Earth and Planetary, Graduate School of Science, The University of Tokyo, 3. National Institute of Polar Research, 4. Institute of Materials Structure Science, High-Energy Accelerator Research Organization, 5. Department of Earth Sciences, Graduate School of Science, Tohoku University

Mars rover Curiosity found manganese (Mn) concentrated in the sediments of the Gale crater. Mn can have six kinds of valence: +2 ~ +7. The valence of Mn depends on the pH-Eh conditions of the fluid that precipitated Mn-oxides and -hydroxides. Hence, Mn can become an important clue for clarifying ancient Martian surface conditions. However, few previous works have worked on Mn-oxides and -hydroxides in a Martian meteorite. The Yamato (Y) 000593, 749, and 802 are the members of nakhlites. Previous works reported that many kinds of alteration minerals occur in Y 000593 and 749 (e.g. [1]). In contrast, the alteration minerals in Y 000802 were not investigated so far. Accordingly, we described the alteration minerals in Y 000802, especially focused on the Mn concentrated to clarify the alteration process and condition.

Y 000802 consisted of olivine, clinopyroxene, and mesostasis. The mesostasis consisted of plagioclase, K-feldspar, tridymite, pyrrhotite, phosphate mineral, and titanomagnetite. The alteration texture named iddingsite was distinctive along with the fractures and grain-boundaries of the olivine grains. Laihunite, magnetite, opal, and jarosite occurred in the iddingsite. We found alteration minerals and Mn-concentrated portions in the mesostasis. The alteration occurred in veinlets crossing the mesostasis. Ferroan saponite (+ opal) replaced the plagioclase and K-feldspar grains with maintaining their original crystal habits. Pyrrhotite and phosphate mineral grains showed a dissolution texture. Jarosite, iron oxides, and iron hydroxides also occurred in the veinlets.

There are two different types of Mn-concentrated portions between the feldspar grains replaced with ferroan saponite (+ opal). One of them is an ultra-high-Mn-concentrated portion and the other is a high-Mn-concentrated portion. Mn-concentrated portions accompanied iron. The Mn/Fe atomic ratios of the ultra-high-Mn- and high-Mn-concentration portions are ~3 and ~1, respectively. Mn L-edge XANES spectra showed the existence of Mn^{2+}, Mn^{3+}, and Mn^{4+} in the Mn-concentrated portions. Mn^{3+} along with Mn^{2+} is dominant in the ultra-high-Mn-concentrated portions, whereas Mn^{2+} (and trace Mn^{4+}) is dominant in the high-Mn concentrated portions. The weak peak of O K-edge XANES at 534 eV and C K-edge XANES at 290 eV also appeared in the Mn-concentrated portions, implying the existence of CO_3^{2-}. Based on TEM and STXM analysis, the Mn-concentrated portions consisted of hausmannite ($Mn^{2+}Mn^{3+}{}_2O_4$), and trace amounts of manganite (γ-MnOOH), rhodochrosite ($MnCO_3$), and pyrolusite (MnO_2). The Mn-concentrated portions included trace amounts of sulfur.

We expect that high-temperature fluid (400–700 ˚C) ascending in the nakhlite body induced the alteration from olivine to laihunite (+ opal and iron oxides/hydroxides). Mn ion dissolved from olivine (and probably pyroxene) through the formation of laihunite and precipitated as hausmannite + rhodochrosite assemblage in the mesostasis. Considering the pH-Eh diagram in the C-S-O-H system, the Eh and pH of the fluid that precipitated the assemblage are ~0 and 9.5–11.5, respectively. Simultaneously, plagioclase was replaced with ferroan saponite by the fluid.

©2020. Japan Geoscience Union. All Right Reserved.

Subsequently, an acidic fluid, which is due to the dissolution of pyrrhotite, induced the alteration of the hausmannite + rhodochrosite assemblage, thus leading to form manganite and pyrolusite. SO_4^{2-} and Fe^{2+} released by the dissolution of pyrrhotite and K released from K-feldspar by the acidic fluid precipitated as jarosite. We expect that these alterations occurred mainly on Earth as a terrestrial contaminant because pyrrhotite can dissolve easily.

Reference [1] Shiraishi et al. (2018) Aqueous alteration of Yamato 000749 based on multi-probe microscopic observation. The Ninth Symposium on Polar Science, abstract.

Keywords: Mars, Nakhlites, Aqueous alteration

©2020. Japan Geoscience Union. All Right Reserved.

[J] Poster | P (Space and Planetary Sciences)：P-CG Complex & General

[P-CG26] New Developments of Planetary Sciences with ALMA

convener:Tetsuo Hasegawa(National Astronomical Observatory of Japan, National Institutes of Natural Sciences), Takayuki Muto(Division of Liberal Arts, Kogakuin University), Takahiro IINO(Information Technology Center, the University of Tokyo), Masumi Shimojo(National Astronomical Observatory of Japan)

The Atacama Large Millimeter/Submillimeter Array (ALMA) started its science operation in 2011, and long-baseline observations have been available since 2014. With its high sensitivity and spatial resolution, ALMA has provided us with transformational information on star and planet formation and our Solar System bodies. For example, in the observations of protoplanetary disks, ring-like structures have been commonly found and the structures with the scale of several-AU are discovered in several systems. In our solar system, scientific achievements which utilizing high capability of ALMA such as detections of new molecules on Titan and Pluto and derivation of 3-D structure of the gas giants with continuum observation have been reported. As of Cycle 4, Solar observations have become available, enabling us, for example, to determine the physical parameters of plasmoid quantitatively. In this session, we overview the latest results of ALMA observations in the broad field of planetary sciences. We also accept theoretical and experimental works that are closely related to the observations and discuss the impact on the planetary science community.

[PCG26-P01] Difficulties in planetary formation theories revisited in light of ALMA observations

*Tetsuo Hasegawa[1] (1.National Astronomical Observatory of Japan, National Institutes of Natural Sciences)

[PCG26-P02] Recent progresses of the observational study on planet formation with ALMA and the future prospects including the connection with ngVLA

*Munetake Momose[1] (1.The College of Science, Ibaraki University)

[PCG26-P03] Three-dimensionl Simulations of Head-on/Oblique Collisions of Sintered Dust Aggregates

*Hidekazu Tanaka[1], Satoshi Okuzumi[2], Koji Wada[3] (1.Tohoku University, 2.Tokyo Institute of Technology, 3.Chiba Institute of Technology)

[PCG26-P04] Collisional Growth from dust to Planets and Protoplanetary Disks Observed by ALMA

*Hiroshi Kobayashi[1], Satoshi Ohashi[2] (1.Department of Physics, Nagoya University, 2.RIKEN)

[PCG26-P05] ALMA High Resolution Observations of GW Ori

Jiaqing Bi[2], Ruobing Dong[2], *Takayuki Muto[1] (1.Division of Liberal Arts, Kogakuin University, 2.University of Victoria)

[PCG26-P06] Dust grain growth in asymmetrical protoplanetary disk of V1247 Ori

*Kohki Gotoh[1], Misato Fukagawa[2], Takayuki Muto[3] (1.The university of Tokyo, 2.NAOJ, 3.Kogakuin University)

[PCG26-P07] Structure of Protoplanetary disk around WW Chameleon

*Kazuhiro Kanagawa[1], Jun Hashimoto[2], Takayuki Muto[3] (1.The University of Tokyo, 2.National Astronomical Observatory of Japan, 3.Kogakuin University)

[PCG26-P08] High-resolution ALMA and NIR Imaging of Protoplanetary Disk around T Tauri star

*Mihoko Konishi[1], Jun Hashimoto[2], Takayuki Muto[3] (1.Oita University, 2.Astrobiology Center, 3.Kogakuin University)

[PCG26-P09] Recent advances in the solar system science brought by ALMA observations

*Hideo Sagawa[1], Takahiro IINO[2] (1.Kyoto Sangyo University, 2.The University of Tokyo)

[PCG26-P10] Current status and prospects of solar observations with ALMA

*Masumi Shimojo[1] (1.National Astronomical Observatory of Japan)

Difficulties in planetary formation theories revisited in light of ALMA observations

*Tetsuo Hasegawa[1]

1. National Astronomical Observatory of Japan, National Institutes of Natural Sciences

ALMA has revolutionarized the study of planetary system formation by providing unprecedented images of protoplanetary disks, the sites of planet formation, at the spatial resolution as good as a few au. On the other hand, some basic difficulties have been recognized in the theories of planet formation. In this paper, we review new observational information from ALMA in this context, and examine whether the new observations give clues to the solution of the difficulties such as; 1) dust growth and planetesimal formation (dust infall problem, turbulence in the disk), 2) migration of planets (planet infall problem).

Keywords: protoplanetary disk, ALMA

©2020. Japan Geoscience Union. All Right Reserved.

Recent progresses of the observational study on planet formation with ALMA and the future prospects including the connection with ngVLA

*Munetake Momose[1]

1. The College of Science, Ibaraki University

Observations of protoplanetary disks are essential in understanding the origins of diversity found in the exoplanets. In the last few years, ALMA observations have made significant progress in two directions. First, ALMA observations reveal that ring-gap structure is ubiquitous in the protoplanetary disks. The ALMA Large Program ” DSHARP" detected gaps potentially carved by a planet in ~20 protoplanetary disks. Secondly, ALMA has obtained several hints of a circum-planetary disk, which can be regarded as direct evidence for a forming planet in the protoplanetary disks. Small-scale dust continuum sources, possibly corresponding to circumplanetary disks, were detected around the two T Tauri stars TW Hya and PDS 70. A feature indicative of meridional flows, an accretion flows nearly vertically towards the surface of a circum-planetary disk, may also be detected in the disk around HD163296 by CO observations with ALMA. All these results strongly suggest that planet formation is taking place in the protoplanetary disks, but the parameters for putative planets estimated from the observed ring-gap structure in the disks do not well match the statistics of expolanets. In order to make direct comparisons between exoplanets and gaps in the disks, both the planet search at larger orbital radii and further gap search in the inner disk regions will be required. In this presentation, I also discuss the importance of the next generation Very Large Array (ngVLA) in the studies of exoplanets and planet formation in the future. While ALMA will remain powerful instrument to search for a gap in a low-surface-density regions, ngVLA will explore high-surface-density regions in dust continuum emission at longer wavelengths (3mm-15mm) at higher angular resolution (< 10 milli-arcseconds). These two instruments will be complementary with each other in search for planetary gaps, allowing us to study the formation of a planetary system consisting of more than two planets. The above observed wavelength range of ngVLA also contains molecular lines of large organic molecules and ammonia, the most important building block of N-bearing species such as formamide and glycine. These will be precious probes for protoplanetary disks to enhance synergies with astrobiology and satellite mission for asteroids in our solar-system.

Keywords: Protoplaneary disks, Exoplanets, Radio observations, ALMA, ngVLA

©2020. Japan Geoscience Union. All Right Reserved.

Three-dimensionl Simulations of Head-on/Oblique Collisions of Sintered Dust Aggregates

*Hidekazu Tanaka[1], Satoshi Okuzumi[2], Koji Wada[3]

1. Tohoku University, 2. Tokyo Institute of Technology, 3. Chiba Institute of Technology

The ring structures in protoplanetary disks observed by ALMA can be explained by the effect of sintering on dust aggregates, which causes rebounds of dust aggregates rather than sticking growth. Polarization of protoplanetary disks recently observed by ALMA also indicates that dust aggregates have a rather compact structure. Since such compact structures can be formed through rebounds at their collisions, collisional properties of the sintered dust aggregates are important to examine the origin of compact dust aggregates in planetary disks.
In this study, we investigate the collisional properties of sintered dust aggregates, through 3D numerical simulations. Sirono and Ueno (2017) performed similar simulations for sintered dust aggregates and found that their collisional outcomes depend mainly on the the number of contacts in colliding aggregates (or the coordination number). However, their simulations are limited to head-on collisions of two-dimensional dust aggregates. In this study, on the other hand, we perform 3D simulations, including oblique collisions.
As initial colliding aggregates in our simulations, we use BPCA with the coordination number of 2 and BAM1 with the coordination number of 4. As initial aggregates with intermediate coordination numbers, we also use compressed aggregates obtained from collisions of BPCAs. Our simulations show that sintered dust aggregates with larger coordination numbers are apt to rebound rather than sticking with a higher rate. This result is consistent with Sirono and Ueno (2017). We also find that the rebound is frequent when the coordination number is equal to or larger than 3. Thus we have to clarify the evolution of the coordination number during dust collisional growth. We also discuss such evolution, using our simulation results on the increases in the coordination number.

Keywords: planet formation, protoplanetary disk, sintered dust

©2020. Japan Geoscience Union. All Right Reserved.

Collisional Growth from dust to Planets and Protoplanetary Disks Observed by ALMA

*Hiroshi Kobayashi[1], Satoshi Ohashi[2]

1. Department of Physics, Nagoya University, 2. RIKEN

We carried out a simulation for planet formation from dust to planets directly via collisions. The growth of dust results in a bright ring in a protoplanetary disk, which is called the growth front. The radial profile around the dust front depends on collisional outcomes for mm-sized or larger dust particles. We discuss it using ALMA data.

Keywords: Planet Formation, Protoplanetary disk

©2020. Japan Geoscience Union. All Right Reserved.

ALMA High Resolution Observations of GW Ori

Jiaqing Bi[2], Ruobing Dong[2], *Takayuki Muto[1]

1. Division of Liberal Arts, Kogakuin University, 2. University of Victoria

We report the results of high spatial resolution observations of GW Ori. This is a hierarchical triple system at a distance of ~402 pc. Two of the stars (2.7 Msun and 1.7 Msun) compose a spectroscopic binary with a separation of ~1 AU. A tertiary component (0.9 Msun) was detected by near-infrared interferometry at a projected distance of ~8 AU. The system harbours a circumtriple protoplanetary disk with dust extending to ~400 AU and with gas extending to ~1300 AU. We observe the disk with dust continuum emission and with CO isotope lines. We discover three dust rings in the disk, which have different inclinations and centers. Both dust and gas emission strongly indicate that the disk has misaligned parts, and the dust emission suggests that the innermost dust ring is eccentric. We interpret these as evidence of ongoing dynamical interactions between the triple stars and the circumtriple disk. This presentation is based on the submitted paper by Bi, van der Marel, Dong, Muto, Martin, Smallwood, Hashimoto, Liu, Nomura, Hasegawa, Takami, Konishi, Momose, Kanagawa, Kataoka, Ono, Sitko, Takahashi, Tomida and Tsukagoshi.

Keywords: protoplanetary disks, ALMA, sub-mm observations, disk dynamics

©2020. Japan Geoscience Union. All Right Reserved.

Dust grain growth in asymmetrical protoplanetary disk of V1247 Ori

*Kohki Gotoh[1], Misato Fukagawa[2], Takayuki Muto[3]

1. The university of Tokyo, 2. NAOJ, 3. Kogakuin University

It has been known in the planet formation in protoplanetary disks that dust fall into the central star before dust particles grow up to planetesimals assuming the uniform density and temperature distribution in disks. To solve this problem, the hypothesis is proposed, where dust grains are trapped in the pressure maxima and prevented from falling into the central star. In addition, it is thought that the region could work as the place of dust sticking, growing, and finally making planetesimals. V1247 Ori, a Herbig Ae star, is known to have the asymmetrical protoplanetary disk that contains the ring (the distance from the central star is about 54 au) and crescent (the distance from the star is about 120 au) in the ALMA Band 7 (870 micron) continuum observations. In the previous study, dust traps were suggested in the whole region of the crescent and the south-eastern region of the ring due to the hypothetical planet orbiting in the gap between the ring and crescent. In this study, we made the map of the opacity index β to evaluate the distribution of dust size using the continuum images with the spatial resolution of 0.09” (about 29 au) at 2.1 mm (Band 4) and 870 micron (Band 7). The signal-to-noise ratio is about 2.7 times larger than the previous study in Band 7. As a result, β in the northern part of the crescent is lower than other regions, which indicates that the growth of dust is observed only in the northern region of the crescent. This is inconsistent with the suggestion from the previous study. In this poster presentation, we discuss the properties (such as surface density) and the origin of the candidate dust trap in the asymmetrical protoplanetary disk of V1247 Ori.

Keywords: protoplanetary disks, radio continuum: planetary systems, opacity

©2020. Japan Geoscience Union. All Right Reserved.

Structure of Protoplanetary disk around WW Chameleon

*Kazuhiro Kanagawa[1], Jun Hashimoto[2], Takayuki Muto[3]

1. The University of Tokyo, 2. National Astronomical Observatory of Japan, 3. Kogakuin University

Recent observations by ALMA have revealed substructures such as gap and ring in protoplanetary disk. These substructures could be clues how planets form within the disk. We present the ALMA observation of the disk around WW Chameleon in Band 6 in Cycle 6. WW Chameleon is a young sstar (age is about 0.2 Myr) with about solar mass, and its distance is about 192 pc, and it is known to be a high accretor with a massive disk. WW Chameleon is also reported to be probable spectroscopic binary. The modeling of SED in the previous study suggested the large cavity with the radius of about 50 AU. If the large cavity opens, our observation with the beam size of ~10 AU could resolve it. However, an image given by our observation does not show such a large cavity. Moreover, although the large-scale spiral arms were detected in the image of NIR observation given by SPHERE, the structure looks axisymmetric in the ALMA image. We modeled the structure of the disk by fitting the visibility and found that the inner cavity can be very small (~a few AU). This visibility fitting also suggest several rings and steep cliff of the dust thermal emission. Assuming the temperature distributions, we also estimated the distribution of the dust density. In this poster, we present the results of our analysis and discuss the origin of these structures.

Keywords: Protoplanetary disk, WW Cha

©2020. Japan Geoscience Union. All Right Reserved.

High-resolution ALMA and NIR Imaging of Protoplanetary Disk around T Tauri star

*Mihoko Konishi[1], Jun Hashimoto[2], Takayuki Muto[3]

1. Oita University, 2. Astrobiology Center, 3. Kogakuin University

Protoplanetary disks have a wealth of substructures such as gaps/rings structures, spiral arms, and asymmetries. Multi-wavelength observations can reveal the dust distributions of different grain sizes, which will give us information to discuss the origin to produce such disk structures. This presentation focuses on T Tauri star HP Cha system (distance: ~190 pc; age: ~2 Myr) observed in submillimeter wavelengths and near infrared. Our submillimeter observations were conducted with ALMA at Band 6 to detect the dust continuum and CO gas isotopes (project code: 2017.1.01460.S). In addition, we obtained the scattered light from the disk with SPHERE IRDIS DPI (Dual-Polarization Imaging) mode in J band, and searched point-like sources by using SPHERE IFS in YJH band (program ID: 0102.C-0561). The 1.3 mm continuum image (beam size: 53 mas x 30 mas) first revealed a ring-disk structure with the width of ~0.1 arcsec (~19 au) at the radius of ~0.27 arcsec (~51 au), while the polarized light was detected within ~0.23 arcsec (~44 au). The results would indicate the clear evidence of dust filtration in HP Cha disk. We will discuss the detail properties and origins of observed dust distribution. It is noted that there is no point-like source around HP Cha except known companions.

Keywords: Protoplanetary Disk

©2020. Japan Geoscience Union. All Right Reserved.

Recent advances in the solar system science brought by ALMA observations

*Hideo Sagawa[1], Takahiro IINO[2]

1. Kyoto Sangyo University, 2. The University of Tokyo

A large number of successful discoveries has been constantly produced by ALMA. Its powerfulness is not only limited to the cosmological or astronomical fields but also can be applied to solar system planetary science. This paper reviews the recent advances in the solar system sciences achieved by ALMA observations.
ALMA’s high sensitivity enables us to observe thermal emission from small minor bodies located at the far distance in our solar system (e.g., TNOs [Lellouch et al., 2017]; Pluto [Lellouch et al., 2017]), and the high spatial resolution provides a quite unique remote-sensing capability to spatially-resolve Jovian icy moons (e.g., Europa [Trumbo et al. 2018]) and asteroids (Juno [ALMA partnership, 2015]). Moreover, heterodyne receiver’s high frequency resolution is one the most interesting observation techniques for the planetary atmospheric study. It can precisely measure the spectral line shape of molecular absorption, from which we can derive the abundances of minor chemical species even with the concentration as low as part-per-billion (e.g., nitriles and hydrocarbons in Titan [e.g., Thelen et al., 2019]). The atmospheric wind can be derived via observing the Doppler-shift of the molecular lines (e.g., super-rotation of Titan thermosphere [Lellouch et al., 2019]).
In addition, we will discuss ALMA’s potential synergetic sciences with the planned space-born explorations such as JUICE and MMX and with future optical/infrared telescopes such as TMT and JWST.

Keywords: ALMA, solar system science, planetary atmosphere

©2020. Japan Geoscience Union. All Right Reserved.

Current status and prospects of solar observations with ALMA

*Masumi Shimojo[1]

1. National Astronomical Observatory of Japan

Solar observations with ALMA have been offered since ALMA-Cycle4 (2016-2017), but scientific results were smaller than predicts, unfortunately. It is caused mainly by the difficulties of solar image synthesis. However, the situation is gradually changing by the efforts of the solar radio community. Actually, seven papers using ALMA solar data were accepted or published by the leading astronomical journals within only these three months(Nov. 2019 - Jan. 2020), despite the number of the Grade-A or B solar programs in each Cycle was less than 10.

We cannot use the full functions of ALMA for solar observations due to the particularity of the observing target. The limitations are also reducing gradually, and the Band7 and Band 5 for solar observations were opened in Cycle 7 and Cycle 8, respectively. The international development team of ALMA solar observations is working on realizing Stokes-V measurement with Band3, now.

In the poster, we summary the achievements of ALMA solar observations and present the current status of the development. Finally, we discuss the prospect of observing the Sun with ALMA, toward the next solar maximum.

Keywords: ALMA, Sun, solar activity

©2020. Japan Geoscience Union. All Right Reserved.

[J] Poster | P (Space and Planetary Sciences)：P-CG Complex & General

[P-CG27] Origin and evolution of materials in space

convener:Hideko Nomura(Division of Science, National Astronomical Observatory of Japan), Takafumi Ootsubo(Institute of Space and Astronautical Science, Japan Aerospace Exploration Agency), Hitoshi Miura(Graduate School of Natural Sciences, Department of Information and Basic Science, Nagoya City University), Aki Takigawa(Department of Earth and Planetary Science, The University of Tokyo)

Recent progress of astronomical observations, laboratory experiments, solar-system exploration, and theoretical work have enabled us to attempt to understand the origin and evolution of materials (dust and gas) in space in the context of material science. It is thus important to link further planetary material science and astronomy for a comprehensive understanding of dust and gas in space and their role in the evolution of galaxies, stars, and planetary systems. Infrared observations with future large satellites/telescopes, such as SPICA and TMT, are suitable for the study of gas and dust, and are expected to bring a new frontier of gas/dust study. In this session, based on the latest results on astronomical observations (ALMA, etc.), experiments, and theoretical studies on materials in space, we discuss the next steps in science for materials in space to maximize the outcome of the observations with the future satellites/telescopes.

[PCG27-P01] Diffusion mechanisms of H^+ in interface between forsterite glass and amorphous ice

*Ayane Kubo[1], Junya Nishizawa[1], Tomoko Ikeda-Fukazawa[1] (1.Department of Applied Chemistry, Meiji University, Japan)

[PCG27-P02] Effects of deposition temperature on structure of amorphous ice

*Yui Ono[1], Kengo Oki, Tomoko Fukazawa[1,2] (1.Meiji University, 2.The Japanese Society of Snow and ice)

[PCG27-P03] Study of formation processes of $C_2H_2N_2$ by quantum chemical calculation

*Teppei Yonetsu[1], Hiroyuki Maezawa[1] (1.Osaka Prefecture University)

[PCG27-P04] Formation of Complex Organic Molecules via Ice Mantle Reactions in Protoplanetary Disks

Chen-En Wei[1], *Hideko Nomura[2], Catherine Walsh[3], Patrice Theule[4] (1.Department of Earth and Planetary Sciences, Tokyo Institute of Technology, 2.Division of Science, National Astronomical Observatory of Japan, 3.University of Leeds, 4.Aix-Marseille Universite)

[PCG27-P05] Complex organic molecules in comet 21P/Giacobini-Zinner

*Takafumi Ootsubo[1], Hideyo Kawakita[2], Shinnaka Yoshiharu[2], Jun-ichi Watanabe[3], Mitsuhiko Honda[4] (1.Institute of Space and Astronautical Science, Japan Aerospace Exploration Agency, 2.Kyoto Sangyo University, 3.National Astronomical Observatory of Japan, 4.Okayama University of Science)

Diffusion mechanisms of H^+ in interface between forsterite glass and amorphous ice

*Ayane Kubo[1], Junya Nishizawa[1], Tomoko Ikeda-Fukazawa[1]

1. Department of Applied Chemistry, Meiji University, Japan

Forsterite (Mg_2SiO_4) glass exists as dust grains in interstellar molecular clouds [1]. In interstellar molecular clouds, elements such as hydrogen, oxygen, carbon, and nitrogen deposit on the dust grains, and form various molecules (e.g., H_2O, CO, CO_2, NH_3, CH_4, H_2CO, CH_3OH, and so on) [2]. These molecules undergo chemical evolutions to organic molecules through various processes on the surface of the dust grains [2]. The structure of forsterite glass is one of the important factors governing the chemical evolutions in interstellar molecular clouds. However, there are few studies for effects of molecular adsorption on the structure and properties of forsterite glass [3]. To investigate the diffusion mechanisms of proton, we performed molecular dynamics calculations of forsterite glass with amorphous ice, molecular dynamics (MD) calculations were performed.

The MD calculations were performed using an atom-atom potential model with MXDORTO program [4]. The potential parameters were empirically determined by constraining the structure to reproduce the experimental results of density, thermal expansion coefficient, and bulk modulus for forsterite crystal and ice polymorphs [5,6]. A fundamental orthorhombic cell consisting of 1176 Mg_2SiO_4 with two-dimensional periodic boundary conditions was used as the initial structure. The glass structure was prepared by quenching the liquid phase from 3000 to 10 K with 2 K/fs in rate. Then, amorphous ice layer with 3311 H_2O, which was prepared by quenching a liquid phase from 290 to 10 K, was adsorbed on the glass surface. The MD code was run with NTP ensemble in a temperature range of 10–300 K at 0.1 MPa.

The result shows that the coordination number of Mg in the forsterite-ice interface is larger than that of forsterite surface without water phase. At temperatures above 200 K, furthermore, a decomposition phenomenon of H_2O molecule to hydroxide and hydrogen ions was observed. From an observation of the trajectories of the ions, the diffusion mechanism was analyzed. The result shows that the hydrogen ion diffuses in the internal part of forsterite glass via repeated formation and decomposition of MgO_xH_y or SiO_4H_z structures. No diffusion was observed for the hydroxide ion, because the hydroxide ion becomes a stable state due to formation of covalent bonds with Mg or Si in forsterite. The diffusion processes have important implications for chemical evolution in interstellar spaces.

References

[1] J. P. Bradley, L. P. Keller, T. P. Snow, M. S. Hanner, G. J. Flynn, J. C. Geno, S. J. Clemett, D.E. Broenlee, J. E. Bowey, *Science* **285** (1999) 1716.
[2] N. Watanabe, A. Kouchi, *Prog. Surf. Sci.* **83** (2008) 439.
[3] J. A. Tangeman, B. L. Phillips, A. Navrotsky, J. K. R. Weber, A. D. Hixson, T. S. Key, *Geophys. Res. Lett.* **28** (2001) 2517.
[4] K. Kawamura, MXDORTO, *Japan Chemistry Program Exchange*, #029 (1990).
[5] T. Ikeda-Fukazawa, *J. Soc. Inorg. Mater. Jpn* **23** (2016) 130.
[6] Y. Kumagai, T. Ikeda-Fukazawa, *Chem. Phys. Lett.* **678** (2017) 154.

Keywords: Forsterite, Amorphous ice, Interface, Molecular dynamics

©2020. Japan Geoscience Union. All Right Reserved.

©2020. Japan Geoscience Union. All Right Reserved.

Effects of deposition temperature on structure of amorphous ice

*Yui Ono[1], Kengo Oki, Tomoko Fukazawa[1,2]

1. Meiji University, 2. The Japanese Society of Snow and ice

In interstellar molecular clouds, elements such as hydrogen, oxygen, carbon, and nitrogen deposit on dust grains, and forms various molecules such as H_2O, CO_2, NH_3, CH_4, H_2CO, CH_3OH, and so on. The deposited water exists as amorphous ice. Because molecules undergo chemical evolutions through various processes on amorphous ice, amorphous ice has an important role for the chemical evolutions in the universe. Amorphous ice formed from a vapor deposition is principally classified into two types: low-density amorphous (LDA) and high-density amorphous (HDA) ices. HDA ice is transformed into LDA ice with warming [1]. However, the mechanism of the phase transition is less conclusive, because the transition temperature depends on experiments [2]. To investigate the effects of thermal history on structure of amorphous ice, a dependence of deposition temperature on infrared spectrum of amorphous ice was analyzed.

Amorphous ice was prepared with vapor deposition of distilled and degassed water on a substrate of oxygen-free copper at a temperature of 43.5–120.5 K. The total pressure in the vacuum chamber was kept at about 5.0×10^{-5} Pa during the deposition. After the deposition of amorphous ice, the substrate was cooled to 43.5 K at a rate of 2 K/min. Then, the sample was warmed to 176 K at a rate of 1–4 K/min. The IR spectra were measured using Shimadzu IRPrestage-21 at every 15 seconds during deposition, and measured at 2 K intervals during cooling and warming.

The effects of the deposition temperature on the structure of amorphous ice was analyzed using the spectra at 43.5 K after cooling from their deposited temperatures. The result shows that the wave number of the O–H symmetric stretching mode depends on the deposition temperature. The wave number gradually decreases as the deposition temperature increases at temperature below 107 K. The decreasing rate changes at 63 and 76 K. This indicates that the HDA ice is transformed into LDA ice via an intermediate structure in the temperature range of 63–76 K. Furthermore, a significant decrease in the wave number was observed at 108 K. This decrease is associated with the transition from the LDA ice to crystalline cubic ice (Ic). The transition point is lower than that observed in the warming process from the HDA ice (i.e., 145–160 K [1]). The lower shift in the transition point is caused by a roughness of its surface. A liquid-like structure in a rough surface can be a cause of the lower shift of the transition point, because the rearrangement motion of water molecules is enhanced with an increase in amplitudes of the thermal vibrations [3].

References

[1] P. Jenniskens, D. F. Blake, *Astrophys. J.* **473** (1996) 1104.

©2020. Japan Geoscience Union. All Right Reserved.

[2] K. Amann-Winkel, C. Gainaru, P. H. Handle, M. Seidl, H. Nelson, R. Böhmer, T. Loerting, *Proc. Natl. Acad. Sci. USA* **110** (2013) 17720.

[3] Y. Kumagai, T. Ikeda-Fukazawa, *Chem. Phys. Lett.* **678** (2017) 154.

Keywords: Amorphous ice, Infrared spectroscopy

©2020. Japan Geoscience Union. All Right Reserved.

Study of formation processes of $C_2H_2N_2$ by quantum chemical calculation

*Teppei Yonetsu[1], Hiroyuki Maezawa[1]

1. Osaka Prefecture University

The amino acids that make proteins in organisms have left-handed enantiomers. This homochirality has also been detected in amino acids detected from meteorites, leading to discussions about the possibility that the origin of life on Earth may have originated in space. On the other hand, the origin of nucleobases which are important components of DNA, the blueprint for life on Earth, are not yet well understood. It is known that organisms can make nucleic acids from de novo synthesis by themselves. However, since nucleobases have also been detected in meteorites, it may be possible that some of the nucleobases of early life originated in space. Although the various laboratory experiments for the formation of nucleobases have been actively demonstrated on the surface of ice, in plasma discharges, and by the high energy particles by many researchers, how the nucleobases are formed is still an enigma. In the synthesizing process of one of the nucleobases, adenine $C_5H_5N_5$ with our plasma system the mass 54 corresponding to the same mass as $C_2H_2N_2$ is detected by a quadrupole mass spectrometer. This suggests that the formation of $C_5H_5N_5$ may be via $C_2H_2N_2$. Observations of E-HNCHCN have also been attempted toward Sgr B2 (N) by Zaleski et al. (2013). HNCHCN can be probably formed by polymerization of HCN, but the activation energy of the reaction is high, therefore this reaction is considered to be difficult to proceed at least in the gas phase in molecular cloud cores.

In this study, the possibility of the formation processes of E-HNCHCN and Z-HNCHCN other than the polymerization of HCN was examined by the quantum chemical calculation with the Hartree-Fock method. 6 -31 G (d, p) of the DZP basis was used as the basis function. As a result, it was found that, for example, NH_2CH_2CN is firstly formed from CH_3CN + NH and CH_2CN + NH_2 by the exothermic reactions and then E- and Z-HNCHCN are formed via a transition state with high activation energy, or via the intermediate molecule, NH_3CHCN and the some transition states with low activation energy. In this presentation, we will report the results of these analyses.

Keywords: Nucleobases, Interstellar medium, Plasma reaction, Quantum chemical calculation

©2020. Japan Geoscience Union. All Right Reserved.

Formation of Complex Organic Molecules via Ice Mantle Reactions in Protoplanetary Disks

Chen-En Wei[1], *Hideko Nomura[2], Catherine Walsh[3], Patrice Theule[4]

1. Department of Earth and Planetary Sciences, Tokyo Institute of Technology, 2. Division of Science, National Astronomical Observatory of Japan, 3. University of Leeds, 4. Aix-Marseille Universite

We have contracted chemical reaction network with ice mantle reactions in addition to gas-phase reactions, gas-grain interaction, and grain-surface reactions in order to investigate their effect on formation of complex organic molecules in protoplanetary disks. As the reaction rate of the ice mantle reactions, we have developed a formula based on the recent laboratory experiments which suggest crystallization of water ice induces the mantle reactions. Periodic FU Ori-type outbursts, which sometimes observed in young protostellar objects, are considered as a heat source required for the ice mantle reaction. Our calculations show that the ice mantle reactions occur efficiently at the temperature of >120K, where the time scale of the ice mantle reaction is sufficiently shorter than the time scale of the outbursts, and produce sufficient amount of ammonium carbamate, which accounts for the broad absorption features observed in the reflected spectra of the comet 67P/Churyumov-Gerasimenko in the Rosetta mission. We simply estimate the temperature of possible comet forming regions in the protoplanetary disks, showing that the mass accretion rate of 10^{-5} solar mass per year is required in order to explain the heating source to produce the ammonium carbamate by FU Ori-type outbursts. The effect of the ice mantle reactions depends on the structure of ices, namely the thermal history of small bodies and has room for further improvement in future work.

Keywords: protoplanetary disks, astrochemistry, formation of organic molecules

©2020. Japan Geoscience Union. All Right Reserved.

Complex organic molecules in comet 21P/Giacobini-Zinner

*Takafumi Ootsubo[1], Hideyo Kawakita[2], Shinnaka Yoshiharu[2], Jun-ichi Watanabe[3], Mitsuhiko Honda[4]

1. Institute of Space and Astronautical Science, Japan Aerospace Exploration Agency, 2. Kyoto Sangyo University, 3. National Astronomical Observatory of Japan, 4. Okayama University of Science

Comet 21P/Giacobini-Zinner is a Jupiter-family comet with an orbital period of ~6.6 years, which is considered a parent body of the October Draconids meteor shower. It is very important to study comet 21P because the comet is peculiar; (i) it is depleted in carbon-chain molecules, NH2, and highly volatile species, and (ii) has a negative linear polarization gradient produced by grains.

We observed comet 21P/G-Z in the mid-infrared with the Cooled Mid-infrared Camera and Spectrometer (COMICS) on the 8.2 m Subaru Telescope on Mauna Kea, Hawaii, on UT 2005 July 5, just after the perihelion passage. The heliocentric and geocentric distances of the comet were 1.04 and 1.43 au, respectively. The spectrum of comet 21P/G-Z shows distinct emission peaks at approximately 8.5, 9.2, and 11.2 micron and weak peaks at approximately 8.2, 11.6, 11.9, and 12.7 micron. The thermal emission model commonly used for cometary dust grains failed to reproduce the observed spectrum of comet 21P. More materials, in addition to silicate materials, are needed to reproduce the emission peaks at 8.2, 8.5, 9.2, and 12.7micron. Those unidentified infrared (UIR) band features have never been observed in previous mid-infrared observations of other comets. The features at ~8.2, ~8.5, ~11.2, and ~12.7 micron could be attributed to polycyclic aromatic hydrocarbons (PAHs) or hydrogenated amorphous carbons (HACs) contaminated by N- or O-atoms, although part of the feature at ~11.2 micron comes from crystalline olivine. The UIR features found in the mid-infrared spectra of classical novae are similar to the emission features in the spectrum of 21P/G-Z.

Laboratory experiments suggest that the carrier of the ~9.2 micron feature observed in the spectrum of comet 21P/G-Z may be some organic molecules contaminated with nitrogen, including aliphatic hydrocarbons that experienced several hundred-K. Comet 21P is depleted in simple organic molecules but enriched in complex organic molecules. The birthplace of comet 21P/G-Z in the solar nebula might be warmer or closer to the Sun than the birthplace of other comets (usually considered to be ~5–30 au from the Sun). The mass fraction of the crystalline component in silicate is, however, typical (~0.45) for comet 21P/G-Z. This indicates that comet 21P/G-Z formed at a similar distance from the Sun in the solar nebula as other comets formed. From this point of views, we propose that the comet might have originated from a circumplanetary disk of giant planets (similar to Jupiter and Saturn) where was warmer than the typical comet-forming region (5–30 au from the Sun) and was suitable for the formation of complex organic molecules.

Keywords: comets, organics, meteors

©2020. Japan Geoscience Union. All Right Reserved.

[J] Poster | A (Atmospheric and Hydrospheric Sciences)：A-AS Atmospheric Sciences, Meteorology & Atmospheric Environment

[A-AS15] Progress in dense observation and numerical modeling of micro-scale meteorology

convener:Junshi Ito(Atmosphere and Ocean Research Institute, The University of Tokyo), Kentaro Araki(Meteorological Research Institute), Nobumitsu Tsunematsu(Tokyo Metropolitan Research Institute for Environmental Protection), Keigo Matsuda(Japan Agency for Marine-Earth Science and Technology)

Progresses in observations and numerical simulations enable to unveil details in micro- or sub-kilometer scale meteorology. For example, low level convergences and heat island effects in the micro-scale may be sometimes associated with extreme atmospheric phenomena such as wind gusts and torrential rainfalls. Numerical simulations with very fine resolution may even predict occurrences of such phenomena. This session is welcome to researches and future scopes in the field of micro-scale meteorology.

[AAS15-P01] Preliminary consideration of the wind and pressure balance in multigrid assimilation scheme

*weiyu ding[1] (1.Institute of Tropical and Marine Meteorology, CMA, Guangzhou, China)

[AAS15-P02] Micro-Scale Atmospheric Pressure Measurement on the Campus of J. F. Oberlin University

*Atsushi Mori[1] (1.J. F. Oberlin University)

[AAS15-P03] **Statistical reconstruction of the heterogeneity of a dense urban wind field using a sparse network of weather stations**

*Ziv Klausner[1], Eyal Fattal[1] (1.Israel Institute for Biological Research)

[AAS15-P04] **Polarimetric Observations of Precipitating and Non-precipitating Stratiform Clouds**

*Kenneth Allan Sinclair[1] (1.NASA Goddard Institute for Space Studies)

[AAS15-P05] Numerical simlation of tornado occured at Nobeoka accompanied by TC1917

*Junshi Ito[1], Hiroshi Niino[1] (1.Atmosphere and Ocean Research Institute, The University of Tokyo)

[AAS15-P06] Quantifying the Impact of Future Urbanization on Urban Microclimate Over Mumbai Metropolitan Region, India.

*Vinayak Nitin Bhanage[1], Han Soo Lee[1], Shirishkumar Gedam[2] (1.CSRE,Indian Institute of Technology,Bombay,India. and Graduate School for International Development and cooperation,Hiroshima University,Japan, 2.CSRE,Indian Institute of Technology,Bombay,India)

[AAS15-P07] Characteristics of Variation of the Atmospheric Boundary Layer Affected by the Gust Fronts

*jie lan Xie[1,2,3], Shao jia Fan[1,2,3] (1.School of Atmospheric Sciences, Sun-Yatsen University, 2.Observation and Research Station for Climate Environment and Air Quality Change in the Pearl River Estuary, 3.Southern Marine Science and Engineering Guangdong Laboratory(Zhuhai))

[AAS15-P08] Development process of convective boundary layer and turbulence characteristic above urban canopy with heterogeneous heating at building and street surface

*Yasuo Hattori[1], Shuji Ishihara[2], Hitoshi Suto[1], Keisuke Nakao[1], Yuma Hasebe[2], Hiromaru Hirakuchi[1] (1.Central Research Institute of Electric Power Industry, 2.Denryoku Computing Center)

Preliminary consideration of the wind and pressure balance in multigrid assimilation scheme

*weiyu ding[1]

1. Institute of Tropical and Marine Meteorology, CMA, Guangzhou, China

In the variational assimilation system, the statistics of the background error covariance matrix needs a huge amount of computation and storage, the geostrophic balance or linear balance is usually constructed to simplify wind and pressure relationship in the background error covariance matrix during the process of minimizing the cost function. With the improvement of model resolution and the assimilation of dense ground observation data, more and more small-scale information needs to be assimilated into the initial value of the model. Geostrophic balance or linear balance cannot describe the balance of local wind and pressure field. In this study, based on the multi-grid assimilation scheme, the sounding data and Atmosphere Motion Vector data are assimilated in the coarse grid with geostrophic balance, and the automatic weather station data are assimilated in fine grid with no wind pressure balance constraint. In this research, a case of squall line process in Guangdong China is studied, and the impact to 2-meter temperature and precipitation simulation are analyzed.

Keywords: wind and pressure balance, multigrid assimilation scheme

©2020. Japan Geoscience Union. All Right Reserved.

Micro-Scale Atmospheric Pressure Measurement on the Campus of J. F. Oberlin University

*Atsushi Mori[1]

1. J. F. Oberlin University

In recent years, MEMS technology has made small and inexpensive barometric pressure sensors available. Using these, observation project has been started in the area around Machida Campus in Machida City, Tokyo. The objective is to capture phenomena related to keywords such as gust front, movement of the precipitation zone, gravitational current, and internal gravity waves. To capture them, the observation is designed with a time resolution of 1 second and a spatial resolution of several hundred meters. At the Meteorological Society of Japan 2019 Fall Meeting, he presented his initial results. In this presentation, I will present an attempt to correct the pressure fluctuation of each sensor. Since each sensor has different characteristics, it is thought that the raw measurement results should not be used directly for data analysis. The pressure at each observation point differs individually. However, it can be expected that there will be no difference between observations in short ranges for fluctuations with a very long period. Therefore, the data is calibrated so that the standard deviation of the low-pass filtered atmospheric pressure data becomes the same. Detailed results will be shown on the day.

Keywords: measurement of atmospheric pressure, MEMS, internet

©2020. Japan Geoscience Union. All Right Reserved.

Statistical reconstruction of the heterogeneity of a dense urban wind field using a sparse network of weather stations

*Ziv Klausner[1], Eyal Fattal[1]

1. Israel Institute for Biological Research

The vectorial wind field is a major factor in the transport and dispersion of air pollution in urban regions. This field is frequently characterized by an inherent spatial heterogeneity. This heterogeneity may be manifested by noticeable differences between rooftop level measurements in adjacent locations. Quite often the degree of heterogeneity changes through the day.

A possible way to obtain real-time information on the current state of the urban wind field is to use a dense weather stations' network. Such endeavor is expansive and technically demanding. This leads to networks that are too sparse to accurately describe the changing degree of the urban wind vectors' heterogeneity.

In situations where there is not sufficient information regarding a specific urban region, it is possible to conduct a two phase scheme. First, deploy a dense weather stations network for a limited time. Then leave a sparse network to continuously monitor the region. Such scheme requires the use of statistical methods in order to estimate essential features of the dense wind field from the sparse network's measurements.

A useful method can be a tolerance region that contains a given proportion of the wind vectors' spatial realizations. For bivariate normal distributed vectors, an ellipse shaped tolerance region can be constructed using an analytical Mahalanobis distance function. However, because actual measurements of urban wind vectors does not always follow this distribution, another approach is required.
This study used wind data collected in the metropolitan area of Tel-Aviv using a network of more than 20 weather stations that were separated by less than a kilometer from each other. The results show that the spatial wind distribution can be very well represented by a small sample of merely four stations. Based on this sample stations, empirical Mahalanobis distance functions were calculated for each season. These functions were found to fit well the logistic distribution. Using these functions, tolerance regions were applied on a different data set in order to validate the statistical projection.

Keywords: micrometeorology, spatial wind distribution, sparse meteorological network, Mahalanobis distance

©2020. Japan Geoscience Union. All Right Reserved.

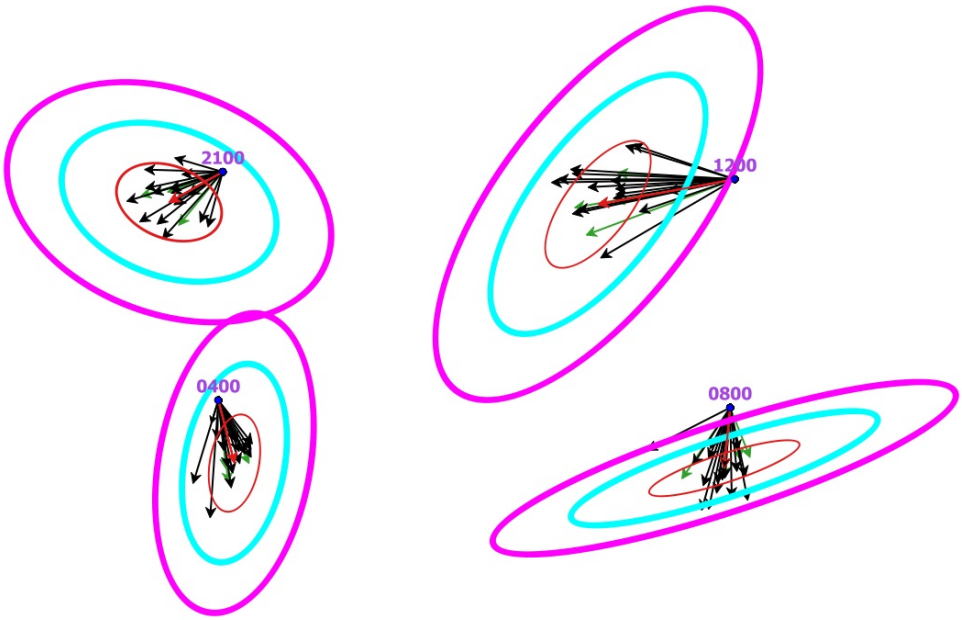

©2020. Japan Geoscience Union. All Right Reserved.

Polarimetric Observations of Precipitating and Non-precipitating Stratiform Clouds

*Kenneth Allan Sinclair[1]

1. NASA Goddard Institute for Space Studies

We present an analysis using polarimetric observations of precipitating clouds. Polarized reflectances originate from single scattering events near cloud top are nearly unaffected by multiple scattering within a cloud. These polarized reflectances as a function scattering angle in the rainbow angular range and droplet radius are integral transforms, allowing the shape of the droplet size distribution to be retrieved without a priori knowledge. Studies of droplet size distribution variability have remained challenging because observational studies have traditionally been limited to *in situ* measurements made by cloud probes on aircraft while profiling clouds. These studies focusing on how dispersion varies with other cloud properties, aerosols and atmospheric state parameters have yielded contradicting results.

We present observations from NASA’ s Research Scanning Polarimeter (RSP) during the NASA-led Observations of Aerosols Above Clouds and their Interactions (ORALCES) campaign. We present the summary of a study investigating variability between cloud properties and precipitation. Precipitation rates using in this study are measured by the Advanced Precipitation Radar, which was flown alongside the RSP during ORACLES. We observe a broad or bimodal feature in the droplet size distribution is commonly observed in the most strongly precipitating cases indicating that precipitating and non-precipitating clouds can be discerned using polarimetric observations from near cloud-top.

Keywords: Polarization, Precipitation, Clouds, Remote Sensing, Rainbow Fourier transform

©2020. Japan Geoscience Union. All Right Reserved.

Numerical simlation of tornado occured at Nobeoka accompanied by TC1917

*Junshi Ito[1], Hiroshi Niino[1]

1. Atmosphere and Ocean Research Institute, The University of Tokyo

A tornedo occurred around 0830 JST on 22 September 2019 accompanied by the tropical cyclone 1917 in the Nobeoka, Miyazaki, Japan. Its strength was the JEF scale of 2. A regional weather prediction model, JMA-NHM (Japan Meteorological Agency’ s Non-Hydrostatic Model) is used to simulate the tornado. A simulation with horizontal resolution 2 km is conducted by use of JMA’ s meso-scale analysis for its initial and boundary values. Other runs with horizontal resolution of 400 m and 80 m or 50 m are conducted by nested in coarser resolution results of every 2 minutes. In the finest resolution, strong winds with counter-clockwise rotation exceeding 70 m/s occur near the surface, and this corresponds to the tornadoes. This tornado is accompanied by meso-cyclone in a rain-band of the tropical cyclone. It is initiated 20 km away from the sea-shore, and approaches the Nobeoka city.

Keywords: Tornado, Tropical cyclone, Gusty wind, Numerical weather prediction

©2020. Japan Geoscience Union. All Right Reserved.

Quantifying the Impact of Future Urbanization on Urban Microclimate Over Mumbai Metropolitan Region, India.

*Vinayak Nitin Bhanage[1], Han Soo Lee[1], Shirishkumar Gedam[2]

1. CSRE,Indian Institute of Technology,Bombay,India. and Graduate School for International Development and cooperation,Hiroshima University,Japan, 2. CSRE,Indian Institute of Technology,Bombay,India

Mumbai Metropolitan Region(MMR) is one of the fastest-growing metropolitan regions in India and experiencing rapid Urban Expansion. According to the 2011 census report, the population of MMR is more than 23.15 million, while this number is expected to increase by up to 30 million by the year 2031. This increment in population and the process of urban expansion will induce the significant alterations in the Land Use Land Cover (LULC) distribution of the MMR further; it will adversely influence the Urban Microclimate of the region. To address this issue, the current study has been carried out to enumerate the effect of the future LULC on urban climate over the MMR. In the first part of the study, we have derived the distribution of current (2018) LULC by processing the latest satellite images obtained from the Landsat, while the future (2050) LULC was simulated using an ANN-based CA-Markov algorithm. In the later part of the study, the estimated LULC dataset was ingested into the WRF-UCM model, and two separate simulations were performed for current and future LULC scenarios under the same exceedingly hot conditions of May 2018. During these simulations, we assigned the fixed initial and lateral boundary conditions, which were acquired from the NCEP FNL dataset. The output from a WRF-UCM model for the current scenario was validated with the in-situ observations. The validation results for near-surface air temperature, relative humidity, and wind speed showed a more significant correlation ($r>0.70$) with observed in situ datasets. Comparative analysis of these simulations conducted for the current and future scenarios shows that by 2050 due to the expansion of urban areas, the mean surface air temperature over the urban areas of MMR will increase by 2.39˚c the mean surface air temperature of the rapidly growing urban centers like Kalyan, Ambarnath, Ulhas Nagar will increase by 4-5˚c.

Keywords: WRF-UCM, LULC, Urban Microclimate, Mumbai

©2020. Japan Geoscience Union. All Right Reserved.

Characteristics of Variation of the Atmospheric Boundary Layer Affected by the Gust Fronts

*jie lan Xie[1,2,3], Shao jia Fan[1,2,3]

1. School of Atmospheric Sciences, Sun-Yatsen University, 2. Observation and Research Station for Climate Environment and Air Quality Change in the Pearl River Estuary, 3. Southern Marine Science and Engineering Guangdong Laboratory(Zhuhai)

Based on the meteorological data and the eddy covariance data obtained from the 356-meter meteorology tower in Shenzhen, China, the characteristics of the vertical variation of the atmospheric boundary layer affected by the gust fronts were analysed. Our study found that the gust fronts had a significant impact on the low-level structure of the atmospheric boundary layer in the eastern Pearl River Estuary. The near-surface boundary layer changed from an unstable boundary layer to a stable boundary layer quickly, accompanied by a short-term drastic reduction in temperature, as well as enhancement in humidity and wind speed, and abrupt change in wind direction. The turbulent kinetic energy and the friction velocity in the lower boundary layer increase significantly, the vertical wind speed fluctuates sharply, and the vertical wind shear increases during the passing of the gust fronts. Our research will help to deepen the understanding of the vertical structure of the gust front in the coastal city, and provides a reference for the forecast and early warning of the strength of the near-surface gale caused by the gust fronts.

Keywords: 356-meter meteorology tower in Shenzhen, gust front, atmospheric boundary layer

©2020. Japan Geoscience Union. All Right Reserved.

Development process of convective boundary layer and turbulence characteristic above urban canopy with heterogeneous heating at building and street surface

*Yasuo Hattori[1], Shuji Ishihara[2], Hitoshi Suto[1], Keisuke Nakao[1], Yuma Hasebe[2], Hiromaru Hirakuchi[1]

1. Central Research Institute of Electric Power Industry, 2. Denryoku Computing Center

An accurate description of turbulence thermal transport processes in convective boundary layer developed above an urban canopy can be used for applications such as development of numerical weather prediction models. However, a detailed analysis of the effects of heterogeneity in the thermal conditions of building and street surfaces has not been reported, while many studies have investigated turbulence characteristics in urban canopies.

In this study, we performed large-eddy simulations (LESs) for a thermally convective flow developed above an urban canopy with buildings and streets under a heterogeneous surface heating condition, which mimics heat fluxes with insolation. The conditions of convective boundary layer and the configurations of urban canopy were set according to previous studies by Moeng and Sullivan (1994), Kanda (2006). An open source CFD code, OpenFOAM, was used. The present simulation was based on a LES version with PIMPLEfoam of OpenFOAM, in which the option of RANS model was adopted to represent the subgrid-scale diffusion. The central differencing scheme and the 2nd-order back Euler scheme for time integration were chosen.
We discussed the vertical profiles of turbulence fluxes in thermal and flow fields of the convective boundary layer. The urban canopy yielded the increased in thermal turbulence fluxes, while the effects of urban canopy on the flow fields were quite small, suggesting that the urban canopy enhanced a dissimilarity between thermal and flow fields. Such a dissimilarity was caused by differences of coherence structures developed above the urban canopy between thermal and flow fields, i.e., the thermal and flow fields were controlled by roll and streaky structures, respectively, which were visualized by contours of instantaneous temperature and velocity fluctuations in horizontal planes.

Keywords: Atmospheric boundary layer, Buoyancy, Coherence structure, LES, Unstable stratification

©2020. Japan Geoscience Union. All Right Reserved.

[J] Poster | A (Atmospheric and Hydrospheric Sciences)：A-OS Ocean Sciences & Ocean Environment

[A-OS18] Coastal circulation and material cycle and freshwater discharge through rivers

convener:Shinichiro Kida(Research Institute for Applied Mechanics, Kyushu University), Kiyoshi Tanaka(University of Tokyo), Dai Yamazaki(Institute of Industrial Sciences, The University of Tokyo), Yuichi Hayami(Saga University)

Coastal seas have high biodiversity and high productivity, while various environmental problems such as eutrophication, red tide, and hypoxia are caused by human activity. In order to understand the material cycle and various phenomena, and to maintain sustainable environment in coastal seas, interdisciplinary research is needed. Coastal processes are also affected by the water cycle from land to the ocean, involving complex dynamics of rivers and buoyancy-driven flows in estuaries and the ocean. Recent progress in satellite observations and numerical models are beginning to illuminate how this water cycle occurs on various time scales globally and regionally.
This session welcomes researchers who are interested in physical phenomena, material cycle, biological responsive dynamics, and their interactions in coastal seas as well as the freshwater cycle from land to the ocean such as surface runoff, river transport, estuarine circulation, and coastal river plumes. Neither study area nor study method is confined. We welcome studies on wide range of topics to communize our knowledge, including presentations in English.

[AOS18-P01] A regional river-ocean seamless model for Kyushu

*Shinichiro Kida[1], Takahiro Tsutsumi[2], Yosuke Alexandre Yamashiki[3], Ryusuke Kuroki[3] (1.Research Institute for Applied Mechanics, Kyushu University, 2.Interdisciplinary Graduate School of Engineering Science, Kyushu University, 3.Graduate School of Advanced Integrated Studies in Human Survivability, Kyoto University)

[AOS18-P02] Relationship between environment and macrobenthos distribution in the coastal area of Kashima city in Ariake Sea

*Yuichi Hayami[1], Naoki Fujii[1] (1.Saga University)

[AOS18-P03] SST variability in Suruga Bay and its surrounding area due to Kuroshio path variability

*Yuya Hirano[1], Kazuyuki Uehara[1] (1.The Graduate School of Geo-environmental Science, Tokai University)

[AOS18-P04] The seasonal cycle of phytoplankton biomass concentration along the coast of Japan

*Shimada Hiroaki[1], Shinichiro Kida[2] (1.Interdisciplinary Graduate School of Engineering Sciences , Kyushu University, 2.Research Institute for Applied Mechanics , Kyushu University)

[AOS18-P05] **Modelling Study of the Zhe-Min Coastal current**

*yang zhang[1], min bao[1] (1.Second Institute of Oceanography, MNR)

[AOS18-P06] Sea surface temperature and chlorophyll *a* variations in the Sanriku Coastal area and their influence on the environment of Otsuchi Bay

*XUANYU LIU[1], Sachihiko Itoh[1], Eisuke Tsutsumi[1], Kiyoshi Tanaka[1] (1.University of Tokyo)

[AOS18-P07] Multi-layer temperature variability at Kurasawa on the back of Suruga Bay.

*Mito Nakamura[1], Kazuyuki Uehara[1] (1.tokai university the graduate school of marine science and technology)

A regional river-ocean seamless model for Kyushu

*Shinichiro Kida[1], Takahiro Tsutsumi[2], Yosuke Alexandre Yamashiki[3], Ryusuke Kuroki[3]

1. Research Institute for Applied Mechanics, Kyushu University, 2. Interdisciplinary Graduate School of Engineering Science, Kyushu University, 3. Graduate School of Advanced Integrated Studies in Human Survivability, Kyoto University

A regional river-ocean seamless model is developed for the island of Kyushu, Japan. Extreme rainfalls cause severe flooding and alter the oceanic environment along the coast. In Japan, rainfalls often occur on a regional scale, which includes multiple river basins. The coast is thus affected by river discharges from multiple rivers that differ in magnitude and time variability. This research aims to develop a numerical model to capture this hydrological cycle from land to the ocean seamlessly. We will present model results from a model that focuses on the island of Kyushu and several heavy rain events in the summer of 2015. We find the model to capture the increase and decrease in transport reasonably compared to observations, but with a delay in peak discharge time. The bias in the magnitude of the river discharge differed for each river basins and suggests the need to implement a sophisticated land surface model.

Keywords: River-Ocean coupled model, Hydrological cycle

©2020. Japan Geoscience Union. All Right Reserved.

Relationship between environment and macrobenthos distribution in the coastal area of Kashima city in Ariake Sea

*Yuichi Hayami[1], Naoki Fujii[1]

1. Saga University

In the coastal area of Kashima City in Ariake Sea, there are wide spread of mud flats and many endemic species including goggle-eyed goby live. Also, active commercial fishing is conducted including laver culture, oyster and arkshell farming. Red tide and hypoxic water mass sometimes happened recently in this area and became a problem. However, there are no data of detailed distribution of water quality, bottom sediment quality and organisms including both subtidal and intertidal area. The “Hizen-Kashima Higata” which locates in the northern part of this area was listed as a site of Ramsar Convention in 2015. Therefore, in order to clarify the environmental features and ecosystem of this area and construct a suitable conservation program, we started environmental monitoring in 2015. Water qualities were measured at 18 stations with a multi-parameter water quality meter in summer and winter. Measurements were conducted in spring tide and neap tide. Temperature, salinity, turbidity, chlorophyll fluorescence and DO were measured. Bottom sediment and macrobenthos sampling was carried out at the same 18 stations with a grab sampler in summer and winter. Bottom sediment and macrobentos sampling was also carried out at 5 stations along the coast on the mudflat. Water content, organic carbon, total nitrogen AVS and ORP were measured. The sediment for collecting macrobenthos was sieved through a 1-mm mesh and the residue was fixed in 70 % ethanol. The macrobenthos samples were sorted and identified in the laboratory. Based on these data, the average distributions of water and sediment quality are clarified and their relationships between macrobenthos distribution was investigated.

The results of the analysis of the data between 2015 and 2018 were as follows. The Hizen-Kashima Higata is a mudflat that had most strong influence of fresh water and temperature variation in the mudflats in Kashima City. The turbidity was highest in the Hizen-Kashima Higata and chlorophyll was relatively low. These results suggest that the Hizen-Kashima Higata is a most harsh environment for organisms among the mudflats in Kashima City. The DO concentration in the subtidal zone was low and sometimes become hypoxic in neap tide in summer. The sediment ORP was low and AVS was high in this area. These results suggest that the subtidal zone is a harsh environment for organisms. However, the macrobenthos species and abundance were higher in the subtidal area than other areas both in summer and winter. The species and abundance of macrobenthos were lowest in the Hizen-Kashima HIgata. There was a high negative correlation between water temperature and macrobenthos species and abundance in winter suggesting that the distribution of macrobenthos was strongly influenced by temperature. In summer, there was no significant correlation between ORP and the macrobenthos species and abundance. AVS has also no significant correlation between macrobenthos species and abundance. The reasons for these results are unknown now. The Hizen-Kashima Higata was a most harsh environment for organisms and the macrobenthos fauna was poorest in the mudflats in Kashima City. Therefore, for the conservation of mudflat ecosystem, it is sufficient to extend the conservation area. We will show the results including the monitoring in 2019-20 in the session.

This study was conducted under the financial support from Kashima City as a program “Coastal sea environmental monitoring program of Kashima City”.

©2020. Japan Geoscience Union. All Right Reserved.

Keywords: Ariake Sea, macrobenthos, bottom sediment quality, water quality, Kashima City

©2020. Japan Geoscience Union. All Right Reserved.

SST variability in Suruga Bay and its surrounding area due to Kuroshio path variability

*Yuya Hirano[1], Kazuyuki Uehara[1]

1. The Graduate School of Geo-environmental Science, Tokai University

The mouth of Suruga Bay is deep exceeding about 2500-m and wide open to the southward. Outer waters such as Kuroshio and Oyashio water can be, therefore, exchanged from not only surface layers but also intermediate and deep layers. And then the outer waters are mixed by the inner waters in Suruga Bay. This suggests that interactions between the outer and the inner seawaters are very important for understanding the thermohaline structure of Suruga Bay.

For thermohaline structure in Suruga Bay, Nakamura (1977) clarified basic temperature and salinity seasonal variations in the uppper 300-m layer of Suruga Bay using observational data from 1964 to 1974. Kimura and Sugimoto (1990) investigated the inflow process of Kuroshio warm water into Kumano and Ensyu Nada. In the results they pointed out that the periodic fluctuations in water temperature around 20 days in this coastal area were associated with the periodic inflow of the warm water separated from the Kuroshio water. Besides, Kutsuwada et al.(2007) showed that long term variabilities of temperature and salinity in the upper 200-m layer in Suruga Bay had relatively high correlations with the Kuroshio path. Relationships between the inner of Suruga Bay and Kuroshio have gradually been clarified from these studies.

However, the time interval of previous studies was monthly, which was too rough to resolve 10-60 days of timescales related to Kuroshio path fluctuations. In this presentation, we focus two Kuroshio large meader paths and Suruga Bay, and analyze the daily time series of Kuroshio’s current axes defined by absolute dynamic topography (AVISO) and of daily sea surface temperature fields derived by JMA.

Keywords: Kuroshio, Suruga Bay, SST, absolute dynamic topography

©2020. Japan Geoscience Union. All Right Reserved.

The seasonal cycle of phytoplankton biomass concentration along the coast of Japan

*Shimada Hiroaki[1], Shinichiro Kida[2]

1. Interdisciplinary Graduate School of Engineering Sciences , Kyushu University, 2. Research Institute for Applied Mechanics , Kyushu University

The seasonal cycle of phytoplankton biomass concentration was investigated along the coast of Japan using chlorophyll-a concentrations observed by Himawari8 from 2016 to 2019. Phytoplankton blooms are major oceanic events that support marine biological production. The growth rate of phytoplankton is known to vary depending on various factors, such as the thickness of the mixed layer, the strength of convection and turbulence, and the zooplankton biomass concentration. Observations show spring blooms occurring along the coastal region of Japan from late February to April and autumn blooms occurring from late August to October. We also found that the concentration was high in Ise Bay, Suruga Bay and off Kushiro throughout the year. In high-latitude waters, the timing of spring bloom is delayed and the timing of autumn bloom is earlier compared to lower latitude waters. Observations further show the inter-annual variability in the timing of spring and autumn blooms and we plan to investigate the mechanism behind these variabilities.

©2020. Japan Geoscience Union. All Right Reserved.

Modelling Study of the Zhe-Min Coastal current

*yang zhang[1], min bao[1]

1. Second Institute of Oceanography, MNR

Zhe-Min Coastal current is oriented from the Changjiang river estuary. It is driven by the Northeast monsoon in Winter and flow Southwestward along the Zhe-min coastal region. Zhe-min Coastal current carries abundant nutrients and fresh water from Changjiang river discharge, which is critical important for the evolution of coastal pelagic ecosystem and aquaculture. A SCHISM model is established to study the seasonal variation and extent of the Zhe-min coastal current. Besides the classic coastal branch, it is indicated by the model that after mixing with KETe, Zhe-min coastal current water will spread in the Taiwan strait and fresh the east side of the strait. The control mechanisms of the seasonal and annual variation of the Zhemin Coastal current are also analyzed.

Keywords: Zhe-min coastal current, control mechanism, unstructured model

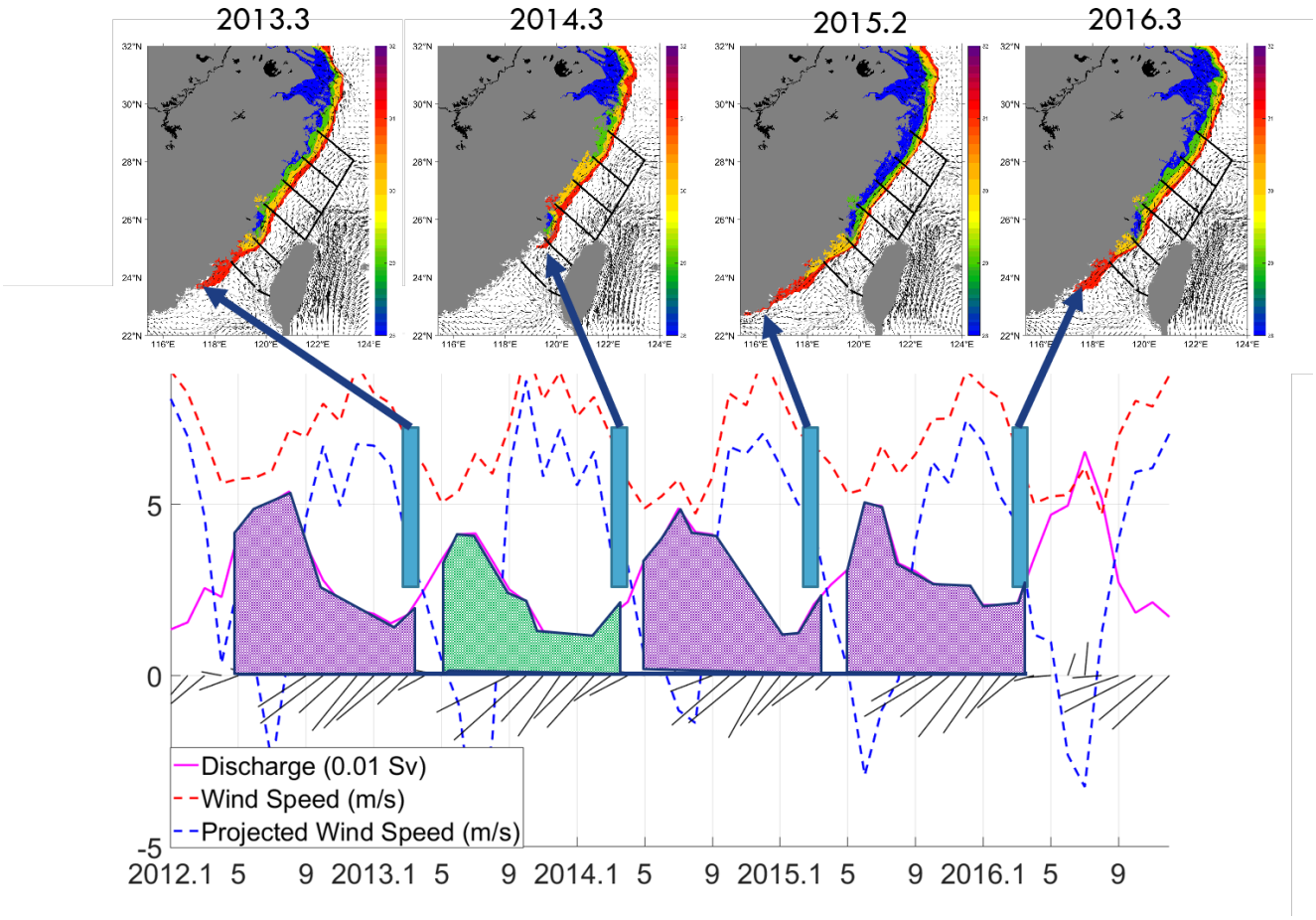

©2020. Japan Geoscience Union. All Right Reserved.

Sea surface temperature and chlorophyll *a* variations in the Sanriku Coastal area and their influence on the environment of Otsuchi Bay

*XUANYU LIU[1], Sachihiko Itoh[1], Eisuke Tsutsumi[1], Kiyoshi Tanaka[1]

1. University of Tokyo

Otsuchi bay is a typical Ria-type bay in the mid Sanriku Coast, and its high productivity and the bay topography are utilized to set net fisheries and aquacultures. Being semi-open to the offshore, the biological productivity of Otsuchi bay depends not only on the river discharge but also on the waters from the Tsugaru Warm Current, the Oyashio, and the Kuroshio (warm-core rings) outside the bay. A recent study conducting continuous observations at the bay mouth and inner bay revealed prominent seasonal variability in temperature and salinity in the bay, which was apparently corresponding to the seasonal fluctuations of the offshore currents. However, relationship between water mass and low-trophic productivity outside the bay and the environment inside the bay has yet to be investigated. Therefore, this study aims at capturing characteristics of water mass and chlorophyll a variability outside the bay, and clarifying their linkage to the environment inside the bay. Sea surface temperature (SST) and chlorophyll a concentration data from Himawari 8 and MODIS Aqua were analyzed and compared with the temperature time series from the Akahama monitoring station of Otsuchi Bay. According to the monthly long-term mean of MODIS Aqua from 2003 to 2018, a prominent boundary of the sea surface temperature was formed around 39–39.5˚N during summer and fall. At the same time, the chlorophyll a concentration increased from the southeast to the northwest. These features in the SST and the chlorophyll a concentration likely reflected the contrast between the Tsugaru Warm Current flowing southward from summer to fall and the Oyashio at the northwest. In winter, the SST was high and the chlorophyll a concentration was low in the coastal areas, consistent with the occurrence of the coastal mode of the Tsugaru Warm Current. The SST and subsurface temperature in the bay showed marked difference at a seasonal scale, suggesting the injection of the offshore water to the subsurface layer of the bay.

Keywords: Sanriku Coastal, Otsuchi Bay, Data analysis

©2020. Japan Geoscience Union. All Right Reserved.

Multi-layer temperature variability at Kurasawa on the back of Suruga Bay.

*Mito Nakamura[1], Kazuyuki Uehara[1]

1. tokai university the graduate school of marine science and technology

For the first time, Nakamura (1977) found the summer subsurface temperature drop in Suruga Bay from the 10-year mean monthly variability in temperature and salinity vertical profiles. He called this summer temperature drop ” Secondary Temperature Minimum” . In this study, we analyzed the time series obtained from the multi-layer water temperature system installed at Kurasawa, from 2008 to 2017 which was observed at a ten-minute interval. As a result, we found that the multi-layer temperature time series is devided into five parts concerning the time change. That is, 1. uniform heating period (April), 2.heating and stratification period (May to the middle of August), 3. surface cooling period (September to October), 4.temperature decrease period, and 5. the lowest temperature period (February and March). We, here, focus the second part, ” heating and stratification period” (May to the middle of August). In this period, the water temperature at a depth of 5-m increases due to surface heating, but decreases below deeper than 20-m. These phenomena are thought to be ” Secondary Temperature Minimum” pointed out by Nakamura (1977). Moreover, these subsurface temperature drops have time scale fluctuations smaller than a month and are very comlicated. We would like to discuss the variabilities of these phenomena in this presentation.

Keywords: Suruga Bay, Characteristics of water temperature, Coastal environment

©2020. Japan Geoscience Union. All Right Reserved.

[J] Poster | A (Atmospheric and Hydrospheric Sciences)：A-OS Ocean Sciences & Ocean Environment

[A-OS26] Global ocean observing systems, their recent status, research results and future directions

convener:Shigeki Hosoda(Japan Marine-Earth Science and Technology), Shuhei Masuda(Japan Agency for Marine-Earth Science and Technology), Yosuke Fujii(Meteorological Research Institute, Japan Meteorological Agency), Fujiki Tetsuichi(Japan Agency for Marine-Earth Science and Technology)

Ocean observing system has been grown up and is now at the turning point. The OceanObs19 was held in September 2019, which was discussed about status and questions of ocean observing system and their future direction in the next decade, introducing many fruitful research results. The importance of sustaining operating ocean observing systems such as Argo, GOSHIP and OceanSITE and expanding the observing system to other research fields or areas with improvement of technologies were discussed and highlighted, and then sustainably expanding and improving the global ocean observing systems were agreed with lots of researchers and users. Especially, since sustaining and expanding ocean observing systems are necessary to promote new researches and techniques based on a lot of accumulated data, developments of useful products for end users and efficiency investigations of the existing observing systems related to the Observing System Evaluations (OSEs) are recommended. On the other hand, there are still lacks of sharing knowledge and communications among observing communities, although creating such research and technical innovations must require collaborations among other communities and users. In this session, current status, recent research results, future works of the global/ basin-scale ocean observing systems will be discussed related to the context of OceanObs19, especially focusing on future directions of the oceanic observing system in coming next decade. Presentations and discussions of variable fields, areas, researches and techniques of the ocean are welcomed in this session.

[AOS26-P02] Introduction of bio-chemilcal observation data on GCM assimilation with a lower ecosystem model

*Takashi SETOU[1], Takeshi OKUNISHI[1], Hiroshi Kuroda[1], Naoki Yoshie[3], Shin-ichi Ito[2], Kiyotaka Hidaka[1], Taketoshi Kodama[1], Yugo SHIMIZU[1], Daiki Ito[1] (1.Fisheries Research and Education Agency, 2.University of Tokyou, 3.Ehime University)

[AOS26-P03] Progress of the decadal scale anthropogenic CO_2 in the Southern Ocean

*BOFENG LI[1], Xianliang Pan[1], Shun Yunoki[1], Yutaka Watanabe[1] (1.Hokkaido University)

[AOS26-P04] Spatiotemporal distribution of anthropogenic nitrogen and internal nitrogen dynamics in the Southern Ocean

*Xianliang Pan[1], Bofeng Li[1], Zhigang Chen[1], Yutaka Watanabe[1] (1.Hokkaido University)

[AOS26-P05] Initiation of biogeochemical float observations in the western North Pacific

*Fujiki Tetsuichi[1], Shigeki Hosoda[1] (1.Japan Agency for Marine-Earth Science and Technology)

[AOS26-P06] Small water mass transport across the Kuroshio Extension region in the thermocline by Seaglider and BGC Argo floats: Hints of integrated ocean observations

*Shigeki Hosoda[1], Ryu Inoue[1], Masami Nonaka[1], Hideharu Sasaki[1], Yoshikazu Sasai[1], Mizue Hirano[1] (1.Japan Marine-Earth Science and Technology)

[AOS26-P07] Halocline Structures in the Subarctic North Pacific Detected by Argo Data

*Shota Katsura[1], Ueno Hiromichi[2], Humio Mitsudera[3], Shinya Kouketsu[4] (1.Scripps Institution of Oceanography, University of California, San Diego, 2.Faculty of Fisheries Science, Hokkaido University, 3.Institute of Low Temperature Science, Hokkaido University, 4.Japan Agency for Marine-Earth Science and Technology)

[AOS26-P08] The propagation of spiciness anomalies in the upper North Pacific

*Tong Wang[1], Toshio Suga[1,2], Shinya Kouketsu[2] (1.Graduate School of Science, Tohoku University, 2. Japan Agency for Marine-Earth Science and Technology)

[AOS26-P09] Release of Deep Argo floats' salinity correction dataset

*Kanako Sato[1], Taiyo Kobayashi[1], Shigeki Hosoda[1], Shuhei Masuda[1] (1.Japan Agency for Marine-Earth Science and Technology)

[AOS26-P10] Boundaries of Physical Structures in the Mid-latitude Northwest Pacific Ocean Identified based on Unsupervised Clustering

*Fumika Sambe[1], Toshio Suga[1,2] (1.Graduate School of Science, Tohoku University, 2.JAMSTEC)

Introduction of bio-chemilcal observation data on GCM assimilation with a lower ecosystem model

*Takashi SETOU[1], Takeshi OKUNISHI[1], Hiroshi Kuroda[1], Naoki Yoshie[3], Shin-ichi Ito[2], Kiyotaka Hidaka[1], Taketoshi Kodama[1], Yugo SHIMIZU[1], Daiki Ito[1]

1. Fisheries Research and Education Agency, 2. University of Tokyou, 3. Ehime University

The sensitivity experiments has been carried out to assess the impact of bio-chemical data data in addition to the temperature and salinity on a GCM assimilation coupled with a lower ecosystem model. The data were obtained along 138E south of Japan by a research vessels Soyo-maru of NRIFS. It was found an introduction of the data to the coupled model enabled finely to represent some important events such as the occurrence of phytoplankton at the surface.

Keywords: lower ecosystem model, bio-chemical data

©2020. Japan Geoscience Union. All Right Reserved.

Progress of the decadal scale anthropogenic CO_2 in the Southern Ocean

*BOFENG LI[1], Xianliang Pan[1], Shun Yunoki[1], Yutaka Watanabe[1]

1. Hokkaido University

In this study, large CO_2 disequilibrium (C_{diseq}) was found in the range of −70 to −10 μmol kg^{-1} in the Southern Ocean (SO). When we tried to formulate this C_{diseq}, C_{diseq} had a strong correlation with the potential water temperature (θ) (C_{diseq} = 1.766θ −45.07; R = 0.71, RMSE = 9.05 μmol kg^{-1}). This equation was applied to the vertical data obtained in the cruise of KARE22_UM-18-08. From the distributions of C_{diseq} and anthropogenic CO_2 (C_{ant}) in the north-south direction, we found that a large amount of C_{anth} is absorbed from the atmosphere to the ocean surface in high-latitude where high-density seawater exists.

Then, we constructed simple equations to predict dissolved inorganic carbon (DIC) and pH with high precision in the entire SO (south of 30° S) by using a hydrographic general dataset for dissolved oxygen, water temperature, salinity, and pressure. To estimate ΔC_{ant} variation in the SO, we applied a new method (that combined the parameterization technics with observational data (*Watanabe et al.*, 2018)) to high-resolution grid data constructed based on ship-based observations from 1990 to 2017. As a result, we determined the ocean uptake of C_{ant} in the SO over the past two decades. DIC increases by anthropogenic effect account for 60% of the variation of DIC in the SO.

Keywords: Southern Ocean, Air-sea CO2 disequilibrium, Anthropogenic CO2

©2020. Japan Geoscience Union. All Right Reserved.

Spatiotemporal distribution of anthropogenic nitrogen and internal nitrogen dynamics in the Southern Ocean

*Xianliang Pan[1], Bofeng Li[1], Zhigang Chen[1], Yutaka Watanabe[1]

1. Hokkaido University

The oceanic external nitrogen (N_{ex}) deposition to the global ocean is expected to rise significantly owing to human activities. The Southern Ocean (SO) is an important pathway, which brings external influences into the ocean. It touches the borders of several developing countries that emit a large amount of anthropogenic nitrogen. To comprehend the dynamics of N_{ex} in the SO, We developed a new method to assess the change in the oceanic uptake of N_{ex} (ΔN_{ex}) in the entire SO. We obtained the spatiotemporal distribution of ΔN_{ex} in the SO by applying this method to a high-resolution grid data constructed using ship-based observations. During the 1990s to the 2010s, N_{ex} increased significantly by 67±1 Tg-N $year^{-1}$ in the SO. By comparing this with the rate of N_{ex} deposition to the ocean, the SO has received ~ 70% of N_{ex} deposition to the global ocean, indicating that it is the largest uptake region of anthropogenic nitrogen into the ocean interior. Additionally, in order to comprehensively understand the impact of natural nitrogen dynamics on N_{ex} transportation in the ocean interior, We have also quantified the nitrogen budget over the 110°E line using the chemical tracer N_2^*. The natural nitrogen balance of SO was found to be controlled primarily by physical processes, rather than being consumed by living organisms. As a result, N_{ex} is also possibly spreading from the SO to the global ocean through transportation of water mass.

Keywords: Southern Ocean, Anthropogenic nitrogen, Decadal variation, Nitrogen budget

©2020. Japan Geoscience Union. All Right Reserved.

Initiation of biogeochemical float observations in the western North Pacific

*Fujiki Tetsuichi[1], Shigeki Hosoda[1]

1. Japan Agency for Marine-Earth Science and Technology

One of the goals in present-day ocean biogeochemistry is to gain a better understanding of the variability in phytoplankton productivity with changing physical and chemical structure of the upper ocean. However, ship-based studies of the open ocean have been limited in their ability to conduct high-frequency observations for understanding variations in phytoplankton productivity and environmental parameters. Also, satellite image analysis is a powerful tool for measuring phytoplankton productivity and environmental parameters, but the information on satellite data is limited to the near-surface layers. To overcome these problems, we started using profiling floats incorporating biogeochemical sensors which enable *in situ* measurements of phytoplankton productivity and environmental parameters over high vertical and temporal resolutions, and have carried out time-series observations in the western North Pacific. Here, we show the results of observations in the western North Pacific by the biogeochemical floats.

Keywords: BGC Argo floats, phytoplankton, western North Pacific

©2020. Japan Geoscience Union. All Right Reserved.

Small water mass transport across the Kuroshio Extension region in the thermocline by Seaglider and BGC Argo floats: Hints of integrated ocean observations

*Shigeki Hosoda[1], Ryu Inoue[1], Masami Nonaka[1], Hideharu Sasaki[1], Yoshikazu Sasai[1], Mizue Hirano[1]

1. Japan Marine-Earth Science and Technology

Integrated ocean observations make it possible to realize detailed information of water mass modifications or their exchanges rather than any single observation only. Regarding water mass across the Kuroshio Extension, clarifying not only their physical mechanisms but also their spatial and time scales are crucial to understand heat, freshwater and materials budget. Especially in the northwestern North Pacific Ocean, deep mixed layer is actively formed by strong winter cooling, and major water masses, such as STMW, CMW, and NPIW, are broadly produced. Based on the situation, we observed small water mass characteristics and their changes by autonomous in-situ measurement tools. One was BGC Argo floats and the other was a Seaglider. In 2011-2012, over 30 BGC-Argo floats with dissolved oxygen sensors had been deployed around 30N,145E within a framework of S1-INBOX project in JAMSTEC, which aimed to clarify small scale physical and geochemical processes of a mesoscale eddy. Further, the Seaglider had launched in 2014 around the south of Kuroshio Extension to investigate water mass formation and modification process, continuously operating for 4 months. The Seaglider is able to measure sea water temperature, salinity and dissolved oxygen every 4-6 hours, diving from surface to 1000 dbar. The profiling data were also delivered every 1-10 km of fine horizontal resolution. From these observations, we obtained detailed temperature, salinity and oxygen data with dense spatial and temporal resolutions in the Kuroshio Extension. The analysis of the Seaglider data shows that small water mass with low salinity and/or low dissolved oxygen were observed in the lower thermocline (26.0- 26.8 $\sigma\ \theta$) during middle of April to early May, whose scales were ~ a few ten kilometers for horizontal width and ~ a few ten meters for vertical thickness. Based on apparent oxygen utility (AOU) analysis, the small water mass had characteristics of less amount of oxygen consumption, suggesting that the water mass took shorter time after contacting atmosphere than surrounded water. Also, the water parcels subducted from subpolar northwestern North Pacific region to the north of the Kuroshio Extension. Similar small water parcels with the same characteristics had been observed by the BGC Argo floats operating in the S1-INBOX project. Here we discuss a possibility of integrated ocean observations with BGC- Argo and Seaglider to clarify a detailed oceanic variability more than ever, showing scientific results based on the individual tools and comparing with a high-resolution numerical model.

Keywords: Dissolved oxygen, BGC Argo, Integrated ocean observation

©2020. Japan Geoscience Union. All Right Reserved.

Halocline Structures in the Subarctic North Pacific Detected by Argo Data

*Shota Katsura[1], Ueno Hiromichi[2], Humio Mitsudera[3], Shinya Kouketsu[4]

1. Scripps Institution of Oceanography, University of California, San Diego, 2. Faculty of Fisheries Science, Hokkaido University, 3. Institute of Low Temperature Science, Hokkaido University, 4. Japan Agency for Marine-Earth Science and Technology

The halocline is a region with a strong vertical salinity gradient, occurring between an overlying low-salinity layer and an underlying high-salinity layer. When the halocline has the dominant contribution to density stratification and thus creates a coinciding pycnocline, the vertical exchange of heat and substances such as nutrients is limited. In the subarctic North Pacific (SNP), a sharp halocline forms a pycnocline and dominates the vertical distribution of heat and biogeochemical parameters. This feature is thought to play an important role in air-sea interaction and biological production. However, the SNP halocline has been far less studied due to the limited availability of salinity data. Recent accumulation of Argo profiling float data has enabled expansive investigation of the halocline structure over the entire SNP. The spatial distribution and seasonality of the halocline in the SNP were investigated using Argo profiling float data. The permanent halocline (PH) showed zonal patterns in the spatial distribution of its depth and intensity. The PH tended to be shallow and strong in the eastern SNP but deep and weak in the west. Mean distributions of the PH depth and intensity corresponded to the winter mixed layer depth and sea surface salinity, respectively. In the Western Subarctic Gyre and Alaskan Gyre, where a relatively strong PH formed, PH intensity and depth showed clear seasonal variations, and deepening of the mixed layer compressed the underlying PH during the cooling period, resulting in intensification and development of the PH in late winter. In both regions, upwelling of high-salinity water also contributed to PH intensification. These results indicate the formation of PH through vertical winter mixing and upwelling. The summer seasonal halocline (SH) showed distinct zonal differences in frequency and intensity, which were opposite to the PH distribution. While an SH formed in the western and central SNP, it was seldom present in the eastern area. This zonal contrast of SH corresponded to freshening of the mixed layer during the warming period, primarily reflecting surface freshwater flux.

Keywords: Pacific, Subarctic Region, Halocline

©2020. Japan Geoscience Union. All Right Reserved.

The propagation of spiciness anomalies in the upper North Pacific

*Tong Wang[1], Toshio Suga[1,2], Shinya Kouketsu[2]

1. Graduate School of Science, Tohoku University, 2. Japan Agency for Marine-Earth Science and Technology

The density-compensated temperature and salinity anomalies, referred to as spiciness anomalies, measure the variations of water mass properties on isopycnals. With the improvement of observing systems, spiciness anomalies have been detected in global ocean, and some recent studies discovered the propagation of spiciness anomalies, but limited to certain regions and relatively short periods. Some numerical models separated and quantified different processes in propagating spiciness signals. However, the quantitative interpretation of the propagation of spiciness anomalies by observational study is still lacking.

Using Argo float observations during 2004~2015, this study investigates spiciness anomalies in the upper North Pacific on neutral density surfaces. Firstly, we explored three major water masses in the upper North Pacific, Subtropical Mode Water (STMW), Eastern Subtropical Mode Water (ESTMW), and Central Mode Water (CMW). Interannual or decadal variability of spiciness are detected, as well as their propagation. To explain the propagation of spiciness anomalies, we calculated the geostrophic velocity on neutral density surfaces, and trace the spiciness anomalies along the mean geostrophic streamlines in the subtropical gyre. Despite high-frequency spiciness variability near the outcrop region, low-frequency spiciness signals of each phase propagate and decay downstream the mean geostrophic streamlines. The propagation paths of spiciness anomalies are highly consistent with the mean flows, but the propagation speeds of spiciness signals are faster than those of the mean advection, especially in regions where the zonal component of geostrophic current is westward. This difference of speeds implies the influences of anomalous advection and other processes.

Furthermore, to quantify the different processes in propagating spiciness signals, we used a conservation equation for salinity anomalies on isopycnal surfaces, and integrated each term along the geostrophic streamlines. As a result, the mean advection of the anomalous spiciness gradient is dominant along the propagation paths, the anomalous advection of the mean salinity gradient is important in generating local signals, and there are also influences of the covarying velocity and spiciness anomalies fields. The total sum of above terms should equal to the spiciness anomaly variability in an eddy-resolving model. However, there is a meaningful difference, which could be caused by estimating the advection only by geostrophic currents in 1°×1° observation resolution, suggesting the effects of processes such as mesoscale/submesoscale eddies. Here, we could interpret this difference in terms of bolus velocity and others.

Keywords: mode water, salinity anomalies, Argo

©2020. Japan Geoscience Union. All Right Reserved.

Release of Deep Argo floats' salinity correction dataset

*Kanako Sato[1], Taiyo Kobayashi[1], Shigeki Hosoda[1], Shuhei Masuda[1]

1. Japan Agency for Marine-Earth Science and Technology

Introduction

Thanks to the broad-scale global array of temperature/salinity profiling floats, known as Argo, temperature and salinity data from sea surface to 2000dbar, which is half of the average ocean depth, has been accumulated, and the temporal changes in ocean heat storage etc. have become apparent. On the other hand, ship-based high-quality hydrography such as GO-SHIP have revealed that the effects of changes in the deep ocean are not negligible to the global environment.

For this reason, the necessity of broad-scale monitoring of the deep ocean has been recognized, and as one method, profiling floats for deep ocean have been recently developed. The Japan Agency for Marine-Earth Science and Technology (hereafter, JAMSTEC) has developed and is operating deep-sea profiling floats “Deep NINJA” with Tsurumi-Seiki Co., Ltd. In addition, in order for monitoring up to 6000dbar, JAMSTEC has deployed another deep-sea profiling floats “APEX-Deep” developed in the United States since November, 2017. As of 14 February, 2020, 23 APEX-Deep floats are in operation in Pacific, Indian and Southern Oceans.

APEX-Deep float has a CTD sensor developed for deep-sea profiling floats. It was recently found that the anomaly between salinity measured by this CTD sensor and the ship-board salinity at float deployment has negative pressure dependence (Kobayashi and Sato (in preparation)). Therefore, we corrected the salinity data measured by APEX-Deep floats. Here, we introduce the dataset and report the temporal variation of salinity anomaly.

APEX-Deep floats

APEX-Deep floats are profiling floats for deep sea manufactured and sold by TELEDYNE MARINE, USA. APEX-Deep float can measure up to 6000dbar and have the CTD sensor for deep sea, SBE61, manufactured by Sea Bird Scientific of the United States.

APEX-Deep salinity correction method

We compared salinity measured by APEX-Deep with ship-board salinity data at float deployment. As a result, we confirmed negative pressure dependence (the higher pressure, the lower salinity) (Kobayashi and Sato (in preparation)). Since salinity anomaly and pressure are close to a linear relationship, salinity measured by APEX-Deep were corrected by assuming a regression line of the pressure. As a result, corrected salinity deeper than 2200dbar had an accuracy of ±0.001. In addition, the salinity anomaly in the deep layer was stable for about 3 months.

APEX-Deep floats’ salinity correction dataset

We release the salinity dataset corrected by the method described above. Of the APEX-Deep floats deployed so far, floats with obvious defects in the CTD sensors have been excluded from correction

©2020. Japan Geoscience Union. All Right Reserved.

targets. Furthermore, for floats in which a failure occurred in the CTD sensors during operation, profiles acquired after the failure occurred were excluded from correction targets. The dataset included APEX-Deep floats data for which the ship-board CTD data at their deployments are available. As soon as ship-board CTD data at float deployment is available, salinity measured by APEX-Deep will be corrected and added to this dataset. Since many APEX-Deep floats are in operation, the dataset should be updated once a month. The dataset will be released in two formats, csv and netcdf. We will introduce URL of dataset in our presentation.

Keywords: Argo floats, Deep sea, Salinity

©2020. Japan Geoscience Union. All Right Reserved.

Boundaries of Physical Structures in the Mid-latitude Northwest Pacific Ocean Identified based on Unsupervised Clustering

*Fumika Sambe[1], Toshio Suga[1,2]

1. Graduate School of Science, Tohoku University, 2. JAMSTEC

The mid-latitude Northwest Pacific Ocean is a region where waters of subtropical and subarctic origin collide, and has been characterized by many boundaries of the spatial distribution of seawater properties, such as the Kuroshio Extension front. It is important to understand the nature of these boundaries correctly, because the location of these boundaries varies seasonally and interannually, and may lead to changes in property of atmosphere-ocean interaction and ecosystem. Until now, a boundary in the mid-latitude Northwest Pacific has been defined as a specific isotherm or isohaline over a specific depth plane, such as the 12˚C isotherm over a 300-m depth plane for the Kuroshio Extension. Such a boundary definition was defined about 40 years ago, when spatiotemporal distribution of ocean data was insufficient, so that the boundary could be determined from temperature and salinity information at only a specific depth, such as 100 or 300 m. Today, the marine environment is changing due to climate change, and the 40-year-old definition may not correctly identify the boundaries. In addition, with the expansion of Argo float array since 2000, a large amount of vertically multi-layered oceanic data is now evenly available in space and time, and it is now possible to identify the boundaries with new methods. In this study, we classified the ocean area using Profile Classification Model (PCM), a method for classifying profile shapes by applying unsupervised clustering, a type of machine learning, to Argo data, and aimed to identify the boundary by focusing on the border of these areas. PCM was developed by Dr. Guillaume Maze at the Ifremer. Previous research has shown that when this method is applied to Argo data for the North Atlantic and the Southern Ocean, the distribution of each class is concentrated in a specific region on the map. Therefore, it is possible to objectively investigate where the seawater with certain properties is located and where the boundaries where the properties of the seawater change are located. We used approximately 20 years of vertical temperature and salinity data from Argo floats in the mid-latitude Northwest Pacific (30-60˚N and 140-180˚E) at depths of 5-1000 m. As a result of performing PCM with the number of classes being set to 5~9, it was observed that each class constitutes a specific area in each case, and the area was subdivided as the number of classes increased. When the number of classes was set to 7, the locations of the borders of each class generally coincided with the four boundaries of the Kuroshio Extension, the Kuroshio Extension Northern Branch, Subarctic Boundary, and Subarctic Front. This suggests that PCM is an effective method to identify the boundaries.

Keywords: Mid-latitude Northwest Pacific Ocean, Kuroshio Extension front, Subarctic Boundary, Argo float, Unsupervised Clustering, Machine Learning

©2020. Japan Geoscience Union. All Right Reserved.

[J] Poster | A (Atmospheric and Hydrospheric Sciences)：A-OS Ocean Sciences & Ocean Environment

[A-OS27] Chemical and Biological Oceanography

convener:Kazuhiro Misumi(Environmental Science Research Laboratory, Central Research Institute of Electric Power Industry), Sayaka Yasunaka(Japan Agency for Marine-Earth Science and Technology)

This session invites presentations on a wide variety of topics related to chemical and biological oceanography.

[AOS27-P01] Evaluation of uncertainty of nutrient measurements

*Daisuke Sasano[1], Michio Aoyama[2,3], Toshiya Nakano[4], Naoki Nagai[1] (1.Japan Meteorological Agency, 2.University of Tsukuba, 3.JAMSTEC, 4.Nagasaki Meteorological Office)

[AOS27-P02] Effect of ocean acidification on bioavailability of iron bound to natural iron-complexing ligands

*Shigenobu Takeda[1], Koichi Hideshima[1], Yoshiko Kondo[1], Mitsuhide Sato[1] (1.Nagasaki University)

[AOS27-P03] Radiocesium in the Kuroshio region and the Taiwan Strait from 2017 to 2018

*Wei-Jen Huang[1], Chen-Tung Arthur Chen[1], Ming-An Lee[2], Sen Jan[3], Yiing-Jang Yang[3] (1.National Sun Yat-sen University, 2.National Taiwan Ocean University, 3.National Taiwan University)

[AOS27-P05] pH measurement of transparent exoplymeric particles secreted by oceanic diatoms

*Tasuku Akagi[1], Rin Ito[2], Takeshi Ishihara[3] (1.Department of Earth and Planetary Sciences, Kyushu University, 2.Department of Earth and Planetary Sciences, Faculty of Sciences, Kyushu University, 3.Department of Biology, Kyushu University)

Evaluation of uncertainty of nutrient measurements

*Daisuke Sasano[1], Michio Aoyama[2,3], Toshiya Nakano[4], Naoki Nagai[1]

1. Japan Meteorological Agency, 2. University of Tsukuba, 3. JAMSTEC, 4. Nagasaki Meteorological Office

Nutrient is one of the fundamental parameters in the biogeochemistry of the ocean. It reflects biogeochemical cycle through biological activities. Because changes in nutrient concentrations reflect changes in the physical and biological processes, it is useful as a tracer to detect the changes in the ocean. However, because nutrient data includes a systematic error in analysis due to the lack of comparability among stations and cruises, it is difficult to detect the difference of nutrient in the ocean. Nutrient certified reference materials (CRMs) have been available since about 10 years ago. With measurement of CRMs, the comparability can be ensured among stations and cruises. Additionally, uncertainty of measurement of nutrient can be evaluated. Through comparison of nutrient data with uncertainty, it is possible to detect a significant change in nutrient concentration. The Japan Meteorological Agency has measured nutrient concentrations in ocean observations. Since April 2010, nutrient CRMs have been analyzed at all stations to ensure comparability between cruises and stations. In this presentation, we show our quality control in the nutrient measurement, and discuss the factors of uncertainty. Additionally, we examine nutrients change using our data acquired in the Japan Sea, where significant oxygen decrease has been observed recently.

Keywords: nutrient, uncertainty, CRM

©2020. Japan Geoscience Union. All Right Reserved.

Effect of ocean acidification on bioavailability of iron bound to natural iron-complexing ligands

*Shigenobu Takeda[1], Koichi Hideshima[1], Yoshiko Kondo[1], Mitsuhide Sato[1]

1. Nagasaki University

Ocean acidification will affect the chemistry and biology of future oceans, and may change the availability of iron to phytoplankton. Iron is a limiting micronutrient in large oceanic regions, including High Nitrate Low Chlorophyll (HNLC) subarctic Pacific, and a critical factor in many nearshore regions such as the coastal California upwelling system. Most of the iron dissolved in seawater is known to be strongly complexed by natural organic ligands. The potential effect of a decrease in pH on iron availability is mainly due to changing the chemical equilibria among free, inorganic iron species and the organic complexes. The limited data on how ocean acidification affects iron availability imply that phytoplankton respond to ocean acidification differently in different ocean regions with a mechanistical link to differences in the character of the iron-complexing organic ligands.
We performed laboratory culture experiments using a marine diatom *Thalassiosira* sp. isolated from the HNLC water of the western subarctic Pacific, and its growth responses at low and high pH/pCO_2 were compared between surface waters collected from the western and eastern subarctic Pacific and subsurface water of the California coastal upwelling region. Before the inoculation of iron-limited diatom cells, the filtered seawater was spiked with 0.5 nM $FeCl_3$ and allowed to equilibrate for 24 hour with natural iron-binding ligand, and pH/pCO_2 was manipulated by bubbling the CO_2:air mixed gases.
The specific growth rate of diatom in the surface water from the western subarctic Pacific (Stn. K2) decreased with decreasing pH from 7.9-8.0 to 7.5-7.6. The observed increase in the consumption ratio of silicic acid and nitrate (Si/N) supports decreased iron availability at lower pH. Opposite trend was observed in the subsurface water of California coastal region. Decreasing the pH increased the specific growth rate, indicating increased iron availability. The relatively low growth rate observed at higher pH suggests that diatoms can not efficiently use iron bound to natural iron-complexing ligands in the subsurface water. The effect of pH in experiments using surface seawater collected from the eastern subarctic Pacific (Stn. P) was not statistically significant, but there was an increasing trend in the specific growth rate with decreasing pH. These results suggest that ocean acidification over the next century will alter the availability of iron in these surface waters differently and may affect future primary production.

Keywords: Ocean acidification, Iron, Phytoplankton, Organic ligand

©2020. Japan Geoscience Union. All Right Reserved.

Radiocesium in the Kuroshio region and the Taiwan Strait from 2017 to 2018

*Wei-Jen Huang[1], Chen-Tung Arthur Chen[1], Ming-An Lee[2], Sen Jan[3], Yiing-Jang Yang[3]

1. National Sun Yat-sen University, 2. National Taiwan Ocean University, 3. National Taiwan University

Anthropogenic radiocesium, such as, long half-lives ^{137}Cs (30.2 yr) and short half-lives ^{134}Cs (2.06 yr), were exported to the Pacific Ocean through atmospheric deposition and direct discharge by the global fallout from atmospheric nuclear weapons testing (which peaked in the early 1960s) and the Fukushima Daiichi nuclear power plants (FDNPPs) accident in 21 century. However, the spatial distribution of ^{137}Cs and ^{134}Cs around the Kuroshio Current and the Taiwan Strait is still unclear. This study collects near-surface waters (shallower than 5 m depth) and subsurface to deep waters (10 m to deeper than 200 m) to analyze ^{134}Cs and ^{137}Cs in the region among 116-123˚E and 20-27˚N from 2018 to 2019. The result displays that ^{134}Cs activity in all samples was below the detection limit (0.6 Bq·m^{-3}). The average of ^{137}Cs activity in the near-surface water was 1.2±0.3 Bq·m^{-3} and was among the range reported by previous studies in the near-surface water at the western North Pacific Ocean. A maxima value of ^{137}Cs in the subsurface water was 2.2 mBq·m^{-3} at 200 m depth. We analyze the water temperature, salinity, and density with ^{137}Cs activity and suggest that the distribution of ^{137}Cs activity was related to the water mass transportation in this study area.

Keywords: cesium-137, cesium-134, Fukushima

©2020. Japan Geoscience Union. All Right Reserved.

pH measurement of transparent exoplymeric particles secreted by oceanic diatoms

*Tasuku Akagi[1], Rin Ito[2], Takeshi Ishihara[3]

1. Department of Earth and Planetary Sciences, Kyushu University, 2. Department of Earth and Planetary Sciences, Faculty of Sciences, Kyushu University, 3. Department of Biology, Kyushu University

The benefitial roles of transparent exopolymer particles (TEP) to secreting diatoms are open to question. TEP are known to be secreted in a greater amount when the nutrient condition is poorer. They are more viscous at deficient nutrient conditions. In this study we measured pH of TEP using flourescent indicators under a microscope. pH of TEP attached to living diatoms was found very low, whereas that from isolated TEP was moderate. In the presentation, the peripheral observation using microscopes, which seems relevant to physilogical roles of diatomaceous TEP will also be shown and discussed.

Keywords: diatom, transparent exopolymer particles, pH

©2020. Japan Geoscience Union. All Right Reserved.

[J] Poster | A (Atmospheric and Hydrospheric Sciences)：A-OS Ocean Sciences & Ocean Environment

[A-OS28] Physical Oceanography (General)

convener:Yoshimi Kawai(Research Institute for Global Change, Japan Agency for Marine-Earth Science and Technology), Kitade Yujiro(Tokyo University of Marine Science and Technology)

This session invites presentations on a wide variety of topics related to physical oceanography, including observation, theory, technology, and numerical modeling.

[AOS28-P01] Upper-Ocean Circulation Anomalies of the Western Equatorial Pacific Observed in 2016 Summer

★Invited Papers

*Yilong Lyu[1] (1.Institute of Oceanology, Chinese Academy of Sciences)

[AOS28-P02] **Seasonal variability of the Upper Mixed Layer Temperature in Sulawesi Sea**

*Xiaofang Wan[1], Aijun Pan[1] (1.Third Institute of Oceanography, Ministry of Natural Resources,China)

[AOS28-P04] **Response of Near-Inertial Shear to Wind Stress Curl and Sea Level**

*Jing Gao[1,2], Jianing Wang[1,3], Fan Wang[1,2,3] (1.Institute of Oceanology, Chinese Academy of Sciences, 2.University of Chinese Academy of Sciences, 3. Laboratory for Ocean and Climate Dynamics, Qingdao National Laboratory for Marine Science and Technology)

[AOS28-P05] **The ocean-atmosphere interaction over a summer upwelling system in the South China Sea**

*Yi Yu[1], Yuntao Wang[1] (1.State Key Laboratory of Satellite Ocean Environment Dynamics, Second Institute of Oceanography, Ministry of Natural Resources)

[AOS28-P06] Tracking Experiment of adrift object using Surface Drifter in Southeast coast 2019

*SeungYun HA[1], YoungTaeg Kim[1], SeokJae Kwon[1], JaeMin Kim[1], JooEun KIM[1], Ho-Kyun Kim[1] (1.Korea Hydrographic and Oceanographic Agency, Busan, Republic of Korea)

[AOS28-P07] Prediction of Storm Surge due to Typhoon passing Korea using by Machine Learning

*Boonsoon Kang[1], Jongjib Park[2], Wanhee Cho[3], Jongyoon Mun[3], Seokjae Kwon[1], Eunil Lee[1] (1.Ocean Research Division, Korea Hydrographic and Oceanographic Agency(KHOA), 2.Department of Coastal Management, Geosystem Research Corporatio, 3.Oceanographic Division, Marine information Technology Corporation)

[AOS28-P08] Impact of applying tidal correction to marginal-sea bathymetry dataset

*Katsuto Uehara[1] (1.Kyushu University)

[AOS28-P09] Changes of the obduction and subduction rates accompanied by anomalous winters

*Yoshimi Kawai[1], Kazuyuki Uehara[2], Shigeki Hosoda[1] (1.Research Institute for Global Change, Japan Agency for Marine-Earth Science and Technology, 2.School of Marine Science and Technology, Tokai University)

[AOS28-P12] Estimation of duration for 2017 Kuroshio large meander

*Takashi SETOU[1], Yugo SHIMIZU[1], Akira KUSAKA[1], Daisuke AMBE[1], Daiki Ito[1], Takuhiko KAMEDA[1] (1.Fisheries Research and Education Agency)

[AOS28-P13] **Baroclinic vertical modes around the East Asian seas**

*You-Soon Chang[1], Byeong-Jun Lim[1], Do-Youn Kim[2] (1.Kongju National University, 2.Ara Consulting & Technology)

Upper-Ocean Circulation Anomalies of the Western Equatorial Pacific Observed in 2016 Summer

*Yilong Lyu[1]

1. Institute of Oceanology, Chinese Academy of Sciences

Mooring measurements at ~140°E in the western equatorial Pacific documented greatly intensified eastward subsurface currents, which largely represents the nascent Equatorial Undercurrent (EUC), to ~67 cm s^{-1} in boreal summer of 2016. The eastward currents occupied the entire upper 500 m, with the westward surface currents nearly diminished. Similar variations were also observed during previous El Niño events, as suggested by historical in-situ data. Further analysis combining satellite and reanalysis data reveals that the eastward currents observed at ~140°E are a component of an anomalous counterclockwise circulation straddling the equator, with westward current anomalies retroflecting near the western boundary and feeding southeastward current anomalies along New Guinea coast. A 1.5-layer reduced-gravity ocean (RGO) model is able to crudely reproduce these variations, and a hierarchy of sensitivity experiments are performed to understand the underlying dynamics. The observed circulation anomalies are largely the delayed ocean response to the strong equatorial wind anomalies over the central-to-eastern Pacific basin emerging in the mature stage of El Niño (September-April). Downwelling equatorial Rossby waves are generated by the reflection of equatorial Kelvin waves and easterly wind anomalies in the eastern Pacific. Upon reaching western Pacific, the Southern Hemisphere lobe of Rossby waves encounter the slanted New Guinea island and deflects equatorward, establishing a local sea surface height maximum near the equator and leading to the detour of westward currents flowing from the Pacific interior. Additional experiments with edited western boundary geometry confirm the importance of topography in regulating the structure of this cross-equatorial anomalous circulation.

Keywords: ENSO, OCEAN CIRCULATION, OCEAN OBSERVATION

©2020. Japan Geoscience Union. All Right Reserved.

Seasonal variability of the Upper Mixed Layer Temperature in Sulawesi Sea

*Xiaofang Wan[1], Aijun Pan[1]

1. Third Institute of Oceanography, Ministry of Natural Resources,China

Using all available data, including remotely sensed SST, rainfall, surface winds, sea level anomaly and assimilated temperature product, seasonal changes of the upper ocean hydrodynamic features are investigated in Sulawesi Sea. It reveals that Sulawesi Sea maintains a high SST exceeding 28.5℃ all-year round and specifically, a cold tongue-like SST pattern emanating from eastern gap between Philippines and Sangihe Islands can be detected in wet season and which, is assumed to be a branch of the ITF intrusion under favorable northeast monsoon forcing.
Further by employing an thermal equilibrium equation, contributions from Surface heat forcing, Ekman advection, Geostrophic advection and Vertical entrainment to the mixed layer temperature tendency are diagnosed quantitatively. It presents that upper mixed layer temperature has drastic seasonality in Sulawesi Sea. As regard to the wet season, Surface heat forcing, Ekman advection and Geostrophic advection all tends to warm the mixed layer during the cooling period (October-January), except the Vertical entrainment, which acts to cool the mixed layer with -0.14℃/month cooling rate. Comparatively, Surface heat forcing contributes over 79% to the mixed layer warming in the warming phase from February to April. As for the dry season, Ekman advection and Vertical entrainment contributes -0.23℃/month and -0.25℃/month, respectively, to the mixed layer cooling and largely offsets warming effect induced by Surface heat forcing in the cooling phase of the mixed layer. And for the warming period, again, Surface heat forcing is testified to be a dominant contributor, with 0.27℃/month warming effect. Further exploration suggests that impacts from Geostrophic advection on the mixed layer temperature exists throughout the whole calender year, but with relatively subtle contribution.

Keywords: Sulawesi Sea, mixed layer, surface heat forcing, geostrophic advection, vertical entrainment

©2020. Japan Geoscience Union. All Right Reserved.

Response of Near-Inertial Shear to Wind Stress Curl and Sea Level

*Jing Gao[1,2], Jianing Wang[1,3], Fan Wang[1,2,3]

1. Institute of Oceanology, Chinese Academy of Sciences, 2. University of Chinese Academy of Sciences, 3. Laboratory for Ocean and Climate Dynamics, Qingdao National Laboratory for Marine Science and Technology

Near-inertial waves (NIWs) contain a pronounced portion of shear energy in the internal wave field and is of great importance to deep ocean mixing. However, accurate simulation of NIWs remains a challenge. Here we analyzed 3-year long mooring observation of velocity profiles over 80-800 m to study the responses of near-inertial downward shear to varying wind stress curls and sea level anomalies (SLAs). It is demonstrated that moderate (even weak) cyclone makes more contributions to enhanced shear below the pycnocline than very strong cyclone. Because very strong curl can stall the downward propagation of large shear. The large positive and negative SLAs cause the accumulation of large shear in the lower and upper parts of the pycnocline through inducing downwelling and upwelling motions, respectively. Time variation of near-inertial shear was strongly influenced by cases of large curls and interannual variation of SLA, and thus did not follow the seasonal variation of wind stress. Our analyses suggest that matched fields of wind stress curl and SLA, and well representing the ocean response to moderate cyclone are needed in simulating the role of NIWs on mixing.

Keywords: near-inertial shear, wind stress curl, sea level

©2020. Japan Geoscience Union. All Right Reserved.

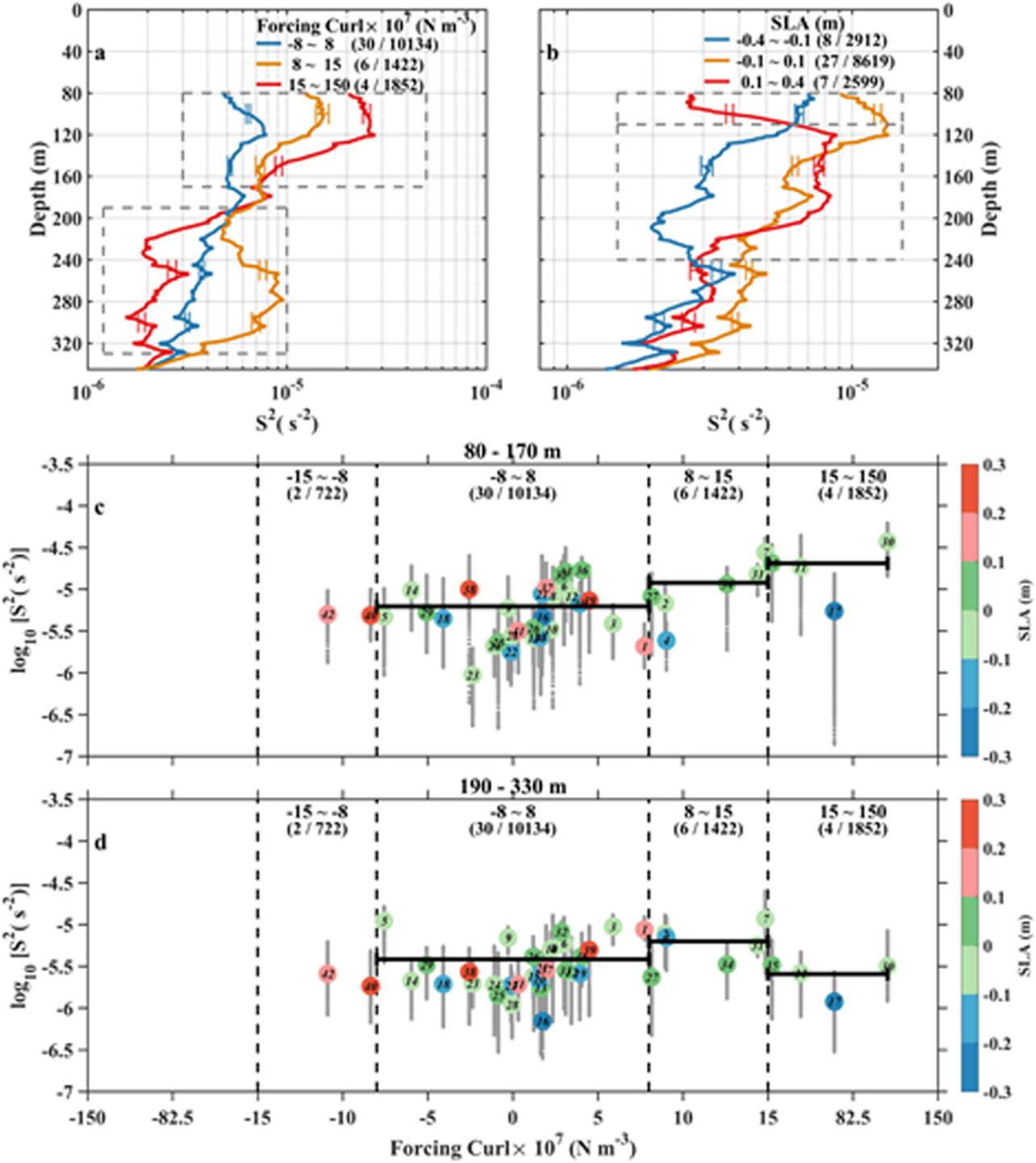

©2020. Japan Geoscience Union. All Right Reserved.

©2020. Japan Geoscience Union. All Right Reserved.

The ocean-atmosphere interaction over a summer upwelling system in the South China Sea

*Yi Yu[1], Yuntao Wang[1]

1. State Key Laboratory of Satellite Ocean Environment Dynamics, Second Institute of Oceanography, Ministry of Natural Resources

The ocean-atmosphere interaction over a summer upwelling system is investigated in the South China Sea (SCS). A strong positive correlation between sea surface temperature (SST) and wind stress is observed near the southeast of Vietnam, where strong SST fronts occur during summertime. This air-sea coupling relationship indicates that the ocean is forcing the atmosphere at oceanic mesoscales, which is the opposite of the negative correlation at large scales. Our results reveal that the SST-induced wind stress curl anomalies have a feedback effect on SST itself. A regression analysis suggests that the wind stress curl anomalies can alter the SST magnitude by as much as 0.5˚C. The coupled system in the southeast of Vietnam is initiated by wind-induced Ekman transport. The Ekman pumping induced by the wind stress curl is subsequently developed over frontal regions, which is approximately half of the Ekman transport. Then the upwelling can enhance the strength of SST fronts. The factors influencing strength and interannual variability in air-sea interaction are also explored in the present study. The wind stress directional steadiness (WSDS) plays an important role in air-sea interaction over the SST frontal regions. The coupling between the wind stress and SST can fully develop, which is consistent with highly stable WSDS. Furthermore, our results suggest that interannual variabilities of air-sea interaction are largely impacted by the El Niño events through influencing the regional winds. The influence of a strong El Niño event on the summer upwelling system is characterized by SST warming and declining winds, which were associated with weakened SST gradients and mesoscale air-sea coupling during the 2010 summer. Current study offers a comprehensive description for the ocean-atmosphere interaction in a typical upwelling system and can be further applied in other global coastal regions.

Keywords: Ocean-atmosphere interaction, Sea surface temperature fronts, El Niño

©2020. Japan Geoscience Union. All Right Reserved.

Tracking Experiment of adrift object using Surface Drifter in Southeast coast 2019

*SeungYun HA[1], YoungTaeg Kim[1], SeokJae Kwon[1], JaeMin Kim[1], JooEun KIM[1], Ho-Kyun Kim[1]

1. Korea Hydrographic and Oceanographic Agency, Busan, Republic of Korea

To understand the effects of tidal current and general surface current on the travel patterns of floats around the Jeju Island and southern area of East Sea. We monitored the tracks of 15 surface drifters deployed on July 25 at the southern area of East Sea. and indentified the several main drifter tracks up to January 15, 2020. In addition, from December 3, 2019 to January 14 2020, we deployed 5 surfeace drifters near the Jeju Island.

Most drifters of 15 drifters, except for on driter(212), were moved by the well know currents of the Korea Strait, such as East Korea Warm Current(EKWC) and Offshre Branch of Tsushima Warm Current(OB), and a couple of mosescale eddied as well. Other drifter(202, 205, 206, 207, 211, 214) were entrapped by mesoscale eddy at the southern area of East Sea(offshore region from Pohang) and parts of then moved again northeastward along the OB. Particularly, drifter 202 followed by Nearshore Branch of Tsushima Warm Current(NB) passed through Tsugaru Strait after October 10, 2019, and now reached Northwest Pacific Ocean. We identified again the dominant effects of Tsushima Warm Current(TWC) at the southern area of East Sea. And, mesoscale eddies are inferred owing to various forces including wind force. On the other hand, 5 drifters deployed near the Jeju Island moved southward. It was believed to be shifted due to the northerly wind effect during the observation period.

Both results show that the influence of the wind is dominant in the surface current in the observation area. Particularly, many turning points were found during the movements. The occurrence of the turning point is thought to be attributed to the influence of the tidal current, and the rotational motion at the turning point was evident when the wind speeds were low.

Keywords: Surface Drifter, Surface Current, Tidal Current, Adrift object tracking experiment, mesoscale eddies

©2020. Japan Geoscience Union. All Right Reserved.

Tracking Experiment of adrift object using Surface Drifter in Southeast Coast 2019 Summer

Seung Yun Ha[1] · Young Taeg Kim[1] · Seok Jae Kwon[1]
· Jae Min Kim[1] · Joo Eun Kim[1] · Ho Kyun Kim[1]

1) Korea Hydrographic and Oceanographic Agency, Busan, Republic of Korea

Abstract

To understand the effects of tidal current and general surface current on the travel patterns of floats around the Jeju Island and southern area of East Sea, we monitored the tracks of 15 surface drifters deployed on July 25 at the southern area of East Sea, and identified the several main drifter tracks up to January 15, 2020. In addition, from December 3, 2019 to January 14 2020, we deployed 5 surface drifters near the Jeju Island.

Most drifters of 15 drifters, except for one drifter(212), were moved by the well-know currents of the Korea Strait, such as East Korea Warm Current(EKWC) and Offshore Branch of Tsushima Warm Current (OB), and a couple of mesoscale eddies as well. Other drifter(202, 205, 206, 207, 211, 214) were entrapped by mesoscale eddy at the southern area of East Sea(offshore region fromF Pohang) and parts of them moved again northeastward along the OB. Particularly, drifter 202 followed by Nearshore Branch of Tsushima Warm Current(NB) passed through Tsugaru Strait after October 10, 2019, and now reached Northwest Pacific Ocean. We identified again the dominant effects of Tsushima Warm Current(TWC) at the southern area of East Sea. And, mesoscale eddies are inferred owing to various forces including wind force. On the other hand, 5 drifters deployed near the Jeju Island moved southward. It was believed to be shifted due to the northerly wind effect during the observation period.

Both results show that the influence of the wind is dominant in the surface current in the observation area. Particularly, many turning points were found during the movements. The occurrence of the turning point is thought to be attributed to the influence of the tidal current, and the rotational motion at the turning point was evident when the wind speeds were low.

Keywords : Surface drifter, Surface current, Tidal current, Adrift object tracking experiment, mesoscale eddies

©2020. Japan Geoscience Union. All Right Reserved.

Prediction of Storm Surge due to Typhoon passing Korea using by Machine Learning

*Boonsoon Kang[1], Jongjib Park[2], Wanhee Cho[3], Jongyoon Mun[3], Seokjae Kwon[1], Eunil Lee[1]

1. Ocean Research Division, Korea Hydrographic and Oceanographic Agency(KHOA), 2. Department of Coastal Management, Geosystem Research Corporatio, 3. Oceanographic Division, Marine information Technology Corporation

There have been growing interests in the coastal regions exposed to the threats by typhoons, storm surges, high waves and so on. Recently, the external threats seem to be intensified with global warming and effect on the human life suffering more than that ever before. As one of the policies to protect coastal areas, the Korea Hydrographic and Oceanographic Agency (KHOA) has provided the maps of Coastal Flooding Forecast by Typhoon, indicating flooding coastal areas due to storm surges by Typhoon, to the local governments with coastal areas.

In this study, the machine learning method using Artificial Neural Network (ANN) is conducted to predict the storm surges with two scenarios of typhoons passing the Korean peninsula. The first is the scenario with the straightened path and central pressure of typhoons artificially created. It is a hypothetical scenario that is slightly different from the typhoons really occurred in paths and central pressure. The second is a stochastic scenario with possible typhoons based on the occurred typhoons, that is created by the TCRM(Tropical Cyclone Risk Model) developed in Geoscience Australia(Geoscience Australia, 2018; William, 2019).

The numerical simulations for storm surges were performed under the two scenarios. The results of the simulations were used in the ANN as learning data, and then the predicted storm surge heights obtained the machine learning were analyzed. Both scenarios represent the results of storm surge prediction that are in much better agreements with the measured data in the southern Korean coasts than those in the western coasts.

The difference between the prediction results by the hypothetical and stochastic scenarios is dominant in the western coasts where typhoons occur with more complicated pathway than that in the southern coasts. The accuracy of storm surge prediction for the stochastic case is higher than that for the hypothetical case, meaning that the accuracy of the machine learning forecast depends on the quality of the input data.

* Ref. : Geoscience Australia: Tropical Cyclone Risk Model, https://github.com/GeoscienceAustralia/tcrm. William C. Arthur, A statistical-parametric model of tropical cyclones for hazard assessment, Natural Hazards and Earth System Sciences, https://doi/10.5194/nhess-2019-192.

Keywords: Storm Surge, Prediction, Typhoon, Machine Learning

©2020. Japan Geoscience Union. All Right Reserved.

Impact of applying tidal correction to marginal-sea bathymetry dataset

*Katsuto Uehara[1]

1. Kyushu University

The impact of different vertical datum adopted in bathymetric grid datasets, a difference between depths referred to the chart datum that roughly corresponds to the low-tide level and those referred to the mean sea level, on the performance of the tidal simulation covering the East China Sea and the South China Sea has been verified by conducting two numerical simulations using model bathymetries derived either from raw depths indicated in navigational charts or from converted depths which refer to the mean sea level. The conversion of the zero-depth level was made by referring to the tidal-correction offsets (z0) at nearby ports listed in tide tables issued by Japan, U.K., China and South Korea. It was found that the difference in M2 tidal amplitudes obtained by the numerical simulations were small at many regions including those adjacent to Japanese coasts, where z0 were mostly less than 1 m and the predicted M2 amplitude differences were generally smaller than 3 cm. In some areas where tidal amplitudes are large, e.g., along the west coast of the Korean Peninsula and the southwestern coast of the Borneo Island, the M2 amplitude difference ranged as large as tens of centimeters and some differences in the spatial pattern of tidal amplitudes were identified. By using the model bathymetry which has removed the tidal-correction offsets, the RMS difference between the model-predicted and observed M2 amplitudes has decreased by about 20 percent for the East China Sea case. It was also found that some global bathymetric grid datasets such as GEBCO 2019, which also incorporate sounding information derived from ENCs, currently does not consider the difference in vertical levels and a care must be taken when applying such bathymetry data to regions having large tidal amplitudes.

Keywords: Bathymetry, Tides, Vertical datum

©2020. Japan Geoscience Union. All Right Reserved.

Changes of the obduction and subduction rates accompanied by anomalous winters

*Yoshimi Kawai[1], Kazuyuki Uehara[2], Shigeki Hosoda[1]

1. Research Institute for Global Change, Japan Agency for Marine-Earth Science and Technology, 2. School of Marine Science and Technology, Tokai University

The mean temperature of the global upper ocean has been increasing, and the warming has already extended to the middle and deep layers. Besides the long-term warming trend, extreme high sea surface temperature (SST) events that persist for days to months within a limited region, which are referred to as “marine heatwaves”, often occur. The frequency and duration of the marine heatwave events are expected to increase under global warming. Anomalous warming with a relatively short period can have devastating impacts on ecosystem, and maybe the ocean circulation. The exchanges of heat, freshwater and materials between the upper ocean and the interior, however, has not been investigated sufficiently. The author calculated subduction and obduction rates with the Eulerian definition, which enabled us to easily evaluate the contribution of obduction to the mixed layer (ML) heat and salinity budgets and to trace water masses below the ML. The MOAA GPV dataset, which is produced mainly from Argo data, plus other CTD data, was used for the calculation. Surface heat, freshwater, and momentum fluxes were obtained from the ERA-interim dataset.
The authors showed in a previous study that the southwestern Bering Sea is one of the regions where the contribution of obduction to the ML salinity budget is large. The interannual variation of the salinizing effect by obducted waters is also significant in this region. From 2013 to 2016 in the southwestern Bering Sea, the obduction rate and its heating/salinizing effects were at a low level. In 2014 and 2015 the ML salinity was low and the temperature increased, leading to low density less than 26.35 δ_θ. This warming appeared to be spillover of the 2014-2016 Pacific blob event that occurred in the northeastern North Pacific. The northeastern North Atlantic off Europe is also one of the most interesting regions from the viewpoint of the obduction effects on the ML budget. The “Atlantic cold blob” was observed simultaneously with the Pacific blob, and the wintertime ML in 2014 became the deepest and coldest since 2005, resulting in the largest obduction rate. The cooling and freshening effects by obuction were also prominent this year. The ML depth and obduction rate largely decreased in 2015-2016 even though the ML density did not decline very much. The decreases were due to a rise of isopycnal surfaces. The authors will other cases related with anomalous winters in the presentation.

Keywords: obduction, subduction, Argo data, marine heatwave

©2020. Japan Geoscience Union. All Right Reserved.

Estimation of duration for 2017 Kuroshio large meander

*Takashi SETOU[1], Yugo SHIMIZU[1], Akira KUSAKA[1], Daisuke AMBE[1], Daiki Ito[1], Takuhiko KAMEDA[1]

1. Fisheries Research and Education Agency

Duration of the 2017 Kuroshio Large Meander event have been estimated by three statistical models based on some scientific materials. All the models have proposed three years or more, which is relatively longer than that of recent events. We will discuss it concretely at the meeting.

Keywords: Kuroshio, large meander, duration

©2020. Japan Geoscience Union. All Right Reserved.

Baroclinic vertical modes around the East Asian seas

*You-Soon Chang[1], Byeong-Jun Lim[1], Do-Youn Kim[2]

1. Kongju National University, 2. Ara Consulting & Technology

Determination of appropriate spatial resolution is important for configuring regional models. First baroclinic Rossby radius of deformation serves as an objective length-scale for ensuring the horizontal grid spacing, while little equivalent quantifiable standard exists for the vertical grid. Stewart et al. (2017) proposed a method to determine vertical grids based on analysis of baroclinic modes commensurate with the theoretical capabilities of a given horizontal grid. Many models adopted this method, but most focuses are placed in the global ocean or ideal case. Therefore, we analyzed baroclinic vertical modes around the East Asian seas by using serial observation data provided by Korean Oceanographic Data Center (KODC).
Results show that at least 3 vertical levels between surface and 20 m are required to resolve the first baroclinic mode for a regional model with 1/20° horizontal grid in this area. For the second baroclinic mode, the regional model needs at least 3 vertical levels between surface and 10 m and another 3 vertical levels between 10 m and 30 m depth. However, this criterion is different by each sub-region and season.

Acknowledgement: This study was supported by the research year project of Kongju National University.

Keywords: Baroclinic mode, East Asian seas, Regional ocean model, Vertical grid

©2020. Japan Geoscience Union. All Right Reserved.

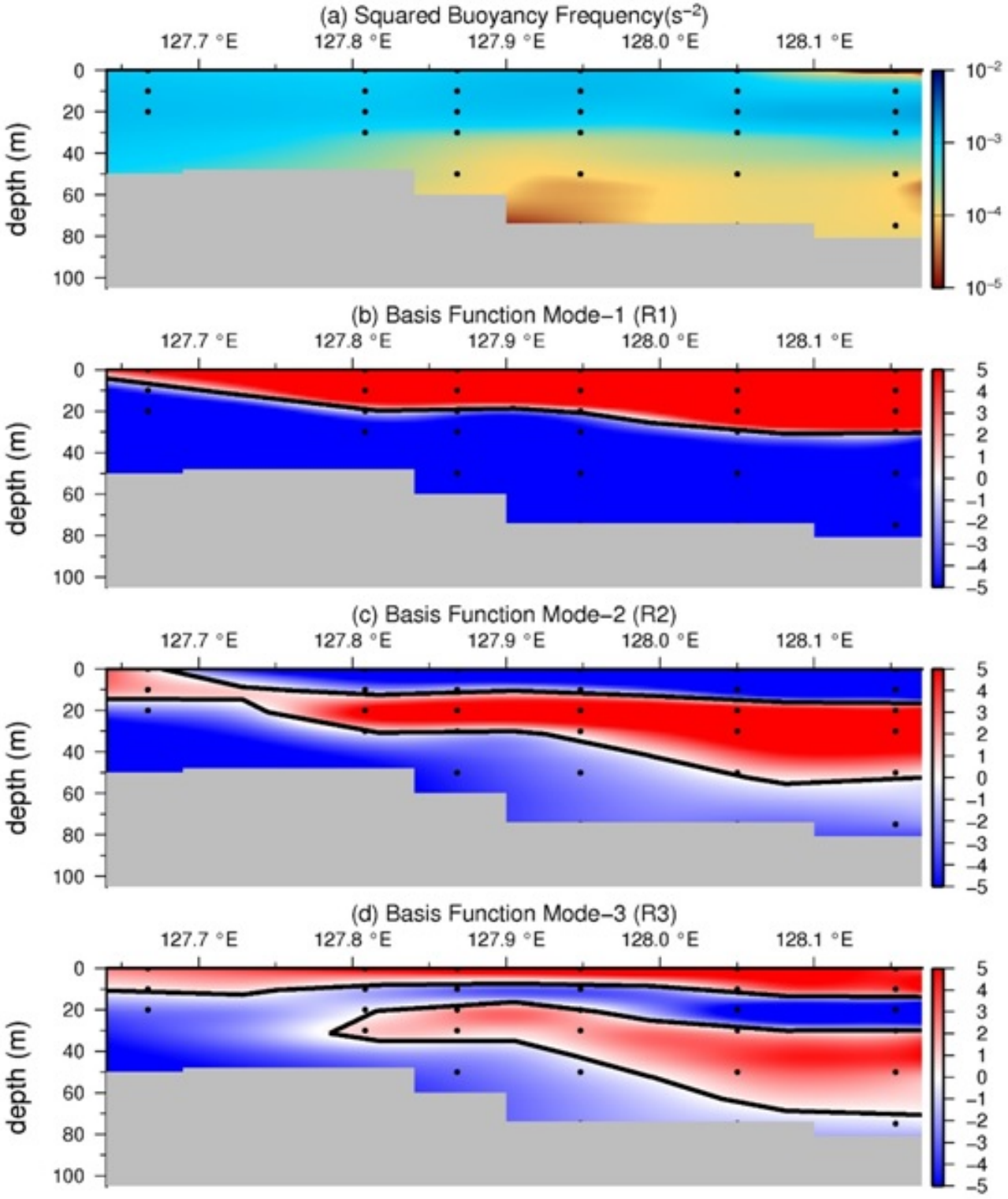

©2020. Japan Geoscience Union. All Right Reserved.

[J] Poster | A (Atmospheric and Hydrospheric Sciences)：A-OS Ocean Sciences & Ocean Environment

[A-OS29] Ocean Research Planning for UN Decade of Ocean Science for Sustainable Developments (2021-2030)

convener:Kentaro Ando(Japan Agency for Marine and Earth Science and Technology), Yoshiko Kondo(Nagasaki University), Eitarou Oka(Atmosphere and Ocean Research Institute, The University of Tokyo), Sanae Chiba(JAMSTEC)

The 72nd United Nation General Assembly (UNGA) held in December 2017 proclaimed "UN Decade of Ocean Science for Sustainable Development (2021-2030, hereafter the UN Decade)", and the IOC/UNESCO has started preparatory actions as a responsible organization to develop implementation plan of UN Decade to submit the plan at the 75th UNGA in the fall of 2020. In the series of preparatory actions and meetings, internationally Japanese government hosted the North Pacific Regional Workshop together with PICES and IOC/WESTPAC from July 31st to August 2nd, 2019 in Tokyo, and domestically after September 2019 Japan Oceanographic Society and Science Council of Japan hosted several symposiums to foster dialogues among communities.
In this session, followed by several lectures about the UN Decade and on the progress of preparations of the UN Decade, we will foster discussion and dialogues for the purposes to seek directions of activities of ocean sciences for the UN Decade in a free, open-minded, and positive atmosphere among ocean scientists and stakeholders by using ideas of ocean science plans to be submitted by individual scientists.
We expect to have submissions about ocean scientific plans in association with the UN Decade as many as possible, and in particular we strongly encourage the proposals by younger generations and early carrier scientists, who will bear the ocean science during the period of the UN Decade. We will also welcome the trans-disciplinary plans bearing in the mind of SDGs, and the participatory plans from multi-sector including private sectors.

[AOS29-P01] Reports on the UN Ocean Science Decade Regional Planning Workshop for the North Pacific and Western Pacific Marginal Seas in the last August and recent activities for the UN Decade in the IOC/WESTPAC region

*Kentaro Ando[1], Wenxi Zhu[2] (1.Japan Agency for Marine and Earth Science and Technology, 2.IOC/WESTPAC secretariat)

[AOS29-P03] Toward an attractive “UN Decade of Ocean Science”

*Sayaka Yasunaka[1], Kaoru Kubokawa[2], Naomi Harada[1] (1.Japan Agency for Marine-Earth Science and Technology, 2.Teikyo University)

Reports on the UN Ocean Science Decade Regional Planning Workshop for the North Pacific and Western Pacific Marginal Seas in the last August and recent activities for the UN Decade in the IOC/WESTPAC region

*Kentaro Ando[1], Wenxi Zhu[2]

1. Japan Agency for Marine and Earth Science and Technology, 2. IOC/WESTPAC secretariat

In collaboration with the Japanese government (MEXT), PICES, AORI and JAMSTEC, the IOC/WESTPAC held the UN Ocean Science Decade Regional Planning Workshop for the North Pacific and Western pacific Marginal Seas in Tokyo from July 31st to August 2nd, 2019. In the planning workshop, more than 160 participants joined from 18 countries, spanning communities from ocean policy and management, ocean science and technology, business and industry, NGOs and civil society, donors and foundations, and various intergovernmental and international bodies/programmes.

This Regional Planning Workshop (RPW) was designed to build dialogues amongst various ocean stakeholders in the region, focusing on the co-development of solution-oriented research strategies to address the Decade six societal outcomes: a clean ocean, a healthy and resilient ocean, a predicted ocean, a safe ocean, a sustainably harvested and productive ocean, and a transparent and accessible ocean. After three days discussion from six working groups, expert leads from the Decade six societal outcomes reported their outputs, and their summary was published at https://www.oceandecade.org/resource/66/Summary-Report-of-the-Regional-Planning-Workshop-for-the-North-Pacific-and-Western-Pacific-Marginal-Seas, and http://iocwestpac.org/calendar/905.html
We will report the outputs from the RPW for the North Pacific and Western pacific Marginal Seas, as well as recent activities and advancements at national and regional levels for the UN Decade in the IOC/WESTPAC region by shar

Keywords: UN Decade of Ocean Science, IOC, Japan National Commission for UNESCO

©2020. Japan Geoscience Union. All Right Reserved.

Toward an attractive “UN Decade of Ocean Science”

*Sayaka Yasunaka[1], Kaoru Kubokawa[2], Naomi Harada[1]

1. Japan Agency for Marine-Earth Science and Technology, 2. Teikyo University

Female scientists comprise on average 38 % of the researchers specializing in oceanography in the world [kk1] (Global Ocean Science Report 2017). In the United States, more than 40% of doctoral degrees are earned by women, and the percentages of women at all levels have increased by roughly 5% to 15% in the past decade (Women in Oceanography 2015). By contrast, the percentage of women in members of The Oceanographic Society of Japan increases from less than 5% in the 1990s to more than 10% in the 2000s, but plateaus around 12% since the late 2000s. According to the report of Cabinet Office in 2019, an organization attracts more job-seeking students, gets longer serving employees, and better economic indicators if it emphasizes the diversity. Ensuring the diversity is important so that ocean science remains an attractive sector. Of course, public relations activities are also important. We hope a lot of women participate and take the leadership in “UN Decade of Ocean Science” and promote the achievement in attractive way.

Considering women in ocean science are still minority, “Women for One Ocean” in 2018 were established. It is characterized by participants from a variety of sectors and with a variety of professions; from natural science to social science and from science to journalism. We are having monthly web meetings, publishing newsletters, providing information through SNS and website, holding outreach events, and so on. Personal connections developed in the network are quite helpful for individualized activities, too. We plan to include the programs and achievements of “UN Decade of Ocean Science” in the social activities, and support research projects of each member contributing to “UN Decade of Ocean Science”.

Keywords: UN Decade of Ocean Science, Gender Equality, Women for One Ocean

海の女性ネットワーク
Women for One Ocean

©2020. Japan Geoscience Union. All Right Reserved.

[J] Poster | A (Atmospheric and Hydrospheric Sciences)：A-HW Hydrology & Water Environment

[A-HW34] Isotope Hydrology 2020

convener:Masaya Yasuhara(Rissho Univ.), Kohei Kazahaya(Geological Survey of Japan, AIST), Shinji Ohsawa(Institute for Geothermal Sciences, Graduate School of Science, Kyoto University), Kazuyoshi Asai(Geo Science Laboratory)

The purpose of the session is to review the present state of knowledge of isotope
hydrology, by bringing together hydrologists, geologists, volcanologists, geochemists, agronomists, ecologists, engineers and so on.

[AHW34-P01] Establishment of accurate estimation method of heavy metal loads in an agricultural river and origins of heavy metals in Fuku River, Saitama, Japan

*Manatsu Kimura[1], Masaya Yasuhara[2], Seongwon Lee[2] (1.Graduate Cource in Environment Systems of Geo-Environmental Science RISSHO University, 2.Environment Systems of Geo-Environmental Science RISSHO University)

[AHW34-P02] The influence of geology on river water quality and chemical loads in Oshika Village, Nagano, Japan

Miyuki Mori[1], *Masaya Yasuhara[1], Seongwon Lee[1], Yuri Hirano[1], Fumitake Kusuhara[2], Noritoshi Morikawa[3], Kohei Kazahaya[3] (1.Rissho Univ., 2.Central Research Institute of Electric Power Industry, 3.Geological Survey of Japan, AIST)

[AHW34-P03] A study on life cycle of freshwater copepod in Chino-ike(Bloody lake), an ephemeral lake on the top of Mt.Akagi, central Japan

*Yuri Hirano[1], Masaya Yasuhara[2], Seongwon Lee[2], Nozomu Iwasaki[2], Yasuhiro Funyu[3], Natumi Simota[4] (1.Rissho University(undergraduate student), 2.Rissho University, 3.Graduate School of Geo-environmental Science, Rissho University, 4.Corporation Belc)

[AHW34-P04] Estimation of Excess Air in groundwater using dissolved Nitrogen and Argon

Kazuyoshi Asai[1], *Kazumi Asai[1] (1.Chikyukagakukenkyusho inc)

[AHW34-P05] Vertical distribution of stable isotopes in deep groundwater of Kofu basin

*Ruri Isobe[1], Takashi Nakamura[1] (1.International Research Center for River Basin Environment, University of YAMANASHI)

[AHW34-P06] On balance of chloride ion in Kanna river aroud Wataruse area, Kamikawa, Saitama, Japan

*Taketoshi Hasegawa[1], Masaya Yasuhara[2], Seongwon Lee[2], Noritoshi Morikawa[3], Tsukamoto Hitoshi[3] (1.KYODO ENGINEERING Corp., 2.Rissho University of Geo-environmental science, 3.Geological Survey of Japan, AIST)

[AHW34-P07] Estimation of groundwater residence time in Mt. Iwaki

Kazumi Asai[1], Seiichiro Ioka[2], *Kazuyoshi Asai[1] (1.Geo Science Laboratory, 2.Hirosaki University)

[AHW34-P08] Isotope tracing for mountain groundwater recharges in volcanic and non-volcanic mountains

*Takashi Nakamura[1], sano anna[1], Kei Nishida[1] (1.International Research Center for River Basin Environment, University of YAMANASHI)

[AHW34-P09] Water chemistry of shallow groundwater and its evolution processes in southern parts of Okinawa island, Japan

Kaede Shimoji[1], *Masaya Yasuhara[1], Seongwon Lee[1], Takashi Nakamura[2], Kazuyoshi Asai[3] (1.Rissho Univ., 2.Yamanishi Univ., 3.Geoscience Laboratory)

[AHW34-P10] Depleting trend of deuterium excess in precipitation observed from 1998 to 2018 at Tiksi, Russia

*Kimpei Ichiyanagi[1], Hotaek Park[2], Masahiro Tanoue[3], Takayuki Uesugi[1] (1.Kumamoto University, 2.JAMSTEC, 3.National Institute for Environmental Studies)

[AHW34-P11] Groundwater recharge in the Kurobe River Alluvial Fan and the nutrient dynamics using chemical compositions, oxygen and hydrogen isotopes: influence by land-use and climate changes over the past 30 years

*YUNYE LIU[1], JING ZHANG[2], Saki KATAZAKAI[1], Yuhei Nakayasu[1], Rezedan Aray[1] (1.Graduate School of Science and Engineering, University of Toyama, 2.Faculty of Science, Academic Assembly, University of Toyama)

Establishment of accurate estimation method of heavy metal loads in an agricultural river and origins of heavy metals in Fuku River, Saitama, Japan

*Manatsu Kimura[1], Masaya Yasuhara[2], Seongwon Lee[2]

1. Graduate Cource in Environment Systems of Geo-Environmental Science RISSHO University, 2. Environment Systems of Geo-Environmental Science RISSHO University

Heavy metals of both dissolved and particulate forms in agricultural rivers are receiving particular attention especially for those potential effects on water environment and aquatic biota of the lower reaches. In this context, it is essential to know not only the heavy metal concentration in river water but also the load which is a product of the concentration of a given heavy metal and river flow rate. In the study for the river cross section 7.7 m wide and ca. 0.3 m~1.0 m deep in Fuku River, Saitama, Japan, the accurate estimation method of heavy metal loads in an agricultural river was established on the basis of high-density flow velocity and concentration measurements across the river cross section.
On the other hand, water level, chemistry and isotope data allowed us to separate the river flow rate of 183,000 m^3/day in late June, 2019 into 1) 160, 000 m^3/day (86 %) from creek water inflow including paddy drain, and 2) 23, 000m^3/day (14 %) from groundwater (base flow). The above-mentioned newly established method in this study was used to estimate heavy metal loads across the river cross section. As the result, creek water inflow including paddy drain proved to contribute 160 kg of Al, 160 kg of Fe, 6.7 kg of Mn, 0.52 kg of Ni, 0.29 kg of Cu, 2.1 kg of Zn, and 0.22 kg of Pb per day to Fuku river. These amounts are 2.2 to about 70 times those from groundwater. This research carried out in summer (June-August, 2019) indicates creek water inflow including paddy drain plays an overwhelming role as an origin of heavy metal loads in Fuku river.

Keywords: River water, River cross section, Heavy metals, Cross-sectional distribution, Dissolved load

©2020. Japan Geoscience Union. All Right Reserved.

The influence of geology on river water quality and chemical loads in Oshika Village, Nagano, Japan

Miyuki Mori[1], *Masaya Yasuhara[1], Seongwon Lee[1], Yuri Hirano[1], Fumitake Kusuhara[2], Noritoshi Morikawa[3], Kohei Kazahaya[3]

1. Rissho Univ., 2. Central Research Institute of Electric Power Industry, 3. Geological Survey of Japan, AIST

Ohshika Village, Nagano Prefecture, central Japan is characterized by various types of rocks with different chemical composition, different grade of metamorphism, ages and origins. It is expected that these rocks and geological conditions may control water quality and chemical loads of the rivers across the village. The purpose of this study is to clarify the relationship between the river water quality/loads and geology through analyses for major ions and heavy metals.
From the trilinear diagram, water quality in the study area proved to be characterized by the Cl^-, Ca^{2+} and Mg^{2+} concentration. A large amount of Cl^- is loaded from the pelitic schist and green schist, while Mg^{2+} from the serpentinite. Also, a large amount of SiO_2 is loaded from the diorite, gneiss, sandstone and mudstone, and Ni is loaded when the river flows down the area composed of the serpentinite, pelitic schist, sandstone and mudstone. Little loading of SiO_2 was found from the serpentinite. The higher the areal proportion of the serpentinite in the drainage basin, the higher the Mg^{2+} concentration and the lower the Ca^{2+} and SiO_2 concentration of the river water.

Keywords: geology, river water quality and load, heavy metal, ultramafic rock, crystalline schist, granite

©2020. Japan Geoscience Union. All Right Reserved.

A study on life cycle of freshwater copepod in Chino-ike(Bloody lake), an ephemeral lake on the top of Mt.Akagi, central Japan

*Yuri Hirano[1], Masaya Yasuhara[2], Seongwon Lee[2], Nozomu Iwasaki[2], Yasuhiro Funyu[3], Natumi Simota[4]

1. Rissho University(undergraduate student), 2. Rissho University, 3. Graduate School of Geo-environmental Science, Rissho University, 4. Corporation Belc

Chino-ike, located on the top of Mt. Akagi at an elevation of ca. 1450 m, is known as an ephemeral lake in which water only appears from early summer to late autumn. Because of being an ephemeral lake, no fish exists there and its ecosystem is mainly composed of plankton.The species of plankton representative of Chino-ike is *Acanthodiaptomus pacificus*. This study aims to clarify the ecosystem in Chino-ike with special emphasis on the life cycle of *A. pacificus*.
The survey was conducted in June, October and December in 2018 and July, September, November and December in 2019. In 2018, lake water appeared on October 1 and lasted until on October 19. In 2019, lake water appeared on June 22 and lasted until September 29, and reappeared on October 12 and lasted until mid-December. In 2018, the maximum water depth of 98 cm was recorded on October 3.In 2019, the maximum water depths of about 180 cm and 200 cm and more were recorded on August 29 and on mid-October, respectively.The survey was conducted in October 2018 and in July, September, November and December 2019. Plankton samples were collected from 13 points (17 samples in total with different depths) in 2018 and 3 or 4 points (4-21 samples in total with different depths) in 2019. The number of plankton in a given volume of lake water was counted on the samples in the laboratory. For the surveys in June and December 2018 when the lake dried up, surface soil samples were collected at the same locations for counting the number of dormant eggs and plankton. Sedimentation traps were installed at two locations on the lake bottom to collect dormant eggs from September 26 to December 8, 2019.
As a result of the study, for adult and copepodite larvae, a higher population density was found at deeper water depths. Nauplius larva showed a higher population density at the surface water to the contrary. The optimal water temperature for *A. pacificus* growth proved to be 17℃, hatching and growing into adults in about two weeks. Additional findings including the life cycle of *A. pacificus* are to be discussed at the conference.
A reconnaissance analysis of nitrogen and carbon isotopes indicates one of the reasons why the lake water in Chino-ike turned red in late autumn is the mixing of *A. pacificus* and lake water. We are also elucidating food habits of *A. pacificus* in more detail on the basis of nitrogen and carbon isotopes from now on.

Keywords: Mt. Akagi, freshwater copepod, carbon and nitrogen isotopes, ephemeral lake, Acanthodiaptomus pacificus, aquatic ecology

©2020. Japan Geoscience Union. All Right Reserved.

Estimation of Excess Air in groundwater using dissolved Nitrogen and Argon

Kazuyoshi Asai[1], *Kazumi Asai[1]

1. Chikyukagakukenkyusho inc

To evaluate distribution of the excess air is vital for groundwater dating using SF6. For the estimation of excess air value, we used dissolved Nitrogen and Argon data. Water samples were collected from 49 springs and 22 wells in the Chubu region. We will present estimated excess air values and discuss its impact for SF_6 groundwater age.

Keywords: Excess air, groundwater, Nitrogen, Argon, SF6 age

©2020. Japan Geoscience Union. All Right Reserved.

Vertical distribution of stable isotopes in deep groundwater of Kofu basin

*Ruri Isobe[1], Takashi Nakamura[1]

1. International Research Center for River Basin Environment, University of YAMANASHI

To identify the deep groundwater (until 1500m depth) recharge sources and flow path in basin-scale hydrology, the hydrogen and oxygen stable isotope distributions were analyzed for 307 deep groundwater samples collected from hot spring water wells in Kofu Basin.
The results of chemical and isotope analysis were suggesting that some of the samples contain the Slab related water at north-west Kofu Basin while the other samples collected representing the whole Kofu Basin showed isotopically local precipitation origin. However, these samples contain relatively high NaCl which suggests the mixing with seawater (fossil saltwater). The groundwater hydrogen isotope values of the precipitation originated were estimated using the mass-balance model. The hydrogen isotope values in deep groundwater (precipitation originated) were slightly decreasing with the depth of wells until 1100m. The estimated recharge elevation using the local recharge line in Kofu Basin were ranged from approximately 1000m to 1600m.

Keywords: water isotope, deep groundwater, basin

©2020. Japan Geoscience Union. All Right Reserved.

On balance of chloride ion in Kanna river aroud Wataruse area, Kamikawa, Saitama, Japan

*Taketoshi Hasegawa[1], Masaya Yasuhara[2], Seongwon Lee[2], Noritoshi Morikawa[3], Tsukamoto Hitoshi[3]

1. KYODO ENGINEERING Corp., 2. Rissho University of Geo-environmental science, 3. Geological Survey of Japan, AIST

Shallow groundwater in the Wataruse area contains high concentrations of chloride ions (6.2 mg/L-284.4 mg/L) in February 2019. This chloride ion is due to the deep-seated fluid that rises from the underground and passes through the basement. Hasegawa et al. (2019) estimated the origin of deep fluids using stable isotope ratios of oxygen and hydrogen. As a result, the origin of the deep fluid was presumed to be a mixture of long-term stagnant water and slab-originated water. The helium isotope ratio revealed that deep-seated fluids of the same origin in the Wataruse area and the Joboji area increased in area. In this study, a more detailed study was conducted on the rise and mixing of deep-seated fluid.

Keywords: stream water, chloride ion, dissolved load, deep-seated fluid, income and outgo

©2020. Japan Geoscience Union. All Right Reserved.

Estimation of groundwater residence time in Mt. Iwaki

Kazumi Asai[1], Seiichiro Ioka[2], *Kazuyoshi Asai[1]

1. Geo Science Laboratory, 2. Hirosaki University

Mt. Iwate, called Tsugaru-Fuji, is a stratovolcano located to the southwest of Hirosaki City. Many springs distribute at the foot of volcano body. We used transient tracers such as ^{3}H, CFCs and SF_6, to estimate the residence time of the springs. Based on the CFCs and SF_6 results, the residence time of the springs in Mt. Iwaki were estimated to be 20 to 30 years.

Keywords: Mt. Iwaki, groudwater age, Tritium, CFCs, SF6

©2020. Japan Geoscience Union. All Right Reserved.

Isotope tracing for mountain groundwater recharges in volcanic and non-volcanic mountains

*Takashi Nakamura[1], sano anna[1], Kei Nishida[1]

1. International Research Center for River Basin Environment, University of YAMANASHI

To identify the characteristics of mountain groundwater recharges on different mountains, deep groundwater was collected from two mountain-plain area on the volcanic and non-volcanic area at Kofu Basin during 2011 to 2013 and 2018. Hydrogen and oxygen stable isotope values of groundwater samples increased slightly with decreasing altitudes in foot of volcanic mountain which suggested occurrence of groundwater recharge in the large area from the gradual-slope of the volcanic mountain, while the steep non-volcanic mountain groundwater flow was confirmed from foot of mountain to plain area. The results revealed topography of the mountain watershed as one of the important factor for groundwater recharges and flow characteristics.

Keywords: water isotope, mountain groundwater, volcanic mountain, non-volcanic mountain

©2020. Japan Geoscience Union. All Right Reserved.

Water chemistry of shallow groundwater and its evolution processes in southern parts of Okinawa island, Japan

Kaede Shimoji[1], *Masaya Yasuhara[1], Seongwon Lee[1], Takashi Nakamura[2], Kazuyoshi Asai[3]

1. Rissho Univ., 2. Yamanishi Univ., 3. Geoscience Laboratory

The southern parts of Okinawa island consist of the less-permeable Shimajiri Group mainly composed of siltstone and the Ryukyu Group composed of the permeable Ryukyu limestone. It is widely recognized that chemical fertilizers continuously used exclusively or in excess in sugarcane fields have significantly increased the nitrate concentration in shallow groundwater in recent years. To elucidate the current state of shallow groundwater quality and its evolution process, we investigated 25 groundwater samples for water quality, stable isotopes of nitrogen and oxygen of nitrate ($\delta^{15}N$ and $\delta^{18}O$) and residence times based on SF_6.
Groundwater quality in the study area proved to be of Ca-HCO_3 type, and considerable contamination by nitrate was observed in the whole survey area. A wide range of $\delta^{15}N$ values from 4 to 20 ‰implies nitrate contamination is caused by diverse sources such as chemical fertilizers, organic fertilizers, livestock manure, and domestic wastewater. SF_6 concentration of groundwater indicates the residence time of groundwater of 7-19 years. The relationship between $\delta^{15}N$ value and concentration of nitrate nitrogen shows two processes, that is denitrification and mixing, play important roles in the evolution of groundwater quality. Taking into account denitrification and mixing, we classified groundwater quality evolution processes in the southern parts of Okinawa island into 4 cases.

Keywords: Ryukyu limestone formation, shallow groundwater, nitrate nitrogen, nitrogen isotope, residence time, evolution of water chemistry

©2020. Japan Geoscience Union. All Right Reserved.

Depleting trend of deuterium excess in precipitation observed from 1998 to 2018 at Tiksi, Russia

*Kimpei Ichiyanagi[1], Hotaek Park[2], Masahiro Tanoue[3], Takayuki Uesugi[1]

1. Kumamoto University, 2. JAMSTEC, 3. National Institute for Environmental Studies

Stable isotopes in precipitation have been widely used in hydrological and meteorological studies as a natural tracer for atmospheric water cycle. From 1998 to 2018, daily precipitation samples were intermittently collected at Tiksi, northern Siberia, Russia. Totally 1,024 samples for $\delta^{2}H$ and 1,519 samples for $\delta^{18}O$ were analyzed by the Isotope Ratio Mass Spectrometry by the 2007 and by the Cavity Ring-Down Spectroscopy after 2008. Daily air temperature data was obtained from the Archive of Tiksi standard meteorological observations, Arctic and Antarctic Research Institute. Results of the quality control of isotopic compositions by using d-excess values (> -10‰) and relationships between $\delta^{18}O$ and air temperature (temperature effect), 637 samples for $\delta^{2}H$ and 1,105 samples for $\delta^{18}O$ were available. Isotopic compositions of $\delta^{2}H$, $\delta^{18}O$, and d-excess were ranged from -337.01 to -79.18‰, from -42.51 to -6.07‰, and from -9.90 to 34.12‰, respectively, and the Local Meteoric Water Line is $\delta^{2}H=7.83*\delta^{18}O-0.3$ (r=0.98). Air temperature at Tiksi was ranged from -47.8 to 24.1℃, and temperature effects for $\delta^{18}O$ was 0.50 (r=0.90). From the temporal analysis in the monthly basis, increasing trend of $\delta^{18}O$ in March and April and depleting trend of d-excess in October and November were significant. The difference in air temperature, evaporation, and 850hPa winds fields between first 5 years (1998-2002) and last 5 years (2014-2018) of the observation period were investigated by using the NCEP reanalysis. In March and April, positive anomalies in air temperature, evaporation, and southwesterly wind anomalies were found in the northern Siberian continent. On the other hand, positive anomalies in air temperature, evaporation along the Siberian coast of the Arctic Ocean, and north wind anomalies were found in October and November. The depleting trend in d-excess might be caused by the moisture source evaporated from the open water in the Arctic Ocean.

Keywords: precipitation, d-excess, Siberia

©2020. Japan Geoscience Union. All Right Reserved.

Groundwater recharge in the Kurobe River Alluvial Fan and the nutrient dynamics using chemical compositions, oxygen and hydrogen isotopes: influence by land-use and climate changes over the past 30 years

*YUNYE LIU[1], JING ZHANG[2], Saki KATAZAKAI[1], Yuhei Nakayasu[1], Rezedan Aray[1]

1. Graduate School of Science and Engineering, University of Toyama, 2. Faculty of Science, Academic Assembly, University of Toyama

Kurobe River Alluvial Fan is the largest one in Japan and is located in the eastern Toyama Prefecture. This region has been known as rich in groundwater, and infiltration water from the Kurobe River plays an important role in the preservation of groundwater. However, it is reported that the groundwater level of the Kurobe River Alluvial Fan has continuously declined over the past 30 years. The decline in groundwater level will cause the change in groundwater quality. In order to sustain groundwater usage effectively, it is essential to grasp the groundwater quality changes and clarify the relationships between climate change, land-use, groundwater usage, and groundwater quality. For a better understanding of the effects of climate change and land-use change on the groundwater quality of the Kurobe River Alluvial Fan, this study focused on nutrient concentration in groundwater and river water and their dynamics and long-time changes were discussed.

Data and water samples of groundwater and river water were collected during the 4 seasons in 2018-2019 (in April, July, November, and December). The major ion components (Na^+, K^+, Ca^{2+}, Mg^{2+}, HCO_3^-, Cl^-, SO_4^{2-}), nutrients (NO_3, PO_4, SiO_2) and water isotopes $\delta^{18}O$ and δD (The analytical precisions were ±0.07‰ for δD and ±0.05‰ for $\delta^{18}O$) in the samples were measured. To evaluate the long-term changes, the previous data set in our research group from 1989,2003-2004, and 2011-2012 was also re-analyzed. The changes in land-use for the past 30 years were examined using Geographic Information System (GIS).

Our future work will investigate how the changes in the amount of nutrients in groundwater and river water influence the nutrient supply to the surface seawater, and affect the primary production in the coastal environment.

Keywords: groundwater, isotope, nutrients, climate change, land-use

©2020. Japan Geoscience Union. All Right Reserved.

[J] Poster | A (Atmospheric and Hydrospheric Sciences)：A-HW Hydrology & Water Environment

[A-HW35] Perspectives on Surface- and subsurface-water resources, society, and the environment

convener: Abhishek(Tokyo Institute of Technology), Tsuyoshi Kinouchi(Tokyo Institute of Technology), Brijesh K yadav(Indian Institute of Technology Roorkee)

Major demographic transition of the developing world from rural to urban societies because of the industrialization and associated employment opportunities has caused unprecedented stress on the available water resources. Massive population growth has further deteriorated the prevailing environmental conditions and has hindered the sustainable growth of the economies. The scope of this session is to create an interdisciplinary forum by providing a common platform for the researchers from academia, industry, and the government belonging to wide geographic diversity to discuss recent scientific results of surface water and groundwater resources related to the society and the enirvironment. More specifically, this session welcomes the presentations related to but not limited to:

1) Surface water and groundwater resources, their pollution, and interaction.
2) Numerical and physical modelling of near-surface and subsurface processes.
3) Societal influence on the governance and management of water resources.
4) Impacts of urbanization on groundwater: quantity and quality aspects.
5) Quantifying the influence of water resources' pollution on human health.

[AHW35-P01] **Why full overturning in Lake Biwa was incomplete in spring 2019? : Simulation study**

*Satoshi Nakada[1], Kenta Yamada[2], Takahiro Okamoto[2], Haruki Yamamoto[2], Koichi Shimotori[1], Akio Imai[1] (1.National Institute for Environmental Studies, 2.Lake Biwa Environmental Research Institute)

[AHW35-P02] Groundwater Resource Assessment using Geophysical Investigation and Hydrological Modelling in Vindhyan-Ganga Sedimentary Formations

*Manik Goel[1], Pankaj Kumar Gupta[2], Brijesh K yadav[1] (1.Indian Institute of Technology Roorkee, Roorkee, India, 2.University of Waterloo, Waterloo, ON, Canada)

[AHW35-P03] **Data Selection for Parameter Estimation Robust to Changing Climatic Conditions**

*Avantika Rathore[1], Joseph H. A. Guillaume[2], Anthony J. Jakeman[2] (1.Indian Institute of Technology Roorkee, 2. Australian National University, Australia)

[AHW35-P04] Impact of mining on water quality and heavy metal dynamics in southern Lao PDR : A brief report

Nanthana Boungnaphalom[1], JING ZHANG[1], *Saki KATAZAKAI[1] (1.Graduate school of science and endneering, University of Toyama)

[AHW35-P05] **GIS-based spring potential mapping in Beijing using machine learning methods**

*Huixiang Li[1], Yun Pan[1], Ying Sun[2] (1.Capital Normal University, 2.Beijing Institute of Hydrogeology and Engineering Geology)

[AHW35-P06] **Greening and browning analysis in Peninsular India detected by change in Leaf Area Index and its relation to the climatic conditions**

*Bageshree K[1], Tsuyoshi Kinouchi[1] (1.Tokyo Institute of Technology)

[AHW35-P07] **Hydrochemical characteristics and sources of brines in the Sua Pans, Botswana.**

*Fiona Segolame Motswaiso[1], Kengo Nakamura[1], Noriaki Watanabe[1], Takeshi Komai[1] (1.Tohoku Univeristy Graduate School of Environmental Studies)

Why full overturning in Lake Biwa was incomplete in spring 2019? : Simulation study

*Satoshi Nakada[1], Kenta Yamada[2], Takahiro Okamoto[2], Haruki Yamamoto[2], Koichi Shimotori[1], Akio Imai[1]

1. National Institute for Environmental Studies, 2. Lake Biwa Environmental Research Institute

This study addresses the reason why the seasonal full-overturning or monomictic-mixing in Lake Biwa was partially incomplete in spring 2019 based on the heat budget analysis using the numerical simulation. The overturning induced by convection or turbulent mixing in lakes vertically provides dissolved oxygen and materials to lake water, and dominantly influences water environment associated with biota such as fishes and aquatic plants. In particular, the monomictic-mixing that reaches to the lake bottom in the water column increases dissolved oxygen in the bentic zone and determines the survival of benthos. However, previous studies reported that many monomictic lakes possibly mix less or become permanently stratified lakes in response to climate change. Recently, Lake Biwa Environmental Research Institute reported that the monomictic-mixing in Lake Biwa was partially incomplete in spring 2019. On the other hand, the monomictic-mixing in spring 2018 occurred in late January. We analyzed the heat budgets of the whole lake focusing on the wintertime cooling in both years based on the numerical simulation. The simulation reproduced the seasonal overturning and spatiotemporal distribution of water temperature of Lake Biwa in the cooling period from summer to next spring in 2017-2018 and 2018-2019. Our analysis indicated that the surface cooling in 2018-2019 was weaker than that in 2017-2018 because the latent and sensible heat fluxes in 2018-2019 is smaller than 2017-2018. The smaller latent and sensible heat fluxes were attributed to the higher air temperature and weaker wind speed, respectively, in 2018-2019 than in 2017-2018. As a result, the simulated whole heat quantity of Lake Biwa in 2018-2019 never fell below approximately 1000 PJ, meanwhile, the heat quantity in 2017-2019 underran below 1000 PJ from January to March in 2018. We proposes a heat quantity index (~1000 PJ) that the seasonal overturning can complete the monomictic-mixing in Lake Biwa. The index suggests Lake Biwa that is currently monomictic can change into the meromictic lake in the future climate or the oligomictic lake that turnovers every few years.

Keywords: Lake Biwa, full-overturning, surface cooling, heat quantity, lake surface wind, latent heat flux

©2020. Japan Geoscience Union. All Right Reserved.

Groundwater Resource Assessment using Geophysical Investigation and Hydrological Modelling in Vindhyan-Ganga Sedimentary Formations

*Manik Goel[1], Pankaj Kumar Gupta[2], Brijesh K yadav[1]

1. Indian Institute of Technology Roorkee, Roorkee, India, 2. University of Waterloo, Waterloo, ON, Canada

Owing to the accessibility and quality of groundwater, it is a crucial component of water resources for the living being. Despite the immense effort in the field of groundwater management, there is an annual depletion of 19.2 Gigatons in northern India itself. In this study, stress on the existing groundwater resources for meeting the groundwater demand is assessed along with its complete quality assessment over the Indo-Gangetic plain in the Vindhyan-Ganga Sedimentary formations. An extensive field study is carried performing 12 Vertical Electrical Soundings (VES) for geophysical investigation and two aquifer tests for characterization of the hydraulic properties of the study area. The survey locations are identified based on the topography and underlain geology of the area. The aquifer systems in the area are classified based on the input from the aquifer test and geophysical investigation surveys conducted. The stages of groundwater development is calculated from the annual groundwater use and recharge computed by analyzing the 10-year groundwater table fluctuation data along with other critical meteorological parameters for the area. The total rechargeable area is calculated by considering the landscape slope determined by the Digital Elevation Model (DEM) prepared from Landsat 8 OLI data. In addition to the in-situ measurements of various physical quality parameters, 10 groundwater samples are analyzed using AAS (Atomic Absorption Spectroscopy) for heavy metals and other major ions. Correlation between different water quality parameters is established using Principal Component Analysis (PCA). Findings of VES are used to simulate the contaminant plume transport through the vadose zone using a hydrological model. The classical advection-dispersion equation, coupled with the Richards' equation, is numerically simulated at different locations for assessing the intrinsic vulnerability of the region. The study concludes that total annual groundwater extraction is 13.89 MCM, with the annual groundwater recharge of 51.96 MCM. The majority of sites are having a concentration of Cd, Pb, As, and Fe more than their recommended WHO limits. Several patches of high vulnerable zones are found out in the south-eastern and western parts of the study area. The findings of this study will assist in decision related to the planning of industrial locations and developing groundwater remediation strategies that would ultimately lead to the improvement in living standards of the people and enhanced health safety of the community by collective efforts of local administration.

Keywords: Groundwater estimation, Vindhyan-Ganga Sedimentary Formations , Vertical Electrical Sounding, Atomic Absorption Spectroscopy, Hydrological Modelling

©2020. Japan Geoscience Union. All Right Reserved.

Data Selection for Parameter Estimation Robust to Changing Climatic Conditions

*Avantika Rathore[1], Joseph H. A. Guillaume[2], Anthony J. Jakeman[2]

1. Indian Institute of Technology Roorkee, 2. Australian National University, Australia

Hydrological models are commonly used for water resource management and making predictions under climate change. Parameters of these models usually depend on the input data. Under climate change, parameter values estimated from the historical record and existing model structures may prove inadequate to simulate the desired output for future conditions. This results in a need to develop methods for improving the robustness of parameter estimation to these changing climatic conditions. In this study, a stress testing approach was used for parameter estimation - identifying specific historically observed transitions between conditions that a model predicts poorly, and using this to inform improvements in the model. Four methods were examined to investigate the relationship between data and estimated parameters: 1) sensitivity analysis for independent time periods using Morris and Sobol2002 methods, 2) time-varying sensitivity analysis using Morris, 3) estimation of predictive uncertainty across periods using Generalised Likelihood Uncertainty Estimation (GLUE), 4) estimation of parameter uncertainty across periods using GLUE. The study was carried out on the Cotter River and Queanbeyan River catchments in the Australian Capital Territory, Australia. All work was undertaken with the hydromad R package (http://hydromad.catchment.org/). The results provided important datasets, i.e. periods where the model predictive uncertainty poorly covers the observations, periods where the most important parameters are very different or periods with different feasible parameter estimates, that could be tested to develop new hydrological models for making predictions under climate change. Sensitivity of mean flow to model parameters was evaluated using Morris and Sobol2002 method for initial 1000 days of Cotter data using GR4J model which gave similar results. 2-D probability distribution of two feasible parameters of CWI model i.e. f and tw in different time periods (1974-1976 & 1980-1982) on Queanbeyan dataset was done. It was observed that the data was less overlapping meaning that these time periods are useful for testing models that make predictions under climate change.

Keywords: Parameter estimation, Hydrological modelling, Sensitivity analysis, Uncertainty estimation

©2020. Japan Geoscience Union. All Right Reserved.

Impact of mining on water quality and heavy metal dynamics in southern Lao PDR : A brief report

Nanthana Boungnaphalom[1], JING ZHANG[1], *Saki KATAZAKAI[1]

1. Graduate school of science and endneering, University of Toyama

Though mining is one of the important industries that contribute to the economic development of country. It sometimes gets worse the environment. By raining a large volume of waste water, it can give a negative impact on the environment, especially water resources. Lao PDR is the developing country and well-endowed with the potential mineral resources. Lao’ s mineral sector has been a strong economic driver of the Lao PDR during the last decade and plays an increasingly important role in the country’ s economic development. It is rapidly becoming an important source of economic growth, national revenue and a driver for local community development and planning of poverty alleviation. Mining industries range from a small scale made by the local peoples to a large scale made by investors. This is expected to cause impacts the local water quality due to different management in each area. For the sustainable development with a good balance between industry and environment in Laos, it is necessary to understand the water systems and the impact of management on material transport characteristics based on scientific evidence. This study focus on two area: one is the Sepon Gold and Copper Mine (manage by Australia investors with a good mining system) and another is the mining area in Hinboun district (many small scales of mining made by local peoples and investors with not good systematic) to evaluate water quality under different management. Our presentation shows a brief report using chemical concentration and isotope composition.

Keywords: Water pollution, Waste water from mining

©2020. Japan Geoscience Union. All Right Reserved.

GIS-based spring potential mapping in Beijing using machine learning methods

*Huixiang Li[1], Yun Pan[1], Ying Sun[2]

1. Capital Normal University, 2. Beijing Institute of Hydrogeology and Engineering Geology

The emergence of spring is usually difficult to be monitored due to mountainous terrain. In this study we investigated the performance of two statistical models (frequency ratio (FR), and weight of evidence (WOE) and two machine learning models (random forest and classification regression tree) in generating spring potential map in Beijing. A total of 1378 springs from field survey were used for simulation, with a consideration of impacting factors including elevation, slope angle, slope aspect, topographic wetness index (TWI), stream power index (SPI), distance to rivers, distance to faults, lithology, normalized difference vegetation index (NDVI) and land use. The results demonstrate the well potential of machine learning method on investigating spring distributions, as well as on understanding its evolution under both climatic and anthropogenic impacts.

Keywords: Groundwater spring potential map, weight of evidence, frequency ratio, random forest, classification regression tree, Beijing

©2020. Japan Geoscience Union. All Right Reserved.

Greening and browning analysis in Peninsular India detected by change in Leaf Area Index and its relation to the climatic conditions

*Bageshree K[1], Tsuyoshi Kinouchi[1]

1. Tokyo Institute of Technology

Leaf Area Index (LAI) gives the amount of photosynthetically active foliage underlying a vegetation canopy. The trend in LAI is a good indicator of vegetation greening or browning. This trend statistics is also an important aspect to know the change in amount of carbon sink of the region. Nonparametric statistical trend tests have been widely used by researchers for time series analysis of vegetation indices. This study analyses the LAI trend in Maharashtra state of India to identify the greening clusters and browning hotspots. We use nonparametric Mann-Kendall trend test along with Theil Sen’ s slope method to find the magnitude of the trend. In this study, the greening and browning are presented in the form Z statistics with 95% significance level over time period of 12 years and the net change in leaf area is found out for the respective clusters. We use Moderate resolution Imaging Spectroradiometer MOD15A2H LAI/FPAR 500m 8 daily composite product to discuss the positive and negative trend using monthly time step. Previous researches have linked the greening in India to land use for agriculture practices. Our results confirm this with 66% of greening and 95% of browning clusters being located in the agricultural zones. The results show that about 5% area of Maharashtra shows greening and about 2% shows browning trend. We further discuss the region wise trend statistics and their possible causes. The browning clusters are observed in the drought prone areas which is a cause of concern considering the agriculture failure related farmer suicides in the region.

Keywords: Trend analysis, Greening and browning, Mann-Kendall test, Leaf Area Index

©2020. Japan Geoscience Union. All Right Reserved.

Hydrochemical characteristics and sources of brines in the Sua Pans, Botswana.

*Fiona Segolame Motswaiso[1], Kengo Nakamura[1], Noriaki Watanabe[1], Takeshi Komai[1]

1. Tohoku Univeristy Graduate School of Environmental Studies

Sua Pan is a basin of internal drainage located in northern Botswana in the easternmost part of the greater Makgadigadi pans area and contains a substantial amount of brine in which sodium chloride/common salt is the main constituent. A brine production wellfield managed by Botswana Ash (Pty) Ltd lies to the north of the westerly trending sand spit between the Nata and Mosetse rivers, extracting brine at a rate of 2880m3/hour. However, the origin of the abundant salt and potash resources remains highly contested. The main objective of the current study is to investigate the processes of brine formation/present-day recharge mechanisms at Sua Pan if any, including possible interactions of the solar evaporation ponds and brine resources.

A total of 39 brine, well and river samples were collected. Physical parameters of the samples such as electrical conductivity, pH, Temperature and salinity were also studied. Water temperatures on sampling varied between 23.8 and 29°C across the pans. The TDS concentration is highest 118400 ppm (mxw028) at the northeastern and within the pan. The TDS concentration is decreased to 41.28ppm (mxw011) at the wells between Ntwetwe pan and Sua pans outside the main wellfield. The lowest EC value was from borehole Mxw011 located on the western side of the project area. The vegetation is also more prominent in this area, indicating the potential for a perennially sustained freshwater regime. To a greater or lesser extent, the boreholes outside the pan reveal relatively fresh (or less saline) water overlying stronger saline water as observed from salinity profiling of monitoring boreholes. Major and minor elements were analyzed using Inductively Coupled Plasma–Atomic Emission Spectrometry (ICP–OES) and ion chromatography.

Keywords: hydrochemical characteristics, origin of brines, Sua pans

©2020. Japan Geoscience Union. All Right Reserved.

[J] Poster | A (Atmospheric and Hydrospheric Sciences)：A-HW Hydrology & Water Environment

[A-HW36] Water Environment and Geology in Urban Areas

convener:Takeshi Hayashi(Faculty of Education and Human Studies, Akita University)

The scope of this session is to create an interdisciplinary forum on the most recent advances in water environment and environmental geology research in urban areas. Various kinds of studies concerning environmental issues on water and geology in urban areas (e.g. water balance, water cycle, water resource development and management, inundations, hydrogeology, pollution and remediation, geohazard, basic law on the water cycle) are welcome from academia, industry, and government as well as wider geographic diversity.

[AHW36-P01] Evaluation of subsurface warming in the Tokyo metropolitan area: characteristics of long-term change in subsurface temperature beneath Yokohama and Kawasaki areas

*Akinobu Miyakoshi[1], Takeshi Hayashi[2] (1.Geological Survey of Japan, AIST, 2.Faculty of Education and Human Studies, Akita University)

[AHW36-P02] Development of multi-tracer method for evaluation of water cycle process in urban area

*Takeshi Hayashi[1], Masaya Yasuhara[2], Takashi Nakamura[3] (1.Faculty of Education and Human Studies, Akita University, 2.Faculty of Geo-environmental science, Rissho University, 3.Graduate Faculty of Interdisciplinary Research Faculty of Engineering, University of Yamanashi)

[AHW36-P03] Water supply system and environmental impacts of chemical release accidents caused by the major earthquake

*Lisa Ito[1], Akihiro Tokai[1], Toyohiko Nakakubo[2] (1.Graduate School of Engineering, Osaka University, 2.Natural Science Division, Fuculty of Core Reserch, Ochanomizu University)

[AHW36-P04] **Exploring the linkage between urban flood risk and spatial characteristics in small urbanized catchments of Beijing, China**

*Lei Yao[1] (1.Shandong Normal University)

[AHW36-P05] Flood disasters and river management in the downstream of Tama River following 2019 Typhoon Hagibis (JMA Typhoon No. 19)

*Jiro Komori[1] (1.Teikyo Heisei University)

[AHW36-P06] Development of a detailed land surface state estimation method toward usage in weather prediction

*Yuuki Myo[1], Kazuyoshi Souma[1] (1.University of Yamanashi)

Evaluation of subsurface warming in the Tokyo metropolitan area: characteristics of long-term change in subsurface temperature beneath Yokohama and Kawasaki areas

*Akinobu Miyakoshi[1], Takeshi Hayashi[2]

1. Geological Survey of Japan, AIST, 2. Faculty of Education and Human Studies, Akita University

Recent research investigations have provided insights regarding the subsurface warming in the Tokyo metropolitan area that widely spreads not only over the urban center but also the suburbs (e.g., Miyakoshi et al., 2019). Based on the results of repeated measurements of temperature–depth profiles (since 2000) and subsurface temperature monitoring (since 2009) at observation wells in Tokyo and Saitama areas, it is found that the long-term warming trend of subsurface temperature mainly changes at shallow depths. Distinct regional differences in the subsurface temperature distribution and secular changes are observed, and the warming trend in the urban center is noted to be considerably larger than that in suburban areas. Subsurface warming is also observed at the deep parts of areas with large groundwater development (e.g., Musashino Upland) because of the effects of anthropogenic groundwater flow. Subsurface warming has been generated by the complex combination of effects of temperature increases at the ground surface and shallow subsurface induced by urbanization and groundwater flow changes caused by pumping and global warming.

The temperature–depth profiles were observed from November 2018 to March 2019 at 20 observation wells in Yokohama and Kawasaki areas, which are located in the southern Tokyo metropolitan area. Observations at the same wells were also conducted; 14 of these were measured in 2001 or 2004. The evaluation of subsurface temperature distribution and the calculation of gradients of long-term subsurface temperature changes for the past 14–17 years are based on the datasets derived from the foregoing observations.

By comparing the past and present datasets, the occurrence of subsurface warming is detected in all 14 wells. Regional differences in warming trend are also noted, and particularly high increases are observed at four wells located inland. Except for these four, the subsurface warming trends are estimated to be approximately 1.6×10^{-2}–2.9×10^{-2} ℃/year and 1.0×10^{-2}–2.0×10^{-2} ℃/year at depths of 30 and 40 m, respectively. These warming trends decrease with depth, and a higher warming trend is observed at the wells in or around the urban center located in the coastal area. A particularly high warming trend of 3.0×10^{-2} ℃/year at a depth of 30–40 m is found at the four wells in the inland area. The subsurface warming trend at these wells indicates the maximum value at a certain depth. It is assumed that the temperature variations are caused by the effects of groundwater pumping in comparison with the geological structure.

The spatial scale of the groundwater flow system in or around this area is smaller than that in the central part of Kanto Plain. It is observed, however, that subsurface warming widely spreads, and the probable factor for such a spread is presumed to be the combined effects of urbanization, changes in groundwater flow, and global warming. The characteristics of subsurface temperature changes in the Yokohama and Kawasaki areas will be compared with those of the other Tokyo bay areas.

The use of observation wells to measure temperature-depth profiles in this study was supported by Environmental Science Research Institute, Environmental Planning Bureau, City of Yokohama, and Water

©2020. Japan Geoscience Union. All Right Reserved.

Quality Section, Environmental Policy Department, Environmental Protection Bureau, Kawasaki City.

Keywords: temperature-depth profile, subsurface warming, groundwater flow, groundwater development, urbanization, Tokyo metropolitan area

©2020. Japan Geoscience Union. All Right Reserved.

Development of multi-tracer method for evaluation of water cycle process in urban area

*Takeshi Hayashi[1], Masaya Yasuhara[2], Takashi Nakamura[3]

1. Faculty of Education and Human Studies, Akita University, 2. Faculty of Geo-environmental science, Rissho University, 3. Graduate Faculty of Interdisciplinary Research Faculty of Engineering, University of Yamanashi

The water cycle in urban areas has been changing quantitatively and qualitatively by urbanization. Urbanization such as reducing of croplands, covering of ground surface by concrete and asphalt, covering of riverbed, and development of sewer system reduces the flux of water cycle. Contrary, leakage from the water pipes and sewers increases the flux. On the other hand, groundwater development is possible to change the groundwater flow system. These kinds of water environment change occur in variety depending on the stage of urbanization.
Enormous hydrological studies have been done widely to evaluate the water cycle in urban areas using various kinds of tracers such as dissolved ions and environmental isotopes. However, it still is difficult to evaluate the water cycle, because the water cycle has been changed continuously with the development of urban areas. We focus on the PPCPs and artificial sweeteners as new tracers to develop a multi-tracers method in this study. In Japan, various artificial sweeteners have been used and the major kinds of them have been changed with the times. Thus, it is expected that the artificial sweeteners are useful not only for tracers but also indicators of the groundwater age. We will show the outline of this study in the presentation. This work was supported by JSPS KAKENHI Grant Number 19K12293-00.

Keywords: urban area, water cycle, multi-tracer, PPCPs, Artificial sweeteners

©2020. Japan Geoscience Union. All Right Reserved.

Water supply system and environmental impacts of chemical release accidents caused by the major earthquake

*Lisa Ito[1], Akihiro Tokai[1], Toyohiko Nakakubo[2]

1. Graduate School of Engineering, Osaka University, 2. Natural Science Division, Fuculty of Core Reserch, Ochanomizu University

Natural hazard triggering technological disasters (Natech) cause pronounced impacts on both society and the environment. In Japan, the Great East Japan Earthquake is an example of such event, when radioactive cesium-137 spread to the air and soil and finally to the river, which raised concerns on environmental and human health impacts (Takahashi et al., 2017). Caused by unexpected earthquakes or other extreme natural events, Natech is a rising concern given the increasing number of handled chemicals. Under these situations, measures to prevent serious accidents involving such toxic chemicals are highly important. However, after the accident, both impacts for the environment and urban infrastructure, such as the water purification system, have not been clarified quantitatively, especially under unstable situations such as major earthquakes. In addition, the effectiveness of each measure against the accidents has not been clarified systematically and comprehensively. Therefore, this study aims to clarify the behavior of toxic chemicals that are accidentally released into the river due to the seismic motion, and to evaluate countermeasures in terms of their efficiency to prevent the release itself or the removability of chemicals from the water after the release accident.

As the research target area, Yodo River basin in Osaka is selected for its large density of chemical facilities and high risks of liquefaction because of the sandy sediment. Yodo River is also an essential water resource that supports urban infrastructure in the Kansai area. Therefore, significant social impacts are expected in the case of an accident. Pollutant Release and Transfer Register (PRTR) chemicals, which could possibly grasp the actual handling amount, are selected for the simulation. Specifically, PRTR registered chemicals (e.g., acrylonitrile and formaldehyde, among others) with high toxicity and difficult to remove at water treatment plants were selected for the worst-case simulation. The model based on AIST-SHANEL (Standardized hydrology-based assessment tool for chemical exposure load) with improved time resolution and flow rate calculation was used. As the risk evaluation endpoints of this study, we set two standards, (i) subacute toxicity to humans in purified water and (ii) acute toxicity to aquatic organisms in river water. Both emergency shut-off valves set in the chemical facilities and activated carbon treatments in the water purification plant are the countermeasures of (i), and only the former is that of (ii). As a result, out of target substances such as formaldehyde, three chemicals exceeded the standard of subacute toxicity to humans in purified water, which would cause the suspension of water supply. We found that the activated carbon adsorption treatment effectively removes the chemicals with high organicity value that is related to the carbon structure (Fujita and Akatsuka, 1984) or the ones with octanol/water partition greater than 1.5. Otherwise, released chemicals are difficult to remove using the water purification treatment; therefore, precautionary measures such as the emergency shut-off valve are necessary. In terms of protecting aquatic organisms in the river, six chemicals such as acrylic acid presented risks and exceeded the standard of acute toxicity to such organisms. An emergency shut-off valve installed in advance can reduce the amount of released chemicals to 1 to 2%, which decreases the possibility of affecting the most vulnerable aquatic organisms even at the water-intake point that is closest to the accident site.

From these analyses, we conclude that precautionary measures at industrial facilities effectively protect both aquatic organisms and water supply system, given that they can be applied to the chemicals that are difficult to remove using the absorption treatment.

©2020. Japan Geoscience Union. All Right Reserved.

Keywords: Chemical contamination, Water supply system, Earthquake, Environmental dynamic analysis, Environmental impacts

©2020. Japan Geoscience Union. All Right Reserved.

Exploring the linkage between urban flood risk and spatial characteristics in small urbanized catchments of Beijing, China

*Lei Yao[1]

1. Shandong Normal University

In the context of global urbanization, urban flood risk in many cities has become a seriously environmental issue, threatening health of public residents and environments. A number of hydrological studies have linked urban flooding issues closely to the spectrum of spatial patterns of urbanization, but relatively little attention has been given to small-scaled catchments within the realm of urban systems. This study aims to explore the hydrological effects of small-scaled urbanized catchments assigned with various landscape patterns. Twelve typical residential catchments in Beijing were selected as the study areas. Total impervious area (TIA), directly connected impervious area (DCIA), and a drainage index were used as the catchment spatial metrics. Three scenarios were designed as different spatial arrangement of catchment imperviousness. Runoff variables including total and peak runoff depth (Q_t and Q_p) were simulated by using SWMM model. The relationship between catchment spatial patterns and runoff variables were determined, and the results demonstrated that, spatial patterns have inherent influences on flood risks in small urbanized catchments. Specifically, (1) Imperviousness acts as effective indicators in affecting both Q_t and Q_p; (2) Increasing the size of drainage area dominated by each drainage inlet will benefit the catchment peak flow mitigation; (3) Different spatial concentrations of impervious surfaces have inherent influences on Q_p. These findings may provide insights into the role of urban spatial patterns in driving rainfall-runoff processes in small urbanized catchments, which is essential for urban planning and flood management.

Keywords: SWMM, Urban flood risk, Spatial pattern, Imperviousness, Rainfall-runoff

©2020. Japan Geoscience Union. All Right Reserved.

Flood disasters and river management in the downstream of Tama River following 2019 Typhoon Hagibis (JMA Typhoon No. 19)

*Jiro Komori[1]

1. Teikyo Heisei University

The typhoon No.19 caused inundation damage in 15 areas along the lower Tama River. This study presents the results of field survey in these area.

The causes of the inundation are classified in following three backward flow, 1) flowback from Tama River (main stream) via sluiceway, 2) backwater from Tama River to a tributary, 3) overflow at the levee crown of a gate. Most of the damaged areas in the track of the river are geologically classified into braided and meandering stream. As for inspection for the river management at the sluiceways and the present hazard map of Tama River are necessary in future.

Keywords: heavy rain disaster, flood gate, backwater, fluvial topography, post-disaster survey, hazard map

©2020. Japan Geoscience Union. All Right Reserved.

Development of a detailed land surface state estimation method toward usage in weather prediction

*Yuuki Myo[1], Kazuyoshi Souma[1]

1. University of Yamanashi

In Japan, localized heavy rainfalls have caused severe damages in recent years. It is indicated that the effects of the land surface states including urban activities on local heavy rainfall. Thus, the detailed land surface processes including urban activities are introduced into the numerical meteorological models used for weather prediction. Introduction of the detailed initial land surface state (land surface temperature, etc.) is required for such numerical meteorological models. Therefore, it will be effective to estimate the land surface state using detailed solar radiation and precipitation data, with advanced urban activity information.

In this study, we will develop a method which estimates realistic land surface states based on a detailed land surface model, introducing solar radiation data based on geostationary meteorological satellites, rainfall data provided by Japan Meteorological Agency (JMA), and detailed urban activity information data. We also estimate the land surface state for about one month in the Keihanshin region to validate the developed method.

In this study, in order to give the boundary conditions of the atmosphere, the initial values of the JMA meso objective analysis data (5km horizontal resolution) were used. For the distribution of precipitation, the Radar-Raingauge Analyzed Precipitation data provided by JMA (1km horizontal resolution) were used. For the distribution of solar radiation, the solar radiation consortium data (1km spatial resolution) were used. For land use including artificial land cover in each cell was calculated from the digital national land information (based on the 2009 survey; around 100m horizontal resolution) provided by GSI. As advanced urban activity data, the anthropogenic sensible heat distribution (Noyori et al., in press; 1km horizontal resolution), and the building height distribution based on the Zmap-AREA II 2010-2 version were also introduced. The introduction of the advanced urban activity data and the ability to support arbitrary grids can be indicated as the improvement compared with previous studies.

These data were introduced into a detailed land surface model called as Simple Biosphere model including Urban Canopy (SiBUC), which consists of the green area, water body, and urban area sub-models. The calculation of each sub-model is carried out based on the heat, radiative, and water budget equations.
In this study, the developed method was applied to the Keihanshin region for 31 days from 09:00 JST on the 1st August 2018 within a domain (480km x 480km; horizontal resolution about 2km), which is the same as that used in a weather prediction experiment by Takayama et al. (2016). In August 2018, an intensified observation of localized heavy rainfalls was conducted. For validation, the time series of roof surface temperature was extracted from within the cell closest to the Sumiyoshi Elementary School in Kobe City, where University of Yamanashi conducted field observations. In the validation, the maximum, minimum, and average roof surface temperatures for each day were extracted from estimated and observed values, to calculate mean error (ME), root mean squared error (RMSE), and correlation coefficient (CC). Regarding the CC, all (the daily maximum, minimum average roof temperature) showed high correlation exceeding 0.8. The ME and RMSE become higher in the order of daily maximum, average, minimum roof surface temperature. The reason for the higher ME and RMSE in the daily maximum roof

©2020. Japan Geoscience Union. All Right Reserved.

surface temperature is expected to be that the ground heat flux (the heat penetrates building) was overestimated. The SiBUC model considers the anthropogenic sensible heat by adding that to the net radiation when calculating the heat budget, that will be resulted in the overestimation of ground heat flux. It is also possible that the roof surface albedo (reflectance) value used in the estimation was lower than that on the roof of the observation site.

Keywords: Land surface state estimation, land surface temperature, Land surface model (SiBUC), Solar radiation consortium data, Advanced urban activity data

©2020. Japan Geoscience Union. All Right Reserved.

[J] Poster | A (Atmospheric and Hydrospheric Sciences)：A-CC Cryospheric Sciences & Cold District Environment

[A-CC39] Glaciology

convener:Takayuki Nuimura(Tokyo Denki University), Ishikawa Mamoru(Hokkaido University), Kzutaka Tateyama(National University Corporation Kitami Institute of Technology), Hiroto Nagai(Waseda Univ., School of Education)

The cryosphere is a fundamental component of the earth system. It is a region where snow and ice exist in the form of glacier/ice sheet, snow cover and snowfall, frozen ground, sea ice and fresh water ice, and they play a critical role in the global environment under the interactions with atmosphere, ocean, ecosystem and others. In this session, research results on physical and chemical characteristics of snow and ice, variations and dynamics of cryospheric environment, roles of the cryosphere on the earth and other planets will be discussed broadly, regardless of the research method.

[ACC39-P01] Estimation of mass balance of glaciers in the Northern Japanese Alps using SfM-MVS

*Kenshiro Arie[1], Chiyuki Narama[1], Kotaro FUKUI[2], Hajime IIDA[2] (1.Niigata University, 2.Tateyama Caldera Sabo Museum)

[ACC39-P02] Glacier flow velocity changes near the border of Alaska-Yukon detected by the Sentinel-1B SAR images

*Natsuki Muto[1] (1.Department of Natural History Sciences, Hokkaido University)

[ACC39-P03] Drainage from short-lived glacial lake in the Tien Shan, Central Asia.

Mirlan Daiyrov[1], *Chiyuki Narama[2], Tsutomu Yamanokuchi[3] (1.Central-Asian Institute for Applied Geosciences (CAIAG), 2.Niigata University, Department of Science, 3.RESTEC)

[ACC39-P04] Ice cliff dynamics in Trakarding Glacier, Nepal Himalaya

*Yota Sato[1], Koji Fujita[1], Hiroshi Inoue[2], Sojiro Sunako[2], Akiko Sakai[1], Akane Tsushima[3], Evgeny A. Podolskiy[4,5], Berthier Etienne[6], Kayastha Rijan[7] (1.Graduate School of Environmental Studies, Nagoya University, 2.National Research Institute for Earth Science and Disaster Resilience, 3.Meteorological Research Institute, 4. Arctic Research Center, Hokkaido University, 5.Global Station for Arctic Research, Global Institution for Collaborative Research and Education, Hokkaido University, 6.Université de Toulouse, 7. School of Science, Kathmandu University)

[ACC39-P05] Normally collapse of hanging glaciers at Mt. Langtang Lirung in Nepal

*Kosuke Matsumoto[2], Chiyuki Narama[1], Honami Watanabe[3], Katsuhisa Kawashima[1], Hiroshi YAGI[4], Daisuke Higaki[5], Akihiko Wakai[6] (1.Niigata University, 2.Graduate school of Niigata University, 3.RESTEC, 4.Yamagata University, 5.Hirosaki University, 6.Gunma University)

[ACC39-P06] The surface change of glacier-derived rock glacier in the northern Tien Shan

*Shun Okuyama[1], Chiyuki Narama[1], Hideyuki Takadama[2] (1.Niigata University, 2.PASCO Co.)

[ACC39-P07] Estimation of snow surface patterns between Showa Station and Dome-Fuji Station of Antarctica using camera images

*Konosuke Sugiura[1], Hirotaka Tomita[1], Kengo Watanabe[1], Naohiko Hirasawa[2], Kenji Kawamura[2], Fumio Nakazawa[2], Hiroshi Ohno[3], Shuji Fujita[2], Ikumi Oyabu[2], Takashi Yamanouchi[2], Hideaki Motoyama[2] (1.University of Toyama, 2.National Institute of Polar Research, 3.Kitami Institute of Technology)

[ACC39-P08] **Temporal and spatial variations of melting and Rain-On-Snow event on the sheets detected by Microwave observation**

Nuerasimuguli Alimasi[1], *Hiroyuki Enomoto[1], Naohiko Hirasawa[1] (1.National Institute of Polar Research)

[ACC39-P09] Monitoring Snow Avalanches by Infrasonic and Seismic Sensors on Mt.Fuji in 2018-2019 Winter Season

*Wataru Ikeda[1], Mie Ichihara[1], Ryo Honda[2], Hiroshi Aoyama[3], Shin'ichi Sakai[1] (1.Earthquake Research Institute, University of Tokyo, 2.Mount Fuji Research Institute, Yamanashi Perfectual Government, 3.Institute of Seismology and Volcanology, Faculty of Science, Hokkaido University)

[ACC39-P10] Application of SGLI and MSI sensor to estimate ice breakup dates on Lake Suwa

*Takashi Nonaka[1], Tomohiro Nakazawa[1] (1.College of Industrial Technology, Nihon University)

[ACC39-P11] Microplastics in rime-ice observed in Kyushu Mountain area, Japan

*Osamu Nagafuchi[1], Koyomi Nakazawa[1], kenichi Shinozuka[1], Koji KaneFuji[2] (1.Fukuoka Institute of Technology , 2.The Institute of Statistical Mathematics)

[ACC39-P12] The relationship between distribution of snow algae and vegetation: Mt. Naeba, Japan.

*Tsubasa Takahashi[1], Suzuki Takumi[1], Nozomu Takeuchi[1] (1.Chiba University)

Estimation of mass balance of glaciers in the Northern Japanese Alps using SfM-MVS

*Kenshiro Arie[1], Chiyuki Narama[1], Kotaro FUKUI[2], Hajime IIDA[2]

1. Niigata University, 2. Tateyama Caldera Sabo Museum

1. Introduction

Fukui and Iida (2012), Fukui et al. (2018), and Arie et al. (2019) measured ice thickness and flow in a perennial snow patches in the northern Japanese Alps, and confirmed seven perennial snow patches are extant glaciers.However, the characteristics of glaciers such as glacier mass balance and flow mechanism are not clear.

In this study, we calculated the mass balance, snow depth, and snowmelt depth of glaciers in the northern Japanese Alps for a total of four years from 2015 to 2019 using geodetic methods using SfM-MVS technology.

2. method

In this study, continuous aerial photographs of the glaciers area and topographic around the glacier area were taken from the Cessna during 2015-2019 at the end of snowmelt season (late September-early October) and during the maximum snowfall (late March-early April). Multi-period glacier DSM (digital surface model) was created using aerial photographs taken from Cessna and SfM-MVS software.The mass balance of a glacier can be obtained by calculating the relative volume change from a comparison of the two periods of DSM and integrating the snow volume with the relative volume change.We calculated the annual mass balance of five glaciers in the northern Japanese Alps from 2015/16 to 2018/19 by comparing the DSM at the end of snowmelt season in the year. In addition, the snow depth and melting depth of the glaciers from 2015/16 to 2018/19 were calculated from the comparison between DSM at the maximum snow season and DSM at the end of snowmelt season.

3. result

Fig. 1 shows the relative altitude change of glacier obtained from the difference of DSM at the end of snowmelt for each glacier and each year. In Fig. 1, the relative altitude change calculated from the DSM difference data is expressed in red as it is positive, green as it is negative, and yellow if there is almost no change.Furthermore, there is no partial difference in the relative altitude change on the glacier.Figure 2 shows the calculated annual mass balance, snow depth, and snowmelt depth for each glacier and each year. Figure 2 shows that there is a proportional relationship between the annual change of the annual mass balance and the annual change of the snow depth.Based on the above, the annual mass balance of glaciers in the northern Japanese Alps depends on the snow depth in that year, in heavy snowy years, the entire glacier is accumulation area, in light snowy years the entire glacier is ablation area.The mass balance characteristics of this Japanese glaciers are different from those of general mountain glaciers which have an accumulation area in upstream and an ablation area in downstream.

Keywords: Glacier, Mass-balance, SfM-MVS

©2020. Japan Geoscience Union. All Right Reserved.

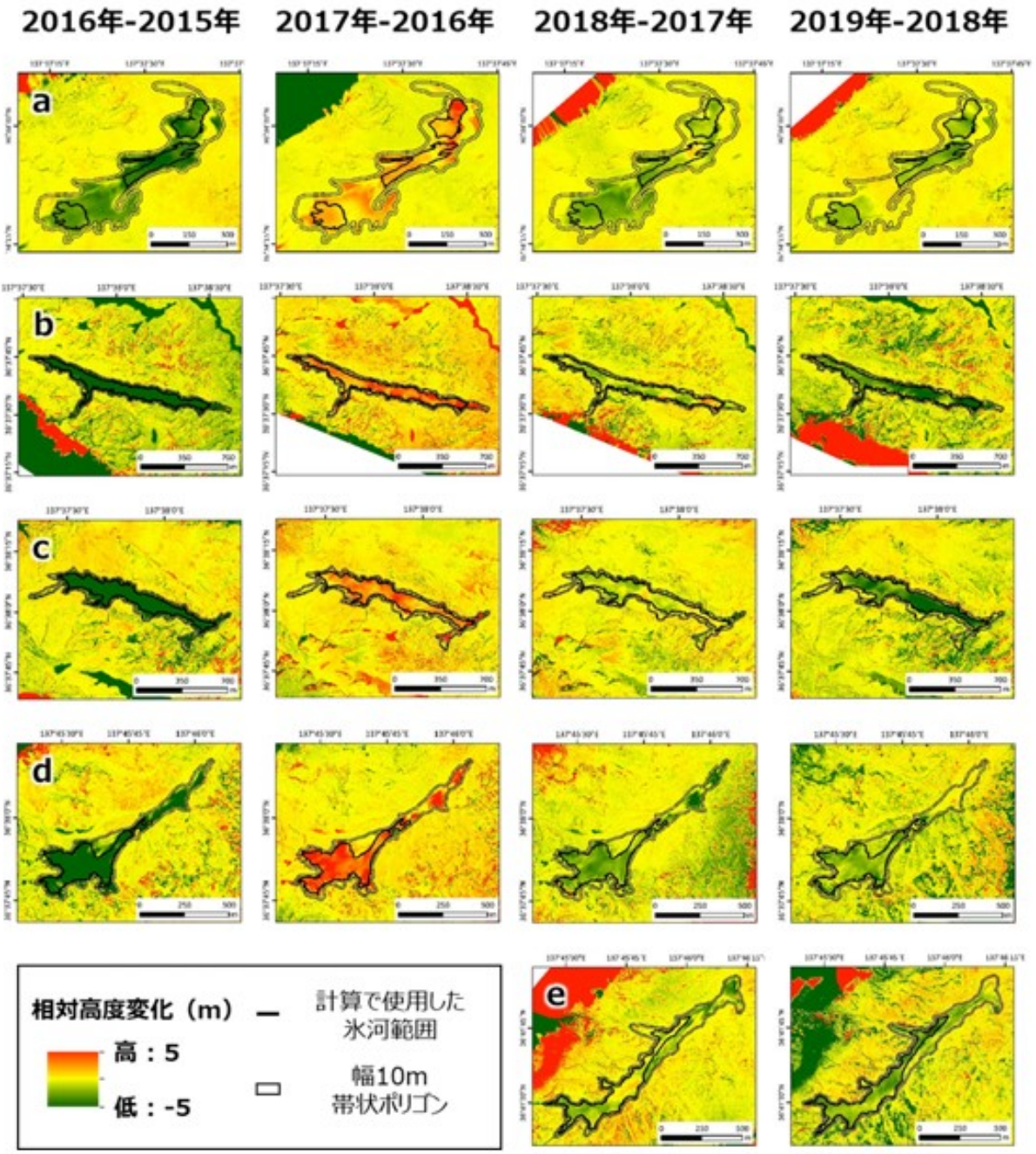

Fig. 1: Relative altitude change for each glacier and each year, obtained from the DSM difference at the end of snowmelt season. a: gozenzawa glacier b: sannnomado glacier c: Komado glacier d: Kakunesato glacier e: Karamatsuzawa glacier.

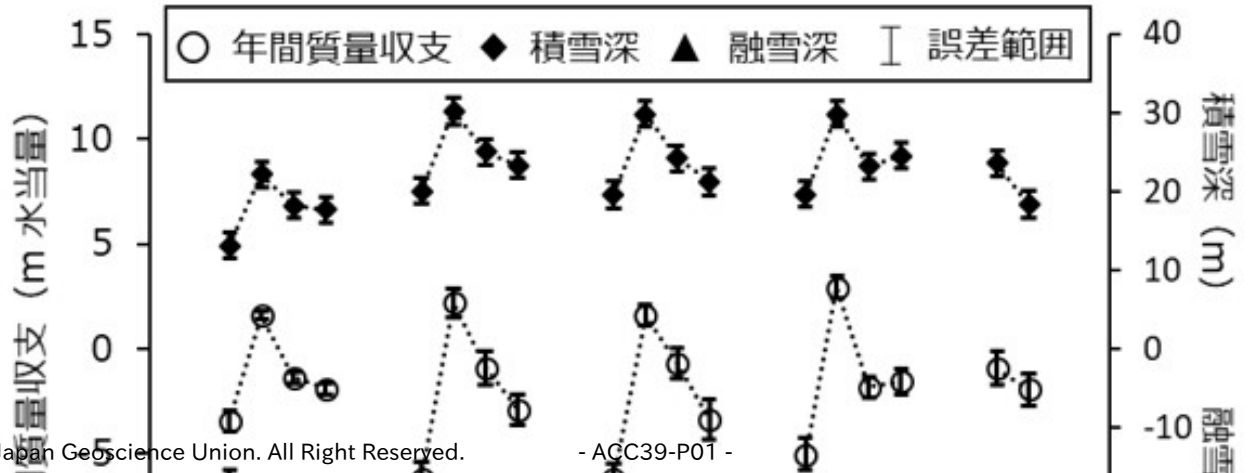

©2020. Japan Geoscience Union. All Right Reserved.

©2020. Japan Geoscience Union. All Right Reserved.

Glacier flow velocity changes near the border of Alaska-Yukon detected by the Sentinel-1B SAR images

*Natsuki Muto[1]

1. Department of Natural History Sciences, Hokkaido University

Recently, diverse spatial and temporal changes in the flow velocity of mountain glaciers have been reported by data analysis of synthetic aperture radar images. Near the border of Alaska, USA, and the Yukon, Canada, numerous surge-type glaciers are present, which are known to exhibit orders-of-magnitude speed-up together with km-scale terminus advance every several decades; the exact recurrent interval depends on each glacier. It is well known that glacier surges often initiate in winter, but its mechanisms remain unclear, in contrast to those for spring-summer speedups that are widely known on normal glaciers. Comprehensive velocity measurements are relatively scarce during winter season, especially in the middle to upper reaches of mountain glaciers, and further measurements are needed to better understand glacier dynamics.

The spatial and temporal velocity changes of mountain glaciers near the border of Alaska-Yukon from 2006 to 2011 were investigated using ALOS / PALSAR data (Abe and Furuya, 2015). Abe and Furuya (2015) reported that, at many of the quiescent surge-type glaciers around the St. Elias Mountains, upstream accelerations occurred from autumn to winter and then propagated towards downstream.

In this study, we applied offset tracking to Sentinel-1B / C-band SAR data on glaciers near the border of Alaska-Yukon to examine their spatial and temporal velocity changes. As a result, we have confirmed winter acceleration on the Anderson, Chitina and Klutlan glaciers, which is consistent with the finding by Abe and Furuya (2015).

Keywords: Ice flow

©2020. Japan Geoscience Union. All Right Reserved.

Drainage from short-lived glacial lake in the Tien Shan, Central Asia.

Mirlan Daiyrov[1], *Chiyuki Narama[2], Tsutomu Yamanokuchi[3]

1. Central-Asian Institute for Applied Geosciences (CAIAG), 2. Niigata University, Department of Science, 3. RESTEC

Many small glacial lakes are located at glacier fronts in the northern Tien Shan in the Kyrgyz Republic, Central Asia. In the region of the Issyk-Kul Basin, four large drainages occurred between 2006, 2008, 2013 and 2014 (Narama et al., 2010, 2018). These large drainages were caused by the “short-lived type” of glacial lakes which rapidly grew and drained within a few months (Narama et al., 2010, 2018; Daiyrov et al., 2018, 2019). To investigate drainage phenomena from short-lived lake, we set water level data logger and interval camera at the Korumdu Glacier, the northern Tien Shan. We got hydrograph of drainage from short-lived lake in 2017, 2018 and 2019.

Keywords: short-lived glacial lake, hydrograph, ice tunnel, Tien Shan

©2020. Japan Geoscience Union. All Right Reserved.

Ice cliff dynamics in Trakarding Glacier, Nepal Himalaya

*Yota Sato[1], Koji Fujita[1], Hiroshi Inoue[2], Sojiro Sunako[2], Akiko Sakai[1], Akane Tsushima[3], Evgeny A. Podolskiy[4,5], Berthier Etienne[6], Kayastha Rijan[7]

1. Graduate School of Environmental Studies, Nagoya University, 2. National Research Institute for Earth Science and Disaster Resilience, 3. Meteorological Research Institute, 4. Arctic Research Center, Hokkaido University, 5. Global Station for Arctic Research, Global Institution for Collaborative Research and Education, Hokkaido University, 6. Université de Toulouse, 7. School of Science, Kathmandu University

Glaciers in High Mountain Asia are valuable indicator of climate change, and their meltwater have an important role for the regional water resources (e.g. Pritchard, 2019). We thus need to estimate Himalayan glacier fluctuation. However, the lower part of large Himalayan glaciers is generally covered with debris mantle, which makes the melting process complicated. Several previous works pointed out a role of ice cliffs that promote local enhancement of the ice melting (e.g. Sakai et al., 1998; Brun et al., 2018). The ice cliff' s spatio-temporal distribution and their dynamics (evolution and decay) are important to understand debris-covered glaciers melting process.
In this study, we generated high resolution digital elevation models (DEMs) and orthomosaic images from aerial photographs taken at four different times at the Trakarding glacier, Nepal Himalaya in order to trace ice cliff dynamics.
In-situ observations and aerial photogrammetry surveys were carried out in 2007, 2017, 2018, 2019 post-monsoon seasons over the entire debris-covered area. These photographs were analyzed using Structure from Motion technology and created high resolution (0.2 - 2.0 m) terrain data. From each image, about 500 ice cliffs were extracted and analyzed these ridge lengths, slope areas, gradients, aspects and spatial distributions.
DEM differencing indicate that the surface mass balance has been strongly negative (-1.65 m w.e. yr^{-1}) from 2007 to 2019. Spatially, we observed that the more significant surface lowering happens, the higher cliff density is remarked. The result suggests the ice cliff locally enhances glacier melting. In addition, a significant correlation between ice cliff length and its slope area was observed, which means that it is possible to estimate the slope area of cliff from the cliff length using coarser satellite data. Analysis of ice cliff aspect elucidated that north-west facing ice cliffs are predominant. And their aspects had heterogeneous distribution. Finally, we estimated ice cliff dynamics and its mechanism from the results of spatial cliff density, aspect and elevation change analysis in Trakarding Glacier.

Keywords: Glacier, Himalaya, Remote Sensing, UAV

©2020. Japan Geoscience Union. All Right Reserved.

Normally collapse of hanging glaciers at Mt. Langtang Lirung in Nepal

*Kosuke Matsumoto[2], Chiyuki Narama[1], Honami Watanabe[3], Katsuhisa Kawashima[1], Hiroshi YAGI[4], Daisuke Higaki[5], Akihiko Wakai[6]

1. Niigata University, 2. Graduate school of Niigata University, 3. RESTEC, 4. Yamagata University, 5. Hirosaki University, 6. Gunma University

In April 2015, a huge earthquake called the Gorka Earthquake occurred near Kathmandu, the capital of Nepal. The Gorka earthquake triggered the collapse of hanging glaciers at Mt. Langtang Lirung. and caused severe damage in the Langtang village located at the bottom of the valley due to the avalanche of snow and ice debris(Kargel et al., 2015). A hanging glacier is a glacier that sticks to a steep hillside or overhangs a cliff. Because a hanging glacier exist in unstable places, they have the characteristic that they collapse in normal times without earthquakes, and the shape of the glaciers is maintained by repeated collapse. Taconnaz hanging glacier in the French Alps has been shown to have a collapse cycle of only half a year(Le Meur and Vincent, 2006). In Europe, the damage caused by the collapse of hanging glaciers in normal times has been reported, and hanging glaciers can cause disasters even in normal times without external factors such as earthquakes. The monitoring hanging glaciers collapse has been performed only in a few places in the European Alps. The amount of collapses, the cycle of collapses, and the topographic features of collapses are not clear in 7000m-class mountainous regions such as the Himalayas.In this study, I created orthophotos and DSM from helicopter aerial images taken in June and October 2015, November 2018, and November 2019, targeting hanging glaciers at Mt. Langtang Lirung in Nepal. By comparing each period, the amount and cycle of the collapse of hanging glaciers in normal times were investigated, and the characteristics of the collapse were considered.

Keywords: hanging glaciers, collapse, Mt. Langtang Lirung, SfM

©2020. Japan Geoscience Union. All Right Reserved.

The surface change of glacier-derived rock glacier in the northern Tien Shan

*Shun Okuyama[1], Chiyuki Narama[1], Hideyuki Takadama[2]

1. Niigata University, 2. PASCO Co.

Rock glacier is known as indicator landforms for mountain permafrost. The surface is covered with debris about boulders, and the interior is composed of permafrost mixed with ice and debris. Rock glacier, like glacier, is one of the periglacial landform that flows due to creep of internal ice. Rock glacier is classified into "talus-derived type" and "glacier-derived type" based on the source of debris and internal ice (Matsuoka,1998)."talus-derived type" is a type in which residual snow or underground water becomes a source of permafrost and develops on the cliff formed by gravel supplied from the bedrock behind it. "glacier-derived type" is a type in which a glacier exists superior of a rock glacier and develops from glacier ice and melted water from the glacier. "talus-derived type" is found worldwide and there are many research cases, but the distribution of "glacier-derived type" rock glaciers is limited, and its development process is not clear. In this study, in the northern Tien Shan, the surface flow of "glacier-derived type" rock glaciers was separated using DInSAR (Differential Interferometry SAR) and image matching, and the surface flow of the "glacial-derived type" was considered.

Keywords: rock glacier, mountain permafrost, DInSAR, image matching, Tien Shan

©2020. Japan Geoscience Union. All Right Reserved.

Estimation of snow surface patterns between Showa Station and Dome-Fuji Station of Antarctica using camera images

*Konosuke Sugiura[1], Hirotaka Tomita[1], Kengo Watanabe[1], Naohiko Hirasawa[2], Kenji Kawamura[2], Fumio Nakazawa[2], Hiroshi Ohno[3], Shuji Fujita[2], Ikumi Oyabu[2], Takashi Yamanouchi[2], Hideaki Motoyama[2]

1. University of Toyama, 2. National Institute of Polar Research, 3. Kitami Institute of Technology

Snow surface patterns in Antarctica are of practical concern and are important from the standpoint of developing an optimum route in Antarctica. In this study, we estimate snow surface patterns between the coast and the inland of Antarctica using camera images during JARE-59. The interval camera was used to capture the image of snow surface. Snow surface was photographed from November 13, 2017 to January 24, 2018. One screen was divided into eight zones to distinguish a small-scale snow surface pattern. The pattern of snow surface was classified in three kinds such as 1) sastrugi, 2) snow dune/barchan, and 3) snow ripple. We judged the snow surface patterns by sight. The frequency of the three patterns of round-trip snow surface was obtained. The analyzed results of altitude dependence agreed with the previous research qualitatively. However, the altitude of the spot where large sastrugi appeared became higher than a previous research. From this point we might go on to an even more detailed research of a time scale of the surface pattern changes.

Keywords: sastrugi, snow dune, snow barchan, snow ripple

©2020. Japan Geoscience Union. All Right Reserved.

Temporal and spatial variations of melting and Rain-On-Snow event on the sheets detected by Microwave observation

Nuerasimuguli Alimasi[1], *Hiroyuki Enomoto[1], Naohiko Hirasawa[1]

1. National Institute of Polar Research

The Arctic is experiencing rapid environmental change due to climate warming, resulting in snow condition changes [1]. Melting of ice sheets has been observed, and recently Rain-on-snow has become a new focus as it indicates evidence of warming and causes disaster in the snow-covered region [2] [3]. Chages in the Antarctica has been occurig, however systematic moitorings are few.

This study presents the temporal and spatial variation of ice sheet melting on the slopes of Antarctic and Greenland ice sheets, based on satellite microwave observations. The research in Antarctica focused on the coastal marginal zone and inland traverse route near Syowa Station, Antarctica, from the S17 site (608 m a.s.l.) to the H128 site (1376 m a.s.l.). Melting was detected using diurnal amplitude variation (DAV). Data from AMSR-E, for 2002–2012, and AMSR2, for 2012–2017, showed a variation in DAV over time. The greatest extent of melting was estimated to have occurred during the 2003/2004 summer. DAV rose inland, until the H92 site (1268 m a.s.l). In contrast, DAV decreased in the case of rain, which was reported by the Japanese Antarctic Research Expedition in 2004 and 2012. This is due to the rise of nighttime brightness temperature (TB). The signal from rain was limited to the area between the S17 and H24 sites (832 m a.s.l.). Coastal zones showed a low TB locally around S17. The refrozen ice lenses under the coastal snow layers seem to have caused the low coastal emissions. The DAV can be significant as daytime and nighttime contrast increase from this low TB.

This study compares the research in the Greenland Ice Sheet [4]. We set the transect from the coast to ridge area in the northen region and the central regions of the Greenland ice sheet.

References

[1] N. Alimasi, A Review: Microwave observations of snow-covered areas over complex Arctic terrain, *Bulletin of Glaciological Research* **36**, 1-13, (2018)

[2] H. Enomoto, N. Alimasi, Changes in Antarctic and Arctic sea ice in 2016-2017 and snow and ice conditions in the surrounding regions, Journal of Japanese Society of Snow and Ice 79(5), 451-463, (2017).

[3] N. Alimasi, H. Enomoto, N. Hirasawa, Summer melting observation at the marginal region of the Antarctic ice sheet by microwave radiometer, *Journal of Japanese Society of Snow and Ice*, **80**(5), 481-499 (2018).

[4] N. Alimasi, H. Enomoto, Arctic snow monitoring by satellite microwave observation, *Journal of Japanese Society of Snow and Ice* **79**(1), 17-30, (2017).

Keywords: Arctic, Antarctic, melting

©2020. Japan Geoscience Union. All Right Reserved.

©2020. Japan Geoscience Union. All Right Reserved.

Monitoring Snow Avalanches by Infrasonic and Seismic Sensors on Mt.Fuji in 2018-2019 Winter Season

*Wataru Ikeda[1], Mie Ichihara[1], Ryo Honda[2], Hiroshi Aoyama[3], Shin'ichi Sakai[1]

1. Earthquake Research Institute, University of Tokyo, 2. Mount Fuji Research Institute, Yamanashi Perfectual Government, 3. Institute of Seismology and Volcanology, Faculty of Science, Hokkaido University

While infrasonic studies of snow avalanches were already reported (e.g., Arai et al.,2017), few observations have been carried out to analyze seismic and infrasonic waves at the same time. Kogelning et al. (2011) reported that big avalanches generated infrasonic waves before the seismic waves. They interpreted it as that a snow avalanche started as low-density snow debris and increased its density when it got big in the last stage. They suggested that infrasonic signals are useful to detect the beginning of the avalanche, and seismic signals are to estimate its end. Therefore, separation of seismic and infrasonic signal is essential to determine the beginning and ending time, location and type of the avalanche.

In this study, we set infrasonic and seismic sensors around Mt. Fuji for a whole winter season. We used signals detected by the multiple sensors to identify events and estimate the direction of sources by calculating the delay of signals. We also compared the power spectra between the data recorded by an infrasonic sensor and a collocated seismometer for each event to distinguish seismic signals and infrasonic signals and to determine the location and type of the avalanche.

We set two infrasonic stations with a relative distance of 1km, each of which consists of a pair of microphones separated about 10m. Two 3-component seismometers and three 1-component seismometers were also installed, as shown in fig1. At AKD station, both infrasonic and seismic sensors were installed. Observations were carried out from December 2018 to May 2019, with a sampling rate of 100Hz. We also installed a probe-like thermometer that had three elements in vertical 40-cm grids next to the infrasonic sensors in AKD to record the temperature and snow depth.

We calculated cross correlation in the frequency band of 1-10 Hz for the data recorded by the microphone pair at each of AKD and KMT to mitigate the signals generated by wind noise. Then, we extracted events whose correlations of the microphone pairs were higher than 0.8 at the both stations. Around 50 samples were selected as likely signals of avalanches after excluding earthquake and artificial signals.

Seismic sensors record both seismic waves and infrasonic waves, and so do infrasonic sensors. In order to distinguish the ground motion triggered by infrasound from seismic waves, we analyzed the data of AKD where seismic and infrasonic sensors were both installed. The response function of the seismometer to infrasound waves was calculated by averaging the power spectral ratios between the seismic and infrasonic records of clear infrasonic signals from the nearby military exercises. Ten events of military exercises were used in the analysis. Then, we used the response function to normalize the seismic-to-infrasonic ratio of the power spectra in the 50 events of likely avalanches. If the seismic sensors detect only infrasonic waves, the normalized ratio ideally goes to 1. In the case of seismic waves, however, it becomes much larger. We focused on this point and found that most of the events only had infrasonic signals. Still, infrasonic and seismic signals were both recorded in 4 events.

The infrasonic part of the signals was recorded by the multiple infrasonic and seismic stations. The

©2020. Japan Geoscience Union. All Right Reserved.

relative arrival times were estimated by the cross-correlation analyses for the microphone pairs and by the amplitude delay among the different stations. They indicate similar source directions for most of the cases, though the resolution was poor. In some cases, we found evidence that the sources were moving. Based on these results, we believe that the signals were generated by snow avalanches. In the 4 events which had both infrasonic and seismic signals individually, we recognized the seismic signals only at a few stations, and could not observe their propagation over the stations. The 4 events occurred from 16th to 27th of April. The thermometer data showed that there was more than 30-cm snowfall from 10th to 11th of April, and the temperature rapidly rose after that. It is possible that the weather conditions made the avalanches denser in the four events.

Currently, the observation of snow avalanches in the 2019-2020 winter season is going on. This winter, we set 4 microphones in a 100-m scale array, the seismic stations, and two probe thermometers. Further detailed observation and analyses will help understanding snow avalanches.

Keywords: Avalanche, Infrasound, Seismology

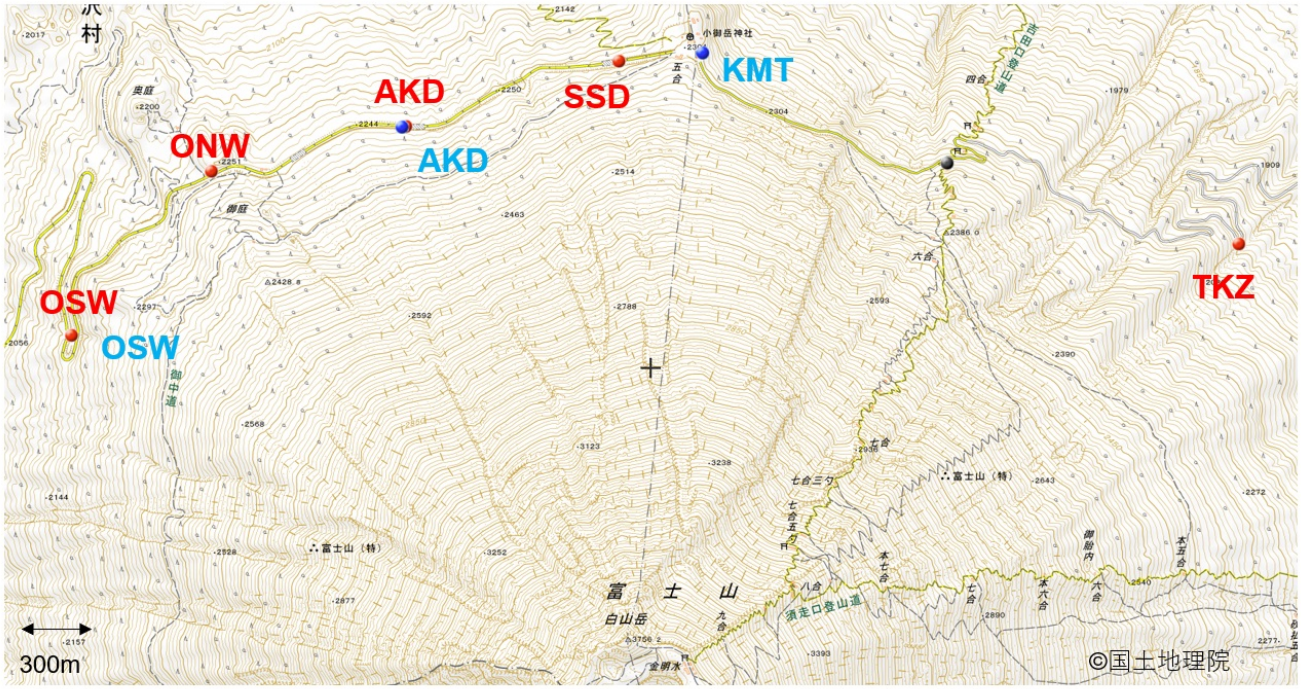

Fig1: Placement of seismic and infrasonic sensors

Infrasound Sensors
Seismic Sensors

©2020. Japan Geoscience Union. All Right Reserved.

Application of SGLI and MSI sensor to estimate ice breakup dates on Lake Suwa

*Takashi Nonaka[1], Tomohiro Nakazawa[1]

1. College of Industrial Technology, Nihon University

The freeze-up and breakup dates for lakes are important indicator of climate change. Freezing point on the lakes were observed in Europe and North America, while there is not enough record of freeze-up and breakup dates of the Japanese lakes. Lake Suwa in Nagano Prefecture in Japan, which is critical due to the frozen surface located in the middle latitude, had observed those freeze-up dates until 1994, however there is no records after that. Even lakes without record are observable utilizing satellite data. In previous studies, we used MODIS sensor mounted on the Terra satellite which can observe the same spot every day, and estimated the surface condition of Lake Suwa. As a result, we successfully classified the surface condition into ice and water using both surface reflectance and water temperature data acquired by MODIS. However, the spatial resolution (1 km) was coarse to observe the small lakes. In addition, selecting different satellites allow more frequent observation.

The present study focused on “Second generation Global Imager (SGLI)” on “Global Change Observation Mission –Climate (GCOM-C)” satellite, an optical sensor with resolution of 250 m, which was launched on December 23, 2017. The objective of this study was to acquire the knowledge for the application of SGLI to estimate the ice breakup dates. Before the examination of the method, we revealed about the accuracy of “Sea Surface Temperature (SST)” and “Normalized Water Leaving Radiance (NWLR)” products quantitatively. The result showed that SST had the accuracy better than 1 degree, though the reflectance of NWLR was underestimated. Therefore, we proposed a method to use the reflectance of Multispectral Imager (MSI) on Sentinel-2 instead of SGLI. We applied the proposed method to analyze 2018 data, and tried to grasp the surface status and ice breakup dates on Lake Suwa. It showed that the reflectance was fluctuated at 2 degree or less same as the previous study using MODIS data. In addition, we revealed that the result acquired by SGLI/MSI complemented the surface status acquired only by MODIS, and shortened the range of the ice breakup dates of Lake Suwa. We intend to develop the methodology to estimate the ice breakup dates using water temperature trend by SGLI data in the future study.

Keywords: Reflectance, Surface temperature, Freezing state, Lake Suwa

©2020. Japan Geoscience Union. All Right Reserved.

Microplastics in rime-ice observed in Kyushu Mountain area, Japan

*Osamu Nagafuchi[1], Koyomi Nakazawa[1], kenichi Shinozuka[1], Koji KaneFuji[2]

1. Fukuoka Institute of Technology , 2. The Institute of Statistical Mathematics

In order to clarify the long-range transport of microplastic litter in Asian region, we have collected rime-ice and snow samples in mountainous area of Japan. We have observed microplastics using raman imaging microscope and FTIR microscopy. We will discuss about the difference of characteristics of microplastics in rime ice and snow. In addition, we will perform back trajectory analysis to discuss about the long range transport of microprastics.

Keywords: rime ice, microplastics

©2020. Japan Geoscience Union. All Right Reserved.

The relationship between distribution of snow algae and vegetation: Mt. Naeba, Japan.

*Tsubasa Takahashi[1], Suzuki Takumi[1], Nozomu Takeuchi[1]

1. Chiba University

Ecosystems of snowy mountains in Japan are composed of unique biological communities. Snow algae are typical microorganisms growing on the snow surface in such ecosystems. They photosynthetically grow in the low temperature condition of the snow surface. They can visibly be observed as colored snow and distribute widely from the lower coniferous or deciduous forests to the alpine zone above timber line. Growth and community structure of snow algae may vary in different vegetation since nutrients and light conditions on the snow surface are affected by the vegetation. However, there is little information on the relationship between snow algae and vegetation in mountain regions in Japan. This study describes spatial and temporal variations of snow algae across a mountain slope from lower forest to upper alpine zone and examines the relationship between snow algae and vegetation.
Fieldworks were carried out three times in mid-April (from 13 to 14 April), end of April (29 to 30 April) and early May (9 to 11 May) in 2019 in Mt. Naeba located in Niigata prefecture, Japan. Surface snow samples were collected at ten sites (S1-S10) of different elevations of the western slope of the mountain. Chlorophyll a concentrations and chemical solutes in the snow samples were analyzed in a laboratory in Chiba University. The chlorophyll a concentration significantly increased from mid-April to early May. It was higher at lowest two sites (S1 and S2) in the end of April to early May, and was also higher at site S7 in early May. The higher Chlorophyll a concentration at the lowest sites are probably due to more abundant snow algae caused by longer duration of snow melt. However, the high chlorophyll a concentration at the higher site (S7) suggests that the factor other than snow melt duration affects the algal growth. The chemical solutes in the snow surface showed that PO_4^{3-} was higher at the sites where the chlorophyll a concentration was high. The difference of PO_4^{3-}concentration in the snow surface may be due to the vegetation at the sites. The vegetation are coniferous trees (Cedar and Abies Mariesii) at sites S1 ,2, 7, are broad leaf trees (Beech and Birch) at S3, 4, 5, 8 and are above timber line at S9 and 10. The PO_4^{3-} concentration in the surface snow greatly increased only at the sites of coniferous trees, suggesting that PO_4^{3-} was supplied from the trees. Since PO_4^{3-} was one of the essential nutrients for snow algae, it is likely to induce the growth of snow algae in the forest. The coniferous trees are typical vegetation in the heavy snow area in mountainous regions of Japan, and thus they are likely to provide favorable conditions for snow algal growth in the regions.

Keywords: Snow algae, Vegetation, Snow mountains

©2020. Japan Geoscience Union. All Right Reserved.

[J] Poster | A (Atmospheric and Hydrospheric Sciences)：A-CG Complex & General

[A-CG54] Biogeochemical cycles in Land Ecosystem

convener:Tomomichi Kato(Research Faculty of Agriculture, Hokkaido University), Kazuhito Ichii(Chiba University), Takeshi Ise(FSERC, Kyoto University), Munemasa Teramoto(Arid Land Research Center, Tottori University)

Terrestrial ecosystem influences global climate through cycles of water, carbon, and nitrogen between land surface and atmosphere. For better understanding of those behaviors, a great effort has been paid for developing varieties of approaches and techniques such as biometric survey, eddy and chamber methods, near and satellite remote sensing, biosphere modeling and so on.
 In particular, the JapanFlux, founded in 2006 as a researchers network of CO2, H2O and other trace gas flux measurement, has promoted the multi-disciplinal studies not only for flux measurement community, but also for remote sensing and biosphere modeling communities. Moreover, the Research-Group-on-Integrated-Land-Processes, which was founded in 2006, also has contributed to build networks between Japanese researchers to better understanding of physical and biological processes on interactions between terrestrial surface and atmosphere.
 This session unites those multi-disciplinal activities, and promotes the oral and poster presentations on the role of terrestrial ecosystem in material circulations of water, carbon, nitrogen, energy and other substances by any approaches and technics. This session takes over the former session in last year: A-CG39

[ACG54-P01] Long-term observations of plant phenology, and land cover and land use change by satellite remote-sensing in Asia

*Shin Nagai[1], Taku M Saitoh[2] (1.Earth Surface System Research Center, Research Institute for Global Change, Japan Agency for Marine-Earth Science and Technology, 2.River Basin Research Center, Gifu University)

[ACG54-P02] Carbon emission estimation through tropical peatland subsidence using interferometric synthetic aperture radar analysis

*Tomohiro Shiraishi[1], Ryuichi Hirata[1], Masato Hayashi[2], Takashi Hirano[3] (1.National Institute for Environmental Studies, 2.Japan Aerospace Exploration Agency, 3.Research Faculty of Agriculture, Hokkaido University)

[ACG54-P03] Effect of global warming on forest ecosystem in Japan: Data analysis using tree-rings, satellite images and earth system model

*Shunsuke Tei[1] (1.Arctic Research Center, Hokkaido University)

[ACG54-P04] A large-scale evaluation of bamboo stand expansion using deep learning and its effect on ecosystem carbon storage

*Yurika Oba[1], Takeshi Ise[2] (1.Center for the Promotion of Interdisciplinary Education and Research, Kyoto University, 2.Field Science Education and Research Center, kyoto University)

[ACG54-P05] Subdaily natural CO_2 flux simulation in Kantō area to support inversion analysis of Tokyo's anthropogenic CO_2 emission

*Qiao Wang[1], Ryoichi Imasu[1], Yutaka Arai[1], Satoshi Ito[1], Takahiro Sasai[2], Hiroaki Kondo[3] (1.AORI, The University of Tokyo, 2.Department of Geophysics, Tohoku University, 3.National Institute of Advanced Industrial Science and Technology)

[ACG54-P06] A long term evaluation of carbon balance in a managed urban forest in central Japan using a Forest Biogeochemical Model (BGC-ES)

Guochao Wang[4], *Tomotsugu Yazaki[1], Makoto Ooba[2], Toshio Kume[4], Takamitsu Kai[3] (1.School of Agriculture, Meiji University, 2.National Institute for Environmental Studies, 3.Kurokawa Field Science Center, Meiji University, 4.Graduate School of Agriculture, Meiji University)

[ACG54-P07] **The long-term observation of PRI and LUE and phenology changes in a temperate Japanese cypress forest at Kiryu Japan.**

*CHEN SIYU[1], Yoshiko Kosugi[1], Tatsuro Nakaji[2], Hibiki M Noda[3], Kenlo Nishida Nasahara[4], Kouki Hikosaka[5] (1.Graduate school of agriculture,Kyoto University, 2.Hokkaido University, 3.National Institute for Environmental Studie, 4.University of Tsukuba, 5.Tohoku University)

[ACG54-P08] **Challenging the detection of solar-induced fluorescence from lower resolution field-measured spectrum in Japan**

*Naohisa Nakashima[1], Tomoki Morozumi[1], KANOKRAT BUAREAL[3], Tomomichi Kato[1], Katsuto Tsujimoto[2], Tomoko Akitsu[4], Kenlo Nasahara[4], Keisuke Ono[5], Hiroyuki Muraoka[6] (1.Research Faculty of Agriculture, Hokkaido University, 2.Graduate School of Life Sciences, Tohoku University, 3.Graduate School of Global Food Resources, Hokkaido University, 4.Faculty of Life and Environmental Sciences, University of Tsukuba, 5.National Institute for Agro-Environmental Sciences, 6.River Basin Research Center, Gifu University)

[ACG54-P09] Influence of climatic fluctuations on crop production for 135 years in Japan

*Tomomichi Kato[1], Moeka Ono[1], Daiki Watanabe[1] (1.Research Faculty of Agriculture, Hokkaido University)

[ACG54-P10] Long-term warming effect on soil carbon fluxes in a red pine forest in Tsukuba

*Munemasa Teramoto[1], Naishen Liang[1], Jiye Zeng[1], Jun Koarashi[2], Toshiaki Kondo[3], Mariko Atarashi-Andoh[2], Takafumi Aramaki[1], Xin Zhao [1] (1.National Institute for Environmental Studies, 2.Japan Atomic Energy Agency, 3.Japan International Research Center for Agricultural Sciences)

Long-term observations of plant phenology, and land cover and land use change by satellite remote-sensing in Asia

*Shin Nagai[1], Taku M Saitoh[2]

1. Earth Surface System Research Center, Research Institute for Global Change, Japan Agency for Marine-Earth Science and Technology, 2. River Basin Research Center, Gifu University

Accurate monitoring of spatio-temporal variability of plant phenology, and land cover and land use change (LCLUC) is one of important tasks to evaluate ecosystem functions (photosynthesis and evapotranspiration) and services, and biodiversity under global change (climate change and anthropogenic activities). Towards this aim, despite coarse spatial resolution (250-1000 m), analysis of Terra and Aqua/MODIS satellites-observed vegetation index data at a daily time step is useful. We evaluated the year-to-year variability of the conventional start (SGS: the timing of leaf flush) and end of growing season (EGS; the timing of leaf fall) in Japan and LCLUC (deforestation) in insular Southeast Asia by analysing time-series in daily Terra and Aqua/MODIS satellites-observed green-red vegetation index (GRVI) for a decadal scale. SGS was defined as the first day when GRVI was greater than or equal to 0 in spring and EGS was defined as the first day when GRVI was less than zero in autumn. We calculated the ratio of number of days of minus GRVI values with clear sky conditions to those of all GRVI values with clear sky conditions for each pixel at a yearly time step. Then deforestation was defined as the ratio was greater than 0.8. SGS and EGS showed the year-to-year variability along the horizontal and elevational gradients. Deforestation for palm oil and acacia plantation was shown in Sumatra, near-coast region of Sarawak, and Central Kalimantan. In this presentation, we show the latest result and discuss the characteristics of spatio-temporal variability of SGS and EGS in Japan, and deforestation in insular Southeast Asia.

Keywords: remote-sensing, plant phenology, land cover and land use change

©2020. Japan Geoscience Union. All Right Reserved.

Carbon emission estimation through tropical peatland subsidence using interferometric synthetic aperture radar analysis

*Tomohiro Shiraishi[1], Ryuichi Hirata[1], Masato Hayashi[2], Takashi Hirano[3]

1. National Institute for Environmental Studies, 2. Japan Aerospace Exploration Agency, 3. Research Faculty of Agriculture, Hokkaido University

The tropical peat swamp forests have been deforested by the rapid expansion of oil palm plantations in Borneo. As a result of drainage by the plantation development, land subsidence occurs through a series of steps of compaction, shrinkage, consolidation, and oxidative peat decomposition. Carbon is emitted through the peat decomposition. We estimated the ground displacement of a newly developed oil palm plantation from a peat swamp forest in Sarawak, Malaysia, using interferometric synthetic aperture radar (InSAR) analysis. The used data were C-band SAR data by Sentinel-1A operated by ESA. The analysis of ground displacement (subsidence) was conducted for approximately nine months from 31 August 2017 to 22 May 2018. The measured subsidence by InSAR analysis was 13.7 cm (18.3 cm $year^{-1}$) on average of the test site (2143 ha). Carbon emissions through the subsidence were estimated by multiplying the subsidence depth by peat bulk density of 0.1 Mg m^{-3} (Ishikura et al., 2019), peat carbon content of 52.8% (Ishikura et al., 2018), and the contribution rate of oxidative peat decomposition at 50%. Total carbon emissions were estimated 48.3 t C ha^{-1} $year^{-1}$. This presentation reports the estimation results and the comparing evaluations with previous studies.

Keywords: carbon emissions, peat decomposition, C-band SAR, interferometric SAR

©2020. Japan Geoscience Union. All Right Reserved.

Effect of global warming on forest ecosystem in Japan: Data analysis using tree-rings, satellite images and earth system model

*Shunsuke Tei[1]

1. Arctic Research Center, Hokkaido University

Global warming not only changes long term trend of temperature and precipitation, but also increases the frequency and intensity of extreme weathers. These changes possibly affect forest ecosystem, and in some cases the ecosystem may be adversely affected. In order to maintain diverse functions of forest ecosystem (ecosystem services) in the future, the effect of global warming on forest ecosystem should be fully understand. However, it has not been obtained yet.

The purpose of this study is to (1) clarify the past effects of long/short term climate change due to recent warming on forest ecosystems in Japan by using tree-ring parameters, satellite images and gridded climate dataset, (2) predict the likelihood of future occurrence for long/short term climate change (e.g., warming trends and intensity/frequency of severe drought) from an earth system model, and (3) evaluate the future risk of forest ecosystems in Japan. In this presentation, we intend to show the preliminary results on this.

Keywords: Global warming, Forest ecosystem, ecosystem service

©2020. Japan Geoscience Union. All Right Reserved.

A large-scale evaluation of bamboo stand expansion using deep learning and its effect on ecosystem carbon storage

*Yurika Oba[1], Takeshi Ise[2]

1. Center for the Promotion of Interdisciplinary Education and Research, Kyoto University, 2. Field Science Education and Research Center, kyoto University

The expansion of bamboo stands causes a serious problem in various parts of Japan. Especially in the warmer regions west of the Kanto region, the rapid expansion of bamboo stands in satoyama ecosystems has reduced ecosystem services such as conservation of biodiversity. Most of the bamboo species in Japan are considered to be exotic species. Until recently, bamboo stand has been planted and managed as a valuable resource that is used as a material for household goods such as baskets and colanders. With the rise of industrial products, bamboo stands have been left in satoyama without management. Bamboos reproduce mainly by the rhizome, thus the rate of shoot proliferation is extremely high. Consequently, bamboo overwhelms tree and shrub species common in satoyama and can significantly change the ecosystem in several years. In this research, low-cost, large-scale, near-real-time identification of bamboo stand for Google Earth is performed by using the chopped picture method of image identification technology based on deep learning, which has attracted attention in recent years. This allows us to quantify the dynamics of bamboo stand expansion in recent years. In addition, a scenario-based analysis was conducted to clarify changes in ecosystem carbon storages according to different management policies of bamboo stand.

Keywords: deep learning, bamboo stand, carbon storage

©2020. Japan Geoscience Union. All Right Reserved.

Subdaily natural CO_2 flux simulation in Kantō area to support inversion analysis of Tokyo’s anthropogenic CO_2 emission

*Qiao Wang[1], Ryoichi Imasu[1], Yutaka Arai[1], Satoshi Ito[1], Takahiro Sasai[2], Hiroaki Kondo[3]

1. AORI, The University of Tokyo, 2. Department of Geophysics, Tohoku University, 3. National Institute of Advanced Industrial Science and Technology

Previous ground monitoring data analysis (Imasu and Tanabe 2018) suggests both diurnal and seasonal variations of atmospheric CO_2 concentration in greater Tokyo area. Such spatiotemporal variability is attribute to a combination of atmospheric processes, human activities and land-atmosphere CO_2 exchange. In this study, we prepare a subdaily version of BEAMS (Biosphere model integrating Eco-physiological And Mechanistic approaches using Satellite data, Sasai et al. 2016) at regional scale to estimate gross primary production (GPP), net primary production (NPP) and net ecosystem production (NEP) in Kanto plain. After calibration and validation, we supply these hourly biogenic CO_2 flux data to the atmospheric transport model AIST-MM (Kondo et al. 2001) to study CO_2 emission from Tokyo.

References :
Imasu and Tanabe, 2018, https://doi.org/10.3390/atmos9100367
Kondo *et al.* 2001, https://doi.org/10.2151/jmsj.79.11
Sasai *et al.* 2016, https://doi.org/10.1002/2015JG003157

Keywords: GPP, NPP, NEP, BEAMS, diurnal variation

©2020. Japan Geoscience Union. All Right Reserved.

A long term evaluation of carbon balance in a managed urban forest in central Japan using a Forest Biogeochemical Model (BGC-ES)

Guochao Wang[4], *Tomotsugu Yazaki[1], Makoto Ooba[2], Toshio Kume[4], Takamitsu Kai[3]

1. School of Agriculture, Meiji University, 2. National Institute for Environmental Studies, 3. Kurokawa Field Science Center, Meiji University, 4. Graduate School of Agriculture, Meiji University

Carbon sink function in urban forests has been attracted attention a mitigation strategy of global warming. Urban forests are usually managed (removing dead and damaged trees, and undergrowth) for preserving scenery and securing safety. Removing trees (thinning) in urban forests of Kanto region, central Japan, unlike the forestry thinning, the thinning is characterized by low intensity and high frequency. Here, we aimed to clarify the effects of these managements on the carbon balance of deciduous broadleaf vorest, and to clarify how we can reduce carbon emission from the urban forest management. We calculated the carbon balances under different management scenarios using a forest biogeochemical model (BGC-ES model) to elucidate effects of urban forest management on carbon sink function.

Keywords: urban green spaces, deciduous broadleaf forest, removal of dead and damaged trees, soil carbon, biomass carbon, carbon sequestration

©2020. Japan Geoscience Union. All Right Reserved.

The long-term observation of PRI and LUE and phenology changes in a temperate Japanese cypress forest at Kiryu Japan.

*CHEN SIYU[1], Yoshiko Kosugi[1], Tatsuro Nakaji[2], Hibiki M Noda[3], Kenlo Nishida Nasahara[4], Kouki Hikosaka[5]

1. Graduate school of agriculture,Kyoto University, 2. Hokkaido University, 3. National Institute for Environmental Studie, 4. University of Tsukuba, 5. Tohoku University

The light-use efficiency (LUE) of vegetation is one of the most essential parameters in production estimation models for terrestrial ecosystems. LUE generally expressed as the ratio of gross primary production (GPP) to absorbed photosynthetically active radiation (APAR). Due to the characteristic of photochemical reflectance index (PRI), which is sensitive to changes in carotenoid pigments (e.g. xanthophyll pigments) in live foliage. We recorded the canopy spectral reflectance data onto hemispherical spectroradiometers to calculate the PRI. Then we sorted and analyzed the diurnal, seasonal, and inter-annual changes of PRI to try to figure out the LUE in temperate Japanese cypress forest. We measured and recorded the CO_2 flux data onto the canopy by using the eddy covariance method to calculate the GPP. We also documented the micrometeorological data of the temperate Japanese cypress forest such as temperature, wind speed and photosynthetically active radiation (PAR) since 2014.

We made use of the digital camera to monitor the canopy phenology changes. The digital camera takes photos in 3 hours interval, and we extracted the RGB channels of image data to calculate the greenness indices.

Combining with the vegetation indices data and the phenology changes data can allow us to figure out the Japanese cypress forest phenology changes patterns and deeply knowledgeable about the relationships between PRI and LUE.

Our findings demonstrated that LUE has a good relationship with the PRI. Correlation coefficient calculated results shows that LUE and PRI significantly associated in 297 fine days ($R>0.75$). During the monitoring period, apparent seasonal and diurnal change of the PRI observed at temperate Japanese cypress forest. Furthermore, the PRI was observed that reaches the peak in September and the valley in February. We also found out distinct phenology changes patterns with the phenological analysis results. The greenness index showed similar seasonal changes with that of PRI. When the redness index reaches the peak, the PRI reaches the valley. It suggested that leaf redding phenomena causes the decline of PRI and LUE.

Keywords: Japanese cypress, photochemical reflectance index (PRI), photosynthetic light use efficiency(LUE), phenological analysis

©2020. Japan Geoscience Union. All Right Reserved.

Challenging the detection of solar-induced fluorescence from lower resolution field-measured spectrum in Japan

*Naohisa Nakashima[1], Tomoki Morozumi[1], KANOKRAT BUAREAL[3], Tomomichi Kato[1], Katsuto Tsujimoto[2], Tomoko Akitsu[4], Kenlo Nasahara[4], Keisuke Ono[5], Hiroyuki Muraoka[6]

1. Research Faculty of Agriculture, Hokkaido University, 2. Graduate School of Life Sciences, Tohoku University, 3. Graduate School of Global Food Resources, Hokkaido University, 4. Faculty of Life and Environmental Sciences, University of Tsukuba, 5. National Institute for Agro-Environmental Sciences, 6. River Basin Research Center, Gifu University

Solar-induced chlorophyll fluorescence (SIF) is considered as more direct remote sensing index to monitor photosynthetic activity than conventional vegetation indices. To detect the SIF, it has been suggested that an ultrafine spectral resolution (SR; full width at half maximum: FWHM < 0.3 nm) is generally required for the usual retrieval algorithms, e.g., Fraunhofer Line Depth (FLD) principle and spectral fitting method (SFM). However, the requirement of such high SR instrument suppresses the expansion of ground-based SIF measurement sites to be comparable as eddy flux tower network. On the other hand, the long-term spectral observations over multiple ecosystem types has been conducted under Phenological Eyes Network (PEN) by relatively lower SR spectroradiometer with the FWHM of 10 nm. Recently-proposed algorithm, area-ratio FLD (aFLD; Tsujimoto et al., in submission), demonstrated the consistent scaling ratio of SIF by aFLD from low SR spectrum to those by conventional algorithms from high SR spectrum in the green house experiments. In this study, therefore, we examined the applicability of aFLD to PEN data for SIF detection under the cross-validation of calculated SIFs using both an ultrafine- and a low- SR spectroradiometer data in two ecosystems: forest and grass in Japan.
Both low and high SR spectra have been recorded by MS-700 (Eko limited inc: FWHM = 10 nm) at 10 minutes interval and by QEPro (Ocean Optics, Inc., FWHM = 0.24 nm) at 5 to 15 minutes interval, respectively, since 2019 in both Takayama deciduous broad-leaf forest site in Takayama (TKY), and Mase rice paddy field site in Tsukuba (MSE), Japan. SIF values were calculated by aFLD for low SR, and by 3FLD and SFM for high SR data at 30 min interval during the growing season from April to September. To investigate the influence of SR on SIF value, virtual spectra in same SR as MS700 were also generated from QEPro data by resampling via moving average assumed of Gaussian distribution.
To reduce the inconsistency in the data quality among instruments, our analyses were conducted on the SIF values only in stable sky condition, eliminating those in rapidly crossing cloud quantitatively with outlier, true reflectance (not contaminated by fluorescence) of less than 0.4 and more than 0.8 calculated from QEPro, and/or with captured cloud passing visually by an automatic-capturing digital fisheye camera (ADFC).
In TKY site, the SIF values obtained from low SR by aFLD showed a strong correlationship with the reference SIF obtained from high SR by 3FLD (r^2 = 0.706, slope = 0.269). Although correlation coefficient between aFLD from low SR and SFM from QEP was still low (r^2 = 0.389), the slope of liner equation (= 0.130) was within the same range between 0.120 and 0.130.
This result suggested that we can easily obtain accurate values using a scaling factor although its absolute values of the retrieved SIF are higher than correct values. The analysis on the data in MSE site would be added on presentation day.

Keywords: Solar-induced chlorophyll fluorescence, Remote sensing, Spectral resolution

©2020. Japan Geoscience Union. All Right Reserved.

Influence of climatic fluctuations on crop production for 135 years in Japan

*Tomomichi Kato[1], Moeka Ono[1], Daiki Watanabe[1]

1. Research Faculty of Agriculture, Hokkaido University

Growing population requires more food supply under the projection of future climate change, which would give a large impact on agricultural production (IPCC, 2017). Avoiding the catastrophic situation induced by food shortage reminds us the importance of wise investment of limited economical and environmental resources onto the social infrastructure to secure the local-to-global sustainability. Global scale analysis, based on national crop statistics, showed that recent climate variation affected the crop production (Lobell et al, 2008, Hertel et al., 2010, etc.). However, conventional analyses are mostly based on the country-level data during the relatively short period, from 3 to 5 decades.
Japan’ s governmental department of agricultural administration (current Ministry of Agriculture, Forestry and Fishery) publishes long-term crop production data in the annual reports from 1883 to present for all 47 prefectures. To elucidate the long-term trend of crop production evolution and its correlation to climatic fluctuations, here we compiled the 135 year record during 1883-2017 on the production of six major crops (rice, wheat, barley, soybean, potato, sweet potato) in 46 out of total 47 prefectures, eliminating Okinawa prefecture, due to too low surface area of 6 nationally major crop cultivation and almost no record for few crops in pre WWII time to keep the consistency in statistical analysis. We analyzed those data on the following two topics, 1) The spatiotemporal distribution of growth crop production growth and potential stagnation, 2) The effect of climate on year to year fluctuation of crop production.
Annual production and area values of six major crops for each prefecture are collected from the printed books on National crop statistics as the photo copies through the National Diet Library Digital Collections (http://dl.ndl.go.jp) from 1883 to 1957, and from the Statistics repository e-Stat (www.e-stat.go.jp). Though long-term averaged yields all showed temporally gradual evolution, prefectural stagnation sign shows spatio-temporal variation in maturity of production evolution (Fig. 1). Potato and sweet potato show clear nation-wide stagnation in recent 4 decades (1981-2017). Correlation coefficients of yields to CRU-based climatology show remarkably that rice, soybean and sweet potato yields respond very positively to air temperature for long-term, and rice to precipitation in last 4 decades. Other wheat, barley and potato do not show particularly long-term climatic sensitivity. Cloudiness does not affect significantly to all 6 crops.

Keywords: national statistics, teleconnection, stagnation

©2020. Japan Geoscience Union. All Right Reserved.

Long-term warming effect on soil carbon fluxes in a red pine forest in Tsukuba

*Munemasa Teramoto[1], Naishen Liang[1], Jiye Zeng[1], Jun Koarashi[2], Toshiaki Kondo[3], Mariko Atarashi-Andoh[2], Takafumi Aramaki[1], Xin Zhao [1]

1. National Institute for Environmental Studies, 2. Japan Atomic Energy Agency, 3. Japan International Research Center for Agricultural Sciences

Globally, soil contains about 3000 Gt of organic carbon. Annually, about 98 GtC is released to the atmosphere from soil as CO_2 (soil respiration, R_s). R_s consists of root respiration and heterotrophic respiration (R_h), and R_h contributes to more than the half of soil respiration. On the other hand, upland soil uptakes CH_4. Therefore, soil (especially forest soil) is a large source for CO_2 and sink for CH_4. Long-term response of those soil carbon fluxes to warmer environment is a key for mitigation and adaptation for future climate change. However, long-term continuous monitoring data for those soil carbon fluxes are totally limited.

To examine the long-term response of R_h to global warming in Asian monsoon forests, we set multi-channel automated chamber measurement system in a red pine forest in Tsukuba in February 2006. We prepared 12 trenched chambers (90 cm ×90 cm ×50 cm) to continuously measure R_h. Half of those trenched chambers were artificially warmed by infrared heaters 1.6 m above the soil surface (+2.5˚C), and influence of soil warming on R_h was examined by comparing control plots and warming plots. In July 2009, we added 8 chambers to measure R_s. Further, we started continuous measurement of soil CH_4 flux in June 2019 using the same chamber measurement system by connecting control unit with CH_4 analyzer (915-0011, Los Gatos Research, Inc., USA).

Remarkable exponential relationships between soil temperature and soil CO_2 effluxes (R_s and R_h) were confirmed every year. In addition, soil CO_2 effluxes were observed to be related with soil moisture especially in summer period from July to September. On the other hand, we found that soil CH_4 was negatively related with soil moisture. Those observations suggest that soil temperature is the primary factor controlling soil CO_2 effluxes, whereas soil moisture is the main factor controlling soil CH_4 uptake in our study site.

Keywords: Soil respiration, CH4, Chamber, Global warming

©2020. Japan Geoscience Union. All Right Reserved.

[J] Poster | A (Atmospheric and Hydrospheric Sciences)：A-CG Complex & General

[A-CG55] Coastal Ecosystems - 1. Water Cycle and Land-Ocean Interactions

convener:Makoto Yamada(Faculty of Economics, Ryukoku University), Ryo Sugimoto(Faculty of Marine Biosciences, Fukui Prefectural University), Masahiko Fujii(Faculty of Environmental Earth Science)

Substances from land which are brought by river and/or submarine groundwater discharge are important for the process of biological production in coastal areas. This session focuses on land-ocean interactions through water cycle. The aim of this session is to create interdisciplinary discussions on the research of connectivity of ecosystems, water cycles in terrestrial and coastal areas, fishery resources and biodiversity. Comprehensive discussion on the mechanisms that promote productivity and biodiversity in coastal ecosystems will be made from the viewpoint of land-ocean interactions. Presentations on water-material cycle in terrestrial and coastal areas, fishery resources, biodiversity and connectivity of the ecosystems are encouraged.
A companion session proposed as "Coastal Ecosystems - 2. Coral reefs, seagrass meadows, and mangroves" focuses on benthic communities in shallow-water ecosystems such as coral reefs, seagrass meadows and mangroves and is dedicated to promote researches on comprehensive assessment and monitoring of ecosystem functions and development of effective means for conservation and restoration. Main focuses of these two sessions are different. However, there are much of information that covers both sessions. Scientists who work on the related field will be able to obtain information and share them with other scientists if they attend to both of these sessions.

[ACG55-P01] Reconstitution of the environment of Submarine Groundwater Discharge (SGD) in the near past by using carbon and oxygen stable isotope ratio in the shell of bivalve

*Osamu Tominaga[1], Seira Tobe[1], Tatsuhiro Ishida[1] (1.Fukui Prefectural University)

[ACG55-P02] Effects of the inflow of hot spring drainage into rivers in Beppu City, Oita Prefecture on benthos in the estuary area.

*Kazuya Shimizu[1], Makoto Yamada[1], Makoto Uenishi[1], Shinji Ohsawa[2] (1.Ryukoku University, 2.Institute for Geothermal Sciences, Kyoto University)

[ACG55-P03] Spatial and seasonal variation of water quality in Batan Bay, Philippines

*Toshihiro Miyajima[1], Ryan Basina[2], Charissa M. Ferrera[3], Naoko Morimoto[1], Yasmin H. Primavera Tirol[2], Maria Lourdes San Diego-McGlone[3], Masami Hamaguchi[4] (1.Marine Biogeochemistry Group, Division of Ocean-Earth System Science, Atmosphere and Ocean Research Institute, The University of Tokyo, 2.Aklan State University New Washington, 3.Marine Science Institute, University of the Philippines Diliman, 4.National Research Institute of Fisheries and Environment of Inland Sea, Japan Fisheries Research and Education Agency)

[ACG55-P04] Influence of River Discharge on the Spatial and Temporal Variability of Chlorophyll-a in the Toyama Bay

*Eligio de Raus Maure[1], Genki Terauchi[1], Yasuyuki Harada[1] (1.Northwest Pacific Region Environmental Cooperation Center)

Reconstitution of the environment of Submarine Groundwater Discharge (SGD) in the near past by using carbon and oxygen stable isotope ratio in the shell of bivalve

*Osamu Tominaga[1], Seira Tobe[1], Tatsuhiro Ishida[1]

1. Fukui Prefectural University

We tried to reconstitute the environmental condition of Submarine Groundwater Discharge (SGD) in the near past by using carbon and oxygen stable isotope ratio in the shell of Manila clam (*Ruditapes philippinarum*). We conducted the rearing experiments of Manila clam collected at Mie Prefecture under field conditions. The field experiment was carried out at 5 sites under different SGD condition in Obama Bay, Japan from September 5th to October 24th 2019. A small piece of the shell was cut from the shell edge along the major growth axis. A cross section (1mm thick) was then cut . Calcium carbonates samples were drilled to a depth of 500 μm in the middle of the prismatic layer using a high-precision micromill "GEOMILL326" fitted with a 300 μm diameter drill bit. The contribution rates (FGRc and FGRo) of SGD were calculated by using the two end member mixing equation. In Obama Bay, The FGRc estimated from the shell were well consistent with that estimated from the $\delta^{13}C$ of ambient water. However, FGRo (which was calculated by $\delta^{18}O$) was not always consistent. Possible reason for the error as follows; the water temperature substituted in the equation which was used for estimating the $\delta^{18}O$ in the ambient water in the near past was not suitable.

Keywords: Submarine groundwater discharge, Carbon stable isotope, Oxygen stable isotope, Shell

©2020. Japan Geoscience Union. All Right Reserved.

Effects of the inflow of hot spring drainage into rivers in Beppu City, Oita Prefecture on benthos in the estuary area.

*Kazuya Shimizu[1], Makoto Yamada[1], Makoto Uenishi[1], Shinji Ohsawa[2]

1. Ryukoku University, 2. Institute for Geothermal Sciences, Kyoto University

Beppu City, Oita Prefecture, is one of Japan’ s leading hot spring resorts, and people receive the benefits in various ways, including bath and heat utilization. Hot spring also very useful as a tourist resource, and it contributes to inbound. On the other hand, there have been cases where hot spring water that used or not used is discharged to surrounding rivers. Moreover previous research shows that it is affecting the ecosystems of rivers and estuaries. Although in their previous research describe the drainage from the hot spring is affecting fish. It is not clear that the extent of the impact by the hot spring drainage for benthos because the previous research uninvestigated about benthos. Therefore, we conducted a survey of the population of the benthos in the estuary area in order to clarify the impact of hot spring drainage on the benthos.

The survey was conducted in the non-tidal and tidal areas of major two rivers in Beppu City, Oita Prefecture. One is the Hirata River where hot spring drainage flows in. The other is the Hiyakawa River where hot spring drainage does not flow in among major rivers in. Ten areas of a 1-meter square at each point were randomly set and living things within those areas were collected using hand nets. After that, the samples were fixed with alcohol and brought back to the laboratory to identify the species of the benthos (crustaceans and shellfish).

Shrimps are often found in the Hirata River, especially a lot of Palaemon serrifer in the tidal area. On the other hand, Crabby was very common in the Hiyakawa River, especially in the non-tidal area. For shellfish, there is a big difference in Clithon retropictus and that was very common in the Hiyakawa River, especially in the non-tidal area. We found that Semisulcospira libertina libertina is common in the Hiyakawa River and Melanoides tuberculate Muller is common in the Hirata River.

Focusing on the results of shellfish observations, Melanoides tuberculate Muller lived in more places in the Hirata River, where hot spring drainage flows than in the Hiyakawa River. Melanoides tuberculate Muller is a hot drainage liking species known to be common in rivers with high water temperatures. From this habitat condition, we suggest that the effects of the drainage of the hot spring water may be exerted on benthos as well as on exogenous fish such as tilapia, which was previously studied.

Keywords: hot spring drainage, benthos, estuary area

©2020. Japan Geoscience Union. All Right Reserved.

Spatial and seasonal variation of water quality in Batan Bay, Philippines

*Toshihiro Miyajima[1], Ryan Basina[2], Charissa M. Ferrera[3], Naoko Morimoto[1], Yasmin H. Primavera Tirol[2], Maria Lourdes San Diego-McGlone[3], Masami Hamaguchi[4]

1. Marine Biogeochemistry Group, Division of Ocean-Earth System Science, Atmosphere and Ocean Research Institute, The University of Tokyo, 2. Aklan State University New Washington, 3. Marine Science Institute, University of the Philippines Diliman, 4. National Research Institute of Fisheries and Environment of Inland Sea, Japan Fisheries Research and Education Agency

Batan Bay and Tinago Lake are shallow embayments connected to each other, located on the north of Panay Island, central Philippines (11.53˚ –11.67˚N, 122.38˚ –122.52˚E). Although they had been originally surrounded by dense mangrove forest till the middle of the last century, mangroves have been mostly cleared and converted into fish and shrimp ponds. Recently, shelves and rafts for cultivating oysters and green mussels have become widespread in the shallow areas of the embayments (see Figure as an example). Replantation of mangroves is also ongoing in limited areas of Batan Bay. We are conducting researches there focusing on ecosystem services of mangroves and seagrass meadows, especially in relation to carbon sequestration and aquaculture production. In this presentation, we report preliminary survey results on environmental conditions that may influence growth and survival of cultivated bivalves, such as freshwater inputs and potential food resources. The survey was conducted in both dry season (February 2019) and rainy season (November 2019). Although the salinity gradient across the bay due to freshwater input was evident in both seasons, the oxygen isotope ratio of seawater indicated that evaporation overwhelmed in inner bay sites in the dry season. Concentrations of chlorophyll and suspended particulate organic matter (POM), i.e. potential food source for bivalves, were high in the inner bay area. Carbon stable isotope ratio (δ^{13}C) of dissolved organic carbon (DIC) and POM showed spatial gradient from the bay mouth (high) to inner sites (low), indicating the influence of riverine DIC and POM inputs. However, the δ^{13}C of oysters (adductor muscle) was consistently higher than POM and showed no clear spatial gradient. The δ^{13}C of oysters was relatively higher for individuals collected from inside or edge of seagrass meadows than those collected in open areas. These results suggest that oysters assimilate only a specific fraction of POM relatively enriched in ^{13}C (i.e. marine-origin POM) and that seagrass meadows support growth of oysters by providing additional food source (e.g. attached microalgae that are abundant on seagrass blades).

Keywords: Oyster aquaculture, Seagrass meadows, Suspended particulate organic matter

©2020. Japan Geoscience Union. All Right Reserved.

©2020. Japan Geoscience Union. All Right Reserved.

Influence of River Discharge on the Spatial and Temporal Variability of Chlorophyll-a in the Toyama Bay

*Eligio de Raus Maure[1], Genki Terauchi[1], Yasuyuki Harada[1]

1. Northwest Pacific Region Environmental Cooperation Center

Toyama Bay, located in the Japan Sea, is a very dynamic bay, generally with depths greater than 200 m confined in a narrow shelf, and with many rivers flowing into the sea. The outflow from rivers plays an important role in the physical and biological dynamics of coastal waters. Thus, it is important to understand the spatial and temporal variations of the river discharge influence on material cycle and productivity in nearshore waters. In the Toyama Bay, the Jinzu River is one of the major in discharge amount, averaging to > 500 $m^3 s^{-1}$ during the peak months. Previous research based on satellite observations of chlorophyll-*a* concentration investigated the phytoplankton seasonality and reported the typical annual cycle of temperate regions dominated by spring and autumn blooms. In the shelf regions where the influence of river discharge is high, the seasonality of phytoplankton was reported to be dominated by a long summer peak that correlated well with river discharge. Although the river discharge can also be high in seasons other than summer, it is not yet clear what is the influence of that river discharge on spatial and temporal variations of phytoplankton during non-summer periods. To understand the seasonal and interannual variability of phytoplankton in relation to river discharge, *in situ* observations of temperature, salinity, chlorophyll-*a*, dissolved inorganic nitrogen and phosphate have been conducted by the NPEC since 2004 for the four main seasons, namely, Spring, Summer, Autumn and Winter. In this study, we employ *in situ* observations to discuss the influence of river discharge on spatial and temporal variations of phytoplankton in the Toyama Bay.

Keywords: Phytoplankton, River Discharge, Toyama Bay

©2020. Japan Geoscience Union. All Right Reserved.

[J] Poster | A (Atmospheric and Hydrospheric Sciences)：A-CG Complex & General

[A-CG56] Coastal Ecosystems-2. Coral reefs, seagrass and macroalgal beds, and mangroves

convener:Yu Umezawa(Tokyo University of Agriculture and Technology), Toshihiro Miyajima(Marine Biogeochemistry Group, Division of Ocean-Earth System Science, Atmosphere and Ocean Research Institute, The University of Tokyo), Atsushi Watanabe(The ocean policy research institute, The Sasakawa peace foundation), Tomihiko Higuchi(Atmosphere and Ocean Research Institute, The University of Tokyo)

Coastal marine ecosystems are complex open system interacting with surrounding watersheds, outer ocean, and the atmosphere, providing a wealth of various ecosystem services to human life. Simultaneously, they are also influenced strongly and often negatively by human activities. This session, together with a companion session dedicated for the water cycle and land-ocean interactions, aims to provide a platform for interdisciplinary discussion covering various aspects of frontiers in coastal ecosystem sciences. This session particularly focuses shallow-water benthic communities ranging from temperate to tropical regions, such as coral reefs, seagrass and macroalgal beds, mangroves, intertidal flats, and saltmarshes. All these communities are characterized by intrinsically high primary production, active material cycling, and biodiversity hot spots. However, increasing human demand for coastal marine resources and industrial development concentrating on coastal regions incur the risk of rapid degradation and diminishment. Comprehensive assessment and monitoring of ecosystem functions and development of effective means for conservation and restoration are urgently needed for such communities. This session is dedicated to organizing and promoting such research and management activities by sharing state-of-the-art science and technology among ecologists, geologists, geochemists, biogeographers, etc. Field-based and modeling studies concerning the following topics are especially welcome: material cycling and ecosystem functions; community connectivity; environmental changes such as global warming, ocean acidification, and sea-level rise; ecosystem services such as carbon sequestration, nutrient regulation, and fisheries production; broad-scale comparison; long-term ecological researches.

[ACG56-P01] Nano-SIMS analysis can highlight the effect of symbiotic zooxanthellae on sulfur utilization of corals

*Tomihiko Higuchi[1], Kentaro Tanaka[1], Kotaro Shirai[1], Ikuko Yuyama[2], Takuma Mezaki[3], Naoto Takahata[1], Yuji Sano[1] (1.Atmosphere and Ocean Research Institute, The University of Tokyo, 2.University of Tsukuba, 3.Kuroshio Biological Research Foundation)

[ACG56-P02] Compound specific stable nitrogen isotope analysis of amino acids and sulfur-containing component analysis of reef corals: Toward method development for the prevention of coral bleaching and for recovering from damaged status.

*Yohei Matsui[1,2], Toshihiro Miyajima[1], Tomihiko Higuchi[1], Kentaro Tanaka[1], Naoko Morimoto[1], Yanhui Yang[1], Hiroyuki Fujimura[3], Naoko Yasuda[3], Sylvain Agostini[4], Ikuko Yuyama[4], Takashi Nakamura[5], Masahiro Yuki[6], Shingo Kato[6], Wataru Fujisaki[2] (1.Atmosphere and Ocean Research Institute (AORI), The University of Tokyo, 2.Japan Agency for Marine-Earth Science and Techonology (JAMSTEC), 3.University of the Ryukyus, 4.University of Tsukuba, 5.Tokyo Institute of Technology, 6.RIKEN)

[ACG56-P03] Examination of potential effects of nitrogen supply on nitrogen content and decomposition characteristics of eelgrass (*Zostera marina*)

*Toru Miyata[1], Yu Umezawa[1], Makoto Watanabe[1], Yoshiki Horikawa[1], Masahiro Nakaoka[2] (1.Tokyo University of Agriculture and Technology, 2.Hokkaido University)

[ACG56-P04] Macroalgal metabolism and carbon budgets affect atmospheric CO_2 uptake in a temperate *Sargassum* bed

*Kenta Watanabe[1], Goro Yoshida[2], Masakazu Hori[2], Yu Umezawa[3], Hirotada Moki[1], Tomohiro Kuwae[1] (1.Port and Airport Research Institute, 2.National Research Institute of Fisheries and Environment of Inland Sea, 3.Tokyo University of Agriculture and Technology)

[ACG56-P05] Degradation characteristics of large brown algae *Ecklonia cava* according to environmental conditions

*Takunari Ida[1], Yu Umezawa[1], Shigeki Wada[2], Horikawa Yoshiki[1] (1.Tokyo University of Agriculture and Technology, 2.University of Tsukuba)

Nano-SIMS analysis can highlight the effect of symbiotic zooxanthellae on sulfur utilization of corals

*Tomihiko Higuchi[1], Kentaro Tanaka[1], Kotaro Shirai[1], Ikuko Yuyama[2], Takuma Mezaki[3], Naoto Takahata[1], Yuji Sano[1]

1. Atmosphere and Ocean Research Institute, The University of Tokyo, 2. University of Tsukuba, 3. Kuroshio Biological Research Foundation

Despite sulfur is the main component in the ocean as sulfate ions, little is known about utilization in living organisms. Genome analysis has revealed that corals, which are host animals, do not have a system for synthesizing cysteine, essential amino acid and one of the sulfur-containing amino acids (Shinzato et al. 2011, Nature). This suggests that corals may receive cysteine synthesized by zooxanthellae, or may obtain and use it heterotrophically. It has been confirmed that sulfur is concentrated in zooxanthellae by autoradiography using radioactive isotope ^{35}S. In addition, the amount of ^{35}S accumulated in the coral animal tissues, zooxanthellae, and skeletons was examined. As the exposure time to ^{35}S in seawater increased, the amount of radioactive sulfur accumulated in coral tissues and zooxanthellae increased. (Yuyama et al. 2016, Biol Open). In this study, a stable isotope labeling experiment was conducted and analyzed by NanoSIMS (NS 50, Cameca) to clarify how sulfate ions in seawater are taken up by corals and zooxanthellae. In the experiment, a juvenile polyp of genus *Acropora* (approximately 1 month old) was used to create a zooxanthellae symbiotic polyp with infection of *Durusdinium* (Clade D) and an apo-symbiotic polyp without infection of zooxanthellae. Corals were incubated in filtered seawater with $Na_2{}^{34}SO_4$ (sulfur isotope ratio +1000 ‰) for 2 days. Individuals that had been isotopically labeled for two days were returned to normal seawater and incubated for two days. After incubation, juvenile corals were embedded with resin and cutting and polishing were conducted for NanoSIMS analysis. When the sulfur isotopes ^{32}S and ^{34}S were mapped using NanoSIMS, high ^{34}S points were found in the coral soft tissue. This study reconfirmed that coral uptakes sulfur from seawater as sulfate ions. In particular, ^{34}S-labeled sites were found in the presence of zooxanthellae and in coral animals close to seawater. In addition, the aposymbiotic polyps showed a ^{34}S label in the host part, indicating that the host corals assimilate sulfate ions without passing through the symbiotic algae. Furthermore, even after returning to normal seawater for 2 days after the ^{34}S label, the ^{34}S label was clearly seen in both symbiotic and aposymbiotic polyps, indicating that assimilated sulfur was preserved for at least 2 days.

Keywords: Coral, Symbiosis, Sulfur

©2020. Japan Geoscience Union. All Right Reserved.

Compound specific stable nitrogen isotope analysis of amino acids and sulfur-containing component analysis of reef corals: Toward method development for the prevention of coral bleaching and for recovering from damaged status.

*Yohei Matsui[1,2], Toshihiro Miyajima[1], Tomihiko Higuchi[1], Kentaro Tanaka[1], Naoko Morimoto[1], Yanhui Yang[1], Hiroyuki Fujimura[3], Naoko Yasuda[3], Sylvain Agostini[4], Ikuko Yuyama[4], Takashi Nakamura[5], Masahiro Yuki[6], Shingo Kato[6], Wataru Fujisaki[2]

1. Atmosphere and Ocean Research Institute (AORI), The University of Tokyo, 2. Japan Agency for Marine-Earth Science and Techonology (JAMSTEC), 3. University of the Ryukyus, 4. University of Tsukuba, 5. Tokyo Institute of Technology, 6. RIKEN

To save reef corals from bleaching event, we investigated possibility of enhancement of tolerance and resilience of corals against temperature stress by controlled feeding. By analyzing bulk stable carbon and nitrogen isotope ratios, as well as compound specific isotope analysis of amino acids of coral animal host and symbiotic algae under natural condition, we aim for enhancing our understanding of the major nutrition source and pathway, and for proposing coral bleaching vulnerability indicators for coral reef ecology. Sulfur containing protein and sulfate minerals were also analyzed by GC-MS and X-ray diffractometer. Although compound specific isotope analysis of amino acids is an established analytical method, accomplishing good derivatization of carboxyl and amine functional groups without generating incomplete derivatization or fragmental/recoupled impure molecules gain experience. Analytical machine side, internal/external leak, oxidation/reduction capability of reactors, surface area of catalyst, and degree of gas flow easiness inside of the reactor tubings are considered essential for stable and precise analytical campaign. Coral species used for this experiment (*Acropora hyacinthus* and *Acropora* cf. *glauca*) contain large number of cnidocytes, such as spirocysts and type b-mastigophores. To isolate symbionts from nematocysts, we applied flow cytometry technique with cell sorting function. Parameters, such as side scatter, forward scatter, green fluorescent, and chlorophyll autofluorescent induced by 488-nm blue laser emission were used for the isolation. By establishing those isolation and precise isotope analysis technique, we have developed evaluation roadmap to confirm an effect of nutrition control for the reef corals.

Keywords: Coral bleaching, Stable nitrogen isotope ratio of amino acids, Sulfur

©2020. Japan Geoscience Union. All Right Reserved.

Examination of potential effects of nitrogen supply on nitrogen content and decomposition characteristics of eelgrass (*Zostera marina*)

*Toru Miyata[1], Yu Umezawa[1], Makoto Watanabe[1], Yoshiki Horikawa[1], Masahiro Nakaoka[2]

1. Tokyo University of Agriculture and Technology, 2. Hokkaido University

Nitrogen is one of the elements that can limit the primary production of plants, therefore nitrogen supply potentially affects coastal primary production. On the other hand, it is known that some secondary metabolites such as phenolic compounds that are not directly involved in growth and catabolism such as photosynthesis, respiration, and assimilation act as protective compounds against predators and pathogens. Some report that the abundance of these substances varies with the supply of nitrogen. Thus, differences in nitrogen supply may contribute not only to the growth of these plants, but also to the biodegradation properties of the plant.

In this study, we focused on the eelgrass (*Zostera marina*) widely distributed in the coastal area of Japan, and examined the followings, potential effects of the nitrogen supply in the coastal area on the function as “blue carbon”.

1) Nitrogen content of eelgrass leaves at several locations with potentially different nitrogen supply

The relationship between nitrogen content in sediments and nutrients in the water column in the eelgrass beds were measured along the coast in the temperate zone and in the subarctic zone and compared with the nitrogen content of the eelgrass leaf.

2) Possibility of measuring nitrogen content in eelgrass leaf using portable nitrogen meter

The measured values of multiple portable nitrogen meters for land herbs were compared with the chlorophyll content and actual nitrogen content of the eelgrass *Z. marina*. Conditions that enable us to effectively estimate the nitrogen content of eelgrass are discussed.

3) Relationship between nitrogen content and the amount of structural and repellent substances in the eelgrass leaves

The amount of structural substances and repellent substances of eelgrass plants were evaluated using chemical (KOH, $NaClO_2$, and NaOH) treatments and Folin-ciocalteu method, respectively, and compared with the nitrogen content in each part of the leave.

Keywords: seagrass meadow, eelgrass (Zostera marina), portable nitrogen measurement device

©2020. Japan Geoscience Union. All Right Reserved.

Macroalgal metabolism and carbon budgets affect atmospheric CO_2 uptake in a temperate *Sargassum* bed

*Kenta Watanabe[1], Goro Yoshida[2], Masakazu Hori[2], Yu Umezawa[3], Hirotada Moki[1], Tomohiro Kuwae[1]

1. Port and Airport Research Institute, 2. National Research Institute of Fisheries and Environment of Inland Sea, 3. Tokyo University of Agriculture and Technology

Macroalgal beds are considered to be one of the vegetated coastal ecosystems (i.e., blue carbon ecosystems) that act as atmospheric CO_2 sinks. Macroalgal metabolisms and carbon budgets affect CO_2 sequestration by macroalgal beds, but its relationships are still poorly understood. In this study, we investigated air–water CO_2 exchange and budgets of dissolved inorganic carbon, total alkalinity, and dissolved organic carbon (DOC) in a temperate *Sargassum* bed during the productive winter. We estimated the metabolism of macroalgae and carbon budgets by using a field-bag method, a degradation experiment, and mass balance modelling over a diurnal cycle. Our results showed that macroalgal metabolism and carbon budgets affected atmospheric CO_2 uptake in and around the *Sargassum* bed. The macroalgal metabolism formed water with low CO_2 and high DOC that was then exported offshore. This export process potentially promotes CO_2 uptake in and around macroalgal beds.

Keywords: macroalgal bed, CO2 sink, metabolism, blue carbon, carbon dynamics

©2020. Japan Geoscience Union. All Right Reserved.

Degradation characteristics of large brown algae *Ecklonia cava* according to environmental conditions

*Takunari Ida[1], Yu Umezawa[1], Shigeki Wada[2], Horikawa Yoshiki[1]

1. Tokyo University of Agriculture and Technology, 2. University of Tsukuba

As a method of reducing atmospheric carbon dioxide, which is one of the causes of global warming, utilization of “blue carbon”, which is carbon fixed by marine ecosystems, has attracted attention. Seaweed have a particularly high production rate and a large area in Japan, but there are few studies on quantification and processes of carbon fixation. Mechanisms of carbon sequestration in macroalgal beds include long-term transfer of deciduous algal tissues and DOC released into water to a deep layer isolated from the atmosphere, and deposition into surrounding sediments. However, because these algae-derived materials are microbially decomposed during transportation, the amount of refractory substances contained in seaweed is important to fix carbon more efficiently in the ocean ecosystem. In addition, the environment in which decomposition occurs varies in the ocean, and the components differ depending on the parts of the algal bodies. Therefore, the decomposition characteristics must be carefully considered in these viewpoints. Therefore, in this study, we focused on “Kajime” (*Ecklonia cava*), a brown algae of the family Laminariaceae, and its related species, “Alame” (*Eisenia bicyclis*). The decomposition characteristics of large brown algae were evaluated by performing decomposition experiments controlling environmental conditions such as dissolved oxygen and nutrients.
The results of this study suggest that it is important to understand where algae-derived organic matter accumulate due to seawater circulation, and to understand the dynamics of refractory DOM, when evaluating macroalgal function as “blue carbon”.

Keywords: seaweed bed, Ecklonia cava, degradation characteristics

©2020. Japan Geoscience Union. All Right Reserved.

[J] Poster | A (Atmospheric and Hydrospheric Sciences)：A-CG Complex & General

[A-CG57] Science in the Arctic Region

convener:Masashi Niwano(Meteorological Research Institute), Shunsuke Tei(Arctic Research Center, Hokkaido University), Tetsu Nakamura(Faculty of Environmental Earth Science, Hokkaido University), Jun Ono(Atmosphere and Ocean Research Institude, The University of Tokyo)

The Arctic and circumpolar region is the key area for the study of global change because the anthropogenic impact is projected to be the largest in this area due to the complicated feedback processes of the nature. A number of international and interdisciplinary research projects have been conducted for the studies on the land-atmosphere-ocean system. In order to understand the feedback processes occurring in the Arctic and to project the global warming in the future, we need to establish the intense observational network and to exchange the knowledge and information by combining the different scientific communities under the common interest of the Arctic. The objectives of this session are 1) to exchange our knowledge on the observational facts and integrated modelling and 2) to deepen our understanding on wide range of natural sciences related to the Arctic and the circumpolar region. Studies on humanities, social sciences, and interdisciplinary fields are also welcomed.

[ACG57-P01] A hemispheric extreme cold winter in 2017/18 controlled by the lowest extent of Chukchi sea-ice

*Keisuke Ota[1], Yoshihiro Tachibana[1], Yuta Ando[1] (1.Graduate School of Bioresources, Mie University)

[ACG57-P02] Detection of a weakening of the polar night jet in early winter and its relation to cooling over Siberia

*Yuta Ando[1], Koji Yamazaki[2], Yoshihiro Tachibana[1], Masayo Ogi[3], Jinro Ukita[4] (1.Graduate School of Bioresources, Mie University, 2.Hokkaido University, 3.Centre for Earth Observation Science, University of Manitoba, 4.Faculty of Science, Niigata University)

[ACG57-P03] Trends of summer precipitation over northern Eurasia in historical simulations with MIROC6

*Manabu Abe[1], Hironari Kanamori[2], Hatsuki Fujinami[2], Tetsuya Hiyama[2], Hiroaki Tatebe[1] (1.Japan Agency for Marine-Earth Science and Technology, 2.Institute for Space-Earth Environmental Research)

[ACG57-P04] External drivers on the Arctic warming and associated sea ice reduction in the early 20th century in a new climate model MRI-ESM2.0

*Takuro Aizawa[1,2], Masayoshi Ishii[2], Naga Oshima[2], Seiji Yukimoto[2], Hiroyasu Hasumi[1] (1.Atmosphere and Ocean Research Institute, University of Tokyo, 2.Meteorological Research Institute)

[ACG57-P05] Meteorological and snow/ice data around the Greenland ice sheet (1980-2019) calculated by the high-resolution polar regional climate model NHM-SMAP

*Masashi Niwano[1], Akihiro Hashimoto[1] (1.Meteorological Research Institute)

[ACG57-P06] **Surface elevation changes of glaciers along the coast of Prudhoe Land, northwestern Greenland, from 1985 to 2018**

*YEFAN WANG[1,2], Shin Sugiyama[1], Daiki Sakakibara[3] (1.Institute of Low Temperature Science, Hokkaido University, 2.Graduate School of Environmental science, Hokkaido University, 3.Arctic Research Center, Hokkaido University)

[ACG57-P07] **Quantifying Chukchi Polynya Occurrence Using Passive Microwave and Local Indigenous Observational Data**

*Pacifica Kitrea Mai Takata-Glushkoff[1,2], Angela C. Bliss[2] (1.Bowdoin College Earth and Oceanographic Science, 2.Oregon State University College of Earth, Ocean, and Atmospheric Sciences)

[ACG57-P08] Increasing Zooplankton Biomass Associated with Sea Ice Loss in the Western Arctic Ocean

*Motoyo Itoh[1], Minoru Kitamura[1], Amane Fujiwara[1], Eddy Carmack[2], Kazuo Amakasu[3], Koichi Ara[4], Mario Uchimiya[5], Toru Hirawake[6], Jonaotaro Onodera[1], Shigeto Nishino[1], Takashi Kikuchi[1] (1.Japan Agency for Marine-Earth Science and Technology, 2.Fisheries and Ocean Canada, Institute of Ocean Science, 3.Tokyo University of Marine Science and Technology, 4.Nihon University, 5.Riken, 6.Hokkaido University)

[ACG57-P09] Influence of physical oceanographic condition to transportation of biosiliceous particles in the Pacific side of the Arctic Ocean

*Jonaotaro Onodera[1], Eiji Watanabe[1], Satoshi Kimura[1], Kohei Mizobata[2], Yuichiro Tanaka[3], Naomi Harada[1] (1.Research and Development Center for Global Change, JAMSTEC, 2.Dept. Ocean Sciences, School of Marine Life Science, TUMSAT, 3.Geological Survey of Japan, AIST)

[ACG57-P10] Surface Waves Under the Arctic Sea Ice Observed by Drifting Wave Buoys

*Tsubasa Kodaira[1], Takuji Waseda[1], Takehiko Nose[1], Kazutoshi Sato[2], Jun Inoue[3] (1.The University of Tokyo, 2.KITAMI INSTITUTE OF TECHNOLOGY, 3.National Institute of Polar Research)

[ACG57-P11] Covariability between Atmospheric Teleconnections and GDP Growth Rates

*Akane Kato[1], Yoshihiro Tachibana[1], Kensuke K. Komatsu[1], Yuta Ando[1] (1.Faculty of Bioresources, Mie University)

[ACG57-P12] Remote influence on extreme weather in mid and high latitudes over the Northern Hemisphere driven by deep convection over Sahel

*Tomoe Nakanishi[1], Yoshihiro Tachibana[1], Yuta Ando[1] (1.Graduate School of Bioresources, Mie University)

[ACG57-P13] Recent Increase of Extreming Snowfall events in Kanto and its Relation to the Shift of Large-scale Atmospheric Circulations.

*Yuki Nakamura[1], Yoshihiro Tachibana[1] (1.Fac. of Bioresources, Mie Univ)

A hemispheric extreme cold winter in 2017/18 controlled by the lowest extent of Chukchi sea-ice

*Keisuke Ota[1], Yoshihiro Tachibana[1], Yuta Ando[1]

1. Graduate School of Bioresources, Mie University

In East Asia 2017/18 winter, the seasonal mean temperature was the lowest recorded since 1988/89. The sea-ice extent of the Chukchi Sea was the lowest in 2017/18. We investigated the influence of the Chukchi sea-ice decline on the hemispheric cold winter viewing from statistical analysis. The Chukchi sea-ice decline was statistically related to East Asia cold winter. Some studies showed that La Niña and sea-ice decline in the Barents and Kara Sea statistically affect to cold winter. We examine the relationship between the statistical effects of the sea-ice decline in the Chukchi Sea and these other factors in 2017/18. The factors of La Niña and the sea-ice decline in the Barents and Kara Sea were not enough as the explanation for abnormal winter in 2017/18. In addition to these two factors, the sea-ice decline in the Chukchi Sea was the well explanation for the cold winter over East Asia in 2017/18. The sea-ice extent of the Chukchi Sea was abnormal in 2017/18. The abnormal sea-ice decline in the Chukchi Sea might statistically affect the cold winter over East Asia in 2017/18.

Keywords: Chukchi Sea, sea-ice

©2020. Japan Geoscience Union. All Right Reserved.

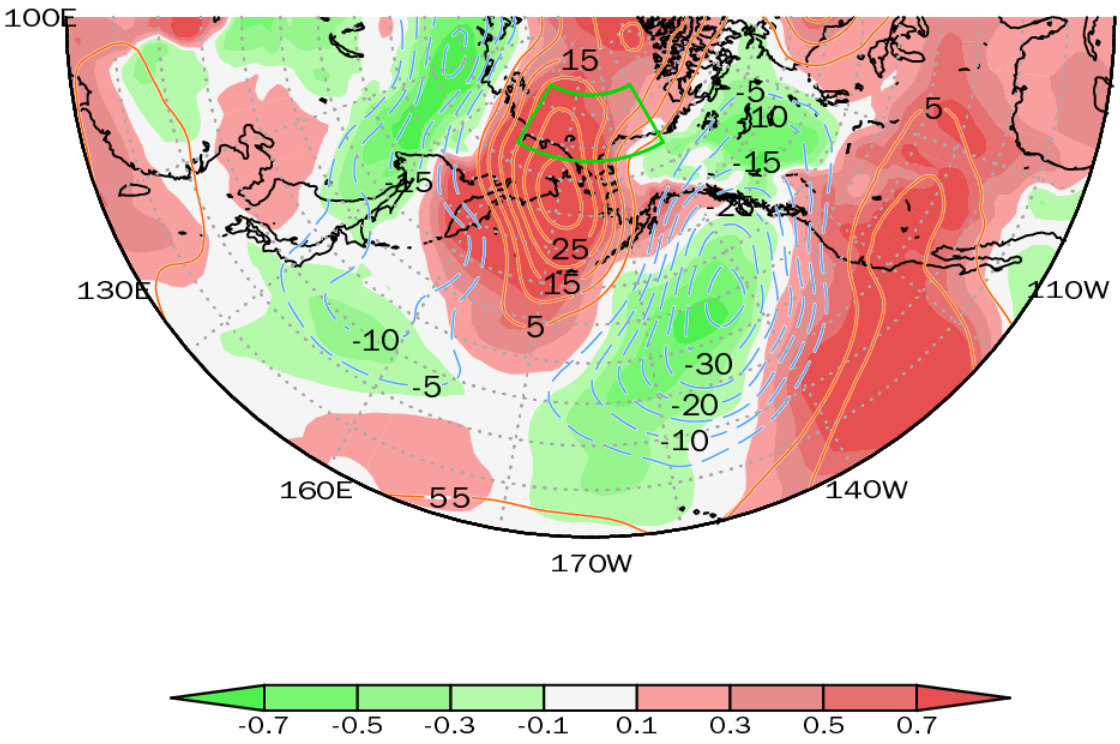

©2020. Japan Geoscience Union. All Right Reserved.

Detection of a weakening of the polar night jet in early winter and its relation to cooling over Siberia

*Yuta Ando[1], Koji Yamazaki[2], Yoshihiro Tachibana[1], Masayo Ogi[3], Jinro Ukita[4]

1. Graduate School of Bioresources, Mie University, 2. Hokkaido University, 3. Centre for Earth Observation Science, University of Manitoba, 4. Faculty of Science, Niigata University

The polar night jet (PNJ) is a strong stratospheric westerly circumpolar wind at around 65°N in winter, and the strength of the PNJ is widely recognized to increase from October through late December. Remarkably, the PNJ temporarily stops increasing during late November. A detailed understanding of the weakening of the PNJ in late November is important in terms of the dynamic meteorology of intraseasonal variations in the stratosphere. No previous studies explicitly showed this weakening of the PNJ, nor have yet been addressed in terms of dynamic meteorology. We thus examined this weakening of the PNJ in terms of the atmospheric dynamical balance and the interannual variability. Examination of the atmospheric dynamical balance showed that an increase in upward propagation of planetary waves from the troposphere to the stratosphere in late November is accompanied by convergence of the Eliassen–Palm (EP) flux in the lower stratosphere, which brings about this weakening of the PNJ. The upward propagation of Rossby (planetary) waves over Siberia from the troposphere to the stratosphere is a dominant cause of the weakening of the PNJ. This upward propagation of planetary-scale Rossby waves at high latitudes is associated with amplification of eddy geopotential height and air temperature, that is, with a strengthening of the trough over Siberia. Further, we inferred that this strengthening of the trough is forced by the high-latitude land–sea thermal contrast caused by their different heat capacities. The interannual variability of the weakening of the PNJ is associated with that of the high-latitude land–sea thermal contrast.

The part of this presentation was published as the article, Ando et al. (2018).

Ando, Y., K. Yamazaki, Y. Tachibana, M. Ogi, and J. Ukita, 2018: Detection of a climatological short break in the polar night jet in early winter and its relation to cooling over Siberia. Atmospheric Chemistry and Physics, 18, 12639-12661, doi:10.5194/acp-18-12639-2018.

Keywords: Stratosphere, Rossby wave, Land–sea heating contrast, Interannual variability

©2020. Japan Geoscience Union. All Right Reserved.

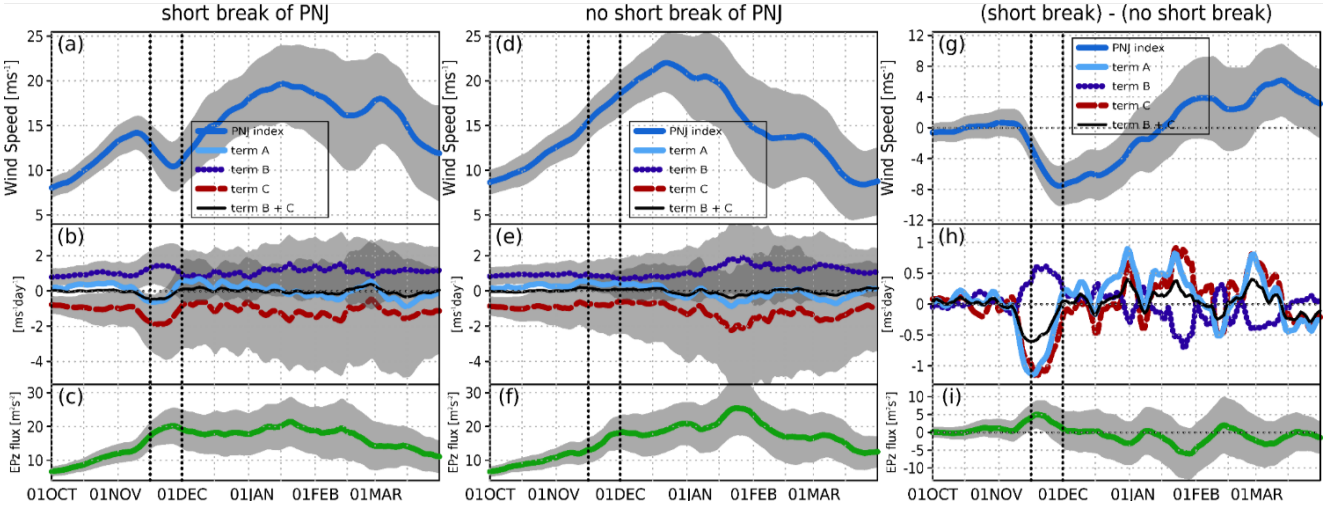

©2020. Japan Geoscience Union. All Right Reserved.

Trends of summer precipitation over northern Eurasia in historical simulations with MIROC6

*Manabu Abe[1], Hironari Kanamori[2], Hatsuki Fujinami[2], Tetsuya Hiyama[2], Hiroaki Tatebe[1]

1. Japan Agency for Marine-Earth Science and Technology, 2. Institute for Space-Earth Environmental Research

It is well known that many models developed by organizations around the world have simulated past climate changes and projected future climate changes (e.g., Eyring et al, 2016). However, in northern Eurasia, features and uncertainties of long-term trends simulated in the models are not sufficiently evaluated. Therefore, in this study, the features and the uncertainties of the variability of summer mean precipitation over northern Eurasia in the historical simulations by MIROC6 are investigated. We analyzed data from 50 members of the historical simulation (1850-2014) with MIROC6 under CMIP6 protocol. In the regions (north more than 60N) and Northeast Asia, the ensemble averages of temporal trends of summer precipitation for 1951-1980 among the 50 members were negative, approximately -0.04 ~ -0.02 mm day^{-1} $decade^{-1}$. However, for 1971-2000, the trend changed to positive. For 1990-2014, the positive trends in eastern Siberia became significant, but the negative trends in the southern part of western Siberia also appeared. In the presentation, we discuss uncertainties in the trends of summer precipitation as well as changes in atmospheric circulation and sea ice conditions which could relate to the trends of summer precipitation.

References:
Eyring, V., Bony, S., Meehl, G. A., Senior, C. A., Stevens, B., Stouffer, R. J., and Taylor, K. E. (2016), Overview of the Coupled Model Intercomparison Project Phase 6 (CMIP6) experimental design and organization, Geosci. Model Dev., 9, 1937-1958, doi:10.5194/gmd-9-1937-2016.

©2020. Japan Geoscience Union. All Right Reserved.

External drivers on the Arctic warming and associated sea ice reduction in the early 20th century in a new climate model MRI-ESM2.0

*Takuro Aizawa[1,2], Masayoshi Ishii[2], Naga Oshima[2], Seiji Yukimoto[2], Hiroyasu Hasumi[1]

1. Atmosphere and Ocean Research Institute, University of Tokyo, 2. Meteorological Research Institute

In the first half of the 20th century, some observational records show that there was significant warming called the early twentieth century warming (ETCW) comparable to that presently occurred. The characteristic of that warming is to appear only in the Arctic. Furthermore, a recent reconstructed sea ice dataset and some observational studies indicate a reduction on Arctic sea ice extent associated with the higher temperatures in the ETCW period. But large uncertainties remain in both the observation and the previous model simulations.

We investigated the external drivers of the temperature changes in the Arctic and the associated sea ice changes especially in the first half of the 20th century by DAMIP experiments using a new climate model MRI-ESM2.0. We conducted a pre-industrial control experiment (CNTL), the historical experiments and the DAMIP experiment to evaluate the cause of historical climate change. The DAMIP experiments consist of historical simulations with well-mixed greenhouse gasses (hist-GHG) only, anthropogenic aerosols only (hist-aer), solar irradiance and volcanic aerosol only (hist-nat), and solar irradiance only (hist-sol). The historical experiments of this study consist of five ensemble members with initial conditions taken at 50-yr intervals from January 1st of years 1 of the CNTL. Each of the DAMIP experiments has three ensemble members with the same initial conditions as those of the original historical experiments.

Climate simulations by MRI-ESM2.0 showed the historical temperature changes including the ETCW more realistically. The DAMIP experiments imply that the natural forcing of long-term low volcanic activity in the ETCW is attributed one of the major factors on the temperature rise and associated the sea ice reduction. Some kinds of feedback mechanisms, such as ice-albedo feedback or ice-ocean-albedo feedback could be acting on amplifying the temperature increase in the ETCW period.

Keywords: Early Twentieth Century Warming , Arctic, Sea ice, Earth System Model

©2020. Japan Geoscience Union. All Right Reserved.

Meteorological and snow/ice data around the Greenland ice sheet (1980-2019) calculated by the high-resolution polar regional climate model NHM-SMAP

*Masashi Niwano[1], Akihiro Hashimoto[1]

1. Meteorological Research Institute

In order to understand the ongoing abrupt changes in the climate conditions around the Greenland ice sheet (GrIS), we have developed the physically based high-resolution (1 hr interval and 5 km horizontal resolution) polar regional climate model NHM-SMAP (Niwano et al., 2018, 2019). Recently, we have conducted long-term climatic calculations from 1980 to 2019 around the GrIS using the model, and submitted the data to the GrIS surface mass balance model intercomparison project GrSMBMIP (Fettweis et al., in review). Now, the data are available for a wide variety of studies around the GrIS. In this contribution, we present available meteorological and snow/ice physical properties from the data, and discuss possible future collaborations using the data.

References:

Fettweis, X., Hofer, S., Krebs-Kanzow, U., Amory, C., Aoki, T., Berends, C. J., Born, A., Box, J. E., Delhasse, A., Fujita, K., Gierz, P., Goelzer, H., Hanna, E., Hashimoto, A., Huybrechts, P., Kapsch, M.-L., King, M. D., Kittel, C., Lang, C., Langen, P. L., Lenaerts, J. T. M., Liston, G. E., Lohmann, G., Mernild, S. H., Mikolajewicz, U., Modali, K., Mottram, R. H., Niwano, M., Noël, B., Ryan, J. C., Smith, A., Streffing, J., Tedesco, M., van de Berg, W. J., van den Broeke, M., van de Wal, R. S. W., van Kampenhout, L., Wilton, D., Wouters, B., Ziemen, F., and Zolles, T. (in review, 2020): GrSMBMIP: Intercomparison of the modelled 1980–2012 surface mass balance over the Greenland Ice sheet, *The Cryosphere Discuss.*, doi:10.5194/tc-2019-321.

Niwano, M., Aoki, T., Hashimoto, A., Matoba, S., Yamaguchi, S., Tanikawa, T., Fujita, K., Tsushima, A., Iizuka, Y., Shimada, R., and Hori, M. (2018): NHM–SMAP: spatially and temporally high-resolution nonhydrostatic atmospheric model coupled with detailed snow process model for Greenland Ice Sheet. *The Cryosphere*, 12, 635-655, doi:10.5194/tc-12-635-2018.

Niwano, M., Hashimoto, A., and Aoki, T., 2019: Cloud-driven modulations of Greenland ice sheet surface melt, *Sci. Rep.*, 9, 10380, doi:10.1038/s41598-019-46152-5.

Keywords: Greenland ice sheet, polar meteorology, polar climatology, glaciology, surface mass balance, polar regional climate model

©2020. Japan Geoscience Union. All Right Reserved.

Surface elevation changes of glaciers along the coast of Prudhoe Land, northwestern Greenland, from 1985 to 2018

*YEFAN WANG[1,2], Shin Sugiyama[1], Daiki Sakakibara[3]

1. Institute of Low Temperature Science, Hokkaido University, 2. Graduate School of Environmental science, Hokkaido University, 3. Arctic Research Center, Hokkaido University

In recent decades, the Greenland Ice Sheet has been a major contributor to global sea-level rise as a consequence of accelerating mass loss. Numerous studies have described spatiotemporal heterogeneity in glacier terminus retreat, flow speed variations, surface elevation change in a scale covering the entire ice sheet. However, details of the changes and heterogeneity of individual glaciers remain uncertain. Therefore, detailed investigations in a finer spatial scale are required. Here we show the surface elevation changes of 16 outlet glaciers along the coast of Prudhoe Land, northwestern Greenland, derived from multi-source DEMs (digital elevation models) (1985 (t0) aerial photograph DEM, ASTER DEMs in 2001–2003 (t1) and 2016–2018 (t2)), for the last 30 years.

We observed a mean surface lowering rate of −0.55±0.22 m a^{-1} over the past three decades (t0–t2) for the whole studied glaciers. The most rapid surface lowering (−3.08 m a^{-1}) was observed near the glacier termini (elevation band 0–50 m), and the slowest surface lowering rate (−0.14 m a^{-1}) is found on the elevation band 800–850 m. The rates varied among the periods. The mean rate showed a slightly positive value of 0.14±0.16 m a^{-1} during t0 –t1, and no distinct altitudinal variations was observed in this period. Strongly negative elevation change rates (−1.31±0.19 m a^{-1}) were detected during the second subperiod (t1– t2). The most rapid thinning (−5.47 m a^{-1}) occurred near the frontal areas (elevation band 0–50 m), and slower but significant thinning at a rate −0.57 m a^{-1} was observed inland areas (elevation band 800–850 m). For individual glaciers, most glaciers have exhibited no significant change or slight surface thickening during the period t0 –t1. Obvious thinning happened only in the frontal areas of Tracy, Farquhar, Sharp and Sun Glaciers. During the period t1– t2, all the studied glaciers experienced thinning in different magnitudes. Tracy (−3.91±0.12 m a^{-1}) and Farquhar (−2.91±0.15 m a^{-1}) Glaciers experienced most significant thinning, while Heilprin Glacier, adjacent to Tracy, showed a moderate thinning rate (−0.51±0.12 m a^{-1}). Interestingly, there is no obvious change at Verhoeff Glacier both in t0 –t1 and t1– t2. Outlet glaciers terminating in Inglefield Bredning showed a mean thinning rate of −1.07 ±0.18 m a^{-1}, which was 67% greater than those of glaciers terminating in Baffin Bay (−0.64 ±0.24 m a^{-1}) during t1–t2.

The elevation changes are generally correlated with atmospheric and oceanic warming in the region. Nevertheless, considerably large heterogeneity was observed among individual glaciers, which may be attributed to the control of the fjord bathymetry and glacier bed topography on the submarine melting and ice dynamics.

Keywords: Greenland, Glaicer, Elevation change

©2020. Japan Geoscience Union. All Right Reserved.

Quantifying Chukchi Polynya Occurrence Using Passive Microwave and Local Indigenous Observational Data

*Pacifica Kitrea Mai Takata-Glushkoff[1,2], Angela C. Bliss[2]

1. Bowdoin College Earth and Oceanographic Science, 2. Oregon State University College of Earth, Ocean, and Atmospheric Sciences

Polynyas are recurring areas where sea ice thins or opens to reveal an ocean-atmosphere interface. They have the potential to affect moisture and heat flux, warming local temperatures, and initiating feedbacks on Arctic atmospheric and oceanographic systems. The Barrow Coastal Polynya and the Chukchi Polynya, found in the Northeastern Chukchi Sea off the Alaskan coast, have widespread implications as they foster the survival of biodiverse marine animals and impact Iñupiat sea ice hunting practices. We develop a database of the timing and spatial extent of the Barrow Coastal Polynya (between Pt. Barrow and Icy Cape, Alaska) and Chukchi Polynya (between Icy Cape and Cape Lisburne) between November 1 and May 31, for the years 2002 through 2019 using 12.5 km resolution satellite passive microwave data from the Japan Aerospace Exploration Agency’ s Advanced Microwave Scanning Radiometer (AMSR-E/AMSR-2) sensors. An automated system identifies polynya events based on annual time series of total water percent over each polynya’ s domain area. Polynya timing and spatial characteristics are verified with sea ice concentration maps, and integrated with local Iñupiat observations from near Utqiagvik, Alaska using the Seasonal Ice Zone Observing Network and Alaska Arctic Observatory & Knowledge Hub. This database of polynya events reveals inter-annual variability in the timing and frequency of both polynyas in response to synoptic scale wind forcing. Between 2002 and 2019 the Chukchi Polynya has typically opened more frequently, but with lower total water coverage than the Barrow Coastal Polynya. Comparing passive microwave-derived polynya identifications to local observations of polynya indicators reveal that these two datasets should be used in tandem to thoroughly characterize the polynyas. By accurately quantifying these polynya events, we lay the groundwork to understand the impacts of coastal polynyas on regional wintertime atmospheric moisture and heat flux.

Keywords: Cryosphere, Sea Ice, Polynya, Local Observations, Passive Microwave, Satellite Observations

©2020. Japan Geoscience Union. All Right Reserved.

Increasing Zooplankton Biomass Associated with Sea Ice Loss in the Western Arctic Ocean

*Motoyo Itoh[1], Minoru Kitamura[1], Amane Fujiwara[1], Eddy Carmack[2], Kazuo Amakasu[3], Koichi Ara[4], Mario Uchimiya[5], Toru Hirawake[6], Jonaotaro Onodera[1], Shigeto Nishino[1], Takashi Kikuchi[1]

1. Japan Agency for Marine-Earth Science and Technology, 2. Fisheries and Ocean Canada, Institute of Ocean Science, 3. Tokyo University of Marine Science and Technology, 4. Nihon University, 5. Riken, 6. Hokkaido University

Sea ice cover is rapidly declining due to global warming accompanied by sea surface temperature warming and an increase in phytoplankton primary production in the western Arctic Ocean. Although these trends are well documented, their influences on marine ecosystems remain unclear because few studies have conducted long-term ecological monitoring at decadal time scales. Using mooring-based acoustic backscattering data collected during periods of both high (2000-2003) and low sea ice coverage (2010-2013) in the Chukchi Sea, western Arctic Ocean, we show that the annual mean zooplankton biomass increased 1.6-fold between the two periods. This biomass change would have increased the grazing pressure on phytoplankton by zooplankton, which, in turn, decreased the supply of sinking carbon to benthic organisms during summer, even though phytoplankton production would have increased. Thus, the Chukchi Sea ecosystem is now shifting away from a pelagic-benthic coupled ecosystem towards one that is pelagic-dominated, in which the primary production is not directly connected to the benthic carbon cycle due to increased pelagic zooplankton grazing.

Keywords: Arctic, sea ice, zooplankton

©2020. Japan Geoscience Union. All Right Reserved.

Influence of physical oceanographic condition to transportation of biosiliceous particles in the Pacific side of the Arctic Ocean

*Jonaotaro Onodera[1], Eiji Watanabe[1], Satoshi Kimura[1], Kohei Mizobata[2], Yuichiro Tanaka[3], Naomi Harada[1]

1. Research and Development Center for Global Change, JAMSTEC, 2. Dept. Ocean Sciences, School of Marine Life Science, TUMSAT, 3. Geological Survey of Japan, AIST

Under the changing physical oceanographic condition in the Arctic Ocean, transport condition of biogenic particles from shelf to basin in addition to vertical settlement of in situ biogenic particles may affect the ecosystems for deeper water mass and sea floor in the southwestern Canada Basin. In order to monitor the lower-trophic marine ecosystems in changing Arctic Ocean, we have studied the relationship between physical oceanographic condition and settling fluxes of biogenic particles mainly composed of diatom and silicoflagellate. Settling particle samples were collected using time-series sediment trap off the north of Barrow Canyon (NBC: 72.472N 155.407W, 2000 m water depth) and the northern part of Hanna Canyon (NHC: 73.303N 160.782W, 450 m water depth) in the southwestern Canada Basin from fall 2015 to summer 2017. Diatom settling flux increased in summer as a reflection of seasonal productivity increase. The assemblages of settling diatom particles at NBC for the first and second deployment periods was characterized by relative dominance of *Thalassionema nitzschioides*, which is sometimes observed in southwestern Canada Basin water, and sea-ice related species such as *Fossula arctica*, respectively. The relative abundance of sea-ice related species was higher at NHC, probably because of the NHC mooring position in more nutrient-rich condition compared to that at NBC. Diatom and silicoflagellate settling-fluxes at NBC also increased with particulate organic carbon in early winter 2016/2017. This reflected the temporal lateral advection of Pacific-origin waters from shelf to basin as the result of temporal changes in atmospheric and physical oceanographic condition.

Keywords: Arctic Ocean, Settling particles, Diatoms

©2020. Japan Geoscience Union. All Right Reserved.

Surface Waves Under the Arctic Sea Ice Observed by Drifting Wave Buoys

*Tsubasa Kodaira[1], Takuji Waseda[1], Takehiko Nose[1], Kazutoshi Sato[2], Jun Inoue[3]

1. The University of Tokyo, 2. KITAMI INSTITUTE OF TECHNOLOGY, 3. National Institute of Polar Research

Surface ocean waves are potentially one of the key physical processes to influence on the sea ice extent. To study the generation, propagation, and attenuation of surface ocean waves under the sea ice, two drifting wave buoys were deployed in the marginal ice zone in the western Arctic during R/V Mirai cruise 2019. The first buoy was deployed in the pancake-ice covered area and the second one in the open ocean. The distance between the two buoys at the deployment was approximately 40km. The comparison of the wave bulk statistic measured by the two buoys shows how the surface waves transform under the sea-ice.

During the measurements, both of the on-ice and off-ice wind conditions emerged. Under the on-ice condition, high-frequency waves attenuated significantly as the waves penetrate to the sea ice. The attenuation of the wind waves were also inferred from the SAR images. The low-frequency waves were, however, barely changed its energy level. The results indicate that the surface waves may not necessarily attenuate by the sea-ice if the wind speed is sufficiently high. On the other hand, under the off-ice conditions, the wave development was not clear, and the swells determined the significant wave direction.

Keywords: Surface Wave, Sea Ice , R/V Mirari

©2020. Japan Geoscience Union. All Right Reserved.

Covariability between Atmospheric Teleconnections and GDP Growth Rates

*Akane Kato[1], Yoshihiro Tachibana[1], Kensuke K. Komatsu[1], Yuta Ando[1]

1. Faculty of Bioresources, Mie University

Weather can have effects on local and global economies. Weather in one region can affect weather in another region, such as the El Niño phenomenon or Arctic Oscillation. Similarly, the economy of one country can affect the economy of another country. Therefore, it is necessary to study from a global perspective. The purpose of this study is to investigate the relationship between atmospheric teleconnections and the GDP growth rates of each country, and to clarify the teleconnection patterns closely related to economic activity.
It is suggested that the GDP growth rates were statistically related with Pacific Decadal Oscillation (PDO) index (negative correlation) or Southern Oscillation index (SOI) (positive correlation). In addition, we performed an empirical orthogonal function (EOF) analysis of the GDP growth rates. The first mode represents the pattern of gap between developing countries and developed countries. The first mode index was significantly correlated with the PDO index or SOI. From the above, it is suggested that the pattern of gap between developing and developed countries may be related to these teleconnection patterns.

Keywords: Gross Domestic Product, Southern Oscillation, Pacific Decadal Oscillation

©2020. Japan Geoscience Union. All Right Reserved.

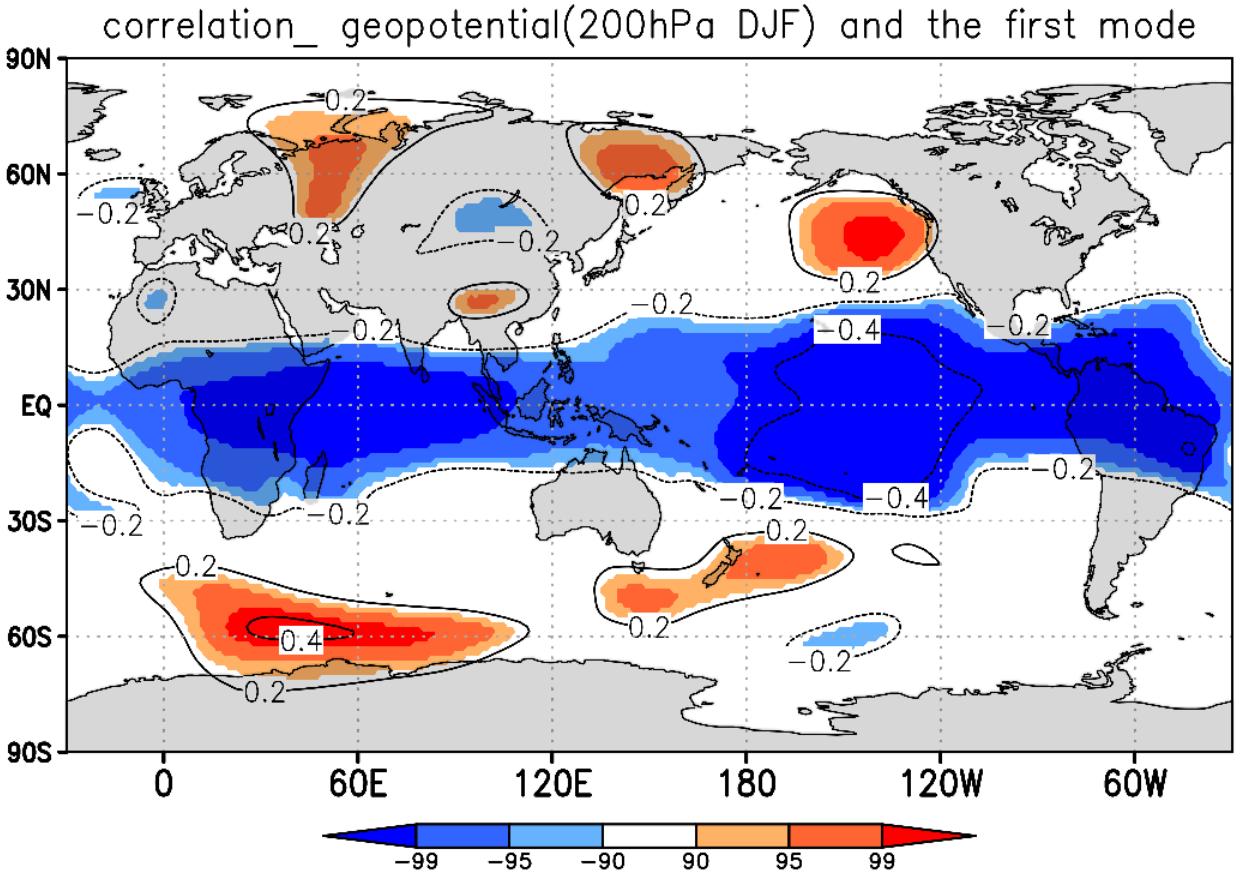

©2020. Japan Geoscience Union. All Right Reserved.

Remote influence on extreme weather in mid and high latitudes over the Northern Hemisphere driven by deep convection over Sahel

*Tomoe Nakanishi[1], Yoshihiro Tachibana[1], Yuta Ando[1]

1. Graduate School of Bioresources, Mie University

The Sahel region, which is located between tropical rainforest Africa and Sahara Desert, has large interannual variability of rainfall in association with extremely deep convection. This deep convection with large vapor condensation heating has a possibility of a remote influence on extreme weather in mid and high latitudes as the well-known influences of tropical oceanic convective clouds upon global climate. Remote influence of convective activity over the land is much less progressive than over the ocean although the both should be equally evaluated. We hypothesize that the deep convection over Sahel initiates a semi-circum teleconnection from Sahel to East Eurasia. Statistical analysis and simple numerical experiments indicate the possible existence of the semi-circum teleconnection in the interannual time.

Keywords: Teleconnection, Convective activity, Rossby wave, Wave train pattern, Linear regression

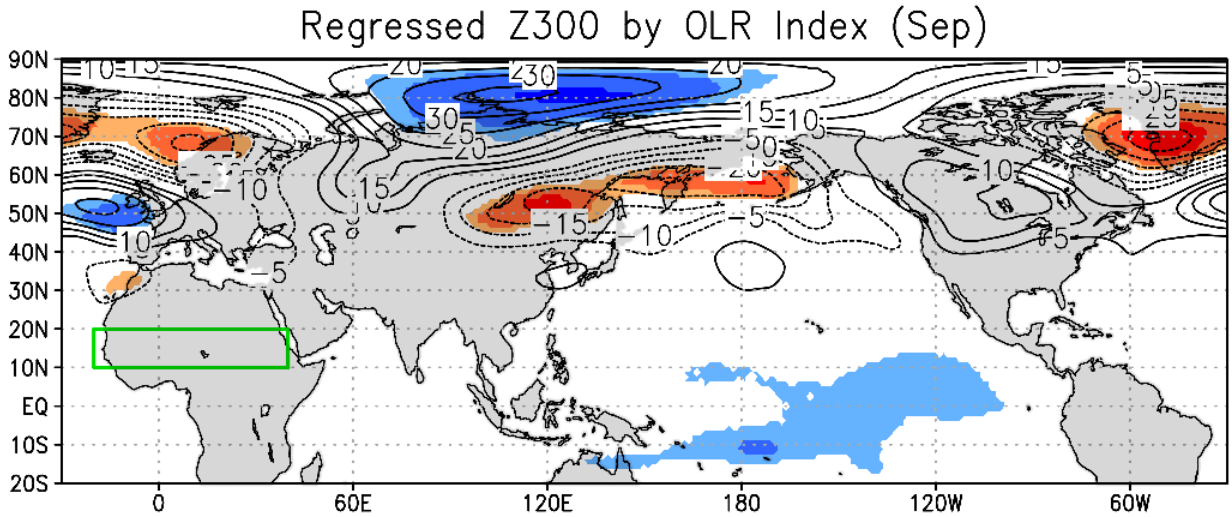

©2020. Japan Geoscience Union. All Right Reserved.

Recent Increase of Extreming Snowfall events in Kanto and its Relation to the Shift of Large-scale Atmospheric Circulations.

*Yuki Nakamura[1], Yoshihiro Tachibana[1]

1. Fac. of Bioresources, Mie Univ

The Kanto region does not snow much throughout the winter, and the measures against snow are weak compared with the Hokuriku region, which is a heavy snowfall region, compared to the Sea of Japan side. Therefore, once snowfall occurs, it has a great impact on lifelines. As an example, in February 2014, 72 people were injured when a train that stopped braking due to heavy snow collided with a preceding train stopped at a station.
Such snow and ice accidents may occur in the future, and it is necessary to predict future snowfall in the Kanto region. Some studies have used numerical models to predict future snowfall. In order to predict the future, it is good to look at a virtual world such as a numerical model, but first it is necessary to know what is happening up to the present and how it has changed between the past and recent years.
Therefore, the purpose of this study is to statistically compare the environmental fields of January and February in the Kanto region, which has a great social impact due to snowfall and snowfall, and to examine how environmental fields have changed in the past and in recent years.

First, in order to confirm whether there is a difference in the total amount of snowfall between the past and recent years, we looked at the changes in the total amount of snowfall in the Kanto region during the 58 years from 1961 to 2018 in January and February of each year.
Then, once every few years, there was a year that greatly exceeded the normal value. However, let before 1988 is first half and after 1989 is second half, there was no significant difference in the annual average snowfall in the past and recent years, not in the first half or the second half of the period. Well, the regime shift occurred at the border of 1988/89, and the climate changed greatly. Therefore, when the years were sorted in descending order of total snowfall, the years after the regime shift that occurred in the latter half of the 1980s were particularly high (Fig. 1).

Therefore, the factors in which the years after 1989 stand out are considered by comparing the difference of the average of each meteorological field on a snowy day by using the composite map analysis. In order to extract snowfall cases due to the South Coast Cyclones, the definition of the snowfall day was defined as the day on which more than 1 cm of snowfall was observed at 5 out of 8 locations in the Meteorological Office of the prefectural capital and Tateno (Ibaraki Prefecture). In addition, in order to consider the factors that have more snowfall years in recent years, we selected the extracted cases as “extreme cases” when the total of 8 points was 100 cm or more, and “normal cases” except the extreme cases. We investigated from two cases, the increase / decrease in the number of extreme cases and the increase / decrease in the amount of snow (precipitation) per case in both extreme and ordinary cases.

The total number of extracted cases was 40 in the last 30 years, and in recent 28 years was 30, totaling 70 cases, and the total number of cases was reduced from 40 to 30. However, Fig. 1 shows that the total amount of snowfall in January and February of each year is higher in recent years, and the number of extreme cases has increased in the past 5 cases, 9 cases in recent years.
Then, to consider why the number of extreme cases increased to confirm the change of the storm track, it became stronger from the South Sea to the East Sea of Japan. At the same location, the north-south temperature gradient of sea surface temperature also increased.

©2020. Japan Geoscience Union. All Right Reserved.

Next, the amount of snowfall (precipitation) in each of the extreme and ordinary cases was examined, there was a significant increase in precipitation in both cases.

Based on the fact that the storm track has been strengthening in recent years, we are considering the factors, in the past and in recent years fields, focusing on the entire Northern Hemisphere and the Arctic region, the snowy years and the number of extreme cases have increased in recent years. This analysis will be announced on the day.

Keywords: South Coast Cyclones, storm tracks, Regime shift

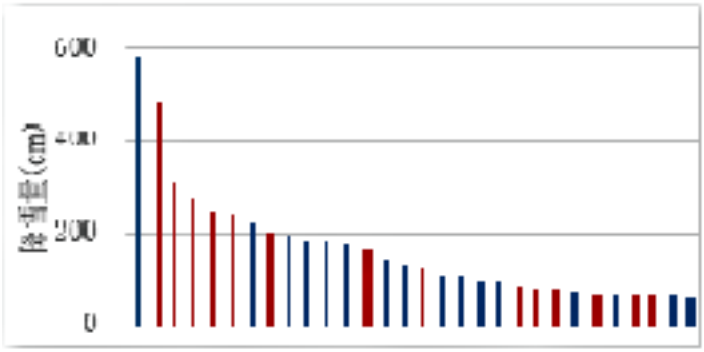

図 1　1961~2018 年の 58 年間の各年 1,2 月総降雪量[cm]を多い順に上位 30 年並べた．赤は 1989 年以降，青は 1988 年以前を表す

©2020. Japan Geoscience Union. All Right Reserved.

[J] Poster | A (Atmospheric and Hydrospheric Sciences)：A-CG Complex & General

[A-CG58] Aircraft and UAV Observations for Earth-planetary sciences

convener:Nobuhiro Takahashi(Institute for Space-Earth Environmental Research, Nagoya University), Makoto Koike(Department of Earth and Planetary Science, Graduate School of Science, The University of Tokyo), Toshinobu Machida(National Institute for Environmental Studies), Taro Shinoda(Institute for Space-Earth Environmental Research, Nagoya University)

The global climate change, especially for global warming is a big issue throughout the Earth and planetary sciences. To confront this problem, progresses of the observations both for continuous monitoring of the Earth and for the process studies as well as the numerical climate modeling become more important. Aircraft observation has the great advantages on the promptness/timeliness and direct (in-situ) observation which cannot be achieved by Earth observing satellites or ground-based observations. Recently, the importance of aircraft observation is increasing in "in-situ measurements" such as concentration of greenhouse gases, aerosol and cloud particle size distribution, and chemical composition, and "remote sensing" such as three-dimensional observation typhoons and observation on forests and vegetation for better understanding of the detailed process of the global warming and its impacts on the global climate and weather. In addition, the application of aircraft observation including the unmanned aerial vehicle (UAV) to geodesy, studies on earthquakes and volcanoes are also progressing. However, operational and/or extensive aircraft observations to fulfill the requirements in Japan are not realized at the present time even though the aircraft observations technologies in Japan has been leading the world. In order to realize more comprehensive/extensive researches by the aircraft observations, it is necessary to have close collaborations among researchers. In this session, we will discuss the future promotion of aircraft and UAV observation through the latest research results using aircraft.

[ACG58-P01] Estimation of Turbulence Kinetic Energy dissipation rate (ε) using High-Resolution Pitot differential pressure sensor onboard a Small Unmanned Aircraft System (sUAS)

*Abhiram Doddi[1], Dale Lawrence[1], Lakshmi Kantha[1], Hubert Luce[2] (1.University of Colorado Boulder, USA, 2.Université de Toulon, France)

[ACG58-P02] Development of Method for Turbulence Simulation using Onboard LIDAR Data Assimilation

*Ryoichi Yoshimura[1], Aiko Yakeno[1], Ryota Kikuchi[3], Takashi Misaka[2], Shigeru Obayashi[1] (1.Institute of Fluid Science, Tohoku University, 2.National Institute of Advanced Industrial Science and Technology , 3.DoerResearch, Inc.)

[ACG58-P04] Characteristic analysis of measurement error in GNSS-R UAV Altimeter

*wang chuanbing[1], Kaoru Ichikawa[1] (1.Kyushu University)

[ACG58-P05] NICT third generation airborne SAR system

*Shoichiro Kojima[1], Junpei Uemoto[1], Yuya Arima[1], Masanori Gocho[1] (1.National Institute of Information and Communications Technology)

[ACG58-P06] Variation of ultra fine particle concentrations within the winter boundary layer observed by a Multicopter UAV

*Masahiko Hayashi[1], Akihiro Yasunaga[1], Ryohei Haraguchi[2] (1.Faculty of Science, Fukuoka University, 2.Graduate school of Fukuoka University)

[ACG58-P07] Proposal to the master plan 2020: Promotion of Scientific Research on Climate and Earth System Sciences Using Aircrafts

*Nobuhiro Takahashi[1], Makoto Koike[2] (1.Institute for Space-Earth Environmental Research, Nagoya University, 2.School of Science, The University of Tokyo)

Estimation of Turbulence Kinetic Energy dissipation rate (ε) using High-Resolution Pitot differential pressure sensor onboard a Small Unmanned Aircraft System (sUAS)

*Abhiram Doddi[1], Dale Lawrence[1], Lakshmi Kantha[1], Hubert Luce[2]

1. University of Colorado Boulder, USA, 2. Université de Toulon, France

The measurement of Turbulence Kinetic Energy (TKE) dissipation rate (ε) and structure function parameters of temperature {C_{t}}^{2} and refractivity {C_{n}}^{2} have been used as immaculate evidence to confirm the presence of turbulence in the atmosphere. The spatial-temporal variability in the measurements of ε and {C_{t}}^{2} help understand the morphology of atmospheric turbulence. We restrict the discussion to the process of estimation of only ε , simply because of the congruence in the procedures for estimating ε , {C_{t}}^{2} and {C_{n}}^{2}

The estimation of ε requires that the airspeed fluctuations be sampled at sufficiently high temporal resolution to characterize the inertial sub-range in the Power Spectral Density (PSD) of the airspeed fluctuations. The DataHawk sUAS has successfully demonstrated the ability to observe targeted atmospheric columns while employing co-located Hotwire Anemometer and Pitot differential pressure sensor, both with a bandwidth of 800Hz serving as independent measurement sources.

Here, we outline the procedure of estimation and the caveats and limitations in accurately estimating high and low intensity ε using the measurements from the digital Pitot differential pressure sensor exclusively. In doing so, the factors deteriorating the quality of the spectral samples are identified and characterized. The effect of airfoil induced flow acceleration and the motor induced vibrations on the Pitot fluctuation intensity and the resulting spectra are carefully explored. The algorithms used for precisely identifying the frequency range of the inertial sub-range energy cascade in the PSD is also described. The effect of high and low turbulence intensities on the quality of ε estimates are explored. The Pitot derived ε_P is validated using the Hotwire derived ε_{HW} and a model derived ε_m using the estimates of temperature structure function parameter {C_{t}}^{2}

Keywords: Turbulence Kinetic Energy Dissipation , In-Situ measurements, Estimation

©2020. Japan Geoscience Union. All Right Reserved.

Development of Method for Turbulence Simulation using Onboard LIDAR Data Assimilation

*Ryoichi Yoshimura[1], Aiko Yakeno[1], Ryota Kikuchi[3], Takashi Misaka[2], Shigeru Obayashi[1]

1. Institute of Fluid Science, Tohoku University, 2. National Institute of Advanced Industrial Science and Technology , 3. DoerResearch, Inc.

Air turbulence is one of the major causes of airborne accidents. The Japan Transport Safety Board reported that 46% of accidents in the last ten years were caused by turbulence. In particular, clear air turbulence (CAT) is a serious issue because it occurs without a warning sign, such as a thunderstorm.

As a practical action against turbulence risk, Airbus and Tamarack developed a wing tip device to alleviate gust wind-induced wing load variation. ATLAS^{TM} Active Winglet from Tamarack Aerospace has a control surface that automatically moves to generate a force opposite to that of the detected wing load. This device can reduce the wing load concurrently with a turbulence encounter. The Japan Aerospace Exploration Agency (JAXA) has also engaged in a program to reduce the risk of accidents by detecting turbulence using the Doppler light detection and ranging (LIDAR) Systems, developed by Mitsubishi Electric.

However, airborne LIDAR measurements are insufficient for a precise estimation of turbulence in terms of spatial resolution. Although computational fluid dynamics (CFD) can solve this problem, its initial and boundary conditions for meteorological phenomena, including CAT, are usually unknown. Consequently, there is a lack of precise turbulence-structure reproduction techniques.

Data assimilation (DA) is a powerful tool for CAT prediction that estimates the optimal initial condition for an N-S solver by integrating airborne observations and output from the simulation. DA modifies the output of an N-S solver on the basis of observed data, and variables around the observed points are bound by the governing equation of the fluid. This implies that DA can facilitate CFD reproducing a flow field close to the airborne wind observation, and the modified flow fields are physically consistent. In our study, a square root filter (SRF) was employed for the DA process.

In the DA experiments, we assumed that the vortices generated by the shear layer instability were the CAT. Air turbulence was simulated in a non-terrain domain with an in-house compressible Navier-Stokes solver. We placed a wind shear layer on the initial flow field and induced Kelvin-Helmholtz (K–H) instability. In the prognostic chart of significant weather, provided by the Japan Meteorological Agency, the region with a high possibility of CAT existence often emerges along with the jet stream at high altitude. Additionally, it is known that CAT is mainly caused by strong wind shear due to meteorological phenomena, such as jet streams and low-pressure areas.

In this study, roll vortices that simulate CAT were estimated using the DA and a pseudo wind observation. Wind observation was conducted in the LIDAR configuration, in which forward winds were observed in a straight line from an aircraft. We validated the performance of the DA by the identical twin experiment; the true state and the wind observation were generated numerically.

As a result of the identical twin experiment in the 3D flow configuration, observation of horizontal and vertical wind elements that could compose the K-H vortex were critical in capturing the roll vortices.

©2020. Japan Geoscience Union. All Right Reserved.

Observation of only the horizontal wind did not improve the estimation. Additionally, we solved the two-dimensional Poisson equation before the DA procedure to approximate pressure from the observation of horizontal and vertical winds. By the assimilation of horizontal and vertical winds and the derived pressure, the accuracy of the estimation improved in comparison with the estimation without assimilating pressure. These results suggest that the vortices were well-captured owing to the increase in the observation-based information, and the DA could correctly filter out the observation errors from the derived pressure.

To summarize, we proposed a method for CAT reproduction using LIDAR observation and CFD. We validated the method numerically in an identical-twin experiment, estimating the turbulence in 3D flow configuration.

Keywords: Clear Air Turbulence, LIDAR, Data Assimilation

©2020. Japan Geoscience Union. All Right Reserved.

Characteristic analysis of measurement error in GNSS-R UAV Altimeter

*wang chuanbing[1], Kaoru Ichikawa[1]

1. Kyushu University

The GNSS signal reflected from the water surface is longer than the signal path that arrives directly from the GNSS satellite. The method of measuring altitude from the distance difference between them is called GNSS-R altimetry. In Ichikawa et al. (2019), the drone is equipped with a GNSS signal receiver, estimates the height of the drone based on the GNSS-R height measurement method, performs a time average of about 7 minutes, and performs an accuracy of about several cm. Achieved. This system uses independent signal receivers for direct and reflected signals to reduce cost. Therefore, a time difference occurs between the receivers (hereinafter referred to as “receiver time difference”), and it is necessary to obtain both the altitude and the receiver time difference as unknowns for each epoch. Since these unknowns are amounts common to a plurality of satellites received at the same time, they can be estimated by using the least squares method for observation data of a plurality of satellites for each epoch. When the altitude and receiver time difference were actually calculated for each epoch of 5 Hz, it was suggested that the receiver time difference did not show a rapid change between epochs, but fluctuated slowly and continuously over time. If the receiver time difference can be approximated by a long-period function and corrected as a known value, the only unknown value for each epoch is the altitude, and an estimate of the altitude (including the observation error) of each satellite must be obtained. Can be. Therefore, in this study, first, the receiver time difference obtained by Ichikawa et al. (2019) is approximated and corrected by a quadratic function of time, and an altitude estimate is obtained for each satellite at each epoch. The error component included in the value is extracted. After that, what kind of time-varying characteristics of the obtained error component has is examined, and the relation with the elevation angle of each satellite is examined. Specifically, in a study by Ichikawa et al. (2019), UAV hovered at altitudes above 100 m and measured relatively stably for 3 minutes from 12:27 to 12:30 on January 7, 2017 Was analyzed. The number of satellites during this time was almost 5, and the elevation angles were 9.8 degrees, 11.3 degrees, 43.3 degrees, 44.3 degrees, and 58 degrees. The error distribution of the estimated value was obtained from the difference from the estimated altitude of each satellite, using the UAV height separately measured by precision positioning as the true value. The error is distributed differently for each satellite. For a satellite with a high elevation angle, the error analyzed for 3 minutes is only a slow fluctuation and does not include a short-period change, but as the elevation angle decreases, the period increases. Both the frequency and amplitude of occurrence of short-term fluctuations of about 1-2 seconds increased. For the lowest elevation satellites, the short-term error amplitude reached 60 m. However, extremely short periods shorter than one second were not significantly included even in a satellite having a low elevation angle. The characteristics of the period of such a short-period fluctuation component suggest that this error is due to the effect of waves on the water surface. The GNSS-R height measurement method solves geometrically by assuming that the reflected water surface is horizontal, but if the water surface is inclined by the wave, the reflection point deviates from the assumption, so the actually measured reflected wave Path becomes large, causing an error. Furthermore, even with the same wavefront tilt, this error increases as the elevation angle of the satellite decreases, so that there is no contradiction that the amplitude of the error of the short-period fluctuation increases as the elevation angle of the satellite decreases.

Keywords: GNSS−R, Altimeter, UAV, Satellite elevation, Wavefront gradient

©2020. Japan Geoscience Union. All Right Reserved.

©2020. Japan Geoscience Union. All Right Reserved.

NICT third generation airborne SAR system

*Shoichiro Kojima[1], Junpei Uemoto[1], Yuya Arima[1], Masanori Gocho[1]

1. National Institute of Information and Communications Technology

National institute of Information and Communications Technology (NICT) developed the second generation polarimetric and interferometric X-band airborne synthetic aperture radar in 2008. NICT has carried out the observation for the application research such as environmental and disaster monitoring since 2011. For example, the Tsunami hit areas in Tohoku region and the crater after the eruption were observed. In addition, the wave height distribution was estimated from the sea surface velocity measured by the along track interferometric mode in the Pi-SAR X2.

Now, NICT is developing the third generation polarimetric and interferometric X-band SAR system. This system is designed to acquire a high-quality SAR image, high performance single and repeat track interferometric SAR data and high performance along track interferometric SAR data. In this study, the expected function and performance of the Pi-SAR X3 is reported. Fig.1 shows the observation targets. NICT plan to perform the disaster monitoring such as the Tsunami hit areas and the crater after the eruption and environmental measurement such as ocean and agriculture by using the Pi-SAR X3. To measure these targets with high precision, 3 performances of the Pi-SAR X2 will be improved and a new function will be added. A basic performance such as the spatial resolution and sensitivity will be improved to enhance the visibility of the image. The accuracy of the elevation measured by the single-track interferometry will be improved. We aim to reduce the estimation error in the elevation to less than 2m. The range of the velocity measured by the along track interferometry will be improved to measure high wave under the typhoon. The repeat-track interferometric observations such as CCD, DinSAR and topography will be realized by controlling the flight course precisely, and the ground deformation and the artificial structure deformation such as a building and bridge will be able to detect.

Keywords: SAR, Disaster monitoring, Environmental measurement

©2020. Japan Geoscience Union. All Right Reserved.

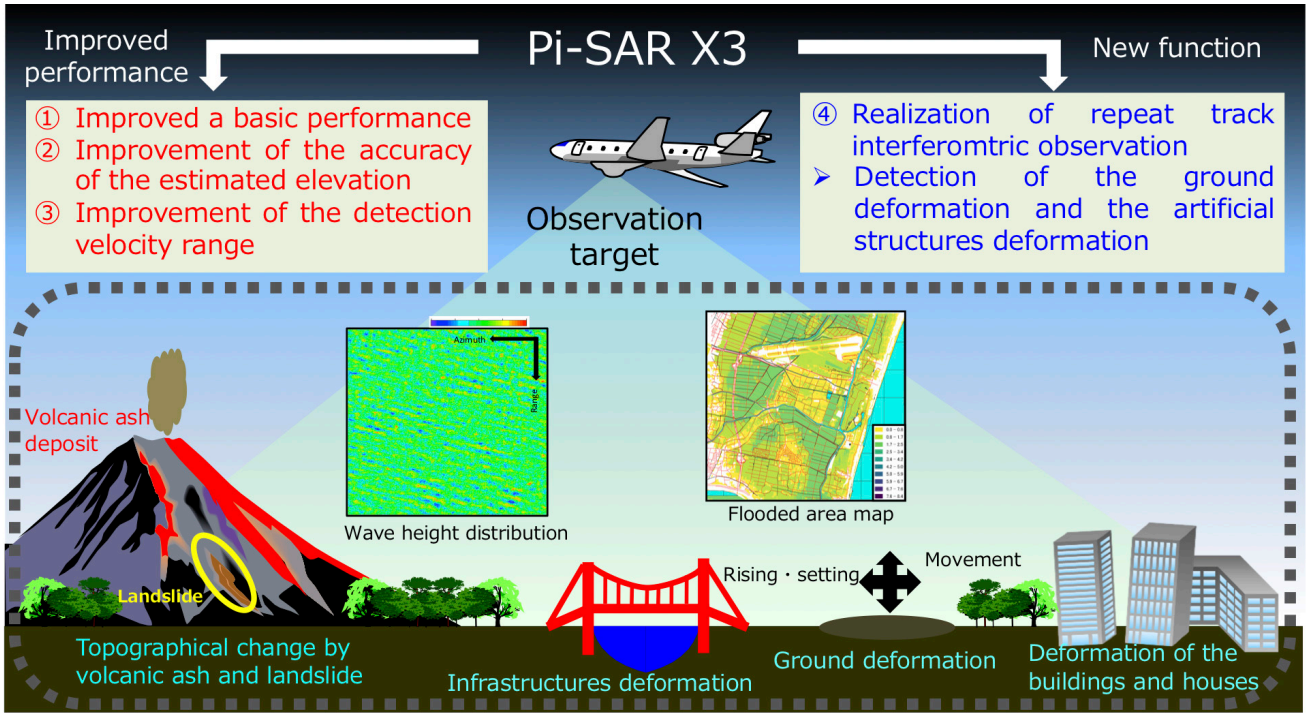

©2020. Japan Geoscience Union. All Right Reserved.

Variation of ultra fine particle concentrations within the winter boundary layer observed by a Multicopter UAV

*Masahiko Hayashi[1], Akihiro Yasunaga[1], Ryohei Haraguchi[2]

1. Faculty of Science, Fukuoka University, 2. Graduate school of Fukuoka University

A CPC (Condensation Particle Counter), which measure number concentrations of Ultra Fine Particles (UFP) with diameter of 10-100 nm was mounted on multicopter manufactured by DJI Co. Ltd., and temperature, humidity and pressure were measured simulteneously. UAV flought until 200m above ground by manual control at Tamura Hanatae field (33.54°N, 130.32°E) and Ikino-matsubara coast (33.58 °N, 130.58°E), both located around boundary of city area and rural area. Operations were carried out Nov. 29th, 30th, Dec. 8th and 9th in 2019. vertical profiles were obtained every 30-40 minuite from sunrise ot sunset on Nov. 29th and from sunrise to noon on other 3 days.
Similar variations were observed from sunrise to noon for all 4 days. High concentrations of UFP, exceed 10000 particles /cm^3 appeared in surface layer and low concentrations of UFP, 2000-5000 particles/cm^3 , were observed in residual layers above surface layers at sunrise. Thickeness of surface layer with high concentration of UFP grew with time until around 11:00, and surface layer disappeared and concentration of UFP decreased at the time. Concentrations of UFP after 11:00 show different level, which seem to refrect the conditon of field located in upstream direction of surface wind. Lifetimes of UFP were estimated as around 5 hours, based on aerosol size distributions observed at Fukuoa University, and they are consistent with low concentration of UFP in resudual layer for all 4 days.

Keywords: multicopter UAV, boundary layer, ultra fine particles, high tempo-spatial resolution

©2020. Japan Geoscience Union. All Right Reserved.

©2020. Japan Geoscience Union. All Right Reserved.

Proposal to the master plan 2020: Promotion of Scientific Research on Climate and Earth System Sciences Using Aircrafts

*Nobuhiro Takahashi[1], Makoto Koike[2]

1. Institute for Space-Earth Environmental Research, Nagoya University, 2. School of Science, The University of Tokyo

This research plan is the proposal to the Master Plan 2020 of the Science Council of Japan by the Meteorological Society of Japan jointly with the Japan Society of Atmospheric Chemistry, and the Japan Society for Aeronautics and Space Sciences as a fusion study between engineering and atmospheric science with the use of unmanned aerial vehicles for earth observation. This proposal is supported by 10 societies such as the Japan Geoscience Union (Atmospheric and Hydrospheric Sciences Section). This proposal is selected as one of priority areas (16 new themes).

The purpose of this research is to promote climate and earth system science research across all earth science fields, including the atmosphere, ocean, vegetation, snow and ice, and the solid earth, by introducing Japan's first aircraft dedicated to earth observation.

Changes in the global environment, including global warming, are progressing rapidly, and are exerting a great influence on human economic and social activities and the basics of life such as water and food supply. However, in order to understand the behavior as a system of climate and environment (fluctuation of macroscopic amount), it is indispensable to understand the microscopic amount and elementary processes such as the concentration of greenhouse gases, the particle size and chemical composition of clouds and aerosols. It can be said that various fields of earth science face this scale gap problem in common. Only aircraft observations can measure micro quantities of less than 100m, including wide areas and altitude distributions, which cannot be captured by satellites or ground-based observations. In other words, aircraft observation is a means of obtaining an entirely new insight of observation, instead of increasing the accuracy of conventional observation. This research aims to a paradigm shift in the earth sciences field to realize the understanding of climate and earth system behavior based on the understanding of microscopic quantities and elementary processes by aircraft observation. With an emphasis on aircraft observations, we aim to establish an integrated earth science framework that crosses the fields of the atmosphere, ocean, land vegetation, snow and ice, and the solid earth. In particular, we will conduct observational research focusing on Asia and the Arctic region, which are gaps in aircraft observations, even as rapid environmental changes become apparent.

Until now, there has been no aircraft dedicated to earth observation in Japan. No systematic aircraft observations were carried out in Asian region even Japan has been leading observation technology. In order to take advantage of Japan's strengths, this study will introduce Japan's first aircraft dedicated to earth observation, based on a joint use system that enables researchers in a wide range of fields to use aircraft from a long-term perspective and establish a researcher-centered operation system. Through long-term operation (10 years), systematic observations and research on important themes in earth science will be achieved with innovative results, as well as strategic equipment development and human resource development. For observation, we will rent Gulfstream-IV class jets aircraft owned by private companies for exclusive use. Furthermore, the use of unmanned aerial vehicles, which have undergone rapid technological progress in recent years, will be strongly promoted.

As for the implementation organization, the Center for Orbital and Suborbital Observations, Institute of

©2020. Japan Geoscience Union. All Right Reserved.

Space-Earth Environmental Research, Nagoya University, will be the operating base of the joint use. The ownership and operation of the aircraft is outsourced to a private company. In addition, JAXA will provide support for the flight technology. In this research, the Aircraft Observation Promotion Committee, consisting of researchers from all over the research fields of atmosphere, ocean, terrestrial ecosystem, snow and ice, earthquake and volcano, will be established to support observational research. In the planning of this plan, 22 academic societies contributed for establish a 224-page research plan.

This research also aims to contribute to the society of disaster prevention and mitigation by improving the accuracy of typhoon forecast and torrential rainfall and understanding the mechanism of disasters such as floods. Through such research, we aim to contribute to the United Nations' SDGs and Future Earth.

Keywords: Climate change, Aircraft observation

©2020. Japan Geoscience Union. All Right Reserved.

[J] Poster | A (Atmospheric and Hydrospheric Sciences)：A-CG Complex & General

[A-CG59] Biogeochemical linkages between the surface ocean and atmosphere

convener:Sohiko Kameyama(Hokkaido University), Yoko Iwamoto(Graduate School of Integrated Sciences for Life, Hiroshima University), Maki Aita Noguchi(Japan Agency for Marine-Earth Science and Technology), Daisuke Sasano(Japan Meteorological Agency)

Multi-scale vertical and horizontal ocean mixing processes can strongly influence the distribution of dissolved and suspended substances including macro- and micro-nutrients, and may impact on the global carbon cycles. The changes in nutrient dynamics generally affect the abundance, composition and metabolic activity of marine organisms such as phytoplankton and bacteria during the bloom. Marine phytoplankton can produce volatile organic compounds (VOCs) and marine atmospheric aerosols, which strongly influence on atmospheric chemistry. Primary and secondary organic and inorganic components produced via marine phytoplankton activity can contribute to the Earth's radiative forcing, and in turn marine ecosystems including biogeochemical processes directly or indirectly. Therefore, the biogeochemical cycles have a tight linkage between the ocean and the atmosphere. In order to understand physical, chemical and biological processes relevant to phytoplankton bloom formation in the ocean, dynamics of VOCs and marine aerosols in the atmosphere, and the biogeochemical linkage between the ocean and the atmosphere, we welcome new interdisciplinary presentations and active discussions on physical, chemical, and biological sciences both from ocean and atmospheric fields in this session. Studies linked to the Surface Ocean-Lower Atmosphere Study (SOLAS) project are good examples, but other related studies are also invited.

[ACG59-P01] Model analysis of atmospheric concentrations and depositions on the Eastern Indian Ocean observed by R/V Hakuho Maru

*Kazuyo Yamaji[1], Katsuhiro Kawamoto[1], Moe Tauchi[1], Yoko Iwamoto[2], Kazuhiko Matsumoto[3], Makio Honda[3], Yugo Kanaya[3], Takashi Sekiya[3], Maki Noguchi Aita[3], Tomoki Nakayama[4], Satoru Chatani[5], Fumikazu Taketani[3] (1.Kobe University, 2.Hiroshima University, 3.Japan Agency for Marine-Earth Science and Technology, 4.Nagasaki University, 5.National Institute for Environmental Studies)

[ACG59-P02] Influence of deposition of atmospheric nitrogen compounds on the surface marine ecosystem at the Japan Sea

*Fumikazu Taketani[1], Maki Noguchi Aita[1], Takashi Sekiya[1], Kazuyo Yamaji[1,2], Kohei Ikeda[3], Makio Honda[1], Kazuhiko Matsumoto[1], Kosei Sasaoka[1], Yugo Kanaya[1] (1.Japan Agency for Marine-Earth Science and Technology, 2.Kobe University, 3.National Institute for Environmental Studies)

[ACG59-P03] Estimation of atmospheric nitrogen deposition over the Kuroshio region in the Autumn of 2015

*Yoko Iwamoto[1,3], Kazuki Kamezaki[2], Shohei Hattori[2], Mako Hirota[1], Shuei Kaizuka[1], Kazuhiko Takeda[1], Kazuhiko Miura[3], Mitsuo Uematsu[4,5] (1.Hiroshima University, 2.Tokyo Institute of Technology, 3.Tokyo University of Science, 4.Atmosphere and Ocean Research Institute, the University of Tokyo, 5.Center of Environment Science in Saitama)

Model analysis of atmospheric concentrations and depositions on the Eastern Indian Ocean observed by R/V Hakuho Maru

*Kazuyo Yamaji[1], Katsuhiro Kawamoto[1], Moe Tauchi[1], Yoko Iwamoto[2], Kazuhiko Matsumoto[3], Makio Honda[3], Yugo Kanaya[3], Takashi Sekiya[3], Maki Noguchi Aita[3], Tomoki Nakayama[4], Satoru Chatani[5], Fumikazu Taketani[3]

1. Kobe University, 2. Hiroshima University, 3. Japan Agency for Marine-Earth Science and Technology, 4. Nagasaki University, 5. National Institute for Environmental Studies

Recently, significant air pollution over South Asia has been attentions from the globe. Especially in the dry season (from October to February), the pollution level has gone bad at mega-cities in India due to enhanced anthropogenic emissions and changed meteorological conditions. On the same season, additionally, it is concerned that the continental pollution transport due to changing air-mass flow coming from the ocean breeze to the land breeze will affect the marine ecosystem in the Bay of Bengal and the Indian Ocean.

On-board atmospheric observations over the Bay of Bengal and the Southeast Indian Ocean during the R/V Hakuho Maru KH-18-6 cruise performed in the early dry season succeeded to capture the heavily polluted air-masses likely including atmospheric pollutants (Iwamoto et al, 2019, 2020). Their aerosol and rainwater samples also provided the possibilities of continental nitrogen deposition into the Ocean.

We tried to investigate the sources and reasons observed enhanced concentrations of gas and aerosol species and these depositions by using a regional chemical transport model, WRF/CMAQ.

CMAQ generally captured well changing of the observed gas and aerosol concentrations in the Bay of Bengal. The increased concentrations of gaseous and particulate pollutants after the Cyclone passing was simulated well in the model, although the model sometime could not reproduce concentrations of individual species. Both observed and simulated relative high concentrations at around 5N might be associated with not only transports from the South part of India, but the Middle East ship route.

Keywords: regional chemical transport model, South Asia, the Bay of Bengal, the Indian Ocean, gaseous pollutants, particulate pollutants

©2020. Japan Geoscience Union. All Right Reserved.

Influence of deposition of atmospheric nitrogen compounds on the surface marine ecosystem at the Japan Sea

*Fumikazu Taketani[1], Maki Noguchi Aita[1], Takashi Sekiya[1], Kazuyo Yamaji[1,2], Kohei Ikeda[3], Makio Honda[1], Kazuhiko Matsumoto[1], Kosei Sasaoka[1], Yugo Kanaya[1]

1. Japan Agency for Marine-Earth Science and Technology, 2. Kobe University, 3. National Institute for Environmental Studies

The sensitivity of the atmospheric deposition of inorganic nitrogen compounds to the surface chlorophyll-a mass concentration at the Japan Sea was investigated using a 3-D lower trophic-marine ecosystem model (NEMURO) combined with an atmospheric regional chemical transport model (WRF-CMAQ). The monthly mean values for the wet and dry deposition of nitrogen compounds including gases (HNO3 and NH3) and aerosol particles (NO3- and NH4+) over the Japan Sea were determined using the WRF-CMAQ, indicating that wet deposition was dominant in all seasons. These values were input into the surface of ocean of NEMURO as a new nitrogen source. The annual average of surface chlorophyll-a mass concentration at the Japan Sea was increased from 0.26 to 0.35 mg/m3. The growth ratios of chlorophyll-a mass concentration in summer was factor of ~2.1, while that in wintertime was factor of ~1.1, indicating that the atmospheric deposition of inorganic nitrogen compounds highly influence to the surface chlorophyll-a mass concentration in summer.

Keywords: Nitrogen compounds, deposition, Japan Sea, marine ecosystem

©2020. Japan Geoscience Union. All Right Reserved.

Estimation of atmospheric nitrogen deposition over the Kuroshio region in the Autumn of 2015

*Yoko Iwamoto[1,3], Kazuki Kamezaki[2], Shohei Hattori[2], Mako Hirota[1], Shuei Kaizuka[1], Kazuhiko Takeda[1], Kazuhiko Miura[3], Mitsuo Uematsu[4,5]

1. Hiroshima University, 2. Tokyo Institute of Technology, 3. Tokyo University of Science, 4. Atmosphere and Ocean Research Institute, the University of Tokyo, 5. Center of Environment Science in Saitama

The Kuroshio has its origin in the subtropical water of high water temperature and oligotrophy, and it is considered to form the ecosystem with high productivity by taking in nutrients from continental shelf and coastal area in the transport process. However, there are many unclear points on the supply mechanism of nutrients to the Kuroshio region. Since the Kuroshio Current is located on the leeward side of the East Asian coastal area, which is a hot spot for air pollutants, the supply of nitrogen components, which are nutrients for marine phytoplankton, through the atmosphere cannot be ignored. In addition, it is predicted that the marine ecosystem in the western North Pacific including the Kuroshio region changes with the increase in the atmospheric emission of anthropogenic nitrogen in the East Asia. The purpose of this study is to clarify the impact of atmospheric nitrogen deposition on the ecosystem in the Kuroshio region from the east coast of Taiwan to the Kanto offshore, Japan.
Atmospheric observations were carried out on the academic research ship Hakuho Maru KH -15-4 cruise. Atmospheric aerosol were collected using a filter pack method and a high volume air sampler during the cruise. These samples were analyzed for water-soluble ions by ion chromatography.
As a result of backward trajectory analysis, it was found that the beginning of the voyage was affected by the oceanic atmosphere, while the other periods were affected by air masses along the coast of East Asia or via the Japanese Islands. Nitrate concentrations in atmospheric aerosols were 1.2 ±0.8 $\mu g\ m^{-3}$, similar to those reported in previous studies of 1.8 ±1.2 $\mu g\ m^{-3}$ in the East China Sea, an order of magnitude higher than 0.17 ±0.09 $\mu g\ m^{-3}$ in the western North Pacific. We will discuss about the dry deposition of atmospheric nitrogen and its impact on primary production.

Keywords: Aerosol, Nitrogen deposition flux, Kuroshio

©2020. Japan Geoscience Union. All Right Reserved.

[J] Poster | A (Atmospheric and Hydrospheric Sciences)：A-CG Complex & General

[A-CG60] Adaptation for climate change and social implementation

convener:Yoichi Ishikawa(JAPAN Agency for Marine-Earth Science and Technology), Hiroya Yamano(National Institute for Environmental Studies), KOJI DAIRAKU(University of Tsukuba), Shingo Watanabe(Japan Agency for Marine-Earth Science and Technology)

The impacts of climate change will increase in the risk of natural disasters such as typhoons and torrential rains, change in the distribution of organisms, deterioration in quality and yield in the agriculture, forestry and fisheries. "Climate Change Adaptation Act" was enforced in 2018, aiming to minimize or avoid the damage caused by climate change, and to build a sustainable society.
In this session, we will discuss about climate change adaptation based on scientific knowledge, including creation of climate change projection data, assessment of the impacts and risks of climate change in various fields, and tackle social implementation of adaptation plan by co-creation with stakeholders.

[ACG60-P01] Possible historical impact of urbanization on the surface air temperature in Sofia, Bulgaria

*Lidia Lazarova Vitanova[1,2], Hiroyuki Kusaka[1] (1.Center for Computational Sciences, University of Tsukuba, 2.Nikken Sekkei Research Institute)

[ACG60-P02] High school Investigation activities for the Carbonates quantities interaction between the ocean lives' shells and atmosphere-ocean.

*Ryo S Nakamura[1] (1.Miyagi Rifu high school)

[ACG60-P03] Prediction of future soil erosion risk in Japan considering climate change

*Gen Machida[1], Kazutoshi Osawa[2], Taku Nishimura[3] (1.Graduate School of Regional Development and Creativity, Utsunomiya University, 2.School of Agriculture, Utsunomiya University, 3.School of Agriculture, Tokyo University)

Possible historical impact of urbanization on the surface air temperature in Sofia, Bulgaria

*Lidia Lazarova Vitanova[1,2], Hiroyuki Kusaka[1]

1. Center for Computational Sciences, University of Tsukuba, 2. Nikken Sekkei Research Institute

This study investigates the possible historical impact of the urbanization in Sofia, Bulgaria. This is the first attempt to be numerically investigated the impact on urbanization on the surface temperature between 1878 and 2012. In this study we use the Weather Research and Forecasting (WRF) model with 1-km horizontal resolution for three separated months of July (2011 –2013) in two cases: past land-use (URB1878) and present land-use (URB2012). First, we verify the results of the control simulation (URB2012) against observations. The results show that the WRF model reproduces reasonably the diurnal temperature distributions for both high-urbanized and low-urbanized / rural areas. The mean model biases ranged from −0.6 to 0.6 ˚C. Second, the impacts of the urbanization on the surface air temperatures are evaluated. The results show significant nocturnal temperature increases by 3.1 ˚C in the URB2012 case compared to those in the URB1878 case in Sofia respectively. Third, the surface air temperatures between high and low-urbanized / rural areas are evaluated. The results showed significant nocturnal temperature increases by 3.6 ˚C between Sofia and its suburbs.

Keywords: urbanization, WRF model, surface air temperature

©2020. Japan Geoscience Union. All Right Reserved.

High school Investigation activities for the Carbonates quantities interaction between the ocean lives' shells and atmosphere-ocean.

*Ryo S Nakamura[1]

1. Miyagi Rifu high school

Carbondioxide CO2 has been risen up to 420ppm lat 30 years(Japan Meteorological Agency).
CO2 is binding with Ca cation and forms Calcite CaCO3 in the seawater in long terrestrial history. In my teaching school, I and my students have investigated ocean saline components includes Ca cation. Ca cation is easy reminded to bind with CO3.Indeed, we confirmed the seasonal fluctuate the Ca cation in the sea water.

From 2019, we investigate CO2 quantikties from osean Oyster from seaside in my area Hamada warf, CO2 values fluctuate 45 wt.% in autumn to 55 wt.% in winter.

In my presentation, I will report the way haw to measure the CO2 quantities from the ocean biological shells and how did we make the discussion activities in the high school.

Keywords: Fixing CO2 in the ocean, Atmosphere and ocean interaction, Ca cation

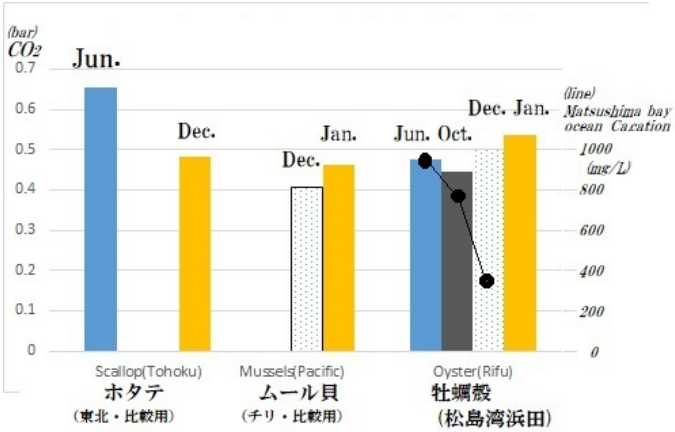

Fig.1 CO_2 degassing from shells (weight ratio)
牡蠣殻のCO_2脱ガス量季節変化と海水Ca^{2+}イオン濃度変化

Fig.2 松島湾浜田産牡蠣殻

©2020. Japan Geoscience Union. All Right Reserved.

Prediction of future soil erosion risk in Japan considering climate change

*Gen Machida[1], Kazutoshi Osawa[2], Taku Nishimura[3]

1. Graduate School of Regional Development and Creativity, Utsunomiya University, 2. School of Agriculture, Utsunomiya University, 3. School of Agriculture, Tokyo University

Approximately 70% of crop land in Japan is classified as hilly or mountainous areas, and soil erosion occurs in these lands due to heavy rains. Under such circumstances, prediction of future climate change in Japan was reported that the frequency of short-term heavy rains with daily precipitation exceeding 50mm will increase nationwide by an average of 25% at the end of this century. From this report, it is expected that soil erosion will be more severe in the whole of Japan in the future, and it is urgent task to understanding future erosion risk in crop land and to consider countermeasures. From above background, the purpose of this study is to predict future soil erosion using a process based model Water Erosion Prediction Project, WEPP, in consideration of future climate change in Japan.

The current and future weather prediction data was used from MarkSim (DSSAT weather generator), NARO (Agro-Metorological Grid Square Data), and ELPIS-jp data set (prepared National Agriculture and Food Research Organization). These data sets include spatially downscaled daily precipitation, temperature, and solar radiation from GCM output. As a tentative result, for data of MarkSim and NARO, future daily precipitation decreased. This trend does not match the original GCM output due to insufficient spatial resolution and time intervals of the dataset. Therefore, it is suggested that the MarkSim and NARO may not represent the future increase of heavy rain in Japan. On the other hand, for data of ELPIS-jp, future precipitation is increasing nationwide and the number of rainy days is decreasing. It is similar trends as in GCM original output. Therefore, the ELPIS-jp is a better database comparing above two databases to represent the increasing of heavy rainfall events with climate change. For the final results, WEPP simulations using CLIGEN data created by ELPIS-jp are to be executed. The results will be used to identify rainfall factors related to changes in erosion amount and areas requiring countermeasures.

Keywords: WEPP Model, MarkSim, NARO, ELPIS-jp, Global warming

©2020. Japan Geoscience Union. All Right Reserved.

[J] Poster | H (Human Geosciences)：H-GG Geography

[H-GG01] Use, change, management of natural resources and environment: Interdisciplinary perspectives

convener:Toru Sasaki(Miyagi University of Education), Gen Ueda(Graduate School of Social Sciences, Hitotsubashi University), Takahisa Furuichi(Miyagi University of Education), Yoshinori OTSUKI(Institute of Geography, Graduate School of Science, Tohoku University)

(Language of the session is Japanese and English with no priority.) In this session, the situation and history of use, changes and management of natural resources and environment from various regions under diverse socio-economic and natural conditions are reported. Findings from local-scale fieldwork and feedbacks on their methodology and/or research concepts are particularly encouraged to be shared and discussed. A variety of research topics are covered through both human-ecological and earth-scientific perspectives, including local knowledge of natural resources and environment, environmental and climatic history, environmental geography, environmental degradation through resource use and/or management, effects of climate change, related socio-economic changes and adaptation for livelihood security, political ecology, and issues for overcoming gaps in linking between local and broader-scale (national, regional and global) studies.

[HGG01-P01] Climatological study of the wind hole in Shodoshima Island

*Masaki HORIUCHI[1], Takako YAMAGUCHI[2] (1.Hosei University, Graduate School of Humanities, 2.Hosei University)

[HGG01-P02] Evaluation of geoheritage for protection

*Kuniyasu Mokudai[1] (1.Tohoku Gakuin University)

[HGG01-P03] Vegetation changes in under semi-arid climate, central Kenya, using opal phytolith analysis

*Asaka Konno[1], Yoshinori OTSUKI[2] (1.Tokoha University, 2.Tohoku University)

[HGG01-P04] Sand harvesting in soil-eroded area under semi-arid climate, central Kenya

*Yoshinori OTSUKI[1], Matheaus Kioko KAUTI[2], Asaka KONNO[3], Miharu TANAKA[4] (1.Institute of Geography, Graduate School of Science, Tohoku University, 2.Southeast Kenya University, 3.Tokoha University, 4.Kanto Regional Development Bureau, Ministry of Land, Infrastructure, Transport and Tourism)

[HGG01-P05] Exploring the Spatial-temporal Coupling Pattern of Grain Yield and Fertilization from Historical Practice for Better Future Application: A Case in the North China Plain

Wenjia Yu[2], *Yaojie Yue[1,2] (1.Key Laboratory of Environmental Change and Natural Disaster of Ministry of Education of China, 2.Faculty of Geographical Science, Beijing Normal University, China)

[HGG01-P06] Land use patterns optimization research under climate change adaptation and mitigation strategies—A case study in China

*Ying Xu[1] (1.Shandong Jiaotong University)

[HGG01-P07] A STUDY ON SAND INDUSTRY IN THE MU US SAND LAND

*Yue Wang[1], Xuemin Liu[1], Shushan Du[1], Ruiyin Dou[1] (1.Beijing Normal University)

Climatological study of the wind hole in Shodoshima Island

*Masaki HORIUCHI[1], Takako YAMAGUCHI[2]

1. Hosei University, Graduate School of Humanities, 2. Hosei University

1.Introduction
A windhole is a place where cold wind blows out of a mountain slope in summer and such a phenomenon (Shimizu et al., 2015).
An example of application in Japan is the storage of silkworm species. Overseas, in Europe, such as the Swiss and Northern Alps, the use of milk in a refrigerated hut can be seen (Sato, 2008).
In recent years, due to growing interest in natural energy, the value of windhole as a natural cold source has been re-recognized, and many windhole have become cool spots for sightseeing and tours. In some areas, practical refrigerators are used to store seedlings, vegetables, pickles, fruits, etc., and demand is increasing.
It is indispensable to clarify the nature of such windholes, and many studies have been conducted over the fields of climate, topography, geology, and vegetation since the Meiji era. In Tanaka et al. (2004), convection caused by the relatively low temperature inside the talus in summer compared to the outside air caused cool air to blow out from the lower windhole, and the inside of the talus was relatively hot in winter. This reveals that warm air blows out from the upper windhole. In this paper, the windhole that blow cold air in summer are called “cold windhole”, and the windhole that blow hot air in winter are called “warm windhole”.
Many examples of such air hole research have been reported in cold regions such as the Tohoku-Hokkaido region and high altitude regions. However, the temperature rarely drops below 0 ˚C, and warm regions where ice does not form inside the windhole. Although there are Hagi (Mori and Sone, 2009) and Kozushima (Suzuki, 2019), there are not many research cases.
In the future, it is considered that the thermal environment of the ground surface will be affected by the rise in temperature due to global warming (Bogdan et al., 2012), and the thermal environment of the windhole may change in the same way. Therefore, conducting a survey in a warm region at the present time is considered important in considering the effects of global warming on the flora and fauna and flora inhabiting the flora.

2.Method
In this study, a windhole (100m above sea level) located on Shodoshima, Kagawa Prefecture, facing the Seto Inland Sea and having a mild climate. A thermometer (TandD: RTR-502, measured at 10-minute intervals) was installed at the windhole and the surrounding area, and the long-term temperature fluctuation was recorded.
A hot-wire anemometer (CUSTOM: WS-03SD) was installed in the windhole from August to November to observe daily changes in wind speed.

3.Result
From the start of the observation (June 8, 2019) to the beginning of October, the temperature of the cold windhole was around 11-14 ˚C, and gradually increased while keeping the temperature lower than the outside temperature. In addition, a temporary rise in the temperature of the cold windhole was observed during a mass precipitation event. This is probably because warm rainwater flowed into the cold windhole, causing the temperature inside to rise temporarily.
Comparing the cold windhole temperature between 11:00 on June 9 (11.3 ˚C) and 11:00 on October

©2020. Japan Geoscience Union. All Right Reserved.

1(14.1 ˚C), the effect of precipitation and outside air intrusion was small and it seems that cold wind was blowing stably. The temperature difference was 2.8 ℃, and the temperature rise rate of the cold windhole during this period was 0.025 ℃ day^{-1}.
According to the wind speed observation results, a relatively good correlation was found between the cold windhole wind speed and the temperature difference inside and outside the cold windhole, and it was found that the wind speed increased as the temperature difference increased. This supports the mechanism (Takahashi et al., 1991) that the wind in the windhole is caused by the density difference between the outside air and the air inside the windhole.
Later, from mid-October, the number of days when the difference between the cold windhole air temperature and the outside air temperature became small at night increased, and in early November, the nighttime temperature difference almost every day became very small. During the winter, the heat stored in the talus in the summer creates an upward air current inside the turf, and the wind blown out of the cool windhole turns into a suction in the summer. Synchronization is considered to capture this suction phenomenon. In addition, in the survey conducted in December, the wind direction of the windhole was actually replaced by suction, which proved that the air temperature was synchronized with the outside temperature.
In addition, the hot windhole was discovered by measuring the surrounding ground surface temperature with a radiation thermometer in winter (December 27, 2019), and observation was started.

Keywords: Windhole, Warm region, air circulation, Observation

©2020. Japan Geoscience Union. All Right Reserved.

Evaluation of geoheritage for protection

*Kuniyasu Mokudai[1]

1. Tohoku Gakuin University

In biology, many attempts have been made to evaluate the rarity or representativeness of biological species and to examine indicators to protect species. On the other hand, in geology and geomorphology, such evaluations are not sufficiently performed. In recent years, geopark activities in Japan have been examining evaluation items for the protection of local geoheritage. There are uniqueness, prominence, representativeness, typicality, vulnerability and scarcity and so on.

Keywords: geosite, natural conservation, inventory

©2020. Japan Geoscience Union. All Right Reserved.

Vegetation changes in under semi-arid climate, central Kenya, using opal phytolith analysis

*Asaka Konno[1], Yoshinori OTSUKI[2]

1. Tokoha University, 2. Tohoku University

We aim at clarifying vegetation changes using opal phytolith analysis in Il Polei, Laikipia County, Rift Valley Province, Kenya. The gully erosion has extended in this region and the present vegetation is scattered. Trees mainly consist of *Acacia* spp., whereas herbs consist *Opuntia* spp. and *Sansevieria* spp..
The deposits from surface to approximatry 2 meters underground are analyzed at 10 or 20 cm interval. The amount of opal phytolith which represents to vegetation coverage is vastly different characteristics in each depth, the amount of opal phytolith at the middle part is about 6 times as much as the one of the upper and lower parts. The 14C age of the humic soil in of the middle part of the deposits is modern (IAAA-191131). However, as the age of humic soil at 3 meters underground investigated in adjacent this study sites indicates 1,600 years ago (Otsuki et al., 2016), this vegetation history is estimated to exhibit the term before 2,000 at least. Thus, the coverage of vegetation in this region considerably decreased in present. We will show the specific details of vegetation history and discuss the possibility that people's natural resource contributed the vegetation changes.

Keywords: Kenya, Vegetation change, Opal phytolith analysis

©2020. Japan Geoscience Union. All Right Reserved.

Sand harvesting in soil-eroded area under semi-arid climate, central Kenya

*Yoshinori OTSUKI[1], Matheaus Kioko KAUTI[2], Asaka KONNO[3], Miharu TANAKA[4]

1. Institute of Geography, Graduate School of Science, Tohoku University, 2. Southeast Kenya University, 3. Tokoha University, 4. Kanto Regional Development Bureau, Ministry of Land, Infrastructure, Transport and Tourism

The objectives of our presentation are to show geomorphological and environmental geographical conditions, and to clarify people’ s sand harvesting in the semi-arid pastoral area, Laikipia North sub-county. The investigated area, the Il Polei sub-location (N 0˚21'56", E 37˚04'32"), has an altitude of 1,750 to 1,850 m. According to previous literatures, a mean annual rainfall at the Mukogodo Station, close to the study area, is 362 and/or 371 mm; tree coverage is extremely low, which comprises sparse woods and shrub consisting mainly of Acacia genus. The area is underlain by Proterozoic gneiss, migmatite, quartzite, and schist, belonging to the Mozambique Belt, and inselberg-pediment systems are regionally identifiable with widespread distribution of pediplain.
Below piedmont angle of the system, near the central settlement, 1.5- to 2-km long gullies exist on the pediment. According to our topographic measurements since March 2015, the maximum retreat rates range from 1.1 to 25.6 m/yr. Sheet erosion extensively predominates in the whole area, in relation to the gullying. Recently, harmful pioneering plants, that is, *Opuntia* spp. and *Ipomoea* spp., etc., are allegedly invading the region.
In this area, local people manage sand harvesting for the construction demand in urban areas, while building cooperated society on the basis of group ranches. We will also show maintaining processes of the management, and quantitative trend of mining, under the above-stated environmental geographical condition in the presentation.

Keywords: sand harvest, soil erosion, gully, semi-arid, Kenya, environmental geography

©2020. Japan Geoscience Union. All Right Reserved.

Exploring the Spatial-temporal Coupling Pattern of Grain Yield and Fertilization from Historical Practice for Better Future Application: A Case in the North China Plain

Wenjia Yu[2], *Yaojie Yue[1,2]

1. Key Laboratory of Environmental Change and Natural Disaster of Ministry of Education of China, 2. Faculty of Geographical Science, Beijing Normal University, China

Fertilization, especially the application of chemical fertilizer, is one of the important measures to promote grain yield. However, the increasing input of chemical fertilizer has led to a variety of pollutions, such as soil pollution and water pollution, which has a serious negative impact on the ecological environment. Therefore, the scientific application of chemical fertilizer plays a vital role in both increasing grain yield and maintaining the ecological environment. This brings an urgent scientific problem, that is, how to find the clue of rational fertilization from the coupling pattern between fertilization and grain yield to guide the future fertilization strategy. However, previous studies rarely focus on the spatial-temporal coupling pattern of grain yield and fertilization from the perspective of large-scale and long-term. In other words, how to find the spatial-temporal coupling pattern between grain yield and fertilization on the large-scale and long-term, so as to provide scientific support for rational and effective fertilization, the relevant research is still lacking. In this study, an analytical method for analyzing the spatial-temporal coupling pattern of grain yield-fertilization based on large-area, long-term serial grain yield, and fertilization data were constructed. Taking the North China Plain as an example, the spatial-temporal coupling pattern, regional differentiation rule and dynamic evolution trend of grain yield and fertilization during 1990-2015 were revealed by using this method. The results show that: (1) the overall grain production in the North China Plain maintained a steady growth trend, while the fertilization intensity increased and then decreased. The coupling pattern between them showed characteristics of non-stationarity in time and space. At the same time, with the increased fertilizer application, its contribution to the increase of grain yield decreased. (2) Different types of food crops responded differently to different types of chemical fertilizers. Among them, the effect of nitrogen fertilizer on increasing yield of rice and wheat was far greater than that of phosphate fertilizer and potassium fertilizer. Since 2010, the effect of fertilization intensity on maize yield has become more and more clearly coupled in time and space, but not before. (3) The effect of the double fertilizers on grain yield was better than a single fertilizer. It is suggested that in the future, it is necessary to comprehensively consider fertilization strategies such as improving the utilization rate of chemical fertilizer, applying fertilizer according to local conditions and applying multiple fertilizers together, so as to achieve better yield increasing effect.

Keywords: grain yield and fertilization, spatial-temporal coupling pattern, geographically weighted regression, geographic detector, the North China Plain

©2020. Japan Geoscience Union. All Right Reserved.

Land use patterns optimization research under climate change adaptation and mitigation strategies—A case study in China

*Ying Xu[1]

1. Shandong Jiaotong University

Land use and land cover change is a main driving force of regional and global climate change, there is growing attraction about the climate change adaptation and mitigation strategies in land use and management. Yet the mitigation and adaptation strategies are handled separately at different dimension and spatial level. In this paper, we present a land use optimization model that integrated climate change adaptation and mitigation, then the model was applied to a case study at regional level—Huailai country whose environmental and socioeconomic conditions are sensitive to climate change. The regional land use optimization model is composited by Linear Programming Model and Cellular Automata Model, which incorporated the climate change adaptation and mitigation constraints of land use, include ecological water demand, spatial suitability and carbon sequestration. The model optimization result show that most region of study area could adapt and mitigate to climate change with constant land use pattern, and the land use conversion region under different climate change scenarios are mainly located in the topography transition region. In addition, model results also reveal the tradeoff relationships between climate change adaptation and mitigation, manifested as increase in carbon sequestration and ecological water demand are accompanied by decrease in net income of agricultural production. It is necessary to incorporated climate change adaptation and mitigation simultaneous into land use optimization and management, and the model proposed in this paper provide a feasible method to incorporate them and balance the tradeoff of them in land use pattern optimization at regional scale.

Keywords: Regional land use optimization model, Climate change adaptation and mitigation, Land use optimization and management, rural mountain–basin watershed

©2020. Japan Geoscience Union. All Right Reserved.

A STUDY ON SAND INDUSTRY IN THE MU US SAND LAND

*Yue Wang[1], Xuemin Liu[1], Shushan Du[1], Ruiyin Dou[1]

1. Beijing Normal University

Desert is an important part of the ecosystem, but desertification can harm the environment productivity and human health; thus, desertification control is extremely necessary. Traditional desertification control projects such as afforestation and grass square plantation can hardly cooperate with resource exploitation, economic development and prosperity growth, so they are difficult to develop sustainably. Hence, it has both practical significance and theoretical value to analyze a whole new desertification control method which can combine ecological construction, industrial development and living standard improvement together.

The Mu Us Sand Land is located in the north part of China, and which is a typical sand land formed because of unreasonable production methods and life style. Therefore, we studied the sand industry development in the Mu Us Sand Land to find a general industrialized ecological management method, which can scientifically guide sustainable desertification control in arid region. In this paper, we analyzed water resources carrying capacity, companies, industrial chains, industry classification, production value, and industrial benefits of sand industry in the Mu Us Sand Land. According to these empirical and quantitative studies, we built a basic development pattern of sand industry.

The main conclusions of this paper are as follows: Water resources shortage is the key reason as well as crucial constraint of sand industry development. It is significant to build proper industrial chains to promote sand industry development. Sand industry should combine economic benefits, ecological benefits, and social benefits together with emphasis on the social ones. The basic pattern of sand industry development is to build a complete industry system under resources constraints, and eventually maximize the benefits output. In order to solve the issues of sand industry development, governments and companies should increase R&D investment, build mixed industrial chains, internalize positive externality, establish a new type of consumer market, and develop desert tourism.

Keywords: Desertification control, Sand industry, The Mu Us sand land, industrial benefits

©2020. Japan Geoscience Union. All Right Reserved.

[J] Poster | H (Human Geosciences)：H-GM Geomorphology

[H-GM03] Geomorphology

convener:Tsuyoshi Hattanji(Faculty of Life and Environmental Sciences, University of Tsukuba), Masayuki Seto(Fukushima Future Center for Regional Revitalization, Fukushima University)

The main subject of this session is the whole range of themes relating to geomorphology, especially geomorphic processes, landform development and its relation to environmental changes, geomorphological hazards and their mitigation and reports of recent events of disaster occurred in Japan, various kind of hazard maps, relationships among geomorphic processes, other natural phenomena and human activities, and various techniques of geomorphological measurements and automatic landform classification. Japanese can be used in this session.

[HGM03-P03] Chemical and physical weathering processes of hydrothermally-altered sandstone: changes of hydraulic and mechanical properties

*Miho Kikuchi[1], Yuki Matsushi[1] (1.Disaster Prevention Research Institute, Kyoto University)

[HGM03-P04] Behavior of the sediments and detritus transported by floodwater on the embanked riverside land and its depositional record in the lower reaches of the Natori River

*Hiroshi Shimazu[1], Takako UTSUGAWA[1] (1.Department of Geography, Faculty of Geo-Environmental Science, Rissho University)

[HGM03-P05] Channel migration in the middle Tama River, central Japan, affected by Typhoon 1919 estimated from the sedimentological characteristics

*Takako UTSUGAWA[1], Masaaki Shirai[2] (1.Department of Geography, Faculty of Geo-Environmental Sciences, Rissho University, 2.Department of Geography, Tokyo Metropolitan University)

[HGM03-P06] Elevation change in a river park flooded by the typhoon Hagibis in 2019

*Keisuke Taniguchi[1], Hirotsugu Arai[1], Hirofumi Yoshita[1], Kazuki Fujita[1], Takuhei Yamasaki[1], Akihiro Maekawa[1], Noritaka Endo[2] (1.Centre for Environmental Creation Fukushima Prefecture, 2.Kanazawa University)

[HGM03-P07] Terrain analysis of terrace spread in Shinano River basin, Niigata Prefecture using detailed DEM data

*Toshifumi Koseki[1], Mamoru Koarai[2] (1.Graduate school of Science and Technology, Ibaraki University, 2.earth science course, college of sciense, Ibaraki University)

[HGM03-P08] Distribution map of subsurface Late Pleistocene fluvial terraces in the lower Sagami Plain, central Japan

*Yoshiki Sato[1], Sumiko KUBO[2] (1.Geological Survey of Japan, Advanced Industrial Science and Technology, 2.School of Education, Waseda University)

[HGM03-P09] **GPR survey for estimating the internal structure of the beach levee formed in the coastal lowland of Enshunada Sea**

*Takayuki Nakano[1], Nobuhisa Matsuta[2], Kazuaki Hori[3], Daisuke Hirouchi[4], Nobuhiko Sugito[5], Yoshiki Sato[6], Tatsuya Ishiyama[7] (1.GSI of Japan, 2.Okayama Univ., 3.Nagoya Univ., 4.Shinshu Univ., 5.Hosei Univ., 6.AIST, 7.ERI, Univ. of Tokyo)

[HGM03-P10] Geomorphic analysis of the active fault in volcanic area based on GIS

*Daisaku Kawabata[1], Haruo Kimura[2], Yasuhira Aoyagi[2] (1.Institute of Geology and Geoinformation, Geological Survey of Japan, AIST, 2.Central Research Institute of Electric Power Industry)

[HGM03-P11] Acquisition of detailed topographic data for active volcano using UAV LiDAR

*Takayama Toko[1], Takayuki Hashimoto[1], Naijia Zhang[1], Yuto Nomura[1] (1.Asia Air Survey Co.,Ltd.)

[HGM03-P12] Effect of past human activities on the 2009 shallow landslide hazard in the Houfu District, western Japan

*Hiromu Daimaru[1] (1.Forestry and Forest Products Research Institute)

Chemical and physical weathering processes of hydrothermally-altered sandstone: changes of hydraulic and mechanical properties

*Miho Kikuchi[1], Yuki Matsushi[1]

1. Disaster Prevention Research Institute, Kyoto University

This study reveals chemical and physical weathering processes and weathering profile of sandstone (graywacke) in accretionary complex affected weakly by hydrothermal alteration. Network of white veins that consist mainly of calcite and laumontite influences the weathering mechanisms leading to changes of hydraulic and mechanical properties of the rock. Our study site is located in Uwajima, Ehime Prefecture in Shikoku, SW Japan. This area is underlain by alternating beds of sandstone and mudstone called Hokezu land block, in the Cretaceous Shimanto group. Many shallow soil slips (< 1 m deep) and bedrock landslides (< 10 m deep) occurred in July, 2018, by heavy rainfall with maximum hourly intensity of 36 mm/h, and total rainfall of 540 mm/4 days. In this area, we conducted geological survey for weathering grade of bedrock, and measured rock strength by using a Schmidt hammer. We obtained a 25 m-long boring core at a selected typical hillslope with a 6 m-deep bedrock landslide to investigate subsurface weathering profile. The bedrock is characterized by well-developed meshes of white veins formed by hydrothermal alteration, consisting of calcite and laumontite. We categorized the weathering grade of the bedrock to the following seven stages: 0) fresh rock; 1) pore formation within the vein; 2) oxidation along joints; 3) color changing into whole rock block; 4) open fracturing; 5) soft saprolite with closed fractures; and 6) soil. Rock strength are drastically decreased at the stage 4. We found that calcite vanished at stage 1. The interacting chemical and physical weathering and strength reduction may have promoted through calcite dissolution at the initial stage of weathering as well as the subsequent expansion and shrinking of laumontite via wet and dry cycles, resulting in the formation and connection of open fractures. The hypothesis of weathering mechanisms and changes of hydraulic properties of bedrock will be tested by lab experiments and hydrological monitoring in hillslopes.

Keywords: chemical weathering, physical weathering, graywacke, hydrothermal alteration, bedrock landslide, rainfall disaster

©2020. Japan Geoscience Union. All Right Reserved.

Behavior of the sediments and detritus transported by floodwater on the embanked riverside land and its depositional record in the lower reaches of the Natori River

*Hiroshi Shimazu[1], Takako UTSUGAWA[1]

1. Department of Geography, Faculty of Geo-Environmental Science, Rissho University

The Natori River flows down in the Sendai Plain. After World War II the lower reaches of the Natori River the floodplain was divided into the riverside land and the habitable floodplain by construction of the continuous embankments. After that as the high water channel of the riverside land was used for private farmland without artificial landform change, the original micro-landform and small forests have been preserved. The high water channel is inundated with various detritus during the flood stage. Some of that was deposited on the high water channel. The flood stage caused by the Typhoon 1919 in 2019 was above about 2m on the surface of the farmland. Although the surface of some farmlands was eroded, fine sediments were deposited on the surface of the most farmlands. The large amount of detritus was caught on the upper side of the small forest. The forest played screening effects as well as flood control forest. The cliffs between the high water channel and river channel were partially eroded by the flood, so that the sand and gravel layers mainly constituting the high water channel were exposed. Based on the observation of characteristics of their sediments, some man-made materials in the layers, vegetation on the high water channel around the outcrops and the root distributions of the trees and grass in the layers, the subsurface sedimentological structure of high water channel and history of sedimentation were examined.

Keywords: embanked floodplain, flooding, deposition, micro-landform, Natori River, Sendai Plain

©2020. Japan Geoscience Union. All Right Reserved.

Channel migration in the middle Tama River, central Japan, affected by Typhoon 1919 estimated from the sedimentological characteristics

*Takako UTSUGAWA[1], Masaaki Shirai[2]

1. Department of Geography, Faculty of Geo-Environmental Sciences, Rissho University, 2. Department of Geography, Tokyo Metropolitan University

The channel migration process in the middle Tama River, central Japan, affected to the Typhoon 1919 occurred on October 12, 2019 was revealed from the observed sedimentological features. The reformation of gravel bar in river accompanying with the changing river channel due to swelling torrent affected by a storm such as a typhoon is well known. While the regional and consecutive report is indispensable as Sakamoto (2015) and Shimazu (2018, 2019).

The Tama River originates in Mt. Kasatoriyama (1,953 m a.s.l.) in the Kanto mountainous region, central Japan, flows into the Kanto Plain at Ome City, Tokyo Metropolis, and runs along the southwestern side of Musashino Upland to Tokyo Bay. This river is a meandering river having alternating bars from the upstream reaches. We researched the location of bars utilizing GPS survey to compare the topography before the swollen and the gravel size distribution on several bars from Ome to Tachikawa Cities, Tokyo Metropolis (18 km in long) in the middle Tama River. Characteristic bedforms on gravel bar, imbrication of gravels, and partially the aerial photography provided by Geospatial Information Authority of Japan are useful to discuss the channel migration process in the swollen occurred on October 12, 2019. The basement of the Tama River, Kazusa Group (ca. 2.5-1.6 Ma) mainly composed of mudstone was exposed especially in downstream of the surveyed area, and deeply eroded in the direction across the usual stream. This direction of erosion and the scour observed on the surface of basement were also helpful to discuss. Many sands to boulders transported as swept away the vegetation usually formed many bedforms having obviously imbrication on the water high level zone in the Tama River. At the 2.2 km downstream site from an intake weir, a conspicuous quantity of boulders probably deposited on the bottom of river may have redeposited on the surface of bars by the swollen. And the gravel bars around the trees (3 to 5 m in high) grew on the water high level zone as well as the bridge pies were significantly scoured by the swollen.

References

Sakamoto, T. 2015. Abstract of annual meeting of the Geological Society of Japan. 492.
Shimazu, H. 2018. Abstract of JpGU 2018: HGM03-O7.
Shimazu, H. 2019. Abstract of JpGU 2019: MIS20-O6.

Keywords: channel migration, chute flow, imbrication, gravel, Typhoon 1919, the Tama River

©2020. Japan Geoscience Union. All Right Reserved.

Elevation change in a river park flooded by the typhoon Hagibis in 2019

*Keisuke Taniguchi[1], Hirotsugu Arai[1], Hirofumi Yoshita[1], Kazuki Fujita[1], Takuhei Yamasaki[1], Akihiro Maekawa[1], Noritaka Endo[2]

1. Centre for Environmental Creation Fukushima Prefecture, 2. Kanazawa University

The typhoon Hagibis, which landed in Japan in October 2019, caused severe damage in a wide area of eastern Japan, including Fukushima Prefecture. In the Niida River basin, which drains into the coastal area of Fukushima Prefecture, heavy rains of over 300 mm were observed between Oct. 11 and 12. As a result, a river park near the confluence of the Niida River and its tributary, the Kitagawa River, was severely damaged by large-scale erosion and sedimentation. In this study, we aimed to evaluate the elevation change due to the flood event based on the detailed DSM obtained by photogrammetry using UAV.
Five hundred and eighty three photo images were obtained with a UAV (Phantom 4 ver.2, DJI) flying at a height of 50 m on November 28, 2019. In addition, the latitude & longitude and the altitude of eleven ground-control-points (GCPs) were measured with a differential GPS receiver (GIR1600, Sokkia) and an auto level (AP-8, Nikon), respectively. Using the above data, a 50 cm-digital surface model (DSM) was created with a MfS software, Agisoft photoscan 1.4.5.
Five survey lines were set in the observation area, and comparison was conducted between the cross sections of the 50 cm-DSM obtained in the present study and a 1 m-digital elevation model (DEM) based on the laser survey performed by Geographical Survey Institute in 2012. At the left bank of the Niida River, the edge of the river park was greatly eroded up to 26 m horizontally, while new gravels were deposited near the right bank.

Keywords: River, Typhoon Hagibis, UAV

©2020. Japan Geoscience Union. All Right Reserved.

Terrain analysis of terrace spread in Shinano River basin, Niigata Prefecture using detailed DEM data

*Toshifumi Koseki[1], Mamoru Koarai[2]

1. Graduate school of Science and Technology, Ibaraki University, 2. earth science course, college of sciense, Ibaraki University

The Shinano River basin in Niigata Prefecture has long been known as an active folding area. It is said that the river terrace along the watershed has an abnormal slope on the upstream and mountain sides. In the Chuetsu earthquake in 2004, an uplift of about 1 m was reported near the Higashiyama Anticline. In these backgrounds,geomorphological, geological and geodetic studies have been conducted in this area.

In this study, landform classification was performed on the terrace near the confluence of Shinano River and Uono River. While, topographic analysis was performed to visualize characteristic terrain surfaces and to consider landform evolution using 1m grid DEM by Lidar data which provided by Geospatial Information Authority of Japan (measurement period: May 2005) was used. In addition, DEM difference between two periods was calculated and the value was calculated as the amount of erosion in 6 years. (another measurement time: November 2011)

As the result of aerial photograph interpretation, field surveys, and reference of preceding studies, river terraces in this area was divided into 15 terraces consisting of M1 to M4 and L1 to L11 terrace in total. In the topographic analysis, a micro topographic map was created using Arc GIS with reference to Toda (2014), and a water network map and watershed map were created using hydrological analysis tools.

The calculated erosion amount clearly shows the erosion on the attack slope side and the accumulation on sand bars. As the result of overlay between erosion map and geological map by GIS. erosion sites were concentrated in the Uonuma Formation near the boundary between the Uonuma Formation and the Wanazu Formation.

For field survey, it is considered that there is room for further discussion on the relationship between geology and erosion at the geological boundary and the amount of uplift by crustal deformation. For topographical analysis, we plan to create maps using tools other than hydrological analysis, and to consider landform evolution.

Keywords: Terrain analysis, Lidar data, Shinano River, River terrace, Arc GIS

©2020. Japan Geoscience Union. All Right Reserved.

Distribution map of subsurface Late Pleistocene fluvial terraces in the lower Sagami Plain, central Japan

*Yoshiki Sato[1], Sumiko KUBO[2]

1. Geological Survey of Japan, Advanced Industrial Science and Technology, 2. School of Education, Waseda University

The lower Sagami Plain is a fluvial plain facing Sagami Bay, central Japan, with about 15 km width and 33 km length, and bounded by the Oiso and Tama Hills and Tanzawa Mountains. In this plain, there are many Middle to Late Pleistocene fluvial terraces, Sagamihara, Nakatasuhara, Tanahara and Minahara Terraces from older to younger, which had been formed by Sagami River depending on sea level fluctuations (Oya et al., 1991; Kubo, 1997). These terraces are distributed beneath alluvial lowland toward downward from about 15 km from the present coastline. Although general distribution of them is shown by Kubo (1997), there is few quantitative analyses using bore hole logs. In this study, we attempt to show distribution of buried terraces based on the result of interpolation on bore hole logs and drilled core samples (Sato et al., 2017).

Bore hole longs were collected from local governments and government agencies. We identified alluvial base, which is not only the top of alluvium base gravel but top of volcanic loess (Kanto Loam) overlying buried terrace, and thickness of loam layer with help of grain size, N value and distribution pattern shown in cross sections. As a result, 3,890 and 2,033 elevation of bore hole logs were obtained for alluvial basement and Kanto Loam layer thickness respectively. Spatial interpolation was performed using the Kriging method on these elevation data with ArcGIS 10.3.1. Grid size of interpolation was ~140 m. Based on distribution pattern and differences in thickness of Kanto Loam layers, we demonstrated the dissected incised valley and buried terraces.

Thickness of Knato Loam layer overlying subaerial fluvial terrace surface, shown by Kubo (1997) and so on, was estimated from boring data and shown their frequency distribution. As a result, there is a significant difference in the average value between the terraces. In addition, the frequency distribution indicate that thickness of Knato Loam layer is 13–20 m for Sagami Terraces, 7.5–13 m for Nakatsuhara Terraces, 3.5–7.5 m for Tanahara Terraces, and 0–3.5 m for Minahara Terraces. We referred conveniently these values as the typical thickness of Knato Loam layer of each terrace for comparison.

Based on distribution pattern of buried flat surface of alluvium basement and thickness of loam layer, we dissected incised valley and buried terrace of Sagami River. The incised valleys are distributed along the eastern margin of the present alluvial lowland with slightly meandering. It is presumed that the paleo-Sagami River Valley joined the paleo-Kaname River Valley in southern part of the plain, and then flowed south to southeastward into the Sagami Bay. Although distribution of buried fluvial terraces is almost consistent with Kubo (1997), following two points were newly suggested; the Minahara Terraces may be distributed more widely, wave cut terraces are distributed widely along the Kaname River. Longitudinal riverbed section estimated from bore hole logs indicate that elevation of the Minahara Terrace is presumed to be about −110 m around the southern margin of the plain, which suggesting approximately the sea level during the formation period of this terrace, at least after AT tephra (29-30 ka) and before the Last Glacial Maximum (ca. 20ka) (Kubo, 1997). This suggestion is consistent with estimated value of global eustatic sea level during 20–30 ka, about −110 m (Yokoyama et al., 2018).

Reference

Kubo, S. (1997) The Quaternary Research (Daiyonki-Kenyu), 36, 147–163.

Oya, M. et al. (1991) Geomorphological Land Classification Map of the Northern Coast of the Sagami Bay,

©2020. Japan Geoscience Union. All Right Reserved.

Keihin River Office of the Ministry of Construction.
Sato, Y. et al (2017) Annual Report of Investigations on Geology and Active Faults in the Coastal Zone of Japan (FY2016), 97–110.
Yokoyama, Y. et al. (2018) Nature, 559, 603–607.

Keywords: buried terrace, Kanto Loam, geomorphological development, fluvial terrace, sea level change

©2020. Japan Geoscience Union. All Right Reserved.

GPR survey for estimating the internal structure of the beach levee formed in the coastal lowland of Enshunada Sea

*Takayuki Nakano[1], Nobuhisa Matsuta[2], Kazuaki Hori[3], Daisuke Hirouchi[4], Nobuhiko Sugito[5], Yoshiki Sato[6], Tatsuya Ishiyama[7]

1. GSI of Japan, 2. Okayama Univ., 3. Nagoya Univ., 4. Shinshu Univ., 5. Hosei Univ., 6. AIST, 7. ERI, Univ. of Tokyo

1. Introduction

Since the 2011 off the Pacific coast of Tohoku Earthquake, it has been pointed out that it is necessary to reconsider the unique seismic theory at the plate boundary, and that would require similar considerations in the case of the Nankai Trough. Therefore, we are conducting study to clarify the diversity of Nankai Trough earthquakes by reconstructing the crustal deformation during and between earthquakes from the development history of Holocene terrain in the coastal lowlands of Enshunada Sea. In order to clarify the development process of the topography of the beach levee, it is necessary to understand the internal structure of it. Therefore, we applied GPR (ground-penetrating radar) survey to beach levees, and the performance of identifying the internal structure was examined.

2. Study outline

Fig. 1 shows the survey area and GPR survey lines. GPR survey was conducted from March 26 to 27, 2019. The red lines are the survey lines. Twenty survey lines were set, and the total length was about 10,160 m. These survey lines were zoned to the six sites shown in Fig. 1. GPR survey was performed using Noggin Plus system of Sensors & Software Inc. with an antenna center frequency of 250 MHz. The data was analyzed with EKKO_Project5 software. In the analysis, basic processing (Gain recovery processing etc.) was performed.

Bristow et al. (2006), Takagawa et al. (2008), etc., show examples of GPR surveys for beach topography, and they indicated that GPR survey is effective for estimating the internal structure of the beach topography. However, our survey area in this study was basically an asphalt road in the urban area or paddy field, which means that the survey conditions were not good.

3. Result & Discussion

Representative results are reported for the Tarosuke site and the Yokosuna site.

At the Tarosuke site, on the long survey line crossing the artificial sand dunes and the interdune lowland from the beach, a clear reflection structures that descends toward the sea side were identified at 2 to 5 m underground of the seaside slope of the sand dune near the coast, the depression formed on the sand dune and the seaside margin of the low relative height sand dune. This is similar to the structure seen in the sand dune shown in Takagawa et al. (2008) and is thought to indicate the sedimentary structure of the past shoreline advance. Although Matsuta et al. (2016) argued that these sand dunes are artificial dunes, it is possible that natural sand dunes were formed on the base.

On a survey line of the Yokosuna site, a reflection structure that descends toward the sea side was identified at a 1 to 3 m underground on the seaside slope near the top of the beach levee. Also, in another survey line, a folded reflection structure that descends toward the land side was identified at a 1 to 3 m underground on the land side slope near the top of the beach levee. Although these may indicate the natural sedimentary structure at the time of the formation of the beach ridge, houses are lined up on the beach bank of this site and the depth of the reflection structure is shallow, which suggests that it may be the structure by artificial modification.

©2020. Japan Geoscience Union. All Right Reserved.

4. Challenges

There is few direct underground structure data such as boring data in the GPR survey area. In the future, we would like to conduct GPR survey even at location where boring data exists, and try to interpret the survey results more accurately.

Acknowledgements: This work was supported by JSPS KAKENHI Grand Number JP18H00765. The GPR devices used for the survey was borrowed from Prof. Yasuhiro Suzuki of Nagoya University.

References:

Bristow et al. (2006): Sedimentology, 53, 769-788; Matusta et al. (2016): 15th Academic Research Grant Report of Japan Geographic Data Center; Takagawa et al. (2008): Proceedings of Coastal Engineering, JSCE, 55, 681-685.

Keywords: beach levee, GPR survey, Enshunada Sea, Nankai Trough

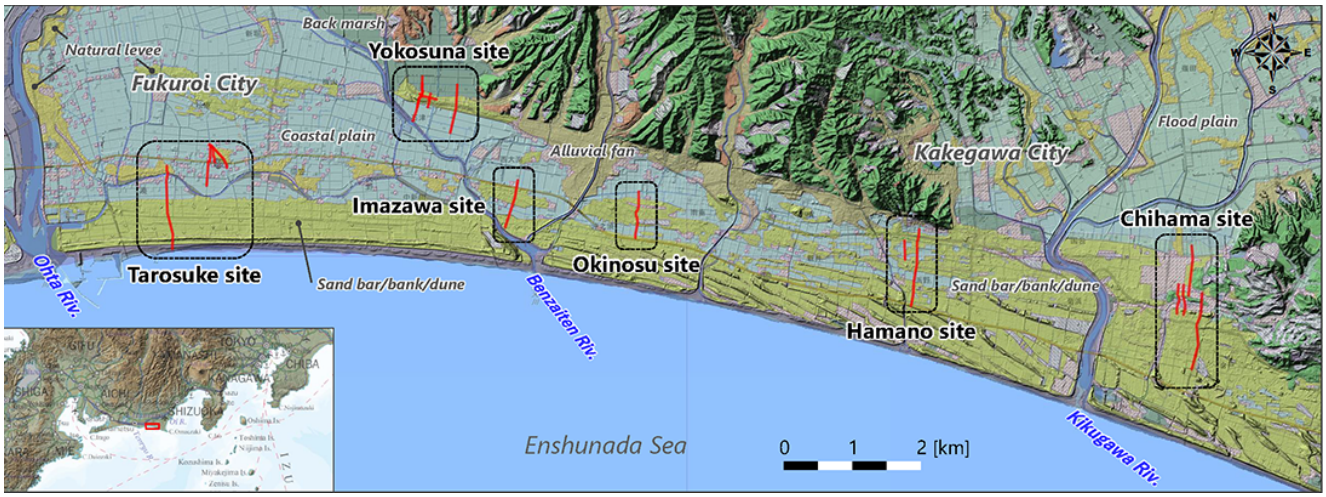

©2020. Japan Geoscience Union. All Right Reserved.

Geomorphic analysis of the active fault in volcanic area based on GIS

*Daisaku Kawabata[1], Haruo Kimura[2], Yasuhira Aoyagi[2]

1. Institute of Geology and Geoinformation, Geological Survey of Japan, AIST, 2. Central Research Institute of Electric Power Industry

The movement of active faults due to inland earthquakes often involves surface displacement. In Japan, where many active faults are distributed, fault displacements are often accumulated and effected on the current topography. However, volcanic rock areas in Japan are difficult to find evidence of fault activity accumulation in the terrain, and it is difficult to find fault traces on the surface. In this study, in order to investigate the characteristics of the river topography around the active fault, geomorphic analysis was examined using a high-precision DEM of the southern region of Iwate Prefecture based on GIS. The target area is mainly covered by Miocene to Pleistocene volcanic rocks. In this area, despite significant earthquakes occurring since 1896, there is little apparent surface displacement. This study clarified the details of the geomorphic quantity of the target area. As a result, SPI value tends to be higher in the area where surface displacement was observed in 2008.

Keywords: geomorphic analysis, GIS, active fault

©2020. Japan Geoscience Union. All Right Reserved.

Acquisition of detailed topographic data for active volcano using UAV LiDAR

*Takayama Toko[1], Takayuki Hashimoto[1], Naijia Zhang[1], Yuto Nomura[1]

1. Asia Air Survey Co.,Ltd.

In Mt. Hakone, an active volcano, volcanic landslides have occurred in the Owakudani and Sounzan areas in the past, and countermeasures have been taken. However, due to the influence of volcanic activity, it is difficult to detail survey.
Therefore, in order to provide basic data for the landslide prevention, the authors prepared floor plans, cross-sectional plans, and a ground temperature distribution map of about 0.8 km2 of Owakudani and Sounzan mountains using a laser scanner and an infrared camera equipped with a UAV (Unmanned Aerial Vehicle).
The survey was carried out from March to April, 2019, and three-dimensional point group data of 400 points/m2 were acquired by a high-density laser scanner.
As a result, it became possible to express detailed microtopography of crater and fumarole, and it was also possible to confirm the deformation and small collapse of countermeasure works such as the crack of hillside work.
Continuous measurement in the future is considered to be effective as a monitoring method.

Keywords: Unmanned Aerial Vehicle, LiDAR, Landslide, Volcano

©2020. Japan Geoscience Union. All Right Reserved.

©2020. Japan Geoscience Union. All Right Reserved.

Effect of past human activities on the 2009 shallow landslide hazard in the Houfu District, western Japan

*Hiromu Daimaru[1]

1. Forestry and Forest Products Research Institute

The heavy rainfall on 21 July 2009 has triggered numerous shallow landslides on the mountains in the Houfu District, western Japan. Effects of geographical factors on the landslide such as topography, vegetation and rainfall amount were evaluated by using machine learning algorithm (random forest and decision tree classifiers).
Vegetation height was the most important factor. Many landslides were occurred in sites with thin vegetation cover, such as young planted conifer forest and open forest accompanied by fern meadow that was believed to be induced by artificial burning.
Many shallow landslides initiated in the narrow valleys filled by granitic sand. The radiocarbon age of the valley fill deposit was Cal AD 1200 - 1600yrs, suggesting that serious erosion and sediment yield prevailed since the 13th period. Buffer zone analysis of the landslide indicates that many landslides occurred on slopes 10 - 30m apart from the past denudated hills. Distribution of soil thickness indicated that reworked material in valley head hollows produced by past human-induced erosion has played an important role in the 2009 landslides.
These evidences indicated that effects of past human activities such as burning and land degradation played important roles in the shallow landslides in this area.

Keywords: shallow landslide, land degradation, hageyama, radiocarbon age, machine learning

©2020. Japan Geoscience Union. All Right Reserved.

[J] Poster | H (Human Geosciences)：H-QR Quaternary research

[H-QR05] Natural hazard and human activity recorded in underwater geoarchaeological structure

convener:Wataru Tanikawa(Japan Agency for Marine-Earth Science and Technology, Kochi Instutute for Core Sample Research), Tokuyama Hidekazu(Center for advanced marine core research, Kochi University), Shintaro Yamasaki(Disaster Prevention Research Institute, Kyoto University)

Human-made tools and architectures on seafloors or submerged under marine sediments at coastal sites teach us not only history of human activities but records of natural disasters which associate with human activities. For instance, tsunami, caused by 1498 Meio earthquake and sector collapse of Mt. Bandai in Japan (1888) caused submergence of villages in sub-lacustrine (Lake Hamanako and Lake Hibara). Volcanic eruption of Mt. Fugen (known as Shimabara Taihen) changed underwater topographic features at a coastal site. Therefore, underwater archaeological subjects may record historical natural disasters and inform their scale and characters However, underwater archaeological study in Japan considerably falls behind the other countries. For instance, Japanese government officially marks about 300 underwater remains, whereas more than 36000 sites are identified as underwater remains in UK. Underwater geoarchaeological study has difficulties for accessibility, high cost, and limitation of analytical method and tools. On the contrary, submerged material are sometimes less weathered, and less artificial modification. Therefore, we may obtain very pure data. Recently, innovative underwater techniques and tools are developing, though, they are not enough applied to underwater geoarchaeological studies. Therefore, this session provides an opportunity to meet the various communities between earth science, archaeology, and geoengineering to discuss current problems and future scopes in underwater disaster geoarchaeology.

[HQR05-P01] Underwater geoarchaeological research at the coastal area of Kochi prefecture to reveal the traditional tale of “Kurodagori”

*Wataru Tanikawa[1], Tokuyama Hidekazu[2], Yuhji Yamamoto[2], Masafumi MURAYAMA[2], Kouki Tanaka[2], Akira Ijiri[1], Tatsuhiko Hoshino[1] (1.Japan Agency for Marine-Earth Science and Technology, Kochi Instutute for Core Sample Research, 2.Kochi University)

[HQR05-P02] Characteristics and its significance of marine cores collected from inner Uranouchi Bay, Kochi Prefecture

*Masafumi MURAYAMA[1], Wataru Tanikawa[2], Akira Ijiri[2], Tatsuhiko Hoshino[2], Takehiro Hirose[2], Toshiya Fujiwara[2], Kazuya Kitada[2], Kastuya Nejigaki[3], Tokuyama Hidekazu[4], Go-Ichiro Uramoto[4], Kazuno Arai[4], Kondo Yasuo[3], Yuhji Yamamoto[4], Research Member Kurodagoori[4] (1.Faculty of Agriculture and Marine Science, Kochi University, 2.JAMSTEC, 3.Graduate School of Integrated Arts and Sciences, Kochi University, 4.Center for Advanced Marine Core Research, Kochi University)

[HQR05-P03] A case study on 3D measurement of underwater structure by using digital image data taken with a digital camera

*Akira Ijiri[1], Wataru Tanikawa[1], Masafumi MURAYAMA[2], Tokuyama Hidekazu[2] (1.Japan Agency for Marine-Earth Science and Technology, 2.Kochi University)

[HQR05-P04] Environmental change over the past 2000 years in Lake Kawahara and Ryuuoo in southern Japan

*Cho Ara[1], Kota Katsuki[2], Jonathan D Woodruff[3], Kaoru Kashima[1], Hannah Elizabeth Baranes[3], Caroline Ladlow[3] (1.Kyushu University, 2.Shimane University, 3.University of Massachusetts)

[HQR05-P05] Application of Boxfish ROV and Boxfish 360 camera to Underwater Archaeological Survey

*Yuka Masaki[1], Hideki Sezoko[2], Masayuki Nagayama[3], Wataru Tanikawa[4], Yuhji Yamamoto[5], Shinichiro Ito[1] (1.COSMOS SHOJI Co., Ltd., 2.Nippon Marine Enterprises, Ltd., 3.360 Planet, 4.Japan Agency for Marine-Earth Science and Technology, 5.Kochi University)

Underwater geoarchaeological research at the coastal area of Kochi prefecture to reveal the traditional tale of “Kurodagori”

*Wataru Tanikawa[1], Tokuyama Hidekazu[2], Yuhji Yamamoto[2], Masafumi MURAYAMA[2], Kouki Tanaka[2], Akira Ijiri[1], Tatsuhiko Hoshino[1]

1. Japan Agency for Marine-Earth Science and Technology, Kochi Instutute for Core Sample Research, 2. Kochi University

Historical records and oral traditions mention submerged villages and buildings due to great natural disasters along the coast in Japan. For instance, 1498 Meio Tokai Earthquake induced the submergence of local villages at southern area of Lake Hamanako, 1585 earthquake caused a subsidence of villages at West Nagahama, and 1888 volcanic eruption of Mt. Bandai submerged a local village into a lake. A traditional tale about a village named Kuroda-gori, which was probably submerged during the Hakuho Nankai earthquake of 684 CE has been passed down orally. To reveal the tales of Kurodagori, academic and private researches had been carried out at multiple sites along the coast of Kochi Prefecture. However, the previous research did not record the results and data clearly, therefore it is difficult to understand what they discovered about Kurodagori.
Therefore, Kochi University and JAMSTEC launched the new project to reveal the mystery of Kurodagori from 2013. The project performed underwater survey at 6 sites along the coast of Kochi Prefecture (Tochi, Nomi-bay, Urano-uchi bay, Okitsu, Tsumajiro, and Kashiwajima). Unfortunately, we did not find any evidence of Kurodagori at all 6 sites until now. On the other hand, the project treats underwater artifacts as potential records of natural disasters, therefore this project may contribute on the understanding of historical natural disasters at Kochi prefecture. A summary of the project and detail of the preliminary results at three sites (Nimi-bay, Tsumajiro, and Kashiwajima) are introduced in this presentation.
Heshima remains (Yayoi period: 300 BC to 300 AD) are found at Heshima Island located at southern parts of Nomi bay, and there are many local witnesses of a drinking well at the seafloor near Heshima Island. Therefore, Nomi-bay has been thought as the most promising candidate site of Kurodagori. Our research discovered the very flat abrasion platform that has 200 m width. Therefore, we may estimate the history of co-seismic subsidence at this area by dating of the platform.
Nearly 30 stone pillars, that appear artifacts, were observed on seafloor at Tsumajiro beach, Tosashimizu city. Our study discovered that the pillars were used as stone works (stone step and building stone foundation) at local village nearby the coast. Moreover, historical earthquake tsunami wave and water flood by high tides contributed on the transport of the pillars from inland to seabed.
A 200 m long stone wall, that is composed of boulders and matrix and appears as a stone bank, are observed at the northern coastal site of Kashiwajima at Hata county. The underwater wall is located along the coastal line that is parallel to the old stone bank in Kashiwajima village (constructed by the director Kenzan Nonaka), therefore, local citizen considered the wall as the submerged stone bank. However, dating and mineral composition data of the stone wall suggest that the wall is probably beachrock. Beachrock is an intertidal deposit forming in the zone where carbonate saturated meteoric and marine water mix, therefore, the history of the submergence by earthquakes at this site can be approximated based on the dating of beachrock.
This project introduces new idea to evaluate the record of the historical natural disasters based on the underwater structures and artifacts.

This research is supported by a grant from Kochi-bank foundation for the promotion of regional economy.

©2020. Japan Geoscience Union. All Right Reserved.

Reference
A review on estimation of subsidence records of Nankai earthquakes from the tradition of the submerged village “Kuroda-gori”, Rekishi Jishin, 31, 17-26

Keywords: Kurodagori, Nankai earthquake, Coseismic subsidence, Kochi Prefecture, Tsunami, Underwater geoarchaeology

©2020. Japan Geoscience Union. All Right Reserved.

Characteristics and its significance of marine cores collected from inner Uranouchi Bay, Kochi Prefecture

*Masafumi MURAYAMA[1], Wataru Tanikawa[2], Akira Ijiri[2], Tatsuhiko Hoshino[2], Takehiro Hirose[2], Toshiya Fujiwara[2], Kazuya Kitada[2], Kastuya Nejigaki[3], Tokuyama Hidekazu[4], Go-Ichiro Uramoto[4], Kazuno Arai[4], Kondo Yasuo[3], Yuhji Yamamoto[4], Research Member Kurodagoori[4]

1. Faculty of Agriculture and Marine Science, Kochi University, 2. JAMSTEC, 3. Graduate School of Integrated Arts and Sciences, Kochi University, 4. Center for Advanced Marine Core Research, Kochi University

For the purpose of the Kuroda-Gori archeological survey, sediment cores collected from the inner part (10m depth) of Uranouchi Bay, Kochi Prefecture, were analyzed. The history of changes in the marine environment and biota at that time was also restored. Uranouchi Bay, located in the central part of Tosa Bay, Kochi Prefecture, faces the north side of the Yokonami Peninsula, is elongated in the east and west, and is known as a sinking bay with a depth of 12 km. A 4-m sediment core was collected by vibro coring using the Kochi University research vessel "Nechun". Since the sampling point was not affected by the surrounding river, this core sample is considered to have recorded detailed environmental changes in the bay. The collected core samples were subjected to X-ray CT and MSCL analysis, and then halved to describe the naked eye and to collect and identify frequently occurring shellfish. The lithology of the sediment is olive-colored sity clay, which generally contains many shell pieces. The area near the upper part of the core was dark and had a strong hydrogen sulfide odor. In addition, event deposits with well-developed grains are observed in the lower part of the core, and the origin of the deposits will be examined in the future.

Keywords: Kuroda-Gori archeological survey, Uranouchi Bay, Event Sediments

©2020. Japan Geoscience Union. All Right Reserved.

A case study on 3D measurement of underwater structure by using digital image data taken with a digital camera

*Akira Ijiri[1], Wataru Tanikawa[1], Masafumi MURAYAMA[2], Tokuyama Hidekazu[2]

1. Japan Agency for Marine-Earth Science and Technology, 2. Kochi University

In recent years, it is possible to handle 3D reconstruction of various objects by using images from multiple viewpoints due to improvement of image processing (Structure from Motion = SfM). The SfM technique is used in geographical and archaeological researches to reconstruct topographical maps using UAV images or to record historical remains. This technique is also applied to record war remains and coral reefs in underwater study, though the examples are not enough to discuss the accuracy of 3D model. Kochi University and JAMSTEC (Japan Agency for Marine-Earth Science and Technology) launched a underwater geoarchaeological research to discover “Kurodagori”, which is a village at coastal area of Kochi Prefecture submerged under water by 684 Hakuho Earthquake. Shape and size of underwater materials must be recorded and measured from seafloor survey, and these data can be obtained by a sonic survey and a direct measurement by divers. However, when the target object is very small located at very shallow depth, these methods are very useless. On the contrary, SfM technique has a potential to solve these problems.

Therefore, in this study, we applied SfM technique for 3D reconstruction of underwater objects by using underwater photo during Kurodagori project. Compact digital camera (TG series, Olympus Corporation) was used to take photos. A commercial software Metashape (Agisoft) was used to construct the 3D models. We succeeded to construct the geographical data at a local spot of Nomi-bay by using about 30 photos. On the contrary, we failed to construct the 3D model of octopus trap pot, probably due to low visibility of undersea.

In this study, we compare 3D models of the pillars at Tsumajiro area and the octopus pot at Nomi-bay by using underwater photo to those by using photo at surface. We also improve the method to construct 3D models that original photo data is difficult to take due to high reflectivity of sunlight from the surface of the objects.

This research is supported by a grant from Kochi-bank foundation for the promotion of regional economy.

Keywords: SfM, 3D model, metashape, underwater geoarchaeology, Kurodagori

©2020. Japan Geoscience Union. All Right Reserved.

Environmental change over the past 2000 years in Lake Kawahara and Ryuuoo in southern Japan

*Cho Ara[1], Kota Katsuki[2], Jonathan D Woodruff[3], Kaoru Kashima[1], Hannah Elizabeth Baranes[3], Caroline Ladlow[3]

1. Kyushu University, 2. Shimane University, 3. University of Massachusetts

The lagoon environment is strongly controlled by relative sea-level (RSL) fluctuation and climate change. The sediment in the lagoon in Japan was continuously deposited and provide high-resolution results of paleoclimate change and RSL fluctuation. Furthermore, the typhoon and tsunami deposit were reconstructed from Lake Kawahara and Ryuuoo. Therefore, those sediment core is good enough to reconstruct the change of climate and sea-level. The environmental change was reconstructed from Lake Kawahara and Lake Ryuuoo based on diatom assemblage, sedimentary facies, and radiocarbon dating. The drastic environmental change happened approximately 1000 years ago. Marine diatom disappeared from Lake Kawahara and the lithology changed from laminated layer to gray clay with sand layer from Lake Ryuuoo. It can indicate the RSL fell down until the past 1000 years. Although freshwater diatom already dominated in Lake Ryuuoo before C.E 1000, the bromine (Br) which is an indicator of marine organic carbon content and salinity suggests the lake was still brackish lagoon. Therefore, both lakes were affected by RSL until C.E 1000. After C.E 1000, the environment of both lakes changed to freshwater conditions. Between C.E 1000 and 1700, the total diatom increased in Lake Kawahara and the and layers were deposited frequently in Lake Ryuuoo. It might be generated by a high amount of precipitation induced by the intense summer monsoon, which is related to the positive phase of the Asain-Pacific Oscillation (APO). After C.E 1700, both lakes changed to the modern condition

Keywords: diatom, environment change, lagoon

©2020. Japan Geoscience Union. All Right Reserved.

Application of Boxfish ROV and Boxfish 360 camera to Underwater Archaeological Survey

*Yuka Masaki[1], Hideki Sezoko[2], Masayuki Nagayama[3], Wataru Tanikawa[4], Yuhji Yamamoto[5], Shinichiro Ito[1]

1. COSMOS SHOJI Co., Ltd., 2. Nippon Marine Enterprises, Ltd., 3. 360 Planet, 4. Japan Agency for Marine-Earth Science and Technology, 5. Kochi University

In 1912, the Titanic sank colliding by an iceberg as a virgin voyage from Southampton to New York. 1517 people died because of this tragedy. It was later turned into a film by James Cameron and became one of the smash hit movies around the world, and what was used to shoot was an unmanned subsea robot ROV (Remotely Operated Vehicle).

The sunk Titanic cannot be preserved as it was eternally due to decay. In August 2019, Triton Submarine surveyed the Titanic in 4K image (underwater) video. In recent years, it has been increasing in the importance of underwater archaeological surveys with using ROV worldwide.

Tokyo submarine canyon, is located at Sagami trough in the vicinity of Tokyo and Sagami Bay, where the Philippine Sea Plate is subducting beneath the North American Plate. Geological and environmental seafloor surveys were conducted with Boxfish ROV (Boxfish Research) and Boxfish 360 camera at the depth of 300 meters on February in 2020. The surveys were technically very challenging because of the rapid current in this site. In this presentation, we will show the example of underwater archaeological survey with Boxfish ROV and Boxfish 360 camera.

It is considered that there are a lot of underwater archaeological sites around Japan due to the rapid current and earthquakes. However, there have not been many surveys with using ROV and the archeological sites are not well comprehended. It is expected that the underwater archaeological surveys with using ROV and underwater 360 spherical cameras will be used more practically in the future.

Keywords: Boxfish ROV, Boxfish360 camera, Underwater Archaeological Survey

©2020. Japan Geoscience Union. All Right Reserved.

[J] Poster | H (Human Geosciences)：H-QR Quaternary research

[H-QR06] Quaternary, Diachronic dynamics of human-environment interactions

convener:Mamoru Koarai(Earth Science course, College of Science, Ibaraki University), Yusuke Yokoyama(Atmosphere and Ocean Research Institute, University of Tokyo), Koji Okumura(Graduate School of Letters, Hiroshima University), Yasufumi Satoguchi(Lake Biwa Museum)

Humans have attained their specific development by indigenous cultures and evolved through environmental adaptation. The session raises issues of human-environmental interactions, views from diverse changes of climate, ocean, land and biota having made striking influence on humans. It welcomes various fields from human-environment change and their chronometric dating among Quaternary disciplines.

[HQR06-P01] **Radiocarbon ages of tsunami deposits from the Lake Harutori in Kushiro City along the Pacific coast of eastern Hokkaido, northeastern Japan**

*Kiyoyuki Shigeno[1], Toshimichi Nakanishi[2], Wan Hong[3], Futoshi Nanayama[4,5] (1.Meiji consultant co.,Ltd., 2.Tono Geoscience Center, Japan Atomic Energy Agency, 3.Geochemical Analysis Center, Korea Institute of Geoscience & Mineral Resources, 4.Geological Survey of Japan,AIST, 5.CWMD, Kumamoto University)

[HQR06-P03] Characteristics of gradient of valley plaine in Ibaraki Prefecture

*Mamoru Koarai[1], Tomoya Sekine[1], Takayuki Nakano[2] (1.Earth Science course, College of Science, Ibaraki University, 2.Geospatial Information Authority of Japan)

[HQR06-P04] Grain Size Composition of Crevasse Spray Sediments in the middle part of Kinu River

*Yoshiki Sato[1], Atsushi Urabe[2] (1.Geological Survey of Japan, Advanced Industrial Science and Technology, 2.Research Institute for Natural Hazards and Disaster Recovery, Niigata University)

[HQR06-P05] Geomorphic development of the Takaragi terrace since the Last Interglacial Period in the North Central Part of Kanto Plain, Japan

*Taiga Kimori[1], Toshihiko Sugai[1], Tatsuki Miyamoto[1], Tetsuya Komatsu[2], Nakanishi Toshimichi[2] (1.The University of Tokyo,Graduate School of Frontier Sciences, 2.Japan Atomic Energy Agency)

[HQR06-P06] Characteristics of the Fuji-Sagamigawa Lahar deposit at the upper reaches of Sagami River, central Japan

*Masaaki Shirai[1], Makoto Kobayashi[2], Takako UTSUGAWA[3], Kiyokazu Kawajiri[4], Takayuki Takahashi[1] (1.Tokyo Metropolitan University, 2.Mt. Fuji World Heritage Centre, Shizuoka, 3.Rissho University, 4.Sagamihara Cuty Museum)

[HQR06-P07] Landform Evolution of Budokubo Area, Niigata Prefecture, Japan

*Kosuke Sasamori[1], Mamoru Koarai[1] (1.Department of Earth Sciences, College of Science, Ibaraki University)

[HQR06-P08] Middle Holocene changes in relative sea-level on western Shikoku Island, Japan

*Tatsuhiko Yamaguchi[1], Tomohiro Tsuji[2], Futoshi Nanayama[3,4], Toshimichi Nakanishi[9], Michiharu Ikeda[8], Yasuo Kondo[5], Michiko Miwa[6], Yohei Hamada[7] (1.Nation. Mus. Nat. Sci., 2.Yamaguchi Univ., 3.AIST, 4.Kumamoto Univ., 5.Kochi Univ., 6.JAPEX, 7.JAMSTEC, 8.Shikoku Research Institute Inc, 9.Japan Atomic Energy Agency)

[HQR06-P09] Depositional sequence of the Post-LGM incised-valley fill controlled by seismic crustal deformation and large-scale lahars: An example of SKM core obtained from the Sukumo coastal lowland along the Nankai Trough, Japan

*Futoshi Nanayama[1,2], Tatsuhiko Yamaguchi[3], Nakanishi Toshimichi[4], Tomohiro Tsuji[5], Michiharu Ikeda[5], Kondo Yasuo[6], Michiko Miwa[7], Shinji Sugiyama[8], Kazunari Kimura[9] (1.Geological Survey of Japan, AIST, 2.CWMD, Kumamoto University, 3.National Museum of Nature and Science, 4.Japan Atomic Energy Agency, 5.Shikoku Research Institute Inc., 6.Kochi University, 7.JAPEX Research Center, 8.Paleo Environment Research Center, 9.Naiba Ehime Branch)

Radiocarbon ages of tsunami deposits from the Lake Harutori in Kushiro City along the Pacific coast of eastern Hokkaido, northeastern Japan

*Kiyoyuki Shigeno[1], Toshimichi Nakanishi[2], Wan Hong[3], Futoshi Nanayama[4,5]

1. Meiji consultant co.,Ltd., 2. Tono Geoscience Center, Japan Atomic Energy Agency, 3. Geochemical Analysis Center, Korea Institute of Geoscience & Mineral Resources, 4. Geological Survey of Japan,AIST, 5. CWMD, Kumamoto University

To estimate the sedimentary process of chronological samples in tsunami deposits, the radiocarbon ages of 10 pairs of marine shells and terrestrial plants were measured from one core obtained of lagoon lake sediments from the Lake Harutori in Kushiro City, eastern Hokkaido. This core of 12.6 meters length was obtained in the central part of the frozen lake in winter, which locates on a tectonic active region in the southwestern Kuril arc. Based on analyses of lithology, molluscan assemblages, and radiocarbon dating, we interpreted three units in order of decreasing age: transgressive tidal flat, transgressive lagoon, deltaic lagoon sediments. The lagoon sediments consisted thin silt layers of varve with terrestrial plant fragments and intercalating some event deposits by 22 sand layers of tsunamis and 6 volcanic ashes (Nanayama et al., 2003, Soeda and Nanayama, 2005). This structure was imaged by a core scanning of a computed tomography (CT) and X-ray fluorescence (ITRAX). The radiocarbon ages from the tsunami deposits were more than 1000-4000 years older than the depositional curve constructed by previous radiocarbon ages and tephrochronology. It clearly suggests that these materials were reworked from older sediments by catastrophic tsunamis. This effect was remarkable on plant samples. The core scanning of CT and ITRAX was performed under the cooperative research program of Center for Advanced Marine Core Research, Kochi University (Accept No. 18B061). This work was supported by KAKENHI Grant-in-Aid for Scientific Research number JP18H01310 and JP 18K03767.

Keywords: Reservoir effect, Lagoon sediments, Lake Harutor, Kushiro City, Pacific coast of Hokkaido

©2020. Japan Geoscience Union. All Right Reserved.

Characteristics of gradient of valley plaine in Ibaraki Prefecture

*Mamoru Koarai[1], Tomoya Sekine[1], Takayuki Nakano[2]

1. Earth Science course, College of Science, Ibaraki University, 2. Geospatial Information Authority of Japan

In the liquefaction risk assessment using landform classification, Nakano et al. (2015) divided the valley plain/flood plain into two parts with a gradient of 1/100, but the reason is not described clearly. The gradient of all valley plain/flood plain in the Land Condition Map in Ibaraki Prefecture was measured using the section function of “GSI Maps”. In addition, we sampled a valley plain with hand auger and investigated the relationship between gradient and particle size of structure materials.

As a result, the valley plain/flood plain steeper than gradient 1/100 accounted for only less than 10 percent by the extended, and its location was limited to a valley head. The gradient of the valley plain dissecting the plateau is steeper than roughly 1/500. Liquefaction caused by the 2011 off the Pacific coast of Tohoku Earthquake didn't occur at the valley plain steeper than gradient 1/500.

On the other hand, most of the flood plain along great rivers in Ibaraki Prefecture have a gentler gradient than the gradient of approximately 1/500, and no particular correlation was found between the liquefaction occurrence spots and the gradient.

For the liquefaction risk assessment based on the landform classification, the valley plain/flood plain needs to be divided into the flood plain along the great rivers and the valley plain dissecting the plateau, and the valley plain has a gradient more than 1/500.

In addition, as a result of sampling using a hand auger and particle size analysis in the valley bottom plain dissecting the plateau, coarse sand was dominant at a deeper than 3 m in the upstream core with a gradient more than 1/100. The result of analysis is supporting the supposition that a rough grain-size deposits are accumulated at steeper valley plains.

Acknowledgements

Prof. Naofumi Yamaguchi of Ibaraki University lent us bowling machinery. Miss. Kaho Hashimoto who is Ibaraki University student and her family had been very kind for an offer in land of sampling sites.

Keywords: valley plaine, garadient, liquefaction

©2020. Japan Geoscience Union. All Right Reserved.

Grain Size Composition of Crevasse Spray Sediments in the middle part of Kinu River

*Yoshiki Sato[1], Atsushi Urabe[2]

1. Geological Survey of Japan, Advanced Industrial Science and Technology, 2. Research Institute for Natural Hazards and Disaster Recovery, Niigata University

Crevasses splays are distributed along the left bank in the middle part of the Kinu River, central Japan. Although Sadakata (1972) suggested that crevasse splays had been formed during the 200–300 years around the 13th century, detail geomorphological development process has not been clarified due to the lack of their grain size composition and formation age. The purpose of this study is to clarify detail sedimentary process of crevasse splays based on coring survey, radiocarbon dating and grain size analysis of three boring cores, GS-JIS-6 to 8, drilled on a crevasse spray around the Ishige district, Joso City. Grain size analysis was performed at 1 cm intervals using a laser diffraction particle size distribution analyzer of Niigata University.

Sediments found in GS-JIS-6 to 8 cores are roughly classified into three units, Units 1 to 3 in ascending order. The Unit 1, 9.0 to 12.5 m T.P., consists of organic silt and silt with fine sand, and presumed to be back marsh sediment. Radiocarbon ages of 2,797–2,953 cal BP and 3,576–3,695 cal BP were obtained from this unit. The Unit 2 is found around 11 to 12 m T.P., which overlies the Unit 1, in only GS-JIS-8 core and consists of medium sand with granules. Coarser sand including plant fragments suggests that this unit is river channel sediment. Radiocarbon ages of 1,175–1,280 cal BP and 1,289–1,348 cal BP were obtained from the Unit 2. The Unit 3 composes of alternating layers of very fine to medium sand and silt and is found above 12 to 13.5 m T.P. Higher and thicker distribution toward west suggest that this unit should be crevasse spray deposits. From the bottom of the Unit 3, radiocarbon ages of 731–903 cal BP to 798–955 cal BP were obtained.

Number of sandy layers in the Unit 3 suggest that crevasse spray was formed by at least three flooding events. Thickness of each sand layer ranges between 2 cm and 1.1 m, and increases upward, which suggesting that the crevasse spray prograded eastward, from river channel to floodplain side. Radiocarbon ages of Unit 3 indicate that crevasse splay deposits deposited after ca. 700–900 cal BP, which is consistent with Sadakata (1972). Thin sand layers at the base of Unit 3 with a thickness of 2 to 4 cm consist of vary fine to fine sand with thin mud drape. Geometric mean [GM] of grain size of these thin layers range between 40 and 240 μm, showing coarsening upward. Thick sand layers distributed above thin layers can be subdivided into two or three subunits, Subunits A to C in ascending order, based on grain size composition. Subunit A, with 5–10 cm thickness, consists of very fine sand to fine sand coarsening upward as well as thin sand layers, and Geometric Standard Deviation [GSD] is around 4. Subunit B consists of fine to medium sand with about 10 cm thickness. GSD of this subunit is around 4–7, indicating poorer sorted deposit compared to other subunits. The Subunit C consists of fine to medium sand with granules, showing upward fining. Thickness of this subunit, around 20 to 100 cm, is largest in the Unit3 sediments. In addition, GSD is measured to be around 2–3 and increasing upward, which indicates that sorting becomes poorer upward. Composition of these thick sand layers shows differences among coring sites. For example, Subunit B was found only in the GS-JIS-6 core. This subunit may be corresponding to the upward fining sandy sediment immediately after the Kinu River breaching during the 2015 flooding (Sato et al. 2017).

Acknowledgements

This study was funded by the JSPS KAKENHI Grant (Project Number 16K16352).

©2020. Japan Geoscience Union. All Right Reserved.

References

Sadakata, N. (1971) Geographic Sciences (Chiri-Kagaku), 18, 13–22.

Sato, Y. et al (2017) The Quaternary Research (Daiyonki-Kenyu), 56, 37–50.

Keywords: Crevasse spla, flood, grain size analysis, Holocene

©2020. Japan Geoscience Union. All Right Reserved.

Geomorphic development of the Takaragi terrace since the Last Interglacial Period in the North Central Part of Kanto Plain, Japan

*Taiga Kimori[1], Toshihiko Sugai[1], Tatsuki Miyamoto[1], Tetsuya Komatsu[2], Nakanishi Toshimichi[2]

1. The University of Tokyo,Graduate School of Frontier Sciences, 2. Japan Atomic Energy Agency

1.Introduction
Takaragi terrace is located in the northern part of the Kanto Plain, where Late Quaternary tectonic movements are relatively inactive (Kaizuka 1987; Suzuki and Koike 2000). There have been few studies of landform development in this region. And the terrain boundary between Takaragi terrace and Sashima terrace that ranging to the south has not been clarified in detail.The purpose of this study is to clarify the landform evolution in the Takaragi-Sashima terraces after MIS5e by the terrain analysis using GIS and analysis of borehole core sediment.

2. Methods
Slope gradation map, hillshade map, Rainbow Contour map (Suginaka et al. 2018), and valley density map were made from 5m and 10m DEM using by ArcGIS10.6. Based on these maps and aerial photography interpretation the Takaragi-Sashima terraces and incised valleys were recognized.The following analyses were performed on four drilling core samples collected from the Takaragi Terrace: facies analysis using by Surface Peel Specimens, grain analysis and measurement of magnetic susceptibility. Based on these results, borehole cores were divided into several sedimentary units Tephra layers collected from the borehole cores were compared with key marker tephras distributed in Kinu River Lowland by analyzing the mineral components, sedimentary Units, shape and chemical composition of the volcanic glass.

3.Results and Discussion
As a result of aerial photography interpretation and DEM analysis, distribution of Takaragi-Sashima terrace and the incised valleys were confirmed from Utsunomiya to Toride. The flow direction of incised valleys on the Takaragi terrace surface has a tendency to change from north-south to northwest-southeast near Koga city. And the valley density becomes higher on the downstream side of Koga city.
Borehole core sediments were divided into five sedimentary units(U1:aeolian sediments with volcanic ash, U2: mudflow sediments, U3:braided river sediments, U4:meandering river sediments, U5:delta front sediments). And the thickness of meandering river sediments(U4) reaches 15~20m, and piles up riverbed sediments, natural levee sediments, back marsh sediments and interbeds many pumice layers.On the other hand, braided river sediments(U3) cannot be confirmed in NG1.
AT(30ka:Machida,Arai2003)and Ag-KP(44ka)were identified in aeolian sediments (unit 1), and Ag-MzP1(60ka)in fluvial deposits of unit 3.
These results suggest following geomorphic development: sea area (Paleo-Tokyo Bay) expanded to at least near the Oyama city at the Marine Oxygen Isotope Stage (MIS) 5e. After that, marine regression has started (U5), and on the delta plane, flooding of the Paleo-Kinu River was repeated, meandering river zone has formed (U4). During the last glacial period, the Paleo-kinu River transported gravels and formed an alluvial fan (U3). The alluvial fan expanded to the south, but when the fan toe reached between GC-OY1 and GC-NG1, it turned to an erosion trend, and terrace was affected by intermittent overflows.
After that, the southern part of the Takaragi terrace (from Oyama to Nogi), it is considered that the Takaragi terrace formed (U2) during the fall age of Ag-KP(44ka)(U1).
In addition, terrain analysis and distribution of tephra suggest that the boundary of the Takaragi and Sashima terraces could be set near Koga and Shimotsuma city.

©2020. Japan Geoscience Union. All Right Reserved.

Acknowledgments: This study was carried out under a contract with METI (Ministry of Economy, Trade and Industry)as part of its R&D supporting program for developing geological disposal technology.

References:Akiyama et.al(2019) Journal of Geography 128(6),905-920.Kaizuka(1987) Journal of Geography 96(4).217-240. Suginaka et.al(2018) Jpgu2018 HQR04-15. Suzuki and Koike(2000)Regional Geomorphology of the Japanese Islands,4 Kanto and Izu-Ogasawara University of Tokyo Press,180-183. Machida and Moriyama(2003) University of Tokyo Press

Keywords: Kanto basin forming movement, Marine Isotope Stage, Fluvial terrace, Terrain Analysis, Borehole Analysis, Tephrochronology

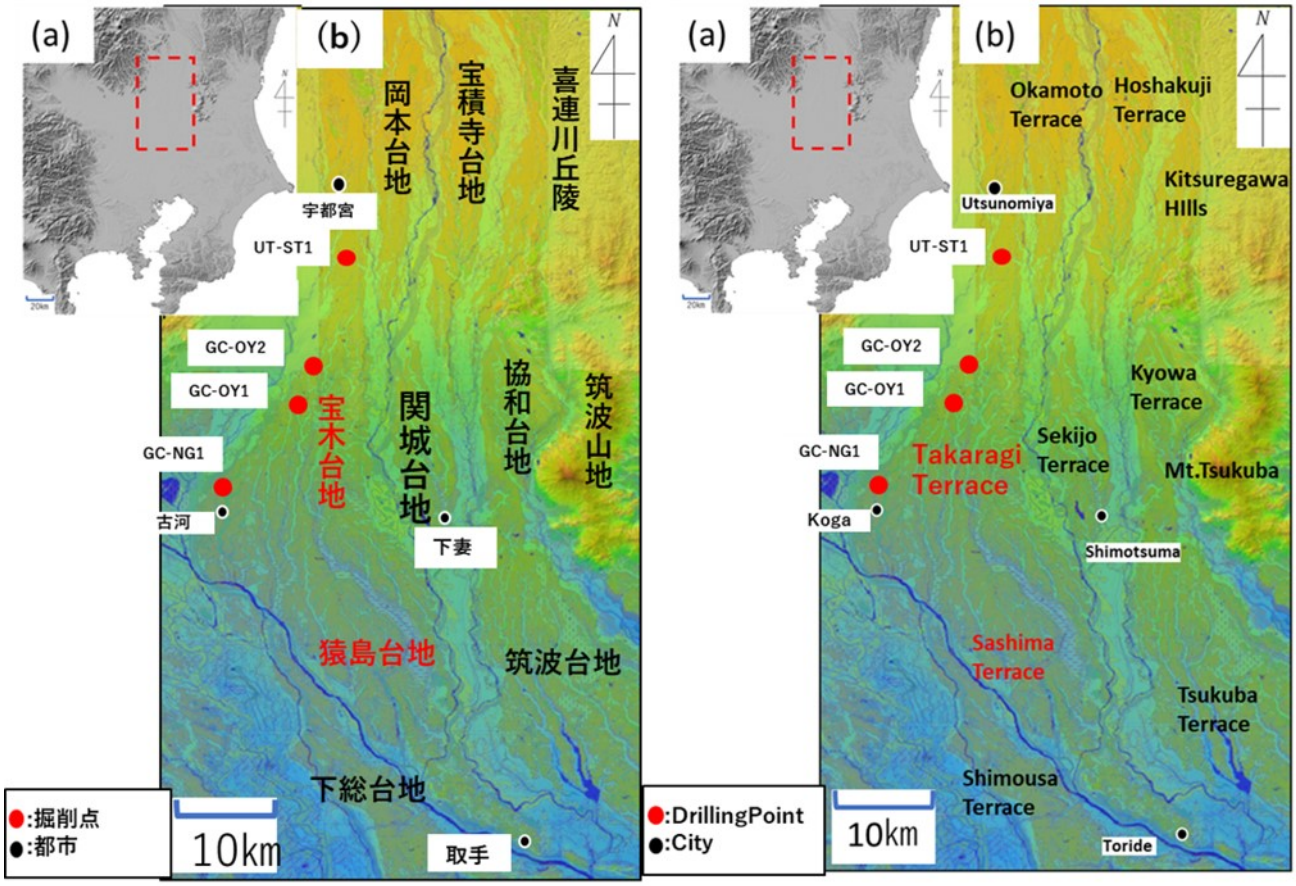

©2020. Japan Geoscience Union. All Right Reserved.

Characteristics of the Fuji-Sagamigawa Lahar deposit at the upper reaches of Sagami River, central Japan

*Masaaki Shirai[1], Makoto Kobayashi[2], Takako UTSUGAWA[3], Kiyokazu Kawajiri[4], Takayuki Takahashi[1]

1. Tokyo Metropolitan University, 2. Mt. Fuji World Heritage Centre, Shizuoka, 3. Rissho University, 4. Sagamihara Cuty Museum

Lahar is a general term for a rapidly flowing mixture of rock debris and water (other than normal stream flow) from a volcano (Smith and Fritz, 1989). Fuji Sagamigawa Mud Flow (Lahar) originated from the Fuji Volcano (Older Fuji) around 22 ka (Machida, 2009) distributes along the Sagami River Valley. The lahar deposits have been reported from Tsuru City, Yamanashi Prefecture to Zama City, Kanagawa Prefecture which apart ca. 90 km from the present Fuji Volcano summit. Although more than 3 events have been recognized based on field surveys by Geographical and Geological Research Group in Sagamihara City (1990), detailed description of Fuji Sagamigawa lahar deposit at the upper reaches of Katsura River (Sagami River) has not been published yet.

Detailed investigation of the lahar deposits in the upper reaches of the Katsura River and Shakunagare River located on northern margin of the Katsura River valley revealed that (i) the lahar deposit would bury the Katsura River valley entirely with more than 20 m thick, (ii) the deposit at upperstream area is characterized by frequent silt layers intercalation, and (iii) several debris flow deposit layers are transformed into hyperconcentrated flow deposit.

Acknowledgment

We thank to Tsuru University permitting us to use the boring data for constructing buildings.

References

Geographical and Geological Research Group in Sagamihara City (1990) Report of Geographical and Geological Survey on Sagamihara (4). Education Board of Sagamihara City, 63p.

Smith and Fritz (1989) Geology, 17, 375-376.

Machida (2009) Nature in History of Sagamihara City. Sagamihara City, 159-165.

Keywords: lahar deposit, Fuji-Sagami River Mud Flow, Katsura River (Sagami River)

©2020. Japan Geoscience Union. All Right Reserved.

Landform Evolution of Budokubo Area, Niigata Prefecture, Japan

*Kosuke Sasamori[1], Mamoru Koarai[1]

1. Department of Earth Sciences, College of Science, Ibaraki University

Shinano River basin was considered an active folding area in Niigata prefecture by 1940’s study(Ikebe,1942,etc.). Then, many studies of tectonic geomorphology have been researched by the field of geology, geomorphology and geodesy. Also,river terraces spread in this area. It reported that some of these river terraces are deformed by active folding. Budokubo region (Study area) is located north of the junction of Shinano River and Uono River. River terraces formed after 26-29ka also spread in this region. Although it was already reported about classification of the river terraces and landform evolution, the theory is controversial. Furthermore, there is an epicenter of the 2004 Mid-Niigata Prefecture Earthquake near this area. For that reason, it is meaningful of disaster prevention to discuss landform evolution of this area. In this study, aerial photograph interpretation, field surveys, and terrain analysis using GIS were carried out to discuss it.

As a result of aerial photograph interpretation and terrain analysis, comparison with previous studies, the river terraces in this area were classified 10(M1~M3, L1~L7). Cross-section figure (northeast-southwest direction) by using 1m grid DEM by LiDAR data shows that most of the terraces decline from northeast to southwest or horizontality distribution. L1 terrace has incline from northeast to Southwest due to uplift. In addition, microtopographic map and the slope direction map. These maps clearly show the terrace cliff and tilting on L1 terrace. Also, the slope direction map shows a meandering counterclockwise of old Shinano River while this river was flowing into this area.

Based on the distribution of the terrace in the riverbed profile and comparison with previous studies, it is considered that the terraces in this area were formed by the Shinano River after merging with the Uono River. Based on the above results, it was considered that the landform evolution of this area associated with the transition of the Shinano River. First, after the AT descent period, the Shinano River flowed into this area with NE-SW direction components. After the forming and deforming of the L1 terrace by uplift, the Shinano River meandered to surround the area counterclockwise, and the L2 and L3 terraces sequentially formed. After the L3 terrace formed, the inflow of the main flow of the Shinano River was cut off, and the meandering part became an abandoned river. The abandoned river was accompanied by forming L4 and L5 terraces. At the same time, the main flow changed its flow again in the NE-SW direction, and it was accompanied by forming L5 terraces. After that, the L6 and L7 terraces formed sequentially, suggesting that they formed the current terrain.

Keywords: Budokubo, Shinano River, River terrace, Landform Evolution, Digital Elevation Model

©2020. Japan Geoscience Union. All Right Reserved.

Middle Holocene changes in relative sea-level on western Shikoku Island, Japan

*Tatsuhiko Yamaguchi[1], Tomohiro Tsuji[2], Futoshi Nanayama[3,4], Toshimichi Nakanishi[9], Michiharu Ikeda[8], Yasuo Kondo[5], Michiko Miwa[6], Yohei Hamada[7]

1. Nation. Mus. Nat. Sci., 2. Yamaguchi Univ., 3. AIST, 4. Kumamoto Univ., 5. Kochi Univ., 6. JAPEX, 7. JAMSTEC, 8. Shikoku Research Institute Inc, 9. Japan Atomic Energy Agency

Shikoku Island is situated 150 km northwest of the Nankai trough that has developed in response to the convergence of the subducting Philippine Sea Plate and overriding Eurasian Plate. This tectonism causes deformation of the island, megathrust earthquakes, and tsunamis. Shikoku Island experiences coseismic and interseismic deformation. The middle Holocene tectonics of the island are still poorly understood. Relative sea-level (RSL) changes indicated by coastal sediments potentially record seismic uplift and subsidence. To infer RSL changes between 8 and 4 cal. kyr BP, we studied Holocene ostracode assemblages from the SKM drill core in Sukumo, southwest Shikoku Island (Tsuji et al., 2018, JpGU, MIS11-P19), and from six cores in the northern part of the island (Yasuhara et al., 2005, Palaeo3, 222, 285–312; Yasuhara and Seto, 2006, Paleontol. Res. 10, 99–116). To estimate paleo-water depth and RSL, we employed the ostracode assemblages and modern analog technique. The SKM core sediments are composed of conglomerate, ash, and mud chiefly. Its geological age was examined, using the ^{14}C dating method (Nakanishi et al., 2019, Radiocarbon, 61, 1939–1950). The ostracode assemblages occur from mud sediments. They are divided into three biofacies, indicating the mud bottom of a central bay with influence of open-sea water during the period of 8.7–8.1 cal. kyr BP, a central bay with intensified influence of open-sea water in the interval of 8.1–7.4 cal. kyr BP, and the brackish condition of a bayhead during the period of 7.0–4.5 cal. kyr BP. The RSL decreases from +4.7 to -5.8 m in elevation between 8.0 and 7.0 cal. kyr BP, fluctuated between -5.8 and +8.8 m from 7.0 to 6.1 cal. kyr BP, and then gradually decreased to -2.4 m until 4.7 cal. kyr BP. The eustatic sea-level (ESL) changes of Okuno et al. (2014, Quat. Sci. Rev. 91, 42–61) indicates a gradual rise from -12 to -2 m in elevation in the period from 8 to 4.5 cal. kyr BP. Hence the RSL reflects uplift to 4.7 cal. kyr BP in the southwestern Shikoku Island, in contrast to north of Shikoku Island. In north of the island, the RSL were slightly lower than the ESL and increases in parallel to the ESL rise. The RSL changes reflect the subsidence between 8 and 4 cal. kyr BP. The differences in RSL across the island suggest tilting of the island, possibly due to convergence of the Philippine Sea Plate.

Keywords: Ostracoda, Nankai Trough, Tectonics

©2020. Japan Geoscience Union. All Right Reserved.

Depositional sequence of the Post-LGM incised-valley fill controlled by seismic crustal deformation and large-scale lahars: An example of SKM core obtained from the Sukumo coastal lowland along the Nankai Trough, Japan

*Futoshi Nanayama[1,2], Tatsuhiko Yamaguchi[3], Nakanishi Toshimichi[4], Tomohiro Tsuji[5], Michiharu Ikeda[5], Kondo Yasuo[6], Michiko Miwa[7], Shinji Sugiyama[8], Kazunari Kimura[9]

1. Geological Survey of Japan, AIST, 2. CWMD, Kumamoto University, 3. National Museum of Nature and Science, 4. Japan Atomic Energy Agency, 5. Shikoku Research Institute Inc., 6. Kochi University, 7. JAPEX Research Center, 8. Paleo Environment Research Center, 9. Naiba Ehime Branch

The characteristics of the post-LGM incised valley fills and the depositional sequence were examined the SKM core collected in the Sukumo coastal lowland, where is expected to huge seismic subsidence due to the Nankai Trough great earthquakes. Our sedimentological, radiocarbon dating and paleoenvironmental results are as bellows. Sediments of the SKM core clearly show a succession influenced by post-glacial sea level change. The Matsuda River incised valley was formed in LGM and filled by fluvial sand and gravels in late Pleistocene. After the postglacial transgression, sea level reached -30 m (a.s.l.) at 9.8 ka and the incised valley changed to an estuary environment. The sea level continued to rise and it became an inner bay mud bottom environment, and reaching a maximum water depth was at 7.5 ka. The 7.3 ka Kikai caldera eruption in southern Kyushu caused heavy K-Ah ash fall in southwestern Shikoku, and then large-scale lahars frequently occurred immediately after the ash fall because of the vicinity of volcanic source. After ash fall, the K-Ah secondary sediments rapidly deposited on the inner bay environment and caused forced regression. After 7.0 ka, the growth of the delta became active ahead of the other regions, which may be due to the large K-Ah ash fall. At 5 ka, the sea level reached + 2.5 m (a.s.l.) estimated by the Sukumo midden and this altitude is recognized as the Holocene marine limit in this area. The information on relative sea level change during the past 10000 years has revealed that the Sukumo Bay area has not subsided due to seismic crustal deformation.

AMS^{14}C dating was supported by JSPS KAKENHI Grant Number JP 18H01310.

Keywords: post-LGM incised valley fills, Upper Pleistocene to Holocene, sequence stratigraphy, AMS14C age, sedimentary environment, Sukumo coastal lowland

©2020. Japan Geoscience Union. All Right Reserved.

[J] Poster | H (Human Geosciences)：H-SC Social Earth Sciences & Civil/Urban System Sciences

[H-SC07] CCUS (Carbon Dioxide Capture, Utilization, and Storage) for Climate Mitigation

convener:Masao Sorai(Institute for Geo-Resources and Environment, National Institute of Advanced Industrial Science and Technology), Ziqiu Xue(Research Institute of Innovative Tech for the Earth), Masaatsu Aichi(Graduate School of Frontier Sciences, University of Tokyo), Yoshihiro Konno(The University of Tokyo)

The prevention of the global warming, which is the urgent challenge facing the world, requires the full-out efforts of science and technology. This session focuses on the CCUS (Carbon Dioxide Capture, Utilization, and Storage) as one of the useful countermeasures for the CO2 emission reduction. It not only targets various scientific phenomenon caused by the capture and storage of CO2, CO2 utilization, and CO2-EOR/EGR, but also discusses the latest R&D developments of each method for the environmental impact assessment, safety assessment, the measuring, monitoring and verification (MMV), and public acceptance. The main theme is the recognition of key issues toward the practical use of CCUS, in addition to the deepening of our knowledge about the CO2 behavior on the underground.

[HSC07-P01] On the relationship between Vp and CO_2 saturation in the logging data at the Nagaoka site

*Takahiro Nakajima[1,2], Ziqiu Xue[1,2] (1.Research Institute of Innovative Technology for the Earth, 2.Geological Carbon Dioxide Storage Technology Research Association)

[HSC07-P02] Changes in hydraulic properties associated with fault development in sedimentary rocks from the Otway Basin using true triaxial testing techniques

*Takato Takemura[1], Eric Tenthorey[2,3], Hinako Hosono[1], Minoru Sato[4,5], Daisuke Asahina[4] (1.Nihon University, 2.Geoscience Australia, 3.CO2CRC, 4.Geological Survey of Japan, AIST, 5.Central Research Institute of Electric Power Industry)

[HSC07-P04] Fiber-optic sensing for CO_2-induced strain detection

*Hyuck Park[1], Yankun Sun[1], Yi Zhang[1], Ziqiu Xue[1] (1.Research Institute of Innovative Technology for the Earth)

[HSC07-P05] Feasibility of Distributed Fiber Optic Vibration Sensing for seismicity monitoring

*Takayuki Miyoshi[1], Takahiro Nakajima[1], Ziqiu Xue[1] (1.Research Institute of Innovative Technology for the Earth)

[HSC07-P06] Derivation of contact angle for evaluation of caprock's sealing performance

*Masao Sorai[1,2], Katsuya Honda[3] (1.Geological Carbon Dioxide Storage Technology Research Association, 2.Institute for Geo-Resources and Environment, National Institute of Advanced Industrial Science and Technology, 3.VALUENEX Japan Inc.)

[HSC07-P07] Molecular Dynamics Study on the Dynamic Contact Angle of CO_2/H_2O/Mineral System in Nano Pore Throat

*Masashige Shiga[1,2], Masao Sorai[1], Masaatsu Aichi[2], Hiromi Honda[2] (1.The National Institute of Advanced Industrial Science and Technology, 2.The University of Tokyo)

[HSC07-P08] Numerical study on leakage suppression of CO_2 stored in sub-seabed strata by gas hydrate formation

*TAKUYA WAKO[1], Toru Sato[1], Yousuke Sawano[1] (1.The University of Tokyo Graduate School of Frontier Sciences Department of Ocean Technology, Policy, and Environment)

[HSC07-P09] Access to Chinese rural landscapes from the perspective of Satoyama environmental education - a case study of Japanese undergraduate students

*XIANG QIONGYING[1], SHIXIAN LUO[1], Katsunori Furuya[1] (1.Chiba University)

[HSC07-P10] **Relationship between the impact of flower viewing tourism and residents' attitude**

*SHIXIAN LUO[1], JING XIE[2], Katsunori Furuya[1] (1.Chiba Univ., 2.Sichuan Agricultural Univ.)

[HSC07-P11] Analyze the impact of the climate change and human activity to the Ulz river basin and compare the protection methods

*Bayanjargal Darkhijav[1], Khulan Myagmar[1], Tsolmon Renchin[1], Bayanmunkh Norovsuren[1], Tsolmon Altanchimeg[1] (1.National University of Mongolia, Mongolia)

On the relationship between Vp and CO_2 saturation in the logging data at the Nagaoka site

*Takahiro Nakajima[1,2], Ziqiu Xue[1,2]

1. Research Institute of Innovative Technology for the Earth, 2. Geological Carbon Dioxide Storage Technology Research Association

This paper discusses the relationship between seismic P-wave velocity (Vp) and CO_2 saturation.in the field scale observation at the Nagaoka site. This dependency is important to evaluate the stored CO_2 in the ground using seismic exploration methods. There are many reports which examined and modeled the relationship. However, most of the reports studied drainage processes, where pore water is replaced by injected CO_2. In this paper, we investigate the relationships during drainage and imbibition processes using the time-lapse logging data at the Nagaoka site. Nagaoka site is the first CO_2 injection site in Japan, and CO_2 was injected between July 2003 and January 2005. Time-lapse loggings have been conduction at the observation wells in order to monitor the injected CO_2. The period of the post-injection monitoring is almost 15 years, so the monitoring data provide information on the imbibition process.
The monitoring data at a down-dip direction showed that CO_2 saturation increased at the injection period, became maximum one year after the end of the injection, and was gradually approaching at a certain value. The latest data is thought to be the residual saturation state. Vp change in the sonic logging data represented that the Vp decreased uniformly during the drainage process but the trajectories during the imbibition process have facies dependencies. This facies dependency means that there is hysteresis in the relationship between Vp and CO_2 saturation, the hysteresis is stronger in the silty stone than the sandy stone at the Nagaoka site.
Physical meanings of these behaviors were considered. The relationship at the drainage process is thought to be modified patchy saturation as Azuma et al., (2013) pointed out. However, during the imbibition process, it became more uniform relationship. The reason of this difference is thought to be come from that injected CO_2 would be invading from the large pore space, while the residual CO_2 would exist only in small pore space, which is thought to be uniformly spread out than large pore space. This supports that the silty layer worked like a uniform medium at the imbibition process.
The results of these analyses indicate that the evaluation of CO_2 saturation from seismic methods needs to be more careful at the post-injection period.

Keywords: Geological CO2 storage, Sonic logging, P-wave velocity, Histeresis, Nagaoka site

©2020. Japan Geoscience Union. All Right Reserved.

Changes in hydraulic properties associated with fault development in sedimentary rocks from the Otway Basin using true triaxial testing techniques

*Takato Takemura[1], Eric Tenthorey[2,3], Hinako Hosono[1], Minoru Sato[4,5], Daisuke Asahina[4]

1. Nihon University, 2. Geoscience Australia, 3. CO2CRC, 4. Geological Survey of Japan, AIST, 5. Central Research Institute of Electric Power Industry

Increases in fluid pressure or tectonic stresses deep underground can trigger fault formation or reactivation. Newly formed faults or existing faults that have reactivated may be potential pathways for migrating fluids such as stored carbon dioxide associated with CCS, which can potentially migrate upward toward the surface. Fluid migration associated with such fault development is therefore important when considering the feasibility of a CCS project. Surprisingly, there are few reports documenting the changes in permeability associated with fault development due to the technical difficulty of such experiments. In this study, we measure the permeability in the direction parallel to the fault plane during fault development under true triaxial stress conditions. In addition, the P-wave velocity in the direction across the fault plane was measured simultaneously with the permeability. In the experiments, sandstone, siltstone and mudstone samples collected from CO2CRC drill core from the Otway Basin, Australia were used. The observed change in permeability with fault development was different for each rock type. In the sandstone, the permeability changes are small even if a fault is formed, which is due to the high permeability of the host rock. In siltstone and mudstone, fault gouges were formed, and fracture zones with higher permeability than the host rock resulted. Therefore, even if a fault gouge develops, fluid migration will occur in a direction parallel to the fault plane through the damage zone. In addition, in the siltstone specimen after the experiment, slip in the carbonate layer was confirmed from observation, which suggests that the friction coefficient of the carbonate layer is extremely low.

Keywords: Fault, Permeability

©2020. Japan Geoscience Union. All Right Reserved.

Fiber-optic sensing for CO_2-induced strain detection

*Hyuck Park[1], Yankun Sun[1], Yi Zhang[1], Ziqiu Xue[1]

1. Research Institute of Innovative Technology for the Earth

For CO_2-induced strain detection, we carried out a laboratory experiment of CO_2 flooding in a core scale sandstone. Single optical fiber was used as distributed fiber optic sensors in this study. X-ray CT imaging was used to measure the CO_2 saturation. We compared the CO_2 transfer by X-ray CT imaging and the response of the optical fiber. Sarukawa sandstone (diameter: 34.83mm, length: 179.50mm) was used in this study. It has a relatively homogeneous structure and has irregularly shaped grains and voids. Microbubble filter (diameter: 34.33mm, length: 5.02mm) was located in between distributor and core specimen in the upstream side. Porosity of the specimen determined by X-ray CT imaging is 23.38%. The permeability is about 7.3 mDarcy. The experiment was conducted under the pressure and temperature conditions that simulate underground environments; pore pressure: 10MPa, temperature: 40 degrees Celsius. The confining pressure selected in this study was 12MPa. The specimen was first saturated with KI aqueous solution (11.5 wt%). The permeability was confirmed using the KI aqueous solution. The upstream pump was prepared at 10.5 MPa for differential pressure of 0.5MPa. Optical fiber measurement and X-ray CT imaging were performed in all experimental steps. Breakthrough occurred after about 0.2PV (pore volume) CO_2 injection. It took about 8 minutes in this study. The CO_2 saturation obtained by the X-ray CT was about 19.58%. When comparing the front of CO_2 saturation and the front of optical fiber frequency difference, they showed good agreement. This suggests that the frequency information of optical fiber can play a role as a sensor representing the behavior of CO_2 in rock.

Keywords: Fiber-optic sensing, X-ray CT imaging, CO2-induced strain, CO2 saturation

©2020. Japan Geoscience Union. All Right Reserved.

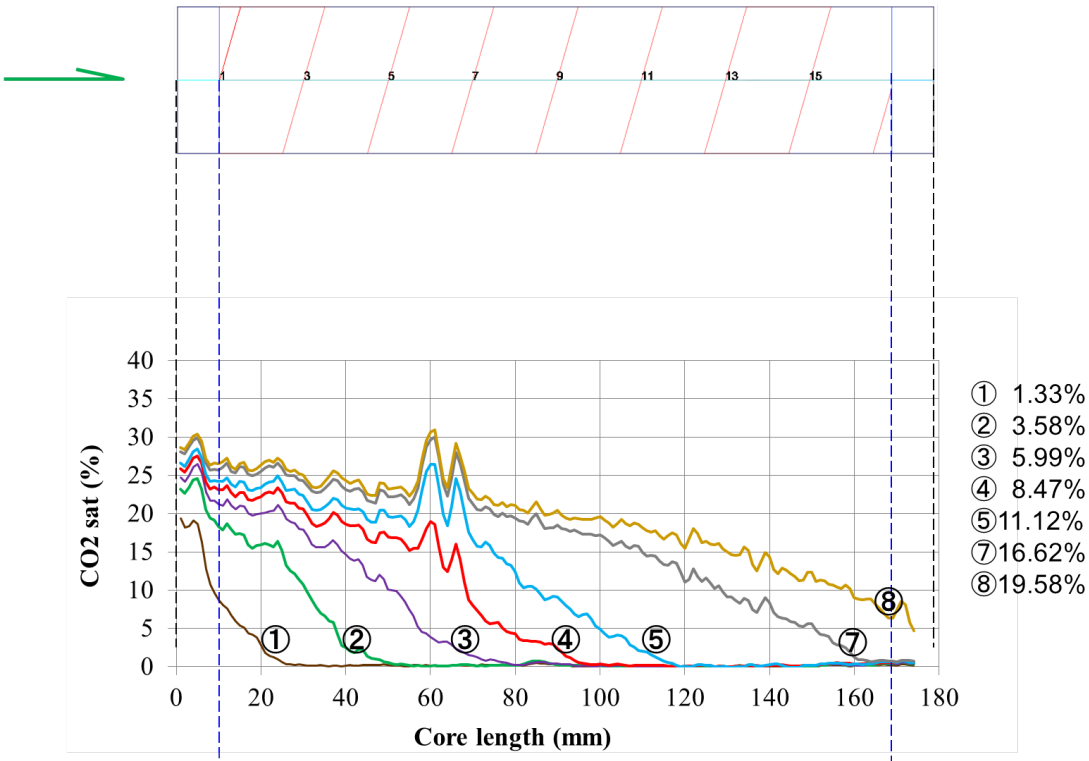

X-ray CT imaging result (CO_2 saturation)

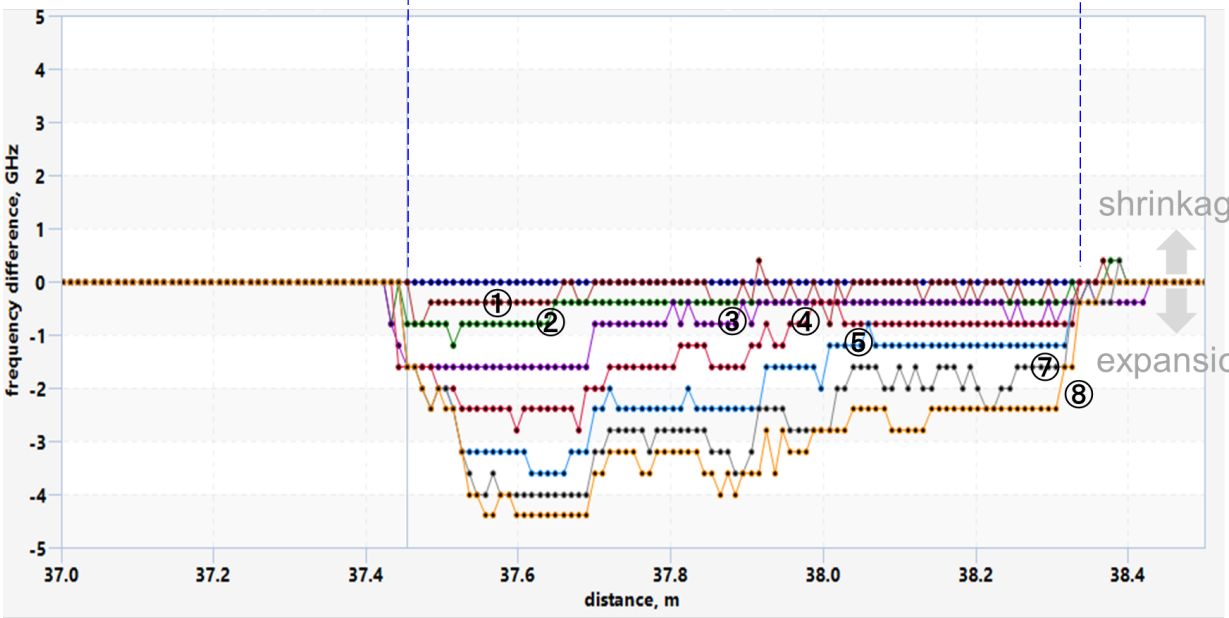

Fiber-optic sensing result (CO_2-induced strain)

©2020. Japan Geoscience Union. All Right Reserved.

Feasibility of Distributed Fiber Optic Vibration Sensing for seismicity monitoring

*Takayuki Miyoshi[1], Takahiro Nakajima[1], Ziqiu Xue[1]

1. Research Institute of Innovative Technology for the Earth

Geological CO_2 storage requires long-term monitoring not only for a plume of injected CO_2 but also area of pressure/strain propagation far away from the plume. The Distributed Fiber Optic Sensing (DFOS) is one of the major technologies capable of acquiring spatially continuous recording. The optical fibers for vibration sensing are used as receivers for the 4D VSP (Vertical Seismic Profiles) techniques in order to image the plume of injected CO_2, and also as passive seismometers for natural/induced seismicity. The sensitivity of optical fibers is not as good as typical geophones/seismometers. We conducted the long-term observation for natural earthquakes using the strain-sensing fiber cables installed behind the casing along the vertical wellbore in order to evaluate the sensitivity of the fiber cables.

A single channel record of the fiber optical sensing captured the ground motion of relatively large earthquake events. Whereas, the earthquake events within 20 km epi-distance listed on the JMA website location were all detected using the fiber records along the 880m well. Considering to the area of monitoring in the geological CO_2 storage (~10km), the fiber optic vibration sensing is one of the feasible options for seismicity monitoring.

Keywords: Geological CO2 Storage, Fiber Optic Sensing, Seismicity

©2020. Japan Geoscience Union. All Right Reserved.

Derivation of contact angle for evaluation of caprock's sealing performance

*Masao Sorai[1,2], Katsuya Honda[3]

1. Geological Carbon Dioxide Storage Technology Research Association, 2. Institute for Geo-Resources and Environment, National Institute of Advanced Industrial Science and Technology, 3. VALUENEX Japan Inc.

Geological CO_2 storage assumes that a caprock retains injected CO_2 stably within a reservoir. However, if geochemical reactions, especially the slight alteration of mineral surfaces, change the contact angle θ, it is expected that the caprock's sealing performance would be reduced. This study aims to verify whether such a scenario is possible. For this purpose, dataset of θ with high accuracy is required, but θ values measured using traditional droplet method usually have a large margin of error. Alternatively, we propose novel method to derive θ based on the capillary pressure equation, $P_c^{th} = 2\sigma \cos\theta / r$, where P_c^{th} is the threshold pressure, σ is the interfacial tension, and r is the pore throat radius. In this method, the P_c^{th} of micro pores around 20 μm diameter drilled in target samples is measured, and then the θ is calculated from above equation applying reference value of σ.

The target samples are five kinds of minerals (quartz, albite, chlorite, calcite, and gypsum) and two types of rocks (malrite and mudstone). These samples were available for breakthrough experiments of supercritical CO_2 at 10 MPa and 40˚C. Then, θ was calculated using measured P_c^{th}. Results showed that our method enabled to derive θ in a reproducible fashion. However, some samples led to $\cos\theta > 1$, in which the θ cannot be defined. Such an inconsistency is caused by the high sensitivity of σ to θ. Therefore, we should examine more accurate data of σ, hereafter. In either case, we can estimate the magnitude relationship of each sample's θ from calculated $\cos\theta$. The study revealed that silicate minerals such as quartz, albite and chlorite, and rocks mainly composed of clay minerals such as marlite and mudstones had a wetting surface (i.e., low θ). In contrast, both calcite as a carbonate mineral and gypsum as a sulfate mineral showed a relatively non-wetting surface (i.e., high θ).

Keywords: Geological CO2 storage, Contact angle, Sealing performance, Threshold pressure, Caprock

©2020. Japan Geoscience Union. All Right Reserved.

Molecular Dynamics Study on the Dynamic Contact Angle of CO_2/H_2O/Mineral System in Nano Pore Throat

*Masashige Shiga[1,2], Masao Sorai[1], Masaatsu Aichi[2], Hiromi Honda[2]

1. The National Institute of Advanced Industrial Science and Technology, 2. The University of Tokyo

CO_2 Geological Storage (CGS) is one of the most promising technologies to reduce the amount of CO_2 emissions into the atmosphere. Enhanced oil recovery in addition to the sequestration in the geological formation has been actively studied, and these are considered to be a significant strategy for sustainable energy development. In order to conduct the project safely, it is necessary to predict and understand the sealing performance of the caprock. This is evaluated by the threshold value of the capillary pressure. This pressure is formulated as Young Laplace equation; the capillary pressure is proportional to $2\Gamma\cos\theta/a$. (Γ : interfacial tension between CO_2 and brine, θ : contact angle, a: radius of the pore throat) Water-receding contact angle, which is represents the wetting behaviors in the drainage process, should be evaluated. Therefore, there have been a lot of experimental measurements of the dynamic contact angle. However, there is no data in the nano scale, which is the actual scale of the caprock in the CGS site. CO_2 and H_2O confined in the nano pore throat is likely to behave in a different manner. This is because the effect of the surface forces working on the fluid phases from the mineral surface is much larger than those in the macroscopic systems.

Considering the importance of studying the wettability in nano scale and its difficulty in direct measurements, we calculated the contact angle by using molecular dynamics simulation. We obtained both advancing and receding contact angles. Moreover, we studied the shape of the interface both at meniscus and film regions, which have crucial roles in wettability alteration.

Keywords: CO2 Geological Storage, Wettability, Molecular Dynamics

©2020. Japan Geoscience Union. All Right Reserved.

Numerical study on leakage suppression of CO_2 stored in sub-seabed strata by gas hydrate formation

*TAKUYA WAKO[1], Toru Sato[1], Yousuke Sawano[1]

1. The University of Tokyo Graduate School of Frontier Sciences Department of Ocean Technology, Policy, and Environment

The Paris Agreement in 2015 stated that the issue was to keep the temperature rise below 1.5 ℃ after pre-industrial average temperature and IPCC (Intergovernmental Panel on Climate Change) presented a scenario in which the future temperature will change depending on the choices that we will tackle in the future. So, we need to solve global warming issue as soon as possible. But, the transition of capital investment against the global warming takes a long time. Therefore, we need to capture the CO2 and store it in deep underground as countermeasure for the CO2 emitted that time. For that reason, CCS(Carbon dioxide Capture and Storage)is spreading around the world.

In the storage under the seafloor, it is conceivable the stable storage becomes possible by forming gas hydrate under the conditions of high pressure and low temperature.

Hydrate storage leads to further expansion of storage potential. This study aims to visualize the behavior of CO2 in the stratum, using numerical simulation.

As a previous study, Yu et al. (2016) proposed a new model of hydrate formation was developed depending on the microscopic position. The hydrate formation simulation on the reservoir scale was performed with coupling the hydrate formation model with GETFLOWS (General purpose Terrestrial fluid-FLOW Simulator). We carried out the simulations using the physical conditions of Sleipner, Snøhvit, and Tomakomai, which are typical seafloor storages, such as seafloor depth, seafloor temperature, geothermal gradient, injection rate, and permeability.

As a result, it was found that the diffusion of the hydrate formation heat made it difficult to form hydrate around the area where hydrate had already been formed, and that the hydrate might leak to the seafloor. Whether it is possible to classify cases that can be stored and cases that lead to leakage depends on the conditions.

Keywords: CO2 hydrate blocking, CCS, Leakage suppression, Reservoir-scale simulation

©2020. Japan Geoscience Union. All Right Reserved.

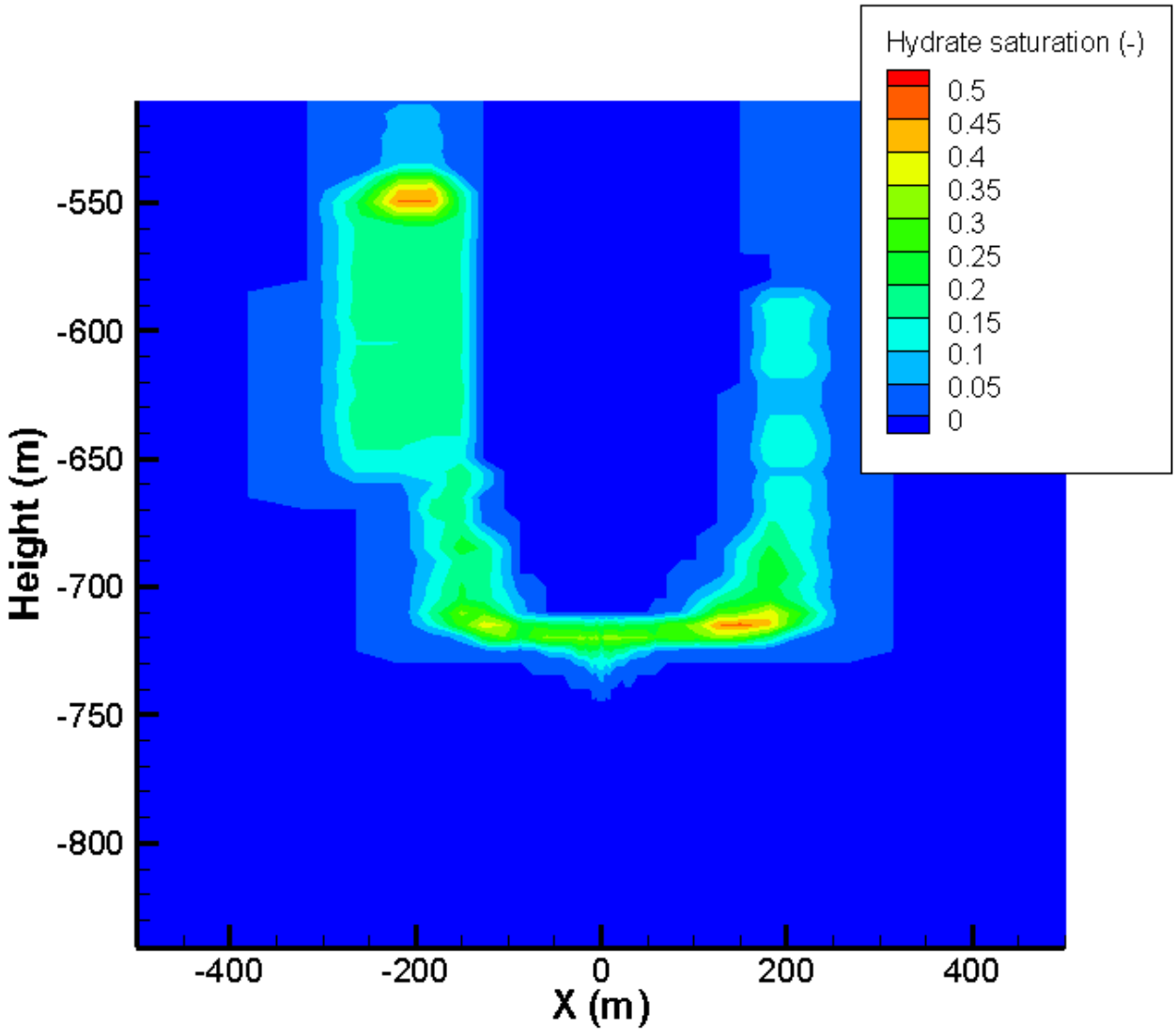

©2020. Japan Geoscience Union. All Right Reserved.

Access to Chinese rural landscapes from the perspective of Satoyama environmental education - a case study of Japanese undergraduate students

*XIANG QIONGYING[1], SHIXIAN LUO[1], Katsunori Furuya[1]

1. Chiba University

With increasing urbanization in China in recent years, the rural landscape has declined. In China, rural landscapes are valued mostly for their development potential, and there is little environmental education, that could allow the younger generation to better understand and value local culture and the rural landscape. In Japan, Satoyama is a relatively mature environmental education system, which leaves a deep impression on young people (especially college students). As the new generation, they have their own opinions and recommendations for improvements in Satoyama. In this study, students from Chiba University in Japan (n=132) were invited to participate in a workshop discussion, fill out a questionnaire on April 23rd and May 24th. At last, we used KH CODER to analyze the vocabulary provided by the respondents. Drawing on the students' memorable experiences of Satoyama's environmental education, the main problems and solutions for the future development of China's rural landscapes are explored. It is hoped that this research will provide an effective reference for the future study of the links between cultural services in ecosystem services.

Keywords: Satoyama, environmental education, rural landscape, KH CODER, workshop

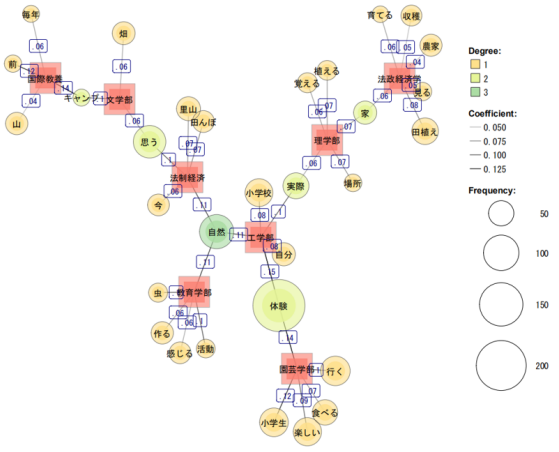

Figure 1. the coefficient and frequency between disciplines

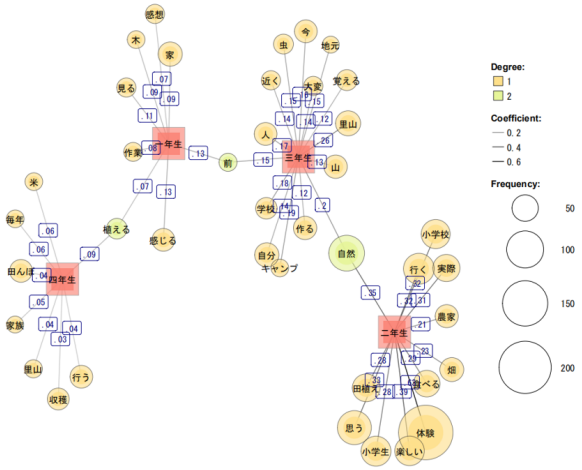

Figure2. the coefficient and frequency between grades

©2020. Japan Geoscience Union. All Right Reserved.

Relationship between the impact of flower viewing tourism and residents' attitude

*SHIXIAN LUO[1], JING XIE[2], Katsunori Furuya[1]

1. Chiba Univ., 2. Sichuan Agricultural Univ.

Plant viewing tourism (PVT) and the impact of tourism on destinations are often discussed, but research on flower viewing tourism (FVT) in the region is still less relevant. The purpose of this study is to highlight the tourism based on flower viewing and to find the impact on flower viewing tourism and perceptions and attitudes of residents. The data comes from a questionnaire survey of 305 residents living in Chengdu City. The questionnaire designed a total of 17 items, and three main dimensions of influencing factors were constructed after performing exploratory factor analysis, which are environment, economy, and sociocultural. Then, SEM was used to examine the relationship between these dimensions and the attitudes of residents. The results show that residents' positive attitudes towards flower viewing tourism can be reflected by the positive response of economic and environmental impacts, while no significant correlation has been found between sociocultural impacts and attitudes. Finally, the data results are discussed and analyzed in-depth, and four conclusions of this study are proposed. This study systematically analyzes for the first time the impact of flower viewing tourism on the region and the attitudes of residents and proposes an effective model that can measure this relationship, so it is meaningful and contributing. Meanwhile, it is one of the few studies in this field. These results can provide suggestions for the future development direction of cities and the formulation of tourism policies, and promote regional sustainable tourism development.

Keywords: Flower viewing tourism, tourism impact, residents' attitudes, structural modeling, sustainable tourism development

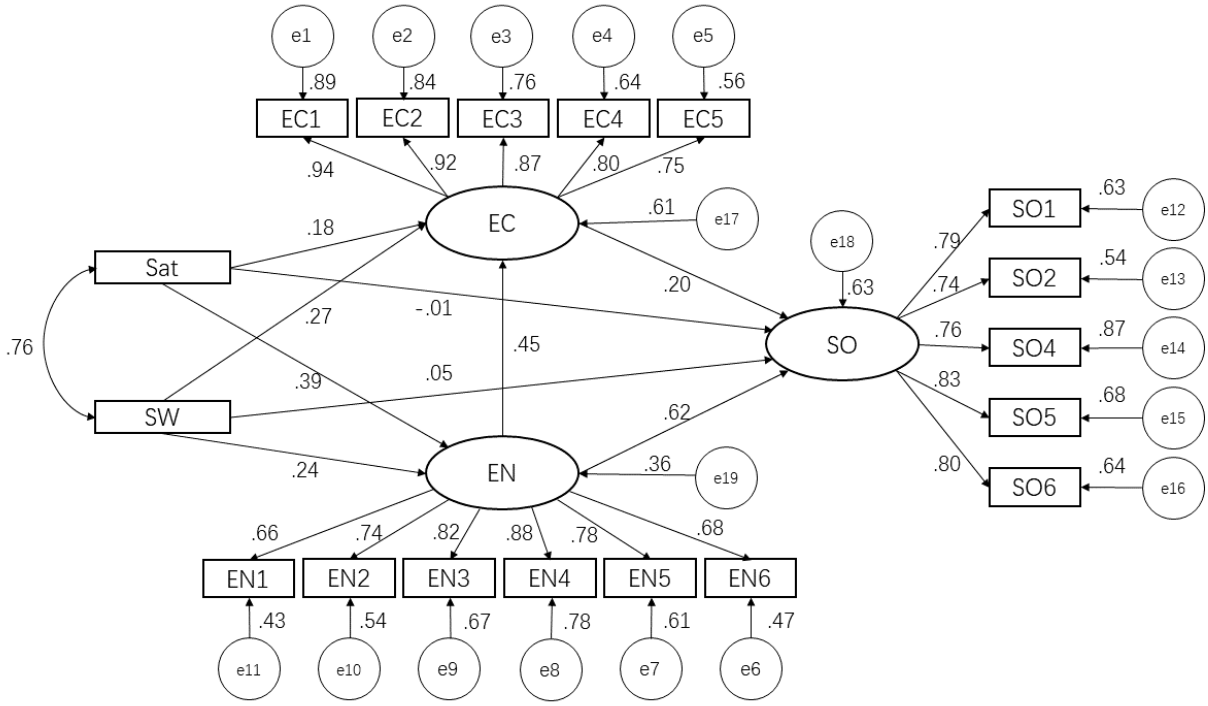

©2020. Japan Geoscience Union. All Right Reserved.

Analyze the impact of the climate change and human activity to the Ulz river basin and compare the protection methods

*Bayanjargal Darkhijav[1], Khulan Myagmar[1], Tsolmon Renchin[1], Bayanmunkh Norovsuren[1], Tsolmon Altanchimeg[1]

1. National University of Mongolia, Mongolia

The purpose of the study is to determine the impact of the climate change and human activity to the Ulz river basin of Mongolia. The study area is located in the taiga, forest steppe region of Mongolia, which is suitable habitat for some animal species originated in Siberia, Mongolia and Manchurian.

In this study we used two methodologies. Firstly, The MaxEnt is based on the maximum-entropy approach for modeling species niches and distribution. Secondly, we carried out Cost-Benefit Analysis (CBA) on the most suitable two scenarios to protect the buffer zone in the Ulz river basin. The cost benefit analysis estimates all costs and benefits in monetary terms and it allows to compare relatively the costs and benefits of a given activities or sectors to be ranked. We also compared potential protection methods to establish the buffer zone.

The result of MaxEnt modeling shows that the core habitat area of the animals would be distributed in our targeted area in the future 40 years using satellite and climate data. Estimating the cost-benefit analysis for two scenarios the total costs consist of economic cost, environmental cost and total benefits includes economic benefit, social benefit and environmental benefit for the year. As results of the analysis indicate the most economically and environmentally beneficial one is Scenario-1. Because three values of the analysis for the scenarios to be compared and it illustrates Scenario-1 has much higher, NVP is 6.2 million dollars than Scenario-2 from 2018 to 2030. The cost benefit analysis is potential method to evaluate competitive scenarios for implementing activities in the long run.

According to the result of the research, it can be seen that by establishing buffer zone using satellite data and GIS techniques can support household’ s income due to rehabilitation and protection of ecosystem in the study area.

Keywords: Buffer zone, satellite data, cost-benefit analysis

©2020. Japan Geoscience Union. All Right Reserved.

[J] Poster | H (Human Geosciences)：H-DS Disaster geosciences

[H-DS12] Geohazards in humid, tectonically active countries and their precursors

convener:Satoru Kojima(Department of Civil Engineering, Gifu University), Hiroshi YAGI(Faculty of Art, Science and Education, Yamagata University), Taro Uchida(University of Tsukuba), Yoshihiko Kariya(Department of Environmental Geography, Senshu University)

This session covers mass movements of landslide, slope failure, debris flow, and gravitational slope deformation in tectonically active, humid countries, and aims to discuss on their mechanisms, characteristics of occurrence sites, the significance in geological time scale, and the methodology to mitigate their affects by researchers with various related research fields.

[HDS12-P01] Geomorphological and geological details of the Mizore large-scale landslide and its causal link to AD1586 Tensho Earthquake in Gifu Prefecture, central Japan

★Invited Papers

*Takahiro Kurimoto[1], Yoshihiko Kariya[2], Kuniyasu Mokudai[3], Ryuji Yamada[4], Takashi Kimura[5], Masaki Sano[6], Akane Tsushima[7], Zhen Li[8], Takeshi Nakatsuka[8] (1.Graduate student , Senshu Univ., 2.Senshu Univ., 3.Tohoku Gakuin Univ., 4.NIED, 5.Ehime Univ., 6.Waseda Univ., 7.MRI, 8.Nagoya Univ.)

[HDS12-P02] Deep-seated gravitational slope deformation process deduced from composition and age of sediments accumulated in a linear depression of Nishifuruike on the ridge near Kamikochi, Northern Japan Alps

*Satoru Kojima[1], Hidehisa Nagata[2] (1.Department of Civil Engineering, Gifu University, 2.Fu-Sui-Do Company Limited)

[HDS12-P03] Gravitational deformation on mountain slope to the northeast of Tokugotoge Pass, Nagano Prefecture, Japan

*Hidehisa Nagata[1], Satoru Kojima[2] (1.Fu-Sui-Do Company Limited, 2.Department od Civil Engineering, Gifu University)

[HDS12-P04] Holocene gravitational rock slope deformation and large-scale landslide features in the western Kamikochi Valley, northern Japanese Alps

*Yoshihiko Kariya[1], Sadao Takaoka[1] (1.Department of Environmental Geography, Senshu University)

[HDS12-P05] Surface changes of rock slopes in the Shirouma-Daisekkei Valley, the Northern Japanese Alps

*Hirotaka Sugiyama[1], Chiyuki Narama[1], Hiroshi Inoue[2] (1.Niigata University, 2.National Research Institute for Earth Science and Disaster Resilience)

[HDS12-P06] Surface changes of Ganpei landslide in Joetsu region

*Yutaka Inoue[3], Chiyuki Narama[1], Chunxiang Wang[2], Eiji Takita[2] (1.Niigata University, 2.KITAK Corporation, 3.Graduate Student,Niigata University)

[HDS12-P07] The characteristic of ground motion amplification based on the Fourier spectrum ratio between surface and underground of the KiK-net seismic observation points - Basic study of landslides caused by earthquakes -

*Tomoyuki Iida[1], Chi-Wen Chen[1], Masato SATO[1], Hidemitsu Tokui[2], Tetsuya Onodera[2], Hiroshi Kawabe, Ryuji Yamada[1] (1.National Research Institute for Earth Science and Disaster Prevention, 2.Technicallinc Kabushiki kaisya)

[HDS12-P08] Gigantic landslides distributed in the upper course of Marsyandhi river in Nepal Great Himalaya

*Hiroshi YAGI[1], Yuki Matsushi[2], Hiroshi P Sato[3], Akihiko Wakai[4] (1.Faculty of Art, Science and Education, Yamagata University, 2.DPRI, Kyoto University, 3.College of Humanities and Sciences, Nihon University,

4.Faculty of Technology, Gunma University)

Geomorphological and geological details of the Mizore large-scale landslide and its causal link to AD1586 Tensho Earthquake in Gifu Prefecture, central Japan

*Takahiro Kurimoto[1], Yoshihiko Kariya[2], Kuniyasu Mokudai[3], Ryuji Yamada[4], Takashi Kimura[5], Masaki Sano[6], Akane Tsushima[7], Zhen Li[8], Takeshi Nakatsuka[8]

1. Graduate student , Senshu Univ., 2. Senshu Univ., 3. Tohoku Gakuin Univ., 4. NIED, 5. Ehime Univ., 6. Waseda Univ., 7. MRI, 8. Nagoya Univ.

A large-scale landslide (V=2.2×10^7 m^3) called the ” Mizore-no Oware(landslide) “ is present around the southern tip of Shokawa-active fault zone. ML is believed to be caused by the AD1586 Tensho-earthquake (est. M 7 to 8) based on historical documents. However, a few researches regarding geological and geomorphological characteristics of ML have been carried out. Based on field investigation and geomorphological analysis by using GIS, we clarified the geological and geomorphological features of ML. The main conclusions are as follows.; a) The ML holds a set of three dissected head scarps and three landslide bodies both showing multiple landslide events. ; b) The ML shows unique geological and geomorphological features such as a jigsaw crack structure and “patchwork structure” in the landslide materials and hummocks/depression upon the ground surface of the landslide bodies; c) Materials of landslide body involve paleosol and fossil logs that enable us to date the landslide event; d) According to ^{14}C dates of logs in paleosol, the latest landslide event is likely occur cal AD1493-1645; e) Also, one wood log sampled from dammed-lake deposits indicated cal AD 1514 to 1618 by ^{14}C and AD1615 to 1620 by tree-ring ^{18}O methods; f)The latest landslide event should be triggered by AD1586 Tensho-earthquake (estimated M=7 to 8) generated from the Shokawa fault zone close to northern of ML.

Keywords: AD1586 Tensho-earthquake, Shokawa fault zone, Large-scale landslide, Dammed lake, Paleo-earthquake

©2020. Japan Geoscience Union. All Right Reserved.

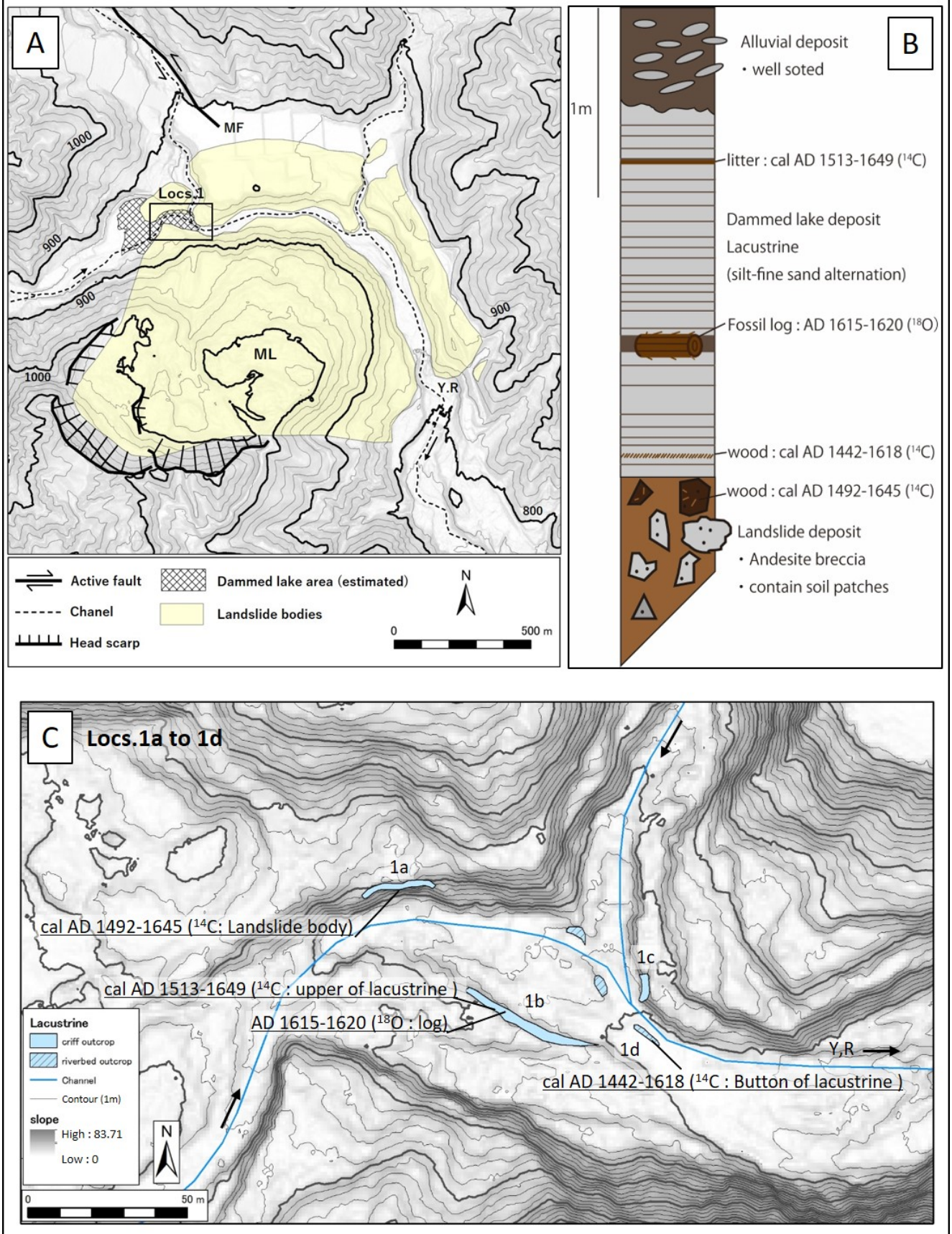

Figures A to C ; A) Topography of the study area. Contour interval is 20 m. B) Integrated geological column of Locs. 1a to 1d. C) Outcrop localities of samples for age determination (Locs.1a to 1d) . MF:Miogo Fault, ML : Mizore Landslide , Y,R : Yoshida River

©2020. Japan Geoscience Union. All Right Reserved.

Deep-seated gravitational slope deformation process deduced from composition and age of sediments accumulated in a linear depression of Nishifuruike on the ridge near Kamikochi, Northern Japan Alps

*Satoru Kojima[1], Hidehisa Nagata[2]

1. Department of Civil Engineering, Gifu University, 2. Fu-Sui-Do Company Limited

Kamikochi is located about 1,500 m in altitude on a wide riverbed of the Azusagawa River. The ridges extending NE-SW direction from Mt. Ohtakiyama (2616 m) to Tokugo Pass (2140 m) on the left side of Azusagawa River have wide crests with low relief and also have 2 to 3 lines of narrow depressions parallel to the ridges, which were regarded to be formed by the deep-seated gravitational slope deformation. The depressions are, in part, pond, swamp, and wet lowland with no trees unlike the surrounding coniferous forests, and are filled with fine-grained sediments. We have drilled 7 cores in Nishifuruike, one of the depressions, in order to clarify the development history of the depression. The cores are common in sedimentary facies, and are composed of the upper dark-brown silt and mud rich in organic materials covering the lower alternating coarse-grained volcanic sands, laminated silt and fine-grained sand, and silt. The sediments were sampled with about 5 cm-thick intervals, and their very fine-grained fractions have been observed under microscope, most of which consist of eolian volcaniclastic materials: volcanic glasses and minerals. The facts that the volcanic glasses are mainly composed of microlite- and pumice-type glasses and the sediments are coarse-grained volcanic materials such as granule-size clasts indicate the sediments were derived from the Yakedake volcano about 8 km west from the Nishifuruike. The last large-scale magmatic eruption of Yakedake volcano is recorded by the 2.3 ka Nakao pyroclastic flow deposits; this indicates the depression had been formed at or before 2.3 ka.

Keywords: deep-seated gravitational slope deformation, Northern Japan Alps, tephrochronology

©2020. Japan Geoscience Union. All Right Reserved.

Gravitational deformation on mountain slope to the northeast of Tokugotoge Pass, Nagano Prefecture, Japan

*Hidehisa Nagata[1], Satoru Kojima[2]

1. Fu-Sui-Do Company Limited, 2. Department od Civil Engineering, Gifu University

Multiple ridges and linear depressions continue about 12 km along the ridge from Tokugotoge Pass to Mount Chogatake. We examined geomorphic development of mountain slope from Tokugotoge to Tokusawa by means of interpretation on the precise DEM by airborne LIDAR, analysis of sediments in a linear depression and geological reconnaissance.

Micro landforms suggested deep seated gravitational slope deformation (DSGSD) such as linear depressions, uphill-facing scarplets and mid-slope steplets are widely developed in this area. They are unevenly distributed, are widespread on the northwest facing slope and are limited near the main ridge on the southwest facing slope. This tendency indicates that gravitational deformation ware formed under control of geologic structure of the Mino Belt. On the other hand, the micro landforms are developed concordantly with the bending of ridge from E-W to N-S trend, and are also recognized around the branching ridge with NW-SE trend, which means that the gravitational deformation originated after main geomorphic framework ware formed.

Result of geological reconnaissance reveals that the bedding plane of strata trends NE-SW and dips northwestward steeply, however, tends to dip southeast at the foot of slope facing to Azusagawa River. The bedrock is loosened intensely near the ridge top and the foot of slope. Furthermore, as the rock is loosened, the bedding plane dips gently, which suggests buckling or flow deformation of the rock mass. Predominant rock loosening restricted to the tributary valley bottom, though the depth of loose zone reaches over 100 m.

Horseshoe-shaped landslide scarps with a few hundred meters wide and tens of meters relative height are also developed in this area, whereas distinguished features of deep-seated landslide toe are hardly recognized. So it is assumed that the gravitationally deformed mass originated by rock loosening did not form deep-seated landslide body separated from sliding surface, but disintegrated into smaller scale surface rock failures.

Gravitational deformation arose after LGM at the latest because the DSGSD features are also seen on the lower slope to “Dissection front in Postglacial age.” Azusagawa River cut down into deep gorge at the foot of the slope until the damming by Akandana Volcano effusives 12.4 ka. The deformation is inferred to start at the time when the relative height to the ridge was larger than present. Since pyroclastic fall deposit from Yakedake Volcano before 2.3 ka buried ridge top depressions, then the depressions were already formed.

Keywords: precise DEM, gravitational slope deformation, geologic structural control, rock loosening, geomorphic development

©2020. Japan Geoscience Union. All Right Reserved.

Holocene gravitational rock slope deformation and large-scale landslide features in the western Kamikochi Valley, northern Japanese Alps

*Yoshihiko Kariya[1], Sadao Takaoka[1]

1. Department of Environmental Geography, Senshu University

Deep-seated gravitational slope deformation (DSGSD) is a remarkable precursor of catastrophic landslide phenomena in mountain areas. Also, DSGSD-derived micro-scale topographies such as linear depressions, unti-scarplets, and hummocks have been thought to be important elements for their creational role forming complex natural environments (i.e., differences in soil moisture, temperature, geomorphic processes, microclimates etc.). However, few attempts have been made to clarify historical development of DSGSD and related landforms in the Japanese high mountains. We carried out drilling survey using a portable auger and could obtain two cores from two linear depressions on Mount Nishihotaka-dake, both of which are developed on periglaciated DSGSD slopes of granodiorite (core: KNG-2017 and NSH-2018). Both cores contain altered layers of peat, humic silt, sand and gravel as well as tephras from a nearby volcano. Based on soil facies, age-depth models with ^{14}C and tephra dates, the onset of topographic formations and pedogenes would be back to the middle Holocene around 4000-5000 cal BP. During this period, according to previous authors, two events of large-scale catastrophic rock slide occurred just below the drilling sites, and paleoclimates had being recovered from minor unstable and cool periods. Formation and changes around the linear depressions were probably caused by coupling of local topographic changes and climate variability. Our data indicate long-term ($> 10^3$ y) slope changes in the alpin-subalpine zones.

Keywords: Deep-seated gravitational slope deformation, Rock avalanche, Granodiorite, Geomorphic change in alpine environments

©2020. Japan Geoscience Union. All Right Reserved.

Surface changes of rock slopes in the Shirouma-Daisekkei Valley, the Northern Japanese Alps

*Hirotaka Sugiyama[1], Chiyuki Narama[1], Hiroshi Inoue[2]

1. Niigata University, 2. National Research Institute for Earth Science and Disaster Resilience

In order to understand the geomorphological characteristics of slope failure points on rock slopes of the Shirouma-Daisekkei valley, we investigated the surface changes of rock slopes using three-dimensional topographic models based on SfM (structure from motion) with digital aerial images from the airplane, drone (Phantom4) and Cessna. Slope failure points and these surface changes were extracted by comparing three-dimensional topographic models. We clarified a difference in the slope depending on the slope direction at Mt.shakushi. The number and area of collapses have been more pronounced on southeast slopes than northeast slopes since 1976. For large slope failure in 2005, we clarified the rock mass of 60 m height and 10 m thickness was collapsed. In recent years, based on remote sensing and field investigations, rock slope retreat was confirmed in areas where joints developed more densely than surrounding those areas.

Keywords: rockfall, rock failure, SfM, Hakuba-Daisekkei, UAV

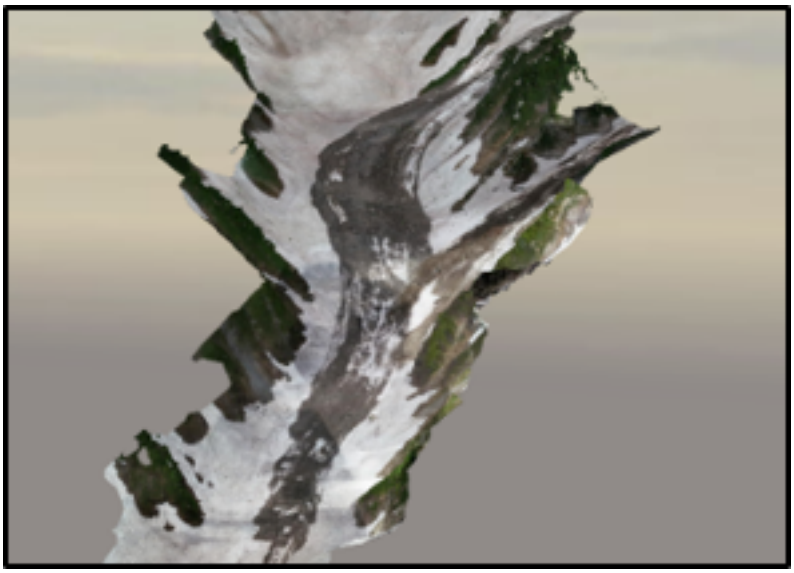

©2020. Japan Geoscience Union. All Right Reserved.

Surface changes of Ganpei landslide in Joetsu region

*Yutaka Inoue[3], Chiyuki Narama[1], Chunxiang Wang[2], Eiji Takita[2]

1. Niigata University, 2. KITAK Corporation, 3. Graduate Student,Niigata University

In a sliding landslide, surface change is not only an indicator of landslide topography extraction by remote sensing, but also a material for estimating the internal structure and landslide form of the landslide.However, at present, few studies have investigated the time series change of the landslide surface with high temporal resolution.

In this study, UAV aerial photographs and field surveys of the Ganpei landslide located in the eastern part of the Takada Plain, Joetsu City, Niigata Prefecture were conducted periodically to investigate the relationship between changes in surface topography and landslides.

Keywords: Landslide, GNSS, DInSAR, Surface change

©2020. Japan Geoscience Union. All Right Reserved.

The characteristic of ground motion amplification based on the Fourier spectrum ratio between surface and underground of the KiK-net seismic observation points - Basic study of landslides caused by earthquakes -

*Tomoyuki Iida[1], Chi-Wen Chen[1], Masato SATO[1], Hidemitsu Tokui[2], Tetsuya Onodera[2], Hiroshi Kawabe, Ryuji Yamada[1]

1. National Research Institute for Earth Science and Disaster Prevention, 2. Technicallinc Kabushiki kaisya

To evaluate ground motion amplification properties of earthquakes in the mountainous area is essential for a mechanism elucidation of landslides caused by earthquakes. Surface and underground seismometry records have been accumulated for more than 20 years after the 1995 Hyogo-ken-nambu Earthquake at the KiK-net observation points of the nationwide seismometry network. In the mountainous area, it is expected that the ground motion will be amplified by both the topography effect and by the ground effect. Nevertheless, the seismometry record of earthquakes in the mountainous area is hardly provided until now because there are very few observation points in the mountainous area.

A large number of small- and medium-scale earthquake data are provided by long-term observation of 14 KiK-net observation points located in mountainous areas. In addition, large earthquakes that triggered a large number of landslides can be successfully observed at some observation points in non-mountainous areas. The useful information about ground motion amplification properties of earthquakes in the mountainous area may be provided by combining these KiK-net observation data.

We collected acceleration records with PGA> 20 gal and analyzed the Fourier spectrum of ground motions (acceleration) at each KiK-net observation point by the following procedure.

1) For each earthquake, we calculated the Fourier spectrum of NS, EW, and UD components at the surface and underground.

2) For the surface and underground, we calculated the composition Fourier spectrum (the square root of the sum of squares of NS, EW, and UD components).

3) We calculated the ratio of the composition Fourier spectrum between the surface and underground for each frequency, which we call the amplification ratio spectrum. We then calculated the arithmetic mean of the amplification ratio spectrum of all earthquakes for each observation point, and call it the mean amplification ratio spectrum. We can consider it to be a kind of transfer function.

The following results were obtained.

1) The composition Fourier spectrum of the surface and underground changes according to the scale of earthquakes, but the amplification ratio spectrum does not change. The mean amplification ratio spectrum is considered to be an index in relation to the dominant frequency and amplification properties of each observation point.

2) The mean amplification ratio at frequency around 1 Hz is closed to 1, which means that there is no

©2020. Japan Geoscience Union. All Right Reserved.

amplification.

3) The 14 KiK-net observation points at mountainous areas can be separated into three groups A, B, and C. In the case of group A, the dominant frequency (5-10 Hz) is relatively clear, and the maximum mean amplification ratio is more than 10, which means that the ground is easy to shake. In the case of group B, the dominant frequency is not clear, and the maximum mean amplification ratio is less than 10, which means that the ground is relatively difficult to shake.

These findings may provide important information on landslides caused by earthquakes.

Keywords: Ground motion, KiK-net, Amplification property, Fourier spectrum, Transfer function

©2020. Japan Geoscience Union. All Right Reserved.

Gigantic landslides distributed in the upper course of Marsyandhi river in Nepal Great Himalaya

*Hiroshi YAGI[1], Yuki Matsushi[2], Hiroshi P Sato[3], Akihiko Wakai[4]

1. Faculty of Art, Science and Education, Yamagata University, 2. DPRI, Kyoto University, 3. College of Humanities and Sciences, Nihon University, 4. Faculty of Technology, Gunma University

There develop gigantic landslides of which scale are more than half billion cubic meters along the upper course of Marsyandhi river in the Nepal Great Himalaya just behind the Annapurna Himal. Landslides in scale of million cubic meters are also sporadically distributed along the gorge which the Marsyandhi divides Annapurna & Manasul massifs. Some of them are absence of their detritus. Such phenomena indicate that the huge volume of detritus were flushed away to the down stream as debris flow.

Keywords: Nepal Great Himalaya, gigantic landslide, Marsyandhi river

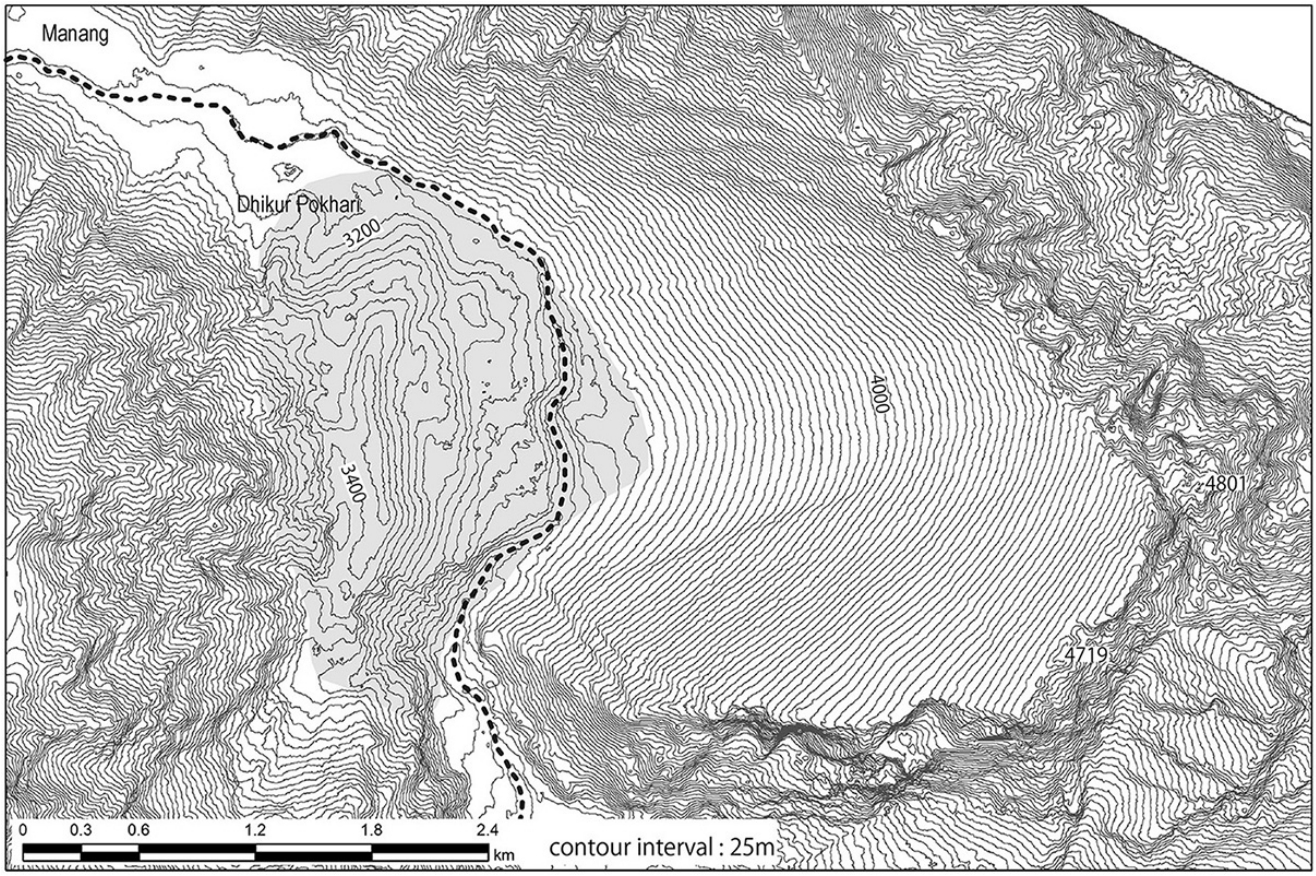

©2020. Japan Geoscience Union. All Right Reserved.

[J] Poster | H (Human Geosciences)：H-RE Resource and Engineering Geology

[H-RE13] Resource Geology

convener:Tsubasa Otake(Division of Sustainable Resources Engineering, Faculty of Engineering, Hokkaido University), Ryohei Takahashi(Graduate School of International Resource Sciences, Akita University), Tatsuo Nozaki(Submarine Resources Research Center, Research Institute for Marine Resources Utilization, Japan Agency for Marine-Earth Science and Technology), Kenzo Sanematsu(Mineral Resource Research Group, Institute for Geo-Resources and Environment, Geological Survey of Japan, National Institute of Advanced Industrial Science and Technology)

Ore deposits containing valuable elements and minerals at high concentrations in supracrustal rocks are formed by the Earth's dynamics including magmatism, hydrothermal activity, metamorphism, and weathering. The formation of ore deposits is also closely associated with global environmental changes and biological evolution in the Earth's history. Involvement of difference academic fields in earth sciences including geology, petrology, geochemistry, mineralogy, and microbiology is required to understand the genesis of ore deposits. The field of resource geology is essential not only for efficient exploration and development of ore deposits but also for better understanding and assessment of hazardous elements that may be caused by the resource development. This session widely covers various topics of field investigation and observation, laboratory experiments, theoretical calculation, development of analytical methods and others related to the supracrustal migration and concentration of elements.

[HRE13-P01] Brecciation event elucidate the high energy processes involved in porphyry copper deposit

*Geri Agroli[1], Atsushi Okamoto[1], Masaoki Uno[1], Noriyoshi Tsuchiya[1] (1.Tohoku University)

[HRE13-P02] **Geology and geochemistry of the Chifumbazi and Mugomo gold prospects, Tete province, Mozambique**

*Euclesia Paulina Francisco Cossa[1], Ryohei Takahashi[1], Andrea Agangi[1], Pearlyn Manalo[1], Hinako Sato[1], Akira Imai[2] (1.Akita Univ. , 2.Kyushu Univ.)

[HRE13-P03] **High Temperature Silicified Zone as a Potential Caprocks for Supercritical Geothermal Reservoir**

*Fajar Febiani Amanda[1], Ryoichi Yamada[1], Masaoki Uno[1], Noriyoshi Tsuchiya[1] (1.Graduate School of Environmental Studies, Tohoku University)

[HRE13-P04] **The zircon Hf-isotope constraints on the distribution of mineral deposits in the Sukhothai Fold Belt, Thailand**

*Apivut Veeravinantanakul[1], Ryohei Takahashi[1], Andrea Agangi[1], Tsukasa Ohba[1], Yasushi Watanabe[1], Marlina Elburg[2], Henriette Ueckermann[2], Punya Charusiri[3,4] (1.Akita Univ., 2.Univ. of Johannesburg, 3.Chulalongkorn Univ., 4.DMR)

[HRE13-P05] Subseafloor mineralization in the Shimokawa Cu-Zn ore deposits in Hokkaido

*Masahito Ikeda[1], Tsubasa Otake[2], Nakayama Ken[3], Tsutomu Sato[2] (1.Division of Sustainable Resource Engineering, Graduate School of Engineering, Hokkaido University, 2.Division of Sustainable Resource Engineering, Faculty of Engineering, Hokkaido University, 3.Center for Advanced Marine Core Research, Kochi University)

[HRE13-P06] Contemporaneous occurrence of spheroidal dolomites and framboidal pyrites in the Shimokawa deposit, Hokkaido, Japan

*Ken Nakayama[1], Masafumi MURAYAMA[2] (1.Center for Advanced Marine Research, Kochi Univ., 2.Faculty of Agriculture and Marine Sciences, Kochi Univ.)

[HRE13-P07] Magnetite Ore Deposit of the Naka-Osaka Mine (Shimonita, Gunma Pref.) is probably IOA (Kiruna) type

*Atsushi MIYASHITA[1], Hiroyasu MURAKAMI[2], Wataru FUJITA[1], Masakazu RIKITA[3], Takashi ICHIKAWA[4], Tomohiko SEKIYA[5] (1.Seikei University, 2.Waseda University, 3.Shimonita Nature School, 4.Keyaki Special Support School, 5.Shimonita Geopark)

Brecciation event elucidate the high energy processes involved in porphyry copper deposit

*Geri Agroli[1], Atsushi Okamoto[1], Masaoki Uno[1], Noriyoshi Tsuchiya[1]

1. Tohoku University

Breccia is a common texture found in the subvolcanic environment, and vast amounts of mechanisms govern the formation of each individual texture. Scholars relate the breccia texture with high energy input in the magmatic-hydrothermal environment, and somehow, it marks the transient pressure shift from lithostatic to hydrostatic fluid regime. We conducted an investigation on breccia texture from Erdenet deposit, Mongolia, to deduce the formation mechanism and how energy release after magma emplacement. The previous study also mentions the initial intrusive body followed by the explosive brecciation on this deposit.

We retrieved ±700 m drilling samples from Erdenet Porphyry Cu-Mo. This porphyry was a product of the Permian-Early Triassic volcanic product situated in Orkhon-Selenge trough and its collision product of Siberian Craton and the Northern Mongolian block and generated vast amounts of intrusive activity. The breccia is a distinct texture observed at some depth along with the core samples at a depth of 8 m, 315 m, 679 m, where respective breccia exhibits different characteristics of matrices and clasts. The samples from 8 m depth consist of clast supported breccia where matrices comprise of Gp+Qz±Cal, and the clast consist of monolithic component of quartz porphyry+Qz. The 315 m samples depth shows the monolithic component composed of Qz+Pl+Chl+Py of aphanitic texture enclosed by the matrix of Cal+Qz. This breccia is matrix-supported, and the last breccia occurrences at a depth of 679 m consist of heterolithic clast of granodiorite porphyry+Qz+Ab+Cal+Chl+Kfs+Py. The matrices comprise of Py+Ccp+Qz+Bt. Ti-in-Qz geothermometer was performed on the matrix-quartz show that the deep breccia (679m) has Ti-content of 4-87 ppm correspond to the temperature at 471-731˚C while the sample from 315 m no Ti was detected from the matrix-quartz correspond to the temperature <400˚C.

This preliminary investigation gives us the general idea that the brecciation in the Erdenet system occurs in several stages; it could be related to the overpressurized-fluid release that traps under the impermeable layer since the impermeable sealing can present at several depths perhaps breccia form at variable circumstances within the upper crust. We suggest that 679 m breccia mark the first brecciation processes where the quartz that precipitates upon initial magma cooling (pre-mineralization), which underwent the fragmentation together with the host granodiorite porphyry. The subsequent brecciation (315 m) took place at lower P-T conditions (syn/post mineralization), and 8 m breccia mark the late stages of brecciation since the gypsum is the latest product of hydrothermal activity on Erdenet system (post mineralization).

Keywords: Erdenet Porphyry Cu-Mo, Breccia, Cathodoluminescence, High-Energy Processes

©2020. Japan Geoscience Union. All Right Reserved.

Geology and geochemistry of the Chifumbazi and Mugomo gold prospects, Tete province, Mozambique

*Euclesia Paulina Francisco Cossa[1], Ryohei Takahashi[1], Andrea Agangi[1], Pearlyn Manalo[1], Hinako Sato[1], Akira Imai[2]

1. Akita Univ. , 2. Kyushu Univ.

The Chifumbazi and Mugomo Au prospects are located in the northwestern part of Tete province [1,2]. The studied areas belong to the southern Irumide Belt consisting of the Proterozoic Mualadzi Group and the Furancungo Suite [1,3]. Gold mineralization of the Chifumbazi and Mugomo prospects has not been characterized yet and the processes of mineralization are still unresolved. Thus, this study aims to characterize the geology, gold mineralization and related hydrothermal alteration based on petrography, geochemical, fluid inclusion and sulfur isotope analyses of the host rocks, veins and ore minerals.

The host rocks of the Mugomo prospect are metavolcanic rocks, schist and silicified rocks cross-cut by quartz veins and epidote veins and veinlets. Pyrite, chalcopyrite, sphalerite, galena and bornite with minor Ag-Te and Bi-Te minerals occur within the quartz-epidote veins, as well as dissemination in the metavolcanic and silicified rocks.

The Chifumbazi prospect is characterized by carbonate quartz-chlorite and quartz veins hosted in granodiorite. Pyrite, chalcopyrite, arsenopyrite, pyrrhotite and bornite with minor sphalerite, covellite, galena and magnetite, occur both in the chlorite, quartz and carbonate-quartz veins and as dissemination in the granodiorite. The mineralization is related to the shear zone associated to a fracture system in different directions. The quartz veins are sub-horizontal, but in some cases, they dip to the south.

The metavolcanic rocks and schist at the Mugomo prospect were altered to quartz, chlorite and epidote, while the granodiorite at the Chifumbazi prospect was altered to illite, calcite and chlorite. Significant Au concentration was measured in the metavolcanic rocks in the Mugomo prospect (2 ppm) and in the quartz-carbonate veins in the Chifumbazi prospect (5 ppm). Sulfur isotopic compositions of sulfides in the Mugomo prospect ($\delta^{34}S$ = +2.5 to +4.0 ‰) are slightly higher than those in the Chifumbazi prospect ($\delta^{34}S$ = +1.0 to +2.5 ‰).

Keywords: Chifumbazi and Mugomo prospects, hydrothermal alteration, Gold, sulfur isotope

©2020. Japan Geoscience Union. All Right Reserved.

High Temperature Silicified Zone as a Potential Caprocks for Supercritical Geothermal Reservoir

*Fajar Febiani Amanda[1], Ryoichi Yamada[1], Masaoki Uno[1], Noriyoshi Tsuchiya[1]

1. Graduate School of Environmental Studies, Tohoku University

A supercritical geothermal reservoir is a promising energy resource for the future. The previous researchers have studied the availability of such a reservoir, including the presence of fluid and the permeability. However, the characteristic of the cap-rock as an entrapment structure of the heat is yet to be known. Silica is the most abundant material in the earth's crust, and its solubility in water is dependent on the pressure and temperature. Silica in the form of quartz commonly occurs as veins, whether it generated from the up-flow of the deep-seated fluid trough the fracture network or the diffusion from the host rock. It is also found in the form of a narrow zone or lenses of relatively impermeable rock as cement at the transition between brittle and plastic zone. In this study, we research the silicified zone in the porphyry-Cu deposit as a potential caprock for a supercritical geothermal reservoir.
The study was conducted in Tazawako Granite Complex, Akita Prefecture, Tohoku District. The area consisted of volcano-sedimentary rock sequences of Paleogene to Neogene age were deposited around a basement of Cretaceous granitoid (Osawa et al., 1981). The silicified rocks are commonly granitoid with porphyritic texture; Quartz and Feldspar as a major phenocryst in the aphanitic quartz matrix. SEM-CL (Cathodoluminescence) was taken to provide a better image of the internal structure of the quartz in the silicified rock. The quartz can be divided into the primary quartz, which is the relic of former granodiorite, and precipitated at the magmatic stage. The brittle failure observed intensively crisscrossing the quartz. The temperature of host quartz determined by Ti-in Quartz geothermometer (Wark and Watson, 2006) is 601 –675^{0}C and the homogenization temperature of fluid inclusion in this quartz is ~360 ^{0}C. The secondary quartz occurred as filling in the microfracture, identified by the dark and weak luminescence, and as an overgrowth of the primary quartz showing bright luminescence and weak zoning. The absence of Titanium and very low Titanium content were observed at this quartz. The fluid inclusion micro-thermometry conducted on secondary quartz shows a homogenization temperature of ~300^{0}C. The supercritical geothermal reservoir has a temperature typically at > 400^{0}C, which lies beyond the brittle region. The possible cap-rock for this system is the impermeable layer that formed between the brittle-plastic transition with a temperature of 370 –400^{0}C (Fournier, 1999). The homogenization temperature of fluid inclusion in the secondary quartz is relatively high (~300^{0}C) compared to hydrothermal quartz vein (~240^{0}C) found in the study area, and low compared to the primary quartz (~360 ^{0}C) of host granodiorite. Although the homogenization temperature cannot show the actual temperature of quartz formation, it can describe that the secondary quartz in silicified zone formed at the temperature lower than the granodiorite (601 –675^{0}C) which formed in lithostatic condition, but higher than the hydrothermal quartz vein which formed at the hydrostatic condition. The condition of the secondary quartz formation may explain the absent or very low detection of the Titanium content of this quartz.

Keywords: Fluid inclusion, Supercritical Geothermal, Silicified zone

©2020. Japan Geoscience Union. All Right Reserved.

The zircon Hf-isotope constraints on the distribution of mineral deposits in the Sukhothai Fold Belt, Thailand

*Apivut Veeravinantanakul[1], Ryohei Takahashi[1], Andrea Agangi[1], Tsukasa Ohba[1], Yasushi Watanabe[1], Marlina Elburg[2], Henriette Ueckermann[2], Punya Charusiri[3,4]

1. Akita Univ., 2. Univ. of Johannesburg, 3. Chulalongkorn Univ., 4. DMR

The Sukhothai Fold Belt (SFB) hosts several vein-type gold-antimony-base metal deposits and tungsten-antimony breccia-type deposits. Copper-antimony-lead sulfide minerals occurred at the contact zone of the youngest granite phase of the Tak Batholith [7], [8] which raises possibility of gold and sulfide minerals being genetically related to the intrusion of Late Triassic granitoids [1].

In this study, we use U-Pb dating and Hf isotope analysis of zircon in the granitoids in the SFB to discuss the relationship between magma sources and the associated mineralization. The granitoids in the SFB consist of granodiorites and granites, which occur mainly in the east and west of the belt, respectively. The results of U-Pb dating show that in the northern part of the SFB, the granitoids yielded an age of 243-227 Ma, while an age of 204 Ma was obtained from the granitoid in the southeastern part of the SFB. The Hf-isotope composition of granitoids in the SFB is characterized by both positive- ε Hf initial values (0.0 to +9.2) and negative- ε Hf initial values (-6.1 to 0.0), which indicate mixed source of magma, which include juvenile mantle and reworked crustal components.

A zircon Hf-isotope compilation including the data obtained in this study and previously reported ones [2], [3], [4], [5], [6], [9], [10] were used to prepare a map, that allows a comparison between magmatic source and mineral deposit distribution in Thailand. The magmatic source for the granitoids in the Loei Fold Belt is dominated by juvenile mantle-derived components, as shown by positive- ε Hf initial values (+4.1 to +11.0) [2], and contributed to porphyry system. In contrast, the Sibumasu Block and Inthanon Zone originated from reworked old crustal materials, as indicated by negative- ε Hf initial values (-27.1 to -5.4) [2], [3], [4], [5] [6], [9], and produced S-type granite-related tin-tungsten mineralization. On the other hand, the various ε Hf initial values (-8.1 to +9.2) [this study], [2], [3], [9], [10] from the intrusions in the SFB suggest mixed sources including evolved and juvenile magma materials, which generated the gold, antimony, and base metal vein deposits and tungsten-antimony breccia-type deposits.

Reference

[1] Crow and Khin Zaw. in Ridd. The Geol. Soc. 2011.
[2] Dew et al. Lithos. 2018.
[3] Dew et al. Data Brief. 2018.
[4] Gardiner et al. Gondwana Res. 2016.
[5] Gardiner et al. Sci. Rep. 2017.
[6] Gardiner et al. Gondwana Res. 2018.
[7] Mahawat et al. J. Southeast Asian Earth Sci. 1990.
[8] Pongsapich and Mahawat. Geol. Soc. Malaysia Bull. 1977.
[9] Wang et al. Gondwana Res. 2016.
[10] Wang et al. Lithos. 2016.

Keywords: Sukhothai Fold Belt, granitoid, zircon, U-Pb dating, Hf isotopes

©2020. Japan Geoscience Union. All Right Reserved.

©2020. Japan Geoscience Union. All Right Reserved.

Subseafloor mineralization in the Shimokawa Cu-Zn ore deposits in Hokkaido

*Masahito Ikeda[1], Tsubasa Otake[2], Nakayama Ken[3], Tsutomu Sato[2]

1. Division of Sustainable Resource Engineering, Graduate School of Engineering, Hokkaido University, 2. Division of Sustainable Resource Engineering, Faculty of Engineering, Hokkaido University, 3. Center for Advanced Marine Core Research, Kochi University

Many base metal deposits currently mined in the world were formed by ancient submarine hydrothermal activities, most of which have been considered to form on the seafloor as stratabound deposits. Recently, however, a replacement model, in which sulfide minerals were precipitated and concentrated by alteration and replacement of sediments beneath the seafloor, has been proposed in some sulfide deposits both for ancient and modern submarine hydrothermal ore deposits. Although, there is no such deposit reported in Japan, one example may be the Shimokawa base metal (e.g., cupper and zinc) deposit located in the northern part of Hokkaido, which was previously considered to be Bessi-type volcanogenic massive sulfide deposit. Therefore, objective of this study is to examine whether Shimokawa ore deposits were formed in the sub-seafloor based on distribution and petrographic characteristics of ore minerals and alteration products (e.g. clay minerals and decomposed organic matter) of both hanging and footwall rocks. Shimokawa ore deposits consist of Nakanosawa and Ochiaizawa ore bodies. Ore samples and slates from the hanging and footwall rocks used for the analyses were obtained from drill cores on Nakanosawa ore body and crosscut to Ochiaizawa ore body.

X-ray diffraction (XRD) results of the analyzed host rock samples show that chloritization and sericitization took place, not only in the footwall but also hanging wall samples, possibly by hydrothermal alteration. This is supported by increasing iron content in chlorite, which was indicated by its second to first intensity peak ratio in their XRD profiles. Furthermore, results of microscopic observation demonstrated that the hydrothermal activity responsible for the mineralization was divided into two stages: the early stage in which iron was mainly concentrated and the later stage in which copper and zinc was mainly concentrated. Distribution of the ore minerals formed by the later stage hydrothermal fluid, which flowed along diabase sill, indicates that the mineralization occurred epigenetically, after the formation of the sills. These results suggest that Shimokawa ore deposits were formed by hydrothermal activity beneath the seafloor and are, therefore, likely to represent sub-seafloor replacement ore deposits.

Keywords: submarine hydrothermal activity, copper, chlorite, marine sediments

©2020. Japan Geoscience Union. All Right Reserved.

Contemporaneous occurrence of spheroidal dolomites and framboidal pyrites in the Shimokawa deposit, Hokkaido, Japan

*Ken Nakayama[1], Masafumi MURAYAMA[2]

1. Center for Advanced Marine Research, Kochi Univ., 2. Faculty of Agriculture and Marine Sciences, Kochi Univ.

Primary dolomites are commonly associated with SEDEX deposits hosted in clastic rocks, but only known for volcanogenic massive sulfide deposits such as bimodal felsic, bimodal mafic and siliciclastic mafic sub-type deposits(1). It has slightly been reported in the submarine hydrothermal deposits and active hydrothermal fields such as the Middle Valley(2), Kagoshima Bay(3) and the Okinawa Trough (4). It became clear for the first time that spheroidal dolomites (SDs) containing framoidal pyrites (FPs) made up the carbonate matrix of pyrite ores in the Shimokawa deposit that was originated from the submarine hydrothermal deposit. This kind of pyrite ores containing SDs and FPs also occur in layered sulfides intercalated in argillites. The SDs with uniform diameter of 0.5 mm (±) are consisted of fibro radial dolomites and calcites infill the interstices of dolomites. Clear maltese crosses (black cross extinction) were observed under crossed polars. Fibrous dolomite crystals have a large number of inclusions and pores arranged parallel to the direction of fibers, and at the same time, pores that are arranged concentrically in the direction perpendicular to fibers. A ring nearly 10 μm width consisting of fine talc crystals develops inside the SD. FPs embedded within the dolomite cements range in diameter from 2.4 to 20.3 μm and relatively larger than that of syngenetic FPs (2.9~10.1 μm) in unaltered argillites away from the sulfide deposits. FPs are overgrown by petal-like pyrite crystals with a length of ~31.5 μm just like a sunflower and make aggregates. However no obvious spatial relationship between FP and SD is observed. TOC of argillites indicates 0.4-0.8wt%, whereas that of baked argillites adjacent to diabase sills records almost 0wt% due to thermal degradation of organic matter. Consequently CO_2, CH_4 and NH_3 caused by intrusion of sill are thought to have ascended via the interstices of the clastic particles and fissures, and seeped to the seafloor. The $\delta^{13}C_{PDB}$ of organic carbon in argillites shows -25.7‰ (n=53), whereas the $\delta^{13}C_{PDB}$ of matrix dolomites and calcites indicates -5.5 ‰(n=15) and -5.2‰ (n=4) respectively. That reflects the influence of pore seawater in unconsolidated sediments, which contain nearly 0‰ $\delta^{13}C_{PDB}$. Since dolomite is highly ordered crystal, it is necessary to overcome the kinetic barrier which prevents the dolomite nucleation(5). As indicated by the reaction as $CH_4 + SO_4^{2-} \rightarrow (HCO_3)^- + HS^- + H_2O$, decrease of SO_4^{2-}, increase in alkalinity and Mg^{2+}/Ca^{2+} caused by methane oxidation and bacterial sulfate reduction possibly promote the nucleation of dolomites and contemporaneous crystallization of FP. Although there have been reports that microbes were involved in the formation of spheroidal textures (6), but there is no positive evidence of microbial involvement in this study, and it is thought that heterogeneous nucleation due to increased supersaturation and rapid crystal growth, such as spherulites formed by polymers and quenched basaltic melts. We postulate that sulfide ores containing FPs and SDs in the Shimokawa deposit were precipitated under reduced environment just beneath the seafloor prior to the high temperature mineralization rich in chalcopyrites, pyrrhotites and sphalerites.

References

(1)Franklin *et al.*(2005) Economic Geology 100th Anniversary Volume,523-560., (2)Fouquet *et al.*(1998) ODP Initial Report 169,153-203., (3)Yamanaka *et al.*(2013) JVGR, 258, 74-84., (4)Miyoshi *et al.*(2014) Springer Open,567-586., (5)James and Jones (2015) AGU, 446p., (6)Gunatilaka(1989) JSP, 57, 922-927.

©2020. Japan Geoscience Union. All Right Reserved.

Keywords: Shimokawa deposit, spheroidal dolomite, sunflower framboidal pyrite, talc, sulfate reduction

©2020. Japan Geoscience Union. All Right Reserved.

Magnetite Ore Deposit of the Naka-Osaka Mine (Shimonita, Gunma Pref.) is probably IOA (Kiruna) type

*Atsushi MIYASHITA[1], Hiroyasu MURAKAMI[2], Wataru FUJITA[1], Masakazu RIKITA[3], Takashi ICHIKAWA[4], Tomohiko SEKIYA[5]

1. Seikei University, 2. Waseda University, 3. Shimonita Nature School, 4. Keyaki Special Support School, 5. Shimonita Geopark

The Naka-Osaka Mine in Shimonita, Gunma Prefecture, Japan, is the geosite of the Shimonita Geopark. This mine is also an industrial heritage site where iron manufacturing was carried out in the early Meiji era in Japan. It was produced high-grade magnetite ore. The Naka-Osaka Mine is located on the north side of the Ookitano-Iwayama tectonic line (the Median Tectonic Line of Japan). The iron ore deposit is composed of small but high-grade magnetite ore bodies, and are embedded in both the Nanjai Formation and the Namee Granite. The Nanjai Formation is correlative with the Jurassic Tanba-Mino accretionary complex. The 70Ma Namee Granite is correlative with the Cretaceous Ryoke I-type granite. The magnetite ore bodies are lenticular and/or vein shaped with wide alteration zones which are composed actinolite or hydro-biotite + chlorite with carbonate stock-work veinlets. Magnetite contains Si up to 3 wt.% and often contains euhedral Cl-apatite micro inclusions(Fig. 1). The small amount of sulfides (mainly pyrrhotite) is associated with the magnetite ore suggesting a low sulfidation state. The composite grain of loellingite and arsenopyrite often found with magnetite, and arsenopyrite contains high arsenic around 36 mol.%. The filling temperatures of primary fluid inclusions in fine fluorite veins are above 500˚C, which is a higher-temperature as compared with common hydrothermal deposits. Actinolite, hydro-biotite, and chlorite associated with magnetite contains up to 1 wt.% chlorine. These altered zones are not accompanied by acidic altered index minerals, such as alunite or kaolinite. Magnetite with apatite in a neutral to alkaline alteration zone at high temperatures above 500˚C in close to the large-scale tectonic line. These features of the Naka-Osaka mine strongly suggests that the magnetite ore deposit belongs to the iron oxide-apatite (IOA or Kiruna) type. The formation age of the ore deposit is younger than 70 Ma, which is one of the youngest IOA types in the world.

Keywords: Naka-Osaka Mine, Magnetite, Iron-Oxide Apatite Type, Kiruna Type, IOA Type, Shimonita Geopark

©2020. Japan Geoscience Union. All Right Reserved.

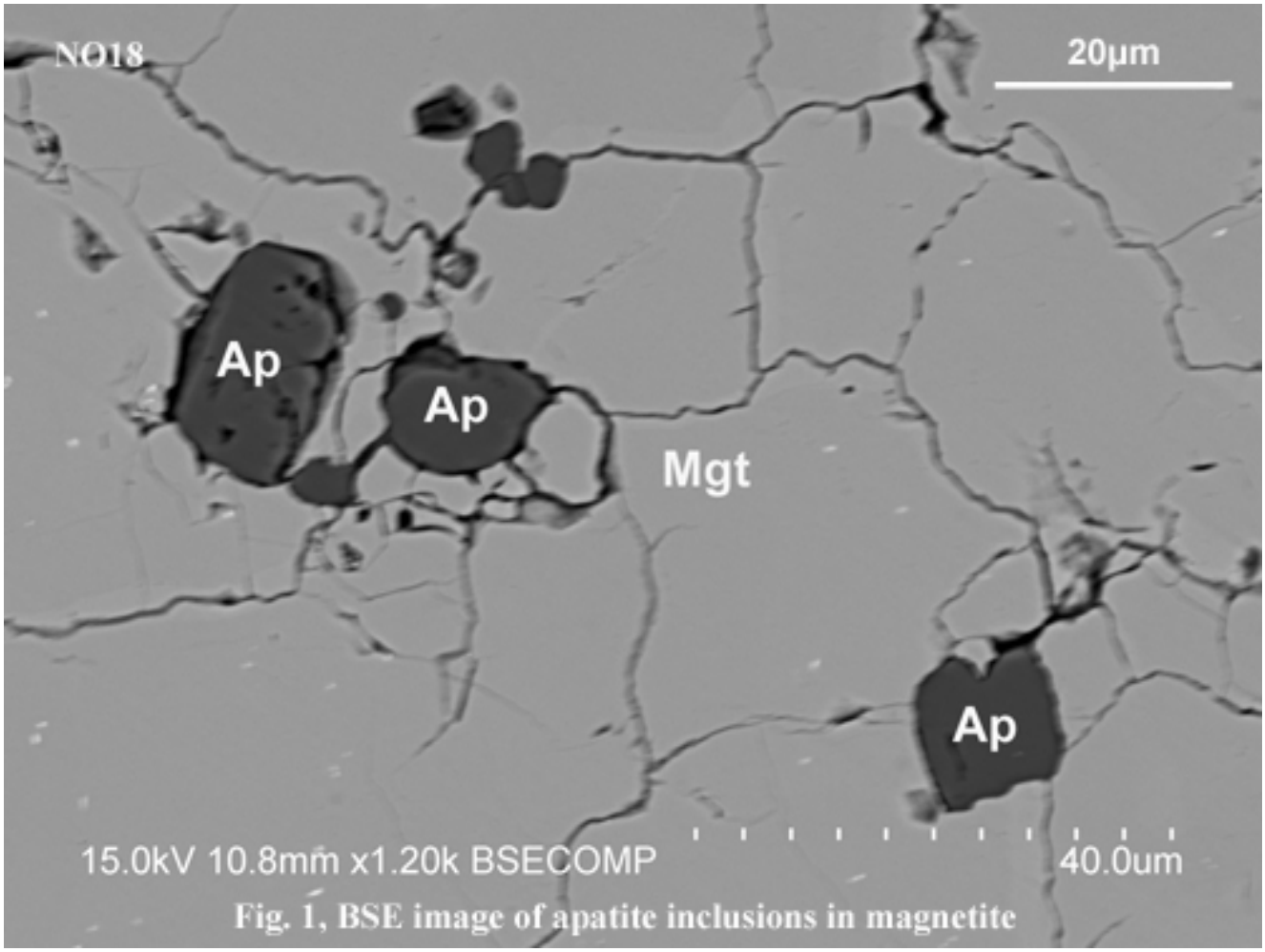

Fig. 1, BSE image of apatite inclusions in magnetite

©2020. Japan Geoscience Union. All Right Reserved.

[J] Poster | H (Human Geosciences)：H-TT Technology & Techniques

[H-TT16] Development and application of environmental traceability methods

convener:Ichiro Tayasu(Research Institute for Humanity and Nature), Ki-Cheol Shin(Research Institute for Humanity and Nature), Katsuyuki Yamashita(Graduate School of Natural Science and Technology, Okayama University)

Modern society uses almost all the elements present in the natural world. Although there have long been calls for the sustainable use of the resources that provide these elements and the building of human societies that are in harmony with the environment, the survival of the human race is increasingly at risk as a result of qualitative changes to the environment as a whole. Implementation by the society of methodologies for diagnosing and tracking these various elements of the natural environment and their relationships with humans are now required.
 Elements cycle within and among the Earth system spheres, human society and the human body. Information on the concentrations and stable isotopes of elements is powerful tool for tracing this cycling and has been applied in studies of atmosphere-hydrosphere circulation, ecological systems, and the life, health and history of humans. We propose a session to discuss development and applications of environmental traceability methods toward the goal of establishing traceability in natural and human systems.
 We encourage the presentation of research integrating isotopic information in various disciplines, such as geochemistry, hydrology, ecology, geology, mineralogy, anthropology, food science, and forensics.

[HTT16-P01] Comparative study of elementary runoff in the Tohoku basin and watershed based on numerical geographic information

*Yusuke Hataya[1] (1.Fukushima university)

[HTT16-P02] Neutralization of acid discharged water from the Kusatsu hot spring area of Japan utilizing industrial by-products

*Takeshi Saito[1], Naoki Watanabe[2] (1.Graduate School of Science and Engineering, Saitama University, 2.Research Institute for Natural Hazards and Disaster Recovery, Niigata University)

[HTT16-P03] Experimental and Simulation Study on the Migration Rule of Arsenic in the Soil of Surface Karst Zone in Southwest China

*bin zeng[1] (1.China University of Geosciences)

[HTT16-P04] Effects of natural and anthropogenic substances on atmospheric deposition in the Kyoto-Osaka-Kobe area using strontium and lead isotope ratios

Ryota Ando[1], *Yoriko Yokoo[1], Naoto Ishikawa[2], Ki-Cheol SHIN[3] (1.Faculty of Science and Engineering, Doshisha University, 2.Faculty of Sustainable Design, Toyama University, 3.RIHN)

[HTT16-P05] Analysis of nitrogen and phosphorus loading in Saijo Plain using trace elements as tracer

*Minoru TOKUMASU[1], Ki-Cheol SHIN[2], Yoshihiro YAMADA[3] (1.The United Graduate School of Agricultural Sciences, Ehime University, 2.The Research Institute for Humanity and Nature, 3.The Faculty of Agriculture of Kagawa University)

[HTT16-P06] Sulfur and Oxygen Isotopic Ratios of Rain Water Sulfate at Tottori-Okayama and Water-soluble Sulfate Ion in Suspended Particulate Matter at Okayama City

*Hitoshi CHIBA[1], Tatsuya Fujiike[1], Tsubasa Yamamoto[1] (1.Department of Earth Sciences, Okayama University)

[HTT16-P08] Characteristics of stable isotopes in monthly precipitation at Oshino village and northern slope of Mt. Fuji from Dec. 2016 to Mar. 2020

*Shiho Yabusaki[1], Makoto Taniguchi[1], Ichiro Tayasu[1], Tomoya Akimichi[1], Noboru Ohomori[2], Souichirou Watanabe[2], Hisamaru Osada[2], Ken Goto[2] (1. Research Institute for Humanity and Nature, 2.Oshino Village office)

Comparative study of elementary runoff in the Tohoku basin and watershed based on numerical geographic information

*Yusuke Hataya[1]

1. Fukushima university

In this study, we tried to obtain the relationship between the regional characteristics (climate, topography, geology, soil) of the basin and the chemical data obtained from the observation using numerical geographic information, and tried to analyze the current environmental conditions. The regional characteristics of the basin based on the digital geographic information were classified by cluster analysis to handle a large amount of data. Chemical data were obtained by analyzing water samples by inductively coupled plasma mass spectrometry (ICP-MS). Analysis of both data clarified the characteristics of the basin. By developing this data, the reference value of the current base can be set. By coexisting with monitoring, it is possible to identify the impact on the watershed in response to environmental changes such as land development. Therefore, useful databases for sustainable development are being developed. The target area is several rivers (upstream and downstream) in the Tohoku region.

The results of multi-element analysis of the reservoir outflow area (upstream area) and the end of a first-class river (downstream area) are shown. Regarding the total amount of multi-elements, the upstream basin tends to increase in proportion to the basin area. In the lower basin, the Natori River showed a high total amount despite its small basin area (939 km2). Concentrations of material components per unit area tended to be higher in the Pacific Ocean on the upstream side. In the lower basin, there was no particular geographical trend, but the results showed that the Natori River was nearly three times higher than the other rivers.

According to the cluster analysis, in the upper basin, the climate was divided into four groups, six in land cover, four in topography, and nine in geology. In the river basin, the climate was divided into three categories: four for land cover, four for topography, and three for geology. In general, the number of sections in the upstream area increases, and it becomes clear that dense features are less likely to appear in wider areas. Due to this effect, similar results were obtained in the upstream basin, but similar regions could not be extracted in the river basin.
In comparison with the results of multi-element analysis, watershed conditions with a higher elemental load per unit area were obtained for the upstream basin and river basin. In the upper basin, the climate is heavy basin with annual precipitation of 2,500 mm or more and heavy snowfall with a snow depth of 250 cm or more (Group 5), and the land cover is occupied by natural vegetation in the beech class area and deciduous broad-leaved forest zones by compensated vegetation Watersheds including high alpine and subalpine belts (Group5), topography is about 20km in length, and riverbeds have moderate riverbed gradients (Group4). Geology is occupation ratio of specific geology such as granite and pumice. Became a large basin (Group4). In the river basin, the climate is relatively low rainfall with an annual rainfall of about 2000 mm, the basin with a snow depth of less than 160 cm (Group 1), and the land cover is the riverside and wetlands. The watershed (Group 1), which includes many swamps and dune vegetation, and has relatively many other (human activity areas), the topography is small, with a watershed area of 1,000 km2 or less and a channel length of 70 km or less, and exhibits a steep slope with a riverbed gradient of 0.0016 or more. The basin (Group 4) and the geology became the basin (Group 3) where the occupation ratio of mud, mudstone and tuff was large.

©2020. Japan Geoscience Union. All Right Reserved.

The commonality of the large basins with large chemical effluent components per unit area in the upstream basin was relatively clear, while the commonality in the downstream basin was unclear. However, as a commonality of the relationship between the regional characteristics of the upstream and downstream basins and the increase in chemical runoff components, the basins with a high geological distribution occupation ratio that tend to be finer in both the upstream and downstream basins tend to have higher loads per unit area. It was revealed that there was. Due to the fine particle size, the solubility is high, and it is assumed that the process easily contributes to the increase in the load of chemical components.

Keywords: ipc-ms, multivariate analysis, geographic information system

©2020. Japan Geoscience Union. All Right Reserved.

Neutralization of acid discharged water from the Kusatsu hot spring area of Japan utilizing industrial by-products

*Takeshi Saito[1], Naoki Watanabe[2]

1. Graduate School of Science and Engineering, Saitama University, 2. Research Institute for Natural Hazards and Disaster Recovery, Niigata University

The Kusatsu hot spring as one of the most famous acidic hot springs in Japan and closed mines taking Sulphur are located in the Eastern foot of Mt. Kusatsu-Shirane as an active volcano. The Yukawa river composed of the acid discharged water from the hot spring area is characterized by low pH value (less than 2.0) and high concentration of harmful chemical constituents such as Arsenic (As), Lead (Pb), and Fluorine (F). The neutralization treatment utilizing crushed limestone has been continuously carried out by the Ministry of Land, Infrastructure, Transport and Tourism (government of Japan) over 50 years. In this study, temporal and spatial variations of water quality in the Kusatsu hot spring area were investigated and the applicability of industrial by-products as alternative liming agents was experimentally examined. Acid discharged water and river water were obtained from the Kusatsu hot spring area. Water temperature, pH, and electric conductivity were performed at the sampling site. Concentration of major ions and heavy metals was measured after filtering the water samples. The batch neutralization experiment was conducted for the acid discharged water from the Kusatsu hot spring utilizing industrial by-products including fly ash, clinker ash, steel slug, autoclaved lightweight aerated concrete, and recycled concrete. Centrifuge tubes with 50 mL volume were filled with 4 g or 0.4 g of each waste material and 40 mL of the acid discharged water. The prepared tubes were shaken for 10 minutes, 1 hour, 3 hours, 12 hours, and 24 hours. Measurements of pH and heavy metal concentration were immediately performed. The acid discharged water showed significantly lower pH value (1.6 to 2.0) and relatively high concentration of As and Pb. Based on the result of batch neutralization experiment, steel slug and recycled concrete showed relatively high neutralization performance if compared to limestone used in the Kusatsu hot spring area.

Keywords: Kusatsu hot spring area, Acid discharged water, Water quality, Neutralization, Industrial by-products

©2020. Japan Geoscience Union. All Right Reserved.

Experimental and Simulation Study on the Migration Rule of Arsenic in the Soil of Surface Karst Zone in Southwest China

*bin zeng[1]

1. China University of Geosciences

Karst Underground River is an important water source in southwest China. In addition to entering and polluting the groundwater directly through the sinkholes, arsenic pollutants produced from the industrial production process will also adsorb, remain, and concentrate in the dissolution cracks and gaps in the surface karst zone, and remigrate under certain conditions to become a "secondary pollution source". Taking an arsenic pollution event in Guangxi province as an example, the dynamic adsorption and desorption experiments of arsenic were carried out by using narrow slot physical model device, and the migration rule of arsenic contamination in the soil of surface karst zone was studied, combined with geochemical simulation. The experimental results show that the adsorption of arsenic in the surface karst zone is mainly physical adsorption (diffusion process), and the desorption rate is slow compared with the adsorption process, while the acid solution can promote the desorption process of arsenic compared with deionized water. The results of geochemical simulation show that goethite contributes most to arsenic adsorption in soil minerals, while acid solution weakens the ability of arsenic adsorption by corroding goethite and other minerals. It is concluded that in the karst area of southwest China, once the surface karst zone system is integrated with arsenic pollutants, the desorption process is slow, and it is easy to form the retention and enrichment of arsenic pollutants; while the accelerated desorption and migration process of arsenic under acid rain will increase the pollution risk of groundwater system.

Keywords: surface karst zone, arsenic pollution, physical model experiment, geochemical simulation

©2020. Japan Geoscience Union. All Right Reserved.

Effects of natural and anthropogenic substances on atmospheric deposition in the Kyoto-Osaka-Kobe area using strontium and lead isotope ratios

Ryota Ando[1], *Yoriko Yokoo[1], Naoto Ishikawa[2], Ki-Cheol SHIN[3]

1. Faculty of Science and Engineering, Doshisha University, 2. Faculty of Sustainable Design, Toyama University, 3. RIHN

In order to evaluate the atmospheric environment, strontium and lead isotope ratios of monthly soluble particles (precipitation; < 0.2 μm) and solid particles (air dust; > 0.2 μm) in rainwater samples were determined. Rainwater samples were collected in Kyoto city and Kyotanabe city (Kyoto prefecture), in Neyagawa city (Osaka prefecture) and in Nishinomiya city (Hyogo prefecture) from January 2010 to December 2011. Sr isotope ratios ($^{87}Sr/^{86}Sr$) and Pb isotope ratios ($^{207}Pb/^{206}Pb$, $^{208}Pb/^{206}Pb$) of the precipitation and the dust after filtering rainwater samples were analyzed using MC-ICPMS.

Monthly $^{87}Sr/^{86}Sr$ of the precipitation ranged from 0.7087 to 0.7107 and monthly $^{87}Sr/^{86}Sr$ of the dust ranged from 0.7081 to 0.7171. Both $^{87}Sr/^{86}Sr$ were higher during spring, and lower during summer and autumn. Higher $^{87}Sr/^{86}Sr$ during spring showed the close value of Chinese loess which is an origin substance of yellow sand. The maximum $^{87}Sr/^{86}Sr$ in Kyotanabe in 2010 was higher than that in 2011. According to the Meteorological Agency, yellow sand was transported much in the spring of 2010 compared to 2011. These results indicate that yellow sand is one of the origin of the dust and the influence of yellow sand on the dust varied depending on the year.

Monthly $^{207}Pb/^{206}Pb$ of the precipitation ranged from 0.859 to 0.889 and $^{208}Pb/^{206}Pb$ ranged from 2.093 to 2.137. Monthly $^{207}Pb/^{206}Pb$ of the dust ranged from 0.851 to 0.891 and $^{208}Pb/^{206}Pb$ ranged from 2.084 to 2.140. Pb isotope ratios of precipitation and dust were almost the same. Monthly $^{207}Pb/^{206}Pb$ and $^{208}Pb/^{206}Pb$ increased in the order of Kyoto, Kyotanabe, Neyagawa, and with Nishinomiya having the most increase. Values varied depending on the sampling seasons. In Kyoto, monthly Pb isotope ratios of the precipitation and the dust had a narrow range; $^{207}Pb/^{206}Pb$ ranged from 0.859 to 0.866 and $^{208}Pb/^{206}Pb$ ranged from 2.097 to 2.109. These indicated that Pb in the precipitation and dust at Kyoto had one substance with a certain Pbisotope ratio or had multiple Pb sources mixed at the same rate throughout the year. Kyoto is located in a mountain basin, and the inflow and outflow of air could be less than that of the other three locations. Therefore, monthly Pb isotope ratios may have changed less throughout the year. On the other hand, in Kyotanabe, Neyagawa and Nishinomiya, Pb isotope ratios varied widely depending on the sampling seasons. These results show that there were multiple sources of Pb in both precipitation and the dust and the mixing ratio changed depending on the season. In Kyotanabe and Nishinomiya, precipitation and dust showed higher Pb isotope ratios in winter, suggesting that they are affected by the transported Pb with high isotope ratio from the Asian continent.

Keywords: rainwater, Sr isotope, Pb isotope

©2020. Japan Geoscience Union. All Right Reserved.

Analysis of nitrogen and phosphorus loading in Saijo Plain using trace elements as tracer

*Minoru TOKUMASU[1], Ki-Cheol SHIN[2], Yoshihiro YAMADA[3]

1. The United Graduate School of Agricultural Sciences, Ehime University, 2. The Research Institute for Humanity and Nature, 3. The Faculty of Agriculture of Kagawa University

1. Introduction
River water sources in the Saijo Plain, Ehime Prefecture, are diverse irrigation water directly conducted from the Kamo River, shallow groundwater recharged from the Kamo River, and deep groundwater supplied from the hinterland of the Saijo Plain. Although it is difficult to grasp the water source quantitatively, Tokumasu et al. (2018) proposed a method of quantitatively analyzing the origin of river water using antimony as an index. In this study, using this method, we analyzed the origin of river water and clarified the effects of nitrogen and phosphorus loads from each water source and the effects of artificial loads from plains.

2. Materials and methods
On April 19 and 20, 2019, surface water was sampled at 43 small and medium rivers and waterways in the Saijo Plain on the right bank of the Kamo River, and each flows was measured by an electromagnetic velocimeter. The collected water was analyzed by ICP-MS for multi-elements, and the analysis of total nitrogen and total phosphorus was analyzed by the spectrophotometric method.

3. Results and Discussion
Using the antimony concentration of each water source (irrigation water, shallow groundwater, deep groundwater), the ratio of the water source at each point was calculated, and by multiplying the nitrogen and phosphorus concentration of each water source, the concentrations of natural resources without any human influence was obtained. The natural load was determined by multiplying the concentration of natural resources at each point by the flow rate. The lowest points are Stn. 11, 22, 23, 32, 33, 34, 36, 38 and 39.
Total nitrogen concentration was about 1 mg / L for irrigation water from Kamo River, and about 0.5 mg / L for shallow and deep groundwater. The concentration of natural resources estimated from the resource rate of water at the lowest point was 579 μg / L on average, and the load was 104 kg / day. On the other hand, the measured average concentration was 532 μg / L and the load was 95 kg / day, slightly lower than the natural load, and there was no increase in the balance due to the artificial load. This indicates that the artificial increase is within the range of natural purification such as trapping of particles in the riverbed, absorption by aquatic plants, and denitrification.
The total phosphorus concentration was about 10 μg / L for irrigation water from Kamo River, and about 10-30 μg / L for shallow and deep groundwater. Similarly to nitrogen, the natural concentration estimated from the resource ratio of the most downstream water was 21 μg / L, and the load was 3.7 kg / day. On the other hand, the measured average concentration was 36 μg / L, and the load was 6.4 kg / day and was 1.7 times the natural load. As for phosphorus, the balance shows that 0.7 times the natural load of phosphorus is present in the river water, indicating that there is an artificial load that exceeds natural purification.
Nitrogen has a mechanism of removal from water, such as denitrification. The nitrogen / phosphorus ratio of chemical fertilizers used for agriculture is approximately 1: 1 by weight, which is higher than the nitrogen / phosphorus ratio of biological substances. These are thought to be the causes of phosphorus

©2020. Japan Geoscience Union. All Right Reserved.

remaining in river water more easily than nitrogen due to artificial load.

Keywords: environmental tracer, antimony, artificial load

©2020. Japan Geoscience Union. All Right Reserved.

Sulfur and Oxygen Isotopic Ratios of Rain Water Sulfate at Tottori-Okayama and Water-soluble Sulfate Ion in Suspended Particulate Matter at Okayama City

*Hitoshi CHIBA[1], Tatsuya Fujiike[1], Tsubasa Yamamoto[1]

1. Department of Earth Sciences, Okayama University

In order to investigate secular change of cross-border pollution from China, we have collected monthly rain water samples at 7 sampling stations in Tottori and Okayama Prefectures and analyzed for their chemistry, isotopic compositions of water and sulfate ion. Also, we have collected suspended particulate matter (SPM) at Okayama University and analyzed their sulfur and oxygen isotopic compositions of water-soluble sulfate ion in order to evaluate contribution of SPM to rain water sulfate.

Rain water samples are collected as monthly composite. SPM is collected more than twice a month using high-volume sampler. The sampling duration of SPM is 4 days for each sampling. Therefore, data for rain water samples represents a monthly average value, and each data of SPM represents an event within 4 days.

Annual sulfur isotopic composition of nss-sulfate in rain water is higher at the Sea of Japan side and lower at the Seto Inland Sea side. This means only small amount of the cross-border pollution originating from coal combustion in China reaches Set Inland Sea area by crossing Chugoku Mountains. Sulfur isotopic ratios of nss-sulfate is generally high in winter and low in summer, indicating cross border pollution from China mainly occurs in winter. However, this phenomenon is not clear in some year, especially in 2018.

Oxygen isotopic composition of nss-sulfate in rain water is high in spring at all the sampling stations. This may be due to the yellow sand events in spring.

Sulfur isotopic composition of water-soluble sulfate in SPM is similar or slightly lower than that of rain water sulfate. Oxygen isotopic composition of SPM is also similar or slightly lower than that of rain water sulfate in summer, autumn and winter. However, it is higher than that of rain water sulfate sometimes in spring. The timing when oxygen isotopic composition of SPM becomes higher that of rain water sulfate coincides with the period of high oxygen isotopic composition of rain water sulfate and yellow sand event. Therefore, high oxygen isotopic composition of rain water sulfate likely indicates the contribution of water-soluble component of yellow sand.

Keywords: Rain water sulfate, Sulfate ion in Suspended Particulate Matter, Sulfur isotope ratio, Oxygen isotope ratio, Okayama

©2020. Japan Geoscience Union. All Right Reserved.

Characteristics of stable isotopes in monthly precipitation at Oshino village and northern slope of Mt. Fuji from Dec. 2016 to Mar. 2020

*Shiho Yabusaki[1], Makoto Taniguchi[1], Ichiro Tayasu[1], Tomoya Akimichi[1], Noboru Ohomori[2], Souichirou Watanabe[2], Hisamaru Osada[2], Ken Goto[2]

1. Research Institute for Humanity and Nature, 2. Oshino Village office

Monthly precipitation has been sampled at 11 sites, whose altitude is from 953 m to 2296 m, in Oshino village and northern slope of Mt. Fuji since December 2016 for using to estimate the recharge area of springs and groundwater in Oshino village. Temporal variation of isotope ratios ($\delta^{18}O$ and $\delta^{2}H$) in monthly precipitation at 11 sites indicates almost same tendency. Isotope ratios are relatively low on June and December-January, because of rainy season and snow event. The d-excess values show a seasonal variation clearly, that is low in the warm period (from April to September) and high in the cold period (from October to March). The $\delta^{18}O$- $\delta^{2}H$ regression line (LMWL) is $\delta^{2}H = 7.7\,\delta^{18}O + 10.2$ (r^2=0.921), and almost all data in monthly precipitation are plotted along the LMWL. For dividing into the warm period (Apr.-Sep.) and cold period (Oct.-Mar.), regression line is $\delta^{2}H = 7.9\,\delta^{18}O + 9.0$ (r^2=0.975) and $\delta^{2}H = 7.8\,\delta^{18}O + 15.5$ (r^2=0.945), respectively. As a result of comparison between monthly precipitation amount and isotope ratios, the relation is not clearly, nevertheless, in the case when using the average values of all observed data, negative correlation is recognized clearly. Relation between air temperature and isotope ratios using the average values of all observed data also show strong positive correlation. From these results, thus it can be said that there is an amount effect and temperature effect when long-term data is used. On the other hand, isotope ratios of monthly precipitation decrease with increasing the altitude, therefore altitude effect is recognized. The altitude effect is -0.18 ‰/100 m for $\delta^{18}O$ and -1.43 ‰/100 m for $\delta^{2}H$, respectively.
In future, we will attempt to estimate the recharge area of Oshino-Hakkai springs and shallow and deep groundwater in Oshino village by using these observed isotope ratios of precipitation.

Keywords: Mt. Fuji, Oshino Village, precipitation, oxygen and hydrogen stable isotopes, altitude effect

©2020. Japan Geoscience Union. All Right Reserved.

[J] Poster | H (Human Geosciences)：H-TT Technology & Techniques

[H-TT17] Environmental Remote Sensing

convener:Hiroto Shimazaki(National Institute of Technology, Kisarazu College), Akihiko Kondoh(Center for Environmental Remote Sensing, Chiba University), HASEGAWA Hitoshi(Kokushikan University), Teppei Ishiuchi(Miyagi University)

Measuring environmental changes at various spatio-temporal scales is the key to improv
e our understanding of the relationship between human activities and environmental pro
blems. Remote sensing is a powerful tool to acquire information on the earth's surface fr
equently and repeatedly over a broad spatial scale, enabling us to find the changes whic
h might be related to the cause and consequence of environmental degradation. This ses
sion discusses the applications of remote sensing to the detection and monitoring of envi
ronmental changes in time and space, and aims to promote the knowledge-sharing for b
etter management of the environmental problems and natural disaster in any place in th
e world.

[HTT17-P01] Application of the Gaussian fitting for mineral composition mapping using airborne hyperspectral sensor data

*Yoshitoshi Tochikura[1], Yasushi Yamaguchi[1], Yukie Asano[2], Shuho Noda[2], Yuu Kawakami[2], Kazuo Masuda[2] (1.Nagoya Univ., 2.JOGMEC)

[HTT17-P02] **Analysis of vegetation recovery after shallow landslides: a comparative study between the Toyota City and the Shōbara City, Japan**

*CHENXI ZHONG[1], Wei Yang[2], Akihiko Kondoh[2] (1.Graduate School of Science and Engineering, Chiba University, 2.Center for Environment Remote Sensing, Chiba University)

[HTT17-P03] **Land Use and Land Cover Change and Its Factor Analysis in Dakhla Oasis and Kharga Oasis in New Valley Province, Egypt**

*Xuechen Wang[1], Akihiko Kondoh[2] (1.Graduate School of Science and Engineering, Chiba University, 2.Center for Environmental Remote Sensing, Chiba University)

[HTT17-P04] High-Resolution Irrigated Area Mapping in Dakhla and Kharga Oasis, Egypt, from 2015 to 2019 Using Sentinel-2 Data

*AYIHUMAIER HALIPU[1], Akihiko Kondoh[2] (1.Graduate School of Science and Engineering, 2.Center for Environmental Remote Sensing Chiba University)

Application of the Gaussian fitting for mineral composition mapping using airborne hyperspectral sensor data

*Yoshitoshi Tochikura[1], Yasushi Yamaguchi[1], Yukie Asano[2], Shuho Noda[2], Yuu Kawakami[2], Kazuo Masuda[2]

1. Nagoya Univ., 2. JOGMEC

Mineralogical and lithological mapping by remote sensing widely used in the early stages of metals exploration to narrow down the area with high resource potential. Since clay and carbonate minerals have diagnostic absorption features in the visible to short-wavelength-infrared regions, we can know the types and chemical compositions of these minerals at a target area by determining the wavelength of absorption features observed by remote sensing. The change in absorption associated with difference in mineral types is usually larger than several tens of nanometers. Also, slight change (< 10 nm) in the absorption center can be observed depending on variation of solid solution composition of a mineral.

Today, spaceborne and airborne hyperspectral sensors with higher spectral resolution is available, but still have a spectral resolution of only 5 to 15 nm that is not high enough to detect the slight change for the purpose of mineral mapping. The objectives of this study are to develop a method that allows us to accurately detect the absorption center wavelength from a reflectance spectrum obtained by the hyperspectral sensor and to evaluated the performance of the proposed method.

In this study, it is assumed that the absorption by a single factor in the mineral could be expressed by a Gaussian function, and that the reflectance spectrum observed by the sensor could be expressed by the sum of multiple Gaussian functions. The outline of the proposed method is as follows: First, Continuum Removal (CR) is applied to the observed reflectance spectrum to enhance absorption peaks. Thereafter, the approximate wavelength of the absorption peaks is obtained from the continuous transformation, and is used as the initial value for Gaussian fitting. The number of Gaussian functions used for fitting is gradually increased, and the fitting is terminated based on the error after fitting and the fitting parameters. Each Gaussian function is regarded as an absorption caused by each absorption factor in the mineral.

The performance of the proposed method was evaluated from two viewpoint. Firstly, we evaluated how accurately the proposed method could restore the original spectrum from the convolved and noise-added spectrum, simulated to correspond to the observation by a satellite or an aircraft sensor. Secondly, we evaluated how accurately the proposed method could detect the absorption peaks. A spectrum with known peaks was prepared and convolved to a simulated spectrum with lower spectral resolution in the same manner as the first evaluation. The original spectrum was compared with the simulated spectrum processed by the proposed method. These two performance evaluations showed the effectiveness of the proposed method and the accuracy of the absorption peak detection.
Finally, the proposed method was applied to actual image data obtained by airborne hyperspectral sensors (AVIRIS and AVIRIS-NG) and we compared the results with the field survey verification. To present the result obtained by the proposed method as an image, we employed the HSV color model by assigning absorption center wavelength to H (hue), absorption depth to S (saturation) and V (lightness), respectively. The Cuprite and Goldfield areas in Nevada, USA, and the Mountain Pass area in California, USA, were selected as test sites. The target minerals are epidote in the Cuprite area, alunite in the Goldfield area, and carbonate minerals in the Mountain Pass area. It was proven that the proposed method could successfully show the gradual shifts of the absorption center wavelength of these minerals

©2020. Japan Geoscience Union. All Right Reserved.

corresponding to the variation of chemical compositions. We also confirmed that the result was consistent with the field observations.

Keywords: Remote sensing, Geological mapping, Gaussian fitting

©2020. Japan Geoscience Union. All Right Reserved.

Analysis of vegetation recovery after shallow landslides: a comparative study between the Toyota City and the Shōbara City, Japan

*CHENXI ZHONG[1], Wei Yang[2], Akihiko Kondoh[2]

1. Graduate School of Science and Engineering, Chiba University, 2. Center for Environment Remote Sensing, Chiba University

Shallow landslides are instability events that lead to dramatic soil and vegetation mass wasting in sloping areas and are commonly triggered by intense rainfall episodes. Vegetation significantly affects hillslope hydrological and mechanical properties related to shallow landslides triggering. Vegetation recovery at shallow landslides sites not only plays an important role in reducing soil erosion and increasing land stability but also records the transformation of loose, exposed landslide surfaces into stable hillslopes during the post-landslide years. Therefore, it is important to evaluate the natural vegetation recovery processes and provide basic information on ecological aspects of the recovering environment after the shallow landslides. However, little is known about the vegetation recovery process or its influencing factors. The objective of this study is to clarify the relationship between vegetation recovery and topographic characteristics which include slope gradient and slope aspect after the shallow landslides, and to assess the influence of different geological structure on vegetation recovery. The comparative analysis was conducted at the shallow landslides areas of the Toyota City and the Shōbara City, which provide different geological structures of granite and rhyolite, respectively. With regard to monitoring of the vegetation recovery conditions, it is essential to develop the quantitative index coupled with remote sensing and Digital Elevation Model (DEM) for long-term assessment at shallow landslide sites. In this study we extracted the damage areas based on post-landslide and pre-landslide aerial photography. Using the long-term time series Landsat data, we calculated the post-landslide annual Fractional Vegetation Coverage (FVC), which was estimated from normalized difference vegetation index (NDVI). The FVC was then applied to determine the rate of vegetation recovery. We also evaluated topographic characteristics from DEM. Then analyzed the correlation between vegetation recovery rate and topographic characteristics in different geological structures. The results indicated that the vegetation recovery rate in the range of 10-20˚on slope gradient presented an increasing trend while that in the range of 23-30˚ showed a decreasing trend. In terms of slope aspect, the vegetation recovery rate in north and northeast was lower than others. The conclusion in this study would enable decision-making and policy-planning in disaster rehabilitation work.

Keywords: Shallow landslides, Remote sensing, Vegetation recovery, Topography, aerial photography

©2020. Japan Geoscience Union. All Right Reserved.

Land Use and Land Cover Change and Its Factor Analysis in Dakhla Oasis and Kharga Oasis in New Valley Province, Egypt

*Xuechen Wang[1], Akihiko Kondoh[2]

1. Graduate School of Science and Engineering, Chiba University, 2. Center for Environmental Remote Sensing, Chiba University

The only available water resource in extremely arid areas is groundwater, which is a limiting factor for agriculture. Understanding land use and land cover change (LUCC) and its driving factors is a crucial challenge for predicting the sustainability of livelihoods in extremely arid areas. The purpose of this study is to analyze land use and land cover changes in the typical extremely arid regions of Dakhla Oasis and Kharga Oasis (New Valley Province, Egypt) for 46 years (1973-2019) and their driving factors. In this study, we used Landsat MSS (1973-1976), TM (1984-2011), and OLI (2014-2019) satellite images, and used the object-based image classification method (OBIA) for obtaining land use and land cover maps. We achieved the high classification accuracy and performed LUCC analysis. In this study, five land cover types (i.e., cropland, urban, waterbody, trees, and desert) were divided, and the land use and land cover changes of Dakhla Oasis and Kharga Oasis were extracted. During the1973-2019, the cropland and urban areas of the Dakhla Oasis and Kharga Oasis gradually increased, changing from desert into cropland is an obvious land cover change. The type of land use/land cover change. The increase in cropland area implied that groundwater consumption is accelerating in the Dakhla Oasis and Kharga Oasis with almost no precipitation. The results from this study will provide useful information for the sustainable development of Dakhla Oasis and Kharga Oasis.

Keywords: Extremely arid area, LUCC, Image classification

©2020. Japan Geoscience Union. All Right Reserved.

High-Resolution Irrigated Area Mapping in Dakhla and Kharga Oasis, Egypt, from 2015 to 2019 Using Sentinel-2 Data

*AYIHUMAIER HALIPU[1], Akihiko Kondoh[2]

1. Graduate School of Science and Engineering, 2. Center for Environmental Remote Sensing Chiba University

With over 95% of the country's land being a vast desert, Egypt's agricultural land is limited to the Nile Valley, Delta, Oasis, and some arable land in Sinai. Agriculture in the Nile Valley and Delta area is strongly related to the Nile River, whereas agriculture in the oasis area is based on groundwater. Egypt's groundwater resources depend mainly on the Nubian sandstone aquifer system.
Unmanaged groundwater extraction in Dakhla and Kharga Oasis had led to several changes which can be seen in the hydraulic head patterns, and noticeable cones of depression have appeared since the beginning of the new valley project in the 1960s. (Iwasaki, 2013, Gad M.I,2011).
Water resources planning and managing in agriculture requires spatially specified information of irrigated area for various crop types and crop growing seasons. For arid areas like Egypt's oasis, making irrigation maps with the high spatiotemporal resolution is extremely paramount in formulating agricultural development, water resource utilization and management plans in this area.
Using a 10 m normalized difference vegetation index (NDVI) and normalized difference moisture index (NDMI) data from Sentinel 2, high-resolution irrigated area maps are developed for all the agroecological zones in Dakhla and Kharga Oasis in Egypt for the period of 2015-2019.
The irrigation maps were evaluated by using agricultural statistics from ground surveys and showed sufficient accuracy when compared to previously developed irrigation maps. It was demonstrated that irrigation was conducted twice a year in the study area, and the irrigation water volume relatively increased while the irrigation area increased year by year. According to statistical data, groundwater use in 2016 increased by 1.5 thousand square meters from 2015.
Based on this irrigation mapping, irrigation water usage on agricultural land in the study area can be determined, and information can be obtained which is useful for planning and managing water resources and building a sustainable water system in North Africa.

Keywords: Egypt, Oasis, Sentinel-2, Irrigation mapping

©2020. Japan Geoscience Union. All Right Reserved.

[J] Poster | H (Human Geosciences)：H-TT Technology & Techniques

[H-TT18] New Developments in Shallow Geophysics

convener:Kyosuke Onishi(Public Works Research Institute), Kunio Aoike(Oyo corporation), Tishiyuki Yokota(National Institute of Advanced Industrial Science and Technology), KEISUKE INOUE(National Agriculture and Food Research Organization)

The session of shallow geophysics calls various research topics to contribute on geophysical exploration techniques for the near surface. The shallow geophysics uses many types of methods to survey various targets. This session does not restrict any survey methods and targets of your research but restrict the target depth in the zones from 5 cm to 30 m (or from 2 in to 100 ft) below the surface of the ground. The shallow part under the ground may be the closest and unknown territory for human society, and advanced societies cannot have controlled it yet to avoid disasters caused by dynamics in the near surface. Peoples require techniques to manage levee, landslide and earth constructions and knowledge to control groundwater, liquefaction and soil pollution. The near surface faces many geotechnical, environmental and hydrogeologic problems. Major survey techniques are surface wave method, electric exploration, ground-penetrating radar and microtremor survey, but any methods can be discussed if your target is located in the shallow depths. This session also welcomes to discuss laboratory tests and rock physics for unconsolidated porous media in the vadose zone. Additionally, we will welcome not only cutting-edge technologies but also usual works, if the knowledge and skills is useful for human living. 3D will be one of main subjects in this year.

[HTT18-P01] An integrated GIS and Geophysical-based approach for geohazards risk assessment in coastal region: a Case study in Suez city, Egypt

*Youssef Mohammed Youssef[1,2], Michiaki - Sugita[2], Khaled Sayed Gemail [3], Saada Ahmed Saada[4], Mostafa - Teama[1], Mohammed ElBarqawy [5] (1.Department of Science and Mathematical Engineering, Faculty of Petroleum and Mining Engineering, Suez University, Suez 43518, Egypt, 2.Faculty of Life and Environmental Sciences, University of Tsukuba, Tsukuba 305-8572, Japan, 3.Environmental Geophysics Lab (ZEGL) Department of Geology, Faculty of Science, Zagazig University, Zagazig 44519, Egypt, 4.Department of Geology, Faculty of Science, Suez University, Suez 43518, Egypt, 5.Department of Geological Engineering, Faculty of Petroleum and Mining Engineering, Suez University, Suez 43518, Egypt)

[HTT18-P02] Shallow seismic imaging of the active fault integrated with other geophysical methods

*Nomin-Erdene Erdenetsogt[1], Tseedulam Khuut[2], Batsaikhan Tserenpil[1], Nyambayar Tsend-Ayush[1], Bayarsaikhan Enkhee[1] (1.Institute of Astronomy and Geophysics, Mongolian Academy of Sciences, 2.Mongolian University of Science and Technology)

[HTT18-P03] Shallow geophysical survey in Goshougake geothermal area.

*Yuya Tada[1], Shin'ya Sakanaka[1], Ryuichi Takei[1], Tomoya Moriwaki[1], Shogo Uechi[1], Shinpei Suzuki[1], Shinzi Ikuta[1] (1.Akita university)

[HTT18-P04] Seismic response characteristics in Fukuyama plain estimated by using the microtremor measurements

*Atsushi Mukai[1], Yukihiko Tsutsumi[1], Hiromu Ishio[1], Yuki Sawada[1] (1.Faculty of Urban Management, Fukuyama City University)

[HTT18-P05] Effects of Surface Geology on Seismic Motion of The 2011 Tohoku Earthquake in Monou-Cho, Ishinomaki

*Keisuke Mizutani[1], Yoshiya Oda[1] (1.Tokyo Metropolitan University)

[HTT18-P06] Data acquisition and analysis of three-dimensional resistivity survey by means of a distributed resistivity measurement system

*Hiroshi Kisanuki[1], Ken Sakurai[1] (1.OYO corporation)

[HTT18-P07] **An attempt to estimate the water level change of undamaged groundwater by earth resistance (II) - Preliminary observations at the PTU borehole in Musashino Upland -**

*Kunihiro Ryoki[1] (1.Polytechnic University)

[HTT18-P08] Development of 3D self-potential tomography for visualization of groundwater condition

*ayaka ishikawa[1], Katsumi Hattori[1] (1.chiba university)

[HTT18-P09] Development of nuclear magnetic resonance scanners for the nondestructive measurement of water fractions in boring cores

*Yoshito Nakashima[1] (1.National Institute of Advanced Industrial Science and Technology)

[HTT18-P10] A case study of 3-D GPR survey and the ground truth at test sites for detection of buried objects

*Takanori Ogahara[1], Kunio Aoike[1] (1.OYO Corporation)

[HTT18-P11] Identifying wetting areas of a concrete deck slab by time-lapse surveys using ground-penetrating radar

*Kyosuke Onishi[1], Takayuki Kobayashi[1], Tadashi Matsumoto[1], Tsubasa Noda[1] (1.Public Works Research Institute)

[HTT18-P12] Conjecture of sourcing wavelet conditions suitable for the simultaneous sourcing 3D seismic survey with the underwater speakers

*Mayu Ogawa[1], Seishiro Furuyama[1], Tetsuro Tsuru[1] (1.Tokyo University of Marine Science and Technology)

An integrated GIS and Geophysical-based approach for geohazards risk assessment in coastal region: a Case study in Suez city, Egypt

*Youssef Mohammed Youssef[1,2], Michiaki - Sugita[2], Khaled Sayed Gemail [3], Saada Ahmed Saada[4], Mostafa - Teama[1], Mohammed ElBarqawy [5]

1. Department of Science and Mathematical Engineering, Faculty of Petroleum and Mining Engineering, Suez University, Suez 43518, Egypt, 2. Faculty of Life and Environmental Sciences, University of Tsukuba, Tsukuba 305-8572, Japan, 3. Environmental Geophysics Lab (ZEGL) Department of Geology, Faculty of Science, Zagazig University, Zagazig 44519, Egypt, 4. Department of Geology, Faculty of Science, Suez University, Suez 43518, Egypt, 5. Department of Geological Engineering, Faculty of Petroleum and Mining Engineering, Suez University, Suez 43518, Egypt

In coastal regions, more precaution for urban expansion should be considered regarding hidden geological hazard from the existence of expansive clay soil and shallow groundwater level. These conditions cause huge damage to engineering constructions that leads to losses of human lives and financial property. However, very little studies were focused on hazard assessment of swelling clay potentiality using GIS approach, because its natures as occur slowly by time. The purpose of the present work is the analysis of geological–geotechnical factors to present a geo-hazard risk assessment model for the identification of high risk-prone regions in the coastal zone using an integrated GIS statistical system and Electrical Resistivity Tomography (ERT) mapping. Suez city (the case study area) is located in the northwest of the Gulf of Suez that has a vital and attractive global location for trading and investment. The geo-hazard model was created in a GIS environment by integrating thematic maps of possible controlling factors from ALOS-DEM image and available geological and geotechnical boreholes. These factors showed a varied ranges: slope (0-35˚), elevation (0-50 m), superficial soil (Conglomerate to silty clay), clay thickness (0-25 m), depth to groundwater (0-20 m), TDS (1000-35000 ppm), Cl-1 (500-17000 ppm), So4 (250-9000 ppm) and pH (6.8-8.7) and in conjunction with swelling potentiality (Liquid Limit (LL) (35-88 %), Plastic Index (PI) (12-62 %) and free Swelling (Sf) (35-150 %)). Assessment these factors causes kind of uncertainty during the evaluation procedure, thus all thematic maps were scored and weighted according to specified criteria to produce severity distributions maps. The crucial relationships between surface and subsurface factors were identified by employing geospatial qualitative and Pearson' correlation analysis. In the considered case, the clay soil is an inorganic cohesive type of high to a very high swelling degree. Among tested factors, the existence of clay soil and its thickness seem to play an important role to increase groundwater level that approach surface in several sites of Suez city, hence rising the risks of Total Dissolved Salts (TDS), Chloride (Cl-1), and augmenting swelling potential. Accordingly, the designed suitable relative weights were determined and all thematic maps were combined to produce a geo-hazard map using Simple Weighting Overlay (SWO) method. This approach illustrates the significant factors and the arithmetic weights assigned to each level of severity, and therefore they should be considered in similar studies. Geo-hazard map was produced with four degrees of severity for urban development: low, marginal, severe and very severe comprising 36.38, 40.28, 22.13 and 1.2 %, respectively, of the study area. The very severe area was observed mainly around El Kapanon district. An extensive field survey was performed, noted significantly high saline groundwater move into the sewage system. Seven 2D- ERT profiles were executed in this region using Dipole-Dipole (DD) array that integrated with available boreholes to establish a clear image for subsurface layers. The topsoil identified as gravelly sand (> 30 Ωm) extending down to - 3 m (a.s.l). A low resistivity layer (< 4 Ωm) attribute to thick silty clay observed underlined this topsoil, the clay behaviour in this area characterized by high swelling potentiality as indicated from near boreholes SZ-3 to SZ-7. The inverted sections were

©2020. Japan Geoscience Union. All Right Reserved.

used to create a 3D visualization by fitting all DD profiles. The result displays the existence of a buried channel of gravelly sand extending from the shoreline to city and underlined by thick clay soil more than 10 m that reduced the vertical infiltration rate. This suggested a lateral invasion of seawater usually occurred from a coastal part to the residential area during high tidal events in winter seasons. This continuous wetting caused the high salinity values and clay swelling measurements in this site. Therefore, government and urban planning should seriously consider treating proper action for current problematic conditions, before they become worse and affect the future development plan in this area. Overall, the results obtained in this study suggest that the GIS-based hazard model combined with localized ERT survey can be a vigorous tool for planning and management, by identifying the appropriate sites for environmental interventions and/or engineering risks.

Keywords: Geographic Information System, Geo-engineering , Electric Resistivity Tomography , Swelling , Geo-hazard map , Seawater

©2020. Japan Geoscience Union. All Right Reserved.

Shallow seismic imaging of the active fault integrated with other geophysical methods

*Nomin-Erdene Erdenetsogt[1], Tseedulam Khuut[2], Batsaikhan Tserenpil[1], Nyambayar Tsend-Ayush[1], Bayarsaikhan Enkhee[1]

1. Institute of Astronomy and Geophysics, Mongolian Academy of Sciences, 2. Mongolian University of Science and Technology

As the framework of 60 years of development of Astronomical and Geophysical science in modern Mongolia, various geophysical methods(electrical tomography, ground-penetrating radar and high resolution reflection-refraction seismic profiles) were used to imaging an active fault in depth range between few decimeters to few tens meters. An active fault was fractured by an earthquake magnitude 7.6 in 1967. After geophysical investigations, trench excavations were done at the sites to expose fault surfaces. The complex geophysical survey in the Mogod fault, Bulgan region of central Mongolia shows an interpretable reflection arrivals range of 5 m to 50 m with the potential for increased resolution. Reflection profiles were used to help interpret the significance of neotectonic surface deformation at the earthquake active fault. The interpreted profiles show a range of shallow fault structures and provide subsurface evidence with support of paleoseismologic trenching photos, electrical surveys, GPR sections.

Keywords: seismic reflection-refraction survey, seismic processing, shallow geophysical survey, Mogod fault

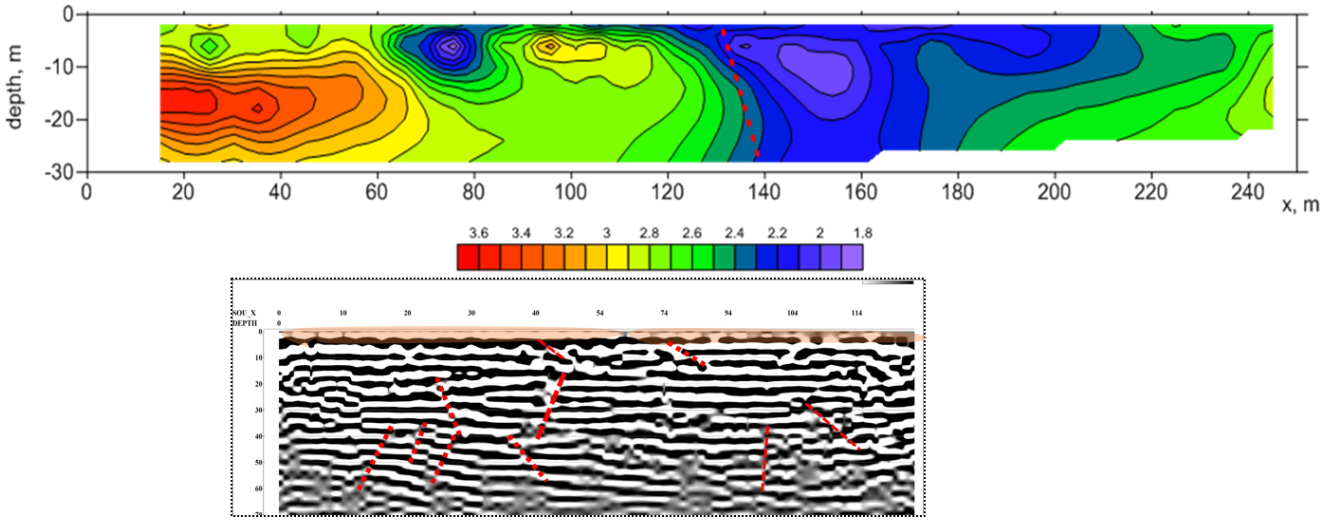

©2020. Japan Geoscience Union. All Right Reserved.

Shallow geophysical survey in Goshougake geothermal area.

*Yuya Tada[1], Shin'ya Sakanaka[1], Ryuichi Takei[1], Tomoya Moriwaki[1], Shogo Uechi[1], Shinpei Suzuki[1], Shinzi Ikuta[1]

1. Akita university

Mud volcanoes in Goshougake geothermal area are classified as high-temperature mud volcanoes, which related to magmatic volcanism of Akita Yakeyama volcano. There are various thermal features including fumaroles and hot spring in and around this area. The promenade in this place was broken by extruded mud and closed in fall 2017. For this reason, geophysical surveys were conducted to detect the pre-eruption mud volcanos.

In this field, ground penetrating radar survey has been performed and it has been reported that clear reflection groups appear locally on part of the survey line (Inoue et al., 2019). ERT and IP measurement by dipole-dipole arrangement were attempted several times in order to obtain the resistivity and the chargeability. However, there was a problem in data quality since enough potential difference could not be obtained. In this time, we performed ERT survey using a Wenner-Schramberger arrangement and obtained a higher-quality resistivity data. We used the ERT system of SYSCAL PRO with 48 electrodes at 2 m intervals. From this result, it was found that reflections of GPR became clear at a thick position of the high resistivity layer on the subsurface.

New survey lines were set along with the mud pots, which is located in a significant alteration zone in 2019. We used the ERT system of Handy-Arm with 32 electrodes at 0.75 m intervals to obtain data of the subsurface zone. From the results, it is clear that there is a low resistivity below 1 ohm m beneath this area, and it is inferred the relationship with the mud volcanoes.

In addition, Self-potential data were acquired along the promenade in the Goshougake Nature Research Road. Positive anomalies were found near Oname Motome and Oyunuma, while negative anomalies were found near Oodorokazan located on the east side, with a maximum potential difference of 85 mV. We are planning to measure more detail SP data again.

Keywords: GPR, ERT, Goshougake, Mud volcano

©2020. Japan Geoscience Union. All Right Reserved.

Seismic response characteristics in Fukuyama plain estimated by using the microtremor measurements

*Atsushi Mukai[1], Yukihiko Tsutsumi[1], Hiromu Ishio[1], Yuki Sawada[1]

1. Faculty of Urban Management, Fukuyama City University

Fukuyama plain had been reclaimed from the lagoon and has the complicated underground structure with the former shore reef areas and the former river beds. We performed the microtremor measurements in the plain and estimated the spatial distribution of seismic response characteristics. Major part of the plain has the low dominant frequency due to soft surface layer in the thickness of a few 10 m, while the dominant frequency in the former shore reef area is high (over 10 Hz). The estimated dominant frequencies in the plain show the complicated spatial distribution.

Fukuyama plain had filled up the lagoon with some shore reefs in the Edo era. The river branch of the Ashida river in the city was reclaimed in Taisho era as well. In this way, the Fukuyama plain has the complicated geological structure, although the plain is flat less than 5m above the sea level.

We can list the human damage and the structure damage due to the amplified seismic motions and the liquefaction as the serious natural disasters in the reclaimed ground. It is necessary to predict the seismic response characteristics and the liquefaction risk in order to reduce the disaster damage for the inhabitants. The adjacent areas in the plain might have large discrepancy in such a risk because of the complicated underground structure. Therefore, we performed the microtremor measurements in Fukuyama plains and estimated the dense spatial distribution in the seismic response characteristics. The measurements were mainly executed in the parks which density is about 10 parks to a square kilometer. The outputs from the accelerometers were filtered through the low-pass filter with cut-off frequency 40 Hz and were recorded at 100 Hz for ten minutes.

We used the H/V spectrum method developed by Nakamura et al.(1986) to estimate the seismic response characteristics by using the microtremor measurements. The H/V spectrum ratio is the amplitude ratio between the horizontal motion and the vertical motion. We can find two dominant frequencies in the H/V spectrum ratio obtained in Fukuyama plain. The higher dominant frequencies show the wide range in 1-20 Hz and could vary greatly even in small areas. The frequencies in the skirts of mountains and the former shore reef areas were obtained to be higher than 10 Hz, while those in major part of the plain were just a few Hz. On the other hand, the lower dominant frequencies show similar values about 0.7-0.9 Hz at every points.
It is considered that the higher dominant frequencies are mainly affected by the soft surface layer. We estimated the geological structure by using the H/V spectrum ratios. The thickness in the surface layer was obtained to be about 1-10 m at the former shore reef areas, while that was about 40-50 m in other areas. We found the underground structure due to the former river beds as well. The Fukuyama plain has the complicated distribution of geological structure and seismic response characteristics.

Keywords: microtremor measurement, Fukuyama plain, seismic response characteristics

©2020. Japan Geoscience Union. All Right Reserved.

Effects of Surface Geology on Seismic Motion of The 2011 Tohoku Earthquake in Monou-Cho, Ishinomaki

*Keisuke Mizutani[1], Yoshiya Oda[1]

1. Tokyo Metropolitan University

Monou-cho is located in Ishinomaki, Miyagi Prefecture. Oda and Toda (2011) conducted single microtremor measurements at 46 points along the Higashihama-Kaido in Ishinomaki, and investigated the predominant frequency from the H/V. In addition, damage investigation was conducted in same area using the method of Yahata and Yamazaki (2008), and the 310 houses in this area were visually ranked from A to F. This method and H/V were compared and evaluating the relationship between H/V and house damage. As a result, they revealed that predominant frequencies of area received significant destruction have multiplex peaks or broad range from 2 Hz to 4 Hz. However, the damage was not serious at all points where the predominant frequency was 2.5 Hz or higher. There was a fact that the damage was small in the area with predominant frequency around 1 Hz, which caused great damage during the Southern Hyogo Earthquake1995. From the above facts, issues such as the need to clarify the detailed underground structure and amplification characteristics in Monou-cho remain.

In this study, we evaluate the amplification of seismic motion in Momo-cho by comparing the house damage during the 2011 The Tohoku Earthquake investigated in Oda and Toda (2011), S-wave velocity structures obtained by using microtremor miniature array method and the seismic response of the 2011 The Tohoku Earthquake.

In this study, microtremor array observations were performed at 27 points, approximately 4km along the Higashihama-Kaido. Based on these observations, a dispersion curve is calculated by the Centerless Circular Array (CCA) method (Cho et. al., 2006). Then, S-wave velocity structures at each point were estimated by Simulated Annealing. The initial models for Simulated Annealing were generated from SIM (Simplified Inversion Method) (Pelekis and Athanasopoulos, 2011) and the nearby borehole data. Using these results, we analyzed the seismic response characteristics of the 2011 Tohoku Earthquake in Monou-cho using the equivalent linear analysis program (SHAKE91) based on the one-dimensional multi-reflection theory. In this analysis, we focused mainly on the acceleration response spectrum and the transfer function from basement to ground surface.

As a result of the estimation of the S-wave velocity structure, it was found that the basement was found at shallower location in the center of Monou-cho, and the basement was found deeper toward the north and south. In addition, it was found that the basement of the southern Monou-cho had a larger drop, and the basement was found deeper than the northern area. This basement is almost the same depth of the Onuki Formation in comparison with borehole data.

As a result of comparing S-wave velocity structure and the seismic response characteristics, the rank of the damage increased in the center of Monou-cho despite the small value of AVS30. A comparison between the acceleration response spectrum of the 2011 Tohoku Earthquake, the transfer function and the distribution of house damage, it is found that response acceleration in the range of 0.25 to 0.5 seconds was larger in the center of Monou-cho where house damage was larger. However, this is inconsistent with the conventional interpretation that the acceleration response spectrum with a period of 1-2 seconds affects house damage.

©2020. Japan Geoscience Union. All Right Reserved.

The acceleration response spectrum of the 1995 Hyogo-ken Nanbu Earthquake, the 2004 Chūetsu Earthquake and 2011 The Tohoku Earthquake at Nakatsuyama Daini Elementary School have peaks at the period of 1 second. It was found that peaks can be also confirmed around 0.25 to 0.5 seconds. In other words, the acceleration response around 0.25 to 0.5 seconds and 1 to 2 seconds may affect the damage of the wooden house. Near surface structure in the center of Monou-cho which amplify the ground motion around 2-3Hz (about 0.3-0.5 seconds) could be the factor that caused serious damage.

Keywords: Microtremor array method, Basement, Seismic response characteristics, Acceleration response spectrum, Transfer function, Local damage

©2020. Japan Geoscience Union. All Right Reserved.

Data acquisition and analysis of three-dimensional resistivity survey by means of a distributed resistivity measurement system

*Hiroshi Kisanuki[1], Ken Sakurai[1]

1. OYO corporation

Three-dimensional resistivity survey by means of a distributed resistivity measurement system was conducted to assess a usability of this new measurement system. Three-dimensional survey is the most effective method for evaluating underground structure accurately compared to one-dimensional and two-dimensional surveys. However, there are some issues for applying three-dimensional survey to geological investigation. For example, it requires a lot of measuring tools and takes a lot of time for data acquisition and processing.

The new system consists of two independent measuring parts which are transmission and reception ones (Truffert et al., 2017). The two parts are synchronized each other with GPS clock. Therefore, this system doesn’ t need to connect all electrodes with measuring instruments. In other words, long and heavy multichannel cables are unnecessary. We expected that this point enables us to save a quantity of work dramatically.

The survey was carried out at OYO Tsukuba site. The survey area was 48 m in length and 48 m in width. We used a total of 16 receivers and injected current at 40 points. One receiver can record 2 channels by using three electrodes. They were set in L-shape at 4 m spacing.

As a result, a total of 1280 data was obtained. A few data showed negative apparent resistivity. Generally, resistivity inversion uses the logarithm of apparent resistivity as the data parameter. If negative value contains in the data, inversion process fails. In order to solve this problem, the new inversion process was proposed by Loke et al(2019). In this process, the data were converted to amplitude and direction by composition of two direction data which was obtained by one receiver. We incorporated this new inversion process to our software which we have been developing. The inversion process could execute stably because amplitude showed always positive value.

In conclusion, the new measurement system was useful for designing electrode arrangement and setting measurement tools because this doesn't need to connect all electrodes with several multichannel cables. In addition, the new inversion process was effective for the dataset which contained negative apparent resistivity.

References:
Truffert, C.M., 2017, A new distributed and cable less system for large 3D electrical resistivity ERT and induced polarization tomography : 9th Congress of the Balkan geophysical society.
Loke, M.H., Gance, J., Truffert, C. and Leite, O., 2019, The inversion of vector array data sets for 3-D resistivity and I.P. surveys : 25th European meeting of environmental and engineering geophysics.

Keywords: resistivity survey, three-dimensional

©2020. Japan Geoscience Union. All Right Reserved.

An attempt to estimate the water level change of undamaged groundwater by earth resistance (II) - Preliminary observations at the PTU borehole in Musashino Upland -

*Kunihiro Ryoki[1]

1. Polytechnic University

1.Introduction

Under the Musashino plateau, which is covered by the highly permeable Kanto loam, there is a Musashino gravel layer several meters thick. The level of non-confined groundwater, staying here, has large seasonal fluctuations, and often rises to the upper loam (Kokubun,2005). Sumida(2017) pointed out that there is perchied water on the loam layer, where clay-like impermeable layers are scattered. When this water level rises, flooding may occur on the surface (Tokyo Geotechnical Consultants Association,2000).
Formerly, the author pointed out the need to prepare for floods by observing groundwater level fluctuations at many points. And as an observation method, it was investigated that a method of estimating the groundwater level based on the change in grounding resistance (Ryoki,2019a). In this study, it is reported that the results of preliminary observations on the verification of this estimation method.

2.Measurement

It was pointed out that the ground resistance changed with the groundwater level , based on the relationship between the layer thickness of the first layer and the equivalent ground resistance in a horizontal two-layer structure, as Fig.1 (Ryoki,2019b). And it was thought that the groundwater level fluctuation could be known by monitoring the fluctuation of the grounding resistance. To verify this phenomenon, an observation well was installed in the Musashino Plateau, and the fluctuation of the groundwater level was measured at 10-minute intervals. Near the observation well, It was started that the grounding resistance was measured at a safety ground electrode of the electrical equipment repeatedly. At the observation well, the temperature and electrical conductivity of groundwater were measured at 10-minute intervals. Table.1 shows the specifications of observation wells and measuring equipment.

3.Result

Fig.2 shows the groundwater level from April 2, 2019 to February 1, 2020. Observations of groundwater temperature and electrical conductivity were very stable, and only fluctuations of the resolution of the measuring instrument were recorded. According to Fig.2, there is no significant change from the start of observation to the rainy season. The groundwater level started to rise from early June. At the end of the rainy season, the water level stabilized around -12m. After that, the groundwater level rised some time due to intensive precipitation caused by the typhoon. In the season with relatively little precipitation since late autumn, the groundwater level had decreased almost linearly.
Fig.3 shows the grounding resistance in Class A grounding, which is attached a 4-story reinforced concrete building, measured during this period. The measured value on May 13, 2019 is very different from the others, but the other ones fluctuate slowly.
To compare Fig.2 and Fig.3, it is shown that the grounding resistance tended to increase when the groundwater level was low. The relationships each other were harmonious.

4. Future plans

©2020. Japan Geoscience Union. All Right Reserved.

It is being advanced that preparation for acquiring the ground resistance and the apparent resistivity of the earth at one-hour intervals.

References

Kokubun, K.(2005): A Hydrological Study of Ground-water and Springs on Musashino-upland by the Heavy Rainfall, *Annu. Re., I.C.E. of TMG 2005*, 201-208.
Ryoki,K.(2019a): An Attempt to Estimate the Level of Non-confind Groundwater by Earthing Resistance (I) -Outline of Theory-, *Proc. Jap. Geosci. U. 2019*, HTT22-03.
Ryoki,K.(2019b): A Theory of Water Level Estimation to Focus on the Change of Earthing Resistance for the Prediction of Flood Occurrence, *Jour. of Polytech. Sci.*, 35, 30-35.
Sumida, K.(2017): Landform and Unconfined Grandwater in the Center of Musashino Upland, Tokyo, *Komazawa Jour. Geog.*, 53, 35-53.
Tokyo Geotechnical Consultants Association (2000): Uplift of Shin-Kodaira Station on the JR Musashino Line, Underground structures and groundwater levels, *Tech. Re.*, 30, 21.

Keywords: electrical equipment, Musashino district, loam layers, perchied water, flood damage, equivalent earthing resistance

©2020. Japan Geoscience Union. All Right Reserved.

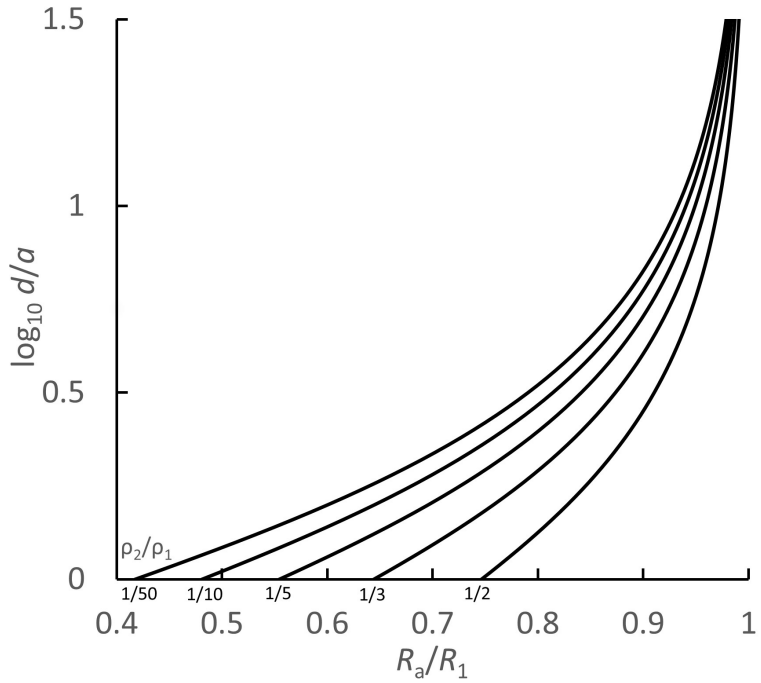

図 1 水平二層構造での第一層の層厚と等価接地抵抗の関係(領木(2019b)に加筆)

Fig.1 Relationship between the layer thickness of the first layer and the equivalent ground resistance in a horizontal two-layer structure (after Ryoki, 2019b)

表 1 観測井および測定機器の諸元

Table 1 shows the specifications of observation wells and measuring equipment

観測井	位置	35° 44' 19.2" N 139° 29' 41" E
	孔口標高	81.92m
	孔長	30.17m
	内径	50.0mm
水位計	応用地質社製	S&DL miniEC 10m計
接地抵抗計	横河製作所製	3235型

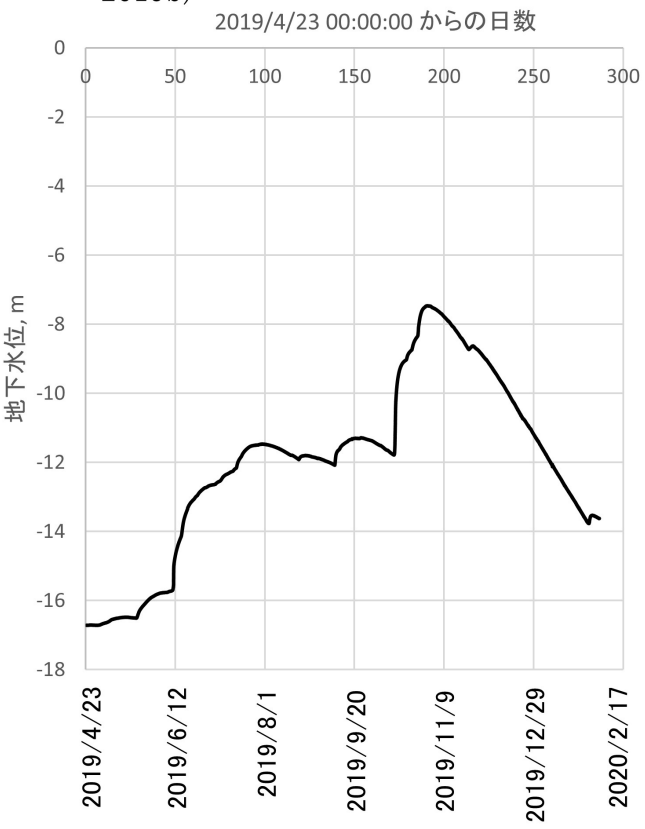

図 2 観測井PTUでの地下水位の変化

Fig. 2 Variation in groundwater level at the observation well PTU

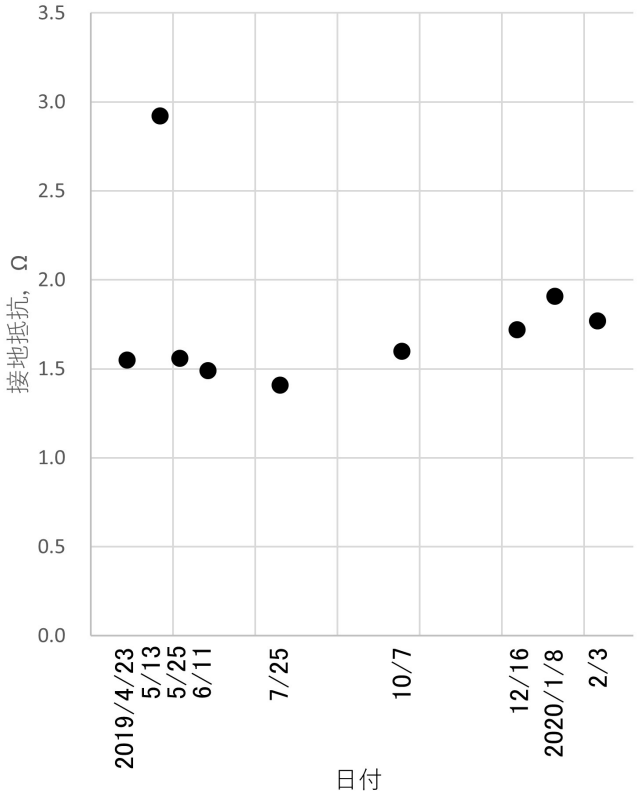

図 3 観測井PTU近傍における接地抵抗の変化

Fig. 3 Transition of grounding resistance near the observation well PTU

©2020. Japan Geoscience Union. All Right Reserved.

Development of 3D self-potential tomography for visualization of groundwater condition

*ayaka ishikawa[1], Katsumi Hattori[1]

1. chiba university

In recent years, as the frequency of torrential rain increases, the number of landslides tends to increase. It is important to understand the process of slope failure triggered by rainfall, monitor the slope, and forecast the occurrence time of failure. We are trying to develop an early warning system for rainfall-induced landslide by the Self-potential (SP) method. The SP method is a passive method to measure the electric potential naturally generated by groundwater dynamics using electrodes buried near the ground surface. This method has an advantage that the cost can be reduced and the observation can be performed over a wide range easily, compared with the observation using a pore pressure gauge with a borehole. From the results of the laboratory experiments to date, it has been confirmed that there is a relationship between the movement of water and the displacement of the soil layer and the SP changes (the electro-kinetic effect is the source of SP). Furthermore, in the sandbox experiments, visualization of groundwater dynamics using the SP method (two-dimensional SP tomography) was verified to be effective. However, application to real slopes requires 3D tomography technology. In this paper, we tried to develop a self-potential tomography to realize three-dimensional visualization of groundwater dynamics using a sandbox experiment. Specifically, the consistency of the estimation of the SP generated by groundwater flow by numerical simulation (direct problem) and the inverse problem of estimating the groundwater dynamics (pressure head and water flow) from the natural potential generated by the simulation described above are examined. A computer experiment was performed, and an actual sandbox experiment was performed using the same parameters as the numerical experiments. Here, the computer and the actual experiment are injection experiments: water is poured into the sandbox in which sand is uniformly spread over and water is injected from the lower part of the side of the box. The parameters related to the sand in the soil layer, such as the permeability coefficient, etc., were measured in other experiments.
First, the reconstructed results of pore water pressure (pressure head) and water flow obtained by the forward problem and the inverse problem by computer experiments are harmonious, and the constructed tomography algorithm and its effectiveness have been demonstrated. Also, compared with the reconstruction results by 2D tomography in the previous study, the errors of the pressure head and the magnitude of the flow vector were smaller and the results of 3D tomography were good. Next, an actual experiment of the same scheme as the above computer experiment was performed, and the head and water flow were inversely analyzed from the observed self-potential data. As a result, in the actual experiment, it was found that the pressure head distribution was different from the ideal distribution by the simulation due to the effect of the unevenness of the soil layer. For the reconstructed water flow, it was found that the flow direction by the tracer in the actual experiment and the direction of the reconstructed vector were generally consistent. The self-potential generation model based on the electrokinetic effect, the developed tomography algorithm and its effectiveness were demonstrated. The application to multi-layer structures and practical slopes is an important issue for the future, but it is expected to be applied to the visualization of groundwater dynamics below the slope. Details will be given in the presentation.

©2020. Japan Geoscience Union. All Right Reserved.

Development of nuclear magnetic resonance scanners for the nondestructive measurement of water fractions in boring cores

*Yoshito Nakashima[1]

1. National Institute of Advanced Industrial Science and Technology

Boring cores are often obtained to test the prediction by the geophysical explorations and to support the geophysical data analyses. Because pore water contents affect the physical properties of rocks and soils, the quantification of the water volume fraction in the cores is one of the most important subjects in the on-site or laboratory core analysis. I am developing a nondestructive core scanner to measure the water volume fraction along porous wet cores. The low-field time-domain proton nuclear magnetic resonance technique is employed for the scanner. Water protons in a static magnetic field produced by permanent magnets are excited by the radio-frequency coil, and the resultant proton transverse relaxation signals are acquired as raw data, which can be translated into water volume fractions, and pore-size distributions and permeabilities of the porous media. The previous version of the on-site core scanner [1] shown in the figure is being improved by employing a new design, single-sided magnetic circuit [2-3], to increase the accuracy and operationability. The current status and future perspective of the new scanner being developed would be presented.

References:
[1] Nakashima, Y. et al. (2011) Non-destructive Analysis of Oil-Contaminated Soil Core Samples by X-ray Computed Tomography and Low-Field Nuclear Magnetic Resonance Relaxometry: a Case Study. Water Air & Soil Pollution, 214, 681-698. http://dx.doi.org/10.1007/s11270-010-0473-2
[2] Nakashima, Y. (2019) Non-Destructive Quantification of Lipid and Water in Fresh Tuna Meat by a Single-Sided Nuclear Magnetic Resonance Scanner. Journal of Aquatic Food Product Technology 28, 241-252. https://doi.org/10.1080/10498850.2019.1569742
[3] Nakashima, Y. et al. (2020) Nondestructive quantification of moisture in powdered low-rank coal by a unilateral nuclear magnetic resonance scanner. International Journal of Coal Preparation and Utilization (in press). https://doi.org/10.1080/19392699.2020.1722656

Keywords: water volume fraction, nondestructive measurement, boring core

©2020. Japan Geoscience Union. All Right Reserved.

A soil core (diameter, 4cm) is being scanned by NMR. [1]

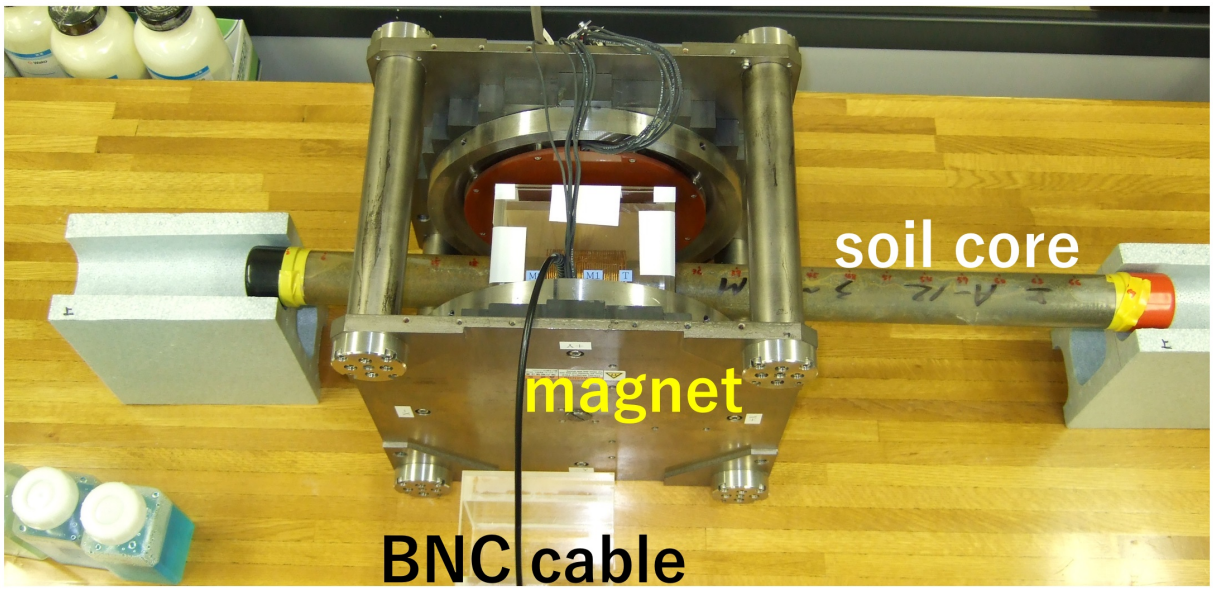

©2020. Japan Geoscience Union. All Right Reserved.

A case study of 3-D GPR survey and the ground truth at test sites for detection of buried objects

*Takanori Ogahara[1], Kunio Aoike[1]

1. OYO Corporation

Various lifelines such as water and sewage, electricity, gas, telecommunications, etc. are located in the shallow underground of urban areas, but due to inaccurate information in that area, there are many accidents cutting buried objects during excavation. Therefore, in order to prevent those accidents , it is essential to acquire more accurate locations and construct a 3-D model of the underground. Geophysical techniques are effective methods for modeling the buried objects. We constructed a test facility to develop and evaluate the method reconstructing the 3-D model of the buried objects. In this presentation, we introduce the outline of the constructed facility and report a case study of 3-D GPR (Ground Penetrating Radar).

The test facility's road is approximately 408 meters in total length and 5 meters wide, designed to drive with the speed up to 60 km/h, and divided into three main sites where objects were buried. At Site 1, various buried objects supposed under the ground of urban areas were installed (Fig. 1 a). These include the buried objects such as manholes, sewer pipes, gas pipes, flexible electrical conduits, void models, steel sheet piles, concrete blocks, wooden piles, dummy unexploded ordnances, and bricks. At Site 2, void models and VP pipes (uPVC; unplasticized polyvinyl chloride pipes) were installed (Fig. 1 b). The 28 void models which were made of Styrofoam and composed of four sizes were buried under from just below the pavement to the maximum depth of 3.5 m. The 4 VP pipes with different inner diameters were laid, and had the structure which enable us to inject and drain water. At Site 3, Hume concrete pipes were installed (Fig. 1 c). The Hume pipes with two different inner diameters were used and arrayed various patterns. The maximum depth of the bottom is 2.7 m.

We used a terrestrial laser scanner to obtain point clouds data that captured the exact position and shape of the buried objects before soil covering so as to realize 3-D comparison between the survey results and the actual burial situation. For the construction records, 3-D models were created by aerially photographing the buried object using a UAV and a rod of 6m for camera. Furthermore, considering seasonal fluctuations in soil condition, we have been so far observed not only rainfall on the ground but soil moistures, temperatures, and electrical conductivities of six different depths at a monitoring point.

We conducted highly dense GPR survey for the Site 1 and the Site 3. The survey lines were spaced at intervals of about 25 cm in the longitudinal and transversal directions of the road. Assuming that the hyperbolic curve to the data obtained by surveying the buried pipes is a travel time curve from a point reflection, we can calculate the propagation velocity so that maximized the semblance along the curve. As the results of visualizing the spatial distribution of the semblance, the characteristic feature of the buried pipes could be visualized.

Now, the Ministry of Land, Infrastructure, Transport and Tourism Japan has promoted BIM/CIM to improve the productivity by integrally sharing and utilizing 3-D models with related parties throughout the processes of design, construction and maintenance. In that trend, 3-D modeling of buried objects is in the midst of a validation.

We aim to accelerate the open innovation of 3-D survey technology and diffuse it as an effective use for BIM/CIM by sharing and utilizing this facility with other research institutions and companies in the future.

Keywords: GPR, buried objects, test sites, 3D model

©2020. Japan Geoscience Union. All Right Reserved.

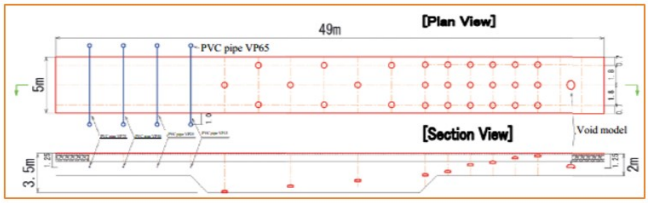

(b) Site2

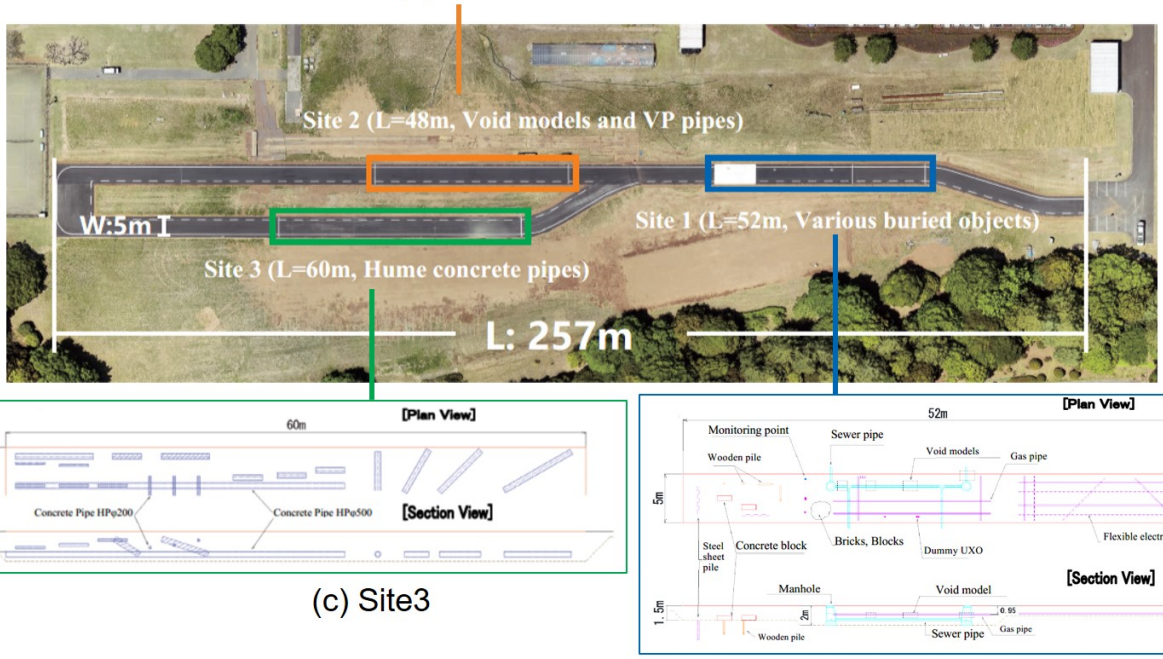

(c) Site3

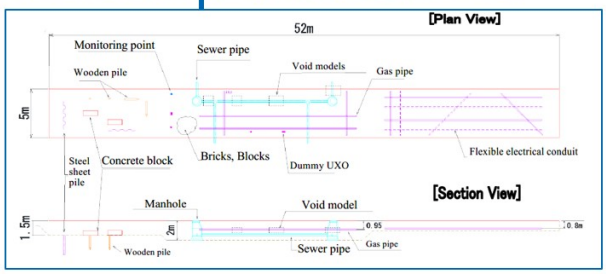

(a) Site1

Fig. 1 View of the test facility

©2020. Japan Geoscience Union. All Right Reserved.

Identifying wetting areas of a concrete deck slab by time-lapse surveys using ground-penetrating radar

*Kyosuke Onishi[1], Takayuki Kobayashi[1], Tadashi Matsumoto[1], Tsubasa Noda[1]

1. Public Works Research Institute

Concrete deck slabs of bridges are damaged by moisture and wheel loads and they are sometimes rapidly deteriorated. The rapid deterioration sometimes progresses under repaired areas with overlaid asphalt. We cannot sometimes identify the deteriorated area from the surface by visual judgements. Therefore, non-destructive survey methods are desired to be developed. Ground-penetrating radar (GPR), which has a fine quality of resolution, is one of promising techniques. However, the standard way to identify deteriorated areas from anomalous areas on GPR sections frequently mistakes the deteriorated areas, because the phase shift of GPR reflection waves is influenced by many causes, moisture, a thickness of pavement, material types of pavement, undulation, and so on. Thus, we propose a new way to identify different areas using time-lapse surveys. Rapid deterioration of concrete deck slabs has an influence of moisture. Water content of a concrete slab will fluctuate. We can identify different areas to analyze records acquired between in dry season and after raining. This report first shows a result of an infiltration region estimated by two records, which were acquired before and after pouring water on a concrete slab model. Second, we show a survey result of an infiltration region of bridge slab in service. We could estimate an infiltration region using time-lapse records and shows a result compared to a deteriorated area determined by excavation. In this results, time-lapse method can clearly identify regions of changing water content. However, high degrees of accuracy for survey positions are required to apply subtraction analysis.

Keywords: GPR, concrete deck slab, time-lapse survey

©2020. Japan Geoscience Union. All Right Reserved.

Conjecture of sourcing wavelet conditions suitable for the simultaneous sourcing 3D seismic survey with the underwater speakers

*Mayu Ogawa[1], Seishiro Furuyama[1], Tetsuro Tsuru[1]

1. Tokyo University of Marine Science and Technology

In Japan, active faults in coastal areas cause an earthquake such as the Noto Peninsula Earthquake (M6.9), and it has become increasingly important to understand geological information at that area. In recent years, a 3D seismic reflection survey (OGP & IACG, 2011) can recognize the structure under sea bottom spatially, and therefore provide more information than that of a 2D seismic reflection survey. However, a 3D seismic reflection survey requires high-cost and large-scale because of a large-capacity air gun and numerous cables. These problems make it for a 3D seismic reflection survey difficult to investigate in the coastal area. The simultaneous sourcing 3D seismic reflection survey system with multiple underwater speakers and one streamer cable (Tokyo University of Marine Science and Technology, 2018) was developed to resolve these problems and simplify a survey at coastal areas. An underwater speaker (200 ×65 mm, 4.5 kg) that is greatly smaller than airgun is able to survey with small-scale and therefore reduce a survey cost. Also, the maximum instantaneous sound pressure of an underwater speaker of 130 dB re 1 μPa at 1m (Tsuru et al., 2019) is very small compared to an airgun that is 210 dB re 1 μPa at 1m (IAGC, 2002). Additionally, an air gun with high sound pressure could cause environmental stress to marine life (Lokkeborg & Soldal, 1993; Cerchio et al., 2014) and it is necessary to reduce that stress (Mougenot et al., 2017). An underwater speaker with small-scale and small sound pressure contributes to resolving influences on marine life.
Our research group has been developing the sourcing wavelet of an underwater speaker to make a more accurate and stable observation (Ogawa et al., 2019). The underwater speaker system uses different non-pulse waves created by MATLAB (MathWorks) as sound source and makes a sound by signal generators. Adjustment of sourcing wavelets such as Marine Vibrator (Orji et al., 2020) is one of the advantages of an underwater speaker. In this research, we create two types of wavelets that are sweep waves and random waves to estimate the optimal wavelet conditions for the underwater speaker system. Sweep waves are generally used in ocean acoustic surveys and land seismic surveys, and random waves are generated by pseudo-random numbers (e.g. Dean, 2013). These two types of wavelets were created for each of the three frequency bands and a total of six wavelets were used for a test at sea. Our results show that the random wavelet is more suitable for the underwater speaker system than the sweep wavelet because the random wave has a higher signal to noise ratio after cross-correlation. Also, the penetration depth of the random wavelet was deeper though the sound pressure was smaller than that of the sweep wavelet. Finally, the seismic profile with more 100-200 Hz band was the most accurate in seismic profiles filtered at 50-100 Hz, 100-200 Hz, and 200-300 Hz.

Keywords: reflection survey, 3D seismic reflection survey, sourcing wavelet

©2020. Japan Geoscience Union. All Right Reserved.

[J] Poster | H (Human Geosciences)：H-TT Technology & Techniques

[H-TT19] Geographic Information System and Cartography

convener:Mamoru Koarai(Earth Science course, College of Science, Ibaraki University), Kazunari Tanka(Department of Civil Engineering and Urban Design, Faculty of Engineering, Osaka Institute of Technology), Kazuhiko W. Nakamura(The University of Tokyo)

This session discusses various methods which acquire, store, analyze and visualize geospatial data, and presents the outcomes of empirical studies using GIS or mapping methods. The session also deals with applications of digital data, GIS, and mapping to various fields of earth and planetary science and human society. All presentations and discussion of this session are made in Japanese.

[HTT19-P01] Consideration of essential information and understandable representation method for liquefaction hazard map: Opinions from local government staffs and residents

*Ryo Endo[1], Takayuki Nakano[1], Takashi Ishii[2], Takashi Hoshikawa[2], Seina Yamanaka[3], Yukiko Takeuchi[3], Shingo Watanabe[4], Keita Takada[4], Takuma Fujita[4] (1.GSI of Japan, 2.City Bureau, Ministry of Land, Infrastructure and Tourism, 3.Kumamoto University, 4.Fukken Co., Ltd.)

[HTT19-P02] Introductions of Evaluation method of chart adequacy using satellite derived bathymetry "Nautical Chart Adequacy Evaluation Procedure" and a trial case study in the waters around Japan

*Haruka Ogawa[1], Takahumi Hashimoto[1], MASANAO SUMIYOSHI[1], Hirokazu Mori[2] (1.Technology Planing and International Affairs Divixion Hydrographic and Oceanographic Department Japan Coast Guard , 2.Hydrograhpic Surveys Division Hydrographic and Oceanographic Department Japan Coast Guard)

[HTT19-P03] **Applications of Stereoscopic viewer for the Seamless Geographical Information System and its Prospect**

*Kunihiro Ryoki[1] (1.Polytechnic University)

[HTT19-P04] Green structural analysis by hierarchical cluster analysis and linear model regression analysis
and evaluation of green environment for continuous cityscape using green visibility and green coverage

*Taiichiro Watanabe[1], Tatsuto Aoki[2] (1.Kanazawa University , 2.Kanazawa University)

[HTT19-P05] Initiatives for an initial disaster response by townspeople using a drone: "Chisan chibou project", a locally operated countermeasure for natural hazards in Jinsekikogen Town, Japan

*Shoichiro Uchiyama[1] (1.National Research Institute for Earth Science and Disaster Resilience)

[HTT19-P06] Effect of topographic expression in Geopark Map

*Mamoru Koarai[1], Naoki Takeda[2], Kazuki Kidoguchi[1], Taiga Suzuki[1], Miteki Sato[1], Kasumi Kobayashi[1], Yuusuke Yokoro[1], Takumi Sekiya[1], Shiori Sugitake[1], Naoki Yamada[1], Misaki Kawamata[1], Shiori Watanabe[1], Miu Ogawa[1], yoshihiro Kurihara[1], Misa Tanaka[1] (1.Earth Science course, College of Science, Ibaraki University, 2.Geopark promotion office, Ibaraki University)

[HTT19-P07] Changes in movements of people to prevent the spread of COVID-19 in Japan since January 2020 based on geotagged Twitter data

*Takashi Kirimura[1] (1.Kogakkan University)

Consideration of essential information and understandable representation method for liquefaction hazard map: Opinions from local government staffs and residents

*Ryo Endo[1], Takayuki Nakano[1], Takashi Ishii[2], Takashi Hoshikawa[2], Seina Yamanaka[3], Yukiko Takeuchi[3], Shingo Watanabe[4], Keita Takada[4], Takuma Fujita[4]

1. GSI of Japan, 2. City Bureau, Ministry of Land, Infrastructure and Tourism, 3. Kumamoto University, 4. Fukken Co., Ltd.

Ministry of Land, Infrastructure and Tourism has been conducting the General Technology Development Project "Study on liquefaction hazard map creation method for risk communication" in order to promote pre-disaster prevention of liquefaction and reduce its damage. In this project, we consider the essential information and understandable representation method for liquefaction hazard map. Based on the contents of consideration, several prototypes of liquefaction hazard maps were producesd, and we have collected opinions from local government staffs and residents through workshops and questionnaire sheets.

The size of prototype hazard maps is A1 size. They have "map part" and "learning and information part" to use them as basic data for risk communication. In the map part, the map is at the scale of 1:25,000 and based on topographic map of the Geospatial Informattion Authority of Japan. It includes the following information: possibility of liquefaction, risk of damage to houses by liquefaction, emergency transportation road, evacuation sites and railroads. We prepared maps with five color schemes in order to evaluate the relationship between visibility and color scheme. The learning and information part includes information such as what is liquefaction phenomenon, and the damage caused by it, and control methods of liquefaction to reduce the damage; which is considered necessary to increase awareness and understanding for liquefaction in conjunction with the map part.

We conducted workshops in Kumamoto city and Urayasu city to collect opinions from local government staffs. 8 people (including one university student) participated in Kumamoto city and 18 people in Urayasu city. 11 people in Kumamoto and 20 people in Urayasu (including audiences) answered the questionnaire. We also distributed questionnaires to 400 households and received 76 (19%) answers in Chikami and Kaminogo, Kumamoto city. In addition, we collected opinions from 4 residents of Akitsu-machi Akita by hearing.

Here, we show the opinions of local government staffs. They listed the following list as essential information of the map part: liquefaction risk, evacuation site, main road, main building, contact information in case of disaster and evacuation route. They also pointed out that it was easy to understand when warm color scheme was used to show the possibility of liquefaction and cold color scheme for water area. On the other hand, they pointed out the difficulty of understanding the explanation about the possibility of liquefaction and the risk of damage to houses by liquefaction. It can be said that both plain expression and visual clarity is necessary. For the learning and information part, they listed liquefaction mechanism, examples of liquefaction damage in the past, impact of liquefaction on daily lives, how to read hazard maps, etc. The result suggests that it is difficult for residents to understand the information on the map part due to lack of knowledge and awareness of liquefaction. This means that they require not only information that allow to imagine liquefaction and the damage caused by it, but also ingenious plans for residents to understand the role and way of utilization of liquefaction hazard map itself.

For future work, we will collect opinions from local government staffs who have never experienced liquefaction damage. Thus, we will make a manual for liquefaction hazard map creation based on these

©2020. Japan Geoscience Union. All Right Reserved.

opinions.

Keywords: Liquefaction hazard map, Workshop, Questionnaire

©2020. Japan Geoscience Union. All Right Reserved.

Introductions of Evaluation method of chart adequacy using satellite derived bathymetry "Nautical Chart Adequacy Evaluation Procedure" and a trial case study in the waters around Japan

*Haruka Ogawa[1], Takahumi Hashimoto[1], MASANAO SUMIYOSHI[1], Hirokazu Mori[2]

1. Technology Planing and International Affairs Divixion Hydrographic and Oceanographic Department Japan Coast Guard , 2. Hydrograhpic Surveys Division Hydrographic and Oceanographic Department Japan Coast Guard

In this study, we introduced "Nautical Chart Adequacy Evaluation Procedure" (Klem et la.2016)(hereinafter referred to as the NCAE procedure) and the results of a trial of the NACE procedure in the waters around Japan.
The validity of the chart (Chart Adequacy) refers to the effectiveness of the information necessary for the safety of navigation, including the depth of water and seafloor topography described in the chart. Proper evaluation of the validity of the chart is one of the important aspects of determining the priority of hydrographic survey.

The NCAE procedure is a method which performs raster operation using four elements of the water depth change, vessel traffic, reference depth and quality information of depth described in the chart to quantify the chart adequacy by using ArcGIS.

In order to perform the NCAE procedure in the waters around Japan, it was necessary to make some changes because the data set in Japan was different. In addition, it was suggested that the NCAE procedure is effective by making improvements in the waters around Japan.

Keywords: Satellite Derived Bathymetry, Chart Adequacy, ArcGIS

©2020. Japan Geoscience Union. All Right Reserved.

Applications of Stereoscopic viewer for the Seamless Geographical Information System and its Prospect

*Kunihiro Ryoki[1]

1. Polytechnic University

1.Introduction

Stereoscopic Viewer (Ryoki,2019a), that displays the GSI Globe (Geospatial Information Authority of Japan,2017), facilitates understanding of geological information appearing in topographic maps and aerial photographs.This viewer displays a single image of a rotating object. It can display 3D images of mineral crystal structures, molecular models, civil engineering structures, etc. (Ryoki,2019b). Therefore, it is expected to be used in education or vocational development (Ryoki,2019c). It is described that An example of using the seamless geological map (Geological Survey of Japan,2019) or images shot from drones, etc. in this paper.

2.Overview of the stereoscopic viewer

Stereoscopic vision is perceived by displaying two images of the target from both pupil locations, one at a time, and performing high-order image processing in the brain (Tanabe and Fujita,2004). The video of the rotating body is recorded by one video camera. When the video is played as two images with a short delay and watchied with left and right eyes, it enables stereoscopic vision (Ryoki,2019a). The viewer, called Stereoscopic Viewer (Fig.1), was coded in HTML and JavaScript in this study.

3.Stereoscopic viewing of geological information

When viewing long active faults expressed in GSI Globe, it is not possible continuously to watch stereoscopic viewing in a range beyond the PC monitor. This is because there are restrictions due to security issues in HTML describing Stereoscopic Viewer. In such a case, the following procedure is possible. First, display only a map of GSI Globe on some browser and move it horizontally with the mouse. At this time, the mouse can be moved to the full width of the monitor regardless of the browser. This window is recorded by a captor application and saved as a very long video file in the horizontal direction. And when this file is browsed with Stereoscopic Viewer, it is able to view seamlessly all of the saved sections in stereoscopic viewing. The same treatment can be used when displaying seamless geological maps.

4.Stereoscopic viewing of moving image

When the video taken from a drone horizontally or rotate, it can be viewed stereoscopically. Even when the video moves vertically, it can be viewed stereoscopically if it is converted horizontally by some video processing application (Fig.2). The animation tool "Google Earth Studio" can created a video file of geographic information image (Google LLC,2020). The file can be viewed with Stereoscopic Viewer. This is suitable not only for horizontal and vertical shooting but also for bird's-eye view or looking-up view.

5.Future plans

In GSI Globe, the map tiles are read from the GSI server each time when they are browsed. For this reason, it cannot be viewed in out of communication area. Therefore, it is planed to improve Stereoscopic Viewer so that the tiles of the required area are downloaded in advance.

References

©2020. Japan Geoscience Union. All Right Reserved.

Geological Survey of Japan(2019): Seamless Digital Geological Map of Japan 1:200,000, AIST, *https://gbank.gsj.jp/seamless/*
Geospatial Information Authority of Japan(2017): Official release of GSI Map Globe, *http://www.gsi.go.jp/common/000185126.pdf*
Google LLC(2020): Introduction,Google Earth Stadio, *https://earth.google.com/studio/docs/ja/*
Ryoki,K.(2019a): A Seamless Stereoscopic Viewer for 3D Browsing of GSI Globe, *Ab. Geoinfor. 2019 Annu. Meet.*, 31-32.
Ryoki,K.(2019b): A stereoscopic viewer of GSI Map Globe for the geographic information system, *Pro. Chiriin Chizu Partner Network 11th confer.*, 15.
Ryoki,K.(2019c): Construction of stereoscopic viewer with rotating images -Development in Education or Vocational Training, and Its Application to Practice-, *Pro. PTU Forum 2019*, 30-J-5.
Tanabe,S. and Fujita,I.(2004): The Neural Representation of Stereoscopic Depth, *Jour. Jap. Neu. Net. Soc.* , 11, 2, 64-73.
Ueki,T. and Sakai,A.(2007): Geological Map of Japan 1:50,000, Ome, GSJ, AIST.
Watanabe,K.(2019): Drone recording in PTU (unpublished).

Keywords: Stereo vision, HTML, Crossing method, rotating body, topographic map, Geological map

©2020. Japan Geoscience Union. All Right Reserved.

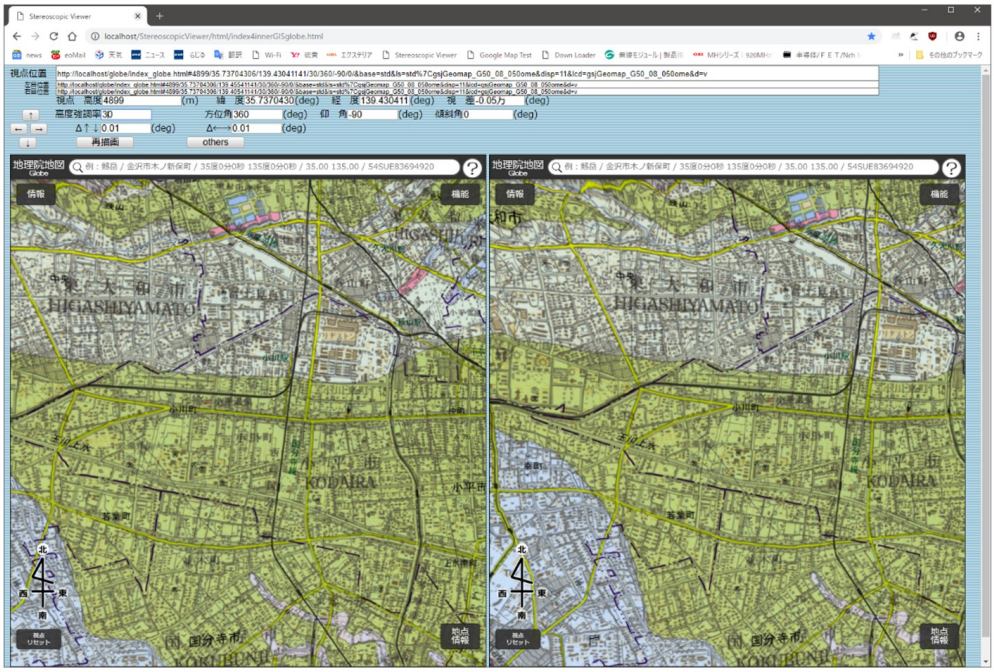

図 1　Stereoscopic Viewerによる地質図の立体表示例　5万分の1地質図福「青梅」(植木・酒井, 2007)の一部を地理院地図Globe(国土地理院, 2017)上に描いて用いた．交差法による．

Fig. 1　3D display of geological map by Stereoscopic Viewer　A part of 1:50,000 geological map “Ome” (Ueki and Sakai, 2007) is drawn on GSI Map Globe (Geospatial Information Authority of Japan, 2017). See with intersection method.

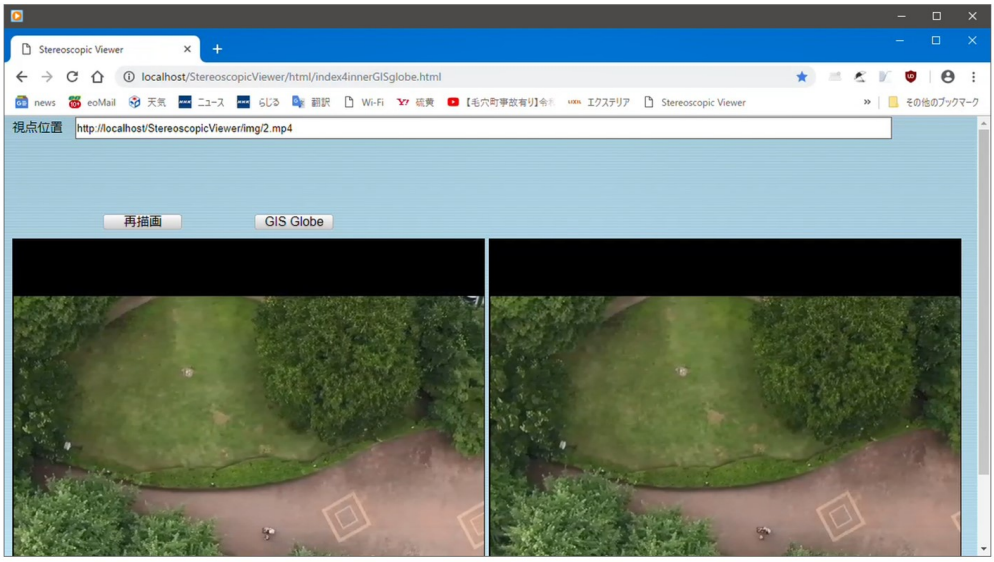

図 2　Stereoscopic Viewsrによる空撮映像の立体表示例　渡邉(2019, 未公表)のドローンによる録画映像を描画．交差法による．

Fig. 2　3D display of aerial video by Stereoscopic Viewer　These screens display the movie of view from a drone recorded by Watanabe (2019, unpublished). See with intersection method.

©2020. Japan Geoscience Union. All Right Reserved.

Green structural analysis by hierarchical cluster analysis and linear model regression analysis and evaluation of green environment for continuous cityscape using green visibility and green coverage

*Taiichiro Watanabe[1], Tatsuto Aoki[2]

1. Kanazawa University , 2. Kanazawa University

Introduction
The purpose of this study is to analyze and consider green environment, which is a finite resource indispensable for sustainable town development, from the viewpoint of landscape. By combining the green coverage rate, which indicates the planar spread of the green environment, and the green viewing rate, which indicates the visual situation, it becomes possible to understand the green environment three-dimensionally and to analyze the image data necessary for analysis. We try to improve the efficiency of data acquisition and analysis by acquiring from remote sensing and big data archives. The green coverage and NDVI values obtained from Landsat 8 and the green visibility and sky occupancy calculated using images obtained from the Google Street View Image API were used as the data to be analyzed. For NDVI, thresholds of 1.0 and 2.0 are set and used as indicators of the distribution of green spaces and the distribution of high-quality green spaces, respectively. In addition, the image analysis of the supervised classification is used to calculate the green viewing rate.

Analysis and Results
1) Cluster analysis
R, which is an open source programming language, is used with variables green coverage (NDVI>1.0), green coverage (NDVI>2.0), green viewing ratio, and sky occupancy obtained from each survey point. A cluster analysis was performed using the Ward method. All the 42 points analyzed were classified into four clusters at height=4 based on the clustering results. They were classified and positioned as city. Next, the cluster with the highest percentage of green was positioned as Suburban, and the two clusters with values between them were named Middle Region A and Middle Region B. Mid-area A has a superior green coverage rate (average green coverage rate 13.20%, average green coverage rate 37.94%) and a higher sky occupancy rate (average 41.72%) than the green visibility rate, and has a good view of green in the horizontal direction Environment has been deployed, and Mid Region B has a vertical green environment with a superior green visibility rate (average green visibility rate 20.79%, average green coverage rate 19.75%) compared to the green coverage rate. Mid-area B looks more lush than middle-area A with only the green-vision rate, which indicates the visual characteristics of the green environment. It can be said that it is a green area, and the sky occupancy is high considering the disaster prevention aspect (Intermediate area A average: 41.72%, Intermediate point B average: 30.11%) Intermediate area A is more suitable for housing there is a possibility. From this, it can be said that when discussing the change of the green environment in continuity, it is important to consider not only the apparent environment but also the spatial environment.

2)Regression analysis between variables
There were three significant correlations between each variable.
There was a certain positive correlation between green visibility in front of block and green visibility in NDVI0.1. It can be guessed that this is because the green in the suburban area is calculated from the

©2020. Japan Geoscience Union. All Right Reserved.

green of the distant green area, the field, and the thicket forest.
There is a negative correlation with Green Visibility in NDVI0.1, although Path Green-Visibility is rough with P value=0.1to0.2. It can be guessed that this is because much of the green on the route is calculated from narrow street trees that do not spread horizontally.
The green viewing rate is highly significant and positively correlated with the route and the front of the block. This is thought to be because the panorama of the urban area passes through 360 degrees and a homogeneous panorama is developed. In Tokyo, the concept of borrowed scenery seen in other urban areas cannot exist, so the buildings are so superb. It indicates that it is dense and complicated. This correlation is particularly strong as compared to the others, and it is considered that the correlation clearly shows the regionality of a large city located in a large plain called Tokyo.

Conclusion

The landscape in Tokyo's green environment was found to be nested with multiple layers of single structures that changed while drawing a wavy gradation in the course of the road connecting the central business district terminal and the large-scale suburban terminal.

Keywords: Big Data Archive, Remote sensing, Hierarchical cluster analysis, Urban landscape, Urban green environment

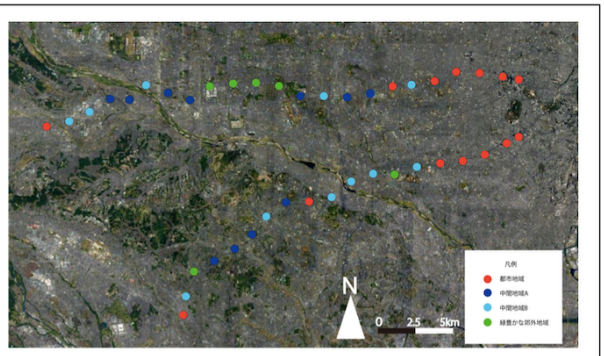

図１　分析対象地点

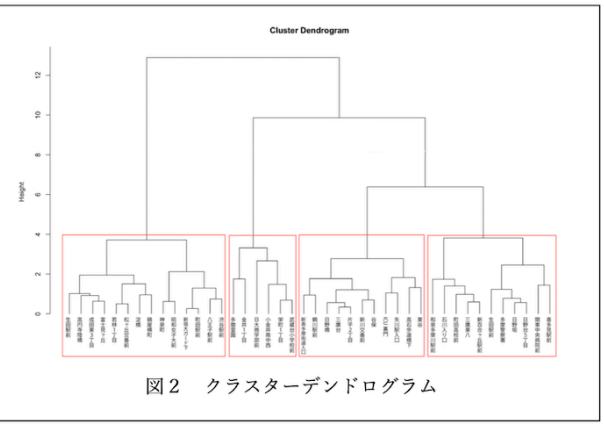

図２　クラスターデンドログラム

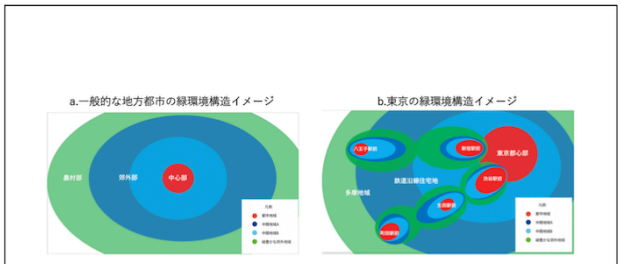

図３　緑環境構造イメージ

©2020. Japan Geoscience Union. All Right Reserved.

Initiatives for an initial disaster response by townspeople using a drone: "Chisan chibou project”, a locally operated countermeasure for natural hazards in Jinsekikogen Town, Japan

*Shoichiro Uchiyama[1]

1. National Research Institute for Earth Science and Disaster Resilience

The "Chisan chibou" project was implemented in Jinsekikogen Town in Hiroshima Prefecture. The aim of this project is drone operation by local townspeople. Five townspeople underwent drone operation training. The five trained operators conducted a demonstration, a disaster situation awareness demonstration as an initial disaster response. In the disaster situation awareness demonstration, orthographic images were created with DroneDeploy (cloud software), and the images were uploaded to a comparison application developed independently as part of the project. As a result, it was possible to compare ortho-images obtained before and after a disaster and share information obtained from the disaster site with the town hall. As a future development, the project has proposed activities involving the daily use of drones. Namely the implementation of disaster prevention drills using drones and the incorporation of initial disaster situation awareness into disaster response schemes in the town. The town and the operators must cooperate and create a system that can function in the real world.

Keywords: drone, townspeople in charge of drone operation, initial disaster response, disaster situation awareness

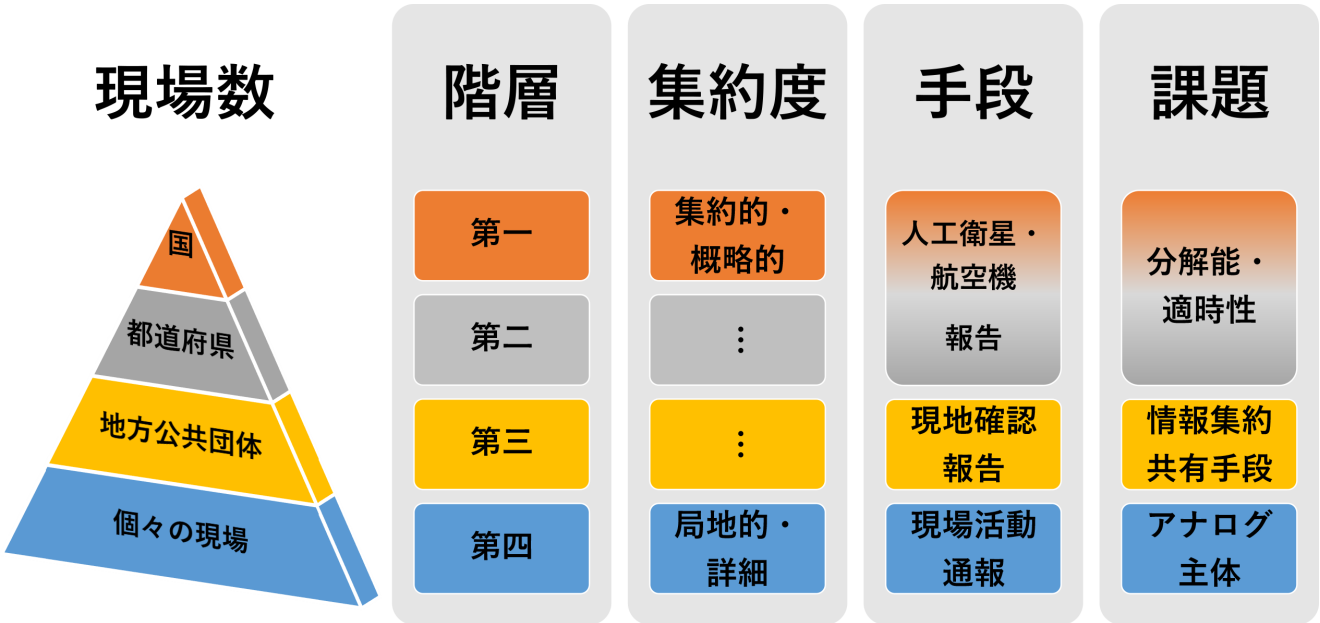

©2020. Japan Geoscience Union. All Right Reserved.

Effect of topographic expression in Geopark Map

*Mamoru Koarai[1], Naoki Takeda[2], Kazuki Kidoguchi[1], Taiga Suzuki[1], Miteki Sato[1], Kasumi Kobayashi[1], Yuusuke Yokoro[1], Takumi Sekiya[1], Shiori Sugitake[1], Naoki Yamada[1], Misaki Kawamata[1], Shiori Watanabe[1], Miu Ogawa[1], yoshihiro Kurihara[1], Misa Tanaka[1]

1. Earth Science course, College of Science, Ibaraki University, 2. Geopark promotion office, Ibaraki University

A geological information map (Geo-site map) had been produced in the "geological information utilization project" which is being performed as student project of Ibaraki University in the North Ibaraki Geopark, but a topography expression in these maps was not performed appropriately. Therefore Imaizumi (2018MS) had consideration of topography expression in Geopark map, and produced trial geo-site map in Mito Semba Lake Geo-site, Omiya Terrace Geo-site and Tanakura Fault Geo-site.

A Color-Shaded Relief Map created with Multiple Light Sources most highly regarded by the questionnaire survey performed in Imaizumi (2018MS) was adopted as topographic expression of three renewal geo-site maps of Mito-Semba Lake, Hiraiso and Tanakura Fault geo-sites.

The authors have been carried out a questionnaire survey about the effect of topographic expression of geo-site map for the general public and tour guide who participant in the Kairakuen and Senba Lake geo-tour using old and new Mito-Senba Lake geo-site map. As a full revise of Hitachi geo-site map is scheduled, the authors carried out a questionnaire survey about request of the revise contents for tour guide who participant in the Hitachi geo-tour using old Hitachi geo-site map.

In this presentation, the authors will report the results of the questionnaire survey, and discuss the effects of topographic expression in geo-sit maps and the problem in future.

Keywords: North Ibaraki Geopark, geo-site map, topograhic expression

©2020. Japan Geoscience Union. All Right Reserved.

Changes in movements of people to prevent the spread of COVID-19 in Japan since January 2020 based on geotagged Twitter data

*Takashi Kirimura[1]

1. Kogakkan University

In order to curb the spread of COVID-19, the prefectural governors in Japan began requesting that inhabitants avoid going out, and the Japanese government also issued the declaration of a state of emergency. As a result, the daily movement of people had been substantially restricted. Although the declaration of a state of emergency has been lifted along with the decrease in the number of new cases of COVID-19, it is expected that the movement of people will continue to decrease to some extent due to the practice of the "new lifestyle." Therefore, this paper clarifies a part of the decrease in the movement of people due to the request for avoiding going out after the end of February 2020 and the declaration of a state of emergency after April 2020 using geotagged Twitter data. In particular, this study focuses on the difference in movement between weekdays and holidays, and the difference in movement according to the time of day on weekdays, because the avoiding going out on weekends and working from home on weekdays are mainly required. It is considered that the decrease in daily commuting, going to school and shopping and sightseeing activities especially on weekends, will have a great impact on functional regional connections and regional economies.

As a result of the analysis, before the request of avoiding going out, Twitter users tended to move more easily on holidays than on weekdays. However, after the end of February when there were requests for avoiding going out by the prefectural governors, they became less mobile on holidays rather than weekdays. Also, in the two metropolitan areas of Tokyo and Osaka, the ratio of the number of Twitter users in the daytime to the number of them in the nighttime on weekdays increased even in the suburbs due to the spread of working from home. In the central areas of the two major cities, the proportion of users staying in the early morning is increasing due to the effects of staggered working hours.

Keywords: COVID-19, avoiding going-out, declaration of a state of emergency, geotagged tweets, metropolitan area

©2020. Japan Geoscience Union. All Right Reserved.

[J] Poster | H (Human Geosciences)：H-CG Complex & General

[H-CG28] Nuclear Energy and Geoscience

convener:Eiji Sasao(Tono Geoscience Center, Japan Atomic Energy Agency), Ryuta Hataya(Central Research Institute of Electric Power Industry), Shinji Takeuchi(Department of Earth and Environmental Sciences, College of Humanities & Sciences, Nihon University)

Handling of geological hazard assessments represent a major environmental concern in the modern society due to constructing nuclear facilities and their radioactive wastes, and also related to the management of contaminated biosphere after nuclear disasters of Fukushima-Daiichi Nuclear Power Plant. The session rational is to provide a forum to deal with various aspects of scientific and engineering aspects of nuclear power. The session in this year focuses on radioactive waste disposal and covers not only scientific aspect such as characterization of geological environment but also engineering aspects such as microbe-nuclide, mineral-water, and cement-water interactions. In addition to this, themes on seismic hazards at nuclear facilities, environmental behavior of radionuclides emitted from disabled nuclear plants, and volume reduction and reuse of cesium contaminated soils are welcomed. Through these presentations, we aim to promote intercultural communication and collaboration between science, engineering and social science.

[HCG28-P01] Collection and Organization of Geoscientific Information for Improvement of Impacts Assessment Model of Seismic and Fault Activities for HLW Geological Disposal

*Makoto Kawamura[1] (1.Japan Atomic Energy Agency)

[HCG28-P02] Systematization from Case Studies of Natural Phenomena to Impacts Assessment on a HLW Geological Disposal

*Makoto Kawamura[1], Tsuneari Ishimaru[1], Masakazu Niwa[1], Tetsuya Komatsu[1] (1.Japan Atomic Energy Agency)

[HCG28-P03] Advanced examination technique for crustal deformation in stable area: a case study of the Kanto Plain, Japan

*Nakanishi Toshimichi[1], Tetsuya Komatsu[1], Misao Hongo[2], Marie Noguchi[3], Tatsuki Miyamoto[4], Taiga Kimori[4], Toshihiko Sugai[4] (1.Japan Atomic Energy Agency, 2.Alps Technical Research Lab. Co. Ltd., 3.Paleo Labo Co. Ltd., 4.Univ. Tokyo)

[HCG28-P04] Distribution map of erosion rates on timescales of 10^2–10^4 years in the Japanese Islands

*Yuki Hiura[1], Tetsuya Komatsu[1], Shigeru Sueoka[1], You Kitamura[2], Tomoji Sanga[2] (1.Japan Atomic Energy Agency, 2.JX Nippon Exploration and Development co. Ltd.)

[HCG28-P05] Machine learning for activity evaluation of crush zones using chemical composition: introduction of examples

*Koji Shimada[1], Ryo Tateishi[2] (1.Japan Atomic Energy Agency, 2.University of Toyama)

[HCG28-P06] Trial of domain segmentation of granite based on fracture orientations using Dip Azimuth Vector plot

*Shuji Terusawa[1], Koji Shimada[2] (1.OYO CORPORATION, 2.Japan Atomic Energy Agency)

[HCG28-P07] Hydrothermal alteration in the Toki granitic body, central Japan
-Mass transfer associated with precipitation of carbonate minerals-

*Hatsukawa Haruka[1], Nakashima Kazuo[2], Yuguchi Takashi[1] (1.Yamagata University Graduate School, 2.ASN Co., Ltd.)

[HCG28-P08] Hydrogeological structures of hydraulic conductive fractures at a depth of 300 m

*Ai Hamada[1] (1.Central Research Institute of Electric Power Industry)

[HCG28-P09] Properties of precipitates in alkaline Fe^{2+}-SiO_2-H_2O systems

*Yuki Sakuma[1], Yuto Nishiki[1], Ryosuke Kikuchi[2], Tsubasa Otake[2], Tsutomu Sato[2] (1.Graduate school of Engineering, Hokkaido university, 2.Faculty of Engineering, Hokkaido University)

Collection and Organization of Geoscientific Information for Improvement of Impacts Assessment Model of Seismic and Fault Activities for HLW Geological Disposal

*Makoto Kawamura[1]

1. Japan Atomic Energy Agency

To evaluate the hydraulic and mechanical effects associated with seismic and fault activities, "conceptual model of seismic and fault activities" has been developed. This conceptual model is, however, a qualitative method focused on general versatility; therefore, possible numerical data applied to parameter setting for numerical analysis has not been organized.As for the seismic and fault activities, distribution of active faults in particular, is characterized by surface surveys using topographical and geological methods. With the surface surveys, investigation and observations are available for visible range from ground such as surface outcrop; though, the continuity to the deep underground exceeding 1,000 m below ground required for geological disposal R & D is not characterized. Moreover, it is very difficult to characterize the behavior and extent of the damage zone that considered to have been formed around the fault, especially here in Japan, where there is a lot of vegetation on the surface ground. In this study, we collected and organized the information on the large earthquakes and fault activities occurred in the past, which are published by research institutions including the Japan Meteorological Agency and universities, and then specified the information that contributes to improvement of the conceptual model. As a result, we obtained the prospect of developing more specific conceptual model by combining geophysical methods such as seismic observation with the information obtained from conventional topographic and geological methods. Acknowledgements: This study was carried out under a contract with METI (Ministry of Economy, Trade and Industry) as part of its R&D supporting program for developing geological disposal technology.

Keywords: HLW Geological Disposal, Seismic and Fault Activities, Conceptual Model, Impacts Assessment Model

©2020. Japan Geoscience Union. All Right Reserved.

Systematization from Case Studies of Natural Phenomena to Impacts Assessment on a HLW Geological Disposal

*Makoto Kawamura[1], Tsuneari Ishimaru[1], Masakazu Niwa[1], Tetsuya Komatsu[1]

1. Japan Atomic Energy Agency

Regarding the selection of suitable geological environment for geological disposal, it is not only necessary to evaluate characteristic of natural phenomena currently occurred, but also to predict the long-term occurrence and changes of natural phenomena over tens of thousands of years after disposal. Moreover, it is essential properly to assess the potential impacts of natural phenomena on the geological environmental conditions. For the appropriate assessment of the impacts, impact assessment model and scenario will be developed. In order to ensure their reliability, validity of scientific evidences should be clarified based on the results of case studies. As a method to demonstrate the validity, a method based on argument diagram has been proposed. In this study, we devised its simplified argument diagram, set the theme then organized the flow of information. As a result, it has made it possible to define the research contents and results information on the natural phenomena and geological environmental conditions that required for the setting theme, and to clarify the flow of the results information for constructing conceptual models and scenarios that adopted as the impact assessment. In addition, since the evaluation scenario was constructed based on the demonstrated conceptual model, we obtained the prospect that we will be able to objectively judge the validity of the scenario. Acknowledgements: This study was carried out under a contract with METI (Ministry of Economy, Trade and Industry) as part of its R&D supporting program for developing geological disposal technology.

Keywords: HLW Geological Disposal, Natural Phenomena, Geological Environment, Evaluation Model / Scenario, Argument diagram

©2020. Japan Geoscience Union. All Right Reserved.

Advanced examination technique for crustal deformation in stable area: a case study of the Kanto Plain, Japan

*Nakanishi Toshimichi[1], Tetsuya Komatsu[1], Misao Hongo[2], Marie Noguchi[3], Tatsuki Miyamoto[4], Taiga Kimori[4], Toshihiko Sugai[4]

1. Japan Atomic Energy Agency, 2. Alps Technical Research Lab. Co. Ltd., 3. Paleo Labo Co. Ltd., 4. Univ. Tokyo

Evidence of uplift and subsidence are scarce in a tectonic stable area, because the topography and strata due to glacial sea-level changes had been difficult to accumulate. To recognize them in such area, comprehensive consideration would be needed based on the uplifted terraces and drilling logs. In order to quantitatively verify the uncertainty of the above issues, the following research was conducted on the northern part of the Kanto Plain where there is few existing information (Tajikara, 2000; Sugai et al., 2013). To identify the distribution of the Marine Isotope Stage (MIS), three drilling cores were drilled at the Takagi Plateau (emerged at MIS 4; Kaizuka et al., 2000) along the Kinugawa River. These drilling sites are located from upstream to downstream in the order of GC-OY-2, GC-OY-1, and GC-NG-1, with hole elevations of 34.0 m, 29.5 m, 20.6 m and excavation length of 86.0 m, 90.0 m and 74.6 m, respectively. Using these cores, lithology, assemblages of diatom and pollen, and tephra analysis were performed. Drilling cores are mainly composed of Pleistocene sediments formed in various sedimentary environments from land to sea. The upper part has transitioned to the loam layer, and a mud bed with severely alteration (Kazusa Group) is distributed below the depth of 79.43 m of the GC-OY-2 core at the uppermost stream. In addition, many vitreous ash layers, pumice layers and scoria layers were found in the three cores. The Pleistocene at a depth of less than 90 m was divided into beach, upper outer, lower outer, inner bay, meandering river and reticulated river. As a result of diatom and pollen analysis, high sea level sediments corresponding to MIS5e and a dominant layer of Quercus spp. Corresponding to MIS11 were identified. Many strata corresponding to these are also found in the central part of the Kanto Plain (Nakazawa and Endo, 2000; Nakazawa and Tanabe, 2011; Naya and Yasuhara, 2014). Examining their distribution and sedimentary environments, we want to establish a method for estimating crustal deformation in the uplift / subsidence boundary area. This study is conducted in collaboration with the University of Tokyo. Topographical development since MIS5 and sea level change before MIS6 have been presented by Kimori et al. (2020) and Miyamoto et al. (2020) at this conference, respectively. We hope fruitful discussion with you.

Acknowledgments: This study was carried out under a contract with the Agency of Natural Resources and Energy, part of the Ministry of Economy, Trade and Industry of Japan as part of its R&D program supporting development of technology for geological disposal of high-level radioactive waste.

References:

Kaizuka, S., Koike, K., Endo, K., Yamasaki, H., Suzuki, T., Regional geomorphology of the Japanese Islands vol. 4 Geomorphology of Kanto and Izu-Ogasawara, Univ. of Tokyo Press, 349p (in Japanese with English abstract), 2000.

Kimori, T., Sugai, T., Miyamoto, T., Komatsu, T., Nakanishi, T., Geomorphic development of the Takaragi terrace since the Last Interglacial period in the north central part of Kanto Plain, Japan, JpGU –AGU Joint Meeting, H-QR06 Session, 2020.

©2020. Japan Geoscience Union. All Right Reserved.

Miyamoto, T., Sugai, T., Kimori, T., Komatsu, T., Nakanishi, T., Paleogeographical changes based on sedimentary facies analysis of the Kinugawa lowland, central Japan, JpGU –AGU Joint Meeting, H-QR06 Session, 2020.
Nakazawa, T., Endo, H., Depositional sequences related to tectonic movements of the shallow subsurface Pleistocene successions in the central Kanto Plain, central Japan, Journal of the Sedimentological Society of Japan, vol.51, pp.23-38 (in Japanese with English abstract), 2000.
Nakazawa, T., Tanabe, S., Geology of Noda district. Quadrangle Series, 1:50000, Geological Survey of Japan, AIST, 72p. (in Japanese with English abstract), 2011.
Naya, T., Yasuhara, M., Geology of Kounosu district. Quadrangle Series, 1:50000, Geological Survey of Japan, AIST, 82p. (in Japanese with English abstract), 2014.
Sugai T., Matsushima (Ogami), H., Mizuno K., Last 400 ka landform evolution of the Kanto Plain: Under the influence of concurrent glacio-eustatic sea level changes and tectonic activity, Journal of Geography (Chigaku Zasshi), vol.122, pp.921-948 (in Japanese with English abstract), 2013.
Tajikara, M., Late Quaternary crustal movement around Kanto mountains, Japan, Proceedings of the Hokudan International Symposium and School on Active Faulting - Active Fault Research for the New Millenium –, pp.503-505, 2000.

Keywords: Sea-level change, crustal deformation, chronology, late Quaternary, Kanto Plain

©2020. Japan Geoscience Union. All Right Reserved.

Distribution map of erosion rates on timescales of 10^2–10^4 years in the Japanese Islands

*Yuki Hiura[1], Tetsuya Komatsu[1], Shigeru Sueoka[1], You Kitamura[2], Tomoji Sanga[2]

1. Japan Atomic Energy Agency, 2. JX Nippon Exploration and Development co. Ltd.

Distribution map of erosion rates on geological timescales should be prepared to evaluate the long-term stability of geological environments. Previous distribution maps of erosion rates were constructed based on deposition rates in artificial dams on multi-decadal timescales. This study aims to construct a new distribution map of erosion rates on timescales of 10^2–10^4 years by using reported data derived from terrestrial cosmogenic nuclide (TCN) methods. This study presents the method for constructing the new distribution map of erosion rate and the results of comparing it with the previous one.

Acknowledgments: This study was carried out under a contract with METI (Ministry of Economy, Trade and Industry) as part of its R&D supporting program for developing geological disposal technology.

Keywords: erosion rate, reservoir sedimentation, terrestrial cosmogenic nuclides, Japanese Islands, GIS

©2020. Japan Geoscience Union. All Right Reserved.

Machine learning for activity evaluation of crush zones using chemical composition: introduction of examples

*Koji Shimada[1], Ryo Tateishi[2]

1. Japan Atomic Energy Agency, 2. University of Toyama

We need a method to assess the activity of crush zones alternative to the application of overlying sediments (Hataya et al., 1992), because the zones encountered in underground tunnels and boring have unknown extensions to the ground surface. Until now, a cease of crush zone activity has been proven by the existence of (a) disagreement of current stress field and slip direction, (b) not-destroyed dike, vein, minerals on the basis of cross-cutting relation, and (c) high-temperature condition of deformation microstructures or mineralization generated when these incidents occurred accompanied with water-rock interaction (NRA, 2015; Ishiwatari, 2016; Niwa et al., 2016; Shimada et al., 2016). These methods have been advanced as being applicable in the field, but ambiguity or inconsistency of evaluation, even among experts, are exist. So, there is room for further evaluation method development.

The method to be developed is one in which the result is objective and independent of the person, which helps professional judgment. In addition, implementation, dissemination and verification must be executable by a general geological engineer. Ideally, it should be as easy as possible to be understood by non-experts. In light of these goals, the whole-rock chemical composition of the fault gouge along a principal slip zone of the crush zone is attractive. In underground tunnels, the time for geological observation may be limited due to construction and safety measures, whereas sampling for whole-rock chemical composition can be done in a relatively short time. Considering the case of widespread use in the future, the hurdle of sampling is low even when a sample is provided by a volunteer. Furthermore, there is a possibility that non-destructive in-situ measurement can be performed by portable XRF. Chemical analysis data is quantitative data that can be disclosed in literatures, and the database can be continuously expanded and repeatedly verified. Then, is there any difference in the chemical composition of fault rocks between active and inactive faults? Is there a solution worth asking this question?

Kuwatani et al. (2014) show that the chemical composition of tsunami deposits and non-tsunami deposits from the 2011 off the Pacific coast of Tohoku Earthquake can be separated with high probability by machine learning (multivariate analysis). We thought this idea could be a solution. Therefore, following this concept, we collected literature values of the chemical composition of fault gouges for faults with known activities, and began searching for a primary equation that distinguishes active from non-active faults by multivariate analysis in 2018. The explanatory variable is a chemical composition which is a quantitative variable, and the objective variable to be predicted is a fault property (active fault or non-active fault) which is a qualitative variable. See Tateishi et al. (2020) for details of the results. The results of studies on granitic rocks show that there are multiple discriminants that separate active and non-active faults with a discrimination rate of 100%. In the process of searching for a discriminant with high generalization performance that is not specialized for teacher data, elements that greatly contribute to discrimination between the two groups are being found. In other words, it is an element that characterizes active faults, and clues are being obtained for solving the nature of chemical composition change associated with continuous activity or activity cessation. In the presentation, we would like to introduce the current status of initiatives, including past case studies.

This study was funded by METI, Japan as part of its R&D program supporting development of technology

©2020. Japan Geoscience Union. All Right Reserved.

for geological disposal of HLW.
References are shown in Japanese abstract.

Keywords: machine learning, crush zone, chemical composition

©2020. Japan Geoscience Union. All Right Reserved.

Trial of domain segmentation of granite based on fracture orientations using Dip Azimuth Vector plot

*Shuji Terusawa[1], Koji Shimada[2]

1. OYO CORPORATION, 2. Japan Atomic Energy Agency

In geological disposal of radioactive waste, it is important to develop a method to extract as much information as possible from one borehole. Here we show the results of a trial of domain segmentation of granite using the Dip Azimuth Vector plot, which is often used in resource exploration drilling, according to the dominant fracture direction in each part observed by BHTV. The term “domain segmentation” means that, for example, a fracture dominant region having a NE-oriented strike and a high-angle NW dip is distributed 50 m in borehole length, and a deeper section is distributed in a section in another direction. In crystalline rocks such as granite, cracks are the main flow path of groundwater. Improving the method of quickly grasping the fracture dominant direction and the intersection of fracture systems at domain boundaries will contribute to the refinement of groundwater flow models.

The data used was strike and dip of about 800 fractures obtained from a 240m borehole TV image taken at the MBC-2 hole drilled on the site of the Japan Atomic Energy Agency's prototype fast breeder reactor Monju. The Dip Azimuth Vector plot (also called the Walkout plot) accumulates the sine and cosine of each data from the dip direction (360-degree dip direction), the cumulative sine on the vertical axis and the cumulative cosine on the horizontal axis on the Cartesian coordinates. This is a method of observing the trend and its change by the dip direction of planer structures, and is used to divide the geological structure in the borehole direction (eg Ciupercă et al., 2018). Here, the origin is the ground surface, and the depth at which the trend is bent, that is, the domain boundary (m; rounded off to the decimal point) and domains A to L are shown (Fig. 1). They have the following characteristics:

Domain A (section length 75m, the same applies hereafter)-Slope direction SSW trend (the same applies below) showing large variations. Domain B (37m)-Small variation in SE trend. Domain C (12m) -NE trend showing small variations. Domain D (18m) -SE trend showing small variations, and the trend matches the domain B. Domain E (11m) -SSW trend showing large variations. Domain F (9m) –WNW trend showing small variations. Domain G (37m) - SE trend, same as B and D, showing small variations. Domain H (11m) -E trend showing small variations. Domain I (4m) -WNW trend, same as F, showing small variations. Domain J (13m) -ESE trend showing small variations. Domain K (2m) -NNW trend showing small variations. Domain L (10m) -ESE trend, same as J, showing small variations. The median of the section length excluding the domain A and L is 11.5 m, and the average value is about 15 m. The average dip of the fracture is about 47 degrees since the cumulative dip angle is 37226 degrees with respect to the number of fractures of 794, and the variation in each domain is small. Domains B, C and D, for example, have the strike and dip of, B and D; N29E47E, C; N45W47E. Intersection lines of the domain boundaries, i.e., intersection of the two dominant fracture orientations, dips 41 degrees into 82 degrees of azimuth, as a possible pipe-like flow path of groundwater.
We present some results of domain division analyses using a few neighboring boring hole data.

©2020. Japan Geoscience Union. All Right Reserved.

Hydrothermal alteration in the Toki granitic body, central Japan -Mass transfer associated with precipitation of carbonate minerals-

*Hatsukawa Haruka[1], Nakashima Kazuo[2], Yuguchi Takashi[1]

1. Yamagata University Graduate School, 2. ASN Co., Ltd.

The hydrothermal alteration has been observed ubiquitously in granitic rocks. In the Toki granitic body, Nishimoto et al. (2008) and Nishimoto and Yoshida (2010) described how the hydrothermal alteration in the granitic rock is constrained mainly by the dissolution –precipitation process during the infiltration of hydrothermal fluid. The hydrothermal alteration of the granite progressed through three successive stages: 1) biotite chloritization, 2) plagioclase alteration, and 3) precipitation of carbonate mineral. Yuguchi et al. (2015 and 2019) also described quantitative discussions about mass transfer associated with biotite chloritization and plagioclase alteration, respectively. Thus, this study focuses on the mass transfer between carbonate mineral and hydrothermal fluid in the Toki granite, which corresponds to final phenomena in the hydrothermal alteration processes.

The Toki granite in the Tono district, Central Japan, is one of the Late Cretaceous plutonic intrusives in the Sanyo Belt, the Inner Zone of Southwest Japan. The Toki granite, a zoned pluton, has three rock facies grading from muscovite-biotite granite at the margin through hornblende-biotite granite to biotite granite in the interior. The samples were collected from the rock mass around 500 m depth in Mizunami Underground Research Laboratory (MIU).

The carbonate minerals were observed by pluralization microscope and scanning electron microscope (SEM), which are categorized into massive (patchy) occurrence and vein (fracture-filling) occurrence, and then are subdivided in terms of their shape and alteration degree. The carbonate minerals were observed by cathodoluminescence image in order to evaluate the growth process and the chemistry of the carbonate minerals were analyzed by EPMA.

Our study presents A) the classification of growth patterns of carbonate minerals and B) the minute amounts of components including the carbonate mineral. In case of the carbonate mineral in contact the altered chlorite, iron and manganese occurs, which may be outflux components derived from previous alteration processes such as biotite chloritization and plagioclase alteration.

Keywords: Carbonate minerals, SEM, Cathode luminescence image, Minor elements, EPMA, Mass transfer

©2020. Japan Geoscience Union. All Right Reserved.

Hydrogeological structures of hydraulic conductive fractures at a depth of 300 m

*Ai Hamada[1]

1. Central Research Institute of Electric Power Industry

In geological disposal of high-level nuclear waste, hydraulic conductive fractures in crystalline rock such as granite have been considered as a main pathway for radionuclides. Diffusion and absorption of radionuclide through microstructure in rock matrix can make mass transport to retard. Because the change of the characteristics of microstructure in rock matrix by structural movement and hydrothermal alteration have an effect on mass transport, it is important to understand the distribution and the structures of hydrogeological continuity of fractures as well as their characteristics of microstructure in rock matrix. There are three directions of fractures commonly distributed in the western and the eastern rock around GL −300 m Measurement Niche off Ventilation Shaft of Mizunami Underground Research Laboratory of JAEA: NW strike and high dip angle fracture (NW fracture), NE strike and high dip angle fracture (NE fracture) and low dip angle fracture, which is distributed around the Upper fracture zone in Toki Granite. The hydraulic conductive fractures across multiple boreholes to the west sides, which mainly show NW fracture have two types of characteristics: euhedral calcite-filled fractures with highly matrix chloritization including sphalerite and epidote and the fractures with poor filling minerals which is formed along cataclastic vein texture. In the former case, it is possible that the druse, which was formed after mineralization, plays a water channel. In the latter case, the fracture was formed along the cataclastic texture consisting of fractured rock-forming minerals. Each NW fracture is well continuous in hydrogeological aspects between the boreholes. Since being measured hydraulic pressure response between these NW fractures, it can be presumed that there is low dip angle fracture to connect the water channel according to the result of the in-situ resin injection test. The transmissibility coefficients in both types of fractures are measured about 10^{-7}-$10^{-5}m^2/s$. NE fractures in the western side are poorly permeable because of highly alteration in matrix filling with sericite, chlorite and smectite. On the other hand, the east side tends to have a larger number of fractures compared to the west side, especially in low dip angle fractures. In the northeast region, the fracture density is high and the fractures have filling minerals such as calcite and smectite with alteration in matrix. This is interpreted as being close to the damage zone associated with the formation of the main shaft fault (Tsuruta et al., 2012) and being affected by alteration along the fault. Hydraulic conductive fractures on the east side are NW fractures, NE fractures and low dip angle fractures, however, there is no remarkably continuous in geological characteristics between the boreholes. Low dip angle fractures have poorly engagement between fracture surfaces in the core samples and the druse forming needle-like or plate-like euhedral calcite crystals. The water pressure response among the three holes in the east side tends to be dispersed over a wide range, not only in the fractures with a large amount of water during drilling. The transmissibility coefficients in both types of fractures are measured about 10^{-8}-$10^{-5}m^2/s$. As a summary, in the rock around GL −300 m Measurement Niche off Ventilation Shaft, on the west side, NW fractures with hydrogeological continuity form higher-permeability zone through low dip angle fractures. On the east side, a large number of low dip angle fractures intersect between the fractures which has a large amount of spring water and may form a network of hydraulic conductive fractures. In addition, the results of the behavior of diffusion and sorption in rock matrix around the hydraulic conductive fractures will be reported. This study is commissioned by the Agency for Natural Resources and Energy in the Ministry of Economy, Trade and Industry. Core sampling were conducted as a part of a collaborative research with JAEA.

©2020. Japan Geoscience Union. All Right Reserved.

Keywords: geological disposal, hydrogeological structure, hydraulic conductive fracture, Toki Granite, Mizunami Underground Research Laboratory, high-level nuclear waste

©2020. Japan Geoscience Union. All Right Reserved.

Properties of precipitates in alkaline Fe^{2+}-SiO_2-H_2O systems

*Yuki Sakuma[1], Yuto Nishiki[1], Ryosuke Kikuchi[2], Tsubasa Otake[2], Tsutomu Sato[2]

1. Graduate school of Engineering, Hokkaido university, 2. Faculty of Engineering, Hokkaido University

Understanding the alteration of the constituent materials of multi-barrier system is crucial for long-term safety assessments of high-level radioactive waste disposal. Whereas previous studies have aimed to understand respective properties and alteration of materials such as stainless steel and glass, few studies have focused on the interaction between these materials due to the difficulty of the experiments under anoxic condition. If secondary phases formed between these materials consume both of dissolved Fe^{2+} from the steel and dissolved silica from the glass, the secondary phases should be considered in addition to kinetics of glass dissolution and native iron magnetization. Hence, this study focuses on the interface and aim to understand properties of precipitates in Fe^{2+}-SiO_2-H_2O systems.
Laboratory experiments with different conditions (Fe^{2+}/Si(initial molar concentration) = 0.4, 0.7, 1.0, 1.3, 1.5 and pH = 7, 10, 12) were conducted in a N_2 or Ar gas filled globe box to maintain reducing environment. After mixing of Fe^{2+}- and silica-bearing solution under all experimental condition, light greenish materials formed. X-ray diffraction (XRD) and infrared (IR) spectroscopy revealed the formation of Fe-bearing hydrated silicate which has similar XRD and IR spectra with those of magnesium silicate hydrate (M-S-H) under all experimental conditions. Therefore, the precipitate may be ferrous silicate hydrate (F-S-H) in Fe^{2+}- SiO_2-H_2O system. Furthermore, the XRD results showed formation of ferrous hydroxides at high Fe/Si condition (Fe/Si ≧1.3) whereas the results showed formation of amorphous silica at low Fe/Si condition (Fe/Si=0.4, pH=10). This suggests that F-S-H has preferable range of Fe/Si like M-S-H. Consequently, ferrous hydroxides or amorphous silica prefer to be formed when Fe^{2+} or silica is excessively dissolved in the system, respectively. Solution chemistry after precipitation under alkaline conditions (pH = 10, 12) indicated that both Fe^{2+} and Si were almost entirely consumed for precipitation of F-S-H. On the other hand, under the condition with pH7, F-S-H precipitated but Fe^{2+} and Si are still present in solution. This reveals that alkaline condition is absolutely essential for formation of F-S-H.
This study implies that F-S-H can form at glass-steel interfaces when disposal environment is alkaline condition. If so, kinetics of F-S-H formation and alteration of F-S-H should be considered to understand evolution of the barrier interface between glass and steel and positive and negative impacts of F-S-H phases.

Keywords: Nuclear waste disposal, Ferrous silicate hydrate , Ferrous iron

©2020. Japan Geoscience Union. All Right Reserved.

[J] Poster | H (Human Geosciences)：H-CG Complex & General

[H-CG29] Role of scientists in rehabilitation of nuclear disaster areas

convener:Taku Nishimura(Deptartment of Biological and Environmental Engineering, Graduate School of Agricultural and Life Sciences, University of Tokyo), Masaru Mizoguchi(Graduate school of Agricultural and Life Sciences, The University of Tokyo), Kosuke Noborio(Meiji University)

Nine years have passed since nuclear power plant accident at Fukushima after Great East Japan Earthquake on March 2011. Memory of the accident is getting less while several governmental actions accelerating the reconstruction of Fukushima from the nuclear disaster have been implement. Still we have many unsolved problems in the disaster area, such as restart of agricultural activities as well as management of radioactive material polluted waste water. Pure natural and social scientific issues such as multiscale mass (including radioactive materials) circulation and rehabilitation policy for depopulated areas after the accident are essential for the reconstruction.
This session aims to discuss cooperation of activities of scientific research, education and implement of outcomes of them in the disaster area. Considering international collaborations at disaster areas we will invite a foreign guest speaker to promote the discussion. This issue is not limited to nuclear disaster areas rather it is a core issue at areas of depopulation and aging community in Japan. So that discussion would not be limited in Fukushima.

[HCG29-P01] Evaluation of water erosion of Andisol under climate chage

*Sotaro Makino[1], Shoichiro Hamamoto[1], Kazutoshi Osawa[2], Onishi Taisuke[3], Taku Nishimura[1] (1.The University of Tokyo, 2.Utsunomiya University, 3.NTC International Inc.)

[HCG29-P02] **Analysis of radiocesium discharge distribution using GeoWEPP in Iitate village, Fukushima**

*Seigo Fujiwara[1], Mari Saito[2], Kazutoshi Osawa[2], Hiroyuki Matsui[2] (1.Center for Research in Isotopes and Environmental Dynamics, University of Tsukuba, 2.School of Agriculture, Utsunomiya University)

[HCG29-P03] Temporal and Spatial Transport of Radiocesium on a Slope after Scraping Surface Soil Off

*Yuki Sunakawa[1], Yuki Ito[2], Yuki Takagi[1], Ryuta Honda[3], Taku Nishimura[4], Masaru Mizoguchi[4], Kosuke Noborio[3] (1.Graduate School of Agriculture, Meiji University , 2.Gilat Research Center, Agricultural Research Organization, Israel, 3.School of Agriculture, Meiji University, 4.Graduate School of Agriculture and Life Sciences, The University of Tokyo)

[HCG29-P04] A study on the run-off of dissolved ^{137}Cs from contaminated slopes to an irrigation canal after the Fukushima Dai-ichi Nuclear Power Plant accident

*Satoshi Tajima[1], Shuichiro Yoshida[1], Taku Fukui[1], Naoto Nihei[2] (1.The Univ. of Tokyo, 2.Fukushima Univ.)

[HCG29-P05] Radioactive cesium binding to dissolved organic matter extracted from litter collected at forest in Fukushima prefecture

*Takahiro Tatsuno[1], Shoichiro Hamamoto[1], Naoto Nihei[2], Taku Nishimura[1] (1.Deptartment of Biological and Environmental Engineering, Graduate School of Agricultural and Life Sciences, University of Tokyo, 2.The Faculty of Food and Agricultural Sciences, Fukushima University)

[HCG29-P06] **Overview of Academic Studies on Iitate Village and its Revival Knowledge**

Hiroaki Sugino[1], *Masaru Mizoguchi[1] (1.Graduate school of Agricultural and Life Sciences, The University of Tokyo)

Evaluation of water erosion of Andisol under climate chage

*Sotaro Makino[1], Shoichiro Hamamoto[1], Kazutoshi Osawa[2], Onishi Taisuke[3], Taku Nishimura[1]

1. The University of Tokyo, 2. Utsunomiya University, 3. NTC International Inc.

Radioactive materials have been distributed after the accident of Fukushima dai-ichi Nuclear Power Plant at March 2011. Decontamination works have been conducted and thus most of arable lands and residential areas have been decontaminated. However, forest was not the target of decontamination plan, and pasture lands are still under planning. Still a possibility of redistribution of radioactive materials from those contaminated area to decontaminated area is discussing.

Water erosion is an important agent of the redistribution. Universal Soil Loss Equation which is a de facto standard soil erosion model in Japan may predict annual soil loss from agricultural lands. It has been extended to describe soil loss from pasture lands and forests. However, it still can predict only annual soil loss even though rainfall characteristics such as rainfall intensity and frequency of a rainfall event alters under effects of the climate change. Soil loss prediction and evaluation for each rainfall event would be important however USLE does not have a performance to do it. So, we tried to use Water Erosion Prediction Project (WEPP) and Cligen combined with Marksim to simulate future rainfall events and soil loss under those rainfall events.

Simulated rainfall by Cligen with Marksim cannot wholly represent a trend of shorter but heavier recent rainfall events. However, results of soil simulations suggested extent of surface runoff during a rainfall event is an important factor to consider soil loss and thus redistribution of radioactive materials. This would suggest soil treatment to avoid reduction of infiltration and management of surface runoff will be effective to reduce redistribution of radioactive materials.

This work was supported by JSPS grant number 15H02467. Also, we would appreciate suports from Fukushima Innovation Coast Framework Promotion Organization to our project (Project leader: Masaru Mizoguchi, UTokyo) .

Keywords: soil erosion, climate change, redistribution of radioactive materials, WEPP

©2020. Japan Geoscience Union. All Right Reserved.

Analysis of radiocesium discharge distribution using GeoWEPP in Iitate village, Fukushima

*Seigo Fujiwara[1], Mari Saito[2], Kazutoshi Osawa[2], Hiroyuki Matsui[2]

1. Center for Research in Isotopes and Environmental Dynamics, University of Tsukuba, 2. School of Agriculture, Utsunomiya University

Background

On March 11th, 2011, a massive tsunami inundated the Fukushima Dai-ichi Nuclear Power Plant, which resulted in an enormous amount of radioactive fallout and deposition on the soil in and around Fukushima Prefecture. Radiocesium deposited on the soil is predicted to be discharged into coastal and fluvial areas during rainfall events. Especially, the half-life of radiocesium137 (^{137}Cs) is 30.2 years. Thus, the effects in Fukushima Prefecture is an ongoing, long-term issue to the local population. On April 1st, 2017, the evacuation order in Iitate Village was lifted except the difficult-to-return zone. However, few forest areas were included in the so-called rational and efficient decontamination. Thus, a large amount of radiocesium remains in upland forests on the plateau. Since most ^{137}Cs is in the depth of 0-5 (cm), the remaining radiocesium has been redistributed with water and sediment transport. The aims of this study are (i) to detect the ^{137}Cs discharge dynamics with river monitoring, which was conducted on two rivers, Mano river and Hiso river, in Iitate village, Fukushima Prefecture from 2013 to 2018 using the Geospatial Interface for the Water Erosion Prediction Project (GeoWEPP), and (ii) to identify the sources of the ^{137}Cs discharge in the watersheds.

Method

GeoWEPP fundamental data and observed data were modified to run analyses on GeoWEPP. Moreover, the data of laboratory experiments about soil erosion were collected to calibrate the estimated values by WEPP. After finishing the data processing, the calibration of effective hydraulic conductivity (K_e) and rill erodibility (K_r) was conducted. Observed and simulated streamflow and sediment yield were compared at annual and whole-simulated time step, by means of model evaluation statistics. The applied statistics were the Nash–Sutcliffe efficiency (NSE), the root mean squared error (RMSE), the percent bias (PBIAS), and the deviation of runoff volume (Dv). At last, the calculation of ^{137}Cs discharge was conducted with the influence of radioactive decay and the decontamination efforts in the residential areas and agricultural lands without the ‘difficult-to-return’ area.

Results

The study areas experienced significant variation in annual precipitation. The annual field-observed streamflow ranged from 62 in 2016 to 215 (mm) in 2015 at Mano river, 65 in 2018 to 179 (mm) in 2015 at Hiso river. In both cases, there is a maximum value in 2015 because there was a big typhoon that caused flood around Fukushima and other prefectures in Japan.

Overall, the GeoWEPP model simulation values were in good agreement with the observed values due to the calibration of streamflow and sediment yield. In terms of streamflow after K_e calibration at both rivers, evaluation results at annual and whole-simulated time step showed better or maintained close values. In the case of sediment yield after K_e and K_r calibration at both rivers, the majority of the simulated years showed ‘satisfactory’ and evaluation results for the whole-simulated years were better. Lastly, the sources of the ^{137}Cs discharge in the watersheds were determined and verified with multiple sampling ^{137}Cs discharge data.

©2020. Japan Geoscience Union. All Right Reserved.

Discussion

The ^{137}Cs discharge was adjusted with the land-use data to introduce the influence of the decontamination works. However, the land-use data are 100m×100m cell size. If there were more fine mesh land-use data, the ^{137}Cs discharge maps would be very helpful to understand the sources of the ^{137}Cs discharge.

Keywords: Radiocesium, Soil erosion, Modelling, GeoWEPP

©2020. Japan Geoscience Union. All Right Reserved.

Temporal and Spatial Transport of Radiocesium on a Slope after Scraping Surface Soil Off

*Yuki Sunakawa[1], Yuki Ito[2], Yuki Takagi[1], Ryuta Honda[3], Taku Nishimura[4], Masaru Mizoguchi[4], Kosuke Noborio[3]

1. Graduate School of Agriculture, Meiji University , 2. Gilat Research Center, Agricultural Research Organization, Israel, 3. School of Agriculture, Meiji University, 4. Graduate School of Agriculture and Life Sciences, The University of Tokyo

In March 2011, radioactive materials, including radiocesium (Cs) were released into the surrounding environments by the accident of Fukushima Daiichi Nuclear Power Plant and contaminated forests and houses. To reduce external gamma exposure, Cs on houses including the surrounding area within a 20m distance from the houses was removed. However, areas beyond the 20m distance at a higher elevation on the backyard mountain slope remained uncleaned. Remaining Cs at the higher elevation on the backyard mountain slope might move down on the slope surface to the lower elevation,
where Cs had been removed, by the surface runoff. The objective of this study was to investigate how Cs was transported on the slope after the removal of Cs. On the south-facing slope located in the north of the houses in Iitate Village, Fukushima Prefecture, topsoil with a litter was collected several times a year from April 2015 to November 2019. The concentrations of ^{134}Cs and ^{137}Cs were measured using a γ-ray spectrometer equipped with a Ge semiconductor detector. The topsoil sampling locations were chosen at Cs-remained, upper Cs-removed, middle Cs-removed, and lower Cs-removed areas along the backyard hill slope, and the lowest Cs-removed area was added in April 2016. Sampling locations were triplicated at a similar elevation to one another. Since the temporal gradients of cumulative rainfall and Cs concentrations at all the locations tended to correspond, Cs might be transported along the slope with surface runoff. When the half-lives of ^{137}Cs (approximately 30 years) were taken into account, the concentration of ^{137}Cs at the lower and the lowest Cs-removed area was often lower than estimates accounting for natural decay. Since the slope of the graph of accumulated ^{137}Cs concentration after 2017 is small at the same areas, Cs might move vertically in the soil while flowing down the slope surface.

Keywords: Radiocesium, Decontamination, Slope

©2020. Japan Geoscience Union. All Right Reserved.

A study on the run-off of dissolved ^{137}Cs from contaminated slopes to an irrigation canal after the Fukushima Dai-ichi Nuclear Power Plant accident

*Satoshi Tajima[1], Shuichiro Yoshida[1], Taku Fukui[1], Naoto Nihei[2]

1. The Univ. of Tokyo, 2. Fukushima Univ.

After the large earthquake and the tsunami disaster hit north-east Japan on March 11, 2011, a variety of radionuclides were released from the Fukushima Dai-ichi Nuclear Power Plant (FDNPP) accident. Among the nuclides, ^{137}Cs has been regarded to have persistent effects on the environment from its relatively long half-life (30.1 y). In the aquatic environment, there are two forms of radiocesium: a 'particulate' form that is strongly combined with suspended sediment, and a 'dissolved' form. Preceding studies reported that there was a tendency of radiocesium in river water to redistribute mostly in the particulate fraction, which was suggested to be a consequence of strong adsorption of radiocesium by clay minerals in soil or sediment in rivers. Nevertheless, dissolved radiocesium may not be ignorable, because it can be imbibed by plants more efficiently than that in particulate form, thereby accumulating in the ecosystem and circulating biologically. Although dissolved radiocesium has been still constantly flowing out from catchments even in a small but certain amount under base-flow condition, the major sources of it have not been completely confirmed.

We focused on the possible risk of remaining ^{137}Cs in the environment around paddy fields. Severe contamination of radiocesium in paddy fields has been removed by the decontamination project. However, slopes of agricultural canals and bunds of paddy fields have not been subject to the decontamination. Since soil can strongly adsorb radiocesium as was mentioned above, litter covering the slopes probably plays a substantial role in supplying dissolved ^{137}Cs.

The objectives of this study were to (1) clarify the trend in the discharge and the redistribution of ^{137}Cs from contaminated slopes along an agricultural canal by directly collecting the overland flow, and (2) analyze the possible mechanisms of the discharge of dissolved ^{137}Cs by investigating and partitioning the forms of ^{137}Cs in the litter samples from the slopes.

The sample of the overland flow was filtered through glass filters and 0.45 μm membrane filters. ^{137}Cs in the filtrate was defined as a dissolved fraction, while in the residue as a particulate fraction. ^{137}Cs in the litter samples were partitioned by employing the sequential extraction method. ^{137}Cs extracted by deionized water (H_2O) was defined as a water-soluble fraction, by ammonium acetate (CH_3COONH_4) as an ion-exchangeable fraction, by alkalis ($Na_2P_4O_7$, NaOH) as a fraction that associated with humic and fluvic acid, and hydrogen peroxide (H_2O_2) as a fraction that associate with other organic matters, such as lignin.

The results showed that dissolved ^{137}Cs constantly and stably ran out of the catchments, while a large proportion of particulate ^{137}Cs ran out exclusively under storm conditions. The annual discharges of dissolved radiocesium ranged between 0.063 –4.7 Bq m^{-2} y^{-1}, and K_d values (ratio of particulate to dissolved radioactivity concentrations) under base-flow condition were in the order of 104 L kg^{-1}, which were less than the geometric mean of the K_ds for forest streams and major rivers reported in the preceding studies.

Storages of currently water-soluble ^{137}Cs in the litter of the slopes were estimated to be 2.2 –32 Bq m^{-2}, and the surface run-off rates of precipitation were 1.8 –8.3%. From these observed values, the discharges of dissolved ^{137}Cs from the catchments were estimated to be 0.040 –2.0 Bq m^{-2} y^{-1}, which roughly corresponded to the observed values. Because there were also ^{137}Cs in the ion-exchangeable form or forms associating with the humic substances, they have potentially become a water-soluble form after

©2020. Japan Geoscience Union. All Right Reserved.

each runoff event to keep the concentration of dissolved ^{137}Cs within the observed range for years. This evidence and discussion suggest that water-soluble ^{137}Cs in the litter layer on the catchments might be one of the major sources of dissolved ^{137}Cs that has been discharged from the contaminated paddy environment.

Keywords: Fukushima Dai-ichi Nuclear Power Plant accident, Radiocesium, Paddy fields, Sequential extraction

©2020. Japan Geoscience Union. All Right Reserved.

Radioactive cesium binding to dissolved organic matter extracted from litter collected at forest in Fukushima prefecture

*Takahiro Tatsuno[1], Shoichiro Hamamoto[1], Naoto Nihei[2], Taku Nishimura[1]

1. Deptartment of Biological and Environmental Engineering, Graduate School of Agricultural and Life Sciences, University of Tokyo, 2. The Faculty of Food and Agricultural Sciences, Fukushima University

Introduction

To understand migration of radioactive cesium (RCs) in soils is an important issue after the accident of Fukushima Dai-ichi nuclear power plant, Japan. Dissolved organic matters (DOM) possibility bind with RCs and alters the migration of RCs in soils. DOM is negatively charged at pH 3-11 owing to the dissociation of hydrogen ion from the functional group, enable to adsorb metal cations. Most of the DOM is composed of humic substances. Humic substances are classified into humic acid (HA), which is acid-insoluble and alkaline-soluble, and Fulvic acid (FA), which is soluble in both acid and alkaline solution. Previous studies showed soil organic samples adsorbed with Cs by using stable Cs solution with high concentration. However, it is not clear whether RCs binds to DOM in the condition with low RCs concentration typically observed in Fukushima. In this study, we evaluated effects of co-existing cations and difference in types of organic matter on RCs binding to organic matters based on adsorption batch experiment.

Materials and Methods

DOM and humic substance (e.g. HA and FA) were extracted from a litter which was collected at an abandoned forest in Iitate, Fukushima, Japan. DOM solution was filtrate solution made by filtering the litter and pure water mixture through 0.45 μm membrane filter. HA and FA were extracted according to the method of the International Humic Substance Society (IHSS). The RCs solution was made by diluting ^{137}Cs stock solution.

The mixture of each organic matter and RCs solution was shaken for 72 hours. DOC concentration in the mixture was adjusted to 20 mg-C L^{-1}, while Cs concentration in the mixture was adjusted to 2.27 $\times 10^{-11}$ mol L^{-1}. Furthermore, in order to evaluate the effect of Na ion on Cs binding to DOM, the concentration of Na ion in the mixture was adjusted to 0, 1×10^{-13}, 1×10^{-11}, 1×10^{-10}, 1×10^{-7}, 1×10^{-4}, 1×10^{-1} by adding NaBr solution to the mixture. After mixing, water-soluble RCs and RCs bound to DOM (hereinafter called RCs-organic form) were separated by ultrafiltration. RCs concentration in the sample was measured by NaI scintillation counter (2480 WIZARD2, Perkin Elmer).

Results and Discussions

As a preliminary experiment, adsorption experiment of RCs and DOM was conducted using DOM solution extracted from litter collected from the forest floor at university forest of the University of Tokyo in Chichibu city, Saitama prefecture, Japan. In the mixture without adding Na ion, 30% of RCs in the mixture bound to DOM. However, as the concentration of Na ion in the mixture increased, the RCs-organic form in the mixture decreased. When Na concentration was more than 1×10^{-3} mol L^{-1}, there was no RCs-organic form in the mixture. These results indicated that Na ion depressed RCs binding to DOM.

Acknnowledgement

This work was supported by JSPS grant number 15H02467and academic fund of The Japanese Society of Irrigation, Drainage and Rural Engineering. Also, we would appreciate supports from Fukushima Innovation Coast Framework Promotion Organization to our project (Project leader: Masaru Mizoguchi, UTokyo)

©2020. Japan Geoscience Union. All Right Reserved.

Keywords: Fukushima, Cesium-137, Dissolved organic matter , humic substance

©2020. Japan Geoscience Union. All Right Reserved.

Overview of Academic Studies on Iitate Village and its Revival Knowledge

Hiroaki Sugino[1], *Masaru Mizoguchi[1]

1. Graduate school of Agricultural and Life Sciences, The University of Tokyo

Much academic research has been conducted in the background of the recovery from the Great East Japan Earthquake. The knowledge accumulated from these studies should be used not only for the reconstruction of this earthquake, but also for building social resilience that will contribute to recovery in an expected large-scale disaster in Japan. This presentation will illustrate the accumulation of knowledge obtained from academic research in Iitate Village since 2011. Topic extraction using the LDA (Latent Dirichlet Allocation) method was performed on meta-information (titles, keywords, abstracts, etc.) of 486 papers whose study location was Iitate village. After visualizing the temporal flow and change of research topics since 2011, required research and knowledge in the future will be discussed.

Keywords: revival agriculture, Iitate village, Fukushima, web scraping, topic modelling

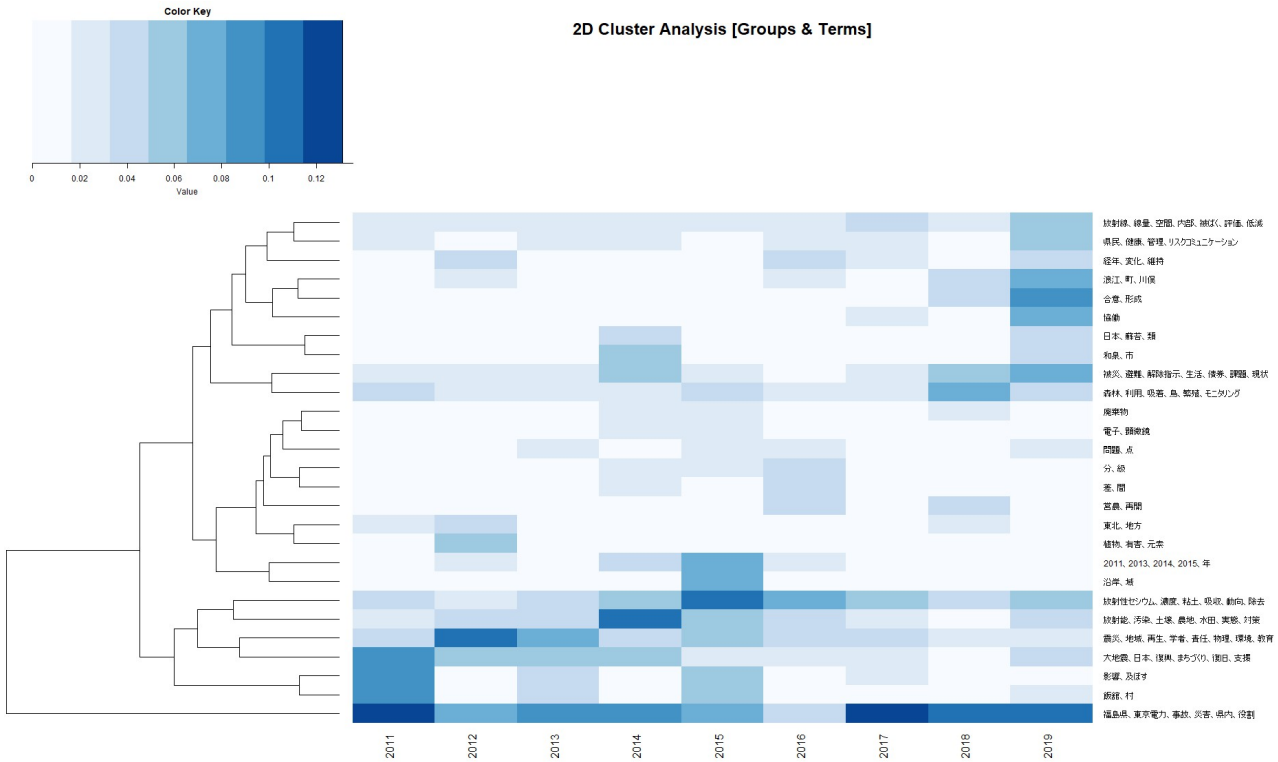

©2020. Japan Geoscience Union. All Right Reserved.

[J] Poster | H (Human Geosciences)：H-CG Complex & General

[H-CG30] Archeological Science: Earth Sciences and Archaeology

convener:Yorinao Shitaoka(Department of Environment System, Faculty of Geo-environmental Science, Rissho University), Tadahiro Hatakeyama(Information Processing Center, Okayama University of Science), Masataka Hakozaki(National Museum of Japanese History)

Archaeological science, which analyzes remains and archaeological sites using geoscientific approaches, has become an invaluable research method to advance research in archaeology by the examination of "things" left behind by earlier humans. Research methods of a wide range, including age determination and paleoenvironmental reconstruction, geophysical exploration, and material analysis, have been applied in archaeological science as methods using geoscientific approaches. Clay body analysis using a stable isotope ratio and research to ascertain the dynamics of humans and livestock are also progressing. This session is aimed at promoting scientific archaeological research to enable further contributions to archaeology. For that purpose, we accumulate the latest knowledge by bringing together all results of archaeological scientific research conducted to restore the history of humankind and to address related fields in an interdisciplinary manner.

[HCG30-P01] Significance of detection of ancent city of Phasis with Earth Sciences and Archaeology

*Satoru Oishi[1], Vakhtang Licheli[2] (1.Research Center for Urban Safety and Security Kobe University, 2.Iv. Javakhishvili Tbilisi State University)

[HCG30-P02] High-precision chronology of paleoenvironmental changes by utilizing Jomon pottery types

*Koji Umeda[1], Masatoshi Shiba[1], Misaki Kondo[1], Tatsuhito Sekine[2], Kodai Igarashi[3], Mizuki Takeuchi[3] (1.Graduate School of Science and Technology, Hirosaki University, 2.Faculty of Humanities and Social Sciences, Hirosaki University, 3.Faculty of Science and Technology, Hirosaki University)

[HCG30-P05] Development of the ultra-high resolution photography for detecting the abnormal tree-rings

*Masataka Hakozaki[1] (1.National Museum of Japanese History)

[HCG30-P06] Middle Paleolithic records of control fire events in north-central India

*Deepak Kumar Jha[1], Rahul Samrat[1], Prasanta Sanyal[1] (1.Department of Earth Sciences, Indian Institute of Science Education and Research Kolkata, India)

[HCG30-P07] Magnetic surveys for archaeology

*Tadahiro Hatakeyama[1,2], Yu Kitahara[3], Nobutatsu Mochizuki[4] (1.Information Processing Center, Okayama University of Science, 2.Graduate School of Biosphere-Geosphere Science, Okayama University of Science, 3.Graduate School of Social and Cultural Studies, Kyushu University, 4.Faculty of Advanced Science and Technology, Kumamoto University)

[HCG30-P08] Analyzing the early 19th century's local geographical points in latitude and longitude of 0.2 second level and geomagnetic declination through Japan from Tadataka Inoh's magnetic survey azimuth ledger simultaneously.

*Motohiro Tsujimoto[1], Akitoshi - Omotani[2] (1.none, 2.San-in.System Consultant Co.Ltd)

[HCG30-P09] What can archaeomagnetism contribute for Southeast Asian archeology?

*Yu Kitahara[1], Mariko Yamagata[2], Masao Ohno[1], Yuhji Yamamoto[3], Tadahiro Hatakeyama[4] (1.Faculty of Social and Cultural Studies, Kyushu University, 2.Faculty of Management, Okayama University of Science, 3.Center for Advanced Marine Core Research, Kochi University, 4.Information Processing Center, Okayama University of Science)

[HCG30-P10] Archeological material and archeo-sediment analysis using luminescence method

*Yorinao Shitaoka[1] (1.Department of Environment System, Faculty of Geo-environmental Science, Rissho University)

[HCG30-P11] Interpreting the Ancient Legend “Descent of Ganga” of India as a Historical Record of a Comet Impact 6000 years ago.

*Mahesh Uday Patil

[HCG30-P12] A human exploitation of obsidian in Pre-Hispanic Tenerife, Canary Islands, Spain: A preliminary result of obsidian sourcing based on pedestrian survey and geochemical analysis

*Yuichi Nakazawa[1], Cristina Vega Maeso[2], Mari Sumita[3], Eduardo Carmona-Ballestero[4], John Rissetto[5], Alberto Berzosa Ordaz[4], Yasuo Naoe[6], Kensho Dohi[7], Mina Araya[7], Mercedes del Arco-Aguilar[8], Hans-Ulrich Schmincke[3] (1.Faculty of Medicine / Hokkaido University, Japan, 2.University of Cantabria, Spain, 3.GEOMAR Helmholtz Centre for Ocean Research Kiel, Germany, 4.University of Burgos, Spain, 5.Nebraska State Historical Society, USA, 6.Chitose Board of Education, Japan, 7.Hokkaido Archaeological Operations Center, Japan, 8.Tenerife Archaeological Museum, Spain)

Significance of detection of ancent city of Phasis with Earth Sciences and Archaeology

*Satoru Oishi[1], Vakhtang Licheli[2]

1. Research Center for Urban Safety and Security Kobe University, 2. Iv. Javakhishvili Tbilisi State University

The ancient city of Phasis was one of the colonies of Ionian Greeks, who made more than 90 colonies in the Caucasus region during the period between 6th and 4th centuries BC. Phasis is assumed to be located somewhere around Poti, which is a Georgian town on the East coast of the Black Sea. However, the exact location of Phasis is still unknown, even BRUN(1880) had discussed, and GAMKRELIDZE(2012) listed twelve candidates of Phasis.
By recognizing the location of Phasis and digging the remaining materials, we could understand cultures and communications of the 6th to 4th century BC leading the expansion of our understanding of cultural propagation.

Lichelli (2016) proposed the possible location of Phasis by taking peat, earthquake and ancient scripts into consideration. He pointed out that the possible location as follows, Supsa river as a southern end, Black sea coast which should be deferent from the current one as a western end, and a meridian line passing Sagvichio town in Georgia as an eastern end. Moreover, he suggested that Phais is located inside a triangle with edges consisting of three intersectional points between Supsa river and Black sea coast, Rioni river and Black sea coast, the meridian line passing Sagvichio and Pichori river. The area of the triangle is 150 square km.

According to the ancient scripts, Phasis was a city on wet-land, based on artificial hills. The settlement consists of one central island having 60m of radius, 7-8 m high, and other small islands locating the area surrounded by wet-land and the Black sea from the western side, rivers, and lake. It is assumed that the islands had 300m times 300m scale, and the area is 0.06% of the triangle. This place was found in 60-ies of the last century as an ordinary settlement, but due to the absence of a coordinate system, identification of the settlement is impossible in the high density forests and wet-lands. Therefore, we made a plan to find out the city. We need to determine the coastal line of 5th century BC, determine the river-meandering area by river-morphology, and we have to take experiments of sedimentation to know which type of shape would appear on the surface of sediment having islands/artificial hill in its beneath. Then, we will find the shape by satellite images of ALOS-2, SAR.

This project is very precious because it leads to the propagation of copper, iron, and litters in Eurasia.

Keywords: Phasis, archaeological sites, detection

©2020. Japan Geoscience Union. All Right Reserved.

High-precision chronology of paleoenvironmental changes by utilizing Jomon pottery types

*Koji Umeda[1], Masatoshi Shiba[1], Misaki Kondo[1], Tatsuhito Sekine[2], Kodai Igarashi[3], Mizuki Takeuchi[3]

1. Graduate School of Science and Technology, Hirosaki University, 2. Faculty of Humanities and Social Sciences, Hirosaki University, 3. Faculty of Science and Technology, Hirosaki University

We examined detrital materials included in Jomon potteries as a proxy for the reconstruction of environment changes.

Keywords: Jomon pottery, paleoenvironmental changes, chronology

©2020. Japan Geoscience Union. All Right Reserved.

Development of the ultra-high resolution photography for detecting the abnormal tree-rings

*Masataka Hakozaki[1]

1. National Museum of Japanese History

Dendrochronology is a scientific dating method that can determine the calendar year of timber materials without error, and is useful for grasping the ages of archeological sites and old buildings with high accuracy. Premise of tree-ring dating is accurate tree ring discrimination. However, the tree-rings may include abnormal rings such as discontinuous rings and false rings. If they cannot be identified, there is a risk of dating failure or reporting the wrong date.
Abnormal rings can be detected by precise observation of cell size and cell wall thickness. However, observation at the cell level requires use the optical microscope or a digital microscope, which is troublesome and costly. Therefore, in this study, we developed a method to easily take ultra-high resolution images that can observe cells with a commercially available digital camera.
Our method can also be applied to the construction of cell tree-ring chronologies and the study of climate reconstruction based on it. Although it is known that cell chronology can be applied to high resolution reconstruction of summer temperature and precipitation, little research has been conducted in Japan. If climate information can be obtained on a monthly or weekly basis, comparisons with historical events can be made easier, and this can lead to thinking about causal relationships.

Keywords: Dendrochronology, False ring, Cell tree-ring chronology

©2020. Japan Geoscience Union. All Right Reserved.

Middle Paleolithic records of control fire events in north-central India

*Deepak Kumar Jha[1], Rahul Samrat[1], Prasanta Sanyal[1]

1. Department of Earth Sciences, Indian Institute of Science Education and Research Kolkata, India

The paleosols preserved in the fluvial cliff sections of the Belan valley, situated in north-central India, provide a gradual change in typotechnology from the Lower Paleolithic (~100 ka) to Neolithic (~3 ka). These archaeological sites would provide a platform to comprehend the hominin landscape and fire activities during the Late Quaternary. The wildfire in modern ecosystem acts as a vital component in shaping the vegetation composition and land surface process and dynamics. Thus, the identification of fire use events in paleo-records would improve our understanding of the prehistoric human-environment in India. However, apart from climate and vegetation, prehistoric humans could have equally contributed to past fire activity. Therefore, disentangling the wildfire from prehistoric human-induced fire is crucial to comprehend the environmental conditions at a regional and global scale.
In this study, paleosol samples were collected from six archaeological sites of the Belan River valley. The samples were used for analyses of macro-charcoal (CHAR) to reconstruct the past fire events. CHAR values suggest paleofire events at i) ~58 ka, ii) ~26 ka and iii) ~8 ka. Our previous study based on isotopic studies of *n*-alkanes biomarker has shown that high rainfall events occurred at i) ~60 ka, ii) ~26 ka and iii) ~10-3 ka, which is contemporaneous to observed fire activities. The period between ~30 and 25 ka indicates the dominance of grassland (C_4 plants) in a cool and dry environment, which was a suitable condition for natural fires to occur. The CHAR peaks observed in this study overlap with high rainfall conditions, which were an unconducive condition for wildfires. Additionally, fire disturbance surges during the early-Holocene to mid-Holocene correspondence to the timing of agricultural practices in the Belan valley. Therefore, this study suggests that prehistoric humans controlled fire during the Middle Paleolithic phase.

Keywords: Archaeology, Charcoal, Fire, Middle Paleolithic

©2020. Japan Geoscience Union. All Right Reserved.

Magnetic surveys for archaeology

*Tadahiro Hatakeyama[1,2], Yu Kitahara[3], Nobutatsu Mochizuki[4]

1. Information Processing Center, Okayama University of Science, 2. Graduate School of Biosphere-Geosphere Science, Okayama University of Science, 3. Graduate School of Social and Cultural Studies, Kyushu University, 4. Faculty of Advanced Science and Technology, Kumamoto University

In archaeology, methods of physical surveys have been used to detect archaeological sites and relics buried in the soils. Survyes of electric waves (ground radar), elastic waves, electric field, magnetic filed and other variables are used in archaeological surveys as well as in geophysical surveys. However, the target depth of the archaeological surveys is much shallower than that of geophysical surveys. In the shallow region, the inhomogeneous structure tends to force the complecated interpretation of the results. For archaeological purpose, we have been measured the magnetic properties observed on the surface, magnetic field (anomaly) and susceptibility, which are the indicatives of the magnetization indicating the exposure to the heat and contents of magnetic (iron minerals).
Here we introduce recent our works on magnetic field survey and magnetic suscepbility survey to find buried/surface fired sites, especially with the paleomagnetic and rock magnetic points of view.

Keywords: Magnetic survey, Magnetic susceptibility survey, Physical survey, Archaeology

©2020. Japan Geoscience Union. All Right Reserved.

Analyzing the early 19th century's local geographical points in latitude and longitude of 0.2 second level and geomagnetic declination through Japan from Tadataka Inoh's magnetic survey azimuth ledger simultaneously.

*Motohiro Tsujimoto[1], Akitoshi - Omotani[2]

1. none, 2. San-in.System Consultant Co.Ltd

The Santou-Houi-Ki is a national treasure of Japan recorded by Japanese cartographic surveyor Tadataka Inoh in 1800 to 1816,consist of 67 volumes survey ledger to produce the first survey map of Japan ,called "Maps of Japanese Coastal Area "(1:216000) or Inoh Map(1:36000,1:216000,1:432000). In the Santou-Houi-Ki estimate 200,000 magnetic compass survey azimuth data by accuracy of 0degree 05minute unit were recorded,with the name or short description of magnetic compass survey execution reference point and target points. Inoh's team carried out the survey did not apply the correction of magnetic declination. Because before the start of his survey, Inoh tried to observe magnetic declination in Edo(Tokyo) was nearly zero. Inoh conducted the survey on the assumption that the influence of magnetic declination to his survey map of Japan is at least. The surveyed region extends from North eastern coast of Hokkaido Island to Yakushima Island in western Japan.However the geomagnetic declination at each province were different in long Japanese archipelago. We start the analysis,check the outline position of the survey execution reference point and target points from magnetic survey azimuth,or name of places recorded in Santou-Houi-Ki, Inoh Map,or from the description of places in Inoh's Survey Diary,early modern survey maps, today's digital maps,GPS,or local source books or maps etc. It is able to calcurate backward the precise position of survey execution reference point,where the value of geomagnetic declination,subtracting the magnetic survey azimuth from the true azimuth to any target points are similar or approximate by using excell formula. Check the source books or maps of local history,and adjust the precise detail position. We must execute interdisciplinary and simultaneous analysis of precise position of the survey execution reference point (aim to latitude and longitude 0.2 second level), target points,real azimuth,geomagnetic declination from national treasure Santou-Houi-Ki. We cannot read the precise content of national treasure Santou-Houi-Ki or Inoh Map without this interdiiciplinary simultaneous analysis. The importance to restore the precise position of the survey execution reference points and target points and geomagnetic declination in early 19th century's Japan from Tadataka Inoh's Santou-Houi-Ki must elucidate.

Keywords: Cartographic surveyor Tadataka Inoh, Inoh Map, magnetic survey azimuth, National treasure Santou-Houi-Ki, geomagnetic declination, interdisciplinary simultaneous analysis

©2020. Japan Geoscience Union. All Right Reserved.

What can archaeomagnetism contribute for Southeast Asian archeology?

*Yu Kitahara[1], Mariko Yamagata[2], Masao Ohno[1], Yuhji Yamamoto[3], Tadahiro Hatakeyama[4]

1. Faculty of Social and Cultural Studies, Kyushu University, 2. Faculty of Management, Okayama University of Science, 3. Center for Advanced Marine Core Research, Kochi University, 4. Information Processing Center, Okayama University of Science

Southeast Asia has various ethnic and cultural groups with rich historical traditions. The elucidation of the history in Southeast Asia has progressing rapidly since the middle of the 19th century, when archeological research by European researchers began. However, many details of the relationship between the archeological sites are still unclear. One of the reasons is that the relationship between the relative ages of the archeological artifacts from each archeological site is still unclear. Because if the designs of the archeological artifacts are significantly different, it will be difficult to construct one series based on typology. However, the physical quantities such as archaeomagnetic data are just numerical values, they are less susceptible to cultural differences and may be used to construct relative chronologies that can link many archeological sites distributed in a wide area.
On these backgrounds, we are currently planning a research to construct a dataset combining archaeology, art history and archaeomagnetism, then to create a foundation for applying to the elucidation of cultural and social structural changes in Southeast Asia, and finally to reapply the results to geoscientific research. Specifically, we plan to study the following three themes; (1) A more detailed description of the history of two cultures from the 4th century BC to the 15th century AD in central Vietnam (Sa Huynh Culture and the culture of the kingdom of Champa), (2) Age estimation of an unknown archaeological site from southern Vietnam, and (3) Construction of a secular variation curve of geomagnetic two components (intensity and inclination) in Vietnam.
In this presentation, we will introduce the outline of this research project and consider its potential.

Keywords: Archaeomagnetism, Southeast Asian Archaeology, Vietnam, Sa Huynh Culture, Kingdom of Champa

©2020. Japan Geoscience Union. All Right Reserved.

Archeological material and archeo-sediment analysis using luminescence method

*Yorinao Shitaoka[1]

1. Department of Environment System, Faculty of Geo-environmental Science, Rissho University

Thermoluminescence (TL) and optically stimulated luminescence (OSL) methods have served important roles in providing a chronology in support of archaeological science studies. These methods have been used for dating, and assessment of firing temperatures.
For this study, TL dating of a burnt block was performed. The burnt block was found at the Tako-Gunga ancient country office site in Gunma, Japan. The site is granary of an ancient country office that was destroyed by fire as result of the archeological excavation. The date of burning shows evidence of fire, because TL signal is reset by heating. Quartz inclusion method was used to estimate the paleodose and achieve TL dating. Results suggest the TL age as 1.29±0.25 ka. The horizon at which the burnt block was found was below the tephra layer (Asama-B), inferred as A.D. 1108, which means that this TL age is consistent with stratigraphy.

Keywords: archaeological science studies, dating, assessment of firing temperatures, thermoluminescence, optically stimulated luminescence

©2020. Japan Geoscience Union. All Right Reserved.

Interpreting the Ancient Legend “Descent of Ganga” of India as a Historical Record of a Comet Impact 6000 years ago.

*Mahesh Uday Patil

Placer deposits of the YarlungZangbo Suture Zone of Tibet are rich with finds like coesite, stishovite, microdiamonds, osbornite, high pressure nitrides, TiO_2 II and other minerals. These finds are usually only associated with hypervelocity impact sites (1). However in the absence of impact evidence some have suggested that they originate from a mantle origin, even though such a mantle origin has many challenges making it difficult to accept. Tibetan lakes behind Mount Kailash between the latitudes of 82°, 30’ E and 90°, 30’ E and 29° N and 33° N are the main source of Yarlung Zangbo River. It is desirable to study this area for possible impact craters.

The ancient legend “Descent of Ganga” which describes a story of a celestial icy body traveling with great velocity and descending on earth, along with other ancient records suggests a possible comet impact near Mount Kailash. Many aspects of this legend such as the description of the events, appearance, descent path, and effects at the time of descent are similar to what one would expect with an impact event by a comet. Ancient Stone carvings and paintings of the time can be viewed as depictions of records of the celestial movement and impact event. Vedas like Rigveda, Atharvaveda refer to comets as “Dhumketu”. Certain hymns and verses of the Vedas are in the form of eye witness accounts of an impact event that is being observed and recorded. In this poster, we will present ancient symbolism, descriptions, and artwork comparing them with expected comet impact appearances being described in the legends, and will review some geological features of the region and attempt to show that a comet broke apart into small pieces and impacted in the Southern Tibet about 6000 years ago.

The image shows an ancient carving depicting "ketu". In Sanskrit, comet is known as "Dhumketu" or "ketu". Its translated as Dhum means "smoke" and Ketu is depicted as" Tail of demon serpent".

(1) E. M. Shoemaker et al., First Natural Occurrence of Coesite, Science 22 Jul 1960,Vol. 132, Issue3421, pp.220-222, DOI: 10.1126/science.132.3421.220

Keywords: Impact, crater, legends

©2020. Japan Geoscience Union. All Right Reserved.

©2020. Japan Geoscience Union. All Right Reserved.

©2020. Japan Geoscience Union. All Right Reserved.

A human exploitation of obsidian in Pre-Hispanic Tenerife, Canary Islands, Spain: A preliminary result of obsidian sourcing based on pedestrian survey and geochemical analysis

*Yuichi Nakazawa[1], Cristina Vega Maeso[2], Mari Sumita[3], Eduardo Carmona-Ballestero[4], John Rissetto[5], Alberto Berzosa Ordaz[4], Yasuo Naoe[6], Kensho Dohi[7], Mina Araya[7], Mercedes del Arco-Aguilar[8], Hans-Ulrich Schmincke[3]

1. Faculty of Medicine / Hokkaido University, Japan, 2. University of Cantabria, Spain, 3. GEOMAR Helmholtz Centre for Ocean Research Kiel, Germany, 4. University of Burgos, Spain, 5. Nebraska State Historical Society, USA, 6. Chitose Board of Education, Japan, 7. Hokkaido Archaeological Operations Center, Japan, 8. Tenerife Archaeological Museum, Spain

The Canary archipelago comprises seven major islands located approximately 27 –29 degrees N, stretching for 490 km on the eastern Atlantic, off the shore of northwestern North Africa. Tenerife, the highest and largest volcanic island among the Canary Islands was occupied by the indigenous people called the Guanches, until the 15th Century when the Spanish colonizers arrived. In November 2016, a group of the authors have conducted a pedestrian survey of obsidian outcrops and archaeological sites on the surface of Tenerife, as well as an observation on excavated obsidian artifacts from major archaeological sites at the Tenerife Archaeological Museum. The purpose of this research was to investigate the human exploitation of obsidian to elucidate how the Guanches survived in this active volcanic landscape during the Pre-Hispanic times. Island of Tenerife provides an ideal setting to address this research question, because of its unique biogeographic settings: diverse ecological zones characterized by northern humid region and southern dryland, and altitudinal difference created by Mt. Teide (3718m asl) in the middle of the Island. The survey was conducted at the southern dryland (“barranco”) of Tenerife, and we identified a total of 32 artifact scatters, principally consisting of obsidian artifacts, pot sherds, and marine shells. Among the surface scatters, 29 of them have obsidian artifacts. Besides these archaeological surface scatters, we also located three obsidian outcrops: Tabonal Negro (a part of phonolitic dome in Mt. Teide), Tabonal los Guanches (northern skirt of Mt. Teide), and Chalco de Viento (north coast). Some obsidian artifacts were collected for further geochemical study of obsidian and hydration measurements. Besides, obsidian artifacts from Estacas 1 and Guargacho were also sampled for comparison. Among these samples, we specifically chose 11 samples from a combination of surface localities, excavated archaeological sites, and obsidian outcrops. In this paper, we report a preliminary result of EPMA and Laser ICP-MS analysis of these obsidian samples. The result will provide a variation in geochemical signatures of obsidian and an implication of Pre-Hispanic human use of obsidian in Tenerife.

Keywords: Canary Islands, Tenerife, pedestrian survey, obsidian, EPMA, L-ICP-MS

©2020. Japan Geoscience Union. All Right Reserved.

[J] Poster | H (Human Geosciences)：H-CG Complex & General

[H-CG31] Coastal wetlands: geomorphologic, biologic and anthropogenic processes

convener:Kiyoshi Fujimoto(Nanzan University), Toyohiko Miyagi(Advantechnology Co., Ltd.)

Coastal wetlands are very fragile environment against external environmental changes such as sea-level rise and anthropogenic impacts. On the other hand, coastal wetlands have a significant role as a place for carbon sequestration in the belowground as well as the aboveground. This session will discuss the geomorphologic, biologic and anthropogenic processes on the coastal wetlands in the various climate zones during the Holocene. For example, coastal wetlands in the tropics have evolved with the development of wetland forests such as mangrove forest, peat swamp forest and fresh water swamp forest. The most significant process for habitat formation and maintenance of the former two forests are peat production and decomposition, which are also significant processes on the coastal lowlands in the temperate and subarctic zones, though the mechanism of the processes might be different. Geomorphological processes such as sedimentation and erosion by fluvial and marine processes are also important for all of coastal wetlands. However, the environment of coastal wetlands has been destroyed by various human activities such as deforestation, agriculture land development, peat mining, and shrimp firming in and around mangrove forests in recent years. We would like to invite the wide discipline of research papers on not only the natural processes but also the anthropogenic processes in order to offer the scientific basis for creating sustainable management systems on the coastal wetlands in the future.

[HCG31-P01] Emerging influences of rapid sea-level rise on Micronesian mangrove forests: Ground level dynamics in the main communities and prop roots dynamics of a *Rhizophora stylosa* community

*Kiyoshi Fujimoto[1], Kenji Ono[2], Shin Watanabe[3], Shingo Taniguchi[3], Keita Furukawa[4], Yasumasa Hirata[5], Kodai Hasada[6], Renpei Suwa[7], Saimon Lihpai[8] (1.Nanzan University, 2.Tohoku Research Center, FFPRI, 3.The University of Ryukyus, 4.Association for Shore Environment Creation, 5.FFPRI, 6.Hosei University, 7.JIRCAS, 8.Pohnpei State Government)

[HCG31-P02] Consideration of sea level rise effect on sediment transport process in mangrove forest

*Keita Furukawa[1], Kiyoshi Fujimoto[2], ONO Kenji[3], Shin Watanabe[4], Shingo Taniguchi[4], Yasumasa Hirata[3], Kodai Hasada[5], Renpei Suwa[7], Saimon Lihpai[6] (1.Association for Shore Environemt Createion, 2.Nanzan University, 3.Forestry and Forest Productis Research Institute, 4.Universtiy of the Ryukyu, 5.Hosei University, 6.Pohnpei State Government, 7.Japan International Research Center for Agricultural Sciences)

[HCG31-P03] Comparison of belowground root production of the mangrove forests in the Western Pacific Ocean islands among tropical and subtropical regions and mangrove species.

*Kenji ONO[1], Kiyoshi FUJIMOTO[2], Rempei SUWA[3], Rene ROLLON[4], Ariel C. BLANCO[4], Giannina MARIE G. ALBANO[4], Green ANN A. CRUZ[4], Yasmin H. PRIMAVERA-TIROL[5], Ronald J. MALIO,[5], Ryan M. BASINA[5], Shingo TANIGUCHI[7], Shin WATANABE[7], Yasumasa HIRATA[1], Saimon LIHPAI[6,8], Kazuo NADAOKA[6] (1.Forestry and Forest Products Research Insititute, 2.Nanzan University, 3.Japan International Research Center of Agricultural Science, 4.University of the Philippines, 5.Aklan State University, 6.Tokyo Institute of Technology, 7.University of the Rhyukyu, 8.Pohnpei State Government, FSM)

[HCG31-P04] Mangrove swamp distribution mapping by the whole earth directsensing approach

*Toyohiko Miyagi[1], Shigeyuki Baba[2], Tomomi Inoue[3], Yasuo Akaji[3], Gakugun Chou[3], Keita Furukawa[4], Hideaki Yanagisawa[5] (1.NIES・Tohoku-Gakuin Univ., 2.ISME, 3.NIES, 4.PEMSEA, 5.Tohoku-Gakuin University)

Emerging influences of rapid sea-level rise on Micronesian mangrove forests: Ground level dynamics in the main communities and prop roots dynamics of a *Rhizophora stylosa* community

*Kiyoshi Fujimoto[1], Kenji Ono[2], Shin Watanabe[3], Shingo Taniguchi[3], Keita Furukawa[4], Yasumasa Hirata[5], Kodai Hasada[6], Renpei Suwa[7], Saimon Lihpai[8]

1. Nanzan University, 2. Tohoku Research Center, FFPRI, 3. The University of Ryukyus, 4. Association for Shore Environment Creation, 5. FFPRI, 6. Hosei University, 7. JIRCAS, 8. Pohnpei State Government

In the western Pacific low-latitude region between the Philippines and Micronesia, the sea level has been rising at over 10 mm/yr (IPCC 2013). In the mangrove habitat situated in the low sediment inflow environment, *Rhizophora* pure forest is generally formed as a pioneer community and mangrove peat is created. However, the mangrove peat accumulation rate is considered to decrease with the vegetation succession because of the decline of tree density of *Rhizophora* sp. The mangrove communities decreased mangrove peat accumulation rate is possibly affected by sea-level rise first. In Pohnpei Island, Micronesia, the surface erosion is not recognized in the *Rhizophora stylosa* and *Rhizophora apiculata* communities, while it is recognized in the communities dominated by other species.

We will report first the ground level dynamics for the main mangrove communities in Pohnpei based on the observation data using the erosion/accumulation observation piles installed into the peat deposits up to the base and secondary the forest dynamics including prop roots of a *R. stylosa* community using the monitoring data for 16 years from 2003 to 2019.

We set five stainless piles with 5 mm in diameter for each observation plot. The observation plots were established seaward and landward sites of four permanent plots, i.e., PR , PC, PS and PK, whose dominant species are *R. stylosa*, *R. apiculata*, *Sonneratia alba* and *Bruguiera gymnorrhiza*, respectively. The landward plot of PK was set between buttress roots of *Xylocarpus granatum*. The ground level dynamics rate (cm/year) of seaward and landward sites for each plot was 0.76±0.48 and 0.28±0.34 for PR, 0.34± 0.22 and 0.23±0.19 for PC, -0.28±0.68 and -0.04±0.36 for PS, -0.42±0.56 and 0.01±0.14 for PK. Namely, accumulation trend in *Rhizophora* communities and erosion trend in *Sonneratia* and *Bruguiera* communities were observed.

The aboveground biomass of PR was estimated using the allometric equation of Komiyama et al. (1988) for *R. stylosa* except prop roots and Komiyama et al. (2005) for *B. gyminorrhiza*. The biomass of densely developed prop roots of *R. stylosa* was estimated by the following procedure because the existed allometric equations are inaplicable, i.e.,1) 5 meters square plots were set at seaward side, central part and landward side of PR, 2) the length and diameter were measured for all prop roots, which were divided into lignified hard one and unlignified soft one, in each plot and the total volume was calculated, and 3) the prop roots biomass was calculated by multiplying the each volume on the each density.

The aboveground biomass in PR increased from 235 t/ha (*R. stylosa*: 212 t/ha, *B. gymnorrhiza*: 23 t/ha) at 2003 to 327 t/ha (*R. stylosa*: 304 t/ha, *B. gymonorrhiza*: 23 t/ha) at 2019. The prop roots biomass of *R. stylosa* increased from 120 t/ha at 2003 to 198 t/ha at 2019. The soft roots increased constantly from 2 t/ha to 41 t/ha during the 16 years, while the hard roots decreased from 137 t/ha to 87 t/ha between 2011 and 2015 and increased again to 158 t/ha at 2019. The total prop roots biomass also decreased

©2020. Japan Geoscience Union. All Right Reserved.

between 2011 and 2015 with the decrease of hard ones. The prop roots dynamics possible suggests that the *R. stylosa* forests are trying to maintain the ground level by accelerating the mangrove peat accumulation rate against the rapid sea-level rise by producing much more new prop roots.

Keywords: Mangrove forest, Mangrove peat, Sea-level rise, Surface erosion, Forest dynamics

©2020. Japan Geoscience Union. All Right Reserved.

Consideration of sea level rise effect on sediment transport process in mangrove forest

*Keita Furukawa[1], Kiyoshi Fujimoto[2], ONO Kenji[3], Shin Watanabe[4], Shingo Taniguchi[4], Yasumasa Hirata[3], Kodai Hasada[5], Renpei Suwa[7], Saimon Lihpai[6]

1. Association for Shore Environemt Createion, 2. Nanzan University, 3. Forestry and Forest Productis Research Institute, 4. Universtiy of the Ryukyu, 5. Hosei University, 6. Pohnpei State Government, 7. Japan International Research Center for Agricultural Sciences

Preliminary measurement for detecting sea level rise (SLR) effects on mangrove forests has been observed at Iriomote Island, Japan and Ponpei Island, Federal States of Micronesia since 2018. The short term SLR effects were measured by surface erosion and sedimentation. If sedimentation rate on a mangrove forest floor is faster enough to catch up with SLR, the forest will adapt on the change (Fujimoto et.al. 1989). Nevertheless, if it is slower than SLR, or erosion rate becomes greater than sedimentation rate, the forest will NOT adapt on the change (Furukawa et.al. 2002).

According to the observations, existence of following sediment transport mechanisms was suggested i.e. the existence of a sheet-flow transport mechanism in a short period of time when seawater is flooded and drained, the occurrence of steady erosion due to tidal transports, and the temporally and spatially uneven transport mechanism (Furukawa et al. 2019). In particular, it is necessary to clarify the effects of sediment supply from the upstream and micro-topography (creeks) existing on the forest floor.

Therefore, we attempted to measure two-dimensional sedimentation rate and sediment transport in the plot with complex topography conditions in 2019 (Pompeii PK plot: Fujimoto et al. 2019). In order to study the effects of tides and rainfall, observations were made during the spring tide (clear weather) and the ebb tide (rainfall).

The observation results were categorized, and the data obtained in the PK plot suggests a net sediment export from the forest to the sea. In particular following three points were noted, 1) sediment transport was remarkably different between the creek area and the flat forest floor area, 2) during the spring tide, sediment is supplied from both upstream and downstream in the creek, and the sediment tends to be slightly deposited, and 3) during the neap tide and rainfall, it was observed that the supply from the upstream side was dominant in the creek and the sedimentation in the forest increased, furthermore net sediment runoff occurred.

This research has been done as a part of “Mangrove forests community situation understanding against SLR.”

Keywords: mangrove forests, sediment transport, sea level rise, micro topography

©2020. Japan Geoscience Union. All Right Reserved.

Comparison of belowground root production of the mangrove forests in the Western Pacific Ocean islands among tropical and subtropical regions and mangrove species.

*Kenji ONO[1], Kiyoshi FUJIMOTO[2], Rempei SUWA[3], Rene ROLLON[4], Ariel C. BLANCO[4], Giannina MARIE G. ALBANO[4], Green ANN A. CRUZ[4], Yasmin H. PRIMAVERA-TIROL[5], Ronald J. MALIO,[5], Ryan M. BASINA[5], Shingo TANIGUCHI[7], Shin WATANABE[7], Yasumasa HIRATA[1], Saimon LIHPAI[6,8], Kazuo NADAOKA[6]

1. Forestry and Forest Products Research Insititute, 2. Nanzan University, 3. Japan International Research Center of Agricultural Science, 4. University of the Philippines, 5. Aklan State University, 6. Tokyo Institute of Technology, 7. University of the Rhyukyu, 8. Pohnpei State Government, FSM

Mangroves with high productivity of belowground roots accumulate the organic matter in their substrata as mangrove peat, create their growth foundations by themselves, and consequently expand their habitat in intertidal zones. Our earlier studies estimated that the mangrove forests including above- and below-grounds generally have a great amount of organic carbon (OC) storage compared with general terrestrial forests. To accurately evaluate sequestration and storage of OC in mangrove ecosystems across tropical and subtropical regions, it is necessary to determine the root productivity in mangrove forests, being because their root productivity highly contributes huge OC storage in their ecosystem, including the substratum. In the present study, we aimed to clarify the variations of the root production in the several types of mangrove ecosystems among the species and the regions. We conducted the ingrowth core experiment according to Fujimaki et al. (2004 PLSO) to estimate the annual root production rates in soils of 30-cm deep by mangrove stands in Micronesia (FSM), Philippines, and Japan. More than three mesh cores filled with root-free sands, i.e., ingrowth cores, were put on the forest floors at interior and seaside positions, respectively, with different frequency of water immersion by daily tide in each forest. From the cores collected from the sites, all fine roots were picked up their mass determined, and their annual production rates estimated. Annual root productions (30-cm deep) in the mangrove stands ranged from 1.9 to 16.9 Mg ha^{-1} yr^{-1} (Table 1). Mangroves in FSM, located in 5.8˚N, showed relatively higher root productivity than those in Philippines and Japan (11.8˚N and 24.4˚N, respectively). There was no clear differences of the root production among the species and between landward and seaward positions based on current data on hand. We continuously proceed with the detailed analyses of samples and data comparison and will report the results in this presentation.

Keywords: fine root production, mangrove, Pacific Ocean Islands

©2020. Japan Geoscience Union. All Right Reserved.

Table 1. Annual root production of mangrove stands (30-cm deep) at the tropical and subtropical regions in the West Pacific Ocean.

Dominant Species	Annual root pruduction ($Mg\ ha^{-1}\ yr^{-1}$)			
	Landward		Seaward	
	ave.	s.d.	ave.	s.d.
	Pohnpei Is., FSM			
Rhizophora apiculata	8.1	2.3	6.2	2.7
R. stylosa	2.4	1.2	6.3	5.1
Bruguiera gymnorrhiza	7.6	3.6	6.7	3.1
Xylocarpus granatum	8.0	2.6	6.6	2.4
Sonneratia alba	5.2	2.0	16.9	2.6
	Panay Is., Philippines			
Avicennia rumphiana	4.9	2.6	4.0	2.0
	Iriomote Is., Japan			
R. stylosa	3.5	1.0	3.5	1.0
B. gymnorrhiza	1.9	1.1	2.0	0.7

©2020. Japan Geoscience Union. All Right Reserved.

Mangrove swamp distribution mapping by the whole earth directsensing approach

*Toyohiko Miyagi[1], Shigeyuki Baba[2], Tomomi Inoue[3], Yasuo Akaji[3], Gakugun Chou[3], Keita Furukawa[4], Hideaki Yanagisawa[5]

1. NIES・Tohoku-Gakuin Univ., 2. ISME, 3. NIES, 4. PEMSEA, 5. Tohoku-Gakuin University

In those several years have remarkable new deployment of a sensing tool and technology. The direct sensing basedon the data base such as the google earth and world imargery is also getting popular. Our groups accumulate a number of field investigation experiences of world mangrove forests in last half century.
The team are carring the data base construction by GIS and World Imargry. We like to explain the current result of the Indochina coastmangrove mapping as the case study.

Keywords: Mangrove Forest, Whole earth direct sensing, Indochina peninsula

©2020. Japan Geoscience Union. All Right Reserved.

[J] Poster | H (Human Geosciences)：H-CG Complex & General

[H-CG32] Risk of Nuclear Technology and Geoscience: Dialogue with Engineers

convener:Kohta Juraku(Department of Humanities, Social and Health Sciences, School of Engineering, Tokyo Denki University), Satoshi Kaneshima(Department of Earth and Planetary Sciences, Kyushu University), Takeshi Sagiya(Disaster Mitigation Research Center, Nagoya University), Daisuke Suetsugu(institute for Marine Geodynamics, Japan Agency for Marine-Earth Science and Technology)

We have organized sessions in the JpGU meeting on the risk of nuclear power utilization in Japan mainly from the point of view of geoscience since 2013. It has shed new light on various aspects of the risk of nuclear power related to earthquakes, volcanic activities and tsunamis. We have also repeatedly acknowledged the differences of standpoints between scientists and engineers on those risks. Last year, our panelists from earthquake science raised the issues centering on the risk of inland earthquakes on nuclear power station and its uncertainty. It is closely relevant to the recent decision of the nuclear regulatory agency (NRA) on the method of inland earthquake risk on nuclear power stations. Public debates on this issue is still on-going.
In the 2020 JpGU meeting, we propose the session to deepen the dialogue between scientists and engineers more. What should geoscience take the stance on the issue of scientific uncertainty and nuclear risk? How could scientist and engineers work together for public goods? We would especially encourage paper submission by engineers to make it fruitful. We are also welcome to papers of other topics relevant to relationship of earthquake science and nuclear power plants.

[HCG32-P01] Communication gap between scientists and the society associated with uncertain risk information

*Takeshi Sagiya[1] (1.Disaster Mitigation Research Center, Nagoya University)

[HCG32-P02] Summary of 2019 JPGU session about strong ground motions anticipated at nuclear power plants in Japan

*Satoshi Kaneshima[1] (1.Department of Earth and Planetary Sciences, Kyushu University)

[HCG32-P03] A review: Earthquake activity of the Median Tectonic Line, Japan

*Daisuke Suetsugu[1] (1.institute for Marine Geodynamics, Japan Agency for Marine-Earth Science and Technology)

[HCG32-P04] Does Science Give Us THE Answer? Issues Centering on Risk and Social Decision-Making

*Kohta Juraku[1] (1.Department of Humanities, Social and Health Sciences, School of Engineering, Tokyo Denki University)

Communication gap between scientists and the society associated with uncertain risk information

*Takeshi Sagiya[1]

1. Disaster Mitigation Research Center, Nagoya University

Many geoscientists are working on natural hazard. Sometimes it is an important responsibility for them to communicate with non-scientists, engineers, decision makers, the media, and citizens, to provide information about future natural hazard. A problem of such risk information is its uncertainty. Some scientists are careful enough and provide risk information deliberately. But such information does not satisfy needs of non-scientists. On the other hand, there some people (sometimes pretending themselves as scientists) provides specific risk information that does not have enough scientific evidence. But sometimes such information is widely accepted. Earthquake hazard is one of such typical examples because of its very low probability. How to communicate with non-scientsts has been a difficult problem for scientists and we should always pay attention to the way how scientific result will be accepted.

Keywords: risk information, communication gap, seismic hazard

©2020. Japan Geoscience Union. All Right Reserved.

Summary of 2019 JPGU session about strong ground motions anticipated at nuclear power plants in Japan

*Satoshi Kaneshima[1]

1. Department of Earth and Planetary Sciences, Kyushu University

In this poster I revisit and summarize the discussions in the session about strong ground motions anticipated to hit Japanese nuclear power plants in the future, which was held at the 2019 JPGU meeting. This session was motivated by the occurrence of a strong crustal earthquake at Iburi, Hokkaido a year ago and generated unexpectedly high ground motions without clear signs of an active fault at the surface. Although it did not cause damages on a nuclear power plant nearby, we anticipated it was timely to discuss about the problem of strong motions expected at nuclear plants in Japan in general. Several geophysical and geological issues associated with this problem were discussed. Starting with a review about current estimates of the thickness of the seismogenic zone that has a potential to generate earthquakes with strong seismic ground motions at surface, the cause of strong ground motions caused by the Hokkaido-Iburi earthquake was discussed. The lack of ability to evaluate complex structures of active faults hidden under ground was elucidated, especially for the case of Kumamoto earthquake in 2016. The presentations given by the experts of each issue and the following discussions elucidated difficulty in making reliable scientific predictions that ensure accurate ground motion evaluations.

Keywords: Nuclear power plants, Strong ground motions, Large earthquake

©2020. Japan Geoscience Union. All Right Reserved.

A review: Earthquake activity of the Median Tectonic Line, Japan

*Daisuke Suetsugu[1]

1. institute for Marine Geodynamics, Japan Agency for Marine-Earth Science and Technology

In January 2020, the Hiroshima High Court ordered Shikoku Electric Power Co. to suspend a reactor of the Ikata Nuclear Power Plant, which is placed a few kilometers from a greatest active fault in Japan, the Median Tectonic Line. The decision was based on a risk from earthquakes of the fault and volcanoes in Kyushu. We provide a review of research and survey for activity of the Median Tectonic Line.

Keywords: Median Tectonic Line, Earthquake activity

©2020. Japan Geoscience Union. All Right Reserved.

Does Science Give Us THE Answer? Issues Centering on Risk and Social Decision-Making

*Kohta Juraku[1]

1. Department of Humanities, Social and Health Sciences, School of Engineering, Tokyo Denki University

It has been discussed the relationship between the risk of nuclear utilization and geoscience, the role of scientist and engineer in the previous sessions. The author has analyzed those issues from the perspectives of interactions and gaps between science and engineering, their views on risk and safety behind the social mechanism and their senses of vocation, and pursued the better way to overcome the obstacles centering on them

However, there has been the counter argument that the fundamental problem is ethics and conscience of scientists and engineers as the relevant professional, or problematic policies and institutional designs which lead moral hazards of them (e.g. Funabashi 2013, Shimazono 2013, Ishibashi 2019 and so on).

These different views are, from the point of view of STS (science and technology studies), caused by the difference of understanding on the nature and role of "science" itself. Does scientific knowledge directly tell us the best answer for social decision on safety (risk) of some technology? And is it an ideal of our way to make decision? Or, it doesn’ t the case, and we need some special articulation to bridge and organize the heterogeneous elements (of course, including scientific knowledge) to make appropriate decision? These different views lead different analysis –to understand the problem from ethical perspective, or communication and social mechanism perspectives.
In this paper, the author would like to illustrate a picture to understand and discuss the issues on "science and engineering relationship" in organized way, and to contribute to encourage substantial dialogue between them, citing his own case study on the "SPEEDI" (System for Prediction of Environmental Emergency Dose Information) controversy which was presented at the 2019 JpGU meeting.

Keywords: Science and Engineering, STS (Science and Technology Studies)

©2020. Japan Geoscience Union. All Right Reserved.

[J] Poster | H (Human Geosciences)：H-CG Complex & General

[H-CG33] Improvement of Integrated Research on Disaster Risk

convener:Keiji Kimura(Department of Geography, Nara University)

The Agenda for Sustainable Development 2030 (SDGs), which was resolved at the UN General Assembly resolution in 2015, has a common goal for the world by 2030.During this period, based on the path to understanding and improving the problems of the Human Geosciences that are becoming clear from the results of the ICSU Global Challenge that began in 2010, the enhancement of Human Geosciences-education and global expansion ensure flow. At the same time, research will be promoted within the framework of Future Earth. In this session, discussions will be held interdisciplinarily on the topics of disaster cause investigation, data integration, human social aspects of risk, disaster resilience, and social collaboration.

[HCG33-P01] Risk Assessment of Tropical Cyclone Disaster over the Seas around China under Climate Change

*Xin Li[1,2], Ren Zhang[1], Ju Wang[1], Mei Hong[1], Xueliang Zhou[1] (1. College of Meteorology and Oceanography, National University of Defense Technology, China, 2.State Key Laboratory of Numerical Modeling for Atmospheric Sciences and Geophysical Fluid Dynamics (LASG), Institute of Atmospheric Physics, Chinese Academy of Sciences)

[HCG33-P02] Wildfire risk prediction in Indonesia with the soil water by the numerical meteorological simulation WRF

*Keiji Kimura[1], Natsuki Takano[4], Mitsuru Osaki[2], Albertus Sulaiman[3], Pribadi Awal[3] (1.Department of Geography, Nara University, 2.Faculty of Agriculture, Hokkaido University, 3.Agency for the Assessment and Application of Technology, Indonesia, 4.Riso Kagaku Co.Ltd.(Graduated student, Nara University))

[HCG33-P03] Evaluation framework of health impacts caused by massive earthquakes in Osaka

*Koki Adachi[1], Lisa Ito[1], Akihiro Tokai[1] (1.Graduate School of Engineering, Osaka University)

[HCG33-P04] Promoting pre-disaster prevention actions in cooperation with school, boards of education, and researchers Part 2: Proposal of procedure manual to read hazard map

*Tatsuto Aoki[1], Kiyomi Hayashi[1] (1.School of Regional Development Studies, Kanazawa University)

Risk Assessment of Tropical Cyclone Disaster over the Seas around China under Climate Change

*Xin Li[1,2], Ren Zhang[1], Ju Wang[1], Mei Hong[1], Xueliang Zhou[1]

1. College of Meteorology and Oceanography, National University of Defense Technology, China, 2. State Key Laboratory of Numerical Modeling for Atmospheric Sciences and Geophysical Fluid Dynamics (LASG), Institute of Atmospheric Physics, Chinese Academy of Sciences

In order to understand the variation trends and disaster risk of tropical cyclone in the background of climate change, this paper investigated the characteristics of intensity and frequency of tropical cyclones over China’s surrounding sea and assessment its risk based on CMA-ST tropical cyclone path set and ship track data. From the point of view of risk analysis, a conceptual framework of tropical cyclone disaster risk was constructed. Then, an index system and assessment model was developed. Finally, the calculation and zoning of the risk of tropical cyclone disasters in the surrounding waters of China was carried out through GIS technology. The results show that the frequency and the extreme peak wind-speed of tropical cyclones were slightly declined during 1950-2010 when the typhoon and strong wind were rising significantly in the first 10 years in 21st-century. Taking into account the danger of tropical cyclones, the vulnerability of disaster-bearing bodies (such as marine vessel) and the ability of disaster prevention and mitigation, the risk of tropical cyclone is the highest over the central and northern parts of the South China Sea and the Philippine Sea, while the risk is very low in the southern part of the South China Sea, in the north-central Yellow Sea and in the Bohai Sea.

Keywords: Meteorological Disaster, Tropical Cyclone, Risk Assessment, GIS Regionalization

©2020. Japan Geoscience Union. All Right Reserved.

Wildfire risk prediction in Indonesia with the soil water by the numerical meteorological simulation WRF

*Keiji Kimura[1], Natsuki Takano[4], Mitsuru Osaki[2], Albertus Sulaiman[3], Pribadi Awal[3]

1. Department of Geography, Nara University, 2. Faculty of Agriculture, Hokkaido University, 3. Agency for the Assessment and Application of Technology, Indonesia, 4. Riso Kagaku Co.Ltd.(Graduated student, Nara University)

In Indonesia, the rain decreases in the El Nino year, and it is said that wildfire increases. When a lot of tropical peat is distributed over Indonesia, and ground water level(GWL) is deepened than 15cm, it is said that the wildfire increase at a stretch. Around Palankalaya city of the middle southern Kalimantan Island, a plan to develop peat area about 1,500,000ha from 1995 through 1999 as a rice field was pushed forward, but, as a result, was over for failure. The land which was about to be developed was left as the farming inappropriate ground. Drainage is continuing now, and the desiccation of the peat goes ahead through the artificated stream which was made to lower GWL.
In this study, we perform the systems construction with the goal of predicting GWL of around 5 days later with the numerical meteorological simulation WRF. The study area was around the GWL observation point that BPPT set up in the suburbs of parang Kalla-ya city under the ground and used data in August, 2017 as application of the simulation by data in August, 2015 and February, 2017 for simulation construction. Weather simulation WRF assumed NCL data of NCEP as initial data and calculated adomains, in mesh size 27km, 9km, 3km, and 1km, for each 31*31 mesh and calculated the soil mousiture of four levels. And we made a correlative expression with the GWL of the target day and decided to use it for a prediction.
The calculation result of August, 2015:
$y=0.5877x_1-1.9520x_2+25.6019x_3+181.4307x_4-54.4165$ Eq(1)
where y :ground water level (cm), x_1 - x_4: the soil moisture contents of between lebel 1 and 4 by WRF.
As for the coefficient, it was certainly revealed that it was predicted by 0.9639 and very good correlation with this expression.
Similarly, the calculation result of February, 2017:
$y=0.082993x_1+25.97913x_4-7.90892$ Eq(2)
where y :ground water level (cm), x_1 and x_4:the soil moisture contents of level 1 and 4 by WRF.
As for the coefficient, it was certainly revealed that I could predict it by 0.9267 and the correlation that after all was very good when I used this expression.
A form, expression coefficients are totally different when Eq(2) with Eq(1) is compared. Therefore, we performed three following calculations to inspect simulation-style generality: at first Eq(1) to data of February, 2017; secondary, Eq(2) in August, 2015; and thirdly to apply to the data of August, 2017. As a result, the correlation had low all cases, and it turned out that it was not usable in a prediction.
As a result, it was revealed that we must make a prediction type every short term and must apply it without being able to make the expression that generalized time to predict the water level of this study point under the ground. However, absolute calculation understood that the expression that we could predict approximately surely more than 0.9 was put up if we made a short-term predictive expression in this way. The point that we intended for calculates only for three months during one spot, the period, but it will be thought that a characteristic to be seen in a prediction-type coefficient is clarified in future by performing that we lengthen a period and increase target points.

Keywords: wildfire, Indonesia, the numerical meteorological simulation WRF

©2020. Japan Geoscience Union. All Right Reserved.

Evaluation framework of health impacts caused by massive earthquakes in Osaka

*Koki Adachi[1], Lisa Ito[1], Akihiro Tokai[1]

1. Graduate School of Engineering, Osaka University

When a high-intensity earthquake occurs, human damages occur at different timelines, as follows: i) deaths and wounds caused by the collapse of buildings or tsunami that comes immediately after the earthquake, ii) health damages caused by acute exposure to chemicals spilled from factories, or iii) deterioration of medical functions caused by the impact of lifeline damage. For this reason, we need to consider these human damages in the sequence of events to enact measures to minimize these damages. In this research, we aim to condense the human damages during the Nankai Trough Earthquake to the above three timelines and evaluate them quantitatively in a time-series of the duration of damage from the time immediately after the earthquake to the recovery period.
In this research, we consider health damages caused by acute exposure to chemicals spilled from one factory suffering tsunami damages. As such, the target area is Konohana-ku, where the factory used the largest number of Pollutant Release and Transfer Register (PRTR) method-designated volatile substances. Regarding the number of deaths caused by the collapse of buildings or tsunami, we used the Nankai Trough Earthquake data and methods for calculating damages published by the Cabinet Office. Moreover, we calculated the number of deaths caused by the tsunami using the tsunami evacuation buildings specified in the target area as an evacuation destination and determined whether evacuation to that building is possible.

We assumed that Toluene, the largest chemical at the target factory, spilled and that immediately after the factory was damaged by the tsunami, two weeks worth of the annual handling volume all flowed out at once. For exposure scenario, Toluene volatilized after the spillage was exposed from the atmosphere after people evacuated to the roof of the tsunami evacuation buildings. In addition, we analyzed the Toluene dynamics for using CAMEO-ALOHA and checked the transition of substances density. The Acute Exposure Guideline Level (AEGL) was used for evaluations for human health damages, which were assumed to be caused by the Toluene density as the tsunami evacuation buildings passed through the AEGL.
We calculated how much the above two human damages were buffered by treatment measures considering the impact of lifeline damages each day. Still, medical treatment completely recovers the human damages. In addition, these damage transitions were converted to Disability Adjusted Life-Years (DALY) for each day. DALY is one of the indicators of the time lost due to disability or premature death and is the sum of the years of life loss (YLL) and the years with disability (YLD). Each sum of DALY such as human damages caused by the collapse, tsunami, and health damages caused by substances were 1.30E+08, 04.12E+04, 5.16E+03 [day/day], respectively. The number of victims was the largest among human damages and the accident value was also the largest, and thus DALY about YLL is much larger than other damages. Human damages caused by substances lasted seven days after the earthquakes occurred despite the assumption that medical treatment enables people to recover completely. Thus, large damages negate the medical function if all of Toluene spilled. In this way, we could check the impacts for human damages, from the differences regarding the target area, degradation of medical function, earthquake, and the earthquake intensity using DALY.
Using the same index, we developed methods to evaluate three types of human damages that occur in different periods from the incidence of the earthquake to the recovery period. In addition, we found that the target area had sufficient medical function for the injured immediately after the earthquake and that

©2020. Japan Geoscience Union. All Right Reserved.

treating the severely ill persons from chemical substances lasted several days. As a future task, the damage to tourists visiting the target area could be considered.

Keywords: NATECH, the Nankai Trough earthquake, DALY, indirect damage, health hazard after earthquakes

©2020. Japan Geoscience Union. All Right Reserved.

Promoting pre-disaster prevention actions in cooperation with school, boards of education, and researchers Part 2: Proposal of procedure manual to read hazard map

*Tatsuto Aoki[1], Kiyomi Hayashi[1]

1. School of Regional Development Studies, Kanazawa University

I Background

The case of Okawa Elementary School in Ishinomaki City, Miyagi Prefecture, which tsunami attacked in the Great East Japan Earthquake in 2011, had a great impact on people involved in school disaster prevention. The judgment issued by the Sendai High Court in April 2018 was finalized in October 2019 when the Supreme Court dismissed the appeals in Miyagi Prefecture and Ishinomaki City. As already pointed out, a major point of this decision is that the importance of "pre-disaster prevention" has been pointed out.

> Principals are required to have a much higher level of disaster prevention knowledge and experience than local residents in order to ensure child safety. According to the published hazard map, Okawa Small was outside the tsunami inundation area and was designated as an evacuation site in the event of a tsunami, but the principals could predict tsunami damage if the school location was examined in detail.
> The principals neglected to be required to revise the crisis management manual according to the school situation. The Municipal Board of Education also neglected guidance such as correcting inadequacies in the manual.

This means that in the future, the standard for disaster response at school sites will be "pre-disaster prevention", and it will be necessary to formulate an appropriate crisis management manual after individually reviewing the assumptions of hazard maps. And this means that the bord of education must check the school's crisis management manual for flaws. If this is not sufficient, and if a natural disaster causes damage to under school-managed children, the school and the Board of Education will definitely be found defective.
With the flow of work style reforms at educational sites, it is more difficult than ever to put a burden on school sites. It is indispensable to support schools to collect and judge information efficiently with minimum load. In addition, it is necessary to provide support to the board of education of the local government, which has to verify the crisis management manuals of all schools by limited human resources.

II For the support of the school and the Board of Education

Based on the above awareness, the authors, who are Ishikawa Prefectural School Disaster Prevention Advisors, are preparing to implement the following in collaboration with the Ishikawa Prefectural Board of Education.

1. Create work manuals and checklists to enable school sites to read hazard maps properly.
2. Create a checklist for the local government's board of education to check each school's crisis management manual

©2020. Japan Geoscience Union. All Right Reserved.

3. Establish a channel for prefectural schools and researchers to provide professional support to schools and schools

The immediate issue is 1. Manuals and checklists can be used to screen "schools that are predicted to be damaged by hazard map information" and "schools that are not likely to be damaged" from a large number of schools and extract gray zone cases. In this presentation, based on the presentation at the Association of Japanese Geographers held in March, we present a flowchart and checklist for screening for earthquake disasters and floods.

Keywords: Pre-disaster prevention actions, Hazard Map, Boards of education, Damage estimations

©2020. Japan Geoscience Union. All Right Reserved.

[J] Poster | H (Human Geosciences)：H-CG Complex & General

[H-CG34] Human social activities and earth and planetary sciences

convener:Kazuo Amano(Center for Spatial Information Science, The University of Tokyo), Takashi Oguchi(Center for Spatial Information Science, The University of Tokyo), Masaki Ito(Institute of Industrial Science, the University of Tokyo), Kayoko Yamamoto(University of Elctro-Communications)

The previous session "Social Media and Earth and Planetary Sciences" has been held nine times in the past, targeting the utilization of social media (SNS) for earth and planetary sciences, and many novel research results have been reported. On the other hand, the development of SNS in the meantime is also remarkable, and the importance of research linked with other information systems is increasing. In addition to the use of conventional SNSsocial media, we would like to call a wide range of papers aimed at the development of earth and planetary sciences in relation to human social activities such as applications of navigation systems and action support systems etc. Furthermore, we welcome broad topics relevant to the session title, including research in human geography on nature and human interactions and social utilization of geologic materials.

[HCG34-P01] Tourism and education utilizing local resources in the sand dunes and lagoon area of the San’in Kaigan UNESCO Global Geopark

*Kyoko Kanayama[1], Akira Kaigo[2], Yuki Iwamoto[3], Noritaka Matsubara[4], Aya Genseki[5], Emiko Sawa[5], Juna Nakagawa[6], Kitamura Sayaka[7], Kagari Ikezoe[7] (1.San'in Kaigan Geopark Museum of the Earth and Sea, Tottori Prefectural Government, 2.Hamayuyama and Tanegaike Vitalization Committee, 3.Secretariat of San'in Kaigan Geopark Promotion Council, 4.Graduate School of Regional Resource Management, University of Hyogo, 5.Uradome Ranger Office, Kinki Regional Environment Office, Ministry of the Environment Government of Japan, 6.Tottori Sand Dunes Visitor Center, San’in Kaigan National Park, 7.Tourism and Geopark Promotion Division, Tottori City Hall)

[HCG34-P02] Balloon Bomb Tour in the North Ibaraki Geopark Plan

*Kazuo Amano[1,2], North Ibaraki Geopark Plan Geonet Kitaibaraki (1.Center for Spatial Information Science, The University of Tokyo , 2.Amano Geological Laboratory, Japan)

[HCG34-P03] Identification of historical building stones and their distribution on the basis of magnetic susceptibility of granites

*Tohru Sakiyama[1] (1.Institute of Geo History, Japan Geochronology Network)

[HCG34-P04] Geology, soils, and wine

*Takashi Oguchi[1] (1.Center for Spatial Information Science, The University of Tokyo)

[HCG34-P05] Social Media Mapping for Disaster Prevention and Reduction

*Kayoko Yamamoto[1] (1.University of Elctro-Communications)

[HCG34-P06] Vulnerable people and hazard map

*SATOSHI KANAGURI[1], Kazuo Amano[2] (1.Amano Geological Laboratory, JAPAN, 2.Center for Spatial Information Science, The University of Tokyo)

[HCG34-P07] Development of Web Portal to Support for Remote Island

*Kayoko Yamamoto[1] (1.University of Elctro-Communications)

[HCG34-P08] The latest state of community formation through online/offline interaction

*Masaki Ito[1] (1.Institute of Industrial Science, the University of Tokyo)

Tourism and education utilizing local resources in the sand dunes and lagoon area of the San’in Kaigan UNESCO Global Geopark

*Kyoko Kanayama[1], Akira Kaigo[2], Yuki Iwamoto[3], Noritaka Matsubara[4], Aya Genseki[5], Emiko Sawa[5], Juna Nakagawa[6], Kitamura Sayaka[7], Kagari Ikezoe[7]

1. San'in Kaigan Geopark Museum of the Earth and Sea, Tottori Prefectural Government, 2. Hamayuyama and Tanegaike Vitalization Committee, 3. Secretariat of San'in Kaigan Geopark Promotion Council, 4. Graduate School of Regional Resource Management, University of Hyogo, 5. Uradome Ranger Office, Kinki Regional Environment Office, Ministry of the Environment Government of Japan, 6. Tottori Sand Dunes Visitor Center, San’in Kaigan National Park, 7. Tourism and Geopark Promotion Division, Tottori City Hall

The area facing the Sea of Japan in the western part of the San’in Kaigan Geopark is characterized by sand dunes and the lagoons/wetlands formed behind them. The Tanegaike Lake, located south of Tottori Sand Dunes which extend 16 km east and west, is a dam lake created by the formation of dunes in front of the valley in the late Pleistocene. On the northeast side of Tanegaike Lake, there was a lagoon once called Yuyamaike. Locals made an underground waterway between Tamanga Pond at 16m above sea level and Yuyama Pond at almost 0m above sea level. Then the water of Tanegaike Lake and the sand of the dunes was poured into Yuyama Pond to reclaim Yuyama Pond. With the project, it took about 100 years to make a 50-hectare paddy field from the early 19th century to the early 20th century. The underground waterway that was created at that time is still used, and supplies water from Tanegaike Lake to farmland in the Yuyama area. Tanegaike Lake has been carefully preserved as an indispensable place for people to survive in this area, so precious ecosystems, shrines and folklore remain.
To attract visitors to Tanegaike Lake, a working group had been organized by Mr. Kaigo from the Hamayuyama and Tanegaike Vitalization Committee and people from the San'in Kaigan Geopark from 2018 to 2019. The group members examined Tanegaike Lake and found the attractions, for example, "Changing sand dunes and people's lives" and "The beauty of the color contrast between the sand dunes and the lake". In order to convey these attractions to tourists, we first created a leaflet, which was included such the information as the history of the formation of Tanegaike Lake, the history of reclamation of Yuyamaike, Tanegaike Shrine, and folklore, “Otane”. By placing them in the Tottori Sand Dunes Visitor Center and the Sand Museum, we created an opportunity for tourists to visit Tanegaike Lake. In this presentation, we will report the details and progress of the project as well as other tourism and educational efforts utilizing the local resources of the sand dunes and lagoons.

Keywords: geopark, tourism, education, sand dunes, lagoon, San'in Kaigan

©2020. Japan Geoscience Union. All Right Reserved.

Balloon Bomb Tour in the North Ibaraki Geopark Plan

*Kazuo Amano[1,2], North Ibaraki Geopark Plan Geonet Kitaibaraki

1. Center for Spatial Information Science, The University of Tokyo , 2. Amano Geological Laboratory, Japan

The North Ibaraki Geopark Plan has been conducting tours at the Izura Kaigan geosite, highlighting the balloon bomb launching base, since its certification of the Japan Geopark Network in 2011. By making the war heritage the main subject of the tour, it became a unique tour unlike any other geoparks. In the beginning, some critics argued that it was unsuitable for a tour in a geopark because it was based on the negative legacy of war. However, considering that "dark tourism" is gaining attention as a sightseeing tour of war heritage today, balloon bomb tours may be ahead of the times. In this presentation, we will introduce the actual balloon bomb tour and consider the significance of introducing dark tourism to a geopark.

Balloon bombs were planned by the Japanese Army in the late Pacific War as a mission to use jet streams to attack the continental United States directly. Between November 1944 and April 1945, it is estimated that 9,300 shots were released, of which at least 1,000 reached the North American continent. At the time, balloons were launched from 42 launch pads at the bases on the Pacific coast near Otsu, Ibaraki Prefecture, near Nakoso, Fukushima Prefecture, and at Ichinomiya Beach in Chiba Prefecture. The only surviving launch pad is Otsu at the Izura Kaigan geosite.

In the balloon bomb tour, the only remaining launch pad will be visited, the natural conditions selected as the launch base will be examined while observing the surrounding landform, etc., and the principle will be explained using a balloon bomb scale model. At the same time, it introduces the social impact of the area when the base was set up. From a geological point of view, the sand on the shore used for the weight mounted on the balloon bomb is presented. The U.S. military performed a geological analysis of the sand to determine where the balloon bombs were launched . The launch location could not always be pinpointed, but a rough estimate of the Pacific coast of eastern Japan was being made. Geology is one example of the use of war. Balloon bomb launch pad is a negative legacy of war, but it is important to observe it and consider the relationship between war and academic research and contribute to world peace.

Dark tourism is a new concept of tourism proposed at the end of the 20th century, and is defined as a journey through memories of tragedies such as wars and disasters. In recent years, tours to learn about natural disasters in geoparks in Japan have been attracting attention. However, memories of war are hard to incorporate into tourism in the traditional sense, and have not been actively incorporated into geoparks. We want to expand the possibilities of geoparks by incorporating a new tourism concept called dark tourism, which is attracting worldwide attention, into geoparks.

(Geonet Kitaibaraki members: Shuya KAKEFUDA, Noboru KOBAYASHI, Kenichiro MATSUMOTO, Wakako MURATA, Hiroo NAKAI, Toshiyuki NAMEKAWA, Masayoshi NEMOTO, Akira NUMATA, Koichiro OZAWA, Tatsuhiro SEKI, Seichi SUZUKI and Yasuyuki WADA)

Keywords: geopark, balloon bomb, dark tourism

©2020. Japan Geoscience Union. All Right Reserved.

Identification of historical building stones and their distribution on the basis of magnetic susceptibility of granites

*Tohru Sakiyama[1]

1. Institute of Geo History, Japan Geochronology Network

Determination of quarrying area of historical stone materials is effective for researches on social condition, culture and so on. In particular, granite stones are widely distributed in various historical times. However, observation of stone materials tends to be qualitative and subjective, because of necessity of nondestructive inspection. Accordingly, I applied measurement of magnetic susceptibility and color index of granitic stone materials and their out crop in some quarries for the quantitative determination. Islands and coastal area of Seto Inland Sea are major production area of granitic stones. They are composed of ilmenite-series granites with low magnetic susceptibility but ranges of magnetic susceptibility of each intrusive mass are slightly different. Magnetic susceptibility reflects iron contents and oxygen fugacity of granite magma. Magma compositions of granites are reflected in contents of mafic minerals. Diagram of magnetic susceptibility and color index is more effective to identification of granitic stones and their product area.

Identification of product area of granite stones revealed following change history of their quarrying and distributions.

(1) Surrounding area of Rokko Mountains is main producing area of granitic stones at 14th to 16th century. They have been used mainly tomb stones and memorial towers of influential persons.

(2) Quarrying sites were extended to entire area of Seto Inland Sea after construction of Osaka Castle at 17th century.

(3) Large amount of granitic stone materials transferred from Seto Inland Sea area to shrines and temples in Sea of Japan area by cargo ships (Kitamae-bune) at 17th to 19th century.
(4) Especially, Onomichi area was raised major production area and quarrying in Rokko Mountains was declined at 19th century.

Keywords: granite, historical stone materials, magnetic susceptibility, granitic stones

©2020. Japan Geoscience Union. All Right Reserved.

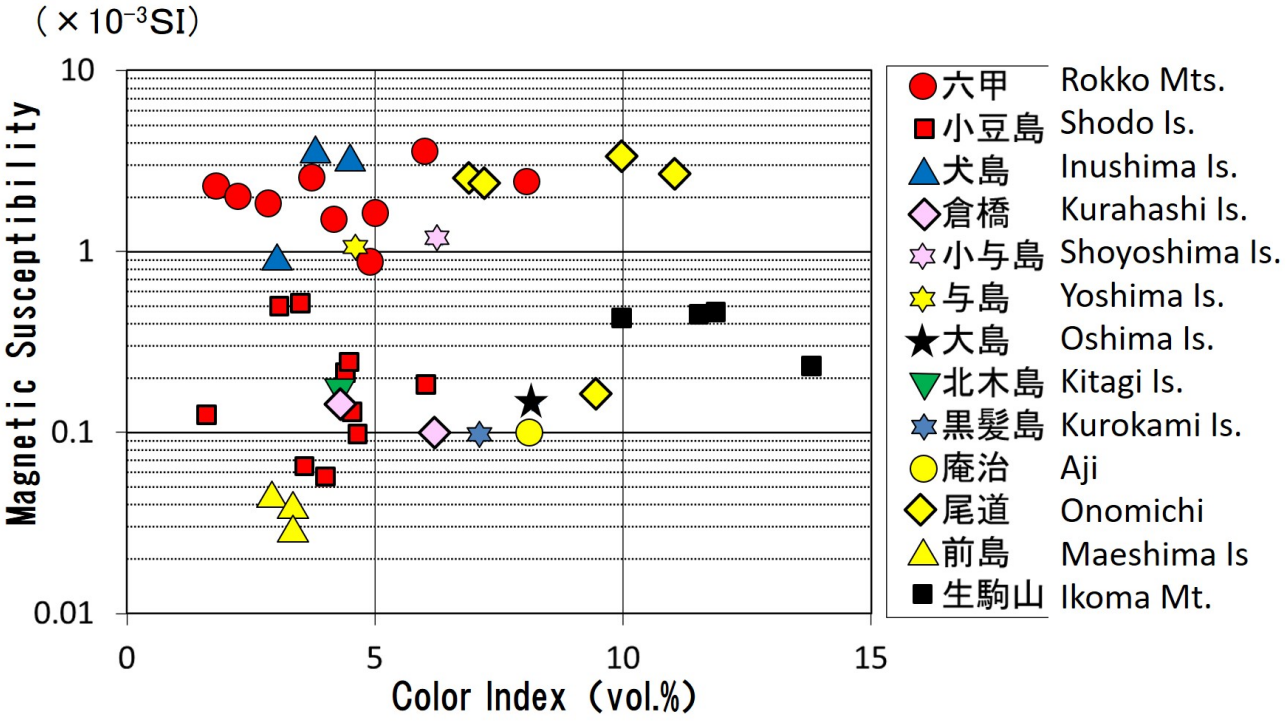

©2020. Japan Geoscience Union. All Right Reserved.

Geology, soils, and wine

*Takashi Oguchi[1]

1. Center for Spatial Information Science, The University of Tokyo

It is widely known that growth of grapes for wine is affected by climate. Some suggest that bedrock geology and soils also affect the characteristics of grapes and wine. A recent book by an American journalist focuses on the effects of geology and soils on grapes and wine, and I supervised its Japanese translation. This presentation introduces some hypotheses to relate wine with geology and soils.

Keywords: Wine, Grape, Bedrock, Soil

©2020. Japan Geoscience Union. All Right Reserved.

Social Media Mapping for Disaster Prevention and Reduction

*Kayoko Yamamoto[1]

1. University of Elctro-Communications

The cloud computing society where everyone can access the Internet using various information tools has been already developed all over the world, and it is the times of IoT (Internet of Things) and IoE (Internet of Everything) when various things were connected to the Internet. On the other hand, in recent years, because the occurrence frequency of meteorological disasters such as typhoon, local heavy rain and heavy snow in attrition to earthquake and volcanic eruption tremendously increased, it is the most important issue to adopt the effective measures for disaster prevention and reduction around the world. Additionally, as the digital infrastructures are toughened in the above measures, the importance of information and communication technologies (ICT) and internet environment is widely recognized especially in recent Japan. At the time of the Heavy Rain Disaster in western Japan in July, 2018, it was possible to gather and accumulate various disaster information using the function of social media mapping included in the spatiotemporal information system developed by the author's lab. Taking up the above social media mapping, the present study described the issues related to the development and utilization of digital infrastructures as one of the measures for disaster prevention and reduction.
In the advanced information society such as Japan, a great variety of information is transmitted via the internet and such information can easily be transmitted, received and shared at “anytime”, “anywhere” and with “anyone” through various ICT. In such a society, as the virtual space is closely involved with the real space, these mutually influence. Accordingly, when a disaster occurs in the real space, submission and reception of the related information using a variety of means (including both mass media and social media) are started approximately at the same time in the virtual space. Due to the close relationship between the real and virtual spaces, it is possible to rescue and support victims, and cause excessive information and confusion. Additionally, it is essential to effectively utilize the information included in the virtual space at the time of disaster. Specifically, it is an important issue to make use of the information in social media for rescue in the real space. For example, it is hopeful to assign the persons without the damaged areas who can appropriately choose the important information to report it to the local governments within the damaged areas and national government. Furthermore, it is essential to take the measures for the people vulnerable to disaster who require the disaster information most. For this, it is necessary to prepare a variety of ICT in addition to oral communication.

Keywords: Disaster Prevention and Reduction, Social Media Mapping, Digital Map, Heavy Rain Disaster in Western Japan in 2018

©2020. Japan Geoscience Union. All Right Reserved.

Vulnerable people and hazard map

*SATOSHI KANAGURI[1], Kazuo Amano[2]

1. Amano Geological Laboratory, JAPAN, 2. Center for Spatial Information Science, The University of Tokyo

In the 2011 off the Pacific coast of Tohoku Earthquake on March 11, 2011, more than 22,000 people were killed or missing, and about 90% of deaths were caused by tsunamis. The death rate of people aged over 65 was accounted for 60% of the total, and the mortality rate of persons with disabilities was twice that of the entire population. Based on self-examination on many victims of the handicapped of this earthquake, the government has mandated that local governments create a list of vulnerable people in disasters. It is recommended that an “individual evacuation plan” will be created on the basis of the list. However, there is a shortage of supporters due to the aging of residents and the weight of responsibility, and the preparation of “individual evacuation plans” has not progressed.

In recent years, attempts have been made to protect vulnerable people from disasters. Attempts to achieve visually impaired people’s understanding of hazard maps have begun in various places. The NPO "Nippon Volunteer Network Active in Disaster" is promoting a preparation for the tsunami caused by the Nankai Trough Mega Earthquake by holding a workshop for these people showing the heaped tsunami inundation area on hazard maps. At the Kure City Association for the Visually impaired in Hiroshima Prefecture, a reading volunteer recorded the contents of the hazard map on a CD, and a study session was held in which visually impaired persons checked the location of shelters near their homes and the location of landslide warning areas. The Headquarters for Earthquake Research Promotion has created a "Probabilistic Seismic Hazard Map for Japan " that takes into account the color scheme so that people with color vision impairment can easily understand it. These efforts have given hope to the visually impaired who have given up on evacuation.

In 2017, the NPO “Hyogo Center for the Disabled” conducted a questionnaire survey of persons with disabilities in the prefecture, and nearly half of those answered that they did not know the hazard map. This result showed that the importance of the hazard map was not visible. In recent years, the flooding of rivers caused by heavy rain has caused flooding of facilities and hospitals for the elderly. Many of these facilities are located in estimated flood areas on hazard maps. Such facilities for the vulnerable people of the disaster should be located in a safe place, but safe areas on the hazard map have high land prices, and the relocation of these facilities to a safe place is not progressing.

Under these circumstances, it is necessary to repeat evacuation drills in order to protect the vulnerable people from disasters. In a disaster, for the handicapped who are not in the facilities, the local residents around them will be reliable. It is important that vulnerable people and neighboring residents cooperate with each other to conduct evacuation drills. The organizer of the evacuation drill must actively encourage the vulnerable people to participate. By evacuation training, it is expected that the hazard map will be widely known. In elderly facilities, daily evacuation drills are important because dozens to hundreds of elderly people must be evacuated to a safe building outside facilities or to over second floors inside facilities. We must note that disasters larger than predicted on the hazard map can occur to determine whether the evacuation site is safe enough.

The most necessary thing to protect the vulnerable from disasters is "Mental barrier-free". Mental barrier-free refers to thinking and acting as a person who can understand the feelings of vulnerable

©2020. Japan Geoscience Union. All Right Reserved.

people in disasters.

Keywords: vulnerable to disaster, hazard map, mental barrier-free

©2020. Japan Geoscience Union. All Right Reserved.

Development of Web Portal to Support for Remote Island

*Kayoko Yamamoto[1]

1. University of Elctro-Communications

According to the survey conducted by the Ministry of Land, Infrastructure, Transport and Tourism in 2015, Japan is composed of 6,852 islands including Hokkaido, Honshu, Shikoku, Kyusyu and Okinawa islands. Among the islands, excluding these large-scale islands, the numbers of remote islands which are manned and unmanned are respectively 418 and 6,430. Approximately 420 thousand people, equivalent to approximately 1.4% of total Japanese population, live in the manned remote islands. Nevertheless, the remote islands play an important role in the protection and increase of the profits for Japan and Japanese people in terms of its territory and the exclusive economic zones, the use of marine resources, the succession of a variety of cultures, the preservation of nature environments, etc.
However, the population of the islands has been continually in the decrease since 1955. Additionally, in 2013, the aging rates of the whole Japan and under population areas are respectively 22.7% and 33.0%, while that of the remote islands is 35.0%. Most remote islands as well as the whole nation suffer from the problem of the declining birth rate and aging population. Furthermore, most remote islands had tremendously serious problems related to declining birth rate and aging population in particular. Though the main industry of the remote island is fishery, there has been lack of new blood and insufficient human resources to carry on such an occupation.
On the other hand, in recent years, more tourists visit remote islands. With the increase of the tourists visiting remote islands from the inside and outside of Japan, it is possible to promote the sustainable development and local revitalization in remote islands. However, there are very few guidebooks and websites which introduce remote islands. Additionally, the islanders could hardly transmit sightseeing information related to their islands by themselves. Therefore, it is difficult for tourists to obtain the information related to the remote islands. Against such a backdrop, in order to support the tourists in the remote islands, the present study aims to develop a web portal to support the islanders to transmit sightseeing information. The web portal is developed using web-geographic information systems (Web-GIS), and connecting with external SNS (Social Networking Services).

Keywords: Support for Remote Island, Web Portal, Digital Map, Social Media, Twitter

©2020. Japan Geoscience Union. All Right Reserved.

The latest state of community formation through online/offline interaction

*Masaki Ito[1]

1. Institute of Industrial Science, the University of Tokyo

The author reported an arising online community to exchange GIS technical information based on social media in the past conference in 2011. This kind of community formation, which had begun at the time, continues to connect new people to create value in society in a new way. In this presentation, I will introduce the latest situation of such community formation with examples around the author. In particular, the author reports the impact of new trends in this field, such as the relay of conferences which become easier with the spread of smartphones and LTE, and a social networking service with real names such as Facebook.

Keywords: SNS, online service, community formation

©2020. Japan Geoscience Union. All Right Reserved.

[J] Poster | H (Human Geosciences)：H-CG Complex & General

[H-CG35] Advanced life support systems with closed bio-ecosystems and thier applications

convener:Masanori Shinohara(Teikyo University of Science), Kaori Tomita-Yokotani(Faculty of Life and Environmental Sciences University of Tsukuba), Hiroshi Katoh(Division of Plant Functional Genomics, Advanced Science Research Promotion Center, Organization for the Promotion of Regional Innovation, Mie University)

In this session, since 2011, we and invited researchers have been introducing and discussing about practical and useful life-support systems in closed bio-ecosystems for inhabitation on extraterrestrial environments. Not only biological studies but also engineering ones
including broad research fields are our target. And also, we assume that it is indispensable to discuss about these interdisciplinary fields beyond the generation for inheriting to our next generation and for developing our field. Theme from old and basic to current and applicative from senior to youth including undergraduate are welcomed.

[HCG35-P03] Identification of proteins found in the process of slow dehydration in a terrestrial cyanobacterium, *Nostoc* sp. HK-01

*Hiroko Tanaka[1], Nagamine Myu[1], Tomoko Abe[1], Shunta Kimura[2], Hiroshi Katoh[3], Kaori Tomita-Yokotani[4] (1.School of Science and Engineering, Tokyo Denki University, 2.Graduate School of Agricultural and Life Sciences, The University of Tokyo, 3.Organization for the Promotion of Regional Innovation, Mie University, 4.Faculty of Life and Environmental Sciences, University of Tsukuba)

[HCG35-P04] Usefulness of an organic wastewater treatment focused on bacteria of the genus *Bacillus*

Chika Watanabe[1], Toshiharu Takayama[2], Tomoyuki Kuribayashi[2], *Tomoko Abe[1] (1.School of Science and Engineering, Tokyo Denki University, 2.KPS-3IV New Applications Research Center, KOA Corporation)

[HCG35-P05] What’s life? Wandering about life from the viewpoint of “transition” of evolutions.

*Masanori Shinohara[1] (1.Teikyo University of Science)

Identification of proteins found in the process of slow dehydration in a terrestrial cyanobacterium, *Nostoc* sp. HK-01

*Hiroko Tanaka[1], Nagamine Myu[1], Tomoko Abe[1], Shunta Kimura[2], Hiroshi Katoh[3], Kaori Tomita-Yokotani[4]

1. School of Science and Engineering, Tokyo Denki University, 2. Graduate School of Agricultural and Life Sciences, The University of Tokyo, 3. Organization for the Promotion of Regional Innovation, Mie University, 4. Faculty of Life and Environmental Sciences, University of Tsukuba

*Nosto*c sp. HK-01 could be used for bio-chemical circulation in a closed ecosystem, including space. Because, it is one of terrestrial cyanobacterium having a tolerance to desiccation stress and it has ability of usefulness as a food. We have been exploring macromolecular substances that would be involved in a mechanism for desiccation tolerance in *Nosto*c sp. HK-01.
In this study, to detect cellular proteins of *Nostoc* sp. HK-01 during slow dehydration, proteins extracted from the cells in the course of the dehydration were applied to SDS-polyacrylamide gel electrophoresis. In comparison with the wet cells, the abundance of some proteins changed after dehydration. Genes of some of them were identified and functional analyses of them are in progress.

Keywords: cyanobacteria, desiccation tolerance, stress protein

©2020. Japan Geoscience Union. All Right Reserved.

Usefulness of an organic wastewater treatment focused on bacteria of the genus *Bacillus*

Chika Watanabe[1], Toshiharu Takayama[2], Tomoyuki Kuribayashi[2], *Tomoko Abe[1]

1. School of Science and Engineering, Tokyo Denki University, 2. KPS-3IV New Applications Research Center, KOA Corporation

Construction of energy-saving and space-saving wastewater treatment systems is one of the important issues for closed bio-ecosystems. In this study, we investigated the usefulness of wastewater treatment by activated sludge focused on the domination of a bacteria group mainly comprising of bacteria of the genus *Bacillus.* In addition, effective utilization of the wastewater treated by this activated sludge were examined.
We revealed that the activated sludge focused on *Bacillus* contained microorganisms had high organic matter decomposition activity (amylase activity, protease activity, lipase activity, cellulase activity). Furthermore, we found some microorganisms that have antimicrobial activity against pathogenic microorganisms, such as plant pathogenic fungi and food poisoning bacteria, in this activated sludge.

Keywords: wastewater treatment, Bacillus, closed bio-ecosystems

©2020. Japan Geoscience Union. All Right Reserved.

What’s life? Wandering about life from the viewpoint of “transition” of evolutions.

*Masanori Shinohara[1]

1. Teikyo University of Science

What’s life?

From various academic standpoint, this theme has been discussed. Here, I try to set up them as changeable style from the viewpoint of “transition” of evolutions and from TegMark’s “LIFE 3.0”.

Keywords: life, evolution, transition

©2020. Japan Geoscience Union. All Right Reserved.

[J] Poster | S (Solid Earth Sciences)：S-GD Geodesy

[S-GD02] Geodesy

convener:Koji Matsuo(Geospatial Information Authority of Japan), Yusuke Yokota(Institute of Industrial Science, The University of Tokyo), Daisuke Oka(Geological Survey of Hokkaido, Environmental and Geological Research Department, Local Independent Administrative Agency, Hokkaido Research Organization)

In this session, we call for wide range of papers concerned with geodesy and its application to geoscience. Topics of interest will include but not limited to recent advances in measurement techniques, data analysis, numerical modeling or theoretical studies of the Earth's geometry, gravity/geoid, and rotation. In addition, this session also welcomes topics of interdisciplinary studies on geoscience using ground-based geodetic techniques (spirit leveling, absolute/relative gravimeter, strain meter and so on) or space geodetic techniques (GNSS, GRACE, satellite altimetry and so on).

[SGD02-P01] Projected Barzilai-Borwein method for the acceleration of gravity field data inversion

*wei li[1,2,3,4], zhao hai meng[5,6], hao wen yan[1,2,3] (1.Faculty of Geomatics, Lanzhou Jiaotong University, Lanzhou 730070, China, 2.National-Local Joint Engineering Research Center of Technologies and Applications for National Geographic State Monitoring, Lanzhou 730070, China, 3.Gansu Provincial Engineering Laboratory for National Geographic State Monitoring, Lanzhou 730070, China, 4.School of Civil Engineering, Lanzhou Jiaotong University, Lanzhou 730070, China, 5.Tianjin Navigation Instrument Research Institute, Tianjin 300131,China, 6.Institute of Geology and Geophysics, Chinese Academy of Sciences, Beijing 100083, China)

[SGD02-P02] **Post-seismic gravity change modelling based on spectral finite element method**

*Changda Yan[1], SHINICHI MIYAZAKI[1] (1.Graduate School of Science, Kyoto University)

[SGD02-P03] Preliminary result of gravimetric geoid computation using airborne gravity data over the Boso peninsula

*Koji Matsuo[1] (1.GSI of Japan)

[SGD02-P04] Mesurement for vertical gravity gradient by CG-5 Autograv Gravimeter

*Masami Handa[1], Akira Tomiyama[1], Tokuro Kodama[1], Shinobu Kurihara[1], Kumikazu Ochi[1], Shuichi Omori[1] (1.GSI of Japan)

[SGD02-P05] An attempt to detect the variation of attractive forces from deep belowground using the Vertical Gravimeter Array.

*Toshiyuki Tanaka[1] (1.Tono Research Institute of Earthquake Science, Association for the Development of Earthquake Prediction)

[SGD02-P06] An attempt to observe gravity fluctuations caused by groundwater table response to tidal fluctuations by continuous gravity measurement near the coast

*Hiroki Goto[1,2], Mituhiko Sugihara[1,2], Yuji Nishi[1,2], Hiroshi Ikeda[2] (1.Geological Carbon Dioxide Storage Technology Research Association, 2.National Institute of Advanced Industrial Science and Technology)

[SGD02-P07] Effect of seasonal snow-mass change on geodetic solutions at Syowa Station: elastic deformation and gravitational attraction

*Akihisa Hattori[1], Yuichi Aoyama[2,1], Koichiro Doi[2,1], Jun'ichi Okuno[2,1] (1.The Graduate University for Advanced Studies (SOKENDAI), 2.The National Institute of Polar Research)

[SGD02-P08] Calculation method of the compliance parameters of the Earth's rotation: Influence of the fluid core and the solid inner core

*Yuji Harada[1,2], Shuhei Okubo[3,4] (1.State Key Laboratory of Lunar and Planetary Science, Space Science Institute, Macau University of Science and Technology, 2.Ocean Hemisphere Research Center, Earthquake Research Institute, University of Tokyo, 3.Department of Surveying and Geoinformatics, Faculty of Geosciences and Environmental Engineering, Southwest Jiaotong University, 4.University of Tokyo)

[SGD02-P09] Utilization of Interferometric Synthetic Aperture Radar Technology for Disaster Prevention

*Takako Nakamura[1], Shuichi Rokugawa[1] (1.The University of Tokyo)

[SGD02-P10] **Postseismic crustal deformation of the 2011 Tohoku earthquake, obtained from tidal data analysis**

*Kei Ishikawa[1], Takahito Kazama[1] (1.Graduate School of Science, Kyoto University)

[SGD02-P11] Performance assessment of the GNSS carrier phase to fault slip approach and its feasibility for seismic monitoring

*Yusuke Tanaka[1], Yusaku Ohta[1] (1.Tohoku University)

[SGD02-P12] Consideration of antenna phase calibration for new GEONET analysis

*Kazuyuki OHASHI[1], Hiroki MURAMATSU[1], Tomoaki FURUYA[1], Yasuaki KAKIAGE[1] (1.GSI of Japan)

[SGD02-P13] Research on the development of rapid and accurate GNSS routine analysis system (3)

*Hiroyuki Nakagawa[1] (1.GSI of Japan)

[SGD02-P14] Proposal to avoid inserting leap seconds

*Kozo Takahashi

Projected Barzilai-Borwein method for the acceleration of gravity field data inversion

*wei li[1,2,3,4], zhao hai meng[5,6], hao wen yan[1,2,3]

1. Faculty of Geomatics, Lanzhou Jiaotong University, Lanzhou 730070, China, 2. National-Local Joint Engineering Research Center of Technologies and Applications for National Geographic State Monitoring, Lanzhou 730070, China, 3. Gansu Provincial Engineering Laboratory for National Geographic State Monitoring, Lanzhou 730070, China, 4. School of Civil Engineering, Lanzhou Jiaotong University, Lanzhou 730070, China, 5. Tianjin Navigation Instrument Research Institute, Tianjin 300131,China, 6. Institute of Geology and Geophysics, Chinese Academy of Sciences, Beijing 100083, China

The recovery of 3D volume of density from gravity field data is a key point for geophysical and geological interpretations. Inversion of gravity field data involves solving an underdetermined problem. Therefore, large-scale data inversion is costly in time and memory consumption. The calculation efficiency is a primary concern for gravity field data inversion. Multiple methods are considered and applied to increase the inversion efficiency. The solution for an inversion problem was formulated by incorporating constraints to obtain stable inversion results, and a new projected Barzilai-Borwein iterative algorithm was applied to accelerate convergence of the inversion method. To test the potential application of the projected Barzilai-Borwein iterative method, synthetic gravity data simulations and real data applications were performed. Numerical performances and practical application indicate that the fast convergence of projected Barzilai-Borwein iterative method increases calculated efficiency of geophysical applications.

Keywords: gravity data, inversion algorithm, exploration methodologies, geophysical application

©2020. Japan Geoscience Union. All Right Reserved.

Post-seismic gravity change modelling based on spectral finite element method

*Changda Yan[1], SHINICHI MIYAZAKI[1]

1. Graduate School of Science, Kyoto University

Simulation of gravity change in post-seismic condition serves as an explanation for gravimetry data acquired from space and land. Recent development of space gravimetry technology, which includes the application of GRACE and GRACE-FO satellites, provides a new source of data in the research of post-seismic problems. This would help us understand more about what may happen after a major earthquake strikes. Some reports show that the rise of sea level after an earthquake, which is linked to post-seismic change, could be a great threat for island countries close to seismic active zones. If we could improve the estimation of the rate of displacement of the land after an earthquake in decades, it would be very helpful for disaster prevention and risk estimation.

Former research presented several ways of calculating the gravity change in post-seismic stage. However, many methods only consider of the change caused by visco-elastic deformation. The other two main mechanisms: after-slip and poroelasticity is not well included. To serve for further discussion of the mechanisms behind the post-seismic gravity change, we attempt to develop a way of unified explanation containing all three mechanisms. This unified model would be a flexible tool for use in the post-seismic gravity change explanation.

Here, we present examples of post-seismic gravity change modelling based on the spectral finite element method (FEM). Our work mostly covers the interpretation of gravity change after the 2011 M9.0 Tohoku-oki earthquake and 2010 M8.8 Chile Maule earthquake. A new program was written for the application of the method. It could serve as a tool for future interpretation of GRACE-FO mission recorded gravity changes after major earthquakes. Still, it could provide another way of explaining the observation of ground displacement recorded by the GPS network.

Keywords: Post-seismic, gravity, GRACE

©2020. Japan Geoscience Union. All Right Reserved.

Preliminary result of gravimetric geoid computation using airborne gravity data over the Boso peninsula

*Koji Matsuo[1]

1. GSI of Japan

The Geospatial Information Authority of Japan (GSI) plans to conduct nation-wide airborne gravity surveys over Japan from 2019 to 2022, with the aim of shifting the current leveling system based on leveling to a new system based on GNSS and Geoid. In this project, GSI aims to develop the 3-cm accurate geoid model over Japan, to quickly and uniformly derive an orthometric height with the same accuracy as the current system from GNSS positioning. Airborne gravity surveys were carried out over the Kanto region in December 2019, and airborne gravity data useful for improving the accuracy of the geoid model were obtained (Iio et al., 2020). In this study, we made the preliminary computation of the gravitational geoid model over the Boso peninsula, the eastern area of the Kanto region, using the airborne gravity data collected in this survey. The computation results suggested that the airborne gravity data was particularly effective along the coastal areas, and showed a difference of up to 15 cm in the calculated geoid height before and after the incorporation of the airborne gravity data. The consistency between the computed geoid model and the GNSS/level geoid height was improved from 3.8 cm to 3.1 cm in standard deviation by incorporating the airborne gravity data. In the future, more accurate gravimetric geoid model is expected to be developed with the addition of new airborne gravity data.

Keywords: Geoid, Gravity, Airborne gravity survey, Height reference system

©2020. Japan Geoscience Union. All Right Reserved.

Mesurement for vertical gravity gradient by CG-5 Autograv Gravimeter

*Masami Handa[1], Akira Tomiyama[1], Tokuro Kodama[1], Shinobu Kurihara[1], Kumikazu Ochi[1], Shuichi Omori[1]

1. GSI of Japan

The Geospatial Information Authority of Japan (GSI) has determined the vertical gravity gradient (hereafter, “VGG”) which is the spatial rate of vertical change of gravity by several times of manual measurements at two different heights using LaCoste & Romberg G-type relative gravimeter (hereafter, LaCoste gravimeter), in order to convert the gravity data at 1.2 m above the ground surface measured by FG5 absolute gravimeter. Due to the start of the airborne gravity survey, at several airports in Japan, the measurement of VGG in the several airports is required for the purpose of conversion from the gravity at the surface of ground to that at the height of the gravimeter mounted on an aircraft. For the improvement of the work efficiency in the measurement of VGG, we tried to introduce the Autograv CG5 relative gravimeter (hereafter, “CG5”) enabling automated measurement. The simultaneous measurement at the lower and upper heights above a gravity point with two CG-5s saves the time of the measurement, and a large amount of gravity data can be collected by the continuous measurement. On the other hand, occasionally CG-5 has unstableness such as nonlinear mechanical drift on measured data according to the change in the ambient temperature and mechanical incline. Then, we considered the method of the VGG measurement by CG-5 and verified the measured VGG comparing with that measured by LaCoste gravimeter.

As a result of the measurement at the Ishioka Geodetic Observing Station, the measured VGG by CG-5 and that by LaCoste gravimeter were 0.353 ±0.004 mGal/m and 0.357 ±0.009 mGal/m respectively. Since the difference between two measured VGG is smaller than the difference among individual LaCoste gravimeters of the VGG measurement in the past decade, the VGG measured by CG-5 is considered reliable.
In this presentation, the process of consideration of the VGG measurement method and the result of verification of its precision will be reported.

Keywords: Vertical gravity gradient, Relative gravimeter

©2020. Japan Geoscience Union. All Right Reserved.

An attempt to detect the variation of attractive forces from deep belowground using the Vertical Gravimeter Array.

*Toshiyuki Tanaka[1]

1. Tono Research Institute of Earthquake Science, Association for the Development of Earthquake Prediction

The author has conducted continuous gravity observations at both aboveground and belowground (Vertical Gravimeter Array, VGA) in the Mizunami Underground Research Laboratory (MIU) in order to detect underground mass fluctuations related to seismic activity. The VGA observation was completed in October 2019 for backfilling the MIU, and approximately 5 years of the data has been accumulated. The sum of the aboveground and belowground gravity values, after the atmospheric corrections, reflects the gravitational effect from below the underground gravimeter position (Tanaka and Honda, 2018, ESS). I hereinafter refer to it as SUM. Tanaka (2019, JgGU) introduced the Local-scale objective analysis (LANAL) for atmospheric correction of VGA observation data for 90 days from May 21, 2018. The statistical values in the abstract were too large due to an accidental time lag and are corrected as follows: the simultaneous values between MANAL and LANAL is 0.13 (not 0.66) microGal, the maximum amplitude from the median is 0.6 (not 2.4) microGal. Therefore, the migration from MANAL (3-hour value) to LANAL (1-hour value) is an appropriate evolution. As for the amplitude ration of atmospheric corrections, the gravitational effect near the observation point was calculated as 97% (14 microGal peak-to-peak), and the other effects were calculated as 3% (0.4 microGal peak-to-peak, the correlation coefficient with the former was 0.48). Therefore, we adopted the latter as a product of the former multiplied by 0.03 for convenience. The conclusion of the following discussion did not change even if the admittance factor method was used for atmospheric correction. And, the gravity step caused by the Osaka-Fu Hokubu Earthquake (17 June 22:58 UTC) was manually corrected. As a result, the SUM (Fig. A) and the "de-tide" confined-groundwater level of TGR350m Borehole (Fig. B) showed an inverse correlation and had the correlation coefficient -0.95. The interpretation of the inverse relationship was described in Tanaka et al. (2006, Gcubed). Therefore, the SUM correctly reflects underground mass fluctuations. Next, the author removed the groundwater-level correlated component from the SUM and tried to extract gravity changes other than groundwater. Here, the residual gravity value was obtained by linear regression using the least-squares method (Fig. C). In late June, a slow slip event occurred in the Tokai region (Monthly Report on Earthquake and Volcano in Japan, JMA), but no particular change looks observed. The gravity change in Mizunami caused by a M5-class slow slip event of the Tokai region is on the order of sub-microgals, and it might be difficult to separate it from background noises.

Keywords: gravity, groundwater, Vertical Gravimeter Array, Local-scale objective analysis

©2020. Japan Geoscience Union. All Right Reserved.

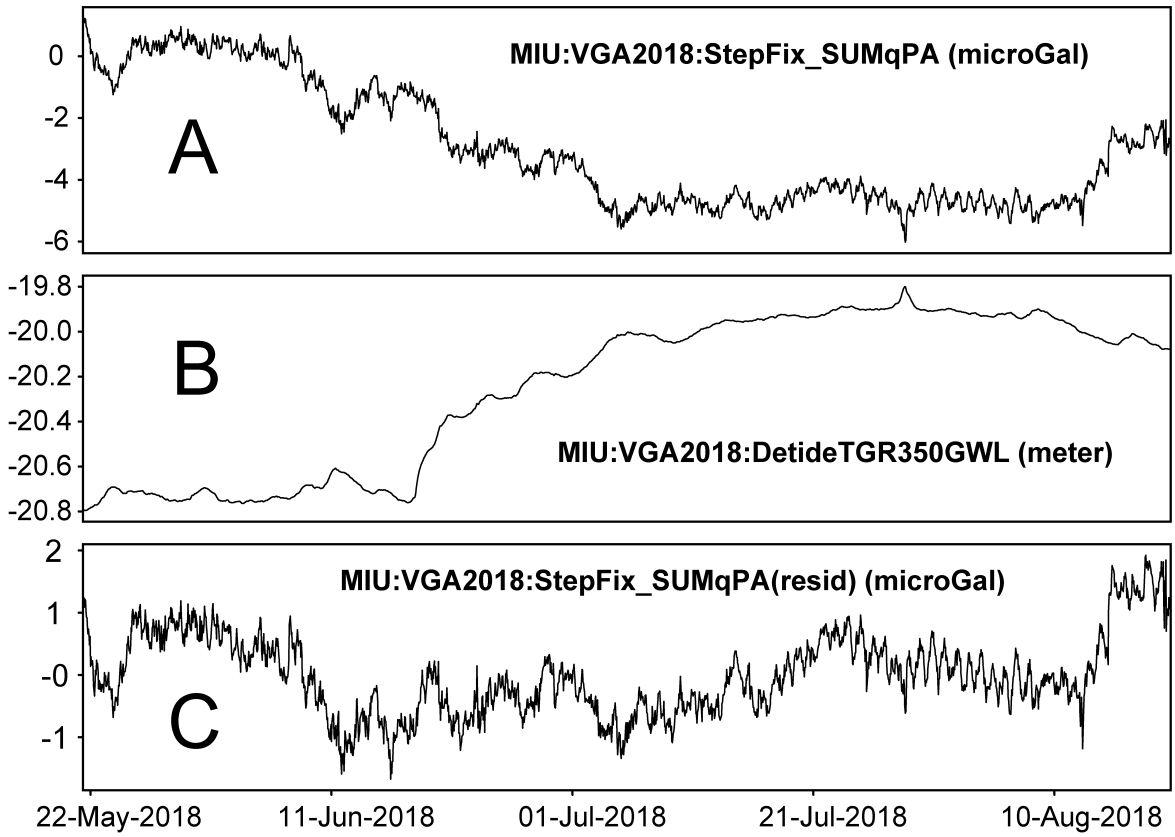

©2020. Japan Geoscience Union. All Right Reserved.

An attempt to observe gravity fluctuations caused by groundwater table response to tidal fluctuations by continuous gravity measurement near the coast

*Hiroki Goto[1,2], Mituhiko Sugihara[1,2], Yuji Nishi[1,2], Hiroshi Ikeda[2]

1. Geological Carbon Dioxide Storage Technology Research Association, 2. National Institute of Advanced Industrial Science and Technology

Groundwater levels in coastal unconfined aquifers respond to tidal fluctuations. Therefore, gravity data obtained near the coast is expected to include gravity fluctuations caused by the tidal response to the groundwater table. We measured gravity and groundwater level continuously near the coast of Tomakomai, Hokkaido, and tried to observe the gravity fluctuation caused by the tidal response of the groundwater table. Two superconducting gravimeters were installed at two points 70 and 80 m from the coast. The elevation at both locations is 8 m. The scale factors of the two gravimeters were determined by comparison with another superconducting gravimeter whose scale factor had already been determined. Water level sensors were installed in wells drilled at two points 60 and 90 m from the coast. The observed groundwater levels showed diurnal and semi-diurnal variations. The amplitude was larger as the distance from the coast was shorter, suggesting that the tidal response of the groundwater table was observed. After removing the effects of ocean loading, diurnal and semi-diurnal fluctuations were found in the difference in gravity measured at the two points. In addition, a phase difference was observed between the fluctuation of the gravity difference and that of gravity from each gravimeter. This gravity fluctuation is considered to be due to the difference in amplitude and phase of the tidal response of the groundwater level below each measurement point. It is shown that information on gravity fluctuations caused by the tidal response of the groundwater table can be obtained by observing the difference in gravity at points at different distances from the coast.

Keywords: superconducting gravimeter, groundwater table, tide, coastal area, unconfined groundwater

©2020. Japan Geoscience Union. All Right Reserved.

Effect of seasonal snow-mass change on geodetic solutions at Syowa Station: elastic deformation and gravitational attraction

*Akihisa Hattori[1], Yuichi Aoyama[2,1], Koichiro Doi[2,1], Jun'ichi Okuno[2,1]

1. The Graduate University for Advanced Studies (SOKENDAI), 2. The National Institute of Polar Research

In the Japanese Antarctic Station "Syowa," located at 69°0.2646’ S 39°34.9074’ E in East Ongul Island, East Antarctica, three different space geodetic observations (GNSS, DORIS, and VLBI) and gravity observation by superconducting gravimeter have been conducted. These geodetic observations are assumed to capture the glacial isostatic adjustment (GIA) effect caused by the melting of the Antarctic ice sheet since the last glacial maximum; however, the GIA response around Syowa Station is predicted to be small (about -2~2 mm/year) from GIA models. On the other hand, a large seasonal variation of the snowpack depth distribution occurs at Syowa Station. Therefore, it is necessary to accurately evaluate and correct the accumulated snow effect for detecting GIA signal precisely from these geodetic observations.

In this study, we derived seasonal variations of snowpack depth in Syowa Station from the time-series of the surface topography obtained by unmanned aerial vehicle (UAV) photographic survey. We evaluated the effects of snow mass close at the observation points on those geodetic solutions: elastic deformation, and gravitational attraction.

We made the digital surface models (DSMs) from the aerial photographs taken by UAV during the 59th Japanese Antarctic Research Expedition (JARE59) activity (2017-2019) with structure from motion (SfM) method. This aerial photogrammetry was conducted with the fixed-wing UAV "senseFly eBee Plus" and the rotary-wing UAV "DJI Inspire 2" and "DJI Phantom" about every once a month.

We generated the DSMs and the orthomosaic images from aerial photographs using the SfM software "Pix4Dmapper." Then, the time-series variation of snowpack depth distribution at Syowa Station was extracted as the change in the height of DSM after the correction using the corresponding orthomosaic image (Hattori et al., 2019 JpGU). With this obtained snow depth distribution and the assumption of snow density, the elastic deformation and gravitational effects caused by the snow mass close to the geodetic observation points were evaluated.

This analysis reveals that the seasonal accumulated snow mass change at Syowa Station causes vertical variation of about 1mm on GNSS observation and of about 0.1-0.3 μGal (1 μGal = 10^{-8} m/s^2) on gravity observation. In this presentation, we show the details of observed changes in snowpack depth distribution, and discuss the comparison between the estimated elastic deformation and gravity effect of local snow accumulation and the geodetic solution derived from each geodetic facility.

Keywords: Elastic deformation, UAV, structure from motion

©2020. Japan Geoscience Union. All Right Reserved.

Calculation method of the compliance parameters of the Earth's rotation: Influence of the fluid core and the solid inner core

*Yuji Harada[1,2], Shuhei Okubo[3,4]

1. State Key Laboratory of Lunar and Planetary Science, Space Science Institute, Macau University of Science and Technology, 2. Ocean Hemisphere Research Center, Earthquake Research Institute, University of Tokyo, 3. Department of Surveying and Geoinformatics, Faculty of Geosciences and Environmental Engineering, Southwest Jiaotong University, 4. University of Tokyo

Effect of non-rigidity of the solid Earth exerted on the tide and rotation is significant for understanding dynamical behavior of the core and mantle. The influence of the fluid core on the Earth's rotational motion is predictable with high precision based on the semi-analytic theory developed by Sasao et al. (the so-called Sasao-Okubo-Saito theory). This theory was expanded afterward into the theory incorporating not only the influence of the fluid core but also that of the solid inner core through a series of theoretical studies by Mathews et al. (the so-called Mathews-Herring-Buffett theory). Within the previous papers completing these SOS and MHB theories, however, there may exist a few unexplicit parts in terms of numerical procedures. It is considered to be valuable to re-definitize the above-mentioned semi-analytic theory. The present study, therefore, describes how to compute each of the important parameters included in the SOS and MHB theories semi-analytically by means of Saito's calculation method of quasi-static deformation in as much detail as possible. As a result of the computation, most of the individual parameters listed in the previous studies can be reproduced almost perfectly.

This work was financially supported by the Research Funding Projects (No. 007/2016/A1, No. 043/2016/A2, No. 119/2017/A3, and No. 187/2017/A3) at the Science and Technology Development Fund, the Macau Special Administrative Region.

Keywords: Earth's rotation, Earth's tide, Earth's interior

©2020. Japan Geoscience Union. All Right Reserved.

Utilization of Interferometric Synthetic Aperture Radar Technology for Disaster Prevention

*Takako Nakamura[1], Shuichi Rokugawa[1]

1. The University of Tokyo

The purpose of this research is to investigate the possibility of extraction and monitoring of ground deformation before and after disasters such as landslides using interference synthetic aperture radar (InSAR) analysis. In flood area extractions, we will introduce analysis results using Sentinel-1A /1B VH cross-polarized images and ALOS-2/PALSAR-2 images. The analysis area was defined as a place where a disaster occurred in the past; satellite image data used for the analysis were obtained before and after the disaster. Based on the results, it may be possible to obtain useful information for responding to a disaster or to predict the timing of a disaster to some extent. Several disaster-affected regions were considered and an analysis was performed on a model area using InSAR analysis technology. The study region covers a wide area such as the northern part of the Hokkaido Iburi region, Miyagi, the northern Kanto region, Nagano, the southwestern part of Hiroshima, southern Okayama, as well as the Ehime and Saga prefectures. In recent years, these areas have been hit by floods caused by typhoons, heavy rain, and sediment-related disasters caused by earthquakes and heavy rainfall. The image data of an HH polarized wave with an incident angle of 34.3˚, acquired during the satellite operation period, was retrieved from the archive data of ALOS/PALSAR and analyzed. In addition, ALOS-2/PALSAR-2 (level 1.1, polarization: HH, incident angle: 34.3 ˚) and Sentinel-1A/1B (VV: horizontal polarization and VH: cross polarization) were used. Interference SAR time series analysis enables the detection of minute fluctuations using a smoothing restraint inversion method to integrally analyze the interference images of multiple orbits. During these analyses, strong displacements were observed not only at the collapsed points but also at the uncollapsed ones. These uncollapsed displacement points suggest a high possibility of subsequent collapse points. The flood distribution area was accurately extracted from the VH cross-polarized images of Sentinel-1A/1B, showing adequate agreement with the hazard map. This resulting image is an intensity image generated at the initial stage of image analysis, does not require complicated analysis, and can be created from a single original image. Therefore, if an image taken at a good timing can be obtained, it is likely to be useful in quickly grasping the current situation of the target area. To implement monitoring using InSAR analysis, it is important to sufficiently consider the geology of the target area and its topographical features as well as accumulate and maintain the base information on a regular basis. In case of emergencies, the latest observation data can be obtained immediately by performing independent analyses or additional analyses together with archived data.

Keywords: InSAR, disaster prevention, heavy rain, sediment-related disaster

©2020. Japan Geoscience Union. All Right Reserved.

Postseismic crustal deformation of the 2011 Tohoku earthquake, obtained from tidal data analysis

*Kei Ishikawa[1], Takahito Kazama[1]

1. Graduate School of Science, Kyoto University

Introduction

Tidal observation data had been used for monitoring crustal deformation before 1990s. For example, Kato and Tsumura (1979) estimated long-term variations in vertical crustal deformation along Japan's coasts, by subtracting regional oceanic disturbances from observed tidal data. However, tidal data have not been used for crustal deformation analysis frequently these days because of the advance of satellite geodetic technology; in the case of the 2011 Tohoku earthquake, crustal deformation fields in Japan were understood by GNSS and InSAR data in detail (e.g., Ozawa et al., 2011; Kobayashi et al., 2011). It should be discussed whether tidal observation data can be utilized for understanding crustal deformation fields associated with the Tohoku earthquake.

Long-term tidal change at Katsuura, Chiba Prefecture

Thus, we analyzed tidal data observed along Japan's coasts in order to obtain vertical crustal deformation associated with the 2011 Tohoku earthquake. The tidal data observed at Katsuura (Chiba Prefecture) from 2003 to 2018 was chosen for our initial analysis, because the data have been continuously collected there even around the time of the earthquake. The effects of earth tide and barometric pressure change were first removed from the original tidal data, using the BAYTAP-G software (Tamura et al., 1991). The time series of the residual tidal change (i.e., the TREND component in the BAYTAP-G's result) was then used for estimating the annual, semi-annual and secular tidal changes under the least-squares method. The secular rate of the tidal change was estimated to be +0.4746 cm/year for the time series before the Tohoku earthquake, which mainly reflects the effects of plate motion and global sea level change. The secular rate was found to change to -0.7880 cm/year (i.e., by -1.2626 cm/year) after the Tohoku earthquake due to postseismic deformation.

Comparison with GPS data

We also estimated the secular variation rates of vertical coordinate from 2003 to 2018 at the Katsuura GEONET station (station number: 93041), using the F3 solution provided by Geospatial Information Authority of Japan. The secular variation rate of the vertical component was estimated to be +0.2609 cm/year for the time series before the Tohoku earthquake, which mainly reflects the plate motion effect. The variation rate was found to change to +1.5543 cm/year (i.e., by +1.2933 cm/year) after the Tohoku earthquake due to postseismic deformation. The postseismic rate of the vertical deformation (= +1.2933 cm/year) well agrees with that of the tidal change (= -1.2626 cm/year), although these signs are reversed since the tidal level is measured from the uplifting ground. This result means that the postseismic deformation due to the Tohoku earthquake can be accurately extracted from the tidal data observed at Katsuura.

Future works

We will next analyze the tidal data acquired at Ayukawa (Miyagi Prefecture) in the same process as described above, since significant crustal deformation has been observed due to the Tohoku earthquake near the tidal station (e.g., Ozawa et al., 2011). We will also compare spatial patterns of the secular variations between the tidal and GPS data, after analyzing tidal data acquired at many other stations along

©2020. Japan Geoscience Union. All Right Reserved.

the Pacific coast. In addition, we will verify the consistency of the spatiotemporal tidal variations with the crustal deformation model of Tobita (2016).

Keywords: tide, postseismic deformation, Tohoku earthquake, GNSS

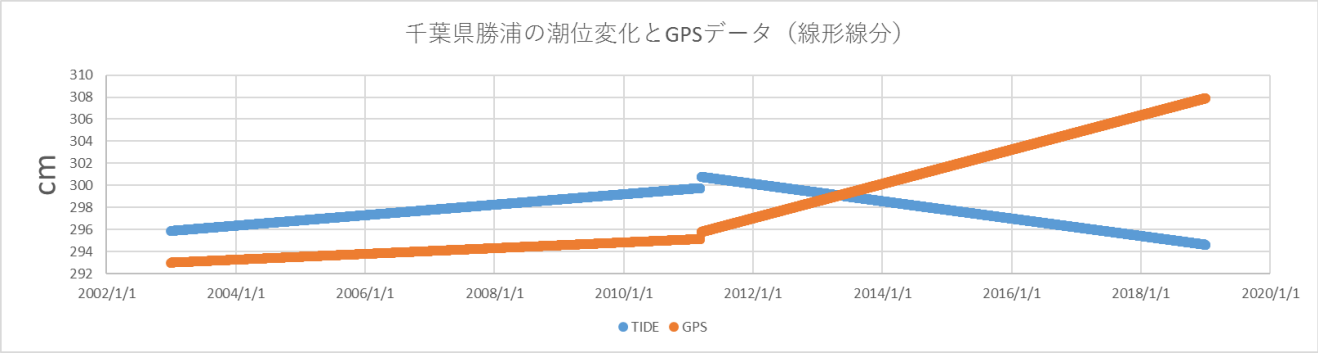

©2020. Japan Geoscience Union. All Right Reserved.

Performance assessment of the GNSS carrier phase to fault slip approach and its feasibility for seismic monitoring

*Yusuke Tanaka[1], Yusaku Ohta[1]

1. Tohoku University

Seismic monitoring based on conventional positioning analysis requires huge computational cost and strongly depends on external precise orbit information. Additionally, using coordinate time series for observation prevents us from evaluating accuracy of separation between fault slip and other unknown parameters such as tropospheric delay. Regarding these problems, we investigate the feasibility of the GNSS carrier phase to fault slip approach for seismic monitoring in subduction zone. This method, which we call PTS (Phase To Slip), relates fault slip directly to relative change of GNSS carrier phase. As PTS method estimates all unknown parameters in parallel, computational costs for real-time seismic monitoring can be reduced. Tanaka et al. (GRL, 2019) applied the PTS method to the 2016 Kumamoto earthquake and they proposed that PTS can work without external high-quality orbit because it relies on relative changes in azimuthal site-to-satellite ranges.

Here we applied the PTS method to the sequence of the 2011 Tohoku-Oki earthquake. In the analysis, we used both precise orbit which is provided by International GNSS Service (IGS) and broadcast orbit submitted from satellite without any network connection. As a result, in the case of IGS orbit, we obtained coseismic slip distribution of the mainshock that well agree with estimation result using conventional positioning analysis time series, such as shown by Iinuma et al. (2011). Although the estimated moment magnitude 8.8 is slight smaller than those by previous studies, calculated displacement field shows good consistency with that derived from positioning analysis. Moreover, we could also detect coseismic slip of subsequent two large aftershocks that occurred in the off Iwate and the off Ibaraki region. These results suggest that we can make use of the PTS method for continuous seismic monitoring in subduction zone.
In case of using broadcast orbit, the long-term stability of the estimated slip time series become much worse. However, if we focus on their relative change within 10 minutes after the earthquakes, we can obtain very similar slip behaviors compared to using IGS orbit. Differences between the slip distributions of two cases became just around one meter or less, which is smaller than the estimated standard deviation of fault slip. These results indicate that the PTS method can be useful as a supplementary system of current monitoring system, which does not depend on any external information.
In the presentation, we will describe detail of these results. Additionally, we will also evaluate O-C fitness and accuracy of parameter separation quantitatively in the dimension of carrier phase, which is used as observation in PTS analysis. Then, we will discuss characteristics of the PTS and future works for refined seismic monitoring using this method.

©2020. Japan Geoscience Union. All Right Reserved.

Consideration of antenna phase calibration for new GEONET analysis

*Kazuyuki OHASHI[1], Hiroki MURAMATSU[1], Tomoaki FURUYA[1], Yasuaki KAKIAGE[1]

1. GSI of Japan

Geospatial Information Authority of Japan (GSI) has been operating GEONET (GNSS Earth observation Network System) to estimate the daily coordinates for the purpose of monitoring crustal deformation in Japan. GEONET analysis strategy was updated four times, and we started 5th version from 2020. One of the improved points is the update of the reference frame to ITRF2014 from ITRF2005. Domes and monuments for GEONET stations are unique types of GSI. Therefore, we used original antenna phase calibration models based on ITRF2005up until now. In response to the update of reference frame, we calculated new models corresponding to ITRF2014. We will show the method of calculation of phase calibration models and results of daily coordinates based on the new GEONET analysis strategy.

We calculated phase calibration models using Bernese. We calculated combinations of two GNSS antennas “TPSCR.G5” and “TRM59800.80”, and three types of monuments. First of all, we installed rover stations, whose phase calibration models are unknown, on monuments without dome, and installed a reference station whose phase calibration model is known on a tripod. After 24-hour continuous observation, we covered rover station’s antenna with dome, and performed continuous observation again.

We took two steps to calculate phase calibration models, the calculation of baseline vectors from double difference data, and the estimation of phase center offsets and phase center variations. For the calculation of baseline vectors, we obtained the coordinates of the reference station by the static analysis from the TSKB station, which is registered to the International GNSS Service, using L1 wave of first day’s data. After that, we calculated baseline vectors between rover stations and the reference station by static analysis using L1 wave of first day’s data too. Note that we corrected ellipsoid height of rover stations by leveling results between the reference station and rover stations. Subsequently, we analyzed phase calibration models for each L1 and L2 wave using second day’s data (hereinafter called “Calculated model“). With regards to other antennas or combinations of domes and monuments, we estimated models by adding differences between “AOAD/M_T”’s phase calibration models corresponding to ITRF2005 and ITRF2014 to the current models (hereinafter called “Converted model“). In order to confirm the consistency of those two methods, we calculated the Converted model for all combinations.

As a result, differences between the Calculated model and the Converted model were within 1mm for both PCO and PCV in any combinations of antennas, domes and monuments, that is, we confirmed the consistency between two models obtained by two different ways.

Keywords: GNSS, Antenna phase calibration model

©2020. Japan Geoscience Union. All Right Reserved.

Research on the development of rapid and accurate GNSS routine analysis system (3)

*Hiroyuki Nakagawa[1]

1. GSI of Japan

The Geospatial Information Authority of Japan (GSI) routinely analyzes GNSS data obtained by GEONET, i.e. Japanese nationwide CORS array of about 1300 stations, and monitoring crustal deformation all over Japan. The results are used as fundamental data in the field of such as evaluating earthquake activity or monitoring volcanic activity. However, depending on the timing of earthquake occurrence or speed of deformation of mountain body, even up-to-date GEONET routine analysis might not always have enough rapidness or time resolution. New analysis method that is more rapid and with higher time resolution are required.

So GSI started a three-year research project on the April of 2017 to develop more rapid and accurate GNSS analysis method than present based on Precise Point Positioning with Ambiguity Resolution, or PPP-AR, and make prototype system implementing this method. PPP-AR can calculate position of a site for each epoch as accurate as those derived by interferometric analysis with much lighter calculation load. As such, we set an objective of developing a prototype system that can calculate twenty-four-hour-long time series of coordinates of all the GEONET stations by post-processing PPP-AR with one second interval, within two hours after data acquisition, and of the repeatability less than 1cm for horizontal component.

Until March, 2020, we have gotten results as below. In this presentation, we show these in detail.

1. A prototype system that can calculate time series of coordinates for all the GEONET station nationwide in one second interval by post-processing PPP-AR. This system consist of two steps as bellow: First, using last 24-hour observation data from global GNSS observation network operating by organizations such as IGS or UNAVCO, estimating information required for PPP-AR such as precise satellite orbits, satellite clocks and other corrections. Then, using these information and GEONET observation data of last 24 hours, calculating 24-hour long time series of coordinates for all GEONET stations by PPP-AR.

2. Using the prototype system, in good condition, we found to be able to get time series of coordinates for all GEONET stations in about 2 and half hours.

3. We evaluate the quality of GPS orbit estimated by the prototype system by means of the difference from IGS final orbit for one year test period from July 2018 to June 2019. Comparing the error with the error for IGS ultra-rapid orbit w.r.t. IGS final orbit, we found that the error for our GPS orbit is smaller than that of predicted part of IGS ultra-rapid orbit because our orbit does not contain predicted part. Although the error is larger than that of observation part of IGS ultra-rapid orbit, our system can calculate orbits for about 20 minutes, much shorter than IGS ultra-rapid orbits (about three hours).

4. To evaluate the quality of final result, that is, daily time series of all GEONET station position, calculating standard deviations of horizontal component during the same test period as item before. The average of all the standard deviation for all the period is about 1cm. The mean standard deviation is found to be larger in summer season and smaller in winter season.

©2020. Japan Geoscience Union. All Right Reserved.

5. Using prototype system, calculating ground deformation for foreshock of 2016 Kumamoto earthquake and “the largest aftershock of the foreshock” which occurred about three hours after the foreshock. We found that our result can divide those ground deformations, which GEONET routine analysis cannot.

Keywords: GNSS, PPP-AR, GEONET, GEONET routine analysis

©2020. Japan Geoscience Union. All Right Reserved.

Proposal to avoid inserting leap seconds

*Kozo Takahashi

In the following ** mearns 'power
O means omega
P: pi

Introduction
The leap seconds are introuced to fill the diffrence between UTC and UT1, and have been inserted 27 times during past 45 years.
Decrease of Earth rotation rate
T ; rotation period,
O ; angular speed,
i; means equal,
P; means pi.

Present definition of one second is that 9192631770 times multiply of one period of Cs radiation f = 9.192631770 GHz. As 27 times leap seconds are inserted during 45 years, the leap seconds become unnecessary where the time is made longer by 27 seconds during 45 years. Namely f is made to be fc = 9.192631673. Because
T = 2 P/O
dT/dt = 27 sec / 45 year
= 19.01 * 10**-8
f * dT/dt = 97 Hz
9192631770 / 9192631673 = 1 + 1.055 * 10**-8
This means one second becomes longer by 1.055 * 10**-8 sec
The definiton of light speed c changes, as the definition of time changed, the value is unchanged because the speed and time duration are offset.
Calculation showes that present half life of the anular speed becomes shorter than that of the ancient one. This will be caused by the increse of the moment inersia of the earth which is caused by the global warming.

Although astronomical observation has shown the decrease of the earth rotation rate, this paper shows the rate has become larger, and the reason is the global warming. And the change of the definition of time makes the insertion of leap seconds unnecessary (Refer to attached figure).

Keywords: leap scond, avoid leap seconds, global warming

©2020. Japan Geoscience Union. All Right Reserved.

(In the following, ** : power, * : multiply)
Where T : period of Earth rotation
ω : angular speed of Earth rotation,
T = 2 π / ω (1) dT/dt=-T d ω/dt/ω (1)'
ω = (ω o) exp{- k t} k : atten. coef. (2)
i.e. log {ω / (ω o)} = − k t (2)'
d ω/dt = -k (ω o) exp{-k t} = -k ω (2)"
k = {dT/dt}/T (3) r * (ω o)**2 = g
r=6378100m, g = 9.80665 m/s**2、
(ω o)−1.2400 * 10**-3 rad/sec−107 rad/day (2)"
ω − 7.292115 × 10**-5 rad/sec (2)'"
ω / (ω o)−(7.292 * 10**-5)/1.240 * 10**-3
= 0.05889 i.e. log{ω/(ω o)} = − 2.832
k −2.832/45.5hund.mill.years=0.06224/hun.mil.y (4)
Half-life :Th log{ω/(ω o)} > − k Th
Th < 0.6931/0.06224hun.mil.y−11.14 hun.mil.y (6)
dT/dt 27 sec/45y− 1.901 * 10** 8 (1)"
k − (1.901 × 10 * * − − 8) / T (3)"
= (1.901 × 10**− 8) / year (3)'"
Th=0.6931/k− {0.6931/1.1901 × 10 − 8)} / year
−0.363 × 10**8) year−0.365 hun. mil. y

f = 1 / T Δ f varia of f, T Δ f ≒ − f Δ T
Δ f ≒ − f Δ T/T Δ f ≒ (1.901 × 10** 8) f
Δ f ≒ 174.75 / sec (7'")
Cs: f =9.192631770 GHz. Cs is made to be 9.192631695 GHz.
(9192631770-174.75) / 9192631770−1-19.01 × 10**-9,
i.e. One second gets longer by 19.01 * 10**-9,
i.e. during 45 years, the time gets longer by 27 secs.

The above mentioned proposal makes influence to basic unit other than time.

Present attenuation coefficient k is (3)'", on the contrary last one is (4), there is much difference. This will show that the earth rotation rate recently gets larger because of the global warning caused by the increase of moment of inertia of the earth.

Althou it has been shown the decrease of the earth rotation rate by the astronomical observation, this paper shows the rate has get larger, and the reason is the global warming. Unnecessary.

©2020. Japan Geoscience Union. All Right Reserved.

©2020. Japan Geoscience Union. All Right Reserved.

[J] Poster | S (Solid Earth Sciences)：S-SS Seismology

[S-SS11] Crustal Structure

convener:Kazuo Nakahigashi(Tokyo University of Marine Science and Technology)

The aim of this session is to cover seismological and geophysical studies on the Earth's crust. Contribution on seismological and geophysical structure of the crust, processes that develop in the crust which include earthquakes, volcanoes and geological descriptions of the crust are welcomed. We also welcome theoretical and methodological studies that will serve as basics in such explorations.

[SSS11-P01] Measurement of seismic velocity anisotropy in the Tohoku region, NE Japan by shear wave splitting analysis

*Tatsuya Mizuta[1], Tomomi Okada[1], Martha K Savage[2], Ryota Takagi[1], Keisuke Yoshida[1], Hiroshi Yakiwara[3], Takeshi Matsushima[4], Hiroshi Katao[5], Yoshiko Yamanaka[6], Masahiro Kosuga[7], Kei Katsumata[8], Mako Ohzono[8], Takashi NAKAYAMA[1], Satoshi Hirahara[1], Toshio Kono[1], Toru Matsuzawa[1], Group for the aftershock observations of the 2011 off the Pacific coast of Tohoku Earthquake (1.Tohoku University , 2.Victoria University of Wellington, 3.Kagoshima University, 4.kyushu University, 5.Kyoto University, 6.Nagoya University, 7.Hirosaki University, 8.Hokkaido University)

[SSS11-P02] An attempt to estimate the migration pathway of slab-derived fluid using shear wave splitting analysis

*Shinya Hiratsuka[1], Koichi Asamori[1], Atsushi Saiga[1] (1.Japan Atomic Energy Agency)

[SSS11-P03] **Estimation of crust and upper mantle velocity structure of the Himalayas and North-Eastern part of India using surface wave data**

*Mradula Vashishtha[1], Sagarika Mukhopadhyay[1] (1.Department of Earth Sciences, Indian Institute of Technology Roorkee, Roorkee- 247667, India)

[SSS11-P04] 1-D layered crustal and uppermost mantle structure beneath Botswana

*Admore Phindani Mpuang[1], Takuo Shibutani[2] (1.Graduate School of Science, Kyoto University, 2.Research Center for Earthquake Prediction, Disaster Prevention Research Institute, Kyoto University)

[SSS11-P05] Receiver function imaging of the Philippine Sea plate subducting beneath Shikoku (2)

*Takuo Shibutani[1], Nakagawa Jun[1], Nagaoka Airi[1], Tsutomu Miura[1], Yusuke Yamashita[1], Ken'ichi Yamazaki[1], Shintaro Komatsu[1] (1.Kyoto University)

[SSS11-P06] 3D Seismic Reflection Imaging with Microearthquake Sources recorded by Dense Nodal Arrays

*Larry D Brown[1], Doyeon Kim[2], Diego Quiros[3] (1.Cornell Univ, 2.Univ Maryland, 3.Capetown Univ)

[SSS11-P07] Imaging of S wave reflector in the crust obtained from a dense seismic array at the southern
part of Abukuma Plateau

*Yuta Usuda[1], Takashi Iidaka[2], Toshihiro Igarashi[2], Kazushige Obara[2], Shin'ichi Sakai[2], Shigeki Nakagawa[2], Tetsuya Takeda[3] (1.UNIC Corporation, 2.Earthquake Research Institute, University of Tokyo, 3.National Research Institute for Earth Science and Disaster Resilience)

[SSS11-P08] Stability of H/V spectra of ambient noise from ocean bottom seismometers (OBS) near the Japan Trench

*Atikul Haque Farazi[1], Yoshihiro Ito, Emmanuel Soliman M Garcia (1.Disaster Prevention Research Institute, Kyoto University)

[SSS11-P09] Moho depth of the Korean Peninsula via P-coda autocorrelation analysis

*Hyejeong Cho[1], Sang-Jun Lee[1], Junkee Rhie[1], Seongryong Kim[2] (1.Seoul National Univ., 2.Chungnam National Univ.)

[SSS11-P10] The gravity anomaly of western offshore of Noto peninsula and the estimation of basement structure

*Akihiro Sawada[1], Yoshihiro Hiramatsu[1] (1.Geosciences and Civil Engineering, College of Science and Engineering, Kanazawa University)

[SSS11-P11] Study of subsurface and geological structure around the Togi–gawa Nangan Fault based on integrated analysis of seismic reflection method and gravity exploration

*Wataru Kobayashi[1], Masaaki Hamada[1], Yasuhisa Tanaka[2], Shinji Kawasaki[2], Takuya Murakami[3], Manabu Sakashita[3], Akihiro Sawada[4], Yoshihiro Hiramatsu[4] (1.Hokuriku Electric Power Company, 2.JGI, Inc., 3.DIA Consultants, 4.Kanazawa Univ.)

Measurement of seismic velocity anisotropy in the Tohoku region, NE Japan by shear wave splitting analysis

*Tatsuya Mizuta[1], Tomomi Okada[1], Martha K Savage[2], Ryota Takagi[1], Keisuke Yoshida[1], Hiroshi Yakiwara[3], Takeshi Matsushima[4], Hiroshi Katao[5], Yoshiko Yamanaka[6], Masahiro Kosuga[7], Kei Katsumata[8], Mako Ohzono[8], Takashi NAKAYAMA[1], Satoshi Hirahara[1], Toshio Kono[1], Toru Matsuzawa[1], _ Group for the aftershock observations of the 2011 off the Pacific coast of Tohoku Earthquake

1. Tohoku University , 2. Victoria University of Wellington, 3. Kagoshima University, 4. kyushu University, 5. Kyoto University, 6. Nagoya University, 7. Hirosaki University, 8. Hokkaido University

Shear wave polarization anisotropy in the Tohoku region was measured using shear wave splitting, which is a phenomenon in which a shear wave splits into fast and slow shear waves when seismic waves pass through an anisotropic medium. The method used in this study was Multiple Filter Automatic Splitting Technique (MFAST; Savage et al., 2010). In this method, by inputting the three components of the seismic waveform observed at the observation station, the optimum filter is selected from the 14 filters prepared by MFAST. The orientation and magnitude of the anisotropy is measured in a number of time windows by the method of SC91 (Silver and Chan, 1991). Then, quality evaluation is performed using cluster analysis (Teanby et al., 2004) from many measured values measured from multiple time windows. MFAST is a program that automates this sequence, so it can process large amounts of data automatically and more quickly than conventional methods, and can obtain objective and reliable measurements. At first, we tested MFAST against previous measurements in the Tohoku region and confirmed its effectiveness. From December 2008 to November 2013, north-south oriented fast orientations of anisotropy were found in the coastal area (Kitakami mountain range) of the Tohoku region, consistent with the results of previous studies (e.g., Takagi and Okada, 2012). Inhomogeneous polarization anisotropy was observed in a small scale in the inland area of the Tohoku region, especially in the aftershock region of the Iwate-Miyagi Nairiku Earthquake in 2008, and the variation of direction could be explained by the stress field estimated in previous studies (e.g., Yoshida et al., 2014). In addition, we compared the anisotropy before and after the 2011 off the Pacific coast of Tohoku Earthquake, but it was considered that the direction and the delay time didn’ t change significantly during the analysis period.

Acknowledgment: We really appreciate Kohtaro Araragi's help.

©2020. Japan Geoscience Union. All Right Reserved.

An attempt to estimate the migration pathway of slab-derived fluid using shear wave splitting analysis

*Shinya Hiratsuka[1], Koichi Asamori[1], Atsushi Saiga[1]

1. Japan Atomic Energy Agency

It is known that hot springs with high temperature exist in Kii peninsula although it is non-volcanic region. Based on the distribution of high $^{3}He/^{4}He$ ratios in Kii peninsula, Morikawa et al. (2016) pointed out the possibility that slab-derived fluid pass through mantle wedge and ascend along pre-existing faults in the crust. According to seismic tomography, it is suggested that slab-derived fluid serpentinize mantle wedge directly above subducting Philippine Sea slab and contributes to the occurrence of non-volcanic swarm activity near Wakayama city (Kato et al., 2014). This is supported by the existence of highly conductive zone in mantle wedge directly above subducting Philippine Sea slab imaged by magnetotelluric (MT) method (Umeda et al., 2006). Pre-existing faults and highly cracked zone in the crust are candidate for the migration pathway of slab-derived fluid, and they are expected to show more significant seismic anisotropy than surrounding areas. In this study, we attempt to estimate the configuration of pre-existing faults and highly cracked zone as a migration pathway of slab-derived fluid using shear wave splitting analysis.

We used seismic waveform data recorded at stations of Earthquake Research Institute (ERI), University of Tokyo, Japan Meteorological Agency (JMA), Geological Survey of Japan (GSJ) and Hi-net data operated by the National Research Institute for Earth Science and Disaster Resilience (NIED) and analyzed the events occurred from April 2004 to March 2009 with focal depth shallower than 80 km and magnitude from 1.5 to 3.5. We estimated the leading shear wave polarization direction (LSPD) and arrival time difference between leading and lagging shear waves (DT) using the method of Silver and Chan (1991). In order to minimize the effect of phase conversion from S to P waves at the free surface, we restricted ray paths to those having incident angle to ground surface are less than 35˚(Booth and Crampin, 1985).

The results can be summarized as follows. Most of LSPD is trending NW-SE direction in the southern Kii peninsula, which is sub-parallel to convergence direction of Philippine Sea Plate along Nankai trough. This result indicate that tensile cracks are aligned parallel to maximum regional stress direction due to plate convergence. In contrast, from central part of Wakayama prefecture to southwestern side of Nara prefecture, some LSPD is trending ENE-WSW direction. Based on three-dimensional ray tracing, we calculated the normalized DT values per unit path length and investigated the spatial distribution of them. As a result, we found that the normalized DT values in the crust tends to be larger than those in the mantle wedge. Especially large normalized DT values per unit path length tends to be concentrated from central part of Wakayama prefecture to southwestern side of Nara prefecture.

Acknowledgments:
We used the seismic waveform data of Hi-net (NIED), ERI, JMA, and GSJ. This study was carried out under a contract with Agency of Natural Resources and Energy (ANRE), part of Ministry of Economy, Trade and Industry (METI) of Japan as part of its R&D supporting program for developing technology of geological disposal of high-level radioactive waste.

References:
Booth, D. C. and S. Crampin, 1985, Geophys. J. R. astr. Soc., 83, 31-45.

©2020. Japan Geoscience Union. All Right Reserved.

Kato et al., 2014, Earth Planets Space, 66:86.
Morikawa et al., 2016, Geochimica et Cosmochimica Acta, 182, 173-196.
Silver, P. G. and W. W. Chan, 1991, J. Geophys. Res., 96, 16,429-16,454.
Umeda et al., 2006, J. Volcanol. Geotherm. Res., 149, 47-61.

Keywords: Shear wave splitting analysis, Polarization anisotropy of S-wave, Slab-derived fluid

©2020. Japan Geoscience Union. All Right Reserved.

Estimation of crust and upper mantle velocity structure of the Himalayas and North-Eastern part of India using surface wave data

*Mradula Vashishtha[1], Sagarika Mukhopadhyay[1]

1. Department of Earth Sciences, Indian Institute of Technology Roorkee, Roorkee- 247667, India

Characteristics of dispersion curves of Rayleigh and Love waves of 2015 Nepal Earthquake and its aftershocks are utilized to investigate the sub-surface structural variations below the Himalayas and nearby regions. Surface waves of these earthquakes recorded in the broadband seismometers installed at Ajmer, Dehradun and Shimla were used for investigation. We have applied multiple filtering technique to obtain the group velocity curves. It is observed that group velocities for both Rayleigh and Love waves obtained using main shock data are consistently lower at all periods compared to those obtained using data from aftershocks for these three stations which lie in the western/southwestern side of the mainshock epicenter. It is reported by various researchers that during this earthquake slip along the fault was unidirectional, i.e. from west to east. We are investigating if the above observation related to differences in group velocity is anyway related to directionality of the faulting and are analyzing data from the eastern side of the mainshock epicenter. Inversion of dispersion curves of mainshock and aftershocks are performed to investigate subsurface shear wave velocity structure and variation of anisotropy with depth for crust and uppermost mantle.

Keywords: Group velocity, Dispersion curves, Rayleigh wave, Love wave, Himalayas

©2020. Japan Geoscience Union. All Right Reserved.

1-D layered crustal and uppermost mantle structure beneath Botswana

*Admore Phindani Mpuang[1], Takuo Shibutani[2]

1. Graduate School of Science, Kyoto University, 2. Research Center for Earthquake Prediction, Disaster Prevention Research Institute, Kyoto University

Despite a relatively low seismicity, Botswana hosts a south westerly extension of the East African Rift System, postulated by various researchers to be in northern and central Botswana, where most seismicity in the country has been observed. Due to a sedimentary coverage of about 75% (Haddon, 2005) and other limitations, understanding the crustal structure has been a challenge. This has seen limited literature on Botswana’ s crustal and upper mantle structure, as well as contrasting ideas on the causes of seismicity and faulting observed in the country. Providing a better definition of the crustal structure enables earthquakes to be better located, their causes to be delineated and improves our understanding of the associated seismic hazards and risks. In an attempt to provide such a definition, this research aims to define layering in the crust and to study the relation between the crustal structure, tectonics and seismicity in Botswana.

To do this, P-to-S receiver functions are computed from waveform records of teleseismic events from epicentral distances between 30 and 85 degrees recorded at 38 stations located within Botswana, with magnitudes Mw>5.8 to ensure good signal to noise ratios. We carried out a further quality assessment of receiver functions to select only the best quality receiver functions. These receiver functions are then stacked in back azimuth and slowness bins to obtain preliminary results that guide further analysis. The preliminary results reveal a layered crust, uniform with back-azimuth at some stations and with a back-azimuthal variation at others. Delayed first peaks at stations located in sedimentary basins are observed as expected. The receiver functions are then further grouped and stacked based on waveform similarity and relative difference in slowness. A genetic algorithm inversion technique (Sambridge and Drijkoningen, 1992; Shibutani et al., 1996) is then applied to the groups of stacked radial receiver functions to obtain one-dimensional shear wave velocity models for a horizontally layered crust.

The results show lower shallow shear wave velocities in sedimentary basins and a tectonic region average crustal thickness between 32km and 43km. A reduced crustal thickness is observed at stations in the Okavango rift zone in northern Botswana which is attributable to rift related extension that causes seismic activity in the area, while a thickened crust in central-western Botswana may point to a buried ancient craton suggested by Begg et al. (2009). A dipping Moho is suspected where an offset of ~8km in Moho depth is observed on the NE-to-E side of station NE208 in the Limpopo belt due to the mechanism of its formation. In the western part of Kaapvaal craton, the crust is undisturbed and thinner than in eastern part where it is affected by the emplacement of Bushveld complex correlatives (Nguuri et al., 2001) and proximity to the Limpopo belt. In general, the depth to the Moho beneath Botswana averages ~39km.

©2020. Japan Geoscience Union. All Right Reserved.

Receiver function imaging of the Philippine Sea plate subducting beneath Shikoku (2)

*Takuo Shibutani[1], Nakagawa Jun[1], Nagaoka Airi[1], Tsutomu Miura[1], Yusuke Yamashita[1], Ken'ichi Yamazaki[1], Shintaro Komatsu[1]

1. Kyoto University

1. Introduction

We carried out receiver function analysis using the waveforms of teleseismic earthquakes observed at seismic stations on a linear array that crossed Shikoku from Tokushima Prefecture to Ehime Prefecture along the northeast east –west southwest direction. We successfully obtained clear images of the upper boundary and the oceanic Moho of the Philippine Sea plate subducting beneath Shikoku.

The purpose of this study is to estimate accurately the structure of the areas around the Philippine Sea slab, which are the source of the Nankai Trough magaquake, and the propagation path of strong seismic waves. Such information is necessary for accurately estimating the extent of the source area and the strong motion generation area, and improving the prediction of earthquake magnitude and strong motion.

In this presentation, we report the shape of the Philippine Sea slab which is being revealed by receiver function analysis in Shikoku.

2. Linear array observation

On the survey line from Tokushima City to Seiyo City, Ehime Prefecture, 14 temporary stations were deployed, including nearby permanent stations, so that the interval was about 5 km.

At each temporary station, the ground velocity output of a high-sensitivity seismometer (Sercel, L-4-3D) with a natural period of 1 s was continuously recorded to CF cards of a data logger. The data logger was powered by a car battery, which was charged by solar cells.

3. Receiver function analysis

The receiver function is a waveform obtained by extracting PS converted waves generated at S-wave velocity discontinuities below seismic stations.We converted the time axis of the receiver function to the depth axis by using the Japan Meteorological Agency's seismic velocity model JMA2001 (Ueno et al., 2002), and obtained an image of the S-wave velocity discontinuities by stacking the amplitude of the receiver functions obtained for many teleseismic events at the stations. The obtained receiver function image is shown in Fig. 1.

The series of red images behind the red line labeled OM is considered to be the top of a high-velocity layer and can be interpreted as the ocean Moho in the Philippine Sea slab. The blue line labeled ST above it is considered to be the top of the low-velocity oceanic crust, that is the top of the Philippine Sea slab. Here, we assume the thickness of the oceanic crust to be almost constant (about 7 to 8 km), and place the

©2020. Japan Geoscience Union. All Right Reserved.

interpretation line (ST) in a series of blue images above the clear ocean Moho (OM). At -80 < x <50 km, dark blue images are seen above the slab upper surface (ST), which suggest the existence of a low velocity layer. It is thought to be due to slab-derived fluids. The Philippine Sea plate is subducting from the front to the back of the paper while tilting west-southwest.

Acknowledgments

Seismic waveform data from permanent stations at the National Research Institute for Earth Science and Disaster Prevention, the Japan Meteorological Agency, the National Institute of Advanced Industrial Science and Technology, Kochi University, and Kyoto University were used.

Keywords: receiver function, Philippine Sea plate, Shikoku, Nankai Trough megaquake, seismological structure

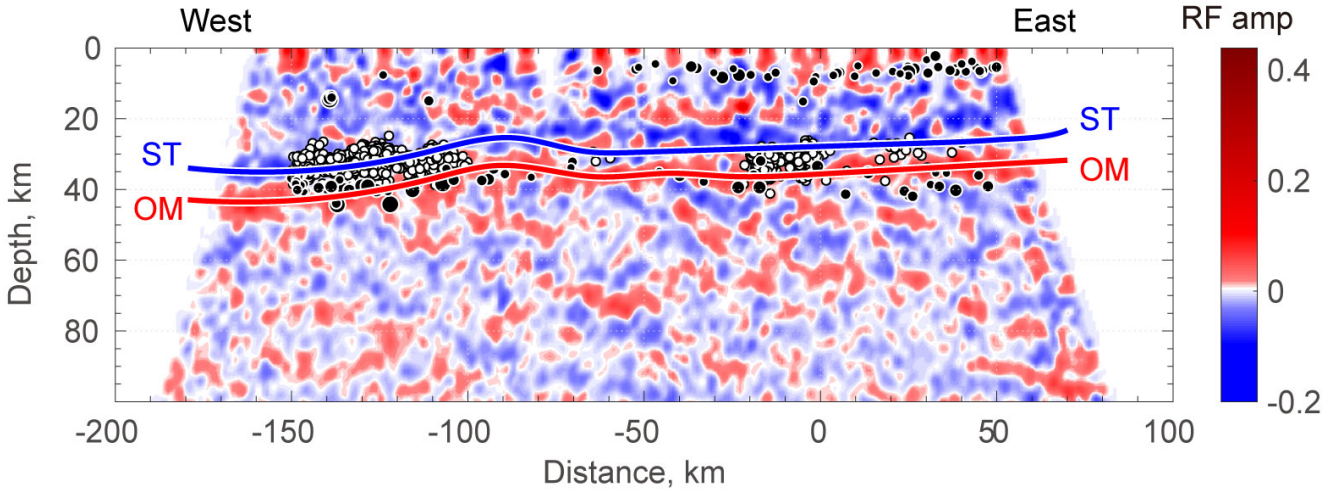

Fig.1 A receiver function image along Tokushima – Seiyo profile in Shikoku. White circles denote deep low frequency events, while black circles show ordinary earthquakes. OM and ST show Oceanic Moho and Slab top, respectively.

©2020. Japan Geoscience Union. All Right Reserved.

3D Seismic Reflection Imaging with Microearthquake Sources recorded by Dense Nodal Arrays

*Larry D Brown[1], Doyeon Kim[2], Diego Quiros[3]

1. Cornell Univ, 2. Univ Maryland, 3. Capetown Univ

Reflection seismology with controlled sources often provides the highest resolution of any seismic technique. However, the application of the reflection method to probe all but the shallowest of structures is often inhibited by the substantial cost of artificial sources as well as logistical barriers to their deployment. Here we describe how reflection processing can be applied to recordings of microearthquakes to produce reflection imagery that approaches the quality of conventional controlled source (CMP) surveys. Such “passive” seismic reflection imaging has only recently become practical with the advent of nodal technology that can simultaneously record spatially dense arrays for substantial lengths of time. Two distinct approaches are illustrated here: re-datuming of microearthquake sources via interferometry and VSP imaging of microearthquakes sources. Examples from the eastern US and Iceland suggest that these methods represent a transformative approach to studying- and monitoring- magma and deep structure in tectonically active areas.

Keywords: Reflection seismology, Crustal seismology, Volcano seismology

©2020. Japan Geoscience Union. All Right Reserved.

Imaging of S wave reflector in the crust obtained from a dense seismic array at the southern part of Abukuma Plateau

*Yuta Usuda[1], Takashi Iidaka[2], Toshihiro Igarashi[2], Kazushige Obara[2], Shin'ichi Sakai[2], Shigeki Nakagawa[2], Tetsuya Takeda[3]

1. UNIC Corporation, 2. Earthquake Research Institute, University of Tokyo, 3. National Research Institute for Earth Science and Disaster Resilience

The 2011 Tohoku-Oki earthquake (Mw9.0) occurred off the Pacific coast of Japan, on March 11, 2011. The seismic activity in Japan changed after the Tohoku-Oki earthquake. It is considered that the stress field in the inland fault zones has changed due to the slip of the main shock and the after slip. Especially in the southern part of Abukuma Plateau (the southern part of Fukushima Prefecture and the northern part of Ibaraki Prefecture), so many earthquakes within the crust has occurred. The largest earthquake in this region is the Fukushima Hamadori earthquake (M7.0), which caused severe damage. In this region, the seismic zone within the crust is divided into two groups. The shallower group earthquakes occurred at a depth of shallower than 15km. The other group earthquakes occurred at a depth rage of 15 km - 25 km. We don’ t know the clear reason that the seismicity is split into two groups.
Earthquake Research Institute, Universities, and other organizations deployed a temporary dense seismic array with 63 seismic stations in this area. We analyzed the 123 earthquakes (Mj2.5~4.0) observed by the array from January, 2012 to December, 2012. We applied AGC (Automatic gain control) to the waveform data. We found two clear later phases after the S wave. In order to clarify the nature of these later phases, we analyzed the particle motion and amplitude of the later phases. The two later phases were reflected wave of the S wave. We estimated the locations of reflection points using reversed VSP (Vertical Seismic Profile) method which is used for seismic exploration. We converted travel time to depth using the velocity structure of JMA (Ueno et al., 2002), and estimated locations of S wave reflection boundary in the crust. As a result, it was found that the two later phases are reflected waves from velocity boundaries located at depths of (1) 15-23km and (2) 27-33km in the crust. The reflection boundary (2), which was located at a depth of 27-33km, was found to be the Moho discontinuity by comparing with previous studies in this region. We compared the location between the reflection boundary (1) and the earthquakes. It was found that the reflection boundary (1) was located just under the hypocenters. The seismic activity in this region started to occur just above the reflection boundary (1). To explain further, this reflection boundary (1) is well consistent with the focal area at the depth of 15-20km which is one of the characteristics of seismic activity in the region. It is suggested that the reflection boundary (1) is significantly related to the cause of the earthquakes occurring at this depth range. The amplitude of the reflected waves from the reflection boundary (1) in the crust is large. The location of the reflection boundary (1) is well consistent with that of the crustal fluids suggested by some previous studies in this region. It is possible that the reflected waves are from the layer including the crustal fluids. In the future, we will estimate the more precise location of the reflection boundary taking into account the migration and the velocity structure estimated in this region. We declare the cause of the earthquakes in this region.

©2020. Japan Geoscience Union. All Right Reserved.

Keywords: Iwaki area, seismic array observation, S wave reflector, crustal structure

©2020. Japan Geoscience Union. All Right Reserved.

Stability of H/V spectra of ambient noise from ocean bottom seismometers (OBS) near the Japan Trench

*Atikul Haque Farazi[1], Yoshihiro Ito, Emmanuel Soliman M Garcia

1. Disaster Prevention Research Institute, Kyoto University

Ocean bottom seismometers (OBS) are being widely used to monitor seismicity of slow earthquakes as well as that of ordinary earthquakes. Seismic velocity structures, especially of S-waves, are essential to estimate hypocenters of them with accuracy. The horizontal to vertical spectral ratio (H/V) method, originally proposed by Nogoshi and Igarashi (1971) and familiarized by Nakamura (1989), is a potential technique to get S-wave velocity structure by inversion of the H/V curve. Here, we aim to use the ambient noise H/V method utilizing OBS data. From this perspective, currently we focus upon spatial and temporal stability of H/V spectra of ambient noise from OBS data as the first step towards future application of this method to estimate S-wave velocity structure deploying the existing OBS stations. We use the Nakamura’s method (1989) for obtaining H/V spectra using a 3-component (H1, H2, and V) OBS array in the Japan Trench area to characterize deep structure above the plate interface near the trench. 21 OBS, 3 broadband and 18 short-period, stations have been used in this study. To retrieve the spectra, processing to the waveform data is applied, the first step of which include removal of instrumental response, and downsampling of the trace to 20Hz, removal of mean and trend from the record, tapering, and filtering. Then, Fourier amplitude spectra of each 3 components are obtained applying fast Fourier transformation (FFT). After that, we applied smoothing to the amplitude spectra following Konno and Ohmachi (1998) method. Next, the 2 horizontal amplitude spectra (H1 and H2) are merged together by taking their quadratic mean (H). Finally, H/V spectral ratio is achieved for the selected time window by dividing the mean of the horizontal components (H) by the vertical component (V). Prior to preprocessing, each 24-hours record was split into 1-hour window, and we selected time windows which are quiet or devoid of any earthquake arrivals so that use of the ambient noise part of the record is ensured. The quiet hours or time windows are selected manually making dayplots (or hourly plots) for each components of a station, from their spectrogram for checking the frequency content, and also from power spectral density (PSD).

The 1-hour H/V spectra of every station are primarily examined to see if their shape indicates similarity suggesting high stability. The 1-hour spectra are then stacked together and averaged in a single window to get each 1-day spectra. These 1-day spectra are also compared for understanding the temporal stability of the H/V spectra from individual OBS station. These 1-day spectra are also stacked and averaged to get the final H/V curve of a single station. The final spectra of a single station is then compared in between stations to discern the spatial stability. Stability of H/V spectra of ambient noise from OBS data is promising for conducting our future work for deeper observation using the ambient noise H/V method.

Keywords: Ambient noise, The H/V method, Ocean bottom seismometer (OBS), Spatial and temporal stability of H/V spectra

©2020. Japan Geoscience Union. All Right Reserved.

Moho depth of the Korean Peninsula via P-coda autocorrelation analysis

*Hyejeong Cho[1], Sang-Jun Lee[1], Junkee Rhie[1], Seongryong Kim[2]

1. Seoul National Univ., 2. Chungnam National Univ.

Moho depths of the South Korean Peninsula (SKP) were constrained via P coda autocorrelation which is developed to extract reflected P waves on discontinuites at depth, such as Moho. Autocorrelation and badpass filtering were applied to each teleseismic events with magnitude≧5.5, occurring in 2010–2017, after spectral whitening being applied. Finally autocorrelograms for about 90 stations were obtained by stacking. The result shows the Moho discontinuity of the SKP is deepening towards Southeast, though Moho has shallow depth in the area where Gyeongsang basin is located. This result is consistant with Moho depth pattern reported in the previous studies analysing receiver function and surface wave dispersion.

Keywords: Moho discontinuity, P coda, autocorrelation

©2020. Japan Geoscience Union. All Right Reserved.

The gravity anomaly of western offshore of Noto peninsula and the estimation of basement structure

*Akihiro Sawada[1], Yoshihiro Hiramatsu[1]

1. Geosciences and Civil Engineering, College of Science and Engineering, Kanazawa University

Estimation of basement structure is important for understanding seismo-tectonics in coastal areas. The gravity anomaly reflects the density structure of the basement, and its analysis provides information on subsurface fault structures. However, it is not easy to conduct gravity measurements in coastal sea areas, and there are often gaps in gravity data. In order to obtain more detailed information on the continuity of the fault structure from land to sea, it is essential to improve gravity measurement points in coastal seas. Hokuriku Electric Power Company performed seafloor gravity measurements on the western coast of the Noto Peninsula from May to June 2018 (Ishida et al., 2018). Seafloor gravity measurements were taken at approximately 40 km along the coast and about 10 km offshore. The measurement interval is about 700 m in the dense area and about 2 km in other areas, and the number of measurement points is 275. Terrain correction (assumed density: 2300 kg/m^3) was performed on these new measurement data using the digital data M7000 series of seafloor topography. In addition, 283 gravity measurements have been conducted on land since 2013. The seafloor gravity data and the marine gravity anomaly data (AIST, 2013), the existing gravity data (Honda et al., 2012; The Gravity Research Group in Southwest Japan, 2001; Yamamoto et al., 2011), and merged new land-based measurement data to create a gravity anomaly distribution map with continuity from land to sea.
The acoustic survey has been conducted along survey lines in the coastal area west of the Noto Peninsula, and the boundary depth distribution of the marine sedimentary layers has been obtained as a profile of the velocity structure along the survey lines. By combining the depth distributions of these sedimentary layer boundaries, we created a three-dimensional density structure model consisting of four layers. Correcting the gravity anomaly caused by the three-dimensional density structure, we obtained a pseudo gravity anomaly due to the two-layer structure consisting of the sedimentary layer and the basement. From the pseudo gravity anomaly, we performed a gravity inversion analysis for a two-layer structure model of the basement and the sedimentary layer.
The inversion analysis revealed the following characteristics of the basement depth distribution off the west coast of the Noto Peninsula. There is a thick sedimentary layer on the west side of the eastern flexure off Hakui and on the west side of the flexure northwest to the eastern flexure. The southern end of the fault along the eastern flexure off Hakui corresponds to a shallow basement extending west from Mt. Hodatsu. The northern end corresponds to the deep basement south of the Amamisaki fault zone. For the western side of the eastern flexure off Hakui, the basement depth is large on the uplift-side. This suggests that the eastern flexure off Hakui is formed by inversion tectonics associated with the change from an extension to a compression field related to the Japan Sea opening.

Keywords: gravity anomaly, basement structure, acoustic survey

©2020. Japan Geoscience Union. All Right Reserved.

Study of subsurface and geological structure around the Togi-gawa Nangan Fault based on integrated analysis of seismic reflection method and gravity exploration

*Wataru Kobayashi[1], Masaaki Hamada[1], Yasuhisa Tanaka[2], Shinji Kawasaki[2], Takuya Murakami[3], Manabu Sakashita[3], Akihiro Sawada[4], Yoshihiro Hiramatsu[4]

1. Hokuriku Electric Power Company, 2. JGI, Inc., 3. DIA Consultants, 4. Kanazawa Univ.

The Togi-gawa Nangan Fault is a 2 km fault with NW-SE strike and uplift on the south-eastern side distributed along the boundary of the mountain and plain along the Togi River, in the Miocene volcanic rock area in the western coast of Noto Peninsula, central Japan, which was reported by Active Fault Research Group (1991). Recently, Imaizumi et al. (2018) suggested that the fault is an estimated active fault of approximately 6 km in length accompanied by right-lateral offset streams. Hiramatsu et al. (2019) conducted an analysis using gravity anomaly, gravity gradient tensor, and two-dimensional Talwani's method (Talwani, 1959) around the fault and revealed that it is a reverse fault dipping 45°–60° to the southeast, and the spatial extent of the fault structure is comparable to the total length of the surface trace of the fault proposed by Imaizumi et al. (2018). In this study, we conducted a borehole and seismic reflection survey around the Togi-gawa Nangan Fault and performed an integrated analysis of the reflection and gravity data of Hiramatsu et al. (2019) to reveal the fault geometry and subsurface and geological structure around the fault.

A borehole survey of 200 m depth was conducted at approximately 50 m southeast of the geomorphologically estimated fault trace. The fault fracture zone within the andesite was penetrated from 134.5 to 135.1 m in depth. It was mainly composed of non-cohesive fine materials with clasts of 0.2–10 cm in diameter and contained a slip surface with slickenside and steeply pitching striation. Reverse fault movement was estimated by the preferred orientation of fragments and the drag of distinct colored muddy layers in the fracture zone. These features indicated that the fault fracture zone is related to the Togi-gawa Nangan Fault estimated by the geomorphic signatures.

A seismic reflection survey was conducted on a 7 km survey line across the Togi-gawa Nangan Fault zone. We deployed 276 seismometers every 25 m on the survey line, and two large vibroseis vehicles shot at every 50 m on the line. The seismic data were processed to obtain reflection seismic profiles. We applied the MDRS (multi-dip reflection surface; Aoki et al., 2010) and CWT (continuous wavelet transform) method to enhance CMP (common mid-point) reflection stacking in the volcanic rock area. The MDRS method produced continuous reflection surfaces in the shallow part and clearly delineated anticlines. The CWT method produced high-resolution reflection surfaces and discontinuities. We delineated seismic discontinuities interpreted as a seismic fault plane having a 50°–60° dip toward south, which is located in the extension of the fault observed in the borehole survey. Furthermore, we applied the refraction tomography method using the first breaks picked from refracted waves. We used the Monte Carlo reliability method for tomographic inversion, which contains randomly produced many initial models to reduce the effect of the dependency on initial models. The tomographic inversion result shows a high velocity zone in the middle of the survey line, which is located on the hanging wall block of the fault.

We calculated the Bouguer gravity anomaly by Talwani's method, using the subsurface density structure determined from the interpretation of the seismic reflection survey. Following Hiramatsu et al. (2019), the

©2020. Japan Geoscience Union. All Right Reserved.

layer densities were set as 1700 kg/m^3, 2300 kg/m^3 and 2650 kg/m^3 from the upper to lower layers, respectively. A layer of 2650 kg/m^3 was assumed to be up-heaved on the hanging wall of the 50˚–60˚ southeast dipping fault plane. As a result, the calculated Bouguer anomalies were substantially comparable with the observed anomalies.
From the results, we concluded that the Togi–gawa Nangan Fault is a steeply southeast dipping reverse fault with an up-heaved and high-density part on its hanging wall.

Keywords: Seismic reflection survey, MDRS method, Gravity survey, Two dimentional Talwani's method, Reverse fault

©2020. Japan Geoscience Union. All Right Reserved.

[J] Poster | S (Solid Earth Sciences)：S-SS Seismology

[S-SS12] Seismic wave propagation: Theory and Application

convener:Kiwamu Nishida(Earthquake Research Institute, University of Tokyo), Kazuya Shiraishi(Japan Agency for Marine-Earth Science and Technology), Takao Nibe(JAPEX), Kaoru Sawazaki(National Research Institute for Earth Science and Disaster Resilience)

Seismic wave propagation provides rich information on earth's heterogeneities and the excitation sources. In order to extract the information, integrated studies are needed among mathematical/numerical studies based on the wave theory, miniature physical experiments using rock specimens, and practical data analyses. Furthermore, it is greatly beneficial to conduct comparative studies of various kinds of waves, such as elastic, acoustic, traveling ionospheric disturbances, and oceanic waves. This session widely invites presentations about the theories and applications related to seismic and other geophysical waves.

[SSS12-P01] Oscillations and traveling perturbations observed from ground to the ionosphere after the 2011 Mw9.0 Tohoku earthquake

*Xiangxiang Yan[1], Yang-Yi Sun[1] (1.Institute of Geophysics and Geomatics, China University of Geosciences)

[SSS12-P02] Waveform feature extraction and similar waveform detection by Locality Sensitive Hashing

*KOMAGATA Ryota[1], Shiro Hirano[1], Hironori Kawakata[1], Makoto Naoi[2] (1.Ritsumeikan University, 2.Kyoto University)

[SSS12-P03] Separation of the temporal variation of the ACROSS signal using independent component analysis

*rina suzuki[1], Koshun Yamaoka[2] (1.Graduate School of Environmental Studies, Nagoya University, 2.Earthquake and Volcano Research Center, Graduate School of Environmental Studies, Nagoya University)

[SSS12-P04] Performance evaluation of methods to estimate temporal changes in attenuation property using active sources

*Shuhei Tsuji[1], Koshun Yamaoka[1], Ryoya Ikuta[2] (1.Graduate School of Environmental Studies, Nagoya University, 2.Faculty of Science, Shizuoka University)

[SSS12-P05] Review and preview of artificial seismic sources of ACROSS

*Koshun Yamaoka[1] (1.Earthquake and Volcano Research Center, Graduate School of Environmental Studies, Nagoya University)

[SSS12-P06] Repeated noises of 7-15 second interval in the seismograms recorded at the seashore landslide

*Issei Doi[1], Sumio Matsuura[1], Hikaru Osawa[3], Tatsuya Shibasaki[2], Shinichi Tosa[2] (1.Disaster Prevention Research Institute, Kyoto University, Japan, 2.Japan Conservation Co. Ltd., 3.Mountain Science Center, University of Tsukuba, Japan)

[SSS12-P07] Towards the detection of the mantle-reflected P wave

*Shota Kato[1], Kiwamu Nishida[1] (1.ERI, University of Tokyo)

[SSS12-P08] Retrieving reflection waves from the Philippine Sea plate boundary using seismic interferometry with the PKIKP phases

*Toshiki Watanabe[1], Naoki Sogawa[1] (1.Graduate School of Environmental Studies, Nagoya University)

[SSS12-P10] **Site classification of recording stations of EEW System for Garhwal region of Uttarakhand, India**

*Pankaj Kumar[1], Ashok Kumar[1], Ajay Gairola[1], Kamal .[1] (1.Indian Institute of Technology Roorkee, India)

[SSS12-P12] Passive seismic imaging of crustal structures: numerical study on acoustic and elastic reverse time migration

*Kazuya Shiraishi[1], Toshiki Watanabe[2] (1.Japan Agency for Marine-Earth Science and Technology, 2.Nagoya University)

[SSS12-P13] Analytical solution of near-field term, intermediate term, far-filed term, and quasi-static displacement due to rectangular fault in a homogeneous whole space

*Kotaro Tarumi[1], Hiroshi Takenaka[1] (1.Okayama University)

[SSS12-P14] Characteristics of teleseismic S-wave response of the Kanto sedimentary basin inferred from dense seismic observation and numerical simulation

*Yue Nakagawa[1], Kazuo Yoshimoto[1], Shunsuke Takemura[2] (1.Yokohama City University, 2.Earthquake Research Institute, the University of Tokyo)

[SSS12-P15] A numerical study on P-wave travel time fluctuation and amplitude fluctuation in the short-wavelength inhomogeneous crustal structure

*Kazuo Yoshimoto[1], Shunsuke Takemura[2] (1.Graduate School of Nanobioscience, Yokohama City University, 2.Earthquake Research Institute, the University of Tokyo)

[SSS12-P16] **Seismic body wave attenuation characteristics within the heterogeneous crust of Northeast India**

*Rabin Das[1], Sagarika Mukhopadhyay[1] (1.Department of Earth Sciences, Indian Institute of Technology Roorkee, Roorkee- 247667, India)

[SSS12-P17] Trans-dimensional imaging or random inhomogeneities at northern Ryukyu arc with a non-diagonal covariance matrix

*Tsutomu Takahashi[1], Yojiro Yamamoto[1], Yasushi Ishihara[1], Koichiro Obana[1], Seiichi Miura[1], Shuichi Kodaira[1], Yoshiyuki Kaneda[2] (1.Japan Agency for Marine-Earth Science and Technology, 2.Kagawa Univ.)

[SSS12-P18] Propagation characteristics of two-dimensional scalar waves in alternating layered structures

*Kazuki Kidoguchi[1], Jun Kawahara[1] (1.Graduate School of Science and Engineering, Ibaraki University)

[SSS12-P19] Angular distribution of energy fluxes of seismic waves in two-dimensional random heterogeneous media

*Kentaro Emoto[1] (1.Graduate School of Science, Tohokuk University)

Oscillations and traveling perturbations observed from ground to the ionosphere after the 2011 Mw9.0 Tohoku earthquake

*Xiangxiang Yan[1], Yang-Yi Sun[1]

1. Institute of Geophysics and Geomatics, China University of Geosciences

This study examined the multi-source data including seismometers, COSMIC radio occultation (RO) soundings of refractivity index (RI) in the lower atmosphere (from 0 to 60 km) and total electron content (TEC) in the ionosphere (from 150 to 550 km), as well as ground-based GNSS TEC after/during the 2011 Mw9.0 Tohoku earthquake/tsunami. The horizontal propagation characteristics of the seismo-traveling ionospheric disturbances were identified combining the seismometers and ground-based GNSS TEC data. The post-seismic ionospheric infrasound and gravity wavefronts were vertically scanned by individual RO TEC profiles. The traveling perturbations indicates that earthquake/tsunami can induce atmospheric acoustic-gravity waves in the Earth’ s upper atmosphere and ionosphere. On the other hand, the RI observations show the first evidence of the Tohoku earthquake/tsunami-induced vertical oscillations in the lower atmosphere. In addition, acoustic resonant oscillations are recorded in ionosphere by ground-based GNSS TEC after Tohoku earthquake, and the spectra are corresponding to the fundamental and harmonic of the atmospheric trapped acoustic modes, which are explained by the normal mode simulation and substantiated using ground seismic data. The study suggests that the coupling between the solid Earth and the atmosphere can excite both the traveling perturbations and harmonic motions from ground to the ionosphere.

Keywords: Tohoku earthquake, oscillations, vertical structure, traveling ionospheric disturbances, radio occultation

©2020. Japan Geoscience Union. All Right Reserved.

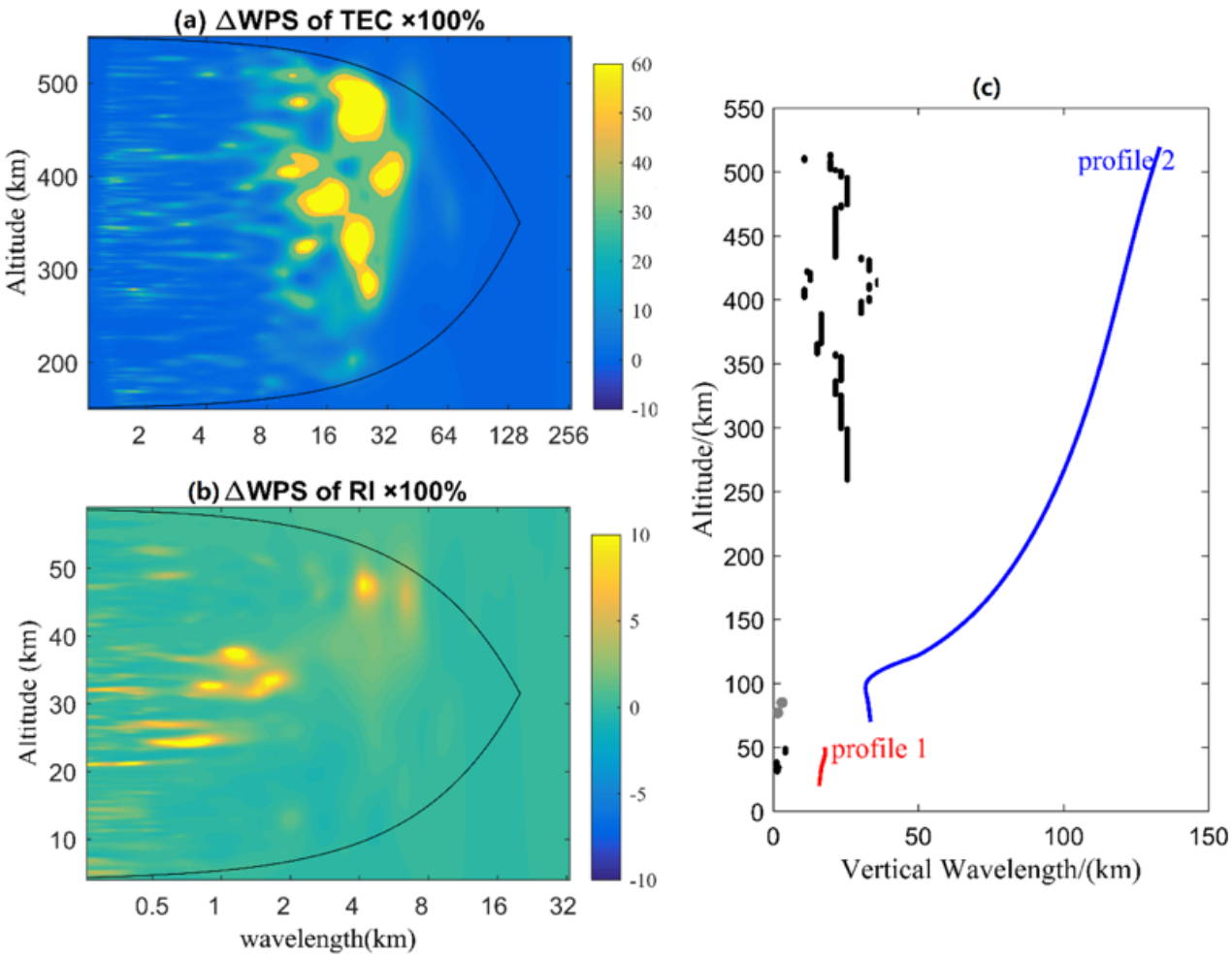

©2020. Japan Geoscience Union. All Right Reserved.

Waveform feature extraction and similar waveform detection by Locality Sensitive Hashing

*KOMAGATA Ryota[1], Shiro Hirano[1], Hironori Kawakata[1], Makoto Naoi[2]

1. Ritsumeikan University, 2. Kyoto University

Even tiny waveforms due to uncataloged earthquakes inform us of the characteristics of an earthquake source, seismic activity, and underground structures. A frequently used method to detect them is the template matching based on a correlation coefficient (CC) among known templates and continuous waveforms (e.g., Doi & Kawakata, 2012; Kato *et al.*, 2012), which is nothing but to find lookalikes of known waveforms. However, if possible, a similarity analysis among all pieces out of the continuous waveforms may enable us to detect more seismic waveforms due to small events.

In this study, we focused on a hashing method without templates to detect similar waveform pairs quickly. Yoon *et al.* (2015) proposed a similar waveform detection method called Fingerprint and Similarity Thresholding (FAST) using Fingerprinting, which is a kind of Locality Sensitive Hashing (LSH) and based on Waveprint proposed for voice search by Baluja & Covell (2008). FAST consists mainly of two components: extraction of waveform features based on an LSH hash function and similarity search based on approximation of the Jaccard coefficient, which is the similarity between the hash values of two waveforms. By using Fingerprinting, many pairs of similar and uncataloged small waveforms can be found. However, FAST needs complicated processing such as spectrogram calculation and a wavelet transform. Thus we proposed two new hash functions with fewer procedures and detected similar waveform pairs by using them and FAST. We compared the performance focusing on the relationship between the similarity of the detected pairs and the CC value and runtime.

Considering that the amplitude of the seismic waveform generally has higher amplitudes than that of the surrounding microtremors, we designed two time-domain hash functions: 2bit-aHash, modified from aHash for image detection by Fei *et al.* (2015) and *k*Hash, a novel method we proposed in this study. 2bit-aHash assigns binaries of "10" and "01" to each sample of a waveform above and below 1 σ, respectively, deviating from the moving averaged continuous waveform , and assigns "00" to the others. *k* Hash assigns binaries "10" and "01" to the top-*k*% amplitudes of the absolute value in the 5-seconds waveform window depending on the sign (i.e., "10" and "01" for the positive and negative outliers, respectively) and assigns "00" to the others.

We analyzed a 24-hours continuous velocity seismogram of the Hi-net Matsumoto Wada station, Japan, of June 29-30, 2011, where an *M*5.4 earthquake and its fore- and aftershocks occurred. As a result, the employment of 2bit-aHash and *k*Hash succeeded in detecting uncataloged similar seismic signal-like waveform pairs. For 2bit-aHash and *k*Hash, each pair showed high CC values, and we observed a good correlation between the similarity and the CC values, which was absent in the case of FAST despite its complicated processing. Also, the overall runtime of both 2bit-aHash and *k*Hash was about 4 to 5 times shorter than FAST, which is not only because their feature extraction is straightforward but also because the similarity search based on them was several tens times faster than FAST. The runtime of similarity search approaches $O(n^2)$ when the data length n becomes very long, so 2bit-aHash and *k*Hash may contribute to a significant improvement in the runtime of similarity searches. In the similarity search, 2bit-aHash and *k*Hash yields extremely low Jaccard coefficients for pairs including noise, which enables to delete dissimilar pairs efficiently from the database that holds many candidates of pairs based on the

©2020. Japan Geoscience Union. All Right Reserved.

Jaccard coefficients, while FAST still holds an enormous amount of noise-noise and signal-noise pairs as candidates. Given the above features, the novel two functions, 2bit-aHash and *k*Hash, have shorter runtime than FAST not only for feature extraction but also for similarity search and have higher CC values between the detected waveform pairs.

Keywords: Earthquake event detection, Waveform similarity, Similarity search, Hash method

©2020. Japan Geoscience Union. All Right Reserved.

Separation of the temporal variation of the ACROSS signal using independent component analysis

*rina suzuki[1], Koshun Yamaoka[2]

1. Graduate School of Environmental Studies, Nagoya University, 2. Earthquake and Volcano Research Center, Graduate School of Environmental Studies, Nagoya University

Transfer functions of the artificial seismic source ACROSS change due to various effects such as stress change before and after earthquakes, barometric pressure, and precipitation. Since the observed temporal variations are influenced by various factors, it is important to separate variations by various factors.

In this study, we performed independent component analysis (ICA) to extract independent variations from the observed transfer function. ICA is a method of extracting statistically independent signal from the records in which multiple signals are mixed. The mixed signal needs to be a linear addition of multiple signals. Assuming that the observed temporal variation of transfer function is a linear addition of independent variations due to several factors, we can extract each variation by ICA.

In this study, we used the ACROSS source installed at Mikawa Observatory of Nagoya University in Toyohashi City, Aichi Prefecture. We used fourteen-month long data for monitoring temporal variation of transfer function at stations around the source. There are six components in the transfer function: up-down, north-west, and east-west components by vertical excitation (Uv, Nv, and Ev component) and those components by horizontal excitation (Uh, Nh, and Eh component). For analysis, we used the transfer function in the frequency domain. We performed preprocessing in which data whitening and dimension compression are made. Data whitening maximizes the performance of signal separation by ICA. Dimension compression is made by principal component analysis to reduce noise that may be included less important components. We applied ICA to the preprocessed transfer function and succeeded to obtain five independent components. Among many methods of ICA, we adopted AMUSE method that is often applied to time series signals.

As a result, we obtained independent components with annual and biannual variations and short-term changes. These independent components were correlated with different kinds of fluid movement, such as ground water level change and rainfall.

Keywords: Artificial source, Seismic wave, Independent component analysis

©2020. Japan Geoscience Union. All Right Reserved.

Performance evaluation of methods to estimate temporal changes in attenuation property using active sources

*Shuhei Tsuji[1], Koshun Yamaoka[1], Ryoya Ikuta[2]

1. Graduate School of Environmental Studies, Nagoya University, 2. Faculty of Science, Shizuoka University

We compare the ability of two methods which are developed for estimating temporal changes in attenuation using signals generated by an artificial seismic source, ACROSS.

Temporal changes in attenuation have not been studied well, probably due to lack of useful methods to detect the change. A lot of studies are reported on temporal changes in travel time all over the world and some of the proposed mechanisms have been suggested on attenuation change. Thus, development of a suitable method on temporal changes in attenuation will contribute to the related study all over the world.

We used an artificial seismic source, ACROSS, to detect temporal changes in attenuation. To find the temporal change in attenuation of a medium, stability of the source is necessary to avoid fake change due to the source instability. ACROSS can excite same signals continuously because it generates seismic waves by rotating eccentric mass under precise phase control. Temporal changes in noise level should also be considered because it may cause fake changes in amplitude. In the ACROSS measurement, noise level is also measurable because frequencies of exciting signals are known. The noise level can be used for estimating the amplitude variation in the following processes.

We developed two methods to estimate temporal changes in attenuation using ACROSS. One method is "simultaneous estimation" (Tsuji et al, 2019, JpGU Meeting), and the other is a method based on wave energy of the signals, named “energy-based estimation”. The simultaneous estimation is a method to estimate variation in travel time and amplitude simultaneously by fitting transfer functions with a specific model in a complex plane. The best-fit parameters are looked for with maximum likelihood method so that minimize square of the length in the complex plane. The energy-based method calculates deviation of energy of transfer functions by reducing the noise energy that is estimated simply by the signal design of ACROSS system.

To assess the performance of the two methods, we applied the methods to a synthetic data in which Gaussian noise of various amplitudes is added to a signal. We compared amplitudes that are estimated with the two methods for the synthetic data. As a result, the simultaneous estimation could estimate smaller variations in amplitude than the energy-based method under a condition of a constant noise level. However, a bias due to noise level is found for the simultaneous estimation. This means results with the simultaneous estimation may contain fake change due to changes in noise level.

Next, we applied the two methods for in-situ data and compared the results. We test the data observed in an ACROSS experiment at Awaji Island that was conducted between January 2000 and April 2001 (Ikuta et al., 2002; Ikuta and Yamaoka, 2004). The previous studies reported sudden delays in travel time in P and S phases at the time of the earthquakes. The amplitude also dropped at the earthquake with a difference between the two methods. The variation with the simultaneous estimation is smaller than that with the energy-based estimation (blue dots of figure) for 1700m borehole seismometer. It may be caused by a difference in noise level between 800m and 1700m sensors. Based on the synthetic test, the simultaneous estimation could work stably in noisy conditions though a bias appears.

©2020. Japan Geoscience Union. All Right Reserved.

Considering the results, the simultaneous estimation is better if the bias due to noise could estimate. Now we are updating the simultaneous estimation by developing a method to estimate the bias. We will show the result in our poster.

Figure Caption:
Variation in amplitude with the simultaneous estimation (left sides) and the energy-based estimation (right sides). Each figure shows one week before and after the occurrence of the 2000 Western Tottori earthquake. Each row shows UD (top), NS (middle) and EW (bottom) component of the sensors at 800m (red) and 1700m (blue) deep.

Keywords: active source, attenuation, ACROSS, Temporal variation

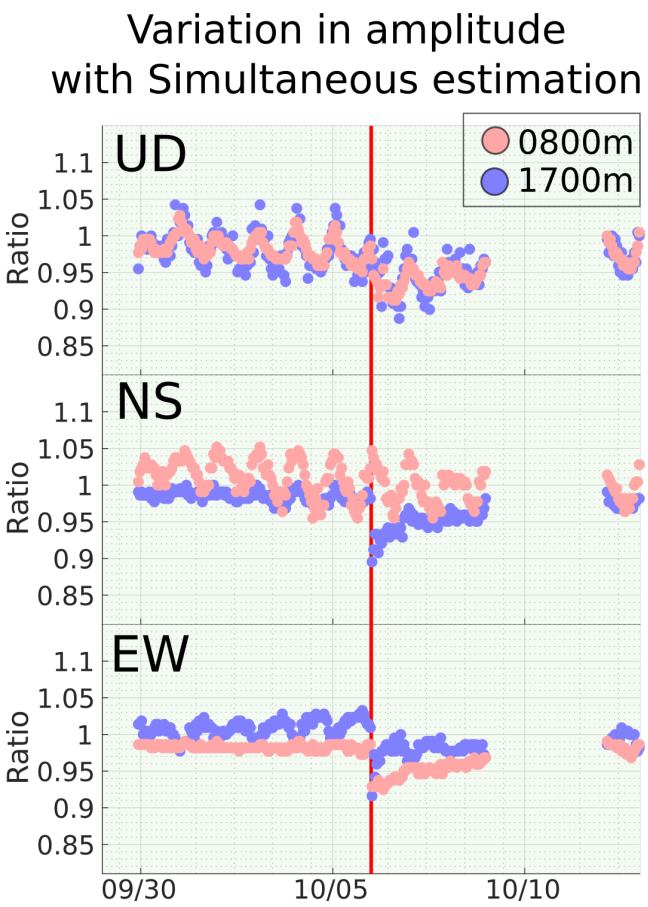

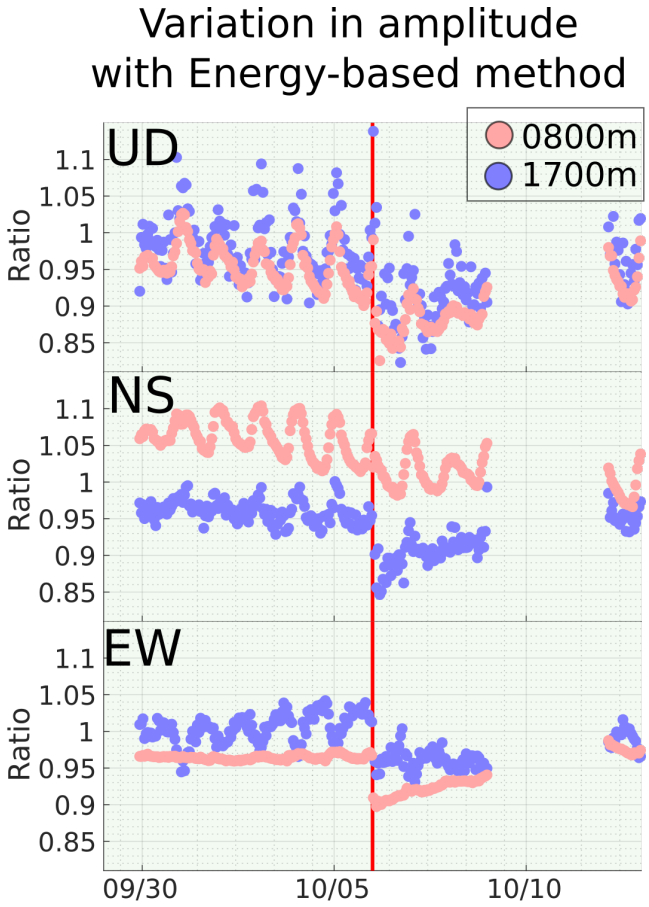

©2020. Japan Geoscience Union. All Right Reserved.

Review and preview of artificial seismic sources of ACROSS

*Koshun Yamaoka[1]

1. Earthquake and Volcano Research Center, Graduate School of Environmental Studies, Nagoya University

Since ACROSS (Accurately-Controlled Routine-Operated Signal System) was proposed, many type of seismic vibrator based on the concept of ACROSS. The following vibrators are representative ones actually used for the research for monitoring the temporal change in the subsurface structure, in which fundamental concept on technical aspect is data stacking with the ability of accurate synchronization between source and receivers.

1) Proto-type ACROSS was created as a rotary source of a laboratory scale in 1994 and was deployed in the campus of Nagoya University. The data stacking is established with synchronization by radio and/or line telemetry.
2) Type-1996 vibrator was created as a first model for practical use, which were deployed in two test site in Awaji island and Toki, Gifu prefecture. It produces 20 tons of sinusoidal force with 25, 35 and 50Hz. As the force is proportional to the square of rotation velocity vibrators of different eccentric moment were made to cover wide frequency range. This type has already removed from the site and stored in Takayama observatory for future usage. (Ikuta et al. 2002, GRL)
3) Type-1999 vibrator was created with similar concept of Type-1996 but without water-cooling circuit, which are deployed in Sakurajima volcano and Toyohashi, Aichi. It can produce 10tons at 20Hz for one unit and is designed to be operated with several units. It was being operated in Toyohashi in more than 10 years. (Yamaoka et al. 2014, EPS)
4) Type-2004 vibrator was created for producing large force in lower frequency range than before. It can produce 20tons at 7.5Hz. It is deployed in Morimachi, Shizuoka and are used to monitor secular change in seismic velocity in this area (Tsuji et al. 2018, EPS).
5) Type-2011 vibrator to produce 40 tons at 50Hz was designed and produced. One is now deployed by JOGMEC in Aquistore project in Canada. Horizontal deployment is regarded as essential in this vibrator to produce P wave efficiently. It is designed, in contrast to the
6) Type 1996, to produce wide frequency range upto 50 Hz with one unit. (See Kasahara and Hasada (2016) published from Gulf Professional Publishing) Type-2014 vibrator was designed to reduce the production and deployment cost of previous ACROSS vibrators, which is a main obstacle to be used. This type is deployed in Toyohashi, Aichi. Small bearing, horizontal emplacement, simple basement and standard unit configuration reduced the initial introduction cost. This new type ACROSS vibrator has been operated without trouble for more than two years now. The same type vibrator is deployed in Kuju, Oita by Kyushu University.
Operation methodologies of ACROSS vibrator were developed in early years of ACROSS development (Kumazawa et al. 2007, JAEA-Research). FM operation and switching operation system were developed and used as a fundamental operation system. The design of the system is based on the technology in 20 years ago, therefore, up-to-date technology is now being employed to reduce the complexity and resultant cost of the system, which will be used in size independent source system or multiple-source operation.

Keywords: artificial source, temporal variation

©2020. Japan Geoscience Union. All Right Reserved.

Repeated noises of 7-15 second interval in the seismograms recorded at the seashore landslide

*Issei Doi[1], Sumio Matsuura[1], Hikaru Osawa[3], Tatsuya Shibasaki[2], Shinichi Tosa[2]

1. Disaster Prevention Research Institute, Kyoto University, Japan, 2. Japan Conservation Co. Ltd., 3. Mountain Science Center, University of Tsukuba, Japan

In recent days, seismic noises are used to estimate subsurface structure and to detect its temporal changes in the methods such as seismic interferometry. It is important to know the characteristics and the generation mechanisms of seismic noises in order to precisely interpret the results for natural phenomena.

We used the seismic data recorded at the station on the seashore landslide in southeastern Hokkaido, Japan. In the seismograms, repeated noises of 7-15 second interval were intermittently found. In order to know the generation mechanisms of these repeated noises, we firstly tried to automatically detect them as follows. 1) We calculated the three-dimensionally synthesized waveform with the length of one hour. 2) We calculated the average of the amplitude of synthesized waveform every one second and obtained its distribution. 3) Fitting the distribution to Gumbel one, we recognized the repeated noise occurence for the waveform with the scale parameter larger than 0.2 empirically. Comparing the timing of the repeated noise occurence and the tide height, it was found that the repeated noises were found mainly at high tide.

©2020. Japan Geoscience Union. All Right Reserved.

Towards the detection of the mantle-reflected P wave

*Shota Kato[1], Kiwamu Nishida[1]

1. ERI, University of Tokyo

The seismic interferometry is the technique which extracts the Green’s function between a station pair by calculating the cross-correlation function (CCF) of random wavefield in a pair of station (e.g. Snieder et al., 2013). The seismic interferometry requires the isotropic and homogeneous source distribution. A microseism, which is excited by ocean swell activities, is a typical example of a random wavefield. Because a microseism is dominated by the surface wave, the seismic interferometry of microseism is suitable for estimating the velocity structure of the crust and upper mantle (e.g. Shapiro et al., 2005). However, recent studies tried to extract the body wave as well as the surface wave by the seismic interferometry. For example, some groups reported reflected P wave at the 410/660 km discontinuities (P410P/P660P) (Poli et al., 2012, Feng et al., 2013), though these studies used the continental stations. The purpose of this study is to extract the P410P/P660P and estimate the depth of discontinuities beneath Japan by application of the seismic interferometry to the vertical motion of Hi-sensitivity Seismograph Network Japan (Hi-net).

The procedures of calculation the CCF are as follows: The dataset in this study is the vertical components of 240 Hi-net stations in Southwest Japan (2007-2018). We down-sampled the original 100 Hz data to 2 Hz. We took the difference between waveforms on two successive days at the same station instead of using the original waveform to suppress the effect of the logger noise (Takagi et al., 2015) on the CCF (Takagi et al., 2019). Next, the 1-day-length waveform was split into 1024-second-length segments, and selected based on the mean square amplitude in 0.05-0.1 Hz and 0.1-0.2 Hz. Then, we calculated CCFs for every pair of station by stacking over all the selected segments with spectral whitening from 0.1 to 1.0 Hz.

Then we calculated the 4th root vespagram (Rost and Thomas 2002) using the CCFs. The vespagram showed the P410P in the 0-300 km offset and the P660P in the 50-100 km offset, with P660P weaker than P410P.

Finally, we applied the Common Middle Point (CMP) stacking to estimate the depth of discontinuity from the extracted P wave (e.g. Stein and Wysession, 2003). Station pairs with the shorter offset than 500 km were categorized into groups according to the location of the reflection point. We applied the CMP stacking with a reference model (JMA2001, Ueno et al., 2002) for each group assuming that the discontinuity depth is constant within the group. We estimated the 410 km discontinuity only, and found the lateral variation on the depth of discontinuity, especially the elevation in the group whose reflection points in 33˚-36˚N 134˚-135˚E. The pattern of the discontinuity depth is consistent with those of previous studies using earthquakes (Tonegawa et al., 2005, Tono et al., 2005).

We estimated the depth of 410 km discontinuity beneath Southwest Japan by the seismic interferometry in this study. In future studies, we will expand the study area to Northeast Japan and will estimate the depth of 660 km discontinuity.

Keywords: seismic interferometry

©2020. Japan Geoscience Union. All Right Reserved.

©2020. Japan Geoscience Union. All Right Reserved.

Retrieving reflection waves from the Philippine Sea plate boundary using seismic interferometry with the PKIKP phases

*Toshiki Watanabe[1], Naoki Sogawa[1]

1. Graduate School of Environmental Studies, Nagoya University

In the Chugoku-Shikoku region of southwestern Japan, associated with the subducting Philippine Sea plate, locked, transitional and steady-slip zones are distributed according to the depth (Obara and Kato, 2016). Various seismic phenomena occurs including slow-slips and deep low-frequency tremors. They are thought to be due to the nature and state of the plate interface. Seismic surveys have suggested a relationship between the state of the plate interface and the amplitude of reflected seismic waves (e.g. Fujie et al., 2002, Sato et al., 2006). Laboratory experiments showed a relationship between the frictional intensity at the interface and the amplitude of the transmitted wave (Nagata et al., 2008). In this study, the reflection waves at the plate boundary were retrieved from the seismic waveform observed at the stationary seismic stations. Then, the spatial distribution of the reflection amplitude on the plate boundary was estimated.

We used seismic interferometry (autocorrelation analysis) to retrieve the reflected waves at the plate boundary from the natural seismic waves. In a one-dimensional wave field, the autocorrelation of a seismic record observed at a single station on surface is equal to the reflected wave response from the virtual source at the station (Claerbout, 1968). In the Chugoku and Shikoku regions, since there are few deep earthquakes below the plate boundary, we used the PKIKP phase which is regarded as a plane wave with a near-vertical incident angle (Ruigrok and Wapenaar, 2012).

From the seismic records of 119 Hi-net stations and 10 F-net stations in the study area observed from 2006 to 2018, 240 earthquakes were found under the condition that the epicenter distance was 140 to 180 (deg) and that the magnitude (Mw) was 6 or more. Among them, 16 events records with high S/N without phases such as PKP and PKiKP were used for analysis. After applying a bandpass filter of 0.1 to 4.0 Hz, the autocorrelation was calculated. The deconvolution was performed to remove the influence of the incident waveform. Then the autocorrelations were stacked for each station. Inelastic attenuation was corrected using the Q-value after Salah and Zhao (2003). Depth conversion was performed using the velocity structure using JMA2001 and the 3-D seismic velocity structure (Matsubara et al., 2019).

In the reflection depth profile, laterally-continuous reflected waves with positive amplitude were recognized which correspond to the Moho (Shiomi et al., 2006) and the upper limit of the hypocenter distribution in the slab. We interpreted them as a oceanic Moho. In the Chugoku region, positive amplitudes corresponding to the land Moho (Shiomi et al., 2006) were also observed. Although not as clear as the oceanic Moho, negative amplitudes were observed that may corresponded to the Philippine Sea plate boundary estimated by Hirose et al. (2008) and Iwasaki et al. (2015) The spatial distribution of the amplitude of the reflected wave, which was interpreted as the plate boundary, shows variation at the same depth. The amplitude decreased with increasing the depth of the plate boundary. There did not seem no clear tendency that the reflected wave amplitude increased in the transition and steady-slip zone compared to the locked zone. In the tremor region, the reflected wave amplitude was large in western Shikoku.

©2020. Japan Geoscience Union. All Right Reserved.

Keywords: Plate boundary, reflected wave

©2020. Japan Geoscience Union. All Right Reserved.

Site classification of recording stations of EEW System for Garhwal region of Uttarakhand, India

*Pankaj Kumar[1], Ashok Kumar[1], Ajay Gairola[1], Kamal .[1]

1. Indian Institute of Technology Roorkee, India

In the present study, site classification study of the 84 stations where accelerometers have been installed in the field, has been carried out. These accelerometers are instrumented in the field as part of Earthquake Early Warning System for Uttarakhand, a province of India. Horizontal to vertical spectral ratio (HVSR) of recorded strong ground motion of earthquakes of *Mw* 2.8 to 7.5 has been carried out to find out the natural period of the ground at the site. Four classification methods have been applied for classification. In the first method, HVSR of Fourier amplitude spectra is performed and natural period corresponding to the HVSR peak is estimated. In the second method 5% damped response spectra is used in HVSR, then the predominant period corresponding to peak of curve is estimated. The estimated time period from method one and two, is used to classify the sites in the range in with the natural period falls in the standard classification schemes (Building Seismic Safety Council, 2003; Japan Road Association, 1980). In the 3rd method, site classification is done by matching the 5% damped response spectra curve to the standard curve and the site index (SI) is estimated using the method proposed by (Zhao et al., 2006). The 4th method uses the Spearman' s rank correlation coefficient as site classification index (Ghasemi et al., 2009). In method 3rd and 4th, the sites are classified in 4 classes. Out of 84 stations, method 1st categorize 44% station in class - B, 27% stations in class -C, 9% stations in class –D and 10% in class –E, method 2 categorize 36 % stations in class –B, 30% stations in class –C, and 5% stations in class- D and 16% in class –E, method 3 categorizes 75% stations in class –B, 10% stations in class –C and 1% in class –D and 3% in class –E, method 4 categorize 46% stations in class –B, 22% stations in class –C, 11% stations in class –D and 10% stations in class –E. Results from method 1st and 4th are consistent and shows the similarity to the classification. Validation of classification is done with the study of ground response analysis carried by (Pandey, 2018).

Keywords: Site classification, EEW System, HVSR, predominant period

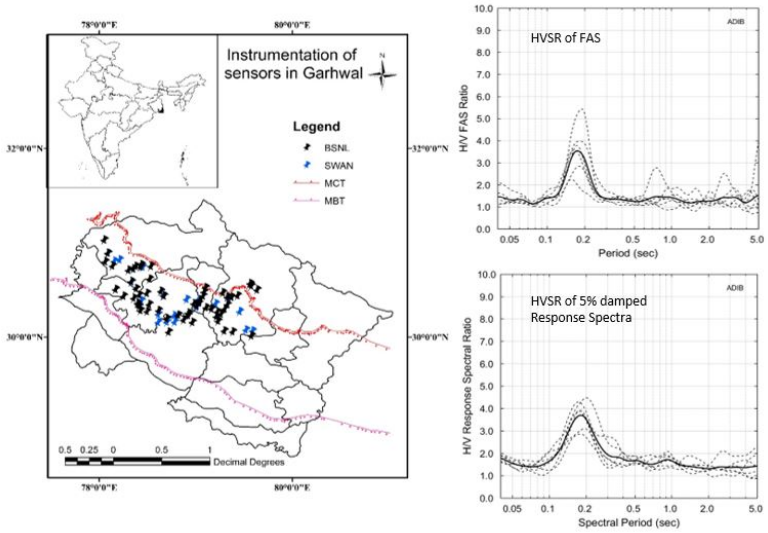

©2020. Japan Geoscience Union. All Right Reserved.

Passive seismic imaging of crustal structures: numerical study on acoustic and elastic reverse time migration

*Kazuya Shiraishi[1], Toshiki Watanabe[2]

1. Japan Agency for Marine-Earth Science and Technology, 2. Nagoya University

Introduction

To image crustal structures from passive seismic data, we propose a reverse-time method using reflection signals in the observed records. We adopted reverse time migration (RTM), which is a powerful technique to image complex structures in active-source seismic imaging, to passive seismic observation. In addition to an acoustic RTM method based on P wave propagation, we developed an elastic RTM method using both P and S waves (Watanabe and Shiraishi, 2019, SEGJ). We conducted numerical study with a regional crustal structure model in SW Japan. The proposed method may become a useful technique for imaging crustal structures and monitoring their conditions from huge amounts of passive seismic data recorded with land-based and offshore seismic station networks and high-dense observation of optic fiber sensing.

Method

We assume a passive observation of seismic waves in the ground: the seismic waves excited at an underground source reflect downward after arriving at one receiver location on the surface, and then reflect upward at the subsurface boundary and arrive at another receiver location. In imaging process from such passive seismic data, we simulate two wavefields, forward in time from one receiver and backward in time from another receiver location, and calculate temporal integration after correlation of the two wavefields of every time step. Stacking the integral results from many records of different sources, we can obtain subsurface images directly from the passive seismic records with undefined source information. In a general acoustic-RTM based on the acoustic wave equation, we deal with only P wave propagation. By adopting elastic wave modeling, we can deal with both P and S wave information in an elastic-RTM. Furthermore, we can obtain two images from P and S waves by means of potential field representation from divergence and rotation computation of the simulated elastic wavefields.

Numerical study

We conducted a numerical study of the proposed method using synthetic data generated with a two-dimensional regional structure model, which was extracted from a plate and crust structure model in SW Japan (Nakanishi et al., 2018). We set a 400-km virtual survey line from Nankai trough off Kumano to Tango Peninsula. We randomly extracted 100 actual sources of local earthquakes from the JMA unified catalog within 35-km range from the survey line, and projected them on the vertical section along the line. We generated synthetic seismic records with 1-Hz dominant frequency using a finite difference method. We compared two observation conditions: ideal dense observation with 400 receivers at 1km intervals, and sparse observation with projected 48 stations to the survey line from Hi-net/F-net/DONET seismic stations within 35-km range from the survey line.

To image the model structures, we applied the acoustic-RTM using only vertical component of the synthetic seismic records and the elastic-RTM using both vertical and horizontal components. In the ideal dense observation, both the acoustic-RTM and elastic-RTM methods can image the subsurface structures. The result from the acoustic RTM, however, shows a degraded image due to S waves in the synthetic records. The elastic RTM with potential representation can overcome this problem by dealing with both P and S waves, and shorter wavelength of S waves than that of P waves is useful for better resolution image in some parts. In the quasi-actual sparse observation, it is difficult to obtain subsurface images by the

©2020. Japan Geoscience Union. All Right Reserved.

present direct imaging approach. In addition to possible illumination improvement by increasing seismic records from different sources, application of compressive sensing may be useful to improve the subsurface images from the actual sparse observation condition.

Acknowledgements
This research is supported by JSPS KAKENHI Kiban-C (JP19K04028). We used information of source location by JMA unified catalog, and seismic stations of Hi-net, F-net, and DONET by NIED.

Keywords: passive seismic imaging, crustal structure, earthquake, reverse time migration, Numerical study

©2020. Japan Geoscience Union. All Right Reserved.

Analytical solution of near-field term, intermediate term, far-filed term, and quasi-static displacement due to rectangular fault in a homogeneous whole space

*Kotaro Tarumi[1], Hiroshi Takenaka[1]

1. Okayama University

Sato (1975, JPE) derived analytical solution on seismic wavefield excited by rectangular fault in whole space, but this solution was not separated into near-field term, intermediate term, far-field term (“separated analytical solution”). The separated analytical solution has not been derived and theoretical analysis on near-field terms (near-field term + intermediate term) has not been performed. The effect of near-field terms or quasi-static deformation nearest fault could be observed at the 2016 Kumamoto earthquake. Here we derived separated analytical solution and investigated the contribution of near-field terms nearest fault with a variety of slip angles. In addition, we derived quasi-static displacements solution in two cases. One of cases is pure quasi-static displacement, the other is quasi-static displacement with S-wave travel time (quasi-static S). Using these analytical solutions, we compared near-field terms with quasi-static displacements.

We consider the fault model which is same as Sato (1975). Rupture front looks like line, whose rupture velocities along strike and dip are constant. Slip time function is ramp function, whose risetime is constant. Here we integrated over strike direction displacement field by point source, near-field term, intermediate term, far-filed term, and quasi-static displacements (e.g. Aki & Richards, 2002).

Fig.1 shows an example of fault model. Numerical calculation setting is P-wave velocity:6.0 km/s, S-wave velocity:3.5 km/s, Length of fault:60 km, Width of fault:15 km, slip amount:2.0m, risetime:2.5 s, slip angle:0˚(strike-slip fault), rupture velocity:2.5 km/s. We consider two cases about the direction of rupture as examples. One of cases (a) is that rupture propagates forward to strike-direction, the other (b) is that rupture propagates upward obliquely. Calculation results are doubled due to the effect of free surface.

Fig.2 shows displacement, near-filed terms, far-field terms and quasi-static displacement in case (a). In case (a), at stations in direction of rupture far-field terms mainly contributes to ground motion in FN component. This shows forward directivity. Near-field terms are not influenced by forward directivity. In case (b), the contribution of far-field terms is nearly equal to that of near-field terms because that of far-field terms becomes smaller than case (a). Quasi-static displacement is different from Near-field terms. In FP component, near-field terms mainly contribute to ground motion in both (a) and (b). Quasi-static displacement is similar to near-field terms compared with FN component and behaviors like ground motion because far-field terms little contributes to ground motion.

Keywords: near-field term, quasi-static displacement, forward directivity, analytical solution, rectangular fault

©2020. Japan Geoscience Union. All Right Reserved.

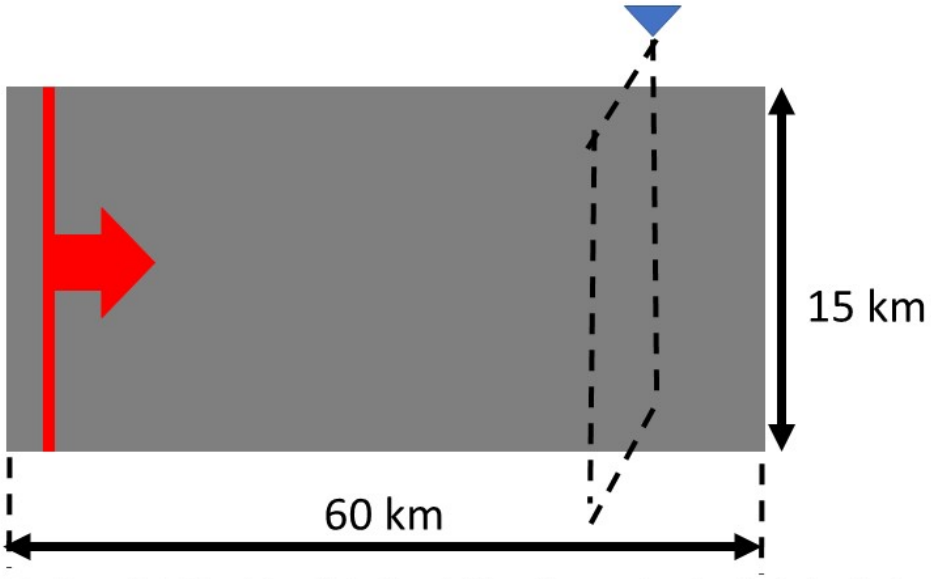

Fig.1 Fault model. Blue triangle is the station. Gray region is whole fault plane. Red line and Vector is rupture front and the direction of rupture.

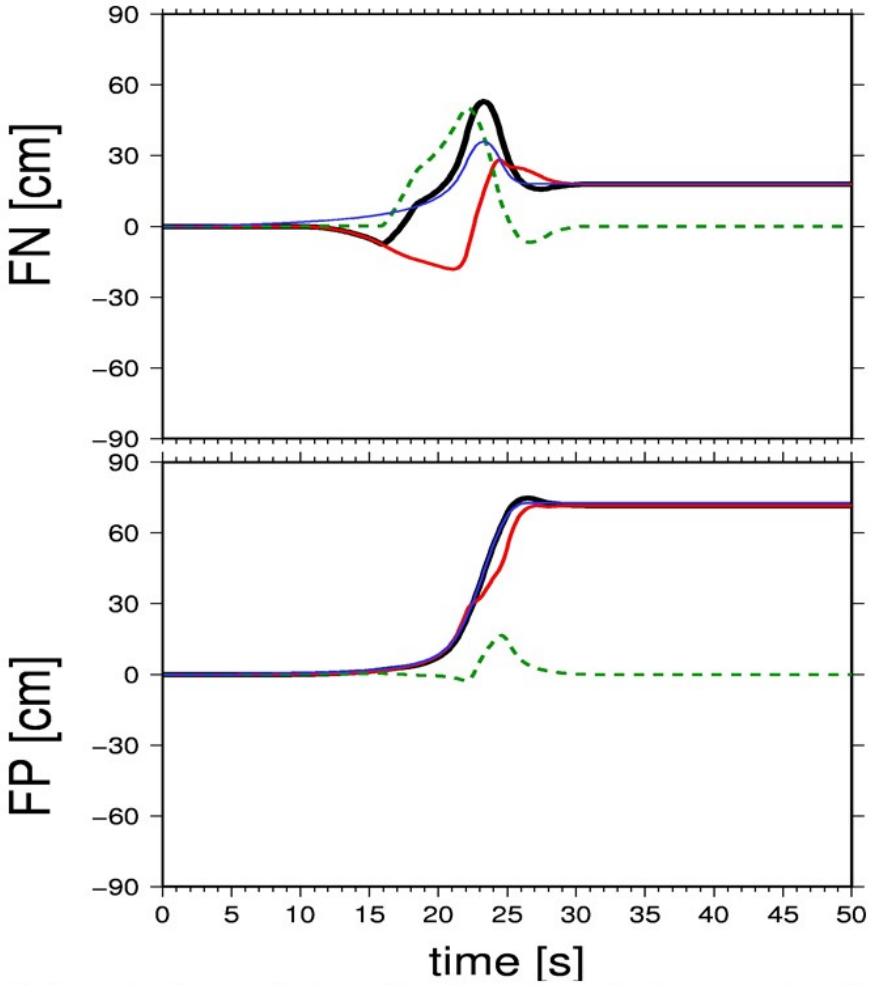

Fig.2 Example of numerical results. . Black line indicates ground motion. Red and green dashed line show near-field terms and far-field terms. Blue line denotes quasi-static deformation.

©2020. Japan Geoscience Union. All Right Reserved.

Characteristics of teleseismic S-wave response of the Kanto sedimentary basin inferred from dense seismic observation and numerical simulation

*Yue Nakagawa[1], Kazuo Yoshimoto[1], Shunsuke Takemura[2]

1. Yokohama City University, 2. Earthquake Research Institute, the University of Tokyo

To investigate characteristics of long-period (> 5 s) ground motions and related structural heterogeneities within the Kanto Basin, we analyzed near-vertical incident teleseismic *S* waves observed at MeSO-net and F-net stations. Comparisons of seismograms between MeSO-net and F-net stations, which are located within/outside the Kanto Basin, allow us to evaluate the long-period (5-20 s) seismic response of the Kanto Basin. Since azimuth and incident angle of teleseismic *S* waves are similar among all stations, differences of observed seismograms at each station could reflect the lateral variation of structural heterogeneities beneath each station.

We selected teleseismic earthquakes with epicentral distances of 30˚-100˚ from the Kanto Basin. We applied a band-pass filter with a passband of 5-20 s to observed seismograms. Seismic energies of direct *S* and later phases were calculated by integrating the three-component squared velocity seismograms for following two time windows; (1) 60 seconds from 10 seconds before the arrival of *S* wave, (2) 50 seconds from 50 seconds after the arrival of *S* wave. First and second time windows are corresponding to those for direct *S* and excited later phases, respectively. To quantify the levels of excited later phases, excitation intensity is calculated by dividing the seismic energy of the later phases by that of the direct waves. We also evaluated the seismic energy ratio between stations within/outside the Kanto Basin. The energy ratio at each MeSO-net station is calculated by dividing the seismic energy at each MeSO-net station by averaged seismic energy of F-net stations. In the case of the *M*w 7.9 Gulf of Alaska earthquake on January 23, 2018, observed seismic energy ratio for horizontal components range 5-20 and excitation intensity exhibits a clear positive correlation with bedrock depth of Koketsu et al. (2012). These results indicate that the later phases are excited by the 3D heterogeneities within the Kanto Basin, such as irregular bedrock topography and complex sedimentary *S*-wave velocity structure.

To explain the observed characteristics of teleseismic *S*-wave response, we conducted FDM simulations using OpenSWPC [Maeda et al. (2017)] and 3D velocity structure model [Koketsu et al. (2012)]. Our simulation model covered a volume of 375×375×250 km^3, which was discretized by a grid interval of 0.25 km. We assumed vertical and inclined incidence of *SH* plane waves. Simulation results roughly explained the observed seismic energy ratio of horizontal ground motions. Simulated excitation intensity increases about 0.1-0.2 per bedrock depth (km). In contrast, simulation results in vertical component did not agree with observed characteristics.

In the presentation, we will discuss a spatial variation of teleseismic *S*-wave response of the Kanto Basin for other teleseismic earthquakes. We will also perform various simulations for *SV*-wave incidence and other teleseismic earthquakes.

Acknowledgment
FDM simulations were conducted on the computer systems of the Earthquake and Volcano Information Center of the Earthquake Research Institute, the University of Tokyo. We used MeSO-net and F-net

©2020. Japan Geoscience Union. All Right Reserved.

continuous seismograms.

Keywords: Kanto sedimentary basin, FDM simulation, Teleseismic earthquake, Long-period ground motion

©2020. Japan Geoscience Union. All Right Reserved.

A numerical study on P-wave travel time fluctuation and amplitude fluctuation in the short-wavelength inhomogeneous crustal structure

*Kazuo Yoshimoto[1], Shunsuke Takemura[2]

1. Graduate School of Nanobioscience, Yokohama City University, 2. Earthquake Research Institute, the University of Tokyo

It is considered that short-wavelength crustal inhomogeneity causes travel time fluctuation and amplitude fluctuation [e.g., Yoshimoto *et al.* (2015)] of high-frequency (> 1 Hz) seismic waves of local earthquakes. However, the characteristics of these phenomena have not yet been fully studied compared to those of teleseismic P-waves [e.g., Butler (1989)]. Thus, we conducted a numerical study on P-wave travel time fluctuation and amplitude fluctuation in the inhomogeneous crustal structure based on 3D FDM simulations.

We conducted 3D FDM simulations for P-wave propagation in different random inhomogeneous media constructed by assuming Birch's law and exponential-type randomness with the correlation distance of 1, 3, and 5 km and the fractional fluctuation of 0.01, 0.02, 0.03, 0.04, and 0.05. Uniform background seismic velocities were assumed to be 6.0 km/s and 3.5 km/s for P wave and S wave, respectively. The medium volume of 204.8×204.8×204.8 km^3 was discretized by a uniform grid spacing of 0.05 km. A double-couple point source of pure strike-slip with an asymmetric cosine source-time function [Ji *et al.* (2003)] with t_s=0.1 s and t_e=0.4 s was set at the center of the model volume. Other technical details are the same as those of Takemura *et al.* (2017). Synthetic velocity seismograms were calculated for stations that were uniformly distributed in the source depth at a grid interval of 2 km. Using simulated seismograms at hypocentral distances less than 60 km, we picked P-wave arrival times (travel times) using an automatic phase-time picker [Maeda (1985)], and measured the maximum amplitudes of filtered seismograms in the passbands of 1-2, 2-4, and 4-8 Hz using a 1 s time window from the P-wave onset. Simulation results show that the travel time fluctuation of P waves increases as the correlation distance and the fractional fluctuation of inhomogeneous media increase. As for the parameter range in our simulations, observed dependency was much more clear for the variation of correlation distance. In the case of our simulation using an inhomogeneous crustal structure model of southwestern Japan [Kobayashi *et al.* (2015); (correlation distance, fractional fluctuation) = (1 km, 0.03)], simulation results showed that travel time fluctuation is about 0.1 s at a hypocentral distance of 50 km. This result implies that the travel time fluctuation due to random inhomogeneity may decrease the accuracy of hypocentral determination of local earthquakes.

Our analysis showed that the travel time fluctuation and the amplitude fluctuation have positive correlation. This indicates that the amplitude of P-waves tends to be small for faster arrival and oppositely to be large for later arrival. This tendency was much clearly observed at low frequencies, and observed for the P-wave propagation in the random inhomogeneous media with large correlation distance and fractional fluctuation. The aforementioned our results imply that velocity perturbation on and around the wave propagation path from the source to receiver affects travel time and also causes focusing and defocusing effects which alter the amplitude of observed P waves.

Acknowledgement

FDM simulations were conducted on the Earth Simulator at the Japan Marine Science and Technology (JAMSTEC). This work was supported by JSPS KAKENHI Grant Number 18K03786.

©2020. Japan Geoscience Union. All Right Reserved.

Keywords: crust, short-wavelength inhomogeneity, P wave, travel time fluctuation, amplitude fluctuation, seismic wave propagation simulation

©2020. Japan Geoscience Union. All Right Reserved.

Seismic body wave attenuation characteristics within the heterogeneous crust of Northeast India

*Rabin Das[1], Sagarika Mukhopadhyay[1]

1. Department of Earth Sciences, Indian Institute of Technology Roorkee, Roorkee- 247667, India

Local earthquakes that occurred during 2011-2013 are used to study body wave attenuation characteristics of Northeast India region. This region is seismically one of the most active zones in the world. The region comprises of tectonically and geologically diverse units like the Eastern Himalayas, Brahmaputra River Basin, Indo-Burma Ranges, Shillong Plateau, and Mikir Hills. The frequency-dependent attenuation of P and S wave has been estimated using the extended coda normalization method. A total of 93 local earthquake waveforms with a magnitude range of 2.8 to 4.5 recorded by the India Meteorological Department (IMD) using six broadband stations were analyzed for this study. The P, S and coda-wave spectra are analyzed for 5 seconds windows at the central frequencies of 1.5, 2, 3, 4, 6, 8, 10 and 12 Hz. Both Qp and Qs values increase with increasing frequency for Northeast India. Qp increases from 50 at 1.5 Hz to 496 at 12 Hz and Qs increases from 116 at 1.5 Hz to 1519 at 12 Hz. The obtained relations for P and S wave are $Qp=31\pm3f^{1.12\pm0.02}$ and $Qs=86\pm12f^{1.16\pm0.06}$. The results obtained for average Qp and Qs in this study show good agreement with those for other studies carried out for tectonically active regions, with high n (~1.0) values and low Q_0 (<200) values, which are characteristic of active regions in terms of seismicity and tectonics. The low values of Qp and Qs obtained for Northeast India and its surroundings correspond to seismically active areas with complex tectonics due to the ongoing underthrusting of the Indian plate below the Himalayas and subduction below the Indo-Burma Ranges that is manifested by the region's high seismicity too. The n values for both Qp and Qs are close to 1 or greater than 1, indicating that the region is highly heterogeneous. Station to station variation in Qp values for Northeast India region, are not exactly similar to that observed for Qs for all frequency range which indicates the presence of high degree of heterogeneities of the subsurface under the study region. The average values of Qs/Qp at different frequencies are greater than 2, which supports this observation.

Keywords: Body wave, Quality factor, Seismic attenuation, Northeast India

©2020. Japan Geoscience Union. All Right Reserved.

Trans-dimensional imaging or random inhomogeneities at northern Ryukyu arc with a non-diagonal covariance matrix

*Tsutomu Takahashi[1], Yojiro Yamamoto[1], Yasushi Ishihara[1], Koichiro Obana[1], Seiichi Miura[1], Shuichi Kodaira[1], Yoshiyuki Kaneda[2]

1. Japan Agency for Marine-Earth Science and Technology, 2. Kagawa Univ.

Crust and uppermost mantle at subduction zones have various structural inhomogeneities over a broad scale range due to accumulations of various tectonic processes such as deformation, faulting, and volcanism. Randomly fluctuating components of velocity inhomogeneity are essential for describing scattered seismic waves at high frequencies (>1 Hz). This study estimated a 3-D spatial variation of random velocity inhomogeneity at northern Ryukyu arc by applying the peak delay time analysis (Takahashi et al. 2013). Study area is off east of Tanegashima and Tokara islands. Seismic waveform data was acquired by a passive survey with 43 short-period ocean bottom seismographs (OBSs) and 4 temporal onshore stations (Yamamoto et al. 2020, EPSL). We measured the delay times of S-wave from rms envelopes of velocity seismograms at 4-8 Hz, 8-16 Hz and 16-32 Hz, and estimated power spectral density of inhomogeneity by assuming the von Karman type function. For a precise imaging of random inhomogeneity, we revised the covariance matrix of likelihood function. The original method uses a diagonal covariance matrix for residuals at all frequency bands. In our revised method, the covariance matrix has non-zero off-diagonal components to make adequate correlations of residuals among different frequencies for each raypath. These non-diagonal terms are quite effective to estimate the exponent of the von Karman type power spectral density function.

Preliminary analysis with a part of observed data imaged weak random inhomogeneity at most of the study area. These weak inhomogeneities commonly have steep spectral gradient. One of strongly inhomogeneous areas was imaged beneath the Tokara islands. Spectral gradient in this area is gentle as with those beneath the Quaternary volcanoes at northeast Japan (Takahashi et al. 2009). Other strongly inhomogeneous areas were found in the forearc side at 10-30 km depth. These anomalies show linear distributions parallel to the Ryukyu trench. Distances from the trench axis are about 80km and 110 km. Vertical extents of these anomalies have large uncertainties due to insufficient data, but it seems to be certain that the former one locates at low seismicity area of regular earthquakes. Correlation with shallow low frequency tremors (e.g., Yamashita et al. 2015) is not clear, then this strong inhomogeneity probably represents structural anomalies of subducting plate rather than those at the plate boundary.

Acknowledgement: This study is supported by “Research Project for Compound Disaster Mitigation on the Great Earthquakes and Tsunamis around the Nankai Trough Region” of the Ministry of Education, Culture, Sports, Science and Technology (MEXT) of Japan. We are grateful for Nishinoomote-city, Minamitane-town and Toshima-village for their kind corporation for onshore seismic observations.

©2020. Japan Geoscience Union. All Right Reserved.

Propagation characteristics of two-dimensional scalar waves in alternating layered structures

*Kazuki Kidoguchi[1], Jun Kawahara[1]

1. Graduate School of Science and Engineering, Ibaraki University

Deep events in the subducting Pacific plate often produce anomalously large intensity on the Pacific seaboard of eastern Japan. The cause was first explained by the Utsu model, assuming a high-Q subducting plate compared with the mantle wedge above it [Utsu, 1967; Utsu and Okada, 1968]. It was shown later that the waveform records in the regions of large intensity show a low-frequency ($f < 0.25$ Hz) onset followed by large-amplitude high-frequency ($f > 2$ Hz) later waves [e.g., Iidaka and Mizoue, 1991; Abers, 2000]. The Utsu model cannot explain this feature. Furumura and Kennett [2005] conducted two-dimensional numerical wave simulations of deep events in the Pacific plate with von Karman-type random heterogeneities. They showed that the heterogeneities with a longer correlation length (10 km) in the downdip direction along the subducting plate and a much shorter correlation length (0.5 km) in thickness reproduced very well the characteristics of the observation. This implies that such a lamina structure acts as an efficient waveguide for high-frequency waves by multiple scattering.

We examined this high-frequency waveguide effect using numerical simulations based on alternating layered structures, which are simplified models of lamina structures. We simulated two-dimensional scalar waves radiated from a point source with a Ricker-wavelet time function, adopting the velocity-stress finite-difference scheme with a staggered grid [Virieux,1984]. An alternating layered structure was made of layers with the same thickness, whose wave velocities was 10% either higher or lower than the mean velocity 4.5 km/s. In every simulation, the total thickness of the layered structure was 59.95 km and the dominant wavelength of the radiated waves (defined as the mean velocity divided by the central frequency of the Ricker wavelet) was 2 km. We changed the layer thickness from 4.95 km down to 0.1 km in respective simulations, thereby changing the wavelength relative to the layer thickness. We deployed 20 km-long receiver arrays from the source in the directions both parallel and normal to the layers (hereafter, horizontal and vertical, respectively).

We obtained the following results. As the relative wavelength became shorter, horizontally propagating waves showed more clearly the dispersion and broadening of waveforms, together with the delay of maximal peaks. These features would denote the high-frequency waveguide effect stated above. For wavelength longer than the layer thickness, vertically propagating waves also showed waveform broadening due to the generation of coda waves, but the forms of the direct waves remained nearly unchanged except for the amplitude attenuation. The generation of coda waves was suppressed as the wavelength became shorter than the layer thickness. We also observed that the propagation velocity for the onset of the horizontally propagating waves became higher than the mean velocity, if the wavelength was shorter than the layer thickness. This would be because the direct waves selected the fastest paths (higher-velocity layers) in the layered structures.

Keywords: alternating layers, scalar waves, wave propagation characteristics

©2020. Japan Geoscience Union. All Right Reserved.

Angular distribution of energy fluxes of seismic waves in two-dimensional random heterogeneous media

*Kentaro Emoto[1]

1. Graduate School of Science, Tohokuk University

Seismic waves propagating in small-scale heterogeneous media have long-lasting coda waves. Coda waves consist of scattered waves coming from various directions. Multiple forward-scattered waves arrive just after the onset of the direct wave and multiple backward-scattered waves arrive at the coda. The coda energy distribution is often approximated by the diffusion process. After the diffusion state, the coda field can be considered as the equipartition state in which the energy flux is isotropic. Emoto (2018, JpGU) investigated the angular distribution of energy fluxes of scalar waves and found that the dependence on the medium parameters is weak in terms of the shape of the angular distribution. Different from the scattering of scalar waves, both P and S waves exist in the seismic waves and conversion scattering occurs between them. Moreover, the ratio of P and S wave energy radiated from the source is different in different directions due to the radiation pattern of the double-couple source. In this study, we investigate the angular distribution of scattered seismic waves by using the finite difference simulation of the seismic wave propagation in two-dimensional small-scale heterogeneous media.

The energy flux of seismic waves can be calculated by taking the product of the velocity and the stress at a certain point. The angular distribution of the energy fluxes, that is the angular spectrum is the ensemble of energy fluxes. The medium size of the finite difference simulation is 384 x 384 km and the grid separation is 100 m. The background velocities are 6.00 and 3.46 km/s for P and S waves, respectively. The random heterogeneous medium is characterized by an exponential type auto-correlation function with the characteristic scale of 0.5 or 5 km and the RMS fractional fluctuation of 5 %. The strike-slip type source located at the center of the medium. The source time function if the Kupper wavelet whose dominant frequency is 3 Hz. Receivers are located at propagation distances 25, 50, 75 and 100 km. At a distance, 8 receivers are located with the interval of the azimuth of 45 degrees. According to the radiation pattern, we stack the energy fluxes of along and perpendicular directions (E90), and oblique directions (E45), respectively. The maximum lapse time of the simulation is 45 s.

The angular spectrum never becomes isotropic within the maximum lapse time of the simulation for both cases (characteristic scales of 0.5 and 5 km). The anisotropy of the angular spectrum at the P coda is stronger than that at the S coda. The difference between the two cases is not strong in terms of the shape of the angular distribution at the S coda. This is the same result as obtained by the scalar wave simulation. Conversely, the angular distribution at the P coda of the case of the characteristic scale of 5 km is anisotropic compared to that of 0.5 km. After the onset of S wave, the angular spectrum approaches the isotropic distribution. This approaching speed of E90 direction is faster than that of E45 direction.

The numerical simulation revealed that the dependence of the angular distribution of scattered waves at

©2020. Japan Geoscience Union. All Right Reserved.

the S coda on the medium parameter is weak. However, at the P coda, P to S scattering plays an important role to determine the angular distribution of the energy flux. We will extend our simulation to three-dimensional heterogeneous media in the future.

Keywords: Scattering, Angular spectrum, coda

©2020. Japan Geoscience Union. All Right Reserved.

[J] Poster | S (Solid Earth Sciences)：S-SS Seismology

[S-SS13] Seismicity

convener:Yasuhiro Yoshida(Meteorological College, Japan Meteorological Agency)

This session aims to improve our understanding on seismicity. Any contribution on behavior of earthquakes as a cluster, such as regional seismicity and aftershocks, is welcomed. We also welcome contribution on temporal and spatial interactions that control seismicity, and tectonic processes, and geological and thermal structures that regulate seismicity.

[SSS13-P01] Visualization of spatial and temporal change in b values and survey for the relationship between b value and the size of next earthquake

*Toshiki Shimbaru[1] (1.Fukuoka Regional Headquarters, JMA)

[SSS13-P02] Spatial and temporal change in b values on the fault plane of the 2016 Kumamoto earthquakes.

*Toshiki Shimbaru[1] (1.Fukuoka Regional Headquarters, JMA)

[SSS13-P03] A discussion of causes of succeeding small and moderate-sized earthquake in a short time -A case study of earthquakes east off the Osumi Peninsula-

*Yuko Yamada[1], Nobuyuki Hirota[2], Toshiki Shimbaru[1] (1.Fukuoka Regional Headquarters Japan Meteorological Agency, 2.Japan Meteorological Agency)

[SSS13-P04] Case study of succeeding earthquakes in the Hyuga-nada Sea, Japan

*Nobuyuki Hirota[1], Yuko Yamada[2], Toshiki Shimbaru[2] (1.Japan Meteorological Agency, 2.Fukuoka Regional Headquarters, JMA)

[SSS13-P05] **Relevalence of seismic activity between the inland crustal earthquakes in Hidaka district, Hokkaido and the great interplate earthquakes along the southern Kuril Trench**

*Tetsuo Takanami[1,2] (1.Hokkaido Research Center of Geology, 2.Carnegie Institution for Science)

[SSS13-P06] Seismic observation for an anomalous activity of shallow low frequency events mixed with normal earthquakes at Hakodate

*Shinako Noguchi[1], Keiji Kasahara[1], Masahiro Kosuga[2], Takuto Maeda[2], Yuta Amezawa[2], Taichi Haruyama[2], Sayumi Ishida[2], Yuki Matsuno[2], Itsuki Orui[3] (1.Association for the Development of Earthquake Prediction, 2.Graduate School of Science and Technology, Hirosaki University , 3.Faculty of Science and Technology, Hirosaki University)

[SSS13-P07] Continuous observation of ocean bottom earthquakes in Suruga Bay. -Hypocenter redetermination using velocity structure model obtained by Air-gun OBS refraction seismic survey.-

*Nakao Nagisa[1], Hisatoshi Baba[1], Takahito Nishimiya[2], Kayoko Tsuruga[3] (1.Graduate School of Oceanography, Tokai University, 2.Meteorological Research Institute,Japan Meteorological Agency, 3.Tokyo University of Marine Science and Technology)

[SSS13-P08] Swarm Activity in the Hida Mountain Range, Central Japan, Started in April 2020.; Comparison with Past Activity

*Shiro Ohmi[1] (1.Earthquake Hazards Division, Disaster Prevention Research Institute, Kyoto University)

Visualization of spatial and temporal change in b values and survey for the relationship between b value and the size of next earthquake

*Toshiki Shimbaru[1]

1. Fukuoka Regional Headquarters, JMA

It has been reported that the b value decreases before a major earthquake occurs in some cases.Nanjo et al.(2012) succeeded in detecting a b value precursor to two M9 - class quakes, at lead time of 10-20 years, and proposed that the b value is an important indicator of an impending great earth quake.
This study exhaustively compared the size of earthquakes occurred in near the boundary between the Pacific and land plates from October 1997 to February 2011 to b value at the epicenter immediately before the event.The result showed that the frequency of large-scale earthquakes is relatively high on the areas with low b value.
This result suggests the universal relationship between b value and the size of next earthquake.

Keywords: 2011 Tohoku-oki earthquake, b value, visualization

©2020. Japan Geoscience Union. All Right Reserved.

Spatial and temporal change in b values on the fault plane of the 2016 Kumamoto earthquakes.

*Toshiki Shimbaru[1]

1. Fukuoka Regional Headquarters, JMA

Since b values are known to be inversely dependent on differential stress (Scholz, 1968, 2015), the observed low b values in the epicenter area was interpreted as an indication of highly stressed area.
This study visualized the spatial and temporal change in b values on the fault plane of the 2016 Kumamoto earthquakes. The result showed that zones of low b value near the epicenter of two events (M6.5 quake on April 14 and M7.3 quake on April 16) overlapped with the slip distribution estimated by the analysis of near-field data of strong ground motions.
This is consistent with the result of Nanjo et al.(2012) on the case of the Tohoku Earthquake on March 11, 2011.

Keywords: 2016 Kumamoto earthquakes, b value, visualization

©2020. Japan Geoscience Union. All Right Reserved.

A discussion of causes of succeeding small and moderate-sized earthquake in a short time -A case study of earthquakes east off the Osumi Peninsula-

*Yuko Yamada[1], Nobuyuki Hirota[2], Toshiki Shimbaru[1]

1. Fukuoka Regional Headquarters Japan Meteorological Agency, 2. Japan Meteorological Agency

In a part of east off the Osumi Peninsula, earthquakes occur successively in a very short period. In order to reveal the mechanism, we analyzed digital seismogram data recorded from January 2001 to March 2019 by calculating cross-correlation coefficients.We detected three groups comprised of repeating earthquakes in the region. However no temporal periodicity of the earthquake occurrence was observed in each group, the earthquakes to belong to one of three groups were included in almost all cases which earthquakes occurred successively in a short period. By accurate hypocenter determination, it is revealed that earthquakes belonging to any group of the three groups are distributed approximately in one place. It may suggests that sources of repeating earthquakes of the each groups are neighboring in the region and when an earthquake occurs at one source, another earthquake successively occurs at another adjacent source by subjecting to stress change accompanying the earthquake.These results indicate that it is useful for assessing the potential of occurrence of earthquakes in the immediate future to grasp adjacent source of repeating earthquakes and check the similarity with the wave form of the earthquake in real time and the past.

Keywords: occurrence of earthquake successively, repeating earthquake, east off the Osumi Peninsula

©2020. Japan Geoscience Union. All Right Reserved.

Case study of succeeding earthquakes in the Hyuga-nada Sea, Japan

*Nobuyuki Hirota[1], Yuko Yamada[2], Toshiki Shimbaru[2]

1. Japan Meteorological Agency, 2. Fukuoka Regional Headquarters, JMA

1.Introduction

In the Hyuga-nada Sea, Japan, two M5.4 earthquakes occurred on March 27, 2019, every few hours. On May 10, 2019, an M5.6 earthquake and an M6.3 earthquake occurred at hourly intervals. In 2016, the Headquarters for Earthquake Research Promotion compiled a report entitled Information on Prospects for Seismic Activity after a Large Earthquake." In this report, succeeding earthquakes all over Japan have been researched, but none of them has been reported in the Hyuga-nada Sea. This is because the results differ depending on the conditions to be extracted. In this report, only large earthquakes were investigated. We researched succeeding earthquakes in the Hyuga-nada Sea including middle class earthquakes.
The Hyuga-nada Sea is the region with the highest seismic activity within the hypocenter area of the Nankai Trough earthquake. In the Hyuga-nada Sea, many earthquakes occur at the plate boundary. This is why it is important to understand the succeeding earthquakes in the Hyuga-nada Sea in detail to monitor seismic activity within the hypocenter area of the Nankai Trough earthquake.

2.Methods

2.1 Data
Hypocenter data: JMA catalog
Period: April 1, 1984 to September 30, 2019
Magnitude: 3.0 or more (M≧3.0)
2.2 Methods
(1)Remove aftershocks
The earthquakes that meet the following conditions is considered aftershocks.And they were removed.
Epicenter distance: within Lkm calculated from Log(L)=0.5M-1.8(Utsu,1961).L means length of fault(km),M means magnitude.
But,if the length of the fault is less than 10km, epicenter distance is 10km.
Period:within 10 days for M≦6.0,within 30 days for M>6.0
Difference of magnitude:0.3 or more
(2)Extract succeeding earthquakes
The earthquakes that meet the following conditions is considered succeeding earthquakes.
Epicenter distance: same condition as for aftershocks
Period: within 1 day
Difference of magnitude: second earthquake magnitude - first earthquake magnitude ≧ -0.2

3.Result

Succeeding earthquakes do not occur evenly throughout the Hyuga-nada Sea, but tend to occur in specific areas of activity.The earthquakes on March 27, 2019 and May 10, 2019 also occurred in areas with a high incidence rate.In areas where these earthquakes occurred, succeeding earthquakes on August 29, 2014(Largest earthquake M6.0)and October 19, 1996(Largest earthquake M6.9)occurred(Fig1).70% of all succeeding earthquakes have the same focal mechanism as earthquakes which occur at the plate boundary in the Hyuga-nada Sea.Many of succeeding earthquakes in the Hyuga-nada Sea may have occurred at the plate boundary.

4.Use in Japan Meteorological Agency

We consider about using result of this research for operation in JMA.We are considering the following two points.

©2020. Japan Geoscience Union. All Right Reserved.

(1)Use for real time monitoring of seismic activity
(2)Use for explanatory materials about earthquake
We report about"(1)Use for real time monitoring of seismic activity".We detected that many succeeding earthquakes in the Hyuga-nada Sea have occurred within 1 day.So, if we could use this result for real time monitoring of seismic activity, we need to analyze about succeeding earthquakes automatically and immediately.We have developed system which analyze and let us know about succeeding earthquakes automatically and immediately when an earthquake occurs.If we had this system when the earthquakes on March 27, 2019 and May 10, 2019 occurred, we could recognize that these earthquakes occurred in areas with a high incidence rate.

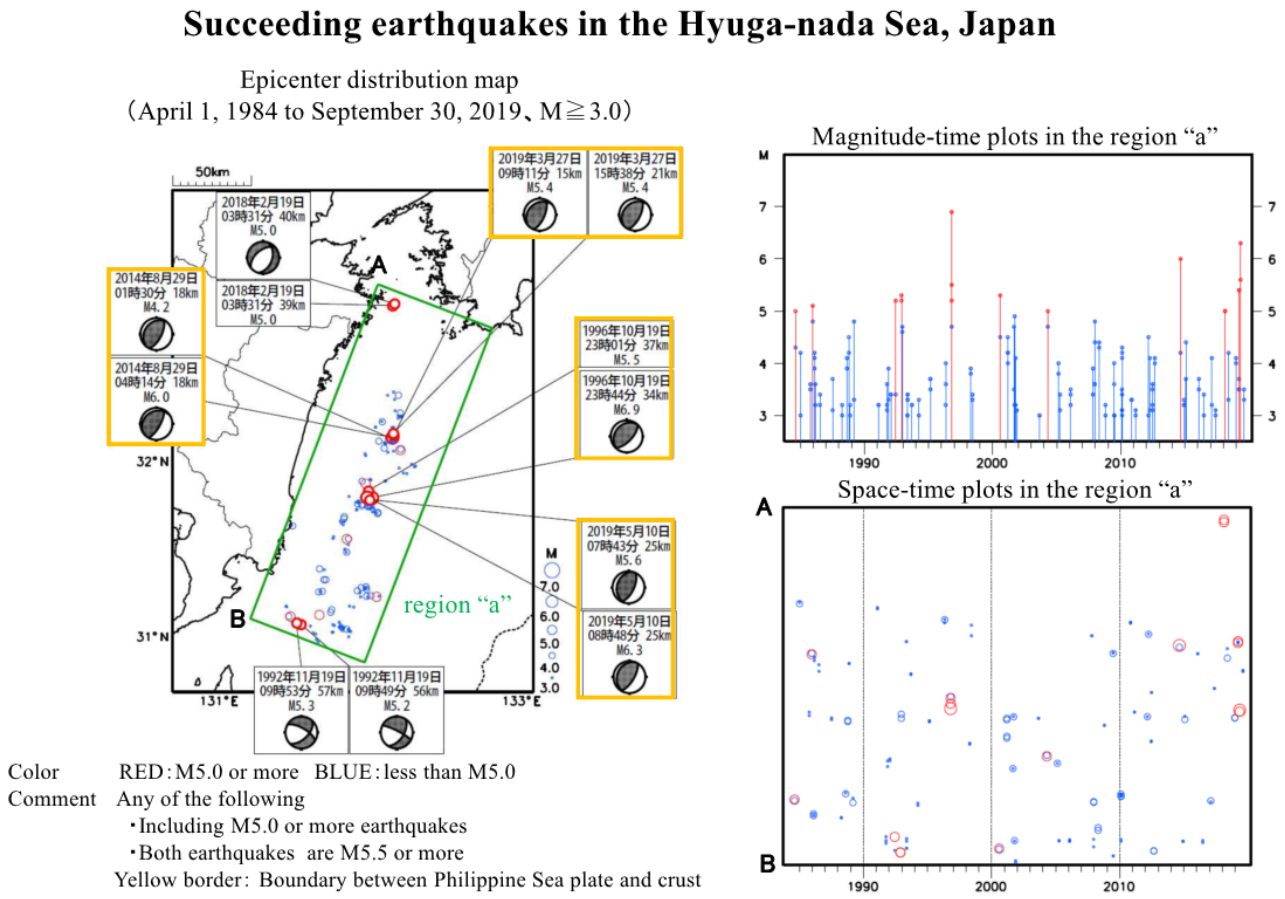

©2020. Japan Geoscience Union. All Right Reserved.

Relevalence of seismic activity between the inland crustal earthquakes in Hidaka district, Hokkaido and the great interplate earthquakes along the southern Kuril Trench

*Tetsuo Takanami[1,2]

1. Hokkaido Research Center of Geology, 2. Carnegie Institution for Science

The Hidaka Mountains in southern Hokkaido may be the result of squeezing deep matter in the collision zone due to the east-west shortening movement of the Kuril forearc since the late Miocene. However, it has been reported that its activity declined in the late Pliocene [1] [2]. On the other hand, the recent activity of inland crustal earthquakes within a depth of about 40 km is high in the Hidaka Mountains and its western region. The 2018 earthquake (Mj6.7) which occurred near the eastern margin fault zone of the Ishikari Lowland, is the largest inland crustal earthquake ever recorded in Hokkaido. According to various observation data, this earthquake is a reverse fault type due to east-west compressive stress, and is a fault motion in harmony with the tectonics of the Hidaka Mountains. So, in order to consider the current tectonics in the Hidaka region, it is important to examine the relationship between the seismic activity along the southern Kuril trench (especially for the interplate earthquake) and that in the Hidaka region. Here, using earthquake data from the 20th century onwards, we examine the chronological relationship of the seismic activity. As a result, it was found that there was a clear difference in seismic activity between the quiet period and the active period each area. However, during the active period of inland seismic activity, there were almost no huge interplate earthquakes along the southern Kuril trench and vice versa and the active periods do not overlap. According to the strain rate map [3] based on the GNSS data from 2005 to 2009, large strain rate values are observed in the coastal area along the southern Kuril trench to the volcanic front, but smaller values are distributed further inland area. Zones where the slightly higher strain rates are locally concentrated include the volcanic belt from Kunashiri island to the Tokachi volcano group, the Abashiri Tectonic Line, the Tokachi Plain adjacent to the epicenter of the 2003 Tokachi-oki earthquake, and the western foothills along the Hidaka mountains, and the epicentral area of the 2018 earthquake. According to the velocity distribution [4] imaged by seismic tomography analysis, the source region of the 2018 earthquake corresponds to the region where the seismic velocity changes significantly. Such a region corresponds to an intensity boundary where a hard part and a soft part are in contact, and implies a region where distortion tends to concentrate. Therefore it can be inferred that a large inland crustal earthquake is likely to occur because the source region is in an environment that accumulated such strains for many years. Moreover the focal mechanism solution supports the westward movement of the Kuril forearc sliver. From the viewpoint of plate tectonics there, the origin of the movement is the collision force acting when the subducting Pacific plate sinks along the southern Kuril trench, which is the combined force of the subducting Pacific plate with slab pull and effective ridge forces [5]. In the case of the southern Kuril forearc, its collision force is decomposed into components parallel and orthogonal to the volcanic front due to oblique subduction of the Pacific plate. The westward movement of the Kuril forearc sliver is caused by a force component parallel to the volcanic front. Therefore, it can be said that the earthquake observed in the west extending area of the southern Kuril forearc, which is moving westward, is closely related to the huge interplate earthquake expected along the southern Kuril trench.

[1] G. Kimura & K. Kusunoki (1997), [2] G. Kawakami et al. (2006), [3] T. Nishimura (2017), [4] M. Matsubara et al. (2017), [5] T. Seno (1999).

©2020. Japan Geoscience Union. All Right Reserved.

Keywords: Inland crustal earthquakes in Hidaka area, Strain concentraiting field in Hidaka area, Huge interplate eartquakes under the southern Kuril forearc.

©2020. Japan Geoscience Union. All Right Reserved.

Seismic observation for an anomalous activity of shallow low frequency events mixed with normal earthquakes at Hakodate

*Shinako Noguchi[1], Keiji Kasahara[1], Masahiro Kosuga[2], Takuto Maeda[2], Yuta Amezawa[2], Taichi Haruyama[2], Sayumi Ishida[2], Yuki Matsuno[2], Itsuki Orui[3]

1. Association for the Development of Earthquake Prediction, 2. Graduate School of Science and Technology, Hirosaki University , 3. Faculty of Science and Technology, Hirosaki University

In this presentation, we report the regional dense seismic observation targeting an anomalous shallow seismic activity consists of both normal earthquakes and low frequency events (LFEs) at near Hakodate, Hokkaido, Japan.
Shallow (<10 km) LFEs have been reported to occur (Noguchi et al., 2018) near Hakodate (A on Fig. 1), which were detected by the AS-net, regional high-sensitive seismic network installed and operated by the Association for the Development of Earthquake Prediction (ADEP). Moreover, normal crustal earthquakes occur quite closely to these LFEs. It is commonly considered that LFEs occur at a depth of 15–40 km, deeper than the depth threshold where normal non-volcanic earthquakes occur. This curious seismic activity near Hakodate conflicts with such common knowledge. Following this report, Nakajima and Hasegawa (2019) reexamined almost a million of shallow crustal earthquakes in Japan to detect another similar shallow activity of LFEs.
It has also been suggested, but not clarified that LFEs can be induced by crustal fluid (water or magma). Additionally, it is known that crustal fluids can also be related to activities of normal crustal earthquakes including destructive ones. It is necessary to investigate the shallow activity near Hakodate in detail to confirm these hypotheses. Particularly, we need to derive highly accurate hypocenter locations and source mechanisms for these events. The density of the existing seismic networks, including AS-net in this region, is not enough for this purpose because the targeted events are too small (M<2).
In order to investigate this shallow seismic activity, ADEP and Hirosaki University started a dense seismic observation around this activity in October 2018 using short-period seismometers. Fourteen stations are operating as of February 2020 (Fig. 1). We intend to install more stations than would normally be required to cover this area in order to compensate for the artificial noise since this activity occurs near the habitation area. We are also targeting another deep LFEs activity occurring 5~10 km to the east of the shallow seismic activity mentioned above (B on Fig. 1). Different from the shallow activity, this deeper LFEs activity is quite similar to the other deep LFEs activities frequently seen in NE Japan. We used Lennartz LD-3lite, three-components seismometers with the natural frequency of 1 Hz. Solar power and/or battery provide power to the sensor and recorder. Data recorded at five distant stations are transmitted via a cell-phone network in real-time. It is expected that real-time data acquisition will make it easier to detect changes in the seismic activities and enable us to accelerate the processing time of our analysis.
According to the JMA catalog, four LFEs and two normal earthquakes have occurred at the shallow target area since the beginning of our observation till the end of 2019. This shallow seismic activity has not been relatively active for decades. When we derive enough event data, we plan to start a highly accurate hypocenter determination procedure using a template matching method. Because of our dense observations, we will be able to detect smaller events compared to the JMA catalog. We also compare the recorded waves of targeting events to the events in the other region. Similar analyses also will be applied to the event data for deep LFEs activity. Based on the results of these analyses, we aim to clarify the detail and mechanism of this anomalous seismic activity near Hakodate.

©2020. Japan Geoscience Union. All Right Reserved.

Acknowledgements
We deeply appreciate a great deal of cooperation from the City of Hakodate and relevant people for our seismic observation.

References

Noguchi, S., S. Sekine, Y. Sawada, K. Kasahara, S. Sasaki, Y. Tazawa, H. Yajima, S. Abe and K. Ishida, Distribution and characteristics of low frequency events observed by AS-net at northern Tohoku and sowthwestern Hokkaido, SSJ Fall Meeting 2018, Koriyama, October 2018, S23-P26. (Japanese)
Nakajima, J. and H. Hasegawa, Detection of shallow low-frequency earthquakes beneath the Japanese Islands, SSJ Fall Meeting 2019, Kyoto, September 2018, S08-09. (Japanese)

Keywords: Shallow low frequency earthquake, Dense seismic observation

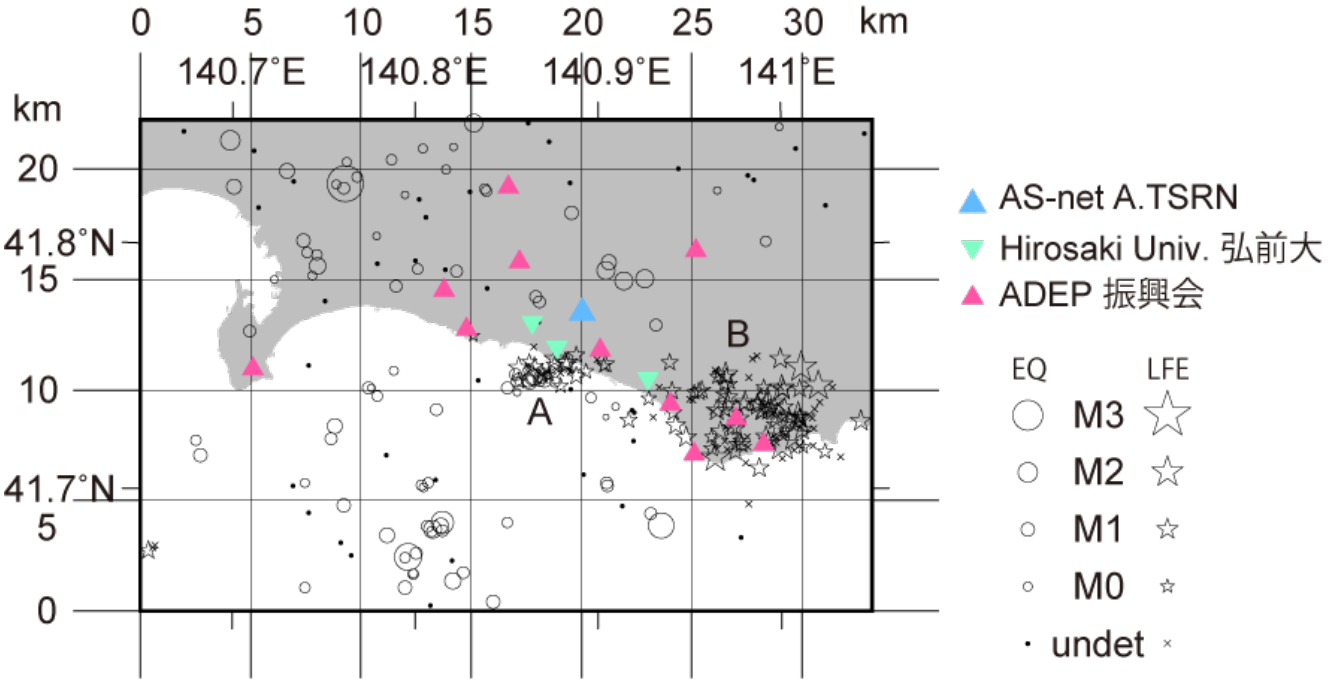

Fig. 1. Distribution of hypocenters and seismic stations around Hakodate.

©2020. Japan Geoscience Union. All Right Reserved.

Continuous observation of ocean bottom earthquakes in Suruga Bay. - Hypocenter redetermination using velocity structure model obtained by Air-gun OBS refraction seismic survey.-

*Nakao Nagisa[1], Hisatoshi Baba[1], Takahito Nishimiya[2], Kayoko Tsuruga[3]

1. Graduate School of Oceanography, Tokai University, 2. Meteorological Research Institute,Japan Meteorological Agency, 3. Tokyo University of Marine Science and Technology

Tokai Univ. and MRI are carrying out the ocean bottom earthquake observations in and around Senoumi Bank near Suruga Trough axial region, using 4 pop-up type Ocean Bottom Seismographs (OBSs) from October, 2011. The seismic activity obtained by these observations proved that most of them were aftershocks of the M 6.5 earthquake occurred in Suruga Bay in 2009.

In 2016, seismic reflection and refraction survey were carried out at Suruga Bay by the research vessel ‘Shinyomaru’ Tokyo University of Marine Science and Technology. 2-D seismic reflection system consists of three 10-ft containers for Air-gun sources, an air compressor, and streamer-cable systems (Tsuruga et al., 2017). We conducted seismic experiments along 4 survey lines located around Suruga Trough. One of the 4 lines, H28-L04 line was set in using OBSs stations, near Senoumi Bank.

Therefore, in order to investigate detailed seismic activity around Senoumi Bank in the central part of Suruga Bay, using velocity structure model obtained by Air-gun OBS refraction seismic survey.
In this presentation, we report characteristics of redetermination hypocenters obtained OBSs.

Keywords: Suruga Trough, Seismicity, Tokai Earthquake

©2020. Japan Geoscience Union. All Right Reserved.

Swarm Activity in the Hida Mountain Range, Central Japan, Started in April 2020.; Comparison with Past Activity

*Shiro Ohmi[1]

1. Earthquake Hazards Division, Disaster Prevention Research Institute, Kyoto University

Intense swarm activity took place in the southern part of Hida mountain range, central Japan, in April 2020. This activity started with an earthquake of Mjma=3.8 on April 22 in Nagano prefecture about 6km apart from the main ridge of Hida mountain range, followed by Mjma=5.5 earthquake on April 23. Focal region of the swarm gradually migrated to the main ridge, which is the prefectural border of Nagano and Gifu prefectures. On May 19, focal region reached to the main ridge and migrated to Gifu prefecture area with an earthquake of Mjma=5.4. As of May 25, 2020, focal area is still migrating to north in Gifu prefecture, which is western side of Hida mountain range. The total extent of the focal area is about 12 km in the NS direction and 8 km in the EW direction as of May 25.

Continual swarm activities have been observed in this region since early 1990’ s. Prominent activities were observed in 1990, 1993, 1998, 2011, 2014, and 2018. One of the characteristic features of these swarm activities is that the focal region of each swarm has not overlapped to each other until 2018 activity. However, in the 2020 activity, the focal region overlaps on that of 1998 activity, which is a unique character of this activity.

In this presentation, we will compare these activities from the view points of focal region, source mechanism, and other phenomenon such as swarm of low frequency earthquakes that follow the shallow swarm activities.

Keywords: Hida Mountain Range, Central Japan, Swarm Activity

©2020. Japan Geoscience Union. All Right Reserved.

[J] Poster | S (Solid Earth Sciences)：S-SS Seismology

[S-SS14] Crustal Deformation

convener:Tadafumi Ochi(Institute of Earthquake and Volcano Geology, Geological Survey of Japan, The National Institute of Advanced Industrial Science and Technology), Masayuki Kano(Graduate school of science, Tohoku University)

Study of crustal deformation plays an extremely important role in the investigation of wide scale earth dynamics those are earthquake and volcanic activity, plate motion and so on. In our session, we discuss the study related to crustal deformation, such as development of observation instrument, observed crustal deformation, analysis method, and simulation study.

[SSS14-P01] The Influence on the Regional Crustal Deformation and Stress Field of the Wenchuan M_S 8.0 Earthquake

*Qi Liu[1], Xueze Wen[2], Zhigang Shao[1] (1.Institute of Earthquake Forecasting, China Earthquake Administration, 2.Institute of Geology, China Earthquake Administration)

[SSS14-P02] **Co-Seismic deformation of the 2017 *Ms*6.6 JingHe, China earthquake derived from Sentinel-1 data and speculate seismogenic fault**

*Wei Feng[1], Ze chao Bai[2], Zhi gang Shao[1], Jian bo Chen[3] (1.Institute of Earthquake Forecasting, China Earthquake Administration, 2.North China University of Technology, 3.Earthquake Administration of Xinjiang Uygur Autonomous Region)

[SSS14-P03] Application of a slow slip objective detection method

*Akio Kobayashi[1] (1.Meteorological Research Institute, Japan Meteorological Agency)

[SSS14-P04] The 2018 Hyuga-nada and Bungo channel long-term SSE detected by GEONET

*Shinzaburo Ozawa[1], Ryoji Kawabata[1], Kensuke Kokado[1], Hiroshi Yarai[1] (1.Geographical Survey Institute of Japan)

[SSS14-P05] Inversion analyses of long-term slow slip events using GNSS and strain data

*Takahiro Tsuyuki[1], Akio Kobayashi[1], Kana Akiyama[2], Reiko Kai[2], Kazuki Miyaoka[2] (1.Meteorological Research Institute, 2.Japan Meteorological Agency)

[SSS14-P06] Spatiotemporal evolution of Slow Slip Events along the southern Ryukyu subduction zone, using GNSS data collected by new stations

*Kazuki Komano[1], Shin'ichi Miyazaki[1], Masayuki Kano[2], Takeshi Matsushima[3], Takuya Nishimura[4] (1.Earth and Planetary Science, School of Science, Kyoto university, 2.Geophysics, School of Science, Tohoku university, 3.Earthquake and Volcano observation center, Kyushu University, 4.DPRI, Kyoto University)

[SSS14-P07] Long-term postseismic deformation at the eastern margin of the Japan Sea implied by temporal changes in areal strain rates and background seismicity rates

*Issei Kosugi[1], Yuta Mitsui[2] (1.Graduate School Of Science and Technology, Shizuoka University , 2.Faculty of Science, Shizuoka University)

[SSS14-P08] Temporal changes of areal strains estimated from three continuous GNSS stations in the vicinity of faults before the 2011 Tohoku and the 2016 Kumamoto earthquake

*Daisuke Sato[1], Masayuki Murase[2] (1.NIHON University Graduate School of Integrated Basic Sciences, 2. Department of Earth and Environmental Sciences, College of Humanities and Sciences, NIHON University)

[SSS14-P09] Seasonal adjustment for tidal data (3)

*Tadafumi Ochi[1] (1.Institute of Earthquake and Volcano Geology, Geological Survey of Japan, The National Institute of Advanced Industrial Science and Technology)

[SSS14-P10] **Vertical annual cyclic movement model of Mainland China and its analysis based on GPS observations**

*Hongbao Liang[1], Wei Zhan[1], Jinwu Li[1,2] (1.First Crust Monitoring and Application Center, CEA, Tianjin 300180, China., 2.School of Geodesy and Geomatics, Wuhan University, Wuhan 430079, China.)

[SSS14-P11] Strain changes due to the co-seismic fault slips observed in Kobe

*Atsushi Mukai[1], Shigeaki Otsuka[2], Yoichi Fukuda[3] (1.Faculty of Urban Management, Fukuyama City University, 2.Former Professor at Kobe Gakuin University, 3.Graduate School of Science, Kyoto Univ.)

[SSS14-P12] Development of the New GEONET Analysis Strategy

*Yasuaki Kakiage[1], Hiroki MURAMATSU[1], Kazuyuki OHASHI[1], Satoshi Abe[1], Tomoaki Furuya[1], Yuki Hatanaka[1] (1.Geospatial Information Authority of Japan)

[SSS14-P13] Estimation of fault models by MCMC method

*Ryoji Kawabata[1] (1.GSI of Japan)

[SSS14-P14] Estimation on fault-slip distributions without smoothing constraints by Reversible-jump MCMC

*Fumiaki Tomita[1], Takeshi Iinuma[1], Ryoichiro Agata[1], Takane Hori[1] (1.Japan Agency for Marine-Earth Science and Technology)

[SSS14-P15] Analysis of ocean bottom pressure gauge data by a hybrid method of MSSA and fitting of a parametric function

*Koichi Murata[1], Toshinori Sato[2], Hajime Shiobara[3], Masanao Shinohara[3], Tomoaki Yamada[4] (1.Graduate School of Science and Engineering, Chiba University, 2.Graduate School of Science, Chiba University, 3. Earthquake Research Institute, University of Tokyo, 4.Japan Meteorological Agency)

[SSS14-P16] **Earthquake potential in Costa Rica estimated by the integration of the interseismic geodetic data with seismicity records and inland faulting traces**

*Luis Alejandro Carvajal Soto[1,2], Takeo Ito[2], Marino Protti[3], Hiroshi Kimura[2] (1.Universidad Latina de Costa Rica, 2.Nagoya University, 3.Universidad Nacional de Costa Rica)

[SSS14-P17] The Fault model of the 2017 M5.6 earthquake estimated from precise leveling survey data in the Eastern flank of the Ontake volcano 2

*Masayuki Murase[1], Fumiaki Kimata[2], Yoshiko Yamanaka[3], Takeshi Matsushima[4], Hitoshi Yamashita Mori[1], Daisuke Sato[1], Takahiro Kunitomo[3], Yuta Maeda[3], Shinichiro Horikawa[3], Takashi OKUDA[3], Kenjoro Matsuhiro[3], Kazushi Tanoue[3], Kazunari Uchida[4], Shin Yoshikawa[5], Hiroyuki Inoue[5], Takahiro Yanada[6], Takahiro Kako[1,6], Hiroyuki Ishimori[6] (1.Department of Earth and Environmental Sciences, College of Humanities and Sciences, NIHON University, 2.Tono Research Institute of Earthquake Science, 3.Earthquake and Volcano Research Center, Graduate School of Environmental Studies, Nagoya University, 4.Institute of Seismology and Volcanology, Kyushu University. , 5.Aso Volcanological Laboratory , Kyoto University, 6.Japan meteorological agency)

[SSS14-P18] Change in area strain around Toyama prefecture during the period of 2005–2018

*Kohei Hotta[1] (1.University of Toyama)

[SSS14-P19] **Estimation of Deformation Fields from GNSS Data Using Basis Function Expansion: Comparison with the Method by Shen et al. (1996)**

*Tomohisa Okazaki[1], Yukitoshi Fukahata[2], Takuya Nishimura[2] (1.Center for Advanced Intelligence Project, RIKEN, 2.Disaster Prevention Research Institute, Kyoto University)

[SSS14-P20] Reconsidered source model of short-term slow slip event by using spatial distribution of strain change

*Noa Mitsui[1], Yasuhiro Asai[1], Satoshi Itaba[2] (1.Tono Research Institute of Earthquake Science, 2.National Institute of Advanced Industrial Science and Technology)

[SSS14-P21] Bayesian l_1 trend filtering for slow slip detection

*Keisuke Yano[1], Masayuki Kano[2] (1.The University of Tokyo, Graduate School of Information Science and Technology, 2.Tohoku university, Graduate School of Science)

[SSS14-P22] Detection of multiple inflection points in time-series of GNSS-acoustic data for a shallow part of the Nankai Trough based on a MCMC method

*Ryoya Igashima[1], Yuta Mitsui[2] (1.Nagoya University, 2.Shizuoka University)

[SSS14-P23] GNSS observation around a shear zone in southern Kyushu, southwest Japan (The fourth report)

*Tsuyoshi Watanabe[1], Koichi Asamori[1], Akiomi Shimada[1], Hiroki Ogawa[1], Atsushi Saiga[1], Koji Umeda[2] (1.Japan Atomic Energy Agency, 2.Hirosaki University)

[SSS14-P24] **Seismic Risk on the Northern Xiaojiang Fault Implied by the Latest and Nearest GPS Observations**

*Zhen Fu[1], Lisheng Xu[1] (1.Institute of Geophysics, China Earthquake Administration)

[SSS14-P26] An Analysis for the Shape of Subducting Oceanic Plate using Shortest-Path Algorithm in GIS

Yuki tsukamoto[1], *Shinsuke Okada[2], Tatsuya Sumita[3], Daisaku Kawabata[3] (1.Graduate School of Science, Tohoku University, 2.International Research Institute of Disaster Science, Tohoku University, 3.Geological Survey of Japan, National Institute of Advanced Industrial Science and Technology)

[SSS14-P27] Toward the development of a kinematic block motion model in Indonesia based on GNSS observation

*Rio Raharja[1], Takeo Ito[1], Hiroshi Kimura[1], Irwan Meilano[2] (1.Graduate School of Environmental Studies, Nagoya University, Japan, 2.Faculty of Earth Sciences and Technology, Bandung Institute of Technology, Indonesia)

[SSS14-P28] Def3D, a three-dimensional FEM tool for modeling deformation near active faults and volcanic centers

*luyuan Huang[1] (1.institute of crustal dynamics,CEA)

[SSS14-P29] The changes of interplate coupling area and the vertical changes at Shikoku before the 1946 Nankai earthquake.

*Yasuhiro Umeda[1] (1.former DPRI Kyoto Univ., former AIST)

The Influence on the Regional Crustal Deformation and Stress Field of the Wenchuan M_S 8.0 Earthquake

*Qi Liu[1], Xueze Wen[2], Zhigang Shao[1]

1. Institute of Earthquake Forecasting, China Earthquake Administration, 2. Institute of Geology, China Earthquake Administration

The long-term impact of coseismic and post-earthquake effects on the crustal deformation field, stress field, fault activity status, and seismic hazard in the surrounding area had attracted more and more attention from the international academic community and had become a hot topic for research in the past two decades. As the first high-angle reversed type 8-magnitude earthquake that occurred in the mainland since the instrument records, the occurrence of the M 8.0 Wenchuan earthquake on May 12, 2008 not only caused serious casualties and economic losses, but also had a continuous and significant impact on the regional tectonic deformation and fault stress accumulation. Carrying out related coseismic and postseismic researches on the Wenchuan earthquake not only favor to understand the rupture characteristics of the earthquake, but also has great significance on analyzing the change of regional crustal deformation and stress field and estimating the future seismic hazards of main active faults. Therefore, we took the Wenchuan earthquake as the research object, based on the dislocation theory and the viscoelastic constitutive relation, carried out the research on the changes of regional deformation field and stress field caused by coseismic dislocation and viscoelastic relaxation of the earthquake. Firstly, we constructed a 3D model of the seismogenic faults of the Wenchuan earthquake by means of comprehensive multidisciplinary data, together with the inversion using multiple coseismic observations, the coseismic slip distribution of the Wenchuan earthquake was obtained. And then, based on the constitutive relation of Burgers' viscoelastic body, with GPS time series as the constraints, with the distribution of coseismic slip in the Wenchuan earthquake as the initial condition, and with the help of finite element numerical simulation, the optimal short-term and long-term effective viscous coefficient of each block in both sides of the Longmenshan fault zone were determined. Finally, the regional deformation field changes caused by coseismic dislocations and viscoelastic relaxation was analyzed, and the earthquake risk of the surrounding active faults in the future was discussed based on the Coulomb stress change.

Keywords: Wenchuan earthquake, crustal deformation, stress evolution, coseismic slip, viscoelastic relaxation, finite element simulation

©2020. Japan Geoscience Union. All Right Reserved.

Co-Seismic deformation of the 2017 *Ms*6.6 JingHe, China earthquake derived from Sentinel-1 data and speculate seismogenic fault

*Wei Feng[1], Ze chao Bai[2], Zhi gang Shao[1], Jian bo Chen[3]

1. Institute of Earthquake Forecasting, China Earthquake Administration, 2. North China University of Technology, 3. Earthquake Administration of Xinjiang Uygur Autonomous Region

An M_S6.6 earthquake hit JingHe County in Bortala Mongol Autonomous Prefecture of Xinjiang Uygur Autonomous region on August9, 2017, with the epicenter (44.3°N, 82.9°E). The earthquake occurred in the eastern part of the Kusongmuxieke front fault in the southwest of Junggar Basin. By using two pairs of coseismic SAR image data for the ascending and descending tracks gained from Sentinel-1 (ESA), according to the 90m SRTM V4 data, this paper remove the topographic phase to get the differential interferograms, and the binomial fitting method is used to remove track residual phase in deformation field, MCF (Minium cost flow) solution is used for phase unwrapping to obtain the data of coseismic deformation field of ascending and descending tracks. The data is used to calculate the fault slip distribution of the earthquake based on the elastic semi-space rectangular dislocation model.

The result shows that this earthquake deformation field has the typical characteristics of thrust seismic deformation. The deformation field is about 28km-long, and 20km-wide, uplift is clear near the epicenter, LOS (Line of Sight) to ascending and descending tracks are 49 mm (20170808-20170814, T85A), 68 mm (20170807-20170813, T63D) respectively, and main slipping dislocation concentrated in depth of 10-14 km , the average momentum is about 0.6 m.

The maximum deformation area is located on the west side of the main earthquake and the characteristics of the unilateral rupture mainly distributed on the west side of the main earthquake are mutually confirmed. Combined with the existing geological knowledge, the existing 2-3 small scale thrust faults with oblique columnar distribution in this area are inferred to be the seismogenic fault of this earthquake.

Keywords: JingHe earthquake, InSAR, Kusongmuxieke front fault

©2020. Japan Geoscience Union. All Right Reserved.

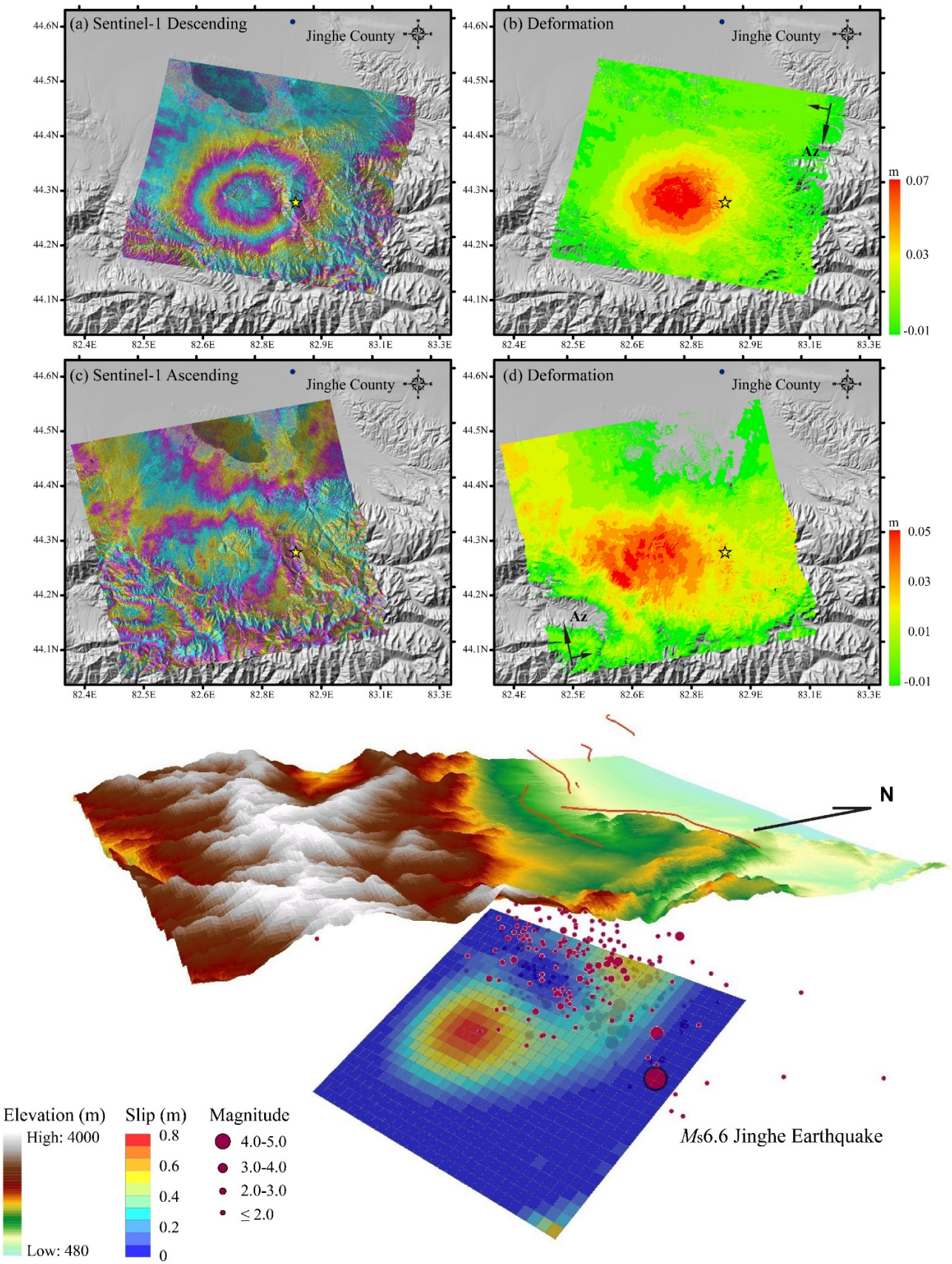

©2020. Japan Geoscience Union. All Right Reserved.

Application of a slow slip objective detection method

*Akio Kobayashi[1]

1. Meteorological Research Institute, Japan Meteorological Agency

In the Nankai Trough, slow earthquakes such as short-term slow slip events (SSEs) and long-term SSEs have been observed. Kobayashi (2017) developed a method for objective detection of long-term SSEs and revealed their spatiotemporal distribution. Here, we tried to estimate the approximate magnitude of long-term SSEs by applying this method.

We used the daily coordinates of the GEONET F3 analysis operated by the Geospatial Information Authority of Japan. We removed linear trend, coseismic and artificial offsets. Chugoku region is close to the Nankai Trough and relatively stable without the influence of long-term SSEs. The median of the coordinates in the Chugoku region was calculated every day and that value was subtracted from the coordinates of all stations. The latitude of the 25-km depth contour of the Philippine Sea plate in the Nankai Trough region was derived at intervals of 0.1˚ from longitude 132.1˚E to 138.0˚E, yielding a line of 60 points. A rectangle measuring 100 km in the direction of plate subduction and 50 km in width, closely matching the strike of the Nankai Trough, was centered on each of the 60 points, and data from the GNSS stations within each of these rectangles were extracted. For each rectangle, the component of motion in the opposite direction from plate subduction was calculated from the mean of the horizontal components of the stations within the rectangle. Then, we obtained cross correlations with a ramp function with 1-year gradient period and change before and after the period.

We assumed a 100 mm slip on a 30 km x 30 km rectangle fault (equivalent to Mw 6.3) centered on the 60 points of the 25-km depth contour. Then, the component of motion in the opposite direction from plate subduction was calculated from the mean of the theoretical displacement of the stations within the 100 km x 50 km rectangle. Assuming that the dimension of the rectangle fault is fixed and only the amount of slip changes, the magnitude of slip was estimated from the ratio of the 1-year change to the theoretical mean displacement.

The magnitude of the long-term SSEs was estimated at Mw 6.3-6.9 at the peak of each event. Except for the Tokai 2000-2005 SSE, these are roughly consistent with the previously analyzed results. Although the duration of Tokai 2000-2005 SSE is long, this method estimates the magnitude per year, so the difference may be large.

Keywords: long-term slow slip event, Nankai Trough, GNSS

©2020. Japan Geoscience Union. All Right Reserved.

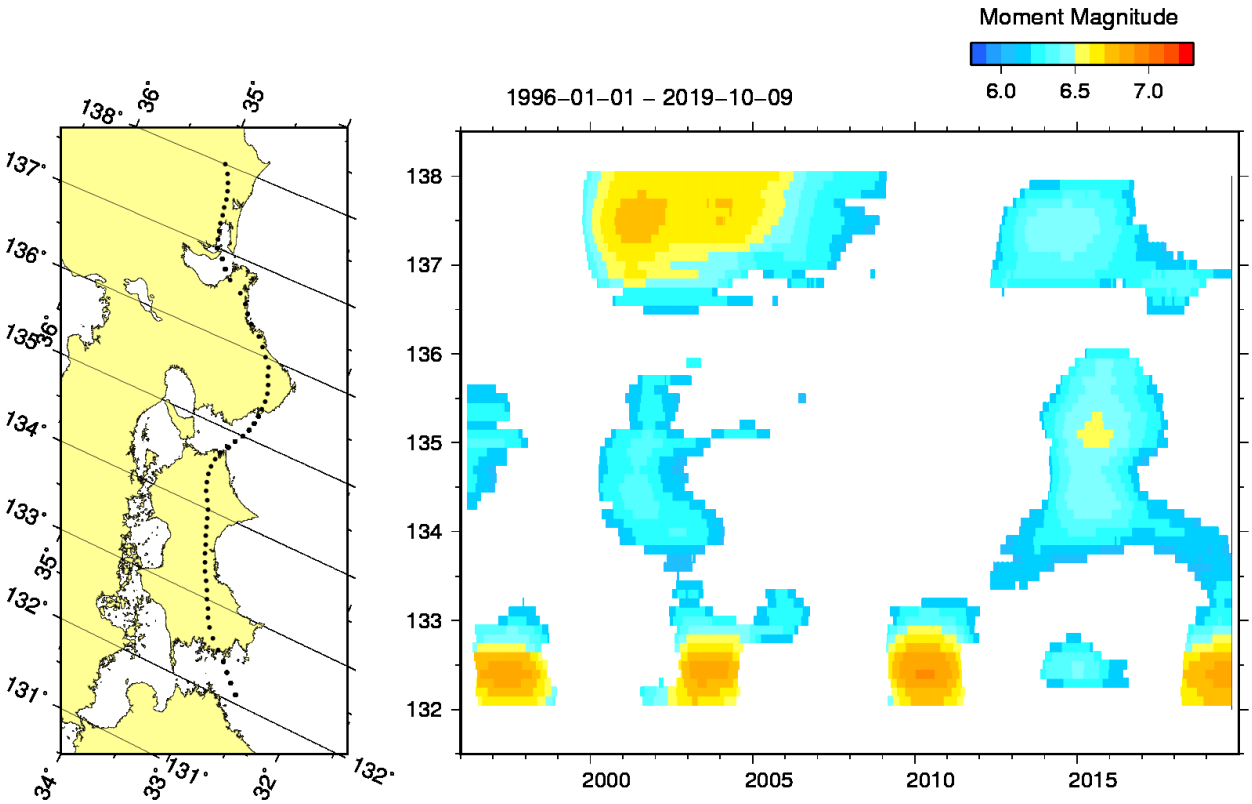

©2020. Japan Geoscience Union. All Right Reserved.

The 2018 Hyuga-nada and Bungo channel long-term SSE detected by GEONET

*Shinzaburo Ozawa[1], Ryoji Kawabata[1], Kensuke Kokado[1], Hiroshi Yarai[1]

1. Geographical Survey Institute of Japan

Abstract

Global Navigation Satellite System (GNSS) network in Japan detected the transient crustal deformation along the Nankai trough, Japan from June 2018. Time dependent inversion analysis shows that the long-term slow slip event in northern Hyuga-nada sea along the Nankai trough, Japan, started from June 2018 and abated in October 2018. From October 2018, slip area appeared in the Bungo channel and expanded to northern Hyuga-nada SEA and southwestern Shikoku. The Bungo channel long-term slow slip continued until around June 2019.

Introduction

Long-term slow slip events repeatedly occurred in the Bungo-channel and northern Hyuga-nada Sea. Just before the 2016 Kumamoto earthquake, long-term SSEs were occurring in northern Hyuga-nada and southwestern Shikoku. Because of the coseismic and postseismic deformation, it remainss unknown whether they continued or ceased after the earthquake. Under the circumstances, transient crustal deformation started in northern Kyushu from June 2018. From October, 2018, the areas neighboring the Bungo-channel showed transients. We estimate spatiotemporal evolution of aseismic interplate slip by inverting position time series detected by GNSS.

Analytical Procedure

We estimated annual and semi-annual components for the period between 2012 and 2019 and subtracted them from the position time series. After this, we estimated a linear trend from 2017 and 2018 and subtracted it from the data without annual and semi-annual components. We conducted the time dependent inversion using east-west, north-south, and up-down components at 250 GNSS sites. We adopted the geometry model estimated by Hirose et al. (2008). Grid spacing is around 40 km. We constrained the slip direction eastward and southward.

Results and Discussion

Long-term slow slip occurred in northern Hyuga-nada from June 2018. After that, slow slip stated in the Bungo-channel and expanded into northern Hyuga-nada and southwest Shikoku. From June 2019, slow slip in the central part of the Bungo-channel abated and neighboring areas show subsidence in August 2019. The estimate rupture propagation is different from those of the past Bungo-channel SSEs. In particular, the 2018-2019 SSE started in northern Hyuga-nada and propagated to the Bungo-channel area and northern Hyuga-nada restarted slow slipping.

©2020. Japan Geoscience Union. All Right Reserved.

It is seven years from the last Bungo-channel SSE and seems to be delayed considering recurrence interval of 5 to 6 years. Furthermore, northern Hyuga-nada SSE occurred twice in 2018-2019 events. These difference in rupture propagation and recurrence interval may be affected by stress perturbation by the 2016 Kumamoto earthquake.

Keywords: Slow slip event, Hyuga-nada Sea, Bungo channel

©2020. Japan Geoscience Union. All Right Reserved.

Inversion analyses of long-term slow slip events using GNSS and strain data

*Takahiro Tsuyuki[1], Akio Kobayashi[1], Kana Akiyama[2], Reiko Kai[2], Kazuki Miyaoka[2]

1. Meteorological Research Institute, 2. Japan Meteorological Agency

Long-term slow slip events (SSEs) have repeatedly occurred along the Nankai Trough, which are mainly detected and analyzed using GNSS data. Although strain observation data has very high detection level for a few days change like short-term SSE, detection level for longer period than a few months or years is conversely low [Yamamoto et al., 2008] and no clear strain change due to the 2001-2007 long-term SSE in the Tokai region has been found in the JMA's strain observation data. [Yoshikawa, 2003: Yamamoto, 2007]. On the other hand, for the 2013-2016 long-term SSE in the Tokai region, its location and slip moment have been estimated by stacking strain data [Miyaoka & Kimura, 2016: JMA & MRI, 2014-2017] and the estimated slip moment accumulation is similar to that estimated from GNSS data. In addition, a rectangular fault model has been estimated for the long-term SSE since 2018 at Bungo Channel using changes of only strain data observed by AIST in the Shikoku region [JMA, 2018-2020]. In any case, only few components of limited stations show clear change of strain and it is not clear that these changes are caused by the long-term SSEs.
In this study, we tried to estimate slip distribution of long-term SSE by joint inversion of GNSS and strain data using ABIC and compare the result with the analyses using GNSS data. Also, we evaluate the error of observed strain change and verify the possibility that strain data change may be due to long-term SSE. If long-term SSE could be detected by strain observation other than GNSS observation, it can support GNSS analysis and prove the certainty of long-term SSE analysis using strain stacking data. We apply a joint inversion method [Garth et al., 2014] to the inversion analyses using strain and GNSS data. Figure shows an example of inversion analysis of long-term SSE at Bungo Channel. This shows consistency with the result from spatio-temporal inversion using GNSS data [GSI, 2018-2020]. Error of strain observation data is estimated about 10^{-11} strain and we have confirmed that the changes of strain observation data are caused by long-term SSE.

Keywords: Strain observation, GNSS, Long-term SSE, Inversion

©2020. Japan Geoscience Union. All Right Reserved.

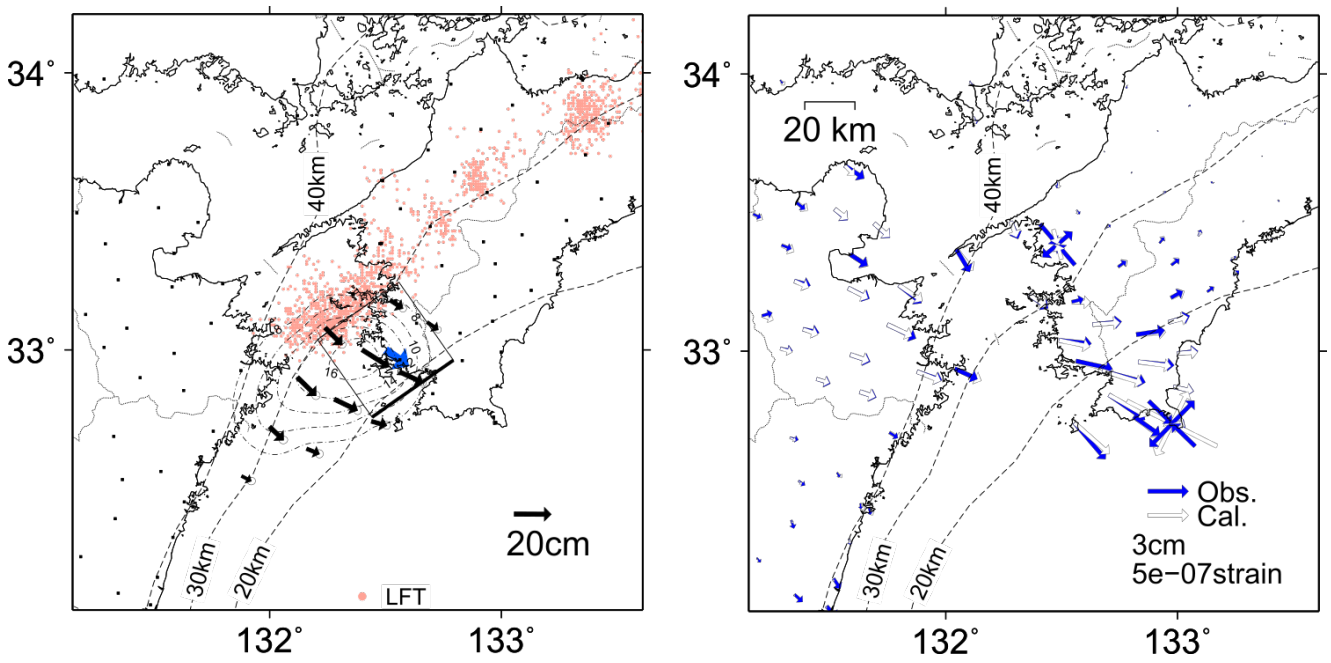

©2020. Japan Geoscience Union. All Right Reserved.

Spatiotemporal evolution of Slow Slip Events along the southern Ryukyu subduction zone, using GNSS data collected by new stations

*Kazuki Komano[1], Shin'ichi Miyazaki[1], Masayuki Kano[2], Takeshi Matsushima[3], Takuya Nishimura[4]

1. Earth and Planetary Science, School of Science, Kyoto university, 2. Geophysics, School of Science, Tohoku university, 3. Earthquake and Volcano observation center, Kyushu University, 4. DPRI, Kyoto University

In the Southwestern Ryukyu Arc, where the Philippine Sea plate subducts into the Amur plate, SSEs (Slow Slip Events) occur about every six months on the plate boundary. It is an important issue to understand the mechanism of SSE, because it has been suggested that the occurrence of SSEs relates the occurrence of earthquakes. Especially in Yaeyama, the Yaeyama earthquake, a large earthquake with a tsunami, occurred in 1771, and SSEs may occur on the same plate boundary this earthquake occurred. We believe that it is necessary to correctly evaluate the possibility of a major earthquake recurring in this region in the future.

Since the SW Ryukyu region is consisted of small islands, there are relatively few GNSS observation points. It is not easy to obtain enough resolution to accurately estimate fault slip at depth. Therefore, in recent years, Kyoto University and Kyushu University have set up many GNSS observation points in SW Ryukyu in addition to the GNSS Earth Observation Network (GEONET). Observation points by Kyoto University are seven points in total: KRSM at Kuroshima Island (observation start in July 2010), OOHR at Ohara in Iriomote Island (February 2011), FNUK at Funauki in Iriomote Island (March 2011), KOHM at Kohama Island (March 2011), YNGJ at Yonaguni Island (March 2018), INDA at Inoda in Ishigaki Island (July 2018), and SRH1 at Shiraho in Ishigaki Island (July 2018). Kyushu University has three observation points: YPNR at Aragusuku Island (September 2017), YKNK at Kanokawa in Iriomote Island (November 2017), and YOGN at Nakanokami Island (November 2017). In addition, we have used one observation point of the Japan Coast Guard. Through this analysis, we try to improve the resolution by using these GNSS observation points.

In this study, we perform inversion analysis of spatiotemporal evolution of SSEs based on Kano et al (2018). This paper reported that the spatiotemporal evolution of slip changes during the events. However, the number of analyzed events is as small as five. So, by increasing the analysis period, we attempted to analyze more events, focusing on the regularity of the temporal change of the moment rate.

Keywords: crustal deformation, slow slip, GNSS

©2020. Japan Geoscience Union. All Right Reserved.

Long-term postseismic deformation at the eastern margin of the Japan Sea implied by temporal changes in areal strain rates and background seismicity rates

*Issei Kosugi[1], Yuta Mitsui[2]

1. Graduate School Of Science and Technology, Shizuoka University , 2. Faculty of Science, Shizuoka University

Magnitude-8 class earthquakes have frequently occurred on the back-arc side of the Tohoku region, especially on the eastern margin of the Japan Sea. For the eastern margin of the Japan Sea, there had been a lot of discussion about its tectonics. For example, Nakamura (1983) hypothesized that the eastern margin of the Japan Sea is a convergence boundary (and beginning trench) between the North American Plate and the Eurasian Plate. Okamura (2002) also hypothesized that the eastern margin of the Japan Sea is a strain concentration zone where a lot of faults had been formed within the plate. In this study, we analyze crustal deformation and seismicity data from recent observation system, to investigate decadal activity of the eastern margin of the Japan Sea before perturbation due to the 2011 Tohoku earthquake.

In terms of crustal deformation analysis, we investigate temporal changes in areal strain of the Tohoku region using the F3 solution of GNSS data provided by Geospatial Information Authority of Japan. We find compressional trends possibly originating from the eastern margin of the Japan Sea especially in the north of the Oga Peninsula. In terms of seismicity analysis, we estimate stress loading rates within the eastern margin of the Japan Sea by applying the ETAS model (Ogata, 1988) to the earthquake catalogue provided by Japan Meteorological Society. These analyses imply that long-term postseismic deformation of two major earthquakes (the 1983 Nihonkai-Chubu earthquake and the 1993 southwest-off Hokkaido earthquake) had continued until around 2010 in the eastern margin of the Japan Sea.

We model this long-term postseismic deformation using a three-dimensional viscoelastic simulation based on Fukahata and Matsu’ura (2006). The result suggests that the asthenosphere beneath the eastern margin of the Japan Sea, especially around the source region of the 1983 Nihonkai-Chubu earthquake, does not have low viscosity as that for the Pacific Plate subduction zone.

Keywords: Japan Sea, GNSS, ETAS model, postseismic deformation

©2020. Japan Geoscience Union. All Right Reserved.

Temporal changes of areal strains estimated from three continuous GNSS stations in the vicinity of faults before the 2011 Tohoku and the 2016 Kumamoto earthquake

*Daisuke Sato[1], Masayuki Murase[2]

1. NIHON University Graduate School of Integrated Basic Sciences, 2. Department of Earth and Environmental Sciences, College of Humanities and Sciences, NIHON University

Temporal changes of areal strains were estimated from three continuous GNSS stations in the Tohoku region and Kumamoto regions. The areal strains for one year in each month were calculated using the 30-days averages of the coordinate values of GEONET F3 solution for the month and the month last year. The areal strain was calculated every month and integrated as time series.
In Tohoku region, the M9.0 huge earthquake occurred in March 2011. In the period before the earthquake from January 1998 to February 2011, the time series were calculated along the coastal area from Aomori to Ibaraki. In Kumamoto region, the M7.3 earthquake occurred in April 2016. The time series were calculated wide area in the period from April 1997 to March 2016. In order to increase the spatial resolution, wide triangle was divided into some small triangles using new GNSS stations and the time series with small triangles were calculated in the period from 2009 to 2016.
Major features of the temporal change of the estimated areal strain are listed below from the northernmost one in the Tohoku region.
At the range of Hachinohe to Kamaishi, the areal strain continued to decrease.
At the range of Kamaishi to Shizugawa, the areal strain had decreased continuously from 1998, however the downward trend of areal strain was changed to stagnant since the beginning of 2007 at the latest.
At the range from Soma to Iwaki, the downward trend of areal strain was changed to stagnant since mid-2006, and in some places it showed the increased trend.
At the range from Iwaki to Kashima(Ibaraki) on the south area, the areal strain did not show significant changes.
At Kumamoto region, the areal strain in the wide area showed decrease and increase repeatedly in a short period of time, then it was changed to the trend of decrease and continued until Kumamoto earthquake. From the analysis of small triangle, Before Kumamoto earthquake, the areal strain decreased continuously in the area around Hinagu Fault, and it became clear that the decrease tendency was large, especially in the triangle including the hypocenter of the main shock.
From the above results of Tohoku region, it is made clear that the downward trend of areal strain was changed to stagnant in some places. In the Tohoku region, there is the general tendency of the shorting to east-west direction due to the subduction of Pacific Plate and areal strain should be showed the decrease continually. Nishimura et al (2012) calculated the de-trend time series of east-west components of GNSS and suggested that deceleration was caused by weakening of the coupling offshore of Fukushima and Ibaraki prefectures. It is generally method to subtract a reference station which is stable during the analysis period from the observation station for calculating the time series of crustal deformation by GNSS. However, in the case of the long-term time series analysis, it is difficult to choose a reference station that be observed stable displacement for a long time. The areal strain of a triangle with three continuous GNSS stations have advantages because of the method without a reference station. The results of the areal strain are consistent with that of Nishimura et al.(2012).
In the Kumamoto region, there are some issues about this study, for example, to elucidate the mechanism of the phenomenon occurred before Kumamoto Earthquake.

©2020. Japan Geoscience Union. All Right Reserved.

We believe that the time series analysis of areal strain is able to detect local space-time variations before an occurrence of an earthquake around a fault.

Keywords: Strain, Tohoku-Oki earthquake , Kumamoto earthquakes

©2020. Japan Geoscience Union. All Right Reserved.

Seasonal adjustment for tidal data (3)

*Tadafumi Ochi[1]

1. Institute of Earthquake and Volcano Geology, Geological Survey of Japan, The National Institute of Advanced Industrial Science and Technology

In this study, long-term tidal records, which contain sea level change data longer than a few months, are considered. Because the change of the tidal record consists of both an oceanic effect and a crustal deformation, it can be used for the monitoring tool of the long-term crustal deformation if we can remove the oceanic effect. The methods introduced by Tsumura (1963) and Kato & Tsumura (1979) overcame the problem under the assumption that the regional crustal deformation can be expressed as a linear change. On the other hand, recent studies revealed that interplate coupling changes not only spatially but also temporally --- sometimes, we regard the change as a long-term slow slip event. Hence a new method that allows a much flexible trend than the linear trend previous studies assumed is required. Ochi (2018, 2019; the meeting of the Geodetic Society of Japan) adopted the seasonal adjustment method to separate the oceanic effects and the crustal deformations from the tidal records and presented the results in southwestern Japan. In this method, I assumed the tidal records to be the sum of non-linear trends, seasonal variations, and residuals. Under the assumption, I ignored the seasonal variation component as the oceanic effect, and only the non-linear trend and residual components are regarded as the vertical crustal deformation. To verify the assumption, I compared the difference of the trend components between the neighboring tidal stations and the GEONET vertical components. The results show that these two data well agree in southwestern Japan, especially along the coast of the Pacific Ocean. In the presentation, I will show the results of the other regions in Japan.

Keywords: Tidal records, Long-term crustal deformation

©2020. Japan Geoscience Union. All Right Reserved.

Vertical annual cyclic movement model of Mainland China and its analysis based on GPS observations

*Hongbao Liang[1], Wei Zhan[1], Jinwu Li[1,2]

1. First Crust Monitoring and Application Center, CEA, Tianjin 300180, China., 2. School of Geodesy and Geomatics, Wuhan University, Wuhan 430079, China.

The annual cyclic deformation of Earth’ s surface can be obtained indirectly using existing models. However, the reliability in local areas is affected by numerous uncertain factors such as indirect observation, inversion algorithms, and complex earth media. In this study, the vertical annual cyclic movement model of Mainland China is built based on the direct observation of deformation by 234 continuous Global Positioning System (GPS) stations and unified data processing using the multisurface function method (referred to as the GPS model). The GPS model shows that the weighted root mean square (WRMS) is reduced for 97% GPS stations after applying the model correction. The average, maximum, and minimum reductions in the WRMS are 11.6%, 37.2%, and -3.6%, respectively. Compared with the global Gravity Recovery and Climate Experiment model and surface loading models, the GPS model is closer to the actual change due to direct and actual deformation observations. Additionally, the GPS model can accurately reflect the detailed motion characteristics of Mainland China, particularly in the neighbouring regions with severe environmental quality changes. The GPS model is extremely important for practical applications and geoscience research, such as the elimination of the nonstructural annual cyclic motion in vertical crustal deformation monitoring, the detection of the annual cyclic changes in glacial ablation, river water levels, and vegetation growth, and the investigation of the relationship between the vertical annual cyclic deformation and microseismic activity.

Keywords: Annual Cyclic Movement, Amplitude, Phase, Global Positioning System, Mainland China

©2020. Japan Geoscience Union. All Right Reserved.

Strain changes due to the co-seismic fault slips observed in Kobe

*Atsushi Mukai[1], Shigeaki Otsuka[2], Yoichi Fukuda[3]

1. Faculty of Urban Management, Fukuyama City University, 2. Former Professor at Kobe Gakuin University, 3. Graduate School of Science, Kyoto Univ.

Significant strain changes due to the 2018 northern Osaka earthquake were observed at Rokko-Takao station about 45 km away from the focus. These strain changes showed the step-like extension in the east-northeast direction for a few seconds just after arrival of the seismic waves. The direction of the maximum principal strain agreed with the calculated one based on the source process reported by Disaster Prevention Research Institute, Kyoto University (2018). We can reproduce the characteristics of the time development of the observed principal strains, if the rupture on the seismic fault had been expanding at 3 km/s from the focus.

Rokko-Takao station in Kobe passes through the fracture zone of Manpukuji fault. We have performed the continuous observation of crustal movements by using the Ishii-type three-component strainmeter and so on. When the 2018 northern Osaka earthquake (M6.1) occurred, we observed the strain changes with time constant of a few minutes and the extension of the order of 0.1 μstrain in the north-northwest direction. This maximum principal strain were far from the calculated one (+0.03 μstrain in the direction of N56°E) based on the source process, and was considered to be caused by the contraction of the fracture zone and the pore pressure increasing (Mukai et al., 2018). As shown by this case, the observation of strain changes at this station is significantly affected by the groundwater migration. However, we can expect to detect the strain step due to the source process just after the arrival of seismic wave, because the groundwater migration starts with some delay.

We observed the linear strain changes just after the arrival of the seismic waves and, as a result, the strain steps of the order of 0.01 μstrain. The maximum and minimum principal strains were +0.06 and -0.03 μstrain, respectively. The direction of the maximum principal strain was N61°E. This direction almost agreed with the calculated one based on the source process, although the magnitudes of the principal strains were about double of the calculated ones. It is considered that these discrepancies in the magnitude were caused by the dynamic properties of the surrounding crust with the fracture zone, and major part of the observed strain steps was caused by the co-seismic fault slips.
It is considered that the linear strain changes just after the arrival of seismic motions showed the crustal movements due to the time development of co-seismic fault slips, that is, the source process. In fact, we can reproduce the characteristics of the observed principal strain changes by using the source process with the rupture velocity of 3 km/s. However, there also remained some negligible discrepancies between the observed and the calculated principal strains. These discrepancies might be caused by the effect of pore pressure changes in the surrounding crust. In this study, we report the investigated results on the strain steps observed at the 2011 off the Pacific coast of Tohoku Earthquake as well.

Keywords: strain changes, fault slip

©2020. Japan Geoscience Union. All Right Reserved.

Development of the New GEONET Analysis Strategy

*Yasuaki Kakiage[1], Hiroki MURAMATSU[1], Kazuyuki OHASHI[1], Satoshi Abe[1], Tomoaki Furuya[1], Yuki Hatanaka[1]

1. Geospatial Information Authority of Japan

Geospatial Information Authority of Japan (GSI) has been operating GEONET (GNSS Earth Observation Network System) since 1996. Daily coordinates of GNSS- based control stations are estimated to monitor crustal deformations throughout Japan. The analysis strategy for daily coordinates of GEONET stations was updated five times so far. The latest fifth generation analysis strategy was developed in 2020. Daily coordinates have been estimated in parallel with the 4th generation analysis strategy which has been in operation since 2009. The main improvements from the previous analysis strategy are: 1. Updating the reference frame, 2. GNSS and GLONASS integration, 3. Improvement of the troposphere model, 4. Implementation of more stable fix-point analysis method for the daily coordinate estimation of the reference station (TSUKUBA1).

The fifth generation analysis strategy is divided into two parts; the "fix-point analysis" and that the “all-point analysis”. The "fix-point analysis" estimates the daily coordinates of the "Tsukuba-1” with respect to IGS (International GNSS Service) sites around the world. Based on the coordinates of the ITRF2014 model as the initial position, the coordinates are estimated by using constraint conditions referred to as No-Net-Translation. We estimated the coordinates of TSUKUBA1 since 1996 by using this analysis condition, but the stability of the coordinates decreased as going back to the past. For this reason, we analyzed the past data using the coordinates of the IGS repro2, which is the products of the IGS second reanalysis campaign from 1994 to 2015 based on ITRF2008. We used the coordinates of the IGS repro2 as the initial coordinates, and estimated the coordinates of TSUKUBA1.

The “all-point analysis” which estimates daily coordinates of each GEONET site based on the estimated coordinates of TSUKUBA1. The “all-point analysis” estimates three types of daily coordinates; GPS based solution, GLONASS based solution, and the coordinates based on the combination of the both systems. The accuracy of all the “all-point analysis” products was evaluated. In this talk, we will report on the stability of the “fix-point analysis” and the results of the verification of accuracy for the “all-point-analysis”.

Keywords: GEONET

©2020. Japan Geoscience Union. All Right Reserved.

Estimation of fault models by MCMC method

*Ryoji Kawabata[1]

1. GSI of Japan

Summary

The Geospatial Information Authority of Japan estimates the fault parameters by using observed coseismic displacement caused by large earthquakes. The fault models are indispensable to evaluate the surface displacement of the whole area, as well as the seismic activities near the source faults. However, we frequently face a difficulty in estimating the fault parameters uniquely due to non-linear dependency of the model parameters and to restriction of the available observation data. In this paper, we show the results of the fault model estimation for some large earthquakes by using Markov Chain Monte Carlo (MCMC) method in order to evaluate the fault parameters probabilistically.

Calculation method

We calculated the surface displacement by rectangular faults with a uniform slip in an elastic half space (Okada 1985). The coseismic displacement data is derived from the F3 solutions of the GEONET sites. We used Metropolis–Hastings algorithm for MCMC calculation to estimate the fault parameters. Parallel tempering (e.g. Sambridge 2013) is also applied to improve the efficiency of the MCMC sampling. All fault parameters are estimated in our analysis while many previous studies constrained some parameters such as fault direction (e.g., Ito et al. 2016, Ohno and Ohta 2018).

Results

In the estimation of the fault parameters of the 2011 off the Pacific coast of Tohoku Earthquake, we used two sectioned faults since single fault model shows systematic difference between the observed and calculated displacement. We found that marginal posterior probability density of the fault parameters show clearly peaked distribution. The calculated displacements by using the averaged values of the estimated parameters can well explain the observed data.

For the earthquake offshore Yamagata prefecture on June 18, 2019, we simultaneously estimate the parameters of two conjugate faults with two different strike angles. The result shows that it is difficult to determine the fault direction only by the GEONET data used in our analysis.

Keywords: Crustal Deformation, Inversion

©2020. Japan Geoscience Union. All Right Reserved.

Estimation on fault-slip distributions without smoothing constraints by Reversible-jump MCMC

*Fumiaki Tomita[1], Takeshi Iinuma[1], Ryoichiro Agata[1], Takane Hori[1]

1. Japan Agency for Marine-Earth Science and Technology

1. Introduction

Estimation of fault-slip distributions from geodetic data is generally performed by least squares methods with a spatial smoothing constraint on the slip distribution based on ABIC or L-curve. However, a viscoelastic inversion simultaneously estimating co- and post-seismic slip distributions [Tomita et al., 2018] require high computational costs due to many hyper-parameters for the spatial smoothing and data weights. Moreover, the inversion also requires non-negative slip constraints. When the non-negative slip constraints are imposed, it is known that ABIC cannot be accurately calculated [Fukuda & Johnson, 2008] and that its computational cost dramatically increases.

Therefore, we have developed a viscoelastic inversion approach using Reversible-jump MCMC (Rj-MCMC) [Green, 1995]. The method can estimate solutions based on a posterior density function (PDF) with non-negative slip constraints and can search numbers of unknown parameters. Tomita et al. [2019, SSJ] applied the Rj-MCMC method to synthetic data and showed that it can estimate slip distributions as well as the conventional ABIC inversion. However, it still has problems on efficiency and convergency of solutions. Here, we developed a Rj-MCMC method using Parallel Tempering (PT) that efficiently searches solutions [e.g., Sambridge, 2013].

2. Method & Data

This study employed the Voronoi-cell spatial separation and the formulations of Bodin & Sambridge [2009]. Because of the Voronoi-cell spatial separation, spatial smoothing constraints are unnecessary. PT prepares multiple replicas with different temperatures and swaps their temperature conditions to avoid local minimum solutions. To accelerate the computational speed, parallel calculation of replicas was performed by MPI.

We calculated synthetic data as responses to assumed fault-slips in an elastic media [Okada, 1992]. To investigate convergency and reproducibility of the slip distribution by Rj-MCMC, we assumed the single window slip distribution in the simple elastic media. The assumed fault geometry is a planer fault (300 km ×500 km) with the dip of 15 degrees imitating a subduction zone, which is composed by 20 km ×20 km subfaults. The assumed slip distribution is a smooth slip with a peak slip of 8 m at 75 km from trench. We prepared two patterns of the observational site distributions: (1) 150 onshore sites & 5 offshore sites and (2) 150 onshore sites & 150 offshore sites assuming the coast line of 200 km from the trench.

3. Results & Discussion

We performed the Rj-MCMC inversion to the above synthetic data with various numbers of PT replicas (4–16), of maximum temperatures (4–16), and of samples (10^5–10^7). As a result, the Rj-MCMC inversion successfully reproduced the assumed slip distribution regardless of the numbers of replicas and maximum temperatures when the samples were over 10^6. Moreover, we found fast convergence of the solutions when the number of replicas was large. Number of unknown parameters was reduced to ~10 for the site distribution (1) and to ~20 for the site distribution (2). This difference reflects their spatial resolutions depending on the site distributions. The PDF for each parameter at a subfault for the site distribution (1) showed a smooth distribution, while that for the site distribution (2) showed multiple steep peaks. This suggests that the site distribution (2) has evident local minimums. However, we successfully reproduced

©2020. Japan Geoscience Union. All Right Reserved.

the assumed slip distribution because ensemble of the multiple replicas prevented the slip distribution from biasing.
In this study, we confirmed that PT improved convergence of the solutions and that Rj-MCMC can reproduce the assumed slip distribution. We'll investigate whether the local minimums for the site distribution (2) can be avoided by changing the numbers of PT replicas and maximum temperatures. Moreover, we'll also investigate reproducibility of the slip distributions by Rj-MCMC assuming various patterns of the assumed slip distribution.

Keywords: Geodetic inversion, Smoothing constraint, Reversible-jump MCMC, Trans-dimensional inversion

©2020. Japan Geoscience Union. All Right Reserved.

Analysis of ocean bottom pressure gauge data by a hybrid method of MSSA and fitting of a parametric function

*Koichi Murata[1], Toshinori Sato[2], Hajime Shiobara[3], Masanao Shinohara[3], Tomoaki Yamada[4]

1. Graduate School of Science and Engineering, Chiba University, 2. Graduate School of Science, Chiba University, 3. Earthquake Research Institute, University of Tokyo, 4. Japan Meteorological Agency

It is known that slow-slip events (SSE) have repeatedly occurred off the Boso Peninsula, with a recurrence interval of several years. Earthquakes are rapid slips on fault surfaces, on the other hand, SSEs are slow slips on them. SSEs are considered one of stress release mechanisms that a fault slips slowly at the plate boundary. Thus, understanding of SSEs is important for a full understanding of tectonic behavior at plate boundaries. To detect vertical motion of ocean floor during the Boso SSEs by using ocean bottom pressure gauge (OBP) data, we propose the following method. First, we applied Multi-channel Singular Spectrum Analysis (MSSA) to extract and remove short-term (up to 20 days) periodic components from the OBP data. Next, we fit a parametric function to the remaining long-term periodic components of the OBP data. The parametric function represents the annual and semi-annual seasonal variations, and the vertical offset due to the Boso SSE. To verify the method, we applied the method to OBP data which include the 2018 Boso SSE.

We observed ocean bottom pressure from August 2016 to September 2018 using 4 OBPs that are composed of pressure gauges of Paroscientific Inc. During of this period, it was clarified that the SSE occurred in June 2018 from the GNSS data.

Sea water depth changes converted from observed pressure changes have not only transient displacements due to the SSE but also several components which affect the sea water depth. First, we removed tidal components and smoothed the time series by calculating a 7 day moving average to remove periodic variations which have up to about several days' periods. Next, to remove periodic variations such as atmospheric pressure changes, oceanic changes, and so on, which have from several to about 20 days periods, we applied MSSA with the window interval of 20 days to the smoothed time series. Results of MSSA extracted principal components (PC) 1 and 2 which about annual to semi-annual periods were distinguished, PC3 and 4 which about 20 days periods were distinguished, and noise components which contributed to the time series lesser than them.

We considered that PC3 and 4 were variations due to atmospheric pressure changes, oceanic changes, and so on. Thus, we removed them as well as noise components. We reconstruct signals by summing the remaining PC1 and 2. We assumed that the long-term periods included in the reconstructed signals were the same as them included in the GNSS time series. Then we fitted a parametric function which represents the annual and semi-annual seasonal variations, and the vertical offset due to the Boso SSE to the reconstructed signals. The fitting results extracted up-lifts of all stations. They (and root-mean-square error) were 15.5 mm (13.8 mm) at BOSO1, 23.6 mm (6.7 mm) at BOSO2, 21.0 mm (6.5 mm) at KAP2, and 13.1 mm (6.9 mm) at KAP3.

To verify the present method, we estimated the slip distributions of the 2018 SSE from displacements extracted from the following two methods. One is the conventional method which only the fitting of the parametric function was performed. The other is the present method. Comparing the RMS of residual of the vertical motion at the OBP stations, the RMS of the present method is 58% smaller than that of the

©2020. Japan Geoscience Union. All Right Reserved.

conventional method. Therefore, we can extract the vertical motion due to the SSE more correctly when MSSA and the parametric fitting are used together.

Acknowledgments
We thank the captains and crew of R/V Kaiyo-maru No.3 and R/V Kaiyo-maru No.5 of Kaiyo-engineering Inc. for their support.
This study utilized the data set "the daily F3 coordinate values of GNSS-based control stations" by the Geospatial Information Authority of Japan.
This work was supported by the Earthquake and Volcano Hazards Observation and Research Program authorized by the Ministry of Education, Culture, Sports, Science and Technology.
This work was supported by JSPS (25287109).

Keywords: Slow Slip Event , ocean bottom pressure gauge, Multi-channel Singular Spectrum Analysis

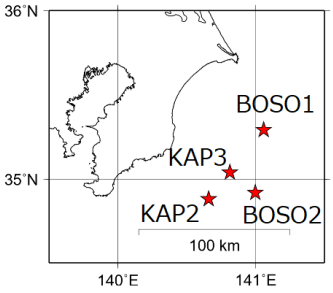

図1.BOSO1、BOSO2、KAP2、KAP3の各観測点の配置

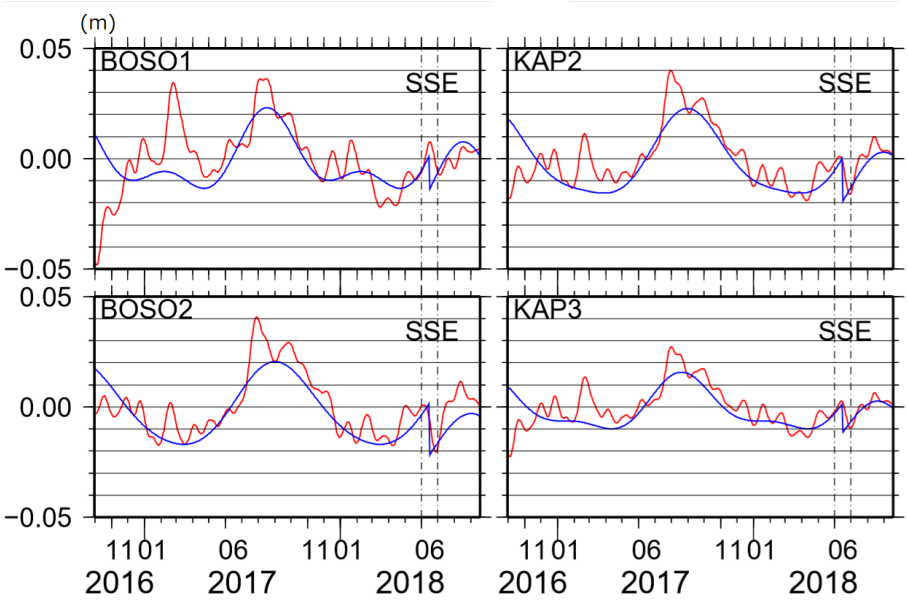

図2.各観測点の再構成信号(赤線)とフィッティング曲線(青線)

©2020. Japan Geoscience Union. All Right Reserved.

Earthquake potential in Costa Rica estimated by the integration of the interseismic geodetic data with seismicity records and inland faulting traces

*Luis Alejandro Carvajal Soto[1,2], Takeo Ito[2], Marino Protti[3], Hiroshi Kimura[2]

1. Universidad Latina de Costa Rica, 2. Nagoya University, 3. Universidad Nacional de Costa Rica

The western border of the Panama Microplate (PM) is presented by the Central Costa Rica Deformed Belt, a diffuse predominant northwest dextral-strike and conjugated northeast sinistral-strike faulting area. This diffuse boundary crosses Central Costa Rica (CCR) from the Caribbean Coast, including the Metropolitan Area (most dense population area in Costa Rica) and the Central Pacific coastline to intersects the Meso American Trench along the subduction of the Cocos Plate (CO).

We use 139 GNSS observation sites located in Nicaragua, Costa Rica and Panama for inversion finding that the crustal deformation in Costa Rica is mainly arranged in three groups: 1). Northwestern Costa Rica is dominated by a northward deformation with rates up to 25 mm/yr, rotating and decreasing up to 12 mm/yr northwestward following the Central American Forearch. 2). Southeastern Costa Rica shows deformation to the North-eastward up to 40 mm/yr (opposite to northwestern Costa Rica). 3). Central Costa Rica is characterized by a diffuse deformation pattern oriented mainly to northward, with deformation rates up to a half of those observed in northwestern and southeastern Costa Rica.

By the integration of the interseismic geodetic data with seismicity records and inland faulting traces, we evaluated the crustal deformation in Costa Rica in 3 kinematic models with different spatial geometries of the tectonic configuration around Central Costa Rica, and determine the earthquake potential in Costa Rica using the best model. Crustal deformation in Costa Rica and surroundings is modeled as result: i) kinematic effects of rigid block motions, ii) elastic deformation due to the interaction on subduction and inland tectonic interfaces and iii) internal strain of each tectonic block. We adopted the Markov Chain –Monte Carlo method in order to estimate the Euler poles of each tectonic block, slip deficit rates (SRD) on block interfaces, and internal strain of each block.

Assuming that the seismic moment in the subduction and inland interfaces is accumulated only as elastic strain and is released co-seismically, the resulting seismic moment accumulated rates in the best model reflect capacity for producing Mw 8.2 earthquakes every 318 ±16 years in southwestern Costa Rica, Mw 7.3 earthquakes every 55 ±7 years beneath CCR, and Mw 8.5 earthquakes every 231 ±21 years in southeastern Costa Rica, as the upper limits of the earthquake potential produced by the Cocos Plate convergence.

Our assumption represents an upper limit of the earthquake potential since additional effects may contribute to the release of accumulated slips, such as the post-seismic deformation, plastic deformation, and the occurrence of slow slip events.

Keywords: Central Costa Rica, Earthquake potential Costa Rica, Crustal Deformation Costa Rica

©2020. Japan Geoscience Union. All Right Reserved.

©2020. Japan Geoscience Union. All Right Reserved.

The Fault model of the 2017 M5.6 earthquake estimated from precise leveling survey data in the Eastern flank of the Ontake volcano 2

*Masayuki Murase[1], Fumiaki Kimata[2], Yoshiko Yamanaka[3], Takeshi Matsushima[4], Hitoshi Yamashita Mori[1], Daisuke Sato[1], Takahiro Kunitomo[3], Yuta Maeda[3], Shinichiro Horikawa[3], Takashi OKUDA[3], Kenjoro Matsuhiro[3], Kazushi Tanoue[3], Kazunari Uchida[4], Shin Yoshikawa[5], Hiroyuki Inoue[5], Takahiro Yanada[6], Takahiro Kako[1,6], Hiroyuki Ishimori[6]

1. Department of Earth and Environmental Sciences, College of Humanities and Sciences, NIHON University, 2. Tono Research Institute of Earthquake Science, 3. Earthquake and Volcano Research Center, Graduate School of Environmental Studies, Nagoya University, 4. Institute of Seismology and Volcanology, Kyushu University. , 5. Aso Volcanological Laboratory , Kyoto University, 6. Japan meteorological agency

The M5.6 earthquake occurred at the Eastern flank of Ontake volcano in June 25, 2017. The fault models were estimated from precise leveling survey data conducted in the Eastern flank of Ontake volcano in the periods including and after the earthquake, respectively.

We conducted the precise leveling surveys after the 2014 eruption in the Ontake volcano. The leveling routes of about 38 km with 98 benchmarks were established on the eastern flank of the Ontake volcano. The main routes were extended to the Yashikino village (Kakehashi and Yashikino routes). In order to improve the spatial layout of the benchmarks, a branched leveling routes were established (Kiso-Onsen, Ontake Ropeway and Nakanoyu routes). The epicenter of the M 5.6 earthquake is located just beneath these leveling routes.

The leveling surveys of all routes were conducted in April 2017, April 2018 and April 2019. In September 2017, the leveling survey was conducted in the Yashikino and Kiso-Onsen routes. The leveling data in April 2017 and September 2017 ware used to detect the vertical deformation associated with the M 5.6 earthquake. The leveling data in the periods during September 2017-April 2018 and during April 2018-April 2019 were used to detect the post-seismic deformations after the M 5.6 earthquake.

Using the detected vertical deformations, a single rectangular fault was estimated. The parameters of the fault geometry were assumed form hypocenter distribution of aftershocks estimated by using DD method. parameters of latitude, longitude and depth were optimized using a genetic algorithm (GA) in order to conform to the vertical deformation during the April 2017 and September 2017. In order to estimate detail slip distribution, the optimal single fault was divided into 12 sub-faults. Akaike's Bayesian information criterion (ABIC) was used to choose the smoothing hyperparameter for the inversion of the sub-fault slips. Using the vertical deformation during September 2017-April 2018, the after-slip distribution was estimated on the assumption that fault geometry of after-slip is the same as that of co-seismic one.

In the results, the benchmarks of the Yashikino and Kiso-Onsen routes showed the uplifts in the period from April 2017 to September 2017. The maximum uplift of 28mm was detected in central part of Yashikino route. In the after-seismic periods during September 2017-April 2018, uplift with maximum of 5 mm was detected in the same region. There is no significant uplift during April 2018-April 2019. As the longest, the post-seismic deformation seem to finish within the 10 months after the earthquake. The slip distribution was suggested mechanism of left lateral with reverse fault in the period from April 2017 to September 2017. Mw 5.2 was calculated from the fault model. The after slip distribution showed the

©2020. Japan Geoscience Union. All Right Reserved.

almost same pattern of co-seismic one.

The left lateral slip was mainly estimated on this fault in our model. According to the centroid moment tensor solution (CMT), the M 5.6 earthquake was estimated as reverse fault mechanism. However, some aftershocks were estimated as mechanism of lateral slip. We believe that the slips of not only reverse slip but also lateral slip occurred in this area. Because of the M 5.6 earthquake estimated as the reverse fault mechanism from CMT, the lateral slip seems to occur as aseismic slip. Ito and Matsuhiro (2018) suggested that it is difficult to explain horizontal deformations detected by GNSS as the reverse fault and also reported that deformation rate of GNSS is changed after the earthquake. The deformations detected GNSS are consistent with the existence of the aseismic slip after the earthquake.

From the above discussion, we believe that the left lateral slip occurred as aseismic slip after the M 5.6 earthquake with the reverse fault. As the longest, the aseismic slip seem to finish within the 10 months after the earthquake.

Keywords: Ontake volcano, fault model, precise leveling

©2020. Japan Geoscience Union. All Right Reserved.

Change in area strain around Toyama prefecture during the period of 2005–2018

*Kohei Hotta[1]

1. University of Toyama

Change in area strain in and around Toyama prefecture during the period of 2005–2018 was examined. Final solutions F3 daily coordinate data from GNSS Earth Observation Network System (GEONET) stations in and around Toyama prefecture (25 stations; operated by Geological Information Authority of Japan) were used. Triangulation of these stations was performed by the TRIANGULATE command of GMT (Wessel and Smith, 1998). Change in area strain within each triangle during the period from October 2006–October 2018 was investigated.

The founding was as follows: (1) Extension in Toyama bay caused by Noto Hanto earthquake in 2007 was still continuing as of 2018. (2) Extension of whole Toyama was detected except around northwest area where contraction was detected in 2011 –when the Great East Japan earthquake and earthquake swarms in west Toyama was occurred in March and October, respectively. (3) After the Kamishiro fault earthquake occurred in November 2014 which caused large strain changes around east to southeast area of Toyama prefecture, contraction detected around northwest area started to proceed. (4) Inflation and the following contraction around Midagahara volcano were found when fumarole activities started in 2012.

Keywords: GEONET, area strain, Toyama

©2020. Japan Geoscience Union. All Right Reserved.

Estimation of Deformation Fields from GNSS Data Using Basis Function Expansion: Comparison with the Method by Shen et al. (1996)

*Tomohisa Okazaki[1], Yukitoshi Fukahata[2], Takuya Nishimura[2]

1. Center for Advanced Intelligence Project, RIKEN, 2. Disaster Prevention Research Institute, Kyoto University

Crustal displacements can be accurately measured by GNSS at observation stations. Many methods have been developed to estimate continuous velocity and strain-rate fields from discrete GNSS data to interpret crustal deformation. Shen et al. (1996) proposed a method to simultaneously estimate velocity and strain-rate fields, in which observed data are weighted according the distance to an estimation point in the least-square calculation. Their method is intuitive and widely used particularly in Japan. From a theoretical viewpoint, however, their method has a serious problem that the estimated strain-rate field does not coincide with the derivative of the estimated velocity field (Okazaki and Fukahata, JpGU 2018). In addition, there is no objective criterion to determine the form of the weighting function in the least-square calculation.

As an alternative consistent method, we present a fitting of velocity fields using basis function expansion. On the estimation of crustal movements, Fukahata et al. (1996) developed a method to reconstruct time variation of vertical crustal movements using levelling data. We modify their formulation to estimate a 2D horizontal velocity field using GNSS data. Since the velocity field is represented by a linear sum of a finite number of basis functions, its derivative, i.e. the strain rate field, can be analytically obtained. A hyperparameter that controls the smoothness of the velocity field can be objectively determined from observed data using ABIC (Yabuki and Matsu'ura, 1992, GJI). In addition to these theoretical advantages, we practically demonstrate the characteristics and merits of this method compared with the method by Shen et al. (1996) by applying them to GNSS velocity data in Japan.

Keywords: GNSS, basis function expansion

©2020. Japan Geoscience Union. All Right Reserved.

Reconsidered source model of short-term slow slip event by using spatial distribution of strain change

*Noa Mitsui[1], Yasuhiro Asai[1], Satoshi Itaba[2]

1. Tono Research Institute of Earthquake Science, 2. National Institute of Advanced Industrial Science and Technology

Various slow earthquakes detected in the subduction zone are modeled as fault slips, just like ordinary earthquakes, but the mechanism generating episodic slow slips is unclear. On the other hand, knowledge of the fault strength suggests that source region of the deep slow earthquakes locates a brittle-ductile transition zone associated with the depth dependence of temperature-pressure conditions. With the transition from brittle to ductile fracture (or ductile flow), plastic deformation increases in plate boundary rocks. The plastic deformation occurs as strain caused by three-dimensional deviatoric stress, and it may not be able to be modeled by using only fault slip. The additional deformation mode can be detected as the normal component to the fault plane. Therefore, in this study, we re-estimate the source model for the short-term slow slip event (S-SSE), which is one of the deep slow earthquakes.

In this re-estimation, the azimuthal coverage of observation points is important. For example, source model of the 2001 Tokai SSE, one of the long-term slow-slip events (Mitsui & Ito, 2019), was re-estimated as tensile deformation normal to the fault plane in addition to fault slip. At the observation point located in the direction of the rake angle (southeastward in the case of Tokai SSE), there was no difference in surface displacement whether the source has tensile deformation or not, while at the observation point located in the opposite direction (northwestward), a remarkable difference was observed mainly in the vertical component of surface displacement.

Although many deep S-SSEs have been reported in the Tokai region (e.g., AIST, 2018), all of the stations used to estimate the source model are located on the coast side (in the direction of rake angle). Therefore, we use additional data of strain meters and stress meters owned by Tono Research Institute of Earthquake Science (TRIES) located in Mizunami City and Toki City, Gifu Prefecture, which is the inland side of the S-SSE source. And we will re-estimate the source model to discuss the existence of non-fault slip component of deformation in the source.

As a preliminary study, we calculated synthetic strain changes at the observation points based on the source model of S-SSE, which occurred in November 2017 (AIST, 2018). We also used a model in which a part of the estimated fault slip amount is reduced and the reduced slip is given as tensile dislocation normal to the fault plane. As a result, the more tensile dislocation increases, the more compressive strain increases causing the change of the direction of the principal strain at the inland observation point. This result suggests that a more appropriate source model can be obtained by using data observed at inland side.

The strain changes due to S-SSE observed by TRIES strain meters and stress meters are consistent with the above synthetic strain changes, and these data are useful for estimating the S-SSE source model.

Keywords: slow slip, strain, source model

©2020. Japan Geoscience Union. All Right Reserved.

Bayesian l_1 trend filtering for slow slip detection

*Keisuke Yano[1], Masayuki Kano[2]

1. The University of Tokyo, Graduate School of Information Science and Technology, 2. Tohoku university, Graduate School of Science

This study focuses on automatic detection for slow slip events (SSEs), which are a geodetical signal of slow earthquakes. SSEs are classified into two types according to their slip durations: long-term SSEs for durations of months to years, and short-term SSEs for durations of a couple of days to weeks. Recent geodetic observations have detected many short-term SSEs in many subduction zones such as Nankai and Cascadia. SSEs are related to the other types of earthquakes including large earthquakes, and therefore refined analysis of SSEs contributes to a better understanding of earthquakes. Detecting SSEs, which is our focus here, is the first important step in the analysis. The automatic detection method based on Akaike Information Criterion (AIC) has been proposed [Nishimura, et al., 2013] and has increased a number of detectable SSEs along the Nankai Trough, southwest Japan.

In this study, we propose a new Bayesian method for detecting short-term SSEs using Global Navigation Satellite System. The proposed method models SSEs as change points of polynomial trends in observations, and employs a Bayesian version of ℓ_1 trend filtering. ℓ_1 trend filtering [Kim, et al., 2009] gives trend estimates that are piecewise polynomial, and hence it fits the analysis of time series having an underlying piecewise polynomial trend. It provides change points of a piecewise polynomial trend and so has been used to detect change points in underlying trends [Rojas and Wahlberg, 2015]. Our Bayesian version of ℓ_1 trend filtering provide not only estimates of change points but also the uncertainty of them. We report the performance comparison of our method to the AIC based detector [Nishimura, et al., 2013] through simulation studies (as well as the real data).

Keywords: Slow slip events, GNSS, Trend filtering

©2020. Japan Geoscience Union. All Right Reserved.

Detection of multiple inflection points in time-series of GNSS-acoustic data for a shallow part of the Nankai Trough based on a MCMC method

*Ryoya Igashima[1], Yuta Mitsui[2]

1. Nagoya University, 2. Shizuoka University

Long-term slow slip events (SSEs) had been detected by onshore GNSS array and mainly estimated at a deeper part of locked zone on subduction plate interface, but recently we are able to estimate long-term SSEs at a shallow part of the subduction zone thanks to development of seafloor GNSS-A measurement (Yokota and Ishikawa, 2020). Here we try to detect unsteady seafloor deformation along the Nankai Trough from the GNSS-A time-series data, using a Markov Chain Monte Carlo (MCMC) method which does not assume a fixed duration (e.g. 1 year) of unsteady deformation. We expect that this method is useful to detect multiple inflection points with uncertainties (as posterior probability distribution). As a result, we find six observation points with unsteady deformation after 2012. One point suffers a very long-term (over five years) undefined event, probably a landslide-like event. Other two points are influenced by previously-reported slow earthquakes based on different observations (Kobayashi, 2014; Araki et al., 2018). In the other three points, the unsteady deformation can be explained by a long-term SSE (~Mw7) in a shallow part along the Nankai Trough as proposed by Yokota and Ishikawa (2020).

Keywords: unsteady deformation, GNSS-acoustic data, MCMC method

©2020. Japan Geoscience Union. All Right Reserved.

GNSS observation around a shear zone in southern Kyushu, southwest Japan (The fourth report)

*Tsuyoshi Watanabe[1], Koichi Asamori[1], Akiomi Shimada[1], Hiroki Ogawa[1], Atsushi Saiga[1], Koji Umeda[2]

1. Japan Atomic Energy Agency, 2. Hirosaki University

Recent strain rate analyses using GNSS velocities detect an active shear zone with high shear strain rate over 10^{-7}/yr in southern Kyushu, where large or moderate-size crustal earthquakes such as the 1997 Northwest Kagoshima earthquakes (M6.5, M6.3) have occurred frequently. However, obvious active faults are not identified there. It suggests that high shear strain rate and sequential earthquakes are responsible for the fault slip in a deep part of the earth’s crust. To investigate the crustal deformation in more detail, we established 10 GNSS observation sites across the shear zone and started observation from March in 2016.

Firstly, we estimated daily site coordinates at above 10 GNSS sites during the period from April 18, 2016 to November 17, 2019 (about 3.6 years) using Bernese GNSS Software (ver.5.2). In this time, 4 GEONET sites operated by Geospatial Information Authority of Japan were utilized as reference points. Then, we corrected the time series of daily site coordinates by subtracting following 3 factors: 1) common mode bias calculated from F3 solutions of about 150 GEONET sites located in Kyushu region, 2) viscoelastic crustal deformation after the 2016 Kumamoto earthquake, and 3) volcanic crustal deformation accompanied with the activity of Sakurajima and Kirishima volcanoes, from original time series of daily site coordinates. After the process, site velocities were estimated along with annual and semi-annual variations.

Secondly, as for interpretation of the obtained site velocities, a vertical strike-slip fault model proposed by Savage and Burford (1973) was applied. This model reproduces the situation that a fault is locked from the earth’s surface to a certain depth, a locking depth, and the fault is slipping at a constant velocity, a slip rate, which is relative rigid block motion below the locking depth. At this time, the surface velocity profile normal to the fault strike is expressed as a function of arctangent across the fault. Although we tentatively assumed the strike of the shear zone to be N110˚E based on the shear strain rate distribution derived from GNSS velocities so far, we estimated the optimum strike direction of the shear zone using the site velocities by conducting a grid search with the range from N90˚E to N120˚E each 0.1˚. As a result, the optimum strike direction was found to be N104.8˚E.

Finally, using the determined strike of the shear zone in this study, the slip rate and locking depth were estimated to be 12.9±1.8 mm/yr and 22.4±6.9 km through a nonlinear least-squares fitting the site velocities to above mentioned fault model (Figure 1). For the analysis, we used the velocities at sites located in the ranges of 60-80 km in north and south and 25 km in east and west from the center of the shear zone (32˚N, 130.5˚E). In addition, we investigated the discrepancy of estimated values (slip rate and locking depth) and estimation errors arose from the difference of the observation period (for 3.6 years and 2.0 years), as an accuracy evaluation about them. The slip rate and locking depth were in good agreement with each other within the errors, and then, we confirmed that the longtime observation reduced the estimation errors and restrained the scattering of site velocities.

Since the strike of the shear zone estimated from observation and analysis in this study is well consistent with the strike of a source fault of the 1997 Northwest Kagoshima earthquakes, which is nearly E-W direction based on the aftershocks distribution, this suggests a possibility that the fault slip in the lower crust is mainly involved in the occurrence of the earthquakes.

©2020. Japan Geoscience Union. All Right Reserved.

This study was carried out by a contract with the Agency of Natural Resources and Energy, part of the Ministry of Economy, Trade and Industry of Japan as part of its R&D program supporting development of technology for geological disposal of high-level radioactive waste.

Keywords: shear zone, slip rate, locking depth, 2016 Kumamoto Earthquake, visco-elastic deformation, GNSS observation

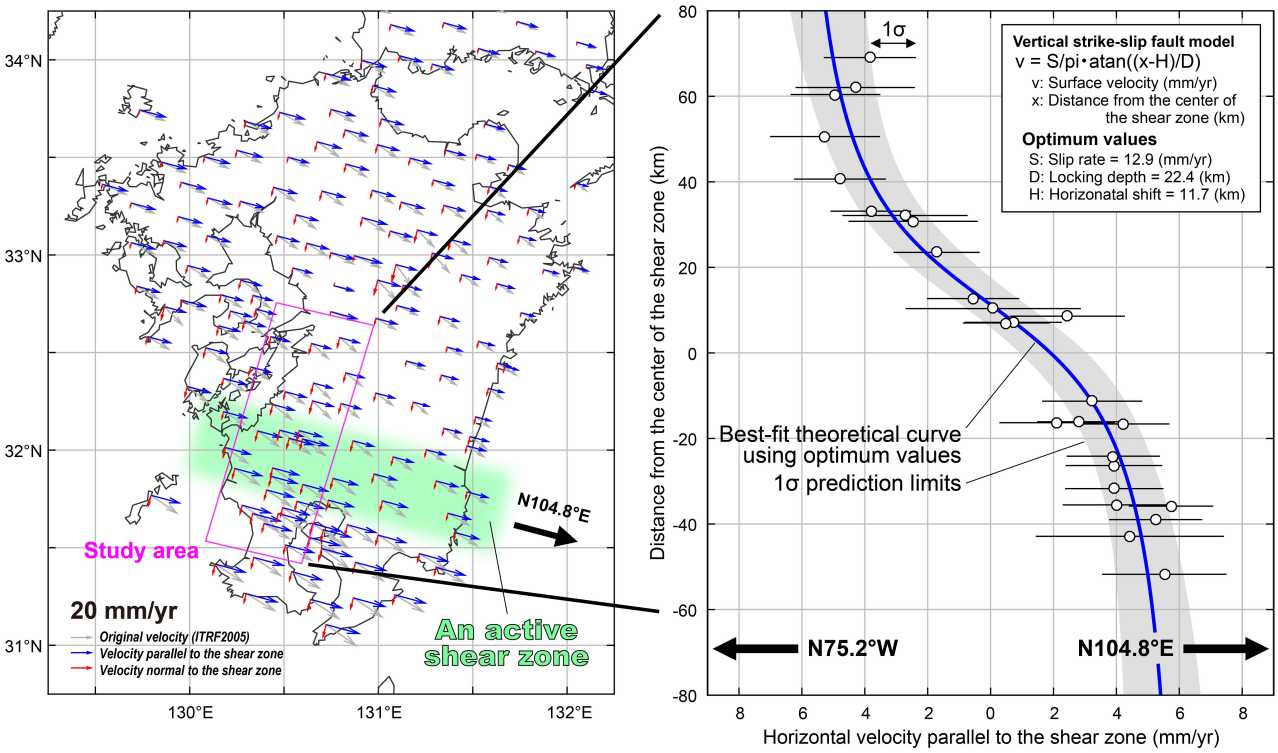

Figure 1) Observed velocities and velocity profile parallel to the shear zone

©2020. Japan Geoscience Union. All Right Reserved.

Seismic Risk on the Northern Xiaojiang Fault Implied by the Latest and Nearest GPS Observations

*Zhen Fu[1], Lisheng Xu[1]

1. Institute of Geophysics, China Earthquake Administration

The Xiaojiang fault zone, part of the southeastern boundary fault zone of the Tibetan Plateau, exhibits high seismic activity due to its complex structure. On the basis of continuous and dense GPS observations covering the northern segment of the Xiaojiang fault zone (n-XJFZ) from March 2012 to March 2016, we present the velocity field, spatiotemporal deformation, slip rate and locking depth of the n-XJFZ. The results provide strong support for achieving a better understanding of the deformation behavior of this fault. The heterogeneity of the GPS velocity field and the relatively nonuniform distribution of seismicity suggest that the observational area is fragmented. Shear strain has been accumulating with an almost constant azimuth, which is consistent with the trends of mapped major faults. The 2014 *M*s 6.5 Ludian earthquake produced a sudden change in the dilatational strain, which was almost constant prior to the event. Despite the nonuniform deformation in the study area, the average strain rates of the whole study area and the northern and southern subareas all increased after the Ludian earthquake, revealing that the n-XJFZ is becoming more locked. These results imply that the seismic risk in the study area is currently rising and that, similar to the 2014 *M*s 6.5 Ludian earthquake, future earthquakes will possibly occur away from mapped faults.

Keywords: GPS, Xiaojiang Fault Zone, seismic risk

©2020. Japan Geoscience Union. All Right Reserved.

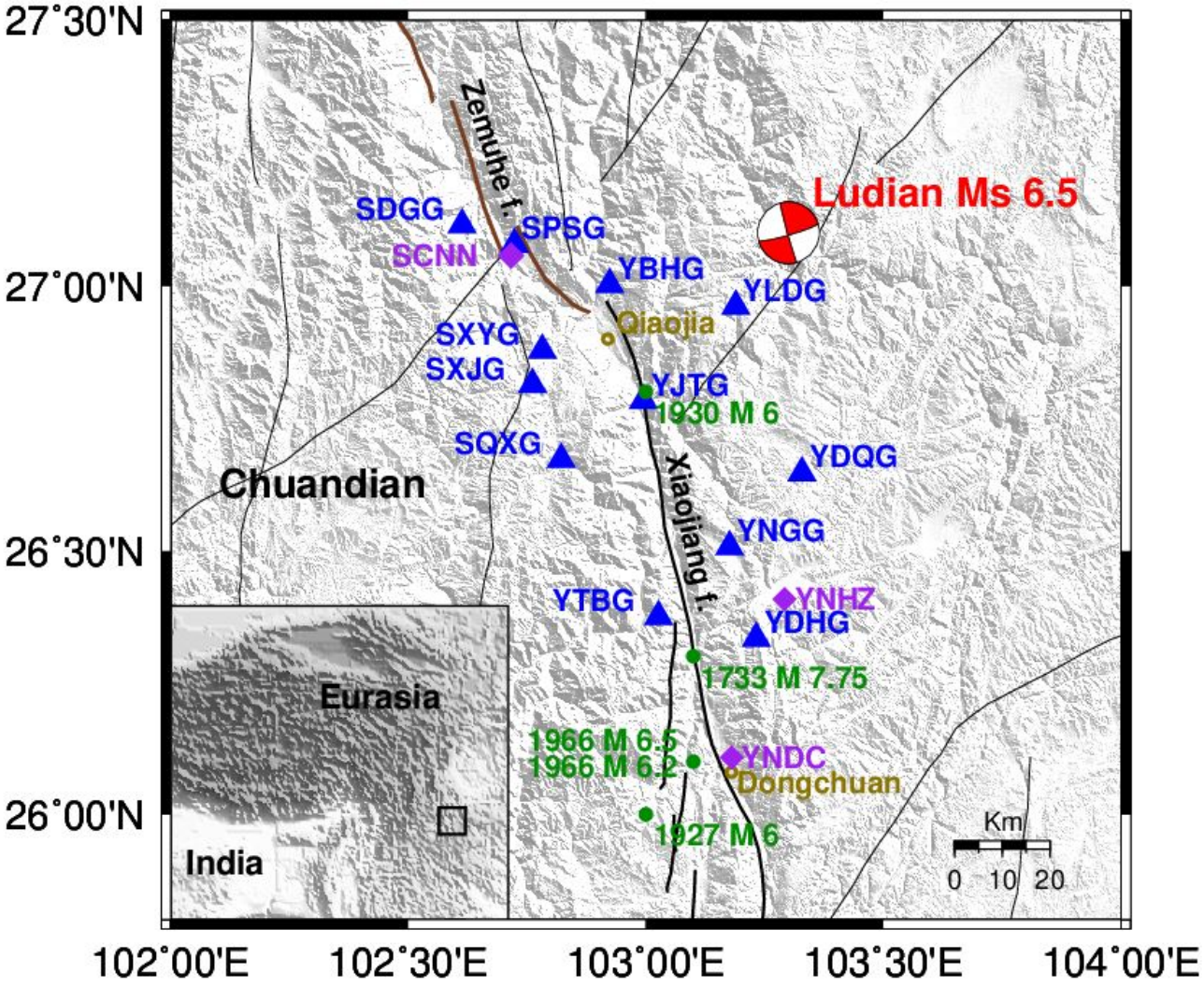

©2020. Japan Geoscience Union. All Right Reserved.

An Analysis for the Shape of Subducting Oceanic Plate using Shortest-Path Algorithm in GIS

Yuki tsukamoto[1], *Shinsuke Okada[2], Tatsuya Sumita[3], Daisaku Kawabata[3]

1. Graduate School of Science, Tohoku University, 2. International Research Institute of Disaster Science, Tohoku University, 3. Geological Survey of Japan, National Institute of Advanced Industrial Science and Technology

Around the Japan arc, plate-boundary earthquakes, intracontinental earthquakes including inland earthquakes, and oceanic plate earthquakes occur. And, the occurrence of these earthquakes is closely related to the subduction of the Pacific and Philippine Sea plates. To understand the tectonics of the island arc, it is important to understand the shape of the subducting plate and to examine its relation to the spatial distribution of the major landforms, active structure, seismicity, and geological structure. In the previous study, the shape of the subducting oceanic plate has been estimated by geophysical methods (seismic activity, seismic tomography, receiver function analysis, etc.). However, in regions without seismic activity, interpolation may have been applied to estimate the shape of subducting plate, the shape of plate is not always accurately captured. Therefore, in this study, we analyze the shape of the subducting plate from a geometric viewpoint different from the geophysical methods. The purpose of this study is to analyzing the shortest distance and shortest path using GIS and evaluate the shape of subducting plate geometrically.

In this study, we first developed a method to analyze the shape of subducting plate using the shortest distance and the shortest path from the starting point of the subduction, assuming the subducting plate as a spherical shell. Next, this analytical method was applied to three types of plate shapes showing normal subduction, rupture, to confirme that our analysis method can evaluate the plate shape. Finally, we applied our analytical method to the shape of subducting Philippine Sea plate, and revealed the distribution of deformation such as rupture and overlapping. The result of deformations was compared with the spatial distribution of inland active faults.

In the analysis of the shortest distance by GIS, the distance between two points is measured along the grid points of the DEM, which is calculated longer than the distance between the two points with a straight line. This effect was corrected by calculating the ratio between the angle of two points and the analysis distance, and incorporated into the analysis method. The analytical method developed in this study (correction applied) was applied to the three shapes of the subduction plate reproduced by the combination of spherical shells, indicating normal subduction, ruptured subduction, and overlapping subduction. The result of these from result, we could confirm that our analytical method developed in this study can evaluate the shape of subducting plate such as rupture and overlapping.

Finally, we applied our analytical method to the shape of the subducting Philippine Sea plate. As a result of Philippine Sea plate, overlapping was confirmed around the Ise Bay area and rupture was observed around the Kii strait. Comparing the results of the plate shape with the distribution of active faults in the Japan arc, it was found that active faults are densely distributed around the Ise Bay area where consistent with overlapping area of the Philippine Sea plate. Especially, the reverse faults in the north-south strike are in harmony with the direction of the compressive stress in the east-west direction due to the overlapping Philippine Sea plate. On the other hand, distribution of the active fault is sparse around the Kii strait and its northwest extension, which is consistent with rupture of the subducting plate. The rupture of plate does not accumulate the strain of crust in the island arc.

©2020. Japan Geoscience Union. All Right Reserved.

In our analysis, we could not analyze the plate shape from the Izu Peninsula to central mountainous region, because the plate boundary (subduction starting point) around the Izu Peninsula is missing in the data used in this study. Setting the subduction starting point with reference to other data and analyzing the plate shape from Izu Peninsula to central mountainous region remained as a future issue.

Keywords: Geographical Inforamtion System (GIS), Shortest path analyst, Plate geometry, Philippine sea plate, Spherical shell tectonics

©2020. Japan Geoscience Union. All Right Reserved.

Toward the development of a kinematic block motion model in Indonesia based on GNSS observation

*Rio Raharja[1], Takeo Ito[1], Hiroshi Kimura[1], Irwan Meilano[2]

1. Graduate School of Environmental Studies, Nagoya University, Japan, 2. Faculty of Earth Sciences and Technology, Bandung Institute of Technology, Indonesia

Indonesia is located in a tectonically complex region and lies in the interaction of four major plates. This interaction resulted in seismic activity in Indonesia and is one of the highest in the world. The earthquake not only occurred along a trench but also in inland fault, which is some of them were destructive. With this condition, research on evaluating the earthquake potential in Indonesia becomes urgent. To assess the earthquake potential, defining the boundaries between each crustal block become fundamental.

In this research, we use GNSS data derived from Indonesia CORS Network (InaCORS) and Sumatran GPS Array (SuGAR). The total number of sites that used in this research is 205 sites with a period from 2008 to 2018. We use Bernese 5.2 software for analyzing the GNSS data and get the velocity field. In order to evaluate the quality of our velocity field, we compare our velocity field with previous study (Koulali et al., 2017). We estimate the euler pole of Koulali's Sunda block. In this estimation, we only used the same sites with Koulali et al. (2017). The biggest difference between our velocity field and Koulali et al. (2017) is about 3 mm/yr. In here we assume that this difference is due to the differences in the observation period and the observation errors.

Our velocity field in the eastern part of Indonesia (from 120°E to the east) is almost completely in line with the block boundaries defined by Bird (2003). In other hand, in the western part (from 120°E to the west), our velocity filed shows disagreement with his block boundaries in Sumatra region. In order to resolve this disagreement, we define new block boundaries in the western part and also make some modification of block boundaries from previous studies in the eastern part.

We employ the MCMC (Markov Chain Monte Carlo) method to generate many kinematic block motion models and choose the optimum model based on AIC (Akaike's Information Criterion). By using the optimum model, we also estimate the relative motion between each block, the euler pole for each block, and the coupling ratio especially in Java region due to subduction of Australian plate that not be done by some previous researches. We also use seismic data in order to evaluate our block boundaries.

©2020. Japan Geoscience Union. All Right Reserved.

Def3D, a three-dimensional FEM tool for modeling deformation near active faults and volcanic centers

*luyuan Huang[1]

1. institute of crustal dynamics,CEA

Calculation of the quasi-static crustal deformation and stress changes plays an important role in geodetic observation’ s interpretation and seismic hazards assessment after mega destructive earthquakes and volcanic intrusions. However, most calculation methods are based on simplified models, such as half space model, 1D flatten model, symmetric spherical Earth model, while the realistic earth is heterogeneous ellipsoid with topography. FEM codes allow for flexibility in distribution of material properties and geometry that is difficult to accommodate in analytical or semi-analytical codes.

In this paper, with high performance computing capacity, we present a Visco-elastic Lateral Heterogeneous model, which includes topography, lateral heterogeneity and curvature of the ellipsoid Earth. Our new model can efficiently calculate visco-elastic deformation and stress changes due to earthquakes and volcanic intrusions. Our new approach is verified by comparisons with Okada's analytical solutions and Mogi's analytical solution in various cases. At last, the performance of the software is shown by case study of 2008 Wenchuan Earthquake and Changbaishan volcanic area.

We calculate visco-elastic deformation, stress changes and the Coulomb Failure Stress changes (ΔCFS) induced by Wenchuan earthquake. The preliminary results show that the coseismic ΔCFS on the hypocenter of Jiuzhaigou earthquake caused by the Wenchuan earthquake is about 0.008 MPa, while the postseismic ΔCFS is up to 0.012~0.016 MPa which means several years advance for Jiuzhaigou earthquake.

The inversion of volcano deformation based on equivalent body force method is first time to be adopted in Changbaishan volcanic area. The surface deformation caused by an ellipsoidal magma chamber fits well with the observed GPS and Leveling data. The Interaction between regional and magma-induced stresses can explain the present stress orientations around the volcano inferred form stress measurements. The Coulomb Failure Stress changes due to magmatic eruption may promote the earthquake swarms with NW fault planes clustering in two regions: in the northeastern part and the southwestern part of the caldera during 2002-2003.

Keywords: FEM, crustal deformation, active faults, volcanic centers

©2020. Japan Geoscience Union. All Right Reserved.

The changes of interplate coupling area and the vertical changes at Shikoku before the 1946 Nankai earthquake.

*Yasuhiro Umeda[1]

1. former DPRI Kyoto Univ., former AIST

If the velocity of the Philippine sea plate is constant and the width of the coupling zone does not change, the rate of vertical change observed on the ground is also constant. If the width of coupling zone changes, the rate of vertical movement also changes. Umeda and Itaba (2011) drew the vertical changes of Shikoku before the 1946 Nankai Earthquake, combining two kinds data of the Geographical Survey Institute and the Hydrographic Bureau (currently Hydrographic and Oceanographic Department Japan Coast Guard). The solid line (Obs.) in Fig.1 is the vertical changes of cape Muroto and Susaki. Before and after 1930, the rate of change is different. To explain this fact, we consider the changes of coupling zone. Fig.2 shows a cross section of the plate boundary that passes through the central part of Shikoku, almost perpendicular to the Nankai Trough. We assume three coupling zones F1, F2, F3 on the plate boundary and Philippine sea plate moves 5 cm per year. The upper plate is dragged 5 m in100 year. The change of the dotted lines are calculated for the following four stages. The change in period (a) shows the case where F1, F2, and F3 in Fig. 2 are coupled and the upper plate is also dragged at 5 cm /y. In the period (b), F1 and F3 slides slowly by 70% (3.5 m) and 80% (4 m) of the total slip. (c) indicates the change by the 1946 Nankai earthquake. Period(d) is after slip by 30% (1.5 m) and 20% (1 m) of the total slip. The slope of the vertical change of the ground surface changes depending on the width of the coupling area. reference:Umeda y. and S. Itaba, 2011, Vertical Crustal Movements along the Pacific Coast of Shikoku before the 1946 Nankai Earthquake, Bull. Geol. Surv. Japan, vol.62(5/6), p.243-257

Keywords: 1946 Nankai earthquake, coupling area, vertical change

©2020. Japan Geoscience Union. All Right Reserved.

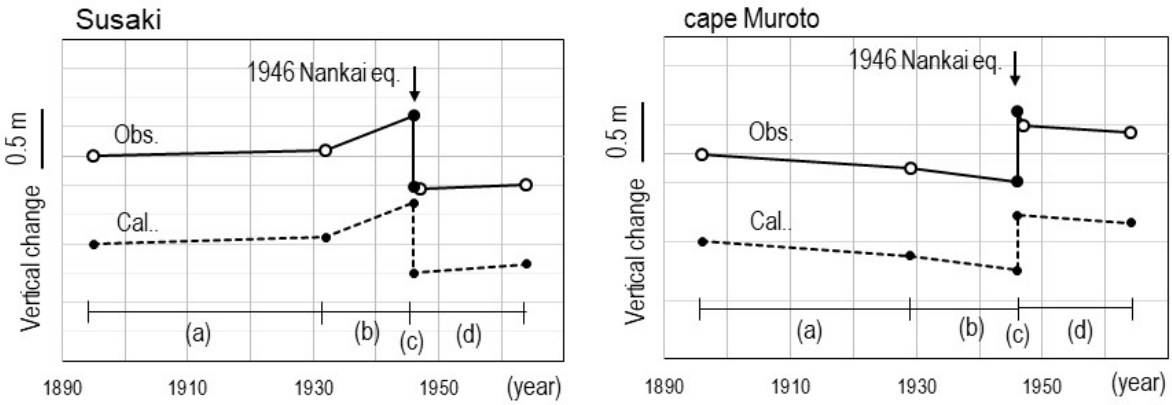

Fig.1 Vertical change of Susaki and cape Muroto before and after the 1946 Nankai earthquake (solid line). The changeof the dotted lines are calculated for the following four stages. The change in period (a) shows the case where F1,F2, and F3 in Fig. 2 are coupled and the upper plate is also dragged at 5 cm /y. In the period (b), F1 and F3 slides slowly by 70% and 80% of the total slip. (c) indicates the change by the 1946 Nankai earthquake. Period(d) is after slip by 30% and 20% of the total slip.

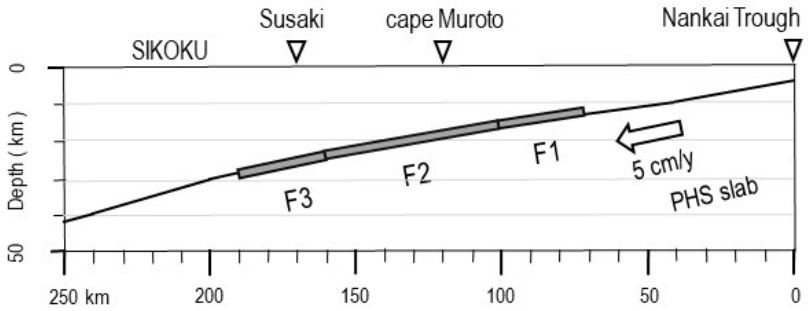

Fig.2 Cross section of the plate boundary perpendicular to the Nankai Trough (solid line). The thick solid lines are the coupled area. The width of F1,F2 ,F3 is 30 km,60 km, 30 km, respectively.

©2020. Japan Geoscience Union. All Right Reserved.

[J] Poster | S (Solid Earth Sciences)：S-SS Seismology

[S-SS15] Fault Rheology and Earthquake Physics

convener:Keisuke Yoshida(Tohoku University), Keishi Okazaki(Japan Agency for Marine-Earth Science and Technology), Shunya Kaneki(Disaster Prevention Research Institute, Kyoto University), Hiroyuki Noda(Kyoto University, Disaster Prevention Research Institute)

The goal of this session is to integrate theoretical, experimental, observational, and numerical perspectives from various fields such as seismology, geodesy, geology, mineralogy, and so on, to define what is known about earthquake source processes and the physical and chemical elementary processes of faulting. This session welcomes studies that address such issues as pre-, co-, and post-seismic processes, the rheology of seismogenic faults and fault rocks, laboratory experiments on elementary processes, numerical models based on frictional laws, and estimates of the stress field in the seismogenic zones. We also welcome studies on fault-zone drilling projects and in situ stress measurements.

[SSS15-P01] Estimation of thermal structure around the Median Tectonic Line in Shikoku, SW Japan

*Hideto Uchida[1], Michiharu Ikeda[1], Takeshi Tsuji[2], Kozo Onishi[3], Naoki Nishizaka[3] (1.Shikoku Research Institute inc., 2.Department of Earth Resources Engineering, Kyushu University, 3.Shikoku Electronic Power)

[SSS15-P02] Pore geometry and elastic moduli of fault rocks accompanied by the Median Tectonic Line in Shikoku, southwestern Japan

*Michiharu Ikeda[1], Kakda Kret[2], Takeshi Tsuji[3], Tatsunori Ikeda[3], Tomohiro Tsuji[4], Kozo Onishi[5], Naoki Nishizaka[5] (1.Department of Civil Engineering, Shikoku Research Institute Incorporated, 2.Institute of Technology of Cambodia, 3.Kyushu University, 4.Yamaguchi University, 5.Shikoku Electoric Power Co. Inc.)

[SSS15-P04] Development of composite-planer fabrics and its physical aspect

Akari Fuke[1], *Tetsuro Hirono[1], Satoshi Yukawa[1] (1.Department of Earth and Space Science, Graduate School of Science, Osaka University)

[SSS15-P05] Evaluation of reactivity under hydrous condition on thermal maturity of carbonaceous materials as a proxy of seismic slip

*Keita Iwagaki[1], Tetsuro Hirono[1] (1.Department of Earth and Space Science, Graduate School of Science, Osaka University)

[SSS15-P06] Experimental investigation of cumulative effect on thermal maturation of carbonaceous material by repeated earthquakes

*Yutaro Shimamura[1], Tetsuro Hirono[1], Hideki Mukoyoshi[2] (1.Department of Earth and Space Science, Graduate School of Science, Osaka University, 2.Department of Geoscience Interdisciplinary Graduate School of Science and Engineering, Shimane University)

[SSS15-P07] Thermal maturation of carbonaceous material as a proxy for earthquake slip: Evaluation of effects by initial maturity, heating rate, and mechanochemical activation

*Shuhei Yamashita[1], Tetsuro Hirono[1] (1.Department of Earth and Space Science, Graduate School of Science, Osaka University)

[SSS15-P08] Effects of initial crack distribution on inner-structures and flow properties of shear deformed rocks

*Yuka Kikuchi[1], Shin-ichi Uehara[1] (1.Toho University)

[SSS15-P09] Frequency characteristics of acoustic emission in granite during triaxial compression tests

*Sueyoshi Kazumasa[1], Manami Kitamura[2], Xinglin Lei[2], Ikuo Katayama[1] (1.Department of Earth and Planetary Systems Science, Hiroshima University, 2.National Institute of Advanced Industrial Science and Technology)

[SSS15-P10] Measurement of shear-wave polarization anisotropy in water-saturated Aji granite during shear experiment

*Jinki Tanaka[1], Ikuo Katayama[1] (1.Hiroshima University)

[SSS15-P11] Relationship between elastic wave velocity and attenuation ; An example of water-saturated granite

*Keiya Yamada[1], Kazuki Sawayama[2], Ikuo Katayama[1] (1.Hiroshima University, 2.Kyushu University)

[SSS15-P12] Development of new rock deformation apparatus with solid confining medium designed to reproduce the Pc-Pp-T condition of the base of the seismogenic zone

*Keishi Okazaki[1], Jun Muto[2], Yohei Hamada[1], Wataru Tanikawa[1], Takehiro Hirose[1] (1.Kochi Institute for Core Sample Research, Japan Agency for Marine-Earth Science and Technology, 2.Department of Earth Sciences, Tohoku University)

[SSS15-P13] Generation mechanism of slow stick slip verified from friction properties of mixed quartz/talc gouges

*Ryota Hibi[1], Risako Shirahige[1], Ken-ichi Hirauchi[1], Takato Takemura[2] (1.Department go Geoscience, Faculty of Science, Shizuoka University, 2.Nihon University)

[SSS15-P14] Effects of ambient temperature on the frictional strength and frictional heating of dolerite

*Michiyo Sawai[1], Yuuki Yokoyama[1], Manami Kitamura[2], Kyuichi Kanagawa[1] (1.Chiba University, 2.Geological Survey of Japan, AIST)

[SSS15-P16] Receiver Function Analysis of Laboratory Frictional Experiments

*Yasunori Sawaki[1], Miyuu Uemura[1], Ikuo Katayama[2], Yoshihiro Ito[3] (1.Graduate School of Science, Kyoto University , 2.Graduate School of Science, Hiroshima University , 3.Disaster Prevention Research Institute, Kyoto University)

[SSS15-P17] Statistical analysis for stick-slip experiments: Effects of inertial term and granular gouge

*Shinichi Oba[1], Yuta Mitsui[2] (1.Graduate School of Science and Tecnology, Shizuoka University, 2.Faculty of Science, Shizuoka University)

[SSS15-P18] System stiffness and unstable slip in the lab and in nature

*Akihiro Shimoda[1], Eiichi Fukuyama[1,2], Futoshi Yamashita[2], Shiqing Xu[2,3] (1.Kyoto Univ., 2.National Research Institute for Earth Science and Disaster Resilience, 3.Southern University of Science and Technology)

[SSS15-P19] Determination of frictional characteristics and evaluation of strong motion by dynamic rupture simulations of the Kamishiro fault at the 2014 Northern Nagano earthquake

*Takeshi Miyamoto[1], Kenichi Tsuda[2], Tetsuro Hirono[1] (1.Department of Earth and Space Science, Graduate School of Science, Osaka University, 2.Institute of Technology, Shimizu Corporation)

[SSS15-P20] Evaluation of ground motions generated from the splay fault of 1896 Rikuu earthquake - Preliminary study by dynamic rupture simulation

*Shuji Kumagai[1], Kiyoshi Hirotani[1], Yuta Mitsuhashi[2], Yusuke Saijo[2] (1.Tohoku Electric Power Co.,Inc., 2.KOZO KEIKAKU ENGINEERING Inc.)

[SSS15-P21] A Study on Dynamic of Strike-slip and Reverse Faults Based on Numerical Simulation

*Arzpeima Samaneh[1], Kenichi Tsuda[2], Sachio Ogawa[1] (1.Ohsaki Research Institute, 2.Shimizu corporation)

[SSS15-P22] Estimation of parameter values for a slip-dependent friction law using slip-stress relations of the Boso slow slips

*Reo Uchida[1], Toshinori Sato[1], Takuma Kobayashi[1,2] (1.Chiba University , 2.Asia Air Survey Co.,Ltd.)

[SSS15-P23] Relationship between the spatiotemporal change of the inelastic strain rate and the state of stress in the aftershock area of the 2016 Kumamoto earthquake sequence

*Ayaho Mitsuoka[1], Satoshi Matsumoto[2], Azusa Shito[2], Hiroshi Shimizu[2], Group for urgent joint seismic observation of the 2016 Kumamoto earthquake (1.Department of Earth and Planetary Sciences, Graduate School of Science, Kyushu University, 2.Institute of Seismology and Volcanology, Faculty of Science, Kyushu University)

[SSS15-P24] Stress tensor inversion in the focal area of the 2016 M_W7.8 Kaikoura earthquake, New Zealand (4)

*Miu Matsuno[1], Tomomi Okada[1], Satoshi Matsumoto[2], Yuta Kawamura[2], Yoshihisa Iio[3], Tadashi Sato[1], Takashi NAKAYAMA[1], Satoshi Hirahara[1], Stephen C Bannister[4], John Ristau[4], Martha K Savage[5], Clifford Thurber[6], Rick Sibson[7] (1.Research Center for Prediction of Earthquakes and Volcanic Eruptions Graduate School of Science, Tohoku University, 2.Institute of Seismology and Volcanology, Faculty of Sciences, Kyushu University, 3.Disater Prevention Research Institute, Kyoto University, 4.GNS Science, Lower Hutt, New Zealand, 5.Victoria University of Wellington, Wellington, New Zealand, 6.University of Wisconsin, Madison, 7.University of Otago, Dunedin, New Zealand)

[SSS15-P25] Stress field in the eastern margin of the Japan Sea and its relationship with faults of recent earthquakes

*Ayaka Tagami[1], Tomomi Okada[1], Shin'ichi Sakai[2], Mako Ohzono[3], Kei Katsumata[3], Masahiro Kosuga[4], Yoshiko Yamanaka[5], Hiroshi Katao[6], Takeshi Matsushima[7], Hiroshi Yakiwara[8], Takashi NAKAYAMA[1], Satoshi Hirahara[1], Toshio Kono[1], Shu'ichiro Hori[1], Toru Matsuzawa[1], Group for the aftershock observations of the 2011 off the Pacific coast of Tohoku Earthquake (1.Research Center for Prediction of Earthquakes and Volcanic Eruptions, Graduate School of Science, Tohoku University., 2.Earthquake Research Institute, University of Tokyo, 3.Institute of Seismology and Volcanology, Graduate School of Science, Hokkaido University, 4.Graduate School of Science and Technology, Hirosaki University, 5.Graduate School of Encironmental Studies, University of NAGOYA, 6.Research Center for Earthquake Prediction, Disaster Prevention Research Institute, Kyoto University, 7.Institute of Seismology and Volcanology, Faculty of Sciences, Kyushu University, 8.Nansei-toko Observatory for Earthquakes and Volcanoes, Kagoshima University)

[SSS15-P26] Stress field estimated from microseismicity in the northeastern edge of the Honshu around the junction between the northeastern Japan arc and the Kurile arc

*Sumire Maeda[1], Toru Matsuzawa[2], Tomomi Okada[2], Takeyoshi Yoshida[2], Masahiro Kosuga[3], Hiroshi Katao[4], Makoto Otsubo[1] (1.Research Institute of Earthquake and Volcano Geology, Geological Survey of Japan/AIST, 2.Graduate School of Science, Tohoku University, 3.Graduate School of Science and Technology, Hirosaki University, 4.Research Center for Earthquake Prediction, Disaster Prevention Research Institute, Kyoto University)

[SSS15-P27] **Monitoring of temporal change in the interseismic plate coupling using misfit angles of focal mechanisms relative to the slip-deficit induced stress field: The Nankai trough**

case

*Kazutoshi Imanishi[1], Akemi Noda[2] (1.Geological Survey of Japan, AIST, 2.National Research Institute for Earth Science and Disaster Resilience)

[SSS15-P28] Early rupture process of the 2019 Off Yamagata earthquake

*Ryo Fujimoto[1], Hirofumi Kowari[1], Masanao Komatsu[1], Hiroshi Takenaka[1] (1.Department of Earth Sciences, Graduate School of Natural Science and Technology, Okayama University)

[SSS15-P29] Development of a non-linear inversion method to estimate fault geometry from teleseismic data

*Kousuke Shimizu[1], Yuji Yagi[2], Ryo Okuwaki[2], Yukitoshi Fukahata[3] (1.Graduate School of Life and Environmental Sciences, University of Tsukuba, 2.Faculty of Life and Environmental Sciences, University of Tsukuba, 3.Disaster Prevention Research Institute, Kyoto University)

[SSS15-P31] Determination of pre-earthquake megathrust strength and frictional properties on seismogenic faults from near-field data

*Hongfeng Yang[1], Suli Yao[1] (1.The Chinese University of Hong Kong)

[SSS15-P32] Comparison of the rupture processes of the repeating earthquake sequences off-Iwate that occurred after the 2011 Tohoku oki earthquake

*Ahyi KIM[1], Naoki UCHIDA[2] (1.Yokohama City University, 2.Tohoku University)

[SSS15-P33] Spatiotemporal change in source parameters of repeating earthquakes due to the 2011 Tohoku-oki earthquake

*Kazuya Tateiwa[1], Tomomi Okada[1], Naoki Uchida[1], Toshio Kono[1] (1.Research Center for Prediction of Earthquakes and Volcanic Eruptions, Graduate School of Science, Tohoku University)

[SSS15-P34] Characteristics of Source Parameter for Aftershocks of the 2016 Kumamoto Earthquake Estimated by the Coda Spectral Ratio Method

*Naoto Maesako[1], Satoshi Matsumoto[2], Ayaho Mitsuoka[1], Group for Urgent Joint Seismic Observation of the 2016 Kumamoto Earthquake (1.Department of Earth and Planetary Sciences, Graduate School of Science, Kyushu University, 2.Institute of Seismology and Volcanology, Faculty of Science, Kyushu University)

[SSS15-P35] Simultaneous estimation of stress drop and rupture directivity of small to medium earthquakes around the Fukushima-Ibaraki border

*Rina Ikeda[1], Keisuke Yoshida[1], Ryo Takahashi[2,1], Toru Matsuzawa[1], Akira Hasegawa[1] (1.Tohoku University, 2.Japan Meteorological Agency)

[SSS15-P36] Estimating and considering the finiteness of small and moderate earthquakes in Iwaki area

*Naoto Yokotani[1], Aitaro Kato[1], Kazushige Obara[1], Shin'ichi Sakai[1], Takashi Iidaka[1], Tetsuya Takeda[2] (1.Earthquake Research Institute, the University of Tokyo, 2.National Research Institute for Earth Science and Disaster Resilience)

[SSS15-P37] Estimation of near-source Q and its temporal varaiation associated with pore pressure change: a case study of the Yamagata-Fukushima border swarm

*Keisuke Yoshida[1] (1.Tohoku University)

[SSS15-P38] Foreshocks immediately before the starting of earthquakes

*Masaki Yamana[1], Aitaro Kato[1] (1.Earthquake Research Institute, the University of Tokyo)

[SSS15-P39] Estimation of P-wave arrival time differences using P-wave first motion similarity with sampling frequency of 10 kHz

*Yuki Noda[1], Yoshihisa Iio[2] (1.Kyoto University Graduate School of Science, 2.Kyoto University Disaster Prevention Research Institute)

Estimation of thermal structure around the Median Tectonic Line in Shikoku, SW Japan

*Hideto Uchida[1], Michiharu Ikeda[1], Takeshi Tsuji[2], Kozo Onishi[3], Naoki Nishizaka[3]

1. Shikoku Research Institute inc., 2. Department of Earth Resources Engineering, Kyushu University, 3. Shikoku Electronic Power

It is important to estimate the thermal structure around the fault zone for understanding fault slip behavior and its strength, because a thermal diffusion during an earthquake is recorded by rocks around the fault zone. (Mori et al.,2015; Kaneki et al.,2018). Recently, various temperature proxies as vitrinite reflectance (Sakaguchi et al.,2011), biomarker maturity (Savage and Polissar, 2019) and carbonaceous materials (CM) (D.G. Henry et al.,2019) have been used to estimate the thermal structure around the fault zone. Especially, Raman spectroscopic analysis on CM is intensively used because CM and graphite commonly exist in sedimentary and metamorphic rocks. In this study, we conducted Raman spectroscopic analysis on CM to estimate a thermal structure around the Median Tectonic Line (MTL).
The MTL extending over 1000 km-long is a geological boundary fault that divides southwest Japan into Inner (mainly the Late Cretaceous Izumi Group and Ryoke granitic to low-P/T metamorphic rocks) and Outer (mainly the Cretaceous Sanbagawa high-P/T metamorphic rocks) zones. The MTL from Shikoku to western Kii Peninsula are dextral active faults revealed by geomorphological and paleo-seismological surveys (e.g., Ikeda et al., 2017). However, the movement history is complex because the MTL is a long-lived fault system from the Middle Cretaceous.
We estimated thermal structure around the MTL using a geological core sample (125 m-long) penetrating the inactive zone of the MTL in Saijyo City, Ehime prefecture (Uchida et al., 2019 JPGU). For Raman spectroscopic analyses, we prepared thin sections which consist of 9 samples from host rock and cataclasite of the Izumi Group at depths of 20–105 m, 8 samples from fault gouge and breccia of the MTL fault zone at depths of 106–110 m and 3 samples from host rock of the Sanbagawa metamorphic rocks at depths of 111–125 m. For each thin section, we measured at 20 ~ 30 points and adopted the averaged results. We adopted equations proposed by Aoya et al (2010) and Kouketsu et al (2014) to estimate the metamorphic temperatures. We then estimated organic matter maturity of the Izumi Group using equation of Henry et al (2019) and estimated temperature of the Izumi Grougp using equation of Barker (1988).
Our results demonstrate that the averaged peak temperatures of the Izumi Group are calculated to be 195 to 211 ±30℃ and those of the Sanbagawa metamorphic rocks are estimated to be 440 to 455 ±30℃. The estimated temperatures (from 218 to 223 ±30℃) of fault breccia in the MTL fault zone are similar to those of the Izumi Group. However, CM of fault gouge in the MTL fault zone show a wide variety of temperatures from 206 to 360 ±30℃. Moreover, estimated temperatures of cataclasite (from 332 to 371 ±30℃) in the MTL fault zone are significantly lower than those of host rocks from the Sanbagawa Metamorphic rocks. The temperatures during coseismic slip generally equal to or higher than those of host rock due to frictional heating. However, our results conflicted with the property that Raman spectra of CM can preserve the maximum temperature. Nakamura et al (2015) suggested that the crystal structure of CM is destructed by shearing during brittle deformation. The changes of R1 ratio (Intensity $_{D1\ band}$ / Intensity $_{G\ band}$) and the G band full width at half maximum of Raman spectra in this study could be explained by destruction of CM crystallinity by shearing. Thermal anomaly due to shear heating was not detected in the Izumi Group to a distance of 70 m from the MTL fault plane at least, while we detected signals of mechanical damage by shearing of the MTL.
Our findings about thermal anomaly and mechanical damage around the MTL can contribute to understanding fault slip behavior of a large crustal fault such as the MTL.

©2020. Japan Geoscience Union. All Right Reserved.

Keywords: thermal structure, Median Tectonic Line, Raman spectroscopic analysis, fault rocks

©2020. Japan Geoscience Union. All Right Reserved.

Pore geometry and elastic moduli of fault rocks accompanied by the Median Tectonic Line in Shikoku, southwestern Japan

*Michiharu Ikeda[1], Kakda Kret[2], Takeshi Tsuji[3], Tatsunori Ikeda[3], Tomohiro Tsuji[4], Kozo Onishi[5], Naoki Nishizaka[5]

1. Department of Civil Engineering, Shikoku Research Institute Incorporated, 2. Institute of Technology of Cambodia, 3. Kyushu University, 4. Yamaguchi University, 5. Shikoku Electoric Power Co. Inc.

Textures or fabrics of fault rocks are basic geological information to estimate maturity and evolution processes of faults. The textures or fabrics are composed of various components: shear planes, matrix, clasts, pores etc. Especially, pores play an important role in evolution processes of fault rocks, because pores strongly control behavior of fluid which promotes alteration of fault rocks and trigger mechanical instability of faults. Pores in fault rocks are mainly composed of intergranular pore, crack pore and clay pore. Fabrics or geometry of pores in mature faults have been subjected to significant modification for a long time. Therefore, the shape of pores in fault rocks can be a good indicator for deformation intensity, evolution stages, and categorization of fault rocks. In this study, we focused on variation of characteristics of pores through fault rocks of the Median Tectonic Line in Shikoku.

The Median Tecotnic Line (hereinafter MTL) is the longest geological terrane boundary fault. The northern and southern parts from the MTL are the Ryoke Belt composed of low P/T metamorphic rocks, granitic rocks and sedimentary rocks and the Sanbagawa metamorphic rocks consisted of high P/T metamorphic rocks, respectively. We drilled a bore hole to obtain a geological core sample penetrating the MTL. The total core length is 250 m-long. The fault plane of the MTL is within 37.45 m-depth. The hanging wall and foot wall zones are the Izumi Group in Ryoke Belt and Sanbagawa metamorphic rocks, respectively.

The fault rocks in the Izumi Group can be classified into three zones, Fractured zone (ca.4–12.5 m-depth), Transition zone (ca.12.5–31.6 m-depth) and Gouge zone (ca.31.6–37.2 m-depth), based on geological observation. On the other hand, the fault rocks of the Sanbagawa metamorphic rocks are cataclasite just below the MTL fault plane (ca.37.5–47 m-depth) and intact rocks in the deeper parts of the core (ca.47–250 m-depth).

We measured seismic velocities and porosities of 53 samples; 24 samples in the Izumi Group and 24 samples in Sanbagawa metramorphic rocks from the core. Because all core samples of the Izumi Group are damaged, 5 samples from outcrops (intact rocks) of the Izumi Group were measured. We estimated the dominant pore aspect ratio (short axes/long axes) and grain elastic moduli from observed velocity-porosity relationships of these samples via the grid-search inversion (Kakda et al., 2018).

Overall, aspect ratios a of pores of intact rocks of the Izumi Group (a=0.005) are distinctly small in comparison to those of damaged rocks of the Izumi Group (a=0.06–0.30). The gouge samples show the largest values of the aspect ratios in the damaged rocks. The aspect ratios of the transition rock samples are slightly higher than those of the fractured rock samples. And then, elastic moduli of intact rocks are remarkably large in comparison to those of damage rocks. The bulk and shear moduli of intact rocks are ca.100 and 60 GPa, respectively, whereas ca.3–5 GPa for both elastic moduli in damage rocks. The gouge samples show largest values of the elastic moduli in the damaged rocks. The elastic moduli of the fractured rock samples are higher than those of the transition rock samples.

The results indicate that destruction of an original rock structure in intact rocks must affect both pore aspect ratios and grain elastic moduli. And then, the variation of the aspect ratios of pores in damaged rocks should depend on combination of the three type pores with each characteristic. On the other hand, the elastic moduli in damaged rocks might be controlled by mixing materials which have different stiffness. The variation of pore aspect ratios and grain elastic moduli along the MTL contribute to

©2020. Japan Geoscience Union. All Right Reserved.

understand evolution processes of fault zone and evaluate petrophysical properties (e.g., permeability or strength) of fault zone.

Keywords: pore geometry, elastic moduli, MedianTectonic Line

©2020. Japan Geoscience Union. All Right Reserved.

Development of composite-planer fabrics and its physical aspect

Akari Fuke[1], *Tetsuro Hirono[1], Satoshi Yukawa[1]

1. Department of Earth and Space Science, Graduate School of Science, Osaka University

The coefficients of friction in rocks have been systematically investigated over a wide range of slip rates from 1 nm/s to 1 m/s. Although the friction coefficients of most rocks fall between 0.6 and 0.85, at high slip rates (above ca. 0.1 m/s) friction coefficients decrease between 0.1-0.4. In order to understand such fault slip behavior, seismic slip has been reproduced in laboratory experiments reproduced seismic slip and microscopic observation have been explored. However, in a wide range of slip speeds of the same rock type, the relationship among slip behavior and mineral assemblage and microstructural fabric remain poorly understood.

Here we conducted laboratory friction experiments using volcaniclastic sediments and characterized their mineralogies and microstructural fabrics before and after the experiments. The samples were sheared at a wide range of slip rates ranging from 0.0002 to 1.0 m/s. As a result, in the low slip rates where the slip weakening did not occur, broken mineral grains and the preferential orientation of elliptical grains parallel to shear planes and shear fabrics such as R1-shear planes were also observed. However, in the high slip rates where the slip weakening occurred, the Y-shear planes developed.

In order to reveal the mechanism of structural development therethically, we simulated the development of shear fabrics with slip by using the numerical model (Distinct Element Method, DEM), and investigated the relationship among the friction behavior, the force on particles, and the relative displacement in adjacent particles. As results, at high slip rates, slip weakening occurred in DEM simulation. Moreover, shear-localized line was formed in parallel with the shear formation. On the other hand, at high slip rates, it was found that the force of particles and the slip between particles were localized, and repeated stick-slip behaviors.

Keywords: composite-planer fabrics

©2020. Japan Geoscience Union. All Right Reserved.

Evaluation of reactivity under hydrous condition on thermal maturity of carbonaceous materials as a proxy of seismic slip

*Keita Iwagaki[1], Tetsuro Hirono[1]

1. Department of Earth and Space Science, Graduate School of Science, Osaka University

The thermal maturity of carbonaceous materials (CM) is often used for evaluation of the frictional heat recorded in faults. However, despite the fault is filled with water, the effect of water on the maturity of CM have not yet been investigated. Thus, here we performed heat treatments on lignite and bituminous coal with some different conditions of CM-water ratio, target temperature, heating rate, and heating holding time, and then evaluated the effect of water. The spectroscopic features by IR and Raman on the heated CMs with various conditions indicated no difference on the maturation (e.g., thermal breaking of aromatic C-H and graphitization). Therefore, the thermal maturation of CM as a proxy for frictional heating in faults is not necessary to consider the presence of water.

Keywords: carbonaceous material, IR spectrometry, Raman spectrometry

©2020. Japan Geoscience Union. All Right Reserved.

Experimental investigation of cumulative effect on thermal maturation of carbonaceous material by repeated earthquakes

*Yutaro Shimamura[1], Tetsuro Hirono[1], Hideki Mukoyoshi[2]

1. Department of Earth and Space Science, Graduate School of Science, Osaka University, 2. Department of Geoscience Interdisciplinary Graduate School of Science and Engineering, Shimane University

Thermal maturation of carbonaceous material (CM) is one of the useful proxies for frictional heat in fault during earthquakes. As temperature rises, CMs release weak chemical bonds and transfer into graphite structure above ca. 800 ˚C. Various techniques (infrared spectroscopy, Raman spectroscopy, mass spectrometry, elemental composition analysis, vitrinite reflectance measurement, etc.) have been used in previous researches. However, it has not been considered whether the effects of repeated seismic events with frictional heating. Thus, in this study, we conducted infrared and Raman spectroscopic analysesand vitrinite reflectance measurements of bituminous coal and anthracite after heating 1, 10, and 100 times at each temperature (100, 300, 500, 700, 900, 1100 and 1300 ˚C).No difference in spectroscopic features depending on the numbers of time. In contrast, bituminous coals heated at 500 ˚C for 8, 16 hours and at 600 ˚C for 8 hours showed a disappearance of aliphatic CH chain. Therefore, it is concluded that thermal maturity hardly progresses under rapid heating such as seismic slip even though the events reached to 100 times and that the maximum temperature recorded, revealed by thermal maturation of CM in fault could correspond to the largest earthquake event experienced.

Keywords: repeated eathquakes, frictional heating, carbonaceous material, spectroscopic analysis

©2020. Japan Geoscience Union. All Right Reserved.

Thermal maturation of carbonaceous material as a proxy for earthquake slip: Evaluation of effects by initial maturity, heating rate, and mechanochemical activation

*Shuhei Yamashita[1], Tetsuro Hirono[1]

1. Department of Earth and Space Science, Graduate School of Science, Osaka University

Thermal maturation of carbonaceous material (CM) has been used as a proxy for frictional heating in a fault zone during an earthquake. CMs have complicated molecular structures and are classified into lignite, bituminous coal, and anthracite depending their initial maturities. During an earthquake, not only temperature in a fault zone rises rapidly but also mineral particles and CMs suffer by shear deformation. However, these factors have not been comprehensively investigated. In this study, we investigated changes in maturity of three types of CMs (lignite, bituminous coal, and anthracite) and graphite. Samples were forced by shear deformation by using a rotary shear apparatus, and then were heated in a tubular electric furnace. The conditions of the friction experiments were as follows: slip rate, 1 mm/s; axial load, 1 and 3 MPa. The target temperatures of the heating experiment were from 300 to 1300 ℃ at 100 ℃ interval and the heating increments were several tens and 0.1 ℃/s. The heated CMs and graphite were analyzed by using infrared (IR) and Raman spectroscopies. The spectrum of heated lignite showed ,a disappearance of C-H chain at ≧ 490 ℃ under slow heating, and at ≧ 890 ℃ under rapid heating. The difference in temperature where the peak was disappeared was 80 ℃ between damaged and undamaged lignite samples. In bituminous coal, disappearances of C-H chain at ≧ 490 ℃ and ≧ 970 ℃ were observed under slow and rapid heatings, respectively. No difference in temperature where the peak was disappeared was observed between damaged and undamaged bituminous samples. In the cases of anthracite and graphite, there was no peak of C-H chain. Raman spectra of lignite sample that unheated and heated showed a difference in the intensity ratio of G and D bands, but no differences were observed in bituminous coal, anthracite, and graphite even though that suffered shear damage. Therefore, thermal maturation of CMs has complicated effects causing from initial maturation, heat rate, and mechanochemical damage and their consideration is needed when the maturation is used as a proxy of frictional heat recorded in faults.

©2020. Japan Geoscience Union. All Right Reserved.

Effects of initial crack distribution on inner-structures and flow properties of shear deformed rocks

*Yuka Kikuchi[1], Shin-ichi Uehara[1]

1. Toho University

Flow properties along a fault strongly depend on the inner structure of the fault zone, such as distribution of damage zone, where crack density is high. One of the possible factors that affects damage zone developments is crack distribution in the host rock. However, it is not necessarily clear how the damage zone development depends on the factor. In this study we operated flow property measurements during uniaxial deformation under confining pressure with rock specimens with various initial crack densities.

We operated the experiment by using rock deformation-flow test apparatus in Toho University. The rock selected for this study was a sandstone from Rajasthan, India, which is mainly composed of 68% quartz, 18% orthoclase and 10% plagioclase. The specimens are cylindrical, 20 mm in diameter and 40 mm in length. To investigate effects of initial crack densities on the results, we prepared cracked specimens (average porosity is 14%) by heating up to 900˚C and cooling down to room temperature, and intact (not heated) rock specimens (average porosity is 14%). The confining pressure was 5 or 10 MPa, the upstream pore pressure was up to 1 MPa and the downstream one was atmospheric pressure. The rock deformation experiments were performed at a constant axial strain rate of 10^{-5} s^{-1}.

In all experiments, sudden brittle failure was observed, and evolutions of flow rate parallel to the axial direction of the specimen until the failure were qualitatively similar to each other: the flow rate was increased from the yielding point till the failure. An increment of flow rate per unit volumetric strain increase for the intact rock specimens were approximately one order larger than that for the heated specimens. This may be because the increment of the flow rate is larger for the specimen with lower initial crack density. The flow rate after the sudden failure was decreased rapidly in the case of the intact rock specimens. In the case of the heated specimens, on the other hand, the flow rate was increased after the failure. We could find the difference in inner-structures of the deformed specimens between the intact and heated rocks: in the case of the intact rock specimens, multi-failure structures were concentrated on the upstream side; in the case of the heated specimens, a single shear fracture connecting the upstream and downstream sides was observed. The flow rate change at the sudden failure may be mainly because of (1) aperture decreases of cracks parallel to the axial direction caused by decreases of differential stress and (2) creation of specimen-scale brittle failure structures. The difference on the flow rate change between the intact and heated rocks probably because the impact of (1) is relatively effective in the case of the intact rocks, and in the case of the heated rocks, the impact of (2) is more effective.

Keywords: Fault zone, Deformation flow test

©2020. Japan Geoscience Union. All Right Reserved.

Frequency characteristics of acoustic emission in granite during triaxial compression tests

*Sueyoshi Kazumasa[1], Manami Kitamura[2], Xinglin Lei[2], Ikuo Katayama[1]

1. Department of Earth and Planetary Systems Science, Hiroshima University, 2. National Institute of Advanced Industrial Science and Technology

Fluid flow-induced seismicity has been observed in various engineering fields such as geothermal system (e.g., Grigoli et al., 2018). Especially, in the Pohang enhanced geothermal systems project, the moment magnitude 5.4 earthquake was induced by fluid injection after the events in the entire period of stimulations (Kim et al., 2018). To understand the generation processes of induced earthquakes due to fluid injection, it is necessary to research the propagation process of pre-existing cracks in thermally damaged granites. The acoustic emission (AE) is defined as elastic waves released by rapid cracking, which is a useful tool for investigating rock fractures. The frequency of AE signals from fracturing contains information about internal structure of a rock. In this study, we measure acoustic emission (AE) and P-wave velocity during triaxial deformation of thermally cracked granite.

We conduct a triaxial compression test on granite at confining pressure of 22.5 MPa and strain rate of 10-5 1/s under dry condition using the loading system at GSJ/AIST (Lei et al., 2011). Cylindrical intermediate-grained Oshima granite and coarse-grained Inada granite (50 mm in diameter and 125 mm in length) which are thermally damaged at 550 ℃ are used as samples. We measure AEs with twenty-eight piezoelectric transducers (PZT) and strains with six strain gauges.

A preliminary result shows that a sample deforms elastically until at 384 MPa. After the peak stress of 438 MPa, post-yield behavior of the sample indicates brittle deformation with drastic stress drop. AE activity was initiated at around 80 % of the peak stress, and increased rapidly after reaching the peak stress. Initiation and growth of cracks inferred from AE events is consistent with the damaging process proposed by Lei (2006). Frequency analysis based on the fast Fourier transform shows that frequency of AE signals released during deformation are in the range of 100-300 kHz. Previous study reported that low-frequency events were dominant as rock approached failure under compression (Ohnaka and Mogi, 1982). However, no clear variation in frequency band was found from the results of this study. This is because AEs were not recorded in a range sufficient to understand the whole trend, and it is necessary to record AE signals from the initial stage of deformation, such as using transducers with different frequency band.

Keywords: acoustic emission, frequency, triaxial compression test

©2020. Japan Geoscience Union. All Right Reserved.

Measurement of shear-wave polarization anisotropy in water-saturated Aji granite during shear experiment

*Jinki Tanaka[1], Ikuo Katayama[1]

1. Hiroshima University

The stress drop at the time of the earthquake not only releases the stress applied to the fault plane but also causes the rotation of the principal stress axis applied to the fault plane. In fact, the change in the direction of the principal stress axis after the earthquake is reported by the mechanism solution of aftershocks and the seismic wave anisotropy(e.g. Tadokoro and Ando 2002; Boness and Zoback 2006). It is thought that this is because the closing (opening) direction of the cracks around the fault plane correspond to the stress axis. Also it is considered that fluid exists in voids such as grain boundaries and cracks in the underground rock. Therefore, in this study, the elastic wave was transmitted during the shear experiment of water-saturated rock and the relation between the shear stress and the principal stress axis and elastic wave velocity was measured in the laboratory. Since the shear-wave polarization anisotropy has a characteristic which is sensitive to the direction of the crack, measurement of different vibration components of S wave is performed in addition to measurement of P wave velocity.

For the experiment, we investigated the change in elastic wave velocity according to shear deformation using a High-T biaxial frictional testing machine in Hiroshima University. For the experimental samples, Aji granite which generated thermal cracks inside by heating to 600 degrees Celsius was used. In the shear test, it was carried out by loading the central rock block at a constant speed while keeping the vertical stress constant. The shear sliding velocity was about 0.9 μm/s and the vertical stress was 5 MPa. For measurement of elastic waves, probes with a resonance frequency of 1 MHz (manufactured by Olympus Corporation) were used, and S wave and P wave were measured by pulse transmission method. The propagation direction of elastic wave is parallel to the shear plane and perpendicular to the shear direction, and for the S wave, we measured two components, wave (SH) oscillating in the plane orthogonal to the shear direction and wave (SV) oscillating parallel to the shear plane.

From the experimental results, with the increase of the shear stress, it is expected that the velocity of SH wave rises earlier and the SV wave rises late. It is also expected that there is a phenomenon in which the initial motion of the SV wave jump suddenly as the shear stress increased. This means that when the shear stress is low and the maximum principal stress axis in the sample is close to the direction of the normal stress, the shear direction cracks are frequently closed and the SH wave velocity increases and the shear stress increases, when the inclination of the maximum principal stress axis becomes steeper with respect to the normal stress, it is considered that the direction of the crack which closes is correspondingly inclined. In this way, since the SH wave and SV wave behave differently due to the increase of the shear stress and the corresponding change of the principal stress axis angle, by utilizing this property, a good index for monitoring the stress state around the fault.

Keywords: Earthquake prediction, Shear-wave polarization anisotropy, Thermal crack

©2020. Japan Geoscience Union. All Right Reserved.

Relationship between elastic wave velocity and attenuation ; An example of water-saturated granite

*Keiya Yamada[1], Kazuki Sawayama[2], Ikuo Katayama[1]

1. Hiroshima University, 2. Kyushu University

Seismic wave attenuation and velocity depend on microcracks and pore fluid in rocks, and these are important physical properties in seismic survey to understand the state of crustal rocks. Especially, excess pore pressure can be the trigger for earthquakes, since effective confining pressure decreases due to the elevated pore pressure. Observing the change of pore pressure is expected to lead to the prediction of earthquakes. Therefore, it is essential to investigate how much seismic wave attenuation and velocity change by the increase of pore pressure quantitatively. Previous experimental studies have measured elastic wave attenuation in sedimentary rocks mainly and the data in igneous rock is poor. Moreover, there are few studies which are focused on the number of microcracks and the change of pore pressure. In this study, we measured elastic wave attenuation and velocity during hydrostatic tests under dry and wet (water-saturated) condition and investigated effects of microcracks and pore fluid on them.
Fine-grained granite, which is collected in Aji region of Kagawa Prefecture, was used in all experiments and its porosity is about 0.8 % under atmospheric pressure. Samples were cored from the same block and formed into cylindrical shape (25 mm in a diameter, 20 mm in a length). Hydrostatic tests were carried out under dry condition at room temperature, using Intra-vessel deformation and fluid-flow apparatus at Hiroshima University. Under dry condition, confining pressure was increased from 5 MPa to 200 MPa. Elastic wave attenuation and velocity were measured by the pulse transmission method, in which the specimen was put in two aluminum spacers with piezoelectric transducers (P- and S-wave) attached. Elastic wave attenuation (Q^{-1}) was estimated from the spectral ratio method using aluminum as a reference spectrum. Elastic wave velocity (V) was calculated by dividing the length of a sample by the travel time passing through it. Axial and radial strains were simultaneously measured by directly attaching a strain gauge to the side of the specimen. Volumetric strain was obtained from them, and the change of porosity was estimated during hydrostatic test quantitatively.
As a result, P-wave attenuation (Qp^{-1}) decreases with increasing confining pressure, while P- and S-wave velocities (Vp, Vs) increases. The change in both attenuation and velocity is large at low confining pressure and it levels off at high pressure. This suggests that the closure and locking of cracks by pressure have an effect on attenuation and velocity. As confining pressure is increased from 5 MPa to 200 MPa, Vp and Vs increase by 18-20 %, whereas Qp^{-1} decreases by 80 %. Therefore, elastic wave attenuation is more sensitive to microcracks in a rock than velocity. In term of porosity, it decreased by 35 % from initial porosity with increasing pressure up to 200 MPa. This result indicates that the closure of microcracks causes the decrease of attenuation and the increase of velocity.
Future tasks are (1)measuring S-wave attenuation (Qs^{-1}), (2)measuring under wet condition, (3)quantitative evaluation of the number of microcracks. By combining these data, we will discuss about the relationship between elastic wave velocity and attenuation under water-saturated condition.

Keywords: Elastic wave attenuation, Elastic wave velocity, Pore pressure, Granite, microcrack

©2020. Japan Geoscience Union. All Right Reserved.

Development of new rock deformation apparatus with solid confining medium designed to reproduce the Pc-Pp-T condition of the base of the seismogenic zone

*Keishi Okazaki[1], Jun Muto[2], Yohei Hamada[1], Wataru Tanikawa[1], Takehiro Hirose[1]

1. Kochi Institute for Core Sample Research, Japan Agency for Marine-Earth Science and Technology, 2. Department of Earth Sciences, Tohoku University

At subduction plate boundaries and inland active faults, most of large earthquakes (Mw >7) occur at the base of the seismogenic zone with a depth of about 10–25 km. The PT conditions of these areas are corresponding to lithostatic pressures ranging 300–800 MPa and temperatures ranging 200–400 degC. In addition, seismological observations indicate that the pore fluid pressure is nearly lithostatic, meaning 300–800 MPa. The presence of high pore fluid pressure has a key role to control the rock rheology, because the frictional strength of the fault is a function of the effective pressure and physico-chemical properties of fluids changes exponentially under high pressure. However, most of rock friction experiments are conducted under pressure lower than 200 MPa. Therefore, understanding of fault rheology at the base of the seismogenic zone is limited by extrapolations of low PT experiments and experiments using analog materials. We recently built two new solid pressure medium apparatuses at Kochi Core Center and Tohoku University. They are capable to increase the confining pressure, the pore pressure and the temperature up to 2 GPa, 1 GPa and 1200 degC, respectively. These apparatuses can reproduce the in-situ or even deeper P-Pp-T conditions of the seismogenic zone. In this presentation, we will report basic performances, calibration data of the apparatuses and initial experimental results.

Keywords: Experimental rock deformation, Rheology, Earthquake

©2020. Japan Geoscience Union. All Right Reserved.

Generation mechanism of slow stick slip verified from friction properties of mixed quartz/talc gouges

*Ryota Hibi[1], Risako Shirahige[1], Ken-ichi Hirauchi[1], Takato Takemura[2]

1. Department go Geoscience, Faculty of Science, Shizuoka University, 2. Nihon University

In order to understand effects of phyllosilicate content on stick-slip behavior of fault zones, we conduct frictional sliding experiments on mixed quartz/talc gouges, using a direct shear apparatus. The experiments are carried out at room temperature, a normal stress of 10 MPa, and sliding velocities of 0.66–2.00 μm/s. Values of the steady-state friction coefficient and ($a-b$) for the quartz/talc gouges decrease with increasing talc content from 0.69 to 0.18 and from 0.0039 to −0.0032, respectively. For the gouges with talc contents of 0–8 wt.%, fast or slow stick slips occur. In slow stick-slip events, duration increases with increasing slip distance (up to 76.8 s), while stress drop decreases with increasing duration (down to 0.0046 MPa). The ratio $K = k/k_c$, where k is the elastic loading stiffness and k_c is the critical rheologic stiffness, slightly increases from 3.88 to 19.76 with increasing talc content. The range of K values (5.81–15.74) obtained for slow stick-slip events is above theoretically estimated K values of ~1 producing them.

Keywords: phyllosilicate, slow stick slip, rate- and state-dependent friction law, stiffness, friction sliding experiments, coefficient of friction

©2020. Japan Geoscience Union. All Right Reserved.

Effects of ambient temperature on the frictional strength and frictional heating of dolerite

*Michiyo Sawai[1], Yuuki Yokoyama[1], Manami Kitamura[2], Kyuichi Kanagawa[1]

1. Chiba University, 2. Geological Survey of Japan, AIST

Frictional properties at intermediate to high slip velocities are essential to understand the earthquake propagation and slip. Coseismic weakening has been observed experimentally at seismic slip velocities for many types of rocks (e.g., Tsutsumi and Shimamoto, 1997; Di Toro et al., 2011). Weakening mechanisms has been controlled by temperature rise including flash heating, melt lubrication or thermal pressurization (e.g., Rice, 2006; Hirose and Shimamoto, 2005). Although the importance of temperature during fault motion are widely recognized, the effects of temperature on frictional properties at intermediate to high velocities remain unknown. We therefore conducted friction experiments at a wide range of temperatures and investigated the effects of temperature on the friction coefficient (μ) and frictional heating.

Experiments were performed on dolerite (Belfast, Northern Ireland) using a rotary shear deformation apparatus at Chiba University. Samples were displaced up to about 20 m at a normal stress of 1 MPa, slip velocities V of 3–300 mm/s, and ambient temperatures T_a of ~20–500°C in an argon atmosphere with an oxygen concentration of 0.3 %. Temperature adjacent to the slip surface T_s was also measured by a thermocouple placed near the slip surface.

At V = 3–30 mm/s, dolerite showed steady-state friction coefficients μ_{ss} of 0.46–0.54 at T_a = 20–100°C. Whereas at T_a = 200–500°C, μ_{ss} increased to 0.64–0.71. At V = 100 mm/s, dolerite showed clear velocity-strengthening with μ_{ss} up to 0.58–0.64 at T_a = 20–100°C, almost constant values with μ_{ss} = 0.65–0.69 at T_a = 200°C and 300°C, and clear velocity-weakening with μ_{ss} = 0.45–0.46 at T_a = 400°C and 500°C. At V = 300 mm/s, dolerite showed strong velocity-weakening at all T_a investigated. In addition, slip-weakening distance (D_c) at V = 100 mm/s and 300 mm/s was smaller at higher T_a. T_s increased with increasing V. The amount of T_s increase (ΔT_s) due to frictional heating was almost the same at all T_a tested at V = 3–30 mm/s (ΔT_s was ~1°C at V = 3 mm/s and ~30°C at V = 30 mm/s). At V = 100 mm/s and 300mm/s, on the other hand, ΔT_s was notably smaller at higher T_a. Thus, the frictional properties and frictional heating of dolerite are affected not only by V but also by T_a. Estimations of temperature distribution during experiments based on three-dimensional finite element modeling are also in progress.

Keywords: frictional strength, frictional heating, temperature dependence, dolerite

©2020. Japan Geoscience Union. All Right Reserved.

Receiver Function Analysis of Laboratory Frictional Experiments

*Yasunori Sawaki[1], Miyuu Uemura[1], Ikuo Katayama[2], Yoshihiro Ito[3]

1. Graduate School of Science, Kyoto University , 2. Graduate School of Science, Hiroshima University , 3. Disaster Prevention Research Institute, Kyoto University

A large number of laboratory frictional experiments have been conducted to clarify the behaviors of frictional slip to understand the occurrences of megathrust earthquakes and slow earthquakes in subduction zones. We apply the receiver function method to biaxial shear experiments to detect a gouge layer as a simulated plate interface; receiver function is one of the effective seismic tools to evaluate velocity discontinuity and detect primary structures such as continental Moho and oceanic crust in subduction zones (e.g., Ammon et al., 1991). Biaxial friction experiments can simulate the fault slip, although it is difficult to measure the temporal changing on a simulate gauge layer with acoustic, or seismological technique, especially using converting wave. Sliding tests can examine the temporal variation of frictional coefficients as shear deformation proceeds. Slide-Hold-Slide (SHS) tests can simulate the fault locking and the effects of aging (i.e., frictional healing). Previous studies have confirmed temporal variations of elastic wave responses from rock interface (e.g., Nagata et al., 2008) and simulated gouge layers (e.g., Scuderi et al., 2016), suggesting that elastic waves can be used as seismic waves and the response may reflect fault structures. Here, we present the preliminary results of the receiver function analysis in biaxial shear experiments.

Sliding and SHS tests with the slip velocity of 1.5 μm/s are conducted using the biaxial slip apparatus at Hiroshima University. We select antigorite serpentinite and Ca-Montmorillonite as simulated gouge layers. We simulate the interface with two sheets of sample powder layers (up to 1.5 mm thickness) by loading 20 kN (~10 MPa) of the normal force in Figure 1. Compressional waves with one cycle of 1 MHz sinusoidal wave are transmitted diagonally to the P and S receivers through the sample layers. The receiver function method is applied by regarding the P-wave receiver as the vertical component and the S-wave receiver as the radial component. The receiver functions are calculated with the Extended-Time Multitaper method (Helffrich, 2006; Shibutani et al., 2008). Frequency dependence is examined by setting Gaussian low-pass parameters; 500 kHz for low-frequency and 800 kHz for high-frequency receiver function.

Some continuous phases around 0.5 to 2 μs and 4 μs are detected in simulated high-frequency receiver functions in Figure 2. These phases are stable in the steady-state frictional condition. Synthetic receiver functions calculated under the velocity model with 1 mm thickness of a low-velocity layer duplicate continuous positive and negative phases around 0.5 to 2 μs and 4 μs, suggesting that the low-velocity sample layer closer to the receivers are detectable by the method. Monitoring of receiver function phases provides a clue to assess faulting processes or the generation of a slow slip on natural faults and plate interfaces, although the input acoustic wave with center frequency of 1 MHz, whose wavelength is around 5 mm in stainless brock, may be relatively low for receiver functions to find out internal structures with 1 mm thickness of the layer.

Keywords: Receiver function, Laboratory frictional experiment, Fault slip, Antigorite

©2020. Japan Geoscience Union. All Right Reserved.

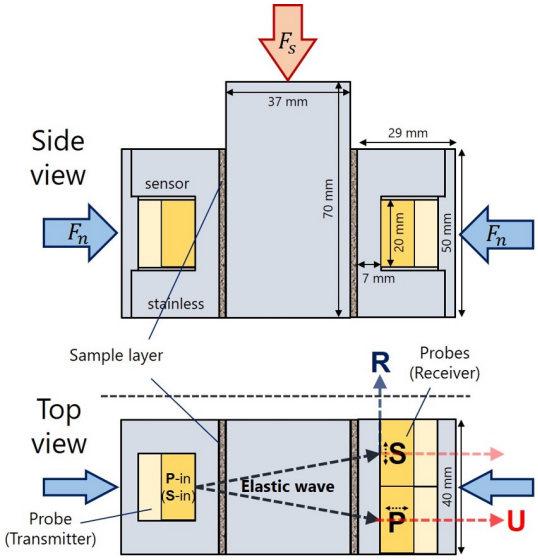

Figure 1. Schematic diagrams of the double-direct shear configuration. The top panel shows the side view, and the bottom panel shows the top view, partially drawn to see through stainless blocks (light blue). Two sheets of powder sample (shown as a rock texture) are sandwiched by stainless blocks. Rectangles colored gold indicate elastic-wave probes; P for compressional waves and S for shear waves. A transmitter probe is located in the center of the block. Two receiver probes are horizontally aligned to be symmetric.

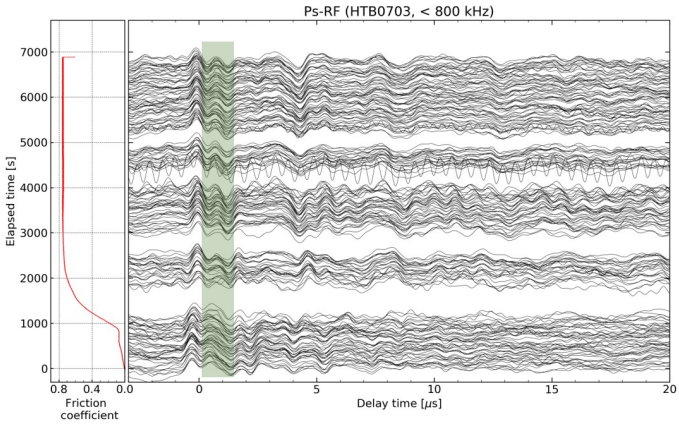

Figure 2. Simulated receiver functions in the sliding test of Antigorite powder (HTB0703) with the frequency content up to 800 kHz (right) and frictional coefficient (left). Horizontal axis denotes the delay time from direct P-wave arrival, and vertical axis denotes the elapsed time from the beginning of shearing. Twenty consecutive waveforms are stacked to calculate each RF trace. Area colored green indicates the conversion phase from the gouge layer on the receiver side. Phases around 4 μs indicate the multiples in the side-block.

©2020. Japan Geoscience Union. All Right Reserved.

Statistical analysis for stick-slip experiments: Effects of inertial term and granular gouge

*Shinichi Oba[1], Yuta Mitsui[2]

1. Graduate School of Science and Tecnology, Shizuoka University, 2. Faculty of Science, Shizuoka University

In natural earthquakes (over km scales), slip displacement D is scaled with fault length L (Scholz, 1982). Laboratory stick-slip experiments have been thought to be analogue of seismic phenomena, but we find that they deviate from the L-D scaling using experimental data from 14 published papers. Namely the experimental data tends to have larger slip displacement than extension of the natural earthquake scaling. We perform correlation analyses to investigate parameters governing the slip displacement D, focusing on gouge thickness and inertia term of frictional system that show high correlation with the slip displacement D. The analyses imply that the slip displacement D for stick-slip experiment is controlled by the characteristic time of inertia (which corresponds to the period of harmonic oscillation) independently of spatial scale.

Keywords: stick-slip, scaling law

©2020. Japan Geoscience Union. All Right Reserved.

System stiffness and unstable slip in the lab and in nature

*Akihiro Shimoda[1], Eiichi Fukuyama[1,2], Futoshi Yamashita[2], Shiqing Xu[2,3]

1. Kyoto Univ., 2. National Research Institute for Earth Science and Disaster Resilience, 3. Southern University of Science and Technology

Unconventional fossil fuel resources such as shale gas and oil have been produced by cracking deep underground rocks with hydraulic fracturing. During this process, induced and triggered earthquakes may occur by injecting fluid into bedrocks. Two M5.5 disastrous earthquakes occurred in Korea, one of which was close to the enhanced geothermal system (EGS) (Grigoli et al., 2018). Induced/triggered earthquakes are caused by the decrease in effective normal stress on the pre-existing fault due to the increase in pore fluid pressure. However, it is very difficult to directly monitor the effective stress change in bedrocks at depth.

In this study, we investigate the relation between system stiffness and fault friction for large scale friction experiments and for natural earthquakes. The purpose of the study is to consider the conditions for safe hydraulic fracturing without causing induced earthquakes at the site. We use the data obtained by the large scale friction experiments at the National Research Institute for Earth Science and Disaster Resilience (NIED). In the experiment, the top metagabbro specimen (1.5 m long, 0.5 m wide and 0.5 m high),was stacked on the bottom metagabbro one (2.0 m long, 0.1 m wide and 0.5 m high), where the nominal contacting area was 1.5 m long and 0.1 m wide. 6.7 MPa normal stress were applied to the stacked rocks, and the shear stress were applied by moving the shaking table horizontally. Macroscopic ratio of the shear stress to the normal stress on the fault was estimated from those measured by the loadcells. The stiffness of the system can be estimated by dividing the amount of stress change before and after the stick slip by the amount of relative displacement during that period (e.g. Shimamoto et al.,1980).In this study, we used four experiments data whose loading velocity was 0.01 mm/s.

The stiffenss values were estimated as 1.88 GPa/m and 1.81 GPa/m based on the data before and after stick slip events, respectively. We confirmed that the stiffness values were approximately the same before and after the stick slip events.

McLaskey & Kilgore(2013) defined the critical stiffness (K_{crit}) based on the the rate- and state- dependent friction law (slip law). We estimated the friction parameters a, b, and Lc from the experiment data using the Runge-Kutta method (Urata et al., 2015). The critical stiffness was estimated as 83.4 GPa/m . This K_{crit} was larger than the estimated stiffness K. Thus we confirmed that unstable slip occurred in the experiments.

We shall infer the condition of the induced earthquake that occurred in October 2017 at EGS in Korea from the critical stiffness. From the seismic moment, stress drop, the width and length of the fault estimated by Grigoli et al., (2018),stiffness can be evaluated. The stiffness becomes 29.4 MPa/m. On the other hand, the critical stiffness is 1.08 GPa/m if we apply the friction parameters for saturated granite in Marone et al. (1990). Because of $K_{crit} > K$ in the induced earthquake in Korea, unstable slip occurs when induced earthquakes occur regardless of the amount of injected fracturing fluid.

Keywords: induced and triggered earthquakes, stiffness, stick slip

©2020. Japan Geoscience Union. All Right Reserved.

©2020. Japan Geoscience Union. All Right Reserved.

Determination of frictional characteristics and evaluation of strong motion by dynamic rupture simulations of the Kamishiro fault at the 2014 Northern Nagano earthquake

*Takeshi Miyamoto[1], Kenichi Tsuda[2], Tetsuro Hirono[1]

1. Department of Earth and Space Science, Graduate School of Science, Osaka University, 2. Institute of Technology, Shimizu Corporation

On 22 Nov. 2014, a large earthquake (M_W 6.2) occurred at the northern of Nagano prefecture. The surface ruptures were observed along the Kamishiro fault, a northern part of the Itoigawa-Shizuoka tectonic line. In order to investigate the relationship between the frictional characteristics of the fault and the seismic waves observed on the surface, we performed friction experiments using the fault-related samples recovered from the Kamishiro fault at the Iida trench, and then evaluated the spatiotemporal evolution of the rupture process during the earthquake by using dynamic simulation on the basis of the friction properties determined. The friction experiments were performed under wet conditions with 1 MPa axial stress and 55 cm/s and 200 μm/s equivalent slip speeds. The initial, peak, and dynamic friction coefficients were determined to be 0.495, 0.708, and 0.269-0.288, respectively. The simulated fault slip near the surface was calculated to be about 10 m, which is well coincided to that analyzed by a previous research. However, the Fourier spectra of the slip velocity showed that the amplitudes have maximum at the smallest frequency and become smaller as frequency becomes larger, which are different from those of the observed ground motion.

Keywords: frictional cahacteristics, dynamic rupture simulation

©2020. Japan Geoscience Union. All Right Reserved.

Evaluation of ground motions generated from the splay fault of 1896 Rikuu earthquake - Preliminary study by dynamic rupture simulation

*Shuji Kumagai[1], Kiyoshi Hirotani[1], Yuta Mitsuhashi[2], Yusuke Saijo[2]

1. Tohoku Electric Power Co.,Inc., 2. KOZO KEIKAKU ENGINEERING Inc.

1 Introduction

In the Tohoku region, there are many reverse fault-type inland crustal earthquakes caused by inversion tectonics, but some of them have east-dip conjugates secondary fault to the west-dip main fault, such as the 2008 Iwate–Miyagi Nairiku earthquake. In the case of the Iwate-Miyagi Nairiku Earthquake, no seismic fault was found on the fault extension on the east-dip fault, but an example of a seismic fault was found on the fault extension on the splay fault was the Kawafune Fault of the 1896 Rikuu Earthquake. It is important to evaluate the seismic motion caused by the activity of the secondary fault on the conjugate side of the main fault in the evaluation of the ground motion located in the upper part of the main fault. The purpose of this study is to evaluate the ground motion generated from the splay fault for the 1896 Rikuu earthquake. As a preliminary study, in the case of the 1896 Rikuu Earthquake, since the measured values of the ground surface displacement were compiled by Matsuda et al. (1980), a dynamic rupture simulation model consistent with these observation data was constructed. The ratio of energy released from the main fault (Senya fault) and the splay fault (Kawafune fault) was evaluated.

2 Analysis Model

A dynamic rupture simulation was performed for the 1896 Rikuu earthquake using a 2D finite element method. The reason for the 2D assumption was that in the 1896 Rikuu Earthquake, the Kawafune fault appears on the eastern part of the Senya fault and the splay fault has occurred in response to the large displacement undergone by the main fault. Such a phenomenon can be simplified and simulated even with a 2D model. Based on the results of the Earthquake Research Institute(2001), an analysis model was made as shown in the figure. The ground near the fault is modeled as a homogeneous except for the surface layer.

3 Simulation analysis of main fault

First, the analysis was performed considering the rupture of only the main fault. At this time, the stress drop in the fault is determined in proportion to the ground stiffness around the fault based on Andrews (1980), and the dynamic parameters such as stress drop and strength excess were set so as to match the measured values of the ground surface displacement reported by Matsuda et al. (1980). As a result, the amount of stress drop was 2.0MPa in the main area.

4 Simulation analysis of main fault and splay fault

Next, the same frictional constitutive law and initial stress as the main fault were applied to the splay fault. A stress drop of 2.0MPa resulted in almost no activity in the splay fault. However at stress drop of 1.0 MPa, the displacement of the splay fault occurred, and the slip on the ground surface of the main fault and ratio of displacement of main fault and splay fault was almost the same as the measured value reported by Matsuda et al. (1980).

Using the analysis results, the sharing ratio of seismic moment generated from each of the main fault and the splay fault was compared. The sharing ratio of the splay fault was found to be more than ten percent. However, since the length of the splay fault in the actual measurement is clearly shorter than that of the main fault, the seismic moment released by the splay fault is expected to be smaller than the result of the

©2020. Japan Geoscience Union. All Right Reserved.

2D model when considering the heterogeneity in the fault length direction. Similar results were obtained for the ground motion near each fault.

5 Future works
For the Rikuu Earthquake, seismic intensity or housing collapse ratio distribution has been studied in detail in previous studies. The results obtained from the dynamic simulation model in the current study will be reflected in the kinematic simulation model, and the ground motions released from the Kawafune fault will be compared to the existing ground motion evaluation and observed seismic ground motion intensity of the 1896 Rikuu earthquake.

Keywords: splay fault, dynamic rupture simulation, Evaluation of ground motion, secondary fault

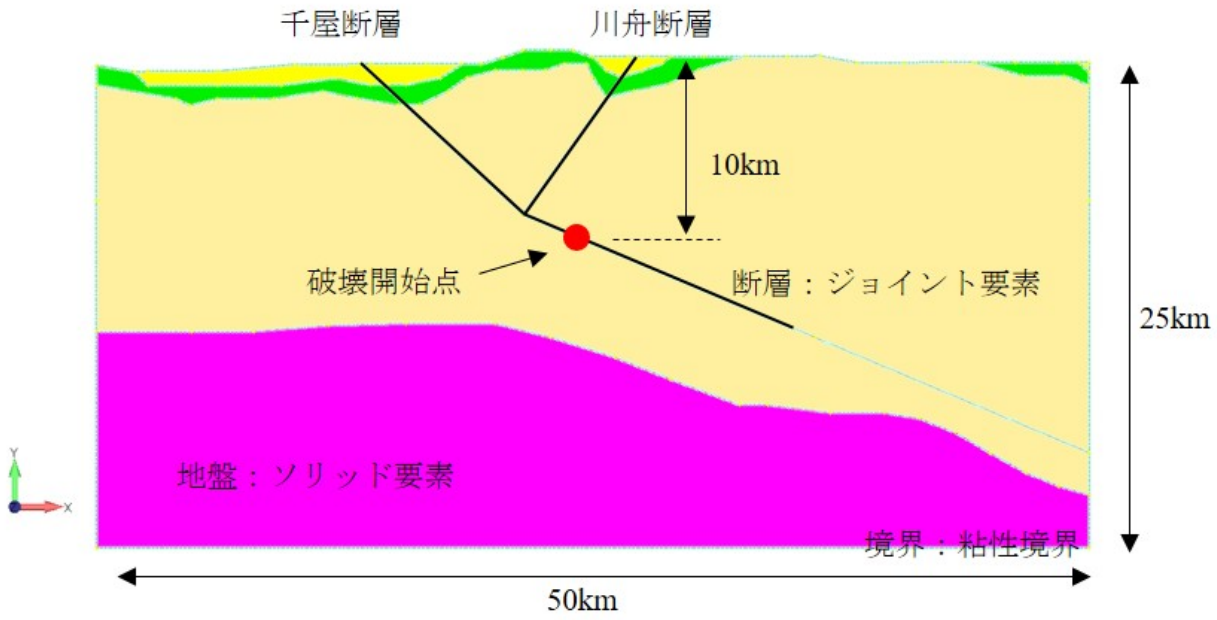

©2020. Japan Geoscience Union. All Right Reserved.

A Study on Dynamic of Strike-slip and Reverse Faults Based on Numerical Simulation

*Arzpeima Samaneh[1], Kenichi Tsuda[2], Sachio Ogawa[1]

1. Ohsaki Research Institute, 2. Shimizu corporation

The use of dynamic rupture models to simulate earthquakes have received considerable attention in recent years among earthquake engineers and seismologists because these models let us deal with the detailed physical processes of rupture dynamics and improve our capability to interpret the kinematic earthquake models derived from seismic recordings. As a consequence, the dynamic rupture models provide a more accurate assessment of the seismic hazard and risk management.

With strike-slip and reverse faulting being the most common type of crustal earthquakes in Japan, we are interested in studying the seismic source process for these two earthquake types.

The purpose of this study is to understand the differences between the rupture of the strike-slip and the reverse fault. For this purpose, we use a 3D numerical approach by adopting the asperity model.

Our hypothetical models consist of faults which are embedded in a semi-infinite homogenous medium and subjected to the same normal stress and frictional parameters. We consider two different depths to represent the shallow and deep earthquakes, we placed one asperity at 5km then at 12km down dip respectively. We assume to have a shallow area, 2 km along the dip, with zero stress drop and a longer dc compare to another area on the fault. The result of our dynamic simulation provides useful clues to understand our question.

Keywords: dynamic simulation, reverse fault, strike-slip fault

©2020. Japan Geoscience Union. All Right Reserved.

Estimation of parameter values for a slip-dependent friction law using slip-stress relations of the Boso slow slips

*Reo Uchida[1], Toshinori Sato[1], Takuma Kobayashi[1,2]

1. Chiba University , 2. Asia Air Survey Co.,Ltd.

Studies on friction laws and effective normal stress on faults is important for understanding fault behavior and earthquake events. Kobayashi and Sato (JpGU, 2019) proposed that relation of slip-rate and stress change for slow slip events can estimate absolute values of effective normal stress on the basis of a rate and state dependent friction law. This presentation proposes an estimation method of parameter values for a slip-dependent friction law from slip-stress relations of slow slip events using that friction force balances shear stress for slow slip events.

To obtain slip-stress relations of slow slip events, we used the daily F3 coordinate values of GNSS stations from the Geospatial Information Authority of Japan. The GNSS data were fitted with a time series model that takes account of the linear trend and seasonal variations in the data, and then the fitted data were smoothed. We made every 3 days transient movements from the smoothed data. From the 3 days data, we estimated slip distributions using ABIC inversion method. We calculated stress changes from the slip distributions using Coulomb 3.3 (in details, see Kobayashi and Sato, JpGU, 2019). We used a slip dependent friction law proposed by Matsu’ ura et al. (Tectonophys, 1992), which considers interaction between statistically self-similar fault surface and abrasion of surface asperities. Important parameters of this friction law are upper fractal limit of wave length on the fault and abrasion rate.

We need to determine a stress scale for comparing observed and theoretical relations between slips and shear stresses. We determined a stress scale from absolute values of effective normal stress estimated by Kobayashi and Sato (JpGU, 2019).

From the comparison of observed and theoretical relations between slips and shear stresses for the Boso slow slip events, we estimate about 100 cm for the upper fractal limit of wave length on the fault and about 0.01~0.1 for the abrasion rate.

Acknowledgements: We used the daily F3 coordinate values by GSI, and Coulomb 3.3 program by USGS.

Keywords: Friction law, slow slip, abrasion rate, fractal limit of wave length

©2020. Japan Geoscience Union. All Right Reserved.

Relationship between the spatiotemporal change of the inelastic strain rate and the state of stress in the aftershock area of the 2016 Kumamoto earthquake sequence

*Ayaho Mitsuoka[1], Satoshi Matsumoto[2], Azusa Shito[2], Hiroshi Shimizu[2], Group for urgent joint seismic observation of the 2016 Kumamoto earthquake

1. Department of Earth and Planetary Sciences, Graduate School of Science, Kyushu University, 2. Institute of Seismology and Volcanology, Faculty of Science, Kyushu University

In order to understand state of stress and strength in the crust, inelastic strain and its rate is a key factor because of contributing stress relaxation. The inelastic deformation in the crust proceeds after a large earthquake occurrence, resulting change in stress field.

In this study, we investigated the spatiotemporal change in the inelastic strain due to seismic activity of the aftershock of the 2016 Kumamoto earthquake sequence, central Kyushu, Japan. The 2016 Kumamoto earthquake sequence occurred at Hinagu and Futagawa fault zones in Kumamoto prefecture, central Kyushu Island, Japan. The activity of the aftershock events of this sequence is high at the hanging-wall side rather than at the foot-wall side. These focal mechanism solutions indicate mostly either the right lateral strike-slip or normal fault types.

We estimated the inelastic strain in a spatial bin using the relationship between the moment tensor density and the inelastic strain tensor [Noda and Matsu’ura, 2010] at several lapse time windows, and calculated the inelastic strain rate with the time length of each time window. In addition, we estimated the stress field before the sequence using seismic moment tensor data and calculated the co-seismic stress change based on co-seismic rupture model [Asano and Iwata, 2016].

In the hypocentral area of the 2016 Kumamoto earthquake sequence, the inelastic strain tensors are more similar to them of the stress field than the co-seismic stress change tensors. Therefore, we could conclude the inelastic strain increased with the stress change having similar tensor to the regional stress condition. In the temporal change in the inelastic strain rate, we obtained that the inelastic strain rate around the faults of the two large earthquakes [Mitsuoka et al., 2019, JpGU Meeting 2019] more rapidly decreased than that at the southern region of the Hinagu fault.

Calculating the tensor product (dT; [Terakawa, 2017]) between the stress field before the present sequence and the co-seismic stress change tensor, we found that the region with the positive dT is correspond to the region showing fast decline in the inelastic strain rate. The positive dT value means that the co-seismic stress change strengthens the magnitude of the stress loaded on the region. This relationship implies there is potential for modeling the temporal change in the strain rate after a large earthquake, if the relationship between the pre-earthquake stress field and the stress change is known. Moreover we discuss the relationships between the inelastic strain rate and the other parameters.

Keywords: inelastic strain rate, stress field, 2016 Kumamoto earthquake sequence

©2020. Japan Geoscience Union. All Right Reserved.

Stress tensor inversion in the focal area of the 2016 M_w7.8 Kaikoura earthquake, New Zealand (4)

*Miu Matsuno[1], Tomomi Okada[1], Satoshi Matsumoto[2], Yuta Kawamura[2], Yoshihisa Iio[3], Tadashi Sato[1], Takashi NAKAYAMA[1], Satoshi Hirahara[1], Stephen C Bannister[4], John Ristau[4], Martha K Savage[5], Clifford Thurber[6], Rick Sibson[7]

1. Research Center for Prediction of Earthquakes and Volcanic Eruptions Graduate School of Science, Tohoku University, 2. Institute of Seismology and Volcanology, Faculty of Sciences, Kyushu University, 3. Disater Prevention Research Institute, Kyoto University, 4. GNS Science, Lower Hutt, New Zealand, 5. Victoria University of Wellington, Wellington, New Zealand, 6. University of Wisconsin, Madison, 7. University of Otago, Dunedin, New Zealand

We study spatio-temporal change of the stress field due to the 2016 Kaikoura earthquake in the northern area of the South Island of New Zealand. Data from both 51 temporary stations and 22 permanent GeoNet stations were used. From these data, we determined focal mechanisms and estimated the stress field before and after the Kaikoura main shock using stress tensor inversion. If there are many aftershocks on the fault plane of the main shock, the fault plane may be distributed with a bias. Therefore, it is necessary to study the effect of focal mechanisms of aftershock that occurred on the fault plane of the main shock. So, we attempted to remove the mechanism solution on the fault plane of the main shock using the fault model of Hamling et al. (2017) and Kagan angle.

We found that the stress field did not change significantly independent of the value of the Kagan angle, and we consider that the effect of the aftershocks occurring on the fault plane of the main shock on the result is small. In addition, we carried out the analysis by dividing the epicenters into several regions. We obtained the following results: 1) In the southwest part of the rupture, the stress field changed from strike-slip before the main shock to a stress field overlapping sigma-2 and sigma-3 (between strike-slip and reverse fault type) after the main shock. The stress ratio (phi) changed from 0.4 to 0.2. 2) In the central part of the rupture, the stress field changed from a stress field overlapping igam-2 and sigma-3 (between strike-slip and reverse type) prior to the main shock, to strike-slip type after the main shock. The stress ratio changed from 0.2 to 0.5. 3) In the northeast part of the rupture, the stress field changed from unstable before the main shock to a more stable strike-slip type afterwards. The stress ratio changed from 0.2 to 0.4. 4) When finely segmenting the stress field after the main shock, the solution of the stress field tended to be unstable in the area near where the strike changed in the fault model of Hamling et al. (2017). The stress ratio typically takes a value between 0 and 0.3 in the area where the solution of the stress field becomes unstable.

When the solution of the stress field becomes unstable and the stress ratio is low, there are two possible causes: the effect of pore fluid pressure (c.f. Warren-Smith et al., 2019) and the heterogeneity of stress due to the main shock. As for the latter, in the southeastern area and fault-intersection area, as shown by the fault model of Hamling et al. (2017), the strike and slip angle of each small fault are not uniform, so inhomogeneous slip may affect the result. Therefore, the change in stress in the depth direction will also need to be examined. We plan to quantitatively determine the ease of movement of each fault by using the obtained stress field and slip tendency.

©2020. Japan Geoscience Union. All Right Reserved.

Stress field in the eastern margin of the Japan Sea and its relationship with faults of recent earthquakes

*Ayaka Tagami[1], Tomomi Okada[1], Shin'ichi Sakai[2], Mako Ohzono[3], Kei Katsumata[3], Masahiro Kosuga[4], Yoshiko Yamanaka[5], Hiroshi Katao[6], Takeshi Matsushima[7], Hiroshi Yakiwara[8], Takashi NAKAYAMA[1], Satoshi Hirahara[1], Toshio Kono[1], Shu'ichiro Hori[1], Toru Matsuzawa[1], _ Group for the aftershock observations of the 2011 off the Pacific coast of Tohoku Earthquake

1. Research Center for Prediction of Earthquakes and Volcanic Eruptions, Graduate School of Science, Tohoku University., 2. Earthquake Research Institute, University of Tokyo, 3. Institute of Seismology and Volcanology, Graduate School of Science, Hokkaido University, 4. Graduate School of Science and Technology, Hirosaki University, 5. Graduate School of Encironmental Studies, University of NAGOYA, 6. Research Center for Earthquake Prediction, Disaster Prevention Research Institute, Kyoto University, 7. Institute of Seismology and Volcanology, Faculty of Sciences, Kyushu University, 8. Nansei-toko Observatory for Earthquakes and Volcanoes, Kagoshima University

Introduction

The M_{jma}6.7 Yamagata-oki earthquake (18 June 2019) occurred in the area where the tectonic belt along the eastern margin of the Japan Sea (EMJS) is located. It is known that many active faults and folds exist along the EMJS. Also, many large to moderate-sized earthquakes have occurred. It is thought that the reverse fault slip is caused by the stress field with the maximum compression axis oriented to an approximately east-west direction (e.g., Terakawa and Matsu’ura, 2010; Okamura, 2019). In this study, we investigate the distribution of focal mechanisms and the stress field to find spatio-temporal changes in a newer time window than in previous studies. Also, we focus on the two large to moderate-sized earthquakes; the Yamagata-oki earthquake and the M_{jma}7.5 Niigata earthquake (12 June 1964).

Data and methods

We use focal mechanism and moment tensor data from the NIED (National Research Institute for Earth Science and Disaster Resilience) f-net and focal mechanisms estimated from P-wave initial motions by Okada et al. (SSJ meeting, 2019). For estimating the regional stress field, we use the stress tensor inversion software SATSI (Spatial And Temporal Stress Inversion; Hardebeck and Michael, 2006). For evaluating the suitability of slip, we use “slip tendency” defined by Morris et al. (1996).

Results

Western coastal area in northeast Japan (included in the EMJS belt)

We analyze earthquake data that occurred during the period from 1 January 1997 to 31 December 2019, located in 37˚N-42˚N, 137˚E-141˚E, with depths of 0-30km to find that the directions of the P-axes vary in the study area.The direction of the P-axis are oriented to NW-SE to the south of about 40˚N (about 39˚N at a depth of the 10-20km), while it becomes to be oriented to E-W to the north. In addition, the percentage of strike-slip type focal mechanisms increases in the northern part (about 40˚N-41˚N) of the study area. Comparison between the Japan Sea areas and Japan inland areas shows that P-axis directions change from NW-SE to E-W as approaching the inland areas.

Next, we estimated the regional stress field using the stress tensor inversion in the study area. The result of the stress inversion shows the change in the stress axis direction. The maximum compressional stress axis direction changes from NW-SE to E-W from south to north. In addition, the stress axis direction changes from to NW-SE to E-W from as approaching the inland areas. We consider that the change in the distribution of the focal mechanisms reflects the change in the stress axis direction.

©2020. Japan Geoscience Union. All Right Reserved.

The slip-tendency analysis for theYamagata-oki earthquake and the Niigata earthquake

For the Yamagata-oki earthquake, we estimate the stress field around the focal area and calculated the slip tendency (Ts) for each focal mechanism. We use focal mechanism data from NIED for Ts analysis and focal mechanism data from Okada et al., (SSJ meeting, 2019) for the stress tensor inversion. For the main shock, the eastward dipping nodal plane shows a high value of Ts. Also, the fault plane with a low dip angle shows high Ts in each focal mechanism of aftershocks. For the Niigata earthquake, we used fault planes from Hirasawa (1965), and we use focal mechanism data from NIED for stress tensor inversion. The eastward dipping fault plane shows a higher value of Ts.

These results are consistent with the idea that these two earthquakes did not occur as reactivation of the high-angle normal faults, which were generated by the tensile stress filed during the Japan Sea formation, but occurred on the reverse faults with low dip angles which generated by the current compressive stress field.

References

Hardebeck, J. L., and A. J. Michael, 2006, J. Geophys. Res., 111, B11310.

Hirasawa, T., 1965, J. Phys. Earth,13, 35-66.

Morris, A., D. A. Ferril, and D.B. Henderson, 1996, Geology, 24, 275-278.

Okamura, Y., 2019, Jour. Seismol. Soc. Japan, Ser. 2, 46, 413-423.

Terakawa, T., and M. Matsu’ura, 2010, Tectonics, 29, TC6008.

Keywords: EMJS, slip tendency, stress field

©2020. Japan Geoscience Union. All Right Reserved.

Stress field estimated from microseismicity in the northeastern edge of the Honshu around the junction between the northeastern Japan arc and the Kurile arc

*Sumire Maeda[1], Toru Matsuzawa[2], Tomomi Okada[2], Takeyoshi Yoshida[2], Masahiro Kosuga[3], Hiroshi Katao[4], Makoto Otsubo[1]

1. Research Institute of Earthquake and Volcano Geology, Geological Survey of Japan/AIST, 2. Graduate School of Science, Tohoku University, 3. Graduate School of Science and Technology, Hirosaki University, 4. Research Center for Earthquake Prediction, Disaster Prevention Research Institute, Kyoto University

We report the present stress field in the northeastern edge of Honshu, NE Japan. The northeastern edge is located around the junction between the northeastern Japan arc and the Kurile arc, and is influenced by the subduction of the Pacific Plate and the southwestward movement of the Kuril Forearc Sliver. However, the seismicity is extremely low in this region. In this study, we investigated focal mechanism solutions of the microearthquakes in the northeast edge of Honshu. The focal mechanisms determined in this study are mainly E-W compressional reverse-fault type in the land area, while N-S compressional reverse-fault type in the sea area. We applied the stress tensor inversions to the focal mechanisms. The estimated stress field is the reverse-faulting type with the NE-SW trending maximum compressional stress axis. The direction of the compressional axis around the junction is rotating even in the result of Terakawa and Matsuura (2010). These results suggest that the northeastern edge of Honshu is largely influencedby the southwestward movement of the Kuril Forearc Sliver. In this presentation, we discuss on the spatiotemporal variations of the stress field there estimated from current microseismicity and the paleostress fields inferred from geological structures.
This research project has been conducted as the regulatory supporting research funded by the Secretariat of Nuclear Regulation Authority (Secretariat of NRA), Japan.

Reference:
Terakawa T, Matsu’ ura M (2010) The 3-D tectonic stress fields in and around Japan inverted from centroid moment tensor data of seismic events. Tectonics 29:TC6008. doi:10.1029/2009TC002626.

©2020. Japan Geoscience Union. All Right Reserved.

Monitoring of temporal change in the interseismic plate coupling using misfit angles of focal mechanisms relative to the slip-deficit induced stress field: The Nankai trough case

*Kazutoshi Imanishi[1], Akemi Noda[2]

1. Geological Survey of Japan, AIST, 2. National Research Institute for Earth Science and Disaster Resilience

The activity of shallow inland earthquakes in the Kinki region, southwest Japan, increased from about 50 yr before to 10 yr after the occurrence of large interplate earthquakes along the Nankai trough (Utsu 1974; Hori & Oike 1999). This observation indicates that the shallow inland earthquakes occur in response to the interseismic plate coupling, facilitating further research on the causal relationship between the inland earthquake activity and the interplate coupling state.

Here we propose a method to monitor the temporal change in the interseismic plate coupling by examining whether the focal mechanisms of inland earthquakes align with the stress field caused by the slip-deficit or not. We expect that earthquakes will preferentially occur on faults whose slip direction is close or in agreement with the slip-deficit induced stress field when the stress buildup due to the plate coupling dominates the regional background stress. Therefore, the misfit angle of focal mechanism solutions (i.e., the angle between the observed slip direction and the tangential traction predicted by the reference stress tensor) is a useful indicator (e.g., Terakawa et al., 2016; Otsubo et al., 2018).

The procedure is summarized as follows:
(1) The stress tensor caused by the slip-deficit is computed every 0.1˚ at the depth of 10 km.
(2) Search the grid point closest to the hypocenter of each focal mechanism, defining a reference stress tensor there.
(3) Calculate the misfit angle of each focal mechanism. Here the smaller angle for each pair of nodal planes is used in subsequent analysis.
(4) Calculate the moving average of the misfit angles for 1-year time window. The error is computed using a bootstrap resampling with replacement over 1000 iterations.

We applied the method to inland earthquakes in the Kinki region and the western Shikoku to evaluate a temporal change in the plate coupling along the Nankai trough. We merged the JUNEC catalog (Ishibe et al. 2014) and the JMA catalog to produce the consolidated one, which spans from 1 July 1985 to 31 December 2019. For the calculation of the slip-deficit induced stress tensor, we adopt the slip-deficit model of Noda et al. (2018). The results show that the average misfit angles fluctuate every 3-5 years. The amplitude of the fluctuation is about 20˚, which is significant even if errors are taken into account. This result may reflect that the interplate coupling periodically becomes strong or weak. Although such cyclic fluctuations have not been reported in the Nankai trough, Uchida et al. (2016) found a quasi-periodic slow-slip behavior (1-6 years period) in the Tohoku subduction zone, which results in the cyclic fluctuations in the interplate coupling. Furthermore, we observe that the average misfit angles tend to decrease since 2012, suggesting a possibility that the plate coupling becomes stronger with time. The recent occurrence of moderate earthquakes, such as the 2013 M_j6.3 Awaji Island, the 2015 M_j5.1 southern Tokushima, and the 2018 M_j6.1 northern Osaka earthquake, may support the hypothesis.

Further studies are needed to verify the above results, but it is likely that the present method has a

©2020. Japan Geoscience Union. All Right Reserved.

capability to detect subtle temporal change in the plate coupling and could be incorporated into earthquake forecasting strategies.

Keywords: stress, monitoring, plate coupling, Nankai trough

©2020. Japan Geoscience Union. All Right Reserved.

Early rupture process of the 2019 Off Yamagata earthquake

*Ryo Fujimoto[1], Hirofumi Kowari[1], Masanao Komatsu[1], Hiroshi Takenaka[1]

1. Department of Earth Sciences, Graduate School of Natural Science and Technology, Okayama University

The earthquake (M_{JMA} 6.7) occurred in Off Yamagata prefecture on June 18th, 2019 (JST). In this study, we investigate the early rupture process during 3.6 seconds after the origin time by source imaging technique (Takenaka *et al* , 2009, EPS). We use P-wave portion before the S-wave arrival on vertical components of velocity waveform data which obtained by integrating the original strong-motion records observed at 15 stations from the seismic networks of NIED, JMA, Yamagata and Niigata prefectures. We assume two fault planes through the hypocenter (38.608˚N, 139.479˚E and 14.0 km depth) reported by the JMA unified catalogue: first one is the plane of strike N26˚E and dip 27˚ from the JMA CMT mechanism solutions; second one is the plane of strike N16˚E and dip 31˚ from the JMA focal mechanism solution using P-wave first motion polarity.
From the result of the source imaging for 3.6 seconds from the origin time (Fig. 1), for either fault planes, the area of large radiation strength was found in north side of the hypocenter. This area corresponds to the large slip region in the result of source inversion conducted by NIED. Two peaks of rupture strength in this area are located 4 km and 10 km northward along the strike from the hypocenter. The snapshots shown in the Fig. 2 image the highest peak of the radiation strength located about 4 km toward north from the hypocenter after 1.2 to 1.8 seconds from the origin time. The rupture in this area extends to north along the strike. Second peak in the area is located 10 km northward from the hypocenter after 3.0 seconds from the origin time.

Acknowledgements: we used the strong motion records of NIED, JMA, and Yamagata and Niigata prefectures.

Keywords: Early rupture process, Source imaging technique, 2019 Off Yamagata earthquake

©2020. Japan Geoscience Union. All Right Reserved.

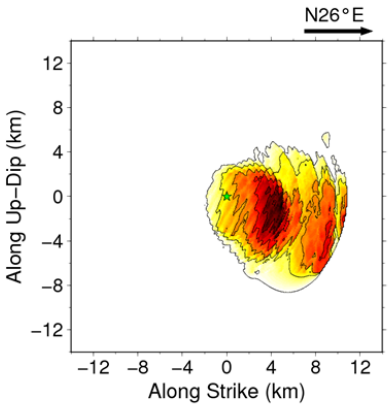

Fig. 1. Radiation strength images on the fault plane given by the JMA CMT solution. Green star indicates the hypocenter.

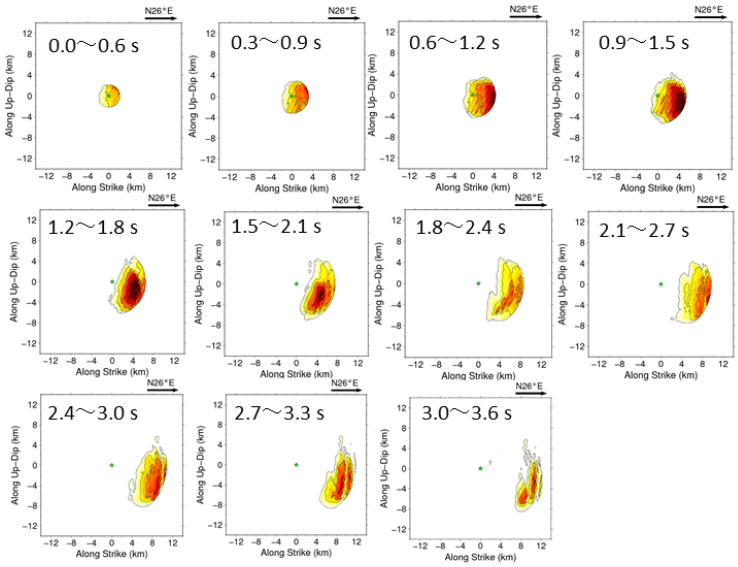

Fig. 2. Snapshot of the radiation strength every 0.3 s. Green star indicates the hypocenter.

©2020. Japan Geoscience Union. All Right Reserved.

Development of a non-linear inversion method to estimate fault geometry from teleseismic data

*Kousuke Shimizu[1], Yuji Yagi[2], Ryo Okuwaki[2], Yukitoshi Fukahata[3]

1. Graduate School of Life and Environmental Sciences, University of Tsukuba, 2. Faculty of Life and Environmental Sciences, University of Tsukuba, 3. Disaster Prevention Research Institute, Kyoto University

A recent advance in developing a new framework of finite-fault modeling, where five basis double-couple components are adopted for representing fault slip along an assumed model-fault plane, has enabled us to construct a source model represented as spatiotemporal distribution of potency density tensor (Shimizu *et al.*, 2020, GJI). The new framework of inversion makes it possible to infer both rupture evolution and fault geometry that are included in teleseismic data. However, the location of resultant potency density tensor along the assumed model plane can be largely deviated from the true location, and hence it is difficult to directly interpret the potency density tensor distribution as a fault geometry. In this study, we propose a way of constructing fault geometry by using only teleseismic data with an iterative process of finite-fault inversion resolving potency density tensor, which is efficient for directly evaluating relationship between rupture propagation and fault geometry. We construct a non-planar model-fault geometry with the following steps: (1) initially inputting a single planar model-fault plane comprising a finite number of flat subfaults, (2) estimating potency density tensor distribution on the input model plane by performing the potency-density inversion, (3) calculating the absolute value of an inner product between the normal vector of each input subfault and that of the fault plane consistent with the estimated potency density tensor on this subfault, and (4) updating the input model-fault geometry to be consistent with the strike and dip angles of the potency density tensor distribution, and then going back to the step (2) unless the average of the absolute value of the inner products at all subfaults becomes acceptably close to 1. We adopted either strike or dip angle distribution for configuring non-planar model plane in order to reduce the number of iterations. Synthetic tests were performed to confirm that our proposed method successfully retrieved an input model-fault geometry with a few iterations for the cases varying either a strike or a dip angle of an input fault. We applied this approach to the M_W 7.7 2013 Balochistan, Pakistan and M_W 7.9 2015 Gorkha, Nepal earthquakes, which are thought to have occurred along a geometrically complex fault system. For the Balochistan and the Gorkha earthquakes, strike angles and dip angles were changed, respectively. The resultant fault models of the Balochistan earthquake showed a curved fault with clockwise rotation of strike angle from northeast to southwest, which was consistent with the location as well as the curved pattern of observed surface rupture distribution of the Balochistan earthquake. The resultant fault model of the Gorkha earthquake showed lower dip angles around the depth of the hypocenter than those in the up- and down-dip regions, which is consistent with the ramp-flat-ramp pattern of fault geometry inferred from the analyses of geodetic and geologic data. These results suggest that this approach works well for constraining geometrically smooth fault of an earthquake.

Keywords: teleseismic waveform, fault geometry, non-linear inversion, finite-fault inversion, 2013 Balochistan Pakistan earthquake, 2015 Gorkha Nepal earthquake

©2020. Japan Geoscience Union. All Right Reserved.

Determination of pre-earthquake megathrust strength and frictional properties on seismogenic faults from near-field data

*Hongfeng Yang[1], Suli Yao[1]

1. The Chinese University of Hong Kong

Frictional properties on seismogenic faults are essential for understanding earthquake nucleation and rupture propagation, as well as ground shaking during earthquakes. However, they are difficult to constrain at seismogenic depths because no direct measurements are available. Frictional strength on faults has been inferred from different approaches, but none of them has reported constraint immediately before a large earthquake. Here, we quantify the frictional strength on seismogenic faults by conducting spontaneous rupture simulations with constraints from near-field observations and kinematic source models. We first estimate stress drop using the kinematic source models, and then conduct a large number of dynamic rupture simulations to search for the best-fit frictional parameters. In the cases of the 2015 Mw 7.8 Nepal and the 2012 Mw 7.6 Nicoya earthquakes, our preferred models show remarkable waveform fit with near-field coseismic displacements and velocities, providing robust constraints of an average strength drop <5MPa. Considering typical ranges for dynamic friction coefficient 0.2 and static friction coefficient , we infer that the maximum value of average effective normal stress and yield stress are ~12.5MPa and ~7.5MPa, respectively. Such low strength is attributed to near-lithostatic pore pressure along the fault interface, which has been implied by seismic studies.

Keywords: Megathrust strength, Frictional properties, Near-field observations

©2020. Japan Geoscience Union. All Right Reserved.

Comparison of the rupture processes of the repeating earthquake sequences off-Iwate that occurred after the 2011 Tohoku oki earthquake

*Ahyi KIM[1], Naoki UCHIDA[2]

1. Yokohama City University, 2. Tohoku University

After the 2011 Tohoku Oki earthquake, both temporal and spatial change of repeating earthquake activity was observed in the off-Iwate area where the large after slip observed. We examined the slip distribution of those various sequences of repeating earthquakes to understand what controls their spatiotemporal changes of the rupture process. We estimated the slip distributions using empirical Green’s function waveform inversion method and compared those results. The results show that, in the same sequence, although the size of rupture area and slip value varies with the magnitude, the main rupture area is overlapped. However, in case of the new sequence appears nearby, the rupture area is reduced so that two rupture areas can be isolated each other. We also compared the peak and average value of the slip for various sequences. In the past study, it was found that average slip value is proportional to the size of earthquake in the wide range (e.g. Chen et. al., 2016). However, in this study, we found that both peak and average slip value is smaller for earthquakes which occurred early stage of the postseismic perios. As time went on, the relationship between the average slip and magnitude becomes comparable with other study. It indicates that the loading rate is one of the factor to control the average slip value and also size of rupture area.

Keywords: repeating earthquake, earthquake rupture process, earthquake slip distribution

©2020. Japan Geoscience Union. All Right Reserved.

Spatiotemporal change in source parameters of repeating earthquakes due to the 2011 Tohoku-oki earthquake

*Kazuya Tateiwa[1], Tomomi Okada[1], Naoki Uchida[1], Toshio Kono[1]

1. Research Center for Prediction of Earthquakes and Volcanic Eruptions, Graduate School of Science, Tohoku University

Many repeating earthquakes occur at Pacific plate boundary in NE Japan. Many studies reported that the behavior of these repeating earthquakes have changed due to afterslip of the 2011 Tohoku-oki earthquake. The numerical simulation showed that recurrence interval, seismic moment, and stress state of repeating earthquakes vary with increment in loading rate (Chen et al., 2010). In this study we systematically investigate on the fluctuation of recurrence of repeating earthquakes occurred at Pacific plate boundary before and after the Tohoku-oki earthquake. We first estimated stress drop of repeating earthquakes by spectral ratio method and investigated characteristics of spatiotemporal distribution of stress drop. Additionally, we estimated aseismic slip rate around seismic patch, verified whether our results are consistent with those of numerical simulation obtained by Chen et al. (2010), and discussed frictional properties of plate boundary.

Stress drops of repeating earthquakes occurred at off-Hidaka and off-Iwate are small. Those at off-Fukushima are high. These characteristic areas are consistent with some previous studies on the general interplate earthquake. Our results showed that many repeating earthquakes whose stress drop is high located in and around asperities of large earthquakes, suggesting the relation between the locked area of large earthquakes and high stress drop area.

We found that seismic moment tends to increase with shortening in recurrence interval when stress drop increases with increment in aseismic slip rate. Also we found that seismic moment tends to decrease with shortening in recurrence interval when stress drop decreases with increment in aseismic slip rate. This trend is consistent with the numerical simulation results of Chen et al. (2010), and we can conclude that we confirmed the usefulness of their numerical simulation.

The slope of regression line for a relationship between recurrence interval and seismic moment (q-value) tends to be negative at off-Iwate and positive at off-Hidaka and Kanto region. Small b-a might be the cause of negative q-value at off-Iwate and high normal stress might be the cause of positive q-value at off-Hidaka and Kanto region.

As described above, it is suggested that spatial changes of source parameters and q-value are closely related with frictional properties of plate boundary.

Keywords: Repeating earthquake, Stress drop

©2020. Japan Geoscience Union. All Right Reserved.

Characteristics of Source Parameter for Aftershocks of the 2016 Kumamoto Earthquake Estimated by the Coda Spectral Ratio Method

*Naoto Maesako[1], Satoshi Matsumoto[2], Ayaho Mitsuoka[1], Group for Urgent Joint Seismic Observation of the 2016 Kumamoto Earthquake

1. Department of Earth and Planetary Sciences, Graduate School of Science, Kyushu University, 2. Institute of Seismology and Volcanology, Faculty of Science, Kyushu University

After the 2016 Kumamoto Earthquake occurrence, a hypocenter distribution along the strike of the Hinagu Fault was found in the aftershock activity deeper than 13 km [Mitsuoka et al., 2019, SSJ fall meeting 2019]. The alignment of the hypocenter has not seen in the distribution before the Kumamoto earthquake. In addition, the activity is located above a low resistivity zone at depth of 18 km [Aizawa et al., 2019], suggesting that the cause of the special activity relates to the resistivity structure.

In order to understand the rupture characteristics of the events, it is essential parameters such as seismic moment (M_0), corner frequency (f_c) and stress drop ($\Delta\sigma$). We estimated M_0 and f_c for 17 aftershocks of the 2016 Kumamoto Earthquake by using a S-wave coda spectral ratio method developed by Somei et al. [2014] and calculated stress drop based on a circular crack model. Then we discussed the spatial variation in stress drops. We investigated the parameters at two groups that were divided the earthquakes into the northern group (11 events) and the southern group (6 events). The parameters for an event were obtained from a processing that we took the spectral ratio of the observed seismogram at a station between an event pair and then stacked among 13 stations to stabilize the ratio. Using the ratio with signal-noise ratio of 2 or more, we estimated seismic moment ratio to the largest event among event of a group and corner frequencies of event pairs by nonlinear least square method.

As the result, we could see the seismic moment and the corner frequency follow the relationship of $M_0 \propto f_c^{-3}$. By adopting seismic moment of the largest earthquake in a group from F-net catalog and assuming a circular clack fault model, we obtained the stress drop [Eshelby, 1957; Brune, 1970,1971]. Stress drops for all 17 events varied between 3.5 and 17 MPa. These were within the range of stress drop for inland earthquake in Japan [Somei et al., 2014]. On the other hand, comparing with similar magnitude earthquakes in Somei et al. [2014], we found stress drops in this study were larger than their results.

In the northern group, we found positive correlation between seismic moment and stress drop (correlation coefficient = 0.78). Geometric average of the stress drops in each group was 6.8 MPa in the northern group, and 12 MPa in the southern group. This is consistent with the previous study that suggest aftershocks in this area caused by shear stress of several MPa to several tens MPa [Mitsuoka et al., 2019, JpGU meeting 2019].

Acknowledgement: Hi-net and F-net were provided by National Research Institute for Earth Science and Disaster Resilience (NIED), Japan. Seismogram data were provided by Hi-net (NIED) and moment tensor solutions were provided by F-net (NIED). The unified earthquake catalog was produced by Japan Meteorological Agency (JMA).

Keywords: The 2016 Kumamoto Earthquake, S-wave spectral ratio method, source scaling, stress drop

©2020. Japan Geoscience Union. All Right Reserved.

Simultaneous estimation of stress drop and rupture directivity of small to medium earthquakes around the Fukushima-Ibaraki border

*Rina Ikeda[1], Keisuke Yoshida[1], Ryo Takahashi[2,1], Toru Matsuzawa[1], Akira Hasegawa[1]

1. Tohoku University, 2. Japan Meteorological Agency

Stress drop is key to understanding the earthquake cycle. Although stress drops of small and medium-size earthquakes have long been estimated by assuming some simple source processes (e.g., Brune, 1970; Sato & Hirasawa, 1973; Madariaga, 1976), developments of recent seismic networks allow us to estimate the rupture propagation process even for small and medium-size earthquakes. In this study, we simultaneously estimated rupture directivities and stress drops of small to medium-size earthquakes (Mw 3.3-5.2) which occurred around the prefectural border between Fukushima and Ibaraki from 11th March 2011 to 31st October 2018.

We first estimated apparent moment rate functions of 348 earthquakes using an empirical Green’s function method. Apparent moment-rate functions were determined at respective seismic stations by the waveform deconvolution method (Ligorria & Ammon, 1999). We used waveforms of nearby smaller earthquakes as empirical Green’s functions. As a result, we found that many of the analyzed earthquakes showed strong directivities of the durations and the amplitudes of apparent moment-rate functions.

Then, by using a generalized rupture model (Dong & Papageorgiou, 2003) that can account for elliptical asymmetry ruptures, we estimated fault sizes, stress drops and rupture directions from the directional dependence of corner frequencies. Introducing asymmetrical rupture of elliptical fault, we succeeded to significantly decrease residuals between observed and synthetic corner frequencies in comparison with analysis assuming symmetrical rupture of circular faults. We found that 306 of 348 earthquakes we analyzed had significant rupture directivities. We also found that fault ruptures tend to propagate in the southeast direction. Stress drops and fault size were systematically larger than those estimated by assuming a symmetrical rupture model.

The median value of the estimated stress drops is 20.2 MPa, which is almost the same as the maximum shear stress estimated by the previous studies in this area (Yoshida et al., 2015a and b). It may suggest that each earthquake released most of the shear stress around its fault plane.

Keywords: stress drop, rupture directivity, crastal earthquakes

©2020. Japan Geoscience Union. All Right Reserved.

Estimating and considering the finiteness of small and moderate earthquakes in Iwaki area

*Naoto Yokotani[1], Aitaro Kato[1], Kazushige Obara[1], Shin'ichi Sakai[1], Takashi Iidaka[1], Tetsuya Takeda[2]

1. Earthquake Research Institute, the University of Tokyo, 2. National Research Institute for Earth Science and Disaster Resilience

In order to understand rupture process of earthquakes more deeply, the parameters that describe spatial and temporal finiteness of earthquakes are important.
Particular models are often assumed so that these parameters can be derived from seismograms.
However, such assumption can make great error when the model does not reflect real rupture process enough.
The second seismic moment gives us these parameters (characteristic rupture duration, fault averaged directivity, and characteristic rupture length) with a few approximations (McGuire 2004).
We applied this second seismic moment approach to waveform data of small to moderate earthquakes in Iwaki area.
We estimated rupture process of these events using waveform data recorded by a dense seismic network (Kato et al., 2013), and discussed spatial variations of these parameters.

Keywords: earthquake rupture, source finitness, second moment

©2020. Japan Geoscience Union. All Right Reserved.

Estimation of near-source Q and its temporal varaiation associated with pore pressure change: a case study of the Yamagata-Fukushima border swarm

*Keisuke Yoshida[1]

1. Tohoku University

Existence of fluids in the crust is key to understanding the occurrence of earthquakes because it affects the fault strength. Given that fluids are intensely distributed in fault zones, anelastic attenuation of seismic waves may be locally high in these regions. The present study examined near-source attenuation in the focal region of the intense swarm activity in the Yamagata-Fukushima border region of Japan by a new simple approach. This earthquake swarm exhibits a distinctive migration behavior of hypocenters similar to fluid-injection induced seismicity and was estimated to be caused by the pore pressure change. Near-source attenuation was estimated by examining the decay of amplitude ratios of nearby earthquake pairs with travel time differences. The obtained *Q-1* was high during the initial ~50 days (with a median value of 0.040 for 2-4 Hz), and significantly decreased to become almost constant for the later period (with a median value of 0.011). This pattern is similar to those independently obtained for background seismicity rate, b-value, stress drop, and fault strength. These patterns can be explained in a consistent manner by the hypothesis that the swarm in question was triggered by fluid movement following the 2011 Tohoku-Oki earthquake, and the source and seismicity characteristics were also affected by this temporal change in pore pressure. Attenuation was high near the earthquake sources than that in the surrounding crust in the initial period of the swarm, indicating the importance of considering the near-source attenuation to correctly estimate the source-effect of an earthquake.

Keywords: attenuation, fluid, swarm

©2020. Japan Geoscience Union. All Right Reserved.

Foreshocks immediately before the starting of earthquakes

*Masaki Yamana[1], Aitaro Kato[1]

1. Earthquake Research Institute, the University of Tokyo

There are many studies describing foreshock activities to understand earthquake initiation process.
On the other hand, few researches remarks on activity immediately before the starting of earthquakes.
For example, Tape et al. (2018) shows simultaneous activity of small earthquakes and very-low-frequency event (VLFE) within 20 seconds before Mw3.7 earthquake in Alaska and discuss the relationship between these events and nucleation process.

In this research, we have visually inspected waveform of shallow crustal earthquakes from 2003 to 2019 with magnitude greater than 3.5 (depth < 15km), in Japan.
From this exploration, we find out that foreshocks occurred immediately before some mainshocks within about 30 seconds.
After detection, we plan to precisely relocate the foreshock and mainshock events applying a double-differential algorithm and discuss the relationship between them.

©2020. Japan Geoscience Union. All Right Reserved.

Estimation of P-wave arrival time differences using P-wave first motion similarity with sampling frequency of 10 kHz

*Yuki Noda[1], Yoshihisa Iio[2]

1. Kyoto University Graduate School of Science, 2. Kyoto University Disaster Prevention Research Institute

In the Western Nagano Prefecture, central Japan, seismic observations with a sampling frequency of 10 kHz have been conducted since June 1995. The seismic stations are located mainly in the eastern part of the aftershock area of the 1984 Western Nagano Prefecture Earthquake, and seismic activity has been high around this area since August 1976. In this area, many earthquakes have shallow focal depths and then large signals can be observed immediately above their hypocenters. Inelastic attenuation is small probably due to homogeneous hard rocks, and the surroundings of the stations are quiet and have low noise levels, so the environment in the area is very suitable for seismic observations. Therefore, we can obtain a large number of microearthquake data and simple waveforms. In addition, the observation with a sampling frequency of 250 Hz of the Manten system has been performed since August 2008.
In this study, we defined mainshocks and their foreshocks of small to moderate earthquakes spatiotemporally based on magnitudes, origin times, and distances between hypocenters. Then, we estimated P-wave arrival time differences of the earthquakes by cross-correlating their P-wave onset waveforms.
We use the vertical component of velocity waveforms. In some spatiotemporally defined foreshock activities, there were many earthquakes that were not similar in the whole waveform but similar in the P-wave initial rise recorded at an identical station. Therefore, we calculated the time differences that maximize cross-correlation coefficients of each pair of earthquakes in a series of foreshock activities, using only windows of a length of 0.01s around P-wave onsets. We treated such time differences as P-wave arrival time differences between two earthquakes at each station. Using these time differences, we will perform relative hypocenter determination with a few meters precision and elucidate the nucleation process of a series of foreshocks which is illustrated by preslip model or cascade model.

Keywords: 10 kHz waveform, cross-correlation, relative hypocenter determination, foreshock

©2020. Japan Geoscience Union. All Right Reserved.

[J] Poster | S (Solid Earth Sciences)：S-SS Seismology

[S-SS16] Active faults and paleoseismology

convener:Mamoru Koarai(Earth Science course, College of Science, Ibaraki University), Hisao Kondo(Geological Survey of Japan, National Institute of Advanced Industrial Science and Technology), Takashi OGAMI(National Institute of Advanced Industrial Science and Technology), Yoshiki Sato(Advanced Industrial Science and Technology, Geological Survey of Japan)

Geologic and historic information on seismic cycles and on the magnitude and source faults of past earthquakes is essential information to understand future large earthquakes. The study of past faulting and seismicity is an important issue for an interdisciplinary community of seismologists, geologists, geomorphologists, archaeologists, and historians.

[SSS16-P02] Discovery of active faults in the Abukuma Mountains, northeast Japan

*Masayoshi Tajikara[1], Takashi Nakata[2], Hideaki Goto[3] (1.Association for the Development of Earthquake Prediction, 2.Hiroshima Univ. Emeritus Prof., 3.Hiroshima Univ.)

[SSS16-P04] Paleoseismology of the northren part of Kamishiro fault, ISTL active fault zone, central Japan

*Daisuke Hirouchi[1], Nobuhisa Matsuta[2], Tatsuya Ishiyama[3], Kenichi Yasue[4], Nobuhiko Sugito[5], Yoshihiro Takeshita[1], Natsuko Fujita[7], Hiroshi Sawa[6], Kotaro Mizutani[8], Kaoru Taniguchi[9] (1.Faculty of Education, Shinshu University, 2.Okayama Univ., 3.Univof Tokyo, 4.Toyama Univ., 5.Hosei Univ., 6.Tsuruoka , 7.JAEA, 8.GRI, 9.Pasco)

[SSS16-P05] Characteristics of the latest slip zone in the near-surface fault zone of the Neodani Fault

Aiki Tsuru[1], *Tomoyuki Ohtani[1], Kazuma Yatabe[1] (1.Department of Civil Engineering, Gifu University)

[SSS16-P06] Holocene tectonic landform of the eastern marginal fault of the Nara basin

*Hiroyuki Tsutsumi[1], Nobuhiko Sugito[2], Noriyoshi Yoshida[1], Haruo Kimura[3] (1.Department of Environmental Systems Science, Faculty of Science and Engineering, Doshisha University, 2.Faculty of Sustainability Studies, Hosei University, 3.Central Research Institute of Electric Power Industry)

[SSS16-P07] Drifted huge boulders by storm surges since 1976 derived from the dike of quartz porphyry in Hashigui-iwa facing the Nankai Trough, Pacific side of central Japan

*Hideaki Maemoku[1], Yuichi Namegaya[2], Masanobu Shishikura[2], Tomoo Echigo[3], Kanae Suzuki[4] (1.Department of Geography, Hosei University, Japan, 2.AIST, Geological Survey of Japan, 3.Geo-Research Institute, Japan, 4.A Graduate of Hosei University)

[SSS16-P08] Densely microtremor observation to estimation of subsurface structure at Shikano fault due to the 1943 Tottori earthquake, Japan

*Tatsuya Noguchi[1], Kasuki Kobayashi[2], Sanri Okano[1], Isamu Nishimura[3], Takao Kagawa[1] (1.Faculty of Engineering, Tottori University, 2.Graduate School of Sustainability Science, Tottori University, 3.Graduate School of Engineering, Tottori University)

[SSS16-P09] Fault history and Trench survey of separated area from surface ruptures in Futagawa fault zone, Kumamoto Prefecture

*Noriyuki Shibuya[1], Masashi Omata[1], Yoshiki Mori[1], Naoto Inoue[2], Naoko Kitada[2], Tonagi Masao[3], Tsutomu Takahama[3] (1.PASCO CORPORATION, 2.Geo-research Institute, 3.KOZO KEIKAKU ENGINEERING Inc.)

[SSS16-P10] Paleoseismic history and horizontal slip of the Futagawa–Hinagu fault zone based on paleoseismological and tectonic geomorphological survey at Hirata, Mashiki Town, Kumamoto Prefecture

*Yoshiya Iwasa[1], Yasuhiro Kumahara[2], Hideaki Goto[3], Masayuki Torii[4] (1.Student of Graduate School of Education, Hiroshima University, 2.Graduate School of Education, Hiroshima University, 3.Graduate School of Letters, Hiroshima University, 4.Center for Water Cycle, Marine Environment and Disaster Management, Kumamoto University)

[SSS16-P11] Compiling descriptions on tsunami accompanied with the 1914 Sakurajima earthquake and inferred causes

*Reiji Kobayashi[1], Kazutoshi Kawano[2], Atsushi Kuroda[2], Keigo Haruta[2], Shunichiro Fujii[2] (1.Graduate School of Science and Engineering, Kagoshima University, 2.Faculty of Science, Kagoshima University)

[SSS16-P12] Tectonic landform and rock-controlled landform along fault trace of the Aceh segment, the northernmost Sumatran Fault

*Yoshio Soeda[1], Hiroyuki Tsutsumi[2], Nobuhisa Matsuta[3], Nazli Ismail[4], Bukhari Ali[4] (1.West Japan Engineering Consultants,Inc., 2.Doshisha University, 3.Okayama University, 4.Syiah Kuala Univ.)

[SSS16-P13] Triggered Surface Faults Associated with Large Earthquakes Detected by L-band SAR Interferometry

*Satoshi Fujiwara[1], Takayuki Nakano[1], Yu Morishita[1] (1.GSI of Japan)

[SSS16-P14] Estimation of fault activity by linear discriminant analysis using chemical composition of fault gouge

*Ryo Tateishi[1], Koji Shimada[2], Mayuko Shimizu[2], Shigeru Sueoka[2], Masakazu Niwa[2], Tsuneari Ishimaru[2] (1.University of Toyama, 2.Japan Atomic Energy Agency)

[SSS16-P16] Study on the structure of sediment covering basement rock in trench survey

*Shiro Tanaka[1], Shingo Kimura[2], Norihiko Sakakura[3] (1.Central Research Institute of Electric Power Industry, 2.Hokuriku Electric Power Company, 3.Dia Consultants Co., Ltd)

[SSS16-P17] Some outcrops along the Ide Fault, a part of the eastern margin fault zone of the Nara basin, central Hoshu.

*Taku Komatsubara[1] (1.Institute of Geology and Geoinformation, Advanced Industrial Science and Technology)

Discovery of active faults in the Abukuma Mountains, northeast Japan

*Masayoshi Tajikara[1], Takashi Nakata[2], Hideaki Goto[3]

1. Association for the Development of Earthquake Prediction, 2. Hiroshima Univ. Emeritus Prof., 3. Hiroshima Univ.

The Abukuma Mountains are located on the Pacific coast of northeastern Japan, approximately 170 km north-south and 50 km east-west. Since the Abukuma Mountains have been considered as a region with gentle crustal deformation, detailed active fault surveys have rarely been conducted. Therefore, active faults are scarcely mapped except for the normal faults around Iwaki and the Futaba fault. We conducted analysis of tectonic landforms using 1/1000 aerial photographs of the 1970s, and found many (presumed) active faults. In this presentation, we will report distribution and properties of these faults.

The faults mapped in this study are mainly strike-slip faults, with a left-lateral slip in the NW-SE strike and a right-lateral slip in the NE-SW strike. Based on slip sense of these faults, we considered that these faults have been formed in east-west compression. In the April 2011 Fukushima Hamadori earthquake, earthquake faults occurred along the Yunotake Fault. These earthquake faults were formed in response to the east-west extension, and its formation mechanism is different from the active faults described in this study. This fact suggests that fault activities that are not induced by huge earthquakes on the megathrust on subduction zone could be occurred in the Abukuma Mountains. Since most of the faults mapped in this study are short, it is unlikely that all of these faults will be seismogenic faults. However, some relatively larger faults may generate M7 class earthquakes.

Keywords: Abukuma Mountains, active fault, mapping, aerial photography

©2020. Japan Geoscience Union. All Right Reserved.

Paleoseismology of the northren part of Kamishiro fault, ISTL active fault zone, central Japan

*Daisuke Hirouchi[1], Nobuhisa Matsuta[2], Tatsuya Ishiyama[3], Kenichi Yasue[4], Nobuhiko Sugito[5], Yoshihiro Takeshita[1], Natsuko Fujita[7], Hiroshi Sawa[6], Kotaro Mizutani[8], Kaoru Taniguchi[9]

1. Faculty of Education, Shinshu University, 2. Okayama Univ., 3. Univof Tokyo, 4. Toyama Univ., 5. Hosei Univ., 6. Tsuruoka , 7. JAEA, 8. GRI, 9. Pasco

The Kamishiro fault is located in the northernmost part of the 150-km-long Itoigawa-Shizuoka Tectonic Line (ISTL) active fault zone, central Japan. Immediately after the destructive Mj 6.7 earthquake of November 22, 2014, which occurred in the north-ern part of the Nagano Prefecture, we conducted trench survey across the northern part of the reverse-faulting Kamishiro fault.

Keywords: ISTL, kamishiro fault, trench servey

©2020. Japan Geoscience Union. All Right Reserved.

Characteristics of the latest slip zone in the near-surface fault zone of the Neodani Fault

Aiki Tsuru[1], *Tomoyuki Ohtani[1], Kazuma Yatabe[1]

1. Department of Civil Engineering, Gifu University

The activity assessment of the active faults basically needs younger sediments. To understand the fault activity in the area with no younger sediments, it is desired to develop the new method which assesses the fault activity from the fault rocks in the basement rocks. The purpose of this study is to clarify the characteristics of the near-surface latest slip plane in the basement rocks based on deformation structure, mineral assemblage and element composition using the active fault with a large displacement during an earthquake.

The study fault is the Neodani Fault ruptured in the 1891 Nobi earthquake. The studied sites are Neo-Nagamine and Hinata, Motosu City, central Japan where left lateral displacements of 3 m and 8 m were occurred in 1891, respectively. The basement rock in the area including the studied sites is the Jurassic mélange with mudstone matrix and blocks of chert, siliceous shale, sandstone and basalt. At the Neo-Nagamine site, black shale and siliceous shale are at the northeast and southwest sides of the latest slip plane, respectively. The fault zone consists of fault breccias and gouges originated from black shale and siliceous shale, and the latest slip plane is the fault gouge of black shale. At the Hinata site, basalt and mudstone are at the northeast and southwest sides of the latest slip plane, respectively. The fault zone consists of fault gouges of them. The latest slip plane shows pale-yellow color and its original rock is not clear from the field observation. These fault zones are covered by the Quaternary river sediments, and the gravels along the latest slip plane are rotated at both sites.

The block samples were collected from the both sites, and deformation structure is observed on the polished slabs. This observation reveals that the gravels are included in the latest slip plane in the basement rocks. These are rounded gravels with 2 mm diameter, and some of them are chert at the Neo-Nagamine site. These are a subrounded chert gravel with 5 cm diameter and a rounded sandstone one with 1 cm diameter at the Hinata site. They do not come from the neighboring fault rocks and intact rocks of the basement.

The powder X-ray diffraction (XRD) and the X-ray fluorescence analysis (XRF) were performed using the powder samples to clarify mineral assemblage and element composition of the fault rocks. Smectite is included in most of the fault gouges at both sites, and kaolinite is detected from the latest slip plane at the Hinata site. Distinctive element mobilization between the latest slip plane, fault rocks and intact rocks is not recognized from the result of XRF.

The gravels including the latest slip plane is considered to come not from the neighboring fault rocks and intact rocks but the river sediments above the basement fault rocks according to the occurrence. Kaolinite in the latest slip plane and no distinctive element mobilization support this idea because Kaolinite is a product of surface weathering. The diameter of gravels in the latest slip plane is larger at the Hinata site with a larger displacement during the 1891 earthquake. This indicates that the wider opening was occurred near the surface at the area with larger displacement. Ring shear experiments under the lower confined pressure by Scaringi et al. (2018) show that clay gouge is more dilated with larger displacement. This suggests that the latest slip plane is opened during the 1981 earthquake due to the dilation of the

©2020. Japan Geoscience Union. All Right Reserved.

slipped fault gouge at the deeper part. Therefore, when the gravels above the sediments are included in the latest slip plane in the basement rocks and the sedimentation age of the gravels is known, the age of the latest faulting is limited after the sedimentation age.

Keywords: latest slip zone, near-surface fault zone, Neodani Fault

©2020. Japan Geoscience Union. All Right Reserved.

Holocene tectonic landform of the eastern marginal fault of the Nara basin

*Hiroyuki Tsutsumi[1], Nobuhiko Sugito[2], Noriyoshi Yoshida[1], Haruo Kimura[3]

1. Department of Environmental Systems Science, Faculty of Science and Engineering, Doshisha University, 2. Faculty of Sustainability Studies, Hosei University, 3. Central Research Institute of Electric Power Industry

The north-trending eastern marginal fault of the Nara basin consists of a series of east-dipping reverse faults at the topographic boundaries between mountains and hills on the east and basins and lowlands on the west. The fault zone poses high seismic hazards to the central Kinki area as it passes nearly Kyoto and Nara metropolitan areas. However, the probability of earthquake occurrence from this fault zone in the next 30 years is very loosely constrained due to considerable uncertainty on the timing of the latest faulting event. The Disaster Prevention Research Institute, Kyoto University, has started a 3-year research project called "Comprehensive Research Project for the Nara-bonchi-toen Fault Zone" that is funded by the Headquarters for Earthquake Research Promotion, MEXT. Doshisha University is responsible for theme 1 of the project that focuses on active fault mapping, slip rate estimation, and obtaining data on the past activity of the fault zone. As part of investigations under theme 1, we acquired 0.5-m-mesh digital elevation data from airborne laser scanning over the fault zone in the northeastern margin of the Nara basin. Besides, we interpreted 1:10,000-scale aerial photographs taken immediately after World War II by the US military. We identified a few localities with tectonic scarp less than a few meters high that are probably related to the most recent movement of the fault. Also, geologic cross-sections using the "Database for Boreholes in the Kansai Area" clearly illuminate the deformation of the Osaka Group and the overlying terrace deposits by the fault strands, which enables us to estimate the vertical offsets of strata and to estimate dip-slip rates.

Keywords: the eastern marginal fault of the Nara basin, airborne laser scanning, tectonic landform, borehole data

©2020. Japan Geoscience Union. All Right Reserved.

Drifted huge boulders by storm surges since 1976 derived from the dike of quartz porphyry in Hashigui-iwa facing the Nankai Trough, Pacific side of central Japan

*Hideaki Maemoku[1], Yuichi Namegaya[2], Masanobu Shishikura[2], Tomoo Echigo[3], Kanae Suzuki[4]

1. Department of Geography, Hosei University, Japan, 2. AIST, Geological Survey of Japan, 3. Geo-Research Institute, Japan, 4. A Graduate of Hosei University

Hashigui-iwa is located seven kilometers northeast of Cape Shiono-misaki facing the Nankai Trough, which is the subduction zone between the Eurasian Plate and the Philippine Sea Plate. It is Neogene dike of quartz porphyry intruded into Neogene sedimentary rocks mainly composed of shale and sandstone. It also seems like a bridge pier composed of 25 individual slab or pillar rocks aligned in a straight line. In the western side of Hashigui-iwa dike, wave-cut benches are well developed on sedimentary rocks during the late Holocene. A few thousands of boulders are scattered on the benches. All boulders are composed of volcanic rock derived from Hashigui-iwa dike. Possible mechanism for transporting the boulders more than several tens of meter from their original position must be inferred as strong wave action due to typhoons or tsunamis. We clarified the main cause for horizontal movement of scattered boulders should have been tsunamis generated by faulting in the Nankai Trough region from numerical analysis on water velocity (Maemoku et al.,2010). This study aims to constrain the maximum dimensions of boulders to be drifted by storm surge using multiple aerial photographs taken in-between 1976 and 2019. We found that at least 19 boulders were moved during the period. The maximum length of the boulders is about 1.85 m (estimated mass is 2.6 ton), and it is classified into light mass of all the boulders. This indicates that the boulders with length larger than 2 m are difficult to be move due to storm surges, but are moved due to large tsunamis.

Keywords: Nansai Trough, tsunami boulder, storm surge

台風	発生日時	通過日時	中心気圧	最大瞬間風速(風向)	最高潮位	有義波高	最大波高
2007年4号	07月09日09時	07月15日06時	962.2hPa	32.8m/s(SSE)	135cm	11.20m	19.70m
2011年06号	07月12日15時	07月20日10時	973.4hPa	33.3m/s(SSE)	138cm	9.45m	15.77m
2011年12号	08月25日09時	09月02日15時	978.6hPa	30.9m/s(ESE)	170cm	11.06m	16.90m
2011年15号	09月13日21時	09月21日09時	961.0hPa	31.6m/s(E)	126cm	8.38m	12.78m
2012年17号	09月21日03時	09月30日15時	959.9hPa	36.4m/s(NE)	178cm	10.56m	16.67m
2014年18号	09月29日15時	10月06日03時	954hPa	39.0m/s(ESE)	224cm	10.92m	17.44m
2016年16号	09月13日03時	09月20日15時	988.2hPa	36.5m/s(WSW)	132cm	10.37m	14.2m
2017年21号	10月16日03時	10月22日18時	960.2hPa	33.7m/s(NWN)	197cm	8.74m	13.0m
2018年21号	08月28日03時	09月04日12時	979.6hPa	35.3m/s(SSE)	173cm	10.84m※	17.7m※
2018年24号	09月21日15時	09月30日15時	958hPa	43.0m/s(SSW)	254cm	9.57m※	13.55m※

©2020. Japan Geoscience Union. All Right Reserved.

Densely microtremor observation to estimation of subsurface structure at Shikano fault due to the 1943 Tottori earthquake, Japan

*Tatsuya Noguchi[1], Kasuki Kobayashi[2], Sanri Okano[1], Isamu Nishimura[3], Takao Kagawa[1]

1. Faculty of Engineering, Tottori University, 2. Graduate School of Sustainability Science, Tottori University, 3. Graduate School of Engineering, Tottori University

The Shikano and Yoshioka fault occurred by the 1943 Tottori earthquake. A geological structure was considered based on previous studies from trench surveys, field surveys, and questionnaire surveys. In this study, we conducted densely microtremor surveys to estimate a subsurface structure and to understand strong ground motion characteristics in closely area of faults.

As a result, microtremor H/V spectra and the distribution of the predominant period were obtained. It was found that the H/V shape was different according to topography and sediment conditions. Furthermore, the H/V shape was different on both sides of the fault surface displacement point, and that it was different in the direction of the horizontal component. The dispersion curve characteristics of the phase velocity were not different according to the fault surface displacement point.

Keywords: microtremor observation, characteristics of ground motion, Shikano fault, 1943 Tottori earthquake

©2020. Japan Geoscience Union. All Right Reserved.

Fault history and Trench survey of separated area from surface ruptures in Futagawa fault zone, Kumamoto Prefecture

*Noriyuki Shibuya[1], Masashi Omata[1], Yoshiki Mori[1], Naoto Inoue[2], Naoko Kitada[2], Tonagi Masao[3], Tsutomu Takahama[3]

1. PASCO CORPORATION, 2. Geo-research Institute, 3. KOZO KEIKAKU ENGINEERING Inc.

A trench survey was conducted at a location away from the main fault (Jinnai area, Otsu-cho, Kikuchi-gun, Kumamoto Prefecture). At least four faulting events were identified on the trench slope, and it was revealed that there were repeated faulting activities in the past at the surface deformation position due to the subsidiary fault that occurred in the 2016 Kumamoto earthquake.
Event I: A ‘crack with an opening’ reaching the ground surface is confirmed. It was formed by the 2016 Kumamoto earthquake.
Event II: On the trench wall, a ‘structure in which the upper stratum enters into a wedge shape’ can be confirmed. It is estimated that the event time is after 9,820 cal.BP and before 3,410 cal.BP.
Event III: On the trench wall (S-plane), ‘a vertical displacement of about 50 cm’ is given to the base layer.It is estimated that the event time is after 11,240 cal.BP and before 10,450 cal.BP.
Event IV: Events can be identified from the shear structure found only in the basement. The activity date and number of activities are unknown.
Therefore, in the Jinnai Trench, fault activity events prior to the 2016 Kumamoto Earthquake is after 9,820 cal.BP and before 3,410 cal.BP. This age coincides with the time of the faulting event, which is confirmed approximately 4,000 to 9,000 years before the main fault of the Futagawa fault.

Keywords: surface rupture, Futagawa fault zone, active fault, subsidiary fault

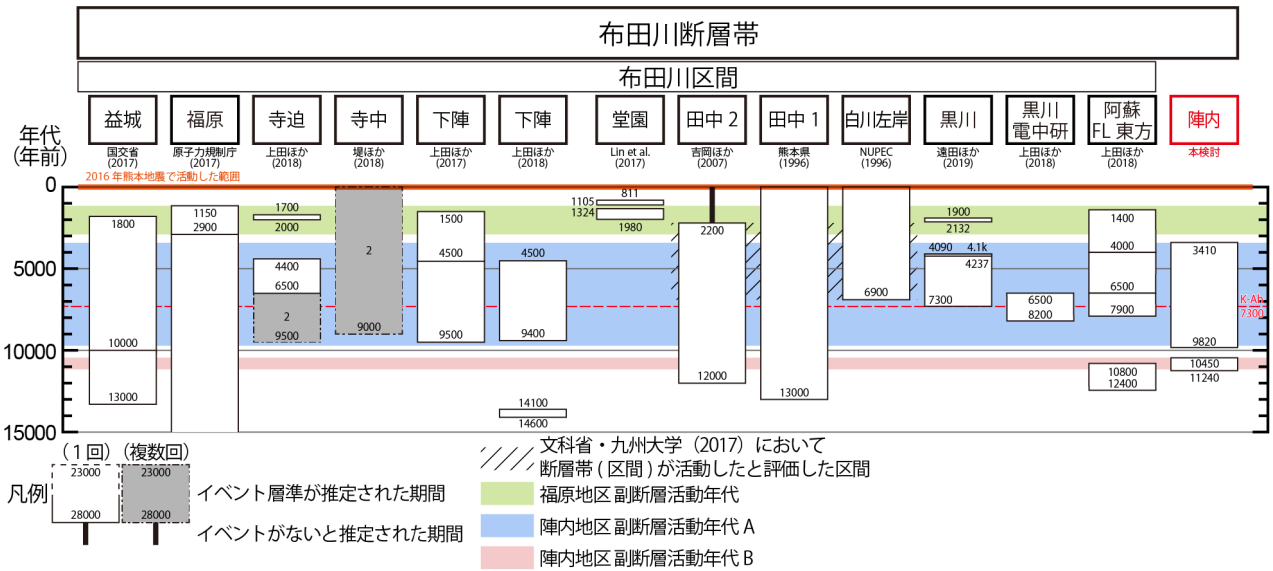

©2020. Japan Geoscience Union. All Right Reserved.

Paleoseismic history and horizontal slip of the Futagawa–Hinagu fault zone based on paleoseismological and tectonic geomorphological survey at Hirata, Mashiki Town, Kumamoto Prefecture

*Yoshiya Iwasa[1], Yasuhiro Kumahara[2], Hideaki Goto[3], Masayuki Torii[4]

1. Student of Graduate School of Education, Hiroshima University, 2. Graduate School of Education, Hiroshima University, 3. Graduate School of Letters, Hiroshima University, 4. Center for Water Cycle, Marine Environment and Disaster Management, Kumamoto University

On the 16 April, 2016 Kumamoto earthquake (Mj7.3), ~31km-long right-lateral surface ruptures appeared along the previously mapped Futagawa-Hinagu fault zone. According to the evaluation by the Earthquake Research Committee of the Headquarters for Earthquake Research Promotion (2013) before the Kumamoto earthquake, the slip rate of the fault zone was 0.1-0.3 mm/yr, and the recurrence interval was 8,100-26,000 years. However, some trenching surveys conducted along surface ruptures after the Kumamoto earthquake showed that the timing of the most recent faulting event before the Kumamoto earthquake was 1,000-4,000 yrBP. Moreover, the horizontal slip rate of the fault zone is 1.5-3.7 mm/yr, and the recurrence interval is 500-2,000 years in the northeastern part of the fault zone based on the investigation of the fault outcrop. On the other hand, it is not enough to examine the paleoseismic history and the slip rate in the central part of the fault zone. Then, we conducted the paleoseismological and tectonic geomorphological study in Hirata, Mashiki Town located in the central part of the fault zone in September, 2019, in order to examine the paleoseismic history and to reveal the horizontal slip rate.
The study site is the formerly cultivated land located east of the Hiratanaka Community Center in Mashiki Town. In the south of the study site, hills consisting of Aso-1 to Aso-4 pyroclastic flow deposit are distributed, and the formerly cultivated land is located at the fan surface formed the outlet of the dissected valley. The dissected valley is dextrally offset about 5m. At the formerly cultivated land, left-stepping surface ruptures appeared associated with the Kumamoto earthquake. The fence dextrally offset about 1.2m in the Hiratanaka community center site. In order to reveal the three-dimensional structure of the strata, we excavated two trenches (trench A and B).
On the trench A wall, surface soil layer, alternation of gravel and silt, and silt layer were mainly exposed. The alternation strata are distributed only on the north side of the wall and sloped to the north. Since it contains many amphiboles, it is considered to be a constitute deposit of fan surface originating from Aso-4. The upper layer of the alternation strata has a 14C age of 10,408-10,229 calBP. The silt layer is distributed only on the south side of the wall. On the trench A wall, the main fault that separates the alternation strata and silt layer and three secondary faults that displace the alternation strata. The main fault has a flower structure branching into several lines in the upper part on the west wall, and the branched fault continues to the opening crack recognized on the surface.
On the wall and the bottom of the trench B, alternation of gravel and silt and fault which bordered the layer and gravel layer covering the alternation strata were exposed. The alternation strata sloped to the north as in the trench A, and the thickness of each single layer was 0.2-0.4 m. It is considered to be the alternation strata exposed on the trench A wall based on the sedimentary facies. It is considered that the gravel layer covering the alternation strata is a debris flow sediment, and it is a sediment which constitutes the fan surface together with the alternation strata. The bottom of the alternation strata has a 14C age of 5,270 -4,871 calBP on trench B wall.
Based on the deformational features of exposed strata of trench A and B, we identified at least two faulting events, including the Kumamoto earthquake after about 10,000 yrBP. Based on the sedimentary and faulting structure and 14C age of the strata, the timing of the penultimate event is considered to be

©2020. Japan Geoscience Union. All Right Reserved.

4,800-10,400 yrBP. In the trenching site, any events after 4800 yrBP cannot be recognized because any strata after 4800 years ago has not been deposited.
On the other hand, the amount of the dextral offset of the alternation strata is at least 2.9m based on the planar structure of the alternation strata. Since this amount of offset is larger than the amount of offset in the Kumamoto earthquake (Approximately 1.2 m), it seems to have faulted multiple times. This survey is being continued even at the time of the manuscript submission, and the horizontal slip rate of the fault zone will be announced on the day.

Keywords: 2016 Kumamoto earthquake, surface rupture, trenching survey, horizontal slip

©2020. Japan Geoscience Union. All Right Reserved.

Compiling descriptions on tsunami accompanied with the 1914 Sakurajima earthquake and inferred causes

*Reiji Kobayashi[1], Kazutoshi Kawano[2], Atsushi Kuroda[2], Keigo Haruta[2], Shunichiro Fujii[2]

1. Graduate School of Science and Engineering, Kagoshima University, 2. Faculty of Science, Kagoshima University

During the 1914 eruption of Sakurajima volcano, a large earthquake (M7.1) occurred at 18:30, January 12 (e.g., Imamura 1920; Omori 1922; Abe 1981). The hypocenter was estimated by previous studies and most of them are located from west to south of Sakurajima. The surface faults have not been found, and the distribution of aftershock hypocenters has also not been estimated. We thus have no information of the source fault.

Tsunami was observed after this earthquake. In general, most tsunamis are caused by uplift and subsidence of seafloor due to fault motion associated with a large earthquake. Thus this tsunami might provide us with the information of the source fault of the earthquake. Kobayashi (2019, Seismological Society of Japan Fall Meeting 2019) compiled descriptions about this tsunami in several reports and papers and inferred its cause.

In this study, further we have added descriptions of the tsunami in scientific reports and in local chronicles of towns and villages along Kagoshima bay. We have also checked the Kagoshima Newspaper published after the eruption, but we have not found news articles about tsunami. The compilation of reports shows that the areas where the tsunami was observed are only coasts of Kagoshima city and Aira town. According to Hasegawa (1914) and Omori (1918), the tsunami arrived 20 minutes or 1 hour after the earthquake. The areas and times of the tsunami arrivals suggest that the tsunami may not occur due to fault motion associated with the earthquake. The cause might be landslide of the seafloor or the coast. Omori (1918) inferred the subsidence of the seafloor.

This research was partly performed as a part of the Science Club for students of Faculty of Science, Kagoshima University.

Keywords: the 1914 Sakurajima earthquake, tsunami, eruption

©2020. Japan Geoscience Union. All Right Reserved.

Tectonic landform and rock-controlled landform along fault trace of the Aceh segment, the northernmost Sumatran Fault

*Yoshio Soeda[1], Hiroyuki Tsutsumi[2], Nobuhisa Matsuta[3], Nazli Ismail[4], Bukhari Ali[4]

1. West Japan Engineering Consultants,Inc., 2. Doshisha University, 3. Okayama University, 4. Syiah Kuala Univ.

The Sumatran fault is a major arc-parallel strike-slip fault that accommodates much of the right-lateral component of oblique subduction of the Indian-Australian plate beneath the Sunda plate. The 1,900-km-long fault is divided into 19 segments (Sieh and Natawidaja, 2000). The Aceh and Seulimeum segments, which are the northernmost segments of the Sumatran fault with a high slip rate (Natawidjaja and Triyoso, 2007; Natawidjaja, 2018), have not ruptured in the past 120 years (Hurukawa et al., 2014). Although the seismic potential of the Aceh and Seulimeum segments is considered to be high, fundamental geologic data on the northernmost Sumatran fault, such as detailed fault trace, late Quaternary slip rate, etc. are poorly documented.

Since 2012, we have conducted tectonic geomorphologic and paleoseismic studies in the northernmost Sumatran fault in Aceh Province. In 2015, we conducted a trenching survey on the Seulimeum segment at Lamtamot where the fault cuts a fluvial terrace. We identified geologic evidence of three seismic events after AD1280 (Tsutsumi et al., 2018).

In the northwestern portion of the Aceh segment, the tectonic geomorphic features are not well documented. In 2019, we carried out the survey in this area. We first conducted topographic interpretation to identify tectonic geomorphic features using stereoscopic images prepared from ALOS PRISM images with a spatial resolution of 2.5 m, and the stereoscopic images prepared from AW3D30, with a spatial resolution of 30 m DEM. We then conducted field geologic observations. During the filed survey, we utilized drone to confirm the topographic features at the sites where the accessibility for field observations was limited.

The Aceh segment with a general strike of N50°W in the study area is the direct northwestern extension of the main fault trace. The active fault line is traced in the lowland (Banda Aceh plain) from south of Jantho toward the northwest until reaching latitude 5°25’ N. The down-to-the southwest scarp and linear troughs are observed in the lowland. From the latitude 5°25’ N to the coastline toward the northwestern direction, active faulted geomorphic features are obscured, though the topographic boundary of the lowland and the Barisan Mountains is apparent.

Along the topographic boundary of the lowland and the Barisan Mountains, alignment of saddles, topographic lineaments and systematic right-lateral offsets of the streams were identified. We observed fracture zones and lithological boundaries of calcareous sand stone and mud stone at the locations of these geomorphic features. We also found an exposure of share zone in the silt-sand stone. The fault in the silt-sand stone do not extend upward to the overlying calcareous sand stone. These geomorphic features identified at the topographic boundary are interpreted to be rock-controlled landform, not active tectonic landform. Although fault lies along the topographic boundary, this fault is interpreted to be inactive in the northwestern portion of the Aceh segment. The active fault is found on the basin side of the topographic boundary of this area.

From the latitude 5°25’ N to the coastline toward the northwestern direction, active faulted geomorphic features are obscured. Ghosal et al. (2012) pointed out that based on marine geophysical data the active fault of the Aceh segment extends toward the northwestern direction offshore. These infers a possibility that the active fault trace of the Aceh segment lies in Banda Aceh plain as a concealed fault. In order to obtain a better understanding of the seismic hazard of the Sumatran fault in Aceh Province, further geoscientific investigations are desirable such as tectonic geomorphology, paleoseismology, and

©2020. Japan Geoscience Union. All Right Reserved.

geophysics.

Acknowledgments: This work was supported by Grants-in-Aid for Scientific Research from the Ministry of Education, Culture, Sports, Science and Technology, Japan to Takao Tabei (No. 17H04577).

Keywords: Sumatran fault, Aceh segment, tectonic landform, rock-controlled landform

©2020. Japan Geoscience Union. All Right Reserved.

Triggered Surface Faults Associated with Large Earthquakes Detected by L-band SAR Interferometry

*Satoshi Fujiwara[1], Takayuki Nakano[1], Yu Morishita[1]

1. GSI of Japan

Interferograms of L-band SAR satellite for large earthquakes generally show elastic deformation caused by the main earthquake as well as numerous complex surface displacements that cannot be explained by the motion of seismic source faults. We have identified linear surface displacements in the interferograms considered to be triggered surface faults for several large earthquakes. These linear surface displacements include shallow extensions of the seismic source faults, however, most of them are located away from the hypocenter and are considered to be triggered surface faults which are not directly connected to the seismic source faults. Since these triggered surface faults have not found evidence of generating large seismic motions, many are unlikely to cause major earthquakes in the future.

However, we found a new example of an active fault that had caused a moment magnitude of 7 class earthquake in the past became a triggered surface fault associated with another moment magnitude of 6 class earthquake of 2018 Northern Osaka.

The emergence of these triggered surface faults associated with large earthquakes is likely a common phenomenon, however, their causes vary and are diverse. For example, in 2016 Kumamoto earthquake sequence, the strain created by the main shock and the motion of the triggered surface fault coincided in a specific area, and it was thought that the main shock directly created the triggered surface faults. Conversely, in another area the movements of the two did not match, and the main shock was just a trigger, and there were also triggered surface faults that have released strain accumulated over a long period from the past.

From these, the following hypothesis is considered. Regardless of the causes, a large earthquake tends to induce the movement of triggered surface faults. Then, the triggered surface faults release the strain by causing fault motions and form linear surface displacements. Once such faulting occurs, they remain as weak fault planes that are easy to move, and will repeatedly move again at the same locations in the future.

Keywords: Triggered surface fault, Kumamoto earthquake, InSAR, Active fault

©2020. Japan Geoscience Union. All Right Reserved.

Triggered surface faults (TSF) associated with large earthquakes

L-band SAR detected large number of TSFs.

Similar TSFs appear to form groups.

Even though they have similar shapes, the causes of different group of TSFs are diverse.

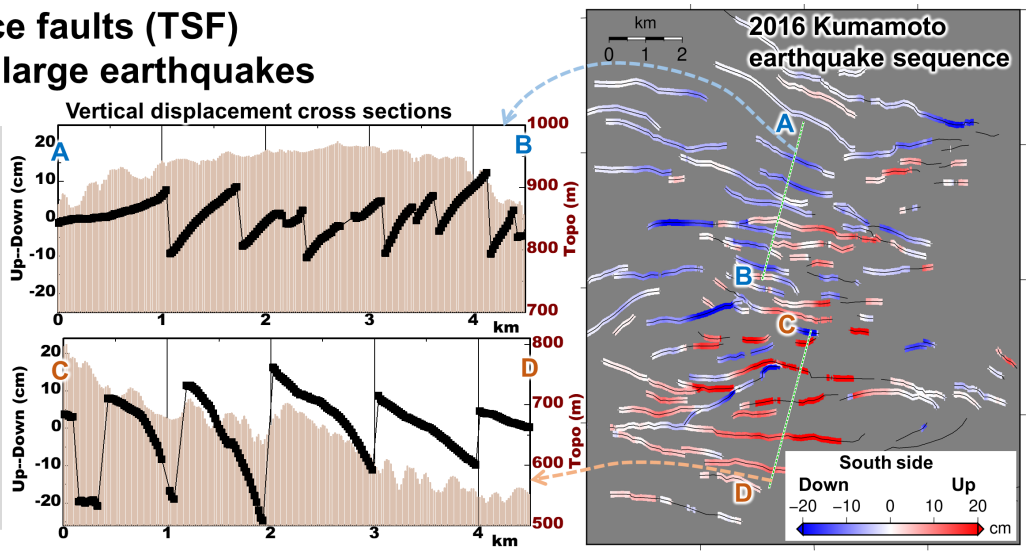

©2020. Japan Geoscience Union. All Right Reserved.

Estimation of fault activity by linear discriminant analysis using chemical composition of fault gouge

*Ryo Tateishi[1], Koji Shimada[2], Mayuko Shimizu[2], Shigeru Sueoka[2], Masakazu Niwa[2], Tsuneari Ishimaru[2]

1. University of Toyama, 2. Japan Atomic Energy Agency

Introduction: The identification of active faults is based on the displacement and deformation of the current topography and the late Quaternary strata. However, in the absence of them at the site, it is quite difficult to determine the fault activity. Tateishi et al. (2019) performed linear discriminant analysis using the chemical composition data of fault gouges of active faults and inactive faults in Japan, and found that the obtained discriminants can identify fault activity without error. It has been shown that the combinations of elements that represent are limited to six elements: TiO_2, Al_2O_3, MgO, Na_2O, P_2O_5, and Ba. In this study, we performed linear discriminant analysis with additional data for the purpose of further narrowing down the elements representing the difference in fault activity and obtaining a better discriminant.

Methods: This research was carried out in the following order; collection of papers, extraction of chemical composition data of fault gouge, addition of new chemical analysis data, formatting of input data, variable selection, linear discriminant analysis. First, chemical composition data of fault gouge of active faults and inactive faults in Japan was extracted from existing publications. The extraction condition is that the fault activity of the analysis target clearly describes and that the basement rock is diverse. In addition, a chemical analysis of the fault gouge sample possessed by the JAEA was carried out, then we created a database that integrates both of them. In this database, in addition to analytical value, 2 categories of fault activity were given to each sample. Next, we extract samples of fault gouges from the database, and select elements to maximize the number of samples. In order to further extract elements suitable for discrimination of fault activity, elements were selected by AIC (Akaike, 1973). Finally, linear discriminant analysis was performed using the combination of elements selected by AIC as explanatory variables.

Results: The chemical composition data of fault rocks was extracted from a database of a total of 276 samples, including the data from collection of 8 publishing papers, 7 JAEA reports, and chemical analysis of 36 fault rocks held by JAEA. Then we selected 15 elements as variable candidates. As a result, a total of 72 samples (48 samples for active faults and 24 samples for inactive faults) were chosen as input data. From these 15 elements, 11 elements were selected as optimum combination of elements in AIC. Then we performed linear discriminant analysis with a following combination of elements; (a) 11 elements selected by AIC, (b) 8 elements with p-value between 0 and 0.01, (c) 6 elements with p-value between 0 and 0.001. The discrimination rate between active faults and inactive faults is 100% in (a), (b) and 97% in (c).

Consideration about the elements representing the difference in fault activity: When the coefficients of the elements in these discriminants are arranged in descending order, the top 6 elements and the top 4 elements were common. Among them, the combination of TiO_2 and P_2O_5, and the combination of Al_2O_3 and Rb show high correlation coefficient with 2 groups. In addition, the distribution patterns of TiO_2, CaO, P_2O_5 and Ba are concentrated at low values on inactive faults, and show a wide distribution at higher values on active faults. Thus, the elements that represent the difference between the 2 groups are top 6 elements. Of these, TiO_2 and P_2O_5, and Al_2O_3 and Rb are considered important, including their respective combinations.

Consideration about better discriminant: Of the (a) and (b) with a discrimination rate of 100%, the number of elements is small in (b). However, (b) includes TiO_2 and P_2O_5, which are considered to be

©2020. Japan Geoscience Union. All Right Reserved.

collinear as above. Therefore, we performed linear discriminant analysis with the combination of elements excluding TiO_2 and P_2O_5 from (b) as (c) and (d), and as a result, the discrimination rate was 99% in each case. From these, it is expected that the ability to discriminate a sample with known activity is the highest at (b), but that the discrimination performance for a sample with unknown activity is higher at (c) or (d). These results will greatly contribute to clarify the mechanism that creates the difference in chemical composition between active and inactive faults.

This study was carried out under a contract with METI (Ministry of Economy, Trade and Industry) as part of its R&D supporting program for developing geological disposal technology.

Referrence: Akaike, H., Proceedings of the 2nd International Symposium on Information Theory, Petrov, B. N., and Caski, F. (eds.), p. 267-281, 1973. ; Tateishi et al., JpGU2019, SSS15-P27, 2019.

Keywords: fault activity, chemical composition of fault gouge, linear discriminant analysis

©2020. Japan Geoscience Union. All Right Reserved.

Study on the structure of sediment covering basement rock in trench survey

*Shiro Tanaka[1], Shingo Kimura[2], Norihiko Sakakura[3]

1. Central Research Institute of Electric Power Industry, 2. Hokuriku Electric Power Company, 3. Dia Consultants Co., Ltd

In the evaluation of fault activity, if there is a step above the fault in the basement rock and the step is covered by the sedimentary layer, it is important to judge whether the fault activity is affecting the overlying sediments. In this presentation, we report the results of detailed observation of the inside structure of the sedimentary layer, taking the case of the outcrop of the sedimentary layer filling the step of the basement formed by erosion. We also report the results of comparison with the fault outcrop.

Keywords: Fault, Trench survey

©2020. Japan Geoscience Union. All Right Reserved.

Some outcrops along the Ide Fault, a part of the eastern margin fault zone of the Nara basin, central Hoshu.

*Taku Komatsubara[1]

1. Institute of Geology and Geoinformation, Advanced Industrial Science and Technology

Introduction
The author found out some outcrops in which the basement Granite thruts upon the basal part of Osaka Group, and several angular unconformities cut and overly in the basal part of Osaka Group near the Ide Fault, north end of the southern part of the eastern margin fault zone of Nara Basin.
Osaka Group near the Ide Fault
The basal part of Osaka Group includes Mushono tephra ca.2.3 Ma, and it is made up by fluvial sand and gravels, mud and sand and fresh water bioturbated lacustrine clay. Gravels in this Group areconsisted mainly by metamorphic rocks and sedimentary rocks. There is little granitic rocks derivered from hinterlands and no Koto rhyolitic gravels in this sand and gravels.
Reverse fault and unconformity in the basal part of Osaka Group near the Ide Fault
The Osaka Group overlies on the basement granit, its unconformity is 50 degree southward dipping at one outcrop in Kamikoma, Kidukawa City. Several unconformities are detectable in the basal part of Osaka Group. A fault outcrop at where basement granit thrusts up to the Osaka Group, and clear angular unconformity is shown in the basal part of Osaka Group at 1 m up from the base of Osaka group.
Significance of angular unconformity in the basal part of Osaka Group
The Ide fault have activated at least since the earliest Gelasian Period. Its initiation era is earlier than Ikoma Fault and Uemachi Fault, which are located west of the parallel to the eastern margin fault zone of the Nara basin. This means the initiation of faulting in southern part of the Kinki Triangle is not same time, but eastern one is earlier than western one. This fact would be accompanied with Neotectonism in central Japan, and with seismic risk evalution.

Keywords: active fault, early Pleistocene, eastern margin fault zone of the Nara Basin, structural evolution, Neotectonics

©2020. Japan Geoscience Union. All Right Reserved.

[J] Poster | S (Solid Earth Sciences)：S-SS Seismology

[S-SS17] Seismology General

convener:Masayuki Obayashi(Japan Agency for Marine-Earth Science and Technology), Kazuo Nakahigashi(Tokyo University of Marine Science and Technology), Tadafumi Ochi(Institute of Earthquake and Volcano Geology, Geological Survey of Japan, The National Institute of Advanced Industrial Science and Technology)

This session provides a forum for scientific presentations and discussion on various themes such as theory, observations, experiments, and simulations related to seismology. We welcome a wide range of presentations and cross-disciplinary discussion, from research to deepen understanding of earthquakes as natural phenomena, research using seismic waves, research on earthquakes as natural disasters, and topics related to social contribution.

[SSS17-P01] Using a Structure Correction Method to Improve the Location Accuracy of the Hotan Seismic Array

*Chunyue Hao[1] (1.Institute of Geophysics, China Earthquake Administration)

[SSS17-P02] Accuracy improvement of DONET seismometer orientations estimated from seismic waveforms

*Takehiro Nishiyama[1], Shuichiro Yada[1], Masaru Nakano[1], Keisuke Ariyoshi[1], Kentaro Sueki[1], Takane Hori[1], Narumi Takahashi[1,2] (1.Japan Agency for Marine-Earth Science and Technology, 2.National Research Institute for Earth Science and Disaster Resilience)

[SSS17-P03] Determination of Current Seismotectonic Properties of Denizli and Its Region

*Dogan Kalafat[1], Yavuz Gunes[1], Mehmet Kara[1], Kivanc Kekovali[1] (1.Bogazici University Kandilli Observatory and Earthquake Research Institute Cengelkoy, Istanbul Turkey)

[SSS17-P04] Analysis of stress drop ratio of slow tsunami earthquake to usual earthquake

*Takahito Nishimiya[1], Akio Katsumata[1] (1.Meteorological Research Institute, Japan Meteorological Agency)

[SSS17-P06] Source process of the 14 April 2016 earthquake (M6.5) in Kumamoto area estimated by back-projection analysis

*Mitsutaka Oshima[1], Hiroshi Takenaka[2], Makoto MATSUBARA[3] (1.Shimizu corporation, 2.Okayama university, 3.Makoto Matsubara)

[SSS17-P07] Analysis on the role of branching angles in dynamic rupture processes on 3-D branching fault system

*Haiming Zhang[1], Jingxing Fang[1], Feng Qian[1] (1.School of Earth and Space Sciences, Peking University)

[SSS17-P08] Estimation of seismic motion at depth from records at a ground surface station without assumption of plane wave incidence

*Tomotsugu Watanabe[1], Hiroshi Takenaka[1], Masanao Komatsu[1], Mitsutaka Oshima[2], Takeshi Nakamura[3] (1.Okayama University , 2.Shimizu Corporation, 3.National Research Institute for Earth Science and Disaster Resilience)

[SSS17-P09] Implosion earthquakes at very shallow level beneath lava dome, Unzen Volcano, Japan

*Tasuku Hashimoto[1], Koki Aizawa[2], Takeshi Matsushima[2], Yuto Hayashida[1], Kaori Tsukamoto[3], Yuto Yamamoto[1], Yuhei Yuasa[1], Kanta Miyano[1], Naoto Maesako[1], Yuta Kawamura[1], Hiroshi Shimizu[2], Satoshi Matsumoto[2], Megumi Kamizono[4], Ayaho Mitsuoka[1] (1.Department of Earth and Planetary Sciences,

Graduate School of Science, Kyushu University, 2.Institute of Seismology and Volcanology, Faculty of Science, Kyushu University, 3.Fukuoka Regional Headquarters, JMA, 4.DIA CONSULTANTS CO., LSD.)

[SSS17-P10] Spatial-temporal and Seismogram Characteristics of Foreshock and Aftershock Activities for Tsunami Earthquakes

*Liu Yifeng[1], Yoshihiro Ito[2], Kazuaki Ohta[3], Satoshi Katakami[1] (1.Kyoto University, 2.Disaster Prevention Research Institude, Kyoto University, 3.NIED)

[SSS17-P11] Screening for elastic multipathing effects on teleseismic body waves

*Melissa J Bernardino[1], Craig H Jones[1] (1.University of Colorado at Boulder)

[SSS17-P12] Signal detection by amplitude distribution and Kullback-Leibler divergence

*Mitsutaka Oshima[1], Hiroshi Takenaka[2] (1.Shimizu corporation, 2.Okayama university)

[SSS17-P13] Re-evaluation of the relation between various magnitude scales

*Nobuo HAMADA[1] (1.none)

[SSS17-P14] The 3-stage earthquake generation process observed during 3 months before the 2011 Tohoku earthquake (4)

*Yoshiki SUE[1] (1.none)

Using a Structure Correction Method to Improve the Location Accuracy of the Hotan Seismic Array

*Chunyue Hao[1]

1. Institute of Geophysics, China Earthquake Administration

A structure correction method is investigated and used to improve the location results of the Wenchuan, Pishan, and 171 other earthquakes using the Hotan seismic array data. Systematic slowness anomalies are found between frequency–wavenumber analysis and the location results from the China Earthquake Network Center, and all slowness error vectors point to about 300 degree. It is found that the back-azimuth and slowness errors change from positive to negative as the back-azimuth of different ray paths turns from north to south and from east to west,respectively. This phenomenon can be attributed to a dipping layer beneath the array with strike, dip, and velocity contrast of 210 degree,45 degree, and 0.78, respectively. After correction for this dipping structure, the location results of the two main sequences are improved by 25.5% and 70.8% in terms of back-azimuth and slowness, respectively. Moreover, the location results of the other 171 earthquakes are improved by 28.5% and 7.1% in terms of back-azimuth and slowness, respectively.

Keywords: Hotan array, systematic error, dipping layer, location improvement

©2020. Japan Geoscience Union. All Right Reserved.

Accuracy improvement of DONET seismometer orientations estimated from seismic waveforms

*Takehiro Nishiyama[1], Shuichiro Yada[1], Masaru Nakano[1], Keisuke Ariyoshi[1], Kentaro Sueki[1], Takane Hori[1], Narumi Takahashi[1,2]

1. Japan Agency for Marine-Earth Science and Technology, 2. National Research Institute for Earth Science and Disaster Resilience

We re-estimated DONET seismometer orientations with 9 years of seismic observation data during the year between 2011 and 2019. With this study, we obtained one digit smaller standard errors of estimated seismometer orientations compared to the former study, thanks to the longer analysis period.

In 2012, Nakano et al. estimated DONET1 seismometer orientations by the 3 types of analysis method as follows: [1]

(1) correlations of long-period seismic waveforms with land seismometer observation
(2) direction of P-wave first motion for distant earthquakes
(3) particle motions of airgun signals

This study shows that the orientation difference compared to the measurement data of ROV video is up to 10 degrees for the most seismometers, while the difference comes up about 50 degrees for some others. Further, Nakano reinforced the information of estimated orientations of seismometers after the construction of DONET2 in 2017 using the method (1) and (2) described in Nakano et al. (2012) as above. Nakano also re-estimated the seismometer orientations of DONET1. [2]

In this study, Nakano shows that the obtained standard errors of estimated seismometer orientations is around 1 to 2 degrees. However, for some seismometers, estimated orientation figures are considered to have a few degrees of error, because of insufficient distant earthquake event that were available during the study. Since DONET2 construction completed in the middle of this study, enough observation period could not be available for these seismometers.

Therefore, it has been expected to re-estimate the DONET seismometer orientations with longer observation period and with sufficient distant earthquake events that can be used for the analysis.
We re-estimated DONET seismometer orientations by the method (2) described in Nakano et al. (2012) with 9 years of DONET data and obtained the latest figures of estimated orientation after the replacement of seismometer at observation point KMC11 in June 2018. We confirmed that the obtained orientations are basically consistent with the previous studies, e.g. Nakano et al. (2012) and Nakano (2017). Also, 9 years of DONET data enables us to obtain the standard errors of estimated orientation with the order of 0.1 degree for most seismometers. We hope that the most up to date and more accurate figures of estimated DONET seismometer orientations will help the concerned scientists and researchers for their studies.

[1] Masaru Nakano, Takashi Tonegawa, and Yoshiyuki Kaneda. Orientations of DONET seismometers estimated from seismic waveforms. JAMSTEC Rep. Res. Dev., Volume 15, September 2012, 77-89
[2] Masaru Nakano, Orientations of DONET2 seismometers estimated from seismic waveforms, JpGU-AGU Joint Meeting 2017, STT59-P03

©2020. Japan Geoscience Union. All Right Reserved.

Keywords: Ocean-bottom seismometer, Nankai trough, DONET, Seismometer orientation

©2020. Japan Geoscience Union. All Right Reserved.

Determination of Current Seismotectonic Properties of Denizli and Its Region

*Dogan Kalafat[1], Yavuz Gunes[1], Mehmet Kara[1], Kivanc Kekovali[1]

1. Bogazici University Kandilli Observatory and Earthquake Research Institute Cengelkoy, Istanbul Turkey

Denizli and its surroundings is one of the most seismically active regions in Turkey. The region is located at the eastern end of the 2 most important graben (Gediz and Buyuk Menderes) in Western Anatolia. Therefore, aktive (living) fault segments producing earthquakes in the region are very scattered and large and contain different zones, which causes intense seismic activity in the region. Particularly in recent years, earthquakes occurring in the region in general are the result of a complex tectonic deformation dominated by the N-S directed extensional tectonic regime in western Anatolia.
The region produced significant earthquakes in historical and instrumental periods. The faults that caused the medium-sized earthquakes occurring in recent years. In this context, the aim of the project is to reveal micro-earthquake activity and young faults in the region. The 4 earthquake stations to be established within the scope of the project will enable the seismicity of the region to be monitored very precisely. Sensitive and healthy monitoring of earthquake activities also provides valuable information about the earthquake pattern of the region. The stations to be established will reveal the characteristics, fault types, stress distributions, directions and earthquake occurrences of tectonic structures causing seismic activity in the region. Thus, scientific results within the scope of the project will make a significant contribution both in reducing earthquake risk, in urban planning and in building a resistant-conscious society in the region. The intense seismic activity occurring in the region in recent years shows that the young tectonic basins in the region continue their tectonic evolution. In this context, the Big Denizli Fault Zone (BDFZ), which is recommended within the scope of the study. It has been suspected that the earthquake activity in the vicinity of such defined faults has not been identified and that there are more active fault segments within the BDFZ. In this regard, micro-earthquake activity in the region should be monitored very regularly and precisely. Unfortunately, there are many active fault segments in the region that have not been identified and cause activity in recent years and the seismic hazard of the region is known to be very high. This is very difficult to do with the existing station distribution. Therefore, the main objective of the project is to monitor the micro-earthquakes occurring during the BDFZ, to enrich the existing seismic network and to increase the seismic threshold (M<2.9) in the region. Calculation of the source parameters of earthquakes in the region from the records to be obtained from digital broad-band earthquake stations to be established, more robust determination of the dominant stress forces and complex tectonic regime in the region, modeling of stress distribution with current data, follow-up of the process before and after the event broad-band stations to be established. In this project, which parts of the BDFZ belong to the ongoing earthquake activity in the region, deformation mechanics, kinematics and seismotectonic relationships of these segments will be investigated.
One of the main objectives of the project is to monitor the earthquake activity occurring in our region in the recent history and which is still going to be expected at the same time and the distribution of the post-earthquake earthquake (aftershocks) that may occur. The data set to be obtained in the project is to investigate whether the geothermal energy and water injections which are being used extensively in the region cause triggered earthquakes.
In this part of Western Anatolia, faults, which are generally oriented in very different directions, play an important role in the tectonic development of the region and the monitoring of the earthquake activities of these faults will add new findings to the known tectonic characteristics of the region. For this purpose, it is aimed to temporarily place 4 broad-band earthquake stations in order to keep the whole region under

©2020. Japan Geoscience Union. All Right Reserved.

control and to operate them for at least 2 years. This study is supported by Bogazici University Research Projects Commission under SRP/BAP project No:16403. We thank to Bogazici University Research Fund Commission and members.

Keywords: Big Denizli Fault Zone, Seismic activity, Broadband seismic station, Earthquake detection threshold, Earthquake source parameters

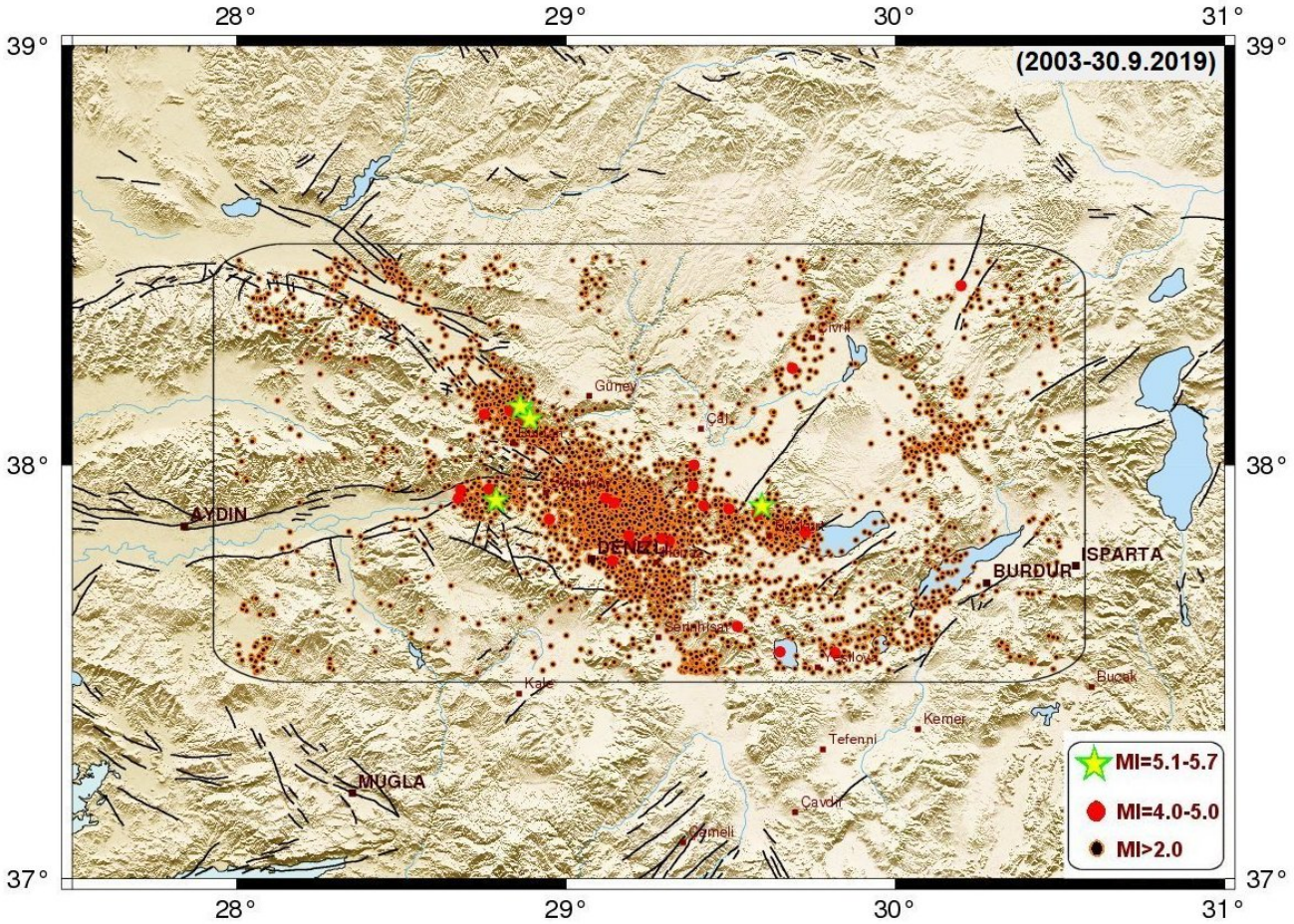

©2020. Japan Geoscience Union. All Right Reserved.

Analysis of stress drop ratio of slow tsunami earthquake to usual earthquake

*Takahito Nishimiya[1], Akio Katsumata[1]

1. Meteorological Research Institute, Japan Meteorological Agency

Characteristics of the slow tsunami earthquake include a long source duration with relative low seismic energy release at high frequencies. It is featured by low corner frequency and small effective stress drop in source spectra analysis on ω^2-model (Polet and Kanamori, 2000).

In the empirical Green's function method (EGFM) in strong ground motion analysis, the source spectrum ratio of the target earthquake to the reference one (or the seismic wave spectrum ratio at each same station) is used. Seismic waves from reference earthquakes which are often aftershocks are regarded as Green's function. In EGFM, it is possible to obtain estimation of the average effective stress drop ratio of the target to the reference (Irikura, 1986, Miyake et al., 1999). Specifically, using the scale parameter N (associated with fault scale based on the scaling law), the source spectral ratio asymptotically approaches CN^3 on the long-period side and CN on the short-period side, and C is the stress drop ratio.

We obtained source spectra of the 1992-Nicaragua-tsunami-earthquake(M_w7.6) and 1994-Java-tsunami-earthquake(M_w7.8) from the P-phase and S-phase of the teleseismic waveform at each station. In addition, we also obtained ones of reference earthquakes. They occurred on the plate boundary with low angle thrust type off the coast of Nicaragua (M_w6.9) on 10/09/2004 and off Java (M_w 5.9) on 11/20/2003. In each case, the spectra approximately could be regarded as the ω^2-model, so we tried to apply the EGFM method. Specifically, the spectrum ratio of the tsunami earthquake to the reference earthquake was calculated for the data at each station, and they were averaged for the P-phase and S-phase. Spectra ratio at the long-period end was fixed by the ratio of seismic moments from GlobalCMT. To them, the optimal corner-frequency (or period) and N was found by the grid search method.
As a result, for the Nicaragua-tsunami-earthquake, the corner-period was 84 sec and the stress drop ratio for the reference earthquake was 1/2.6, and for the Java-tsunami-earthquake, the corner-period was 84 sec and the stress drop rario for the reference earthquake was 1/5.0.

Keywords: tsunami earthquake, souorce spectrum, effective stress drop

©2020. Japan Geoscience Union. All Right Reserved.

Source process of the 14 April 2016 earthquake (M6.5) in Kumamoto area estimated by back-projection analysis

*Mitsutaka Oshima[1], Hiroshi Takenaka[2], Makoto MATSUBARA[3]

1. Shimizu corporation, 2. Okayama university, 3. Makoto Matsubara

The series of seismic activity of the 2016 Kumamoto earthquake began on April 14, with an M6.5 earthquake. There occurred many earthquakes, including an M7.3 earthquake on April 16, followed by three earthquakes of magnitude about 6 on April 16 alone. In this study, the fault rupture process of the M6.5 earthquake on April 14 was estimated by the back-projection method using local strong motion records. In back-projection method, the spatio-temporal distribution of the radiation intensity of seismic waves is obtained, so that the spatio-temporal evolution of the fault rupture can be investigated. With the back-projection method, it is possible to capture the fault rupture process in a higher frequency band than the waveform inversion that is usually performed in frequency of about 0.1 to 1 Hz. Accumulation of analysis of fault rupture processes by the back-projection method are to contribute to the construction of a broadband fault model for ground motion prediction.
For the analysis, the strong motion records of KiK-net underground stations around Kumamoto area were used. The seismograms were corrected for the orientation of the seismometers, removed the offset, and integrated once to obtain the velocity waveform. In the back-projection method, it is not necessary to set the fault plane in advance, however, from the viewpoint of computational efficiency, the fault plane was set in this study. For this earthquake, waveform inversion has already been performed, and the fault plane used for the waveform inversion was also used in the back-projection. The travel time data used for the back-projection method were the observed travel times obtained by Matsubara et al. (2018) using hypocenter relocation using the double-difference method. By spatially interpolating the travel time of near fault plane events, the travel time among the grids on the fault plane and the strong motion stations were obtained. In the spatial interpolation of the travel time data, the values of the free parameters of the interpolation formula were set by performing statistical investigations so as to minimize the interpolation error. Furthermore, the accuracy of the relative position of the seismic wave radiation intensity to the epicenter was improved by performing travel time data processing similar to Takenaka and Yamamoto (2004). The strong motion stations were divided into multiple groups according to the positional relation with the fault plane, back-projection was performed for each group, and the rupture images obtained for each group were integrated to obtain the final rupture image. The integration of multiple back-projection images was performed in consideration of the direction of arrival of the seismic waves.
Our presentation will show the data used, the method, and the fault rupture process of the April 14, 2016 earthquake (M6.5) estimated by the back-projection method.

Acknowledgement: We would like to express the deepest appreciation to NIED for providing us with KiK-net data.

Keywords: The 2016 Kumamoto earthquake, the earthquake occurred on 14 April, 2016, back-projection method

©2020. Japan Geoscience Union. All Right Reserved.

Analysis on the role of branching angles in dynamic rupture processes on 3-D branching fault system

*Haiming Zhang[1], Jingxing Fang[1], Feng Qian[1]

1. School of Earth and Space Sciences, Peking University

Fault branching is one of the geometrical complexities of fault systems and widely exists in nature. It may heavily influence the patterns of rupture propagation of fault systems. In this study, we investigate the effect of branching angle on rupture inclination and the interaction between branch planes in two-fork branching fault systems by numerical simulation and theoretical analysis based on Mohr’ s circle. A friction law dependent on normal stress is used, and special attention is paid to study how ruptures on the upper branch plane and the lower one affect the stress and rupture on each other separately. The results show that the two branch planes affect each other in different patterns and the intensity of the effect changes with the branching angle. The rupture of the upper branch plane has a negative effect on the rupture of the lower branch plane in case of a small branching angle, but almost no negative effect in case of a large branching angle. The rupture of the lower branch plane, however, suppresses the rupture on the upper branch plane no matter the branching angle is large or small.

©2020. Japan Geoscience Union. All Right Reserved.

Estimation of seismic motion at depth from records at a ground surface station without assumption of plane wave incidence

*Tomotsugu Watanabe[1], Hiroshi Takenaka[1], Masanao Komatsu[1], Mitsutaka Oshima[2], Takeshi Nakamura[3]

1. Okayama University , 2. Shimizu Corporation, 3. National Research Institute for Earth Science and Disaster Resilience

To evaluate the seismic stability of shallow subsurface structure and the response of buildings to ground motions, we often need the distribution of seismic wavefield incident on a given subsurface level, which is estimated from the ground motion at a free surface position. It is currently conventional that the incident wavefield at depth is estimated by assuming a vertical incident plane wave for every component. However, this conventional approach assumes that the vertical and horizontal components of the seismic wave independently propagate as P-wave and S-wave, respectively, and the derived seismic motion is then identical at any horizontal positions on the subsurface level. We have proposed a new method to evaluate the subsurface incident wavefield from a surface record without assumption of plane-wave incidence at the previous presentation (Takenaka et al., 2019, SSJ Fall meeting). This method needs a horizontally-layered model including not only the target evaluation depth but also earthquake source. We calculate the synthetic seismogram at the surface station and the incident wave at the subsurface evaluation point. We then deconvolve the subsurface incident wave with the surface synthetic motion to get the transfer function and convolve it with the surface record. Replacing the incident wave at depth by the synthetic seismograms at the subsurface point, we can estimate the seismic motion at this point (Fig. 1).

In this study, we apply the new method to real event records which were observed both at surface and subsurface levels and compare the estimated seismogram by our method with the subsurface record and one obtained by the conventional method to confirm effectiveness of our method. We employ the local strong-motion records at a KiK-net, NIED station in western and central Tottori. We could successfully recover the subsurface records by our method. Fig. 2 shows the comparison of the velocity waveforms at depth of 100 m estimated by the proposed and the conventional methods for the evaluation point with a horizontal offset of 1 km from the surface station. Red and green lines indicate the seismograms estimated by the proposed and the conventional methods, respectively. They have a clear difference in the phase. If the evaluation point is located at a deeper position, each waveform differs both in the phase and the amplitude. This is because the conventional method is not able to consider the effect of the oblique incidence. The proposed method is also very robust to errors in the assumed focal mechanism and the structure model deeper than the evaluation point, and sensitive to the used shallower structure model. We will further discuss about the spectra in the frequency domain and the relationship between the estimated waveform and the shallow structure.

Keywords: seismic motion, plane wave, strong motion, subsurface wavefield

©2020. Japan Geoscience Union. All Right Reserved.

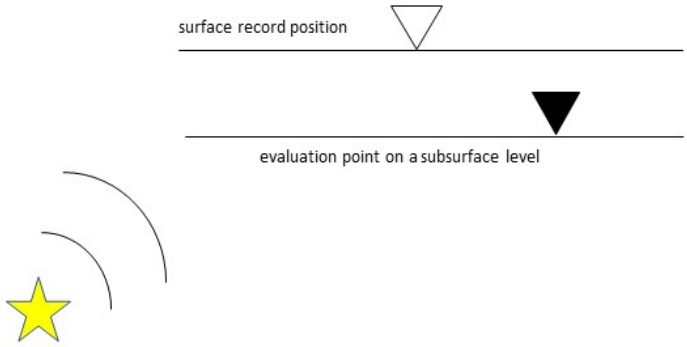

Fig. 1. Schematic view for the proposed method. White and black triangles indicate the surface record position and the evaluation point on a subsurface level, respectively. Star denotes the hypocenter.

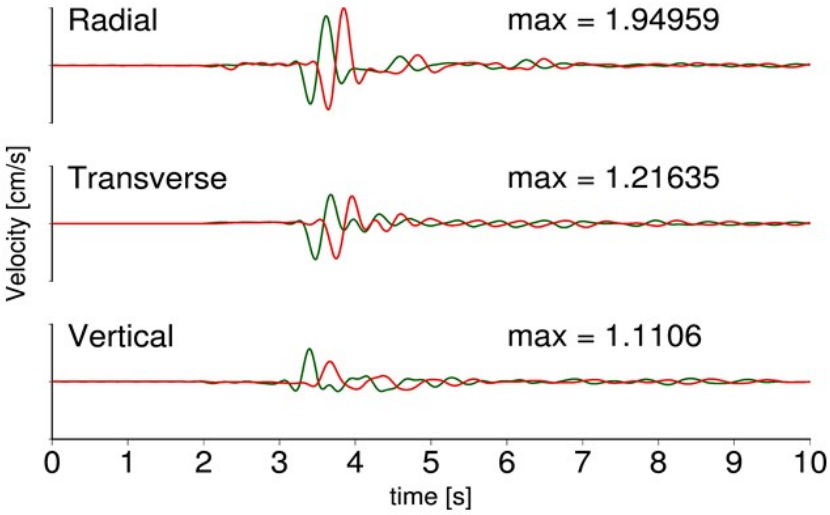

Fig. 2. Comparison of velocity estimated at depth of 100 m by the proposed and the conventional methods at KiK-net station, SMNH01. Red and green lines indicate waveform from the proposed and the conventional methods, respectively. The evaluation point has a horizontal offset at 1 km from the surface station.

©2020. Japan Geoscience Union. All Right Reserved.

Implosion earthquakes at very shallow level beneath lava dome, Unzen Volcano, Japan

*Tasuku Hashimoto[1], Koki Aizawa[2], Takeshi Matsushima[2], Yuto Hayashida[1], Kaori Tsukamoto[3], Yuto Yamamoto[1], Yuhei Yuasa[1], Kanta Miyano[1], Naoto Maesako[1], Yuta Kawamura[1], Hiroshi Shimizu[2], Satoshi Matsumoto[2], Megumi Kamizono[4], Ayaho Mitsuoka[1]

1. Department of Earth and Planetary Sciences, Graduate School of Science, Kyushu University, 2. Institute of Seismology and Volcanology, Faculty of Science, Kyushu University, 3. Fukuoka Regional Headquarters, JMA, 4. DIA CONSULTANTS CO., LSD.

Unzen Volcano is a stratovolcano located in central part of the Shimabara peninsula of Kyushu Island, Japan. During the eruption periods 1991-1995, the seismicity was vigorous at shallow level beneath the Heisein-Shinzan lava dome (Shimizu et al., 1992; Umakoshi et al., 2001), then the number of shallow earthquakes decreased significantly after the eruptions. However, since 2010, the number of shallow earthquakes have been increasing steadily beneath Mt. Fugen and Heiseishinzan lava dome (Japan Metrological Agency (JMA)). The most of the hypocenters were estimated 1~2 km below sea level, while importantly, several earthquakes were located above sea level since February 2017. The P-wave arrivals of the earthquakes above sea level show the downward motion at all stations of JMA, MLIT, and Kyushu university. The coda, which shows relatively longer period oscillation, continues approximately 20 to 40 seconds. According to Japan Meteorlogical Agency (JMA), very shallow earthquakes above sea level were reported 6 times in 2018 and 4 times in 2019.
In order to explore the shallow earthquake activity beneath Unzen volcano, we established 12 seismic stations around Mt. Fugen and Heisei-Shinzan lava dome in August, 2018 (plus 2 stations at Heisei-Shinzen lava dome since April, 2019). In addition, broad-band magnetotelluric (MT) observation was conducted in October and November, 2018 to investigate the contribution of fluids to the earthquakes. From these observations, we found (1) the hypocenters of very shallow earthquakes are relocated 200m depth, which correspond to the boundary between Mt. Fugen and Heisei-Shinzan lava dome and also correspond to the conduits of the 1991-1995 eruptions, (2) very shallow earthquakes not only shows downward P-wave arrivals but shows upward P-wave arrivals at a few seismic stations, (3) very shallow earthquakes sometimes occur repeatedly within 20 seconds, (4) Tensile axes of very shallow earthquakes shows various directions, (5) the zone below very shallow earthquakes shows significantly high resistivity. We conclude that the very shallow earthquakes were generated by the collapse of small voids filled with gas and air at the boundary between Mt. Fugen and Heisei-Shinzan lava dome. We speculate that the recent deflation around the volcanic conduits may generate the voids for the very shallow earthquakes.

Keywords: Unzen Volcano, implosion earthquake, volcanic earthquake, resistivity structure, closing crack, lava dome

©2020. Japan Geoscience Union. All Right Reserved.

Spatial-temporal and Seismogram Characteristics of Foreshock and Aftershock Activities for Tsunami Earthquakes

*Liu Yifeng[1], Yoshihiro Ito[2], Kazuaki Ohta[3], Satoshi Katakami[1]

1. Kyoto University, 2. Disaster Prevention Research Institude, Kyoto University, 3. NIED

Tsunami earthquakes and their source process are one of open questions in earthquake seismology because the tsunami earthquakes are rare events comparing to ordinary earthquakes with the same magnitude. In order to understand a generating mechanism of tsunami earthquakes, we search any small events showing similar properties with tsunami earthquakes happened before and after main shock. We focus on three tsunami earthquakes and their foreshock & aftershock activities, such as Nicaragua(1992/09/02, Mw7.7), Java Island(2006/07/17) and Mentawai Islands(2010/10/25, Mw7.8). We investigate foreshock and aftershock activities from earthquake catalogs with a period of twenty years, published by ISC and USGS. Evaluating the spatiotemporal patterns of their activities in three regions, we have found that four foreshocks near the epicenter of the main shock from August 10 to August 13 in the region of the 1992 Nicaragua earthquake. Moreover, we also observed the migration of their activities heading from the northeast to the southwest. We evaluate the regional and spatiotemporal seismicity in small regions with dividing epicenter area (5 degree * 5 degree) into twenty-five segments and each segment is actually 1 degree * 1 degree. Based on cumulative frequency distributions, we have found out that two seismic quiescence segments existed in Nicaragua, and both of them are near the main shock area. We also investigate amplitude ratio of surface to body waves from their fore- and aftershocks exceeding magnitude 5, with comparing to that from the main shock. Here, after applying a band pass filter (0.01 to 0.1 Hz) to each event, the maximum-amplitude ratio of the surface wave to the SV wave is calculated. We have found that especially three earthquakes (Foreshock 8/11(Mb 5.1) and Aftershock 9/5(Mb 5.3), 9/6(Mb 5.3)) that occurred in the same region of the Nicaragua earthquake showed similar features with the amplitude ratio from the main shock. This suggests that a slightly smaller earthquake with similar characteristics as a tsunami earthquake occurred just before and immediately after the occurrence of the tsunami earthquake.

Keywords: Tsunami Earthquake, Spatial-temporal Characteristics, Seismogram Analysis

©2020. Japan Geoscience Union. All Right Reserved.

Screening for elastic multipathing effects on teleseismic body waves

*Melissa J Bernardino[1], Craig H Jones[1]

1. University of Colorado at Boulder

A growing literature indicates that teleseismic intrinsic attenuation measurements can be contaminated by propagative effects like multipathing and scattering. Upper mantle wavespeed heterogeneities will focus and defocus seismic amplitudes with some dependence on frequency. The Sierra Nevada, California, USA has been one region where upper mantle t* measurements continue to be problematic if interpreted as reflecting intrinsic attenuation. One source for this complexity is the presence of a large, upper mantle, high wavespeed feature termed the “Isabella anomaly”. Conventional attempts at measuring intrinsic attenuation (i.e., using t* from either the spectral ratio method or inverting spectra) in the Sierra Nevada consistently produce estimates of high attenuation for the Isabella anomaly. 2-D waveform modeling of a simple cylinder of similar size to the Isabella anomaly reveals that focusing and defocusing effects from waves traversing this feature effect t* measurements more than those arising from anelastic attenuation.

Seismic waves propagating through heterogeneous material have observable and predictable effects on travel time and arrival amplitude. Body waves arrive earlier when traversing through faster material but also exhibit reduced amplitudes. Thus, if seismic energy is traversing a medium with wavespeed anomalies but uniform intrinsic attenuation, we expect to see early arrival times correlate with low amplitudes and high t* estimates. In contrast, if intrinsic attenuation dominates over multipathing, then we expect a different trend when plotting arrival time versus seismic amplitude. We explore the feasibility of using these trends as a preliminary screen for problematic regions that are more likely to be dominated by multipathing effects. We compare trends of arrival time and seismic amplitude for P-, S-, and SKS-phases at teleseismic distances. We introduce a multipathing scalar value to highlight regions where focusing and defocusing effects are expected to be problematic.

Keywords: seismic attenuation, teleseismic body waves, upper mantle, seismic amplitudes, defocusing effects

©2020. Japan Geoscience Union. All Right Reserved.

Signal detection by amplitude distribution and Kullback-Leibler divergence

*Mitsutaka Oshima[1], Hiroshi Takenaka[2]

1. Shimizu corporation, 2. Okayama university

A variety of methods have been proposed to detect seismic signals from records of seismometers. We have developed a signal detection method that uses amplitude distribution (probability density function: PDF) of seismic records and Kullback-Leibler divergence (KLD) (Oshima and Takenaka, 2020). Records of seismometers that contains no seismic event are comprised of microtemor and electric noises. Namely, such records are assumed to be a summation of random noise. In contrast, according to Fermat’ s principle, the initial portion of seismic waveforms of epicentral distance up to about 100 km is constituted by direct wave that propagated through the shortest path from hypocenter to station. In telecommunications engineering, the sum of random phase waves is called as Rayleigh fading and Rayleigh distribution is known as a PDF of absolute amplitude for Rayleigh fading. According to scattering theory in seismology, the PDF of absolute amplitude for coda waves are shown to be a Rayleigh distribution. On the other hand, the central limit theorem says that the PDF of the sum of samples extracted from independent and identically distributed data becomes a Gaussian distribution. Taking this into account, the PDF of the amplitude of records of seismometers can be approximated by Gaussian or Rayleigh distributions, except the initial part of seismic waves. In information theory, Gaussian distribution is deduced as the statistical distribution with maximum entropy in all of the statistical distributions of the same average and standard deviation. This means that the seismometer records with PDF similar to Gaussian distribution contains no rare phenomenon (e.g., seismic signal emitted by an earthquake) that makes entropy small. Taking the aforementioned theoretical backgrounds into consideration, Oshima and Takenaka (2020) have developed a method to find signals of seismic events in seismometer recordings. The method by Oshima and Takenaka (2020) catches signals of seismic events by following 4 steps. 1. Estimate PDF of amplitudes of seismic records within a time window. 2. Calculate the Gaussian or Rayleigh distribution that have the same average and standard deviation as that obtained at step 1. 3. Quantify the dissimilarity of two PDFs obtained in step 1 and 2 by using KLD. 4. Repeat step 1 through 3 while shifting the time window from the start to the end of the seismometer records. The gained KLD time series takes a large value when the PDF of the seismic records deviates from Gaussian or Rayleigh distributions, namely around the arrival time of seismic waves. Hence we can detect signals of seismic events by searching the peaks of the KLD time series. In our presentation, we show examples of the application of the method.

Acknowledgement: We would like to express our gratitude to NIED for providing us with KiK-net data.

Keywords: signal detection, probability density function, Kullback-Leibler divergence

©2020. Japan Geoscience Union. All Right Reserved.

Re-evaluation of the relation between various magnitude scales

*Nobuo HAMADA[1]

1. none

After Richter(1935) proposed an instrumental earthquake magnitude(ML), various magnitude scales(mB, mb, Ms, Mj and Mw etc.) were proposed by several authors and have been adopted to indicate earthquake size in the earthquake catalogs published by seismological centers. Moment magnitude(Mw) proposed by Kanamori(1977), that is based on the physical parameters of earthquake faulting process, is now widely accepted as the scale to represent accurate size of earthquakes and has been included in many earthquake catalogs. Relations of Mw with conventional magnitudes have been well studied by several authors such as Kanamori(1983) and Utsu(1999). However, changes of seismographs, ways of observation practice, the station distribution etc. would possibly affect the relation between magnitudes for a long years as discussed by Borman and Dewey(2014). Periodical or occasional re-evaluation of the magnitude relation must be desirable to make sure the consistency of magnitude in the catalogs.

Using bulletin of the International Seismological Centre(ISC), I studied relations among Mw and other magnitudes reported by several agencies(ISC, NEIC, JMA and NIED etc.) for earthquakes occurring in and around Japan and some other regions. The result of the study shows that Mws reported by different agency agree well with each other showing universality and robustness of Mw as a scale for earthquake size. Deviations of conventional magnitudes from Mw are generally similar to those reported by Utsu(1999). However, among conventional magnitudes, Mj (Tsuboi(1954), Katsumata(2004)) shows minimum deviation from Mw within the range from Mw=4.0 to 7.0. Mj will be better substitute of Mw when it is not available. Several other interesting results are also to be presented.

Reference

Richter C. F.(1935) An instrumental earthquake magnitude scale, Bull. Seis. Soc. Am. ,25,No.1,1-31.

Kanamori H.(1977)The Energy Release in Great Earthquakes, J. Geophys. Res.82,No20,2981-2987.

Kanamori H.(1983) Magnitude scale and quantification of earthquakes, Tectonophysics, 93, 185- 199.

Utsu, T.(1999) Representation and analysis of the earthquake size distribution: A historical review and some new approaches, Pure Appl. Geophys.,155, 509-535.

Borman P. and Dewey J.W.(2014)The new IASPEI standards for determining magnitudes from digital data and their relation to classical magnitudes, Information Sheets 3.3, New Manual of Seismological Observatory Practice 2 (NMSOP2), G.F.Z.

Keywords: Magnitude, Moment magnitude(Mw), JMA magnitude(Mj)

©2020. Japan Geoscience Union. All Right Reserved.

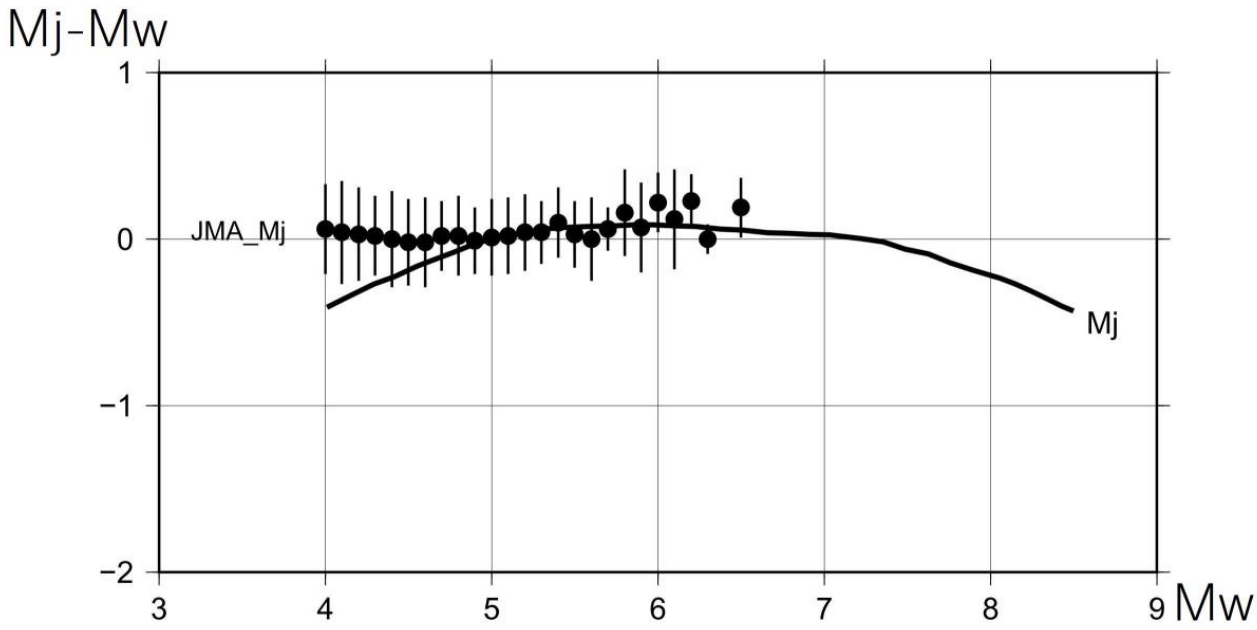

Fig.1 Deviation of Mj from Mw
The solid line shows deviation of Mj from Mw(After Utsu(1999))
Solid symbols and error bars show the result of the present study

©2020. Japan Geoscience Union. All Right Reserved.

The 3-stage earthquake generation process observed during 3 months before the 2011 Tohoku earthquake (4)

*Yoshiki SUE[1]

1. none

1. Introduction
The researcher has conducted the following research on the subject earthquake.
At first, the operational situation of the F-net broadband seismic network was examined, and it was found that number of stations with missing data increased from December 22, 2010 to January 18, 2011 and from February 16, 2011 to March 2, 2011. Especially from February 19 to March 2, they reached the maximum number of 4 stations (Sapporo(HSS), Iwateyamagata(IYG), Kesennuma(KSN), Shiramine(SRN)), of which 3 of them are close to epicenter of the earthquake. (Sue, 2013)
Then, to understand such behavior of the F-net, various reports were collected, and it was found that seismic activity for three months before the earthquake was consisted of three stages shown below.
First stage: This is the final stage of strain accumulation (i.e. compression) of the land-side plate, and the strain accumulation reached the upper limit at the end of this stage.
Second stage: Slow slip started to occur near the epicenter, also the direction of the movement of land-side plate reversed.
Third stage: This is the final stage before the main shock. (Sue, 2017)
As a next step, detailed investigation focused on the events of the first stage (late November, 2011 - around January 28, 2011) was conducted. Large vibrations were found by such instruments as the F-net from January 3 to 18, which preceded the last day of strain accumulation. (Sue, 2018)
The start date of this stage shall be changed to the end of November to include the West off Chichijima island earthquake (M6.9) on November 30, 2010.
Then, the second stage (around January 29, 2011 - around March 2, 2011) was examined. A slow slip started to occur near the epicenter around January 29, and rebound of the land-side plate was also observed. From mid-February to late February, there were strong seismic activities at off Sanriku region. Expansion of the slow-slip area, and increase in F-net stations with missing data were also observed. (Sue, 2019)
As a follow-on step, this paper reports behavior of the third stage (March 6, 2011 - March 11, 2011: the day of main shock) . Note, based on the latest research, the start date of this stage shall be March 6.

2. Analysis
The GEONET shows various parts of the Tohoku region have moved independently since January 29, but from around March 6, a large area in the Tohoku region has moved toward the trench axis simultaneously. At the same time, electromagnetic and thermal abnormal were reported. These movements continued the main shock after the March 9 off Sanriku earthquake M7.3, which is understood as a foreshock. The source of the precursors is presumed to be the boundary of plates near the epicenter.
The events observed at this stage are shown below (items, period, special notes).
GEONET (wide area sliding), 3/6 and later, (Kamiyama, 2012)
VLF / LF electromagnetic anomaly, 3/5-6, (Hayakawa et al., 2012)
ULF / ELF electromagnetic anomaly, 3/6, (Ohta et al., 2013)
ULF electromagnetic anomaly, 3/6, (Hayakawa et al., 2012)
GPSTEC electromagnetic anomaly, 3/7-8, (Hirooka et al., 2016)
GPSTEC electromagnetic anomaly, 3/11, (Heki, 2011)

©2020. Japan Geoscience Union. All Right Reserved.

OLR radiation heat anomaly, 3/7-10, (Ouzounov et al., 2011)

3. Researches to be conducted
In the six days before the earthquake, crustal movements, electromagnetic and thermal changes were observed simultaneously. Therefore, it is necessary to conduct research from view points of each area.

References:
Hayakawa, M. et al., 2012, Ann. Geophysics (Italy), **55**, N. 1, 95-99.
Heki, K., 2011, Geophys. Res. Lett, **38**, L17312.
Kamiyama, M., 2012, Japanese Geotechnical Society, 2012 General assembly of Tohoku branch.
Hirooka, S. et al., 2016, IEEJ Trans. on Fundamentals and Materials, **136**, 5, 265-271.
Sue, Y., 2013, JpGU2013, SSS30-P01.
Sue, Y., 2017, JpGU2017, SSS14-P08.
Sue, Y., 2018, JpGU2018, SSS13-05.
Sue, Y., 2019, JpGU2019, SSS09-P03.
Ohta, K. et al., 2013, Radio Science, **48**, 5, 589-596.
Ouzounov, D. et al., 2011, Earthquake Science, **24**, 6, 557-564.

Keywords: Tohoku Earthquake, Precursor, Electromagnetic anomaly, Thermal anomaly

©2020. Japan Geoscience Union. All Right Reserved.

[J] Poster | S (Solid Earth Sciences)：S-EM Earth's Electromagnetism

[S-EM21] Electromagnetic Induction in the Earth and Planetary Interiors, and Tectono-Electromagnetism

convener:Tetsuo Matsuno(Kobe Ocean Bottom Exploration Center, Kobe University), Maki Hata(Earthquake Research Institute, the University of Tokyo)

This session welcomes papers on electromagnetism in the Earth and planetary interiors. The topics include but not limited to electromagnetic phenomena associated with earthquakes and volcanism, electrical conductivity structure, laboratory experiments, results of simulations, new equipment for observation, and methods of data analysis.

[SEM21-P01] 3-D resistivity models beneath two active volcano groups in a graben by Network-MT data of reticular arrangements (2)

*Maki Hata[1], Makoto Uyeshima[1], Yoshikazu Tanaka[2], Takeshi Hashimoto[3], Ryokei Yoshimura[4], Naoto Oshiman[4] (1.Earthquake Research Institute, the University of Tokyo , 2.Kyoto University, 3.Institute of Seismology and Volcanology, Graduate School of Science, Hokkaido University, 4.Disaster Prevention Research Institute, Kyoto University)

[SEM21-P02] A preliminary resistivity model in the south part of Mt. Ontake volcano

*Shuhei Nishijima[1], Hiroshi Ichihara[1], Shinichiro Horikawa[1], Yuta Maeda[1], Kenjiro Matsuhiro[1], Kazushi Tanoue[1], Takahiro Kunitomo[1] (1.Graduate School of Environmental Studies, Nagoya University)

[SEM21-P03] A research report on the fundamental investigations of an electrical resistivity structure beneath Chugoku and Shikoku regions, southwestern Japan(2019)

*Ichiro Shiozaki[1], Tomofumi Uto[1], Makoto Uyeshima[2], hiroshi hataoka[3], Hideki Murakami[4], Naoto Oshiman[5], Yoshihisa Iio[5], Kazuya Ando[6] (1.Graduate School of Engineering, Tottori University, 2.Earthquake Research Institute, University of Tokyo , 3.Technical Department, Tottori University, 4.Research and Education Faculty , Kochi University, 5.Disaster Prevention Research Institute, Kyoto University, 6.San'in Kaigan Geopark Museum of the Earth and Sea)

[SEM21-P04] Estimation of MT response function to reveal resistivity structure around the Hyuganada area

*Hayato Nakamura[1], Hiroshi Ichihara[1], Tada-nori Goto[2], Tetsuo Matsuno[3], Noriko Tada[4], Shinya Sato[5] (1.Graduate school of environmental studies, Nagoya University, 2.Graduate School of Life Science, University of Hyogo, 3.Kobe Ocean Bottom Exploration Center, Kobe University, 4.Japan Agency for Marine-Earth Science and Technology, 5.Kyoto Univesity, Graduate School of Engineering)

[SEM21-P05] 3D resistivity structure of the Matsukawa geothermal area using magnetotelluric data

*KENTARO AOYAMA[1], Toru Mogi[2], Junna Kanehiro[1], Koichi Suzuki[1] (1.Hokkaido University, 2.Tokyo Institute of Technology)

[SEM21-P06] MT data analysis with Multi-channel Spectrum Analysis (MSSA)

*Shu Kaneko[1], Katsumi Hattori[2], Toru Mogi[2], Chie Yoshino[2] (1.Chiba University Graduate School of Science and Engineering, 2.Chiba University Graduate School of Science)

[SEM21-P07] Effects of source field on MT responses of the flat Earth and the spherical Earth

*Shinya Sato[1] (1.Kyoto Univesity, Graduate School of Engineering)

[SEM21-P08] Electromagnetic field fluctuations recorded in MT data during the eruption of Kirishima Shinmoe-dake in 2018

*Satoru ANIYA[1], Koki Aizawa[2], Takeshi Matsushima[2] (1.Department of Earth and Planetary Sciences,Graduate School of Sciences,Kyushu University, 2.Institute of Seismology and Volcanology,

Facurity of Sciences, Kyushu University)

3-D resistivity models beneath two active volcano groups in a graben by Network-MT data of reticular arrangements (2)

*Maki Hata[1], Makoto Uyeshima[1], Yoshikazu Tanaka[2], Takeshi Hashimoto[3], Ryokei Yoshimura[4], Naoto Oshiman[4]

1. Earthquake Research Institute, the University of Tokyo , 2. Kyoto University, 3. Institute of Seismology and Volcanology, Graduate School of Science, Hokkaido University, 4. Disaster Prevention Research Institute, Kyoto University

Mt. Aso with a large caldera and Mt. Unzen, which are composed by active Quaternary volcanoes, lie at the Beppu-Shimabara graben. The graben travels across the island of Kyushu almost in an E-W direction. Aso caldera was formed at the central part of the graben by a series of huge eruptions, with a volcanic explosivity index of 7, during 270–90 ka. A post-caldera cone of Naka-dake in Aso caldera is a quite active volcano, at which magmatic and phreatomagmatic eruptions occurred during 2014–2016 and ash eruptions (emissions) have continued since July 2019. On the other hand, Unzen, a back-arc volcano at the western edge of the graben showed a dome-forming eruption at Fugen-dake cone during 1990–1995, preceded by a significant eastward migration of volcano-tectonic seismicity from Tachibana bay to the summit. The total amount of extruded dacitic lava was 2×10^8 m^3 DRE, and the repetitive partial collapses generated ~10,000 pyroclastic flows [e.g., Nakada et al., 1999; Yamamoto et al., 1993].
In and around Aso caldera and Unzen volcano, network-MT surveys for measuring the electric potential difference (the electric field) were carried out during 1993–1998 by using long metallic wires/dipoles of the commercial telephone company's networks [e.g., Uyeshima et al., 1995; Tanaka et al., 1998; Hashimoto et al., 1999; Hata et al., 2015]. We determined two components of network-MT response functions between the potential differences for respective dipoles and the two horizontal components of the magnetic field at the Kanoya Geomagnetic Observatory. Three-dimensional (3-D) inversion analyses were performed for obtaining each electrical resistivity model beneath Aso caldera and Unzen volcano. In the inversion analyses, we used a data-space inversion code, which can be taken into account the length and direction of respective dipoles [e.g., Siripunvaraporn et al., 2004]. Moreover, two data sets in a period range from 480 to 20,480 s, which are distributed as to respectively cover the two target regions (Aso caldera and Unzen volcano) with reticular dipole arrangement, were used for obtaining well-resolved 3-D models. In this presentation, we show magma supply systems inferred from the 3-D resistivity models beneath Aso caldera and Unzen volcano.

©2020. Japan Geoscience Union. All Right Reserved.

A preliminary resistivity model in the south part of Mt. Ontake volcano

*Shuhei Nishijima[1], Hiroshi Ichihara[1], Shinichiro Horikawa[1], Yuta Maeda[1], Kenjiro Matsuhiro[1], Kazushi Tanoue[1], Takahiro Kunitomo[1]

1. Graduate School of Environmental Studies, Nagoya University

Investigating underground structure in volcano such as distribution of magma chamber and hydrothermal area is essential to understand mechanisms of eruptions. Around the Mt. Ontake volcano, two previous studies investigated 3-D resistivity distribution. Abd Allah & Mogi (2016) modeled subsurface resistivity distribution beneath the top of Mt. Ontake volcano using the grounded electrical-source airborne transient electromagnetic (GREATEM). They found a conductive zone in the east part of the volcano, the resistive zone at about 1 km deep, and moderately resistive zones in the other most part in the volcano. Ichihara et al. (2018) clarified resistivity distribution below the southeast flank of Mt. Ontake volcano based on the magnetotelluric (MT) investigations. They found two conductive zones interpreted as hydrothermal areas. However, resistivity structures over 1 km deep have not been investigated around the top of Mt. Ontake volcano. In this study, we conducted MT measurements around the top of Mt. Ontake volcano to clarify the 3-D resistivity structure including deep area.

We measured MT data at 9 sites using ADU-07e system from Metronix Geophysis Co. around the top of Mt. Ontake volcano on 10-12 September and 7-11 October, 2019. The sampling frequencies are 32, 1024, 32k, and 524kHz. The data were recorded 1-2 days for the 2 lower frequencies and 1-3 hours for the 2 higher frequencies. We estimated MT impedances at observed site using BIRRP program (Chave & Thomson, 2004). To reduce noise, the remote reference technique was applied. For the 1k, 32k, and 524kHz data, we used horizontal magnetic field data at the observation site which observed the same time with observation site. For the 32Hz data, we used horizontal magnetic field data from site OKR at Okura village, Yamagata Prefecture observed by Geothermal Energy Research & Development Co.

We then estimated preliminary 1-D resistivity structure based on grid search which find minimum RMS misfit between observed impedance and calculated responses. We supposed that resistivity structures consist of horizontal 2 and 3 layers from sounding curves at the site 009 (this study) and the site 305 (Kanehiro et al., 2018), respectively. The obtained resistivity structure beneath the site 305 is consistent to the previous structure by Abd Allah & Mogi (2016). Trend of the resistivity structure is also similar to the model by Abd Allah & Mogi (2016) at the site OTT008 although more conductive resistivity is estimated in this study. We will conduct additional MT surveys and then analyze 3-D resistivity distribution in the future.

Keywords: Ontake, magnetotelluric method

©2020. Japan Geoscience Union. All Right Reserved.

A research report on the fundamental investigations of an electrical resistivity structure beneath Chugoku and Shikoku regions, southwestern Japan(2019)

*Ichiro Shiozaki[1], Tomofumi Uto[1], Makoto Uyeshima[2], hiroshi hataoka[3], Hideki Murakami[4], Naoto Oshiman[5], Yoshihisa Iio[5], Kazuya Ando[6]

1. Graduate School of Engineering, Tottori University, 2. Earthquake Research Institute, University of Tokyo , 3. Technical Department, Tottori University, 4. Research and Education Faculty , Kochi University, 5. Disaster Prevention Research Institute, Kyoto University, 6. San'in Kaigan Geopark Museum of the Earth and Sea

In order to contribute to a reduction in damage caused by earthquakes and volcanic eruptions, heterogeneities of crustal and upper mantle structure should be clarified based on fundamental investigations of electrical resistivity structure in Chugoku and Shikoku regions, southwestern Japan arc. Our research group has shown that there is a clear relationship between resistivity and seismicity in the San'in and Shikoku regions. In the eastern part of San'in region, it was found that a conductive area exists in the deep crust part under the seismic region, which is a resistive area, along with the seismic activity area stretching nearly in the east and west direction. Assuming that inland earthquakes occur because of local stress concentration caused by heterogeneity beneath a seismic activity band(Iio, 2009), it is necessary to improve spatial data and to clarify the heterogeneity in this area hereafter.
On the other hand, in the Shikoku district, it was suggested that the distinctive low resistivity region exists in the upper crust mainly from the survey results in the outer belt, and that there is a clear relation between the low resistivity and low seismicity in the central and the western area. In order to understand the earthquake phenomenon, it is important to clarify the generation environment and the principle as well as the activity style of the slow earthquake (Obara(2017)).

In this background, broadband MT observation was conducted in the eastern part of Chugoku district from late October to late December 2019. The study area is the eastern extension area (seismic activity is relatively weak) of the Shikano-Yoshioka fault, and there are sites that locate near the Amedaki - Kamato faults and the Yamazaki fault zone. The geomagnetic 3 component and electric field 2 component variations were measured at a total of 11 points using the Phoenix instruments MTU-5 and MTU-5 A. As a general feature, shapes of the sounding curves, such as apparent resistivity and phase value, are similar and both curves suggest the existence of a high-resistivity region (At least kΩ m order) in the deep part. Also, the YX component value of the phase difference tends to increase from about several 100 seconds. Assuming the existence of a 2D structure in the EW direction, model analysis was carried out using the code of Ogawa and Uchida (1996). As a preliminary result, the model shows that the crust was generally estimated as a high resistivity region and the deep low resistivity region of 10 Ωm or less indicated in the Sanin region has not been shown except for the shallow part. Seismic activities may appear to have occurred in the higher resistivity region compared to the surrounding resistivity values.
In the Shikoku region, 3-D resistivity model analysis is being carried out by utilizing and integrating existing data. In particular, it is important to clarify the relationship between the resistivity structure and the mode and environment of slow earthquakes in the eastern and western regions of Shikoku.

This study was supported by the Ministry of Education, Culture, Sports, Science and Technology (MEXT) of Japan, under its Observation and Research Program for Prediction of Earthquakes and Volcanic Eruptions and by ERI JURP(2019-A-03(B0102)). We would like to express sincere gratitude for the

©2020. Japan Geoscience Union. All Right Reserved.

Nittetsu Mining Consultants Co. Ltd. kindly let us use their continuous geomagnetic records as remote references. We used equipment of Tokyo Institute of Technology and joint research equipment of Kyoto University Disaster Prevention Research Institute for observation of this research.

Keywords: electrical resistivity, fundamental investigations, Chugoku and Shikoku regions

©2020. Japan Geoscience Union. All Right Reserved.

Estimation of MT response function to reveal resistivity structure around the Hyuganada area

*Hayato Nakamura[1], Hiroshi Ichihara[1], Tada-nori Goto[2], Tetsuo Matsuno[3], Noriko Tada[4], Shinya Sato[5]

1. Graduate school of environmental studies, Nagoya University, 2. Graduate School of Life Science, University of Hyogo, 3. Kobe Ocean Bottom Exploration Center, Kobe University, 4. Japan Agency for Marine-Earth Science and Technology, 5. Kyoto Univesity, Graduate School of Engineering

Hyuganada area is on an interplate earthquake zone between the Eurasian plate and the subducting Philippine Sea plate. Slow earthquakes, such as low frequency tremor (Yamashita et al., 2015) and slow slip event (Nishimura et al., 2014), were also occurred. The differences of these motion types may relate to the existence of fluid and sediments on the plate boundary interface (e.g. Obara, 2009).

Magnetotellurics (MT) is the passive exploration method to reveal underground resistivity structure. Electrical resistivity is a physical property which sensitive to fluid and sediments. To understand the generation mechanism of the regular and slow earthquake, it is necessary to reveal the resistivity structure beneath the Hyuganada area.

In this study, we estimated MT impedance from electromagnetic data observed at ocean bottom sites around Hyuganada.

Electromagnetic data were recorded at twelve stations around Hyuganada by Ocean Bottom Electro-Magnetometer (OBEM). They had surveyed for half to one year between May in 2017 and August in 2019. In addition to three components magnetic field and two horizontal components electric fields, tilt, temperature (at all stations) and pressure (at two stations) had been measured at 8Hz or 60s sampling. We applied the BIRRP code (Chave and Thomson, 2004) to estimate MT impedance from time series data of the electromagnetic fields. The horizontal magnetic field data recorded at Kakioka Geomagnetic Observatory were also used as the data of the remote reference site.

The MT impedances at long periods (more than 3,000s) had poor decision accuracy at four stations whose depths are less than 1,000m. We considered that this is because the electric field was affected by oceanic current and/or tide. At almost stations, apparent resistivity at short periods was smaller than at long periods, and they indicated the tendency regarded as a one-dimensional structure at less than 100s period. This result implied there was a conductive layer just below the seafloor. We assumed this layer to be a sediment layer.

Previous marine MT studies showed that bathymetry near the coast strongly distorts MT impedance as known as coast effect (e.g. Key and Constable, 2011). Therefore, we will perform 3-D forward calculation for resistivity models incorporating with bathymetry to evaluate the coast effect.

©2020. Japan Geoscience Union. All Right Reserved.

Keywords: magnetotellurics, resistivity, Hyuganada, slow earthquake, Nankai trough

©2020. Japan Geoscience Union. All Right Reserved.

3D resistivity structure of the Matsukawa geothermal area using magnetotelluric data

*KENTARO AOYAMA[1], Toru Mogi[2], Junna Kanehiro[1], Koichi Suzuki[1]

1. Hokkaido University, 2. Tokyo Institute of Technology

The Matsukawa area in Iwate Prefecture is located ~30 km northwest of Morioka City and is the only vapor-dominated geothermal area in Japan. A 2D inversion was performed in 2009 using magnetotelluric data to explore the area’ s geothermal structure in detail and identify a new drilling target (TOUSEC, 2009). However, portions of the obtained data indicate strong three-dimensionality and resistivity anomalies may therefore have been falsely generated. In this study, we perform a 3D inversion using ModEM (Egbert and Kelbert, 2012). We used MT data of 45 stations around the Matsukawa Geothermal Power Plant provided by TOUSEC. By considering the calculation conditions as the initial resistivity, a smoothing parameter, and a Lagrange multiplier, we determine an optimized solution according to results obtained with the smallest root mean square value. The results of the 3D inversion are used to confirm the zones of clay alteration and faulting, both of which control the geothermal system in this area. The 3D resistivity structure matches well with electrical logging data obtained from as deep as 1 km and is therefore more reliable than the 2D inversion above sea level where logging data is available.

Keywords: magnetotelluric method

©2020. Japan Geoscience Union. All Right Reserved.

MT data analysis with Multi-channel Spectrum Analysis (MSSA)

*Shu Kaneko[1], Katsumi Hattori[2], Toru Mogi[2], Chie Yoshino[2]

1. Chiba University Graduate School of Science and Engineering, 2. Chiba University Graduate School of Science

Near the Boso Peninsula, there are triple junctions where the Pacific Plate, the Philippine Sea Plate, and the North American Plate gather, and crustal deformation is very active. Off the coast of Boso is the epicenter of the Enpo earthquake, and the southern Boso area is the epicenters of the 1702 Genroku Kanto earthquake and the 1923 Taisho Kanto earthquake. Recently, slow slip events have been confirmed off Katsuura every 5-6 years. In 2014-2016, Chiba University conducted a wide-area MT survey in the Boso Peninsula to investigate the source structure of the past major earthquake and the resistivity structure of the plate boundary. The observations were made at 12 long-term observation points at 1 Hz sampling using U43 and 41 short-term observation points at 2400, 150 and 15 Hz using MTU-5 and MTU-5A. However, in the Boso Peninsula, the influence of artificial noise included in the acquired MT data is extremely large due to leakage current from a DC train, factories, or power lines running around/in the peninsula. A conventional remote reference method using geomagnetic 1 Hz data at Memambetsu station operated by Japan Meteorological Agency was applied to the Boso MT data, but the effect of noise reduction was insufficient. Therefore, in this study, we applied the noise removal of time series data using Multi-channel Singular Spectrum Analysis (MSSA) as preprocessing of MT analysis. MSSA parameters include window length, data length, and principal component grouping. By changing these parameters, the effect of noise removal on Boso MT data was investigated in detail. This time, we report the effect of noise reduction by parameters and the results of MT analysis.

Keywords: noise reduction, Multi-channel Singular Spectrum Analysis, MT method, Boso peninsula

©2020. Japan Geoscience Union. All Right Reserved.

Effects of source field on MT responses of the flat Earth and the spherical Earth

*Shinya Sato[1]

1. Kyoto Univesity, Graduate School of Engineering

Magnetotelluric (MT) method is one of electromagnetic exploration methods using ionospheric and magnetospheric current for source field. Many researchers have discussed the bias of source field on MT responses (e.g., Madden and Nelson, 1964). Such bias should be careful especially in case of the exploration for deep mantle. For the analysis of deep mantle, some studies are undertaken assuming the flat Earth (Baba et al., 2010) and some are assuming the spherical Earth (Grayver et al., 2019). In this study, the MT responses under the flat or spherical Earth when source field is considered are derived. Varying the vertical and horizontal distance from a site, the robustness of MT responses at each coordinate is discussed.
The MT responses when source is considered have been studied by many researches (e.g., Schmucker, 1970). However, the technique of applied mathematics is introduced not enough in the papers. Therefore, at the appendix of poster presentation, such technique is explained.

Keywords: Magnetotelluric, Source field

©2020. Japan Geoscience Union. All Right Reserved.

Electromagnetic field fluctuations recorded in MT data during the eruption of Kirishima Shinmoe-dake in 2018

*Satoru ANIYA[1], Koki Aizawa[2], Takeshi Matsushima[2]

1. Department of Earth and Planetary Sciences,Graduate School of Sciences,Kyushu University, 2. Institute of Seismology and Volcanology, Facurity of Sciences, Kyushu University

Shinmoe-dake is an active volcano located in the center of Kirishima volcanic area in Kyushu. In January 2011, magmatic eruption occurred for the first time in about 300 years, and erupted again in October 2017 and March to June 2018. In this study, we discuss the relationship between electromagnetic signals obtained by broadband MT (magnetotelluric) observation and seismic and infrasound data close to the Shinmoe-dake volcano.
Twenty eruptions during March to June 2018 were selected for an analysis. We use the MT data recorded at two sites ((1) 5.1 km NW of the Shinmoe-dake crater, and (2) 3.2 km WSW of the Shinmoe-dake crater) and a seismic and infrasound observations data recorded at 30 m away from (1) MT site. We obtained MT time series data with physical unit (mV/km, nT) by applying a Fourier transform, incorporating the frequency responses of instruments and inverse Fourier transform. We also got time series data of physical units (μm/s, Pa) from seismic and infrasound data.
At (1) MT sites, the electromagnetic signals of explosive eruptions well synchronized with the seismic vertical motions and infrasound data. The shape of the impulsive compression phase of infrasound data looks very similar to the shape of EM variation at that time. We also concludes that the EM signals are not occurred in the crater but occurred at the area very close to the MT observation sites.
We will carefully investigate the relationship between electromagnetic signals and seismic and infrasound data close to the Shinmoe-dake volcano and discuss why the seismic and infrasound generates electromagnetic variations.

Keywords: electromagnetic signal, explosive eruption, infrasound, seismic motions, Shinmoe-dake

©2020. Japan Geoscience Union. All Right Reserved.

[J] Poster | S (Solid Earth Sciences)：S-EM Earth's Electromagnetism

[S-EM22] Geomagnetism, paleomagnetism and rock magnetism

convener:Masahiko Sato(Department of Earth and Planetary Science, The University of Tokyo), Chie Kato(Faculty of Social and Cultural Studies, Kyushu University)

We are going to discuss the issues on the magnetic fields of the Earth and planets, paleomagnetism, rock-magnetism, and their applications. This session includes following topics: (1) observation and analysis of the magnetic fields of the Earth and planets, (2) paleomagnetic field variations obtained from natural and archaeological materials, (3) numerical simulations on the magnetic fields of the Earth and planets, (4) measurements and theories of magnetic properties of rocks, minerals, meteorites, and other materials, (5) climate changes and surface tectonics based on the paleomagnetic measurements of rocks and sediments, (6) observations of the magnetic anomalies and the crustal magnetization models of the Earth, planets, and satellites, and (7) developments of the measurement method and data analysis. We also encourage papers stimulating an interdisciplinary collaboration relating to establishment of the SEDI-Japan community. The presentation and discussion will be made in Japanese or English in this session.

[SEM22-P01] **The geomagnetic field modeling of different areas of China based on the Three-dimensional Surface Spline model**

*yan feng[1,2], Yi Jiang[1], Shuang Liu[1] (1.The College of Mathematics and Statistics, Nanjing University of Information Science & Technology, Nanjing 210044, China., 2.State Key Laboratory of Space Weather, Chinese Academy of Sciences, Beijing 100190, China.)

[SEM22-P02] Forecasts of geomagnetic secular variation using core surface flow models (2)

*Masaki Matsushima[1], Hisayoshi Shimizu[2], Futoshi Takahashi[3], Takuto Minami[4], Shin ya Nakano[5], Ryosuke Nakashima[3], Hinami Taniguchi[3], Hiroaki TOH[6] (1.Department of Earth and Planetary Sciences, School of Science, Tokyo Institute of Technology, 2.Earthquake Research Institute, University of Tokyo, 3.Department of Earth and Planetary Sciences, Graduate School of Science, Kyushu University, 4.Department of Planetology, Graduate School of Science, Kobe University, 5.Institute of Statistical Mathematics, 6.Data Analysis Center for Geomagnetism and Space Magnetism, Kyoto University)

[SEM22-P03] Statistical property of the polarity reversals in numerical dynamo models with implications for the geomagnetic field reversals

*Futoshi Takahashi[1], Yuhji Yamamoto[2] (1.Faculty of Sciences, Kyushu University, 2.Center for Advanced Marine Core Research, Kochi University)

[SEM22-P04] Investigation of equatorial symmetry of the flow and magnetic fields in numerical dynamos with dipolar reversal

*takumi kera[1], Yuto Katoh[1], Yuki Nishida[1], Hiroaki Matsui[2] (1.tohoku university, 2.Dept. of Earth and Planetary Sciences, University of California, Davis Dept. of Earth and Planetary Sciences, University of California, Davis)

[SEM22-P06] **Magnetic minerals in a speleothem from Tonga, the southern Pacific: Observation from scanning SQUID microscopy and rock magnetism**

*Naoto Fukuyo[1,3], Hirokuni Oda[2], Geoffrey Clark[4], Yusuke Yokoyama[1,3] (1.Atmosphere and Ocean Research Institute, The University of Tokyo, 2.Institute of Geology and Geoinformation, Geological Survey of Japan, AIST, 3. Department of Earth and Planetary Science, The University of Tokyo, 4.College of Asia and the Pacific,The Australian National University)

[SEM22-P07] Paleomagnetic direction of the Paleogene Kobe Group ; the constraints on the paleoposition of Southwest Japan

*Hiroki Senda[1], Akira Hayashida[1] (1.Doshisha Univ.)

[SEM22-P08] A paleomagnetic record of the upper Olduvai polarity transition from the Hata Formation, Chikura Group, in the southernmost part of the Boso Peninsula

*Takahiro Kitamura[1], Makoto Okada[2] (1.Graduate School of Science and Engineering, Ibaraki University, 2.Department of Earth Sciences, Faculty of Science, Ibaraki University)

[SEM22-P09] Paleomagnetic secular variation and rock magnetic characteristics for the last 30 kyrs from the Nankai Trough sediments, Japan

*Ryoya Goto[1], Toshitsugu Yamazaki[1], Natsumi Okutsu[1,2], Juichiro Ashi[1] (1.Atmosphere and Ocean Research Institute, The University of Tokyo, 2.Japan Agency for Marine-Earth Science and Technology)

[SEM22-P10] Paleo-stress analysis of fault gouges using Raman spectroscopy and rock magnetic methods

Yuki Nose[2], *Norihiro Nakamura[1,2], Hiroyuki Nagahama[2] (1.Institute for Excellence in Higher Education, Tohoku University, 2.Department of Earth Science, Tohoku University)

[SEM22-P12] Coercivity- and blocking temperature-dependent remanence properties of single plagioclase crystals with exsolved magnetite

*Yoichi Usui[1], Chie Kato[2] (1.Japan Agency for Marine-Earth Science and Technology, 2.Earth-Life Science Institute, Tokyo Institute of Technology)

[SEM22-P13] Preliminary paleomagnetic study on single plagioclase crystals separated from the anorthositic dike in the Doshi gabbroic body

*Haruka Nagai[1], Masahiko Sato[1], Chie Kato[2], Kazuhito Ozawa[1] (1.The University of Tokyo, 2.Tokyo Institute of Technology)

[SEM22-P14] “On-land investigation of a sea-floor spreading in Ethiopia” Geo-electromagnetic research at the center of a divergent plate boundary in Afar depression, Ethiopia

*Naoto Ishikawa[1], Ryokei Yoshimura[2], Tesfaye Kidane Birke[3], Shin-ichiro Higashino[4], Shin-ichi Kagashima[5], Ameha A. Mulneh[6], Kirika Kitagawa[5], Nobutatsu Mochizuki[12], Masakazu Fujii[7], Mamoru Kadoya[11], Mitsuhiro Iwamoto[11], Noriaki Obara[9], Yo-ichiro Otofuji[8], Minoru Funaki, Tetsu Kogiso[10] (1.Faculty of Sustainable Design, Toyama University, 2.Disaster Prevention Research Institute, Kyoto University., 3.University of KwaZulu Natal, 4.Graduate School of Engineering, Kyushu University, 5.Yamagata University, 6.Addis Ababa University, 7.National Institute of Polar Research, 8.Japan Geochronology Network, 9.Robotista, 10.Graduate School of Human and Environmental Studies, Kyoto University, 11.X-treme Composite Japan, 12.Kumamoto University)

[SEM22-P15] Periodic change of magnetic susceptibility observed in the dolerite

*Masaru Nakamura[1], Kohei Oda[1], Masaaki Tanaka[1], Daisuke Kashima[1], Yuichi Shimizu[1], Koki Takuwa[2], Shimpei Miyamoto[2] (1.The Chugoku Electric Power Co., Inc., 2.Chuden Engineering Consultants Co., Ltd.)

[SEM22-P16] **Shock remanence structure of natural basalt and granite samples**

*Masahiko Sato[1], Kosuke Kurosawa[2], Shota Kato[1], Masashi Ushioda[3], Sunao Hasegawa[4] (1.The University of Tokyo, 2.Chiba Institute of Technology, 3.National Institute of Advanced Industrial Science and Technology, 4.Japan Aerospace Exploration Agency)

The geomagnetic field modeling of different areas of China based on the Three-dimensional Surface Spline model

*yan feng[1,2], Yi Jiang[1], Shuang Liu[1]

1. The College of Mathematics and Statistics, Nanjing University of Information Science & Technology, Nanjing 210044, China., 2. State Key Laboratory of Space Weather, Chinese Academy of Sciences, Beijing 100190, China.

Based on surface observations, satellite data, we create the Three-dimensional Surface Spline (3DSS) model of Chinese mainland. Through this model, the magnetic field analyses of domestic plateau (Qinghai Tibet Plateau 28˚N-38˚N, 78˚E -102˚E), plain (Middle and lower reaches of Yangtze River Plain 27˚N-34˚N, 111˚E-122˚E) and marine (parts of the East and South China Sea 16˚N-30˚N, 123˚E-136˚E) areas have been investigated. In addition, single models of plateau and plain have also been created. In order to compare and verify results, the corresponding Two (2DTY) and Three-dimensional (3DTY) Taylor polynomial models have been derived. Issues like the removal of disturbing geomagnetic fields, the data gap between surface and satellite level, boundary effect are all seriously considered. Aims for evaluate the modeling results, several measuring points are not calculated intentionally while modeling, then calculate the residuals, change rate absolutes, RMSE. Results show that expect East component *Y*, the change rate absolutes of other components are less than 1% both in domestic and single models, which means the modeling result of 3DSS is better than other two models. 3DSS models of plateau and plain reflect fine distribution of magnetic field after comparing domestic distribution. 3DSS model fits the plateau best, plain is second, the worst in the marine area, which implies the creation of a 3DSS model might not need so many points. The modeling precision depends on the number and distribution of measuring points.

Keywords: Geomagnetic field, Three-dimensional model, Surface Spline, CM4

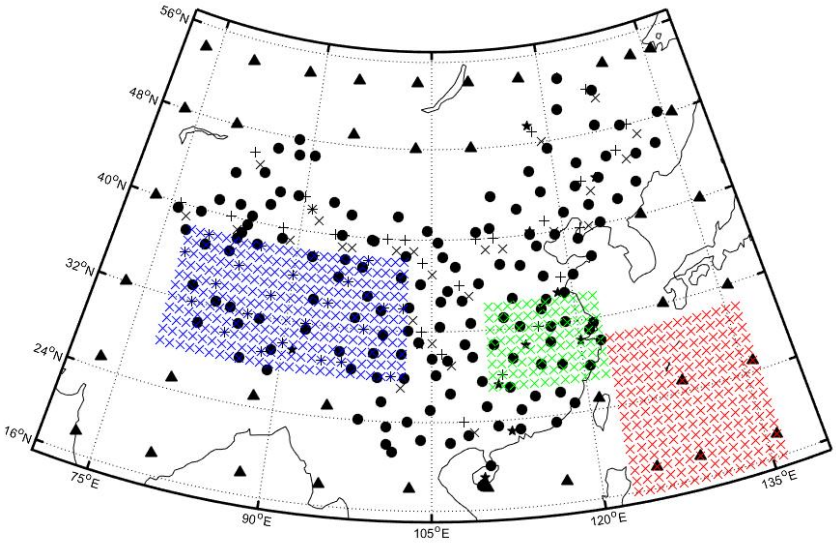

©2020. Japan Geoscience Union. All Right Reserved.

Forecasts of geomagnetic secular variation using core surface flow models (2)

*Masaki Matsushima[1], Hisayoshi Shimizu[2], Futoshi Takahashi[3], Takuto Minami[4], Shin ya Nakano[5], Ryosuke Nakashima[3], Hinami Taniguchi[3], Hiroaki TOH[6]

1. Department of Earth and Planetary Sciences, School of Science, Tokyo Institute of Technology, 2. Earthquake Research Institute, University of Tokyo, 3. Department of Earth and Planetary Sciences, Graduate School of Science, Kyushu University, 4. Department of Planetology, Graduate School of Science, Kobe University, 5. Institute of Statistical Mathematics, 6. Data Analysis Center for Geomagnetism and Space Magnetism, Kyoto University

The International Geomagnetic Reference Field (IGRF) is a standard mathematical description in terms of spherical harmonic coefficients, known as the Gauss coefficients, for the Earth’ s main magnetic field and its secular variation. On December 19, 2019, the working group V-MOD of the International Association of Geomagnetism and Aeronomy (IAGA) released the 13th generation of IGRF, which consists of three constituents; a Definitive IGRF (DGRF) for 2015, an IGRF for 2020, and a secular variation (SV) model from 2020 to 2025. We submitted a candidate model for SV from 2020 to 2025, relying on our strong points, such as geodynamo numerical simulation, data assimilation, and core surface flow modeling.

We can estimate core flow near the core-mantle boundary (CMB)from distribution of geomagnetic field and its secular variation. Such a flow model can be obtained for actual physical parameters of the Earth. However, numerical simulations of geodynamo were carried out for physical parameters far from actual ones. Therefore, a core flow model to be used for data assimilation had to be obtained on a condition relevant to the numerical simulations. To obtain the candidate model for SV, we adjusted time-scale of a geodynamo model (Takahashi 2012, 2014) to that of actual SV of geomagnetic field as given by Christensen and Tilgner (2004).

In this presentation, we first investigate temporal variations of geomagnetic field due to the magnetic diffusion only. Next, we investigate temporal variations of geomagnetic field due to the motional induction caused by some core flow models as well as the magnetic diffusion. Then we compare secular variations of geomagnetic field forecasted by these methods.

Keywords: IGRF, secular variation, core surface flow

©2020. Japan Geoscience Union. All Right Reserved.

Statistical property of the polarity reversals in numerical dynamo models with implications for the geomagnetic field reversals

*Futoshi Takahashi[1], Yuhji Yamamoto[2]

1. Faculty of Sciences, Kyushu University, 2. Center for Advanced Marine Core Research, Kochi University

Geomagnetic secular variation provides a way to characterize dynamo processes in the Earth’ s outer core. Among them, polarity reversals of the Earth’ s dipole have been one of the least understood phenomena. Recent advances in numerical dynamo simulation have enabled us to examine secular variation in both short- and long-period. Here we use numerical dynamo modeling to have general statistical property of the reversals occurred in numerical dynamos. Since we primarily focus on statistical behavior, long-term (typically longer than 1 Myrs) dynamo simulations are required to have a large number of reversals. However, it is tough and enormously time-consuming to perform a long-term dynamo simulation at state-of-the-art parameters. To handle the circumstances, we have to choose a higher value of E (Ekman number) by compromise. Some of the parameters adopted in the present study are fixed at E = 3.25×10^{-3} and 2×10^{-3}, Pr (Prandtl number) = 1, Pm (magnetic Prandtl number) = 20, whereas Ra (Rayleigh number) is varied to see effects of the buoyancy on time variation of the dynamos.
Time-integration is carried out for 30 –40 non-dimensional time unit, which is scaled by the magnetic diffusion time. In each run, we have observed tens to hundreds of reversals during the above intervals. Based on the results, we calculate some statistics and examine their behavior. Preliminary results will be reported.

Keywords: dynamo, reversal, core

©2020. Japan Geoscience Union. All Right Reserved.

Investigation of equatorial symmetry of the flow and magnetic fields in numerical dynamos with dipolar reversal

*takumi kera[1], Yuto Katoh[1], Yuki Nishida[1], Hiroaki Matsui[2]

1. tohoku university, 2. Dept. of Earth and Planetary Sciences, University of California, Davis Dept. of Earth and Planetary Sciences, University of California, Davis

Paleomagnetic observations reveal that the geomagnetic field has reversed its polarity every hundred of thousands to millions of years and each reversal typically takes 2000-12000 years to occur. Numerical dynamo simulations have been performed to gain insight into physical processes that give rise to polarity reversal temporal characteristics. Olson et al. (2011) found a transitional regime between dipolar and multipolar regimes by simulating with different Rayleigh number (*Ra*) and Ekman number (*E*). When dominated by rotation (i.e. models with low *Ra* and low *E*), magnetic field was dipole dominant without reversal. And when dominated by convection (i.e. high *Ra* and high *E*), magnetic field had multipolar structure with frequently reversing dipole component. In the transitional regime, simulations have long stable dipole-dominated chrons separated by relatively short reversals. A polarity reversal in their most Earth-like dynamo has precursory reversal with intensity low for 35 kyr followed by a rapid polarity change for about 400yr, with no postreversal rebound. The overall duration is approximately 50 kyr. However, mechanism for each phase or time scale remain not clear. Olson et al., (2004) analyzed the mechanism of magnetic polarity reversals in a dynamo model. In their model, the reversed flux is produced locally in the convective plumes and the transported from south to north by the meridional circulation. This result suggests that asymmetric flow with respect to equator play a role in reversals.
In the present study, we perform dynamo simulations in order to discuss dynamical processes of the reversal, using a geodynamo code Calypso [Matsui et al., 2014]. In particular, we investigate how equatorial flow asymmetry contributes reversal processes. In the present study, we fix aspect ratio, Ekman, Prandtl and magnetic Prandtl numbers of $r_i/r_o = 0.15, E = 10^{-3}, Pr = 1$ and $Pm = 5$, respectively. The simulations are performed to 4 times of the magnetic diffusion time (t_d) with various Rayleigh number of $Ra = 980$, 1100, 1200 and 1300. Then we examine the dipole tilt angle. Generally, with increasing *Ra*, the tilt angle became more unstable. In $Ra = 980$ case, during simulation time, dipole field was stable without reversal. In $Ra = 1100$ case, dipole field tilts to vicinity of the opposite polarity at near the end of simulation ($t = 4.0 t_d$). In $Ra = 1200$ case, dipole field keeps the normal polarity at $2.0\ t_d < t < 3.5\ t_d$, and flips to the reverse polarity to the end of the simulation. In $Ra = 1300$ case, the dipole field has reverse polarity at $2.0\ t_d < t < 3.5 t_d$, and has normal polarity at $1.0\ t_d < t < 2.0 t_d$ and $3.5\ t_d < t < 4.0 t_d$. And we are performing with aspect ratio of the current Earth's outer and inner cores (i.e. $r_i/r_o = 0.35$), and we analyze the amplitude of symmetric and asymmetric components of flow and magnetic field respectively. For further research, we will also discuss how the equatorial antisymmetric flow component with respect to the equator is generated and maintained, focusing on the energy transfer between the flow and the magnetic field.

Keywords: Geomagnetic field, Geodynamo, Polarity reversals, Equatorial symmetry

©2020. Japan Geoscience Union. All Right Reserved.

Magnetic minerals in a speleothem from Tonga, the southern Pacific: Observation from scanning SQUID microscopy and rock magnetism

*Naoto Fukuyo[1,3], Hirokuni Oda[2], Geoffrey Clark[4], Yusuke Yokoyama[1,3]

1. Atmosphere and Ocean Research Institute, The University of Tokyo, 2. Institute of Geology and Geoinformation, Geological Survey of Japan, AIST, 3. Department of Earth and Planetary Science, The University of Tokyo, 4. College of Asia and the Pacific,The Australian National University

Speleothems could be an ideal archive of paleomagnetism since they retain continuous geomagnetic records in stable conditions as well as their applicability of reliable radiometric datings such as U-series and radiocarbon techniques. Furthermore, speleothems can be useful tools in studies of environmental magnetism. The magnetic minerals in the speleothems can provide records of environmental variability by rock magnetic properties to changes of detrital input reflecting regional and global environmental changes such as paleofloods, precipitation, and anthropogenic influence. However, their weak magnetic signals hinder this archive from being widely used in the field. A scanning SQUID Microscope (SSM) can image very weak magnetic fields with high spatial resolution and hence could potentially solve this obstacle. In this study, we have conducted paleomagnetic measurements based on magnetic mapping with an SSM and rock magnetic measurements on a stalagmite collected at Anahulu cave in Tongatapu Island, the Kingdom of Tonga. We observe a stronger magnetic field above the surface layer compared with that of the inner layers associated with the laminated structures of a speleothem at the submillimeter scale with SSM. Further, rock magnetic measurements show that the concentration of magnetic minerals increased, and maghemite and goethite contents had changed from the inner white layers to the surface black layer of this speleothem. These differences could occur because the depositional environment for the speleothem has been changed to oxidative.

Keywords: Scanning SQUID microscopy, environmental magnetism, speleothem

©2020. Japan Geoscience Union. All Right Reserved.

Paleomagnetic direction of the Paleogene Kobe Group ; the constraints on the paleoposition of Southwest Japan

*Hiroki Senda[1], Akira Hayashida[1]

1. Doshisha Univ.

Paleomagnetic studies of the Miocene and Cretaceous rocks in Southwest Japan since 1980s suggested that Southwest Japan suffered clockwise rotation of about 40˚ relative to the Asian continent in a short period in the Miocene (e.g., Hoshi et al., 2015). Before that, no significant motion is assumed since the late Cretaceous (Uno et al., 2017). However, the apparent polar wander path, that is important to understand drift history of continents or crustal blocks, has not been established for Southwest Japan, particularly due to scarce paleomagnetic data from the Paleogene.

The Kobe Group, distributed in southern part of Hyogo prefecture, was dated at 30-39 Ma (Late Eocene to Early Oligocene) by K-Ar, Ar/Ar and fission-track dating, but its paleomagnetic direction has not been examined yet. In attempt to obtain Paleogene paleomagnetic poles representing Southwest Japan, we collected samples of tuffacious sediments of the Kobe Group in western part of the Sanda basin, where the strata are relatively well exposed. After measuring magnetic susceptibility and its anisotropy with a Kappabridge, we made measurement of remanent magnetizations using a cryogenic magnetometer (2G SRM) and stepwise thermal or alternating field (AF) demagnetizations. In addition, we made stepwise acquisition experiments of anhysteretic remanent magnetization (ARM) and isothermal remanent magnetization (IRM) in order to assess the coercivity spectra.

Results of the thermal and AF demagnetization are classified into three groups characterized by (1) only low temperature or low coecivity components, (2) additional high temperature or high coecivity components and (3) no meaningful components identified. The low temperature/coecivity components were recognized all the sites with the directions close to the present axial dipole field, suggesting overprints of viscous remanent magnetization (VRM). The high temperature/coecivity components, which were identified only at several sites, consistently showed eastward deflections of about 40-60˚ from the true north.

We interpret that the high temperature/coecivity components likely represent primary paleomagnetic direction of the Kobe Group, although the current data may be insufficient to average out the effect of paleosecular variation. The mean direction, however, is consistent with the late-Paleogene paleomagnetic directions reported from the Tonosho Group in Kagawa Prefecture and the KawamotoGranodiolite in Shimane Prefecture, providing the paleomagnetic pole plotted between the early Miocene (20Ma) and the Late Cretaceous poles. This result suggests that Southwest Japan had been a part of the continental block of east Eurasia during 70-20 Ma. Further investigation of the Paleogene paleomagnetic directions in Southwest Japan is expected to give clear constraints for paleogeography of East Asia before the opening of the Japan Sea.

Keywords: Paleogene, Southwest Japan, paleomagnetic direction

©2020. Japan Geoscience Union. All Right Reserved.

A paleomagnetic record of the upper Olduvai polarity transition from the Hata Formation, Chikura Group, in the southernmost part of the Boso Peninsula

*Takahiro Kitamura[1], Makoto Okada[2]

1. Graduate School of Science and Engineering, Ibaraki University, 2. Department of Earth Sciences, Faculty of Science, Ibaraki University

The Chikura Group, located at the southern tip of the Boso Peninsula, is an Upper Pliocene to Lower Pleistocene marine succession. The Chikura Group bears strong and stable paleomagnetic signals because one of the sediment sources is thought to be the Izu-Ogasawara volcanic arc. It is also suitable for biostratigraphic and paleoceanographic studies because it produces abundant microfossils such as foraminifera and calcareous nannofossils.
In the upper Chikura Groupe, an oxygen isotope stratigraphy established using benthic foraminifera, indicated that the upper part of the Hata Formation was corresponded between 1.59 Ma and 1.82 Ma (MIS55 ~ MIS64) including the upper Olduvai boundary (Okada & Furukawa, 2013). However, detailed paleomagnetic records have not been obtained in the upper part of the Hata Formation. Therefore, the purpose of this study is to conduct paleomagnetic studies in the top section of the Hata Formation in the Chikura Group to restore detailed geomagnetic variations across the upper Olduvai boundary.
In the section of the layer thickness of 14 m in the Hata formation thought to include the upper Olduvai boundary, samples for palaeomagnetic measurements were collected basically at every 1 m stratigraphic interval, but at every 0.1 m between 3 and 6.5 m, from a total of 41 horizons.
In this study, a hybrid demagnetization method consisting of a thermal demagnetization at 250 ℃ and a progressive alternating field demagnetization sequence. A relative paleointensity (RPI) was deduced from a hybrid demagnetization of an anhysteretic remanent magnetization (ARM). The measurements were carried out at Center for Advanced Marine Core Research, Kochi University. The variation of the VGP latitudes indicates that the upper Olduvai boundary is situateded between 3.3 m and 4.2 m. On the other hand, since the RPIs exhibit low values in the normal polarity interval below the boundary, a further study has to be done in the lower succession to discuss the starting process of the upper Olduvai reversal.

Reference
Furukawa & Okada, 2013, "Oxygen isotope stratigraphy at the top section of the Hata formation, the Chikura group in the southern part of the Boso Peninsula", the Geological Society of Japan The 120th Annual Meeting

Keywords: Olduvai, polarity transition, Boso Peninsula

©2020. Japan Geoscience Union. All Right Reserved.

Paleomagnetic secular variation and rock magnetic characteristics for the last 30 kyrs from the Nankai Trough sediments, Japan

*Ryoya Goto[1], Toshitsugu Yamazaki[1], Natsumi Okutsu[1,2], Juichiro Ashi[1]

1. Atmosphere and Ocean Research Institute, The University of Tokyo, 2. Japan Agency for Marine-Earth Science and Technology

The geomagnetic field constantly fluctuates in direction and intensity, known as secular variation (PSV). Paleomagnetic studies using marine and lake sediments, and archeological materials have been conducted globally for understanding PSVs over the past several tens of thousands of years. In Japan, Ali *et al*. (1999) presented a Holocene PSV master curve of declination and inclination from Lake Biwa, central Japan. This curve has widely been used to correlate cores and estimate ages. But this master curve has some problems including the accuracy of age axis. In addition, recent progress of paleomagnetism has made it possible to discuss relative paleointensity (RPI) using marine sediments.

For PSV studies using marine sediments, especially for RPI studies, it is desirable that the sediments are magnetically relatively homogeneous and have stable remanent magnetization (Yamazaki *et al*. 2017). In addition, it is necessary that the sediments can be dated and have a sedimentation rate enough for targeted resolution. Seafloor sediments off Kumano in the Nankai Trough are considered to satisfy these conditions based on current knowledge (Okutsu, 2019, Ph.D thesis). On the other hand, it is necessary to take into account intercalated turbidite layers. Okutsu (2019, Ph.D thesis) has identified turbidite layers in the sediment core used in this study from various analyses including particle size analysis, magnetic susceptibility measurement, X-ray CT scan, and XRF core scan (ITRAX).

In this study, we intend to present a new PSV record (declination, inclination and RPI) for the last 30 kyrs from Nankai Trough sediments. We aim to construct a more accurate and reproducible PSV curve in Japan than those of the previous studies, and to newly obtain a RPI record These PSV curves will be useful for inter-core correlation and age estimation of sediments around Japan.

We will introduce mainly the results of paleomagnetic and rock magnetic measurements on 293 discrete samples (7 cc cube) taken from core PC04 of the Hakuho-maru KH-17-2 cruse off Kumano of the Nankai Trough.

Keywords: paleomagnetic secular variation (PSV), relative paleointensity (RPI), rock magnetism, turbidites, the Nankai Trough, Holocene

©2020. Japan Geoscience Union. All Right Reserved.

Paleo-stress analysis of fault gouges using Raman spectroscopy and rock magnetic methods

Yuki Nose[2], *Norihiro Nakamura[1,2], Hiroyuki Nagahama[2]

1. Institute for Excellence in Higher Education, Tohoku University, 2. Department of Earth Science, Tohoku University

Paleo-stress analysis is important for estimating ancient activities of faults only from the information of fault gouge. Mishima et al. (2006) and Fukuzawa et al. (2017) determined the layers of high-temperature slip zone by magnetic methods. Although these studies are powerful to detect slip layers, paleo-stress is not determined. Chou et al. (2002) identified the presence of irregular-shaped pyrite crystals and the absence of framboidal pyrite within the 1999 Chi-Chi principal slip zone. It is thought that such pyrite is associated with alteration of iron sulphide minerals into pyrite at hydrothermal conditions due to coseismic frictional heating during earthquakes. Such pyrite has the potential to record accumulated stress as structural distortions in fault gouge after earthquakes. Therefore, we measured pyrite crystals in the Nojima fault gouge by Raman spectroscopy and analyzed the distortion. We found that systematic shifts of Raman double peak spectrum (Ag, Eg modes) to increase the wavenumber. Non-hydrostatic pressure causes such wavenumber shift according to laboratory pressure experiments. As a result, it is estimated that the maximum magnitude of stress from pyrite is estimated at 600 ~ 1000 MPa, resulting in long-duration after the last earthquake. After determining slip zones by magnetic methods, Raman analysis offers a practical method that could derive paleo-stress to reveal fault activities only from the information of fault gouge.

Keywords: Fault gouge, Raman, Scanning magnetic imaging

©2020. Japan Geoscience Union. All Right Reserved.

Coercivity- and blocking temperature-dependent remanence properties of single plagioclase crystals with exsolved magnetite

*Yoichi Usui[1], Chie Kato[2]

1. Japan Agency for Marine-Earth Science and Technology, 2. Earth-Life Science Institute, Tokyo Institute of Technology

Single-domain particles are fundamental to paleomagnetism. Increasing number of reports verify that exsolved magnetite in plagioclase is close to the non-interacting single-domain state, and pioneering works have successfully used them for both paleodirection and paleointensity studies. On the other hand, anomalously strong magnetic anisotropy and high efficiency of remanence acquisition have been identified as obstacles to accurately interpret paleomagnetic record in exsolved magnetite. However, rock magnetic measurements concerning these properties are still scarce. Moreover, coercivity- and blocking temperature-dependence has been rarely assessed, while stepwise demagnetization is a standard protocol in most of the paleomagnetic applications. In this study, we report systematic measurements of anhysteretic remanence (ARM) and thermoremanence (TRM) at different field directions, field magnitude, and demagnetization steps, for plagioclase crystals separated from oceanic gabbros. Similar to the previous reports, plagioclase crystals showed high coercivity (median destructive field ~60 mT), and sharp unblocking above 560 °C. Both ARM and TRM suggested large anisotropy with deviation of remanence direction from applied field by 10 - 30°. Upon progressive AF and thermal demagnetization, ARM showed 2-3 apparent "components", indicating coercivity- and blocking temperature-dependent anisotropy. The directional patterns were different between AF and thermal demagnetization. There was a tendency that the direction of the low coercivity (<90 mT) "component" is similar to that of the high blocking temperature (>560 °C) “component”. AF demagnetization of TRM was generally similar to that of ARM, except that the high coercivity "component" was larger in TRM. Remanence acquisition was efficient, and both ARM and TRM reached 10-30 % of saturation remanence with bias field of 40 uT. This fraction increased upon AF demagnetization, reflecting smaller AF stability of IRM. Nonetheless, the remanence acquisition curves versus the bias field magnitude seems to be insensitive to coercivity window. The complex pattern in AF demagnetization of ARM and TRM particularly warns the interpretation of data such as those in Shaw-type paleointensity experiments. Thermal demagnetization may be relatively easier to interpret, because the main unblocking above 560 °C seems to be of single “component”. Nevertheless, we emphasize that anisotropy should be determined around the unblocking temperature rather than for total TRM, and precise temperature control would be a next challenge. Nonlinear remanence acquisition may be approximated using total ARM or TRM. We will discuss these observations in light of microscopic texture of exsolved magnetite.

©2020. Japan Geoscience Union. All Right Reserved.

Preliminary paleomagnetic study on single plagioclase crystals separated from the anorthositic dike in the Doshi gabbroic body

*Haruka Nagai[1], Masahiko Sato[1], Chie Kato[2], Kazuhito Ozawa[1]

1. The University of Tokyo, 2. Tokyo Institute of Technology

In order to explore the long-term variation of geomagnetic field paleointensity, studies on plutonic rocks are considered to be suitable since they are likely to record the time-averaged field during their cooling history. We performed a paleomagnetic study on single silicate crystals separated from the plutonic rocks. We measured the intensity of natural remanent magnetization (NRM) of samples from four sites, including the Doshi gabbroic body, Tanzawa tonalitic pluton, central Japan (DOS03D and DOS21D) and the Pankenushi gabbroic complex, Hidaka magmatic belt, central Hokkaido (95100104 and 95092407B). The DOS03D was collected at central part of the Doshi gabbroic body, while the DOS21D was sampled from the anorthositic dike in the Doshi gabbroic body. The sampling site of 95100104 was located at the east margin of the Pankenushi gabbroic complex, and the 952407B was sampled from the felsic vein in the Pankenushi gabbroic complex. The zircon U-Pb ages in the Doshi gabbroic body and the Pankenushi gabbroic complex were reported as ~5 Ma and ~18.5 Ma, respectively. In cases of the Pankenushi gabbroic complex samples, four out of 30 for 95092407B and four out of 20 for 95100104 had larger NRM intensity than the detection limit of the SQUID magnetometer (2G Enterprises Model 755-4.2 cm). Because 47 out of 58 for DOS03D and 79 out of 80 for DOS21D showed larger NRM intensity than the detection limit, we further conducted stepwise alternating field demagnetization on these samples. At relatively high coercivity range, a linear component heading to the origin was recognized in eight out of ten samples of DOS21D. We consider this component as the primary magnetization. We could not detect such linear component in any samples of DOS03D. We selected five samples of DOS21D and conducted paleointensity experiments using the double heating technique of the Shaw method with low-temperature demagnetization (LTD-DHT Shaw method). The result show that no sample passed the sample selection criteria for reliable paleointensity determinations mainly due to the weak anhysteretic remanent magnetization. Alternately, we tried to calculate paleointensity using the ratio of thermoremanent magnetization at the first heating to that at the second heating in the LTD-DHT Shaw paleointensity experiment. The obtained paleointensity was significantly stronger than the averaged paleointensity data during 4.5–5 Ma reported by previous studies on volcanic rocks.

Keywords: Paleointensity, Single plagioclase crystals, Plutonic rocks

©2020. Japan Geoscience Union. All Right Reserved.

“On-land investigation of a sea-floor spreading in Ethiopia” Geo-electromagnetic research at the center of a divergent plate boundary in Afar depression, Ethiopia

*Naoto Ishikawa[1], Ryokei Yoshimura[2], Tesfaye Kidane Birke[3], Shin-ichiro Higashino[4], Shin-ichi Kagashima[5], Ameha A. Mulneh[6], Kirika Kitagawa[5], Nobutatsu Mochizuki[12], Masakazu Fujii[7], Mamoru Kadoya[11], Mitsuhiro Iwamoto[11], Noriaki Obara[9], Yo-ichiro Otofuji[8], Minoru Funaki, Tetsu Kogiso[10]

1. Faculty of Sustainable Design, Toyama University, 2. Disaster Prevention Research Institute, Kyoto University., 3. University of KwaZulu Natal, 4. Graduate School of Engineering, Kyushu University, 5. Yamagata University, 6. Addis Ababa University, 7. National Institute of Polar Research, 8. Japan Geochronology Network, 9. Robotista, 10. Graduate School of Human and Environmental Studies, Kyoto University, 11. X-treme Composite Japan, 12. Kumamoto University

In order to clarify the formation process of magnetic stripes and structure under a sea-floor spreading center at the divergent plate boundary, we are performing an on-land geo-electromagnetic research project in Afar Depression, Ethiopia, where we can investigate into a subaerial sea-floor spreading center directly. We will show the outline of our project, and report our research activities in 2016-2019 fieldworks and preliminary results.

Keywords: divergent plate boundary, sea-floor spreading, magnetic anomaly, geo-electromagnetic surveys, small unmanned aircraft

©2020. Japan Geoscience Union. All Right Reserved.

Periodic change of magnetic susceptibility observed in the dolerite

*Masaru Nakamura[1], Kohei Oda[1], Masaaki Tanaka[1], Daisuke Kashima[1], Yuichi Shimizu[1], Koki Takuwa[2], Shimpei Miyamoto[2]

1. The Chugoku Electric Power Co., Inc., 2. Chuden Engineering Consultants Co., Ltd.

In Shimane Peninsula, located in eastern Shimane Prefecture, sedimentary rocks of the Josoji formation in the Miocene are intruded by dolerite. In this study, we confirmed periodic change of magnetic susceptibility after continuous measurement of magnetic susceptibility using about 8 meters columnar sample from the dolerite which has the thickness of >50 meters. We report this phenomenon.

The columnar sample is part of a borehole core obtained in Kashima, Matsue City, Shimane Prefecture. The intrusion age of dolerite is ca.14 Ma, which produced silicification of tuffaceous shale in the Josoji formation. There is fine grain near the boundary of intrusion, and the grain size gradually increases toward the depth. It is confirmed that the dolerite shows the ophitic texture of plagioclase and clinopyroxene and has opaque minerals in matrix. Part of clinopyroxene has altered to chlorite. The opaque minerals turned out to be magnetite and ilmenite as a result of EPMA.

The magnetic susceptibility of dolerite is on the order of 10^{-3}~10^{-2}SI, and it is nearly one-hundredth of that within one meter of the boundary of intrusion at a depth of 79.33 meters. This measurement value is considered common since it is known that the magnetic susceptibility of basalt rock is most often on the order of 10^{-2}SI and occasionally on the order of 10^{-4}~10^{-1}SI [*Society of Exploration Geophysicists of Japan*, 2012]. The existence of magnetite and ilmenite in the dolerite has been confirmed. Since the susceptibility of magnetite is on the order of 10^{-0}SI [*Society of Exploration Geophysicists of Japan*, 2012], it is possible that these magnetic minerals may affect the susceptibility.

The value of the magnetic susceptibility changes periodically in the range of 7 to 13×10^{-3}SI. At 1 meter from the intrusion boundary at a depth of 81 meters, the period is less than 1 meter, whereas at 6 meters from the intrusion boundary at a depth of 85 meters, the period is about 2 meters. It is confirmed that the period tends to increase with distance from intrusion boundary.

Such a periodic structure is also found near the intrusion boundary of the dolerite exposed at the coastal outcrop about 1.5 km west of the borehole point. It is thought that this dolerite intruded in the same age that the dolerite intruded, whose magnetic susceptibility was measured, and in this place a periodic layered structure having relief parallel to the intrusion boundary is recognized. Atsumi dolerite distributed in Tsuruoka city, Yamagata Prefecture is known as an example of a periodic layered structure having relief of dolerite. This is a layered structure of several tens of centimeters parallel to the intrusion boundary at the coastal outcrop. The structure is formed because the more vesicles there are, the more easily it is eroded by the waves, and the width of the layer increases regularly from the intrusion boundary to the inside [*Toramaru et al.*, 1996]. This structure is explainable on the basis of the idea that, due to the balance between the rate of heat transfer in magma and the diffusion rate of magmatic volatiles in melt, the growth of vesicles such as the Liesegang rings proceeded heterogeneously and with a spatial and temporal periodicity (double diffusion model) [*Takahashi and Ishiwatari*, 2012]. It is thought that these dolerites around the survey site built a periodic structure during magma cooling since a layer structure similar to Atsumi dolerite is found near the intrusion boundary of the dolerite at the coastal outcrop.

©2020. Japan Geoscience Union. All Right Reserved.

Based on the periodic change in magnetic susceptibility that we found in this study, it is possible that periodic growth occurred when magnetic minerals such as magnetite crystallized and grew as matrix during magma cooling, similar to the gas component which caused the layered structure of Atsumi dolerite.

Keywords: dolerite, magnetic susceptibility, periodic change

©2020. Japan Geoscience Union. All Right Reserved.

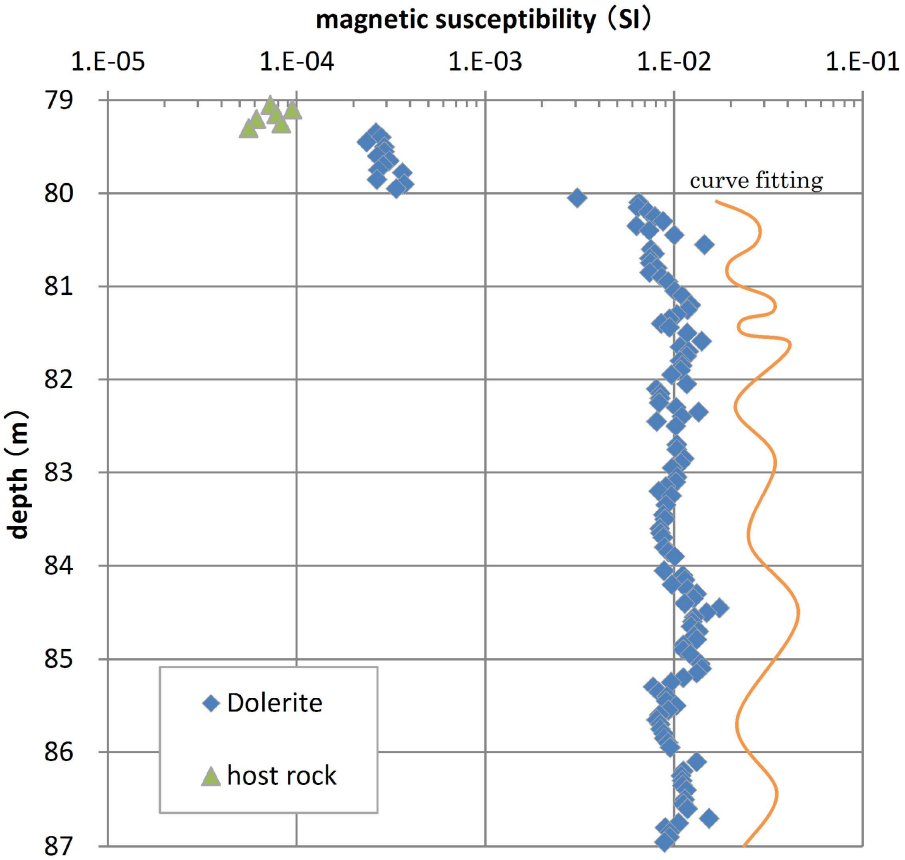

©2020. Japan Geoscience Union. All Right Reserved.

Shock remanence structure of natural basalt and granite samples

*Masahiko Sato[1], Kosuke Kurosawa[2], Shota Kato[1], Masashi Ushioda[3], Sunao Hasegawa[4]

1. The University of Tokyo, 2. Chiba Institute of Technology, 3. National Institute of Advanced Industrial Science and Technology, 4. Japan Aerospace Exploration Agency

Knowledge of the evolution of magnetic field intensity is key to understanding the past evolution of planets. However, magnetic field paleointensity data of terrestrial planets such as Mars and Moon have been poorly obtained because of the lack of appropriate rock samples. To address the problem, we focus on shock remanent magnetization (SRM). There are many impact craters on surface of the terrestrial planets, and the magnetic field originated from the SRM of planetary crust can be measured by spacecraft magnetometer. The magnetic field paleointensity could be estimated using the magnetic field data observed over the impact craters. In order to estimate the magnetic field paleointensity from the observed magnetic field data, it is crucial to know a structure of the SRM, while the structure remains unclear due to the difficulty in experimental techniques. In this study, to reveal the structure of SRM, the SRM imparted sample was cut into a millimetre-sized cube and magnetic measurements were conducted for the cube samples. Basalt samples with cylindrical form and granite parallelepiped samples were used as a target. The basalt samples were subjected to alternating field demagnetization at 80 mT before the SRM acquisition experiments, while the granite samples with natural remanent magnetization were used for the SRM acquisition experiments. The two-stage light gas gun at the Institute of Space and Astronautical Science (ISAS) of Japan Aerospace and Exploration Agency (JAXA) was used for the SRM acquisition experiments. A magnetically shielded cylinder of 32 cm in diameter and 100 cm in length was set in a vacuum experimental chamber of the two-stage light gas gun. The magnetically shielded cylinder was constructed with three μ-metal layers, and the residual field in the cylinder was <0.3 μT. A solenoid coil of 26 cm in diameter was set in the magnetically shielded cylinder. Target sample was placed at the center of the solenoid coil. The applied field was set to be 0–100 μT. An aluminum sphere of 2 mm in diameter was used as the projectile. A nylon slit sabot was used to accelerate the projectile. The impact velocity was ~7 km/s, and the impact angle was fixed at 90° from the horizontal. After the SRM acquisition experiment, the target samples were cut into the cube using a small rock cutter. The stepwise demagnetization and remanence measurement of the cube samples were conducted with the superconducting quantum interference device magnetometer. Systematic changes in the remanence intensity and stability with increasing the distance from impact point were observed for the basalt sample. Now we plan to conduct magnetic measurements of the granite samples. In this talk, we will discuss the structure of SRM based on the results of magnetic measurements of basalt and granite samples.

Keywords: shock remanence, magnetic anomaly, planetary magnetism

©2020. Japan Geoscience Union. All Right Reserved.

[J] Poster | S (Solid Earth Sciences)：S-GL Geology

[S-GL34] Geochronology and Isotope Geology

convener:Takahiro Tagami(Graduate School of Science, Kyoto University), Yuji Sano(Division of Ocean and Earth Systems, Atmosphere and Ocean Research Institute, University of Tokyo)

Reliable reconstruction of geohistory is of primary importance to better envision the present and future of the Earth. Geochronology and isotope geology play major roles in the reconstruction. This session offers an opportunity to present the results of fundamental studies, including the developments / improvements of analytical methods and age calibration, as well as applications to the Earth and planetary materials. We particularly focus on: (1) radiometric dating, bio-stratigraphy, magneto-stratigraphy and stable isotopic time series that provide the age information, (2) radioisotopes and stable isotopes widely employed for analyzing the Earth and planetary systems and (3) hypothesis and numerical modeling that utilize / assimilate the age and isotopic data. We also welcome contributions that integrate a variety of relevant disciplines.

[SGL34-P01] Cellulose oxygen isotopic time series of teak disks collected from Java, Indonesia

★Invited Papers

*Yumiko Watanabe[1], Ryo Hisamochi[1], Masaki Sano[2], Takeshi Nakatsuka[3], Takahiro Tagami[1] (1.Department of Earth and Planetary Scineces, Kyoto University, 2.Faculty of Human Sciences, Waseda University, 3.Nagoya University)

[SGL34-P02] Cellulose oxygen isotopic time series of teak disks collected from Bago Mountains, Myanmar

Wataru Ohmuro[1], *Yumiko Watanabe[1], Zhen Li[2], Takeshi Nakatsuka[2] (1.Department of Earth and Planetary Scineces, Kyoto University, 2.Nagoya University)

[SGL34-P03] Stable Sr isotopes of saline water from non-volcanic Arima-type spring in Japan: Sr isotope fractionation during fluid generation from subducting carbonate?

*Tomomi Kani[1], Keiji Misawa[2], Noritoshi Morikawa[3], Kohei Kazahaya[3], Fumitake Kusuhara[4], Yasutaka Terakado[5] (1.Department of Earth and Environmental Sciences, Kumamoto University, 2.National Institute of Polar Research , 3.Geological Survey of Japan, National Institute of Advanced Industrial Science and Technology (AIST) , 4.Central Research Institute of Electric Power Industry , 5.Graduate School of Human Development and Environment, Kobe University)

[SGL34-P05] Zircon U-Pb age and stratigraphy of some Quaternary tephras around Kagoshima Bay

*Hisatoshi Ito[1], Shimpei Uesawa[1], Futoshi Nanayama[2], Hiroomi Nakazato[3] (1.Central Research Institute of Electric Power Industry, 2.National Institute of Advanced Industrial Science and Technology, 3.National Agriculture and Food Research Organization)

[SGL34-P07] Formation ages of the Konosuyama Formation and the Shinobu Diorite and the provenance of the Douge Formation in the Noto Peninsula, central Japan

*Xianyu Chen[1], Hiroto Ota[1], Koh Kubomi[1], Mitsuhiro Nagata[1], Koshi Yamamoto[2], Shigeru Otoh[3] (1.Graduate School of Science and Engineering, University of Toyama, 2.Graduate School of Department of Earth and Environmental Studies,Nagoya Unversity, 3.Academic Assembly, Faculty of Sutainable Design, University of Toyama)

[SGL34-P08] Late Mesozoic magmatism and associated porphyry Mo mineralization in the the Xiong'ershan area, East Qinling Orogen, China

*Xinkai Hu[1,2], Toshiaki Tsunogae[1] (1.Graduate School of Life and Environmental Sciences, University of Tsukuba, 2.School of Earth Sciences and Resources, China University of Geosciences Beijing)

[SGL34-P09] Paleozoic magmatism in the Alxa Block and its geological implication: constraints from geochronology and geochemistry of the Devonian plutons in the Bayanwulashan area

*Kaiyuan Xu[1,2], Changqing Yin[1,2], Jian Zhang[1,2], Jiahui Qian[1,2], JIngna Liu[1,2] (1.School of Earth Sciences and Engineering, Sun Yat-sen University, Guangzhou 510275, P.R. China, 2.Southern Marine Science and Engineering Guangdong Laboratory (Zhuhai), Zhuhai 519082, P.R. China)

[SGL34-P10] Constraining timing of thrust activity within the Nobeoka Thrust, SW Japan

*Horst Zwingmann[1], Masakazu Niwa[2], Asuka Yamaguchi[3], Koichiro Fujimoto[4] (1.Kyoto University, 2.Tono Geoscience Center, JAEA, 3.Atmosphere and Ocean Research Institute, Tokyo University, 4.Faculty of Education, Tokyo Gakugei University)

[SGL34-P11] Observation result of 3.1Ga Cleaverville Banded Iron Formation in the Coastal Pilbara Craton, Western Australia.

*Kohei Ishikawa[1], Shoichi Kiyokawa[1] (1.Kyushu Univ.)

Cellulose oxygen isotopic time series of teak disks collected from Java, Indonesia

*Yumiko Watanabe[1], Ryo Hisamochi[1], Masaki Sano[2], Takeshi Nakatsuka[3], Takahiro Tagami[1]

1. Department of Earth and Planetary Scineces, Kyoto University, 2. Faculty of Human Sciences, Waseda University, 3. Nagoya University

Tree rings are useful to reconstruct terrestrial paleoclimate because of their precise dating and high time resolution. In the tropics, there are few dendroclimatological studies because it is difficult to collect tree samples with annual rings. In Indonesia, the master chronology of tree ring has been constructed since the study of Berlage (1931) and perfomed correlation analyses with precipitation data (e.g., D'Arrigo et al., 1994). Moreover, previous studies of Poussart et al. (2004) and Schollaen et al. (2013) measured oxygen isotope ratios of Javanese teak, suggesting that it could be an effective proxy of precipitation. However, these previous studies conducted at limited area of Java Island, and thus the spatial coherency still remains unknown. In this study, we measured cellulose oxygen isotopic compositions of ten teak disks collected at four sites in Java, and verified the synchronicity of the time series variations.

Keywords: isotope, oxygen, tree ring, cellulose, Indonesia

©2020. Japan Geoscience Union. All Right Reserved.

Cellulose oxygen isotopic time series of teak disks collected from Bago Mountains, Myanmar

Wataru Ohmuro[1], *Yumiko Watanabe[1], Zhen Li[2], Takeshi Nakatsuka[2]

1. Department of Earth and Planetary Scineces, Kyoto University, 2. Nagoya University

Myanmar is a region that is strongly affected by the Asian monsoon, and past climate information is very important to understand its mid- to long-term fluctuations. However, in Myanmar, there are a few past meteorological data due to its historical background, so an alternative indicator of paleoclimate reconstruction is necessary to obtain long-term weather information. In this study, I focused on the annual ring width and the cellulose oxygen isotopic composition ($\delta^{18}O$) of teak annual rings collected from Bago Mountains in central Myanmar, analyzed the correlation between them and the amount of precipitation, and examined whether they could be an index of paleoclimate restoration.

The samples used were six discs of teak from Bago Mountains with 95-97 tree rings, cut between 2001 and 2003.

First, focusing on the annual ring width, a significant positive correlation was obtained between the annual ring width and the rainy season precipitation in three samples. This is consistent with the results of Pumijumnong (2012), that reported the correlation between teak rings and rainy season precipitation in northwestern Thailand and D 'Arrigo et al. (1994), that reported the same using teak ring widths in Indonesia. This suggests that teak annual ring width well reflects precipitation in rainy season and might be a useful tool for rainfall reconstruction in central Myanmar.

On the other hand, few samples showed a significant correlation between $\delta^{18}O$ and rainy season rainfall. This is a different result from previous studies in Southeast Asia, such as Buajan et al. (2016), that reported a negative correlation between teak-ring $\delta^{18}O$ and rainy season precipitation in northwestern Thailand, or Schollaen et al. (2013), which showed a negative correlation between the two in Indonesia. This might be caused by the difference of the origin of rain fall in rainy season. This means that the origin of precipitation in Bago Mountains changes from Bay of Bengal to South China Sea during the rainy season. In other words, the isotopic composition of precipitation itself is high in the early rainy season and low in the late rainy season due to the different origin of the rainwater and the different isotope fractionation in the process of coming to Bago Mountains. Since the isotopic composition of precipitation has a seasonal change, the annual ring $\delta^{18}O$ response to the rainfall amount is dull in Bago Mountains. Then, for some annual rings, I subdivided one annual ring to six or twelve parts and measured the variation of $\delta^{18}O$ within the same year. As a result, the variation between individuals was matched better, and the tendency was different every year. These suggest that it is difficult to use the $\delta^{18}O$ of the teak annual tree-ring in Bago Mountains to duplicate the amount of annual rainfall itself, but it has the potential to explain the fluctuation of the annual rainfall or the relationship of the seasonal winds that come from different part by subdividing the annual rings.

Keywords: isotope, oxygen, tree ring, cellulose, Myanmar

©2020. Japan Geoscience Union. All Right Reserved.

Stable Sr isotopes of saline water from non-volcanic Arima-type spring in Japan: Sr isotope fractionation during fluid generation from subducting carbonate?

*Tomomi Kani[1], Keiji Misawa[2], Noritoshi Morikawa[3], Kohei Kazahaya[3], Fumitake Kusuhara[4], Yasutaka Terakado[5]

1. Department of Earth and Environmental Sciences, Kumamoto University, 2. National Institute of Polar Research , 3. Geological Survey of Japan, National Institute of Advanced Industrial Science and Technology (AIST) , 4. Central Research Institute of Electric Power Industry , 5. Graduate School of Human Development and Environment, Kobe University

Stable Sr isotope values (δ^{88}Sr) of saline water, which were sampled from Arima-type springs in Japan, were analyzed by TRITON TIMS with correction of isotope fractionation during mass spectrometry with ^{87}Sr-^{84}Sr double spike. The saline water samples were collected from Arima hot spring in Hyogo prefecture and Kashio mineral spring in Nagano prefecture. The Arima-type saline water possibly originated deep fluids derived from subducting slab rather than palaeoseawater buried in an aquifer, based on oxygen, hydrogen, helium and carbon isotopic compositions. The new obtained δ^{88}Sr values (0.11) of the saline water samples from Arima hot spring in this work are lower than those of surrounding Rokko granitoids and tuff (0.2) and the Phanerozoic mean of carbonates (0.16). The obtained δ^{88}Sr value (0.13) of the Kashio saline water is low as much as that of Arima saline water. The low δ^{88}Sr of Arima-type saline water indicate Sr isotope fractionation during fluid extraction from subducting oceanic plate with marine carbonates.

Keywords: slab-fluid, subduction, geofluid, water

©2020. Japan Geoscience Union. All Right Reserved.

Zircon U-Pb age and stratigraphy of some Quaternary tephras around Kagoshima Bay

*Hisatoshi Ito[1], Shimpei Uesawa[1], Futoshi Nanayama[2], Hiroomi Nakazato[3]

1. Central Research Institute of Electric Power Industry, 2. National Institute of Advanced Industrial Science and Technology, 3. National Agriculture and Food Research Organization

It is important to investigate eruption ages of Quaternary widespread tephras originated from in and around Kagoshima Bay, because some of these tephras are assumed to have reached as far as Boso Peninsula (~1,000 km away from the source), and therefore they are essential to establish tephrostratigraphy in Japan and also to evaluate future mega disaster caused by super eruptions. Here we examined and obtained zircon U-Pb ages on some tephras at well-exposed outcrops near Yamada River, one of tributaries of Beppu River, that runs into Kagoshima Bay. We also measured zircon U-Pb ages on some other tephras of regional importance in order to correlate these tephras. The U-Pb data were obtained from 2017 to 2019, and were calculated based on Sakata (2018), which tends to yield relatively older ages for tephras <0.5 Ma, compared to Ito (2014).

We observed Komiyaji pyroclastic flow deposits (pfl) and Oda pfls I and II, in ascending order at the outcrops near Yamada River (Yamada Outcrop). Based on the fact that these tephras are covered by the ~0.34 Ma Kakuto pfl and some biostratigraphic evidence, their eruption ages were assumed to be middle Pleistocene (Kagawa and Otsuka, 2000). We obtained zircon U-Pb ages of 0.67±0.34 Ma (n=5, MSWD=2.8) for Komiyaji pfl and 0.71±0.12 Ma (n=5, MSWD=0.86), 0.61±0.11 Ma (n=8, MSWD=3.2) and 0.40±0.17 Ma (n=6, MSWD=3.6) at three localities of Oda pfls I and II. We also obtained ages of 0.57± 0.09 Ma (n=9, MSWD=1.3) for Nabekura pfl and 0.48±0.14 Ma (n=8, MSWD=2.9) for Hegawa pfl, both of which crop out near the Yamada Outcrop. A zircon U-Pb age of 0.65±0.12 Ma (n=12, MSWD=2.1) was also obtained from Kakuto pfl that cover all the tephras mentioned above.

Therefore, our results indicate that the three lower-most tephras (Komiyaji, Nabekura and Hegawa plfs) were erupted at 0.5–0.6 Ma, which is consistent with the stratigraphy. The 0.4–0.7 Ma Oda pfls I and II and the 0.65 Ma Kakuto pfl ages are older than the stratigraphy, which may indicate that these are not eruption ages but the time when magma crystallized zircons or the tephras may have incorporated older zircons prior to final deposition. We plan to investigate zircon morphology and composition to further examine magmatic conditions that erupted these tephras.

References: Ito, 2014, J. Volcanol. Geotherm. Res., 289, 210–223; Kagawa and Otsuka, 2000, J. Geol. Soc. Japan, 106, 762–782; Sakata, 2018, Geochem. J. 52, 281–286.

Keywords: Quaternary, tephra, zircon, U-Pb dating, Kagoshima

©2020. Japan Geoscience Union. All Right Reserved.

Formation ages of the Konosuyama Formation and the Shinobu Diorite and the provenance of the Douge Formation in the Noto Peninsula, central Japan

*Xianyu Chen[1], Hiroto Ota[1], Koh Kubomi[1], Mitsuhiro Nagata[1], Koshi Yamamoto[2], Shigeru Otoh[3]

1. Graduate School of Science and Engineering, University of Toyama, 2. Graduate School of Department of Earth and Environmental Studies,Nagoya Unversity, 3. Academic Assembly, Faculty of Sutainable Design, University of Toyama

Introduction

The Oligocene or younger volcanic and sedimentary rocks widely occur in the Noto Peninsula. This study aims to explore the formation ages of the Konosuyama Formation and the Shinobu Diorite and the provenance of the Douge Formation in the Noto Peninsula, central Japan. We performed the U-Pb dating of igneous and detrital zircons from these and related geological units.

Geologic setting

In the north of the Noto Peninsula, the Oligocene Konosuyama Formation, consisting mainly of andesite, is widely distributed, and the Shinobu Diorite intrudes into it (Kano, 2018). In the northwest of the Noto Peninsula, on the other hand, the Besshodake Andesite (the former Anamizu Formation) and the Nawamata and Douge formations (e.g. Ozaki, 2010) cover the constituent rocks of the Hida Belt. The Douge Formation unconformably covers the Nawamata Formation and consists mainly of conglomerate, with minor sandstones, mudstones, and dacite tuffs. The conglomerate contains round pebbles to cobbles of mainly andesite, rhyolite, tuff, and granite.

Method

We collected lava of the Konosuyama Formation, the Shinobu Diorite, and a granite cobble and sandstone of the Douge Formation. Moreover, we collected the Shirakawa Granite cutting the Nohi Rhyolite in the Shirakawa Village of Gifu Prefecture. We extracted zircons from these rock samples and conducted U-Pb dating with the LA-ICPMS equipped in the Graduate School of Environmental Studies of Nagoya University. We adopted concordant data with the error ellipse (2σ) on the concordia diagram (a $^{206}Pb/^{238}U$–$^{207}Pb/^{235}U$ plot) intersecting the concordia curve.

Results of the zircon U–Pb dating

The dating results are shown in the attached table.

Discussion

The weighted mean age of the youngest age cluster of the Konosuyama Formation and the Shinobu Diorite was 32.8 ±2.3 Ma and 28.09 ±0.67 Ma, respectively. Hence, the andesite of the Konosuyama Formation likely formed at about 33 Ma, and the Shinobu Diorite intruded into it at about 29 Ma.
Four zircon age clusters of 23 Ma, 59–74 Ma, 173–201 Ma, and 252–267 Ma were obtained from the sandstone sample of the Douge Formation, and the granite cobble from the same outcrop contained 181–206 Ma zircons. The age of this granite cobble is similar to that of the Hida Younger Granites (e.g., Takahashi et al., 2010).In addition, the formation age of the Hida Older Granites was about 266–229 Ma (Horie et al., 2010; Takahashi et al., 2018). Hence, it is likely that 173–201 Ma and 252–267 Ma zircons in the Douge sandstone are from the Hida Granites. The source of 23 Ma zircons in the Douge sandstone is probably the 22–23 Ma Moonstone Rhyolite (Ota et al., 2019; Yamada, 2019) to the south of the study

©2020. Japan Geoscience Union. All Right Reserved.

area. The source of the 59–74 Ma zircons from the Douge sandstone is most likely the Nohi and Futomiyama rhyolites of 66–72 Ma (Hoshi et al., 2016; Kaneko et al., 2019). Moreover, the 60–66 Ma Shirakawa Granite, which cuts the Nohi Rhyolite 100 km to the south of the study area, is a probable source of zircons in the Douge sandstone. In this way, the provenance of Douge sandstone may have covered the distribution areas of the Nohi Rhyolite, Fotomiyama Group, Shirakawa Granite, and Moonstone Rhyolite distributed in the Toyama and Gifu prefectures to the south.
On the other hand, we have not confirmed the zircon supply from the Bessyodake Andesite (K–Ar age of 15–17 Ma: Shibata et al., 1981) covered by the Douge Formation, the Konosuyama Formation, and the Shinobu Diorite, which are widely distributed to the east of the Douge Formation. This result is concordant with the northward paleocurrent direction in the Douge formation (Yoshioka et al.,1984).

Reference

Horie et al., 2018, *Precambrian Res.*, **183**, 145–157 / Hoshi et al., 2016, *35th IGC*, 1512 / Kaneko et al., 2019, *J. Geol. Soc. Japan*, **125**, 781–792 / Kano, 2018, *J. Geol. Soc. Japan*, **124**, 781–803 / Ota et al., 2019, *126th Annu. Meet. Geol. Soc. Japan, Abstr.*, 215 / Ozaki et al., 2010, *Digital Geosci. Map S-1*, Geol. Surv. Japan, AIST / Shibata et al., 1981, *J. Japan. Assoc. Mineral. Petrol. Econ. Geol.*, **76**, 248–252 / Takahashi et al., 2010, *Gondwana Res.*, **17**, 102–115 / Takahashi et al., 2018, *Isl. Arc*, **27**, e12220 / Yamada et al., 2019, *2019 JpGU,* SGL28-P01 / Yoshioka et al., 1984, *84th Annu. Meet. Geol. Soc. Japan, Abstr.*, 288.

Keywords: Miocene, Neogene, U–Pb dating, zircon, SW Japan

Geological unit	Rock type	YSG	YC2σ	dates				
Douge Formation	sandstone	22.9 ± 1.0 Ma		23 Ma	59–74 Ma	172–201Ma	252–267 Ma	
	granite pebble	180.5 ± 3.8 Ma	183.8 ± 0.6 Ma			180–206 Ma	222–226 Ma	464 Ma
Konosuyama Formation	andesite	27.7 ± 6.0 Ma	32.8 ± 2.3 Ma	28–35 Ma				
Shinobu Diorite	diorite	26.5 ± 2.4 Ma	28.09 ± 0.67 Ma	27–32 Ma				
Shirakawa Granite	granite	59.6 ± 3.9 Ma	62.97 ± 0.75 Ma		60–66 Ma			
compile data	plutonic					191–199 Ma	229–265 Ma	
	volcanic			22–23 Ma	66–72 Ma		258 Ma	

Table 1 The U–Pb zircon data in this study and the U–Pb zircon compile data of Neogene–Permian igneous rocks from the Hida Belt.(Horie et al.,2013;Horie et al.,2018; Kaneko et al.,2019; Ota et al.,2019; Takahashi et al.,2010; Takahashi et al.,2018; Takehara and Horie ,2019;Takeuchi et al.,2017; Yamada et al.,2019b; Zhao et al.,2013)

©2020. Japan Geoscience Union. All Right Reserved.

Late Mesozoic magmatism and associated porphyry Mo mineralization in the the Xiong'ershan area, East Qinling Orogen, China

*Xinkai Hu[1,2], Toshiaki Tsunogae[1]

1. Graduate School of Life and Environmental Sciences, University of Tsukuba, 2. School of Earth Sciences and Resources, China University of Geosciences Beijing

The Late Mesozoic granitoids representing prolonged magmatism during 160-108 Ma, are widely distributed in the East Qinling Orogen Belt (EQOB). Previous studies show that the Late Mesozoic molybdenum mineralization in the EQOB is spatially and temporally associated with the Late Mesozoic magmatism. Even so, the petrogenesis of the Late Mesozoic granitoids, magma sources remain debated. This study presents integrated whole-rock geochemistry, zircon U-Pb geochronology and Hf-O isotopes for Late Mesozoic ore-bearing granite porphyry stock (Leimengou granite porphyry) and ore-barren plutons (Haoping and Jinshanmiao plutons) in the Xiong’ershan area of the EQOB. The 130-127 Ma ore-barren granitoids are characterized by high-K subalkaline, metaluminous, and show negative correlations between Al_2O_3, MgO, TiO_2, MnO, CaO, FeO^T and P_2O_5 with SiO_2. However, the Leimengou granite porphyry yield a zircon U-Pb age of 130.9 ±0.4 Ma and is peraluminous, high-K alkaline and shoshonitic, and lacks distinctive linear correlation between major oxides with SiO_2 except Al_2O_3, K_2O and Na_2O. These granitoids are enriched in LREE over HREE with slightly negative europium anomalies. Most samples show enrichment of Rb, Ba, Th, U, K and Pb, and depletion of Nb, Ta, P and Ti, mostly overlapping the ranges of the Taihua Group. The Hf-O isotopic features of zircon from the Leimengou granite porphyry ($\delta\,^{18}O_{zircon}$ = 5.03‰ - 5.86‰, $\varepsilon\,Hf_{(t)}$ = -24.3 to -14.4) are markedly similar with the Haoping pluton ($\delta\,^{18}O_{zircon}$ = 5.17‰ - 5.61‰ and $\varepsilon\,Hf_{(t)}$ = -26.6 to -21.4). Zircon grains from the Jinshanmiao pluton have unique $\delta\,^{18}O_{zircon}$ ranging from 6.01‰ to 8.90‰ and $\varepsilon\,Hf_{(t)}$ from -15.6 to -12.2. We propose that Haoping pluton and Leimengou granite porphyry were derived from mixing of partial melts of the Taihua Group with mantle-derived material, whereas the Jinshanmiao pluton originated from a mixture of Xiong’er Group and mantle-derived material, with minor Taihua Group. The zircon grains from the Leimengou granite porphyry have significant higher Ce^{4+}/Ce^{3+} (mean 547) and δEu (mean 0.65) ratios than those in the ore-barren Haoping pluton (mean 207 and 0.54, Ce^{4+}/Ce^{3+} and δEu, respectively) and the Jinshanmiao pluton (mean 235 and 0.62, respectively). The main controlling factors for porphyry-type Mo mineralization are likely the oxygen fugacity (fO_2) of the magma and input of mantle-derived material in the Xiong'ershan area.

Keywords: Geochemistry, Zircon geochronology, Zircon Hf-O isotope, Late Mesozoic granitoid, East Qinling

©2020. Japan Geoscience Union. All Right Reserved.

Paleozoic magmatism in the Alxa Block and its geological implication: constraints from geochronology and geochemistry of the Devonian plutons in the Bayanwulashan area

*Kaiyuan Xu[1,2], Changqing Yin[1,2], Jian Zhang[1,2], Jiahui Qian[1,2], JIngna Liu[1,2]

1. School of Earth Sciences and Engineering, Sun Yat-sen University, Guangzhou 510275, P.R. China, 2. Southern Marine Science and Engineering Guangdong Laboratory (Zhuhai), Zhuhai 519082, P.R. China

The Alxa Block which surrounded by Tarim Craton (TC), Central Asian Orogenic Belt (CAOB), Qilianshan orogenic belt and Langshan-Bayanwulashan fault zone was long considered as a part of the North China Craton (NCC). However, in the past few years, some scientists considered the Alxa Block as an independent Archean block that did not aggregate into the NCC until Paleozoic. Clarifying multiple Paleozoic magmatic events during the development of the Paleo-Asian Ocean (PAO) in the Alxa Block will be a crucial scientific question in understanding the evolutionary history of the Alxa Block, which will also help to evaluate the relevance among the contemporaneous events in the NCC and Alxa Block. Bayanwulashan area, where both have Paleozoic plutons and Proterozoic basement rocks, locates in the most eastern of the Alxa Block. In our study, results of LA-ICPMS zircon U-Pb dating and whole-rock analysis have revealed an episode of Paleozoic magmatism (ca. 375 Ma) which is the first discovery of Late Devonian plutons in the Alxa Block. Basic plutons with low SiO_2 content (44.19–50.54 wt.%) have a low-temperature crystallization condition (715–796 ℃) and intermediate plutons with higher SiO_2 content (53.90–59.15 wt.%) indicate a higher-temperature crystallization condition (792–849 ℃). All ca. 375 Ma basic-intermediate plutons show arc affinities, indicating a southward subduction system along the northern margin of the Alxa Block. In-situ zircon Hf isotope analysis (ε Hf(t) ranges from -10.3 to -2.9) which was conducted by LA-MC-ICPMS shows that these plutons might share the same source of PAO-related magmatism during Paleozoic. The whole-rock Sr isotope (initial $^{87}Sr/^{86}Sr$ is 0.706374-0.707637) and Nd isotope (initial $^{143}Nd/^{144}Nd$ is 0.511690-0.511783) suggest a mixing source between the lithospheric mantle and lower continental crust. Combining previously published data and our study, we suggest that a large Phanerozoic magmatic arc bordering the northern margin of NCC was westerly extended to the Alxa Block, which might have been involved in the same southward subduction system along the southern margin of PAO lithosphere since the early Paleozoic. Besides, we also believe that the Alxa Block has had the same Proterozoic-Archean basement with the northern margin of NCC and has undergone similar evolutionary history.

Keywords: North China Craton, Alxa Block, U-Pb zircon dating, in-situ Hf isotope, Sr-Nd isotope, Geochemistry

©2020. Japan Geoscience Union. All Right Reserved.

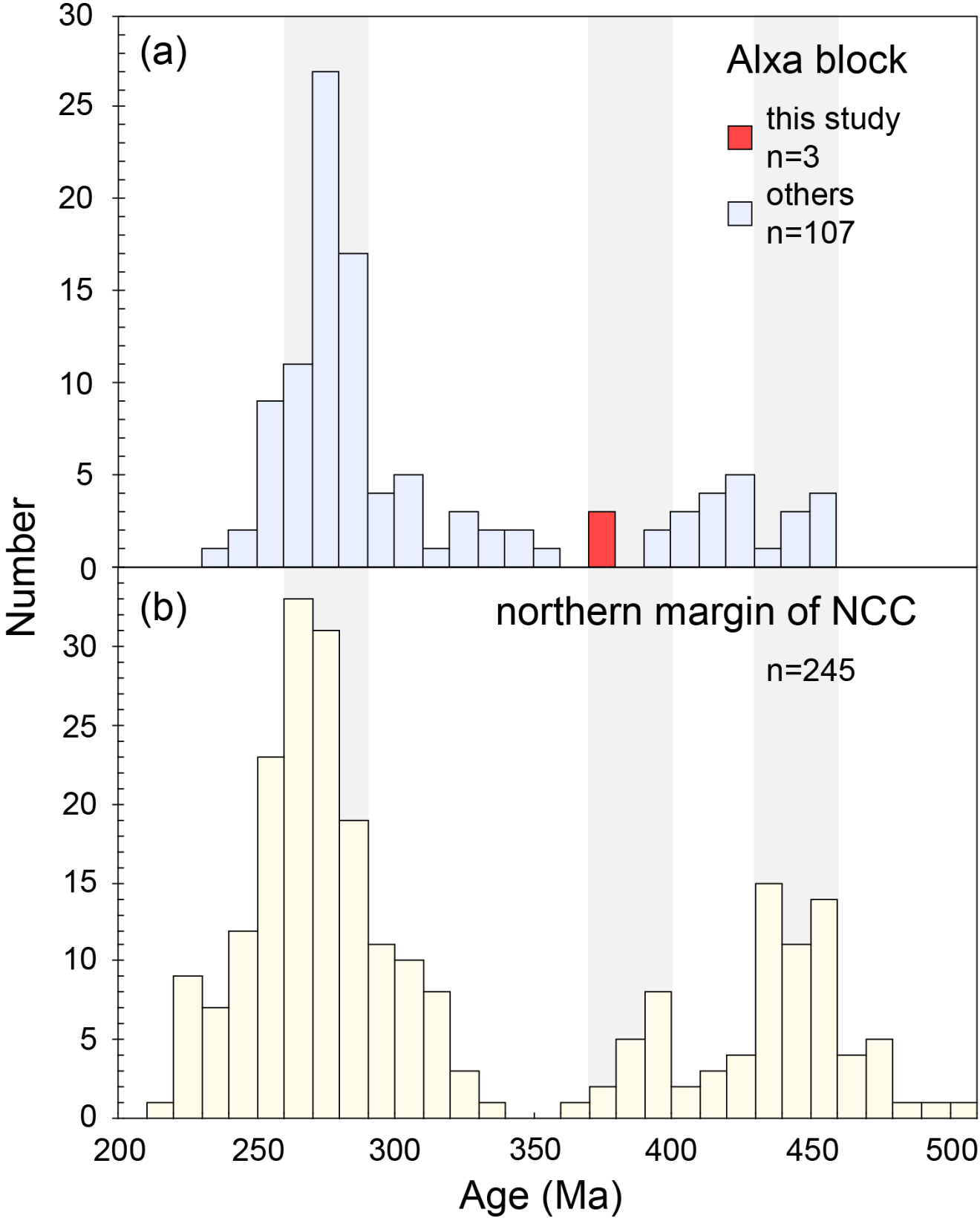

©2020. Japan Geoscience Union. All Right Reserved.

Constraining timing of thrust activity within the Nobeoka Thrust, SW Japan

*Horst Zwingmann[1], Masakazu Niwa[2], Asuka Yamaguchi[3], Koichiro Fujimoto[4]

1. Kyoto University, 2. Tono Geoscience Center, JAEA, 3. Atmosphere and Ocean Research Institute, Tokyo University, 4. Faculty of Education, Tokyo Gakugei University

Studies of the thermal, mechanical and hydrothermal effects of Nobeoka drilling core samples (NOBELL) indicate distinctive changes in the Illite crystallinity between the footwall, main fault zone and hanging wall (Fukuchi et al., 2014). Detailed illite crystallinity investigations of the core samples provide a unique framework to constrain timing of authigenic illite formation within an ancient tectonic boundary thrust system. This pilot study investigates timing of thrust formation by dating of authigenic illite (<2 micron fractions) separated from 2 fresh non- weathered fault core, 3 footwall and 2 hanging wall core samples from the Nobeoka drilling core collected over a depths range of 80 to 30 m below ground surface. The obtained K-Ar ages range from ~ 41 Ma (Paleogene-Eocene-Lutetian) to 28 Ma (Paleogene-Eocene-Chattian) and cover an age range of ~ 14 Ma. The <2 μm age data of the two main fault zone samples range from ~ 32 Ma (Paleogene-Eocene-Rupelian) to ~ 28 Ma (Paleogene-Eocene-Chattian) and will be discussed within the geological background of an ancient tectonic boundary thrust system.

This study was funded by METI, Japan as part of its R&D program supporting development of technology for geological disposal of HLW.

References

Fukuchi et al., 2014. Earth, Planets and Space 2014 66:116.

Keywords: Nobeoka thrust, K-Ar dating, authigenic illite

©2020. Japan Geoscience Union. All Right Reserved.

Observation result of 3.1Ga Cleaverville Banded Iron Formation in the Coastal Pilbara Craton, Western Australia.

*Kohei Ishikawa[1], Shoichi Kiyokawa[1]

1. Kyushu Univ.

The Cleaverville Formation was well identified as Mesoarchean banded iron formation (CL BIF) in the coastal Pilbara terrane in Western Australia (eg. Kiyokawa et al., 2019). The CL BIF was a key formation to know correlation with east and west sedimentary sequence in Pilbara Craton (eg. Hickman, 2012). The CL BIF is also one of the best preserved iron formation before GOE event. Therefore, CL BIF is deposited before oxygen is produced in the atmosphere, so the cause of precipitation of iron is discussed. However, the cause is not clear(Holland et al. 1973). Therefore, CL BIF is one of key formation to estimate 3.1Ga environment. Moreover, we collected fresh core samples from DXCL drilling project in 2007 and 2012 (four cores: DX, CL1, CL2 and CL3). Especially CL 3 core contains flesh BIF and black shale sequence. In this study, we show some result of very detail observed samples of CL3 core, which contains CL BIF, and form very detail stratigraphy, lithological characteristics and some geochemical result. We did core surface description, thin section observation by microscope, and SEM and chemical analysis by EDS, XRD.

Thickness of the Cleaverville Formation is about 370m, and it is composed of the Black Shale Member (about 150m) and BIF Member (about 220m) to top. We collected 210m long core from 60 m below surface. The Black Shale Member contains organic rich black shale with few cm thick volcanic very fine sandstone, which contains cross lamination. The BIF Member composed of siderite/greenish shale unit (SG unit), magnetite/greenish shale unit (MG unit) and siderite/black shale unit (SB unit), and overlay SG unit1, MG unit1, SG unit2, MG unit2, SG unit3 and SB unit.

The SG unit form stratify laminated siderite/chert layer and massive greenish shale layer (about 10cm thickness). Laminated siderite/chert layer is composed clay lamination and white chert lamination alternately (1mm-1cm). Clay lamination is composed siderite corted quartz grain (10-30μm). However, the siderite doesn’ t have idiomorphic. White chert lamination formed fine quartz. Moreover, recristalized idiomorphic siderite is observed at the boundary of clay lamination and white chert lamination. The massive greenish shale is mainly composed siderite and chlorite, and have homogeneous structure.

The MG unit become stratify magnetite/chert layer and massive greenish layer alternately (about 10cm thickness). Moreover, stratify magnetite layers become magnetite lamination and quartz lamination alternately (1mm-1cm). Magnetite lamination is formed idiomorphic cubic magnetites. The idiomorphic magnetite crystals formed only clay layers of siderite/chert layer of SG unit. Quartz layer and the massive greenish shale are similar to that of SG unit.

The SB unit become stratify siderite/chert layer and black shale (about 10cm thickness). There is wave shape organic carbon rich lamination in this sequence.

Therefore, MG unit is made by replacing siderite of clay lamination of SG unit with magnetite. Moreover, the SB unit might be preserved original sedimentary structure to form BIF sequence.

Reference

Formation and a post-accretion pull-apart system in the Cleaverville area, coastal Pilbara Terrane, Pilbara,

©2020. Japan Geoscience Union. All Right Reserved.

Western Australia. Island Arc, Volume 28, Issue 6, 1-23.

Hickman (2012) Review of the Pilbara Craton and Fortescue Basin, Western Australia: crustal Evolution providing environments for early life. Island Arc, volume 21, issue 1, 1-31

Holland (1973) The Oceans; A Possible Source of Iron in Iron-Formations. Economic Geology, Volume 68, Issue 7, p.1169-1172

Keywords: Cleaverville Formation, Banded Iron Formation, siderite

©2020. Japan Geoscience Union. All Right Reserved.

[J] Poster | S (Solid Earth Sciences)：S-VC Volcanology

[S-VC44] Hydrothermal systems of volcanoes

convener:Yasuhiro Fujimitsu(Department of Earth Resources Engineering, Faculty of Engineering, Kyushu University), Wataru Kanda(Volcanic Fluid Research Center, School of Science, Tokyo Institute of Technology), Takeshi Ohba(Department of chemistry, School of Science, Tokia University)

There is a diversity of hydrothermal systems between magmas and the ground surface in various geoscientific environments. Understanding of the hydrothermal systems contributes to understanding of the earth systems, and is essential for utilization of geothermal energy and prediction of volcanic eruption. In this session, we will discuss the topics on subsurface structures and heat and fluid flows of "hydrothermal systems of volcanoes" from the perspectives of geophysics, geochemistry, geology and geothermal reservoir engineering. Any research approaches, theoretical, observational and experimental, are welcome.

[SVC44-P01] Geochemical study of High-T hydrothermal fluid and chimney obtained from Tarama Hydrothermal Vent Field in southern Okinawa Trough

*Toshiro Yamanaka[1], Eri Yokota[1], Kei Okamura[2], Takuro Noguchi[2], Tomohiro Toki[3], Urumu Tsunogai[4], Yuji Onishi[5], Hiroko Makita[1] (1.Tokyo University of Marine Science and Technology, 2.Kochi University, 3.University of Ryukyus, 4.Nagoya University, 5.Kyoto University)

[SVC44-P02] Water chemistry of fluid supplied from subaqueous fumaroles of Yugama crater lake, Kusatsu-Shirane volcano, inferred from geochemical heterogeneities of lake water

*Leona Suzuki[1], Akihiko Terada[1], Muga Yaguchi[2], Masanori Takahashi[1], Takeshi Ohba[3] (1.Tokyo Institute of Technology, 2.Meteorological Research Institute,JMA, 3.Department of chemistry,School of Science,Tokai University)

[SVC44-P03] Preliminary resistivity structure model around Kusatsu-Shirane Volcano revealed by broadband Magnetotellurics

*Yasuo Matsunaga[1], Wataru Kanda[2], Shinichi Takakura[3], Takao Koyama[4], Tatsuji Nishizawa[2] (1.Department of Earth and Planetary Sciences, School of Science, Tokyo Institute of Technology, 2.Volcanic Fluid Research Center, School of Science, Tokyo Institute of Technology, 3.National Institute of Advanced Industrial Science and Technology, 4.Earthquake Research Institute, University of Tokyo)

[SVC44-P04] Geophysical implication of the high Vp/Vs zone at depth of approximately 3.6 km obtained by the DAS measurements at the Medipolis geothermal filed

*Junzo Kasahara[1,2], Yoko Hasada[1,3], Haruyasu Kuzume[1] (1.ENAA, 2.Shizuoka University, 3.Daiwa Exploration and Consulting Co. Ltd.)

[SVC44-P05] Estimation of Temperature and Permeability Distribution in Kakkonda Geothemal Field, Iwate Prefecture, Japan, Using Neural Network

*Ugo Tsubasa[1], Kazuya Ishitsuka[2], Toru Mogi[4], Koichi Suzuki[4], Yosuke Kobayashi[3] (1.Department of Environmental Circulation Systems, Hokkaido University, 2.Kyoto University, 3.Muroran Institute of Technology, 4.Hokkaido University)

[SVC44-P06] Extraction of features of strata using borehole data of geothermal area by multivariate analysisExtraction of features of strata using borehole data of geothermal area by multivariate analysis

*Ojima Hiroki[1], Kazuya Ishitsuka[2], Toru Mogi[1], Kajiwara Tatsuya[3], Takeshi Sugimoto[3], Hiroshi Asanuma[4] (1.Hokkaido University, 2.Kyoto University, 3.Geothermal Engineering Co., Ltd., 4. Fukushima Renewable Energy Institute, AIST)

[SVC44-P07] Geochemical characteristics of silica scales precipitated from the geothermal water at the Onuma geothermal power plant.

*CHEN FEIYANG[1], Mayuko Fukuyama[1] (1.Akita University)

[SVC44-P08] Hydrothermal system around the Iwo-yama fumarolic field in Kuju volcano (Japan) inferred from a 3-D resistivity structure model

*Wataru Kanda[1], Mitsuru Utsugi[2], Hiroyuki Inoue[2], Shogo Komori[3], Tsuneomi Kagiyama[4] (1.Volcanic Fluid Research Center, School of Science, Tokyo Institute of Technology, 2.Aso Volcanological Laboratory, Graduate School of Science, Kyoto University, 3.National Institute of Advanced Industrial Science and Technology (AIST), 4.Aso Geopark Promotion Council)

[SVC44-P09] Gravity changes inferred from hydrothermal simulation before and after the 1995 eruption in Kuju volcano, Oita prefecture

*Jun Nishijima[1], Yoshiyuki Mizusawa[2], Yasuhiro Fujimitsu[1] (1.Department of Earth Resources Engineering, Faculty of Engineering, Kyushu University, 2.Department of Earth Resources Engineering, Graduate School of Engineering, Kyushu University)

[SVC44-P10] **Updating the conceptual model of Tendaho geothermal field, Afar Region, Ethiopia**

*belete ashenafi fekadu, Yasuhiro Fujimitsu, Jun Nishijima, Mitsuo Matsumoto

Geochemical study of High-T hydrothermal fluid and chimney obtained from Tarama Hydrothermal Vent Field in southern Okinawa Trough

*Toshiro Yamanaka[1], Eri Yokota[1], Kei Okamura[2], Takuro Noguchi[2], Tomohiro Toki[3], Urumu Tsunogai[4], Yuji Onishi[5], Hiroko Makita[1]

1. Tokyo University of Marine Science and Technology, 2. Kochi University, 3. University of Ryukyus, 4. Nagoya University, 5. Kyoto University

In 2017, active hydrothermal venting of over 300-deg. fluid was found at 1840 m deep seafloor on the slope of Tarama Knoll in Southern Okinawa Trough during dive survey of DSV/Shinkai 6500. The venting site involved with hydrothermal chimneys was named YZ site. On this knoll warm shimmering site (about 20-deg. higher than the ambient seawater), named Fox Site, involved with sediments rich in iron oxide was found near the summit in 2009, but high-T venting site had not been identified then. This knoll is located slightly south from the main rifting zone of Southern Okinawa Trough and belonging to a volcanic chain of Ishigaki seamounts. During the dive surveys in 2017 hydrothermal chimney fragments and venting fluids were collected and provided for geochemical study.
Chimney fragment samples were obtained from active chimneys by the manipulators of DSV. The samples were observed and analyzed using the microscope, XRD, EPMA. Those samples were classified into three types; (1) arsenic sulfide-rich type, (2) anhydrite-rich type, and (3) metal sulfide-rich type. The mineral composition of each sample was similar to the chimney mineral composition reported from multiple hydrothermal systems in the Okinawa Trough (e.g., Izena Cauldron, Daiyon-Yonaguni Knoll, Hatoma Knoll).
Chemical and isotopic compositions of the sampled hydrothermal fluids and pore fluids from the both sites were measured. Those results indicate significant contribution of sedimentary organic matter, although Tarama Knoll is mainly composed volcaniclastics of felsic rocks. It also suggests that the high-T fluid venting from YZ site has no significant difference in the redox state (oxygen and sulfur fugacities) and the isotopic compositions of methane are comparable with those of other hydrothermal fluids occurring in the Okinawa Trough. In addition, the estimated endmember fluid compositions of each site are different, suggesting that those fluids are supplied from individual hydrothermal reservoirs.

Keywords: Seafloor hydrothermal activity, Tarama Knoll, Southern Okinawa Trough

©2020. Japan Geoscience Union. All Right Reserved.

Water chemistry of fluid supplied from subaqueous fumaroles of Yugama crater lake, Kusatsu-Shirane volcano, inferred from geochemical heterogeneities of lake water

*Leona Suzuki[1], Akihiko Terada[1], Muga Yaguchi[2], Masanori Takahashi[1], Takeshi Ohba[3]

1. Tokyo Institute of Technology, 2. Meteorological Research Institute,JMA, 3. Department of chemistry,School of Science,Tokai University

Yugama crater lake at Kusatsu-Shirane volcano is classified as a high-activity crater lake with a diameter of 200 - 300 m. Water temperatures are 10 –15 degrees Celsius higher than the ambient air temperature because of fluid emissions from subaqueous fumaroles on the lake floor at a depth of 30 m. The lake water has a pH of around 1.0 and contains high concentrations of Cl and SO_4 ions, which show marked changes in response to volcanic activity. Therefore, regular sampling of lake water by hand has been performed at the shore of Yugama crater lake for 50 years, providing valuable data including early warning of an eruption. However, geochemical properties of hydrothermal fluid emitted from subaqueous fumaroles is altered because of mixing with existing lake water and diluted by precipitation input. Surface evaporation cause kinetic fractionation of water stable isotope rate as well as condensation of chemical concentration including Cl and SO_4. To evaluate water chemistry of fluid emitting from subaqueous fumaroles around the center of Yugama crater lake, we have sampled lake water from various depth around the subaqueous fumaroles by a drone (unmanned aircraft system). Our drone (DJI MATRICE 600 PRO) with a winch enables to descend sampling bottles from a drone to the lake surface, without descending a drone itself to lake surface, meaning reduction of the risk of a loss of radio communications between the drone and the operator at a site due to topographic effects. Remote water sampling using a drone have been repeatedly performed from a site located at 1 km southeast from the center of Yugama crater lake in 2019. Isotope compositions of water differ from that of water sampled at the lake shore, while temperature recorded by thermistor attached to a sampling bottle is only 1-2 degrees higher than that of ambient lake water. Our numerical simulation, which takes into account isotope fractionation during surface evaporation, precipitation input and seepage through the lake bottom, indicates the relation between water stable isotope composition of fluid emitted from subaqueous and that of lake water sampled at the shore. Comparing numerical simulation and drone observations, we found that water stable isotope sampled by a drone is consistent with numerical evaluation. Data on temporal changes in lake water chemistry are useful for identifying and predicting volcanic activity. However, it takes enough time to detect temporal changes in lake water chemistry due to large volume of lake relative to mass flux of subaqueous fumaroles. In the case of Yugama crater lake, the residence time is over 1 year indicated by numerical simulation. Therefore, water sampling from subaqueous fumaroles by a drone is useful to evaluate temporal changes in volcanic activity such as changes in hydrothermal reservoir supplying hot water to crater lake.

Keywords: Drone, Unmanned aircraft system, Kusatsu-Shirane volcano, Crater lake, Water stable isotope ratio, Volcano monitoring

©2020. Japan Geoscience Union. All Right Reserved.

Preliminary resistivity structure model around Kusatsu-Shirane Volcano revealed by broadband Magnetotellurics

*Yasuo Matsunaga[1], Wataru Kanda[2], Shinichi Takakura[3], Takao Koyama[4], Tatsuji Nishizawa[2]

1. Department of Earth and Planetary Sciences, School of Science, Tokyo Institute of Technology, 2. Volcanic Fluid Research Center, School of Science, Tokyo Institute of Technology, 3. National Institute of Advanced Industrial Science and Technology, 4. Earthquake Research Institute, University of Tokyo

Kusatsu-Shirane Volcano (KSV) is the active volcano known for its significant hydrothermal activity and producing phreatic eruptions in recent years. A number of geochemical and geophysical studies, conducted around the present active eruption center (Yugama), have been revealed the shallow hydrothermal system mainly around the crater. By geological studies, there were also frequent magmatic eruptions at Mt. Motoshirane, a different pyroclastic cone from that which hosts Yugama, until 1500 years ago. Therefore, it is expected that the magma produced at that time has not yet cooled and solidified. However, the positional information of a magma chamber is still unknown because of lack of deep structural information. Knowing the subsurface structure such as the spatial distribution of the magma-hydrothermal system is essential to discuss the present volcanic activity and the future eruption risk.

As a first step to reveal the whole image of the magma-hydrothermal system of KSV, broadband magnetotelluric (MT) observations centered on Mt. Motoshirane were conducted in 2015 and 2016 (Matsunaga et al., 2020). The 3-D electrical resistivity structure model revealed an extensive low-resistivity layer which was interpreted as a hydrothermal reservoir supplying fluids to the active crater at depths of 1–3 km beneath the summit area. However, no structural features suggestive of the presence of magma have been found beneath this layer. This is because the resolution of the structure deeper than 5 km was not sufficient.

In 2019, we conducted new MT observations covering the entire edifice of KSV. By expanding the observation area to a wider range, it is expected that a more reliable deep resistivity structure will be obtained. In the presentation, we are going to present an improved 3-D resistivity structure of KSV inferred using both new and old MT data, and to discuss the spatial distribution of the magma-hydrothermal system.

Keywords: Kusatsu-Shirane Volcano, magnetotellurics, resistivity structure

©2020. Japan Geoscience Union. All Right Reserved.

Geophysical implication of the high Vp/Vs zone at depth of approximately 3.6 km obtained by the DAS measurements at the Medipolis geothermal filed

*Junzo Kasahara[1,2], Yoko Hasada[1,3], Haruyasu Kuzume[1]

1. ENAA, 2. Shizuoka University, 3. Daiwa Exploration and Consulting Co. Ltd.

We conducted the second seismic and temperature measurement at the Medipolis geothermal field in 2019 using optical fiber system in the borehole down to depth of 1,545 m. Using distributed temperature sensors (DTSs), the temperature in the borehole was measured. The temperature was 272˚C and 155˚C at 918 m and 1,530 m, respectively. Offset VSP data were obtained using distributed acoustic sensors (DASs). We operated the MiniVib seismic source at five locations.

The analysis of the P-to-S conversions observed by surface seismometers at the same geothermal field in 2018 suggested the presence of *Vp/Vs*=3 zone at depth of approximately 4 km (Kasahara *et al*., 2020b) (see Figs.1 & 2). By forward modeling and the migration processing of DAS data in 2019, we obtained *Vp/Vs*=3 zones at depth of approximately 700–900 m, 1,300–1,600 m and 3,600 m (Kasahara *et al*. 2020a). Because ordinary silicate rocks show approximately *Vp/Vs*=1.75 (*e.g*. Hoshino *et al*., 2001), *Vp/Vs*=3 is quite different from other rocks. Vp/V=3 does not mean exact number, but it means that Vp/Vs is much higher than 1.75 which is that for ordinal silicate rocks.

We considered the geophysical meaning of *Vp/Vs* ~3. Using the numerous *Vp* and *Vs* measurements under high pressure and temperature by Kern (1978), Kern and Richter (1981), and Kern *et al*. (1997), most quartz-free rocks showed very small temperature dependence of *Vp* and *Vs*. Rocks including quartz minerals demonstrated large temperature dependence on *Vp* due to that phase change from α to β quartz (Kern and Richter, 1981). For quartz-free rocks, *Vp/Vs* remained constant to be approximately 1.75 and *Vp/Vs* ~3 was not explained. The serpentine rock exhibited large decreases in *Vs* and *Vp* at temperatures higher than 500 ˚C (Kern and Richter, 1981). The amount of velocity decrease at high temperature was explained by the dehydration of antigorite, which is a high temperature-type serpentine mineral. The decrease in *Vs* was larger than that in *Vp*. Water saturation in rocks might be a cause of high *Vp/Vs*. In addition, the *Vp/Vs* is related to the Poisson’s ratio. *Vp/Vs* = 3 corresponds to 0.467 for the Poisson’s ratio. Because the Poisson’s ratio of water is 0.5, the zone at a depth of approximately 3.6–4 km could be filled by water. Winlker and Nur (1985) obtained *Vp/Vs* > 2 for the Massillon sandstone if the sandstone was 100% saturated by water. Considering the above discussion, high *Vp/Vs* suggests the presence of high-water saturation zones at depth of approximately 4 km. Because the temperature at the depth of 914 m is 264 ˚C in the IK-4 well, the zone around 4 km depth might be close to the supercritical state if the zone is filled by low salinity water.

ACKNOWLEDGHMENTS
This article is based on the results obtained from a project commissioned by the New Energy and Industrial Technology Development Organization (NEDO).

References

Hoshino, K., Kato, T., Tanaka, S., Komata, A., Moriguchi, Y., Hattori, M., and Imamura, T., Handbook of mechanical properties of the Japanese rocks under high confining pressure, AIST Geological Survey of Japan Quick report No. 23, (2001).

©2020. Japan Geoscience Union. All Right Reserved.

Kasahara, J., Hasada, Y., Kuzume, H., Mikada, H., and Fujise, Y.: The second seismic study at the geothermal field in southern Kyushu, Japan using an optical fiber system and surface geophones, *Proceedings*, 45th Workshop on Geothermal Reservoir Engineering, Stanford University, Stanford, CA (2020a).

Kasahara, J., Hasada, Y., and Kuzume, Y.: Possibility of high Vp/Vs zone in the geothermal filed suggested by the P-to-S conversion, *Proceedings,* 45th Workshop on Geothermal Reservoir Engineering, Stanford University, Stanford, CA. (2020b).

Kern, H.: The effect of high temperature and high confining pressure on compressional wave velocities I quartz-bearing and quartz-free igneous and metamorphic rocks, Tectonophysics, **44**, (1978), 185-203.

Keywords: geothermal structure, Distributed Acoustic Sensor (DAS), high Vp/Vs, Temperuer effects on seismic velocities, Vp/Vs by water contents, borehole seismic

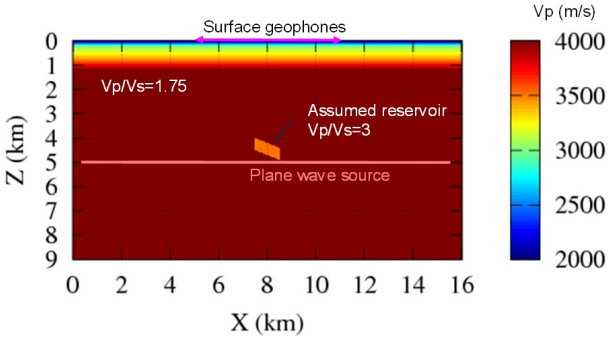

Fig. 1: Model to examine the P-to-S conversion. *Vp/Vs* in the reservoir is assumed to be 3. The plane wave source at 5 km depth. The dip of the reservoir is 20° .

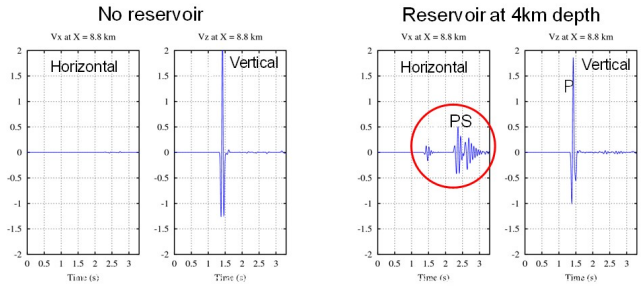

Fig. 2: Waveforms at 8.8 km from the left edge of the model shown in Fig. 5. It is noted that the P-to-S conversion arrival is observed on the horizontal component, but only intense P first arrival is seen on the vertical component for the 4 km-deep reservoir model.

©2020. Japan Geoscience Union. All Right Reserved.

Estimation of Temperature and Permeability Distribution in Kakkonda Geothemal Field, Iwate Prefecture, Japan, Using Neural Network

*Ugo Tsubasa[1], Kazuya Ishitsuka[2], Toru Mogi[4], Koichi Suzuki[4], Yosuke Kobayashi[3]

1. Department of Environmental Circulation Systems, Hokkaido University, 2. Kyoto University, 3. Muroran Institute of Technology, 4. Hokkaido University

Estimation of temperature distribution around a geothermal field is important to understand a geothermal system. A major method for understanding the temperarure structure of the subsurface is to dig a well, but it costs a lot to dig just one well. Previously, temperature distributions were successfully estimated by a neural network based on temperature logs and magnetotelluric (MT) data (Spichak V.V. (2006), Ishitsuka et al., 2018). This method firstly trains the relationship between three-dimensional locations, resistivities and temperatures by a neural network. Then, the optimized neural network is used to estimate temperature distribution based on a resistivity structure obtained by the MT method. But, not only temperature but also permeability are important physical parameters to evaluate a geothermal system. In this study, we developed a method to estimate permeability distribution as well as temperature distribution by a neural network. The methodology was applied to the Kakkonda geothermal field, Japan. We used the temperature and the resistivity logs data provided by Tohoku Sustainable & Renewable Energy Co. Inc.

Since permeability along a well is not generally measured, we created a training data of permeability from existing resistivity data, we first estimated permeability along a well based on porosity deduced from resistivity log using the Archie’ s law. The temperature dependence of the resistivity of water was corrected at the processing. In addition, we assumed that the salt concentration at each depth was equal to the salt concentration of the collected fluid inclusion. Subsequently, the porosity was converted into the permeability by the Kozeny-Carman equation. Data about D 95 and mineral isograds were also added to the training data to further improve the estimation.

We then estimated temperature and permeability distribution around the target area. For training data, we used temperature logs and the estimated permeability logs using resistivity profiles at the 20 wells. To estimate temperature distribution, we used the 3D resistivity structure made by the MT survey (Yamaya et al., 2017).

The result exhibited that both temperature and permeability show a distribution according to the physical law. As for the temperature, the high temperature part assumed to be a heat source was estimated in the deep part, and the permeability showed high values in the low specific resistance part. With the increase in the types of input data, our method enables to estimate more accurate distribution.

©2020. Japan Geoscience Union. All Right Reserved.

Extraction of features of strata using borehole data of geothermal area by multivariate analysisExtraction of features of strata using borehole data of geothermal area by multivariate analysis

*Ojima Hiroki[1], Kazuya Ishitsuka[2], Toru Mogi[1], Kajiwara Tatsuya[3], Takeshi Sugimoto[3], Hiroshi Asanuma[4]

1. Hokkaido University, 2. Kyoto University, 3. Geothermal Engineering Co., Ltd., 4. Fukushima Renewable Energy Institute, AIST

The quartz index is defined as the percentage of the strongest X-ray intensity of a certain mineral in the sample and the intensity of the pure quartz measured under the same experimental conditions. We have developed a method to classify the strata by multivariate analysis and extract the features, in particular the difference in alteration degree, and verified effectiveness of the method in comparison with usual geological analysis. First, applying the principal component analysis data was dimensionally compressed and characteristics were emphasized. and Then classification of the strata by the clustering based on the Gaussian mixture model. In addition, the classification results obtained by this method compared with electric logging and temperature logging data.

In this study, we used the quartz index data obtained from wells in Hachimantai geothermal area of Iwate prefecture. The geology of this area consists of andesite tuff and dacite tuff. The quartz index means the content (% by weight) in the sample for quartz and the relative quantity ratio for the other minerals. To verify the validity of this method, the principal component analysis was performed on the quartz index data of standardized clay minerals and compared with the results of existing geological classification by geological interpretation. As a result of the comparison, the classification results were similar, and this method was verified.

Next, in order to ascertain the effect of dimensional reduction by the principal component analysis, (i) we performed clustering without dimension reduction for all quartz index, and (ii) after the dimensional reduction is applied to all quartz index, we compared the results of clustering. In dimension reduction, we used up to the principal components whose contribution total is 95%. As a result of the comparison, the optimal classification number of the strata was 6 in the case where dimension reduction was not performed (case (i)), but in the case of dimensional reduction (case (ii)), the optimum classification number was 10. As a result, it was found that more detailed features can be extracted from the formation by dimension reduction. In particular, the classification in the depth range from 0 to 1000 m, especially the correspondence between clay minerals and zeolite minerals, became clearer.

©2020. Japan Geoscience Union. All Right Reserved.

Geochemical characteristics of silica scales precipitated from the geothermal water at the Onuma geothermal power plant.

*CHEN FEIYANG[1], Mayuko Fukuyama[1]

1. Akita University

The scale precipitation is a major problem in water-dominated geothermal power plants as it reduces the production rate of geothermal energy. The scale precipitates at different physical and chemical conditions in each geothermal power plant as a result from a fluid-rock interaction for specific conditions of the each plant. Thus it is important to understand the chemical characteristics of the scale and process of scale precipitation from geothermal fluid. Understanding of those will be applied to effective protection against the scale precipitation. On the other hand, information on the process of transportation of metals and its precipitation from hydrothermal fluid will be useful to understand the formation of hydrothermal ore deposit.
In this study, we present the geochemical characteristics of geothermal water and scales from the Onuma geothermal power plant at Akita, Japan. The samples were collected from pipes for transportation of thermal water at the plant. The geothermal water were analyzed major elements by Ion Chromatography (Thermo Fisher Scientific Dionex ICS-2100 and ICS-3000) at Akita Prefecture Industrial Center and trace elements by Q-ICP-MS (Agilent 7700) at Akita University. The silica scale is analyzed for trace elements by Q-ICP-MS (Agilent 7700) at Akita University after the acid digestion of samples.
The scale consists of mainly amorphous silica and/or trace amounts of montmorillonite kaolinite, and/or pyrite. The geothermal water is Cl type.
The scale contains Na (0.63-1.32%), Ca (0.76-1.39 %), Mg (107-7417 μg/g), Fe (0.03-1.44%), Al (3.6-5.4%) and trace amounts of Cu (2-53 μg/g), Zn (3-180 μg/g), and lithophile elements, such as Li (2-11 μg/g), Rb (135-183 μg/g), Sr (173-378 μg/g), and REE. Chondrite-normalized REE patterns of scales in this study showing both of slightly LREE enriched and HREE enriched patterns with positive anomalies of Eu. Yttrium behaves in a similar manner as the HREE, especially Ho, as these elements have similar ionic radii. Yttrium and Ho positively correlate with Y/Ho ratios of 31.2–50.2. It is slightly higher than the upper continental crust Y/Ho value of 27.5 estimated by McLennan (2001).
The analytical results of scales show high Au concentration of 1.5-23.3 μg/g, comparable to the average of gold ore contains few μg/g. Gold is positively correlated with Ag and Pb. The concentrations of Au, Cu, Pb, and Li of scale show the negative correlation with Eu anomalies. The amounts of trace elements correlated with the concentrations of Na, Ca, and Al, suggesting that clay minerals such as montmorillonite and kaolinite can contain significant amounts of the elements. This result indicates that clay minerals could remove trace elements from geothermal water in the pipeline.

Acknowledgements
We appreciate the Mitsubishi Materials Co. Ltd. and Akita Power Generation Co. Ltd. for obtaining scale and geothermal fluid samples from the Onuma geothermal power plant. We would like to thank Dr. Yukio Enda at the Akita Industrial Technology Center for help during ion chromatography analysis. This work was partly supported by JSPS Grants– in– Aid for Scientific Research (C) (19K04008).

Keywords: geothermal, silica scale, trace element

©2020. Japan Geoscience Union. All Right Reserved.

Hydrothermal system around the Iwo-yama fumarolic field in Kuju volcano (Japan) inferred from a 3-D resistivity structure model

*Wataru Kanda[1], Mitsuru Utsugi[2], Hiroyuki Inoue[2], Shogo Komori[3], Tsuneomi Kagiyama[4]

1. Volcanic Fluid Research Center, School of Science, Tokyo Institute of Technology, 2. Aso Volcanological Laboratory, Graduate School of Science, Kyoto University, 3. National Institute of Advanced Industrial Science and Technology (AIST), 4. Aso Geopark Promotion Council

This paper presents an electrical resistivity structure inferred from audio-frequency magnetotelluric (AMT) surveys carried out in the central part of Kuju volcano. Kuju volcano is a composite volcano, consisting of more than 20 lava domes or cones, located in the central part of Kyushu Island, SW Japan. In Oct. 1995, a phreatic explosion occurred after a few hundred years of dormancy with opening of several new vents at the eastern flank of Mt. Hossho, one of the domes of the Kuju complex. The new vents were located about 300m south of an intense fumarolic field called Iwo-yama. After the eruptive activity continued to middle of 1996, a rapid cooling of the volcanic edifice beneath around Iwo-yama was inferred from several geophysical observations. The objective of our AMT surveys is to reveal the shallow electrical structure of the cooling zone relating to the phreatic explosion.

The AMT data were successfully collected at 25 locations around Iwo-yama from 2005 to 2008 and recently interpreted by a 3-D inversion (Usui, 2015). A thin conductive layer less than 100 m thick near the surface and an underlying resistive zone were found beneath Iwo-yama area, which is interpreted as a permeable zone saturated with vapor-rich fluids. The center of cooling zone inferred is located around the lower part of this less conductive zone, where the accumulation of groundwater and the vaporization of hydrothermal fluids are supposed to occur.

Keywords: Resistivity structure, Hydorthermal system, Phreatic eruption

©2020. Japan Geoscience Union. All Right Reserved.

Gravity changes inferred from hydrothermal simulation before and after the 1995 eruption in Kuju volcano, Oita prefecture

*Jun Nishijima[1], Yoshiyuki Mizusawa[2], Yasuhiro Fujimitsu[1]

1. Department of Earth Resources Engineering, Faculty of Engineering, Kyushu University, 2. Department of Earth Resources Engineering, Graduate School of Engineering, Kyushu University

The phreatic eruptions were occurred on October and December 1995, at Kuju Iwoyama, Oita prefecture, Japan. Several hydrothermal models were calculated using Hydrotherm ver. 2.2 (Hayba and Ingebritsen, 1994). The temperature of the fumaroles and heat discharge rate were used for a matching parameter on these models. These models can interpret the hydrothermal flows change before and after the eruption. The steep gravity decreases up to 100 μgal and gradual gravity recovery up to 110 μgal were detected after the eruption by micro-gravity monitoring in Kuju volcano. This result interpreted the mass changes in the geothermal reservoir around the conduit in the Kuju Iwoyama. The objective of this study is to construct a hydrothermal model to satisfy the heat discharge rate and gravity changes for the improvement of the previous hydrothermal model. The numerical modeling is conducted using Hydrotherm ver. 3.2 (Kipp Jr. et al., 2008). This presentation reports the results of the hydrothermal modeling.

Keywords: Hydrothermal modeling, gravity, Heat discharge, Kuju volcano

©2020. Japan Geoscience Union. All Right Reserved.

Updating the conceptual model of Tendaho geothermal field, Afar Region, Ethiopia

*belete ashenafi fekadu, Yasuhiro Fujimitsu, Jun Nishijima, Mitsuo Matsumoto

Developing and understanding the conceptual model of any geothermal system plays a key role to its commercially successful exploration, development and utilization. Conceptual models are mainly based on analysis of geological data, geophysical information, borehole data and information on the chemical content of reservoir fluids. In this paper we compiled the most relevant data for Tendaho geothermal area to visualize the subsurface pattern and to develop the conceptual model using Leapfrog© Geothermal Software. Three shallow and three deep exploration wells have been drilled in the 1990s. Several geophysical investigations also conducted in the past. The geological model of the field is defined from surface geological data, magneto telluric data and borehole information. The result from analysis of the magnetotelluric data indicates low resistivity value <10 Ohm m for the Southwestern part of the drilled exploration wells. The magnetotelluric model shows an uncertainty in depicting the cap rock and the shallow reservoir since both shows a very low resistivity at shallower depth. However, it clearly indicates the the deep conductive body at a depth of 6km. The 3D geologic model is built combining the magnetotelluric measurements and borehole information. The conceptual model updated based on the available information depict the possible heat source which is in the southeastern part of drilled wells, the fluid flow pattern and probable faults.

Keywords: Geothermal, Tendaho graben, Conceptual model, Magnetotelluric, Leapfrog@

©2020. Japan Geoscience Union. All Right Reserved.

[J] Poster | S (Solid Earth Sciences)：S-VC Volcanology

[S-VC45] Active Volcanism

convener:Yuta Maeda(Nagoya University), Takahiro Miwa(National research institute for earth science and disaster prevention), Takeshi Nishimura(Department of Geophysics, Graduate School of Science, Tohoku University)

This session discusses various aspects of active volcanisms including, but not limited to, recent and historical eruptions, various phenomena associated with the volcanic activities, underground structures of the volcanoes, and developments of new instruments based on geophysical, geochemical, geological, and multidiscipline approaches. We also welcome studies on understanding and predicting the transitions of the eruptive activities from observational, theoretical, and experimental approaches.

[SVC45-P01] Unrest event at Nakamachinesiri crater of Meakandake in 2019; insight from total magnetic field observations

*Ryo Tanaka[1] (1.Hokkaido University,Institute of Seismology and Volcanology)

[SVC45-P02] Possible very micro low-frequency earthquakes in the Showa-Shinzan lava dome in the Usu volcanic region captured by dense seismic campaign

*Akiko Takeo[1], Motoko Ishise[1], Kiwamu Nishida[1], Hiroshi Aoyama[2], Yosuke Aoki[1] (1.Earthquake Research Institutute, the University of Tokyo, 2.Institute of Seismology and Volcanology, Faculty of Science, Hokkaido University)

[SVC45-P03] Detection of long-period volcanic earthquakes using continuous wavefield processing system

*Mare Yamamoto[1] (1.Research Center for Prediction of Earthquakes and Volcanic Eruptions, Graduate School of Science, Tohoku University)

[SVC45-P04] Geothermal Activity by Observation using Infrared Thermal Camera during the 2018-19 Volcanic Activity at Azumayama

*Susumu Seki[1], Masayuki Oishi[1], Tomoyuki Matsumura[1] (1.Japan Meteorological Agency)

[SVC45-P05] Reactivation of volcanic activity on May 2019 at Azumayama – Importance of precise ground deformation monitoring near the crater

*Jun Okada[1], Yu Nihara[2], Shin Chikasawa[3], Takuya Yamamura[3], Susumu Seki[3], Koki Sasaki[2], Akimichi Takagi[4], Keiichi Fukui[4] (1.Volcanology Research Department, Meteorological Research Institute, JMA, 2.Regional Volcanic Observation and Warning Center, Sendai Regional Headquarters, JMA, 3.Seismology and Volcanology Division, Sendai Regional Headquarters, JMA, 4.Volcanology Division, Seismology and Volcanology Department, JMA)

[SVC45-P06] Detection of crustal deformation owing to volcanic activity of the Oana crater in the Mt. Azuma area using interferometric synthetic aperture radar and pressure source estimation

*Sota Nagagata[1], Koichi Suzuki[1], Toru Mogi[2] (1.Hokkaido University, 2.Tokyo Institute of Technology)

[SVC45-P07] Consideration of JMA tilt meter data around volcano using boundary element method (2)

*Ryohei Kawaguchi[1] (1.Meteorological Research Institute)

[SVC45-P08] Imaging of the volcanic activity process beneath the Yugama crater at Kusatsu-Shiranesan volcano

*Akimichi Takagi[1], Tsukasa Kobayashi[1], Takahiro Kitagawa[1], Kousuke Takahashi[1], Koji Kato[1], Jun'ichi Miyamura[1] (1.Seismology and Volcanology Department, Japan Meteorological Agency)

[SVC45-P09] Self-potential and geomagnetic total intensity observations at Motoshirane volcano after the 2018 eruption (2)

*Akira Yamazaki[1], Hideki Iino[1], Shin Akira[1], Jun Shimokawa[1] (1.Kakioka Magnetic Observatory)

[SVC45-P10] Crack resonances at an LP source beneath Kusatsu-Shirane volcano triggered by volume changes with vapor condensation

*Kimiko Taguchi[1], Hiroyuki Kumagai[1], Yuta Maeda[1] (1.Nagoya University Environmental Studies)

[SVC45-P11] Forward analysis of seismic waves accompanied by tilt ground motion during the eruption of Mt. Motoshirane, Japan, on January 23, 2018

*Ryohei Takahashi[1], Yuta Maeda[1], Toshiki Watanabe[1] (1.Graduate School of Environmental Studies, Nagoya University)

[SVC45-P12] Real time monitoring of underground temperature in Jigokudani, Midagahara volcano using LPWA devices

*Tohru Watanabe[1] (1.University of Toyama)

[SVC45-P13] Development of a system for FEM-based crustal deformation analysis

*Tomokazu Kobayashi[1], Shinya Yamada[1] (1.GSI of Japan)

[SVC45-P14] Silisic magma reservoirs beneath Fuji Volcano, Japan, constrained from interstitial melt in gabbroic xenoliths

*Megu Otsuka[1], Hidemi Ishibashi[2], Natsumi Hokanishi[3], ATSUSHI YASUDA[3] (1.Graduate School of Integrated Science and Technology, Shizuoka University, 2.Shizuoka University, 3.Earthquake Research Institute,The University of Tokyo)

[SVC45-P15] Corrections of individual properties of relative gravimeters by using cooperative precise gravity measurement data in Izu-Oshima volcano

*Shin'ya Onizawa[1], Ryuichi Nishiyama[2], Shuhei Okubo[2,3], Yutaka Nagaoka[1], Yasuo Hirayama[4], Takanori Ishihara[4], Kensuke Matsuda[4], Yuya Kaneko[4], Yoshihiro Ueda[4], Yuichi Imanishi[2], Atsushi Watanabe[2], Miwako Ando[2], Shikou Sakashita[2] (1.Meteorological Research Institute, JMA, 2.Earthquake Research Institute, The University of Tokyo, 3.Southwest Jiaotong University, 4.Seismological and Volcanological Department, JMA)

[SVC45-P16] Temporal gravity change observed on Izu-Oshima Island in 2010's

*Ryuichi Nishiyama[1], Yuichi Imanishi[1], Shin'ya Onizawa[2], Shuhei Okubo[1,3], Miwako Ando[1], Atsushi Watanabe[1], Shikou Sakashita[1], Yutaka Nagaoka[2], Yoshiyuki Tanaka[4], Hidefumi Watanabe[1,5] (1.Earthquake Research Institute, The University of Tokyo, 2.Volcanology Research Department, Meteorological Research Institute, JMA, 3.Southwest Jiaotong University, 4.Graduate School of Science, The University of Tokyo, 5.Disaster Prevention Division, Tokyo Metropolitan Government)

[SVC45-P18] Vesiculation texture and change in the amount of phenocrysts of the summit eruption of the Izu-Oshima volcano - Comparison between the An'ei and the 1986 eruption -

*Yuya Ikenaga[1], Fukashi Maeno[1], ATSUSHI YASUDA[1] (1.Earthquake Research Institute, The University of Tokyo)

[SVC45-P19] A study on surface displacement and pressure source of Kozushima Island based on InSAR analysis

*Wataru Uehara[1], Yoshiya Oda[1] (1.Tokyo Metropolitan University)

[SVC45-P20] Automatic Seismic Wave Detection with Deep Learning
- Application to temporary observation data at Hachijojima Island -

*Ryohei Tottori[1], Hiroyuki Azuma[1], Yoshiya Oda[1], Toshifumi Matsuoka[2] (1.Tokyo Metropolitan University, 2.Fukada Geological Institute)

[SVC45-P21] Temporary dense seismic observation in Hachijojima Island

*Ryotaro Kanemaru[1], Yoshiya Oda[1], Hiroyuki Azuma[1], Kentaro Omori[1], Syotaro Kanke[1], Toshiki Watanabe[2] (1.Tokyo Metropolitan University, 2.Earthquake and Volcano Research Center Graduate School of Environmental Studies, Nagoya University)

[SVC45-P22] Lava discharge rate in Nishinoshima volcano, Ogasawara Islands revealed using ALOS-2/PALSAR-2

*Shinobu Ando[1], Satoshi Okuyama[2], Shinichi Matsusue[3] (1.Seismology and Tsunami Research Department, Meteorological Research Institute, 2.Volcanology Research Department, Meteorological Research Institute, 3.Volcanology Division, Japan Meteorological Agency)

[SVC45-P23] Spatial variation of magma compositions at the Abu Monogenetic Volcano Group, SW Japan

*Kenyo U[1], Koji Kiyosugi[1], Yasuko Itoh[2], Yoshiyuki Tatsumi[1] (1.Kobe University, 2.Hagi Geopark Promotion Division)

[SVC45-P24] Repeated aeromagnetic survey on Kuju Volcano using drone, unmanned multicopter.

*Mitsuru Utsugi[1], Takeshi Hashimoto[2], Akinori Satoh[2], Noriko Tada[3], Toyonobu Ota[4], Shin Yoshikawa[1], Hiroyuki Inoue[1] (1.Kyoto University, 2.Hokkaido University, 3.JAMSTEC, 4.Tierra Tecnica)

[SVC45-P26] Seismo-acoustic signals before ash emissions at Aso volcano, Japan

*Akihiko Yokoo[1] (1.Graduate School of Science, Kyoto University)

[SVC45-P27] Waveform analysis of infrasound pulses observed before the phreatomagmatic explosion on October 23, 2015

*Yuto Kozawa[1], Akihiko Yokoo[1] (1.Graduate School of Science, Kyoto University)

[SVC45-P28] Melt inclusion constraints on the pre-eruptive process of Kirishima-Ohachi 1235 subplinian eruption

*Yoshiharu Iwaki[1], Hidemi Ishibashi[2], Natsumi Hokanishi[3], ATSUSHI YASUDA[3], Toru Ishikawa[4] (1.Shizuoka University Graduate School of Integrated Science and Technology, 2.Shizuoka University, 3.Earthquake Research Institute,The University of Tokyo, 4.Kirishima Geopark Council)

[SVC45-P29] Temporal and spatial variations of helium isotope ratios in volcanic gases at Kirishima volcanic group

*Hirochika Sumino[1], Kotaro Toyama[1], Takeshi Ohba[2], Muga Yaguchi[3] (1.Department of Basic Science, Graduate School of Arts and Sciences, The University of Tokyo, 2.Department of Chemistry, Tokai University, 3.Meteorological Research Institute)

[SVC45-P30] Vertical ground deformation in Sakurajima volcano measured by precise leveling survey (during Nov. 2018 - Nov. 2019)

*Keigo Yamamoto[1], Takeshi Matsushima[2], Shin Yoshikawa[3], Hiroyuki Inoue[3], Tadaomi Sonoda[1], Taishi Yamada[1], Yichen Tang[2], Koki Yoshinaga[2], Takamitsu Ikegame[4], Hiroshi Kishimoto[4], Takahiro Ohkura[3] (1.Disaster Prevention Research Institute, Kyoto University, 2.Faculty of Sciences, Kyushu University, 3.Graduate School of Science, Kyoto University, 4.Japan Meteorological Agency)

[SVC45-P31] Changes in carrier phase residuals of GPS satellite radio waves following the eruptions of Sakurajima
-Data analysis from 2013 to 2019-

*Yukako Asakura[1], Takeshi Nishimura[1], Yusaku Ohta[1], Masayuki Kano[1] (1.Graduate school of science, Tohoku University)

[SVC45-P32] Detection of volcanic earthquakes and estimation of internal attenuation structure beneath the Kikai submarine caldera

Yasutomo Seto[1], *Hiroko Sugioka[1], Tsutomu Takahashi[2], Yojiro Yamamoto[2] (1.Kobe University, 2.JAMSTEC)

[SVC45-P33] Occurrence and distribution of pyroclastic fall deposits of Kuchinoerabujima volcano 2020 eruption

*Masashi NAGAI[1], Shojiro Nakagawa[2], Yu Iriyama[3], Takahiro Miwa[1], Setsuya Nakada[1] (1. Volcano Research Department, National Research Institute for Earth Science and Disaster Resilience, 2.Yakushima Chigaku Club, 3.Research and Industrial Collaboration Department, Kyushu University)

[SVC45-P34] Three-dimensional resistivity imaging of Taal Volcano, Philippines

*Yusuke Yamaya[1], Paul Alanis[2] (1.National Institute of Advanced Industrial Science and Technology, 2.Philippine Institute of Volcanology and Seismology)

[SVC45-P35] Detection of the volcanic plume by 19 February 2018 eruption of Mount Sinabung deduced from GNSS post-fit phase residual analysis

*Yusaku Ohta[1], Masato Iguchi[2], Gunawan Hendra[3], Umar Rosadi[3], Estu Kriswati[3] (1.Research Center for Prediction of Earthquakes and Volcanic Eruptions, Graduate School of Science, Tohoku University, 2.Sakurajima Volcano Research Center, Disaster Prevention Research Institute, Kyoto University, 3.Center for Volcanology and Geological Hazard Mitigation)

[SVC45-P36] The performance of the back elevation angle estimation of 3-dimensional infrasonic small array observation

*Kazuya Yamakawa[1], Mie Ichihara[1], Claudia Sánchez[2], Wataru Ikeda[1], Giorgio Lacanna[2], Maurizio Ripepe[2] (1.Earthquake Research Institute, University of Tokyo, Japan, 2.Department of Earth Sciences, University of Florence, Italy)

[SVC45-P37] A trial to quantify volcanic activities using the JMA unified earthquake catalog and the ETAS model

*Yuta Maeda[1] (1.Nagoya University)

[SVC45-P38] Temporal relationship between seismic activity and ground deformation by GNSS data with applying the stacking method

*Yo Kanno[1], Akimichi Takagi[1], Takashi YOKOTA[2], Kazuki Miyaoka[1] (1.Seismology and Volcanology Department, Japan meteorological agency, 2.Aichi Institute of Technology)

[SVC45-P39] Multi-sensor system with air blowers for airborne volcanic gas survey using drones: an improvement of a sensor response time

*Kohki Matsuura[1], Akihiko Terada[1], Toshiya Mori[2], Takato Ono[2] (1.Volcanic Fluid Research Center, Tokyo Institute of Technology, 2.Chemical Research Center, Graduate School of Science, The Univercity of Tokyo)

[SVC45-P40] Tephra segregation profiles from Vulcanian eruptions on Sakurajima volcano, Japan, based on settling velocity observations

*Kosei Takishita[1], Masato Iguchi[2], Alexandros Panagiotis Poulidis[2], Tadaomi Sonoda[2] (1.Division of Earth and Planetary Sciences, Graduate School of Science, Kyoto University, 2.Sakurajima Volcano Research Center, DPRI, Kyoto Univ.)

Unrest event at Nakamachinesiri crater of Meakandake in 2019; insight from total magnetic field observations

*Ryo Tanaka[1]

1. Hokkaido University,Institute of Seismology and Volcanology

Mt. Meakan is an active volcano located at the southwestern tip of the Akan Shiretoko volcanic line in eastern Hokkaido. There is a Ponmachineshiri crater on the summit and a Nakamachineshiri crater on the northeastern flank. The eruptions in recorded history include intermittent phreatic explosions at the Nakamachineshiri crater and the Ponmachineshiri crater from 1955 to 1966 and the phreatic eruptions in 1988, 1996, 1998, 2006, 2008 at the Ponmachineshiri crater (Hokkaido Disaster Prevention Council, 1976). Since 2008, seismic activity has been concentrated almost beneath the Ponmachineshiri crater. In 2015, demagnetization and inflation below the Ponmachineshiri crater, and increase in fumarolic activity has been observed. On the other hand, although there is a difference in the density of the observation network between the craters, the ground deformation observations did not capture the activity beneath the Nakamachineshiri crater.

An increase in earthquakes beneath the Nakamachineshiri crater was observed in February and July-August 2019 (JMA, 2019). Prior to this seismic activity, ground deformation that had been observed since 2016, suggesting an expansion of 3 km deep at the northeastern foot of Mt. Meakan, turned to stagnation or deflation in 2018. The purpose in this study is to clarify the mechanisms of the activity beneath the Nakamachineshiri crater in 2019, comparison among the results of repeated magnetic field observations around the Nakamachineshiri crater since 2013, the seismic activity under the Nakamachineshiri crater, the activity of deep pressure sources, and the resistivity structure below the crater.

The observation of the total magnetic field at the Nakamachineshiri crater has not been performed in recent years. However, the Nakamachineshiri crater is still performing the active heat release from fumaroles and hot ponds. The activity under the crater has been expected. The survey of total magnetic field has been performed at 20 sites repeatedly. The data of reference point were provided by the Memambetsu Magnetic Observatory, Japan Meteorological Agency.

As reported by Tanaka et al. (2017, Volcanological Society of Japan), the results of the change in total magnetic field from 2013 to 2017 are modeled by demagnetization with a magnetic moment rate 1–2×10^{6} A m^{2} yr^{-1} at a depth of 200–300 m below the south wall of the Nakamachineshiri crater. No significant changes were observed in the trend from 2017 to 2018 and the amount of the magnetic moment rate. However, the change in the total magnetic field 2018–2019 was modeled with a spherical demagnetizing source, the depth was 360 m and the magnetic moment 9×10^{6} A m^{2} yr^{-1}, indicating that the deeply demagnetization was accelerated.
The comparison between the position of the spherical source of change in total magnetic field and the resistivity structure (Takahashi et al., 2018) reveals that the spherical sources estimated by the results from 2014 to 2018 are located within the low resistivity zone, containing the clay minerals and hydrothermal fluid, just beneath the Nakamachineshiri crater. The comparison also shows that the source of change in total magnetic field between 2018 and 2019 are beneath the low resistivity zone. The epicenter of earthquakes occurred around the Nakamachineshiri crater in 2019 are located at the 0-1 km below sea level which is deeper than the spherical source. There is a possibility that the activity of the

©2020. Japan Geoscience Union. All Right Reserved.

Nakamachineshiri crater in 2019 reflected the process of the fluid supply from the deep source to the shallow source beneath the Nakamachineshiri crater. The quantitative examinations such as the mass valance between the deep and shallow source are required to reveal the mechanisms of the activity beneath the Nakamachineshiri crater in 2019.

Keywords: hydrothermal system, Total magnetic field

©2020. Japan Geoscience Union. All Right Reserved.

Possible very micro low-frequency earthquakes in the Showa-Shinzan lava dome in the Usu volcanic region captured by dense seismic campaign

*Akiko Takeo[1], Motoko Ishise[1], Kiwamu Nishida[1], Hiroshi Aoyama[2], Yosuke Aoki[1]

1. Earthquake Research Institutute, the University of Tokyo, 2. Institute of Seismology and Volcanology, Faculty of Science, Hokkaido University

The Showa-Shinzan lava dome has a unique evolution history grown from a wheat field to an altitude of about 400 m with several eruptions in 1943-1945. To understand its evolution process from shear-wave velocity structure, we deployed 22 short-period seismometers on and around the lava dome from May 9-10 to Jun 6-8, 2018 (Takeo et al. 2019 SSJ meeting) and recorded three-component seismograms at 200 sps. We here report local events near the summit that unexpectedly recorded by this observation.

We first used vertical-component seismograms filtered at a frequency higher than 2 Hz, and manually detected 56 events whose signals are visible at most of the stations on the lava dome. Some events can be recognized at the nearest JMA permanent station located at the southeast of the lava dome. The signal cannot be seen at other permanent stations. Smaller events, visible only at several stations on the dome, were frequently observed for a rate of about 1.5 per hour.

We then picked the first arrival for each event and each station from the envelope function, the moving average of RMS at a frequency higher than 5 Hz with a time window of 0.05 s. The first arrival time is defined at the time when the envelope amplitude becomes 10% of the maximum envelope amplitude. When the maximum-amplitude time and the arrival time differ more than 0.1s, the pick was rejected. After the trial hypocenter determination with various assumed homogeneous velocities in a range of 0.5-5 km/s, we found that the velocity of about 2 km/s is needed to reduce the misfit between picked and theoretical arrival times. This result indicates that the recorded signals are not acoustic waves like the firework signal from the Lake Toya-ko, but are P-waves from seismic events.

We finally determined the hypocenters of 37 events by only analyzing events with more than 10 first arrival measurements. The assumed velocity structure is homogeneous with a P-wave velocity of 2.0 km/s. Most of the events are located near the summit within the lava dome at altitudes of 250-350 m. Some events are located at the east of the summit at altitudes higher than 400 m in the air, indicating the insufficient quality of arrival-time picking and/or the assumed velocity structure. The roughly estimated magnitudes based on the JMA equation are between -3 and -2.5.

Although the validation is still ongoing, the durations of signals indicate that the events are not regular earthquakes but low-frequency earthquakes. The distribution of arrival times further indicates that the hypocenter is not a unique location. Preliminary calculation by the template matching method with one template event shows smaller events are occurring almost constantly. The activity may be thus related to the fumarolic activity continuing near the summit, or the contraction of the dome. To understand its activity and its meaning to the volcanic activity, relocation and template matching analyses are needed in the future.

©2020. Japan Geoscience Union. All Right Reserved.

Keywords: Showa-Shinzan, Usu, Low Frequency Earthquake

©2020. Japan Geoscience Union. All Right Reserved.

Detection of long-period volcanic earthquakes using continuous wavefield processing system

*Mare Yamamoto[1]

1. Research Center for Prediction of Earthquakes and Volcanic Eruptions, Graduate School of Science, Tohoku University

Long-period earthquakes and low-frequency earthquakes observed around active volcanoes are considered to be generated by the movement of volcanic fluid in the shallow hydrothermal system, and the elucidation of these signals are thought to be one of the critical keys to understand the thermal state of hydrothermal system and to evaluate volcanic activities. So far, the observation of long-period signals has been conducted using broadband seismometers close to the focal area around active craters and fumaroles, and it is rather difficult to detect them comprehensively at volcanoes where the observation networks is not sufficient. For example, at Hakkoda volcano, where long-period (10 s) events frequently occurred between 2013 and 2015, the detail of their activity had been unclear until the installation of a broadband seismometer close to the focal area. To systematically detect long-period earthquakes around active volcanoes using the data observed at permanent stations like NIED Hi-net, we have been developing a continuous wavefield processing system as a part of MEXT 'Integrated Program for Next Generation Volcano Research and Human Resource Development'. In this presentation, we report the result of an evaluation test of back projection analysis of the long-period events at Zao volcano.

Our continuous wavefield processing system is being developed to analyze continuous seismic wavefield using seismic interferometry, back projection, and spectral analyses. The back projection analysis in the system is based on the slant stack of wavefield assuming predefined virtual sources, and it is almost similar to the Source-Scanning Algorithm by Kao and Shan (2004). Because the dominant period of long-period events occurring at shallow depth is around 10 s and the observed wavefield at far stations is dominated by surface waves, we stack the observed wavefield assuming the propagation of Rayleigh wave from the virtual source. To obtain the travel times of Rayleigh wave propagating between the focal area and far stations, we use the ambient noise seismic interferometry between the station in the vicinity of postulated source location and far stations.
In this study, to verify the detectability of long-period earthquakes and the robustness of the method, we apply this processing to the analysis of long-period events at Zao volcano. In the analysis, we use the vertical component data at stations operated by Tohoku Univ., JMA, and NIED, and apply the method for several frequency bands. As the result, we find that the method successfully detects almost all the events which are detected by manual inspection, and the estimated source energy well correlates with the amplitude of long-period events observed at nearby stations.

We are now operating the continuous back projection analysis at three volcanoes (Zao, Azuma, and Asama) as a trial, and we expect further optimization of the processing will contribute the monitoring of volcanic activities as well as the systematical detection of long-period events.

Acknowledgments: This work was supported by MEXT Integrated Program for Next Generation Volcano Research and Human Resource Development.

Keywords: volcanic earthquake, seismic wavefield, realtime processing

©2020. Japan Geoscience Union. All Right Reserved.

©2020. Japan Geoscience Union. All Right Reserved.

Geothermal Activity by Observation using Infrared Thermal Camera during the 2018-19 Volcanic Activity at Azumayama

*Susumu Seki[1], Masayuki Oishi[1], Tomoyuki Matsumura[1]

1. Japan Meteorological Agency

Introduction
Ground-fixed infrared thermal camera observation provides the nighttime data without influence of solar radiation besides the images with a fixed angle of view, as compared with mobile observation. It allows us the detailed pixel analysis of the thermal images. We report the expansion of the geothermal area and temperature changes during a series of 2018-19 activities at Azumayama.
Data and Analysis
Japan Meteorological Agency (JMA) has deployed infrared thermal camera at Jododaira, east flank of Azumayama, and performed continuous monitoring since 2016. The infrared thermal camera records thermal images every 5 second and thermal data every hour. Thermal data is a binary file consisting of temperature data for each pixel. We convert this binary data to a CSV file and perform two ways of analysis. One is to extract the maximum temperatures in the specified ranges. The other is to count the number of pixels with a temperature above a specific threshold.
Result
During the 2018-19 activity, the maximum temperature of geothermal area increased and the area expanded around October 2018 at Ooana crater, the main geothermal area in Azumayama with some active fumaroles, and at the NW region from Ooana crater.
Magnetic observation suggests demagnetization at the shallow subsurface around Ooana crater and volcanic gas monitoring (Multi-gas observation data) shows simultaneous increase in the ratio of SO2/H2S during the activity. In addition, the main type of volcanic earthquakes changed from relatively deeper BH-type to shallower low frequency earthquakes and volcanic tremors.
The data collected by geothermal observation using infrared thermal camera will be able to play important roles for evaluation of the volcanic activity by correlating to various data, such as activity of volcanic earthquakes, magnetic total intensity, volcanic gas, and ground deformation.

Keywords: Geothermal area

©2020. Japan Geoscience Union. All Right Reserved.

Reactivation of volcanic activity on May 2019 at Azumayama –Importance of precise ground deformation monitoring near the crater

*Jun Okada[1], Yu Nihara[2], Shin Chikasawa[3], Takuya Yamamura[3], Susumu Seki[3], Koki Sasaki[2], Akimichi Takagi[4], Keiichi Fukui[4]

1. Volcanology Research Department, Meteorological Research Institute, JMA, 2. Regional Volcanic Observation and Warning Center, Sendai Regional Headquarters, JMA, 3. Seismology and Volcanology Division, Sendai Regional Headquarters, JMA, 4. Volcanology Division, Seismology and Volcanology Department, JMA

The volcanic disasters of Ontake eruption in 2014 casted volcanologists an assignment on understanding and predicting phreatic eruption. Since phreatic eruption can be very local phenomena due to the expansion of water into steam at very shallow depth (several hundred meters to 1 km beneath ground), it is very important to have precise ground deformation measurements close to the vent area in order to detect possible eruption precursors. Japan Meteorological Agency (JMA) operates a borehole tiltmeter (100 m in depth) and three GNSS stations within 1 km from Oana crater, where the last phreatic eruption was taken place in 1977 at Azumayama. The 2018-2019 volcanic unrest activity was geophysically well monitored. Okada *et al.* (2019) reported some geophysical similarities between the 2018-2019 and the 2014-2015 activities based on the dataset till April 2019. The volcano reactivated afterwards and "Near-crater Warning" was released on 9 May. This study examines the available dataset by expanding the period of analysis up to the present and discusses about the sequence and the cause of the reactivation episode.

The start of the reactivation can be recognized around 1 May by the occurrence of minor seismicity and the corresponding tilt change recorded at Jododaira, 750 m ESE of Oana crater. Observed tilt changes indicate a ground inflation near Oana crater. The number of earthquakes (mainly high frequency type) increases after 5 May and the tilting rate rises drastically at around 17:30 on 9 May. The inflation signals of the tilt suddenly turns into a deflation at around 19:50 on the same day. A rapid deflation coincides with a sharp drop of high-frequency earthquakes occurs after this deformation reversal. Combining the detrended GNSS data with the tilt data, the volcanic activity on May 2019 can be explained by a single pressure source at very shallow depth, but the deeper sources are not necessarily demanded whereas they are requested by Okada *et al.* (2019) during the main period of the 2018-2019 activity. Our results indicate the reactivation on May 2019 may be a part of the 2018-2019 activity and not accompanied with the new injection of hot volcanic fluids from the depth. This supports that the ratio of SO_2/H_2S of volcanic gases does not show any changes but decreases consistently during the corresponding period. Finally, we also report that the repeated EDM measurements at Jododaira capture a possible deflation of Oana crater during June-September 2019. The existence of this deflation may indicate a relaxation process of the heated ground/aquifers and mark the ending of the 2018-2019 volcanic crisis at Azumayama even though the geothermal activity near the crater remains high. Precise ground deformation measurements such as tilt, GNSS and EDM close to the vent area give an important constrain on understanding the shallow hydrothermal systems, a potential hotbed for phreatic eruptions.

Reference:
Okada *et al.* (2019) Ground deformation associated with the 2014-2015 and the 2018-2019 volcanic activities at Azumayama. SVC38-P02, Japan Geoscience Union Meeting 2019

Keywords: Azumayama, hydrothermal activity, tiltmeter, GNSS, EDM

©2020. Japan Geoscience Union. All Right Reserved.

©2020. Japan Geoscience Union. All Right Reserved.

Detection of crustal deformation owing to volcanic activity of the Oana crater in the Mt. Azuma area using interferometric synthetic aperture radar and pressure source estimation

*Sota Nagagata[1], Koichi Suzuki[1], Toru Mogi[2]

1. Hokkaido University, 2. Tokyo Institute of Technology

The Mt. Azuma area is a group of basalt-andesitic volcanoes located in southern Tohoku on the boundary between Yamagata and Fukushima prefectures and consists of many stratovolcanoes and monogenetic volcanoes. The Sendai District Meteorological Observatory regularly records crustal deformation at the Oana crater and clinometer tilt changes at Jododaira on the eastern side of the Oana crater have been observed since late July 2018, indicating expansion of the shallow part of the crater. We estimate surface displacement associated with volcanic activity, which appears to have been active from July 2018 until May 2019, using data obtained from interferometric synthetic aperture radar (InSAR) analysis. This method offers particular advantages such that observation points on the ground are not required as well as the ability to refine a detailed spatial pattern of surface displacement. We use seven PALSAR-2 datasets collected between May 17, 2017 and October 29, 2019. The results show that as much as 13 cm of surface displacement in the direction approaching the satellite occurred on the Oana crater between October 18, 2018 and May 14, 2019. We apply the Markov chain Monte Carlo method to the spherical source model proposed by Mogi (1958) to estimate the pressure source depth responsible for the surface displacement. Our results indicate a source depth of ~240 m from the ground surface, which is similar to that of 200–600 m estimated reported by Yoshida et al. (2012) from the Mogi model using GPS data. The depth determined here is also in good agreement with that estimated by Yamasaki et al. (2010) (~300 m) using a thermal demagnetization source from total magnetic force observations, and is expected to be a hydrothermal reservoir. Additionally, the composition of sulfur dioxide and hydrogen sulfide has changed since the onset of expansion in July 2018. The displacement is likely caused by the migration of volcanic gas or other pore fluids into the hydrothermal reservoir under the Oana crater.

Keywords: InSAR, crustal deformation, Mt. Azuma

©2020. Japan Geoscience Union. All Right Reserved.

Consideration of JMA tilt meter data around volcano using boundary element method (2)

*Ryohei Kawaguchi[1]

1. Meteorological Research Institute

Small volcano deformations detected by tilt meters installed around carter were important to monitor and evaluate the volcanic activity. Japan Meteorological Agency has been installing the tilt meter station around the crater at active volcano. Because these deformation data observed around crater were affected by the topography of volcanic edifice, it is important to consider the topographic effect for the analysis of the estimation of pressure source. When the location of pressure source was estimated above the observation station, the amount of tilt change was not well calculated by the assumption of elastic half space. In this study, to develop the evaluation tools of volcanic deformation data due to shallow pressure sources, we calculate volcanic deformation due to shallow pressure sources by using the 3-d boundary element method (BRM). The boundary element method could calculate the volcanic deformation on any surface topography by the pressure source of any shapes. We express the topography of Nasudake using the 10 m mesh digital elevation data (DEM). Nasudake has a tilt meter around crater which located a distance of about 600 m from the summit and at an altitude of about 1700 m. We calculate tilt changes on this tilt observation station assuming the spherical pressure sources located above sea level. Our calculation results show that, when the altitude of the pressure source was around sea level, the tilt change observed by the tilt station were larger about several percent compared to the case of assuming the elastic half space. When the altitude of the pressure was higher than 1000m above sea level, the amount of tile changes calculated by the BEM was several times larger than that of the case of assuming the elastic half space. These results indicate that in the analysis of tilt change data due to shallow pressure sources, the effect of topography affects the estimation results such as the depth and amount of change of pressure sources.

Keywords: tilt change, BEM, volcano deformation

©2020. Japan Geoscience Union. All Right Reserved.

Imaging of the volcanic activity process beneath the Yugama crater at Kusatsu-Shiranesan volcano

*Akimichi Takagi[1], Tsukasa Kobayashi[1], Takahiro Kitagawa[1], Kousuke Takahashi[1], Koji Kato[1], Jun’ichi Miyamura[1]

1. Seismology and Volcanology Department, Japan Meteorological Agency

Around the Yugama crater at Kusatsu-Shiranesan, seismic activity, crustal deformation, and other fluctuations have appeared since 2014, and activity has increased. Although a small phreatic eruption occurred at the Moto-Shiranesan crater in 2018, no eruption has occurred from the Yugama crater. The 1983 eruption from the Yugama crater was the last one.

At the Yugama crater, various observations have been conducted since around 1970. From the viewpoint of medium- to long-term activity evaluation, volcanic activity in the past several decades was examined comprehensively by collecting and organizing past geochemical and geophysical observations and research results.

The volcanic phenomenal sources estimated by various observations were plotted. Most of the pressure sources obtained by GNSS and EDM (Takagi et al., 2018), the demagnetization sources obtained by repeated measurements of total magnetic intensity (Takahashi et al., 2014) and the hypocenter of volcanic earthquakes were located in the same area on the northeast side of Yugama crater. The hypocenter was located at an altitude of around 1000 m above sea level, but the pressure sources and demagnetization sources were located at shallower than the earthquake occurrence area. Nurhasan et al. (2006) showed that a low resistivity layer exists in this region shallower than the altitude of around 1000 m above sea level, and proposed that a fluid reservoir exists below this layer.

Based on these observations and the spatio-temporal relationship of various phenomena those have been repeated at the shallow part beneath the Yugama crater, we tried to build a conceptual model of the activity process from the viewpoint of the inflow and outflow of volcanic fluid around the fluid reservoir (Hirabayashi, 2000). And then we consider how to monitor and evaluate volcanic activity of Kusatsu-Shiranesan.

Keywords: Kusatsu-Shiranesan, Yugama crater, phreatic eruption, fluid reservoir

©2020. Japan Geoscience Union. All Right Reserved.

Self-potential and geomagnetic total intensity observations at Motoshirane volcano after the 2018 eruption (2)

*Akira Yamazaki[1], Hideki Iino[1], Shin Akira[1], Jun Shimokawa[1]

1. Kakioka Magnetic Observatory

A phreatic eruption occurred at Kusatsu-Shirane volcano (Motoshirane volcano) on January 23, 2018, and some craters were formed on the Kagamiike crater-floor and the Kagami-ike northern crater. After the eruption, the temporarily activated seismic activity near the crater has declined, and the fumarolic activity has ceased after late February 2018.
In order to estimate geothermal status after the eruption, we carried out self-potential (SP) and repeat geomagnetic total intensity observations at Motoshirane volcano in 2018 to 2019. The first measurements of the SP were conducted at about 130 points around the summit of Motoshirane volcano from June 30 to July 2, 2018. Copper-Copper sulfate electrodes were used, the measurement interval was about 50 m, and the measurement was carried out by the so-called full potential method. The second measurements were conducted form July 2 to July 4, 2019 at the same survey lines as the first. We applied -1.51 mV/m as correlation coefficient for correction of the topographic effect to all the SP measurement stations. As a result of the SP, we detected a positive anomaly, 200-500mV in magnitude, developing around the summit of Motoshirane volcano. By comparison of the result of the 2018 and the 2019 observations, there was no remarkable changes in the SP distribution. In detail, tens of mV decline of the SP voltage was observed during one year around north-east from Kagami-ike northern crater where was main crater of the 2018 eruption. This may suggest to tend to subside of the volcanic activities.
As for the geomagnetic total intensity observation, we made ten repetitive observation stations around the summit of Motoshirane volcano, and carried out five times observations from 2018 to 2019. As a result, no significant changes in the geomagnetic total intensity during those two years. It suggests that thermal demagnetization or magnetization by cooling does not occur at underground of Motoshirane volcano.

Keywords: Kusatsu-Shirane volcano, Motoshirane volcano, Self-potential observation, Geomagnetic total intensity observation, Thermal demagnetization

©2020. Japan Geoscience Union. All Right Reserved.

Crack resonances at an LP source beneath Kusatsu-Shirane volcano triggered by volume changes with vapor condensation

*Kimiko Taguchi[1], Hiroyuki Kumagai[1], Yuta Maeda[1]

1. Nagoya University Environmental Studies

Long-period (LP) events observed at active volcanoes have been considered to be generated by the change of the fluid pressure in a fluid-filled resonator. The frequencies and *Q* factors for decaying oscillations of observed LP waveforms depend on the resonator geometry and fluid properties at the source, and their spectra change with the excitation defined by the area where the fluid pressure change applied. Taguchi et al. (*J. Geophys. Res.*, 2018; AGU Fall Meeting, 2019) developed the method to estimate the resonator geometry and fluid properties simultaneously based on the crack model (Chouet, *J. Geophys. Res.*, 1986), and analyzed LP events at Kusatsu-Shirane volcano, Japan, in 1992 and 1993. From their estimates and dilatational initial motions of the observed waveforms, they interpreted that the LP events were generated by the resonance of an existing crack containing water vapor and mist which was produced by condensation of the vapor within a constant length from the crack edge. However, this triggering process was not discussed quantitatively.

To resolve this problem, we estimated the excitation area where the fluid pressure changed and the fluid volume change for an LP event on 2 November 1992. We first numerically simulated far-field seismograms generated by the crack resonances with various excitation areas, then compared their spectra with those of the observed LP waveforms. In our simulations, we used the values of the crack geometry and fluid properties estimated by Taguchi et al. (2018). The observed spectra showed dominant spectral peaks with the estimated wavelengths of $2L/3$ and $2L/5$, where L is crack length. These peaks were dominantly appeared when we applied the fluid pressure change over a narrow strip located at one edge of the crack length and across the entire width of the crack. This excitation is consistent with that proposed by Taguchi et al. (2018), which suggested that the condensation of water vapor within a constant length from the crack edge triggered the observed event. Next, we estimated the fluid volume change associated with the occurrence of the LP event. The values for crack geometry and fluid properties shown by Taguchi et al. (2018; 2019) were estimated from the decaying parts of the observed waveforms, which were generated by the crack resonances after the condensation and mist generation. Their estimates of crack length, width, and aperture were 160 m, 87 m, and 92 mm, respectively, and the crack volume was estimated to be 1300 m^3, in which the mist occupied 46 m^3. Assuming that all the mists in the crack were vapor, the vapor volume before the occurrence of the LP event was estimated to be 3500 m^3. If we consider that the volume decrease occurred at one edge of the crack length as shown by the estimated excitation area, the crack length was shortened by 280 m due to the condensation. Considering the fact that the decaying oscillations of the observed waveforms started after several seconds from the initial motion, our interpretation of the source process of this LP event is given as follows. First, the existing crack was opened by the supply of water vapor exsolved from magma. Condensation at the edge of the crack was observed as the initial dilatational motions of the observed waveforms and triggered the crack resonances. A part of the vapor became mist by the pressure change in association with the resonances, then the crack was closed from the edge where the first condensation occurred. After the mist generation, the resonances of the remaining part of the crack was observed as the decaying oscillations of the LP waveforms.

©2020. Japan Geoscience Union. All Right Reserved.

Forward analysis of seismic waves accompanied by tilt ground motion during the eruption of Mt. Motoshirane, Japan, on January 23, 2018

*Ryohei Takahashi[1], Yuta Maeda[1], Toshiki Watanabe[1]

1. Graduate School of Environmental Studies, Nagoya University

Mt. Kusatsu-Shirane is an active volcano located in the northwestern part of Gunma Prefecture. It is composed of Mt. Shirane, Mt. Ainomine, and Mt. Motoshirane. Most of the recent activities of this volcano have been seismic activities and crustal deformations near Yugama crater lake (e.g., Japan Meteorological Agency (JMA), 2018, Report of Coordinating Committee for Prediction of Volcanic Eruptions), whereas the last known magmatic eruption at Mt. Motoshirane was 1500 years ago (Nigorikawa et al., 2016, JpGU; Terada, 2018). From 10:02 JST on January 23, 2018, a phreatic eruption occurred at Mt. Motoshirane. New craters were identified along the east-west direction at the northern rim of Kagamiike crater lake after the eruption. Yamada et al. (2019, The Volcanological Society of Japan) investigated the source process of this eruption based on a seismic wave analysis. They applied the moment tensor inversion method of Nakano and Kumagai (2005) to the data in the following two time windows with different frequency bands: a 180-s-long window from 9:59 with a 10-50 s band, and the following 80-s-long-window with a 10-30 s band. Their results from the former and latter time windows were consistent with an open crack at a depth of 700 m and inclined cylindrical focal mechanism at a depth of 1000 m immediately beneath Kagamiike north crater, respectively. The source processes of the signals with periods longer than 50 s have not been investigated yet. Horizontal motions with a period of ~300 s were recorded during the eruption, which seems to mainly represent a tilt motion taking into account the natural period of the seismometer of 240 s. We are planning to investigate the source processes in these long period bands using the waveform inversion method of Maeda et al. (2011), which can take into account both the translational and tilt motions recorded by seismometers. In this presentation, we show the results of our preliminary forward analysis, where the observed waveforms were compared with synthetic ones taking into account both translational and tilt motions caused by a given source mechanism.

In this study, we calculated Green's functions of translational and tilt motions at three station sites, N.KSHV (Hoshimata), N.KSNV (Nikenya), and N.KSYV (Yazawahara)of V-net operated by the National Research Institute for Earth Science and Disaster Resilience. We used a 3D finite-difference method with a mesh size of 40 ×40 ×40 m . We assumed a compressional wave velocity $Vp=2500$ m/s, a shear wave velocity $Vs=1443$ m/s, and a density $\rho=2500$ kg/m^3 as typical structures of Mt. Kusatsu-Shirane and other active volcanoes. As the source mechanism, we used a north-south opening (east-west striking) vertical crack at 1200 m above sea level below the craters, assuming a source time function that changes from inflation to deflation, and calculated the waveforms with a time constant of 250 s. We then convolved the Green's functions with the seismometer's translational and tilt responses to produce synthetic waveforms where the both types of motions are taken into account. Results showed that the shapes and time constants of the synthetic waveforms were consistent with those of observed ones low-pass filtered at 10 s, except for the NS component of N.KSHV and N.KSNV. Especially, the observation that the horizontal components have much larger amplitudes than vertical ones was reproduced by the synthetic waveforms. These results suggest that the characteristics of the observed horizontal and vertical waveforms can be explained by the superposition of translational and tilt motions.

However, the assumed source location and mechanism did not reproduce the observed amplitude ratios

©2020. Japan Geoscience Union. All Right Reserved.

among the components and the polarities of several traces. We will try to explain them by investigating a better source location and mechanism using the waveform inversion method in the future.

This work was supported by JSPS KAKENHI Grant Number 19K04016.

Keywords: source mechanism, tilt motions

©2020. Japan Geoscience Union. All Right Reserved.

Real time monitoring of underground temperature in Jigokudani, Midagahara volcano using LPWA devices

*Tohru Watanabe[1]

1. University of Toyama

Jigokudani is an active geothermal area in Midagahara volcano, Toyama prefecture, central Japan. It was formed as a result of repeated phreatic eruptions over 40,000 years. Increased volcanic activity in this area has been observed since 2011. In order to detect a precursory signal of a phreatic eruption, observations should be conducted on seismicity, ground deformation, geothermal activity, volcanic gas, etc. A real time monitoring system of underground temperature using LPWA (Low Power, Wide Area) devices was tested in Jigokudani first in 2018. The LPWA devices send temperature data every 30 minutes to a gateway to the internet situated in Hotel Tateyama. Underground temperatures were monitored on internet devices. However, the monitoring system was unstable due to the vulnerability of LPWA devices to volcanic gas and rain. Some devices ceased measuring during the test. In 2019, a real time monitoring system was constructed with another LPWA devices. An LPWA device (netvox, R718CX2) has two thermocouples and a transmitter (LoRaWAN). 8 devices were deployed in Jigokudani. Thermocouples were placed at the depths of 10 and 50 cm. Short-period (~10 hours) variations in temperature are remarkable at 10 cm, while quite weak at 50 cm. Short-period variations come from the temporal change in the surface temperature. The heat flux can be estimated from temperatures at different depths.

Keywords: Midagahara volcano, Jigokudani, underground temperature

©2020. Japan Geoscience Union. All Right Reserved.

Development of a system for FEM-based crustal deformation analysis

*Tomokazu Kobayashi[1], Shinya Yamada[1]

1. GSI of Japan

Introduction

It has recently become possible to measure volcanic crustal deformation in a mountainous area in detail with the improvement of volcano observation techniques such as SAR. With this background, it is necessary to improve crustal deformation calculation for source modeling. Effects of topography and inhomogeneous underground structures should be taken into account for crustal deformation calculation at volcanoes. We have developed a crustal deformation analysis system using a three-dimensional (3D) finite element method (FEM) which is specified to volcanoes. In this presentation, we will introduce the outline of the system for FEM-based crustal deformation analysis, and show the effects of crustal deformation calculation incorporating topography and underground structure.

Overview of analysis system

The analysis system mainly consists of three processings: element division in a calculation domain, deformation calculation by 3D-FEM, and estimate of deformation source. Linear elastic deformation based on the infinitesimal deformation theory is considered. Deformation is calculated using Advance/FrontSTR software developed by the Advance Soft Corporation. In this system, 10m-mesh-size digital elevation model released by the Geospatial Information Authority of Japan is implemented, thus users can set up any land in Japan for an analysis domain, and perform crustal deformation calculation and source modeling there. Users can set an analysis domain (latitude, longitude, and depth), the number of element divisions, and the source information by graphical user interface (GUI) operation. In addition, three types of deformation sources; rectangular crack, sphere, and spheroid, which are often used in analyzing volcanic crustal deformation, can be selected from the GUI system. The calculation results are output in a “vtk” format file, and can be displayed and operated in 3D using the visualization software ParaView.

For improving calculation speed

In this study, in order to improve the computational efficiency, which is a disadvantage of FEM, we implemented several techniques such as infinite elements and partial-fine-meshing. In FEM calculation, artificial errors are produced due to the effects of side and bottom surfaces of calculation domain because calculations are performed within a finite area. Therefore, this system implements the function of infinite elements. By setting the infinite element at the horizontal and bottom boundaries excluding the ground surface, the calculation can be performed in the same way as adding a finite element reaching infinity to the boundary of the calculation domain. Furthermore, we implemented a function that finer meshes are set in the proximity of deformation source. By these implementations, we successfully improved the calculation speed without degrading calculation accuracy while preventing an excessive increase in the number of elements.

Effects of calculation incorporating topography and underground structure

The effect of topography and underground structure was investigated through calculations at actual volcanoes. Here we assumed an inflation source within the body of Mt. Ontake volcano, and examined how the ground deformation is affected by the position of the source. As a result, we found that the deformation is strongly affected by the topography when the source is located at the shallow part. We

©2020. Japan Geoscience Union. All Right Reserved.

demonstrated that the uplifted area turned into subsidence and the polarization of tilt turns out to be an opposite direction as the source position changes from deep part to shallow part. In addition, the effect of the underground structure was investigated at Sakurajima volcano. When we calculated the ground deformation with taking into account the underground structure obtained by seismic explorations, we revealed that the surface displacement increases by several tens of percentages in the proximity of the source, compared with the conventional method assuming a homogeneous medium.

Keywords: FEM, volcanic crustal deformation, topography, underground structure

©2020. Japan Geoscience Union. All Right Reserved.

Silisic magma reservoirs beneath Fuji Volcano, Japan, constrained from interstitial melt in gabbroic xenoliths

*Megu Otsuka[1], Hidemi Ishibashi[2], Natsumi Hokanishi[3], ATSUSHI YASUDA[3]

1. Graduate School of Integrated Science and Technology, Shizuoka University, 2. Shizuoka University, 3. Earthquake Research Institute,The University of Tokyo

Gabbroic xenoliths in the deposits of the 1707 eruption of Fuji volcano, Japan, sometimes include interstitial glass filling the space between euhedral mineral grains. These melt-beating gabbros are thought to be fragments of a crystal mush constituting a magma reservoir beneath Fuji volcano. In this study, chemical compositions of interstitial glasses and co-existing minerals in the gabbroic xenoliths are analyzed, and based on the results, pre-eruptive magmatic conditions and processes in the crystal mush are investigated.

The analyzed gabbro samples are classified into two groups, Goup-A and B, based on the interstitial glass compositions. In Group-A gabbros, interstitial glasses are rhyolitic (SiO_2~72.7-77.6wt.%) and homogeneous in each sample. On the other hand, chemical compositions of interstitial glasses in Group-B gabbros vary significantly from basaltic andesitic to dacitic (SiO_2~54.5-74.5wt.%) in each sample. Volume fraction of melt + bubble is higher in Group-A gabbros (23.8-35.2vol.%) than Group-B gabbros (0.8-14.8vol.%). In Group-A gabbros, composition of the interstitial glass coincides with that of the most SiO_2-rich plagioclase-hosted melt inclusions, suggesting that the interstitial melt of Group-A (melt A) is a residual melt of crystallization. In contrast, in Group-B gabbros, plagioclase-hosted melt inclusions are more silicic than the interstitial glasses. In addition, banded flow structure composed of chemically distinct glasses are found in interstitial glasses of Group-B gabbros. These suggested that permeable flow and mixing of chemically distinct melts occurred in Group-B crystal mush. Furthermore, Group-B gabbros are subdivided into two types, Group-B1 and B2; as SiO_2 content of interstitial glass increases, Al_2O_3 content decreases and increases in Group-B1 and B2 gabbros, respectively. These two compositional trends were formed by mixing between the same mafic end-member melt and two distinct silicic end-member melts. The melt-A is the silicic end-member melt in Group-B1 gabbros. In contrast, silicic end-member melt in Group-B2 gabbros is a dacite melt with a SiO_2 content of ~68.0wt.% (melt B). The results suggest that at least three end-member melts of rhyolitic, dacitic and mafic compositions exist in the crystal mush beneath Fuji volcano. Based on Fe-Ti oxide thermometry and plagioclase-melt thermohygrometry, the equilibrium temperatures and H_2O contents are estimated to be ~823℃ and ~7.4wt.% for the melt-A and ~863℃ and ~8.6wt.% for the melt-B, respectively. The estimated H_2O contents correspond to the H_2O-saturated depths of ~8.5km and ~13.5km for the melt-A and B, respectively. The estimated depths coincide with that of the low seismic velocity zone where low frequency earthquakes occur beneath Fuji volcano, suggesting the seismic activity may be related to crystal mush processes.

Keywords: Fuji Volcano, gabbro, interstitial melt, crystal mush, xenolith

©2020. Japan Geoscience Union. All Right Reserved.

Corrections of individual properties of relative gravimeters by using cooperative precise gravity measurement data in Izu-Oshima volcano

*Shin'ya Onizawa[1], Ryuichi Nishiyama[2], Shuhei Okubo[2,3], Yutaka Nagaoka[1], Yasuo Hirayama[4], Takanori Ishihara[4], Kensuke Matsuda[4], Yuya Kaneko[4], Yoshihiro Ueda[4], Yuichi Imanishi[2], Atsushi Watanabe[2], Miwako Ando[2], Shikou Sakashita[2]

1. Meteorological Research Institute, JMA, 2. Earthquake Research Institute, The University of Tokyo, 3. Southwest Jiaotong University, 4. Seismological and Volcanological Department, JMA

1. Introduction

Meteorological Research Institute, JMA (MRI) has conducted repeated microgravity surveys in Izu-Oshima volcano in order to understand volcanic processes. Two relative gravimeters, LCR D#109 and Scintrex CG-5#033, have been used since 2008. However, resultant data contain some uncertainties due to the relative measurements. Earthquake Research Institute, The University of Tokyo (ERI) has conducted hybrid absolute and relative gravity measurements. MRI and ERI started a cooperative observational study of Izu-Oshima volcano in order to help understanding subsurface processes of the volcano. In this presentation, we mainly show correction processes of properties of MRI relative gravimeters and show significances of the cooperative study.

2. Scale Factor Calibrations

As for the two MRI relative gravimeters, absolute scale factors were not well calibrated until recently. Relative scale factors between the gravimeters using maker-suppled scale factors show clear temporal change and its magnitude reaches up to 1,000 ppm within ten years. Since gravity difference in Izu-Oshima is about 180 mGal, this temporal change can lead to about 180 μGal of false gravity changes. Further, it seems the relative scale has a non-linear relationship in low dial ranges of the D#109.

2.1 D#109

MRI conducted calibration measurements of the D#109 at Izu-Oshima in May and June 2017 by visiting the two ERI absolute gravity sites (111 mGal of difference). While the maker-supplied scale factor coincides with the measured one with an accuracy of approximately 10^{-4} in the high dial range, it deviates significantly in the low dial range as expected from the non-linear characteristics of the relative scale factors. Therefore, we reconstructed the scale factor for the low dial ranges by using this calibration measurement data.

2.2 CG-5#033

Six calibration measurements of the CG-5#033 were conducted from 2012 to 2017 using absolute gravity sites of the Japan Gravity Standardization Net (JGSN). According to the dataset, the scale factor depends primarily on the gravity reading ranges regardless of site combinations and observed times. Therefore, the gravity readings can be corrected by introducing a reading-dependent scale factor. Further, even though the scale factor essentially depends on gravity readings and not on time, temporal changes were

©2020. Japan Geoscience Union. All Right Reserved.

recognized during repeated measurements at the same site combinations. A long-term instrumental drift could explain this phenomenon. That is, the calibration shifts during repeated measurements were apparently caused by: 1) the scale factor dependence on the gravity reading ranges, and 2) the shift of the gravity reading ranges due to the instrumental drift (Onizawa, 2019). The temporal changes found in the relative scale factors can be attributed to this apparent calibration shift of the CG-5#033.

2.3 Verifications

A cooperative hybrid measurement was conducted at Izu-Oshima in Nov. 2018. The scale factors of the D#109 and CG-5#033 constructed as mentioned above were checked by using gravity values of the two absolute sites. Gravity differences observed by both the gravimeters coincided well with that of the absolute measurements (1 μGal of difference). The coincidence of the CG-5#033 is particularly important because the reading-dependent scale factor relationship was constructed by completely independent dataset. Further, we could verify that prominent calibration shift did not occur in the D#109.

3. Effect of Vertical Gravity Gradients on Instrumental Height Correction

MRI has conducted *in situ* vertical gravity gradient measurements at Izu-Oshima gravity sites in order to quantify gravity changes due to ground deformations, particularly vertical movements. For over 20 sites where the gradient was measured, the gradients range from 0.30 to 0.44 mGal/m. These vertical gradients play an important role in the instrumental height corrections in case that different types of gravimeters such as LCR and Scintrex are used because of the difference of the effective instrumental height. Uses of inappropriate vertical gradient easily lead biases up to several tenth μGal (e.g. Lederer, 2009). For the 2018 campaign data, we applied site-dependent vertical gravity gradients to the height corrections of both the D#109 and CG-5#033. Except for two sites of about 30 μGal difference, gravity values of the two gravimeters coincide within 14 μGal of difference.

Acknowledgements

We are grateful to the staff of Geodetic Department, The Geospatial Information Authority of Japan, for providing data on the JGSN sites and for consultation on measurements at the sites. This study was supported by ERI JURP 2018-G-12.

Keywords: Izu-Oshima volcano, gravity

©2020. Japan Geoscience Union. All Right Reserved.

Temporal gravity change observed on Izu-Oshima Island in 2010's

*Ryuichi Nishiyama[1], Yuichi Imanishi[1], Shin'ya Onizawa[2], Shuhei Okubo[1,3], Miwako Ando[1], Atsushi Watanabe[1], Shikou Sakashita[1], Yutaka Nagaoka[2], Yoshiyuki Tanaka[4], Hidefumi Watanabe[1,5]

1. Earthquake Research Institute, The University of Tokyo, 2. Volcanology Research Department, Meteorological Research Institute, JMA, 3. Southwest Jiaotong University, 4. Graduate School of Science, The University of Tokyo, 5. Disaster Prevention Division, Tokyo Metropolitan Government

We report on the gravity observation on Izu-Oshima Island during 2010’ s with the aim of detecting mass movement associated with magma accumulation beneath the island. The gravity measurement campaign was performed at around 30 stations on the island in 2012, 2017 and 2018. The result shows a gravity decrease of ~70 microgal at the southern coastal region and a gravity increase of ~90 microgal at the caldera region during 6 years from 2012 to 2018. To interpret these temporal gravity changes into the magma accumulation, the following two gravity contributions must be properly corrected: (i) the free-air gravity change due to the uplift or subsidence of the observation site; (ii) the disturbances caused by rainfall and groundwater. The former can be monitored by performing relative gravity survey at the four GEONET stations on the island. The latter can be corrected with physical modeling and continuous absolute gravity measurements on the island (Nov. 2019 –Mar. 2020).

Keywords: Izu-Oshima Island, gravity, volcano

©2020. Japan Geoscience Union. All Right Reserved.

Vesiculation texture and change in the amount of phenocrysts of the summit eruption of the Izu-Oshima volcano - Comparison between the An'ei and the 1986 eruption -

*Yuya Ikenaga[1], Fukashi Maeno[1], ATSUSHI YASUDA[1]

1. Earthquake Research Institute, The University of Tokyo

Izu-Oshima is one of the most active basaltic volcanoes in Japan that caused eruptions for many times. In 1986, there were Strombolian eruption and lava effusion from the summit crater, and lateral craters caused subplinian eruption and lava effusion for several days (e.g. Endo et al. 1988). The last large-scale eruption, the An’ ei (Y1) eruption, started in 1777 with approximately one-year scoria ejection from the summit crater and lava effusion from the mountainside (basal scoria period) (Nakamura 1964, Tsukui et al. 2009).

There are differences between Y1 and 1986 eruptions in the characteristics of eruption from the summit crater. In the basal scoria period of Y1 eruption, thick scoria layer was formed outside the caldera rim. The amount of plagioclase phenocrysts (Pl) in scoria and the intensity of scoria ejection both increased as the eruption proceeded (Misonou et al 2005, Ikenaga et al. 2018). On the other hand, about the summit eruption in 1986, the amount of Pl was nearly constant (Fujii et al. 1988) and the intensity was weak that almost all scoriae deposited inside the caldera.

In this study, we conducted density measurements and textural observations of scoriae, and compared them between Y1 and 1986 eruptions. In Y1 eruption, the change in the amount of Pl was investigated in detail at the outcrop in the B2 crater of 1986 eruption nearby the summit crater.

The ejecta in the later stage of Y1 eruption (Unit C) contain more dense scoriae than those in the early stage (Unit A). The density of 1986 scoria was lower than those of 2 units of Y1. The scoriae of Unit A contain many small bubbles and some particles are bubbly like reticulite. The scoriae of Unit C also contain small bubbles, but bubbles are surrounded by thick glass walls. The scoriae of 1986 eruption hold larger bubbles than those of Y1. Based on the geological study that Unit C was more intense than Unit A (Ikenaga et al. 2018), it is assumed that there was not enough time to vesiculate because of fast ascent of magma in Unit C, whereas magma vesiculated during slow ascent of magma in Unit A. It is possible that in 1986 eruption large bubbles were formed as a result of expansion and interconnection during slower magma ascent than Y1 eruption.

The amount of Pl in Y1 eruption increased in a step-like form in terms of stratigraphic level. The deposits of Y1 eruption can be divided into several layers in which the clast size is constant, and the steps of Pl amount coincide with boundaries between layers. It is indicated that there is some system in the magma chamber that the amount of Pl increases according to the time that passed since the onset of the eruption, if the boundaries indicate pauses of the eruption. Because of this, it is assumed that the amount of Pl increased in Y1 eruption that the basal scoria period continued for approximately 1 year, and that the amount of Pl was constant in 1986 summit eruption of which the main phase continued for only several days.

©2020. Japan Geoscience Union. All Right Reserved.

Keywords: Izu-Oshima, density of ejecta, vesicularity, change in phenocryst amount

©2020. Japan Geoscience Union. All Right Reserved.

A study on surface displacement and pressure source of Kozushima Island based on InSAR analysis

*Wataru Uehara[1], Yoshiya Oda[1]

1. Tokyo Metropolitan University

Currently, there’re more than 100 active volcanoes in Japan. Volcanic activities such as eruption could cause serious disasters. To prevent volcanic disasters, it’s necessary to know the details of volcanic activity. To evaluate surface displacement of Kozushima Island, a volcanic island belonging to Tokyo, we’ve conducted InSAR (Interferometric Synthetic Aperture Radar) analysis. In addition, we've conducted the inversion analysis to evaluate pressure source position.

InSAR analysis is a technic to conduct interferometric analysis for multiple data observed by SAR mounted on the satellite, and we’re able to grasp the surface displacement from the analysis result. In this study, we used SAR data observed by ALOS-2, Japanese satellite, and Sentinel-1A, European Union satellite.

As a result, from December 4, 2014 to November 29, 2018, we detected surface displacement of approx. 4 cm several times. In particular, relatively large surface displacement was detected around Mt. Tenjosan located in the northeastern part of the island.

Discoloration of seawater around Kozushima Island was also observed several times during the period when such a large surface displacement was detected. If these discoloration of seawater are related to volcanic activity, the large surface displacement around Mt. Tenjosan could be also related to volcanic activity. We confirmed that the deference between the displacements based on InSAR analysis and those of GPS-based control station were within 3 cm and the result of InSAR analysis using Sentinel-1A indicate same trend.

In order to estimate the pressure source position, we’ve conducted an inversion analysis Simulated Annealing algorithm (Kirkpatrick et al., 1983). As the results of inversion using the data of large surface displacement during which the seawater discoloration were observed, spherical pressure sources were estimated at approx. 6 km depth in southeast, approx. 1 km depth in northeast, approx. 7 km depth eastern, and approx. 6 km depth northeast of Kozushima Island. The latter three estimated positions correspond with the higher seismicity area during the period 2013 and November 29,2018.

Keywords: Kozushima Island, InSAR analysis, Evaluation of pressure source

©2020. Japan Geoscience Union. All Right Reserved.

Automatic Seismic Wave Detection with Deep Learning - Application to temporary observation data at Hachijojima Island -

*Ryohei Tottori[1], Hiroyuki Azuma[1], Yoshiya Oda[1], Toshifumi Matsuoka[2]

1. Tokyo Metropolitan University, 2. Fukada Geological Institute

There are 111 active volcanoes in Japan, of which 50 volcanoes have been selected as "volcanoes that require enhanced monitoring and observation systems for volcanic disaster prevention." Geophysical studies using natural earthquakes, such as imaging the crustal structure beneath a volcano, are important for evaluating the eruption risk of a volcano. However, the current seismicity around Hachijojima Island where studying area is low. Therefore, thepurpose of our research is to detect small earthquakes that had not been picked before by seismic wave automatic detection using a deep learning technology.

Machine learning technology, especially deep learning, automatically extracts many features from earthquake data with labels indicating Pwave,Swave, noize. In previous studies using machine learning, because of hardware problems thatthe computational speed was slow, and because of simple network structure, sufficient results could not be achieved.

However, recently due to the development of computational technology such as Graphic Processing Units (GPU), successful results has been obtained.

In this study, we used the Generalized Phase Detection framework (GPD) consisting of a Convolutional Neural Network (CNN) model (Ross et al., 2018). GPD has been trained using earthquakes labeled by analysts at the Southern California Seismic Network (SCSN).

First, we have applied GPD to the continuous seismic waveform data observed by the F-net seismometer at Hachijojima Island, and then GPD was applied to the waveform data obtained by our temporary earthquake observation in Hachijojima Island.

As a result, in both data, we were able to detect more earthquakes than the number of earthquakes currently published by the Japan Meteorological Agency. However, since GPD is a network using CNN and recognizes the waveform as an image, it is picked based on the learned features regardless of the relationship of the P-S time series. Thus, the P-wave-only earthquake and S-wave-only earthquakes were detected.

In the future, we will examine the validity of the detected earthquakes and apply a time series data analysis using the Recurrent Neural Network.

Keywords: Deep Learning, Convolutional Neural Network, Hachijojima Island, Automatic Seismic Wave Detection

©2020. Japan Geoscience Union. All Right Reserved.

Temporary dense seismic observation in Hachijojima Island

*Ryotaro Kanemaru[1], Yoshiya Oda[1], Hiroyuki Azuma[1], Kentaro Omori[1], Syotaro Kanke[1], Toshiki Watanabe[2]

1. Tokyo Metropolitan University, 2. Earthquake and Volcano Research Center Graduate School of Environmental Studies, Nagoya University

There are 111 active volcanoes in Japan and 50 of them are continuously monitored for volcanic disaster prevention. Hachijojima Island is one of the 50 monitored volcanoes.There was no record of eruption after the eruption in 1605, and the volcanic activity was calm. However, a dike intrusion was estimated beneath Nishiyama in Hachijojima Island during the 2002 earthquake swarm (Kimata et al., 2004).
From the above background, Tokyo Metropolitan University is engaged in imaging of volcanic structure beneath Hachijojima Island as part of research project on volcanic disaster mitigation.Temporary dense seismic observation was performed to obtain volcanic structure with enough resolution. We have installed 45 seismographs in Hachijojima Island, mainly around Nishiyama, and 1 seismograph in Hachijokojima. Total number of seismic stations was 46.The observation period was approximately seven months from September 2019 to March 2020. The seismometer we used was a 1 Hz velocity type seismograph (LE-3DLite MkIII) and off-line type data recorder (GSX) for continuous recording at a sampling frequency of 250 Hz.
By this Temporary observation, in addition to earthquakes listed in JMA hypocenter bulletin, it was possible to detect earthquakes that could not be determined from the conventional seismic network.
In this paper, we introduce the outline of the temporary dense seismic observation and preliminary results of the hypocenter determination.

Reference
Fumiaki Kimata, Meilano Irwan and Keita Fukano (2004) Ground Deformation at Hachijo Island, Japan on 1322 August 2002 Observed by GPS Measurements and Estimated Dike Intrusion Model. Volcano, 49, 13-22.

Keywords: Hachijojima Island, Temporary dense seismic observation, hypocenter distribution

©2020. Japan Geoscience Union. All Right Reserved.

Lava discharge rate in Nishinoshima volcano, Ogasawara Islands revealed using ALOS-2/PALSAR-2

*Shinobu Ando[1], Satoshi Okuyama[2], Shinichi Matsusue[3]

1. Seismology and Tsunami Research Department, Meteorological Research Institute, 2. Volcanology Research Department, Meteorological Research Institute, 3. Volcanology Division, Japan Meteorological Agency

Nishinoshima volcano, Ogasawara Islands, where the eruption began in November 2013, the eruptive activity is still continuing to this day. Eruptive activities are roughly classified into the following four phase:
Phase I: Nov.2013–Dec.2015
Phase II: Apr.2017–Aug.2017
Phase III: Jul.2018–Aug.2018
Phase IV: Dec.2019–(ongoing)
The lava flow associated with the eruption activity reached the coast and expanded land area, except for the eruption during the third phase. The land area in Nishinoshima volcano measured from the amplitude images obtained with ALOS-2/PLASAR-2 is approximately 3.2 km^2 as shown in Fig. 1 (as of January 31, 2020).
We have been analyzing mainly crustal deformation around large-scale earthquakes and volcanoes using ALOS-2/PLASAR-2 data since August 2014. ALOS-2/PLASAR-2 has been imaged in multiple observation modes around Nishinoshima. In particular, the spotlight (SPT) mode observation (resolution 3m (range) x 1m (azimuth)) newly installed in PALSAR-2 is observed every 14 days, which is almost equal to the number of regression days. For this reason, high spatial resolution and high temporal resolution observations have been realized in Nishinoshima.
In this presentation, we mainly discuss coherence image analysis using SPT mode observation. The coherence image is obtained by imaging the correlation degree distribution of each pixel unit from 0 to 1 by accurately aligning the observation data of the two periods. If the active volcanic activity continues, its surface will change every moment, and the degree of correlation will decrease significantly over time. However, it was found that the SPT mode data that can be acquired every 14 days maintains a very high degree of correlation when no eruption occurs. Therefore, assuming that the low degree of correlation during the eruption corresponds to the lava flow area, we calculated the lava discharge rate at each interval. The thickness of the lava was assumed to be 2.5–5 m on land and 10 m on the sea area from the report of the Earthquake Research Institute of the University of Tokyo (ERI). As a result, the average lava discharge rate for each eruptive activity period is as follows (see the figure for the time series):
Phase I (Second half: Mar.2015–Dec.2015): 0.09–0.16 x 10^6 m^3/day
Phase II (Apr.2017–Aug.2017): 0.10–0.18 x 10^6 m^3/day
Phase III (Jul.2018–Aug.2018): 0.04–0.07 x 10^6 m^3/day
Phase IV (Dec.2019–Mid-Feb. 2020): 0.21–0.38 x 10^6 m^3/day
Maeno et al (2016) estimates that the average lava discharge rate in Phase I (first 15 months) is 0.2 x 10^6 m^3/day and that in its peak period (September 2014) is 0.5 x 10^6 m^3/day. Comparing our results with these results, we found that the Phase IV eruptive activity, which began in December 2019, has a lava discharge rate comparable to Phase I. We would also like to discuss the distance changes in the satellite line-of-sight extension that are frequently detected near lava flows.
The PALSAR-2 data were prepared by the Japan Aerospace Exploration Agency (JAXA) via Coordinating Committee for the Prediction of Volcanic Eruption as part of the project 'ALOS-2 Domestic Demonstration on Disaster Management Application' of the SAR analysis of volcano Working group. The PALSAR-2 data belongs to JAXA. Gamma and RINC (Ozawa et al, 2016) were used for PALSAR-2 analysis. In the process of

©2020. Japan Geoscience Union. All Right Reserved.

the InSAR, we used ‘the digital elevation map 2.5m-mesh’ provided by the Geospatial Information Authority of Japan (technical data: C1-No.448, 453, 458, 462, 463, 478, 489). We used GMT (Wessel and Smith, 1998) to draw the map.

Keywords: ALOS-2/PALSAR-2, spotlight mode, coherence analysis, lava discharge rate, Nishinoshima

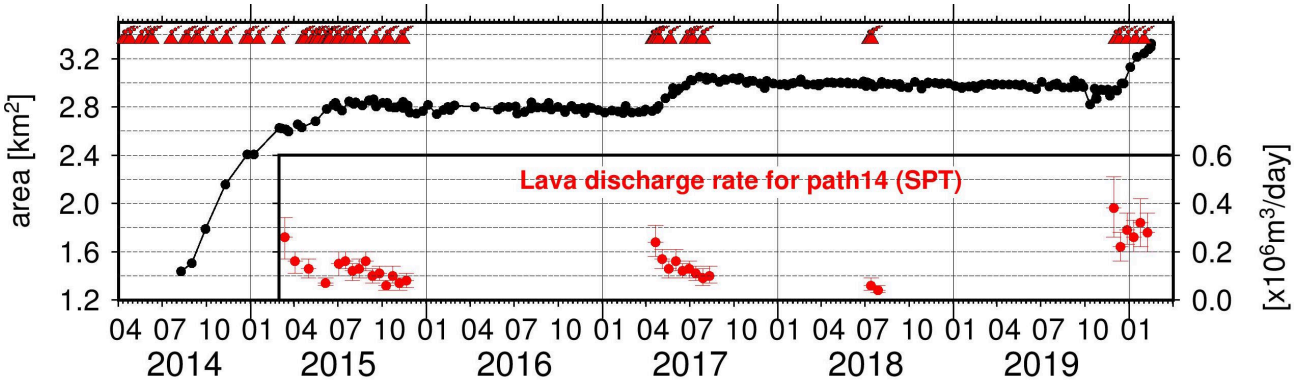

Fig. Time series in a land area of Nishinoshima measured by all ALOS–2/PALSAR–2 amplitude images, and lava discharge rates estimated from coherence images in spotlight mode (Path14).

©2020. Japan Geoscience Union. All Right Reserved.

Spatial variation of magma compositions at the Abu Monogenetic Volcano Group, SW Japan

*Kenyo U[1], Koji Kiyosugi[1], Yasuko Itoh[2], Yoshiyuki Tatsumi[1]

1. Kobe University, 2. Hagi Geopark Promotion Division

To mitigate volcanic hazard of volcanic fields, understanding of temporal-spatial migration of vents and evolution of magma composition is important. The Abu Monogenetic Volcano Group (AMVG) is a late Cenozoic volcanic field composed of basaltic to rhyolitic lava flows distributed over a district of 400 km^2. We investigated the whole rock chemical composition of these lava flows to determine the evolution of magma of the AMVG. It is known that the AMVG classified into early (2-1.6 Ma) and late (<0.8 Ma) period. In this study, we focus on the monogenetic volcanoes in the late period.

Spatial variation of magma composition shows that relatively primitive basaltic magma erupted in the east area of the AMVG, whereas, silicic magma erupted in the west area. The relatively primitive magma has features of extraordinary high Cr content (>120 ppm) and Ni content (>300 ppm), low FeO*/MgO (<=1.1). The silicic magma (SiO_2 <=60 wt%) has features of high Sr content (>600 ppm), low Y content (<= 18 ppm), and low Nb content (<16 ppm). It contains smaller amount of REE than basaltic magma, suggesting that these magmas are originated from different magma source. The chemical composition of volcanoes in the middle area can be explained by mixing of these two end members: the composition gradually changes from east (basaltic) to west (silicic).

These results suggest that magma evolution of volcanic fields is also complicated as that of stratovolcanoes. Further investigation of magma evolution at volcanic fields including the AMVG is required to understand the entire mechanism.

Keywords: Monogenetic Volcano Group, Spatial variation, Whole rock chemical composition, Southwest Japan

©2020. Japan Geoscience Union. All Right Reserved.

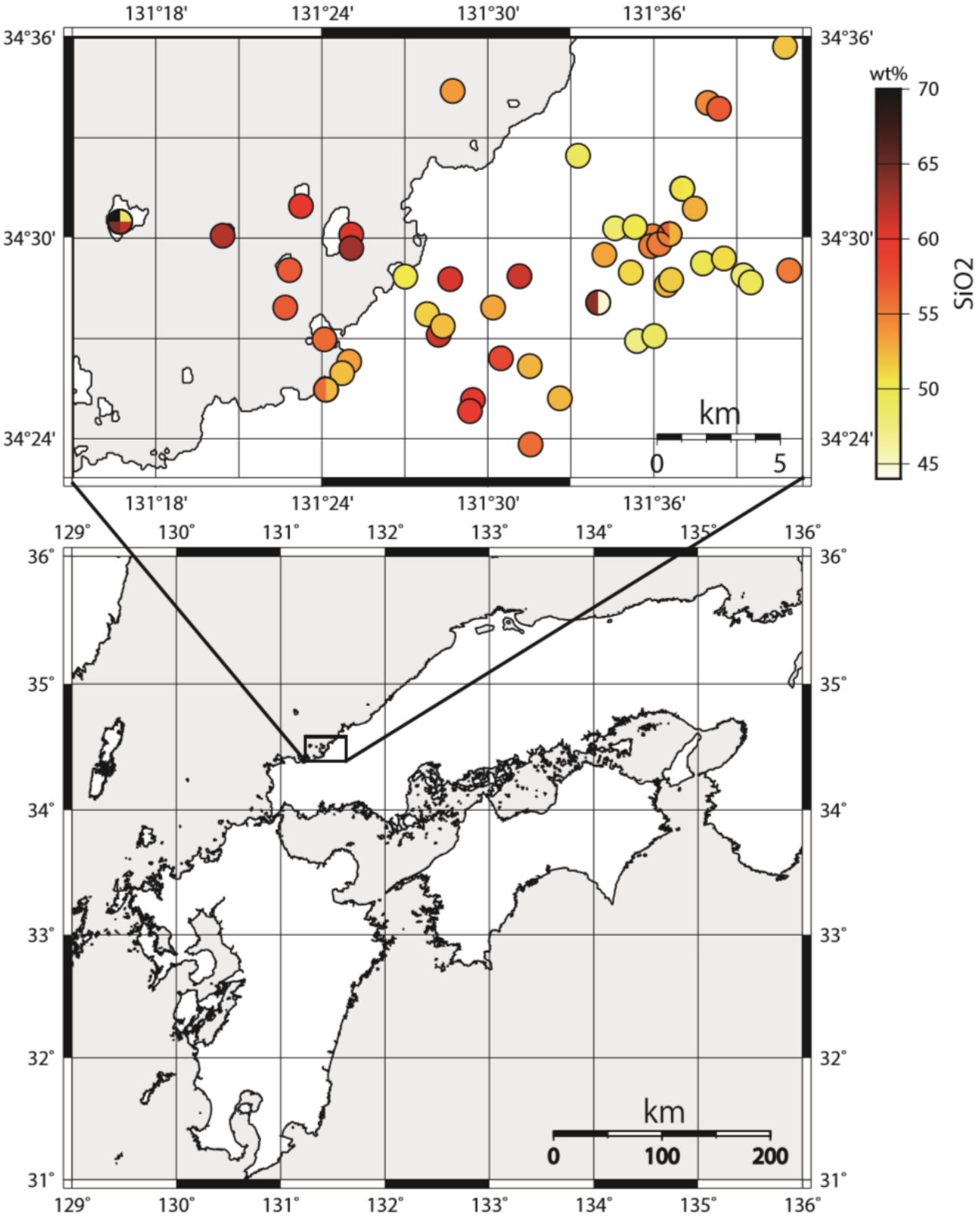

©2020. Japan Geoscience Union. All Right Reserved.

Repeated aeromagnetic survey on Kuju Volcano using drone, unmanned multicopter.

*Mitsuru Utsugi[1], Takeshi Hashimoto[2], Akinori Satoh[2], Noriko Tada[3], Toyonobu Ota[4], Shin Yoshikawa[1], Hiroyuki Inoue[1]

1. Kyoto University, 2. Hokkaido University, 3. JAMSTEC, 4. Tierra Tecnica

On Kuju Volcano, central Kyushu, Japan, the continuous and repeated magnetic observations had been performed since the phreatic explosion in 1995, and a remarkable temporal magnetic field change was observed, which is the increase of the magnetic total force on the south, and the decrease on the north, of the Iwoyama volcano, and this suggests the subsurface rocks were magnetized by cooling.
On this Volcano, Kyoto University conducted a high-density aeromagnetic survey around Iwoyama in December 2004. In this survey, an observation bird equipped with a magnetometer (G858 producted by Geometrix inc.) and GPS was towed by a helicopter, and magnetic anomalies (magnetic total force) were observed in 2 km x 2 km area around Iouyama volcano with an altitude of about 150 m from the ground.
In Oct. 2019, we conducted aeromagnetic survey on this area using a unmanned muiti-copter with the aim of detecting the temporal changes during 2004 to present. In this observation, the magnetic total force was measured using the drone aeromagnetic measurement system GSMP35U-DR of Tera Tecnica inc., which consists of a drone Matrice600pro (DJI), and potassium magnetometer GSMP-35U (GEM system inc.). In order to eliminate the noise generated by the drone, the magnetometer sensor was suspended for about 2.5 m, and the total force was measured at a sampling interval of 0.05 seconds. In addition, the data measured by GPS equipped with Matrice600pro was used as the position data.
Using this observation system, we conducted aeromagnetic survey in the part of the flight route in 2004, which is EW about 1 km, and NS about 2 km around Iwoyama. From the obtained data, we picked out the points whose distance between the nearest point of 2004 survey is less equal 20 m, and compared with their observed data. As a result, we detected the magnetic field change correspondig to the ground survey results, and it is suggesting that our repeated aeromagnetic survey had succesfully detected a temporal change during 2004 to 2019.
At present, in order to further examine this results, a data analysis is being performed using an analysis method based on the mis-tie control method proposed by Nakatsuka et al. (2006). In this presentation, we will show the results of our data processing in detail.

Keywords: Kuju volcano, repeated aeromagnetic survey, drone

©2020. Japan Geoscience Union. All Right Reserved.

Seismo-acoustic signals before ash emissions at Aso volcano, Japan

*Akihiko Yokoo[1]

1. Graduate School of Science, Kyoto University

Aso volcano located in southwest Japan has continued ash venting since July in 2019. We could not identify any stop of emission of ashes for more than several months. At the beginning of this eruption activity, however, clear hiatuses of the emission could sometimes be seen. Before each onset of individual ash venting, characteristic seismo-acoustic signals were recorded. The features are as follows: About half a day before the eruption onset, the amplitude of the continuous tremor (few-10 Hz) gradually increased. Almost at the same time, occurrences of infrasound pulses started to appear. These infrasound pulses have a dominant frequency of 3-10 Hz. To extract individual infrasound pulses from the raw records, the author used the Matched-Filter method with Network Correlation Coefficient. Consequently, a total of 2000-3000 pulses were identified for each event. Both the occurrence frequency and amplitude of the pulses showed a gradual increase with time. They were synchronized with an increase of tremor's amplitude. Two hours before the eruption, infrasound pulses and seismic tremor share a time of peak activity within 10-30 min difference: the peak in the seismic activity, then the infrasound activity. Immediately after the peaks were recorded, the activities decreased sharply and followed by the start of the eruption after a 30-min hiatus. According to the analysis of the tremor's amplitude by the Amplitude Source Location method, the source location of the continuous tremor source is situated at a shallow portion beneath the active crater, <300 m, however slightly off in the horizontal direction (Ichimura et al., 2019, EPS). For cases in 2019, temporal variation of ratios of the amplitude in a network of the station was clearly identified. This observation suggested that the source had moved toward the crater by the time of the eruption. It seems to relate an increase of gaseous fluid flux into the crater. Thus intermittent small gas explosions with infrasound pulses might have occur in the crater. However, each explosion was confirmed not to be associated with a Very-Long-Period earthquake or an explosion earthquake. The following points are also unclear: 1) How to start the ash emission itself after a 30-min hiatus, and 2) physical meaning of such hiatus of seismo-acoustic activity. Understanding these processes will be a clue for our further advancement toward the prediction of an eruption.

©2020. Japan Geoscience Union. All Right Reserved.

Waveform analysis of infrasound pulses observed before the phreatomagmatic explosion on October 23, 2015

*Yuto Kozawa[1], Akihiko Yokoo[1]

1. Graduate School of Science, Kyoto University

A phreatomagmatic explosion is hazardous because it scatters ballistic projectiles and pyroclastic flows around the crater. Therefore, society demands to predict its occurrence. To attempt this, it is necessary to understand the mechanisms of the explosion itself and also related processes progressing beneath the crater before an occurrence of the explosion. In this study, we analyze infrasound pulses of Aso volcano, which were observed several days before explosions in 2015.

At Nakadake 1st crater of Aso volcano in Japan, phreatomagmatic explosions occurred in the early morning of October 23, 2015. Before the occurrence of explosions, tones of infrasound pulses were observed around the crater. These pulses started to appear three days before the explosions. In the beginning, the maximum amplitude of the pulses was 1 Pa at 200 m distance: however, it gradually increased and reached to 60 Pa at 10 hrs before the explosion. The occurrence frequency of the pulses, which was initially small about once every two minutes, increased with each passing day. It consequently reached 20 pulses per min four hrs before the explosion. The waveform of the infrasound pulses of Aso volcano quite resembles that often observed at Stromboli volcano. The pressure increased over ~0.1 s. After reaching the positive pressure peak, the pressure decreased in a short time to be a negative phase. The maximum amplitude of negative pressure was about 50-60% of the positive peak. After that, it returned to the original state while vibrating the pressure for ~1 s. The dominant frequency of the infrasound pulses was about 3-12 Hz.

We analyzed the waveform of the infrasound pulses using a model of Vergniolle and Brandeis (1996): Their model was proposed to interpret mechanism of infrasound radiation for Strombolian explosions. In the model, the size of a large bubble changes with time (the radius of a bubble oscillates) at the surface of the magma in the conduit, which induces the perturbation of the air pressure. The bubble shape surrounding by a fluid (magma) is assumed to be composed of a hemisphere and a cylinder in the upper and lower parts. The overpressure of gas inside the bubbles causes a change of the radius. Given the surrounding fluid density, viscosity, and the thickness of the bubble's membrane at equilibrium, we solve the model equations of motion of the bubble's radius by the fourth-order Runge-Kutta method. We set the density of the surrounding fluid as 1000-3000 kg/m^3 (5 patterns), the viscosity as 10^{-3}-10^3 Pa s (7 patterns), and the bubble film thickness as 1-10 cm (4 patterns). By iterating to minimize the residual between the observed and calculated waveforms, we could estimate three parameters; the radius of the hemispherical part, the length of the cylinder, and the gas overpressure inside the bubble. We applied this method to an initial part of the infrasound pulse, from the onset to the maximum negative pressure.

The result for the pulse at 22:41:07 on October 22 is as follows. The residual was minimized when the fluid density, viscosity, and the film thickness are 2000 kg/m^3, 10^3 Pa s, and 10 cm, respectively. At this case, the estimated radius and the length of the bubble are 0.21 m and 11 m, respectively (the volume is 1.5 m^3). The gas overpressure inside the bubble is 1.2×10^6 Pa. The size of bubble's radius might be confined by the size of the conduit. For time variation of the bubble's film thickness, it is gradually decrease. It indicates that bursting of the bubble occurred when the strength of the film thickness becomes below the critical value.

©2020. Japan Geoscience Union. All Right Reserved.

By applying the same method to all other infrasound pulses observed before the occurrences of explosions, it would be possible to reveal time variations of such parameters of each pulse (size, inner pressure, and the surrounding conditions of the bubble). This gives us a clue to understand the environmental conditions that might control processes leading to a phreatomagmatic explosion.

Keywords: Aso volcano, infrasound pulse

©2020. Japan Geoscience Union. All Right Reserved.

Melt inclusion constraints on the pre-eruptive process of Kirishima-Ohachi 1235 subplinian eruption

*Yoshiharu Iwaki[1], Hidemi Ishibashi[2], Natsumi Hokanishi[3], ATSUSHI YASUDA[3], Toru Ishikawa[4]

1. Shizuoka University Graduate School of Integrated Science and Technology, 2. Shizuoka University, 3. Earthquake Research Institute,The University of Tokyo, 4. Kirishima Geopark Council

In this study, chemical compositions were analyzed for groundmass glasses, melt inclusions (MIs) and their host phenocryst minerals in the scoria and pumice of the 1235 subplinian eruption, Takaharu tephra, of Ohachi volcano, Kirishima, Japan, to clarify the magma plumbing system beneath the volcano and the pre-eruptive process of the eruption. Among the 4 stratigraphic units of the eruption, scoria, pumice and banded pumice in the b layer, which is the tephra of the climactic stage of the eruption, were used. Phenocryst mineral assemblages are plagioclase + olivine + orthopyroxene + clinopyroxene for the scoria and plagioclase + orthopyroxene + clinopyroxene for the pumice, respectively. Although scoria- and pumice-forming mafic and silicic magmas were mingled to form banded pumice, the boundary between mafic and silicic parts is not gradual, suggesting that chemical mixing was minimum. The results of chemical analyses of the MIs and the groundmass glasses revealed that (1) the groundmass glass and plagioclase-hosted MIs in the pumice (melt A) are rhyolitic with SiO_2~74.9wt.%, and (2) the composition variations of MIs in the scoria are mostly explained by post-entrapment crystallization (PEC) of their host phenocrysts from the common initial melt (melt B) with SiO_2~56.9 wt.%. However, the compositional variation of plagioclase-hosted MIs in the scoria, which are opened to the groundmass melt, cannot be explained by PEC, suggesting that a basaltic andesite melt was mixed with the melt B right before the eruption. Pre-eruptive temperature, H_2O content, and pressure conditions were estimated to be ~932℃, ~1.2wt.% and ~12MPa for the melt A and ~1040℃, ~4.6wt.% and ~210MPa for the melt B, respectively, assuming the melts were H_2O-saturated. The estimated pressures correspond to the depths of ~0.5km and ~8.6km for the melt A and B, respectively.

Based on the results, the pre-eruptive process of the 1235 eruption was proposed as follows; initially, there were two magma chambers at the depths of ~0.5km ~8.6km for the melt A and B, respectively. Then, a basaltic andesite melt intruded into the chamber of the melt B. The mafic melts, composing the groundmass of the scoria, was formed by mixing of the two mafic melts and then started ascent. During ascent to the surface, the mafic magma passed the shallow silicic chamber and entrained the melt A mechanically.

The composition of the melt B is similar to olivine-hosted MIs of the Shinmoedake 2011 eruption. Furthermore, the estimated depth of the chamber of the melt B is similar to depth of the mafic magma chamber beneath Shinmoedake inferred by Suzuki et al. (2011). These may suggest that the mafic chamber at the depth of ~8.6km is common beneath Ohachi and Shinmoedake. However, the estimated depths and compositions of the silicic magmas are different between the two volcanoes; the silicic magma of Ohachi is more differentiated, H_2O-poor and viscous. The conditional difference of silicic magmas may cause the systematic compositional difference of erupted magmas between Ohachi and Shinmoedake volcanoes.

Keywords: Ohachi volcano, melt inclusion, Kirishima, magma chamber, banded pumice

©2020. Japan Geoscience Union. All Right Reserved.

Temporal and spatial variations of helium isotope ratios in volcanic gases at Kirishima volcanic group

*Hirochika Sumino[1], Kotaro Toyama[1], Takeshi Ohba[2], Muga Yaguchi[3]

1. Department of Basic Science, Graduate School of Arts and Sciences, The University of Tokyo, 2. Department of Chemistry, Tokai University, 3. Meteorological Research Institute

In Kirishima volcanic group in Kyushu, Southwest Japan, Shinmoe-dake erupted in 2008, 2011, 2017 and 2018, and Iwo-yama also erupted in 2018. For volcanic disaster prevention, forecasting volcanic eruption is required. It is known that temporal variations in chemical and isotopic compositions of volcanic gases are useful to evaluate the present state of volcanic activity [1]. Among them, helium isotope ratio ($^3He/^4He$) has a great potential as a good indicator of volcanic activity, because it exhibits unique values corresponding to the origin (e.g., 7-8 Ra in the mantle and about 0.02 Ra in the crust, where 1 Ra denotes atmospheric $^3He/^4He$ ratio of 1.4×10^{-6} [2]). Some studies have reported pre-eruptive $^3He/^4He$ anomalies, suggesting the increase of the magmatic helium supply into the hydrothermal system preceding eruption [1,3,4].

We report spatial and temporal variations of $^3He/^4He$ ratios of fumaroles and hot spring gases collected from 10 sites in Kirishima volcanic group during 2016 to 2020. The measured $^3He/^4He$ ratios were corrected for atmospheric contamination based on $^4He/^{20}Ne$ ratios. The air-corrected $^3He/^4He$ ratios (6.8 to 7.7 Ra) observed in and around the central craters of the active volcanos (i.e., Iwo-yama, Shinmoe-dake, and Ohata-ike) are higher than those (3.5 to 5.8 Ra) at the other sites. The $^3He/^4He$ ratios of non-crater sites decrease with the increase of their distances to each sampling site from a magma reservoir, location of which is estimated as pressure source of crustal deformation associated with the 2011 Shinmoe-dake eruption. This can be accounted for by an increase of contribution of radiogenic ^4He in old groundwater to the magmatic helium with migration distance of the fluid from the magma to the site [7]. On the other hand, former or present active craters show constant and high $^3He/^4He$ ratios irrespective of the distance from the magma reservoir, indicating there would be pathways of magmatic gas from the magma without or less interaction with the old groundwater.

The $^3He/^4He$ ratios of fumaroles in Iwo-yama slightly increase before Shinmoe-dake eruptions, and decrease after each eruption. This variation cannot be accounted for by the contribution of the radiogenic ^4He relative to total helium in the fumaroles before and after the eruptions, because it is estimated that the amount of radiogenic ^4He which volcanic gas can acquire during its migration from magma to the surface is negligible. Alternatively, the variation results from the change in mixing ratio of gases derived from two reservoirs having high and low $^3He/^4He$ ratios. Assuming that the magma reservoir has high $^3He/^4He$ ratio, the increase of $^3He/^4He$ ratios of the fumaroles before the eruption would result from increase of the supply of the gas from the magma reservoir to the Iwo-yama fumaroles. Once an eruption occurs at Shinmoe-dake, magmatic gas is effectively released through the volcanic vent, resulting in decrease of its supply to the Iwo-yama fumaroles. Thus, the temporal variation of $^3He/^4He$ ratios in volcanic gases may reflect the pressure variation of the magma reservoir. Since the last eruption at Shinmoe-dake in June 2019, the $^3He/^4He$ ratios of Iwo-yama fumaroles have been constant at high values (7.2–7.6 Ra), suggesting magmatic gas has been continuously supplied to Iwo-yama fumaroles at constant rate.

©2020. Japan Geoscience Union. All Right Reserved.

References:

[1] Paonita et al. (2016) Geology. [2] Ozima and Podosek (2002) Noble Gas Geochemistry. [3] Padrón et al. (2013) Geology. [4] Sano et al. (2015) Sci. Rep. [5] Nakao et al. (2013) Earth Planet. Space. [6] Ueda et al. (2013) Earth Planet. Space. [7] Sano et al. (1994) Appl. Geochem.

Keywords: Helium isotopes, Kirishima volcanic group, Volcanic gas

©2020. Japan Geoscience Union. All Right Reserved.

Vertical ground deformation in Sakurajima volcano measured by precise leveling survey (during Nov. 2018 - Nov. 2019)

*Keigo Yamamoto[1], Takeshi Matsushima[2], Shin Yoshikawa[3], Hiroyuki Inoue[3], Tadaomi Sonoda[1], Taishi Yamada[1], Yichen Tang[2], Koki Yoshinaga[2], Takamitsu Ikegame[4], Hiroshi Kishimoto[4], Takahiro Ohkura[3]

1. Disaster Prevention Research Institute, Kyoto University, 2. Faculty of Sciences, Kyushu University, 3. Graduate School of Science, Kyoto University, 4. Japan Meteorological Agency

We conducted the precise leveling survey in Sakurajima volcano, southwest Japan in November 2019. The leveling routes measured in this survey are about 21 km long in total, including Sakurajima western flank route and Sakurajima northern flank route. These leveling routes were measured during the period from November 11 to 15. Mean square errors of the conducted survey were achieved with a good accuracy ranging from ±0.22 to ±0.27 mm/km.
From the measured data, we calculated the relative height of each benchmark referring to the reference benchmark BM.S.17 which is located at the western coast of Sakurajima. The calculated relative heights of the benchmarks were then compared with those of the previous survey conducted in November 2018 (Yamamoto et al., 2019), resulting in the relative vertical displacements of the benchmarks during the period from November 2018 to November 2019.
The resultant displacements indicate that no remarkable vertical displacements are detected at the measured benchmarks, although the minor ground subsidence is seen at benchmarks around the central part of Sakurajima. The results suggest that the inflation of the magma reservoir beneath Aira caldera was not remarkable during the period between November 2018 and November 2019. From the preliminary analysis based on a spherical source model (Mogi, 1958), the deflation source is suggested to exist beneath Minamidake crater. However, the pressure decrease is minor during this period.

Keywords: Sakurajima volcano, precise leveling survey, vertical ground deformation

©2020. Japan Geoscience Union. All Right Reserved.

Changes in carrier phase residuals of GPS satellite radio waves following the eruptions of Sakurajima -Data analysis from 2013 to 2019-

*Yukako Asakura[1], Takeshi Nishimura[1], Yusaku Ohta[1], Masayuki Kano[1]

1. Graduate school of science, Tohoku University

This study, we investigated temporal changes in the mean and variance of GPS carrier phase residuals before and after volcanic eruptions in Sakurajia. Ohta and Iguchi (2015) found that the eruption of higher than 5000 m on July 21, 2012 in Sakurajima was captured by GPS. They monitor ash plumes using the fact that the carrier phase residuals of signals from GPS satellites is delayed by ash plumes.
Based on this study, large eruptions on Sakurajima from 2013 to 2019 were systematically investigated. We focused only on the eruptions whose height of eruptive column was, greater than 4500 m. GPS data were analyzed using Gipsy-X at three GEONET stations provided by the Geospatial Authority of Japan on the mainland of Sakurajima.
As a result, the carrier phase residuals abnormality could not be clearly seen, but the average of the residuals during one hour after the eruption rose 81% than that during one hour before the eruption. The standard deviation of the residuals also increased by 63% after the eruption.
By adding small-scale eruptions, we will examine environmental factors such as weathered magnetic storms, GPS observation points and satellite paths.

Keywords: volcanic eruption , GNSS, Sakurajima

©2020. Japan Geoscience Union. All Right Reserved.

Detection of volcanic earthquakes and estimation of internal attenuation structure beneath the Kikai submarine caldera

Yasutomo Seto[1], *Hiroko Sugioka[1], Tsutomu Takahashi[2], Yojiro Yamamoto[2]

1. Kobe University, 2. JAMSTEC

Kikai submarine caldera is located to the south of the Kyushu and lies astride the volcanic front of the southwestern Japan. It has been recently revealed that giant lava dome with a volume of 32km^3 is created after super eruption at 7.3 K.a. (Tatsumi et al., 2018). Seismic observation had been conducted by five short-period Ocean Bottom Seismometers (OBSs) located above the caldera from October 19, 2016 to March 4, 2017 to obtain continuous data recorded on the three-component seismometers at 100 Hz sampling rate for about 5 months.

We found that volcanic events had been always occurred over during the observation periods. The detected volcanic events are roughly classified into two kinds based on dominant frequency bands. One is the so-called volcanic low-frequency tremor with dominant frequencies at 2-8 Hz, whose waveforms are in the shape of spindle-like. The other is the so-called volcanic high-frequency earthquake with dominant frequencies at over 5 Hz. We determined the hypocenters of the latter earthquakes using and found that most of all locations are concentrated in the shallow part (<10km) beneath the caldera.

The OBSs recorded many earthquakes occurred in the subducted Philippine Sea Plate. We measured the peak delay time in seconds for the S wave using rout mean square (rms) envelope, which were calculated for the sum of two horizontal components in four frequency bands of 2-4, 4-8, 8-16 and 16-32 Hz. High-frequency S-wave envelopes well reflect on the medium heterogeneity beneath the caldera. We defined the peak delay time as the time lag from the direct S-wave onset to the maximum amplitude arrival of the RMS envelope to use the quantity to evaluate the strength of the inhomogeneity along the seismic ray path. The measured peak delay time at the station located near the Satsuma Iojima was much smaller at the lower frequencies of 2-4 Hz and consistently larger at the other higher frequencies of 4-32 Hz, which suggests the existence of medium inhomogeneity stronger at shorter wavelength than around 0.5 km. The frequency dependence is also one of the most important features to speculate the medium inhomogeneity. The peak delay time has negative correlation with frequencies and the amplitude decreases at higher frequencies at the station located at the southern caldera, which effect intrinsic attenuation. Furthermore, the attenuation of the amplitude was significantly recorded on S-wave propagated through the whole caldera. The intrinsic attenuation beneath the caldera may be related to magma chamber.

Keywords: submarine caldera, ocean bottom seismometer, giant supereruption

©2020. Japan Geoscience Union. All Right Reserved.

Occurrence and distribution of pyroclastic fall deposits of Kuchinoerabujima volcano 2020 eruption

*Masashi NAGAI[1], Shojiro Nakagawa[2], Yu Iriyama[3], Takahiro Miwa[1], Setsuya Nakada[1]

1. Volcano Research Department, National Research Institute for Earth Science and Disaster Resilience, 2. Yakushima Chigaku Club, 3. Research and Industrial Collaboration Department, Kyushu University

At Kuchierabujima volcano, eruption began intermittently from January to February 2020. Relatively large eruptions are observed on January 11, 27 and February 3. The ash fall distribution survey was conducted on two eruptions with ash fall on eastern adjacent Islands excluding the January 27 eruption where the ash fall axis was in the south sea direction. We also used survey results provided by Japan Meteorological Agency Kuchinoerabujima Volcano Disaster Prevention Liaison Office and Kagoshima Prefecture Yakushima Office, and interviews with Yakushima Town Office and local residents.
The Ash fall deposits on Yakushima and Tanegashima Islands are all light gray to reddish light gray colored sandy to silty volcanic ash layers, the component are mainly composed of lithic fragments and hydrothermal altered fragments and small amount of fresh vitreous rock fragments. At the eruption of February 3, where the largest one during a series of eruptions, on the ash fall axis extending to the east, 430 g/m^2 of ash deposited in the northwestern part of Yakushima Island, 100 g/m^2 in the northeast part, and 30 g/m^2 in the southern part of Tanegashima Island. In the northern part of Yakushima Island, fine lapilli was also included, and the maximum particle diameter tended to be larger on the north side than the ash fall axis. The deviation between the axis of ash fall axis and the axis of maximum particle diameter distribution can be explained by the difference in wind direction and wind speed at altitude. The distribution of ash fall and maximum particle size was similar to that of the January 17, 2019 eruption, but the distribution was slightly northward and the width of the heavily deposited area was wider.
The amounts of air fall deposits were obtained by the method of Fierstein and Nathenson (1992) using average deposition density of 1000 kg/m^3. Based on the distribution data of distant deposits, they are estimated to be ca.15,000 tons on the January 11 eruption and ca.96,000 tons for the February 3 eruption. These are smaller than the amount of air fall deposit of May 29, 2015 eruption estimated in the same method, ca.120,000 tons. Since 2015, the eruptions of Kuchierabujima shows a positive correlation between eruption column heights and estimated amounts of air fall deposits.

Keywords: tephra, phreatic eruption, Phreatomagmatic eruption, eruption column, Thickness-isopach area curve, Ryukyu arc

©2020. Japan Geoscience Union. All Right Reserved.

Three-dimensional resistivity imaging of Taal Volcano, Philippines

*Yusuke Yamaya[1], Paul Alanis[2]

1. National Institute of Advanced Industrial Science and Technology, 2. Philippine Institute of Volcanology and Seismology

Taal Volcano in the Philippines erupted from the main crater on January 12, 2020. Intense explosions occurred several times generating a 10-15 km tall eruption column, and the following day they shifted to magmatic eruptions fountaining lava. Prior to these eruptions, Yamaya et al. (2013) and Alanis et al. (2013) interpreted the resistivity structure estimated by the magnetotelluric (MT) survey, and suggested that a large hydrothermal reservoir existed beneath the main crater of the volcano, which could cause a magmatic-hydrothermal eruption. Their resistivity structures were estimated by 2D inversion and 3D forward modeling due to the limitations of computers and calculation codes. In recent years, 3D inversion has become practical due to the development of computers and codes, enabling more accurate and objective structure estimation. Therefore, we re-analyzed the resistivity structure by 3D inversion using the MT data of Yamaya et al. (2013) and Alanis et al. (2013). This allowed us to use diagonal components of the MT impedance and transfer functions of the magnetic field that could not be used in 2D analysis. In addition, to assume the 3D distribution of conductive seawater enabled us to use long-period data longer than 100s.

Followings are preliminary results. The estimated 3D resistivity structure was similar to the result of 2D inversion from the surface down to a depth of about 1 km. The conductive layer widely spread and the resistivity beneath the main crater lake was relatively high. At a depth deeper than 1 km, a considerable conductive body was estimated at northeast of the crater lake. Given its large size and extent, this conductor likely indicates another structure being related to volcanic activities rather than the cap rock of the hydrothermal reservoir interpreted in the previous studies.

Keywords: Taal Volcano, resistivity structure, hydrothermal reservoir

©2020. Japan Geoscience Union. All Right Reserved.

Detection of the volcanic plume by 19 February 2018 eruption of Mount Sinabung deduced from GNSS post-fit phase residual analysis

*Yusaku Ohta[1], Masato Iguchi[2], Gunawan Hendra[3], Umar Rosadi[3], Estu Kriswati[3]

1. Research Center for Prediction of Earthquakes and Volcanic Eruptions, Graduate School of Science, Tohoku University, 2. Sakurajima Volcano Research Center, Disaster Prevention Research Institute, Kyoto University, 3. Center for Volcanology and Geological Hazard Mitigation

On 19 February 2018, 08:53 local time, the Indonesian volcano Mt. Sinabung on Sumatra, Indonesia erupted with a high volume of ash that quickly rose to an estimated 15-17 km above sea level. The eruption also generated a pyroclastic flow which mainly ran the southeastern flank of the mountain. Around the Mt. Sinabung, four GNSS sites are located to monitor the crustal deformation. Ohta and Iguchi (2015) investigated the temporal and spatial development of a volcanic plume during the eruptive event at Sakurajima volcano in Japan on July 24, 2012. In this study, we applied the similar approach to detect the volcanic plume caused by the eruption of Mt. Sinabung.

We extracted the post-fit phase residuals (PPR) of ionosphere-free linear combinations for each satellite based on the precise point positioning (PPP) approach. We used GIPSY-OASIS software ver. 6.4 for the analysis. To reduce the multi-path effect which caused by the surrounding environment at each site, we subtracted the PPR time series of previous day with sidereal time sifting. The obtained residual time series clearly shows the PPR anomalies at all GNSS sites. For example, LKWR station, which located the northern flank of the mountain, showed the clear impulsive PPR positive anomaly just three minutes after the eruption relative to SVN62 satellite which was southeastern direction with 34-degree elevation angle. In contrast, SNBG station, which locate the southeastern direction of the mountain, showed very long duration PPR anomaly relative to SVN41 satellite which was northwestern direction with 25-degree elevation angle. This ray-path corresponded to the just above the mountain. Furthermore, MRDG station, which located the southwestern flank of the mountain, also showed long duration PPR anomaly longer than one-hour, relative to SVN62. This ray-path roughly corresponded to the south of the mountain flank. Based on the results from MRDG and SNBG may suggest that the obtained PPR anomaly may reflect the pyroclastic flow after the eruption because the PPR anomaly direction concentrated in the southern direction of the mountain.

In the presentation, we will discuss the more detailed results including the not only PPR analysis but also the signal-to-noise ratio analysis of the GNSS signals.

Keywords: GNSS, plume, Sinabung

©2020. Japan Geoscience Union. All Right Reserved.

The performance of the back elevation angle estimation of 3-dimensional infrasonic small array observation

*Kazuya Yamakawa[1], Mie Ichihara[1], Claudia Sánchez[2], Wataru Ikeda[1], Giorgio Lacanna[2], Maurizio Ripepe[2]

1. Earthquake Research Institute, University of Tokyo, Japan, 2. Department of Earth Sciences, University of Florence, Italy

The infrasonic array technique has been widely used to detect an infrasonic signal and to constrain its source. Yamakawa et al. (GRL, 2018), hereafter referred to as YMK2018, reported that a small array with a 20-m aperture had a practically sufficient back azimuth (BAZ) resolution, but did not resolve the back elevation angle (BEL). The BEL estimation is important in identifying the source from multiple mechanisms. In order to improve the BEL resolution, we tried a small 3D array observation with three sensors on the ground and one sensor 1.9 meters above the ground. Here we examined the performance of the small 3D array of this experiment.

The experiment was conducted at the summit of Stromboli, the same place as YMK2018, from 20 to 21 on June 2019 (Fig. a). We compared the performances for three sensor combinations (Fig. b): (A) the 3D array using all the four sensors, (B) the 2D array the plane of which was inclined to the ground surface by the use of the elevated sensor, and (C) the 2D array using only the sensors on the ground similar to YMK2018.

The MUSIC method [Schmidt, 1986] was used in the array processing. We analyzed 0.5–40 Hz band dividing into narrow bands (central frequency ±10 %) in steps of 0.25 Hz. The infrasound speed was assumed to be 340 m/sec. The directions of arrival (DOAs), which are BAZ and BEL, were picked from the MUSIC spectrum peak.

First, we examined the frequency dependence of the accuracy of DOAs using the data during the observation with a handy camera. We selected 42 explosion signals the source vents of which were confirmed by the images, and 24 one-minute time windows containing only puffing signals with no explosions. A mirror peak was observed at the symmetric BEL with respect to the array plane in each frequency band with the 2D arrays. The 3D configuration effectively reduced the mirror effect in >15 Hz. On the other hand, in BAZ the spatial aliasing effect became significant above 15 Hz. By comparing high and low frequencies, BAZs and BELs were adequately estimated to the vent direction in >8 Hz and >20 Hz, respectively. Then, we selected the peak of each MUSIC spectrum closest to the vent direction as the signal DOAs.

For statistical processing, we analyzed additional 63 explosion signals and 48 one-minute time windows for puffing signals with no images. Of the 105 signals and 72 time windows, we selected 64 signals and 62 time windows the sources of which were estimated either of the three active vents. The standard deviation (STD) of DOAs was calculated for each set of signals from the same vent in each frequency band. Although the STDs significantly increased in < 3 Hz, we could constrain DOAs in ±20˚ down to 1 Hz (Fig. c). Of all the frequency band above 3 Hz and for all of the three source vents, 90 % of STDs of A were in <2.2˚ for BAZ and in <3.9˚ for BEL. B had similar but a bit larger STDs, while those of C were larger (<2.8˚ for BAZ and <7.4˚ for BEL) (Fig. d). Besides, there is a notch in the signal spectra, in which the signal power is very low, in which STDs increased up to 6˚ with A and B, and 10˚ with C. We also found that the BEL

©2020. Japan Geoscience Union. All Right Reserved.

estimations with the 2D configurations (B and C) sometimes concentrated in the dip direction of their array planes.

We also found systematic shifts of DOAs depending on the frequency. Particularly in 3–5 Hz, DOAs were always in the same direction more than 10˚ off the vents regardless of the source. The shifts were observed in all of A, B, and C, and larger than the STDs of either BAZs and BELs, and such shifts were not produced in the numerical tests which used a signal with ideal time lags even with overlapping random noises. We consider the shifts are significant, though the cause needs to be identified.

The performances of A and B were similar and better in BEL resolutions than C. The reason was that their array planes were inclined against the BEL. We conclude that putting a sensor at a high position by only 2 m improved the BEL estimation.

Keywords: Infrasound, Array observation, volcano

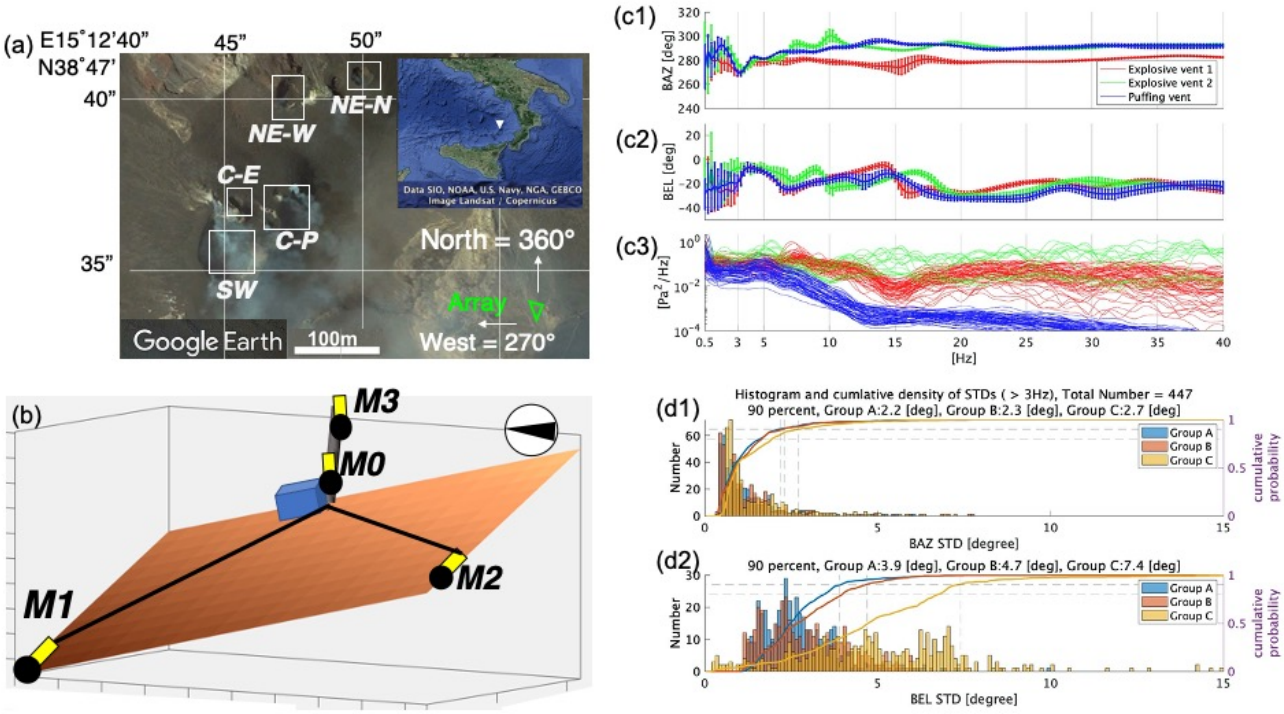

©2020. Japan Geoscience Union. All Right Reserved.

A trial to quantify volcanic activities using the JMA unified earthquake catalog and the ETAS model

*Yuta Maeda[1]

1. Nagoya University

To make judgements for bifurcations on volcanic activities based on precursors, a lot of examples of eruptions and precursors need to be evaluated quantitatively with a common approach. A dataset suitable to this type of analysis would be the unified earthquake catalog issued by Japan Meteorological Agency (JMA), which consists of the origin times, locations, and magnitudes of earthquakes all over Japan since 1923 including volcano-seismic events. To quantitatively relate seismic and volcanic activity levels, it seems that the seismicity level needs to be evaluated without explicitly using a time length and the number of earthquakes, since these quantities in precursory periods differ by eruptions. This requirement could be satisfied by using an Epidemic Type Aftershock-Sequences (ETAS) model (Ogata, 1988), which represents the seismicity by the summation of a background activity and aftershocks of all the preceding earthquakes. When the relation between the cumulative earthquake intensity predicted by the model (a transformed time) and the observed cumulative number of earthquakes do not show a single straight line, a change in the slope of the relation would represent a seismicity level change. In this study, we tried to quantify volcano-seismic activity levels using the unified earthquake catalog and ETAS model.

We first evaluated the volcano seismicity in this catalog by comparing it with that in another catalog around Mt. Ontake volcano created by Nagoya University (NU catalog). Although the number of earthquakes in the unified catalog was ~1/7 of that in the NU one, spatiotemporal characteristics of the seismicities in the both catalogs were essentially consistent to each other.

We next tried to develop a common method and criterion to extract volcano seismicities around the active volcanoes all over Japan from the unified catalog. To do this, we grouped the earthquakes within 20 km east, west, south, and north of each volcano at depths less than 15 km into 15 clusters using a mixed normal distribution model for the 3-D spatial distribution of hypocenters. Then volcano-seismic events are extracted as those in the cluster corresponding to a normal distribution for which the weight center was closest and less than 5 km (horizontal) of the volcano (i.e., the location is close enough to the volcano) and the longest radius of one standard deviation ellipsoid was less than 5 km (i.e., the hypocenters are not too widely scattered). The volcano-seismic events were identified successfully at 45 volcanoes, whereas 36 including Aso and Kirishima did not have a cluster which meet the requirements, and 29 volcanoes in island regions had too few earthquakes to perform the clustering.

We investigated ETAS model parameters for the extracted volcano-seismic events. Plots for the cumulative numbers of earthquakes against transformed times of the ETAS model showed elevated seismicities before 2007 and 2014 eruptions at Mt. Ontake, with a more significant activation in the 2014 case consistent with the eruption size. At Sakurajima, an increased seismicity associated with a dike intrusion on 15 August 2015 followed by several stages of calming down were identified. An intensified seismicity at Hakone in 2015 was most clear in the clusters 2nd and 3rd closest to the volcano. Remaining tasks include an improved extraction of the volcano seismicity, evaluations of the ETAS model at the other volcanoes, and a trial to find out a quantitative relation between the seismic and volcanic activity levels.

This study was supported by the Ministry of Education, Culture, Sports, Science and Technology (MEXT)

©2020. Japan Geoscience Union. All Right Reserved.

of Japan, under its The Second Earthquake and Volcano Hazards Observation and Research Program (subject ID: THK13). We used SASeis2006 software (The Institute of Statistical Mechanics, Japan) for the analyses of the ETAS model.

Keywords: Volcano seismology, Event bifurcation

©2020. Japan Geoscience Union. All Right Reserved.

Temporal relationship between seismic activity and ground deformation by GNSS data with applying the stacking method

*Yo Kanno[1], Akimichi Takagi[1], Takashi YOKOTA[2], Kazuki Miyaoka[1]

1. Seismology and Volcanology Department, Japan meteorological agency, 2. Aichi Institute of Technology

For understanding processes of volcanic activities, it is important to clarify the temporal relationship between ground deformation and seismic activities including their depth. It is reported that baseline changes seem to have started several weeks-to-months prior the earthquake swarms in recent studies. These results show that it is possible to detect volcanic activity changes before an eruption or earthquake swarms.

During the 2007 and 2014 Ontake volcano activity, the changes of stacked GNSS data began in the long stacked data moved to the short stacked data over time. Miyaoka and Takagi (2019) inferred that these data revealed movements of a pressure source to a shallower region from a deeper region (about 5km depth). The same case was reported during the 2013 Hakone volcanic activity, the changes of long stacked data (source depth about 5-10km depth) seem to have started several months prior to the earthquake swarms. Similar cases were reported in the earthquake swarms of Izu-Tobu volcanoes and the changes of GNSS data seem to have about half a day prior to the earthquake swarms (JMA, 2010). It was assumed that only ground deformation were detected when magma ascended in the hot and ductile part at the depth, and the earthquake occurred when magma reached to the shallower part (The headquarters for earthquake research promotion, 2010). Takagi (2019) reported volcanic ground deformation events that were detected at 9 volcanoes in Japan by applying the stacking method to strain measurements along baselines of GEONET, the GNSS network managed by the Geospatial Information Authority of Japan. On the other hand, the relationships between the ground deformation and earthquake activity were still not investigated in Takagi (2019).

In this study, for the purpose of detecting movement of a pressure source, we checked the relationship between earthquake activities and the occurrence of ground deformation based on events caused by deep pressure sources revealed by Takagi (2019). As a result, ground deformations prior to seismic activities were observed at many volcanoes, not only Ontake volcano and Hakone volcano but also Meakandake volcano, Niigata-yakeyama volcano, Asama volcano, Shinmoedake volcano and Aso volcano. Although no eruptions have been observed, it was also observed that ground deformation prior to swarm activity at Zao volcano and Azuma volcano, which had swarm activities in recent years. In particular, at Meakandake volcano and Azuma volcano, it is possible that the slight baseline changes from the long stacked data to the short baseline be seen by using the stacking method of Miyaoka and Takagi (2016). The results of an investigation of the relationship between ground deformation and seismic activity for several volcanoes including above will be shown.

Keywords: Ground deformation, Earthquake activity, GNSS, Stacking method

©2020. Japan Geoscience Union. All Right Reserved.

Multi-sensor system with air blowers for airborne volcanic gas survey using drones: an improvement of a sensor response time

*Kohki Matsuura[1], Akihiko Terada[1], Toshiya Mori[2], Takato Ono[2]

1. Volcanic Fluid Research Center, Tokyo Institute of Technology, 2. Chemical Research Center, Graduate School of Science, The Univercity of Tokyo

Drones (Unoccupied aircraft systems, UAS) are essential tools for understanding and monitoring volcanoes. They can also make measurements for geochemical analysis from hazardous area such as toxic volcanic gas near active vents during initial stages of volcano unrest as well as throughout eruptions. Gas measurements using drones equipt with a multi- gas sensor system have been performed at many volcanoes (Mori et al., 2016; Stix et al., 2018; Liu et al., 2019). Molar ratios in the volcanic gas are evaluated by a slope of regression lines between the one gas concentration and other gas concentration, therefore, a consistency of response time of sensors is critical. Using commercial gas sensors, we have developed a multi-sensor system which includes electrochemical sensors for sulfur species (SO_2 and H_2S, RAE System ToxiREA), a non-dispersive infrared (NDIR, TandD TR-76Ui) sensor for CO_2. Concentration of H_2O is calculated using the relative humidity measured by a capacitive humidity sensor and temperature measured by a thermistor (SENECOM SE-TRH-FS15-SS). Response times of a NDIR CO_2 sensor and a thermistor show marked changes in response to ambient wind speed, probably due to forced convection. In order to adjust response time of all of sensors, we attached small air blowers to a NDIR and thermistor sensors. Our laboratory experiments indicate that sensor response times can be set to around 10 seconds under the condition of ambient wind speed of more than 1.5 m/s. Assuming a linear response, an uncertainty of molar ratios in the volcanic gas is estimated to be less than 30 % in maximum if an exposure time to the volcanic time is 10 seconds, while an uncertainty is estimated to be 120 % in maximum without using air blowers. Exposure time of multi-sensor system to fumarolic gas is limited because of capability of drones. Therefore, air blowers are useful to improve accuracy of evaluations of molar ratios in the volcanic gas, especially in small plume.

Keywords: Volcanic gas, MultiGAS, Drone, Unoccupied aircraft system

©2020. Japan Geoscience Union. All Right Reserved.

Tephra segregation profiles from Vulcanian eruptions on Sakurajima volcano, Japan, based on settling velocity observations

*Kosei Takishita[1], Masato Iguchi[2], Alexandros Panagiotis Poulidis[2], Tadaomi Sonoda[2]

1. Division of Earth and Planetary Sciences, Graduate School of Science, Kyoto University, 2. Sakurajima Volcano Research Center, DPRI, Kyoto Univ.

Ashfall from volcanic eruptions has been predicted by studies using advection-diffusion models based on the wind velocity field and terminal velocity estimated from the particle size of volcanic ash particles. Models calculate the ash fallout distribution considering the advection, diffusion, and descent processes from the plume to the surface. Among the input parameters, plume height, total weight of volcanic ash, wind field, particle size, etc. are given based on observations, and the deposition pattern of ashfall can be faithfully reproduced at distances of tens to hundreds of kilometers, but not at distances of a few kilometers proximal to the crater.
The profile of tephra concentration along a volcanic column is decided by the complex interplay of eruption dynamics and the atmospheric state. Despite its importance in tephra transport and dispersal modelling, large uncertainties remain, mainly due to the lack of direct observations. Here, we investigate tephra segregation profiles (TSPs) from Vulcanian eruptions on Sakurajima volcano, Japan, using a combination of in-situ observations and high-resolution atmospheric and tephra transport modelling.
A total of 17 optical disdrometers (OTT Parsivel2) were installed on the flanks of Sakurajima for the in-situ measurement of tephra fall, allowing for the detailed observation of particles with sizes between 0.25-20 mm and settling velocities under 12.8m/s. Deposit loads for each disdrometer were estimated using an empirical formula that accounts for different densities in the observations. For the reproduction of the observed tephra deposits, we coupled the WRF numerical weather prediction model with a modified version of Tephra2, an advection-diffusion model that estimates the trajectories of the center of particle groups. Improvements made include: the replacement of the diameter distribution with observed terminal velocity distribution, the ability to solve the equations over temporally-evolving three-dimensional meteorological fields (three wind components and air density), and the ability to apply arbitrary TSPs.
A total of 6 Vulcanian eruptions were used for the study, with the plume heights ranging between 1400m and 4700m above the vent. The estimated TSPs were bimodal distributions. The higher peak corresponds to the top of a mushroom-shaped plume, which is made just when an eruption occurs, and the lower one indicates the dominance of segregation from the lower part of plume, which follows the mushroom-shaped plume. The results suggest that TSPs reflect temporal changes of discharge rate of volcanic ash.

Keywords: Tephra segregation profile, disdrometer, Vulcanian eruption, Sakurajima, Parsivel

©2020. Japan Geoscience Union. All Right Reserved.

[J] Poster | S (Solid Earth Sciences)：S-VC Volcanology

[S-VC46] Mitigation of volcanic disasters - basic and applied researches

convener:Shinji Takarada(Geological Survey of Japan, National Institute of Advanced Industrial Science and Technology), Mitsuhiro Yoshimoto(Mount Fuji Research Institute, Yamanashi Prefectural Government), Tatsuro Chiba(Asia Air Survey Co., Ltd.), Tomohiro Kubo(Mount Fuji Research Institute)

Volcanic disasters are caused by wide range of volcanic phenomena including ash fall, pyroclastic flow, debris avalanche, lahar, and lava flow. To mitigate volcanic disasters, wide range of technologies including simulation, data processing on GIS, and communication techniques are required. Researches on volcanic hazards mapping, eruption scenarios, and probabilistic eruption assessments are getting important. This session invites presentations and broad reviews related to these topics. Contributions on database technology, case studies of social and school educations, and specific examples of eruption crisis events are also encouraged.

[SVC46-P01] Research on observation method of volcanic ash accumulation using spaceborne SAR: Quantitative extraction of decorrelation by volcanic ash-fall

*Taku Ozawa[1], Eisuke Fujita[1] (1.National Research Institute for Earth Science and Disaster Resilience)

[SVC46-P02] How to set wind condition data for stochastic ashfall risk assessment?

*Yoshinori TOKIZANE[1], Masatsugu Wakaura[1], Himeka Kikuchi[1] (1.OYO RMS Corporation)

[SVC46-P03] Validity of thickness of Aso-4 tephra fall deposit of the Uwa Basin, western Shikoku

*Chisato Nakamura[1], Tomohiro Tsuji[2], Michiharu Ikeda[3], Naoki Nishizaka[4], Kozo Ohnishi[4], Masayuki Sakakibara[5,6] (1.NAIBA Co. Ltd., 2.Graduate School of Science and Technology for Innovation, Yamaguchi University, 3.Shikoku Research Institute INC., 4.Shikoku Electric Power Co. Ltd., 5.Faculty of Collaborative Regional Innovation, Ehime University, 6.Research Institute for Humanity and Nature)

[SVC46-P04] Improvement of accuracy of DEM generated using UAV -a case study of the central crater of Izu-Oshima volcano, Japan-

*mori takaaki[1], Shunsuke Miura[1], Takumi Mochizuki[1], Shino Naruke[1], Hideki Nonaka[1], Hisashi Sasaki[1], Kenichi Arai[1], Koji Fujita[1], Toshihiro Urayama[1], Tatsuro Chiba[1] (1.ASIA AIR SURVEY CO.,LTD.)

[SVC46-P05] Types and characteristics of evacuation shelters for volcanic eruption in Japan

*Hisashi Sasaki[1], Shino Naruke[1], Hiroyuki Yamada[2] (1.Asia Air Survey Co., Ltd., 2.National Defense Academy)

[SVC46-P06] Disaster prevention using data of climber's movement and tendency in active volcanoes

*Yosuke Miyagi[1], Setsuya Nakada[1], Mitsuhiro Yoshimoto[2], Tomohiro Kubo[2], Ryo Honda[2] (1.National Research Institute for Earth Science and Disaster Resilience, 2.Mount Fuji Research Institute)

[SVC46-P07] Development of Proto-type Educational Web Contents for the Municipalities' Disaster Response Staff

*Tomohiro Kubo[1], Mitsuhiro Yoshimoto[1], Yuki Horiuchi[1], Ryo Honda[1], Yasuhiro Ishimine[1], Yosuke Miyagi[2] (1. Mount Fuji Research Institute, 2.National Research Institute for Earth Science and Disaster Resilience)

Research on observation method of volcanic ash accumulation using spaceborne SAR: Quantitative extraction of decorrelation by volcanic ash-fall

*Taku Ozawa[1], Eisuke Fujita[1]

1. National Research Institute for Earth Science and Disaster Resilience

Volcanic ash often causes heavy disaster due to debris flow. To mitigate such disaster, rapid observation of the volcanic ash distribution and forecast of debris flow from such observation are important. However, rapid observation of the volcanic ash distribution has been carried out mainly by on-site survey, and it is difficult to observe it rapidly. Then development of more rapid observation method are required. As one of solutions resolving such problem, utilization of satellite remote sensing technique is expected. Then, we are researching on observation method of volcanic ash distribution using spaceborne SAR in “Cross-ministerial Strategis Innovation Promotion Program (SIP)-2nd season” as one of development items. In this development, we use InSAR coherence analysis. In InSAR results, clear fringes are seen if the coherence is high. On the other hand, noise is dominant if the coherence is low, and fringe becomes unclear. Generally, loss of coherence (decorrelation) is caused by difference of radar scatter at the pixel for InSAR pair. In a result from an interferometric pair including the eruption occurrence, decorrelation due to radar scatter change caused by volcanic ash accumulation is generally seen around the crater. If the relation between decorrelation and the amount of volcanic ash accumulation becomes clear quantitatively, the amount of volcanic ash accumulation will be obtained from InSAR coherence analysis. Then, in this development, we estimate decorrelation only due to volcanic ash accumulation, using a temporal coherence change model without volcanic ash effect constructed from InSAR coherence time-series analysis. In this presentation, we mention about such an attempt of quantitative extraction of decorrelation by volcanic ash-fall.

Coherence decreases with time due to a change in radar scattering due to a change in ground surface coverage and shape, a change in water content, and so on. We assume such temporal change the exponential function “g = Aexp(Bt) + C”, where g is the coherence, t is the observation interval of the interference pair, and A, B, and C are constants. Fitting this function to observed coherence in Kuchinoerabu-jima by PALSAR-2, large residuals exceeding 0.2 were obtained. Such large residuals are remarkably in dense vegetation area, and therefore, it must have been caused by mis-modeling of decorrelation due to temporal change of the vegetation effect. Since vegetation varies with the seasons, we assume that its component fluctuate annually. Then we modified the model to “g = Aexp(Bt){Csin(2 pai t)+Dcos(2 pai t)+Esin(4 pai t)+Fcos(4 pai t)}+G”, and temporal change of coherence could be explained with residual of less than 0.1. However, fitness of the model for time-series of coherence that reference SAR data is different was not good. Therefore it may be necessary to consider the time variation of the time constant of the exponential function.

Keywords: volcanic ash, SAR, coherence

©2020. Japan Geoscience Union. All Right Reserved.

How to set wind condition data for stochastic ashfall risk assessment?

*Yoshinori TOKIZANE[1], Masatsugu Wakaura[1], Himeka Kikuchi[1]

1. OYO RMS Corporation

The tephra fall (pyroclastic fall) caused by large-scale eruptions is widely advected and diffused by the wind , affecting not only near the vent, but also several hundred kilometers away from the volcano. Regarding the uncertainty by wind, even if the eruption phenomenon itself is the same, the uncertainty due to the difference in the wind direction and wind speed in the sky is large, so in the ashfall risk assessment, appropriately evaluate the diversity of the wind in the sky It is extremely important to do. Therefore, for example, in the recently created ashfall hazard map, efforts have been made to show the maximum thickness by performing ashfall simulation using the wind for the past several years comprehensively (Towada Volcano Disaster Prevention Council, 2018) . In addition, ashfall simulations using wind data from past decades based on long-term reanalysis weather data (JRA-55) have been attempted (Sasaki et al., 2019).
On the other hand, in the probabilistic ashfall risk assessment, it is general to use not only the above-mentioned wind direction and wind speed but also the logic grey, which branches the eruption scale, etc. (Jenkins, 2012). If the long-term wind direction / wind speed is comprehensively applied to this logic tree, the number of branches becomes enormous. Furthermore, when all volcanoes in the world are targeted, it is necessary to reduce the number of branches of the wind direction and speed.
In this study, for the Hoei scale eruption of Mt. Fuji, the conditional excess probability of ashfall was calculated using all wind direction and speed data (n = 10,685) for the past 30 years. Next, it was confirmed that the wind direction and speed were steady data although the seasonality was strong. Therefore, random sampling was performed every month, and a hazard curve was created based on the sampled wind direction and wind speed data. As a result, it was confirmed that there is no effect even if it is reduced to 120 in the east of the crater (Fig. 1). On the other hand, in other directions, more wind data is needed to reproduce the hazard curve based on all wind data, and the amount of ash fall required by wind data of about 240 to 600 is required (Fig. 2).

Keywords: stochastic ashfall risk assessment, Tephra2

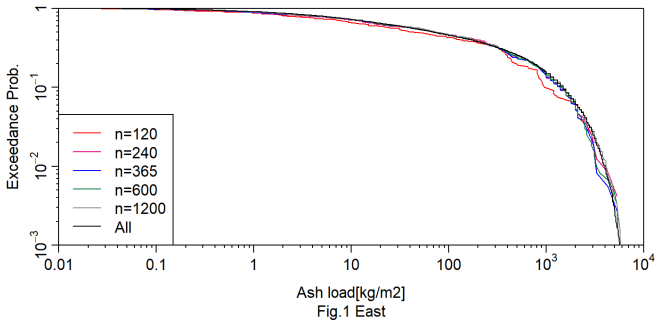

Fig.1 East

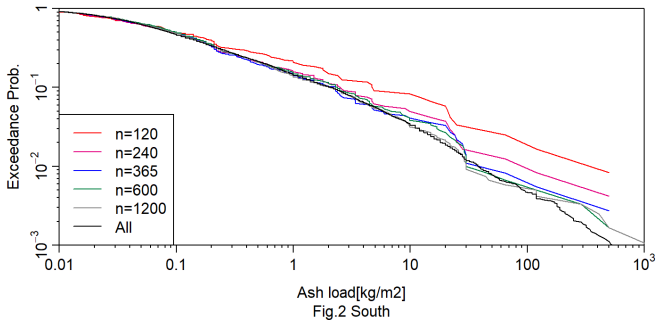

Fig.2 South

©2020. Japan Geoscience Union. All Right Reserved.

Validity of thickness of Aso-4 tephra fall deposit of the Uwa Basin, western Shikoku

*Chisato Nakamura[1], Tomohiro Tsuji[2], Michiharu Ikeda[3], Naoki Nishizaka[4], Kozo Ohnishi[4], Masayuki Sakakibara[5,6]

1. NAIBA Co. Ltd., 2. Graduate School of Science and Technology for Innovation, Yamaguchi University, 3. Shikoku Research Institute INC., 4. Shikoku Electric Power Co. Ltd., 5. Faculty of Collaborative Regional Innovation, Ehime University, 6. Research Institute for Humanity and Nature

The volume of tephra related to the Aso-4 eruption of about 89 ka is estimated to be more than 400 km^3 (Machida and Arai, 2003). It was calculated using an isopach map based on a thickness of 15 cm on eastern Hokkaido. Takarada (2019) recently compiled an isopach map based on previous study data and estimated the volume of the Aso-4 tephra. It is shown that the Aso-4 eruption volume was larger than previously thought. An estimate of the volume of the Aso-4 tephra requires reliable thickness measurements from proximal areas (e.g., Kyushu and Shikoku Islands) to distal them (e.g., Hokkaido Island). In some cases, tephra layers consist of primary and secondary volcaniclastic deposits, which are defined as the “direct” products of volcanic eruptions and the “reworked” products of the former, respectively. This is a problem in evaluating the thickness of tephra layers. Because of an estimate of the volume greatly changes by thickness data, it is necessary to interpret the distinction thickness of primary tephra layers.

The high-quality thickness data of the Aso-4 tephra fall deposit in core UT from the Uwa Basin on western Shikoku was reported to be a 31-cm-thick by Tsuji et al. (2018). The Uwa Basin is in a relatively short distance from Kyushu Island volcanoes. Because tephras of eruption events of various scales are likely to be recorded, many tephra layers are reported in the thick sediments which continuously deposited for 0.7 Myr sediments from the Uwa Basin (e.g., Tsuji et al., 2018).

It is desirable to evaluate the thickness data of the Aso-4 fall deposit with multiple cores from the Uwa Basin. In this study, we obtained the thickness of the Aso-4 fall deposit in the core UT-iwk which sampled at about 500 m north of the core UT to examine the validity of the Aso-4 fall deposit thickness from the Uwa Basin. The thickness of the Aso-4 fall deposit of the core UT-iwk was 20–30 cm, slightly thinner than the core UT. The determination methods of the thickness of primary fall deposits are (1) observation of sedimentary structures by utilizing half cores and surface peel specimens, (2) existence of accidental clasts, and (3) measurement of grain size change of volcanic glass shards. Overall, the Aso-4 fall deposit in the core UT-iwk doesn’t exhibit lamination and includes a minor amount of accidental clasts (<5%). The bottom layer is characterized by a concentration of large pumices; the maximum pumice size of 3 mm. The lower part consists mostly of coarse phenocrysts and pumices. The upper part is weakly sorted; the average size of volcanic glasses decreases slightly towards the top. These detailed descriptions allow the getting of the thickness of primary tephra layers.

Additionally, the core B1 was sampled at a point about 1 km northwest of the core UT. The thickness of the Aso-4 fall deposit in it was about 30 cm (Soyama et al., 2012, Soyama et al., 2013). The bottom altitudes of the Aso-4 fall deposit in the core UT, the core B1, and the core UT-iwk is 206.00 m, 206.93 m, and 206.17 m, respectively. The thicknesses of the Aso-4 fall deposit in all cores have a range of 20–30cm-thick in three sites with about the same altitude. These data suggest the thickness of the Aso-4 fall deposit in western Shikoku is estimated to be 30 cm. The thickness data is useful in calculating the

©2020. Japan Geoscience Union. All Right Reserved.

volume of the Aso-4 fall deposit.

Machida, H. and Arai, F. 2003. Atlas of Tephra in and around Japan (revised edition).
Soyama C., Sakakibara M., Ikeda M. and Tsuji T. 2012 Volcanic petrology of Aso-4 tephra in Unomachi core samples, western Shikoku, southwestern Japan. Programme and abstracts the Volcanological Society of Japan, P56, 155.
Soyama C., Sakakibara M., Sano S., Ikeda M. and Tsuji T. 2013. Volcanic petrology of Aso-4 tephra (ca. 90 ka) in western Shikoku, southwest Japan. Proceeding of 1st International Seminar of Environmental Geoscience in Asia, 1-5.
Takarada S. 2019. Estimation of Eruptive Volume of the Aso-4, Aira and Toya eruptions. Programme and abstracts the Volcanological Society of Japan, A3-14, 46.
Tsuji T., Ikeda M., Furusawa A., Nakamura C., Ichikawa K., Yanagida M., Nishizaka N., Ohnishi K. and Ohno Y. 2018. High resolution record of Quaternary explosive volcanism recorded in fluvio-lacustrine sediments of the Uwa basin, southwest Japan. Quaternary International, 471, 278-297.

Keywords: Aso-4, tephra fall deposit, thickness, Uwa Basin

©2020. Japan Geoscience Union. All Right Reserved.

Improvement of accuracy of DEM generated using UAV -a case study of the central crater of Izu-Oshima volcano, Japan-

*mori takaaki[1], Shunsuke Miura[1], Takumi Mochizuki[1], Shino Naruke[1], Hideki Nonaka[1], Hisashi Sasaki[1], Kenichi Arai[1], Koji Fujita[1], Toshihiro Urayama[1], Tatsuro Chiba[1]

1. ASIA AIR SURVEY CO.,LTD.

1. Introduction

Typhoon No. 19, which occurred on October 6, 2019, landed on the Izu Peninsula with large and strong power and passed through the Kanto region. We prepared a topographic model of the Miharasan central crater using UAV in 2017 in preparation for the next eruption of Izu Oshima. However, the terrain around the central crater of Miharayama may have changed due to the effect of Typhoon No.19, so the latest terrain model around the crater was recreated using UAV. The terrain model was created using SfM / MVS from images taken by UAV. The software used was Metashape.
In this study, in order to evaluate the accuracy of the terrain model, a reference point (GCP: Ground Control Point) was set around the crater, and the position accuracy of the terrain model with and without the reference point was verified. In addition, the volume of the crater was calculated and the state of collapse was confirmed from the created terrain model around the crater.

2.Izu Oshima, Miharayama central crater photography

A demonstration experiment was conducted at Izu Oshima from November 7 to November 8, 2019. The UAV used is Matrice210 (manufactured by DJI) and the camera mounted is ZENMUSE X4S (visible light). The UAV was automatically navigated with the camera oriented vertically to cover the area around the crater. The number of shot images is about 500.

3. Ground Control Point (GCP)

Until now, the position information obtained from the GPS mounted on the UAV was used, but there was a problem with the position accuracy, especially in the height direction, when compared with existing aerial laser surveying. Therefore, in this flight, a reference point was set and the position accuracy of the terrain model was verified. 18 reference points were set along the crater outer ring promenade so as to be uniform over the UAV measurement range. Network-based RTK-GPS positioning (VRS method) was performed on the installed reference points to obtain highly accurate position information.
Comparing the position accuracy (elevation value) of the terrain model with and without the reference point, the terrain model was created with "with reference point (RMS: 0.10 m)" compared to "without reference point (RMS: 24.96 m)" As a result, the result that the error was significantly reduced was obtained. In particular, the accuracy in the height direction was reduced. It is important for the difference analysis of the terrain model that the error of the position accuracy is small, and it is considered important to acquire and accumulate the reference point coordinates of the measurement candidate site before the eruption.

4.Difference analysis

For the image taken last time in 2017, the model was recreated by applying the reference point of 2019, and difference analysis was performed. It was confirmed that a part of the vertical cliff west of the central crater collapsed and accumulated at the bottom of the crater. According to the data of the volcanic eruption prediction series, it was clear that the collapse occurred between September 26 and October 9, which seems to have occurred during the typhoon 19.

©2020. Japan Geoscience Union. All Right Reserved.

5. Summary

A reference point was set around the central crater of Miharayama, and a terrain model with higher positional accuracy than before could be created. The volume of the crater was clarified, so that it was possible to calculate the amount of lava accumulated in the crater from images taken obliquely, even if the crater could not fly over the crater after the eruption. In addition, from the difference analysis of the topographic models of 2017 and 2019, it was confirmed that the landslide had collapsed on the western slope of Miharayama central crater.

Although the reference point was found to be important for the accuracy of the terrain model in the creation of the terrain model, it is practically difficult to enter the vicinity of the crater during the eruption, and it is difficult to set the reference point. The latest UAV has an RTK-GNSS-equipped type, and there is a possibility that the same high-precision terrain model can be created without setting a reference point. Utilizing such technology, we would like to study so that a more accurate terrain model can be created in a short time.

Keywords: UAV, Active Volcano, SfM/MVS

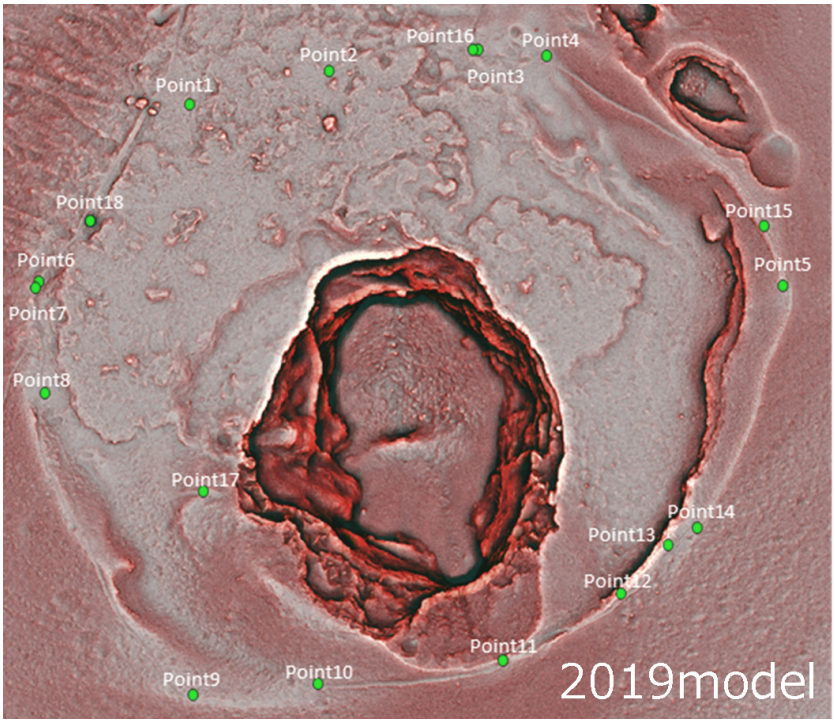

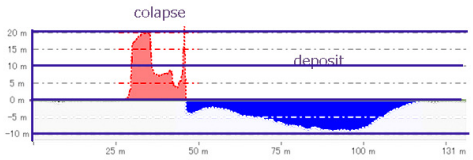

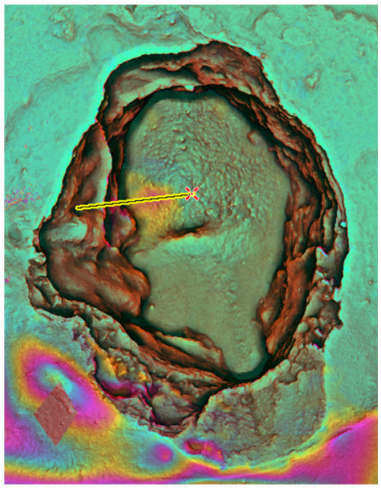

©2020. Japan Geoscience Union. All Right Reserved.

Types and characteristics of evacuation shelters for volcanic eruption in Japan

*Hisashi Sasaki[1], Shino Naruke[1], Hiroyuki Yamada[2]

1. Asia Air Survey Co., Ltd., 2. National Defense Academy

After the sudden eruption of Mount Ontake in September 2014, 58 people were left dead and 5 people were missing. After this eruption, the Cabinet Office, Government of Japan published the “Guide to Enhancing Evacuation Shelters, etc. on Active Volcanoes" (hereafter it is abbreviated as the "shelter guide") in 2015. After this guide was published, the installation of evacuation shelters began around several volcanoes in Japan. Two types of evacuation shelters are installed in Japan. One is a special facility for a volcanic eruption. RC construction (cast-in-place concrete and installation of precast concrete) is common for special facilities. Steel constructions are classified into temporary and permanent types. Both are special facilities for evacuation and remain unused on regular days. The other is a dual-use facility where the shelter function is added to tourist facilities such as rest houses and visitor centers. When an all or part of a tourist facility is turned into a shelter by RC construction, tourists and passengers can evacuate in the event of an eruption. The "shelter guide" demonstrated a method to use aramid fiber to reinforce the roofs or ceilings of wooden buildings. Reinforcement using aramid fiber is currently being undertaken in mountain huts around Japanese volcano.

Keywords: shelter, active volcano, evacuation

©2020. Japan Geoscience Union. All Right Reserved.

Disaster prevention using data of climber’s movement and tendency in active volcanoes

*Yosuke Miyagi[1], Setsuya Nakada[1], Mitsuhiro Yoshimoto[2], Tomohiro Kubo[2], Ryo Honda[2]

1. National Research Institute for Earth Science and Disaster Resilience, 2. Mount Fuji Research Institute

Integrated Program for Next Generation Volcano Research conducted by Ministry of Education, Culture, Sports, Science and Technology, Japan started in 2016. This project takes notice to not only observation and prediction researches but also research for countermeasure technology of volcano disasters. National Research Institute for Earth Science and Disaster Resilience has been in charge of one of the main theme which is named “Development of countermeasure technology for volcano disasters”. In this theme, we develop an information tool for volcano disasters, in which we consider disaster management personnel in local governments as users, and we try to provide appropriate information for them in both the event of disaster and normal times.
In the tragic disaster of Ontake Volcano in 2014, it was difficult for local governments to grasp whereabouts of climbers and to conduct rescue and search for victims. Even recently, climbers can approach to an active vent in many volcanoes in Japan, for example Mt. Fuji, it is quite important to grasp whereabouts of climbers in the event of disaster for proper decision of rescue and search.
Experiments to acquire data of climbers have conducted in Mt. Fuji since 2015 and Mt. Ontake in 2019, named “Mt. Fuji Challenge” and “Mt. Ontake Challenge”. In experiments, we distribute beacons to climbers and receivers which are set in mountain trails detect signals from the beacons, then we can grasp the number and location of climbers who have the beacons. In the experiment in 2018, it took about two hours to grasp locations of 3,000 climbers.
In this research, we are going to use the data for disaster prevention. In the event of disaster, it is possible to reduce the time for grasping climber’s information. In the normal time, local governments can refer the output data to make evacuation plans, including establishment of shelters or evacuation routes.
The information tool developed in our research use the climber’s data as input data, and visualize on GIS like software. As a result, it is possible to grasp whereabouts of climbers on map information, including trails, shelters and hazard information from hazard map. Now we try to promote actions for disaster prevention by local governments around Mt. Fuji and Mt. Ontake, in which there are climber’s data from the experiments, by using our information tool and the climber’s data. In next summer, other experiment will be conducted in Nasudake Volcano.

Keywords: Next Generation Volcano Research, countermeasure technology for volcanic disaster, data of climber’s movement and tendency

©2020. Japan Geoscience Union. All Right Reserved.

Development of Proto-type Educational Web Contents for the Municipalities' Disaster Response Staff

*Tomohiro Kubo[1], Mitsuhiro Yoshimoto[1], Yuki Horiuchi[1], Ryo Honda[1], Yasuhiro Ishimine[1], Yosuke Miyagi[2]

1. Mount Fuji Research Institute, 2. National Research Institute for Earth Science and Disaster Resilience

After 2014 Mt. Ontake eruption, the municipalities which have active volcano are obliged to prepare the evacuation plan following the "Act on Special Measures for Active Volcanoes". As a result, the municipalities are going to prepare the evacuation plan following, but there is less information about the volcano disaster. Because the volcano disaster is low frequency than other nature disaster. Therefore, we develop the proto-type educational web contents for the municipalities' disaster response staff who prepare the evacuation plan and give the residents a lecture of the volcano disaster response.

The web contents consist of the information about the volcano phenomenon and volcano disaster, the applicable laws and regulations, and sharing the disaster prevention events with neighboring municipalities.

We report the web contents and the result of trial utilization by the municipalities' disaster response staff.

Keywords: disaster prevention education, Municipalities' disaster response staff, Volcano Disaster, Web Contents

©2020. Japan Geoscience Union. All Right Reserved.

[J] Poster | S (Solid Earth Sciences)：S-VC Volcanology

[S-VC47] Volcanic and igneous activities, and these long-term forecasting

convener:Teruki Oikawa(GSJ, National Institute of Advanced Industrial Science and Technology), Takeshi Hasegawa(Department of Earth Sciences, College of Science, Ibaraki University), Daisuke MIURA(Department of Physical Science, Graduate School of Science, Osaka Prefecture University), Nobuo Geshi(Geological Survey of Japan, The National Institute of Advanced Industrial Science and Technology)

This session focuses on generation and accumulation processes of magmas, magma-crust interaction and degassing, and modes of eruption, long-term forecast of eruption, dispersal and emplacement of the volcanic products. The discussion spans petrological, geochemical, geophysical, and geological processes related with volcanic activity and products in the past, the present and the future.

[SVC47-P01] Yield strength obtained from tree molds and lava tube caves of Medicine Lake Volcano

*Tsutomu Honda[1] (1.Vulcano-speleological Society)

[SVC47-P02] Phase separation in mushy magma reservoirs

*Christian Huber[1], Matej Pec[2], Olivier Bachmann[3] (1.Brown University, 2.MIT, 3.ETH Zurich)

[SVC47-P03] Age of the Toya caldera eruption

*Akihiko Tomiya[1], Isoji Miyagi[1] (1.Geological Survey of Japan, National Institute of Advanced Industrial Science and Technology)

[SVC47-P04] Stratigraphy and eruption styles of 40 ka Kp I eruption, Kutcharo Volcano, Eastern Hokkaido, Japan

*Shibata Shohei[1], Takeshi Hasegawa[2] (1.Graduate school of Science and Engineering, Ibaraki University, 2.Depeartment of Earth Sciences, College of Science, Ibaraki University)

[SVC47-P05] Volcanic structure and tephrostratigraphy of the Iwate volcano clarified by the determination of collapse source of debris avalanches

*Nobuo Doi[1] (1.Research Center for Regional Disaster Management, Iwate University)

[SVC47-P06] Experimental constraints on magma storage conditions for caldera-forming eruptions of Towada volcano, Japan: a preliminary report

*Takayuki Nakatani[1], Toshihiro Suzuki[1], Takashi Kudo[1], Masashi Ushioda[1], Akihiko Tomiya[1], Akiko Tanaka[1] (1.Geological Survey of Japan, AIST)

[SVC47-P07] Transition sequence of the Y4 Eruption, Izu-Oshima volcano, Japan.

*Yoshihisa Kawanabe[1] (1.Geological Survey of Japan, AIST)

[SVC47-P08] Eruptive stratigraphy and magma compositions of the Tsubota stage (4.0-2.5 ka) in the southern part of the Miyakejima Volcano, Japan

*Shota Watanabe[1], Takeshi Hasegawa[1], Teruki Oikawa[2], Nobuo Geshi[2] (1.Graduate School of Science and Engineering, Ibaraki University, 2.Geological Survey of Japan, The National Institute of Advanced Industrial Science and Technology)

[SVC47-P09] Reconsideration of Late Quaternary tephrostratigraphy on Mikurajima Volcanic Island, Izu Islands.

*Tomohiro Tano[1], Takehiko Suzuki[1,2], Daisuke Ishimura[1,2], Satoshi Terayama[1], Tatsuki Watanabe[1] (1.Department of Geography, Tokyo Metropolitan University , 2.Research Center for Volcanic Hazards and Their Mitigation,Tokyo Metropolitan University)

[SVC47-P10] Holocene volcano of Kazafuki Volcano, Shirouma-Oike volcanoes, central Japan.

*Teruki Oikawa[1], Shun Nakano[1] (1.GSJ, National Institute of Advanced Industrial Science and Technology)

[SVC47-P11] The Omine Tuffite Dike and its Accompanied Andesite Fragments, Central Kii Peninsula, SW Japan

*Yutaka WADA[1], Kohnosuke NISHIMOTO[2] (1.Department of Earth Sciences, Nara University of Education, 2.Heguri Junior High School)

[SVC47-P12] Volcanic activity of the Miocene Basalts in Yatakayama Area, Kibi Plateau, Takahashi City, Okayama Prefecture, SW Japan

*Takumi Nagato[1], Shigeyuki Suzuki[1], Haruo Koami[2], Kotaro Nakai[1], Toru Tachibana[3] (1.Okayama University, 2.Okayama Prefectual Okayama Asahi Senior High School, 3.Soil Engineering Corporation)

[SVC47-P13] Textural observation and chemical analyses of 1716-1717 Kyoho eruption pumice at Shinmoedake, Kirishima volcano group

*Akari Kagawa[1], Atsushi Toramaru[1] (1.Kyushu university)

[SVC47-P14] **Identification of lava flow temperature by lava tube cave structure of Mt.Etna**

*Tsutomu Honda[1] (1.Vulcano-speleological Society)

Yield strength obtained from tree molds and lava tube caves of Medicine Lake Volcano

*Tsutomu Honda[1]

1. Vulcano-speleological Society

1.Introduction: Medicine Lake Volcano in northern California is the largest volcano in the Cascade Range that has erupted nine times over the past 5200 years. On the northeastern flank of this shield volcano, many lava tree molds formed on the lava flow that flowed about 10,000 years ago and many lava caves formed 30,000 to 40,000 years ago are preserved in the Lava-Beds National Monument [1,2,3)]. We measured the depth of these tree molds and the height of the lava tube cave, then, estimated the yield strength of the lava flow. The slope angle was roughly estimated by reading the map contour.

2.Lava tree molds: Lava tree molds are abundant in the btm (basaltic tree mold) lava flow of SiO_2: 51.9wt%, 12,330 yr B.P at an altitude of 2000m, with their diameter range from 15cm to 90cm. Since it is an old lava flow, deposits are accumulated at the bottom of most vertical tree molds, though for the btm-TM-4.2m vertical tree mold,it has been removed for C14 dating[4)]. The position of the tree mold at N41.63854, W121.60744, with diameter: 0.79mx0.91m, depth: 4.2m as shown in Fig.1. . As the tree mold depth is the lava flow thicknessH, the critical limit thickness of lava flow $f_B = H(\rho g \sin\alpha)$ was used to determine the apparent lava yield strength f_B where the gravity acceleration was $g = 980$ cm / s^2, and density was $\rho = 2.5$ g / cm^3. As shown in Table.1, the apparent yield strength: $1.8x10^4$ Pa is obtained from the slope angle α of 9.5 ˚. This apparent yield strength shows a relatively high value for a lava flow of SiO_2 : 51.9wt%, which may be due to lava inflation.

3.Lava tube caves: The heights H of Valentine Cave located in bvc lava flow(SiO_2: 53.0 wt%, 12,260 yr B.P.) and Sentinel Cave located in bmc lava flow(SiO_2: 52.3 wt%, 40Ar / 39Ar age / 36 ±16 ka) are measured. Fig.2 and Fig.3 show photographs of inside of each cave. The lava yield strength f_B was obtained from the flow critical limit condition of the gravity flow in an inclined pipe of slope angle: α,$f_B = H(\rho g \sin\alpha) / 4$. Table 2 shows the lava yield strength obtained from these lava tube caves. The obtained yield strength is in the range of $1.54x10^3$ to $2.8x10^3$ Pa which is a reasonable yield strength as a basaltic lava of SiO_2: 52.0-53.0 wt%.

4.Conclusions: The apparent yield strength obtained from the tree mold depth (lava thickness) is 6 to 12 times higher the yield strength obtained from the lava tube cave height. Even though the btm lava flow is different from the bmc lava flow, this indicates that the lava flow caused lava inflation in general and transitioned from simple flow to inflated flow. This also shows that the lava tube cave is formed through lava inflation.

Acknowledgments: I wish deeply thank to Dr. J. Donnelly-Nolan and Dr. J. Tinsley of the US Geological Survey (USGS) for geological information and the location of lava trees and their excavation status.

References:

1)Johnston, D.A., and Donnelly–Nolan, J.M. eds(1981)., Guides to some volcanic terranes in Washington,

©2020. Japan Geoscience Union. All Right Reserved.

Idaho, Oregon, and northern California: US Geological Survey Circular 838, p143

2)Katie Keller Lynn(2014): Lava Beds National Monument Geologic Resources Inventory Report Natural Resource Report NPS/NRSS/GRD/NRR—2014/804 p22-23

3)http://geotripper.blogspot.com/2010/01/other-california-if-tree-falls-in.html

4)Private communication with Donnelly–Nolan, J.M.,:Jul 16, 2018, on the locations of the carbon-14 samples collected from large tree molds in map units btm, bvc, and bbr.

5)Donnelly–Nolan, J.M (2010):Geologic Map of Medicine Lake Volcano, Northern California:Pamphlet to accompany Scientific Investigations Map 2927,USGS

Keywords: tree mold, lava tube, yield strength, lava flow

Fig.1 4.2m lava tree mold(btm lava flow)

Fig.2 Valentine cave (bvc lava flow)

Fig..3 Sentinel cave(bmc lava flow)

Table.1 Apparent yield strength obtained from lava tree mold depth of btm lava flow(*from ref 5))

btm-TM No. (12,330 yr B.P, SiO_2:51.9wt% *)	Depth:H(lava thickness)	Lava density: ρ	Gravity:g	Slope angle: α (by map contour)	Apparent yield strength: $f_B=H(\rho g \sin\alpha)$
btm-TM-4.2m	4.20m	2500kg/m^3	9.8m/sec^2	9.5°	1.8x10^{4}Pa

Table.2 Yield strength obtained from lava tube cave height of bvc and bmc lava flows(*from ref 5))

Lava flow name and eruption time *	SiO2 wt%*	Slope angle α from contour	Lava tube cave name and height:H	Yield strength $f_B=H(\rho g \sin\alpha)/4$
Valentine Cave (bvc) 12,260 yr B.P	52.9, 52.9, 53.4% avg of 3 samples= 53.0%	6 °	Valentine cave: H= 8-10ft=2.4m~3m	1.54 x10^{3}Pa ~1.93 x10^{3}Pa
Mammoth Crater(bmc) 40Ar/39Ar age is 36±16 ka	48.4–55.9%; avg of 45 samples= 52.3%	3.5°	Sentinel cave：H= 25 ft high=7.5m	2.8x10^{3}Pa

©2020. Japan Geoscience Union. All Right Reserved.

Phase separation in mushy magma reservoirs

*Christian Huber[1], Matej Pec[2], Olivier Bachmann[3]

1. Brown University, 2. MIT, 3. ETH Zurich

Phase separation in crystallizing magma reservoirs plays a fundamental role in the generation of silica-rich magmas and influences the long and short term evolution of volcanic systems. As more evidences suggest that reservoirs are dominantly in a mush state for most of their lifespan, phase separation from permeable but rheologically locked-up reservoirs is likely efficient, despite the high viscosity of the melt and and crystal framework involved in these processes. In this presentation, we use a combination of field data, laboratory experiments and physical modeling to study phase separation in crystal mushes. We specifically focus on the different modes of exsolved volatiles and melt transport through mushy magmas, with an emphasis on constraining the processes and timescales involved. We find that the broad range of crystal volume fraction over which phase separation takes place impacts the mode of mush deformation that accommodates phase separation. Furthermore, these different modes of extraction have distinct efficiencies with some able to operate even with relatively low driving stresses, and are likely to leave different footprints in the rock record.

Keywords: melt extraction, volcanology, crystal mush

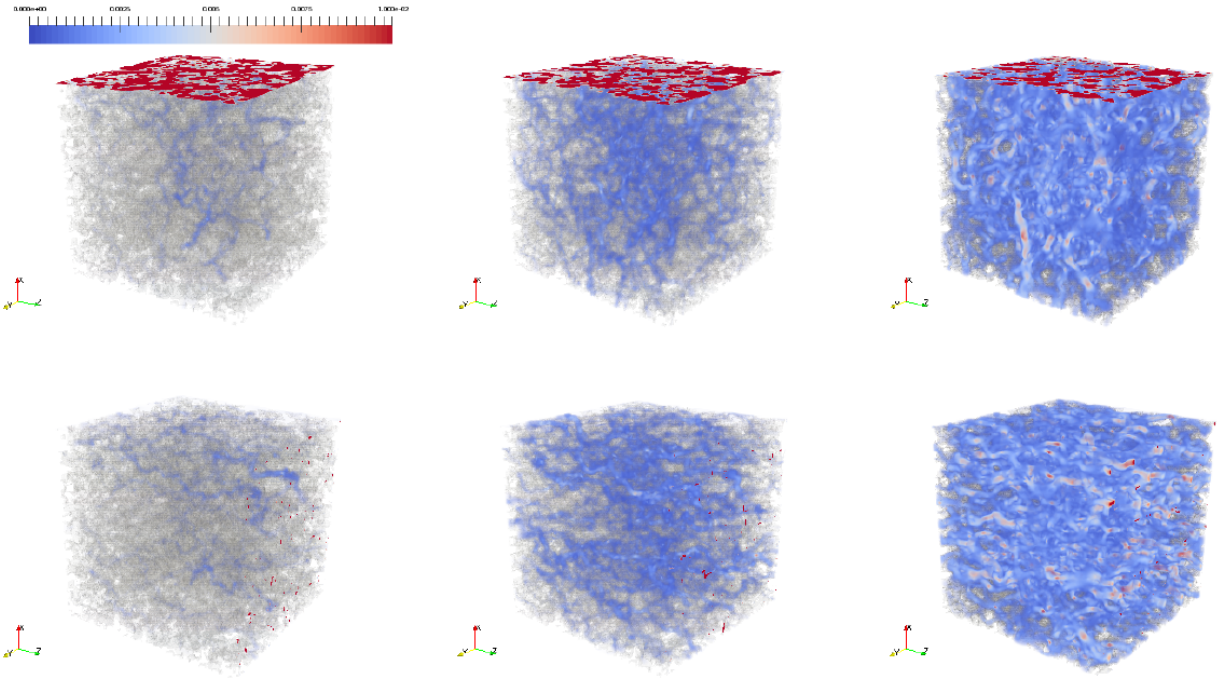

©2020. Japan Geoscience Union. All Right Reserved.

Age of the Toya caldera eruption

*Akihiko Tomiya[1], Isoji Miyagi[1]

1. Geological Survey of Japan, National Institute of Advanced Industrial Science and Technology

1. Introduction

Toya caldera eruption is one of the largest eruptions in Japan, producing Toya ignimbrite (>36.8 km^3; Goto *et al.*, 2018) and Toya ash (Toya; >150km^3; Machida et al., 1987; Takarada, 2019). Toya ash is one of the most useful marker tephras in Japan. The age of Toya eruption, estimated by radiometric and stratigraphic dating, is about 0.11 Ma (see later). However, when looking closer, there is some confusion because the eruption age used differ from researcher to researcher. Precise age determination is valuable since Toya ash is a critical time marker of 0.11 Ma or Marine Isotope Stage (MIS) 5d (5.4) (e.g., Kudo, 2018). Therefore, we compiled and evaluated the reported ages to propose an appropriate age (Tomiya and Miyagi, 2020).

2. Absolute age

Early studies to measure the ^{14}C age (e.g., Minato, 1966) failed because of the much shorter half-life of ^{14}C than the eruption age. There is no K-Ar age reported because of the much longer half-life of ^{40}Ar. The first reported eruption age is 0.13±0.03 Ma by zircon FT (fission track) dating (Okumura and Sangawa, 1984). Then, Takashima *et al.* (1992) reported TL (thermoluminescence) ages of 0.103 to 0.134 Ma with an error of 30%. Ganzawa *et al.* (2007) reported SAR-RTL ages of 113±13 to 132±15 ka, and Ganzawa and Ike (2011) revised them to be 104±15 to 118±15 ka. Recently, Ito (2014) reported U-Pb and U-Th ages of 0.11±0.01 Ma and 108±19 ka, respectively, using laser ablation ICP-MS. Thus, the absolute age is about 0.11 Ma with an error of 0.01-0.02 Ma.

3. Relative age and its conversion

Toya ash overlies the MIS 5e (5.5) terrace and underlies the MIS 5c (5.3) one, indicating that it deposited in the MIS 5d (5.4) (Machida *et al.*, 1987; Machida and Arai, 2003). Combining with the information from deep-sea cores (Shirai, 2001; see later), Machida and Arai (2003) proposed the eruption age to be 112-115 ka.

Shirai *et al.* (1997) and Shirai (2001) studied Toya ash in the sediments recovered from ODP Site 794 (Sea of Japan). They estimated the eruption age to be 112 ka based on the correlation of dark and light layers with a nearby site where oxygen isotope record was available. To convert the stratigraphic position to the absolute age, they applied the oxygen isotope curve by Bassinot et al. (1994), where the peak of MIS 5.4 was 106 ka. Matsu'ura *et al.* (2014) studied Toya ash in the Chikyu C9001C cores (Pacific Ocean), where oxygen isotope record was available (Domitsu *et al.*, 2010, 2011). They clearly showed that the Toya ash deposited in the MIS 5.4. They adopted 106 ka as the eruption age because they considered it to be corresponding to the peak of MIS 5.4 by Bassinot *et al.* (1994) (Matsu'ura, personal comm.).

4. Reexamination of the age

The stratigraphic position of Toya ash is actually above the peak of MIS 5.4, according to the oxygen isotope record at C9001C. The eruption age, therefore, must be younger than that peak. Bioturbation is negligible at this site because the sedimentation rate is high (Domitsu, personal comm.). Furthermore, pollen analysis shows that Toya ash deposited after an extreme cold and dry period corresponding to the peak of MIS 5.4 (Ooi *et al.*, 1997).

Besides, the oxygen isotope curve by Bassinot *et al.* (1994) is not precise for <300 ka (Waelbroeck *et al.*,

©2020. Japan Geoscience Union. All Right Reserved.

2002). Recently, Lisiecki and Raymo (2005) and Thompson and Goldstein (2006) have proposed that the peak of MIS 5.4 is 109 ka, which we consider better.
Considering that the stratigraphic position of Toya is between the peaks of MIS 5.4 and MIS 5.3, we propose that the age of Toya eruption is ca. 106 ka. Even if the stratigraphic position is considered to be merely around the peak of MIS 5.4, the eruption age should be 109±ca.3 ka. These values well agreed to the absolute ages mentioned above.

For detail: Tomiya and Miyagi (2020) Age of the Toya eruption. *Bull. Volcanol. Soc. Japan*, 65(1), in press.

Keywords: Toya caldera, ignimbrite, Toya ash, MIS 5d (5.4), absolute age, relative age

©2020. Japan Geoscience Union. All Right Reserved.

Stratigraphy and eruption styles of 40 ka Kp I eruption, Kutcharo Volcano, Eastern Hokkaido, Japan

*Shibata Shohei[1], Takeshi Hasegawa[2]

1. Graduate school of Science and Engineering, Ibaraki University, 2. Depeartment of Earth Sciences, College of Science, Ibaraki University

Kutcharo volcano is located in eastern Hokkaido and is the location of the largest caldera in Japan (26×20 km). The first eruption associated with the formation of Kutcharo caldera produced the Furuume welded tuff (FWT) at 400 ka. Subsequent caldera-forming eruptions generated Kutcharo pumice flows Ⅷ to Ⅰ (KpⅧ to Kp Ⅰ in ascending order; Katsui and Satoh,1963 : Hasegawa et al.,2011). The shape of the present (26 x 20 km) caldera was mostly defined by the largest Kp IV eruption (175km$^{3:}$ Hasegawa et al.,2016). The Kp Ⅰ eruption (40 ka) is the second largest (125km^3) with its activity caused by large-scale phreatomagmatic explosion (Okumura, 1991,1996). However, detailed eruption stratigraphy, eruption styles and sequences are unknown.

We conducted geological survey to reveal the eruption sequence of Kp Ⅰ. In this study, we provide description of the tephra layers and subdivided stratigraphy. In addition, we performed grain size analysis and component analysis based on the subdivided stratigraphy and examined the evolution of the eruption styles. Grain size analysis was done using an electromagnetic sieve shaker for -5ϕ to 4ϕ. For finer particles (< 4ϕ), the particle size frequency was calculated using laser scattering particle size analyzer and converted to weight percentages. Further, the percentages of various component for 1 mm to 32 mm grains in the samples were determined by visual classification and weight scale.

As a result of the geological survey, Kp Ⅰ deposits are subdivided into Unit 1 to Unit 9 in ascending order. Units 1 and 2 are distributed within 30 km northeast of the caldera. Unit 1 is a yellowish white to white, clast-supported pumice layer, mainly composed of lapilli-sized pumice and lithic fragments with small amounts of isolated crystals and cohesive silty ash. Unit 2 is a white silty ash layer and rich in accretionary lapilli and isolated crystals. Units 3 and 4 are yellowish white to white pumice layer and white silty ash layer, respectively, showing similar facies as Unit 1 and 2. However, the distributions of Units 3 and 4 are wider than those of Units 1 and 2. Unit 5 is a white, clast-supported pumice layer. The pumice in Unit 5 is coarser and highly vesicular compared to those of Units 1 and 3. Unit 5 also rarely includes cauliflower surface pumice. Unit 6 is a white, silty ash layer containing accretionary lapilli with maximum thickness > 2 m and widely spread in eastern Hokkaido, and it can be correlated with Kutcharo-Shoro tephra (Kc-Sr: Machida and Arai, 2003). Unit 7 is a white, non-welded pumice flow deposit, covering aa wide area from northeast to west of the Kutcharo caldera. Unit 7 is the largest in Kp Ⅰ deposits with 2-30 m in thickness, and contains variously vesiculated pumices and cauliflower surface pumice. A heavier components (lithic fragments and crystals) concentration layer, observed at the base of Unit 7, is interpreted as the Ground layer (Walker et al.,1981). The Ground layer includes fresh andesite that is lacking in Unit 6 or lower. Unit 8 is a white silty ash layer with minor lapilli-sized pumices. Unit 9 is a white, non-welded pumice flow deposit. Distribution of Unit 8 and Unit 9 is limited in northern part of the caldera. Mineral assemblages of isolated crystals are plagioclase, pyroxene and olivine are common. On the other hand, few olivine phenocrysts can be recognized in pumice samples.

Grain size distributions of Unit 1 to 3 indicate bimodal distributions. The coarser and finer peaks are around -1 to 0ϕ and 5ϕ, respectively. On the other hand, Units 4 to 6 show unimodal distributions.

©2020. Japan Geoscience Union. All Right Reserved.

Sorting is more uniform in the upper units. Although the percentages of fine particles (≦4ϕ) are commonly 20~45 wt.%, Unit 5 is characteristically poor (4 wt%) in fine particles. Lithic componentry of Units 1, 2 and 3 are 26 wt%, 36 wt%, 37 wt%, respectively. While, those of Unit 4, 5 and 6 are 13 wt%, 3 wt%, 11 wt%, respectively.

It seems that the peaks of very fine particles (5ϕ) commonly recognized in Units 1 to 3 were generated by phreatomagmatic fragmentation. Furthermore, the poorly sorted and lithic rich characters of these units suggest vent-opening processes through an unstable conduit with wet conditions. Wider distribution areas and decreasing the proportions of lithic fragments for Units 4 to 6, indicate the vent system became more stable to form a higher eruption column. Units 6 and 7, account for the majority of the volume of the Kp I , ejected at climax phase. Vent widening and/or sifting resulting in caldera-formation occurred in Unit 7 because lithic types clearly changes from this phase. After the relatively small phases of Units 8 and 9, the explosive activity of KpI eruption terminated.

Keywords: Kutcharo caldera, Large scale pyroclastic flow, Tephra stratigraphy, Phreatomagmatic eruption

©2020. Japan Geoscience Union. All Right Reserved.

Volcanic structure and tephrostratigraphy of the Iwate volcano clarified by the determination of collapse source of debris avalanches

*Nobuo Doi[1]

1. Research Center for Regional Disaster Management, Iwate University

There are seven debris avalanche deposits (DADs) on the foot of Iwate volcano (Doi, 1991). They are Ippongihara DAD (AD915-1686), Hiragasa DAD (ca. 6.7ka), Yamagozawa DAD (ca. 30ka), Koiwai-Oishiwatari DAD (ca. 120ka), Shizukuishi DAD, Aoyamacho DAD (ca. 150ka), and Gohyakumori DAD (ca. 190ka) in descending order. The lower four DADs are in the horizon of Sotoyama Volcanic Ash. The source amphitheater (Amp) of upper three DADs were specified in the Higashi-iwate volcano, and the source of Koiwai-Oishiwatari DAD and Shizukuishi DAD were specified in the Nishi-iwate volcano (Doi, 2000, 2019).
In this study, the source of Aoyamacho DAD, which is newly named as Byobuone Amp, has been discovered in the Nishi-iwate volcano. Three volcanos such as Onimata, Sainokamisawa, and newly named Kometsuka volcano grew up in the Onimata Amp, Sainokamisawa Amp, and Byobuone Amp respectively. The Dogasawa volcano covers the east of Kometsuka volcano, and Kurokura volcano covers the west of Nishi-iwate main volcano. These volcanoes indicate that the Nishi-iwate volcano is composed of several volcanic edifices in the horizon of Sotoyama Volcanic Ash. The Dogasawa volcano erupted the Kaganai scoria falls (ca. 50-60ka) in the lower Shibutami Volcanic Ash. The Nishi-iwate caldera, which was formed by pyroclastic flow eruptions (ca. 30-45ka) at the summit of Nishi-iwate volcano, has a crater ca. 0.7-km in diameter at the center of caldera floor. The postcaldera Onawashiro volcano grew up at the western side in the crater. The crater may show us the mechanism of the summit caldera formation.

Keywords: debris avalanche deposit, amphitheater, Iwate volcano, volcanic structure, tephrostratigraphy

©2020. Japan Geoscience Union. All Right Reserved.

Experimental constraints on magma storage conditions for caldera-forming eruptions of Towada volcano, Japan: a preliminary report

*Takayuki Nakatani[1], Toshihiro Suzuki[1], Takashi Kudo[1], Masashi Ushioda[1], Akihiko Tomiya[1], Akiko Tanaka[1]

1. Geological Survey of Japan, AIST

Towada volcano is an active arc volcano located in the northern part of Northeast Japan and characterized by a large caldera lake with a diameter of ca. 10 km. At this volcano, two extensive eruptions, which are called eruptive episodes N and L, generated Ofudo pyroclastic flow at 36 ka and Hachinohe pyroclastic flow at 15.5 ka, respectively. These eruptions discharged large-volume silicic magma (~20 km^3 dense rock equivalent in each eruption), causing caldera formation. Although the constraints on magma storage conditions for such large-scale eruptions is fundamentally important in terms of risk assessment of future caldera-forming eruptions, precise determination via an experimental approach is still lacking for Towada volcano. From a petrological point of view, amphibole is present in the eruptive product of episode L, but absent in that of episode N. The presence or absence of such hydrous minerals is important because it may reflect the water content in the magma, which controls explosiveness of eruption. However, this has not been understood in terms of the differences in magma storage conditions.

Here we conducted petrological and experimental studies on the silicic endmember pumice from the pyroclastic flow deposits of the eruptive episodes N and L (bulk SiO_2 content: 73.1 wt% for N, 72.0 wt% for L) to understand the magma storage conditions for the caldera-forming eruptions at Towada volcano. The phenocryst mineral assemblages in the silicic endmember pumice of the eruptive episodes N and L are plagioclase (Pl) + orthopyroxene (Opx) + clinopyroxene (Cpx) + Magnetite (Mt) + ilmenite (Ilm) and Pl + Opx + Cpx + Hornblende (Hbl) + Mgt + Ilm, respectively. Magnetite-ilmenite thermo-oxymetry revealed that average temperature and oxygen fugacity of the pre-eruptive silicic endmember magma for the episodes N and L are mostly identical at ~850˚C and ΔNNO (Ni-NiO) = + 1.2.

Phase equilibrium experiments were performed for both episode N and L pumices at 850˚C and 1.5–2.5 kb, and at 875˚C and 2 kb for 5–8 days by using an internally heated pressure vessel (SMC-5000) which has been newly installed at GSJ/AIST. Staring glasses were synthesized by fusing as-is pumice powders at 1250˚C and 2.3 kb for 3 hours. All the phase equilibrium experiments were conducted under a water-saturated condition and oxygen fugacity was buffered with Ni and NiO (i.e., ΔNNO = 0). Magnetite was absent in all the experiments possibly due to the relatively low oxygen fugacity compared to that estimated for the natural magmas. Plagioclase was always present in the L system, but absent at 850˚C and 2.5 kb and 875˚C and 2.0 kb in the N system, which indicates the higher liquidus temperature for plagioclase in the more mafic L system. The assemblage of Pl + Opx + Cpx + Ilm was observed at 850˚C and 1.5 kb (ca. 6 km deep) in both systems; they may correspond to the storage conditions for the episode N magma. Hornblende was crystalized at 850˚C under higher pressures of 2.0 and 2.5 kb in both systems, while it was absent at 875˚C and 2.0 kb. This indicates that hornblende crystallization favors relatively high pressure and low temperature conditions. However, hornblende did not coexist with pyroxenes in all the experiments, implying that further experiments are necessary especially at water-undersaturated conditions to determine the storage conditions for the episode L magma.

©2020. Japan Geoscience Union. All Right Reserved.

This research was supported by the Secretariat of the Nuclear Regulation Authority, Japan.

Keywords: Internally heated pressure vessel, Towada volcano, caldera, phase equilibrium experiment, amphibole

©2020. Japan Geoscience Union. All Right Reserved.

Transition sequence of the Y4 Eruption, Izu-Oshima volcano, Japan.

*Yoshihisa Kawanabe[1]

1. Geological Survey of Japan, AIST

Izu Oshima volcano Y4 eruption is a large-scale eruption that occurred in the first half of the 15th century. In the Y4 eruption, a flank eruption occurred the southeastern part of Izu Oshima. The fissure of Y4 flank craters is approximately 4 km in length in the northwest-southeast direction from the southeastern Imasaki coast to the vicinity of Mabushi Forest Road. In this report, the interpretation of the airborne laser survey data and the on-site geological survey have revealed the distribution of side craters and the transition of eruptions from the tephra.

Of the two pyroclastic cones previously considered N1 flank volcanoes, the northern “Mokkoku” pyroclastic cone has a fresh crater rim and the craters are lined up in the same direction as the Y4 eruption flank craters, and lava flows from the southwestern foot of the cone. The lava flow was confirmed to be Y4, and the "Mokkoku" pyroclastic cone was determined to be a volcano on the Y4 eruption.

On the northwestern extension of the Y4 flank fissure near the Mabushi Forest Road, there is a fissurer-like topography extending across the ridge. In the northwestern extension there is a dike that cuts the N4 pyroclastic cone, and on the southwestern part of the caldera rim, a slightly welded spatter covers the caldera rim on the west of the Suberi-dai. The chemical composition of the welded spatter is consistent with that of the initial eruption product of the Y4 eruption, but not with other eruption products.

From these facts, it is considered that the Y4 eruption crater extended into the caldera. The fissure of the Y4 flank eruption is about 6 km long on the ground, and reaches 10 km including the seafloor (Ishizuka et.al., 2014).

The Y4 eruption tephra is divided into Y4a scoria fall, Y4b ash mainly composed of scoria ash, Y4c scoria fall, and Y4d fall ash with light gray / light brown ash layers. Y4a may be divided into lower Y4a1 scoria fall and Y4a2 scoria fall depending on size change. The Y4a1 is thick in the southeastern part of the island and its distribution is considered to originate mainly from the flank craters. The Y4a2 is thicker on the north side than Y4a1, and it is considered from the distribution axis that it erupted from Mt. Mihara area. This indicates that the flank eruption of Y4 occurred in early stage of the eruption, followed by a scoria discharge eruption at the summit. Y4a1 and Y4a2 fall scoria have almost the same whole-rock chemical composition as the spatters and lava of the early Y4 eruption stage.

Both Y4b and Y4d have no axis in a specific direction. Volcanic ash release may have taken place over a long period of time. Y4c scoria fall which covers Y4b are richer in Al_2O_3 than early eruptives such as Y4a. The axis of distribution extending southeast from Mt. Mihara is clear, but scoria fall with different Al_2O_3 composition is also distributed on the northeast side, suggesting that scoria fall of Y4c was emitted multiple times.

Keywords: Izu Oshima volcano, active volcano, flank eruption

©2020. Japan Geoscience Union. All Right Reserved.

Eruptive stratigraphy and magma compositions of the Tsubota stage (4.0-2.5 ka) in the southern part of the Miyakejima Volcano, Japan

*Shota Watanabe[1], Takeshi Hasegawa[1], Teruki Oikawa[2], Nobuo Geshi[2]

1. Graduate School of Science and Engineering, Ibaraki University, 2. Geological Survey of Japan, The National Institute of Advanced Industrial Science and Technology

Miyakejima Volcano, located on the Izu-Mariana Arc, is one of the most active volcanoes in Japan. Based on the eruption frequency, styles and magma compositions, the development history during the last 10,000 years of the volcano is divided into five stages: the Ofunato stage (10-4 ka: including a dormant period from 7 to 4 ka), the Tsubota stage (4-2.5 ka), the Oyama stage I (2.5-1.3 ka), the Oyama stage II (1.3 ka-AD 1469), the Shinmio stage (AD 1469-1983) (Niihori et al., 2003). Clarifying the stratigraphy and petrologic feature of The Tsubota stage is important for understanding long-term eruption history and magmatism of Miyakejima Volcano, because it is the initial stage after the long dormancy (7-4 ka) and is characterized by relatively differentiated andesite magmas. The Tsubota stage products are distributed in Northwestern and Southern parts of Miyakejima island, and the former (TbN) has been investigated by Tsukui et al. (2005). In this study, we focused on the southern part of ejecta of the Tsubota stage (TbS). Geological survey, radiocarbon dating and petrological analysis of juvenile materials were performed to reveal the eruption stratigraphy and magma compositions of the stage.

TbS can be divided into at least 5 units as TbS-1 to 5 (bottom to top), separated by weathered volcanic ash and/or erosional surfaces that represent significant time intervals between eruptions. TbS-1 consists of a scoria fall and pyroclastic surge deposits. The thickness of the scoria fall is > 200 cm at Tsurune-misaki cape, the western coast of the study area. The ^{14}C dating of charcoal in this layer indicates approximately 3,200 yBP. Although pyroclastic surge deposit comprises of > 10 m thick tuff breccia in Tsurune-misaki cape, the thickness and grain size (lapilli tuff) decrease towards Chotaro-ike, the eastern coast of the study area, suggesting that TbS-1 was derived from the source near Tsurune maar (Tsukui and Suzuki, 1998). Source directions interpreted by the impact sag structures and dune migrations are also consistent. TbS-2 is a lava flow showing different groundmass colors (light to dark gray) in the same rock. The ^{14}C age of charcoal in debris flow deposits just beneath the TbS-2 is approximately 2,600 yBP. TbS-3 (light gray-colored) and 4, 5 (dark gray) are also lava flow units.

Phenocryst contents of juvenile materials are generally up to 6 vol. %, and the assemblages are mainly plagioclase, clinopyroxene, orthopyroxene, and opaque mineral. However, TbS-5 rarely contains olivine phenocrysts. TbS-2 and TbS-3 are andesite (SiO_2 = 58.0-59.0 wt. %), whereas other units are basaltic andesite (SiO_2 = 52.9-54.8 wt. %). Whole-rock Mg#s (= 100×Mg / (Mg + Fe)) of andesite and basaltic andesite samples are 31.2-32.9 and 36.8-43.2, respectively.

TbS 1 to 5 cannot be correlated with TbN (composed of 6 units) described by Tsukui and Suzuki (1998) with respect to lithofacies, stratigraphy and petrological characteristics. Thus, it seems to be at least 11 eruptions occurred at the Tsubota stage during 4,000 to 2,500 yBP. The eruption frequency in this stage can be estimated to be 0.73 times or more per 100 years. This value is significantly lower than other stages of the Miyakejima Volcano (e.g., the Shinmio stage: about 2.53 times).

Niihori et al. (2003) reported the systematic cycles for whole-rock Mg# is the highest during the first eruption and it decreases with time in each stage (except for the Ofunato stage). In this cycle, the Tsubota

©2020. Japan Geoscience Union. All Right Reserved.

stage has been characterized by andesitic (SiO_2 = 55.9-63.2 wt. %) and relatively low Mg# (28.9-38.8) compositions lacking in high Mg# basaltic andesite. However, our data suggest that undifferentiated (high Mg# and basaltic andesite) magmas were ejected around 2,600 yBP and 3,200 yBP in the late Tsubota stage. The banded structure of light and dark gray-colored in TbS-2 lava flow implies the mixing processes of andesite and basaltic andesite magmas in this stage.

References:

Niihori et al. (2003) *Bull.Volcanol.Soc.Japan* **48**, 387-405.

Tsukui and Suzuki (1998) *Bull.Volcanol.Soc.Japan* **43**, 149-166.

Tsukui et al. (2001) *J.Geogr* **110**, 156-167.

Tsukui et al. (2005) *Geological map of volcanoes 12. Geological Survey of Japan, AIST.*

Keywords: Miyakejima Volcano, eruptive stratigraphy, magma composition

©2020. Japan Geoscience Union. All Right Reserved.

Reconsideration of Late Quaternary tephrostratigraphy on Mikurajima Volcanic Island, Izu Islands.

*Tomohiro Tano[1], Takehiko Suzuki[1,2], Daisuke Ishimura[1,2], Satoshi Terayama[1], Tatsuki Watanabe[1]

1. Department of Geography, Tokyo Metropolitan University , 2. Research Center for Volcanic Hazards and Their Mitigation,Tokyo Metropolitan University

Mikurajima Island is a volcanic island located on the Izu-Ogasawara arc, about 200 km south of Tokyo Metropolis. A previous work on the tephrostratigraphy in the Mikurajima Island by Sugihara and Shimada (1999) is not enough because it was based only on refractive indices of volcanic glass shards, distribution, and old documents. Sugiuchi and Fukuoka (2005) and Saito et al. (2007) investigated distribution of rhyolite tephras within the Izu Islands based on the chemical composition of the major element composition of volcanic glass shards. More accurate tephrostratigraphy on the Mikurajima Is. can be established using this method.

In this study, we aimed to identify and correlate tephras distributed and established the tephrostratigraphy on Mikurajima Is. The result can contribute to not only establishing the activity history of Mikurajima volcano, but also to constructing the chronological framework comprehending the Izu Island.

We conducted outcrop observation, a simple drilling survey using a hand-operated auger and analysis of volcanic glass (the morphology, refractive index, and major element components) and revealed several new knowledgments as below.

We totally identified nine tephras on Mikurajima Is. These are Niijima-Mukaiyama tephra (Iz-Nm, AD886), Kozushima-Tenjohsan tephra (Iz-Kt, AD838), Mk-3 tephra, the latest eruption of Mikurajima volcano, (6.3 ka, Geological Survey of Japan 2017), two newly discovered tephras: Mk-2.2, Mk-2.1, Kikai-Akahoya tephra (K-Ah, 7.3 ka), Niijima-Shikinejima tephra (Iz-Sk, about 8 ka), Mk-2 and Mk-1 tephra, originated from Mikurajima volcano tephra, in descending order. Iz-Nm and Iz-Sk are newly recognized in Mikurajima Is. and provide new information on the southern limit of the distribution of each tephra. The stratigraphic relationships of these tephras are consistent with the age of Mk-3 (6.3 ka; on calibrated) reported by Sugihara and Shimada (1999) and Sekiguchi et al. (2001). It was also found that the eruption ages of Mk-2, Mk-1 are older than Iz-Sk (about 8 ka). Between Iz-Kt and Mk-3, we found volcanic glass as cryptotephra. That could be identified Amagi-Kawagodaira tephra (KGP, 3.1 ka).On the other hand, Mk-G, rhyolitic tephra of unknown origin, intercalated between Mk-2 and Mk-1 reported by Sugihara and Shimada (1999) ,could not be discovered in this study.

It was revealed that the Mk-3 eruption change from pyroclastic surge, lava outflow, eruption of lapilli and ash fall, and finally to ejection of pumice fall. This means that the final phase of Mk-3 eruption changed from of all out of the volcanic lapilli and ash to the Plinian eruption causing pumice fall without a geological time gap. As reported by Sugihara and Shimada (1999), it is considered that the vent of Mk-3 located around the lava dome in the southeastern part of the island based on its distribution. On the other hand, we could not find the sources for Mk-2 and Mk-1.

Two newly discovered tephras, Mk-2.1 and Mk-2.2, fell Mk-3 and K-Ah tephras. In this study, we could not determine the source of these two tephras, but if they are originated from Mikurajima volcano, Mikurajima

©2020. Japan Geoscience Union. All Right Reserved.

volcano erupted three times during the period K-Ah and Mk-3 for about 1,000 years. It means that the occurrence of explosive eruption of Mikurajima volcano was more frequent than previous estimation.

Keywords: Mikurajima Volcano, tephrostratigraphy, Kozushima-Tenjohsan tephra , Niijima-Shikinejima tephra

©2020. Japan Geoscience Union. All Right Reserved.

Holocene volcano of Kazafuki Volcano, Shirouma-Oike volcanoes, central Japan.

*Teruki Oikawa[1], Shun Nakano[1]

1. GSJ, National Institute of Advanced Industrial Science and Technology

Kazafuki volcano, central Japan consist with the northeastern part of Shirouma-Oike volcano. It was believed that there was no Holocene eruption at this volcano. Based on geological field survey, the tephra layer for this volcano was newly discovered. The ^{14}C dating result of the soil layer just below the tephra layer that is newly discovered is about 4,000 yr BP. In addition, the latest magmatic eruption unit has a ^{14}C dating result of about 8800 yr BP. It makes be clear that Kazafuki volcano had erupted several times during the Holocene.

Keywords: active volcano, Holocene, eruption, tephra, radiocarbon dating

©2020. Japan Geoscience Union. All Right Reserved.

The Omine Tuffite Dike and its Accompanied Andesite Fragments, Central Kii Peninsula, SW Japan

*Yutaka WADA[1], Kohnosuke NISHIMOTO[2]

1. Department of Earth Sciences, Nara University of Education, 2. Heguri Junior High School

Pyroclastic conduits exposed at the caldera margin give informations about pre-eruptive conditions of the pyroclasts and magma chamber. At the Kii peninsula in southwest Japan multiple caldera eruptions occurred 14 million years ago [(1)], their pyroclastic conduits are exposed (e.g., Nakaoku dike[(2)]; Omine dike [(3)(4)]; Kozagawa dike[(5)]). In this study we report the field occurrence of the Omine dike and its accompanied andesite fragments.

The Omine dike is one of the conduit of the Omine-Odai caldera[(6)], and extends NNE-SSW direction for ca. 30 km. At the Takigawa outcrop in Totsukawa area, the dike is ca. 70 m wide. U-Pb age from the zircon is 14.88±0.45 Ma[(7)].

The dike consists of tuffite, which includes lapilli- to block-sized fragments in welded matrix. There are andesites, sedimentary rocks derived from host rocks, and fiammes as the fragments. The andesite fragments, a few centimeter to 2 m in diameter, are irregular-shaped and have glassy but devitrified margins. The welded matrix includes broken crystals and rock fragments in brown volcanic glass. The brown glass with eutaxitic texture includes lensoidal and bubble-wall type glass fragments.

Field and microscopic observations above indicate that the welding occurred in the closed conduit after explosion and fragmentation, similar to the mechanism at the Nakaoku dike[(8)], the other conduit of the Omine-Odai caldera. On the other hand, the irregular-shaped andesite fragments suggest strongly that they were emplaced as hot magma. One of the trigger for the felsic caldera eruptions may be the injection of mafic magma into felsic magma chamber [(9)]. Therefore, more detailed petrological studies about the andesite fragments are necessary to understand the development of the Omine-Odai caldera eruption.

References

[(1)]Miura and Wada (2007) JVGR, 167, 300.
[(2)]Wada and Iwano (2001) Bull.VSJ, 46, 107.
[(3)]Tajima (1977) Abst. GSJ, p.59.
[(4)]Wada and Nagasawa (2008) Gekkan Chikyu (Gogai), 60, 91.
[(5)]Miura (1999) JVGR, 92, 271.
[(6)]Sato and YORG (2006) Chikyu Kagaku, 60, 403.
[(7)]Shinjoe *et al.* (2019) Geol.Mag., doi: 10.1017/S0016756819000785.
[(8)]Kitajima and Wada (2010) Jour.GSJ, 116, 510.
[(9)]Sparks *et al.* (1977) Nature, 267, 315.

Keywords: caldera, pyroclastic conduit, Miocen volcanism, Kii peninsula, tuffite, mafic magma

©2020. Japan Geoscience Union. All Right Reserved.

Volcanic activity of the Miocene Basalts in Yatakayama Area, Kibi Plateau, Takahashi City, Okayama Prefecture, SW Japan

*Takumi Nagato[1], Shigeyuki Suzuki[1], Haruo Koami[2], Kotaro Nakai[1], Toru Tachibana[3]

1. Okayama University, 2. Okayama Prefectual Okayama Asahi Senior High School, 3. Soil Engineering Corporation

Numbers of basaltic rocks are sporadically distributed in Kibi Plateau, around the border between Okayama Prefecture and Hiroshima Prefecture. These basalts are alkali basalts (Takamura,1973) and formed in late Miocene, 7.4-9.5Ma (Uto,1995). The study areas are Mt. Sushiyama, Mt. Yatakayama, Tachiarai areas which are located in western side of Okayama Prefecture. We discovered contact planes of basaltic intrusive rocks, tuff breccias and lava flow which help to understand volcanic evolution of the Miocene Basalts.

Observed basaltic dikes intruded into the Miocene Bihoku Group and tuff breccia of the Miocene Basalt. The basaltic tuff breccia is composed of lapilli (5mm to 10cm) and matrix (cement and pore). The lava has brecciated nature. Some basaltic fragments have jigsaw-fit structure.

Keywords: Basalt, reconstruction of volcanism, volcanic product, Miocene, field survey

©2020. Japan Geoscience Union. All Right Reserved.

Textural observation and chemical analyses of 1716-1717 Kyoho eruption pumice at Shinmoedake, Kirishima volcano group

*Akari Kagawa[1], Atsushi Toramaru[1]

1. Kyushu university

Volcanic products have the historical eruption Information of magma chamber in their texture. For instance, after classifying volcanic products by the result of textural observation and chemical analysis, we can calculate the rate of magma supply from mantle from the crystal size distribution (CSD) (Yamashita and Toramaru (2019)). Kyoho eruption, occurred in 1716 and 1717 in Kirishima Shinmoedake volcano, produced pumice fall and volcanic ash fall of the total amount of volcanic products of 200 million tons. In this study, I did textural observation and chemical analysis for fall pumice of Kyoho eruption. The aim of this study is to clear how magma chamber exist and act at Kyoho eruption by the result of textural observation and chemical analyses.

Samples are taken at outcrops, located in southeast east Shinmoedake volcanoes. The deposits consist of seven units (from the bottom Sm-Ky1, Sm-Ky2, ⋯, Sm-Ky7), as described by previous studies. We focus on five pumice units except two units (Sm-Ky1 and Sm-Ky3) of ash fall. We conducted particle size analyses, bulk density measurement, textural observation, and chemical analyses. To be specific, we did particle analyses by using sieve for eight sub-layers in each unit. For two pumices in a sub-layers for each unit, we conducted bulk density measurement by using a 3D scanner and electronic weighing instrument. Using thin sections of the pumices, we performed mineral description, calculated phenocryst crystallinity for photos taken by SEM We define the phenocryst crystallinity as the areal fraction of phenocrysts in whole grain area, multiplied by 100 as percent . Similarly, we define phenobubble% as the areal fraction of phenobubble (Phenobubble is defined as bubbles with area larger than 0.01 mm^2 and presummed to be formed in the magma chamber.) We conducted chemical analyses for plagioclase phenocrysts by using FE-EPMA and SEM-EDS .

The result of particle size analyses, all units showed the characteristics of fall deposits. Previous studies said that these units are fall deposits, so this result corresponded to previous studies. The result of bulk density measurement showed that Sm-Ky2 layer’ s pumice had remarkably high density compared with other sub-layers. Mineral description showed that most of phenocrysts in all units are plagioclase and clinopyroxene. The result of crystallinity and phenobubble% of Sm-Ky2 layer also show the different signature. From the histogram of anorthite contents, it is found that core compositions have one peak (near 70(big)) in Sm-Ky2 and Sm-Ky4 layer, whereas they have three peaks (near 55, 70(big), and 85) in Sm-Ky5 and Sm-Ky6 layer, and two peaks (near 60(big) and 80) in Sm-Ky7 layer. Rim compositions have two peaks (near 30 and 70(big)) in Sm-Ky2 layer, 3 peaks (near 30, 70(big), and 80) in Sm-Ky4 and Sm-Ky5 layers, and 3 peaks (near 60, 70(big), and 80) in Sm-Ky6 and Sm-Ky7 layers.

It is found that the relationship between phenobubble% and crystallinity shows different trend between Sm-Ky2 and other layers. This difference can be seen in the relationship between bulk density and phenobubble%. The difference cannot be seen in the relationship between bulk density and crystallinity. From these results, we can draw two conclusions. First, bulk density was affected phenobubble% rather than crystallinity in volcanic deposits of Kyoho eruption . And, from the different trend of correlation diagram, Sm-Ky2 layer and other layers’ magma component are different. So, they came from different magma chamber. From this, it is suggested that Shinmoedake may have more than two magma chambers.

©2020. Japan Geoscience Union. All Right Reserved.

Second, from the result of anorthite contents showing similar distribution for Sm-Ky2 and Sm-Ky4 , we think that plagioclase phenocrysts in Sm-Ky2 and Sm-Ky4 layers formed in the similar condition.

©2020. Japan Geoscience Union. All Right Reserved.

Identification of lava flow temperature by lava tube cave structure of Mt.Etna

*Tsutomu Honda[1]

1. Vulcano-speleological Society

[Introduction]

Like Mt.Fuji, there are many lava tube caves formed in the past on Mt.Etna. An attempt was made to identify the lava flow temperature during the formation of a lava tube by using the yield strength obtained from the height of the lava tube cave at Mt.Etna. The viscosity coefficient of the lava flow was also estimated from the identified temperature.

[Lava yield strength obtained from lava tube cave]

Table 1 shows a list of major lava tube caves at Mt.Etna[1)] along with their length, cavity height, and slope angle. Considering the tube cave as the drain of lava from the inside of the tube, the yield strength can be obtained from the flow limit condition [2)] in the inclined tube:

$f_B = H(\rho g \sin\alpha) / 4$ ·····(eq-1)

where f_B is the yield value, H is the cavity height, ρ is the lava density, g is the gravitational acceleration, and α is the slope angle. The yield strength of the cave obtained from (eq-1) is shown in the rightmost column of Table 1. The yield strength is in the range of $1.6x10^4$~$1.1x10^5$ dyne/cm^2($1.6x10^3$~$1.1x10^4$Pa).

[Temperature change of yield value and viscosity of Etna volcano]

Mt.Etna is the only example where temperature-dependent curves of yield strength and viscous coefficient have been obtained by actual measurement of lava flow[3,4,5)]. The fitting equation from that data can be obtained as follows,

$\log_{10} f_B = 35.1836-0.0289\theta$, ·····(eq-2)

θ is the temperature in degrees Celsius and the yield strength f_B is dyne / cm^2

$\log_{10}\eta_B = 24.0469-0.0175\theta$, ·····(eq-3)

θ is the temperature in degrees Celsius and the viscosity coefficient η_B is poise

The lava tube cave formation temperature is in the range of 1044℃~1073℃ judging from the yield strength-temperature curve (eq-2) according to the yield strength $1.6x10^4$~$1.1x10^5$ dyne/cm^2($1.6x10^3$~$1.1x10^4$Pa)obtained from the cave. According to the viscosity coefficient -temperature curve (eq-3), the lava viscosity coefficient with respect to the temperature is in the range of $1.9x10^5$~$6.2x10^5$ poise($1.9x10^4$~$6.2x10^4$ Pa.s). It should be noted that the temperature of 1056~1067℃ obtained from the yield strength of $2.4x10^3$~$4.8x10^3$Pa and the viscosity coefficient of $2.6x10^4$~$4.0x10^4$Pa.s obtained for the Cutrona cave formed in the 1991-1993 lava flow, are close to the measured temperature 1020 ~ 1080 ℃ and the viscosity coefficient $0.8x10^4$~$1.9x10^4$Pa.s, which were measured in the lava flow at an altitude of 2000m at Serra Pirciata by Calvari et al [6)]

[Conclusion]

It is possible to identify the lava temperature at the time of lava tube cave formation by obtaining the yield strength from the cave by obtaining the temperature change dependence curve of the lava yield value in advance. Moreover, the viscosity coefficient can be obtained from the temperature dependence curve of the lava viscosity coefficient by the temperature. Therefore, it is considered that this method can be used to identify the temperature and viscosity coefficient of lava flow during the formation of a lava tube cave whose temperature has not been measured in the past.

©2020. Japan Geoscience Union. All Right Reserved.

References:

1) S.Calvari, M.Luizzo (1999): ” Excursion Guide, Lava tubes and lava caverns Etna volcano, 1999”, 9th International Symposium on Vulcanospeleology,
Catania, Italy, 11-19 September, 1999.

2) T.Honda(2001): B-10 Mt.Fuji lava cave formation mechanism and findings, 2001 Autumn Meeting of the Volcano Society of Japan.

3) T.Mizuyama, A.Kurihara, K.Kawamura, I.Kitahara (1989): Lava flow simulation and countermeasures, Shinsabo Vol.42 No.4 (165) Nov.1989

4) H.Pinkerton,and R.S.J.Sparks(1978): Field measurements of the rheology of lava., Nature (London), Vol. 2, 76, No. 5686, pp.383-385, 1978.

5) M.Dragoni, M.Bonafede,E.Boschi(1986): Downslope flow models of a Bingham liquid: Implications for lava flows. Jour. Volcanol. Geotherm Res., 30, pp. 305-325, 1986.

6)S.Calvari,M.Coltelli,M.Neri,M.Pompilio,V.Scribano(1994):The 1991-1993 Etna eruption chronology and lava flow field evolution,Acta Vulcanonologica Vol.4 1994 pp1-14

Keywords: lava tube, Etna volcano, lava temperature, yield strength

表１ エトナ火山の溶岩チューブ洞窟に関する形状データと得られた降伏値, 温度, 粘性係数
（形状データは文献 1)の測量図よりチューブ形状部分から読み取っている）

洞窟名 Name of lava tube cave	長さ Cave length	高低差 Cave elevation range	傾斜度 Slope angle α	空洞高さ Cave height H	流動限界条件(eq-1)から得られる降伏値 Yield strength f_B	回帰式(eq-2)からの温度 Temperature	回帰式(eq-3)からの粘性係数 Viscosity η_B
Cutrona Cave (1991~1993 lava flow)	404m	60m	8.5°	2m~4m	$2.4x10^4$ ~$4.8x10^4$dyne/cm^2 ($2.4x10^3$ ~$4.8x10^3$Pa)	1056~1067°C	$2.6x10^5$~$4.0x10^5$poise ($2.6x10^4$~$4.0x10^4$ Pa.s)
La Fenice Cave (1792-1793 lava flow)	80m	15m	10.8°	1m~3m	$1.5x10^4$~$4.5x10^4$ dyne/cm^2 ($1.5x10^3$~$4.5x10^3$Pa)	1057~1073°C	1.9 $x10^5$~$3.8x10^5$poise (1.9 $x10^4$~$3.8x10^4$Pa.s)
Serracozzo Cave (1971 lava flow)	280m	60m	12.4°	3m~6m	$5.3x10^4$~$1.1x10^5$dyne/cm^2 ($5.3x10^3$~$1.1x10^4$Pa)	1044~1054°C	$4.3x10^5$~$6.2x10^5$poise ($4.3x10^4$~$6.2x10^4$Pa.s)
Tre Livelli Cave (1792-1793 lava flow)	1000m	260m	15.1°	~5m	$1.1x10^5$dyne/cm^2 ($1.1x10^4$Pa)	1045°C	$6.2x10^5$poise ($6.2x10^4$Pa.s)
KTM Cave (1792-1793 lava flow)	533m	94m	10.2°	~5m	$7.2x10^4$dyne/cm^2 ($7.2x10^3$Pa)	1051°C	$5.0x10^5$poise ($5.0x10^4$Pa.s)
Cassone Cave (1792-1793 lava flow)	246m	25m	5.9°	~6m	$5.0x10^4$dyne/cm^2 ($5.0x10^3$Pa)	1055°C	$4.1x10^5$poise ($4.1x10^4$ Pa.s)
Intraleo Cave (uncertain dating)	80m	4m	2.9°	~5m	$1.6x10^4$dyne/cm^2 ($1.6x10^3$Pa)	1073°C	$1.9x10^5$poise ($1.9x10^4$ Pa.s)
Abisso di Monte Nero Cave(1923 lava flow)	612m	38m	3.6°	~10m	$3.8x10^4$dyne/cm^2 ($3.8x10^3$Pa)	1059°C	$3.5x10^5$poise ($3.5x10^4$Pa.s)

©2020. Japan Geoscience Union. All Right Reserved.

[J] Poster | S (Solid Earth Sciences)：S-GC Geochemistry

[S-GC49] Solid Earth Geochemistry, Cosmochemistry

convener:Gen Shimoda(Geological Survey of Japan, AIST), Katsuhiko Suzuki(Submarine Resources Research Center, Japan Agency for Marine-Earth Science and Technology), Katsuyuki Yamashita(Graduate School of Natural Science and Technology, Okayama University), Akira Ishikawa(Department of Earth and Planetary Sciences, Tokyo Institute of Technology)

"Solid Earth Geochemistry, Cosmochemistry" session aims at evaluating processes during the 4.6 billion years of the solar system and the Earth. Any approaches to this issue is welcomed, including, geochemistry, geophysics, geology, mineralogy and petrology.

[SGC49-P01] **Particle size control of olivine alteration pathway and rate for simultaneous H_2 generation and CO_2 storage**

*Jiajie Wang[1], Noriaki Watanabe[1], Atsushi Okamoto[1], Kengo Nakamura[1], Takeshi Komai[1] (1.Tohoku University)

[SGC49-P02] Chemical composition of river sediments around Lake Biwa area, southwestern Japan

*Masako Kato[1], Motohiro Tsuboi[1] (1.Kwansei Gakuin University)

[SGC49-P03] Highly siderophile element geochemistry of komatiites from Pilbara Craton, Western Australia

*Shun Nakano[1], Akira Ishikawa[1], Yuichiro Ueno[1], Tetsuya Yokoyama[1] (1.Tokyo Institute of Technology)

[SGC49-P04] Time scale of the separation of molten metal droplets in the magma ocean: implications to metal-metal differentiation during core-mantle segregation

HIrotaro Sagi[1], *Tetsu Kogiso[1] (1.Kyoto Univ.)

[SGC49-P05] Geochemical investigations for magma genesis of Pre-Unzen volcano, Shimabara Peninsula, Kyushu, Japan

*Tomoyuki Shibata[1], Takuma Yoshida[1], Takeshi Sugimoto[2] (1.Graduate School of Science, Hiroshima University, 2.Geothermal Engineering Co., Ltd.)

[SGC49-P08] **Ship Detection Using Synthetic Aperture Radar**

*Kengo Iwata[1] (1.Tokyo Denki University)

Particle size control of olivine alteration pathway and rate for simultaneous H_2 generation and CO_2 storage

*Jiajie Wang[1], Noriaki Watanabe[1], Atsushi Okamoto[1], Kengo Nakamura[1], Takeshi Komai[1]

1. Tohoku University

The hydrothermal alteration of olivine [$(Mg,Fe)_2SiO_4$] has attracted considerable attention as it represents not only a potential way to produce hydrogen (H_2) by the oxidation of Fe(II) in it, but also to store CO_2 by its carbonation. The combination of the strategies of H_2 production and CO_2 storage during H_2O-olivine-CO_2 reaction may be a promising way to contribute to low-carbon society development. During H_2O-olivine-CO_2 reaction, the olivine grain size is a key parameter in controlling olivine dissolution and products generation rates.

In this study, three experiments with olivine particles of 28-53, 53-90 and 90-160 μm were conducted in 0.5 mol/L $NaHCO_3$ solution at 300 ˚C for 72 h. Olivine alteration rate (r, wt%/h) was closely related to its geometric surface area (GS, m^2/g), with the linear relationship of r=4.097GS. H_2 production was much higher with the simultaneous CO_2 storage [in magnesite, $(Mg,Fe)CO_3$] in the experiment with an olivine grain size of 28-53 μm than those with larger olivine grain sizes. The highest cumulative H_2 yield was 118 $mmol/kg_{olivine}$ in 72 h. The inhibited magnesite precipitation in experiments with olivine grain size >53 μm was attributed to the low Mg concentrations caused by the slow olivine dissolutions. The results also suggest olivine serpentinization proceeded faster than carbonation, and the covering of olivine with serpentines [$(Mg,Fe)_3Si_2O_5(OH)_4$] may inhibited further olivine alteration and H_2 production. Therefore, decrease the olivine grain size to < 53 μm is an efficient way not only to enhance olivine alteration with H_2 production but also to realize simultaneous H_2 production and CO_2 storage during H_2O-olivine-CO_2 reaction.

Keywords: Olivine, grain size, hydrogen, carbon storage

©2020. Japan Geoscience Union. All Right Reserved.

Chemical composition of river sediments around Lake Biwa area, southwestern Japan

*Masako Kato[1], Motohiro Tsuboi[1]

1. Kwansei Gakuin University

Lake Biwa is the largest lake in Japan and it supplies daily life water to Kinki area, southwestern Japan. About 118 first-class rivers flow into Lake Biwa, and the lake water only flow out from the Seta River, which locates southern part of the lake. The geology of the watershed area of rivers flowing into Lake Biwa is roughly divided into four areas: 1) granite area, 2) Ko-biwako Group area, 3) slate, chert and sandstone area, and 4) limestone and basic volcanic rock area[1)]. In this study, 14 samples of river sediments were collected from the western part of the lake, where river sediments have not been widely surveyed. 6 samples are collected from the granite area, 3 samples are from the Ko-biwako Group area, and 5 samples are from slate, chert and sandstone area. River sediment samples with a particle size of less than 180 μm were studied. Major and other minor elements were determined by wavelength dispersive X-ray fluorescence spectrometer (XRF). River sediment chemical composition data from geochemical map of sea and land of Japan by AIST[2)] are also compiled in this study. The concentration of P_2O_5 is particularly high in the Koto region, eastern part from the lake. Rice paddy fields are widely distributed in this region. The higher phosphorus value is considered to be affected by the fertilizer eluted from the soil. Mn and Cu concentration distributions are higher at western part from the lake. Manganese mines in this area may affect these elemental distributions[3)]. The alumina saturation index (=(K_2O+CaO+Na_2O)/Al_2O_3) of most collecting river sediments show higher values in the granite area and lower values in the sedimentary rocks area. It is concordant with surrounding geology. River sediment sample reflects chemical characteristics of surrounding geology. Chemical composition of sediments and concentration correlation matrix analysis reveal that the correlation between sediments of inflowing river and lake bottom sediment is low. It may be caused by redistribution of chemical elements such as weathering and ion exchange. The correlation between the sediment of Seta River and lake bottom sediment is also law. Sediments in the Seta river may be more affected by the sediments of surrounding branch inflowing rivers than the lake bottom sediments[4)-8)].

References
1) Mori et al., *Jpn. J. Limnol.*, 1993, 54, 3-10.
2) Imai et al., *Geochemical map of Japan*, 2004.
3) Takase et al., *Bull. Geological Survey of Japan*, 1960, 11, 301-318.
4) Kutsukake et al., *Earth Science*, 1991, 45, 363-367.
5) Omori et al., *Bull. Geological Survey of Japan*, 1968, 19, 103-114.
6) Matsumoto et al., *Memoirs of the Faculty of Education, Shimane Univ.*, 2008, 42, 97-105.
7) Minami et al., *Summaries of Researches Using AMS at Nagoya University XV*, 2004, 181-1980.
8) Yamazaki et al., *Environmental Technology*, 1999, 28, 827-836.

Keywords: Lake Biwa, river sediments, chemical composition

©2020. Japan Geoscience Union. All Right Reserved.

Highly siderophile element geochemistry of komatiites from Pilbara Craton, Western Australia

*Shun Nakano[1], Akira Ishikawa[1], Yuichiro Ueno[1], Tetsuya Yokoyama[1]

1. Tokyo Institute of Technology

The Late veneer hypothesis, which suggests that primitive materials were added to the mantle after core-mantle differentiation, has long been advocated for explaining the excess of highly siderophile elements (HSEs) in the present-day mantle. However, the timing of accretion and mechanisms of subsequent homogenization of the primitive components are not yet well understood. The komatiite magma generated by high degrees of partial melting of mantle is considered to be useful for tracing the chemical evolution of the Archean mantle. Maier et al. (2009) reported that HSE abundances of komatiites in early Archean tend to be lower than those in late Archaean, as a result of the progressive mixing of late veneer materials deep into the mantle. Although this observation and hypothesis may provide a key constraint on the evolution of the Earth’ s mantle, the quality and quantity of data are still not satisfactory enough to reveal secular trends of HSE abundances in komatiite sources.
In this study, to further investigate secular trends of HSE abundances in komatiite sources, we focused on the early Archean komatiites from Pilbara craton, Australia. We performed the analyses of Re-Os isotopes and HSE abundances in a series of komatiite flows in the region by using the Carius tube digestion coupled with isotope dilution mass spectrometry. Our primary objective is to test whether the previous data are biased due to (1) low number of measured samples that may underestimate the effects of crystallization differentiation, and (2)less reliable analytical method used (NiS-fire assay digestion coupled with calibration-curve method).
Our results demonstrate that there are systematic variations in HSE abundances and rock types (basalts, basaltic komatiites, olivine cumulates); Os, Ir and Ru (IPGE) show strong positive correlations against MgO contents, whereas Pt, Pd and Re (PPGE) show weak negative correlations against MgO contents. This is broadly consistent with previous indications that IPGE and PPGE behave as compatible and incompatible elements during crystal fractionation, respectively. However, compositional trends regarding Ru and Pt identified in the studied rocks are significantly different from those observed in well-studied komatiites, implying that crystallizing phases controlling HSE abundances are variable between komatiites of different petrogenetic types of lava flow. Although our new data for the komatiite samples in the Pilbara craton are broadly consistent with the previously reported values, effects of crystallization differentiation, particulallry on Ru, must be carefully examined in order to estimate the composition of primitive magma and the source mantle.

Keywords: Komatiite, Re-Os isotope, highly siderophile element

©2020. Japan Geoscience Union. All Right Reserved.

Time scale of the separation of molten metal droplets in the magma ocean: implications to metal-metal differentiation during core-mantle segregation

HIrotaro Sagi[1], *Tetsu Kogiso[1]

1. Kyoto Univ.

Highly siderophile elements (HSE) in the Earth's interior are thought to have been partitioned into Fe-Ni metal phases in the magma ocean and have segregated into the core during Earth's formation, because high-pressure silicate-metal partitioning experiments have demonstrated that HSE are strongly partitioned into silicate melt when metal and silicate phases are in equilibrium in the magma ocean. On the other hand, recent studies report the existence of HSE-bearing small phases in CAI, chondrules, and matrices in chondrites, suggesting that HSE had been partly included in small HSE phases distinct from Fe-Ni metal phases in the magma ocean. If so, HSE had not fully been partitioned into Fe-Ni metals in the magma ocean. In this study, we have calculated the time scale of separation of metallic droplets in silicate melt of a convecting magma ocean, and examined the condition under which HSE behave separately from Fe-Ni in the magma ocean. We compared the time scale of separation in silicate melt between molten Pt and molten Fe metal droplets, and found that Pt metal droplets can be suspended in silicate melts more likely than Fe metal droplets under a wide range of conditions. This means that HSE discrete phases could have stayed behind after Fe-Ni phases had been separated from silicate melt in the magma ocean. Therefore, the HSE excess in the modern mantle compared with the expectation from high-pressure partitioning would be the result of incomplete separation of HSE phases in the magma ocean.

Keywords: magma ocean, highly siderophile element, core-mantle segregation

©2020. Japan Geoscience Union. All Right Reserved.

Geochemical investigations for magma genesis of Pre-Unzen volcano, Shimabara Peninsula, Kyushu, Japan

*Tomoyuki Shibata[1], Takuma Yoshida[1], Takeshi Sugimoto[2]

1. Graduate School of Science, Hiroshima University, 2. Geothermal Engineering Co., Ltd.

Cenozoic Basalts, which have similar geochemical characteristics to ocean island basalt (OIB)enriched in incompatible elements, are distributed at East Asia along NE China, Korea and Southwest (SW) Japan. The origin of these basalts have been explained by components from mantle plume and stagnant pacific slab (Sakuyama et al., 2014; Kuritani et al., 2011; Kuritani et al., 2017). In the northeast Kyushu, SW Japan, Cenozoic basaltic volcanic activities are observed from Goto Islands (0.5 Ma - 2ka, K - Ar and ^{14}C age; Nakagoka & Furuyama, 2004), Kitamatsura (8.5 - 6 Ma, K –Ar age; Sakuyama et al., 2009). The magma genesis of former is explained by hydrous plume component from the upper mantle (Kuritani et al., 2017), and contribution of plume component from the lower mantle is emphasized to the later (Sakuyama et al., 2014). The reason for the difference of basalt magma genesis from those closed area is still unclear. At the Shimabara Peninsular located between Goto Islands and Kitamatsuura, basaltic Pre - Unzen volcano was active from 4.6 Ma to 0.5 Ma (K - Ar age; Yokoyama et al., 1981, Nakada & Kamaata, 1998, Uto et al., 2002). It is suggested that the geochemical characteristics of Pre-Unzen basalts is similar to that of OIB (Hoang & Uto, 2006). However, detailed geochemical study is not well accumulated. Because Pre-Unzen volcano stands specially and temporally in between Goto Islands and Kitamatsuma, the investigations of magma genesis of Pre - Unzen volcano give us the insight to understanding the Cenozoic mantle processes beneath the NE Kyushu in the respect to the mantle plume and stagnant Pacific slab. Therefore, we analyzed trace element compositions of the basalt from Pre - Unzen volcano. The results and discussions will be presented.

Keywords: Pre - Unzen volcano, stagnant slab, mantle plume

©2020. Japan Geoscience Union. All Right Reserved.

Ship Detection Using Synthetic Aperture Radar

*Kengo Iwata[1]

1. Tokyo Denki University

Synthetic aperture radar image includes waves, internal waves, vessel detection, and tides. With regard to the ship detection, the synthetic aperture radar PALSAR-2 mounted on ALOS-2 and AIS (Automatic Identification System), which transmits and receives identification codes, ship names, positions, speeds, etc., will cooperate. Surveillance is being conducted to identify suspicious vessels.

This study conducted the vessel monitoring in three steps:(1) Measuring the backscattering coefficient (s^0) from the orthocorrected image, and the ship is defined to be detected when the average value ($\sigma Avg.0$) over the small area exceeds the threshold value (σth). (2) Marking the estimated target area, converting the pixels-lines of the area into latitude and longitude, and comparing it with AIS location information.(3) Measurement of the displacement between the ship and the wake wave in azimuth direction, and estimating the line-of-sight component of the ship. This LOS speed is calsucrated also from AIS and used for the comparison.

We used three scenes of November 18, 2019 in the waters from the Pacific Ocean in Wakayama Prefecture to the Kii Suido and Osaka Bay, taking into account the number of vessels traveling and the expected speed of navigation. At the same time, AIS information of the same area was used to compare ship detection and speed calculation.

We performed the supervised classification in adopting Pacific data as a teacher, small areas are 3 pixels per side by trial and error, and the threshold is -8.0 dB. As a result, we obtained that, 1) the number of detected vessels containing AIS position information was 27/29 (95%) and 25/25 (100%). The percentage of detected ships was 31.02% and 8.38%. Because many coastal structures such as artificial islands and bridges were detected in the Kii Channel and Osaka Bay, the number of non-vessel detections increases. The larger number of vessels were found more than in the AIS information is probably due to that some vessels, such as small boats and destroyers, do not need to carry AIS or do not emit AIS. 2) For the velocity estimation, the relative error compared to AIS was -63.3% to 48.8%.

Keywords: Synthetic Aperture Radar, Ship Detection

©2020. Japan Geoscience Union. All Right Reserved.

[J] Poster | S (Solid Earth Sciences)：S-CG Complex & General

[S-CG66] Ocean Floor Geoscience

convener:Kyoko Okino(Atmosphere and Ocean Research Institute, The University of Tokyo)

Most of Earth's volcanism and much of its tectonic activity occur on and beneath the seafloor. Various phenomena on the seafloor are closely linked to plate tectonics, Earth structure and dynamics, and also related to Earth's environments through the hydrosphere and atmosphere. Seafloor rocks and sediments record Earth's evolution and heat and material fluxes on the Earth. Ocean Floor Geoscience session covers a broad range of research on seafloor such as mid-ocean ridge process, subduction dynamics, arc magmatism, hot spot and LIPs, crustal movement and structure etc. Every field of researches and every approaches are welcomed.The session aims to encourage discussion among scientists from different study fields and to integrate our understanding of ocean floor.The session is co-chaired by K. Tadokoro (Nagoya Univ.), O. Ishizuka (AIST), T. Toki (Univ. Ryukyus), and N. Takahashi (JAMSTEC).

[SCG66-P01] Relationship between the oblique opening system in the back-arc basin and Hamilton's principle

*Takao Eguchi

[SCG66-P02] A sand-box experiment for understanding marine self-potential anomalies

*Yoshifumi Kawada[1,2], Takafumi Kasaya[2] (1.International Research Institute of Disaster Science, Tohoku University, 2.Japan Agency for Marine-Earth Science and Technology)

[SCG66-P03] Sandbox analogue experiments to examine how syntectonic sedimentation influence on forearc basin stratigraphy and accretionary wedge growth

*Atsushi Noda[1], Hiroaki Koge[1], Yasuhiro Yamada[2,3,4], Ayumu Miyakawa[1], Juichiro Ashi[5] (1.National Institute of Advanced Industrial Science and Technology, 2.Japan Agency for Marine-Earth Science and Technology, 3.Faculty of Science and Technology, Kochi University, 4.Department of Earth Sciences, Royal Holloway University of London, 5.Atmosphere and Ocean Research Institute, The University of Tokyo)

[SCG66-P04] Geophysics in the R/V Hakuho-maru 2019-2020 expeditions around the world, 30th anniversary

*Masakazu Fujii[1,2], Hiroaki Koge[3], Hiroshi Sato[4], Kyoko Okino[5], Chiori Tamura[5], ZHOU JINYU[5], Kosuke Inoue[5] (1.National Institute of Polar Research, 2.The Graduate University for Advanced Studies, SOKENDAI , 3.AIST, 4.Senshu University, 5.Atmosphere and Ocean Research Institute, UTokyo)

[SCG66-P05] How fracture zones work on subducting lithosphere?

*Nobukazu Seama[1,2], Tomoeki Nakakuki[3] (1.Department of Planetology, Graduate School of Science, Kobe University, 2.Kobe Ocean Bottom Exploration Center, Kobe University, 3.Department of Earth and Planetary Systems Science, Graduate School of Science, Hiroshima University)

[SCG66-P06] Topographic features of rift zones of the seamounts on the Pacific Plate

*Megumi Fujimoto[1], Masao Nakanishi[2] (1.Graduate School of Science and Engineering, Chiba University , 2.Department of Earth Sciences Graduate School of Science, Chiba University)

[SCG66-P07] Dredge cruise on petit-spot volcanoes and IODP drilling earth science -Great discovery : explosion crater (Maar) in the abyssal plane, off Tohoku-

*Teruaki Ishii[1], Makoto Kaneko[2], Naoto Hirano[3], Shiki Machida[4], Asako Matsumoto[4], Norikatsu Akizawa[5], Yuki Sato[3], Taku Yutani[6], Keishiro Azami[5], Yuki Katsuragi[3], Shunta Sakai [3], Yukihiko Nakano[7], Takuya Matsuzaki[8] (1.Center for Integrated Research and Education of Natural Hazards, Sizuoka University, 2.Fukada Geological Institute, 3.Tohoku University, 4.Chiba Institute of Technology, 5.The University of

Tokyo, 6.Tohoku University,University of Bayreuth (Germany), 7.Nippon Marine Enterprises, LTD, 8.Kochi University)

[SCG66-P09] Geophysical analysis of the Yonaguni, Irabu and Tarama knolls

*ZHOU JINYU[1], Kyoko Okino[1], Masakazu Fujii[2] (1. Atmosphere and Ocean Research Institute, The University of Tokyo, 2.National Institute of Polar Research)

[SCG66-P10] **Reflection seismic survey data around ring structures of the submarine Kikai Caldera, south offshore Kyushu, Japan**

*Jih-Hsin Chang[1], Takahiko Inoue[1], Ayanori Misawa[1], Kohsaku Arai[1] (1.Geological Survey of Japan, National Institute of Advanced Industrial and Science Technology.)

[SCG66-P11] Pore fluid chemistry at a small pockmark with liquid CO_2 venting within an active hydrothermal field in the Okinawa Trough

Shunta Ueno[1], Akihi Tsutsumi[1], Akiko Makabe[2], Shinsuke Kawagucci[2], Masahiro Yamamoto[2], *Jun-ichiro Ishibashi[1] (1.Department of Earth and Planetary Sciences, School of Science, Kyushu University, 2.Japan Agency for Marine-Earth Science and Technology)

[SCG66-P12] Precipitation environment and preservation mechanism in formation of iron hydroxide in Satsuma Iwo-jima, Kagoshima, Japan.

*Koki Hori[1], Shoichi Kiyokawa[2] (1.Department of Earth and Planetary Sciences, Graduate School of Sciences, Kyushu University, 2.Kyushu University Earth and Planetary Science)

[SCG66-P14] **Developing efficient methods to collect and observe microfossils of fish teeth (ichthyoliths) from pelagic clay for determining depositional ages of pelagic clay**

*Kazuhide Mimura[1], Shugo Minabe[1], Junichiro Ohta[1,2,3], Kentaro Nakamura[1], Kazutaka Yasukawa[1,2], Koichiro Fujinaga[2,1], Kazuhiro Takao[1], Yasuhiro Kato[1,2] (1.Department of Systems Innovation, School of Engineering, the University of Tokyo, 2.ORCeNG, Chiba Institute of Technology, 3.JAMSTEC)

[SCG66-P15] Chemostratigraphy of ferromanganese crusts based on Independent Component Analysis

*Keishiro Azami[1], Qing Chang[2], Jun-Ichi Kimura[2], Kazutaka Yasukawa[1,3], Kentaro Nakamura[1], Yasuhiro Kato[1,3] (1.Department of System Innovation, Graduate School of Engineering, The University of Tokyo, 2.Japan Agency for Marine-Earth Science and Technology, 3.Chiba Institute of Technology)

[SCG66-P16] Buoy-mounted system for continuous and real-time seafloor crustal deformation measurements

*Keiichi Tadokoro[1], Natsuki Kinugasa[1], Teruyuki Kato[2], Yukihiro Terada[3], Kenjiro Matsuhiro[4] (1.Research Center for Seismology, Volcanology and Earthquake and Volcano Research Center, Nagoya University, 2.Hot Springs Research Institute of Kanagawa Prefectural Government, 3.National Institute of Technology, Kochi College, 4.Technical Center, Nagoya University)

[SCG66-P17] Evaluation of the effects of seafloor station array size on the accuracy of GNSS-A observation using synthetic data

*Yuto Nakamura[1], Yusuke Yokota[2], Tadashi Ishikawa[1], Shun-ichi Watanabe[1] (1.Hydrographic and Oceanographic Department, Japan Coast Guard, 2.Institute of Industrial Science, University of Tokyo)

[SCG66-P18] High-resolution bathymetry and efficient geological survey using submersible SHINKAI 6500 equipped with MBES and SBP in the petit-spot volcanic fields around Minamitorishima Island.

*Junji Kaneko[1], Shiki Machida[2] (1.Japan Agency for Marine-Earth Science and Technology, 2.Chiba Institute of Technology)

[SCG66-P19] An efficient method for high-res deep ocean mapping newly developed in the international unmanned survey competition

*MASANAO SUMIYOSHI[1] (1.Hydrographic and Oceanographic Department, Japan Coast Guard)

[SCG66-P20] Recovery operation of "anchor-recovery type OBSs" – KR19-06C cruise of R/V Kairei, off Yamagata, Japan Sea

*Ryo Miura[1], Tetsuo No[1], Shuichi Kodaira[1], Takuya Maekawa[2], Ikumasa Terada[2], Hidenori Shibata[2], Keiji Okabe[3] (1.Japan Agency for Marine-Earth Science and Technology, 2.Nippon Marine Enterprises, Ltd., 3.Mitsuya, Ltd.)

Relationship between the oblique opening system in the back-arc basin and Hamilton's principle

*Takao Eguchi

Within a certain arc - back-arc system at spherical subduction zones, some spatiotemporal changes in peripheral tectonics, such as collisions at adjacent plate boundaries, or sudden changes in trench axis morphology, would occasionally create an "arc rift system" or "back-arc rift system." As such a rift system grows, a back-arc basin would be formed.
Among active back-arc basins around the world, in the Andaman Sea, the Bismarck Sea, the Lau Basin, etc., active extension tectonics that can be regarded as oblique expansion (expanding in a direction not perpendicular to the ridge axis strike)rather than so-called orthogonal expansion is progressing.
Some successfully developed back-arc opening systems inevitably require the replenishment of the melt materials while actively or passively exciting the upper mantle flow. In other words, the back-arc oblique opening phenomenon is an energy dissipation problem including the dynamics of the upper mantle flow, etc.
The length of the ridge segment of the back-arc oblique extension system is variable. There are also back-arc basins with an echelon-arranged scheme of short parallel ridges, starting from a relatively longer transform faults (e.g., the Andaman sea, Bismarck sea, and Lau basin. In the central Andaman sea, there is a relatively longer oblique opening ridge segment.
We investigated the dynamic background in the length difference of these back-arc oblique opening ridge segments, as an energy dissipation problem including the effect of the upper mantle flow regime.
Specifically, regarding the total energy dissipation in the active back-arc basin with oblique expansion, we discussed by modelling the amount of energy dissipated along the transform fault(s) and the amount of dissipation at ridges. The latter dissipation is strongly associated with the upwelling flow having been originated at a certain depth toward the opening ridge segment(s).
In this study, we discussed the dynamics in the back-arc basins with such an oblique extension system from the viewpoint of Hamilton's principle.

Keywords: back-arc oblique opening, energy dissipation, upwelling flow, Hamilton's principle

©2020. Japan Geoscience Union. All Right Reserved.

A sand-box experiment for understanding marine self-potential anomalies

*Yoshifumi Kawada[1,2], Takafumi Kasaya[2]

1. International Research Institute of Disaster Science, Tohoku University, 2. Japan Agency for Marine-Earth Science and Technology

The marine self-potential method has advantages in detecting hydrothermal ore deposits by its simple observation procedure: Only towing multiple electrodes connected with a voltmeter in the seawater can detect signals from ore deposits up to 100 m above the seafloor. The self-potential signal is negative above ore deposits in most cases (e.g., Sato et al., 2017; Safipour et al., 2017; Kawada and Kasaya, 2017, 2018; Constable et al., 2018). At present, there is only one example of a positive self-potential anomaly observed at the Oomuro-Dashi (Kawada and Kasaya, JpGU2019).

The self-potential signals from ore deposits are probably explained by the geo-battery mechanism of Sato and Mooney (1960), in which an oxidative and reduced environments are connected by an electric conductor. A negative self-potential is expected above the oxidative (upper) side of the conductor; a positive signal is expected below the reduced side, where the conductor is being corroded. In the marine environment, the oxidative environment is maintained by seawater, the reduced environment is due to reduced sub-seafloor sediments, and an ore body crossing these environments can be a conductor. The oxidative-reduced boundary is not necessarily the seafloor itself because the recharge of seawater could deepen the boundary. In this case, a completely buried ore body may be detected above the seafloor. In this presentation, the concept of geo-battery mechanism extending to the marine environment is tested by an analog experiment inspired by Rittgers et al. (2013).

To set up the marine environment, a plastic container of 35 by 50 cm footprint and 30 cm height is filled by a 10-cm-thick sand layer filled with saline water (~3.5 wt%NaCl) mimicking the surface sediment and another 10-cm-thick layer of saline water above the sand layer for the ocean. Steel bars (mostly, 5-cm-long and 2-cm-diameter) mimicking ore deposits are installed in the sand layer with the top 0 to 1cm being exposed from the layer; an exposed ore deposit is approximated. The system is kept at rest for over a month. Two Ag/AgCl electrodes, one fixed at a corner of the plastic container and another moved by hand manipulation within saline water, connected to a voltage logger are used to scan the distribution of self-potential inside the container. Reference electrodes for general chemistry are used because of their small diameter (~2 mm), but electrodes designed for marine electromagnetic surveys (3 cm diameter; manufactured by Clover Tech Inc.) can be used as well.

From the very beginning of the experiment, we can detect negative self-potential anomalies above exposed steel bars, whose order is of the order of 10 microvolts. An almost completely buried steel bar is also accompanied by a negative self-potential anomaly. The results are reproducible including their amplitude, indicating that this is a quasi-steady-state behavior. In this case, steel bars above the sandy layer are not under corrosion but those below the sand are corroding. Though a very rare case, a positive self-potential anomaly was observed near the boundary between the sandy layer and a steel bar. However, this is not always the case, indicating that this is a time-dependent behavior. In this case, corrosion is occurring above the sand or near the boundary. The positive self-potential anomaly observed at the Oomuro-Dashi might be reflected by progressive corrosion occurring at or near the seafloor.

©2020. Japan Geoscience Union. All Right Reserved.

Keywords: hydrothermal ore deposits, marine geo-battery, electrochemistry, geophysical exploration, analog experiment

©2020. Japan Geoscience Union. All Right Reserved.

Sandbox analogue experiments to examine how syntectonic sedimentation influence on forearc basin stratigraphy and accretionary wedge growth

*Atsushi Noda[1], Hiroaki Koge[1], Yasuhiro Yamada[2,3,4], Ayumu Miyakawa[1], Juichiro Ashi[5]

1. National Institute of Advanced Industrial Science and Technology, 2. Japan Agency for Marine-Earth Science and Technology, 3. Faculty of Science and Technology, Kochi University, 4. Department of Earth Sciences, Royal Holloway University of London, 5. Atmosphere and Ocean Research Institute, The University of Tokyo

Forearc basin stratigraphy is expected to record a detailed history of the deformation and growth pattern of an accretionary wedge. However, the relationship between syntectonic basin sedimentation and growth of a wedge remains poorly understood, including (1) how deformation of the wedge modifies the basin stratigraphy and (2) how syntectonic sedimentation influences deformation of the wedge. In this study, we conducted scaled analogue sandbox experiments to reproduce accretionary wedges with and without syntectonic sedimentation. The results show that basin stratigraphy varied with the growth pattern of the accretionary wedge. In the case that wedge growth was dominated by trenchward accretion, the depositional area migrated trenchward. In contrast, prolonged underthrusting caused the sediment layers to be tilted landward and the depocenter to migrate landward. A phase dominated by underthrusting can result in the combining a retro-wedge basin with a wedge-top basin, and yield a wide area of accommodation space in the forearc basin. The occurrence of two types of basin stratigraphy (i.e., trenchward and landward migration of the depocenter) reflects the two different types of deformation style of accretionary wedge (frontal accretion phase and underthrusting phase), and these differences possibly depend on a contrast in strength of the basal shear resistance between the inner and outer parts of the wedge due to sedimentation on the wedge. A change in the magnitude of normal stress acting on the wedge base likely influenced the mode of deformation of the wedge. These results suggest that forearc basin stratigraphy is influenced by the growth pattern of an accretionary wedge that is affected by syntectonic sedimentation.

Keywords: accretionary wedge, forearc basin, analogue experiment

©2020. Japan Geoscience Union. All Right Reserved.

Geophysics in the R/V Hakuho-maru 2019-2020 expeditions around the world, 30th anniversary

*Masakazu Fujii[1,2], Hiroaki Koge[3], Hiroshi Sato[4], Kyoko Okino[5], Chiori Tamura[5], ZHOU JINYU[5], Kosuke Inoue[5]

1. National Institute of Polar Research, 2. The Graduate University for Advanced Studies, SOKENDAI , 3. AIST, 4. Senshu University, 5. Atmosphere and Ocean Research Institute, UTokyo

The seafloor covers more than 70 percent of the solid-earth surface, but most parts have not been explored because of observation difficulty. Significant records of submarine volcanism, dynamic erosion, and sedimentation as well as continental breakup and seafloor spreading are preserved in the seafloor. Here, we present new geophysical observations of ocean floors in southern hemisphere including various tectonic settings such as mid-ocean ridges, fracture zones, subduction systems, and continental slope to margin. We conducted underway geophysical mapping during the R/V *Hakuho-maru* cruises of KH-19-6 Leg 1 (Tokyo to Honolulu, October 2019), KH-19-6 Leg 2 (Honolulu to Valparaiso, October –November 2019), KH-19-6 Leg 3 (Valparaiso to Punta Arenas, November –December 2019), KH-19-6 Leg 4 (Punta Arenas to Cape Town, December 2019 –January 2020), and KH-20-1 (Cape Town to Fremantle, January –February 2020). Multibeam bathymetry, sub-bottom profiler, total and vector magnetic fields, and gravity data were widely acquired except exclusive economic zones. Specific scientific target area were set to 1) the Chile Ridge, southern Mid-Atlantic Ridge, and Southeast Indian Ridge to reveal the seafloor spreading process in the Cenozoic era and the mid-ocean ridge oscillation; 2) South Shetland Trench system, West Antarctica, to understand the formation of accretionary prisms and sediment supply from the continent; 3) Vulcan and Bullard Fracture zones to reveal temporal change of mid-ocean ridge volcanism and mantle heterogeneity; 4) Conrad Rise to understand its origin and surrounding magmatism; and 5) off Cape Darnley, East Antarctica, to reveal relationship between solid-earth processes and presently formed Antarctic bottom water. In this presentation, we overview preliminary geophysical results which were combined with previous data obtained during cruises of the R/V *Hakuho-maru*, Icebreaker *Shirase*, and R/V *Mirai* as well as previous compile study (e.g., Quesnel et al., 2009; Ryan et al., 2009) and satellite gravity insight (e.g., Sandwell et al., 2015; Wessel, 2015). Finally, we discuss geophysical insights into tectonic, volcanic, sedimentation, and glacial processes in Pacific, Atlantic, Indian and Southern Oceans.

Keywords: Marine geophysics, R/V Hakuho-maru, Expeditions around the world, Southern Hemisphere

©2020. Japan Geoscience Union. All Right Reserved.

How fracture zones work on subducting lithosphere?

*Nobukazu Seama[1,2], Tomoeki Nakakuki[3]

1. Department of Planetology, Graduate School of Science, Kobe University, 2. Kobe Ocean Bottom Exploration Center, Kobe University, 3. Department of Earth and Planetary Systems Science, Graduate School of Science, Hiroshima University

A fracture zone extends past a transform fault that is a fault along a plate boundary with predominantly strike-slip movement resulting from the action of offset mid-ocean ridge axis segments. Once the fracture zone is away from the ridge axis, it becomes seismically inactive because both plate segments are moving in the same direction horizontally. On the other hand, the fracture zone cut all through lithosphere vertically and each lithosphere both side of it is expected to independently move in vertical direction due to different ages and different subsidence rates. This suggest that the fracture zone is a mechanically weak linear line in the lithosphere. Then, the fracture zone could work as a slit in the lithosphere where water could be transported through it from the ocean to the lithosphere, which results in further weakening the lithosphere mechanically. We investigate this possible mechanically weak linear line of the fracture zone, and we found characteristic topographic features of the subducting lithospheres with related to the fracture zones: Outer rise that is subtle ridge on the seafloor near an oceanic trench due to bending lithosphere, does not appear (or does appear in much smaller level than others) in two areas: Izu-Ogasawara subduction system, and Tonga-Kermadec Trench subduction system, where the old Pacific lithospheres are subducting. The fracture zones of the old Pacific lithospheres in both two areas shows their directions parallel to the trench. We propose that the fracture zone, which is a mechanically weak linear line in the lithosphere, prevents the subducting lithosphere from making an outer rise; the fracture zone disconnects the stiff core of the lithosphere to transfer bending stress, so that the lithospheric flexure to generate the outer rise is reduced. We will present these results with further investigations on fracture zones with related to subducting lithosphere.

Keywords: fracture zone, lithosphere, subduction

©2020. Japan Geoscience Union. All Right Reserved.

Topographic features of rift zones of the seamounts on the Pacific Plate

*Megumi Fujimoto[1], Masao Nakanishi[2]

1. Graduate School of Science and Engineering, Chiba University , 2. Department of Earth Sciences Graduate School of Science, Chiba University

Several volcanos on land have rift zones. A rift zone is an elongated topography made by intrusion or extrusion of magma. A volcano has usually two or three rift zones that elongate from the crest of the volcano. Several studies indicated that the angle between is about 120° (e.g., Wentworth and Macdonald, 1953; Carracedo, 1994).

Vogt and Smoot (1984) reported that there is a seamount of the Japanese seamounts that has more than three rift zones. However, few studies about rift zones of seamounts have been done because of lack of detailed bathymetric data. The spread of multibeam echo sounder has brought the increase of detailed bathymetric data of seamounts. We examined the topographic expression of seamounts on the Pacific Plate except for the seamounts studied by Vogt and Smoot (1984) using the multibeam data.

©2020. Japan Geoscience Union. All Right Reserved.

Dredge cruise on petit-spot volcanoes and IODP drilling earth science -Great discovery : explosion crater (Maar) in the abyssal plane, off Tohoku-

*Teruaki Ishii[1], Makoto Kaneko[2], Naoto Hirano[3], Shiki Machida[4], Asako Matsumoto[4], Norikatsu Akizawa[5], Yuki Sato[3], Taku Yutani[6], Keishiro Azami[5], Yuki Katsuragi[3], Shunta Sakai [3], Yukihiko Nakano[7], Takuya Matsuzaki[8]

1. Center for Integrated Research and Education of Natural Hazards, Sizuoka University, 2. Fukada Geological Institute, 3. Tohoku University, 4. Chiba Institute of Technology, 5. The University of Tokyo, 6. Tohoku University,University of Bayreuth (Germany), 7. Nippon Marine Enterprises, LTD, 8. Kochi University

The R/V (Research Vessel) Shinsei Maru Cruise KS-18-19 was performed during 10 days from Thursday, August 2, 2018 (Ishinomaki, Miyagi) to , Saturday, August 11, 2018 (Ishinomaki, Miyagi) in the off Tohoku area about 350km east, and was conducted by the chief scientist: Dr. Naoto Hirano (Tohoku University) together with total 12 onboard scientists. The research title is “Distribution of petit-spot submarine volcanoes along the deformation of tectonic plate” which was selected by the Cooperative Research System of the R/V Shinsei Maru, Atmosphere and Ocean Research Institute (AORI), The University of Tokyo. The main research objectives are recovering the igneous rocks from petit-spot volcano, of which magmas originate from the asthenosphere (ductile part of the mantle) immediately below the Pacific Plate with about 70km thick, and assent directly from the deep without petrological change. Research days became less than half, because of escaping from the Typhoon 13, 2018, only 5 times (one with deep sea camera) of dredge hauls were performed to recover igneous rocks, at atop the outer-rise of the Pacific Plate, off Fukushima, NE Japan. Onboard as well as sub-bottom geological and geophysical several observations (ADCP, SBP, MBES, etc.) were also successfully done during the Cruise. Research summaries are shown in the followings:①recovering the very young igneous rocks from three petit-spot volcanoes, originate from the asthenosphere, ② recovering ferromanganese crust related with hydrothermal activity of petit-spot volcanoes, ③ discovery of the petit-spot volcano with explosion crater (=Maar) in the ocean floor about 5500m deep.

New scientific concepts of (A) the petit-spot’s magmas originate from the asthenosphere and (B) the magmas made deep sea explosion crater (=Maar) are great discovery in the earth science (like the Chibanian?) originated from Japan. The concepts will encourage Japanese young geoscientists. The petit-spot volcanoes are the most important scientific target of IODP.

Keywords: explosion crater (=maar) in the deep ocean floor, “petit-spot” volcano, “petit-spot” magma originate from the asthenosphere, outer-rise off Tohoku, ferromanganese crust related “petit-spot” volcanoes, IODP drilling earth science

©2020. Japan Geoscience Union. All Right Reserved.

Geophysical analysis of the Yonaguni, Irabu and Tarama knolls

*ZHOU JINYU[1], Kyoko Okino[1], Masakazu Fujii[2]

1. Atmosphere and Ocean Research Institute, The University of Tokyo, 2. National Institute of Polar Research

This research aims at understanding the subseafloor structure of the Yonaguni, Irabu, and Tarama Knolls, which are volcanos located in the southern Okinawa Trough backarc basin, where the Philippine Sea Plate subducts below the Eurasia Plate. The Okinawa Trough is now in the rifting stage. Through the state of the Yonaguni, Irabu, and Tarama Knolls, we can also infer the dynamics of the southern Okinawa Trough.

We collected bathymetry, gravity, and magnetism data of the Yonaguni Knolls and the adjacent area during the YK11-10 cruise in 2011, in the YK14-16 cruise, collecting the data for the Irabu and Tarama Knolls. The Yonaguni Knolls are located at the western end of the Okinawa Trough (Yaeyama graben), where the water depth is 1700 meters, 200 meters deeper than the area west part of the knolls. The Yonaguni Knolls consists of dozens of knolls, that align in E-W trending three rows parallel to the rift axis. These rows show a right-stepping en-echelon pattern, forming general NE-SW trend, oblique to the rift. The heights of the knolls are among 300-500 meters. Irabu and Tarama knolls at the east of Yonaguni knolls. The water depth surrounding the Irabu and Tarama knolls is about 2000 meters. The heights of the knolls are up to 600 meters. The Tarama Knolls locate in an EW trending rifting zone, and they are at the south of the rifting axis. The Irabu knolls locate in the intersect of the East-West trending rifting zone where Tarama Knolls are and a Northeast-Southwest rifting zone of the Okinawa Trough.

We calculated the Bouguer anomaly to remove the effect of topographic relief, assuming the density contrast between water and crust is 1720kg/m3. In the Yonaguni survey area, the Bouguer anomaly generally decreases from east to west, from 30 mGal to 5 mGal. The eastern part of the survey area showing a high Bouger anomaly (BA) corresponds to the active rifting zone of the Okinawa Trough. The high BA likely indicates the thinner, extended crust by backarc extension. The mantle material has a higher density than the crust, uplifting, causing the higher gravity of the rifting area. The rift axis is segmented and trends NE-SW direction east of the Irabu Knoll. The EW trending Yaeyama Graben is accompanied by positive gravity anomaly, whereas the NE-SW trending rift shows a negative gravity anomaly. It may suggest the difference of the rifting stage.

The influence on the gravity of the knolls seems to be negative. Yonaguni Knolls corresponds to a lower BA approximately 5 mGal than that in the surrounding area. It may be interpreted that volcanoes are active; hot magma has a low density. Gravity analysis on the Tarama knolls shows a similar result to the Yonaguni knolls. Low gravity anomaly beneath the knolls indicates low-density structure beneath the knolls. It is likely due to the active volcanism, where melting occurs. The other possibilities are thinner crust or different material density. There is no distinct gravity anomaly above the Irabu Knolls.

Magnetic anomaly distribution shows that three knolls are accompanied by typical dipole anomalies, and the rift axis shows a positive anomaly larger than 100nT. A positive magnetic anomaly along the rift axis likely indicates the existence of intrusive rocks.
Assuming the magnetization of knolls having the same direction to the ambient field (taken from IGRF), we did the calculation of reduction to pole. The knolls are positively magnetized, suggesting the recent eruption.

©2020. Japan Geoscience Union. All Right Reserved.

The positively magnetized body is located beneath the southern peak of the Tarama Knolls, and it seems that no magnetized body under the northern peak of the Tarama knolls. Magnetized body beneath the Yonaguni and Irabu knolls are well-distributed beneath the knolls. Magnetic anomaly of

Tarama is less than 500nT, whereas Irabu knolls have an up to 1000nT anomaly, which suggests more igneous rocks formed in the Irabu knolls area.

Keywords: Gravity, Magnetism, Back-arc basin, Volcano

©2020. Japan Geoscience Union. All Right Reserved.

Reflection seismic survey data around ring structures of the submarine Kikai Caldera, south offshore Kyushu, Japan

*Jih-Hsin Chang[1], Takahiko Inoue[1], Ayanori Misawa[1], Kohsaku Arai[1]

1. Geological Survey of Japan, National Institute of Advanced Industrial and Science Technology.

Records of volcanic activities may be destroyed by successive explosion especially at center part of caldera and it is thus of great significance to investigate the volcanic history through the volcanic structures around the caldera. Kikai caldera is rhyolitic caldera located at south offshore Kyushu, lying on the volcanic front of the subduction zone of Philippine Sea plate at Nankai trough and Ryukyu trench. It is bounded by the Takeshima island and Satsuma Iwojima island as subaerial parts of a ring structure of caldera to the north and west, and submarine double ring faults to the south and east, representing a trapdoor (asymmetrical) morphology of the caldera. Using reflection seismic data across the Kikai Caldera collected in 80s and archived in Geological Survey of Japan, we investigated the ring structure around the Kikai Caldera.

North of the northern ring structure, a bathymetric bulge is recognized and shows a gentle convex shape on reflection seismic profiles. It is likely to represent the tumescence of the Kikai activities. Beneath the bathymetric bulge, a relatively flat and eastward dipping surface is clearly shown. The formation of this surface is likely to provide us a key to evaluate the of most recent activities of the Kikai Caldera. South of the south ring structure, a funnel-shaped feature is recognized in our reflection seismic data. Based on field perception from Miyakejima Volcano, we interpreted it as a volcanic crater associated structure, probably indicating a phreatomagmatic explosion controlled by the lateral evolution of a feeder dike.

Keywords: Reflection seismic data, Kikai caldera

©2020. Japan Geoscience Union. All Right Reserved.

Pore fluid chemistry at a small pockmark with liquid CO_2 venting within an active hydrothermal field in the Okinawa Trough

Shunta Ueno[1], Akihi Tsutsumi[1], Akiko Makabe[2], Shinsuke Kawagucci[2], Masahiro Yamamoto[2], *Jun-ichiro Ishibashi[1]

1. Department of Earth and Planetary Sciences, School of Science, Kyushu University, 2. Japan Agency for Marine-Earth Science and Technology

Since the first discovery in 1989, liquid CO_2 venting on the seafloor has been observed in several hydrothermal fields in the Okinawa Trough. In Higashi Izena hydrothermal field, a small pockmark about 10-20 meters in diameter covered with white material was discovered during KM 18-08C dive campaign. Venting of liquid CO_2 was observed from the pockmark surface when the sediment was disturbed, which suggests liquid CO_2 accumulation just beneath the surface sediment. During the following KR18-14 dive campaign, short push sediment cores about 20-30 cm in length were collected at and near the small pockmark. The sediment cores were sliced into 3 cm pieces and pore fluid was extracted, onboard. The pore fluids were provided for chemical analysis after return to the laboratory, intended to reveal chemical signature affected by liquid CO_2 accumulation within the sediment. The pore fluid between 15 and 30 cm below the seafloor at the pockmark indicated increase of concentrations in all major ions compared with the seawater. They also showed D-depleted and ^{18}O-depleted signature in the isotopic composition. These results strongly suggest incorporation of H_2O into the CO_2-hydrate formed within the sediment.

Keywords: CO2 hydrate, Vertical profile of chemical composition, phase separation of hydrothermal fluid

©2020. Japan Geoscience Union. All Right Reserved.

Precipitation environment and preservation mechanism in formation of iron hydroxide in Satsuma Iwo-jima, Kagoshima, Japan.

*Koki Hori[1], Shoichi Kiyokawa[2]

1. Department of Earth and Planetary Sciences, Graduate School of Sciences, Kyushu University, 2. Kyushu University Earth and Planetary Science

Satsuma Iwo Jima is a volcanic island located about 50 km south of Makurazaki City, Kagoshima Prefecture, on the northwestern edge of the Kikai caldera, and the size is about 6 km east to west and 3 km north to south. From the seabed of Nagahama Bay, in the southern part of the island, hot spring water rich in dissolved ferrous iron springs out, and red-brown iron hydroxide precipitates due to mixing with seawater. The purpose of this study is to investigate in detail the precipitation environment of iron hydroxide in Nagahama Bay, and to clarify the precipitate process until sediment is preserved as a stratum. For this purpose, we measured the water quality of Nagahama Bay water mass (1) and observed sediments samples collected from Nagahama Bay (2).

<Method>
(1) Water quality measurement: A multi-item water quality meter was dropped from a breakwater in Nagahama Bay, and each item was measured while changing the water depth by 20 to 50 cm. The measurement was performed in August and December in 2017, March in 2018, and April, May and August in 2019. The main measurement items are as below: water temperature, pH, ORP, turbidity.
(2) Sample observation and analysis: Core samples collected in 2018 to 2019 from Nagamama Bay were used. The sample length were 50~100 cm. For observation Smear slide and scanning microscope (SEM) were used. The analysis has been performed by X-CT imaging and gamma ray attenuation (GRA) and susceptibility measurement by MSCL thus far.

<Result>
1) As a general trend, it was confirmed that pH increased and turbidity decreased with increasing depth. Eh showed a trend be low value relatively in the lower part of the body of water, and that increased toward the middle part, and decrease rapidly near the water surface. The measured pH ranged from 5.9 to 8.7, and Eh ranged from +57 to +492 mV.
2) As a result of smear slide observation, the sediments are composed of amorphous iron hydroxide, clastics such as sand and silt supplied from other sources, and volcanic glass. As a result of X-CT and GRA measurements in addition to slide observation, relatively high density parts are rich in relatively large debris. The change of gamma-ray density and the magnetic susceptibility coincide. And additionally, High-magnification observations of sediments using FE-SEM revealed that, in addition to aggregates and debris of iron hydroxide, many stalk-like substances were observed from the middle to the lower part of the cores.

<Discussion>
1) It is presumed that the aggregation of iron hydroxide particles strongly depends on pH change in the water mass of Nagahama Bay. In addition, iron hydroxide is likely to be generated by physicochemical oxidation as an iron precipitation environment considered from pH and Eh, however, depending on conditions, it can be an environment where organisms preferentially oxidize iron. In particular, biological oxidation is likely to occur near the sea surface where both pH and Eh take small values.
2)The analysis results suggest that the content of clastics in iron hydroxide is the main determinant of the

©2020. Japan Geoscience Union. All Right Reserved.

density in sediments. The magnetic susceptibility is thought to indicate mainly the inclusion of detrital material, suggesting that the low-density and low-magnetic-susceptibility part has a high amorphous iron hydroxide content. In addition, the presence of stalk-like substances observed by SEM observation suggests the presence of iron-oxidizing bacteria in sediments. In Nagahama Bay, iron oxidation by the action of bacteria in chimney mounds has been reported before, so the action of iron-oxidizing bacteria may affect the preservation of iron even in the stratum.

Keywords: Satsuma Iwo-jima, iron hydroxide, Iron oxidizing bacteria

©2020. Japan Geoscience Union. All Right Reserved.

Developing efficient methods to collect and observe microfossils of fish teeth (ichthyoliths) from pelagic clay for determining depositional ages of pelagic clay

*Kazuhide Mimura[1], Shugo Minabe[1], Junichiro Ohta[1,2,3], Kentaro Nakamura[1], Kazutaka Yasukawa[1,2], Koichiro Fujinaga[2,1], Kazuhiro Takao[1], Yasuhiro Kato[1,2]

1. Department of Systems Innovation, School of Engineering, the University of Tokyo, 2. ORCeNG, Chiba Institute of Technology, 3. JAMSTEC

Deep-sea sediments record paleo-environmental changes thorough geologic time. Among them, pelagic clay is one of the most widely distributed sediment in global ocean and thus is an important medium recording changes of atmospheric/oceanic circulations and surface ocean productivity that occurred in pelagic realm [1]. Although studies on pelagic clay [e.g. 2] have suggested that pelagic clay has significant variations in bulk geochemistry, possibly reflecting long term environmental changes, less attention has been paid to pelagic clay due to a difficulty in determination of depositional age.
It has long been recognized that determining depositional ages of pelagic clay is a challenge, because age-diagnostic calcareous/siliceous microfossils are seldom contained and paleomagnetic records are often ambiguous. Our studies [2,3] have shown that biostratigraphy of 'ichthyoliths' (microfossils of fish teeth and denticles [e.g. 4]) provide key constraints on depositional age of pelagic clay. However, traditional methods for collection and observations of ichthyoliths were troublesome; ichthyoliths were concentrated from samples by sieving and then manually picked from sieved samples to slide glasses under stereomicroscope. Therefore, observing enough amount of ichthyoliths from various samples is time consuming.
To overcome the problem, we first constructed a new method to concentrate a lot of ichthyoliths in a short time. We found that a combination of elutriation and heavy-liquid separation effectively accumulates ichthyoliths from pelagic clay. We then developed a method for direct detection of ichthyoliths by utilizing a slide scanner and deep learning-based technologies called 'Mask R-CNN' [5]. We are now improving the accuracy of the model. The latest results will be shown in the presentation.

References : [1] Kyte et al. (1993) *Geochim. Cosmochim. Acta* **57**, 1719-1740. [2] Mimura, K et al. (2019) *JpGU Meeting 2019*. [3] Minabe, S et al. (2019) *JpGU Meeting 2019*. [4] Doyle and Riedel (1985) *Init. Repts. DSDP* **86**, 349-366. [5] He et al. (2017) *Proc. IEEE ICVC*, 2961-2969

Keywords: pelagic clay, age determination, microfossils, ichthyolith, deep learning, object detection

©2020. Japan Geoscience Union. All Right Reserved.

Chemostratigraphy of ferromanganese crusts based on Independent Component Analysis

*Keishiro Azami[1], Qing Chang[2], Jun-Ichi Kimura[2], Kazutaka Yasukawa[1,3], Kentaro Nakamura[1], Yasuhiro Kato[1,3]

1. Department of System Innovation, Graduate School of Engineering, The University of Tokyo, 2. Japan Agency for Marine-Earth Science and Technology, 3. Chiba Institute of Technology

Ferromanganese (Fe-Mn) crusts are chemical sedimentary rocks that occur in submarine environment and are composed mainly of Fe-Mn (oxyhydr)oxides[1]. Due to a slow growth rate (1-10 mm/Myr), Fe-Mn crusts are expected to record long-term changes in ocean environments. Therefore, many studies have tried to discuss paleoceanographic environments from chemostratigraphy of Fe-Mn crusts. However, previous approaches by using bulk chemical analysis and EPMA have been severely limited in a spatial (and thus temporal) resolution and number of measurable elements, respectively. In addition, the criteria for sectioning stratigraphy based on chemical composition and growth structure proposed in previous studies are not objective sufficiently.

Here, we show the elemental maps of Fe-Mn crusts analyzed by using femto-second laser ablation (LA)-ICP-MS (iCAP Q). The laser beam was approximately 30 μm in diameter and 10 Hz repetition rate which scanned over sample surface along the growth direction at 70 μm/s, and space between adjacent scan lines was 80 μm. Concentrations of major and trace elements were calculated from standard materials of JMn-1 and Nod-P-1 (issued by GSJ and USGS, respectively) and normalized into 100% of major element oxides. The LA-ICP-MS analysis enables us to discuss the chemostratigraphy of Fe-Mn crusts with a time resolution approximately two orders of magnitude higher than previous works.

Based on the elemental mapping images, distribution patterns of almost all the elements are classified into three types: (1) Mn-oxide type showing the clear column structures, (2) Fe-oxyhydroxide type enriched in the space between the columns and (3) debris type showing spotty high contents between the columns. Several elements (e.g. Ti, Ce, Th) show the compositional changes irrespective of the boundaries of the growth structure, indicating that the sectioning of Fe-Mn crusts' stratigraphy merely based on the growth structure is insufficient. In addition, because the compositional changes are sometimes observed as the layer of submillimeter-scale, it would not be detected by the previous low-resolution bulk chemical analysis.

We also performed independent component analysis (ICA) on the elemental mapping data to section the stratigraphy of Fe-Mn crusts objectively and systematically. Based on the influence of the extracted ICs to each data point (IC scores), we systematically sectioned the chemostratigraphy of Fe-Mn crusts for the first time. In addition, we interpreted the geological meanings of each IC based on the geochemical features of the ICs (IC loadings). The results show that the boundaries of the chemostratigraphy generally coincide with that of the growth structure, but some of the layers showing the same structural character were divided into multiple layers based on geochemical features. Systematic sectioning based on multi-elemental features by using ICA will be a powerful tool to reconstruct paleoceanographic changes from Fe-Mn crusts.

1. Koschinsky & Hein, *Elements* **13**, 177–182 (2017).
2. Hyvärinen & Oja, *Neural Networks* **13**, 411–430 (2000).
3. Iwamori & Nakamura, *Gondwana Research* **27**(3), 1131-1152 (2015).
4. Yasukawa et al., *Sci. Rep.* **6**, 1–12 (2016).

©2020. Japan Geoscience Union. All Right Reserved.

Keywords: Ferromanganese crust, Chemostratigraphy, Independent component analysis

©2020. Japan Geoscience Union. All Right Reserved.

Buoy-mounted system for continuous and real-time seafloor crustal deformation measurements

*Keiichi Tadokoro[1], Natsuki Kinugasa[1], Teruyuki Kato[2], Yukihiro Terada[3], Kenjiro Matsuhiro[4]

1. Research Center for Seismology, Volcanology and Earthquake and Volcano Research Center, Nagoya University, 2. Hot Springs Research Institute of Kanagawa Prefectural Government, 3. National Institute of Technology, Kochi College, 4. Technical Center, Nagoya University

Our research group has been testing a measurement system for the continuous seafloor crustal deformation at a moored buoy site operated by Kochi prefecture from March 2018. We performed continuous acoustic ranging tests for a total of 106 days during the following four periods: March 28–31, June 2–July 12, and November 16–December 17 in 2018; and March 24–April 25, 2019. The tests revealed that the developed system can continuously transmit the acoustic ranging signals and send the acquired data to the on-land station via the satellite link, if sufficient electrical power is supplied. The system on the buoy was able to acquire high-quality acoustic waveforms with extremely high maximum cross-correlation coefficients. We coded a program for detecting the arrival time of direct acoustic wave automatically on the basis of thresholds of cross-correlation coefficient and energy ratio to reduce the capacity of data transferred via satellite communication. More than 99 % of the direct acoustic wave onsets at the buoy were correctly distinguished using our program code even if those waveforms had been corrupted with reflected waves. The above experimental studies show that our software system is capable of continuous real-time measurement of seafloor crustal deformation. However, the acoustic ranging controller and the satellite communication modem frequently experienced power failures during the test phase, and we re-designed the power supply part. We found that some of the solar panels were under the shadow of the mast, constructed on the center of the buoy, due to the stable yaw angle of the buoy. The original system was equipped with five 135-Watt solar panels connected in a series and 24 V valve-regulated stationary lead-acid batteries with a capacity of 300 Ah (10-hour rate). In the newly designed system is equipped with additional three (eight in total) solar panels which are separated to two parallel circuits. The power storage is also reinforced with additional two batteries. The re-installation of the new system was started in December 2019; the establishment is planned to be finished by the end of March, 2020. We report the present status of the continuous measurement using the newly designed system.

©2020. Japan Geoscience Union. All Right Reserved.

Evaluation of the effects of seafloor station array size on the accuracy of GNSS-A observation using synthetic data

*Yuto Nakamura[1], Yusuke Yokota[2], Tadashi Ishikawa[1], Shun-ichi Watanabe[1]

1. Hydrographic and Oceanographic Department, Japan Coast Guard, 2. Institute of Industrial Science, University of Tokyo

The Hydrographic and Oceanographic Department of Japan Coast Guard has been performing seafloor geodetic observations since the early 2000s using the GNSS-Acoustic ranging (GNSS-A) observation technique. With the GNSS-A technique, we measure the acoustic wave travel times between the transducer equipped on the bottom of the survey vessel and the mirror transponders (seafloor stations) installed on the seafloor, while tracking the precise position of the survey vessel using GNSS. By combining and analyzing these data with the survey vessel attitude data and the acoustic velocity profile measurements, we can locate the position of a seafloor reference site in precision of centimeters.
One of the largest consequences of GNSS-A observation is the observation frequency, which is only up to several times per year per seafloor site due to the limited ship time and human resources. The current observation system lacks the temporal resolution to observe phenomena with time scales less than few months. To increase the temporal resolution of GNSS-A observation, it is necessary to improve the observation efficiency to maximize the observation frequency in a limited ship time.
One of the key factors that affects the observation efficiency is the size of the seafloor station array. Four seafloor stations are installed to form a square array, with the seafloor site in the centroid, so the horizontal location of the seafloor site can be well defined compared to when only one station is installed. The size of the seafloor station array has been defined empirically from the early GNSS-A observations; that is, the length of the diagonals of the seafloor station array should be approximately the same as the depth of the seafloor site (Spiess, 1985, GRS). Since the size of the survey line array, which the vessel sails along during the observation, is set to twice the size of the seafloor station array, it is inevitable that the deeper sites take longer observation times compared to the shallower sites. This is a large concern for the new seafloor sites installed in the fiscal year of 2019, which were placed near the Nankai trough axis and have depths of approximately 3000~4000 meters. To improve the observation efficiency, it is necessary to reduce the observation times at these deep seafloor sites, which can be done by reducing the seafloor station array and the survey line array sizes of these sites. However, the effects of reducing the array size on the accuracy of GNSS-A observation have not been evaluated and remain to be unknown.
To evaluate the effects of reducing the seafloor station array size, we conducted an experiment using the GNSS-A observation simulator (Yokota et al. 2015, JpGU) to generate synthetic GNSS-A datasets, inputting different array sizes for each run. Like the actual GNSS-A data, each synthetic dataset was analyzed with an algorithm that alternately estimates the acoustic velocity profile and the seafloor station positions using linearized inversion (Fujita et al. 2006, EPS). In our presentation, we will present the analysis results of the synthetic GNSS-A datasets and discuss the effects of seafloor station array size on the accuracy of GNSS-A observation.

Keywords: GNSS-A observation, GNSS-A simulator, seafloor station array

©2020. Japan Geoscience Union. All Right Reserved.

High-resolution bathymetry and efficient geological survey using submersible SHINKAI 6500 equipped with MBES and SBP in the petit-spot volcanic fields around Minamitorishima Island.

*Junji Kaneko[1], Shiki Machida[2]

1. Japan Agency for Marine-Earth Science and Technology, 2. Chiba Institute of Technology

1.Introduction
Petit-spot volcanoes were first discovered on the old northwestern Pacific plate off Sanriku in Japan (Hirano, N. et al., 2006). Subsequently, it has been reported that such volcanoes were recently discovered on the slope of the Chile, Java trenches and southeastern of Minamitorishima Island (YK10-05 cruise report). The common feature of these areas is the stress field of plate tectonics, where is the plate flexes and fractures before the subducting area. It is necessary to obtain the high-resolution topography and detailed geological structure of regional Petit-spot lava fields to define the relationship between the regional stress field and petit-spot volcanism.

2. Method
We conducted the research cruises (YK18-08, YK19-05S) using submersible SHINKAI 6500 on the southeastern of Minamitorishima Island, where around the petit-spot volcano field. During the research cruise, a broad-area geophysical survey was conducted by R/V Yokosuka. Based on these broad-area geophysical data and previous research data, then the dive point was determined. The submersible SHINKAI 6500 equipped with Multibeam echo sounder (Seabat 7125) and Sub-bottom profiler (Strata Box) to collect detailed topographic and stratigraphic data. The principal results of the dives are summarized as follows.

3.Result
The dives were conducted six times (YK18-08: Dive1520,1521,1522, YK19-05S: Dive1542,1543,1544) and all dives were confirmed to be the petit-spot volcanic field. Four dives were conducted seamount, Dive1521 and 1544 dive points were a place where topographical elevation and large-scale outcrop were not observed by the shipboard survey. Dive1521, condition of the seafloor of landing point was flat, acoustic basement reflection was confirmed below the seafloor. Following the reflection, small outcrops (approximately 1 m) were confirmed. Dive1544 was performed by a one-man pilot dive (one pilot and two observers). During the first half of the dive, a box survey was conducted at an altitude of 50m above the seafloor to map each outcrop and collect geological data between the outcrops. In the latter half, observations and sampling were performed in sequence through the mapped outcrops. Acoustic survey near the seafloor collected high-precision and high-density seafloor topography data including the outcrop and acoustic basement data under the seafloor. SHINKAI 6500 equipped with an acoustic survey system provided efficient and effective dive and we obtained the data to define the relationship between stress field and petit-spot volcanism.

Keywords: high-resolution bathymetry, acoustic survey, petit-spot volcano, minamitorishima Island, submersible SHINKAI 6500, MBES and SBP

©2020. Japan Geoscience Union. All Right Reserved.

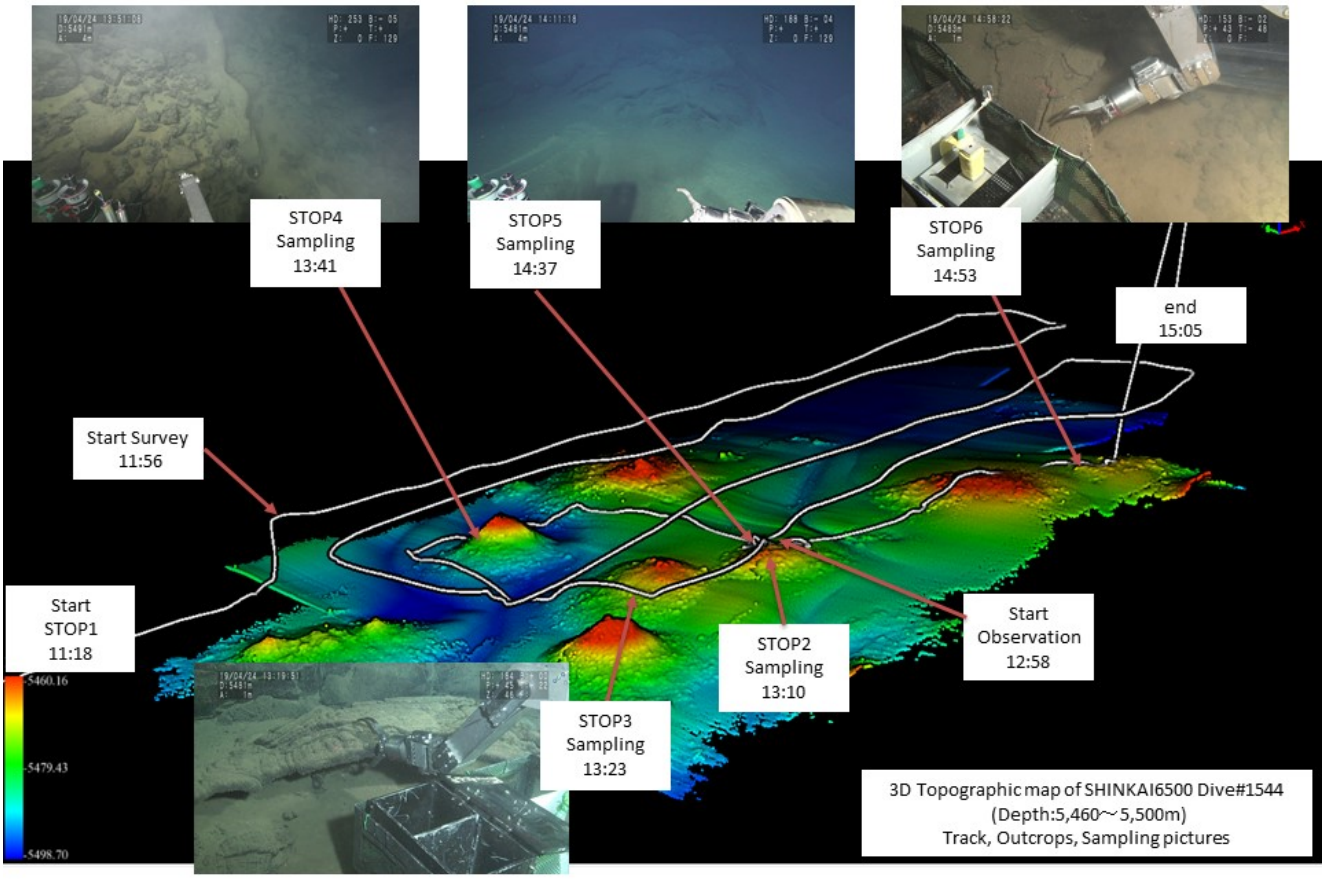

©2020. Japan Geoscience Union. All Right Reserved.

An efficient method for high-res deep ocean mapping newly developed in the international unmanned survey competition

*MASANAO SUMIYOSHI[1]

1. Hydrographic and Oceanographic Department, Japan Coast Guard

Recently, with the spread of high-resolution deep seafloor mapping using Autonomous Underwater Vehicles (AUVs), it has become possible to obtain detailed bathymetric maps at deep waters, as well as those at shallow waters. In the future, in order to further improve the efficiency of deep seafloor mapping, including unmanned launch and recovery of AUV, technological innovation is necesssary. To promote such technological innovation, the Shell Ocean Discovery XPRIZE, an international unmanned bathymetric competition at deep waters, had been held for three years. The GEBCO-Nippon Foundation Alumni team, led by alumni of the bathymetric survey training program at the University of New Hampshire, has won the championships of teams around the world. Through participation in this competition,the team has developed new technologies for creating detailed seafloor bathymetric maps in deep water areas. This paper introduces the technical activities of the GEBCO-Nippon Foundation Alumni team throughout the “Shell Ocean Discovery XPRIZE”, and specifically describes the efficient high-resolution deep sea mapping method developed by this team,including its features and advantages.

Keywords: Shell Ocean Discovery XPRIZE, GEBCO-Nippon Foundation Alumni Team, Bathymetric Survey, Autonomous Underwater Vehicle / Unmanned Surface Vessel, Multibeam Echosounder / Synthetic Aperture Sonar, Bathymetric Data Processing / Analysis

©2020. Japan Geoscience Union. All Right Reserved.

Recovery operation of "anchor-recovery type OBSs" – KR19-06C cruise of R/V Kairei, off Yamagata, Japan Sea

*Ryo Miura[1], Tetsuo No[1], Shuichi Kodaira[1], Takuya Maekawa[2], Ikumasa Terada[2], Hidenori Shibata[2], Keiji Okabe[3]

1. Japan Agency for Marine-Earth Science and Technology, 2. Nippon Marine Enterprises, Ltd., 3. Mitsuya, Ltd.

Many active faults are distributed in the coastal area in the eastern part of the Japan Sea (e.g. Okamura, 2019). In order to understand the seismotectonics of the Japan Sea, it is important to obtain crustal structure images of the coastal area derived from the seismic profile.
In August 2019, we conducted a marine seismic survey to study the crustal structure off Yamagata Prefecture, using 39 ocean bottom seismographs (OBSs) and a tuned air-gun array system of R/V Kairei. The survey covered the areas from the continental shelf to the Yamato Basin and was located near the aftershock area of the earthquake offshore Yamagata Prefecture (M_J 6.7) that occurred on June 18, 2019. The crustal structure is important information to understand the occurrence of this earthquake. However, it is difficult to obtain the structural information in such a coastal area due to economic activities (e.g. fishing activity). To minimize the conflict, we used eight "anchor-recovery type OBSs" in the coastal area. The OBS is connected to the anchor with a rope to wind up the anchor from the seafloor, following the OBS recovery.
In the past, we had some experiences in successfully operating the anchor-recovery type OBSs where the seafloor is shallower than 100 m. However, we had to deploy four anchor-recovery type OBSs deeper than 100 m (max. 646 m) during this survey, and this was our first attempt. To make it possible, we made some improvements to the OBS's recovery system, and conducted experimental tests using a water tank at the JAMSTEC Yokosuka Headquarters.
In addition, we also prepared a sweep-line with grapnel anchors in cases something unexpected happens to the OBS recovery. We designed the sweep-line on the basis of an emergency recovery method for a subsurface observation mooring system which is composed of a main rope, grapnel anchors, depressor weights, and a transponder (e.g. Momma and Hotta, 1986).
During the seismic survey, we recovered eight anchor-recovery type OBSs as well as 31 normal type OBSs after the air-gun shooting. The OBS recovery was carried out as follows: first, R/V Kairei sent an acoustic releasing command to each OBS. Then, surfaced OBS and its anchor connected with a rope were recovered using M/V Hirokai. We recovered seven OBSs with anchor successfully. However, one OBS didn't respond to a releasing command despite a number of trials to make acoustic communication.
For this unreleased OBS, we tried to recover using the towed sweep-line with grapnel anchors. The sweep-line was deployed from the stern of R/V Kairei, and towed around the OBS position with a radius of ~100 m. We monitored the sweep-line navigation data from the transponder and vessel navigation data during the towing. The first trial failed probably because the sweep-line didn't reach the seafloor. For the second trial, we added depressor weights and grapnel anchors to the sweep-line, and towed along multiple elliptic courses. As a result of the second trial, the sweep-line caught the OBS with its anchor, and we recovered them.
In this presentation, we report the operations and emerged problems of the anchor-recovery type OBSs.

[References]
Momma, H. and H. Hotta, 1986, JAMSTEC-TR, 16, 1-14.
Okamura, Y., 2019, Zisin2, 71, 185-199, doi: 10.4294/zisin.2017-21.

©2020. Japan Geoscience Union. All Right Reserved.

Keywords: Ocean Bottom Seismograph (OBS), Off Yamagata, Japan Sea, anchor recovery

©2020. Japan Geoscience Union. All Right Reserved.

[J] Poster | S (Solid Earth Sciences)：S-CG Complex & General

[S-CG67] Crustal fluids and deformation

convener:Yuichi Kitagawa(Tectono-Hydrology Research Group, Geological Survey of Japan, National Institute of Advanced Industrial Science and Technology), Naoji Koizumi(School of Environmental Science,the University of Shiga Prefecture), Koji Umeda(Hirosaki University), Fumiaki Tsunomori(Geochemical Research Center, Graduate School of Science, University of Tokyo)

We will provide an opportunity to discuss about observation and modeling of crustal fluids. Topics of interests include, but not limited to (1) a field of physics and chemistry of fault fluids, which is related to earthquake occurrences and researches physical and chemical changes of the fluids caused by crustal deformation including earthquakes, (2) a field of earthquake hydrology, which estimates crustal deformation from level, pressure and chemistry of groundwater using poroelastic theory, and (3) a field of chemistry of crustal fluids, which concerns chemical and isotopic features of the crustal fluids and try to estimate the flux of them.

[SCG67-P01] **Changes in stream water and spring water after the 2016 Kumamoto earthquake, Japan**

*Naoji Koizumi[1], Shinsuke Minote[2], Tatsuya Tanaka[3], Azumi Mori[4], Takumi Ajiki[5], Tsutomu Sato[6], Hiroshi A Takahashi[6], Norio Matsumoto[6] (1.School of Environmental Science,the University of Shiga Prefecture, 2.Taneya Co.Ltd., 3.JA Lake Otsu, 4.Yodogawa Hu-Tech Co., Ltd., 5.Kinki Eco Science Inc., 6.Geological Survey of Japan, AIST)

[SCG67-P02] Post-seismic slow strain changes and groundwater level changes in the case of the KST observation site of AIST

*Yuichi Kitagawa[1], Satoshi Itaba[1], Norio Matsumoto[1] (1.Tectono-Hydrology Research Group, Geological Survey of Japan, National Institute of Advanced Industrial Science and Technology)

[SCG67-P04] Experimental study on the effect of the oscillating confining pressure on permeability of fractured rock

*Yang Li[1,3], Shogo Kawakita[2], Daisuke Asahina[3], Takato Takemura[4] (1.Integrated Basic Sciences, Nihon Univ., 2.Graduate School of Science & Technology, Nihon Univ., 3.Geological Survey of Japan AIST, 4.Nihon Univ.)

[SCG67-P06] Relationship between geology and ^{222}Rn concentration in hot springs and groundwater around Kagoshima city, Japan

*Kuniyo Kawabata[1], Mai Watanabe[2,3], Ryosuke Nakano[2], Yujin Kitamura[4], Takashi Tomiyasu[4] (1.Institute for Comprehensive Education, KAGOSHIMA UNIVERSITY, 2.Faculty of Science, Kagoshima University, 3.Konica Minolta Planetarium Co., Ltd., 4.Graduate School of Science Engineering, Kagoshima University)

Changes in stream water and spring water after the 2016 Kumamoto earthquake, Japan

*Naoji Koizumi[1], Shinsuke Minote[2], Tatsuya Tanaka[3], Azumi Mori[4], Takumi Ajiki[5], Tsutomu Sato[6], Hiroshi A Takahashi[6], Norio Matsumoto[6]

1. School of Environmental Science,the University of Shiga Prefecture, 2. Taneya Co.Ltd., 3. JA Lake Otsu, 4. Yodogawa Hu-Tech Co., Ltd., 5. Kinki Eco Science Inc., 6. Geological Survey of Japan, AIST

The 2016 Kumamoto earthquake, whose main shock was an M7.3 event on April 16, 2016, 28 hours after a foreshock of M6.5, caused severe damage in and around Kumamoto Prefecture, Japan. It also caused postseismic hydrological changes in Kumamoto Prefecture. In this study, we analyzed daily streamflow data collected by eight observation stations from 2001 to 2017 in regions that experienced strong ground motion during the 2016 Kumamoto earthquake. We also surveyed 11 spring waters in the region several times after the main shock. Streamflow had no or slight change immediately after the earthquake; however, large increases were recorded at some of the eight stations following a heavy rainfall that occurred 2 months after the earthquake. A decrease in the water-holding capacity of the catchment caused by earthquake-induced landslides can explain this delayed streamflow increase. Conversely, earthquake-related changes to the spring flow rate were not so clear. Water temperature and chemical composition of spring waters were also hardly changed. Only the concentration of NO3-, which is usually considered to be supplied from the surface, increased slightly just after the earthquake. These results show that the postseismic hydrological changes were caused mainly by earthquake-induced surface phenomena(Koizumi et al., 2019).

Reference

Koizumi, N., S. Minote, T. Tanaka, A. Mori, T. Ajiki, T. Sato, H. A. Takahashiand N. Matsumoto, Hydrological changes after the 2016 Kumamoto earthquake, Japan, Earth, Planets and Space, 71, https://doi.org/10.1186/s40623-019-1110-y, 2019.

Keywords: Hydrological changes, Kumamoto earthquake, Water-holding capacity, Landslide

©2020. Japan Geoscience Union. All Right Reserved.

Post-seismic slow strain changes and groundwater level changes in the case of the KST observation site of AIST

*Yuichi Kitagawa[1], Satoshi Itaba[1], Norio Matsumoto[1]

1. Tectono-Hydrology Research Group, Geological Survey of Japan, National Institute of Advanced Industrial Science and Technology

In order to research short- and intermediate-term forecast of the Nankai megathrust earthquake, we observe crustal movement and groundwater at observation sites in Aichi Prefecture, Kii Peninsula and Shikoku, in particular focus on monitoring of short-term SSEs on the plate boundary. When the earthquake (M6.3) occurred on May 10, 2019 at the Hyuga-nada, slow strain changes were post-seismically observed at the Tosashimizu-Matsuo (TSS) observation site of AIST, however it is presumed that the post-seismic strain changes at the TSS are likely to be caused by the local changes around the TSS due to the shaking of the earthquakes. We investigated whether similar strain changes were occurred at the Kushimoto-Tsuga (KST) observation site of AIST, which is near the locked part of the plate boundary of the Nankai Trough as with TSS. According to checking of changes of the strain and groundwater level at the KST after the M5 or more earthquakes around the Kii Peninsula and the earthquakes with a seismic intensity of 3 or more in Kushimoto town, five cases of strain changes due to short-term SSEs around KST and one case of post-seismic slow clear strain changes were found. In the latter case, it was found that the groundwater level in the observation well (Hole 2) at the KST had post-seismically risen at the same time. These observation results are introduced.

Keywords: strain, groundwater, post-seismic change

©2020. Japan Geoscience Union. All Right Reserved.

Experimental study on the effect of the oscillating confining pressure on permeability of fractured rock

*Yang Li[1,3], Shogo Kawakita[2], Daisuke Asahina[3], Takato Takemura[4]

1. Integrated Basic Sciences, Nihon Univ., 2. Graduate School of Science & Technology, Nihon Univ., 3. Geological Survey of Japan AIST, 4. Nihon Univ.

The effects of earthquakes on groundwater flow mainly include two changes: pore pressure and permeability of the aquifer. These two changes interact each other and effect the groundwater flow in the aquifer during the earthquake.
In this study, we conducted the experiments to observe the effects of the oscillating confining pressure on the permeability of fractured rocks. Three experimental samples were tested, Shirahama Sandstone, Kimachi Sandstone and Inada Granite. Macro cracks were created by hammering a chisel into the sandstone samples. For granite, a split cylinder test was conducted to generate macro cracks. The permeability was measured through the flow pump method. The confining and pore pressure were set to 7.0 and 3.0 MPa, respectively, and the oscillation period of the confining pressure was 60s. The permeability was measured before and after the confining pressure oscillation. From the experimental results, we discuss the change in pore pressure and permeability on the fault surface due to the oscillating confining pressure during earthquake.

Keywords: Permeability, Laboratory experiments, Earthquake

©2020. Japan Geoscience Union. All Right Reserved.

Relationship between geology and ^{222}Rn concentration in hot springs and groundwater around Kagoshima city, Japan

*Kuniyo Kawabata[1], Mai Watanabe[2,3], Ryosuke Nakano[2], Yujin Kitamura[4], Takashi Tomiyasu[4]

1. Institute for Comprehensive Education, KAGOSHIMA UNIVERSITY, 2. Faculty of Science, Kagoshima University, 3. Konica Minolta Planetarium Co., Ltd., 4. Graduate School of Science Engineering, Kagoshima University

Radon (^{222}Rn) is a radioactive noble gas that occurs naturally in Earth's crust as an intermediate step in the uranium series radioactive decay chain. Radon is highly soluble in water, and thus is very mobile through groundwater and fluid flow in the crust. Radon release rate mainly depends on the physical properties of rocks/aquifers, such as surface area and porosity. Thus, the concentration of radon in crustal fluids and groundwater can provide clues for understanding the state of underground including host rocks, faults and the deformation status. Radon concentrations has been monitored as precursory indicator of earthquakes (e.g. Ulmov and Mavashav, 1971; Wakita et al., 1980; Igarashi et al., 1995; Kuo et al., 2006; Tsunomori and Tanala, 2014). Groundwater radon concentration has come to be used to investigate the existence of active faults, on the basis of the larger surface areas in fault zone than massive rock (Malgrange and Gleeson, 2014; Tsunomori et al., 2017).

We surveyed hot spring and groundwater radon concentrations in the vicinity of Kagoshima city area to examine relationship with the geology such as the formation and active fault. Temperature of hot springs suggested that they conform to popular geothermal gradient, suggesting that the hot springs are currently not affected by heat from magma under Aira caldera and old volcanic ejecta. Higher radon concentration in groundwaters discharged from porous pyroclastic flows than that in hot springs from hard bed rocks are obtained. The radon concentration distribution show that the hot springs along the active faults and faults in bed rock have higher concentration, suggesting that the hot springs may be discharging through active and inactive faults. Several hot springs along the faults are considered to be a mixture of meteoric water and magma related water by stable oxygen and hydrogen isotope data, which means that magma related waters are upwelling through active and inactive faults. These results suggest that radon concentration distribution of the hot springs and groundwater strongly associate with their hosting geology and geological structure. Using the relationship, we also estimate the depth of pollution source in several wells.

Igarashi et al., *Science*, 269, 1995
Kawabata et al., *Rep. Fac. Sci., Kagoshima Univ.,* 51, 2018
Kuo et al., *Ground Water*, 44, 2006
Malgrange and Gleeson, *J. Geophys. Res., Solid Earth*, 119, 2014
Tsunomori and Tanaka, *Radiat. Meas*, 60, 2014
Tsunomori et al., *Radioact.,* 172, 2017
Wakita et al., *Science*, 207, 1980
Ulmov and Mavashav, *Akad. Nauk Uzbek*, 1971

Keywords: Radon, Groundwater, Hot spring, Geology, Active fault, Kagoshima

©2020. Japan Geoscience Union. All Right Reserved.

[J] Poster | S (Solid Earth Sciences)：S-CG Complex & General

[S-CG68] Environment formed and maintained by active faults

convener:Naoji Koizumi(School of Environmental Science,the University of Shiga Prefecture), Makoto Yamano(Earthquake Research Institute, the University of Tokyo), Takafumi Kasaya(Japan Agency for Marine-Earth Science and Technology), Hideki Hamamoto(Center for Environmental Science in Saitama)

An active fault causes a large earthquake at a very low frequency such as once every several thousand to tens of thousands years and destroys the surrounding environment. On the other hand, during the period when the large earthquake or the fault movement does not occur, the unique environments such as mountains, basins, structural lakes, hot springs and mineral deposits are formed and maintained by the topography and hydrogeological structure made by the accumulation of the fault movement. In general, the presence of active faults is recognized as a factor of environmental destruction, but it is also necessary to understand the active faults as a factor of environmental formation and maintenance. In this session, we welcome wide-ranging topics on the role of active faults as a factor for the formation and maintenance of the environment and how to investigate it.

[SCG68-P01] Three-dimensional distinct element (DEM) simulation of shear bands formation and their time development for strike-slip faults

*Satoru Yamaguchi[1], Daigo Furukawa[1], Tada-nori Goto[2] (1.Graduate School of Science, Osaka City University, 2.Graduate school of Life Science, University of Hyogo)

[SCG68-P02] Profiles of magnetic susceptibility and resistivity along an "outcrop" of the Atera fault

Shuhei Sogi[1], *Tada-nori Goto[1] (1.Graduate School of Life Science, University of Hyogo)

[SCG68-P03] **Effect of active faults on the water quality of the Ado river and neighboring spring waters in Shiga Prefecture**

*Naoji Koizumi[1], Keisuke Ishida[1], Natsuko Oshida[1], Masahiro Maruo[1] (1.School of Environmental Science,the University of Shiga Prefecture)

[SCG68-P04] Discussion on the environment formed and maintained by active faults

*Naoji Koizumi[1] (1.School of Environmental Science,the University of Shiga Prefecture)

Three-dimensional distinct element (DEM) simulation of shear bands formation and their time development for strike-slip faults

*Satoru Yamaguchi[1], Daigo Furukawa[1], Tada-nori Goto[2]

1. Graduate School of Science, Osaka City University, 2. Graduate school of Life Science, University of Hyogo

There have been many studies to elucidate shear band formation and its development process with fault displacement using model experiments and numerical simulations employing the finite element or boundary element methods (e.g. Sawada & Ueda, 2009; Taniyama, 2011). Many of these used models with uniform medium and strength.
Fault zone in nature is typical NON-uniform region as fault zone is weaker than its surrounding area. It is interesting where are shear bands formed and how do they develop as fault displacement increases. However, it is difficult to perform model experiments for a non-uniform model, mainly because of difficulty in making a well-controlled non-uniform model.
We performed numerical simulations of shear band formation and its developing process, using a three-dimensional (3D) distinct element method (DEM) for three types of model. Every model has one or two vertical plate-like weak zones in the base model.
(1) Continuous model; one weak plate is located at the center of the base model (Fig.1a)
(2) Gap model: a non-weak part exists in the weak plate (Fig.1b).
(3) Step model: the weak plate displaces in a step (Fig.1c)
First, we examined the effect of the weak zone parameters (weak zone width and bond strength) on spatiotemporal change of shear band as fault displacement increase for the Continuous model.
Next, we examined effect of the gap length on forming shear bands and their spatiotemporal change for the Gap model, further, examined of them on the Step mode.
In this presentation, we show the results of these simulations and what they mean.

Keywords: strike-slip fault, Three-dimensional distinct element method, shear band

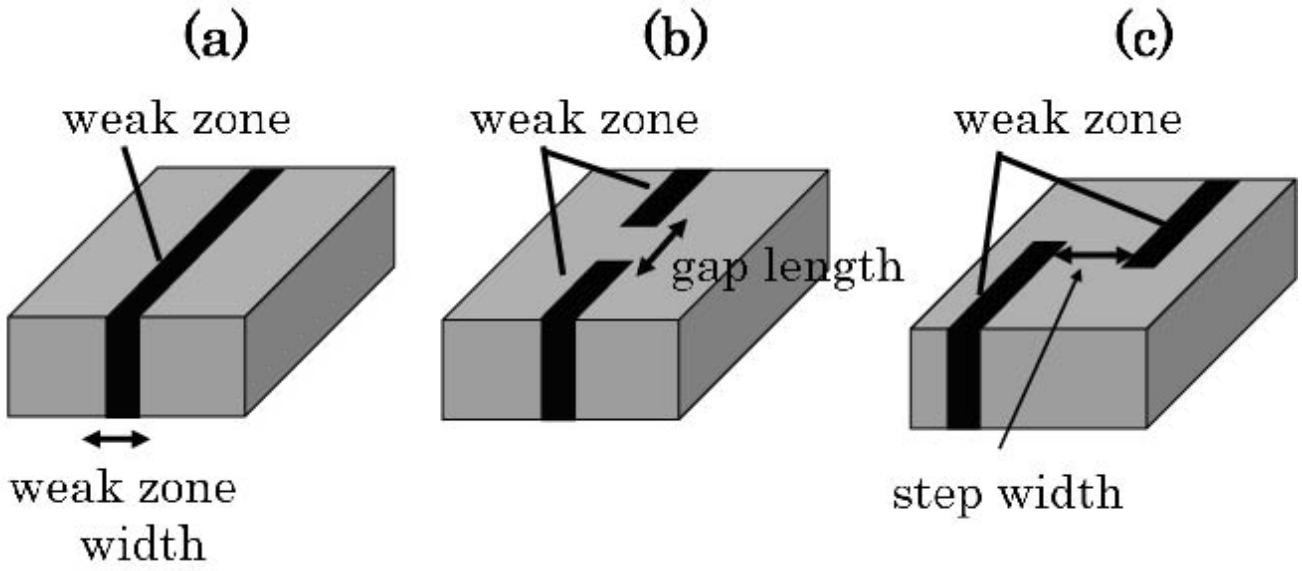

©2020. Japan Geoscience Union. All Right Reserved.

Profiles of magnetic susceptibility and resistivity along an "outcrop" of the Atera fault

Shuhei Sogi[1], *Tada-nori Goto[1]

1. Graduate School of Life Science, University of Hyogo

In this study, we apply portable physical property sensors to geological surveys at outcrops, and investigate how much geological information can be increased by performing high-density in-situ measurements. The Atera Fault in Nakatsugawa City, Gifu Prefecture, was selected as the study area. The Atera Fault is a large active fault, and the local variation of physical properties are expected along the fault core due to rock fracturing caused by fault movement. At the fault outcrop (Kawakami outcrop) in Nakatsugawa city, a two-meter survey profile was placed on the cliff, and in-situ measurements of magnetic susceptibility and resistivity were performed at intervals of 5 cm. As a result, we found 1) the magnetic susceptibility increasing at the fault core, and 2) the resistivity decreasing around the fault core. These features are considered to be involved in rock fracture and mineral formation associated with fault movement. Such fine features were not observable with eyes, demonstrating the usefulness of on-site physical property measurement.

©2020. Japan Geoscience Union. All Right Reserved.

Effect of active faults on the water quality of the Ado river and neighboring spring waters in Shiga Prefecture

*Naoji Koizumi[1], Keisuke Ishida[1], Natsuko Oshida[1], Masahiro Maruo[1]

1. School of Environmental Science,the University of Shiga Prefecture

Along a fault plain, there is a fractured damage zone, which has high permeability. This zone is often become groundwater path from deep to shallow (Faulkner et al., 2010). As a result, the fault-related groundwater stably supplies heat and chemical materials including water itself, which make some effect on the environment in and around the fault zone. For example, hot and mineral springs tends to distribute in and around fault zones(Koizumi et al., 1985; Mino et al.,1985). Since river has a base flow from groundwater, an active fault along or across the river also can have some effects on the water quality of the river by the base flow. The active fault causes a large earthquake at a very low frequency such as once every several thousand to tens of thousands years and destroys the surrounding environment. However, during the period when the large earthquake or the fault movement does not occur, the active fault forms and maintains the environment through the groundwater.

The length of the Ado river, which is located in the western part of Shiga Prefecture, is 58km and the second longest in the rivers which flow into Lake Biwa, which is the largest lake in Japan. The catchment area of the Ado river is 300 km^2 and the third largest in the rivers which flow into Lake Biwa (Shiga Prefecture, 2018). In the part of the upstream and most of the midstream, the Ado river runs along the Hanaore fault. In the downstream the Ado river crosses the Biwako-seigan fault(Fig.1). Both of the faults are the main active faults in the western part of the Shiga Prefecture. In addition the ado river basin is not well developped (Biwa basin study group, 2003). Therefore the Ado river is suitable for investigating the effect of active faults on the river water quality. There are some spring waters in the end of the alluvial fan of the Ado river. There are also some spring waters along the Biwako-seigan fault, which crosses the top of the fan. Hereafter they are called the fan spring water and the fault spring water, respectively.

During the period from 1996 to 1998, the water quality of the Ado river at ADG in Fig.1 was firstly Ca-HCO3 type and later turned mainly into NaHCO3 type or rarely into Na-Cl type (Koizumi et al., 2019). Water quality of the hot springs along the Hanaore fault and Biwako-seigan fault around the Ado river is Na-HCO3 type and its concentration is several times to 10 times larger than that of river water (Koizumi et al., 2019). Therefore it is considered that the major cation should change from Ca^{2+} to Na^{+} when the effect of the hot spring waters through the faults increases.

We surveyed the Ado river during the period from August 12 to August 14 in 2018. Before this period there had been no precipitation for thirteen days. Therefore it is considered that the river water was mainly composed of the base flow. The results showed that the water quality of the Ado river was Ca-HCO3 type from the upstream to the downstream at the period (Koizumi et al., 2019).

We have regularly surveyed the downstream of the Ado river, the fan spring waters and the fault spring waters about once a month since April, 2018 (Fig.1). In this survey, the water quality of the downstream was Ca-HCO3 type until August 2018. However since September 2018, the water quality have been Na-HCO3 type. The water quality of two of the fan spring waters, i.e. HRE and KWS in Fig.1, was also Ca-HCO3 type until August 2018 although it has also been turned into Na-HCO3 type since September 2018. In the presentation we will report the factors for those water quality changes.

©2020. Japan Geoscience Union. All Right Reserved.

Fig.1:Left: Solid circles indicate the sampling points of the Ado river during the period from August 12 to August 14 in 2018. Solid triangles show meteorological observation stations of JMA. Right: Regular sampling points since April 2018. Solid and open squares indicate fault spring waters and fan spring waters, respectively. Background map is from the active faults database of AIST(AIST, 2020).

Keywords: Ado river, Active fault, Water quality, Permeability, Spring water

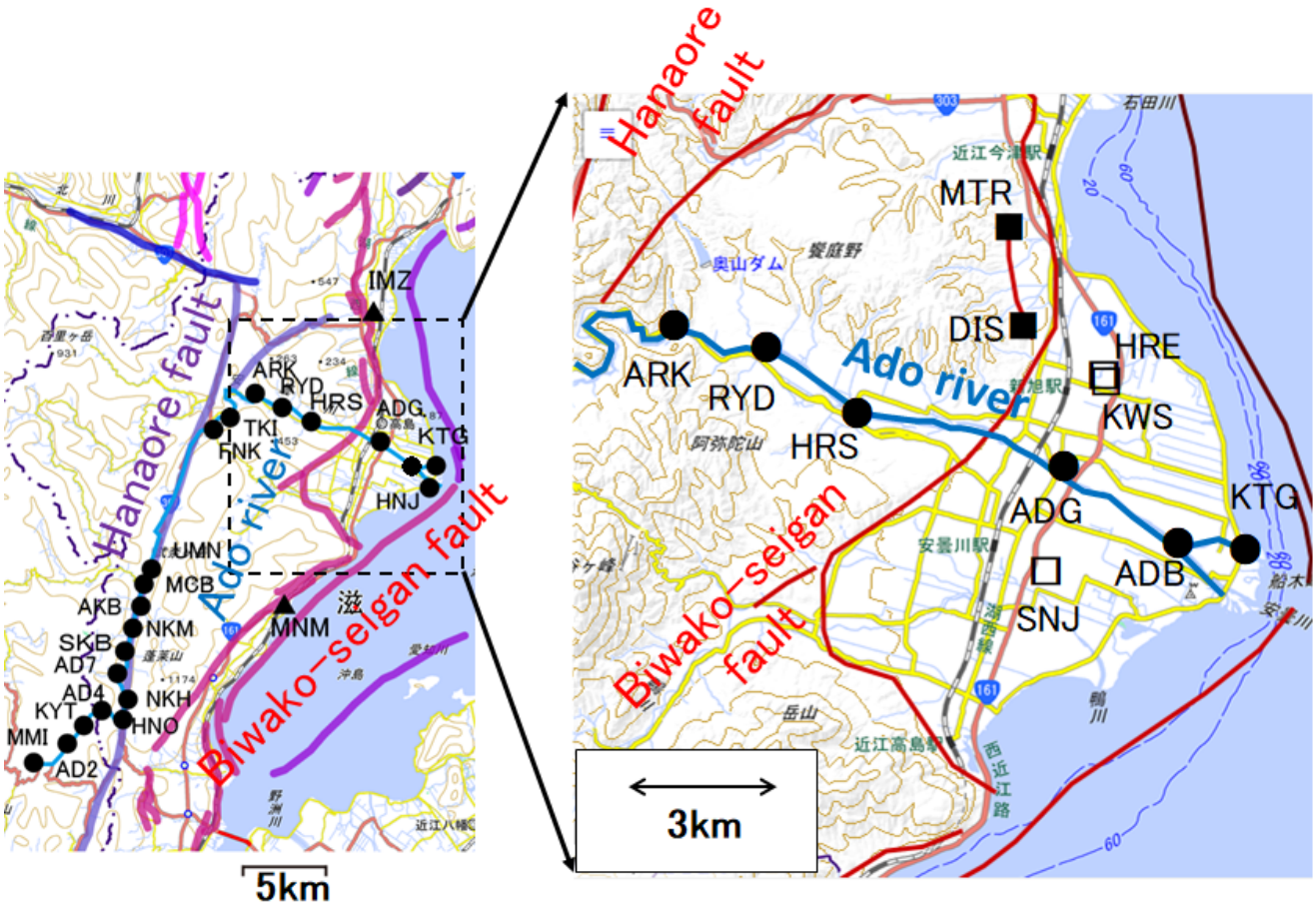

©2020. Japan Geoscience Union. All Right Reserved.

Discussion on the environment formed and maintained by active faults

*Naoji Koizumi[1]

1. School of Environmental Science,the University of Shiga Prefecture

We will discuss on the environment formed and maintained by active faults.

Keywords: Active fault, Environment, Discussion

©2020. Japan Geoscience Union. All Right Reserved.

[J] Poster | S (Solid Earth Sciences)：S-CG Complex & General

[S-CG69] Rheology, fracture and friction in Earth and planetary sciences

convener:Miki Tasaka(Shizuoka University), Osamu Kuwano(Japan Agency for Marine-Earth Science and Technology), Ichiko Shimizu(Division of Earth and Planetary Sciences, Graduate School of Science, Kyoto University), Shintaro Azuma(Department of Earth and Planetary Sciences, School of Science, Tokyo Institute of Technology)

The aim of this session is to join people from various research area in the earth and planetary sciences and to stimulate discussion beyond the boundaries of each research area. Our goal is to deepen our understanding of dynamics in geosciences by looking over whole areas in the earth and planetary sciences from the viewpoint of PHYSICS OF DEFORMATION, FLOW, AND FRACTURE. We welcome any field (e.g., earthquake, volcano, earth surface, crust, mantle and the core, and other planets and satellites) and any approach (e.g., laboratory experiments, numerical simulations, field observations, and theories).

[SCG69-P01] Deformation of dry orthoenstatite under high *P-T* conditions and its implication for the variation in strength of oceanic plates

*Yumiko Tsubokawa[1], Tomohiro Ohuchi[1], Yuji Higo[2], Yoshinori Tange[2], Tetsuo Irifune[1] (1.Ehime University Geodynamics Research Center, 2.Japan Synchrotron Radiation Research Institute)

[SCG69-P02] **Influence of hydration products on brittle deformation of olivine gabbro**

*Yuya Akamatsu[1], Ikuo Katayama[1] (1.Hiroshima University)

[SCG69-P03] Deformation experiments of chlorite at high pressures and temperatures: A preliminary study

*Sachiko Yamauchi[1], Tomoaki Kubo[2], Mori Yuichiro[2], Rei Shiraishi[3], Yuji Higo[4], Yoshinori Tange[4] (1.Department of Earth and Planetary Sciences, Graduate School of Sciences, Kyushu University, 2.Kyushu Univ., 3.Tohoku Univ., 4.JASRI)

[SCG69-P04] Dependency of crack distributions in granite on elastic velocities

Kanami Iwazaki[1], *Shinichi Uehara[1], Miki Takahashi[2], Manami Kitamura[2] (1.Faculty of Science, Toho University, 2.National Institute of Advanced Industrial Science and Technology)

[SCG69-P05] Image analysis on experimentally sheared granitic rocks: Shear zone development at brittle-ductile transition zone

*Shun Arai[1], Jun Muto[1], Takamoto Okudaira[2], Daichi Iwata[1] (1.Department of earth science, Tohoku University, 2.Department of Geosciences, Graduate School of Science, Osaka City University)

[SCG69-P06] Experimental study and numerical simulation of failure of feldspathic-mafic rocks by phase change of fluid

*Katsuya Mizuno[1], Nobuo Hirano[1], Noriyoshi Tsuchiya[1], Atsushi Okamoto[1] (1.Tohoku university)

[SCG69-P07] Continuously sheared granular matter reproduces in detail seismicity laws

*Victor Simon Levy dit Vehel[1], Sebastien Lherminier, Ramon Planet[3], Gilles Simon[1], Knut Jørgen Måløy[2], Loic Vanel[1], Osvanny Ramos[1] (1.Institut Lumiere Matiere Lyon 1, 2.University of Oslo, 3.University of Barcelona)

[SCG69-P08] Response and fracture of a viscoelastic fluid under unsteady shear rate

*Osamu Kuwano[1], Mie Ichihara[2] (1.Japan Agency for Marine-Earth Science and Technology, 2.Earthquake Research Institute, University of Tokyo)

[SCG69-P09] Evolution of size and shape distributions of comminuted particles under shear deformation

*Osamu Kuwano[1], Daisuke Sasakura[2] (1.Japan Agency for Marine-Earth Science and Technology, 2.Malvern Panalytical Japan, Div of Spectris Co., Ltd.)

[SCG69-P10] Microstructural analyses of peridotite xenoliths in Shimane prefecture ~ implications for plastic deformation during Japan Sea opening

*Miki Tasaka[1], Hiroyuki Oma[2], Shunsuke Inagawa[2] (1.Shizuoka University, 2.Shimane University)

[SCG69-P11] Structural and petrological analyses of blocky serpentinite in the Sanbagawa belt, central Shikoku, Japan: Implications for deep slow earthquakes

*Yurina Nagata[1], Kengo Kataoka[1], Ken-ichi Hirauchi[1], Katsuyoshi Michibayashi[2] (1.Department of Geosciences, Faculty of Science, Shizuoka University, 2.Department of Earth and Planetary Sciences, Graduate School of Environmental Studies, Nagoya University)

[SCG69-P12] **Relationship between stylolite and faults in chert**

*Kota Kojima[1], Jun-ichi Ando[1], Kaushik Das[1], Naotaka Tomioka[2] (1.Department of Earth and Planetary Systems Science, Hiroshima University, 2.Kochi Institute for Core Sample Research, Japan Agency for Marine-Earth Science and Technology)

[SCG69-P13] **Textural analyses for K-feldspar inclusions within a micro-shear zone developed in Teshima granite, the Ryoke metamorphic belt**

*Tae-Hoon Uhmb[1], Katsuyoshi Michibayashi[1] (1.Department of Earth and Planetary Sciences, Research group of Petrology and Mineralogy, Nagoya University)

Deformation of dry orthoenstatite under high *P-T* conditions and its implication for the variation in strength of oceanic plates

*Yumiko Tsubokawa[1], Tomohiro Ohuchi[1], Yuji Higo[2], Yoshinori Tange[2], Tetsuo Irifune[1]

1. Ehime University Geodynamics Research Center, 2. Japan Synchrotron Radiation Research Institute

The initiation of subduction is a key element to understand the evolution of terrestrial planets. Because the strength of dry olivine is too strong to allow the operation of plate tectonics (Kohlstedt et al., 1995), the reason why subduction of plates was initiated in the Earth needs to be reconsidered.We hereby experimentally evaluated the creep strength of dry orthoenstatite, which is the 2nd dominant phase in the upper mantle, at pressures of 1.4-8.1 GPa and temperatures of 1290-1470 K using a deformation DIA (D-DIA) apparatus combined with synchrotron X-ray radiation.
At a constant strain rate ranging from 6.7 $\times 10^{-6}$ to 5.2 $\times 10^{-5}$ s^{-1}, steady-state creep strength of orthoenstatite followed the power-law flow law with the stress exponent of 3.1 ±0.3. Transmission electron microscopy observations revealed developments of many dislocations and the main slip system is the [001] glide on either (100) or (010) plane. The flow law for dry orthoenstatite in this study predicts that orthoenstatite is weaker than olivine at lower temperatures due to its low activation energy. Our calculations based on the obtained flow law suggest that two dry harzburgites, which are forming a load-bearing framework of strong olivine and interconnected layers of weak orthoenstatite, give the upper and lower limits of the effective thickness of the oceanic lithosphere in the world. For the onset of plate tectonics in Archean Earth, formation of the interconnected layers of orthoenstatite could allow the initiation of the subduction.

Keywords: Orthoenstatite, Dislocation creep, Oceanic plate

©2020. Japan Geoscience Union. All Right Reserved.

Influence of hydration products on brittle deformation of olivine gabbro

*Yuya Akamatsu[1], Ikuo Katayama[1]

1. Hiroshima University

Hydration of mantle and oceanic crustal rocks plays a key role on several aspects of geodynamical process of the oceanic lithosphere, because hydration products such as serpentine have characteristic physical and mechanical properties. For instance, deformation experiments demonstrate that the small amount of serpentine reduces the strength of peridotite to that of pure serpentinite and hence can weaken the oceanic lithosphere (Escartín et al. 2001). Meanwhile, the influence of hydration on these properties of gabbroic crustal rocks is poorly understood. In this study, we carried out triaxial deformation experiments of gabbroic rocks containing partially serpentinized and/or altered olivine to understand the influence of hydration on the mechanical and physical properties of oceanic crustal rocks.

For deformation experiments, we used gabbro collected from the Oman Ophiolite. These gabbros contain small amount of olivine, where hydration products such as serpentine and chlorite are formed along grain boundaries and intragranular cracks. The experiments were conducted using the intra-vessel deformation and fluid flow apparatus at room temperature, a constant confining pressure of 20 MPa, and a constant strain rate of ~10^{-6} s^{-1}. Compressional and shear waves traveling in a direction normal to the loading axis were measured during deformation. For comparison, additional experiments were conducted using unaltered gabbroic rocks and lizardite serpentinite.

Hydrated olivine gabbros showed maximum differential stress of 200–350 MPa, which was comparable to that of lizardite serpentinite, while unaltered gabbroic rocks showed much higher maximum stress of ~600 MPa. This indicates that small amounts of serpentine and/or chlorite reduce the fracture strength of gabbro. Elastic wave velocity of hydrated olivine gabbros was nearly constant even prior to failure, suggesting that the mode of brittle deformation of these samples were not associated with development of extensile cracks that are commonly recognized in most crystalline rocks and which are responsible for dilatancy (e.g. David et al. 2018). Microstructural observation of these samples recovered after deformation demonstrated that crack damage was limited to the immediate vicinity of the fracture zones, while the regions apart from the shear zones remained nominally undeformed and hence indistinguishable from the starting materials. By combining these data, the fracture strength of gabbro can be weakened by the small amounts of hydration products such as serpentine and chlorite, because the deformation is accommodated primarily by these mechanically weak phyllosilicate minerals (Escartín et al. 1997, Moore & Lockner 2004). Since these hydration minerals are commonly recognized in gabbroic crustal rocks at the various tectonic settings, including mid-ocean ridges and subducting oceanic plates, hydration of gabbro can weaken the oceanic crust and promote further deformation in such regions.

Keywords: Gabbro, Hydrothermal alteration, Brittle deformation, Elastic wave velocity, Serpentine, Chlorite

©2020. Japan Geoscience Union. All Right Reserved.

Deformation experiments of chlorite at high pressures and temperatures: A preliminary study

*Sachiko Yamauchi[1], Tomoaki Kubo[2], Mori Yuichiro[2], Rei Shiraishi[3], Yuji Higo[4], Yoshinori Tange[4]

1. Department of Earth and Planetary Sciences, Graduate School of Sciences, Kyushu University, 2. Kyushu Univ., 3. Tohoku Univ., 4. JASRI

Intermediate-depth earthquakes (IDEQs) occur within subducting oceanic plates at depths of about 60-300 km beyond the brittle-plastic transition. Dehydration embrittlement of serpentine (antigorite) has been considered as one of possible mechanisms for generating IDEQs, however previous studies have not provided sufficient experimental evidences especially at higher pressures than 3.5 GPa (~100km depth) (e.g., Ferrand et al., 2017; Gasc et al., 2017; Ikehara et al., JPGU2019). According to the thermal-petrologic model by Hacker et al. (2003), IDEQs seem to be distributed beyond the dehydration region of serpentine over the stability field of chlorite that dehydrates at higher temperatures. Therefore, the deformation behavior of chlorite might be related to the occurrence of IDEQs. Chlorite has 4 kinds of polytype, I*a*, I*b* (β=90˚), I*b* (β=97˚) and II*b*, and causes discontinuous structural change in the stacking (c-axis) direction during compression at room temperature. (Welch et al., 2004, 2005). For example, the d-value of the c-plane decreases discontinuously at ~6-7 GPa in I*a*, and ~9-10 GPa in II*b*, respectively. The former is accompanied by polytype change to I*b*. Acoustic emission (AE) associated with this structural change was also detected at room temperature (Dobson et al., 2007). However, deformation behaviors in chlorite has not been studied at high pressures and temperatures. In this study, we carried out deformation experiments of chlorite at the P-T conditions under which IDEQs occur, in order to investigate the relationship between the structural change and shear instability.

Uniaxial deformation experiments were conducted at 5 GPa, 230-800℃ using Deformation-DIA apparatuses at SPring-8 (BL04B1). Monochromatic X-rays (60 keV) were used as an incident beam to observe compression behavior, dehydration reaction, and deformation behaviors with recording AEs. The starting material is natural clinochlore from Brazil. We put a powder and a stacking of disk-shaped single crystals (c plane is perpendicular to the compression axis) in tandem in a hBN capsule. Au foils are placed at the upper and lower edges of the sample as a strain marker. Deformation experiments were carried out with a constant anvil displacement rate of 200 μm/h and a temperature ramping rate of 0.1K/s.

In the experiment at 5 GPa, the d_{004} spacing in clinochlore decreased during compression at room temperature and increased with heating. It decreased when the deformation started at 230℃, then increased again above ~500℃. Both powdered and single-crystal samples exhibited similar changes in values of d_{004}. AEs were detected during cold compression, heating, and deformation, whereas no AEs were observed above ~400℃ including during dehydration. These AE activities may be related to the changes in the d_{004} spacing, although we did not observe the abrupt changes implying the structural transition. The strain rate and the final strain in the powdered sample (7.2e-5/s and 37%) were about 8-9 times larger than those of the disk-shaped single crystal sample (8.5e-6/s and 5%), suggesting the large difference in the deformation mechanism during the uniaxial compression. This may also cause the difference in AE activities, which will be discussed after the quantitative determination of AE locations. We are also planning to conduct shear deformation experiments, in which the c-plane of clinochlore is parallel to the shear plane, to investigate deformation-induced structural changes in the stacking layer and shear instability.

©2020. Japan Geoscience Union. All Right Reserved.

Keywords: chlorite, high pressure, shear instability, intermediate-depth earthquakes

©2020. Japan Geoscience Union. All Right Reserved.

Dependency of crack distributions in granite on elastic velocities

Kanami Iwazaki[1], *Shinichi Uehara[1], Miki Takahashi[2], Manami Kitamura[2]

1. Faculty of Science, Toho University, 2. National Institute of Advanced Industrial Science and Technology

Technologies relating to enhanced geothermal systems (EGS) have recently been developed, such as hot rock geothermal power generation in ductile deformation regime, or supercritical geothermal power generation. In these systems, it is planned to create artificially fractured geothermal reservoirs by injecting water into hot rock mass and cooling it. Properties of crack distributions caused by cooling rocks are still not clear. To estimate non-destructively induced fracture distributions at the EGS development, it should be useful to investigate the relationship between elastic wave transmission properties and properties of crack distribution in rock.

In this study, we generate cracks in granite specimens by heating them up to 550℃ or 650℃ then rapidly cooling with ice water, and we clarified the relationship among the crack distribution, porosity and elastic wave transmission properties. Cylindrical specimens (25 mm in the diameter and 30 mm in the length) of granite from Oshima, Ehime Prefecture (initial porosity: 0.46±0.02 %, P and S wave velocity (V_P, V_S) under water saturated condition: 6.12±0.06, 3.17±0.10 km/s, respectively), and granite from Inada, Ibaraki (initial porosity: 0.68±0.02 %, V_P, V_S under water saturated condition: 6.06±0.04, 3.07±0.09 km/s, respectively) were used for the experiments. Average mineral size of Inada granite is larger than Ohshima granite. We operated experiments to transmit P and S wave through the granite specimens which is dry or saturated with water, under atmospheric pressure.

Porosity is increased as a heating temperature is increased. Porosity of Inada granite is approximately 1.3 to 1.5 times larger than that of Ohshima granite for intact and heated rocks. There is no clear difference on the relationship between porosity and V_P, V_S between Inada and Ohshima granite. V_P and V_S are negatively correlated with porosity: in the case of water saturated specimens, as porosity is increased from 0.4% to 4.3%, V_P and V_S is decreased approximately 32% and 55%, respectively. We are planning to evaluate crack distributions in the specimens, and investigate the relationship between the crack distribution and the measurement results.

Keywords: elastic wave velocity, granite, laboratory experiment, cracked rock

©2020. Japan Geoscience Union. All Right Reserved.

Image analysis on experimentally sheared granitic rocks: Shear zone development at brittle-ductile transition zone

*Shun Arai[1], Jun Muto[1], Takamoto Okudaira[2], Daichi Iwata[1]

1. Department of earth science, Tohoku University, 2. Department of Geosciences, Graduate School of Science, Osaka City University

Despite numerous experimental studies focusing on crustal rheology within the transition from brittle to semi-brittle (e.g., Bos and Spiers, 2002; Pec et al., 2012) and fully ductile (Holyoke and Tullis, 2006) regimes, associated with microstructural development including strain partitioning remain poorly understood. We report the results of Griggs-type solid medium deformation experiments using gneiss (Gneiss Minuti, the same material used in Holyoke and Tullis, 2006) composed of 20 ~ 30% quartz, 40 ~ 50% plagioclase, and 20 ~ 40% micas. Samples of ~1.2 mm in thickness are cut into halves in a direction normal to shear direction, after which a strip of Ni is inserted to serve as an in-situ strain marker. At temperature of 800˚C, strain rate of 2 x 10^{-5} s^{-1}, and confining pressure of 1.5 GPa, the peak strength measured 700 ~ 800 MPa at bulk shear strains (γ ≈1.0). The strength monotonously decreased towards 200 MPa, however steady-state flow was not achieved even for bulk γ≈7.2. Electron dispersive spectroscopy in a scanning electron microscope (SEM-EDS) revealed that the sample deformed to bulk γ ≈7.2 developed several narrow shear bands. The shear bands are oriented oblique (20 ~ 30˚) to the shear direction. Using the in-situ strain marker, the strain away from the shear zone is measured to be γ ~ 1.1, while the most of deformation is localized as slip along the shear bands. We analyzed back scattered electron (BSE) images of starting material and sheared samples (γ = 1.4 ~ 7.2) with the software “ImageJ” to analyze their microstructures. Analysis on quartz and biotite revealed the aspect ratio of grains increases, while the cross-sectional area of grains decreases with increase in shear strain. Most of grains are rotated toward shear direction, and the proportion of grains oriented to S-plane increases at high strain. Those microstructural characteristics indicate that grain size reduction and grain rotation progress in the host rock (outside of shear zone) by γ ~ 1.1, then the localized slip along the shear zone becomes dominant at higher strain. In the presentation, we will also report the deformation mechanism of each minerals as a function of strain.

Keywords: Brittle-ductile transition zone, Griggs-type apparatus, Granitic rocks, Shear zone, Image analysis

©2020. Japan Geoscience Union. All Right Reserved.

Experimental study and numerical simulation of failure of feldspathic-mafic rocks by phase change of fluid

*Katsuya Mizuno[1], Nobuo Hirano[1], Noriyoshi Tsuchiya[1], Atsushi Okamoto[1]

1. Tohoku university

BDT (Brittle-Ductile Transition) is the boundary transition of crustal rocks from brittle to ductile. We had thought that especially the BDT of granite is the limit of geothermal developments because granite is one of the most common rocks in the upper crust and the permeability of rocks reduces significantly in the area deeper than BDT of granite. However, recent studies have revealed that geothermal development could be expected even there in that situations. For example, Watanabe et al. (2017) reported that the potentially available resources may exists in the ductile area of granitic rocks at temperature from 375℃ to approximately 460℃. Therefore, we need to think the way to generate the fracture network at that area. For that, we focused on the rock fracturing by the phase change of fluid by rapid decompression of high temperature and high pressure fluid. In this method, we use thermal shock occurred by cooling that caused by fluid decompression. Previous our studies have revealed that quartz was the important factor to make rock more permeable by fracturing because quartz tended to make cracks at the grain boundaries between other minerals and itself due to low thermal expansion coefficient. However, it was unrevealed if cracks will be generated with no quartz.

In this study, we conducted rapid decompression experiments for three times to gabbro, which is common rock in the lower crust and has no quartz, and compared permeability and porosity with those of granite conducted same experiments in the same situation and equation of granite’s permeability and porosity from Watanabe et al. (2017). Moreover, we observed samples after experiments by X-ray CT and SEM. As a result, we found that cracks in gabbro was smaller and less permeable than those in granite. We also conducted numerical simulation using FEM (Finite Element Method) to reveal where stress concentrates during fracturing. We found that stress concentrates at the grain boundaries of ilmenite and other minerals in gabbro, similar to quartz of simulation result of granite.

References

Watanabe et al., 2017. Nature Geoscience 10, 140-144

Keywords: rapid decompression, gabbro, crack, permeability, FEM

©2020. Japan Geoscience Union. All Right Reserved.

Continuously sheared granular matter reproduces in detail seismicity laws

*Victor Simon Levy dit Vehel[1], Sebastien Lherminier, Ramon Planet[3], Gilles Simon[1], Knut Jørgen Måløy[2], Loic Vanel[1], Osvanny Ramos[1]

1. Institut Lumiere Matiere Lyon 1, 2. University of Oslo, 3. University of Barcelona

Earthquake forecast has long been an objective for geoscience, resisting scientific efforts for more than a century. This difficulty stems in part from the very large spectrum of time and energy scales, a feature required of physics-earthquake analogies [1], as well as the complexity of the system producing earthquakes. Efforts to model this phenomenon might aim to reduce the complexity of the mechanisms while preserving the richness of the dynamics. Simple model have been proposed (friction of blocs, granular shearing) with some success over the years, replicating a few features of earthquakes. We propose a continuously sheared granular experiment [1] that marginally increase system complexity (in regard to prior experiments) while achieving quantitative agreements with several key features of earthquake statistics (Gutenberg-Richter law, Omori law, inter-event time distribution [2]). Furthermore, recent upgrades in our setup allows us to track every grain and contact force (through photo-elasticity) as well as the global dilation of the granular medium [3]. We welcome any insight or discussion about analysis and interpretation of the vast amounts of data produced by our experiment.

[1] S. Lherminier, R. Planet, V. Levy dit vehel, G. Simon, K. J. Måløy, L. Vanel & O.Ramos : Continuously sheared granular matter reproduces in detail seismicity laws, Phys. Rev. Lett. 122, 218501 (2019)

[2] A Corral : Long-term clustering, scaling, and universality in the temporal occurrence of earthquakes, Phys. Rev. Lett. 92, 108501 (2004)

[3] V. Levy dit Vehel, F. Dubourg, L. Vanel, K. J. Måløy, & O.Ramos : Evolution of the distance between plates in an experimental granular fault. Implications for earthquake forecast, RNL 2018 proceedings (2018)

Keywords: Earthquake, Shearing, Granular matter, Dilation

©2020. Japan Geoscience Union. All Right Reserved.

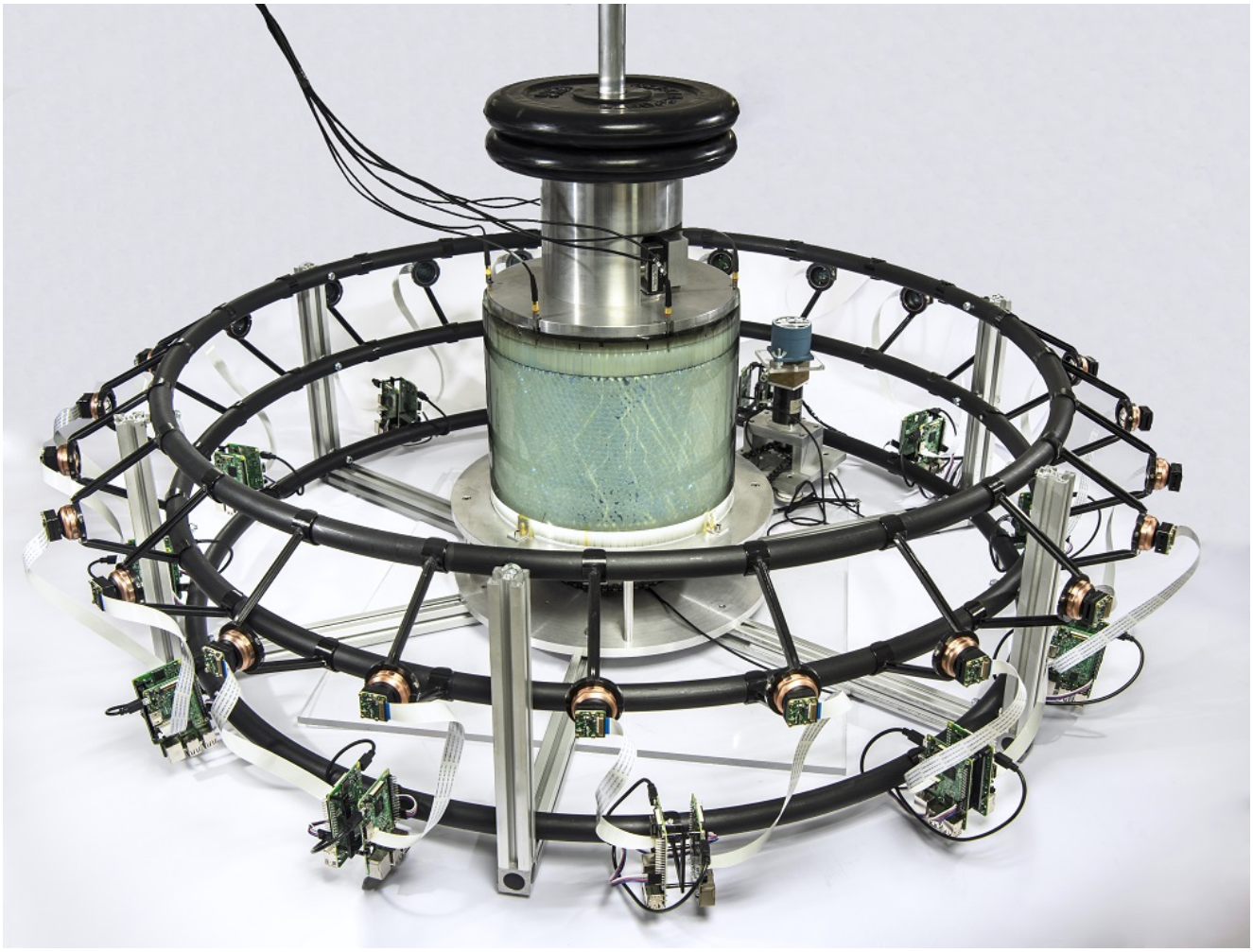

©2020. Japan Geoscience Union. All Right Reserved.

Response and fracture of a viscoelastic fluid under unsteady shear rate

*Osamu Kuwano[1], Mie Ichihara[2]

1. Japan Agency for Marine-Earth Science and Technology, 2. Earthquake Research Institute, University of Tokyo

The transition from flow to brittle fracture (e.g., magma fragmentation in volcanic eruption) is an important and unsolved phenomenon in the modeling of solid earth phenomena. Recently, in the field of soft matter physics, research on the fracture of the complex fluid has been rapidly progressing by new experimental results (e.g., Tabuteau et al., 2011, Soft Matt.). It is pointed out that the viscoelastic properties obtained from conventional measurement (viscosity under steady flow and viscoelastic response under small-amplitude oscillation) cannot express the deformation behavior from the flow to the fracture (Arora et al., 2017, J. Rheol.), because of a remarkably unsteady and large deformation.
We focused on the transition from flow to brittle fracture of the viscoelastic material and changes in physical properties due to an increase in the deformation rate, and started the experiment using soft matter in which viscoelastic effect is easy to measure.
As a viscoelastic test material, we synthesized a gel crosslinking a CpCl microemulsion with polyethylene glycol (Filali et al., 1999, JPhysChem, Ishikawa et al., 2019, JPS abst.). After viscoelastic measurements on a cone plate with a diameter of 25 mm using a rotary rheometer, shear tests were conducted with gradually increasing shear rates at given acceleration (0.1, 1, 10, 100 s^{-2}). In this presentation, we will report the response at each shear acceleration in comparison with the solution for the linear Maxwell fluid. We will also introduce the photoelastic visualization of fracture.

©2020. Japan Geoscience Union. All Right Reserved.

Evolution of size and shape distributions of comminuted particles under shear deformation

*Osamu Kuwano[1], Daisuke Sasakura[2]

1. Japan Agency for Marine-Earth Science and Technology, 2. Malvern Panalytical Japan, Div of Spectris Co., Ltd.

A faults zone contains fine rock powders called gouge that have been ground up by past fault motions. Particle size distribution and particle shape of gouge particles affect the frictional properties of the fault and reflect the comminution process by the past fault motions. It is well known that particle size distribution of fault gouge show power-law distributions. Exponent of this power law is considered to reflect the style and degree of deformation. We did several shear experiments using a rotary shear apparatus with the shear displacement ranges from 10mm to 1m. In this presentation, we will discuss about the relationship between the particle size distribution and the degree of comminution of model particles by particle image analysis.

©2020. Japan Geoscience Union. All Right Reserved.

Microstructural analyses of peridotite xenoliths in Shimane prefecture ~ implications for plastic deformation during Japan Sea opening

*Miki Tasaka[1], Hiroyuki Oma[2], Shunsuke Inagawa[2]

1. Shizuoka University, 2. Shimane University

A number of Cenozoic ultramafic xenoliths are located on the southwest Japan arc. In this study, we conducted microstructural analyses using peridotite xenoliths in Noyama-dake and Kawashimo, Shimane prefecture. The microstructural results imply that these textures are formed by plastic deformation during Japan Sea opening (~15 Ma) with various stress conditions before volcanic eruption (~7 Ma).

The microstructure of peridotites is classified into 2 types, including (1) coarse-grained equigranular texture (~ 1mm), (2) large- and fine-grained combined texture. Based on electron backscattered diffraction (EBSD) analysis, the olivine crystals in (1) coarse-grained equigranular texture have a crystallographic preferred orientation (CPO) with (010)[100] slip systems, indicating plastic deformation during mantle flow. In (2) large- and fine-grained combined texture, large grains have kink band with slip direction (001)[100] or (100)[001]. Further nine-grained aggregates have similar CPOs indicating the fine grains are recrystallized by one large grain.

Based on electron probe micro analyzer (EPMA), both (1) coarse-grained equigranular texture and (2) large- and fine-grained combined texture have origin of residual mantle. Two pyroxene geothermometer (Wells, 1977) indicates that the rock has equilibrium temperature T ~ 1200C, resulting from high temperature at the pressure of spinel stability field (P ~ 1 to 2 GPa). Based on these results, we will discuss the deformation history of the ultramafic xenoliths.

Keywords: ultramafic xenoliths, EBSD, Japan Sea opening

©2020. Japan Geoscience Union. All Right Reserved.

Structural and petrological analyses of blocky serpentinite in the Sanbagawa belt, central Shikoku, Japan: Implications for deep slow earthquakes

*Yurina Nagata[1], Kengo Kataoka[1], Ken-ichi Hirauchi[1], Katsuyoshi Michibayashi[2]

1. Department of Geosciences, Faculty of Science, Shizuoka University, 2. Department of Earth and Planetary Sciences, Graduate School of Environmental Studies, Nagoya University

In southwestern Japan, deep slow earthquakes such as tectonic tremor and slow slip events occur along a plate interface near the tip of the mantle wedge. In order to understand the relationship between deep slow earthquakes and deformation of mantle-wedge serpentinites, we perform structural and petrological analyses of a paleo-mantle-wedge serpentinite body in the Sanbagawa belt, central Shikoku, Japan. The serpentinite body examined was formed at pressure and temperature conditions corresponding to source areas of deep slow earthquakes. The serpentinite exhibits a block-in-matrix structure, formed by open and shear cracking under differential stress conditions. Block size distribution analysis yields fractal dimensions (D=1.3~6.5), indicating that the cracking occurs at various length scales. Antigorite aggregates in the matrix are coarse grained, formed through dissolution and precipitation of antigorite in the blocks. In addition, antigorite aggregates along localized shear planes deform by dislocation creep with a slip system of [010](001). Strength profiles along a subduction plate interface at southwestern Japan, obtained using friction and flow laws of antigorite, indicate these cracking occurs only at near-lithostatic and supra-lithostatic fluid pressures. We therefore suggest that episodic tremor and slip is caused by open and shear cracking following a localized plastic (viscous) deformation in the serpentinized mantle wedge, which is linked with perturbations in fluid pressure.

Keywords: serpentinite, slow earthquake, mantle wedge, Sanbagawa belt, fractal analysis

©2020. Japan Geoscience Union. All Right Reserved.

Relationship between stylolite and faults in chert

*Kota Kojima[1], Jun-ichi Ando[1], Kaushik Das[1], Naotaka Tomioka[2]

1. Department of Earth and Planetary Systems Science, Hiroshima University, 2. Kochi Institute for Core Sample Research, Japan Agency for Marine-Earth Science and Technology

Stylolite is a structure developed mainly in cherts and limestones, which are the main constituent rocks of accretionary complex. Moreover, pressure solution being the formation process of stylolite, is an important plastic deformation mechanism that lowers the crustal strength. In this study, we verified that stylolite develops in the chert block, could act as a weak surface leading to fault formation, through both field and microstructural observations.

Our results suggest that 1) that the fault was formed after stylolite was created, and 2) that the strike and dip of fault are almost same as those of stylolite planes. In other words, it is strongly suggested that stylolite could act as a weak surface leading to fault formation.

Keywords: stylolite, illite, smectite, pressure solution, slickenside

©2020. Japan Geoscience Union. All Right Reserved.

Textural analyses for K-feldspar inclusions within a micro-shear zone developed in Teshima granite, the Ryoke metamorphic belt

*Tae-Hoon Uhmb[1], Katsuyoshi Michibayashi[1]

1. Department of Earth and Planetary Sciences, Research group of Petrology and Mineralogy, Nagoya University

The shape change rate of an inclusion grain is controlled by the rounding process resulting from both interfacial tension and diffusion creep caused by differential stress (Toriumi, 1987). Okamoto and Michibayashi (2005) presented a numerical model which explained the shape change rate of a garnet inclusion within a quartz host grain in accordance with deformation conditions such as differential stress and deformation time. In this study, we determined estimate deformation conditions for a micro-shear zone developed in Teshima granite in the Ryoke metamorphic belt. The sample is a biotite granite which is composed of quartz, K-feldspar, plagioclase and biotite with minor muscovite, containing a micro-shear zone with a few centimeters of width. Foliations are defined by shape preferred orientations of minerals such as biotite. The foliations show gradual change from higher angle to lower angle toward the micro-shear zone in several centimeters as decreasing grain sizes of individual minerals. K-feldspar inclusions occur within quartz host grains. We divided thin section of this sample into five domains based on the distance from the micro-shear zone and measure shape factors of K-feldspar inclusions such as grain size (R) and aspect ratio (L) in each domain. Grain sizes of K-feldspar inclusions range from 1 to 100 μm and aspect ratios vary regardless of their grain sizes. We compare the measured L-R distribution patters with those calculated for K-feldspar inclusions following to Okamoto and Michibayashi (2005) and discuss deformation conditions for the micro-shear zone.

Keywords: Teshima granite, Micro-shear zone, K-feldspar inclusions, Textural analyses

©2020. Japan Geoscience Union. All Right Reserved.

[J] Poster | S (Solid Earth Sciences)：S-CG Complex & General

[S-CG70] Reducing risks from earthquakes, tsunamis & volcanoes: new applications of realtime geophysical data

convener:Masashi Ogiso(Meteorological Research Institute, Japan Meteorological Agency), Masumi Yamada(Disaster Prevention Research Institute, Kyoto University), Naotaka YAMAMOTO CHIKASADA(National Research Institute for Earth Science and Disaster Resilience), Yusaku Ohta(Research Center for Prediction of Earthquakes and Volcanic Eruptions, Graduate School of Science, Tohoku University)

As the number of population centers grows in regions with earthquake, tsunami and volcano hazards, the importance of improving methods for rapid, realtime estimates of activity increases. Realtime monitoring, analysis, and prediction of seismic ground motion, crustal movement and tsunami will be powerful tools to contribute to earthquake and tsunami disaster preparedness/mitigation. Tsunami and Earthquake Early Warning systems exist today in many locations around the world. Now JMA has started to promptly provide Eruption Notices to inform people of impending and beginning volcanic eruptions. Large events like the 2011 Tohoku Earthquake (Mw9.0) have demonstrated some of the shortcomings of existing techniques. In this session, we invite presentations on new ideas, methods and applications of (near) realtime analysis of seismic, geodetic and tsunami data, to the problem of realtime prediction aimed at improving disaster preparedness/mitigation in the fields of earthquake, tsunami and volcano observation. Presentation is encouraged to bring together scientists, engineers, and practitioners from a broad range of backgrounds from around the world, and to promote collaborative communication at the leading edge of the science and technologies.

[SCG70-P01] Estimation of seismic energy sources inferred from Source-Scanning-Algorithm method: Case of the 2018 M6.6 Hokkaido Eastern Iburi Earthquake and the 2019 M6.7 Yamagata-Oki Earthquake

*Mugi Yamamoto[1], Ken Moriwaki[1] (1.Japan Meteorological Agency)

[SCG70-P02] Development of the parallelized code of the numerical shake prediction scheme

*Masashi Ogiso[1] (1.Meteorological Research Institute, Japan Meteorological Agency)

[SCG70-P03] Development of the spatial information data base using building damage of the 2019 Yamagata offshore earthquake

*Shohei Naito[1], Hiromitsu Nakamura[1], Hiroyuki Fujiwara[1], naokazu momma[2], Tetsuya Yamada[2] (1.National Research Institute for Earth Science and Disaster Resilience, 2.PASCO Corporation)

[SCG70-P04] Cluster analysis of tsunami inundation distribution for improvement of tsunami early prediction

*Masato Kamiya[1], Toshitaka Baba[1] (1.Tokushima University)

[SCG70-P05] Long-term evaluation of S-net pressure data for real-time tsunami forecasting

*Naotaka YAMAMOTO CHIKASADA[1], Tatsuya Kubota[1] (1.National Research Institute for Earth Science and Disaster Resilience)

[SCG70-P06] Real–time uncertainties evaluation of coseismic fault models and Tsunami inundation deduced from GNSS observations

Keitaro Ohno[1], *Yusaku Ohta[1] (1.Research Center for Prediction of Earthquakes and Volcanic Eruptions, Graduate School of Science, Tohoku University)

Estimation of seismic energy sources inferred from Source-Scanning-Algorithm method: Case of the 2018 M6.6 Hokkaido Eastern Iburi Earthquake and the 2019 M6.7 Yamagata-Oki Earthquake

*Mugi Yamamoto[1], Ken Moriwaki[1]

1. Japan Meteorological Agency

The Source-Scanning-Algorithm(SSA) has been reported to be an effective method for imaging the distribution of seismic energy sources in time and space (e.g. Kao et al., 2004). SSA calculates the Brightness(Br) value by adding the absolute values of the waveform amplitudes from stations at respective theoretical arrival times, and the distribution of seismic energy sources is identified by the maximum of the Br value. As this approach does not require the knowledge of the actual fault plane, we can see the source distribution immediately.
In this study, we determined the energy source distribution of two significant earthquakes. One is the 2018 M6.6 Hokkaido Eastern Iburi Earthquake and another is the 2019 M6.7 Yamagata-Oki Earthquake. In our analysis, we use waveform data of strong-motion stations (JMA, K-NET, KiK-net and Local government sites) whose epicenter distances are within a certain range so that the respective lengths of one period of all waveforms are about the same. We used the waveforms of the P waves for summing, and then bandpass-filtered from 4.0 to 20.0 Hz to remove low-frequency noise. The grid point whose interval is 1km, are placed around the epicenter. The travel-times of P waves from all grid points to all stations are calculated using JMA2001(Ueno et al.,2001). Finally all Br values are calculated for each grid point by 0.01 sec sampling interval.
The results were compared with the source process determined by JMA to ensure appropriate features of the fault movements. In the case of the 2018 M6.6 Hokkaido Eastern Iburi Earthquake, the maximum of Br value has two peaks both in time and space. At about 1 to 2 sec after the origin time(OT) the distribution of the high Br value is near the epicenter determined by JMA, and then the Br value attenuates, and rises again at about 6 to 8 sec. Although the region with a high Br value has a difference of several km from the one with a large moment release by the source process analysis, two peak times are almost the same. In another case, that is the 2019 Yamagata-Oki Earthquake, at about 4 to 6 sec after OT the distribution of high Br value extends about 8km from the epicenter to the west-northwest. The region of high Br value and the large moment release region almost match although two peak times have a slight difference.
We also used resolution test to ensure spatial and temporal accuracy of an imagining obtained by SSA. Assuming that several test waveforms were emitted from the epicenters (virtually located around the epicenter) and observed at the stations which were used in the actual analysis at the time based on theoretical travel-time, we compared the distribution of the high Br value and the location of the hypocenters. In either case the two positions almost matched.

©2020. Japan Geoscience Union. All Right Reserved.

Development of the parallelized code of the numerical shake prediction scheme

*Masashi Ogiso[1]

1. Meteorological Research Institute, Japan Meteorological Agency

In most of the currently operational real-time ground motion prediction systems, prediction strategy using hypocentral information (location and magnitude) is widely adopted. From the viewpoint of robust prediction, a prediction framework without hypocentral information is required because sometimes the estimation of hypocentral information may be failed. The numerical shake prediction scheme proposed by Hoshiba and Aoki (2015) is one approach to predict ground motion without source parameters. One problem in the numerical shake prediction scheme is a calculation load. To implement the scheme in an operational system, a fast and efficient calculation code is required. Hence, we have begun to develop a parallelized calculation code of the scheme. We use Fortran 90 and OpenMPI.

The numerical shake prediction scheme of Hoshiba and Aoki (2015) consists of two parts: one is the estimation of current seismic energy distribution using data assimilation technique, and the other is the calculation of future seismogram based on a radiative transfer theory. In the estimation of current energy distribution, optimal interpolation is adopted, which is represented as a matrix calculation. In the prediction stage, a Monte Carlo simulation is used because of its flexibility. There are two ways in parallelization strategy. The one is the regional parallelization, which means that the target region is divided into many subregions and each MPI subprocess is assigned to each subregion. The other is the parallelization over particles in a Monte Carlo simulation. The regional parallelization is preferable in a highly parallelized environment, however, it requires some ingenuity to keep consistency with adjacent regions. Calculation time would reach the limit as the number of MPI subprocesses increases in the parallelization over particles, however, it is easier to make a code than the regional parallelization.

When we measure the calculation time of the prototype code, not only the part of the Monte Carlo simulation but also other parts such as communication using MPI functions and initializing arrays contribute the calculation time. To reduce the calculation time in the Monte Carlo simulation, hybrid parallelization using OpenMP would be effective. In the hotspots of communication and array initialization, calculation time would be reduced by minimizing the amount of communication and array size.

Keywords: Real-time ground motion prediction, Parallelized computing

©2020. Japan Geoscience Union. All Right Reserved.

Development of the spatial information data base using building damage of the 2019 Yamagata offshore earthquake

*Shohei Naito[1], Hiromitsu Nakamura[1], Hiroyuki Fujiwara[1], naokazu momma[2], Tetsuya Yamada[2]

1. National Research Institute for Earth Science and Disaster Resilience, 2. PASCO Corporation

Understanding a spatial distribution of damaged buildings caused by an earthquake is important for modeling a relationship of seismic motion and building damages. Furthermore, an accumulation of a building damage inspection result contributes to development of the elaborate damage function, and the real-time damage estimation system based on damage functions is effective both for supporting a decision-making of the disaster response and the contribution for early recovery of infrastructures (Fujiwara et al., 2019).

To this end, we formerly acquired plural building damage inspection results performed by municipalities for the purpose of certification of disaster victims, targeting severely damaged earthquakes such as the 2004 Chuetsu, 2007 Chuetsu offshore, 2008 Iwate-Miyagi, 2011 off the Pacific coast of Tohoku, and 2016 Kumamoto. By using these data, we constructed the spatial information data base with a resolution of 250-meter square meshes, then based on these data base, we developed damage functions of collapsed buildings which are separated from each 2 types of structures and ages (Monma et al, 2018).

These damage functions are available for prediction of the collapsed buildings affected by a severely earthquake corresponding to the seismic intensity 6+ or 7 which is defined by the Japan Meteorological Agency. However, the damage function which is applicable for a partially or moderate damage is also expected to beneficial for disaster responses, because frequency of not so fatal earthquake corresponding to intensity 5+ or 6- is higher.

In this study, we constructed the spatial information database of the 2019 Yamagata offshore earthquake (magnitude 6.7) which occurred at 22:22 of June 18, by using the field inspection results performed by municipalities. The area of this study consists of the Murakami city where intensity 6+ was observed, and the Tsuruoka city where intensity 6- was observed.

Furthermore, we extracted roofs covered by blue plastic sheets using post-earthquake images of 1.5m per pixel resolution taken at July 3 acquired by the SPOT7 satellite, and the ArcGIS is used for automatic image classification. The study area covers the comparatively major damaged districts such as Huya, Gatsugi, Koiwagawa, Ohiwagawa, Nezumigaseki, and Atsumi distirict. We used these extraction results for comparing damage degree of each district.

Additionally, we are going to extract more than partially damaged buildings from the former developed spatial information database, and develop a model between the earthquake motion and the building damage. Moreover, we are going to compare damages of the Yamagata offshore earthquake and the other earthquake, then consider characteristics of each earthquake.

Reference)

©2020. Japan Geoscience Union. All Right Reserved.

H.Fujiwara, H.Nakamura, S.Senna, H.Otani, N.Tomii, K.Ohtake, T.Mori, and S.Kataoka : Development of a real-time damage estimation system, Journal of Disaster Research, Vol.14, No.2, pp.315-332, 2019.

N.Monma, H.Nakamura, H.Fujiwara, S.Naito, H.Shimomura, and T.Yamada : Construction of earthquake building damage information space database and examination of building damage curve, The 15th Japan earthquake engineering symposium, PS1-01-33, December 6-8, 2018, Sendai.

Keywords: Building damage, Damage estimation, Damage function, Spatial information, GIS, Remote sensing

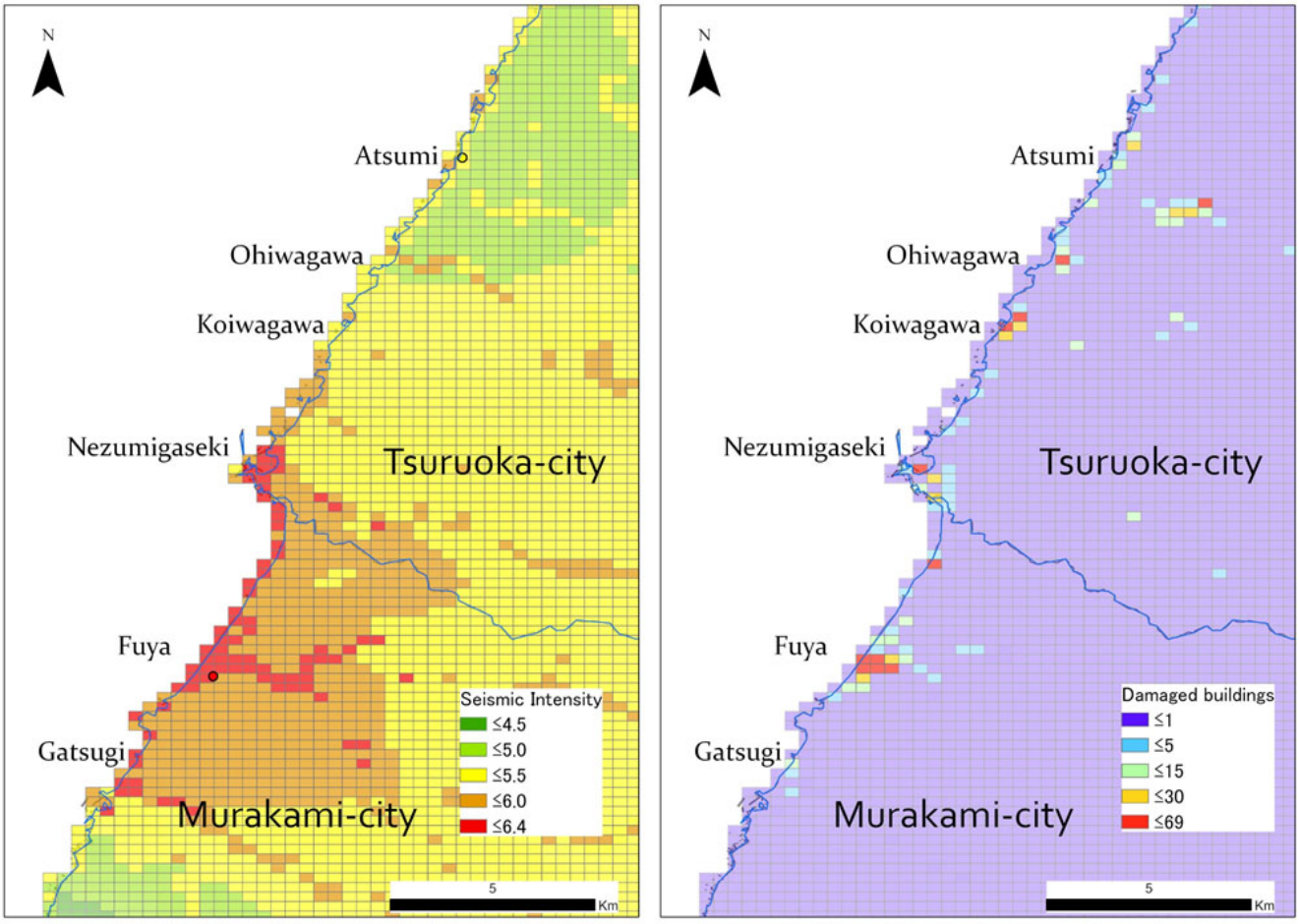

©2020. Japan Geoscience Union. All Right Reserved.

Cluster analysis of tsunami inundation distribution for improvement of tsunami early prediction

*Masato Kamiya[1], Toshitaka Baba[1]

1. Tokushima University

Offshore tsunamis can be observed before arrival at the coast using seafloor pressure gauges or GPS wave meters in Japan. The use of these data with well-known Green's law can predict the height of the tsunami at the coast. Similar methods based on the regression of a large number of simulated tsunami results were proposed by Baba et al. (2014) and Yoshikawa et al. (2019). These models are simple but very practical in use because of good accuracy and short processing time. However, the regression models only predict the height at one point on the shore, while disaster prevention offices in charge of emergency operations after tsunami disaster need the information on the distribution of tsunami inundation. To extend the regression models to estimate the tsunami inundation distribution, we may be able to repeat regression analysis for enormous forecast points. But the processing time becomes longer. As a solution, we attempted to reduce the number of forecast points by pre-grouping areas where the tsunami inundation depths are always similar. Therefore, we applied clustering methods to make the pre-grouping area using tsunami inundation datasets.
In this study, we used the k-means method, which is a typical model of the non-hierarchical method of clustering analysis. The analysis area was near Anan City, Tokushima Prefecture. The tsunami inundation database used in the cluster analysis was created by Takeda (2019), which stores the tsunami calculation results in Tokushima Prefecture from 3967 fault models (M7-9) of the Nankai Trough earthquakes (Hirata et al., 2017). We selected the 18 earthquakes yielding particularly large inundation from the tsunami database. Also, we analyzed 11 cases of tsunami models proposed by the Cabinet Office, which are widely known as the Nankai Trough earthquake scenarios. It is noted that the k-means method requires the analyst to determine the number of clusters in advance. This would cause arbitrariness. Therefore, the x-means method (Ishioka, 2000) which automatically determines the number of clusters was also used.
As a result, the studied area was divided into 10 clusters by the k-means method and 37 clusters by the x-means method. In the Cabinet Office scenarios, the cluster was divided into 6 clusters by the k-means method and 10669 clusters by the x-means method. Prediction accuracy using the regression model was evaluated for tsunami data in a cluster. The RMSE of tsunami height prediction using a regression model for 18 scenarios in the tsunami inundation database (Takeda, 2019) was improved by 4% from 1.164 m of k-means to 1.119 m of x-means. The RMSE for 11 scenarios of the Cabinet Office scenario was calculated to be 1.083 m with the k-means method.

Keywords: cluster analysis, tsunami

©2020. Japan Geoscience Union. All Right Reserved.

Long-term evaluation of S-net pressure data for real-time tsunami forecasting

*Naotaka YAMAMOTO CHIKASADA[1], Tatsuya Kubota[1]

1. National Research Institute for Earth Science and Disaster Resilience

The water pressure gauge data of the Seafloor observation network for earthquakes and tsunamis (S-net) have been released since October 2019 (doi: 10.17598/nied.0007), and an online data request application form have been opened from the website of the ocean bottom earthquake and tsunami observation network of National Research Institute for Earth Science and Disaster Resilience (NIED). On this website, data obtained after August 2016 (for S6 25 stations, after April 2017) can be used for the application, and observation data has been accumulated over a period of three years and more. Therefore, we evaluated the range of between about 100 seconds and several thousand seconds in which the tsunami is dominant, and then we expectedly confirmed coseismic and background noises (Kubota et al, 2020, JpGU S-CG66). We also confirmed tsunami signals (Kubota et al., 2020, GRL). However, we found that there are unexpected continuous noise and unexpected intermittent noise in irregularly. In this presentation, long-term evaluation is presented for all 150 observation stations, and we would like you to discuss together in the poster booth.

Keywords: S-net, Ocean bottom pressure data, Tsunami

©2020. Japan Geoscience Union. All Right Reserved.

Real-time uncertainties evaluation of coseismic fault models and Tsunami inundation deduced from GNSS observations

Keitaro Ohno[1], *Yusaku Ohta[1]

1. Research Center for Prediction of Earthquakes and Volcanic Eruptions, Graduate School of Science, Tohoku University

Rapid understanding of the magnitude of large earthquakes and their associated fault dimensions are extremely important from the viewpoint of immediate tsunami prediction. Since September 2012, Geospatial Information Authority of Japan (GSI) and Tohoku University are jointly developing the GEONET real-time analysis system (REGARD). REGARD system rapidly estimates two types of coseismic fault models, which are slip distribution along the plate interface and single rectangular fault model, using permanent displacement field based on the real-time GNSS time series. In November 2017, the Cabinet Office, Government of Japan, commenced operation of the system for estimation of tsunami inundation and damage. The system is to be adopted as part of the Disaster Information Systems (DIS). The system has been developed based on the results from "The research group of real-time estimation for tsunami inundation" including utilization of the results from the REGARD system.

The REGARD system, however, has a problem that it is difficult to estimate the quantitative uncertainty of the estimated result because of the obtained result should contain both of the observation error of the real-time GNSS time series and modeling error caused by the assumed model settings. Understanding of such uncertainties quantitatively based on the data is important for evaluation of the result for disaster response.

Based on these backgrounds, we develop the method which estimate the coseismic slip distribution and its estimation uncertainties using MCMC (Markov Chain Monte Carlo methods). In the slip distribution model estimation, we focus on Nankai area in Japan where megathrust earthquakes have repeatedly occurred. We utilize the simulated Hoei type earthquake by Todoriki et al. (2013). We divided into 2951 rectangular subfaults along the subducting plate interface and designed Quadtree-like sampling flow by 4-step sequential segmentation. As the result, we successfully obtain the expected slip distribution and its uncertainty as the 95%C.I. of posterior PDF.

Furthermore, we assess how the uncertainty of the fault model estimation can affect the results of the tsunami inundation. Firstly, we extracted the 300 slip distribution models which has the same variance reduction value (99.51%). Based on the extracted models, we calculated the tsunami inundation for Kochi city. In the most models, the inundation area was the same as the result of the assumed fault slip model. However, the several cases clearly show the larger inundation. This result clearly suggest that the obtained tsunami inundation will have large diversity even though we use the results from high VR value models.

Furthermore, we propose visualization procedure which shows the risk of the tsunami inundation as the map with the probability. Firstly, we classify the slip distribution models by the MCMC approach using k-means approach. Secondly, we extracted the median value as the "possible scenario" from each cluster. Finally, we calculate the tsunami inundation using each "possible scenario" and then, we count the number of the tsunami inundation at each inundation point for all of the "possible scenario". The obtained map reflect the uncertainties of the tsunami inundation caused by the uncertainties of the

©2020. Japan Geoscience Union. All Right Reserved.

coseimsic fault estimation using the real-time GNSS data. The map may be useful to understand the possible “worst case” scenario based on the observation.

Keywords: GNSS, Real time, Tsunami inundation

©2020. Japan Geoscience Union. All Right Reserved.

[J] Poster | S (Solid Earth Sciences)：S-CG Complex & General

[S-CG71] Volcanic roots

convener:Naofumi Aso(Tokyo Institute of Technology), Tsuyoshi Iizuka(University of Tokyo), Shuhei Sakata(Earthquake Research Institute, The University of Tokyo), Yohei Yukutake(Hot Springs Research Institute of Kanagawa Prefecture)

The magma transport system beneath volcanoes is a key to understand geodynamics and the evolution of the Earth. To understand the deep volcanic roots around the lower crust, including deep magma chambers, we need to integrate studies based on various approaches. As seismological evidence, deep long-period earthquakes around the Moho beneath active volcanoes are interpreted to relate to the magma transport system. It is therefore essential to investigate seismicity with a high-resolution hypocenter distribution and focal mechanisms of deep long-period earthquakes. Physical understanding of these events will guide us to reveal the role of deep long-period earthquakes in the magma transport system. Also, high-resolution seismic or electrical resistivity imaging is essential to understand physical properties at the depths and to visualize the magma transport system. Besides, the petrological and geochemical properties of igneous rocks provide important information on the origin of magma and its evolutionary processes including fractional crystallization, assimilation, and mixing at the deeper part of the crust. In particular, microscale chemical and isotopic analyses of minerals with compositional zoning provide important constraints on the evolution of magma chambers. We welcome studies to understand volcanic roots from a variety of approaches including but not limited to the methods mentioned above.

[SCG71-P01] Focal Mechanisms of Volcanic Deep Low Frequency Earthquakes in Northeast Japan

*Genki Oikawa[1], Naofumi Aso[1], Junichi Nakajima[1] (1.Tokyo Institute of Technology)

[SCG71-P02] Deep Long-Period Earthquakes in Eastern Shimane

*Naofumi Aso[1] (1.Tokyo Institute of Technology)

[SCG71-P03] S-wave reflectors below the earthquake swarm in the Yonezawa-Kitakata area, NE Japan

*Manami Suzuki [1], Tomomi Okada[1], Akiko Hasemi[1], Toru Matsuzawa[1], Norihito Umino[1], Takashi NAKAYAMA[1], Noriko Tsumura[2], Tadashi Yamashina[3], Group for the aftershock observations of the 2011 off the Pacific of Tohoku Earthquake (1.Research Center for Prediction of Earthquakes and Volcanic Eruptions, Graduate School of Science, Tohoku University, 2.Graduate School of Science, Chiba University, 3.Faculty of Science and Technology, Kochi University)

[SCG71-P04] V_{SV} and V_{SH} structures beneath Asama volcano

*Yutaka Nagaoka[1], Kiwamu Nishida[2], Yosuke Aoki[2], Minoru Takeo[2] (1.Volcanology Research Department, Meteorological Research Institute, 2.Earthquake Research Institute, The University of Tokyo)

[SCG71-P05] Simultaneously determination of U-Pb age and titanium concentration: A case study of the Kurobegawa granite.

*Kozue Ishibashi[1], Shuhei Sakata[2], Hayato Yamazaki[1], Takashi Yuguchi[1] (1.Yamagata University, 2.The University of Tokyo)

[SCG71-P06] Unraveling the generation process of granitoid magmas in the Hidaka Metamorphic Belt by in situ geochemical and Sr isotopic analyses of plagioclase

*Tokiyuki Morohoshi[1], Otaro Kobayashi[1], Tsuyoshi Iizuka[1] (1.University of Tokyo)

Focal Mechanisms of Volcanic Deep Low Frequency Earthquakes in Northeast Japan

*Genki Oikawa[1], Naofumi Aso[1], Junichi Nakajima[1]

1. Tokyo Institute of Technology

Deep low-frequency earthquakes (LFEs) are small events (M<2) with dominant frequencies of 2–8 Hz. LFEs in Northeast Japan mainly occur at depths of 20-40 km around active volcanoes. Many previous studies obtained various focal mechanisms including both double-couple and non-double-couple components. Therefore, physical models related to the movement of magma or crustal fluid have been proposed. However, we need further case studies to constrain their physical mechanisms. Thus, we determine the focal mechanisms of volcanic LFEs beneath 21 volcanic regions and examine the temporal variation of focal mechanisms in relationship to seismicity and large earthquakes.

To analyze the mechanisms of LFEs, we use the amplitude ratios of S-wave to P- wave (S/P ratios). First, the site effect at each station is corrected using the radiation from regular earthquakes with known focal mechanisms. Next, we carry out a grid search to estimate the moment tensor components which minimize the residuals between observed and theoretical S/P ratios. Finally, we select reliable solutions using the Bootstrap test.

We obtain various focal mechanisms of 155 events including significant non-double- couple component, while there are some events with similar focal mechanisms in each region. In order to evaluate the similarity of mechanisms, we perform clustering analysis using the density-based algorithm. Based on the results of clustering, we determine representative focal mechanisms for seven regions. We calculate induced stress tensors from the 2008 Iwate-Miyagi earthquake and the 2011 Tohoku earthquake to quantitatively evaluate the triggering potentials. As a result of this analysis, representative focal mechanisms in seven regions show good agreement with the LFE activity change associated with the 2011 Tohoku earthquake. This result indicates that seismicity of LFEs are controlled by the temporal stress change as well as shallow crustal earthquakes.

Keywords: low-frequency earthquake, the 2011 Tohoku Earthquake

©2020. Japan Geoscience Union. All Right Reserved.

Deep Long-Period Earthquakes in Eastern Shimane

*Naofumi Aso[1]

1. Tokyo Institute of Technology

Deep long-period earthquakes (DLPs) are deep (~10–45 km) earthquakes that radiate long-period (~2–8Hz) seismic waves despite their small magnitude (M<2). As well as low-frequency earthquakes on plate interface (tectonic LFEs), DLPs widely observed in volcanic regions (volcanic DLPs) are potentially essential to understand the slow deformation processes in various tectonic settings. While tectonic LFEs are recognized as slip events, the physical mechanism of volcanic DLPs has not been well understood. Specifically, at least some volcanic DLPs have significant non-double-couple components [Nakamichi et al., 2003; Aso and Ide, 2014; Oikawa et al., 2019].
Volcanic DLPs occur around the Moho not only beneath worldwide volcanoes but also far from active volcanoes [Aso et al., 2011, 2013; Vidale et al., 2014]. Many of these events are located in shear zones [e.g., Nishimura and Takada, 2017], where large inland earthquakes occur. As a candidate mechanism that could explain both DLPs on volcanic front and back-arc DLPs without recent surface volcanic activity, thermal strains produced by a cooling magma body are suggested as a driving force [Aso and Tsai, 2014]. Secondary triggered resonant oscillation may produce harmonic waveforms, which commonly characterize volcanic DLPs.
The seismic source process is fundamentally essential for understanding their genesis. For this purpose, we reanalyze the DLPs in eastern Shimane, where high signal-to-noise (S/N) records are available. We use Hi-net stations, which meet the high S/N standard. We first correct P-wave arrivals based on the waveform similarity among stations. Then, we apply moment tensor inversion for the P-wave windows. We confirm the oscillating source process reported by Aso and Ide (2014). While the middle and the latter part of the P-wave determine the oscillating pattern robustly, the polarity of the oscillation is sensitive to the initial part of the P-wave, which is not constrained well. Therefore we carry out the campaign observation to investigate the very early part of the DLP events.

Keywords: Deep long-period earthquakes

©2020. Japan Geoscience Union. All Right Reserved.

S-wave reflectors below the earthquake swarm in the Yonezawa-Kitakata area, NE Japan

*Manami Suzuki [1], Tomomi Okada[1], Akiko Hasemi[1], Toru Matsuzawa[1], Norihito Umino[1], Takashi NAKAYAMA[1], Noriko Tsumura[2], Tadashi Yamashina[3], Group for the aftershock observations of the 2011 off the Pacific of Tohoku Earthquake

1. Research Center for Prediction of Earthquakes and Volcanic Eruptions, Graduate School of Science, Tohoku University, 2. Graduate School of Science, Chiba University, 3. Faculty of Science and Technology, Kochi University

Studies about distinct S wave reflectors around volcanic regions and inland earthquake faults has been reported for decades. In the NE Japan, S wave reflectors was interpreted as fluid which was dehydrated from melt [e.g., Hasegawa et al., 2005]. In addition, it is pointed out that crustal fluid may be involved in the mechanism of inland earthquake occurrence, and further understanding of the crustal fluid is necessary.

Also in the Yonezawa - Kitakata area, NE Japan, earthquake swarm occurred 7 days after the 2011 off the Pacific coast of Tohoku Earthquake because frictional strengths were estimated to have changed due to fluid diffusion [e.g., Okada et al., 2015]. In the previous studies (e.g., JpGU 2019 Meeting), we have obtained the spatial distribution of the S wave reflectors in Yonezawa - Kitakata area. We used data from the permanent stations by Hi-net and the temporary seismic network deployed by Group of the aftershock observations of 2011 off the Pacific coast of Tohoku Earthquake. We used the hypocenters determined by the Double Difference method using the temporary observation data. First, we carefully picked the travel time of the S wave reflected wave manually. Next, using the travel time, the strike/dip and the position of the reflection point were obtained by the image station method [e.g., Horiuchi et al., 1988]. As a result, the reflectors were located at the depth of 10 - 20 km below the focal area of the swarm.

The internal structure of the S-wave reflector is important for interpreting the origin of seismic reflector. In order to estimate the internal structure of the S-wave reflector, we calculated the spectral amplitude ratio of the reflected S wave to the direct S wave. Each time window sets from -0.1 s to 0.53 s based on the arrival time. The sampling frequency is 100Hz. The station used in this analysis is N.YNZH station deployed by Hi-net. The peak frequency of the obtained spectral amplitude ratio was confirmed at about 3-5 Hz, and the secondary peak could be seen at a multiple of that frequency. This characteristic of spectral amplitude ratio could be explained by a model of thin layer with low seismic velocity as shown by Umino et al., (2002). This result suggests that localized fluid exist below the focal area. Accordingly, it can be interpreted that earthquake swarm occurred due to the presence of fluid around the epicenter.

Keywords: seismic reflector

©2020. Japan Geoscience Union. All Right Reserved.

V_{SV} and V_{SH} structures beneath Asama volcano

*Yutaka Nagaoka[1], Kiwamu Nishida[2], Yosuke Aoki[2], Minoru Takeo[2]

1. Volcanology Research Department, Meteorological Research Institute, 2. Earthquake Research Institute, The University of Tokyo

Recent studies report the existence of the discrepancy between V_{SV} and V_{SH} beneath volcanoes with large calderas such as Toba caldera (Jaxybulatov et al., 2014) and Yellow Stone caldera (Jiang et al., 2018) or volcanoes at the rim of large calderas such as Kirishima volcanoes. Such discrepancies imply the radial anisotropy generated by a sill complex in the magma reservoir. However, it is not clear whether this feature is common only among volcanoes related to large calderas. In this poster, we will present whether there is the same feature beneath a volcano without a large caldera taking an example of Asama volcano for comparison.

The technique we employed is seismic wave interferometry, which extracts the seismic wave propagation between two seismic stations by taking cross correlations of random wavefields, such as the ambient seismic noise or the seismic coda wave. The cross correlations of random wavefields recorded at two stations can be represented as if the source is at one station and the recorder is at the other. This technique is suitable for exploring local structure since the extracted wave is sensitive to the internal structure between the two stations.

We applied this technique to the ambient seismic noise data recorded at 46 seismic stations on and around Asama volcano between July 2005 and July 2007. Rayleigh and Love waves are extracted by taking cross correlations (Rayleigh waves from cross correlation functions of pairs of vertical components, and Love waves from transverse components). We derived the reference dispersion curves of Rayleigh and Love waves, respectively, using all possible pairs of stations, then measured phase velocity anomalies of all possible pairs with respect to the reference in multiple frequency bands (0.1-0.2 Hz, 0.15-0.3 Hz, 0.2-0.4 Hz, and 0.25-0.5 Hz).

The phase velocity maps of Rayleigh and Love waves were obtained by the surface wave phase velocity tomography (Rawlinson and Sambridge, 2005). The phase velocity map of Rayleigh waves in 0.1-0.2 Hz shows a low velocity region in the western part of the volcano. In the frequency bands higher than 0.15 Hz, low velocity regions exist beneath the entire volcano. The phase velocity maps of Love waves exhibit low velocity regions beneath the entire volcano in all frequency bands. Moreover, the intensity of the low velocity is relatively stronger on the east side of the summit crater. We plan to construct the three-dimensional V_{SV} and V_{SH} structures inverted from the phase velocity maps of Rayleigh and Love waves, respectively, by the linearized inversion (Tarantola and Valette, 1982).

Keywords: Asama, magma reservoir, radial anisotropy

©2020. Japan Geoscience Union. All Right Reserved.

Simultaneously determination of U-Pb age and titanium concentration: A case study of the Kurobegawa granite.

*Kozue Ishibashi[1], Shuhei Sakata[2], Hayato Yamazaki[1], Takashi Yuguchi[1]

1. Yamagata University, 2. The University of Tokyo

This study presents procedures and results of simultaneous determination of zircon U-Pb age and titanium concentration for a single ablation pit using LA-ICP-MS, which was employed for clarification of the formation process of the Kurobegawa granite. The Kurobegawa granite in the Hida Mountain Range has zircon U-Pb age of 10–0.8 Ma, and thus which is the Earth’s youngest known exposed granitoid pluton (Ito et al., 2013; 2017). In this study, the youngest zircon samples were collected from the felsic rock mass of the central part (Babadani river) of the Kurobegawa granite, which are same location to the sampling site of ‘KRG03 (< 1 Ma)’ of Ito et al. (2013). The U-Pb age of such young zircon is accompanied with small error, and thus which allow us to discuss the variation of ages within a single zircon crystal.

The simultaneous determination was carried out using the triple quadrupole ICP-MS (Agilent8800) housed at the Gakushuin University. MS/MS mass-shift mode with oxygen reaction gas provides reliable and consistent measurement of titanium as $^{48}Ti^{16}O^{+}$. As a result, zircon U-Pb ages range from 1.07 ±0.09 to 0.63 ±0.12 Ma and the titanium concentrations have a range between 0.92 ±0.08 and 16.99 ±0.84 ppm. The obtained U-Pb ages is consistent with the previous data of Ito et al. (2013). The temperature conditions of zircon crystallization were estimated from the geothermometry of Watson et al. (2006). As assumed as a_{TiO2} = 0.3, the crystallization temperature ranges from about 650 to 920 °C.

Keywords: zircon, U-Pb age, Ti in zircon thermometer, LA-ICP-MS, CL image

©2020. Japan Geoscience Union. All Right Reserved.

Unraveling the generation process of granitoid magmas in the Hidaka Metamorphic Belt by in situ geochemical and Sr isotopic analyses of plagioclase

*Tokiyuki Morohoshi[1], Otaro Kobayashi[1], Tsuyoshi Iizuka[1]

1. University of Tokyo

In order to understand the growth history of continental crust, it is essential to reveal the importance and mechanism of crustal reworking processes. The contribution of pre-existing crustal rocks to granite genesis has been investigated using Sr isotopes because old crustal rocks have higher $^{87}Sr/^{86}Sr$ as compared to juvenile magma. However, since granites often involve multiple magmatic sources, it is difficult to unravel the nature of the sources from whole rock Sr isotope analysis. Nowadays, in situ analysis of minerals for trace elements and isotope ratios becomes popular to overcome these difficulties.

To better understand granitoid genesis and crustal reworking process, we present a combined Sr isotopic and major and trace element geochemistry by in situ analysis of plagioclase in granitoids from the Hidaka Metamorphic Belt (HMB) in Hokkaido. The HMB exposes a cross section of arc crust is exposed and, therefore, lower crustal rocks are available for direct analysis. The HMB is mainly composed of metamorphic rocks reaching to granulite facies and igneous rocks intruding into them. This study focused on the northern part of the HMB where various igneous rocks are exposed. All samples used in this study were collected in the field trip at the northern HMB. Eight samples which represent the typical geological setting of this part are chosen for the analyses.

We performed in situ analyses of plagioclase as well as other minerals for major elements by an electron microprobe micro analyzer (EPMA), for trace elements by a laser ablation inductively coupled plasma quadrupole mass spectrometer (LA-ICP-QMS), and for Sr isotope ratio by a laser ablation multiple collector inductively coupled plasma mass spectrometer (LA-MC-ICP-MS). We analyzed multiple spots in single crystals to evaluate geochemical and isotopic heterogeneities. All Samples were analyzed in solid state as thin section.

The EPMA and LA-ICP-MS data revealed chemical and isotopic zoning in plagioclase crystals. In addition, different grains have different isotope signatures especially in the cores. In a tonalite sample, Sr isotope ratios in the cores split into two parts. By contrast, their rims have similar Sr isotope ratios. Given that the Sr isotopic ratios in the cores represent their source magma compositions, these observations can be interpreted as mixing and homogenization processes in the source magmas having different origins. The higher isotope ratio overlaps those of sedimentary and metamorphic rocks in the HMB (Kojima et al., 2014), whereas the lower ratio overlaps those of mafic igneous rocks (Maeda et al., 2011). These results indicate that the tonalite source magma involves both juvenile and reworked crustal components. Assuming that the distinct core compositions respectively reflect the juvenile and reworked crustal components, we estimated the contribution of the crustal component to be 25% at most. On the other hand, two granite samples show less clear convergence or unified change in plagioclase composition compared to the tonalite sample. Strontium isotope ratios in all plagioclase crystals overlap the compositions of the sedimentary and metamorphic rocks or higher than them. It can be interpreted that these granites were generated dominantly by partial melting of sedimentary and metamorphic rocks.

©2020. Japan Geoscience Union. All Right Reserved.

©2020. Japan Geoscience Union. All Right Reserved.

[J] Poster | B (Biogeosciences)：B-BG Biogeosciences & Geosphere-Biosphere Interactions

[B-BG02] Interaction between Life, Water, Mineral, and Atmosphere

convener:Yuichiro Ueno(Department of Earth and Planetary Sciences, Tokyo Institute of Technology), Takeshi Kakegawa(Graduate School of Science, Tohoku University), Ken Takai(Extremobiosphere Research Center, Japan Agency for Marine-Earth Science & Technology), Yohey Suzuki(Graduate School of Science, The University of Tokyo)

Biological activity on Earth is based on dynamic and diverse physico-chemical processes throughout the history of the Earth. It is essential to study interaction between Life, Water, Mineral and Atmosphere. In order to understand the complex biogeochemical system, it is necessary to communicate various researchers from different disciplines. This session provides an indispensable opportunity to discuss the Earth's biosphere as a whole from wide range of interdisciplinary researches

[BBG02-P01] Analysis of 13C-13C isotopologue of ethane and ethanol by a fluorination method

*Taguchi Koudai [1], Tomonari Yamamoto[1], Mayuko Nakagawa[1,2], Alexis Gilbert[1,2], Yuichiro Ueno[1,2,3] (1.Department of Earth and Planetary Sciences, Tokyo Institute of Technology, 2.Earth-Life Science Institute (WPI-ELSI), Tokyo Institute of Technology, 3.Department of Subsurface Geobiological Analysis and Research (D-SUGAR), Japan Agency for Marine-Earth Science and Technology (JAMSTEC))

[BBG02-P02] Iron isotope fractionation in the 3.2Ga Moodies Banded Iron Formations, Barberton Greenstone Belt, South Africa

*RYOHEI SUGIURA[1], Tsubasa Otake[2], Daizo Yamauchi[1], Yoko Ohtomo[2], Tsutomu Sato[2] (1.Graduate school of Engineering, Hokkaido University, 2.Facility of Engineering, Hokkaido University)

[BBG02-P03] Geochemical studies on the mobilization of phosphorus during seawater/rock interaction of Miocene lava flows in the *Hokuroku* district in Akita, Japan

*Tsukasa Sai[1], Takeshi Kakegawa[1] (1.Graduate School of Science, Tohoku University)

[BBG02-P04] Passive treatment of acid mine drainages containing dissolved iron

*Tatsuya Matsui[1], Sereyroith Tum[1], Frances Chikanda [1], Yoko Ohtomo[2], Tsubasa Otake[2], Ryosuke Kikuchi[2], Tsutomu Sato[2] (1.Graduate School of Engineering, Hokkaido University, 2.Faculty of Engineering, Hokkaido University)

[BBG02-P05] Textual characteristics of laminated silica hot spring deposits in Kagoshima Prefecture

*Chizuru Takashima[1], Tomoyo Okumura[2], Akihiro Kano[3], Susumu Kakubuchi[1] (1.Faculty of Education, Saga University, 2.Center for Advanced Marine Core Research, Kochi University, 3.Department of Earth and Planetary Science The University of Tokyo)

[BBG02-P06] Formation mechanism of halloysite-rich layer by differential weathering of tephra under a reduced condition

*Hirokazu Fukui[1], Yuki Matsushi[2], Tetsuhiro Watanabe[3] (1.Graduate school of Science, Kyoto University, 2.Disaster prrevention research institute, Kyoto university, 3.Graduate School of Agriculture, Kyoto university)

[BBG02-P07] Aquifer Nitrate Concentration and Associated Human Health Risk Assessment of Haridwar District of Uttarakhand, India

*AHTESHYAM AHTESHYAM[1], Shaveta Sawhney[1], Jahangeer -[2] (1.Patanjali Medical College, Haridwar, India, 2.Nebraska Water Center, University of Nebraska Lincoln USA)

[BBG02-P08] Global ocean pigments transport by mesoscale eddies

*xiangguang zhang[1,2,3], yongsheng Xu[1,2,3] (1.Key Laboratory of Ocean Circulation and Waves, Institute of Oceanology, Chinese Academy of Sciences, 2.Center for Ocean Mega-Science, Chinese Academy of

Sciences, 3.Laboratory for Ocean and Climate Dynamics, Qingdao National Laboratory for Marine Science and Technology)

[BBG02-P09] **Screening of Genes from Subseafloor Sediments and Co-Rich Ferromanganese crust Using Substrate-induced Gene Expression (SIGEX) Method.**

*Aki Yoshida[1], Taisuke Wakamatsu[1], Takashi Morisawa[1], Takeshi Terada[3], Shunichi Ishii[2], Yuki Morono[2] (1.Kochi university, 2.Kochi Institute for Core Sample Research, JAMSTEC, 3.Marine Works Japan Ltd.)

[BBG02-P10] Spatial analysis of water quality data to prioritize sites for oyster reef restoration

*Cameron Chase Atkinson[1], James Deemy[1] (1.College of Coastal Georgia)

Analysis of 13C-13C isotopologue of ethane and ethanol by a fluorination method

*Taguchi Koudai [1], Tomonari Yamamoto[1], Mayuko Nakagawa[1,2], Alexis Gilbert[1,2], Yuichiro Ueno [1,2,3]

1. Department of Earth and Planetary Sciences, Tokyo Institute of Technology, 2. Earth-Life Science Institute (WPI-ELSI), Tokyo Institute of Technology, 3. Department of Subsurface Geobiological Analysis and Research (D-SUGAR), Japan Agency for Marine-Earth Science and Technology (JAMSTEC)

Doubly-substituted isotope species (“clumped isotopes”) of a molecule potentially records important biogeochemical information such as its temperature of formation and/or its (bio)synthetic pathway. The abundance of clumped isotopologue can be viewed as a deviation from its stochastic abundance, conventionally denoted as a D value (i.e., $D = (R_{sample}/R_{stochastic} - 1)$). Notably, when an isotope exchange reaction occurs at equilibrium, the abundance of clumped isotopologue reflects its temperature and thus is used as a geothermometer. Recentlly, ^{18}O-^{18}O species in oxygen and ^{15}N-^{15}N in nitrogen have been measured and their abundance helped distinguishing between atmospheric, volcanic and biological sources [1,2]. Recently, Clog et al [3] measured ^{13}C-^{13}C species of ethane from natural gas, highlighting the potential of the approach to study thec biogeochemistry of organic molecules.

Yet, measuring ^{13}C-^{13}C species at natural abundance is not trivial. The common method used to measure the bulk ^{13}C isotopic composition of ethane consists in its combustion to CO_2, which leads to the loss of ethane molecules, and thus of its ^{13}C-^{13}C isotopologue. Clog et al (2018) measured the abundance of clumped isotopologue in ethane in natural gasusing high-resolution gas source mass spectrometer (MAT253 Ultra) which allows the sepoaration and quantification of ^{13}C-^{13}C isotopologues of ethane.

Here, we propose a new alternative method for measuring ^{13}C-^{13}C isotopologue of C2 molecules - not only to ethane but also potentially applicable to various organic compounds - using a conventional isotope ratio mass spactrometer. Because fluorine has only one stable isotope, ^{13}C-^{13}C isotope species in C_2 molecules were measured as C_2F_6 arising from the fluorination of C_2 molecules. This method is applicable to ethane from natural gas samples but also to ethanol from the fermentation of sugars. Ethanol is first converted into ethene through dehydration reaction then fluoridated to C_2F_6.

The fluorination reaction is first conducted at 77K for 10min and then at 173K for 30min using ice ethanol slush adding liquid nitrogen into ethanol. During the fluorination, the mild condition at low temperature is critical to avoid to break the C-C bonding. On the other hand, further fluorination of the intermediate requires higher temperature up to 298K. Therefore, the sample was thawed back to room tempareture for a quantitative conversion.

The yield of fluorination cannnot be strictly contorolled and varies within 5% around the average value. In order to estimate the effect of the conversion efficiency on the $D^{13}C^{13}C$ values, fluorination reactions were conducted at lower yields by changing the amount of fluorine against the starting ethene/ethane. Whereas the $D^{13}C^{13}C$ values of ethane are affected at low yields, the $D^{13}C^{13}C$ valies are constant at the yield above 50%. On the other hand, the $D^{13}C^{13}C$ values of ethene are constant for all yields. Therefore, we can obtain the reproducible $D^{13}C^{13}C$ values at a yield commonly reached 60% or 80% for ethene and ethane, respectively.

©2020. Japan Geoscience Union. All Right Reserved.

Reproducibility of the whole prorocol, including chemical modification steps and measurement of C_2F_6 isotopologues is 0.14‰ for all the compounds. We applied this method to sevral C_2 molecules: ethane from natural gas (thermogenic and abiotic), biologically derived ethanol, as well as abiotic ethane produced experimentally by diverse processes (UV irradiation, spark discharge, Fischer-Tropsch synthesis and Gamma ray irradiation).

Ethane from thermogenic natural gas samples and biologically derived ethanol show a narrow range of D^{13}C^{13}C values varying from 0.72‰ to 0.90‰. In contrast, abiotic ethane, either from natural samples or from experiments shows D^{13}C^{13}C values systematically lower than those of biotic origin. C-C clumping provides new potential (a)biomarkers to the biogeochemistry field.

Reference

[1] Yeung LY, Li S, Kohl IE, et al. Extreme enrichment in atmospheric 15N15N. Sci Adv. 2017;3(11):1-10. doi:10.1126/sciadv.aao6741

[2] Yeung LY, Ash JL, Young ED. Biological signatures in clumped isotopes of O2. Science (80-). 2015;348(6233):431-434.

[3] Clog M, Lawson M, Peterson B, Ferreira AA, Santos Neto E V., Eiler JM. A reconnaissance study of 13C–13C clumping in ethane from natural gas. *Geochim Cosmochim Acta*. 2018;223:229-244. doi:10.1016/j.gca.2017.12.004

Keywords: Clumped isotope, Fluorination, Isotopologue

©2020. Japan Geoscience Union. All Right Reserved.

Iron isotope fractionation in the 3.2Ga Moodies Banded Iron Formations, Barberton Greenstone Belt, South Africa

*RYOHEI SUGIURA[1], Tsubasa Otake[2], Daizo Yamauchi[1], Yoko Ohtomo[2], Tsutomu Sato[2]

1. Graduate school of Engineering, Hokkaido University, 2. Facility of Engineering, Hokkaido University

Iron isotopic signatures in Banded Iron Formations (BIFs) have the potential to provide information about the ocean chemistry and evolution of the marine biosphere on early Earth since they may preserve their biological or abiological formation pathways. However, there are controversies on interpretations of variable iron isotope values recorded in BIFs, such as progressive partial oxidation of hydrothermal fluids following a Rayleigh fractionation-type model or the effect of microbial dissimilatory iron reduction (DIR). In this study, the lower section (MdS1) of the Moodies BIFs, which were deposited in a shallow ocean, including detrital components from the continent, at ~3.2Ga in Barberton Greenstone Belt, South Africa are focused on. Novel relationships of the whole rock Fe isotope data (δ^{56}Fe = -0.58 to +0.56‰) with iron contents and sedimentary environments of different groups of rocks (i.e., magnetite-rich, carbonate-rich, and clastic sedimentary rocks) are presented. The bulk δ^{56}Fe values (δ^{56}Fe = -0.54 to +0.56‰) in magnetite-rich and carbonate-rich groups, which contain much iron from chemical precipitations, tend to increase with increasing of iron contents and as go deeper in the depositional environments. A significant difference in the trend was not observed between magnetite-rich and carbonate-rich groups. These results indicate that the variation in the bulk Fe isotopes reflects precipitation process of a same precursor following a Rayleigh fractionation-type model. Furthermore, Fe isotope fractionation during the formation of Fe(II)-silicates (e.g., greenalite), which have recently been proposed as the primary Fe mineral in BIFs, was also examined by the synthetic experiments. The results demonstrate that the Fe isotope fractionation between Fe(II)-silicates and Fe^{2+}(II) is too small to satisfy the measured range of observed δ^{56}Fe values in the Moodies BIFs. Since oxidative precipitation of dissolved ferrous iron as ferric (Fe(III)) hydroxide (e.g., ferrihydrite) is known to cause large Fe isotope fractionations, the observed variation of δ^{56}Fe values can be only explained by the formation of ferric hydroxide as the primary precipitate. Although ferric hydroxide was transformed, possibly DIR involved, to secondary Fe(II)-bearing minerals, such as magnetite and siderite, via the oxidation of microbial organic carbon, the Fe isotope signatures reflecting the precipitation process following a Rayleigh fractionation-type model were likely preserved in the geological record of the Moodies BIFs.

Keywords: Earth history, isotope, sedimentary rock, microorganism, iron, oxygen

©2020. Japan Geoscience Union. All Right Reserved.

Geochemical studies on the mobilization of phosphorus during seawater/rock interaction of Miocene lava flows in the *Hokuroku* district in Akita, Japan

*Tsukasa Sai[1], Takeshi Kakegawa[1]

1. Graduate School of Science, Tohoku University

The phosphorus is an essential element for biological activity. On the other hand, the phosphorus cycle on the modern surface Earth is often controversial. Many reseachers consider that oceanic crusts scavenge phosphorus by seawater/rock interaction. However, this idea is not supported by global data, in particular fersic submarine lava flows. Thus, the purpose of this study is set to examine phosphorus behavior during seawater/rock interaction of submarine rhyolite. The samples are collected from ca.12 Ma submarine rhyolite lavas which erupted on the seafloor of ancient Japan Sea in the *Hokuroku* basin. The collected samples were categorized into less and extensively altered samples. The less altered samples recorded the simple seawater/lava interaction, and extensively altered samples represent altered rocks by high-temperature submarine hydrothermal fluids. Primary igneous apatite is observed in phenocrysts, such as quartz, plagioclase, magnetite, ilmenite, and zircon. Secondary phosphate minerals are observed in vein, chalcedony in plagioclase pseudomorphs, and Fe-bearing minerals. Secondary phosphate includes 10-100 μm-sized apatite, monazite, and xenotime. Variety of secondary phosphates were found in extensively altered rhyolite, including euhedral and anhedral apatite, monazite, xenotime, corkite, and hinsdalite. In addition, hydrothermal formation of sulfur-bearing apatite was confirmed in plagioclase pseudomorph, groundmass, and altered minerals. Systematic chemical analyses on less altered rhyolite indicate the enrichment of phosphorus in unaltered rocks, followed by extensive phosphorus loss in heavily altered rocks. Therefore, it is concluded that rhyolite can supply phosphorus in ocean water by advanced seawater/rock interaction. Coupling of the initial enrichment and rapid loss of phosphorus in submarine fersic rocks may be important when considering ancient and modern chemoautotrophic vent communities, because our results imply that Kuroko-type venting fluids were rich in phosphorus and could support the benethic ecosystems. This new knowledge is different from a popular hypothesis that oceanic igneous rocks are sink of marine phosphorus.

Keywords: phosphate mineral, seafloor alteration, hydrothermal alteration, apatite

©2020. Japan Geoscience Union. All Right Reserved.

Passive treatment of acid mine drainages containing dissolved iron

*Tatsuya Matsui[1], Sereyroith Tum[1], Frances Chikanda [1], Yoko Ohtomo[2], Tsubasa Otake[2], Ryosuke Kikuchi[2], Tsutomu Sato[2]

1. Graduate School of Engineering, Hokkaido University, 2. Faculty of Engineering, Hokkaido University

Active treatment of the acid mine drainage (AMD) at abandon mine has economically been a big issue. Recently at some of AMD, economic treatments were accomplished by introducing lime channel in the drainage as passive treatment. For sustainable management of the AMD, switch from active to passive treatment should be necessary if available. In south part of Hokkaido, Japan, the abandon Shojin mine discharges AMD to Shojin and Amemasu rivers, containing toxic heavy metals such as iron, arsenic, lead and cadmium. In Shojin river, concentration of the heavy metals is less than environmental standard at monitoring point without treatment. On the other hand, concentration of the heavy metals keeps high in downstream of Amemasu river. In this context, site investigations were conducted in Shojin and Amemasu rivers to identify the geochemical differences for natural attenuation process for passive treatment in Amemasu river.

At the mixing point of AMD with Shojin river, pH of AMD increases to 3.5 from 2.8, where precipitation of schwertmannite was formed due to pH increasing. Concentrations of As is decreased due to the high adsorption capacity of schwertmannite at the pH. Moreover, toxic heavy metals in the AMD was diluted by the river water because flow rate of AMD is relatively less than that of the river water. In contrast, at the mixing point of AMD with Amemasu river, the pH was not changed (pH=2.86), where precipitation was not observed. In addition, heavy metal concentrations of the AMD are not diluted by the river water because flow rate of AMD are not so different from that of Amemasu river water. Consequently, from the difference in flow rate between two rivers, natural attenuation in Shojin river is accomplished by adsorption of newly formed schwertmannite and dilution of AMD. Therefore, precipitation by increasing pH of AMD may firstly considered for passive treatment in Amemasu river. To understand preferable pH for As, Pb and Cd removal, surface complexation modelling was conducted. For schwertmannite precipitation, pH 3.5 is necessary. At pH 3.5, the concentration of As decreases to that less than the standard by adsorption by schwertmannite. Pb may be removed under the standard at pH5.0 by the adsorption while Cd may not be removed until pH 9.0. For passive treatment in Amemasu river, increase of pH more than 5.0 requires a large-scale lime channel, therefore dilution at downward would be expected for lead and cadmium attenuation.

©2020. Japan Geoscience Union. All Right Reserved.

Textual characteristics of laminated silica hot spring deposits in Kagoshima Prefecture

*Chizuru Takashima[1], Tomoyo Okumura[2], Akihiro Kano[3], Susumu Kakubuchi[1]

1. Faculty of Education, Saga University, 2. Center for Advanced Marine Core Research, Kochi University, 3. Department of Earth and Planetary Science The University of Tokyo

The present oxygen-rich global environment was created by the interaction between ancient microorganisms and the environment. However, many mysteries remain in the evolution of microorganisms such as cyanobacteria that first generated oxygen in ancient atmosphere. The key for understanding the origin and evolution of Precambrian organisms is in banded iron formations and stromatolites, which contain components from seawater. As for the formation process of these two laminated sediments, the involvement of microorganisms has been pointed out from stable isotope ratios, biomarkers, or organic structures that are rarely preserved in chart-like parts (e.g., Konhauser et al. 2002). However, in many cases, evidence of microbial communities and activities has been erased by several billion years of metamorphism. Therefore, the origin and periodicity of lamination of stromatolite and banded iron formation are not yet clear. In this study, we focus on hot spring silica deposits, which have a slow deposition rate and have many similarities in ancient laminated sediments. Tamatebako hot spring in Ibusuki City, Kagoshima Prefecture, is a high temperature (about 90 degrees Celsius), neutral pH, and contains many Na^{+}, Ca^{2+}, Cl^{-}. A concentration of Si is about 190 mg/L. Amorphous silica is deposited along the flow path from the vent and have developed over about 170 m^2 due to the decrease in water temperature and evaporation from upstream to downstream. Silica sediment are very hard at upstream and become brittle at downstream. The surface of the sediment is pale pink, and the cross-section of the sediment can be observed with laminations in microns to millimeters of the white and colored layers. The sediments in the uppermost part have strongly colored layers that are alternated with porous white layers. The midstream sediments have clear laminations, and transparent filamentous microorganisms can be found in the pores of the white layers. The thickness of the sediments downstreams is thin, but as the midstream sediments, transparent filamentous microorganisms exist in the pores of the white layers. The elemental mapping showed that the white layers were more silica and the colored layers contained high iron and manganese. The white layer of silica deposits was porous and there were many microorganisms, and microorganisms probably work as the nucleus in silica precipitation. On the other hand, the colored layer was dense and contained a lot of heavy metals, and there were few microorganisms. The cycle of the laminations may reflect a cyclic change in the redox state of hot spring water and/or microbial metabolism, which is likely daily.

Konouser et al., (2002) Can bacteria have formed the Precambrian banded iron formations? Geology, 30(12), 1079-1082.

Keywords: silica, bacteria, hot spring

©2020. Japan Geoscience Union. All Right Reserved.

Formation mechanism of halloysite-rich layer by differential weathering of tephra under a reduced condition

*Hirokazu Fukui[1], Yuki Matsushi[2], Tetsuhiro Watanabe[3]

1. Graduate school of Science, Kyoto University, 2. Disaster prrevention research institute, Kyoto university, 3. Graduate School of Agriculture, Kyoto university

Research focus
The dissolution of the primary minerals and the precipitation of secondary minerals depends on the redox conditions; just below the ground surface, shallower than 1m, an oxidizing condition dominates, while a reduced condition is preferred at deeper soil. As water is vertically percolating into soil, subsurface water behaves heterogeneously in the infiltration and drainage processes. Soil-microbial functions also affect the oxidation-reduction potential by consuming dissolved oxygen. The states and changes in the redox conditions have an impact of the ionic species of iron, that is a ferrous iron or a ferric iron, which is subsequently involved in the formation of secondary minerals.

Our aim of the study is to clarify the distribution of halloysite, which is affected by the hydrological and chemical processes in soil, addressing the dissolution of volcanic glass and the solid and solution chemistry.

Keywords: Tephra, Diffrential weathering, Halloysite, Reduced condition, Ferrous iron, Preferential flow

©2020. Japan Geoscience Union. All Right Reserved.

Aquifer Nitrate Concentration and Associated Human Health Risk Assessment of Haridwar District of Uttarakhand, India

*AHTESHYAM AHTESHYAM[1], Shaveta Sawhney[1], Jahangeer -[2]

1. Patanjali Medical College, Haridwar, India, 2. Nebraska Water Center, University of Nebraska Lincoln USA

Groundwater contamination by nitrate is a matter of global concern and nitrate is a widespread contaminant of ground and surface water worldwide. The aquifer of Haridwar district is mainly contaminated by nitrate-nitrogen. Nitrate contamination associated with N-based fertilizers use, geology of sub-surface of the soil layer, pit latrines, sewerage, industrial effluents, and manure storage Aquifer Nitrate Concentration and Associated Human Health Risk Assessment of Haridwar District of Uttarakhand, India. The study aims to investigate the possible health hazards in local residents of Haridwar, Uttarakhand, India. Amount of nitrate in groundwater of Haridwar region in ranges between 0.1 - 89mgL^{-1} . Some locations showed a high level of nitrate than the safe limits as decided by the Bureau of Indian standards (higher than 45 mgL^{-1}) and the World Health Organization (50 mg L^{-1}). There is strong & a direct relation between drinking water nitrate ingestion and associated health risks like methemoglobinemia (Blue baby syndrome) among infants and specific types of cancer. The crude current rate of cancer in Uttarakhand is 91(incident rate per 100000 in 2016). Nearly 59 deaths are reported due to cancer only in Haridwar district during the year 2018-19. The study tends to show that the people of Haridwar district are at risk of chronic toxicity due to excess intake of nitrate in drinking water. Therefore, this is a call to take some immediate preventive measures to safeguard the health of local residents.

Keywords: Groundwater, Nitrate Pollution , Human Health Risk

©2020. Japan Geoscience Union. All Right Reserved.

Global ocean pigments transport by mesoscale eddies

*xiangguang zhang[1,2,3], yongsheng Xu[1,2,3]

1. Key Laboratory of Ocean Circulation and Waves, Institute of Oceanology, Chinese Academy of Sciences, 2. Center for Ocean Mega-Science, Chinese Academy of Sciences, 3. Laboratory for Ocean and Climate Dynamics, Qingdao National Laboratory for Marine Science and Technology

Mesoscale eddies can trap ocean pigments and move them from one region to another. The concentration of oceanic pigments change with depth. However, satellite can only observe ocean pigments concentration at the sea surface. Here, we estimate eddy-induced ocean pigments transport based on satellite observations, Argo float measurements, and an empirical model of vertical distribution of ocean pigments. In this paper, we focus on the global chlorophyll transportation by mesoscale eddies. The result shows mesoscale eddies have a strong influence on the distribution and transport of ocean pigments, and therefore can have a significant impact on marine ecosystems.

Keywords: Global ocean pigments transportation, Mesoscale eddies, Chlorophyll-a transportation, Ocean pigments vertical distribution, Marine ecosystems

©2020. Japan Geoscience Union. All Right Reserved.

Screening of Genes from Subseafloor Sediments and Co-Rich Ferromanganese crust Using Substrate-induced Gene Expression (SIGEX) Method.

*Aki Yoshida[1], Taisuke Wakamatsu[1], Takashi Morisawa[1], Takeshi Terada[3], Shunichi Ishii[2], Yuki Morono[2]

1. Kochi university, 2. Kochi Institute for Core Sample Research, JAMSTEC, 3. Marine Works Japan Ltd.

The substrate-induced gene expression (SIGEX) method is a gene-screening approach that uses a promoter trap-type vector based on the assumption that general gene expression is induced by substrates/metabolites of catabolic enzymes and that the regulatory elements are often positioned in proximity to the catabolic genes[1]. The DNA fragments from environmental samples are inserted upstream of the gene of green fluorescence protein, and induction-positive clones can be selectively isolated by fluorescence-activated cell sorting in a high-throughput manner. One of the advantages of this method is that we can presume the potential gene-function without relying on its sequence information, which can lead to explore new, unknown functions of DNA sequences buried in environmental metagenomes.
In this study, we applied SIGEX method to metagenomes of ultra-*oligotrophic* South Pacific Gyre (SPG) subseafloor sediment samples and covalt-rich ferromanganese crust from Dakuyo-Daigo seamount. In SPG sample, we tested substrates of methane, sodium acetate, or manganese chloride as inducing compounds, and isolated in total 87 induction-positive clones. We then performed DNA sequencing on 72 clones (CH_4: 13, CH_3COONa: 52, $MnCl_2$: 7). On the other sample, we tested substrates of sodium formate, manganese chloride, manganese sulfate, cobalt chloride, nickel chloride, sodium tangstate, and others metallic ions. We isolated in total 58 induction-positive clones and the inserted sequences of 42 clones were determined (HCOONa: 5, $MnCl_2$: 10, $MnSO_4$: 8, Na_2WO_4: 14, $CoCl_2$: 2, $FeCl_2$(II), $NiCl_2$, Na_2MoO_4:1). Through database search, we often encountered to the situation that the sequence in induction-positive clones show low similarity to the sequences in the database. One of the notable characteristics for the sequences was that there were highly frequent observation of inverted repeat sequences that we similarly identified in previous studies[2,3], but the fragment that we isolated from Takuyo-Daigo seamount didn't have these sequence. We will discuss the results of databases search and functional prediction analyses using available tools for the 114 sequences. The linkage between gene-induction response and gene fragments found in this study indicates that there is still a large room of the unknown genetic function to be explored in the environmental metagenomes.

1)Uchiyama T *et al.*, (2005) *Nat. Biotechnol.*, **23**, 88–93.
2)Futagami T *et al.*, (2013) Philos. Trans. R. Soc. Lond. B Biol. Sci., **368**, 20120249.
3)Wakamatsu T *et al.*, (2018) J. Appl. Microbiol., **125**, 1396-1407.

Keywords: SIGEX, South Pacific Gyre, Takuyo-Daigo seamount

©2020. Japan Geoscience Union. All Right Reserved.

Spatial analysis of water quality data to prioritize sites for oyster reef restoration

*Cameron Chase Atkinson[1], James Deemy[1]

1. College of Coastal Georgia

Water quality data has proved vital in enhancing the understanding of estuarine environments and the biodiversity they support. Oysters are a keystone species in many estuarine environments throughout the globe and contribute to the formation of productive ecosystems. As oysters are sessile filter feeders, they rely upon the maintenance of optimal water quality for their recruitment and propagation. With an emphasis being placed on restoring oyster reefs globally, it is important that water quality data be considered before the onset of restoration projects. Here, we highlight an approach that utilizes water quality data to identify sites of high habitat quality and high restoration suitability for the eastern oyster (*Crassostrea virginica*). Our objectives are to 1) identify critical physicochemical parameters as well as optimal ranges for *C. virginica* establishment and success and 2) create a GIS index that maps low, medium, and high habitat quality for *C. virginica*. Water quality data collected by the Georgia Department of Natural Resources: Coastal Resources Division from 2000-2018 was interpolated to produce a GIS habitat suitability index for *C. virginica.* We found that the water quality analysis of the coast of Georgia (United States of America) indicated distinct sites of high and low habitat/restoration quality for *C. virginica*. Water quality data should be used to drive models for restoring habitat especially for a sessile ecosystem engineer such as *C. virginica*. We believe similar analysis and spatial modeling efforts could improve understanding of ecosystem restoration globally.

Keywords: Water Quality, Oyster Reef Restoration, Spatial Analysis , GIS

©2020. Japan Geoscience Union. All Right Reserved.

[J] Poster | G (General)：General

[G-02] Comprehensive disaster prevention education

convener:Hitoshi Nakai(Kobuchisawa Research Institute for Nature and Education), Jiro Komori(Teikyo Heisei University), Shintaro Hayashi(Akita University Graduate School of Education)

Each time a serious disaster occurs, there are calls for better disaster prevention education in and around the stricken area, and such education is actually implemented. However, it is not extended to other parts of the nation. Although disaster prevention education really is needed across Japan, it tends to be implemented only in the directly affected locality of a catastrophic disaster. Moreover, even in affected areas, when 10 to 20 years have elapsed from a major event, with a decline in the number of survivors, there is less motivation to pass experiences and learning on to the next generation, despite the potential for such disasters to recur, tens or hundreds of years into the future. It is not easy to maintain conversations about disaster experiences through several generations. Consequently, effective disaster prevention education is provided only in the region stricken by a particular event, and it is practiced only for up to 20 years following the last disaster. As a result, provision of disaster prevention education has become less effective in many areas of Japan. This session focuses on the following two questions: (1) What kind of disaster prevention education can be practiced continuously nationwide? (2) How can such disaster prevention education be implemented in schools and educational sessions? We encourage anyone who wishes to help develop new disaster prevention education based on awareness of these issues to make a presentation in this session. Participation is not restricted to geoscientists; any person or group engaged in any domain of disaster prevention is welcome to submit a paper.

[G02-P01] Thinking about Needs for minority victims in Multicultural Collaboration society

*ITOYA NATSUMI[1], MICHITAKA TAHARA[1], SHUNSUKE HAMADA[1] (1.oyo corporation)

[G02-P02] A Proposal of Universal Design Teaching Material for Education of Disaster Risk Reduction

*Haruka Matsuoka[1], Kei Takashima[1], Tsukasa Sano[1], Asako Nakagawa[2], Seiji Hori[1], Minako Noda[1] (1.Faculty of Business and Informatics, Tsukuba Gakuin University, 2.Faculty of Home Economics, Otsuma Women's University)

[G02-P03] Reconsideration of the Cause of the Accident Given in the Tsunami Judgment of Okawa Elementary School

*Mamoru Hayashi[1] (1.University of TOYAMA)

[G02-P04] Case report of education about earthquakes and faults in elementary schools

*Noa Mitsui[1], Kumi Yoshitake[2], Kazuyuki Nakagawa[3] (1.Tono Research Institute of Earthquake Science, 2.University of human environments, 3.Jiji Press)

[G02-P05] Consideration on Education of Disaster Prevention Jointly Practiced with the Field

*Erina Hyuga[1], Ami Pareek[1], Hikari Tanaka[1], Mirei Toba[1], Chisa Funada[1], Satoko Oki[1] (1.Keio University)

[G02-P06] Junior high school students experienced the "Shelter Management Game"

*Takeshi Matsumoto[1] (1.Faculty of Science, University of the Ryukyus)

[G02-P07] What is the "comprehensive" in disaster prevention education?

*Hitoshi Nakai[1] (1.Kobuchisawa Research Institute for Nature and Education)

Thinking about Needs for minority victims in Multicultural Collaboration society

*ITOYA NATSUMI[1], MICHITAKA TAHARA[1], SHUNSUKE HAMADA[1]

1. oyo corporation

In these days, The number of Muslim people living in Japan is increasing year after year, and it’s drawing attention in Japan. The number of international students in Japan has reached 298,900 as at May 1, 2018(Japan Student Services Organization, 2019), There are more than 10,000 international students from countries whose main religion is Islam. In modern Japanese society, it is necessary to understand each other's position as a religious minority and create an environment that can respect cultural and religious diversity. However, there is no detailed discussion on what preparations, actions and cautions Muslims should take during a disaster in disaster countermeasures of the Japanese government.

An important part of a disaster community action plan for small communities is "cohesion." Further It is also important to promote “clarification and sharing of issues” in diverse values. In this study, we focused on "clarification and sharing of issues", and used Yonmenkaigi System Method (YSM), which proposed structuring the process of forming knowledge into action. This Yonmenkaigi System Method is applied in a workshop in which residents and disaster prevention experts cooperate as one of the support methods for action plan by residents. In this study, Muslims and Japanese collaborate using Yonmenkaigi System Method and apply it to the direction to solve the issues.

In order to understand the “clarification of the issues,” we tried to interview two victims (from Bangladesh) of the Great East Japan Earthquake. One of the highlights of the interview was that "Muslims could not imagine living in a shelter." The purpose of making Yonmenkaigi map is to specify the actions and things necessary for Muslims to live in shelter and set the theme "For Muslims to be comfortable in shelters".

Yonmenkaigi System Method applied in this study considers the actions (actions and things) necessary for the issue and the actions (actions and things) to be prepared, and we tried to apply these actions to four dimensions The four dimensions are composed of “organization / money(management)”, “information”, “human resources (Soft Logistics)”, and “physical resources (Hard Logistics)”. Each group (Muslim and Japanese) were in charge of each side, writing ideas(actions) on sticky notes, and clarifying and sharing solutions for the theme issue.

Keywords: Yonmenkaigi System Method, Multicultural Collaboration society, Disaster

©2020. Japan Geoscience Union. All Right Reserved.

A Proposal of Universal Design Teaching Material for Education of Disaster Risk Reduction

*Haruka Matsuoka[1], Kei Takashima[1], Tsukasa Sano[1], Asako Nakagawa[2], Seiji Hori[1], Minako Noda[1]

1. Faculty of Business and Informatics, Tsukuba Gakuin University, 2. Faculty of Home Economics, Otsuma Women's University

Typhoon Hagibis featured Category 5 strength on the Saffir–Simpson hurricane wind scale landed in Japan at 12th October, 2019 and triggered many deadly floods and landslides. In its wake, 99 persons were killed and 484 suffered injuries. Though many media had been reporting in the period, the death of 13 was added in the heavy rainfall occurred at 12 days after the disappearance of the typhoon.

More than seven million people were urged to leave their homes as such a huge storm approached, but it is assumed only 50,000 stayed in shelters. It revealed that the preparation prior to disaster, including the knowledge associated with the force of nature and the evacuation planning, is still insufficient even in Japan as known as a country of frequent natural disasters. The emphasis on education and knowledge for disaster risk reduction should be taken precedence.

Since the 70% of dead persons were over 60 years old in the typhoon mentioned above, we focus the education to the vulnerable person to disasters such as an old aged, a juvenility, and a foreigner in this study. The educational materials for visually understanding without difficult explanations are necessary for them. We propose them featuring pictograms to show actions to take in case of disaster. They could be universal teaching materials and greatly contribute to disaster risk reduction.

Keywords: Disaster Risk Reduction , educational material, universal design

©2020. Japan Geoscience Union. All Right Reserved.

Reconsideration of the Cause of the Accident Given in the Tsunami Judgment of Okawa Elementary School

*Mamoru Hayashi[1]

1. University of TOYAMA

The judgment of the Sendai High Court of April 26, 2018 became final and binding on October 11, 2019, with the Supreme Court's dismissal of the appeal filed by the defendant. The evidence collected by the plaintiffs, including the bereaved families, and the important testimonies of the persons concerned in the trial revealed the causes of the disaster until March 11, 2011, which was a great achievement of the trial. It was found that the life of the child would have been saved if the defendants, Ishinomaki City and Miyagi Prefecture, had taken measures against the earthquake off the coast of Miyagi Prefecture.

However, in a civil trial for the purpose of determining whether or not the accused is liable for damages, no fact-finding can be made that goes back to a deeper background cause. It has not been confirmed yet what measures taken by Miyagi Prefecture and the Japanese government to complement Ishinomaki City made the movement of teachers imperfect. For future school and regional disaster prevention, investigation and sharing of the disaster cause seem to be important.

However, in Ishinomaki City and Miyagi Prefecture after the judgment became final, both the mayors and the governor seem to be reluctant to investigate the cause and prevent recurrence. The Governor of Miyagi Prefecture rejected the proposal of Ishinomaki City Mayor, who requested Miyagi Prefecture to bear an appropriate burden, and said that the responsibility for compensation lies with Ishinomaki City. As the result, the division between the disaster inhabitants of Ishinomaki City continues.

Miyagi Prefecture, which started the 4th earthquake damage estimation in the summer of 2010, decided to exclude the two great historical tsunamis (869 Jogan, 1611 Keicho) from the countermeasures. The lives of many victims would have been protected if the historical fact that Ishinomaki Plain and Sendai Plain were flooded as much as 3 to 4 km from the coastline had been conveyed to the inhabitants as the assumption of local governments. It cannot be said that Miyagi Prefecture has no responsibility for the disaster.

Documents related to the process of Miyagi Prefecture's removal of historical tsunamis from its countermeasures were obtained through a request for disclosure. Together with hearing from expert committee members and persons in charge at that time and related information, large causes of disaster are approached. For disaster prevention education and disaster prevention measures to be promoted through cooperation between the prefecture and the city, and for the resolution of the division between inhabitants, the investigation of the background causes should be indispensable.

Keywords: responsibility of scientists, Okawa Elementary School Accident Investigation Committee, school disaster prevention, subsidiarity principle in local government, large tsunami in 869 and 1611, Responsibility of Miyagi Prefecture

©2020. Japan Geoscience Union. All Right Reserved.

2011年3月11日直前の重要動向

2010年6月17日	宮城県第4次地震被害想定調査業務打合せ（宮城県危機対策課とパシフィックコンサルタンツ株式会社），開示された打合せ記録簿では，「宮城県から福島県の沖合に想定される地震」が検討対象に含まれていた
2010年7月9日	同調査打合せ（同課・同社・東北大今村教授）で「宮城県から福島県の沖合に想定される地震」は資料から削除を決定
2010年7月12日	委員レク（長谷川教授）記録には「宮城県から福島県の沖合に想定される地震」はなし
2010年8月5日	宮城県第1回地震対策等専門部会
2011年1月27日	政府地震本部事務局が長期評価見直しについて宮城県に説明，宮城県の反応「貞観地震等の記載は，科学的事実であり，書かれることは仕方がないが，県としては対応が難しい」
2011年2月1日	宮城県第2回地震対策等専門部会で「第四次地震被害想定調査報告書」（中間報告）発表
2011年2月	大川小で総合防災訓練打合せ：校長が（5mの堤防を）「津波が漏れてというか，越してくるようなことはないんですか」と質問，石巻市河北総合支所担当職員は「計算上，津波は越してこないことになっている」と回答
2011年3月9日	予定されていた長期評価記者発表中止（電力の横やり），牡鹿半島沖地（M7.3）発生で大川小児童ら校庭避難，東北大松澤教授が「ガス抜き」発言
2011年3月11日	東北地方太平洋沖地震発生，東日本大震災津波被災

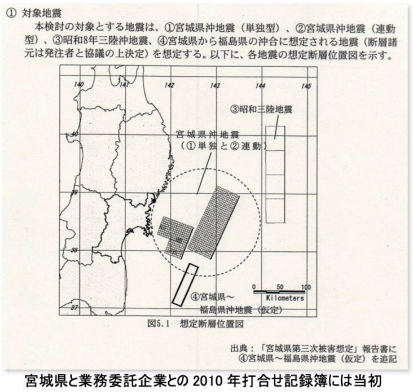

宮城県と業務委託企業との 2010 年打合せ記録簿には当初「宮城県～福島県沖地震」が想定地震として記されていた

2019年10月大川小裁判判決確定後の動向

2018年4月：仙台高裁で原告勝訴，その後，被告（石巻市と宮城県）が上告
石巻市と宮城県に連帯して14億3617万4293円と遅延損害金の支払いを命じた
2019年10月11日：最高裁上告棄却（仙台高裁判決が確定）
（10月12日：台風19号が本州に上陸・北上，石巻市はじめ宮城県内でも被害発生）
10月15日：石巻市長と宮城県知事面会（応分の負担を求める市長提案を知事が拒絶）
宮城県知事の説明：宮城県は給与を負担しただけであり，賠償責任は一義的に石巻市にある（校長等＝大川小校長，教頭，教務主任，石巻市教委の組織的責任）。郡山市行健中学校いじめ事件最高裁判例でも福島県は郡山市に「求償できる」となっている。
10月17日：宮城県議会議員全員協議会（およそ20億円全額を宮城県が立替払し，石巻市が10年で返す案が説明されるが，反対意見も目立つ）
10月18日：石巻市議会議員全員協議会（上記案が市長から説明され，議会は紛糾，臨時議会開催決定）
10月20日：石巻市議会臨時会（反対意見が3名の議員から詳しく述べられたが反対4，賛成25で上記石巻市案を盛り込んだ補正予算案が可決成立）
県議会・市議会での反対意見のポイント：県と市町村が連携する学校防災の事例と過去の判例事例とは異なる。連敗した弁護士に従うだけでなく，連勝した原告弁護団からも意見を聞くべき（市長は調査ならびに県との協議の余地あるのを認める）
10月25日：石巻市と宮城県との覚書締結（不測の事態が生じた場合は両者で協議する旨あり。その後，賠償金が原告に支払われる）
12月1日：亀山紘市長が石巻市河北総合センターで遺族と面会「未来ある尊い命が失われ，取り返しのつかない悲劇を引き起こした。申し訳ありませんでした」と謝罪（＊註）。その後，大川小に移動，遺族と大川小跡地に移動，協力して大川小校舎，校地を震災遺構として活用していくことを確認。石巻市，宮城県の教育長ら幹部も同席。

＊産経新聞ネット版12月1日（16時10分）付は，亀山市長が「公式の話し合いの場で遺族と面会するのは2014年3月以来。市教育委員会や学校はこれまで，法廷での審理を含め，責任の所在を明確にしてこなかった。市教委が招待状を送付した児童74人の遺族のうち27人が参加した。ただ「形だけの謝罪はいらない」として参加しない遺族もいた」と速報している。

名取市津波防災マニュアル(2001)から

©2020. Japan Geoscience Union. All Right Reserved.

Case report of education about earthquakes and faults in elementary schools

*Noa Mitsui[1], Kumi Yoshitake[2], Kazuyuki Nakagawa[3]

1. Tono Research Institute of Earthquake Science, 2. University of human environments, 3. Jiji Press

In general, disaster prevention education conducted in and around the stricken areas focuses on passing down disaster experiences. This education has a difficulty in maintaining their activities because the number of survivors has decreased due to the change of generations.

On the other hand, geoscientific phenomena itself that causes disasters are universal. Therefore, the education, consisting of geoscientific phenomena as main contents and the resulting disasters as additional contents, enables continuous disaster prevention education combining "cause = geoscientific phenomena" and "result = natural disasters". Such education is intended even in the current science education, and it is realistic to determine guidelines for effective teaching methods based on practical examples.

In this study, we focus on earthquakes and the disaster. The importance of disaster prevention education is discussed based on an example of education about earthquake and faults in elementary schools and its effect on the students in time of disaster occurrence (Nakagawa, 2017, JpGU). We also point out that a new result expected from disaster prevention education is that "acquisition of knowledge of geoscientific phenomena in advance mitigates psychological damages caused by disasters".

Keywords: elementary school, education, prevention and mitigation of psychological damages, Kumamoto earthquake

©2020. Japan Geoscience Union. All Right Reserved.

Consideration on Education of Disaster Prevention Jointly Practiced with the Field

*Erina Hyuga[1], Ami Pareek[1], Hikari Tanaka[1], Mirei Toba[1], Chisa Funada[1], Satoko Oki[1]

1. Keio University

1. Background of the Study

The Great East Japan Earthquake in 2011 was an unprecedented catastrophe. It triggered an increase in social demand for disaster prevention education. On the other hand, according to MEXT (2014), disaster prevention education has not been effectively performed in schools. Also, Nagamatsu and Oki (2015) revealed that many teachers are aware of the necessity of disaster prevention education but that it’s difficult for them to carry it out. Based on such situation, Oki Seminar to which the author belongs has examined the ideal way of disaster prevention education jointly with teachers.

2. Field of this Study

The field of this study is schools in Kawagoe City, Saitama Prefecture. Authors and Kawagoe City Board of Education have carried out practical disaster prevention education research jointly since 2017 fiscal year. In FY 2017 and FY 2018, we examined the effects of teacher trainings using narrative approach (Pareek, 2018; Pareek, 2019). In the 2019 fiscal year, 4 schools in Kawagoe city were made to be model schools, and we examined the changes which arose in students and teachers in the model schools.

3. Approach Method and Efforts at Model Schools

We approached both students and teachers through classes and trainings. Using data such as questionnaire surveys before and after the intervention, hearing surveys after the implementation of classes, we would examine and analyze the effects on students and teachers. In this fiscal year, the questionnaire was also carried out to the protectors of all school pupils of the model schools. Teachers who observed the classes of the authors carried out the class in their own grade. The class carried out by the teachers was arranged based on character of the children. It’s a teachers' own strength and we authors do not have that. In addition, the approach which took in the new teaching guideline of the next fiscal year was also introduced such as incorporating disaster prevention in the science class. In the training for teachers, some teachers pointed out that it was necessary to reexamine the ideal way of the current training, which indicates that teachers' consciousness has been changing.

4. Report from Model Schools

The principals of the model schools said that there was a scene in which the consciousness of disaster prevention was improved even in the daily life such as not only the initial action in the training greatly changed, but also the conversation on earthquake and past disaster increased. In addition, it has been reported that teachers became eager to verify the teaching method of safety education. There were many teachers who began to have the question to the evacuation training which merely followed the content of the previous fiscal year.

5. Future Prospect

In the fiscal year end, we will confirm the details of the changes which arose for children, teachers and parents. And, from the 2019 fiscal year, it became possible to carry out the investigation to the schools other than the model schools. We will investigate what kind of effects the challenge of the model schools gives to other schools and will also verify the way to spread disaster prevention education.

©2020. Japan Geoscience Union. All Right Reserved.

References
・Ministry of Education, Culture, Sports, Science and Technology (2014), 'Enhancement of safety education at schools' (summary of deliberations).
・Tosei NAGAMATSU and Satoko OKI (2015), 'Effective disaster prevention education incorporating local risks', Japan Geoscience Union Meeting 2015 24 May -28th MAKUHARI MESSE.
・Ami PAREEK (2018), 'Better disaster prevention training using narratives', Keio University SFC graduation thesis.
・Ami PAREEK (2019), 'Introduction of Narrative Approach for Earthquake Disaster Prevention (BOSAI) Teacher Training: Practice in Saitama Prefecture', Japan Geoscience Union Meeting 2019 May 26th -30th MAKUHARI MESSE.

Keywords: Education of disaster prevention, School, Joint Practice

©2020. Japan Geoscience Union. All Right Reserved.

Junior high school students experienced the "Shelter Management Game"

*Takeshi Matsumoto[1]

1. Faculty of Science, University of the Ryukyus

In disaster prevention education, "how to escape" (avoiding the disaster) is often emphasized. However, depending on the location conditions of schools, it is necessary to prepare the "how to accept" side (setting up and managing shelters, protection of victims, etc.) at all times.

The "Shelter Management Game" (HINANJO HUG) is a game-style shelter management experience tool developed by Shizuoka Prefecture. In the event of a large-scale disaster such as a huge earthquake or tsunami, schools and community centres, which are designated by local governments in advance, become shelters. The people who come to evacuate these disasters are various, such as the elderly, the sick, and the person with small children. Recently tourists from foreign countries led by tourism workers, as well as foreigners living and working in the local area, may come to the shelter. The players of the game is assumed to be in a position to operate the shelter appropriately as an officer of the local community association or the voluntary disaster prevention association. The game uses the "evacuee cards" which are to be placed properly in the school gymnasium and classrooms. The "event cards" including information from the headquarters and requests from evacuation centres are also placed for players to respond properly in the shelter. Teamwork and role-sharing by discussing how to respond to the card are to be required to the player's team.

Once a year, the University of the Ryukyus Junior High School offers special classes for students by university teachers. Therefore, the author gave a special lecture titled "Real Experience! Management of shelters" to the grade 9 junior high school students on November 28, 2019 by use of the "Shelter Management Game".

In the questionnaire after the end of the class, 7 answered "It was easy to understand" and 7 "There were some difficulties, but I could understand mostly" in response to the question "Was the contents of the class easy to understand?". 9 answered "It was very interesting" and 5 "It was interesting" in response to the question "Were you interested in the content of the class?".

When the author facilitated the HUG workshop at a community centre and a school child care facility, the majority of the participants were adult and some high school students participated. This special class was the first trial for the grade 9 junior high school students for the author. One of the purposes of this attempt was to see whether the junior high school students were able to act appropriately in such a situation. As a result, even junior high school students can act almost in the same way as adults. The author was able to be convinced that the junior high school students would be able to cooperate in the shelter management enough even if their school was designated as a shelter.

Keywords: Natural Hazards, Shelter Management

©2020. Japan Geoscience Union. All Right Reserved.

What is the "comprehensive" in disaster prevention education?

*Hitoshi Nakai[1]

1. Kobuchisawa Research Institute for Nature and Education

In a conventional disaster prevention education course, students generally learn how people were affected in previous disasters, and perform disaster drills. Their motives to participate in such programs are their own anxiety about a possible disaster and sympathy for victims. It is, so to speak, education that appeals to their emotions. Due to these characteristics, conventional disaster prevention education can only be carried out in disaster-affected areas and tends to decline in effectiveness when several decades have elapsed since the event and the memory of the suffering endured has grown dimmer. The author argues that a new educational program that appeals to the intellectual side of students by presenting knowledge on disaster prevention in systematic form would be a more effective approach. The new disaster prevention education program is outlined in this paper. It will enable students to acquire a strong awareness of the importance of disaster prevention.

Keywords: comprehensive disaster prevention education, continuous and nationwide disaster prevention education, Systematization of disaster prevention education

©2020. Japan Geoscience Union. All Right Reserved.

[J] Poster | G (General)：General

[G-03] Geoscience education from elementary school to university students

convener:Masatsune Hatakeyama(Seiko Gakuin High School), Yoshihiro Niwa(Center for Ocean Literacy and Education, Graduate School of Education, The University of Tokyo)

We will provide and discuss various educational practices (teachings and procedures) for elementary, junior high school, high school and university students. We also welcome fieldwork reports and outreach reports for all grades. In addition, especially for liberal arts level geoscience education of undergraduate, we will consider the problems and future prospects of our current geoscience situation. Furthermore, we will also think about common teaching material development and sharing of teaching material data.

[G03-P01] Recipe 2.0 for rock thin-section study in a classroom. Part 1. Observation

*Yoshio Okamoto[1] (1.Kamnoetvidya Science Academy, PCSHS Mukdahan, Thailand)

[G03-P02] Recipe 2.0 for rock thin-section study in a classroom. Part 2. Making

*Yoshio Okamoto[1] (1.Kamnoetvidya Science Academy, PCSHS Mukdahan, Thailand)

[G03-P03] Implementing Concept Mapping to Evaluate College Students' Ocean Literacy

*ChengChieh Chang[1], YaHsin Lu[2], LiangTing Tsai[2], KuoChen Chang[2], ChunChieh Hsu[1], MeiChun Lin[2], TingKuang Yeh [3] (1.National Taiwan Ocean University, 2.Taiwan Marine Education Center, 3.National Taiwan Normal University)

[G03-P04] The Oceanographic Society of Japan (JOS) School Visit Program

*Yushi Morioka[1], Naoki Fujii[2], Ueno Hiromichi[3], Akihiro Senda[4], Hideki Kaeriyama[5], Sayaka Yasunaka[1] (1.Japan Agency for Marine-Earth Science and Technology, 2.Saga University, 3.Hokkaido University, 4.The Japan Science Society, 5.Japan Fisheries Research and Education Agency)

[G03-P05] Using a borehole for groundwater observation in junior high school

*takashi morie[1] (1.Faculty of Risk and Crisis Management, Chiba Institute of Science)

[G03-P06] Hands-on learning of science for elementary school students in Kyotango-city,Kyoto Prefecture.

*Makoto Obase[1] (1.kyoto Prefectural Mineyama High School)

[G03-P07] The Logical Thinking Ability that High School Students want to acquire through Inquiry Learning

*Kazuya Kawakatsu[1] (1.Hyogo Prefectural Himeji Higashi senior high school)

[G03-P08] Future Geospatial Information Authority of Japan Geography Education Support Based on Questionnaire Results to High School Geoscience Teachers

*Hiroaki Tanaka[1], Ryouichi Kojiroi[1] (1.Geospatial Infomation Authority of Japan)

[G03-P09] Learning ambient noise analysis with Raspberry Pi and accelerometers

*Naofumi Aso[1], Ritsuya Shibata[1], Junichi Nakajima[1] (1.Tokyo Institute of Technology)

Recipe 2.0 for rock thin-section study in a classroom. Part 1. Observation

*Yoshio Okamoto[1]

1. Kamnoetvidya Science Academy, PCSHS Mukdahan, Thailand

In geoscience education, the thin-section study is a fundamental method to comprehend geology. However, it is tough to carry out a thin-section study in a secondary school classroom. It is difficult for the ordinary school to prepare enough number of polarized microscopes and thin-sections. Therefore we introduce an alternative method to carry out the thin-section study in a secondary school classroom. Our study divided two categories; i) Home-made polarized microscope unit: observing thin-sections and ii) An alternative thin-section making method: using new tools for rock cutting and grinding. The title 2.0 means a sophisticated method rather than a traditional 1.0. Also, I am not a specialist in petrology, so please let me know if mistakes.
In this article, we describe the first method. The making process of thin-sections is described in the next poster. Usually, a polarized microscope is high expensive and not be prepared in the science classroom at secondary school. Therefore, we propose an easy-made polarized unit assembled with a cheap microscope sold at the online shopping site around 160 USD. It has two light systems at the top and the bottom. The alternative USB microscope sold reasonable cost, is also useful to capture photos using this unit.
The unit consists of three parts; 1) turntable; a cheap one purchased from the online net shop (70mm square having 37mm hole in the center, 4 USD) 2) polarized film; purchased from the same shop (10 pieces of 8cm square size, 9 USD) and are used in quarter size. 3) acrylic plates: 70x70mm, 5mm thickness with 25mm center for the turntable, 45x90mm, 3mm thickness for the upper Nicol.
The turntable and two 5mm thick plates are assembled with 4mm bolts sandwiching a polar film. The upper Nicol is made by a 3mm thick plate and a polarized film. It can be turned over the stage. Acrylic glue is used to join the plates. The acrylic end materials are sold at some online shops.
The unit is set on the microscope stage, and thin-sections are placed on the turntable for observing. We made ten units of the units and twenty of more simplified units (the rotation is made by hand) attached with binocular microscopes. The total number of microscopes is 42, including 12 professional polarized microscopes. Forty-two students of our geoscience class can use their microscopes and some thin-sections. The observation time is 50 minutes; the students observe granite, andesite, basalt, and gabbro samples. For help to the observation, we use a USB microscope to show the thin-section images on the big monitor. We presented how to identify the minerals and optical properties: 1) non-color minerals; quartz and feldspar (form, cleavage, twin) 2) colored minerals; biotite, hornblende, pyroxene, olivine (form, cleavage, refractive index, interference color, pleochroism, extinction angle, twins) The students thoroughly enjoyed the observations, sketching their eye view, or taking a picture by smartphones for uploading to their SNS. The questionnaire results also show an excellent performance of this practice. The details of the questionnaire results will be presented at the conference.
The merit of our unit is low cost about 170 USD for a microscope and 20USD for a polarized unit. Also, such cheap microscopes already installed the bottom LED system, so the students can easily carry out their observation. However, their low magnification around 20x to 40x is somewhat insufficient for optical mineralogy, and cheap turntables show some backlashes. Also, our system has no aperture system, so it is hard to recognize Becke lines. Moreover, our system has no subsequent functions of advanced optical mineralogy such as interference plates, or a conoscope imaging system. However, our system has an excellent feature for educational geology, and some improvement for high magnification will increase the

©2020. Japan Geoscience Union. All Right Reserved.

performance in the future. The making process of the thin-sections is presented at our next poster: Part 2.

Keywords: Thin-section, Polarized microcope, observation, classroom

©2020. Japan Geoscience Union. All Right Reserved.

Recipe 2.0 for rock thin-section study in a classroom. Part 2. Making

*Yoshio Okamoto[1]

1. Kamnoetvidya Science Academy, PCSHS Mukdahan, Thailand

In a classroom, for the sufficient study of thin-sections, we have to prepare many samples. However, they are very high expensive, around 20 USD for each thin-section, so we can not purchase enough samples. For this reason, we tried to make home-made tools for the thin section making. Instead of the use of high-cost rock saws or rock-grinders, we try to use inexpensive mass production machines for the base of our system. Easy-making additional tools can complete cheap alternative tools. A table-top bench grinder and a rotary kitchen sharpener are chosen. They can be purchased from a DIY store less than 100USD for each.
In our trial, for the rock saw, we use a 150mm twin bench grinder as a base machine, and one side of the grindstone is removed, including its cover. A water tank with a table made from acrylic plates is fixed to the base of the motor with bolts. For the rock sawing, a cheap diamond blade (160mm to 180mm diameter, 1mm thickness) is mounted on the motor shaft with arbors, which is made using a table-top lathe machine. Except for this lathe operation, most of the processes can be completed with usual electric tools. For the cutting of acrylic plates, we use a hand cutter and glue specialized for acrylic work. On the water tank, an aluminum 3mm thickness board, having a slit for the blade, is fixed as a saw table. Also, at the bottom of the tank, a draincock was drilled.
The rock sawing is carried out with a quarter filled water. For safety, we have to set the ground for the electric system. A 1mm thick diamond blade is useful for the generic rock sawing. We can smoothly cut around the fist-sized rock with enough motor torque. When we cut the glued rock sample attached to the slide-glass, we set a guide for thin rock sawing on the table using a cramped acrylic block. After some training, we can cut the section within 0.5mm thickness. For the rock and glass gluing, a 90-minute hardening "Bond-E" is used. Also, we use a hot-plate for rock warming to make glue more liquidity.
Next is rock grinding. Hand grinding is the primary way of traditional method; however, we use a new grinding machine based on a kitchen knife sharpener, which consists of a rounded wet stone, a water tank, and a motor. A diamond grinding disk, 180mm diameter and 1mm thickness around 15 USD, is set and fixed on the wet stone by an extensional bolt. This tool is used for the rough (#180) and middle (#400) grinding stage, holding the thin-section by your finger to keep on the rotating disk with water poring. After masterly, the thin-section reaches 0.1mm or less thickness for a few to ten minutes. Nevertheless, the final fine grinding is still processed by hand like the traditional method. Because even a finer grit #1000 or much always makes scratch scars on the thin-section surface. In the final hand grinding, #800 carborundum and #1500 alundum + water are used on the glass plates. After completed grinding, a cover glass is glued on the thin section using soft UV resin. UV resin is useful because it causes fewer air bubbles than the traditional Canada balsam. After the cover glassing, the resin is cured with UV light or sunlight. Finally, the surplus resin is removed by a cutter knife and manicure remover (acetone). The name label is put on, and the thin-section is completed.
By our method, the total time is shortened almost around one hour to a couple of hours excepting gluing time, while the traditional way takes almost a half to a full day. This method provides more parallel surfaces and less defective thin-section compared with the traditional making process.
In the future, we try to mechanize the final stage; however, now we can not succeed in solving the scratches problem. After the introduction of our new tools, almost 200 new thin-sections are completed successfully. Such making process of thin sections and machines are not so complicated for a student's practice. So, it may be suitable for the geoscience club activities at the senior high school level.

©2020. Japan Geoscience Union. All Right Reserved.

Keywords: Thin-section making, Rock saw, grinding machine, geoscience club

©2020. Japan Geoscience Union. All Right Reserved.

Implementing Concept Mapping to Evaluate College Students' Ocean Literacy

*ChengChieh Chang[1], YaHsin Lu[2], LiangTing Tsai[2], KuoChen Chang[2], ChunChieh Hsu[1], MeiChun Lin[2], TingKuang Yeh [3]

1. National Taiwan Ocean University, 2. Taiwan Marine Education Center, 3. National Taiwan Normal University

The purpose of the study is to understand freshmen in the university regarding marine science concepts by using concept map method (open-ended tasks) and an open-ended question, and to assess their misconceptions about marine science concepts. A survey method was conducted on students from three departments of National Taiwan Ocean University(NTOU),Taiwan. In pre-test,a total of 305 samples was distributed, and a validity count of 294 was returned.In post-test,a total of 140 samples was distributed, and a validity count of 134 was returned.Using questionnaires as research instruments,the data were subject to concept mapping and SPSS statistics.The results of this study were as follows:
1.The answers provided by the students of NTOU with the assistance of propositional concept maps showed the average mark 63.07 out of 150,indicating only a basic understanding of marine science concepts among these students.
2.The first three terms "Submarine Volcano", "Mid-Ocean Ridge", and "Ocean currents" were the most commonly used by students to express marine science concepts. The first term "Submarine Volcano" was 131 times.The other two terms "Mid-Ocean Ridge" and "Ocean currents"appearred 126 and 113 times, respectively.
3.The marine concepts were more knowledge-oriented in the cognitive domain than attitudes and affective domains.We also observed the knowledge-oriented(46.4%), the affective-oriented(16.0%), the attitude-oriented(11.6%), and misconception-oriented(5.2%).
4.The scores of the post-test propositional concept maps were higher than that of pre-test. Therefore, it's helpful to the ability of marine sciences that students attend in the class of Introduction to Environmental Science Related to Marine. The total scores of ME were $t=-3.166, p<0.01$, and the total scores of MM was $t=-4.092, p<0.001$.
5.The marine science concepts we provided were mostly accuracy-oriented.In accuracy-oriented, the scores of CSE was $t=-4.752, p<0.001$, the scores of CSE was $t=-4.814, p<0.001$, and the scores of MM was $t=-5.950, p<0.001$.
6.The three marine words "Submarine Volcano","Oceanic trench" and "Plate" were most frequently misconstrued by students.
7.The most misconceived statement of the marine misconception assessment was "the relative connections of submarine volcanoes, plate, and mid-ocean ridges","salinity of the ocean","depth of the oceanic trench", and "the difference between tides and ocean currents".

The study can assist researchers and higher education in improving the quality and effectiveness of infusing marine education into curricula and promote ocean literacy.

Keywords: Ocean literacy, marine science, concept map, misconceptions

©2020. Japan Geoscience Union. All Right Reserved.

The Oceanographic Society of Japan (JOS) School Visit Program

*Yushi Morioka[1], Naoki Fujii[2], Ueno Hiromichi[3], Akihiro Senda[4], Hideki Kaeriyama[5], Sayaka Yasunaka[1]

1. Japan Agency for Marine-Earth Science and Technology, 2. Saga University, 3. Hokkaido University, 4. The Japan Science Society, 5. Japan Fisheries Research and Education Agency

Oceanography plays a major role in Earth and Planetary Sciences, but it is not well recognized nor understood among the general public due to few opportunities of learning oceanography at primary-high schools and universities. Give this situation, the Oceanographic Society of Japan (JOS) has initiated a school visit program on oceanography since 2016, by dispatching ocean science professionals to schools and public facilities in order to improve ocean literacy. To date, 40 lectures have been carried out nationwide, involving a wide variety of subjects related to school teaching materials and cutting-edge ocean science. Since 2018, JOS has collaborated with The Japan Science Society (JSS) to accept their school visit program on “Cubic Earth”. In addition, the JOS has performed several outreach activities in the relevant public events. These domestic activities are also expected to contribute to both the Sustainable Development Goals (SDGs) and the UN Decade of Ocean Science for Sustainable Development (2021-2030) from the perspective of ocean education. In this presentation, we will introduce outreach activities in oceanography such as school visits of ocean science and the Cubic Earth.

Keywords: The Oceanographic Society of Japan, Marine Education, School Visit Program

©2020. Japan Geoscience Union. All Right Reserved.

Using a borehole for groundwater observation in junior high school

*takashi morie[1]

1. Faculty of Risk and Crisis Management, Chiba Institute of Science

We used a borehole to understand groundwater for junior high school students in Tokushima Prefecture Southwest Japan. The borehole 10 m in depth was digged for geological survey and located in the school ground. Students observed temperature, smell, resistivity and level of groundwater in one or two hours of science class in November 2012. They realized abundant groundwater around the school and found relationship between groundwater level and daily rainfall amount. Groundwater is an impressive topic in science and environment educations in junior high school.

Keywords: groundwater, junior highi school, borehole

©2020. Japan Geoscience Union. All Right Reserved.

Hands-on learning of science for elementary school students in Kyotango-city,Kyoto Prefecture.

*Makoto Obase[1]

1. kyoto Prefectural Mineyama High School

Hands-on learning of science for elementary school students in Kyotango-city,Kyoto Prefecture. About 5,000 students participated this program in 10 years.

Keywords: elementary school science education, outdoor activity, geopark, stratum and fossil, volcano and earthquake, natural environment and marine garbage

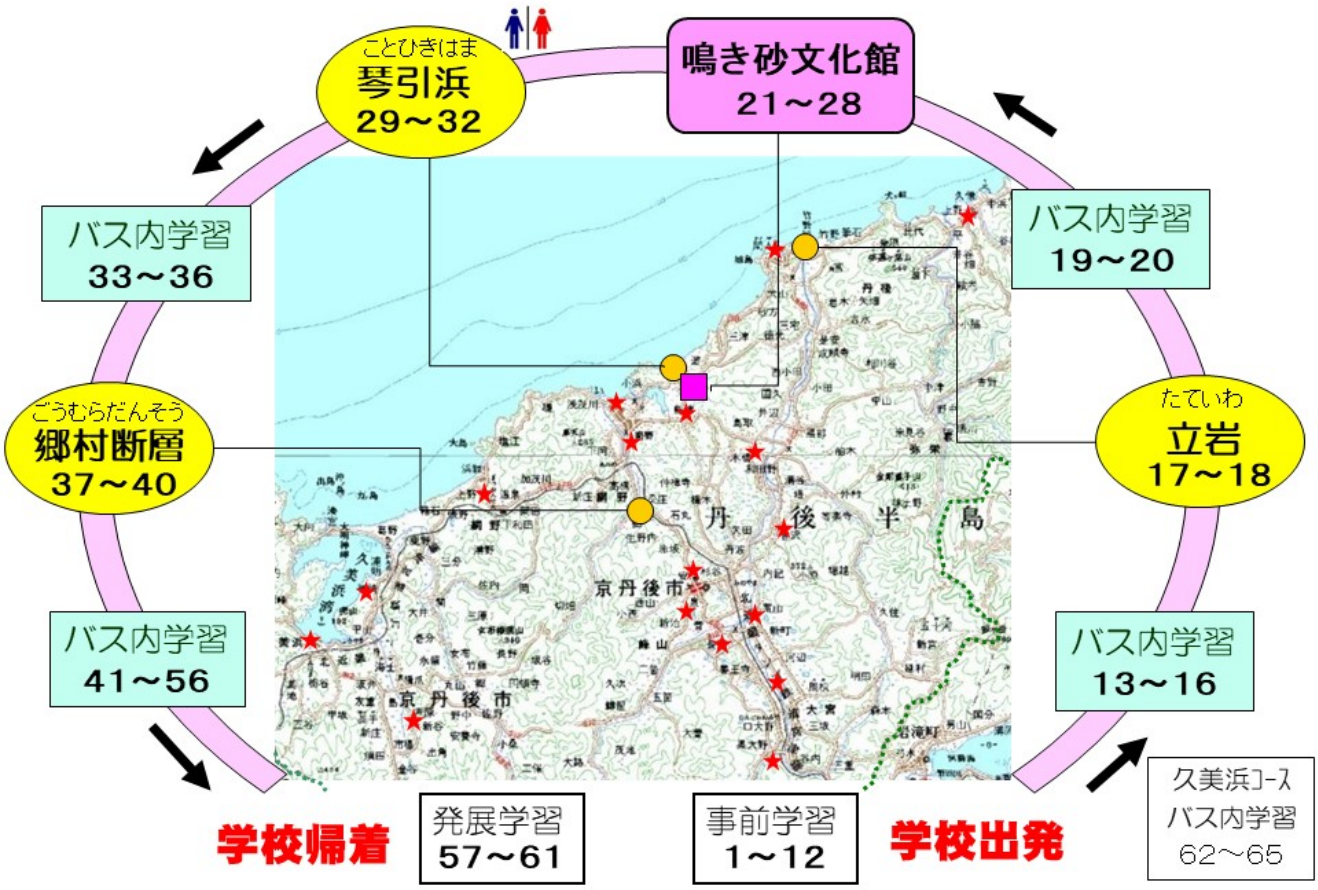

©2020. Japan Geoscience Union. All Right Reserved.

The Logical Thinking Ability that High School Students want to acquire through Inquiry Learning

*Kazuya Kawakatsu[1]

1. Hyogo Prefectural Himeji Higashi senior high school

1. Introduction

In traditional high school education, training has focused on how to quickly and accurately answer a question for which the answer is known. There was an answer in the content of the learning, so there was a set procedure on the way to it, and it was possible to learn manually and it was easy to learn. However, like many phenomena around us, we do not have the experience of thinking about how to solve a question that has no answer or does not know whether there is an answer. There is an urgent need to foster the ability to survive in an AI society, such as the ability to think flexibly, discuss, and communicate to others.

Many teachers themselves have worked on tasks that have answers in their school days, so they don't know how to teach them about unanswered questions. Teachers don't know the answer, so there is no manual on how teachers teach it. Teachers' specialized approaches are often useless. Not sure how to teach, teachers are grappling, despite recognizing the need for inquiry education.

If there is a manual in the process of inquiry, it is as follows. (1) Be interested in familiar phenomena and question various phenomena. (2) Think about how to answer your questions. (3) From the obtained results, consider without prejudice such as guesswork or galling. (4) Write the paper in an objective way using mathematics instead of an impression sentence, and convey it to others.

2. What is required for inquiry learning

The power required for inquiry requires logical thinking ability based on hypothetical deduction. Here I will summarize two points that are not often mentioned. They are logical thinking and ethical thinking.

(1) Statistics

I give the following examples to students. I bought a pack of eggs from the same store on the same day. Eggs packed on the same day. After a while, I was worried that it was not damaged. No, so the rest of the eggs are not damaged? Student's answer is no. So, if you're OK with breaking the second, can you say that the rest is not damaged? Students also answer no. So how many pieces can we say are all eggs intact? The answer is all.

In an information program, an announcer said, iPS cells have been proven to differentiate into various tissues, which is scientifically strange. There is no proof because not all iPS cells can be confirmed to differentiate into tissue. However, the more surveys you make, the more certainty you can get. This is

©2020. Japan Geoscience Union. All Right Reserved.

where students need to learn statistics, whether they are high school students.

(2) Scientific ethics

For scientists, what is technically possible and what can be done are not the same. It is understandable given the social impact of scientists. Even today, when high school students' scientific research has flourished, it is critical that science ethics is not properly learned in high school. In addition to providing guidance and advice on the contents of the research, it is necessary to learn about its ethical considerations.

3. Teachers' attitude toward exploration

Many teachers are new to teaching, have no instruction, and do not know how to work. The points are as follows. (1) If you have any doubts, work on your quest with your students without thinking that you have to achieve results. At this stage it is enough for the teacher to snuggle, interesting and strange, why. (2) Students will naturally bring out new ideas in the discussion. When the results are available, the teacher actively participates in student discussions and verifies the logical consistency of the discussion.

Keywords: Inquiry Learning, Statistics, Scientific Ethics, Logical Thinking

©2020. Japan Geoscience Union. All Right Reserved.

Future Geospatial Information Authority of Japan Geography Education Support Based on Questionnaire Results to High School Geoscience Teachers

*Hiroaki Tanaka[1], Ryouichi Kojiroi[1]

1. Geospatial Infomation Authority of Japan

1.Introduction
Geospatial Information Authority of Japan (hereinafter referred to as "GSI"). Has recently been focusing on geographic education support. However, when I look at the work of the GSI, I consider that its contents will greatly contribute to geoscience education. From this point of view, I recently introduced the GSI map and its contents to teachers of high school geosciences in Saitama and Chiba prefectures, and had the opportunity to conduct a questionnaire (hereinafter referred to as “Saitama” and “Chiba”). Omitted). The results and considerations are introduced.

2. About the questionnaire conducted
The survey targets Saitama Prefecture, which has held meetings every year since 2015 and counts a total of five times, and Chiba Prefecture, which is held for the first time this year.
In the questionnaire, we asked about the awareness of the GSImap and the toolbox for geography education, how they were used, and their requests. As for the implementation method, the people who came to the poster presentation in Saitama Prefecture answered the questionnaire, and Chiba Prefecture distributed it as part of the materials and collected it after the closing ceremony. The number of responses was 16 in Saitama Prefecture and 27 in Chiba.

3. Questionnaire results
Details of the response results will be shown in the announcement. From some results, it was found that as a general tendency, the GSI maps was highly recognized, but the degree of use in classes etc. was low.

4. ConsiderationWhat can be said from the results of the questionnaire is as follows.
Recognition has been raised by past activities to disseminate the Geographical Institute map, and the effects of the dissemination activities are seen. On the other hand, the toolbox for geography education, which was introduced for the first time this year, proved difficult to recognize. Also, if you have used the Geographical Institute's website for actual school activities, Chiba has a higher awareness of the toolbox for geography education than Saitama, and in Saitama how to access the Geographical Institute map directly Therefore, it is probable that he went directly to the Geographical Institute map without looking at the others.
Based on the above, although it is effective for publicity activities, new sites such as tool boxes for geography education are not noticed in the present situation, so to disseminate it not only in the geography field but also in the geology field It is important for teachers and staff members to take an

©2020. Japan Geoscience Union. All Right Reserved.

active role. In addition, I think that it is better to show how to use some killer content in which class to actually use it.

Keywords: Geography Education Support, high school geology, GSI maps, questionnaire

©2020. Japan Geoscience Union. All Right Reserved.

Learning ambient noise analysis with Raspberry Pi and accelerometers

*Naofumi Aso[1], Ritsuya Shibata[1], Junichi Nakajima[1]

1. Tokyo Institute of Technology

Seismograms that we analyze in seismology are not always associated with earthquakes. The Earth's surface is always shaking primarily from oceanic noise due to tidal forces. Analyzing this ambient noise is attracting much attention in seismology for its potential for estimating crustal structure without earthquakes. We developed an educational material to present such a frontier technique in seismology, in which we analyze seismic waves in a more general sense.
Specifically, we connect small accelerometer chips, which are considered to be seismographs, to Raspberry Pi and mimick ambient noise analyses. Two LIS3DH sensors transfer three-dimensional acceleration data to Raspberry Pi through serial communications based on SPI protocol. Raspberry Pi calculates cross-correlation functions of previous five-second seismograms of the station-pair every one second. By multiplying the differential travel time by seismic velocity, we get the distribution of seismic energy as a function of differential travel distances. LEDs connected to the Raspberry Pi display the function so that the system works as a stand-alone real-time source locater. The current system considers two-dimensional data for the simplicity of the system and coding but can be upgraded to three-dimensional as an advanced assignment.
While this tool can be used to determine source location assuming seismic velocity as mentioned above, we can also estimate the seismic velocity using this for a known source. The material perfectly suits for learning frontiers in seismology, including ambient noise analyses and back-projection analyses, but is suitable for learning programming or digital circuit in a more general sense.
We release this material in an outreach event at the Tokyo Institute of Technology in March 2020. We also introduce slow earthquakes, which is another hot topic in seismology, by providing how to analyze seismicity using the "Slow Earthquake Database".

Keywords: Seismology, Raspberry PI, Accelerometer

©2020. Japan Geoscience Union. All Right Reserved.

[J] Poster | G (General)：General

[G-04] Geoscinece Outreach

convener:Jiro Komori(Teikyo Heisei University), Takeyuki Ueki(Faculty of Risk and Crisis Management, Chiba Institute of Science), Naoko HASEGAWA(Ochanomizu University), Satoko Oki(Faculty of Environment and information Studies)

The aims of Outreach and geoscience education are to encourage developments that raise public awareness of geosciences through schools and/or public outreach by not only educators but also researchers. Therefore, any presentation related with these aims will be welcomed to this session. Depending on schedule and venue,some presentation will be changed to Poster presentations.

[G04-P01] Diversity concept of the new curriculum "Inquiry learning"-To increase the number of student's presentations-

Masao Mukoh[2], *Tomoko Goto[1], Kazuyo Nagahama[3], Hideki Ishida[4] (1.Earthquake Research Institute, the University of Tokyo, 2.Tokyo Metropolitan Institute Fuji Senior High School・Junior High School, 3.Mejiro University, 4.Tohoku University)

[G04-P02] Kochi Core School for Asian Young Scientists at Kochi Core Center: new international outreach activity in marine sediment core and related sciences

*Go-Ichiro Uramoto[1], Hiroki Matsui[1], Kazuno Arai[1], Naohisa Nishida[2], Hirofumi Asahi[1], Yusuke Kubo[3], Satoshi Tonai[1], Wataru Tanikawa[3], Yurika Ujiie[1], Yuhji Yamamoto[1], Minoru Ikehara[1] (1.Kochi University, 2.Tokyo Gakugei University, 3.Japan Agency for Marine-Earth Scienct and Technology (JAMSTEC))

[G04-P03] A Pilot Study of an Active Learning Program for the General Public using Radiological Monitors

*Haruka Matsuoka[1] (1.Department of Business and Informatics, Tsukuba Gakuin University)

[G04-P04] Spread of hemispherical multi-touch panel for rear projection type digital globe "Dagik Earth"

*Yukinobu Koyama[1], Akinori Saito[2] (1.KINDAI University Technical College, 2.Graduate School of Science, Kyoto University)

[G04-P05] Practice report of geological excursion for elementary school students using terrain model made by 3-D printer

*Iida Kazuya[1] (1.Komaba-Toho Junior and Senior High School)

[G04-P06] A support activity for field excursion by a voluntary organization “Geo-Education”

*Jiro Komori[1], Tomoaki Kitayama[2], Iida Kazuya[3] (1.Teikyo Heisei University, 2.JAMSTEC, 3.Komaba Toho Junior & Senior High School)

[G04-P07] The report of the International Earth Science Olympiad (IESO) 2020

*Norihito Kawamura[1], Yutaka Takigami (1.School of Regional Resource Management, Graduate School, University of Hyogo)

[G04-P08] Standing on an asteroid: using virtual reality for outreach and education

*Elizabeth Tasker[1], Alexander Kaurov[2,3] (1.Institute of Space and Astronautical Science (ISAS), JAXA, 2.Institute for Advanced Study, 3.OmniScope)

Diversity concept of the new curriculum "Inquiry learning"-To increase the number of student's presentations-

Masao Mukoh[2], *Tomoko Goto[1], Kazuyo Nagahama[3], Hideki Ishida[4]

1. Earthquake Research Institute, the University of Tokyo, 2. Tokyo Metropolitan Institute Fuji Senior High School・Junior High School, 3. Mejiro University, 4. Tohoku University

For “Inquiry learning” (MEXT), we are trying an exploratory approach in “The Society of Environment Project-based Research” (http://kantanken.net/). We need more chance for presentation. We introduce the collaborative studies with some researchers in institutions such as Universities and Research institutes. We discuss about what we need and the evaluation methods that have leveled from our participation in research conferences and awards.

Keywords: Inquiry learning, new curriculum, The Society of Environment Project-based Research

©2020. Japan Geoscience Union. All Right Reserved.

Kochi Core School for Asian Young Scientists at Kochi Core Center: new international outreach activity in marine sediment core and related sciences

*Go-Ichiro Uramoto[1], Hiroki Matsui[1], Kazuno Arai[1], Naohisa Nishida[2], Hirofumi Asahi[1], Yusuke Kubo[3], Satoshi Tonai[1], Wataru Tanikawa[3], Yurika Ujiie[1], Yuhji Yamamoto[1], Minoru Ikehara[1]

1. Kochi University, 2. Tokyo Gakugei University, 3. Japan Agency for Marine-Earth Scienct and Technology (JAMSTEC)

We held “Kochi Core School for Asian Young Scientists 2019” for the first time from 13th to 20th November 2019 at the Kochi Core Center (KCC), Kochi, Japan, by the support of the SAKURA Science Exchange Program (SSP) of Japan Science and Technology Agency (JST). KCC has been acting as one of three major core-repositories of global ocean drilling program for decades (such as International Ocean Drilling Program: IODP), which is as a joint institute of the Center for Advanced Marine Core Research, Kochi University and Kochi Institute of Core Sample Research of JAMSTEC. A wide range of state-of-the-art analytical instruments and scanning methods are available according to the high standards of IODP at KCC.
One of the major goals of the KCC is to train the next generation of scientists and promote IODP-related sciences. To achieve this goal, KCC had offered a unique training opportunity through the Kochi Core School, fully utilizing the comprehensive research/education facilities therein. Using a marine sediment core taken from the Tosa Basin (off Shikoku) as a training material, the training program of the Kochi Core School was implemented in mainly two parts: (1) visual core description and (2) specific measurement of core (physical property and paleomagnetic measurements, and stable isotope measurements of foraminifers). A one-day field trip to the Muroto UNESCO Global Geopark was also included. Nine participants (postgraduate students and postdoctoral researchers from Korea, China, and Taiwan) were invited by the SSP fund, learned the IODP workflows and discussed analytical results.

Keywords: Core School, Scientific drilling, Kochi Core Center

©2020. Japan Geoscience Union. All Right Reserved.

A Pilot Study of an Active Learning Program for the General Public using Radiological Monitors

*Haruka Matsuoka[1]

1. Department of Business and Informatics, Tsukuba Gakuin University

Raising children in a safe and healthy manner is the most important task in our daily life. The nuclear accidents in the Fukushima Daiichi Nuclear Power Plant complex, associated with the horrific earthquake, The Tohoku Earthquake, caused radioactive contamination via nuclear fallout in the eastern region of Japan. Some meteorological agencies in other countries soon released their radioactive material diffusion simulations for the region immediately, whereas the general public in Japan could not obtain enough information about the diffusion for a few weeks because of control by their government. Most parents raising children certainly lacked and sought information about the contamination by nuclear radiation in areas relevant to their daily activities. The author, living in Ibaraki Prefecture next to Fukushima Prefecture, met many parents who sought to measure the radiation doses using radiological monitors at parks, gardens, street, drains/trees etc. Through such measurements done together, they seemed to have learned much about the presence of radioactive material and the mechanism of their accumulation by rain fall and where the relatively safe places for their children were. These experiences triggered the launch of this study.

In this study, an active learning program focused on radiation monitoring for the general public is proposed. The program has been adapted for students at university and improved over a period of three years. It is composed of four parts: previous learning, outdoor measurement, indoor analyses by mapping, and discussion. First, short lectures about radioactivity and the mechanisms of radiological monitors are given. After that, the participants are divided into small groups that set the science targets for each group according to their interests. The outdoor radiation monitoring then is performed collaboratively at various places selected for their targets. Accomplishing these measurements by themselves, they progressively acquire the scale of radiation doses. After all measurements are carried out, they undertake to create the radioactive contamination maps from the obtained profiles. The analyses and discussions about the contrast in contamination levels on maps are carried out in each group. These small group discussions likely contribute to a deeper understanding of radioactive material in rainfall, soil, trees, and other phenomena associated with earth science.

Keywords: active learning, radiological monitoring, civil seminar

©2020. Japan Geoscience Union. All Right Reserved.

Spread of hemispherical multi-touch panel for rear projection type digital globe "Dagik Earth"

*Yukinobu Koyama[1], Akinori Saito[2]

1. KINDAI University Technical College, 2. Graduate School of Science, Kyoto University

As you can see from various organizations already using it for their exhibitions, to use the digital globe "Dagik Earth" is effective for outreach of Solar-Terrestrial Physics. Various user interfaces have been tried from mouse to Switch controller, but hemispherical multi-touch panel has not been realized. Therefore, we have developed hemispherical multi-touch panel for rear projection type digital globe by using inexpensive infrared method. In this presentation, we will demonstrate it, and discuss its dissemination.

Keywords: Digital globe, Hemispherical multi touch panel, Solar-terrestrial physics

©2020. Japan Geoscience Union. All Right Reserved.

Practice report of geological excursion for elementary school students using terrain model made by 3-D printer

*Iida Kazuya[1]

1. Komaba-Toho Junior and Senior High School

In the geological excursion, teaching topographic character in the area is important, because topographic image provides geological history in the area. However, understanding topographic demands reading topographic map, which is difficult for elementary students. In order to solve this problem, we made relief map using 3-D printer.
In this practice, ten elementary students joined to the geological excursion. Relief maps were prepared for each students using 3-d printer.
Questionnaire survey provide after excursion suggest followings.
(1) Although participant’ s school locate in the excursion course, they didn't realize topographic feature of this area.
(2) Participants realize topographic feature after this excursion.

Keywords: 3D printer, elementary school, geological excursion, relief map

©2020. Japan Geoscience Union. All Right Reserved.

A support activity for field excursion by a voluntary organization “Geo-Education”

*Jiro Komori[1], Tomoaki Kitayama[2], Iida Kazuya[3]

1. Teikyo Heisei University, 2. JAMSTEC, 3. Komaba Toho Junior & Senior High School

In the recent school and lifelong education, disaster prevention and environment study with practical instruction are required. On the other hand, there are still many obstacles in education including shortfall in human resources. Our unincorporated group "Geo-Eeducation" supports field excursion of earth science and geography for people in a wide age range in primary school, university student and local residents from April, 2012. In this presentation, we introduce some contents of field excursion and new agenda in response to previous our activity. Furthermore, we will show discussion about the potential of passing of knowledge and skills from practicing and former teachers to younger generations by such voluntary group.

Keywords: earth science education, geographical education, field study, utilization of human resources, voluntary group

©2020. Japan Geoscience Union. All Right Reserved.

The report of the International Earth Science Olympiad (IESO) 2020

*Norihito Kawamura[1], Yutaka Takigami

1. School of Regional Resource Management, Graduate School, University of Hyogo

We will report the outlines of the International Earth Science Olympiad (IESO)

1) From 2007 to 2021

IESO 2007 (Korea) 7 countries and 24 students, Japan was observer

IESO 2008 (Philippine) 6 countries and 24 students, 3 silver and 1 bronze

IESO 2009 (Taiwan) 14 countries and 50 students, 4 silver

IESO 2010 (Indonesia) 17 countries and 63 students, 1 gold and 3 silver

IESO 2011 (Italy) 26 countries and 104 students, 1 gold , 2 silver and 1 bronze

IESO 2012 (Argentina) 17 countries and 66 students, 1 gold and 3 silver

IESO 2013 (India) 23 countries and 90 students, 1 gold and 3 silver

IESO 2014 (Spain) 21 countries and 82 students, 3 gold and 1 bronze

IESO 2015(Brazil) 22 countries and 85 students, 1 gold , 1 silver and 2 bronze

IESO 2016 (Japan) 26 countries and 100 students, 3 gold and 1 silver

IESO 2017(France) 29 countries and 108 students, 2 gold and 2 silver

IESO 2018(Thiland) 38 countries and 139 students, 3 gold and 1 silver

IESO 2019(South Korea) 43 countries and 163 students, 4 gold

IESO 2020(Rossia),

IESO 2021(China)

2)JESO

Application from Sep.1 to Nov.15

©2020. Japan Geoscience Union. All Right Reserved.

1st Selection at Dec. (from about 2000 students to 60 students., about 75 places)

2nd Selection at March (from 60 students to10 students , Tsukuba City)

Final Selection at March (from 10 students to 4 students , Tsukuba City)

Keywords: International Earth Science Olympiad

©2020. Japan Geoscience Union. All Right Reserved.

Standing on an asteroid: using virtual reality for outreach and education

*Elizabeth Tasker[1], Alexander Kaurov[2,3]

1. Institute of Space and Astronautical Science (ISAS), JAXA, 2. Institute for Advanced Study, 3. OmniScope

Virtual reality presentations offer an immersive and interactive environment to share scientific material. From standing on the surface of a planetary body or deep underwater on the ocean floor, to holding three dimensional models of instruments or spacecraft, virtual reality can provide an experience impossible to replicate in classrooms or conference halls.

With museums and planetariums currently unable to welcome large gatherings, the use of virtual worlds can bring their immersive presentations online to reach audiences around the globe, and enable the opportunity to interact with scientists live in virtual meeting spaces. This interaction ability is also applicable to online conferences, which often struggle to replicate the collaboration potential of in-person meetings despite the growing need for remote alternatives due to environmental impact or financial restrictions.

As a proof-of-concept, we developed an experience that covers the Hayabusa2 asteroid exploration mission led by JAXA. This virtual tour contains custom designed scenes that recreate both real and fictitious places, including the asteroid surface and the mythological palace of Ryugu-jo from the tale of Urashima Taro. With the use of the Mozilla Hubs platform, multiple people can share the same virtual space with the lecturer and interact with the environment (exploring the scenes and handling models of the spacecraft) as well as one another. The cross-platform capability of Hubs allows people to connect from almost any system, from a virtual reality headset through to a computer web browser or smart phone. We are currently testing and learning ways to present effectively in the virtual worlds and design new environments for effective learning and sharing of ideas.

Keywords: virtual reality, outreach, education, planetary science

©2020. Japan Geoscience Union. All Right Reserved.

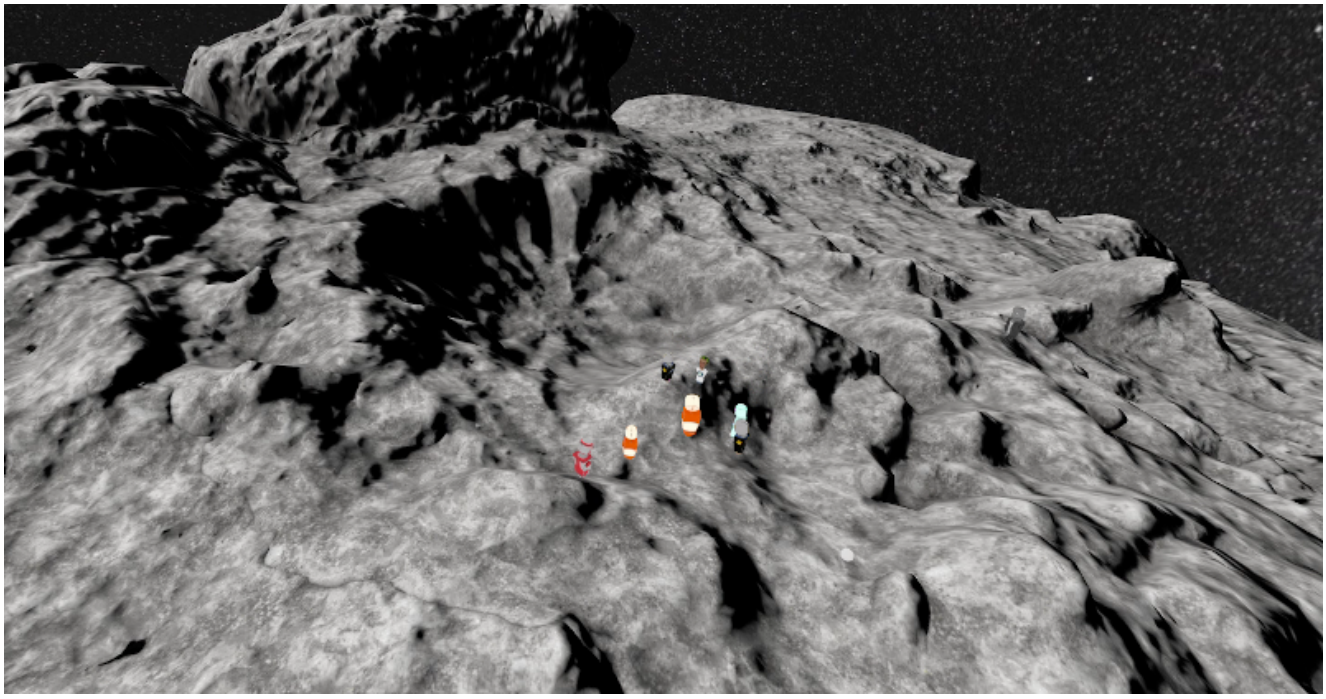

©2020. Japan Geoscience Union. All Right Reserved.

[J] Poster | M (Multidisciplinary and Interdisciplinary)：M-IS Intersection

[M-IS20] Atmospheric Electricity: Lightning discharges and related physical phenomena

convener:Yasuhide Hobara(Graduate School of Information and Engineering Department of Communication Engineering and Informatics, The University of Electro-Communications)

This year's Atmospheric Electrical Session will focus on lightning discharge phenomena and various physical phenomena related to lightning discharges, which are one of the core fields of atmospheric electricity. This session will consist of invited presentations introducing above-mentioned fields by leading experts, and contributed presentations on the latest observational and theoretical research results in these fields. For example, we welcome lightning physics, lightning observation technology, electrical effects of thunderstorms, and lightning related phenomena such as the mesospheric transient luminous events (TLEs), and lightning-related high-energy phenomena that have been actively studied in recent years. We certainly welcome papers regarding all topics on atmospheric electricity including global electric circuit, ion and fair weather electricity, lightning protection, terrestrial electromagnetic noise environment including wave propagation in the magnetosphere and ionosphere.

[MIS20-P02] **Characteristics of Medium-low Frequency Magnetic Fields of Initial Continuous Current in Triggered Lightning**

*Yanfeng Fan[1], Yang Zhang[1], Weitao Lyu[1], Dong Zheng[1], Xiangpeng Fan[1] (1.State Key Laboratory of Severe Weather, Chinese Academy of Meteorological Sciences)

[MIS20-P03] Study on the time development of lightning and precipitation activities by LLS and radar observations

*Takeshi Morimoto[1], Keichiro Boda[1], Yoshitaka Nakamura[2], Hideo Sakai[3], Masahito Shimizu[4] (1.Kindai University, 2.Kobe City College of Technology, 3.University of Toyama, 4.Chubu Electric Power Co. Inc.)

Characteristics of Medium-low Frequency Magnetic Fields of Initial Continuous Current in Triggered Lightning

*Yanfeng Fan[1], Yang Zhang[1], Weitao Lyu[1], Dong Zheng[1], Xiangpeng Fan[1]

1. State Key Laboratory of Severe Weather, Chinese Academy of Meteorological Sciences

Triggered lightning experiment of Field Experiment Base on Lightning Sciences, China Meteorological Administration (CMA-FEBLS) provides a good opportunity to study the discharge process and its related electromagnetic effects. Based on the data obtained by the magnetic antennas around the launch site, the paper analyzes the electromagnetic characteristics of initial continuous current. Benefitting from the expansion of the bandwidth of the antenna, magnetic pulses of the signal quiet period are observed for the first time. The mean pulse width and inter-pulse interval of these pulses are about 1 μs and 14 μs, respectively, which indicating that the propagation of upward leaders during the stage is in the form of small scale breakdown. The magnetic pulse bursts (MPB) can be both observed by close and far antennas, and the mean inter-pulse interval of the MPB (24.5 μs) is larger than that of the signal quiet period pulse. In addition, the channel-base current during the stage of MPB increases to dozens of hundreds of amperes, so it can be included that the electric field condition is conductive to the development of the upward leaders. Furthermore, the measurement of magnetic field can reflect the physical process of the initial continuous current pulse (ICCP) and *M*-component. The regular magnetic pulse (RMP) observed during the stage of ICCP and *M*-component are attributed to the interception of recoil leader with existing lightning channel. The inter-pulse interval of RMP is one order less than that of MPB, which may reflect the differences between the positive polarity breakdown and the negative polarity breakdown of leaders.

Keywords: triggered lightning, initial continuous current, medium-low frequency magnetic fields

©2020. Japan Geoscience Union. All Right Reserved.

Study on the time development of lightning and precipitation activities by LLS and radar observations

*Takeshi Morimoto[1], Keichiro Boda[1], Yoshitaka Nakamura[2], Hideo Sakai[3], Masahito Shimizu[4]

1. Kindai University, 2. Kobe City College of Technology, 3. University of Toyama, 4. Chubu Electric Power Co. Inc.

The lightning and precipitation activities are studied in this paper by Ku-band broadband radar (Ku radar) and Lightning Location System (LLS) observations. The authors have been conducting cooperative lightning observations in Toyama, Japan, in where winter thunderstorm are developed. This paper focuses on the time development of thunderstorm activities.

Ku radar is a low-power high-resolution Doppler radar for meteorological applications. Ku radar employs bi-static system which is composed of a pair of Luneberg Lens Antenna, and solid state amplifier which transmits the wideband signal (80 MHz) in Ku-band. The pulse compression technique, which has the advantage that high range resolution profiles can be acquired by low transmitting power, is applied. Observation time resolution for a full volume scanning and range resolution less than 1 minute and 2.5 m are realized with Ku radar, respectively.

LLS is a passive remote sensing system locating impulsive lightning EM radiation sources associated with lightning return strokes. LLS brings locations and the estimated values of stroke currents.

The comprehensive studies of these observations for the locally and quickly developed thunderstorms indicate the below:

The time development of the peak value, and the top and the most active height of the radar echo are similar with each other.

Most lightning return strokes are located where strong radar echo is noticeable at high altitude.

Keywords: Linghtning, Radar Observations, thunderstorm

©2020. Japan Geoscience Union. All Right Reserved.

[J] Poster | M (Multidisciplinary and Interdisciplinary)：M-IS Intersection

[M-IS21] Geopark

convener:Keiichi Tadokoro(Research Center for Seismology, Volcanology and Earthquake and Volcano Research Center, Nagoya University), Takayuki Ogata(Disaster Prevention Research Center for Island Regions, University of the Ryukyus), Marekazu OHNO(Unzen Volcanic Area Geopark Promotion Office), Takayuki Arima(Yokohama City University)

This session targets interdisciplinary and multidisciplinary discussion on geopark, involving geoheritage, geodiversity, geoconservation, geotourism, sustainable development, governance, risk management, science communication and geoscientific education. These topics contribute to scientific and attractive activities in geoparks.

[MIS21-P01] **Educational application of Geopark in order to better understanding the regional resource management**

*Kyohei Sano[1] (1.Graduate School of Regional Resource Management, University of Hyogo)

[MIS21-P02] Thinking Geopark and Geo-story through an active Learing methode Mystery

*Ryuta YAMAMOTO[1] (1.Center for professional development of teachers Shizuoka University)

[MIS21-P03] Efforts to improve the quality of the sea activity guide through collaboration between the private sector, the government, and experts: San’in Kaigan UNESCO Global Geopark GEO×Activity Project

*Kyoko Kanayama[1], Yuzo Ota[1], Yuki Iwamoto[2], Suzuka Koriyama[2], Akio Yamashita[3], Yoshinori Kodama[4], Yoshiaki SUGAMORI[4], Kyohei Sano[5] (1.San'in Kaigan Geopark Museum of the Earth and Sea, Tottori Prefectural Government, 2.Secretariat of San'in Kaigan Geopark Promotion Council, 3.Develop Surf & Sea, 4.Faculty of Agriculture, Tottori University, 5.Graduate School of Regional Resource Management, University of Hyogo)

[MIS21-P04] Approach of Nanki Kumano Geopark Guided tours add value to tourist destinations Guide to hotel-hosted bus tours

*TAKAMARU NAKAE[1] (1.Japanese Geoparks Network)

[MIS21-P05] Reorganization of “sites” in Unzen Volcanic Area UNESCO Global Geopark ver.2020

*Taku MORIMOTO[1] (1. Unzen Volcanic Area Geopark Promotion Office)

[MIS21-P06] **The Permian–Triassic granitoid and gneiss in the Dinosaur Valley Fukui Katsuyama Geopark and other areas, Fukui Prefecture, Central Japan**

*Sachiho Koizumi[1], Shigeru Otoh[1] (1.Graduate School of Science and Engineering, University of Toyama)

[MIS21-P07] Re-discovering the Lake Towada area as a geological heritage: A key to the revitalization of the local community

*Yusuke Kuwahara[1], Mizuki Ishida[1], Mio Kobayashi[2], Katsuya Ohnuma[3], Yasuhiro Kato[4,1,5] (1.Department of Systems Innovation, School of Engineering, The University of Tokyo, 2.Department of Eco System Studies, School of Agricultural and Life sciences, The University of Tokyo, 3.Department of Physics, School of Science, The University of Tokyo, 4.Frontier Research Center for Energy and Resources, School of Engineering, The University of Tokyo, 5.Ocean Resources Research Center for Next Generation, Chiba Institute of Technology)

[MIS21-P08] 10 years cooperation history of geopark activity between Fossa Magna Museum and Niigata University in Itoigawa geopark.

*Yousuke Ibaraki[1], Ko Takenouchi[1], Takahiko Ogawara[1], Takeo Kobayashi[2], Atsushi Matsuoka[3] (1.Fossa Magna Museum, 2.Itoigawa Geopark Council, 3.Niigata University)

[MIS21-P09] Japan-China Comparison of the Role of Museums in Lifelong Education——To consider the role of education in geoparks

*Qikun Zhou[1] (1.Graduate School of Tourism, Wakayama University)

Educational application of Geopark in order to better understanding the regional resource management

*Kyohei Sano[1]

1. Graduate School of Regional Resource Management, University of Hyogo

Geopark is the program to manage the regional resource with the holistic concept of protection, education, and sustainable development. Geopark contains not only geological and geographical heritage but also ecological and cultural heritage. To develop the Geopark activities in each region, it is important to accumulate the activity report, to share such reports, and to discuss “What is the Geopark?”, “How can the Geopark make a contribution to local society?” in Geopark members.
In the University of Hyogo, Japan, we apply the Geopark and their heritages in order to better understanding regional resource management. For example, the lecture“Introduction to Geopark” for graduate students picks up the effort and system of Geopark as the way to manage the regional resources. In this lecture, we have fieldwork and classroom lectures. In the part of the fieldwork, students visit the museum and Geosite in San’in Kaigan Unesco Global Geopark to study and observe the activity of local people. In the part of the classroom lecture, students study the concept and current situation of Geopark and we discuss such subjects of “What is Geopark?” “What is the Celebrating Earth Heritage?” “Relation between Celebrating Earth Heritage and Sustainable Development”.
This presentation reports educational application and results of the discussion about Geopark in Graduate School of Regional Resource Management, University of Hyogo.

Keywords: San’in Kaigan Unesco Global Geopark, Education

©2020. Japan Geoscience Union. All Right Reserved.

Thinking Geopark and Geo-story through an active Learing methode Mystery

*Ryuta YAMAMOTO[1]

1. Center for professional development of teachers Shizuoka University

Geopark is a UNESCO program promoting SDGs / ESD in the area and also in the school. MEXT revised the national school curriculum in 2018/19 and promotes competence-oriented and active learning at school. Local government and the Geopark Promotion Office emphasizes local awareness of young generation in Geopark education. To adopt these three multi scale context, considering the barrier of acceptance of in-service teacher, the author suggests using a learning method Mystery.

Keywords: Education, Active Learning, SDGs/ESD, Geopark

©2020. Japan Geoscience Union. All Right Reserved.

Efforts to improve the quality of the sea activity guide through collaboration between the private sector, the government, and experts: San’in Kaigan UNESCO Global Geopark GEO×Activity Project

*Kyoko Kanayama[1], Yuzo Ota[1], Yuki Iwamoto[2], Suzuka Koriyama[2], Akio Yamashita[3], Yoshinori Kodama[4], Yoshiaki SUGAMORI[4], Kyohei Sano[5]

1. San'in Kaigan Geopark Museum of the Earth and Sea, Tottori Prefectural Government, 2. Secretariat of San'in Kaigan Geopark Promotion Council, 3. Develop Surf & Sea, 4. Faculty of Agriculture, Tottori University, 5. Graduate School of Regional Resource Management, University of Hyogo

Marine activities such as sea kayaking, stand-up paddleboarding (SUP), snorkeling and surfing have been popular in the Uradome Coast of San’in Kaigan Geopark. Approx. 60 people work as activity guides, and more than 5,600 tourists including students for the school excursion enjoyed these activities in fiscal 2018. The number of participants rose ten times compared to those before San’in Kaigan was designated as a Global Geopark. These days, the demand for a textbook, which covers the features unique to the Uradome Coast such as formations of sea cave, gates and the marine life forms, has increased among the activity guides.

Therefore, the San’in Kaigan Geopark Museum of Sea, the San’in Kaigan Geopark Promotion Council and the local university in partnership with the activity guides conducted lectures as well as creating the textbook which summarized materials for the guides in fiscal 2019. This project is for the guides to learn and enjoy the geopark by mixing guides’ perspective with geographical, geological and biological knowledge. With this textbook and training programs, it is considered that the guiding skills will be improving by sharing these knowledge.

At beginning, we started to conduct a field research to gather information for the textbook from geological and biological perspective. In organizing the survey results, we found a story of geological formations and marine creatures in Uradome Coast across the field of geographical, geology and biology. In addition, we were able to incorporate the contents which the guides can handle for frequently asked questions from customers.

We had training programs in June, September and March in 2019 based on the textbook we had created. We obtained positive comments from the guides as follows: “we were able to learn more about marine life in earth”, “we found stories that we could tell customers right away.” and “we got tips for finding features of the landscapes and the marine creatures easily.”

This project also brought the San’in Kaigan Geopark Promotion Council to a close relation with the activity business operators and the academic experts. We also learned we could find the attractive guiding resources by multiplying the different territories of geographical, geology and biology. Furthermore, we rediscovered that it is essential to organize the knowledge that we had in the research.
We are planning to make the activity programs targeting at tourism and school excursion as well as conduct the regular workshops in partnership with activity guides and experts.

©2020. Japan Geoscience Union. All Right Reserved.

Keywords: geopark, San'in Kaigan, activity, Cooperation, guide

©2020. Japan Geoscience Union. All Right Reserved.

Approach of Nanki Kumano Geopark Guided tours add value to tourist destinations Guide to hotel-hosted bus tours

*TAKAMARU NAKAE[1]

1. Japanese Geoparks Network

Geopark initiatives
Guided tours add value to tourist destinations
Oedo Onsen Monogatari Bus Tour Guide

Guide Association of Nanki Kumano Geopark
Geopark Guide

Nanki Kushimoto Tourist Association
Guide Section Committee Secretary

Tourism is part of sustainable community development, one of the components of Geopark.
We introduce a case where the guide's approach from the perspective of a geopark amplifies the new attraction of a tourist spot.

Oedo Onsen Monogatari, a hotel in Kushimoto-town, operates a cheap round-trip bus from Osaka, Kyoto and Kobe to attract customers on weekdays.
The outbound bus arrives at the hotel shortly after 2:30 pm, and leaves at 3:30 pm with passengers from the previous day.
In other words, They you have to check out by 10:00 am the day after your stay and wait for the bus until 3.30 pm.
In order to keep those customers from getting bored, there are optional tour buses in tourist areas.

The buses change course depending on the season, but on the course around Kozagawa, it is a guided tour.
The course covers the Ichimai-iwa monolith in Koza river, Taki-no-hai waterfall, Mushikui-iwa rock in Takaike, and Hashigui-iwa rock.
The guide for this course is undertaken and dispatched by the Nanki Kushimoto Tourism Association.

However, instead of just looking at the sights, the added value will be enhanced by commentary provided by the Geopark Guide, making it even more attractive.
We are convinced that we can attract more customers.

We want to take the guide activities into the community and connect the Geopark to tourism.

©2020. Japan Geoscience Union. All Right Reserved.

Keywords: Geopark, Sightseeing, Bus tour

©2020. Japan Geoscience Union. All Right Reserved.

Reorganization of “sites” in Unzen Volcanic Area UNESCO Global Geopark ver.2020

*Taku MORIMOTO[1]

1. Unzen Volcanic Area Geopark Promotion Office

In FY2016, the Unzen Volcanic Area Geopark Council reviewed the number of sites from 189 to 130, and classified the sites into four types of categories as follows. 1: geological sites, 2: ecological sites, 3: Historical / cultural sites, 4: composite sites. In particular, the composite site is defined by the Unzen Volcanic Area Geopark Council based on its own standards. The typical site is “Hara Castle Ruins” which is a UNESCO World Cultural Heritage site, and at the same time, the basement rocks that has important geological value. However, in the GGN (Global Geopark Network) self-evaluation sheet, there is no item of composite site, and it is not consistent with the GGN evaluation axis at the time of re-evaluation. Besides that in managing the site (protecting and preserving), it was difficult to clearly communicate the value of the site to local residents and visitors. in managing the site (protecting and preserving), it was difficult to clearly communicate the value of the site to local residents and visitors.

Against this background, from 2018 to 2019, the Unzen Volcanic Area Council decided to reorganize complex sites in the area as following 3 types; geological sites, natural sites and historical / cultural site. At the same time, we reorganized the sites in the point of view of managing the existing 130 sites in the future as follows; whether the location and scope of the sites will not be unclear, whether they will be subject to the nature or cultural property protection system, whether it has potential for using education and tourism activities. As a result, the total number of sites as of March 2020 was 50, of which 16 were geological sites, 6 were natural sites, and 28 were historical / cultural sites. Observation decks and other places where you can observe the scenery of the site are placed as view spots. The 50 sites that have been reorganized are important sites that the Unzen Volcanic Area Geopark Council would like to keep together with local residents, especially for the future. In the future, we will continue to add or modify new sites that need to be protected when they become newly found or when the status of site management changes.

The reorganization and review of the site will be a good opportunity to share the value of the site which can be regarded as a "local treasure," with various stakeholders, such as residents, the government and researchers. In addition, it is important for the strategy for developing geo-tourism, such as changing the content of multilingual commentary boards, general information boards, leaflets and websites. From now on we will create a site record that describes the management and utilization plan of the reorganized site among the stakeholders, and based on this, will carry out activities to take over the site in a sustainable way to the future.

Keywords: Reorganization of sites, Self evaluation, sites values, Usage plan of sites

©2020. Japan Geoscience Union. All Right Reserved.

The Permian–Triassic granitoid and gneiss in the Dinosaur Valley Fukui Katsuyama Geopark and other areas, Fukui Prefecture, Central Japan

*Sachiho Koizumi[1], Shigeru Otoh[1]

1. Graduate School of Science and Engineering, University of Toyama

Introduction

Various studies have been conducted of the Early Cretaceous Tetori Group that yield many dinosaur fossils in the Dinosaur Valley Fukui Katsuyama Geopark. On the other hand, many pre-Cretaceous small rock bodies that sporadically occur in the western part of the Geopark and other areas of Fukui Prefecture remain unstudied. These rock bodies are regarded as the Hida granitoid and Hida gneiss (e.g., Fukui Prefecture, 2010), the basement rocks of the Tetori Group and other Mesozoic to Cenozoic sedimentary units. However, the only petrological or geochronological study is Shibata and Uchiumi (1992), who reported a K–Ar alkali feldspar age of 178 ±5 Ma from the Mt. Murakuniyama granitoid in Echizen City to the southwest of the geopark. Here we present the results of petrographical and geochronological studies that help to characterize the granitoid and gneiss.

Geological Setting

Pre-Cretaceous granitoid and gneiss sporadically occur in the northeastern part of Fukui Prefecture (the Reihoku district), the western part of the Hida Belt. In this study, we investigated the granitoid or gneiss of four areas, the Saragawa– Bandojima area in the geopark, Mt. Genampo area in Ono City, and Mt. Taiheizan and Mt. Murakuniyama areas in Echizen City. (1) Granite, gabbro, orthogneiss, and greenish gneiss crop out in the Saragawa–Bandojima area, covered by the Upper Cretaceous sedimentary rock and felsic tuff or Miocene andesite. (2) Two types granitoid crops out in the Mt. Genampo area: one is partly crushed and crops out in the southern foot of Mt. Genampo, whereas the other is undeformed and crops out in the northern foot of Mt. Genampo and Hokyoji to the north. (3) Granite and gabbro occur in the Mt. Taiheizan area, and (4) granite, diorite, and gabbro crop out in the Mt. Murakuniyama area.

Analytical Methods and Results

We took a granitoid sample from the Saragawa–Bandojima, Mt. Taiheizan, and Mt. Murakuniyama areas, two granitoid samples from the Mt. Genampo area, and a gneiss sample from the Saragawa–Bandojima area. Then we conducted the modal and the zircon U–Pb dating by the LA–ICPMS equipped at Nagoya University. The results are summarized in the attached table.

Discussion

The results of zircon dating indicate that zircons from the granitoid bodies crystallized in the Middle Permian to the Early Triassic. The zircon U–Pb age of the Murakuniyama tonalite (250.9 ±2.5 Ma) is older than the alkali feldspar K–Ar age (178 ±5 Ma: Shibata and Uchiumi, 1992). We consider that the zircons in the Murakuniyama tonalite crystallized at ca. 250 Ma (Early Triassic), and a tectonic thermal event of 200℃ (blocking temperature of alkali feldspar) or more overprinted at ca. 178 Ma (Early Jurassic). The low Th/U ratio of the zircons of the Bandojima orthogneiss body suggests that the zircon age, 231.8 ±1.8 Ma, is metamorphic. A local metamorphic event probably occurred in the Saragawa–Bandojima area around

©2020. Japan Geoscience Union. All Right Reserved.

231 Ma, together with the intrusion of the Saragawa tonalite. From the amount of magnetite of each sample, we consider that the granitoid in the Mt. Genampo and Mt. Taiheizan areas is of magnetite series.

References
Fukui Prefecture, 2010, *Fukui Pref. Publ. Corp. Const. Tech.*, 173p /Shibata and Uchiumi, 1992, *Bull. Geol. Surv. Japan*, **43**, 359–367.

Keywords: Dinosaur Valley Fukui Katsuyama Geopark, Hida Belt

Table Summary of the petrographical and geochronological analyses of five granitoid and one gneiss samples from the geopark and adjacent areas.

Name of rock body	Main constituent minerals	Accessory minerals	Zircon ^{238}U–^{206}Pb ages			Th/U ratio of zircons
			Age range	LPP*	YC age (2σ)**	
Saragawa tonalite	plagioclase, quartz, biotite, chlorite, and muscovite	zircon, monazite, and opaque minerals (magnetite poor)	266–223 Ma	243.8 Ma	230.7 ± 4.1 Ma (n = 7, MSWD = 2.2)	0.15–0.37
Hokyoji granodiorite	undeformed plagioclase, quartz, alkali feldspar, biotite, muscovite, and hornblende	zircon, titanite, and opaque minerals (magnetite rich)	285–248 Ma	267.6 Ma	256.1 ± 1.9 Ma (n = 10, MSWD = 1.6)	0.41–1.21
Genampo tonalite	partly crushed plagioclase, quartz, alkali feldspar, and biotite	zircon, epidote, and opaque minerals (magnetite rich)	295–263 Ma (with a 322 Ma grain)	272.4 Ma	271.9 ± 1.9 Ma (n = 22, MSWD = 1.4)	0.44–0.89
Taiheizan monzonite	plagioclase, alkali feldspar, biotite, and chlorite	zircon, garnet, and opaque minerals (magnetite rich)	249–233 Ma	243.8 Ma	243.0 ± 1.6 Ma (n = 22, MSWD = 1.11)	0.63–1.29
Murakuniyama tonalite	plagioclase, quartz, and muscovite	zircon and opaque minerals (magnetite poor)	289–240 Ma	247.3 Ma	250.9 ± 2.5 Ma (n = 26, MSWD = 1.5)	0.47–1.65
Bandojima orthogneiss	quartz, alkali feldspar, alternation of plagioclase, chlorite, and biotite	zircon, epidote, titanite, garnet, and opaque minerals (magnetite poor)	251–225 Ma	234.9 Ma	231.8 ± 1.8 Ma (n = 12, MSWD = 1.4)	0.01–0.41 (mostly <0.1)

* Largest graphical age peak on an age-probability plot

** Weighted mean of the youngest age-cluster (YC), consisting of the youngest zircon age and the other ages with the error bar (±2σ) overlapping with the youngest age

©2020. Japan Geoscience Union. All Right Reserved.

Re-discovering the Lake Towada area as a geological heritage: A key to the revitalization of the local community

*Yusuke Kuwahara[1], Mizuki Ishida[1], Mio Kobayashi[2], Katsuya Ohnuma[3], Yasuhiro Kato[4,1,5]

1. Department of Systems Innovation, School of Engineering, The University of Tokyo, 2. Department of Eco System Studies, School of Agricultural and Life sciences, The University of Tokyo, 3. Department of Physics, School of Science, The University of Tokyo, 4. Frontier Research Center for Energy and Resources, School of Engineering, The University of Tokyo, 5. Ocean Resources Research Center for Next Generation, Chiba Institute of Technology

In Japan, there are many areas where unique geological features have nourished the areas' distinct ecosystems and cultures. In order for such areas to attract people, it is important to promote the touristic and educational value of geological heritage, as well as natural and cultural heritage. However, the significance of geological heritages can sometimes be "forgotten" by the local communities, leaving the intriguing geological processes behind the landscape be untold. Understanding these fundamental geological processes can help local communities to "re-discover" the true values of that area, gain a sense of pride, and utilize geotourism in boosting local economies.
As a part of the University of Tokyo's program, we visited Lake Towada area in Aomori and Akita prefecture to find clues in revitalizing the local community. With its magnificent landscape created via volcanic activities (e.g. Lake Towada), distinct ecosystem (e.g. bryophyte community in Oirase Gorge), and unique style of living co-exist with nature (e.g. cultivation of Kokanee salmon in Lake Towada), Lake Towada area is an ideal place to learn and appreciate the dynamics of the Earth. However, we realized that the existing educational and touristic activities in the area mostly featured the cultural and natural aspects, and rarely focused on the geological aspects of the area.
Therefore, we organized a special class at a junior high school in the area to demonstrate the educational value of the geological heritages in the area. We explained the formation process of Lake Towada and Oirase Gorge through vivid illustration and simple, easy experiments (e.g. caldera formation experiment using cocoa powder). We also surveyed about the impression of the class. Based on the results of these activities, we discuss some scenarios to maximize the educational and touristic values of geological heritages in the Lake Towada area, to revitalize the local communities.

Keywords: Regional revitalization, Lake Towada, Geotourism

©2020. Japan Geoscience Union. All Right Reserved.

10 years cooperation history of geopark activity between Fossa Magna Museum and Niigata University in Itoigawa geopark.

*Yousuke Ibaraki[1], Ko Takenouchi[1], Takahiko Ogawara[1], Takeo Kobayashi[2], Atsushi Matsuoka[3]

1. Fossa Magna Museum, 2. Itoigawa Geopark Council, 3. Niigata University

dummy

Keywords: Itoigawa UNESCO Global Geopark, Itoigawa Geopark Council, Fossa Magna Museum, Niigata University, cooperation

©2020. Japan Geoscience Union. All Right Reserved.

Japan-China Comparison of the Role of Museums in Lifelong Education——To consider the role of education in geoparks

*Qikun Zhou[1]

1. Graduate School of Tourism, Wakayama University

Whether the role of education that a geopark should fulfill in response to social demands is an issue that cannot be ignored. Geoparks play a very important role not only in Japan but also in China, where lifelong education systems are currently being developed. To examine the role of geoparks in lifelong education, we first look at museums in Japan and China, which are similar to geoparks and are thought to have accumulated examples of lifelong education initiatives.
In Japan and China, there are significant differences like management system and the public perception of the museums. Compared with Japan, where education was spread earlier, education was not yet sufficient in China due to its historical influence. Museums are one of the solutions to that problem. Therefore, in 2008, the Chinese government tried to increase the number of visitors by giving free admission to museums through a grant from the central finances.
Because of these differences, it is thought that the role of each museum in Japan and China in the lifelong education system will be different. Therefore, we will investigate and organize the efforts of the museums on lifelong education in Japan and China.
This time, first, summarize policies and regulations on museums on the websites of each museum and MEXT of Japan (and the Ministry of Education of China) and analyzing previous research on museums and lifelong education. Find out what kind of activities they are doing (especially in social education) and what kind of characteristic efforts they are doing. Based on that, we compare the history of Chinese and Japanese museums and the policies implemented, and summarize the differences in their roles in lifelong education, and examine how they can be applied to the role of geoparks in lifelong education.

Keywords: Geopark, Lifelong education, The role of education in museum, Japan-China Comparison

©2020. Japan Geoscience Union. All Right Reserved.

[J] Poster | M (Multidisciplinary and Interdisciplinary)：M-IS Intersection

[M-IS22] Exploring the origin of space, solar system, earth, moon, plate tectonics, life, etc.

convener:Akira Taneko(SEED SCIENCE Lab.)

SCIENCE has developed and accumulated knowledge and applications, called truths, written in language and character symbols, through the induction and deduction, discovering the laws of motion and chemical reactions in accordance with the elucidation of periodic motion and agreement with experiments and observations. It was. However, the mystery of the origin was difficult to make empirical reasoning, and could not go out of the scope of religion and philosophy.
The biological transformation of organisms is seen as a flow of evolution, but it is also considered as evolution when exploring the origins of astronomy and the earth. If you can explain it, you can solve the mystery of the universe with a paradigm that is close to the truth. Remove interdisciplinary and freely seek discussion of inquiry. There is a theory (hypothesis) and verification is possible for the first time.

[MIS22-P01] Moon, Earth (ocean floor, plate boundary, plate tectonics, driving force), asteroid belt and differentiated meteorites, origin of Jupiter's Great Red Spot, all sources verified by Abduction

★Invited Papers

*Akira Taneko[1] (1.SEED SCIENCE Lab.)

[MIS22-P02] No mechanism to expand Space! Big Bang hypothesis has 't been proven! Red-shift can be explained by New stationary space theory based on Quantum Red-Shift. Neither black holes nor Dark matter are required. Validated by Abuduction

★Invited Papers

*Akira Taneko[1] (1.SEED SCIENCE Lab.)

Moon, Earth (ocean floor, plate boundary, plate tectonics, driving force), asteroid belt and differentiated meteorites, origin of Jupiter's Great Red Spot, all sources verified by Abduction

*Akira Taneko[1]

1. SEED SCIENCE Lab.

Purpose of science is to explain all Mysteries of Universe. So far, Laws of science and Truth have been explored by Induction and Deduction. Since the quest for origin does not go back in time, Initial state was unknown. Creative reasoning and evaluation are important in exploring Origin. It is a method called abduction that is evaluated based on Results of evolution. Specifically, we propose **a New Model** and explain all Results (features) of One-time evolution in a unified manner.

In order to be a mantle-only moon in Giant Impact (GI) hypothesis model, it must accidentally hit Earth at a special angle of 30 degrees at a speed of Vx=7km/s. Calculated Lunar Orbital Energy(3×Re) is only 1/20 of Actual Lunar, (GI) hypothesis could not be tested.

This is a new Hypothesis for Moon Formation Model. Instead of Giant Impact GI model (a protoplanet with a differentiated Mars size), we assumed **An Impactor** (MI) with **Lunar-sized differentiated Only Mantle.** Earth has a core (Fe + Ni) with half Radius, and its outside is covered with a mantle. Discovery that Moon is made of only Mantle is a major feature. In order to reproduce Characteristics even in GI hypothesis, we assumed various angles and velocities and calculated Mechanism of agglomeration without including Core in Debris, and searched for special conditions. However, Lunar orbital energy was only 1/20 of Current value. Impact energy given to Earth is about 2.5 times higher for GI than for MI. Therefore, in Collision of the GI model, Earth is completely deformed to Core, but in Collision of MI model, Core is intact, Earth mantle is missing, and Moon is emitted only in Mantle. In MI hypothesis, when Solar system was observed because of Inevitable formation of a moon-sized mantle impactor, it was found that Planet was missing at Position of the asteroid belt according to Bode's law. Assuming that Missing planet was destroyed by accidental collision, Debris splatters in all directions and cannot aggregate.
"Inevitable Collision Idea" (Core+Mantle change Only Mantle)
Hint is Comet Shoemaker Levi Ninth, which left a line of traces on Jupiter and set a good example of a tidal rupture. Problem is the mechanism by which a circular orbit CERRA (protoplanet of Mars size at Ceres) becomes an elliptical orbit with tidal rupture. Due to Perturbation of a massive gas planet born around Sera, Angular momentum of Serra was absorbed by Jupiter and flattened Serra's orbit. With Law of orbital energy being constant, Serra ruptures due to tidal forces where the attractive forces of Sun and Jupiter balance each other, and Mantle fragments are arranged in a line like a Train and orbit Same elliptical orbit.

Collision with Earth occurs at Intersection of this elliptical orbit and Earth's orbit every meeting cycle. Speed and Angle obtained by theoretical calculation are 12.4 km s and 36.4 degrees. Although Impact velocity is higher than Secondary space velocity of 11.2km/s, Current lunar orbital position can be easily explained by considering Coefficient of restitution. Earth's Mantle is denser near Center, and Ejected Earth Mantle pieces are eccentric and Outer surface is covered with **Mmelting Mantle**. However, Crater formed during Heavy Meteorite Bombing Period becomes a Black Moon Sea when Inner Basaltic Material remelts and flows out. Back side is Same Andesitic Breccia, so Sea is not formed and it becomes a Desert

©2020. Japan Geoscience Union. All Right Reserved.

of Moon.

Emitted Moon is eccentric and Earth rotate each other around Common center of gravity. Heavy side (surface) is stable near Common Center of Gravity. Heavy side (surface) is stable near Common Center of Gravity. So Surface is always facing Earth, so Backside is not visible from Earth.Origin of Earth could all be explained by MI.

In this **“Multi-Impact Hypothesis”** , Origin of Earth is further described as**[Deep ocean floor of Earth]** [plate boundary]**[plate tectonics][driving force]**[rapid change in plate movement direction][start of overlap between plates]**[return Pacific arc shape Explanation of archipelago/back-arc concave basin/trench]** [Antarctica cessation][Transform fault][Hirakawa Formation][Eccentricity of Van Allen Zone][Earth field reversal][Inclination of earth axis] did it.As Origin of Solar system,[feeding zone][asteroid belt][differentiated meteorite][Love pile asteroid] **[Great Red Spot of Jupiter]** [Mantle of Pluto][Core Rich of Mercury],[Impact **velocity** and **angle** of **Mantle fracture**] can be calculated from Theory, and [Moon Eccentricity][Why Lunar sea concentrates on Surface][Reason why Moon always faces Earth] could be explained in a unified manner, which helped to clarify **Missing link** in **End of Hades**.
It can be said that it was **completely verified** by **Abduction**. cf.S-IT25(May 26A05),M-IS22(May 24,201B)

Keywords: The method of examining the mystery of planet origin is an abduction that can come up with a groundbreaking model and unify the multiple present conditions of the results of evolution., Multi-impact hypothesis, Giant impact hypothesis, creative inference of evolution , Origin of Moon,Lunar orbital energy, the moon always faces the earth, the surface has a lunar sea, the mantle only the moon, Origin of Earth's Ocean Bottom and Plate Boundary, Plate Tectonics, Driving Force, Earth's Rotational Axis, Rapid Change in Plate Movement Direction, Start sinking of Plate, Origin of the asteroid belt, Differentiated Meteorite, Jupiter's Red Spot, Pluto, Mercury's core / mantle ratio,, Cardinal Pacific Arc Islands and a back arc ocean basin and the trench, Abduction(Creative reasoning),Induction,Deduction

©2020. Japan Geoscience Union. All Right Reserved.

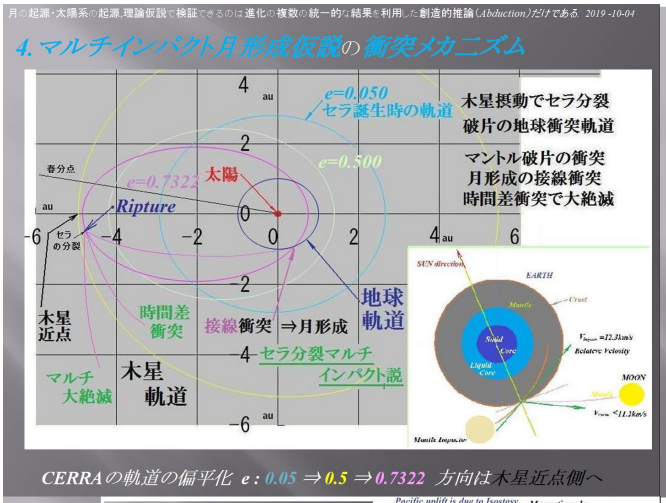

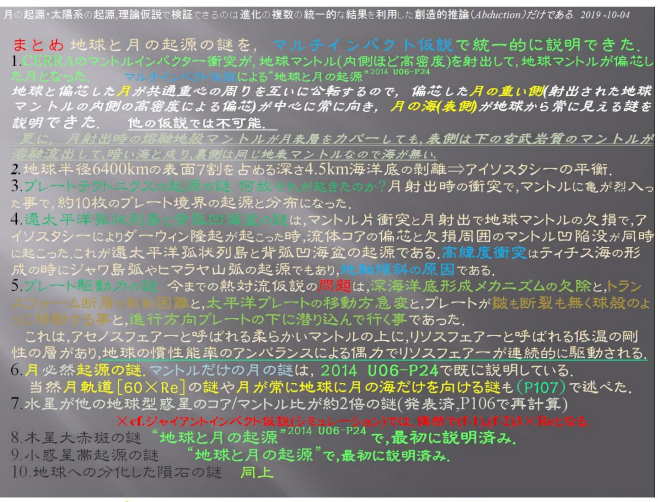

6.地球 Abduction

①環太平洋弧状列島の起源,

②深海洋底の起源とアイソスタシーによる凹プレートの形成メカニズム

③プレート相互の重なり始めのメカニズム

④駆動力(偏芯慣性モーメント)

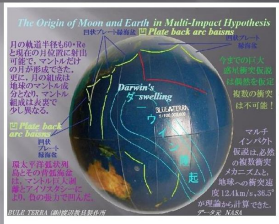

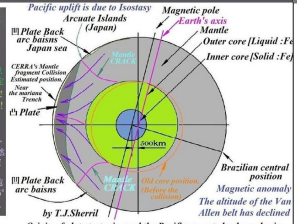

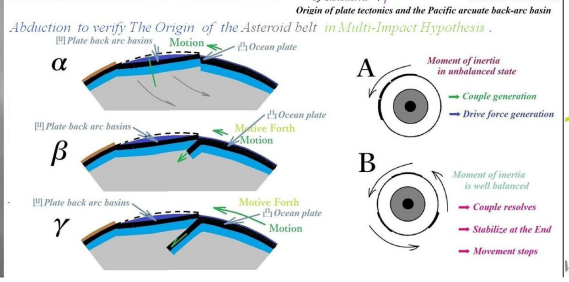

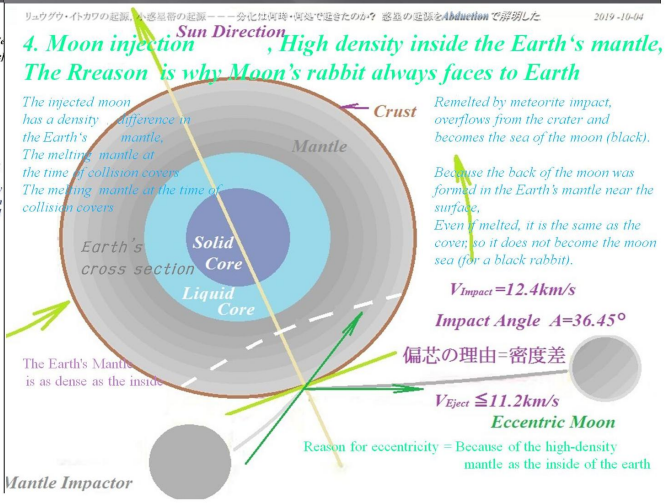

©2020. Japan Geoscience Union. All Right Reserved.

No mechanism to expand Space! Big Bang hypothesis has 't been proven!
Red-shift can be explained by New stationary space theory based on Quantum Red-Shift. Neither black holes nor Dark matter are required. Validated by Abuduction

*Akira Taneko[1]

1. SEED SCIENCE Lab.

"Currently, **various Cosmologies** are proposed. Each of them has a Different Hypothesis, and **None of them has been proved as one.** Reason is that there is no correct Evaluation Method.
Mechanism to expand Space cannot be proved! Big bang is just an **Astronomer's Hypothesis** to explain Red-shift! As a Dogma. Reason why Universe cannot be collapsed is explained by adding an Inexplicable Hypothesis that Expanding energy and Attraction of Dark Matter are balanced. It is unknown who said it, and it is irresponsible. When Traffic Lght is red at Intersection, No one is afraid if everyone crosses Road together. Ignore those who complain that it's weird! Given Laws of conservation of energy, it is Authoritarian to devise Black Holes and Dark Matter and continue Dogma without evidence. Eiichiro Komatsu was able to observe Background Isotropic Radiation of Universe, and Profile was similar to that of Blackbody Radiation at 2.725K. He said in 2014 that Observations were evidence of a Big Bang. Reason why Universe does not collapse is explained by adding an Inexplicable Hypothesis that Expanding Energy and Attraction of Dark Matter are balanced.

However, Observed Background Radiation is described in “Unknown Encyclopedia (1) p91-p100. Rowan Robinson 1980-July” on p95 “Energy Density of this Back Ground Radiation comes from many Galaxies. It is very similar to Average Energy Density of Stars. There is No known way to transform Light of such a Star into a form of Black Body Radiation at 2.7 degrees K. " It has said. Yes, I have observed that Light from a Distance in Universe is "Diluted in Energy according to Lambert's law" and that Frequency shifts to Red. In other words, at Observation point, it can be explained theoretically as a Quantum Mechanical Effect. Furthermore, since Observation point is not at Center of Universe but at Earth, it can show Isotropicity.

[1] Redshift has already been explained in Abduction at Japan Society for Planetary Sciences, "P1-23 Spatial Quantum Redshift Hypothesis and New Stationary Cosmology".
[2] Background Radiation at 3 degrees K can be explained by Fact that Average Solar Frequency Distribution was observed at 3 degrees K, with Peak shifted by Radius of Closed Universe.
[3] Red-shift at Center of Earth is only when Observation Position is Earth.
[4] Reason that Universe cannot be collapsed is explained by Mach Dynamics in a finite Universe, which considers Action (Attraction) and Reaction (Inertial Mass) to be balanced.

Biggest Mystery of Big Bang Hypothesis is that Mechanism of Spatial Expansion has not been Physically Proven. Because Ruler expands with Space, it is impossible to explain Observation of Spatial Expansion. I can't prove it for anyone else, but No Spatial Expansion has been observed. Only way to evaluate Origin of Universe was to analyze and integrate Results, and to estimate them by Induction and Deduction. Now, if you evaluate "How many features of Universe can be explained" as a result of Evolution by abduction, Hypothesis can be easily broken. Black holes,

©2020. Japan Geoscience Union. All Right Reserved.

dark matter and the big bang are no longer needed. Atomic physicists and astronomers on the Big Bang are excellent freeriders. People who construct their own theory based on Big Bang, Black Hole and Dark Matter are free riders, so Grounds are broken. Do not accept Illusion of your predecessor. Search for Truth by myself.
Check Truth of Hypothesis in Current state of Nature.
Earth is also a part of Universe, not Center of Universe. Quantum mechanics has been demonstrated on Earth, and it is used industrially in ICs and LSIs. In quantum mechanics, energy is applied where it is diluted into space. Light arriving from beyond Universe is diluted in Space. In other words, if Energy conservation law and frequency conservation become impossible at the same time, Frequency shifts to Red.
This is Grounds of [1] red-shift.

Space does not need to expand. Before inflating with a big bang, if energy is concentrated on one point, it is a big black hole and cannot explode (laughs). How can we explain Contradiction in which Effect of Space Expansion can be observed with distant light when Space Expansion cannot be observed on Earth?

Origin of Universe.
Until now, Big Bang hypothesis was believed to be correct, even if it had not been substantiated because there was No Hypothesis to compare. Who can actually prove a Big Bang?
There is a theory in Christianity that "God created World".
A similar, Big-Bbang Hypothesis has now been denied. Like Reincarnation of Buddhism, it can be said that Universe has No beginning and is Changing Forever.
Space does not need to expand. How can we explain Contradiction in which Eeffect of space expansion can be observed with distant light when space expansion cannot be observed on Earth?

Keywords: A new evaluation method to elucidate the mystery of infinity, transcending space with abduction to verify the truth, A new evaluation method to elucidate the mystery of origin, transcending time with abduction to verify the truth, Big Bang hypothesis has 't been proven!, Red-shift has already been explained in New Stationary Cosmology with Quantum red-shift., Black holes and dark matter are also Hypotheses., Mechanism for Expanding Space has not been proven !

©2020. Japan Geoscience Union. All Right Reserved.

P1-19 赤方偏移が何故 地球を中心として観測されるのか? 空間量子赤方偏移仮説 2016 09-12

3. 量子赤方偏移Z_qの計算

- エネルギー保存の法則より, 距離 r が大きく成るにつれて S が小さくなり, n より r^2 が大きくなると, 量子効果が現れる. すなわち,
- エネルギー希釈により波長が維持できず, より低エネルギー準位の低い長波長λ'に変換すると仮定する. cf. $\alpha \equiv r'/r_e$ と定義する.
- 逆に, $nh\lambda/r_e^2 \geq 1$ の範囲 $(r \leq r_e)$ では波長が変わらずに観測.
- しかし, エネルギー保存法則を考慮すると, $\lambda = nh/r^2$ となる r_e より遠方 r'では, より長波長λ'に変換される.
- その変換波長λ'を計算すると, $\lambda' = \lambda$, $Z_q = 0$ (但し $0 \leqq \alpha < 1$)
- $\lambda' = \lambda \cdot r'^2/r_e^2 = r \cdot (r'/r_e)^2 = \lambda \cdot \alpha^2$, $Z_q = \alpha^2 - 1$ (但し $1 \leqq \alpha$)

この様に, 量子赤方偏移では波長のズレは地球中心で説明できた.

- 膨張宇宙論Vで後退している星のドップラー効果による波長λ'は, もとの波長λと光速cを用いて $\beta \equiv \lambda'/\lambda$ と定義すると,
- $\lambda' = \lambda(1+V/c)$ [ドップラー効果] Vについて解くと,
- $V = c \cdot (\lambda'/\lambda - 1) = c \cdot (\beta - 1)$ である.
- $Z_d \equiv (\lambda'/\lambda) - 1 = \beta - 1 \equiv V/c$ ただし $2 < \beta$ の範囲で光速を超える.
- ハッブルの測定結果で $Z_d = r \cdot K$ ∴ $K = V/c/r$ rが大きいとVも大.

10. 空間量子赤方偏移のアイデア

エネルギー希釈=量子効果

- 基本仮説の宇宙論 空間量子赤方偏移 → 赤方偏移の観測結果 ← 他の宇宙論(仮説) ドップラー効果による
- 波長シフトアイデア → 観測位置が地球 → 地球中心の観測結果 ← ◆空間の膨張仮説 ◎ビッグバン仮説
- ローワンロビンソンの推定
  - 平均恒星波長シフトと2.7°Kの一致
  - 有限宇宙の仮説
  - 宇宙半径の導出
  - → 宇宙背景輻射 2.7° K等方観測結果 ← ◆膨張の結果の波長シフト(証明) ◎有限宇宙の仮説
  - 物理量が出ない⇒問題
- 有限宇宙バランス マッハ力学による反作用=慣性質量 → 万有引力で宇宙が潰れない謎 ← ◆空間が膨張しているから ◆膨張のエネルギー不明⇒ダークマター

P1-19 赤方偏移が何故 地球を中心として観測されるのか? 空間量子赤方偏移仮説 2016 09-12

0. 結論 赤方偏移を説明するだけの苦し紛れの仮説

空間量子赤方偏移仮説とビックバン仮説との比較検討

比較項目 ＼ 仮説名称	赤方偏移の原因	地球中心で遠方ほど周波数の偏移が大きい理由	3° K背景輻射の説明(証明?) その理由	その他 メリット デメリット
量子赤方偏移仮説 The Quantum Red Shift Hypothesis	・拡散進行波のエネルギーが空間で希釈されると,量子効果で波長が伸びて観測	・観測地点が地球である ・宇宙が宇宙原理を満たし等方均質であるから	閉じた宇宙仮定 ・空間量子赤方偏移による平均恒星のスペクトラムピーク波長が3° Kにシフト	・宇宙半径が計算可能 ・輪廻による宇宙年齢不要 ・コペルニクス的大転換
ビック・バン仮説 The Big Bang Hypothesis	・光のドップラー効果で波長が伸びる ・光源の後退速度に波長が正比例する	・ビックバン時の超高圧?で空間が均等(or.加速的に)に膨張を続けるため ・地球中心の説明のため	閉じた宇宙仮定 ・ビック・バン時のなごりの空間膨張が遠方光源のドップラー効果により波長がシフトする	・空間が膨張するメカニズムと膨張エネルギーの起源と説明が困難 ・暗黒物質の仮定が必要!!

P1-19 赤方偏移が何故 地球を中心として観測されるのか? 空間量子赤方偏移仮説 2016 09-12

4. Z_q計算結果と比較説明

その変換波長 λ'を計算すると,

- $\lambda' = \lambda$, $Z_e = 0$ (但し $0 \leqq \alpha < 1$)
- $\lambda' = \lambda \cdot r'^2/r^2 = r \cdot (r'/r_e)^2 = \lambda \cdot \alpha^2$

$Z_q = \alpha^2 - 1$ (但し $1 \leqq \alpha$)

地球中心の赤方偏移を, 量子赤方偏移仮説では, 計測位置による必然として説明できた.

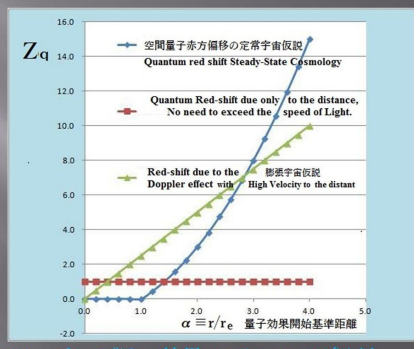

膨張仮説では $\lambda' = \lambda(1+V/c)$ [ドップラー効果] Vについて解くと,

- $V = c \cdot (\lambda'/\lambda - 1) = c \cdot (\beta - 1)$ である. $\beta \equiv \lambda'/\lambda$ と定義すると,
- $Z_d \equiv (\lambda'/\lambda) - 1 = \beta - 1 \equiv V/c$ ただし $2 < \beta$ の範囲で光速を超える.
- ハッブル測定結果で $Z_d = r \cdot K$ ∴ $V = r \cdot c \cdot K$ rが大でVも超光速.

©2020. Japan Geoscience Union. All Right Reserved.

[J] Poster | M (Multidisciplinary and Interdisciplinary)：M-IS Intersection

[M-IS23] Interface- and nano-phenomena on crystal growth and dissolution

convener:Yuki Kimura(Institute of Low Temperature Science, Hokkaido University), Hitoshi Miura(Graduate School of Natural Sciences, Department of Information and Basic Science, Nagoya City University), Hisao Satoh(Low-Level Radioactive Waste Disposal Center, Japan Nuclear Fuel Limited)

Recent developments of observations in nano-scale opened a detail discussion concerning mechanisms of crystal growth and dissolution based on interface phenomena including dynamics. In this session, growth and dissolution mechanisms of crystals will be discussed focusing on interface phenomena of minerals in the fields of biological origin, global environment, planets and space in addition to general minerals.

[MIS23-P01] A new theory of impurity incorporation into a growing crystal

*Hitoshi Miura[1] (1.Graduate School of Natural Sciences, Department of Information and Basic Science, Nagoya City University)

[MIS23-P02] Homogeneous nucleation of iron from saturated vapor by molecular dynamics simulation

*Kyoko Kitakami Tanaka[1,2] (1.Tohoku University, 2.Nihon University)

[MIS23-P03] Homogeneous nucleation of silicate nanoparticles in a microgravity environment using a sounding rocket

*Yuki Kimura[1], Joseph A Nuth[3], Frank Ferguson[4], Yuko Inatomi[2] (1.Institute of Low Temperature Science, Hokkaido University, 2.JAXA/ISAS, 3.NASA's Goddard Space Flight Center, 4.Catholic Univ. America at NASA's Solar System Exploration Division)

[MIS23-P04] Preparation for nucleation experiment of ice nanoparticles by the low-temperature gas evaporation method

*Yuki Kimura[1], Akira Kouchi[1] (1.Institute of Low Temperature Science, Hokkaido University)

[MIS23-P05] Growth of ice crystals via quasi-liquid layers: Effect of nitric acid gas

*Ken Nagashima[1], Josée Maurais[2], Ken-ichiro Murata[1], Yoshinori Furukawa[1], Patrick Ayotte[2], Gen Sazaki[1] (1.The Institute of Low Temperature Science, Hokkaido University, 2.Université de Sherbrooke, Québec, Canada)

[MIS23-P06] Radiolysis-induced crystallization process of salt in liquid cell transmission electron microscopy

*Tomoya Yamazaki[1], Yuki Kimura[1] (1.Institute of Low Temperature Science Hokkkaido University)

[MIS23-P07] Pore space property of clay in the forms of gelled and compacted

*Hisao Satoh[1], Yuki Araki[2], Ken Nagashima[3] (1.Naka Energy Research Laboratory, Mitsubishi Materials Corporation, 2.Department of Physical Sciences, College of Science and Engineering, Ritsumeikan University, 3.The Institute of Low Temperature Science, Hokkaido University)

[MIS23-P08] Growth of SrB_4O_7 crystal fibers with near stoichiometric composition by the micro-pulling-down method

*Harutoshi Asakawa[1], Takaaki Machida[1], Sho Inaba[1], Yu-ki Hamada[1], Hiroshi Uneda[1], Ryuichi Komatsu[1], Arashi Kitakaze[1] (1.Graduate School of Sciences and Technology for Innovation Yamaguchi University)

[MIS23-P09] Thermodynamic stability of norsethite $BaMg(CO_3)_2$ under hydrothermal conditions

*Koki Suga[1], Harutoshi Asakawa[1], Hiroshi Uneda[1], Itaru Echigo[1], Kaoru Isobe[1], Ryuichi Komatsu[1]
(1.Graduate School of Sciences and Technology for Innovation Yamaguchi University)

A new theory of impurity incorporation into a growing crystal

*Hitoshi Miura[1]

1. Graduate School of Natural Sciences, Department of Information and Basic Science, Nagoya City University

Concentration of impurities (or additives) in crystal is an important factor that determines crystal quality and property. For example, the electric conductivity of semiconductor strongly depends on the impurity concentration. Perfection of protein crystals used for X-ray structural analysis is affected by incorporation of impurities. The impurity concentration and its distribution in minerals are important clues to speculate geophysical environments in which these minerals have formed. To understand what factor determines the impurity partition into growing crystals is important to control properties of industrial crystals and to elucidate formation process of rock-forming minerals.

The impurity concentration in crystals is characterized by a partition coefficient, which represents the ratio of impurity fractions in crystal to growth environment. The impurity fractions are defined by a ratio of concentrations of impurity molecules to host molecules. The partition coefficient being unity indicates that the impurity fraction in the growing crystal is the same as that in the growth environment. The partition coefficient depends on the growth condition in general. There are some theories that formulated the relationship between the partition coefficient and the crystal growth velocity such as the BPS theory [1] and Smith model [2]. Both theories have formulated the effect of the concentration field disturbed at around the growing crystal. However, the essence of the crystal growth is the incorporation of molecules to the crystal at its surface. The impurity molecules are also incorporated into the crystal after adhesion on the surface, migration along the surface, and finally incorporated at step edges. This suggests the importance of the surface process on impurity partitioning, but there is no theory that predicts what factors of the surface process affect the impurity distribution and how.

In this study, we propose a new theory of the impurity partition that takes the surface process of impurity molecules into consideration. The canonical theory of crystal growth that consider the surface process of molecules is the BCF theory [3]. This theory formulated the steady distribution of host molecules adsorbed on the crystal surface using a diffusion equation and derived their incorporation rate into step edges, namely, the advancing velocity of steps. What we should consider here is the same process for impurity molecules. The behavior of the impurity molecules on the crystal surface can be described by the same diffusion equation with the host molecules. The difference from the host molecules is the number density of molecules in the crystal; the density of host molecules is fixed, on the other hand, that of impurity molecules is variable. To determine the number density of impurity molecules in the crystal, we added another constraint on the impurity incorporation. We succeeded to formulate the partition coefficient as functions of parameterized quantities that characterize the surface process of impurity molecules. In the talk, we will introduce the outline of our theory and some interesting results on the impurity partition.

The theory that we proposed in this study is a straightforward extension of the BCF theory, so it is applicable for various crystals that exhibit layer-by-layer growth. For example, our theory would be useful to quantitatively analyze the experimental results of growth of semiconductors and protein crystals. Our theory might be able to clarify the importance of the surface process for impurity partition by applying to the experimental results that cannot be interpreted by the BPS theory or the Smith model.

©2020. Japan Geoscience Union. All Right Reserved.

References:
[1] J. A. Burton et al., J. Chem. Phys. 21, 1987-1991 (1953). [2] V. G. Smith et al., Can. J. Phys. 33, 723-745 (1955). [3] W. K. Burton et al., Philos. Thans. R. Soc. London Ser.A 243, 866 (1951).

Keywords: Crystal growth, Impurity partition, Theory, Surface process

©2020. Japan Geoscience Union. All Right Reserved.

Homogeneous nucleation of iron from saturated vapor by molecular dynamics simulation

*Kyoko Kitakami Tanaka[1,2]

1. Tohoku University, 2. Nihon University

Condensation process from vapor to liquid (or solid) via homogeneous nucleation is a fundamental process and plays an important role in many areas of science and technology. Despite the familiarity of the process, serious unreliability remains in model predictions for nucleation rates. Molecular dynamics (MD) simulations are able to directly resolve details of the nucleation process and provide useful test cases for nucleation models. There were a lot of previous studies with MD simulations for the investigation of nucleation in a supersaturated vapor, but only limited type of substances such as rare gas and water have been examined. In this study, we performed the MD simulations of homogeneous nucleation process from a saturated vapor composed of iron atoms. There was an example of MD simulation for iron (Lummen&Kraska2005), but there was no detail comparison with the theory because of the small system with 343-1,331 atoms. In this study, we performed the MD simulations of homogeneous nucleation process from a vapor with 1,000-100,000 iron atoms. The simulations were performed with the Large-scale Atomic/Molecular Massively Parallel Simulator (LAMMPS) code developed at Sandia National Laboratories. We used the embedded atom method (EAM) for modeling the force field acting between the iron atoms (Mendelev et al. 2003). We reproduced the homogeneous nucleation process with the nucleation rate of orders of magnitude lower than the previous study. Comparing the results of our MD simulations with theoretical models requires knowledge of the thermodynamic properties, especially the surface tension and equilibrium vapor pressure. To estimate the quantities we performed a series of equilibrium MD simulations of liquid-vapor systems consisting of a liquid slab with vapor at fixed temperature (NVT) and with periodic boundaries. In the MD simulations, the values of the critical nucleus were almost unity because of high supersaturation ratio, while the nucleation rates were several orders of magnitude lower than the gas kinetic collision limit for nucleation rates. The results may indicate a difficulty of dimerization in the nucleation process.

Keywords: Nucleation, iron, Molecular dynamics simulation

©2020. Japan Geoscience Union. All Right Reserved.

Homogeneous nucleation of silicate nanoparticles in a microgravity environment using a sounding rocket

*Yuki Kimura[1], Joseph A Nuth[3], Frank Ferguson[4], Yuko Inatomi[2]

1. Institute of Low Temperature Science, Hokkaido University, 2. JAXA/ISAS, 3. NASA’s Goddard Space Flight Center, 4. Catholic Univ. America at NASA's Solar System Exploration Division

Silicates are the main mineral group found at the Earth’s surface and are commonly composed of magnesium, iron, silicon and oxygen. Silicates have been observed to form in the outflows of oxygen-rich stars and that source is thought to have provided the building blocks for our solar system. Many silicate minerals can be found in meteorites and isotopic analyses confirm that some grains survived the processes of evaporation, condensation and aqueous alteration in the early solar system: these are presolar silicates. Astronomical observations show that most of the infrared features attributed to silicates in oxygen-rich, circumstellar outflows most likely arise from amorphous silicates. However, some high-mass-loss, oxygen-rich stars show crystalline features in their infrared spectra. The fraction of crystalline silicates is typically on the order of ~10% of the total. Experimentally, the degree of crystallinity has been confirmed to depend on the cooling rate from the gas phase, the Mg/Si ratio, the annealing temperature and time. However, a reasonable explanation for why only 10% of silicates are crystalline in these outflows, and why crystalline silicates are not detected in the gas outflows of low-mass-loss stars is not yet known. The character of the resulting silicate grains would be governed by the initial silicate nucleation process.

We conducted a set of microgravity nucleation experiments using a NASA Black Brant IX sounding rocket on October 7, 2019 to study the nucleation, growth and aggregation of silicate grains. Over a period of 460 seconds in microgravity silicate particles formed following the evaporation of starting materials previously deposited onto tantalum filaments that were resistively heated in six different experimental chambers. Particles formed via homogeneous nucleation from a supersaturated vapor after cooling in a buffer gas of either pure argon or a mixture of argon plus oxygen. The temperature and concentration of the evaporated vapor can be determined by direct imaging of a double-wavelength, Mach-Zehnder type interferometer. In addition, we successfully recovered both the payload and the particles produced during the experiment. We studied these analog presolar silicates using a transmission electron microscope. The particles have a size distribution centered at ~40 nm in diameter and are mostly amorphous but with some small degree of crystallinity in some grains. While some aggregated grains show clear boundaries between the particles, other samples show complete fusion with no observable boundaries remaining. We will discuss the nucleation of presolar grains based on the results of the further analyses of these experiments.

Keywords: Dust, Nucleation, Microgravity, Silicate

©2020. Japan Geoscience Union. All Right Reserved.

Preparation for nucleation experiment of ice nanoparticles by the low-temperature gas evaporation method

*Yuki Kimura[1], Akira Kouchi[1]

1. Institute of Low Temperature Science, Hokkaido University

Nanoparticles with the size of ~100 nm are ubiquitous in space and serve as substrates for molecular formation and become building blocks of planets. Therefore, understanding their composition, size, and abundance is very important to understand material evolution in space. Especially, ice condenses homogeneously or heterogeneously on other mineral particles depending on an environment after a heating event in the early planetary system. Therefore, elucidation of nucleation conditions of ice is essential for discussions on planet formation and astrobiology. In this study, we have established a new experimental method for formation of ice nanoparticles and in-situ observation of its formation environment to determine two important physical parameters (surface free energy and sticking probability) of ice nanoparticles. Here, the concept of our study and experimental system named ALADDIN; Advanced Laboratory Apparatus for Direct Detection of Ice Nucleation, will be presented.

Acknowledgements

This work was partly supported by Grants-in-Aid from KAKENHI for Scientific Research (S) (15H05731).

Keywords: Nanoparticle, Nucleation, Ice

©2020. Japan Geoscience Union. All Right Reserved.

Growth of ice crystals via quasi-liquid layers: Effect of nitric acid gas

*Ken Nagashima[1], Josée Maurais[2], Ken-ichiro Murata[1], Yoshinori Furukawa[1], Patrick Ayotte[2], Gen Sazaki[1]

1. The Institute of Low Temperature Science, Hokkaido University, 2. Université de Sherbrooke, Québec, Canada

Ice is one of the most abundant crystals on the earth, and hence the molecular-level understanding of ice crystal surfaces holds the key to unlocking the secrets of a number of fields. We and Olympus Engineering Co., Ltd. have developed laser confocal microscopy combined with differential interference contrast microscopy (LCM-DIM), by which we succeeded in the direct visualization of 0.37-nm-thick elementary steps on ice for the first time [1]. In addition, we could also visualize the quasi-liquid layers (QLLs) on ice crystal surfaces [2], which are covered with thin liquid layers even below the melting point (0˚C). The direct observations of QLLs under nitrogen gas revealed the appearance temperatures and partial pressure of water vapor [3,4]. On the other hand, we also found that even trace acidic gas induced the stability of QLLs. In this study, we chose HNO_3 as a model atmospheric gas, and directly observed the QLLs on ice basal faces by advanced optical microscopy[5].

Irrespective of the presence/absence of the HNO_3 gas, the pure-QLLs and HNO_3-QLLs appeared with increasing temperature and disappeared with decreasing temperature. The shape of pure-/HNO_3-QLLs showed spherical dome and the contact angle of them on the ice basal face was ~1˚. Although the appearance/disappearance temperatures of the pure-QLLs were not so different (-1.9 and -2.2 ˚C, respectively), there was the large thermal hysteresis between the appearance and disappearance temperatures of HNO_3-QLL (-1.8 and -6.4 ˚C, respectively). The result suggests that the disappearance mechanisms of the pure-/HNO_3-QLLs were different. Our previous paper indicated that the pure-QLLs are kinetically formed, not by the melting of ice surfaces, but by the deposition of supersaturated water vapor on ice surfaces. On the other hand, we found that the HNO_3-QLLs are not composed of pure water, but rather of aqueous HNO_3 solutions, and also that the HNO_3-QLL and the ice crystal were in equilibrium.

When the HNO_3-QLL and the ice crystals were in equilibrium, we suddenly reduced the temperature, which meant that the systems fell out of equilibrium and the HNO_3-QLL became supercooled. At this time, we observed that a macrosteps appeared along the periphery of the HNO_3-QLL. Such growth behavior is well known as the vapor–liquid–solid (VLS) growth mechanism, which usually causes the growth of whisker crystals.

Recently, we studied the effects of hydrogen chloride gas on the behavior of QLLs (HCl-QLLs) on ice basal faces [6,7]. We found that the HCl-QLLs were also aqueous hydrochloric acid solution, and that the temperature and HCl concentration of the HCl-QLLs were also very close to those of a liquidus line: these results were similar to those found in this study. However, the growth of ice started preferentially from droplet–ice–vapor contact lines, thereby causing the HCl-QLLs to become embedded within ice crystals without freezing[7]: no VLS growth occurred contrary to the case of the HNO_3-QLLs. We will present more detail of the difference between the roles of pure-/HNO_3-/HCl-QLLs while ice growth and evaporation.

[1] Sazaki et al. (2010) PNAS 107, 19702.

©2020. Japan Geoscience Union. All Right Reserved.

[2] Sazaki et al. (2012) PNAS 109, 1052.

[3] Asakawa et al. (2015) PNAS 113, 1749.

[4] Murata et al. (2016) PNAS 113, E6741.

[5] Nagashima et al. (2020) Crystals 10, 72.

[6] Nagashima et al. (2016) Cryst. Growth Des. 16, 2225.

[7] Nagashima et al. (2018) Cryst. Growth Des. 18, 4117.

The details of this study are shown in our paper [5]. We will present this study from other viewpoints in "A-AS07 Atmospheric Chemistry" and “A-CC39 Glaciology” sessions.

Keywords: Ice, quasi-liquid layer, nitric acid gas, optical microscopy

©2020. Japan Geoscience Union. All Right Reserved.

Radiolysis-induced crystallization process of salt in liquid cell transmission electron microscopy

*Tomoya Yamazaki[1], Yuki Kimura[1]

1. Institute of Low Temperature Science Hokkkaido University

Crystallization in solution is a ubiquitous process in the earth and is important not only for the production of materials but also for understanding geochemical processes. However, the early stages of crystallization, including nucleation, are still mysterious because of difficulty in visualizing the processes due to the limitation of observation techniques. A promising method for observing these processes is liquid-cell transmission electron microscopy (LC-TEM), which has nanoscale spatial resolution and real-time temporal resolution. On the other hand, capturing the moment of nucleation using this technique is quite difficult because the observable area is very small and controlling supersaturation in the observing area is extremely difficult. We recently found that sodium chloride crystallized when the electron beam was irradiated on a mixture of a little amount of saturated aqueous solution of sodium chlorate and acetone. This experiment suggests that the electron beam causes radiolysis resulting in dissociation of chlorate ion into chloride ion, and acetone works as an antisolvent for sodium chloride and controls supersaturation of its crystal. Here we report further study for understanding the crystallization process using LC-TEM and different antisolvent.

We used the TEM holder which can enclose the vacuum-tight liquid cell. We enclosed a saturated antisolvent solution (e.g. ethanol) of sodium chlorate in the liquid cell. Then we observed the solution by TEM with a field-emission gun at an acceleration voltage of 200 keV. In this presentation, the detailed results of observation which include analysis of the nucleated crystal and mechanisms of the crystallization will be discussed.

Acknowledgement

This work was supported partly by Grant for Basic Science Research Projects from The Sumitomo Foundation (Grant Number 170738) and JSPS KAKENHI Grant Numbers JP15H05731 and JP18J01470.

Keywords: liquid-cell transmission electron microscopy, crystal growth, solution growth, antisolvent crystallization

©2020. Japan Geoscience Union. All Right Reserved.

Pore space property of clay in the forms of gelled and compacted

*Hisao Satoh[1], Yuki Araki[2], Ken Nagashima[3]

1. Naka Energy Research Laboratory, Mitsubishi Materials Corporation, 2. Department of Physical Sciences, College of Science and Engineering, Ritsumeikan University, 3. The Institute of Low Temperature Science, Hokkaido University

Context: Rock and clay are still major constructive materials in the modern ages even for the underground facilities such as radioactive waste repository, due to its long-term robustness. The chemical and mineralogical robustness should be promised by its very low reactivity. Until recently, there are many studies developing the geochemical and engineering models to validate the safety of waste disposal, because the repository has buffer clay as engineered barrier. Dissolution of clay minerals is the first priority information. Direct measurement revealed that dissolution rate of clay is extremely lowered by effective surface area at the reactive (hk0) edge (ESA) exposed to the pore solution as a function of density [1]. Recently, we have successfully formulated the effective ESA as the function of density involving isotropic-nematic transition [2]. Step-interaction also affect the dissolution kinetics [1, 3] which is sometimes explained by the step-dynamic law such as the BCF theory [4]. Explaining the relationship between dissolution and its resultant degradation in water-stopping property such as hydraulic conductivity is required to validate the feasibility in engineered barrier system. Very recently, we have developed an atomistic scale method to evaluate the surface property of hydration structure of clay in groundwater directly [5].

Methods: We used FESEM to observe pores in clay rocks from Tsukinuno mine (Kunimine Industries Co., Dr. M. Itoh, Pers. Comm.). The tomographic observation was also made on this clay with micro X-ray CT (Fig. 1). Direct dissolution measurement by interferometry had been carried out on a purified separate from same clay rock (Kunipia P) under various compaction conditions [1, <1E-12 mol/m^2/s]. To understand the connection between hydraulic property and dissolution, we applied surface force measurement with FM-AFM [6]. This method can realize force curve measurement which reflects interaction between hydrated clay surface and ambient water. The force curve scanning can visualize 3-D development of electric double layer (EDL) over the interface (a few nm). This is a new direct measurement estimating hydraulic property at the very nano-scale pores. Based on the step-dynamics and hydration structure with EDL, we can evaluate evolution of actual pore size during alteration process.

Results and Discussion: Groundwater has passed though these pores while the clay-rock is underlying at the mine. Pores as interstitial space surrounded by clay grains are the flow-path. The actual space is limited by the EDL as well as clay density. FM-AFM exhibited that the EDL over the clay surface is not constant [5], so that the water-path in the compacted clay should be very complicated. Generally, it is understood that the hydraulic conductivity varies as the function of clay density. The density cannot affect only the exposed area of the clay edge at which dissolution mainly occurs [2], but also the hydraulic property by the variety of the EDL in compacted clay. If the clay contains other secondary minerals such as zeolite or silica, the EDL of pores should be changed.

Until now, there are many macroscopic data about clay hydraulic measurements. Realistic pore

©2020. Japan Geoscience Union. All Right Reserved.

observation of natural clay-rock can be currently achieved only by FM-AFM and nano-scale tomography. For better safety management, we need to proceed such a bottom-up approach to explain the large scale phenomena concerning migration issues about waste disposal.

References: [1] Satoh et al. (2013) Clay Min., 48, 285-294.; [2] Terada et al. (2017) Mat. Res. Exp. 6(3) 035514.; [3] Satoh et al. (2007) Am. Min., 92, 503-509.; [4] Burton et al. (1951) Phil. Trans. Royal Soc. London, 243, 299; [5] Satoh et al. (2019), Abst. Migration 2019; [6] Araki et al. (2017) Surf. Sci, 665 32-36.

Figure 1. Micro XCT images of gelled (a, wet) and compacted (b, dry) montmorillonite clay.

Keywords: clay, EDL, hydraulic conductivity

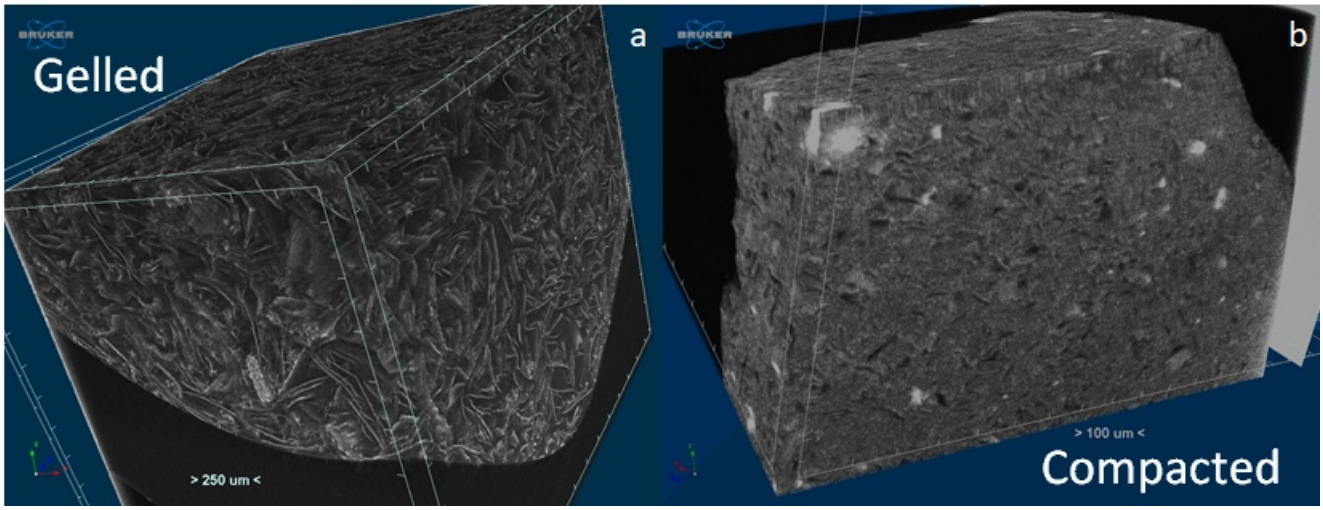

©2020. Japan Geoscience Union. All Right Reserved.

Growth of SrB_4O_7 crystal fibers with near stoichiometric composition by the micro-pulling-down method

*Harutoshi Asakawa[1], Takaaki Machida[1], Sho Inaba[1], Yu-ki Hamada[1], Hiroshi Uneda[1], Ryuichi Komatsu[1], Arashi Kitakaze[1]

1. Graduate School of Sciences and Technology for Innovation Yamaguchi University

SrB_4O_7 (SBO) has recently received much attention as a wavelength-conversion material that can operate into the deepest ultraviolet wavelengths (125 nm). The utilization of SBO for semiconductor lithography and laser ablation requires fully transparent crystals. Here, we show the growth of SBO crystal fibers with near-stoichiometric composition by the μ-pulling-down method. $SrB_{2x}O_{3x+1}$ ceramics sintered with various values of x were evaluated by X-ray diffraction (XRD). The melting point of the SBO ceramics was measured by differential scanning calorimetry (DSC) as 1017 ˚C, and the heat of fusion was 63.3 J/g. Figure 1 shows the external form of SBO crystal fibers grown with various x values. Crystal fibers shown in A and C were opaque due to the formation of growth ridges (black arrows). Also, we succeeded in obtaining transparent SBO crystal fibers by the growth with a stoichiometric composition. Then, we observed SBO crystal fibers grown with various x values by polarized optical microscopy. As a result, even when the deviation from stoichiometric composition was ±−0.1 mol % SrO (x = 2 ±0.004), SrB_2O_4/SrB_6O_{10} appeared. These results demonstrate that SBO shows no solid-solution width and that the stoichiometric composition is equal to the congruent composition. In contrast, since growth ridges including SrB_2O_4/SrB_6O_{10} were formed only on surfaces of the SBO single crystals, SBO crystal fibers grown with nonstoichiometric composition were opaque. We could explain the formation of growth ridges via compositional supercooling on rims.

©2020. Japan Geoscience Union. All Right Reserved.

Thermodynamic stability of norsethite $BaMg(CO_3)_2$ under hydrothermal conditions

*Koki Suga[1], Harutoshi Asakawa[1], Hiroshi Uneda[1], Itaru Echigo[1], Kaoru Isobe[1], Ryuichi Komatsu[1]

1. Graduate School of Sciences and Technology for Innovation Yamaguchi University

Norsesite $BaMg(CO_3)_2$ has piezoelectric properties, and shows a birefringence (0.175) higher than conventional piezoelectric crystals, Hence, it is expected that norsethite is a new-generation material of an acousto-optic device or wavelength conversion element. To reveal the characteristics of the norsethite, it is necessary to grow a crystal of several mm. Under atmospheric pressure, the solubility of norsethite is extremely low, and the growth rate is quite slow (several nm/min). Therefore, the hydrothermal synthesis method is useful as well as the conventional carbonate growth. However, since the hydrothermal synthesis needs a pressure- and heat-resistant container, the crystallization process under hydrothermal conditions is invisible. Recently, we have succeeded in fabricating the chamber that allows the in-situ observation under hydrothermal conditions. As a result, we, for the first time, succeeded in in-situ observing the solution-mediated transition of norsethite under hydrothermal conditions. In this study, we investigated the thermodynamic stability of norsethite under hydrothermal conditions by measuring the solubility to quantitatively understand the solution-mediated transition mechanism of norsethite under hydrothermal conditions.

Pure water at room temperature was circulated by a pump into the in-situ observation chamber under hydrothermal condition containing powdered norsethite for several hours. The pH of the solutions returned to atmospheric pressure from the chamber was measured at 3MPa and individual temperature T. The dissolution equilibrium was confirmed from the change in pH. Ba^{2+}, Mg^{2+}, and CO_3^{2-} concentrations in saturated solutions of norsethite were measured by ICP (Inductively coupled plasma) atomic emission spectrometry and total organic carbon measurement.

Fig.1 shows the temperature dependence of the solubility product K of norsethite under hydrothermal conditions and atmospheric pressure. The curves correspond to the result fitted by the revised van't Hoff equation. At 3 MPa, the solubility product of norsethite increased from room temperature to around 40˚C, and then decreased with increasing temperature as well as atmospheric pressure[2]. In contrast, the solubility product of norsethite under hydrothermal conditions was ca. 5 units lower than that under atmospheric pressure.

To further understand the thermodynamic stability of norsethite, the dissolution enthalpy dH and the dissolution entropy dS under hydrothermal conditions and atmospheric pressure were determined from the fitting parameters. The dissolution enthalpies $dH_{298.15}$ of norsethite and barium carbonate at 30˚C were 78.45 (kJ/mol) and -57.61 (J/mol/K), respectively, and these dissolution entropies $dS_{298.15}$ were 19.88 (kJ/mol) and -126.8(J/mol/K), respectively. Also, the dissolution enthalpies $dH_{363.15}$ of norsethite and barium carbonate at 90˚C were -125.5 (kJ/mol) and -763.5 (J/mol/K),respectively, and dissolution entropies $dS_{363.15}$ were -221.2 (kJ/mol) and -856.3 (J/mol/K), respectively.The dissolution enthalpy and dissolution entropy of norsethite and barium carbonate under hydrothermal conditions decreased with increasing temperature. Using these results, we calculated the difference of the chemical potential between norsethite and barium carbonate. As a result, we revealed that norsethite relatively easily crystallizes under hydrothermal conditions.

©2020. Japan Geoscience Union. All Right Reserved.

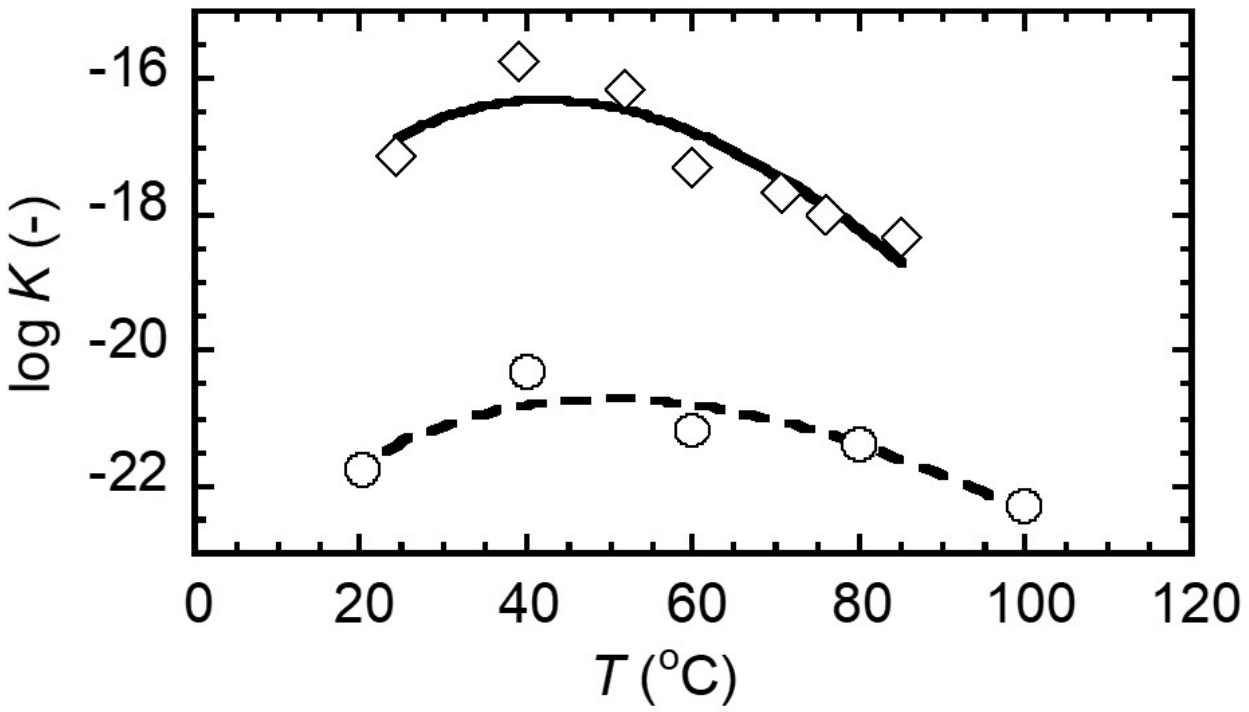

Fig.1 The temperature dependence of the solubility product *K* of norsethite under hydrothermal conditions (: ○) and atmospheric pressure (: ◇)

©2020. Japan Geoscience Union. All Right Reserved.

[J] Poster | M (Multidisciplinary and Interdisciplinary)：M-IS Intersection

[M-IS24] Mountain Science

convener:Keisuke Suzuki(Research Center for Mountain Environment, Shinshu University), Yoshihiko Kariya(Department of Environmental Geography, Senshu University), Akihiko SASAKI(Department of Geography and Environmental Studies, Kokushikan University), Chiyuki Narama(Niigata University, Department of Science)

Mountainous areas provide water resources to the populated downstream areas, protecting the diversity of ecosystem and providing tourism attraction. To access the mountain environment changes and mitigate the impacts of global warming influences, a cross-cutting session is proposed to share the scientific knowledge among various fields; such as climatology, hydrology, geography, glaciology, water/carbon/material cycle, eco-diversity, etc.

[MIS24-P01] Large-scale landslide immediately occurred at the fallout of Aira-Tn tephra (31 cal ka BP) in the northern Tenshu Mountains, central Japan

*Keiju Kimura[1], Yoshihiko Kariya[2] (1.Undergraduate Senshu University, 2.Senshu University)

[MIS24-P02] The effects of temporal continuity of grasslands on plant- and butterfly-communities

*Taiki INOUE[1], Yuki Yaida[2], Yuki Yaida[2], Koki Katsuhara[2], Keiko Takashima[2], Takeharu Seki[1], Yuka Yamamoto[1], Atsushi Ushimaru[2], Tanaka Kenta[1] (1.University of Tsukuba, 2.Kobe University)

[MIS24-P05] Clarification of cause of temporal tracer variations in spring water, Kamikochi, Shinshu

*Yoshitake Nagahata[1], Koichi Sakakibara[1], Keisuke Suzuki[1] (1.Shinshu University)

[MIS24-P06] Hydraulic connectivity between groundwater and surface water in Suwa region, Japan

*Mizuki Hori[1], Koichi Sakakibara[1], Yuichi Miyabara[1], Keisuke Suzuki[1] (1.Shinshu University)

[MIS24-P07] Development of a high-resolution prediction model for spatio-temporal dynamics of snowmelt using time-lapse camera images at west side of Mt. Tateyama

*Reiko Ide[1], Ryotaro Okamoto[2], Hiroyuki Oguma[1], Wataru Shimada[3], Kazuma Aoki[3] (1.National Institute for Environmental Studies, 2.University of Tsukuba , 3.University of Toyama)

[MIS24-P08] Factor that results in a decrease in snow surface albedo that promotes snow melting in the Kamikochi, Taisyoike

*Miu Otsuka[1], Keisuke Suzuki[1], Motoshi NISHIMURA[2] (1.Faculty of Science, SHINSHU UNIVERSITY, 2. Interdisciplinary Graduate School of Science and Technology ,SHINSHU UNIVERSITY)

[MIS24-P09] Spatiotemporal variations in stable isotope ratios of precipitation in the Japanese Alps Region

*Tsukasa Katsuragawa[1], Tsutomu Yamanaka[2], Akihiko SASAKI[3], Yuki Kurokumo[1], Motoshi NISHIMURA[1], Shimizu Hironori[1], Keisuke Suzuki[4] (1.Graduate School of Science and Technology,Shinshu University, 2.Faculty of Life and Environmental Sciences, University of Tsukuba, 3.Kokushikan University, 4.Shinshu University)

[MIS24-P11] Variation of snow in the Japanese Alps

*Keisuke Suzuki[1] (1.Research Center for Mountain Environment, Shinshu University)

Large-scale landslide immediately occurred at the fallout of Aira-Tn tephra (31 cal ka BP) in the northern Tenshu Mountains, central Japan

*Keiju Kimura[1], Yoshihiko Kariya[2]

1. Undergraduate Senshu University, 2. Senshu University

In the Tojiro district (Minobu Town, Yamanashi Prefecture), the northern part of the Tenshu Mountains, there is a remarkable landslide feature. However, its geological and geomorphological details have been uninvestigated yet. We clarified characteristics and historical development of this landslide based on both field and laboratory approaches. [Landforms and geology] Three horseshoe-shaped steep cliffs are present on the left bank of the Tojiro River at an elevation from 800 m to 1600 m. Below these cliffs, a gentle slope ($A=6.0\times10^5$ m^2) , 500 m wide and 1500 m long , is developed. Basaltic gravels larger than 2 m in diameter are seen on the gentle slope. Poorly-sorted debris consisting of basalt clasts is exposed on the eastern and western edge of the gentle slope. Therefore, the steep cliffs are considered to be originated from head scarps by landsliding, and the gentle slopes are landslide emplacement materials. Assuming that an average thickness of the landslide materials is 10 m, the volume of landslide materials is estimated to 6.0×10^6 m^3, equivalent to a large-scale classification of landslide. On the valley side slopes in the right bank of the Tojiro River, poorly-sorted debris correlatable with the landslide materials at Tojiro remain. Around there, a fine vitric tephra was found just above the landslide materials without remarkable uncomformity. This tephra, mainly composed of a bubble-walled to planar type of glass shards, is can be identified with Aira-Tn (AT: 30.8 cal ka BP) on the basis of an analysis of major chemical components. Judging from the stratigraphic relationship with AT, it is considered that the landslide materials was formed immediately at 31 cal ka. [Debris flow terrace] Terraced forms with a relative height of 5 to 6 m from the present riverbed are present on both banks of the Tojiro River downstream of the main landslide gentle slopes. These terraces consist of poorly-sorted subrounded to subangular gravel of basalt and mudstone. Imbrication is also seen. These terraces are thus considered to be debris flow terraces origin, formed simultaneously or lately the large landslide. [Historical development of landslide] Based on the above data, the historical development of the large landslide in Tojiro can be reconstructed as follows: 1) Around 31 cal ka BP, a large-scale landslide occurred on the mountainside slopes south of Tojiro, and a large amount of debris ranout, resulting in headscarp formation. 2) The moved debris formed a gentle slope around the present settlement of Tojiro. Furthermore, a part of debris climbed up to the opposite valley side of the Tojiro River. 3) The gentle slope was dissected to form a terrace feature and debris flow terraces were also formed along the downstream of the Tojiro River.

Keywords: Southern Fossa Magna, Tephrochronology, Aira-Tn tephra, Late Pleistocene

©2020. Japan Geoscience Union. All Right Reserved.

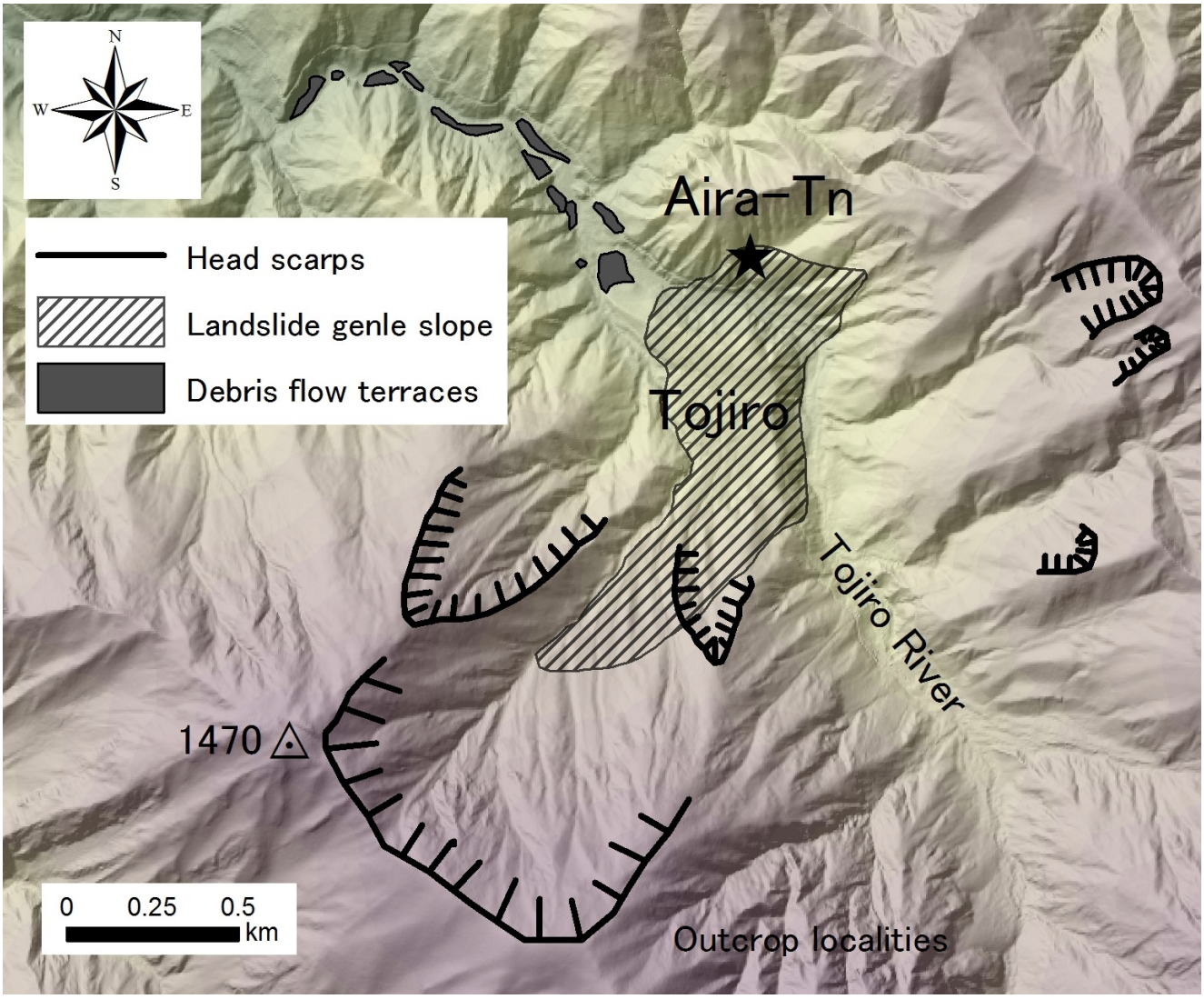

©2020. Japan Geoscience Union. All Right Reserved.

The effects of temporal continuity of grasslands on plant- and butterfly- communities

*Taiki INOUE[1], Yuki Yaida[2], Yuki Yaida[2], Koki Katsuhara[2], Keiko Takashima[2], Takeharu Seki[1], Yuka Yamamoto[1], Atsushi Ushimaru[2], Tanaka Kenta[1]

1. University of Tsukuba, 2. Kobe University

Approximately half grasslands in the world have been converted to farmlands. Temperate grasslands are biodiversity–rich ecosystems that are rapidly decreasing over the world and Japan. For effective biodiversity conservation, it is urgent to identify grasslands that have high biodiversity and thus conservation–priority. Recently, increasing number of studies have shown that the permanence of grassland affects biological communities, suggesting that the past vegetation history can be an effective biodiversity indicator. To establish a identifying method of grasslands with high conservation priority, this study addressed the effects of temporal continuity of grassland, which means that grasslands continue without becoming forests, on biodiversity. We investigated the effects of grassland on species richness and community composition in plants and butterflies, which they are closely related to plants and many endangered species live in grassland.
We traced the change in grassland distribution from the 1910s to the present in three regions in central Japan, i.e. Sugadaira, Hakuba and Kirigamine, using topographic maps and aerial photos. Study sites were "old grassland" that had lasted for more than 100 to 1000 years, "new grassland" generated by deforestation 44 to 73 years ago, and "forest", in the above three regions (total 58 sites). We investigated plant communities at 5–8 sites in each of three types of vegetation. We also studied butterfly communities in the 19 sites in Sugadaira. We sat a 1 ×20 m transect in each study site at least 20 m borders between grasslands and forests. In each transect, we recorded the presence of vascular plant species in July and September. We classified them into grassland–dependent native species and endangered species according to habitat information in guides and appearances in Red lists in each prefecture. For butterfly survey, we sat a 5 ×20 m plot including the plant plot in each study site, and the number of species and individuals was recorded seven times between June and September by one round trip in 12 minutes.
We found that old grasslands had higher numbers of grassland–dependent native plant species and that of grassland–dependent endangered plant species, than the other vegetation in the whole three regions. Plant species compositions were different between old and new grasslands, consistently in the three regions. The plant species compositions of the new grasslands tended to be intermediate between the old grasslands and the forests, suggesting that the influences of forest history still remained on the species composition in the new grasslands. Old grasslands tended to have more indicator plant species. As old grassland indicators, *Cirsium* sp. was common in the three regions, and *Adenophora triphylla* was common in Sugadaira and Kirigamine, on the other hand, no indicator species was common in new grassland. We found that grassland had higher number of butterfly species, and the old grasslands tended to have more species than the new ones. Whilst plant community was affected by the vegetation history of the very study sites, butterfly community was affected by the area of old grassland within 300 m of the study sites, suggesting that the historical butterfly communities depend on large old grasslands. This difference between plant and butterfly may be caused by (1) the difference of required resource and (2) mobility. Butterflies (1) require multiple plant individuals for food throughout the larval and adult stages, and (2) are generally more mobile than plants. Thus, butterflies may be more affected by area of grassland than plants that can maintain a species even if only one individual remains. We propose that grasslands that have long temporal continuity have high conservation value with rich and unique biological communities. because almost all grasslands in this study are managed as ski runs, it is re–recognized that

©2020. Japan Geoscience Union. All Right Reserved.

ski runs are important in grassland conservation.

Keywords: semi-natural grassland, land use history, sky run, indicator species, conservation

©2020. Japan Geoscience Union. All Right Reserved.

Clarification of cause of temporal tracer variations in spring water, Kamikochi, Shinshu

*Yoshitake Nagahata[1], Koichi Sakakibara[1], Keisuke Suzuki[1]

1. Shinshu University

Understanding of groundwater discharge processes in mountain regions is important for the prevention of natural disasters such as flood and landslide. The temporal variation of environmental tracers can characterize the discharge process; hence, the long-term data of environmental tracers should be obtained to describe groundwater discharge processes in mountain regions. However, there are few researches using long-term tracer data on the high-mountain hydrology field due to difficulties of access and severe weather. Therefore, the objective of this study is to investigate the temporal change of environmental tracers and its cause in groundwater in Kamikochi, Shinshu, Japan. For this, field surveys were conducted once every 2 weeks throughout the year (from October 2018 to October 2019). Water samples (4 springs and 1 precipitation) were collected from 4 groundwater discharge points and 1 precipitation sampler location. Then, we measured basic water quality and analyzed dissolved inorganic ion concentrations and oxygen/hydrogen stable isotopic compositions of water.

Water temperature of 3 of 4 springs gradually decreases in autumn and winter seasons. And, that gradually increases in spring and summer seasons. In addition, water temperature of those springs rapidly increases shortly after heavy rainfall events. On the other hand, water temperature of the rest of springs does not change so much throughout the year. These results indicate the groundwater discharge processes of one spring are different from other springs even these discharge locations are close to each other. pH and EC of spring waters have no clear temporal tendencies throughout the year, although EC of some spring waters slightly decreases from May to August.

Water chemistry inferred that calcium-bicarbonate water type was dominant; hence, calcium and bicarbonate ions could be treated as effective tracers in this study. These two ions concentration slightly increases and decreases in winter and spring seasons, respectively. Considering snow conditions, the groundwater recharge process is limited in winter season due to snow-accumulation and that is enhanced in spring season due to snowmelt. This should be the main causes of water chemistry variation.

Stable isotopic compositions of oxygen and hydrogen in precipitation ranged from −21.7‰ to −6.8‰ and from −159.9‰ to −38.0‰, respectively. On the other hand, those of oxygen and hydrogen in spring water ranged from −14.5‰ to −8.5‰ and from −96.0‰ to −76.3‰, respectively. This suggests precipitation may affects some parts of spring water; however, groundwater is discharged as spring some moment after groundwater recharge by precipitation. Therefore, it is necessary to investigate groundwater age for more precise discussion regarding environmental tracer variations.

Keywords: Kamikochi, spring, dissolved ion , oxygen/hydrogen stable isotopes

©2020. Japan Geoscience Union. All Right Reserved.

Hydraulic connectivity between groundwater and surface water in Suwa region, Japan

*Mizuki Hori[1], Koichi Sakakibara[1], Yuichi Miyabara[1], Keisuke Suzuki[1]

1. Shinshu University

Understanding interaction between groundwater and surface water is important to consider a sustainable water resources management. Environmental tracers such as inorganic ions and oxygen/hydrogen stable isotopes have been recognized as useful tracers to obtain an information of connectivity between groundwater and surface water. The people in Suwa region strongly rely on the groundwater for the principal water resource; however, there are few consensuses of water resource recharge processes regarding relationship among precipitation, surface water, and groundwater. Therefore, the objective of this study is to clarify a water resources recharge process through the indication of the hydraulic connectivity between groundwater and surface water in Suwa region, Japan. For this, groundwater table levels in four locations were monitored throughout the year. In addition, lake water, river water, groundwater, and precipitation were periodically sampled to determine the environmental tracer information.

Monitored groundwater table levels presented different trends in space and time. Considering hydraulic potential distribution from mountain side to lake side, the groundwater in mountain side had higher potential than that in lake side throughout the year. This suggests the groundwater mainly flows from mountain side to the lake. Groundwater table level rose a maximum of about 1.3 m in the vicinity of the lake from spring to summer seasons; however, the temporal trend was much different between surface (lake) water and this groundwater. This indicates the lake water and groundwater near the lake might not be hydraulically connected. For more detailed discussion about connectivity between the lake and groundwater, it is necessary to get hydraulic potential data in several wells near the lake.

Stable isotopic compositions of sampled water were plotted near the local meteoric water line on the delta diagram, indicating sampled water (groundwater and surface water) mostly originated from precipitation. However, determined stable isotopic compositions of oxygen and hydrogen in precipitation ranged from −16.5‰ to −7.9‰ and from −121.0‰ to −42.0‰, whereas those in other water ranged from −12.4‰ to −10.0‰ and from −85.6‰ to −69.8‰. This result suggests that although precipitation should contribute groundwater recharge, this process is not fast and direct phenomenon. No clear temporal variation of chemistry in groundwater samples was observed even in the season with large amount of rainfall, supporting that interpretation.

In terms of interaction between groundwater and river water, observed stable isotopic compositions of all groundwater samples had the value within the range of those in river water. This may indicate the groundwater consists of river water affected by the precipitation. However, this interpretation is still weak; thus, the river water role on the groundwater recharge should be examined in the future work in Suwa region.

Keywords: Suwa region, interaction between groundwater and surface water, hydraulic potential, inorganic ions, oxygen/hydrogen stable isotopes

©2020. Japan Geoscience Union. All Right Reserved.

Development of a high-resolution prediction model for spatio-temporal dynamics of snowmelt using time-lapse camera images at west side of Mt. Tateyama

*Reiko Ide[1], Ryotaro Okamoto[2], Hiroyuki Oguma[1], Wataru Shimada[3], Kazuma Aoki[3]

1. National Institute for Environmental Studies, 2. University of Tsukuba , 3. University of Toyama

The vulnerability of alpine ecosystems to climate change was pointed out (IPCC, 2007). The Japanese alpine zone is characterized by extreme snowfall, and snowmelt time is a key factor in the growth of alpine ecosystems. Habitats of alpine plants have high diversity within small areas reflecting complex snow cover distribution due to the complex topography and various environmental conditions. It is required to predict snowmelt timing at high-resolution (i.e. plant community level) for understanding the alpine ecosystems. However, meteorological observations are difficult to perform in alpine zones, in addition, the spatial resolutions of current regional climate models are at most 2km. Therefore, in 2011, the National Institute for Environmental Studies (NIES), Japan, launched long-term monitoring of snowmelt time and ecosystems in the Japanese alpine zone using automated digital time-lapse cameras. Twenty-nine monitoring sites are currently in operation. The objectives of this study were to construct models to predict spatial and temporal dynamics of snowmelt at fine resolution based on image analysis of the time-lapse cameras.

The study area was the west side of Mt. Tateyama range in the Japanese Northern Alps (at c.a. 2400-3000m a.s.l., c.a. 1.8km square). The area was captured within the images of time-lapse camera installed at Tateyama-Murodou-Sansou Mountain Lodge (Toyama Prefecture). We used about two thousand images which were taken by the camera with 21 million pixels in jpeg format every hour during daytime in May to August in year 2015-2017.
First, red, green, and blue (RGB) digital numbers were derived from each pixel within the images automatically, and based on the intensity of the grayscales, snow-cover and snow-free pixels are classified into binary images using a statistical discriminate analysis. Next, pixel-wise snowmelt dates were determined with timeseries of the binary images and demonstrated as snowmelt maps. Then the snowmelt maps were transformed to orthophotos, by being projected on the digital elevation map (DEM) with 5m mesh.

Snow cover distributions showed almost the same spatial pattern among years depending on the local microtopographic characteristics due to strong westerly monsoon. While, the speed of snowmelt differs from year to year depending on yearly meteorological conditions. Therefore, the spatial distribution of snow cover was analyzed statistically in relation to microtopographic parameters, and the snowmelt speed was analyzed using in-situ meteorological parameters, respectively.
As results, spatial distribution of snow cover was well predicted using Random Forest regression with microtopographic parameters such as tilt angle and curvature at various scales of averaged elevation. In addition, snowmelt speed was well regressed with the sum of daily temperature (degree days method) and yearly snow depth (by Univ. of Toyama) using multiple-regression analysis. By these integrated statistical models, daily snow cover distribution at west side of Mt. Tateyama was predicted at 5m-resolution with high accuracy, which was validated by comparison with high-resolution satellite images.

The model enables to predict the spatio-temporal dynamics of snowmelt in alpine zone at high precision by only given snow depth and daily mean temperature data. Although prediction was not performed for

©2020. Japan Geoscience Union. All Right Reserved.

the shaded areas of camera view in this study, modelling for wider area can be realized by similar analyses at various fields and use of satellite images. The assessments for impacts of climate changes on alpine ecosystems are expected by further studies using the local vegetation maps and future climate.

Keywords: Image analysis, Snow discrimination analysis, Microtopography, Random forest, Degree-day method

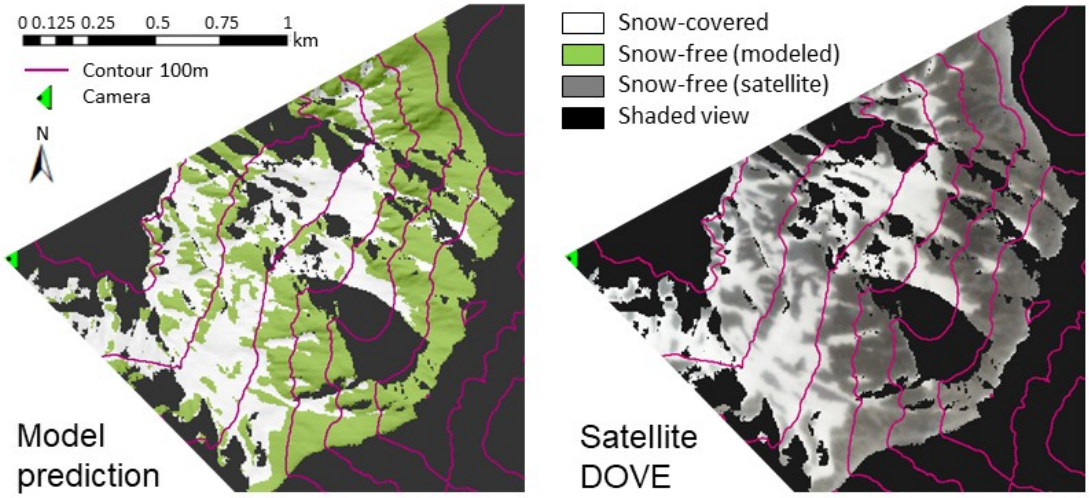

Fig. Snow cover distribution of model prediction (left) and satellite image (right) on 3 July 2019.

©2020. Japan Geoscience Union. All Right Reserved.

Factor that results in a decrease in snow surface albedo that promotes snow melting in the Kamikochi, Taisyoike

*Miu Otsuka[1], Keisuke Suzuki[1], Motoshi NISHIMURA[2]

1. Faculty of Science, SHINSHU UNIVERSITY, 2. Interdisciplinary Graduate School of Science and Technology ,SHINSHU UNIVERSITY

Introduction

The biggest factor in melting snow is solar radiation. The decline in snow surface albedo has an important role in understanding the snow cover melting process, as it determines the amount of solar radiation absorbed on the snow surface. Albedo on the snow surface is known to be particularly heavily dependent on the size (snow particle size) of the snow particles and the dirt (snow covered impurities) on the snow surface. (Warren and Wiscmbe 1980) Black carbon, mineral dust and organic carbon are cited as accumulated snow impurities, but the effect of lowering albedo differs greatly depending on the characteristics of the impurities observed. Although it has already been reported that the main melting heat in the snowfall of Taisho Pond research site in the highlands is an increase in the shortwave radiation balance due to the decrease in Albedo (West Village and other 2018), the factors causing the decrease in Albedo are still unknown. Therefore, the research site of Taishoike in the upper highlands conducted a survey on the double snowfall periods of 2017-2018 and 2018-19 to evaluate the characteristics of the snowfall impurity and the effect of the snowfall impurity on the snow surface albedo, and further evaluate the effect of the snowfall particle size on the snow surface albedo.

Method

During the double snow accumulation period of 2017-2018 and 2018-19, snow accumulation samples were collected and snow accumulation cross section observation (layer structure, density, moisture content, snow quality, particle size) was performed in the vicinity of Taishoike in the upper highlands. The samples were taken back to the clean room, measured electrical conductivity and pH, and analyzed the principal ion concentration using ion chromatography. The concentration of snow-covered impurities (weight concentration) was determined by the strong heat loss test method using a quartz fiber filter, and the analysis was carried out with reference to electron microphotographs. ImageJ, an image analysis software, was used as the particle size of the snow.

Result & Discussion

The snow covered impurities found in the Taisho Pond in the Kamijo highlands were mainly organic matter, plant pollen. As for inorganic matter, yellow sand was found in the incubation period, but soil dust was found in the snow melting season. It has already been reported that organic carbon does not contribute to the reduction of Albedo on the snow surface. According to the results of intensive observation conducted in February 2019, the relationship between inorganic snow impurities and albedo was suggested during the incubation period, but in the overall snow-covered season, the concentration of

©2020. Japan Geoscience Union. All Right Reserved.

snow impurities showed a tendency to rise, but since it flowed out in the latter half of the snow melting season, there was no apparent relationship with albedo. Therefore, it is thought that the snowflake impurity contributes little to the lowering of the snow surface albedo. On the other hand, looking at the relationship between the particle size of the snow and the snow surface albedo, the decision coefficient is high , and it is thought that it is mainly the particle size of the snow surface albedo that affects the snow surface albedo. Further, since the snow accumulation impurity does not contribute to the albedo, it has been found that the cause of the lowering of the albedo accelerating the snow melting is an increase in the snow accumulation particle size caused by the temperature rise.

Keywords: snow surface albedo, snow covered impurities, snow grain size

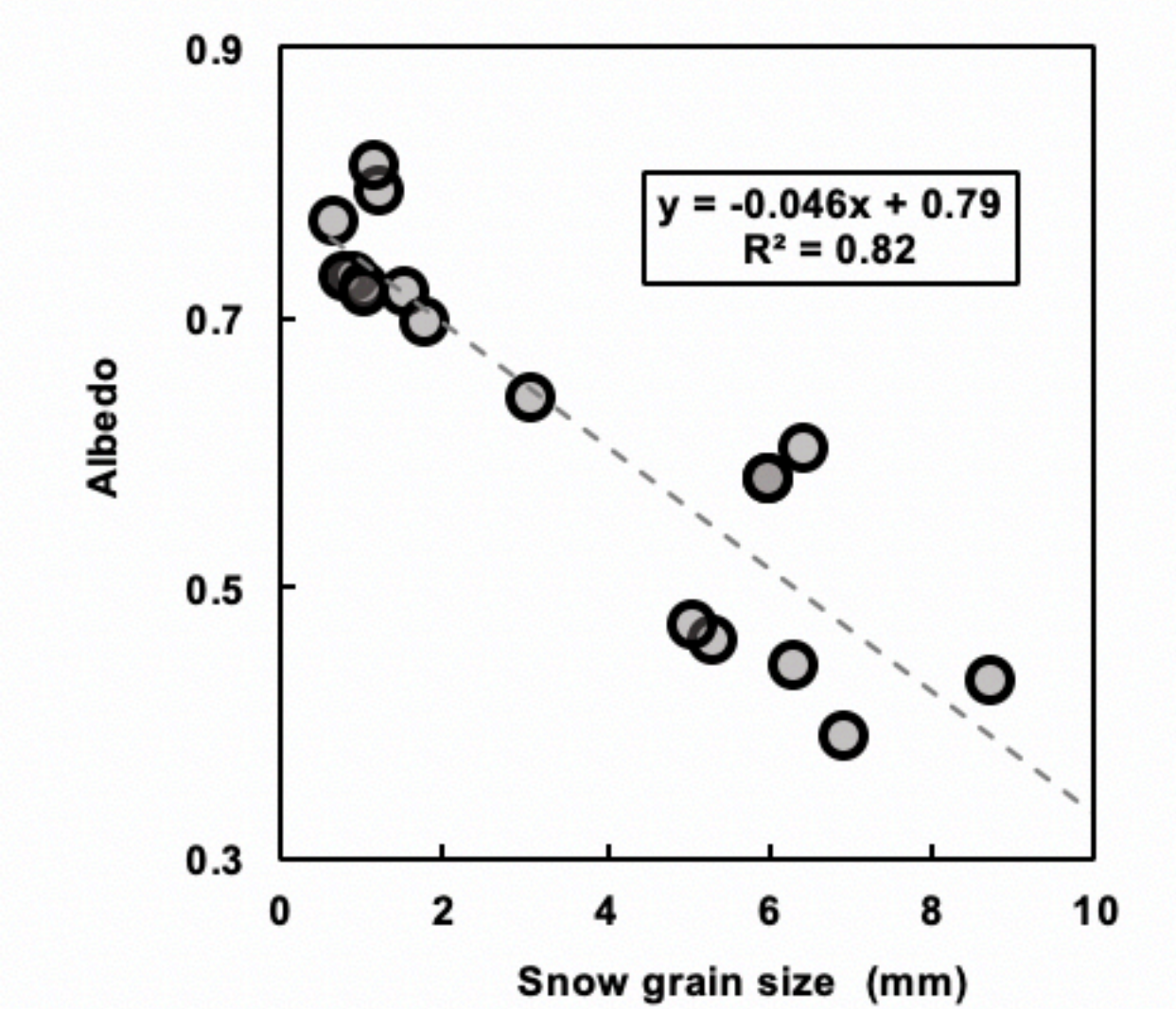

Fig. Snow surface albedo & Snow grain size

©2020. Japan Geoscience Union. All Right Reserved.

Spatiotemporal variations in stable isotope ratios of precipitation in the Japanese Alps Region

*Tsukasa Katsuragawa[1], Tsutomu Yamanaka[2], Akihiko SASAKI[3], Yuki Kurokumo[1], Motoshi NISHIMURA[1], Shimizu Hironori[1], Keisuke Suzuki[4]

1. Graduate School of Science and Technology,Shinshu University, 2. Faculty of Life and Environmental Sciences, University of Tsukuba, 3. Kokushikan University, 4. Shinshu University

We collected precipitation samples and observed weather every month from January 2011 to December 2018 at nine locations in the Japanese Alps Region (Nagano, Matsumoto, Suwa, Omachi, Sugadaira, Norikura, Kamikochi, Shigakogen, Nishihotaka). The collected water samples were brought back to the laboratory to stable isotope analysis to determine δD, δ^{18}O and calculated d-excess. The δ^{18}O in precipitation was weighted average using the amount of precipitation and was taken as the average monthly value. As a result of examining the seasonal variation of δ^{18}O from 2011 to 2018, δ^{18}O showed two peaks in spring and summer. In order to investigate the spatial variation, the coefficient of determination between latitude, longitude, altitude and δ^{18}O was calculated, it clearly correlated with altitude from April to October. d-excess showed seasonal variation which is high in winter and low in summer. As a spatial variation, correlation with altitude is high in summer and correlation with longitude and latitude is high in winter. The correlation between longitude,latitude and d-excess in winter is thought that high d-excess precipitation was brought by the winter pressure pattern to Omachi,Nagano,Sugadaira and Shigakogen in the Northeastern part of the sampling area.

Keywords: precipitation, isotope

©2020. Japan Geoscience Union. All Right Reserved.

Variation of snow in the Japanese Alps

*Keisuke Suzuki[1]

1. Research Center for Mountain Environment, Shinshu University

The Japanese Alps experience exceptionally heavy snowfall, extreme even by global standards, and in spring and summer the melting snow becomes a valuable water resource. The snow effectively acts as a natural dam when it accumulates in watersheds during winter. However, there have been no observations of the amount of snow in high-altitude regions of Japan. Therefore, we cannot discuss the effect of global warming on the change in the amount of snow in these regions based on direct observation data. A network of meteorological observatories has been developed by Shinshu University in the Japanese Alps, which have already started recording observations. In this study, we will discuss the temporal and spatial variability of the snow depth in the Japanese Alps.

Keywords: alpine region, snow fall, snow depth

©2020. Japan Geoscience Union. All Right Reserved.

[J] Poster | M (Multidisciplinary and Interdisciplinary)：M-IS Intersection

[M-IS25] Biogeochemistry

convener:Keisuke Koba(Center for Ecological Research, Kyoto University), Hideaki Shibata(Field Science Center fot Northern Biosphere, Hokkaido University), Naohiko Ohkouchi(Japan Agency for Marine-Earth Science and Technology), Youhei Yamashita(Faculty of Environmental Earth Science, Hokkaido University)

Biogeochemistry is an interdisciplinary study field including ecology, geochemistry, oceanography, limnology, hydrology, soil science, and environmental sciences. Respective researches have tended to be conducted separately so far. This session aims to provide a common platform for biogeochemists of different disciplines, which facilitates the interactive discussion and information exchanges for further development of biogeochemical studies.

[MIS25-P01] Model estimation of natural terrestrial methane emission and their stable carbon isotope ratio at broad scale

*Akihiko Ito[1] (1.National Institute for Environmental Studies)

[MIS25-P02] In-situ determination of denitrification, assimilation, and nitrification rates in urban streams

*Fumiko Nakagawa[1], Kensuke Suzuki[1], Masanori Ito[1], Urumu Tsunogai[1] (1.Graduate School of Environmental Studies, Nagoya University)

[MIS25-P03] Are sediment-derived long-chain *n*-alkanes a reliable paleoenvironmental indicator?

*Vijayananda Sarangi[1], Prasanta Sanyal[1] (1.Indian Institute of Science Education and Research Kolkata)

[MIS25-P04] Nitrate contamination of mountainous headwater streams from adjacent agricultural and pasture lands beyond the watershed boundary in eastern Hokkaido, Japan

*Keitaro Fukushima[1], Kenta Iwasaki[2], Yoshiya Oda[3], Masaru Sakai[4], Yuji Onishi[1], Keisuke Koba[1], Genki Katata[5], Takashi Yamaguchi[2], Tomohiro Kubota[5], Hirohiko Nagano[6], Makoto Watanabe[7], Jun Koarashi[6] (1.Kyoto University, 2.Hokkaido Research Organization, 3.Tokyo Metropolitan University, 4.Chuo University, 5.Ibaraki University, 6.Japan Atomic Energy Agency, 7.Tokyo University of Agriculture and Technology)

[MIS25-P05] Stable carbon and nitrogen isotope analysis of bacterial nucleic acid

*Yuji Onishi[1], Keitaro Fukushima[1], Keisuke Koba[1] (1.Center for Ecological Research, Kyoto University)

[MIS25-P06] Individual specificity of feeding habit analyzed by stable isotope in a group of Japanese macaque.

*Kazuho Funakawa[1], Keisuke Koba[1] (1.Kyoto University)

[MIS25-P07] Geological, anthropogenic and tidal effects for stream water chemistry of the Yoshinogawa river systems in the Shikoku region

*Yoriko Yokoo[1], Saki Nagayama[1], Tomohiro Yoshida[1], Ryo Anma[2] (1.Faculty of Science and Engineering, Doshisha University, 2.Graduate School of Technology, Industrial and Social Sciences, Tokushima University)

[MIS25-P08] Biogeochemistry and benthic community structure of volcanic stream ecosystems in northern Japan

*Kazuki Marumo[1], Tomoya Iwata[1], Kokichi Aoya, Kazumi Tanida[2], Satoko Noda[1], Nozomi Kasai[1], Masahiro Yuki[3] (1.University of Yamanashi, 2.Osaka Museum of Natural History, 3.RIKEN)

[MIS25-P09] Determine of host-parasitic relationship of freshwater parasites using stable isotope analysis

*Kei Kinoshita[1], Keitaro Fukushima[1], Yuji Onishi[1], Keisuke Koba[1] (1.Department of biology, Graduate School of Science, Kyoto University)

[MIS25-P10] **Variation among carbon isotopes of plants growing in mixed evergreen-deciduous ecosystem.**

*AKANKSHA RAI[1], Biswajit Roy[1], Padmasini Behera[1], Prasanta Sanyal[1] (1.INDIAN INSTITUTE OF SCIENCE EDUCATION AND RESEARCH KOLKATA)

[MIS25-P11] Effect of watershed-scale practical forest management on nitrogen leaching in a cool-temperate natural forest in northern Japan

*Karibu Fukuzawa[1] (1.Field Science Center for Northern Biosphere, Hokkaido University)

[MIS25-P12] Interaction between marine bacterial community and dissolved organic matter released by pelagic phytoplankton

*Yuya Tada[1], Koji Suzuki[2], Youhei Yamashita[2] (1. National Institute For Minamata Disease, 2.Hokkaido Univ.)

[MIS25-P13] Relationship of N_2O emission and environmental factor between different vegetation in a cool temperature

*Miwako Nagane[1], Hideaki Shibata[2], Yoshitaka Uchida[3], Ryunosuke Tateno[4], Atsuko Sugimoto[5] (1.Graduate school if Environmental Science, Hokkaido University, 2.Field Science Center for Northern Biosphere, Hokkaido University, 3.Faculty of Agriculture, Hokkaido University, 4.Field Science Education and Research Center, Kyoto University, 5.Arctic Research Center, Hokkaido University)

Model estimation of natural terrestrial methane emission and their stable carbon isotope ratio at broad scale

*Akihiko Ito[1]

1. National Institute for Environmental Studies

Methane (CH_4) is the second potent greenhouse gas and an important short-lived climatic pollutant. However, because of its complicated sources and sinks, there remain large uncertainties in the global and regional budget of methane. In this study, a process-based terrestrial ecosystem model, Vegetation Integrative SImulator for Trace gases (VISIT), was used to simulate CH_4 emission from natural wetlands and CH_4 uptake by upland soil oxidation. The VISIT model captures carbon and nitrogen cycling by using simple box flow schemes and simulates exchange between atmosphere and ecosystem of greenhouse gases in a biogeochemical manner. To separate the observed CH_4 variability into biological and fossil-fuel components, it is effective to use stable carbon isotopes. Biologically-produced methane has lower (more depleted in ^{13}C) stable carbon isotope ratio than that from fossil fuel exploitation, but the ratio varies with substrates used for CH_4 production. Namely, CH_4 produced from carbon dioxide has lower ratio than that produced from acetate, and therefore, wetland CH_4 models should estimate the production rate taking account of its substrate composition. In this presentation, a preliminary result of the spatial distribution and temporal change in $^{13}C/^{12}C$ ratio of CH_4 produced in wetlands. Finally, the present author would discuss possible collaborations with atmospheric observations and future tasks.

Keywords: Methane, Wetland, Stable carbon isotope ratio, Process-based model

©2020. Japan Geoscience Union. All Right Reserved.

In-situ determination of denitrification, assimilation, and nitrification rates in urban streams

*Fumiko Nakagawa[1], Kensuke Suzuki[1], Masanori Ito[1], Urumu Tsunogai[1]

1. Graduate School of Environmental Studies, Nagoya University

Fixed nitrogen, such as NO_3^-, $NH_4^+$and Org-N, controls photosynthesis (primary production) in most of the aquatic environments. In recent decades, human activities have released large amounts of fixed nitrogen into aquatic environments mainly via rivers. As a result, the primary production of rivers, and its downstream lakes and oceans has become excessively higher, leading to disturbance of the ecosystems. In order to properly evaluate the effects of human activities on ecosystems, it is essential to understand the spatiotemporal changes in nitrogen dynamics in rivers including denitrification which is a removal process of fixed nitrogen by converting it to N_2. Fixed nitrogen is often transported downstream as NO_3^-in the oxidative river water. The NO_3^-concentration in river water changes depending on the inflow from outside the river system, nitrification in the river system, and the removal processes such as denitrification and assimilation. Therefore, it is difficult to evaluate the denitrification rates only from the spatiotemporal changes in NO_3^-concentration. Previous studies have attempted to quantify the denitrification rate in river environments using culture methods. However, since the denitrification rate greatly changes due to a small change in the redox environment, it was difficult to reproduce the same environment as the on-site environment in the culture system. However, since a small difference in the redox state greatly changes the denitrification rate, it is difficult to estimate the exact denitrification rate by the culture method.

Here we propose a new tracer called “atmospheric NO_3^-concentration”, which can be calculated from both concentration and triple oxygen isotopic composition ($\Delta^{17}O$ value = $\delta^{17}O - 0.52 \times \delta^{18}O$) of dissolved NO_3^- in river water, to determine the removal rate of NO_3^-(sum of denitrification rate and assimilation rate) in the river environments. We attempt to determine the in-situ denitrification, assimilation, and nitrification ratesin the river waterindividually by tracing the atmospheric NO_3^- concentration together with totalNO_3^-concentration.
In this study, we focused on urban rivers that are significantly affected by human activities. The study was carried out at Tenpaku River (Aichi Prefecture). We selected an observation section where tributaries and other inflows were negligible, and performed observations at the entrance and exit of the section every two hours for 24 hours. The observations were held five times (August, October, December, 2018 and March and July 2019). We first estimated the NO_3^-removal rate from the difference in atmospheric NO_3^- concentration between the two sites and then estimatedthe nitrification rate from the difference in the total NO_3^-concentration between the two sitesand from the determined NO_3^-removal rate. While the denitrification rate was estimated from the NO_3^-removal rate at night, the assimilation rate was estimated from the difference between the NO_3^-removal rate at day and night.As a result, the denitrification rate, assimilation rate, and nitrification rate were estimated to be 2.4 to 4.7 mmol/m^2/h, 0.5 to 2.1 mmol/m^2 /h, and 2.1 to 5.5 mmol/m^2/h, respectively. All the rates showed seasonal changes that increased in summer and decreased in winter. Using the denitrification rate obtained in this study, we found that about 30% of loaded nitrogen that are transported from the Tenpaku River to the ocean was reduced by denitrification in the river.

Keywords: urban streams, denitrification, assimilation, nitrification, triple oxygen isotope

©2020. Japan Geoscience Union. All Right Reserved.

Are sediment-derived long-chain *n*-alkanes a reliable paleoenvironmental indicator?

*Vijayananda Sarangi[1], Prasanta Sanyal[1]

1. Indian Institute of Science Education and Research Kolkata

In soil, the distribution and carbon isotopic composition of *n*-alkane ($d^{13}C_{n\text{-}alk}$) is extremely source-specific. In general, terrestrial higher plants are primary producers of long-chain *n*-alkanes (C_{27}-C_{33}) while short-chain *n*-alkanes (C_{14}-C_{20}) are mainly contributed from microorganisms with distinct $d^{13}C_{n\text{-}alk}$ values. Hence, the distribution and $d^{13}C$ values of *n*-alkane in sediments have been primarily used to characterize the source(s) of organic matter in a given depositional environment as well as to gain insight into paleoenvironmental conditions. However, very little is known about post-depositional modification of plant-derived long-chain n-alkanes within the soil. Therefore, the present study aims to understand the factors affecting the distribution and $d^{13}C$ values of long-chain *n*-alkanes in the soil as well as evaluate their potential as paleoenvironmental indicators. In this context, three soil profiles developed within an oxbow lake setting from the lower Gangetic plain, West Bengal, India has been used. The *n*-alkanes exhibit a bimodal distribution suggesting contributions from both terrestrial higher plants and soil microbes. The concentration of long-chain *n*-alkanes (C_{27}-C_{33}) within the soil profiles decreases with depth, indicating a significant loss of biomarkers during soil-forming processes. In the soil profiles, the $d^{13}C_{n\text{-}alk}$ values exhibit a high degree of variability across the higher molecular weight homologues (C_{27}-C_{33}). On the contrary, the $d^{13}C_{n\text{-}alk}$ values of the modern C_3 and C_4 plants from the study area show minimal variation (~2‰) in the isotopic composition across its homologues (C_{27}-C_{33}). This suggests that the observed variation in the $d^{13}C_{n\text{-}alk}$ values in the soil is a result of microbial degradation of *n*-alkanes during its transfer from leaves to soil. Additionally, the inter-homologue variation in the $d^{13}C_{n\text{-}alk}$ values shows an increasing trend with depth (from 6.0‰ to 9.6‰) suggesting that older soil samples have undergone more microbial alteration compared to the younger ones. As the $d^{13}C$ values of higher molecular weight homologues (C_{27}-C_{33}) have been primarily used to estimate the relative abundance of C_3 and C_4 plants in the past, significant inter-homologue variations in the $d^{13}C_{n\text{-}alk}$ values can result in erroneous paleovegetational interpretations. Therefore, the present study suggests that caution must be exercised while using *n*-alkanes as a paleoenvironmental indicator as the variations in $d^{13}C_{n\text{-}alk}$ values in sediments is a cumulative product of temporal changes in the vegetation composition and post-depositional modifications experienced by the biomarker.

Keywords: Biomarker, Carbon Isotope, Microbial degradation, Paleoenvironment

©2020. Japan Geoscience Union. All Right Reserved.

Nitrate contamination of mountainous headwater streams from adjacent agricultural and pasture lands beyond the watershed boundary in eastern Hokkaido, Japan

*Keitaro Fukushima[1], Kenta Iwasaki[2], Yoshiya Oda[3], Masaru Sakai[4], Yuji Onishi[1], Keisuke Koba[1], Genki Katata[5], Takashi Yamaguchi[2], Tomohiro Kubota[5], Hirohiko Nagano[6], Makoto Watanabe[7], Jun Koarashi[6]

1. Kyoto University, 2. Hokkaido Research Organization, 3. Tokyo Metropolitan University, 4. Chuo University, 5. Ibaraki University, 6. Japan Atomic Energy Agency, 7. Tokyo University of Agriculture and Technology

Introduction

Watershed is a fundamental unit for quantitative understanding of water and nitrogen (N) cycle in forested ecosystem. Nitrogen retention in the forest ecosystem can be mainly evaluated as a balance between input of atmospheric reactive N and hydrological N loss at a watershed scale. As an assumption for the evaluation, it has been proposed that the watershed is completely “closed”, namely, the source of water flowing out from the watershed is rainwater fallen in the watershed. This means that exchange of N transported with water between the watershed and the adjacent watershed beyond the watershed boundary is ignored. However, is this assumption applicable for all forested watersheds? If not, N retention in the watershed may not be evaluated accurately. In our presentation, we aim to elucidate the source of streamwater nitrate-N in the forested watershed whose water balance is not possibly closed.

Material and Methods

This study was conducted in Hokkaido Forest Research Station, Field Science Education and Research Center, Kyoto University, which is located in the eastern part of Hokkaido. The research forest is mainly composed of a cool-temperate deciduous broad-leaved forest and adjacent to the vast agricultural and pasture lands across the watershed. We estimated water and N balance in a gauged watershed (150 ha) within the research forest during 2011-2018. In 2014 and 2017-2019, we collected more than 50 streamwater and stream-bed and bedrock spring water across the forest, and measured nitrate and other major ions, and stable isotopes of nitrate-N and oxygen (O).

Results and Discussion

In the gauged watershed, water discharge rate was 1.5-2.1 times larger than rainfall input, indicating that the watershed is not likely “closed”. It is possible that groundwater derived from areas outside the watershed may spring out. Nitrogen input via throughfall was 4-6 kgN ha^{-1} yr^{-1}, while hydrological N loss from the watershed was estimated as 7-10 kgN ha^{-1} yr^{-1}, indicating low N retention. In the streams across the research forest including the gauged watershed, groundwater spring points were widely observed at the streambed. Groundwater from the streambed had high nitrate and chloride concentrations and high $\delta^{15}N$ of nitrate, implying that the possible source of nitrate is sewage or livestock manure. These results suggest that a large portion of nitrate in streamwater is provided by streambed spring water, which may originate from agricultural and pasture lands adjacent to the research forest.

©2020. Japan Geoscience Union. All Right Reserved.

Keywords: Nitrate, Stable isotope, Groundwater discharge, Streamwater chemistry

©2020. Japan Geoscience Union. All Right Reserved.

Stable carbon and nitrogen isotope analysis of bacterial nucleic acid

*Yuji Onishi[1], Keitaro Fukushima[1], Keisuke Koba[1]

1. Center for Ecological Research, Kyoto University

Conventional stable isotope ecology cannot evaluate the role of microbes in ecosystems. We focus on nucleic acids of microbes, and try to use the carbon and nitrogen isotope ratios of the nucleic acid to the stable isotope ecology. However, the stable carbon and nitrogen isotope ratios of the nucleic acid have not been analyzed. The purpose of this study is to develop the methods for isotope analysis of bacterial nucleic acid and to reveal offsets of isotope ratios between the biomass and nucleic acid.
Nucleic acids were extracted from incubated denitrifying bacteria (*Pseudomonas aureofaciens*) using reagent for nucleic acid extraction, ISOPLANT and ISOPLANT II (Nippon Gene Co., Ltd.). The extractions were precipitated under ethanol, and then were dissolved in water. A part of the solution was used for protein, RNA, and DNA concentrations, and the remain was used for isotope analysis.
The extraction by ISOPLANT II contained a large amount of protein and contaminant, which suggest that the reagent is inadequate foe isotope analysis. On the other hand, protein was not detected in the extraction by ISOPLANT. The extraction almost consists of RNA rather than DNA. Offsets of carbon and nitrogen isotope ratios between biomass and the extraction by ISOPLANT insignificantly varied, which imply that the isotope ratios of bacterial RNA are controlled by those of biomass.

Keywords: Stable isotope, Nucleic acid

©2020. Japan Geoscience Union. All Right Reserved.

Individual specificity of feeding habit analyzed by stable isotope in a group of Japanese macaque.

*Kazuho Funakawa[1], Keisuke Koba[1]

1. Kyoto University

A group of japanese macaque in Arasiyama has been researched for long years, and their ranking, sex, age, family tree and relationship between individuals were recorded. I analyzed their feeding habit by using stable isotope analysis. And I clarified the relationship between each feeding habit and their various characters, then I discussed the society of japanese macaque in Arashiyama in point of their individual feeding habit.

Keywords: stable isotope , feeding habit, japanese macaque

©2020. Japan Geoscience Union. All Right Reserved.

Geological, anthropogenic and tidal effects for stream water chemistry of the Yoshinogawa river systems in the Shikoku region

*Yoriko Yokoo[1], Saki Nagayama[1], Tomohiro Yoshida[1], Ryo Anma[2]

1. Faculty of Science and Engineering, Doshisha University, 2. Graduate School of Technology, Industrial and Social Sciences, Tokushima University

We determined the elemental compositions of stream water of the Yoshinogawa river systems in the Shikoku region. The main stream water, except for samples around the mouth, were enriched in $Ca^{2+}$and HCO_3^-. The tributaries on the right side of the Yoshinogawa river were enriched in $Ca^{2+}$and HCO_3^- and Ca^{2+}, $Mg^{2+}$and HCO_3^-. The river water were rich in $Mg^{2+}$and Si in Sonosegawa, indicating that these ionic compositions are derived mainly from geological inputs from the weathering of green schist in Sanbagawa Belt. On the other hand, the tributaries on the left side of the Yoshinogawa river were rich in Ca^{2+}, HCO_3^- and SO_4^{2-}. The rates of SO_4^{2-} and NO_3^-in anions and the concentrations of Al, P, and Si were higher in Imagirigawa and Kyuyoshinogawa than those of the other tributaries. This ionic composition is largely attributable to anthropogenic effect.

The main stream and tributaries around the mouth were enrich in $Na^+$and Cl^-. Tidal effect was shown in this area. $Na^+$and Cl^- concentrations of tributaries in the center of Tokushima city were higher than those of main stream of the Yoshinogawa river. This result shows that tributaries in the center of Tokushima city are more influenced by tide than main stream. Tamiyagawa, located at the farthest site from the mouth in the center of Tokushima city, had high EC and P, SO_4^{2-} and NO_3^- concentrations. This result is largely attributable to anthropogenic effect due to sewage treatment system.

Keywords: Yoshinogawa river, ionic composition, tidal effect

©2020. Japan Geoscience Union. All Right Reserved.

Biogeochemistry and benthic community structure of volcanic stream ecosystems in northern Japan

*Kazuki Marumo[1], Tomoya Iwata[1], Kokichi Aoya, Kazumi Tanida[2], Satoko Noda[1], Nozomi Kasai[1], Masahiro Yuki[3]

1. University of Yamanashi, 2. Osaka Museum of Natural History, 3. RIKEN

Since the discovery of chemosynthetic ecosystems in deep-sea hydrothermal vents, benthic invertebrate communities sustained by organic matter derived from the chemoautotrophic bacteria have been found in many places of dark, deep-sea floor ecosystems. However, food webs sustained fully by chemoautotrophic primary productivity have never been reported from sunlit terrestrial ecosystems. In streams flowing through active volcanic regions, highly acidic hot-spring water often flows into the stream water, thereby making the stream ecosystems extreme environments. In such ecosystems, algal primary productivity, as well as the supply of terrestrial organic matter from surrounding arid environments, tends to be decreased. However, we found the high density of stream benthic macroinvertebrate community in volcanic streams around Mt. Akita-Yakeyama, where active volcanic activity influences the physicochemical characteristics of streams and rivers in the watershed. Here we report the biogeochemistry and benthic community structure of streams influenced by volcanic hot-spring water. We performed a field survey in three volcanic streams where hot-spring water comes from geothermal environments of Mt. Akita-Yakeyama, and in a nearby reference stream, during June 6 and 8, 2019. In each study stream, we quantified the physico-chemical environments and the abundance of benthic stream communities. In addition, we conducted an in situ incubation experiment in a study stream to estimate the photoautotrophic and chemoautotrophic primary productivity in the stream ecosystem. Our field study showed that water quality variables, such as pH and water temperature, differed greatly among the study streams. In particular, dissolved sulfide concentration was higher in the volcanic streams relative to the reference stream. Moreover, the standing crop of epiphytic algae and benthic particulate organic matter tend to be lower in the volcanic streams. Even in such environments with the decreased availability of basal resources of stream food webs, the density of benthic macroinvertebrates exhibited one to two orders of magnitude higher than that of the nearby reference stream. Moreover, specific taxa (e.g., a Nemourid stonefly larvae and Chironomid midge larvae) tend to predominate in the benthic community of the volcanic streams, suggesting that specific group adapted to extreme environments can be a dominant species in the stream communities under the predator- and competitor-less conditions. The in situ incubation experiment showed that the concentrations of dissolved sulfide and dissolved inorganic carbon (DIC) were significantly decreased in both light and dark chambers. In contrast, dissolved oxygen (DO) did not increased associated with the decrease of DIC, implying that oxygenic and anoxygenic photosynthesis was not responsible for the DIC consumption; chemoautotrophic production by sulfur-oxidizing bacteria is likely to play a primary role in organic matter production of the volcanic stream ecosystems. Based on the change in DIC and DO concentrations, we estimated the rate of chemoautotrophic primary productivity in the stream as 0.75 gC m^{-2} d^{-1}. This organic matter productivity by chemoautotrophs is comparable to the gross photosynthetic production rate reported from the worldwide non-acidic stream and river ecosystems.

Keywords: chemosynthetic ecosystem, sulfur-oxidizing bacteria, volcanic stream

©2020. Japan Geoscience Union. All Right Reserved.

Determine of host-parasitic relationship of freshwater parasites using stable isotope analysis

*Kei Kinoshita[1], Keitaro Fukushima[1], Yuji Onishi[1], Keisuke Koba[1]

1. Department of biology, Graduate School of Science, Kyoto University

There are ubiquity of parasites all ecosystems, and it is said that they account for more than half of the species on earth. In Lake Biwa, more than 100 species of parasites have been reported, including trematoda, cestoda, acanthocephalans, and crustaceans. These parasites cause behavioral changes and trait changes in the host, directly and indirectly affecting the food web structure and material cycle of ecosystems. Stable carbon and nitrogen isotope measurement is widely used as a method to elucidate the material cycle and food web of ecosystems. It is known that the stable isotope ratio between carbon and nitrogen is enriched as the trophic level increases in the predator-prey relationship. On the other hand, it is suggested that the “host-parasite” relationship may be different from the conventional “predator-prey” relationship, even though the host is used as a resource.
Therefore we will measure the trophic relationship between parasites and host organisms using stable isotopes to elucidate the trophic level of parasites.
Cyprinid fish collected in Lake Biwa were dissected, and parasites were collected from the oral cavity, gills, swimwear, and digestive tract. The gills, swimwear, digestive tract, and muscle were removed from the host. All samples were lyophilized, powdered and measured. The measurement was performed using EA / IRMS, and Δ13C and Δ15N of the sample were measured. In addition, EA-IRMS was partially modified to measure microparasites one.
Crustaceans, monogenea, trematoda (larvae, adults), and acanthocephalans were found in *Opsariichthys uncirostris*. Δ13C and δ15N of the collected crustaceans, trematoda and acanthocephalans were measured. All the measured parasites showed negative values in Δ13C and Δ15N. We discuss these results.

©2020. Japan Geoscience Union. All Right Reserved.

Variation among carbon isotopes of plants growing in mixed evergreen-deciduous ecosystem.

*AKANKSHA RAI[1], Biswajit Roy[1], Padmasini Behera[1], Prasanta Sanyal[1]

1. INDIAN INSTITUTE OF SCIENCE EDUCATION AND RESEARCH KOLKATA

The variation of leaf bulk carbon isotope values C_3 plants ($\delta^{13}C_{bulk}$) at a global scale displays strongest dependence on mean annual precipitation (MAP) among all climate variables. However, the MAP- $\delta^{13}C_{bulk}$ relation in regional scale studies displays varying correlation among the two variables. Such studies are conducted across a precipitation gradient, leading to differences in both environmetal factors (soil moisture, topography etc.) as well as species assemblage. Additionally, the observed MAP- $\delta^{13}C_{bulk}$ relation may be a one-time occurrence and not remain constant over time. To understand the MAP- $\delta^{13}C_{bulk}$ relation temporally and minimize environmental variations, 18 naturally occurring plant species were sampled from a single location over a period of six years (2012-18). The study region (22˚57’ N, 88˚ 31’ E) lies in the lower Gangetic floodplain experiencing sub-tropical monsoonal climate which supports mixed deciduous-evergreen vegetation. Among the two plant functional types (deciduous and evergreen), lower $\delta^{13}C_{bulk}$ values were observed in evergreen species at an annual timescale with a difference of 0.9‰ to 1.5 ‰. The dataset compiled in this study shows no correlation among $\delta^{13}C_{bulk}$ and rainfall amount in the months of June, July and August which is the period when maximum rainfall intensity occurs. However, a strong correlation is seen when $\delta^{13}C_{bulk}$ values are correlated with MAP. Deciduous species exhibit a stronger correlation with MAP (r^2=0.55) compared to evergreen (r^2=0.20). The observations can be explained through the difference in leaf growth strategies between deciduous and evergreen species. The higher $\delta^{13}C_{bulk}$ values in deciduous trees indicate a higher water use efficiency leading to lower carbon assimilation. Their dependency on MAP is a result of shorter leaf life-span compared to evergreen trees. In the context of changing climate with predictions of varying precipitation regime, a potential shift in plant community composition can alter the carbon assimilation at a global scale and tend to have an adverse effect on growth of deciduous species.

©2020. Japan Geoscience Union. All Right Reserved.

Effect of watershed-scale practical forest management on nitrogen leaching in a cool-temperate natural forest in northern Japan

*Karibu Fukuzawa[1]

1. Field Science Center for Northern Biosphere, Hokkaido University

Anthropogenic disturbances in forests, such as cutting of trees, alter ecosystem nitrogen (N) cycling, and increase N leaching from the soil to streams. In forests with dense understory vegetation, mechanical site preparation following tree cutting is commonly used to improve the early establishment of tree seedlings. In cool-temperate forests in northern Hokkaido, Japan, dense understory vegetation (mainly comprising *Sasa* dwarf bamboo) inhibits forest regeneration after tree cutting. Soil scarification is a common site preparation technique for eliminating *Sasa* bamboo and improving forest regeneration. However, the effect of the site preparation on the watershed-scale stream chemistry has not been well understood. For 14 years (2003-2016), we observed the stream water chemistry in naturally forested watersheds where various forest managements were conducted in Uryu Experimental Forest of Hokkaido University (North Hokkaido Experimental Forests Site of JaLTER) in northern Japan. The forest management practice in each watershed includes clear-cutting, soil scarification, and soil replacement. We also established control watersheds which are valuable as a background information to analyze the effect of long-term climate, environment, and vegetation changes on stream water chemistry. Water samples were collected from the outlets of ten watersheds. We measured inorganic N concentrations (nitrate and ammonium) after filtering, and pH, and electrical conductivity (EC) in the stream water. We also monitored stream discharge, water level, and stream water temperature in each watershed. Nitrate concentration ranged 0.01-8.68 mg L-1 in all watersheds during study period. Analysis of covariance that nitrate concentration was assigned as objective variable and time and watershed were assigned as explanatory variable revealed that time and watershed affect to nitrate concentration significantly ($P < 0.001$), indicating that nitrate concentration increased during study period and differed between watersheds. However, interaction effect of time and watershed was not significant ($P = 0.37$), suggesting that clear-cutting does not induce nitrate leaching. On the other hand, soil scarification and soil scarification followed by soil replacement increased nitrate concentration. Nitrate concentration reached maximum in seven years after treatment in soil scarification and five years in soil scarification followed by soil replacement. Nitrate concentration after treatment was higher in in soil scarification followed by soil replacement treatment. These results suggest that clear-cutting only does not induce nitrate leaching from forest ecosystem watershed, whereas soil scarification and soil replacement which eliminate bamboo root system promote nitrate leaching. The response time was shorter and the extent of increase was larger in soil scarification followed by soil replacement treatment. This study revealed the role of understory vegetation in retention of N after clear-cutting.

Keywords: nitrate, clear-cutting, soil scarification, Sasa dwarf bamboo

©2020. Japan Geoscience Union. All Right Reserved.

Interaction between marine bacterial community and dissolved organic matter released by pelagic phytoplankton

*Yuya Tada[1], Koji Suzuki[2], Youhei Yamashita[2]

1. National Institute For Minamata Disease, 2. Hokkaido Univ.

Dissolved organic matter (DOM) representing one of the largest reduced carbon pools in the ocean, is strongly involved in the global biogeochemical processes. A large proportion of labile DOM in the marine environments is derived from phytoplankton. Many previous studies have shown that such DOM derived from phytoplankton (DOMP) can affect the bacterial community structure and diversity with concomitant changes in DOM characteristics in aquatic ecosystems. However, little is known about the characteristics of the DOMPs from pelagic phytoplankton, and the community response of marine bacteria to the DOMPs. In this study, we analyzed the characteristics of fluorescent DOM (FDOM) of DOMP derived from two different pelagic phytoplankton cultures, the pelagophyte *Pelagomonas calceolata* (Pelago) and cyanobacterium *Synechococcus* sp. (Synech) using excitation emission matrix fluorescence spectroscopy. To prepare the DOMPs, these phytoplankton cultures were incubated in the L1 medium. Then, the algal cells in the medium were removed by filtration (0.2 μm pore-size Sterivex filter). In addition, we conducted incubation experiments using natural seawater amended with these DOMPs, and analyzed FDOM characteristics, and community and diversity shifts of marine bacteria using 16S rRNA gene (V4 region) tag-sequence. During incubation experiment, we collected FDOM and microbial DNA subsamples on Day 0, 1, and 5.

FDOM analysis for initial samples (Day 0) showed that the fluorescence intensity of humic-like M, C, A from $DOMP_{Synech}$ amendments were higher than those of $DOMP_{Pelago}$. During incubation experiments, fluorescence intensity of protein-like B and T in the $DOMP_{Pelago}$ decreased with time. After incubation (Day 5), decreases in humic-like M intensity were observed both in the $DOMP_{Synech}$ and $DOMP_{Pelago}$ treatments. The 16S rRNA gene tag-sequence revealed the relative abundance of *Oceanospirillales* and *Alteromonadales* (affiliated with Gammaproteobacteria) to total 16S rRNA sequences drastically increased in both DOMP treatments on Day 1. However, an increase in *Rhodobacterales* (affiliated with Alphaproteobacteria) was observed on Day 5. Interestingly, the proliferation of Betaproteobacteria and Deltaproteobacteria (numerically rare lineages in surface seawater) occurred in the $DOMP_{Synech}$ and $DOMP_{Pelago}$ treatments on Day 5, respectively.
These results suggest that the DOMPs released by distinct pelagic phytoplankton can affect the bacterial community structures including numerically rare lineages, and these lineages potentially contribute to the degradation of phytoplankton-derived humic-like materials in seawater.

Keywords: Marine bacteria, Marine phytoplankton, Dissolved organic matter

©2020. Japan Geoscience Union. All Right Reserved.

Relationship of N_2O emission and environmental factor between different vegetation in a cool temperature

*Miwako Nagane[1], Hideaki Shibata[2], Yoshitaka Uchida[3], Ryunosuke Tateno[4], Atsuko Sugimoto[5]

1. Graduate school if Environmental Science, Hokkaido University, 2. Field Science Center for Northern Biosphere, Hokkaido University, 3. Faculty of Agriculture, Hokkaido University, 4. Field Science Education and Research Center, Kyoto University, 5. Arctic Research Center, Hokkaido University

Nitrous oxide (N_2O) is a greenhouse gas, mainly produced by soil microbial processes (i.e., denitrification and nitrification) within nitrogen (N) cycle. The N_2O emissions from soil are controlled by factors such as soil temperature, moisture, pH, and N availability in soil. However, the relative contribution of these environmental factors to N_2O emission vary across different types of ecosystem and climate. Also, microbial functional genes driving N cycle are important as the controlling factors of N_2O emission from soil. We hypothesis that driving factors for N_2O emissions from soils of different vegetation are influenced not only litter quality (CN ratio, residual organic matter) but also factors related to the functional gene abundance of soil microbes and soil related environmental factors (temperature and soil moisture). In this study, we aimed to clarify the spatial and temporal patterns and their driving factors including both environmental and microbial variables (i.e., functional genes in soils) in a cool temperate forest in eastern Hokkaido, northern Japan. We established study plots in two forest types: broad-leaved forest dominated by *Quercus crispula* with *Sasa nipponica* as understory vegetation; and evergreen needle-leaved forest dominated by *Abies sachalinensis* (i.e., total 6 plots = 2 vegetation x 3 replicates). We observed N_2O emission flux from soil using a closed chamber method from April to October in 2019. Soil temperature and moisture were also observed in surface soil near the chamber. We collected soil samples for analysis of inorganic N (NH_4-N and NO_3-N), dissolved organic carbon (DOC), soil pH, and abundance of bacterial and archaeal *amoA* (AOB and AOA), *nirK*, *nirS*, *nosZ1* and *qnorB* (functional genes related to nitrification and denitrification) as copy number in surface soil. We used generalized additive model (GAM) to investigate the driving factors influencing the N_2O emissions in each forest type.

Average N_2O emission rates were 8.75 ug N m^{-2} h^{-1} (± 4.45 SD) in the broad-leaved forest, and 7.41 ug N m^{-2} h^{-1} (± 3.51 SD) in the needle-leaved forest. The highest N_2O emission rates were observed in July, when soil temperature was the highest. The GAM analysis indicated that NH_4-N, *nosZ1* and DOC were selected in the best models in the broad-leaved forest, while soil temperature, soil moisture and *nirK* were selected in the best model in the coniferous forest. DOC is an energy source of soil microbes in the denitrification process. Therefore, it is assumed that it was chosen with nosZ1 as the best model. Since *nosZ1* is a functional gene that reduces N_2O to N_2, it is considered that N_2O was reduced to N_2 by complete denitrification, resulting in a decrease in N_2O emission. On the other hand, factors related to the environment surrounding the soil, such as soil moisture and soil temperature, were selected as the best model for the coniferous forest. From this, it is considered that the change in the physical environment surrounding the coniferous forest soil is relatively large. Since the coniferous forest is an evergreen conifer, the forest canopy is closed, so the soil temperature and soil moisture change greatly in early spring due to the influence of temperature. It is considered that *nirK* involved in nitrite reduction was selected together with soil moisture because it was inhibited when soil moisture was low.
In our result, there was no significant difference in N_2O emission between two forest types, but the results of this study suggested that the factors affecting N_2O emissions differed between two forest types. Soil chemical indicates such as resources for soil microbes (nitrogen and carbon) affect the broad-leaved forest, and physical factors such as soil temperature and soil moisture content and physical factors affect

©2020. Japan Geoscience Union. All Right Reserved.

in the coniferous forest.

Keywords: Nitrous oxide, Forest soil, Soil microbes

©2020. Japan Geoscience Union. All Right Reserved.

[J] Poster | M (Multidisciplinary and Interdisciplinary)：M-IS Intersection

[M-IS26] Electromagnetic phenomena associated with seismic and volcanic activities

convener:Tetsuya Kodama(Research Unit I, Research and Development Directorate, Japan Space Exploration Agency), Toshiyasu Nagao(Institute of Oceanic Research and development, Tokai University)

This session deals with reviews and contributions on the recent studies of electromagnetic (EM) phenomena associated with earthquakes and volcanic eruptions. One of the main targets of the session is to clarify the mechanism of seismo-EM emission and Lithosphere-Atmosphere-Ionosphere (LAI) coupling. Recently, some scientists claim that seismic activities are the critical phenomena. These kinds of approach are also welcome.

[MIS26-P01] An internal/external separation of Sq geomagnetic daily variation on quiet days in January 2011 around Japan

*Tsutomu Ogawa[1] (1.Earthquake Research Institute, the University of Tokyo)

[MIS26-P03] **3D-Tomography of the Ionospheric Anomalies Immediately Before and After the 2011 Tohoku-oki (M_W9.0) Earthquake**

*Ihsan Naufal Muafiry[1,2], Kosuke Heki[1] (1.Hokkaido University, Japan, 2.Universitas Esa Unggul, Indonesia)

An internal/external separation of Sq geomagnetic daily variation on quiet days in January 2011 around Japan

*Tsutomu Ogawa[1]

1. Earthquake Research Institute, the University of Tokyo

It is reported that preceding the 2011 off the Pacific coast of Tohoku earthquake (Mw 9.0), the geomagnetic daily variations on international quiet days in January 2011 around Japan were anomalous by internal/external separation of the geomagnetic field (Liu et al., 2019). The present study reassesses the result.

The 1-minute geomagnetic records at 21 geomagnetic observatories and stations in both the northern and southern hemispheres in the longitude range between 115 and 160 degrees are analyzed. The records on 240 days from the international 5 quiet days per month for 4 years from 2009 to 2012 are resampled to 30-minute records in the local time derived from the longitude. Using the natural orthogonal component (NOC) analysis, Sq components are identified for the north, east and downward components separately. Among the bases, it is found that the first basis represents the daily variations in summer, while the combination of the first and second bases can exhibit the Sq daily variation including its seasonal variation of the phase. In the present study, the combination up to the third basis is treated as the Sq daily variation.

For the internal/external separation, the slice method is adopted to the records in local time, and the equivalent current system is then estimated. In the spherical harmonic analysis, not only the point prediction but also the prediction interval are estimated. The truncation order and degree are chosen so that the mean prediction interval over all the components and the observation points is minimized, which can vary day to day.

The equivalent current systems for days in January and February 2011 do not show prominent difference between one another, especially the vortices below and above the Tohoku district in Japan in January 2011 as Liu et al. (2019) pointed out. The combination of synthetic daily variations with internal and external origins well explain the records considering the prediction interval with the significance level of 5%. Those variations do not show anomalous amplitudes as Liu et al. (2019) pointed out.

Three features of Liu et al. (2019) to consider the cause of the present result different from theirs can be pointed out. 1) Japan standard time is adopted to summarize the records at geomagnetic observatories and stations which distribute in the range of longitude of 45 degrees, instead of the local time depending on the longitude. 2) Only the first basis of the NOC analysis is adopted to represent the Sq daily variation. 3) In the spherical harmonic analysis, the truncation order and degree are so large that the standard error would be large due to the multicollinearity: degree and order up to 67 and 7, respectively.

Keywords: Sq daily variation, spherical harmonic analysis, natural orthogonal component analysis, the 2011 off the Pacific coast of Tohoku earthquake (Mw 9.0)

©2020. Japan Geoscience Union. All Right Reserved.

3D-Tomography of the Ionospheric Anomalies Immediately Before and After the 2011 Tohoku-oki (M_w9.0) Earthquake

*Ihsan Naufal Muafiry[1,2], Kosuke Heki[1]

1. Hokkaido University, Japan, 2. Universitas Esa Unggul, Indonesia

A dense network of ground Global Navigation Satellite System (GNSS) receivers detected ionospheric total electron content (TEC) increase immediately before the 2011 Tohoku-oki (M_w 9.0) earthquake around the ruptured fault. It is also known that coseismic vertical crustal movements trigger acoustic wave propagating upward, reaching the F-layer of the ionosphere after 8-10 minutes. The wave front makes an N-shaped impulsive signature in TEC time series, often followed by electron depletion lasting for tens of minutes. This postseismic TEC drop has been sometimes thought to have caused artificial TEC increase before the earthquake. Our study robustly estimates three-dimensional (3D) distribution of both pre- and postseismic ionospheric anomalies of the 2011 event by performing tomography of electron density anomalies. We set up > 6,000 blocks over the region covering the Japanese Islands, the Japan Sea, and the Korean Peninsula, as large as 1.0° (east-west) x 0.9° (north-south) x 60 km (vertical) up to 840 km altitude. By using TEC residuals of pairs of ~1,200 stations and 8 satellites from reference curves, we estimated electron density anomalies within individual blocks. To stabilize and regularize the solution, we applied two types of constraints, i.e. continuity constraint and altitude-dependent absolute value constraint around zero. The reliability of the solution has been confirmed in various ways including the checkerboard test. Our results showed that the estimated pre- and postseismic electron density anomalies do not overlap each other, i.e. the former occurred above land and the latter occurred above ocean (Figure 1). The preseismic anomalies are composed of a pair of positive (~300 km height) and negative (~600 km height) electron density anomalies along the geomagnetic field. The positive and negative anomalies are well balanced suggesting that the anomalies are caused by electron transportation. They occurred above the land of Northeast Japan without extending offshore, suggesting that the electric field due to surface electric charges are responsible for the preseismic anomaly. Electric field made by the surface charges would have penetrated the ionosphere and have caused downward electron transportation to cancel electric field along the geomagnetic field. On the other hand, the postseismic electron depletion occurred over the sea where coseismic vertical crustal movements were the largest. This supports its origin by vertical movements of the sea surface above the submarine fault. These results demonstrate that the pre- and postseismic ionospheric anomalies are independent not only temporarily but also spatially and certainly in underlying physical mechanisms.

Keywords: Pre-seismic Ionospheric Anomalies, Post-seismic, GPS-TEC, 3D-tomography

©2020. Japan Geoscience Union. All Right Reserved.

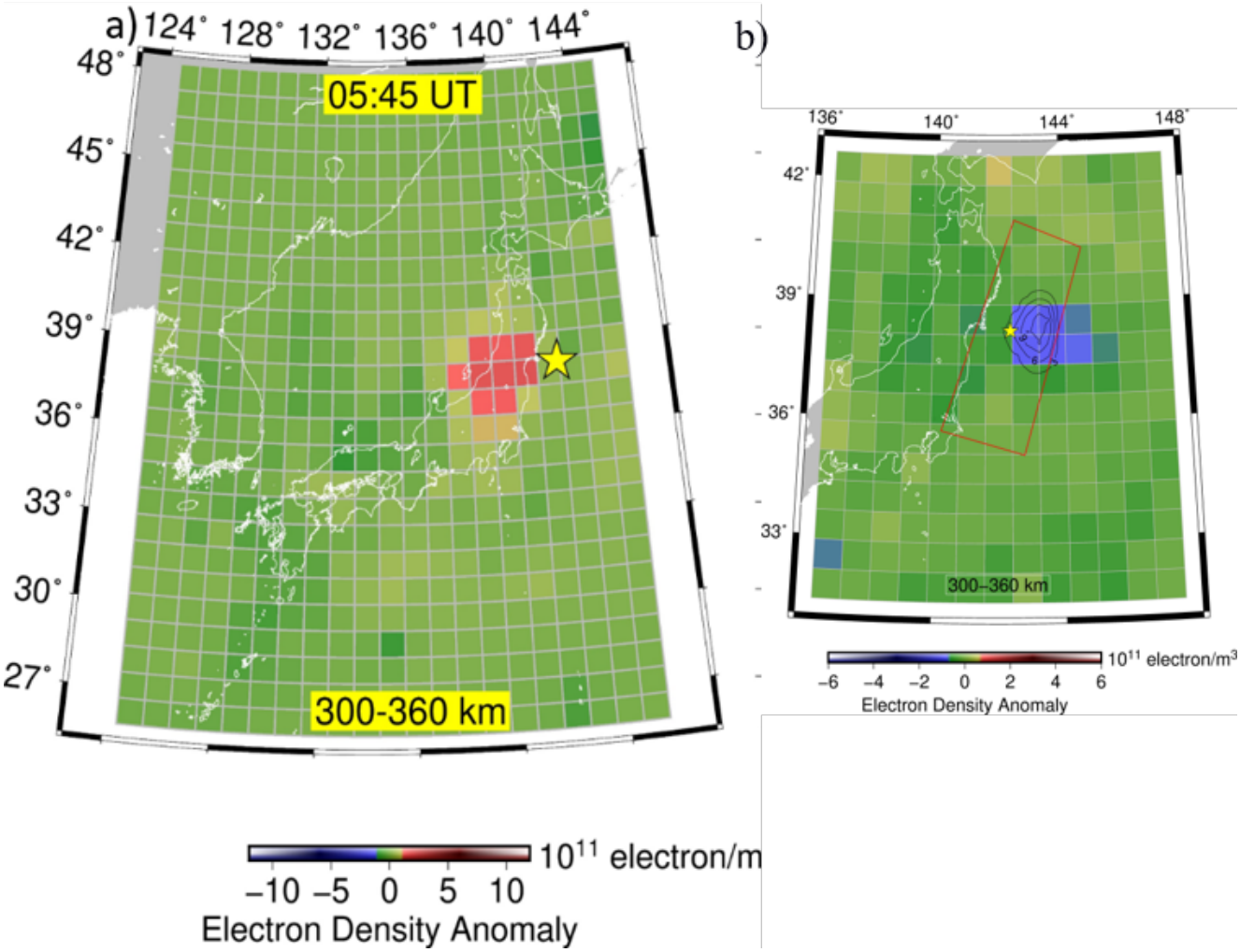

©2020. Japan Geoscience Union. All Right Reserved.

[J] Poster | M (Multidisciplinary and Interdisciplinary)：M-IS Intersection

[M-IS27] Geophysical fluid dynamics-Transfield approach to geoscience

convener:Keita Iga(Atmosphere and Ocean Research Institute, The University of Tokyo), Shigeo Yoshida(Department of Earth and Planetary Sciences, Faculty of Sciences, Kyushu University), Takatoshi Yanagisawa(Research Institute for Marine Geodynamics, Japan Agency for Marine-Earth Science and Technology), Hidenori AIKI(Nagoya University)

This session on geophysical fluid dynamics is open to discussions and researches on fluid phenomena in whatever fields of earth and planetary sciences, e.g., motions in the earth and planetary interior, oceans, atmospheres, volcanoes, and the ionosphere, conducted with whatever methods. Talks intending to stimulate exchange of ideas among multiple fields of researches or those identifying concepts that are commonly applicable to wide range of geophysical fluids are especially welcome.

[MIS27-P01] Transient flow states during convective spin-up

*Daisuke Noto[1], Yuji Tasaka[2], Takatoshi Yanagisawa[3,2], Takehiro Miyagoshi[3], Yuichi Murai[2] (1.Graduate School of Engineering, Hokkaido University, 2.Faculty of Engineering, Hokkaido University, 3.Japan Agency for Marine-Earth Science and Technology (JAMSTEC))

[MIS27-P02] Axial flow characteristics of a liquid metal roll convection under a horizontal magnetic field

Koki Sawada[1], *Yuji Tasaka[1], Takatoshi Yanagisawa[2,1], Yuichi Murai[1], Ataru Sakuraba[3] (1.Faculty of Engineering, Hokkaido University, 2.Japan Agency for Marine-Earth Science and Technology, 3.Department of Earth and Planetary Science, University of Tokyo)

[MIS27-P03] Influence of side-wall Hartmann braking in a liquid metal convection under a horizontal magnetic field

*Takatoshi Yanagisawa[1], Koki Sawada[2], Yuji Tasaka[2], Takehiro Miyagoshi[3], Ataru Sakuraba[4] (1.Research Institute for Marine Geodynamics, Japan Agency for Marine-Earth Science and Technology, 2.Faculty of Engineering, Hokkaido University, 3.Research Institute for Value-Added-Information Generation, Japan Agency for Marine-Earth Science and Technology, 4.Faculty of Science, University of Tokyo)

[MIS27-P04] Shallow water MHD waves trapped in the polar regions on a rotating sphere with an imposed azimuthal magnetic field

*Ryosuke Nakashima[1], Shigeo Yoshida[2] (1.Faculty of Sciences, Kyushu University, 2.Department of Earth and Planetary Sciences, Faculty of Science, Kyushu University)

[MIS27-P05] Sporadic low salinity signals in the oceanic mixed layer observed by the Kuroshio Extension Observatory buoy

Kohei Kameyama[1], *Hidenori AIKI[1], Yuki Kanno[1], Shun Ohishi[2], Hiroyuki Tomita[1], Fukutomi Yoshiki[1] (1.Nagoya University, 2.RIKEN)

[MIS27-P06] Laboratory experiments of vortices and internal waves around oscillating rectangular cylinder in a stratified viscous fluid

*Tatsuo Motoi[1], Shigenori Murakami [1], Nobuyuki Kinoshita[1], Mitsuo Ohizumi[1], Teruyuki Kato[1] (1.Meteorological College)

[MIS27-P07] Resonance between waves propagating on the flow in a cylindrical tank with a rotating bottom

*Keita Iga[1] (1.Atmosphere and Ocean Research Institute, The University of Tokyo)

[MIS27-P08] About the collapse of a huge ice sheet lake on the Laurentide ice sheet.

*SHOUJI Yoshinori

Transient flow states during convective spin-up

*Daisuke Noto[1], Yuji Tasaka[2], Takatoshi Yanagisawa[3,2], Takehiro Miyagoshi[3], Yuichi Murai[2]

1. Graduate School of Engineering, Hokkaido University, 2. Faculty of Engineering, Hokkaido University, 3. Japan Agency for Marine-Earth Science and Technology (JAMSTEC)

Rotating thermal convection is one of the most important topics in the field of fluid dynamics and geo-/astrophysics. Most of the previous efforts on this topic have been dedicated for the explanation of the heat transfer scaling and the exploration of the flow morphologies under the fully developed states, i.e. the equilibrium states of the rotating thermal convection. Accordingly, detailed investigations of transient states during spinning-up of thermal convection are less and many open questions stay up to now.

We have tackled this problem via visualization experiments using water as the test fluid with changing three experimental parameters; aspect ratio of the fluid container, Rayleigh number, and Taylor number. Soon after giving an impulsive rotation to a fully developed thermal turbulence, the convective flow structures are blown away and start to form concentric roll structures. Depending on the thermal and the rotational force intensity, the roll structures were found to take two different states; spiral and ring structures. In both cases, the roll structures were collapsed into azimuthally aligned vortical structures due to the Kelvin-Helmholtz instability. These shear-induced vortical structures, interestingly, possessed the horizontal size equivalent to that of the columnar vortices formed under the equilibrium states of rotating thermal convection, which are originated in the thermal plumes.

Keywords: Natural convection, Rotating field, Flow transition

©2020. Japan Geoscience Union. All Right Reserved.

Axial flow characteristics of a liquid metal roll convection under a horizontal magnetic field

Koki Sawada[1], *Yuji Tasaka[1], Takatoshi Yanagisawa[2,1], Yuichi Murai[1], Ataru Sakuraba[3]

1. Faculty of Engineering, Hokkaido University, 2. Japan Agency for Marine-Earth Science and Technology, 3. Department of Earth and Planetary Science, University of Tokyo

Magneto-convection is one of important flow systems for describing behavior of the earth’ s outer core. It is well known that applying sufficiently strong horizontal magnetic field to thermal convection in a liquid metal layer stabilizes the convections into quasi-two-dimensional rolls aligned parallel to the magnetic field. The corresponding phenomena of convection rolls are, however, not so simple because of existence of side boundaries; pressure gradient nearby the wide wall perpendicular to the magnetic field causes axial flow due to Ekman pumping in Bödewadt layer. And, the flow provides complexity on the convection. We examined axial flow and advection structures on quasi-two-dimensional convection rolls by laboratory experiment using liquid metal layer imposed by horizontal magnetic field. Ultrasonic velocity profiler visualized and quantified roll structures and axial flows by multiple measurement lines set in the fluid layer. The measurements were performed for different Rayleigh and Chandrasekhar numbers and variations of the axial flow velocity were investigated. Visualized flow pattern suggested influence of Lorenz force on the axial flow and scaling law with considering the Lorenz force effect was discussed.

Keywords: Natural convection, Magnetic field, Flow transition

©2020. Japan Geoscience Union. All Right Reserved.

Influence of side-wall Hartmann braking in a liquid metal convection under a horizontal magnetic field

*Takatoshi Yanagisawa[1], Koki Sawada[2], Yuji Tasaka[2], Takehiro Miyagoshi[3], Ataru Sakuraba[4]

1. Research Institute for Marine Geodynamics, Japan Agency for Marine-Earth Science and Technology, 2. Faculty of Engineering, Hokkaido University, 3. Research Institute for Value-Added-Information Generation, Japan Agency for Marine-Earth Science and Technology, 4. Faculty of Science, University of Tokyo

The effect of magnetic field is important for flows occurring in liquid metals. For phenomena confined by solid boundaries, the existence of side wall is also essential. We performed both laboratory experiments and numerical simulations on Rayleigh-Benard convection with a liquid metal as the test fluid under a strong horizontal magnetic field to elucidate influence of side-wall Hartmann braking on the phenomena. Vessels with different length in the direction of magnetic field were examined to modify the influence. In the laboratory experiments, horizontal velocity profiles were measured by ultrasonic velocity profiler to observe behavior of the convection and to quantify it. It was confirmed that there are quasi-two-dimensional rolls aligned parallel to the magnetic field because of sufficiently strong magnetic field and the magnitude of convection was characterized as variation of Reynolds number with respect to Chandrasekhar number, which is the ration of Lorenz force to the viscous damping. Scaling law describing the variation was derived with assumption of balance between buoyancy given by vertical temperature difference and side-wall Hartmann braking, which is viscous dissipation due to thinning of side-wall boundary layer perpendicular to the magnetic field (Hartmann layer) by the Lorentz force. It is expected that as the length scale in the magnetic field becomes narrower, the influence of Hartmann braking becomes stronger. The variations for different Rayleigh number and the length scale were collapsed into a unified curve by normalization according to the scaling law at conditions of relatively strong magnetic field.

Keywords: magnetoconvection, Hartmann boundary layer, roll-like structure

©2020. Japan Geoscience Union. All Right Reserved.

Shallow water MHD waves trapped in the polar regions on a rotating sphere with an imposed azimuthal magnetic field

*Ryosuke Nakashima[1], Shigeo Yoshida[2]

1. Faculty of Sciences, Kyushu University, 2. Department of Earth and Planetary Sciences, Faculty of Science, Kyushu University

Magnetohydrodynamic (MHD) shallow water linear waves are examined on a rotating sphere with a background toroidal magnetic field expressed as $B_{0\Phi}=B_0\sin\theta$, where B_0 is constant, θ is the colatitude and Φ is the azimuth. The MHD shallow water equations are often used in studying the dynamics of the solar tachocline (e.g. Gilman & Dikpati, 2002[1]; Márquez-Artavia et al., 2017[2]) and sometimes the outermost Earth's core (Márquez-Artavia et al., 2017[2]; Nakashima, Ph.D. thesis, 2020[3]) and exoplanetary atmosphere (e.g. Heng & Workman, 2014[4]). In this poster, we especially focus on the propagation mechanisms and the force balances of polar trapped waves and unstable modes (Márquez-Artavia et al., 2017[2]; Nakashima, Ph.D. thesis, 2020[3]).

Comprehensive searches for eigenmodes yield two polar trapped modes when the main magnetic field is weak (the Lehnert number $\alpha=V_A/2\Omega R^2<0.5$, where V_A is the Alfvén wave velocity, Ω is the rotation rate and R is the sphere radius). One is the slow magnetic Rossby waves, which propagate eastward for zonal wave number $m\geqq2$ (Márquez-Artavia et al., 2017[2]). As the Lamb's parameter $\varepsilon=4\Omega^2R^2/gh\rightarrow0$ (where g is the gravity acceleration and h is the equivalent depth), these branches asymptotically approach the eigenvalues of two-dimensional slow magnetic Rossby waves. Another is newly discovered westward polar trapped modes (Nakashima, Ph.D. thesis, 2020[3]).

In the case when $\alpha>0.5$ (the background field is strong), these novel westward modes merge with the westward-propagating fast magnetic Rossby waves. In addition, only when m=1, polar trapped unstable modes appear due to the interaction between these fast magnetic Rossby waves and westward-propagating slow magnetic Rossby waves. These growth modes are believed to be the polar kink (Tayler) instability (Márquez-Artavia et al., 2017[2]).

In order to easily understand the propagation mechanisms and the force balances of polar trapped modes, we investigate a cylindrical model around a pole with an artificial boundary condition. This model provides the approximate dispersion relations and eigenfunctions of polar trapped modes, and indicates that stable polar trapped modes are governed by magnetostrophic balance and that the metric magnetic tension force causes the difference between the slow magnetic Rossby waves and the novel westward modes. For m=1 and $\alpha>0.5$, the balance between Coriolis and Lorentz forces is disrupted and the part of magnetic tension with which Coriolis force can not compete induces kink instability.

[Reference]

[1] Gilman, P. A., Dikpati, M. (2002) *Astrophys. J.*, **576**, 1031. doi: 10.1086/341799
[2] Márquez-Artavia, X., Jones, C. A., Tobias, S. M. (2017) *Geophys. Astrophys. Fluid Dyn.*, **111**, 282. doi: 10.1080/03091929.2017.1301937
[3] Nakashima, R. (2020) Ph.D. thesis, Kyushu University.
http://dyna.geo.kyushu-u.ac.jp/HomePage/nakashima/pdf/doctoral_thesis.pdf
[4] Heng, K., Workman, J. (2014) *Astrophys. J. Sup.*, **213**, 27. doi: 10.1088/0067-0049/213/2/27

©2020. Japan Geoscience Union. All Right Reserved.

Keywords: MHD shallow water, toroidal magnetic field, polar trapped waves, slow magnetic Rossby waves, polar kink instability

©2020. Japan Geoscience Union. All Right Reserved.

Sporadic low salinity signals in the oceanic mixed layer observed by the Kuroshio Extension Observatory buoy

Kohei Kameyama[1], *Hidenori AIKI[1], Yuki Kanno[1], Shun Ohishi[2], Hiroyuki Tomita[1], Fukutomi Yoshiki[1]

1. Nagoya University, 2. RIKEN

The hourly measurements of air-sea interaction parameters made at the Kuroshio Extension Observatory (KEO) buoy since 2004 have produced an extensive dataset that can be used to understand the dynamics of the oceanic mixed-layer under extreme weather conditions. Our analysis of the KEO-buoy measurements reveals the presence of sporadic low-salinity signals (SLSSs) in the mixed-layer when, for example, tropical cyclones (TCs) approach. These intermittent features cannot be reproduced by one-dimensional turbulence closure models. Here SLSS and sporadic low-temperature signals (SLTS) are identified within the buoy data by using flags which are set to unity when the values of normalized salinity and temperature, respectively, fall below -1 (minus one). Application of this definition to the hourly time series of salinity and temperature measured at 10m depth by the KEO buoy has allowed us to identify 244 SLSS events and 191 SLTS events over the 11-year analysis period. A composite time series of the flagged events, constructed with reference to the start time of each SLSS event, shows that these episodes decay monotonically over 1-2 days in all four seasons, a time-scale that is closer to the near-inertial period rather than to the decay-times of instability processes associated with oceanic eddies and currents. Both winter (January-March) and spring (April-June) seasons show a peak in the composite time series of wind velocity diurnal variation (WVDV) near the start time of SLSS events, which indicates that atmospheric cyclones and anticyclones play a role in their genesis. Moreover, SLSS events can be terminated by the entrainment of saltier subsurface water parcels to the mixed-layer in response to storms. The discovery of the WVDV peaks following SLSS commencement is the reason the present study has adopted a time scale of 1 day for WVDV analysis. This temporal resolution has enabled us to identify a TC-related delay in the development of the WVDV peaks, which may represent a fundamental characteristic of the influence of TCs on these events.

Keywords: precipitation, salinity, hourly measurment

©2020. Japan Geoscience Union. All Right Reserved.

Laboratory experiments of vortices and internal waves around oscillating rectangular cylinder in a stratified viscous fluid

*Tatsuo Motoi[1], Shigenori Murakami [1], Nobuyuki Kinoshita[1], Mitsuo Ohizumi[1], Teruyuki Kato[1]

1. Meteorological College

Laboratory experiments of vortices and internal waves around vertically oscillating rectangular cylinder in a uniformly stratified viscous fluid of salt solution were carried out by means of visualization methods. The particle path, streak line and Moiré fringe methods were used as visualization methods. The results from the experiments are summarized as follows.
(1)The vortices were induced around the rectangular cylinder due to viscosity as the square and circular cylinders.
(2)The two vortices were generated at the corner of the rectangular cylinder, rotating in opposite directions in the vicinity to its each side wall.
(3)Associated with the flow by two vortices, the two sources of internal waves were generated at the four corners of rectangular cylinder, and so the internal waves were excited in the total of the eight sources.
(4)The observed fluid particles near the sources of the internal waves moved along elliptic path, which is different from lined path of the resonant direction of linear theory (the direction defined by the forcing frequency of vertically oscillating rectangular cylinder and the characteristic frequency of uniformly stratified viscous fluid (Brunt-Väisälä frequency)), however the velocity fields near the sources included the velocity which had the direction of resonance.
(5)As long as the rectangular cylinder was forced to oscillate vertically, the energy of oscillation was transported outward from the rectangular cylinder along the resonant direction by the movements of pushed and pulled fluid particles near the sources of the internal waves, which resulted in the development of the eight direction rays of internal waves by the two direction rays at the four corners of rectangular cylinder.

Keywords: vortices, internal waves, laboratory experiments

©2020. Japan Geoscience Union. All Right Reserved.

Resonance between waves propagating on the flow in a cylindrical tank with a rotating bottom

*Keita Iga[1]

1. Atmosphere and Ocean Research Institute, The University of Tokyo

In the terrestrial and planetary atmospheres, non-axisymmetric structures are often formed from the axisymmetric environments. We can realize such non-axisymmetric flows in a very simple laboratory experiment using a cylindrical tank filled with water whose bottom rotates rapidly.
For the theoretical analysis of such phenomena, the axisymmetric flow as the basic state is necessary. We have been analyzed the axisymmetric flows using boundary layer theories, and obtained the basic axisymmetric flow, which predicts the water elevation of the axisymmetric regime of the laboratory experiments precisely.
Based on the obtained flow field, instability of the axisymmetric flow is investigated, under the shallow water system, but some differences are found between the results of the stability analysis and the laboratory experiment. The instability is considered using the concept of resonance between couner-propagating waves. The instability is considered to be caused by resonance between a topographic Rossby wave and a gravity wave along the side wall. In pariticular, the propagation of the gravity waves should be estimated considering the finite depth of the water layer.

Keywords: rotating flow, instability, resonance between waves, laboratory experiments

©2020. Japan Geoscience Union. All Right Reserved.

About the collapse of a huge ice sheet lake on the Laurentide ice sheet.

*SHOUJI Yoshinori

In the northern continent of the last glacial era, a huge Laurentide ice sheet of more than 3,000 m thick was formed. There is a theory that a huge ice sheet lake called Lake Agassiz was formed, and its collapse had a significant impact on the global environment. However, the reality of the collapse was not clear. Therefore, I analyzed the topographic data released by NOAA using my own software. As a result, it was found that the water volume of Lake Agassiz was much less than the previous theory. In addition, the surrounding terrain has revealed that Lake Agassiz is not a large-scale catastrophic lake. A sloping map of the North American continent created a terrain near Lake Agassiz that might have been the sign of a massive erosion. This revealed that the Lake Agassiz collapse was caused by another larger ice sheet lake collapse. The purpose of this study is to examine the collapse mechanism and scale of a huge ice sheet lake on the Laurentide ice sheet.

Keywords: Lake Agassiz, Laurentide Ice Sheet, Global cooling, Younger Dryas

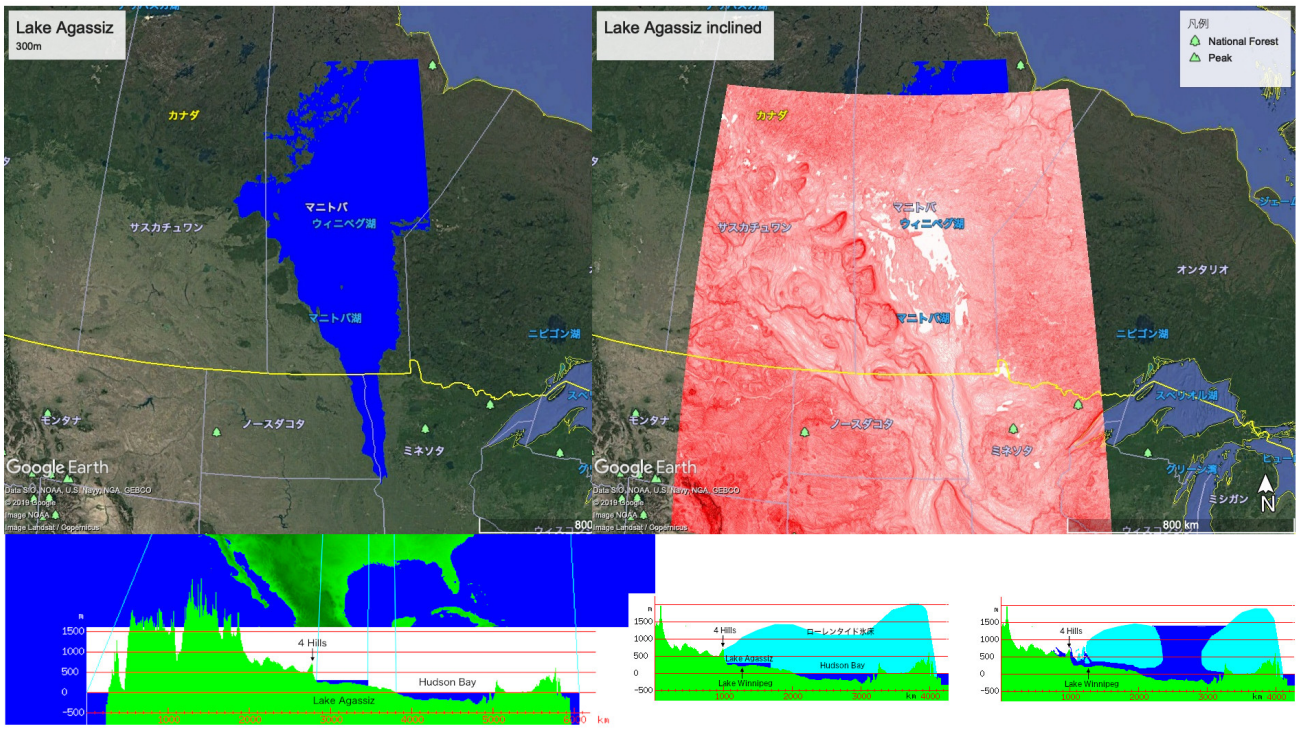

©2020. Japan Geoscience Union. All Right Reserved.

[J] Poster | M (Multidisciplinary and Interdisciplinary)：M-IS Intersection

[M-IS28] History X Earth and Planetary Science

convener:Yasuyuki Kano(Earthquake Research Institute, The University of Tokyo), Hiroaki Isobe(Faculty of Fine Arts, Kyoto City University of Arts), Kei Yoshimura(Institute of Industrial Science, The University of Tokyo), kiyomi iwahashi(National Institute of Japanese Literature)

The history of modern observation in earth and planetary sciences is often far shorter compared with the timescales of their interests. Investigation of the long-term variations and occurrences of extremely rare events requires effective use of information derived from historical documents observed and recorded by pre-modern people. Thus, historical documents have been referred in various fields of earth and planetary sciences such as seismology, climatology, meteorology and astronomy. Sharing their records, methods and experiences will be beneficial for each field and bring new insights. It is also essential to involve experienced historians because one needs to carefully investigate the reliability and the context of each document in order to use it as scientific data. On the other hand, analyzing the record in the historical documents with the eyes of modern science may also bring new insights to the historians. Cooperative work between historians and earth scientists will provide better knowledge on disaster mitigation, and science, technology and society through understanding of human reaction to historical disasters.

In this session we overview the studies using the historical documents in various fields of the earth and planetary sciences as well as the recent advances in related topics such as historical-data assimilation and digital humanities, such as AI character recognition. The aim is to promote the communication and dialogues among the researchers in various background, and thus foster the new ideas and collaborations in the study of "History X EPS."

[MIS28-P01] Recompilation of online data for historical earthquake studies

*Yasuyuki Kano[1] (1.Earthquake Research Institute, The University of Tokyo)

[MIS28-P02] Estimation of the rice production in the early 20th century of China: its explanation and impact in both hydrological and historical ways

★Invited Papers

*CHANG LIU[1], Akiyuki KAWASAKI[1], Tomoko SHIROYAMA[2] (1.Department of Civil Engineering, The University of Tokyo, 2.Graduate School of Economics, The University of Tokyo)

[MIS28-P03] Historical flood disaster in the southern area of Gunma Prefecture infered from the memorial monuments of flood

*Masafumi Aoyama[1] (1.Faculty of Education, Gunma University)

[MIS28-P04] Consideration on problems and classification methods of "Disaster Monument"

*Junzo Ohmura[1] (1.Earthquake Research Institute,The University of Tokyo)

[MIS28-P05] Atmospheric data assimilation which accomodates weather descriptions as observations of solar radiation: Evaluation of performance with a modern one-year case

*Kooiti Masuda[1], Panduka Neluwala[2], Kinya Toride[4,3], Kei Yoshimura[3], Hidenori Tanaka[5], Sho Miyazaki[5], Satoshi Nozawa[5], Mika Ichino[6], Yu Okubo[7,8], Junpei Hirano[7] (1.Department of Geography, Tokyo Metropolitan University, 2.Department of Civil Engineering, University of Peradeniya, 3.Institue of Industrial Science, University of Tokyo, 4.Department of Atmospheric Sciences, University of Washington, 5.Department of Earth Science, College of Science, Ibaraki University, 6.ROIS-DS Center for Open Data in the Humanities, 7.Department of History, Teikyo University, 8.Department of Geography, Senshu University)

[MIS28-P06] Application of Observational Seismology to Historical Seismology (1) A pilot seismic observations in the suburbs to investigate regional variations in seismic intensity from the 1855 Ansei Edo-Earthquake

*Motoko Ishise[1], Ryoichi Nakamura[1], Tomoya Harada[1], Takashi Iidaka[1], Shigeki Nakagawa[1], Ayakia Saiki[1], Kazuhito Hikima[2], Shin'ichi Sakai[1] (1.Earthquake Reseach Institute, University of Tokyo, 2.Tokyo Electric

Power Company Holdings, Inc.)

[MIS28-P07] Sunspot Observation before 1945 in Nagashima Aiseien

*Harufumi Tamazawa[1], Hiroaki Isobe[1] (1.Kyoto City University of Arts)

[MIS28-P08] A Linkage between climatic condition and market economy in the 19th century Japan
- Analysis of solar radiation from historical documents and rice price -

*Mika Ichino[1], Kooiti Masuda[2], Takehiko Mikami[2], Yasuo Takatsuki[3] (1.Center for Open Data in the Humanities, Joint Support-Center for Data Science Research, Research Organization of Information and Systems , 2.Tokyo Metropolitan University, 3.Research Institute for Economics and Business Administration, Kobe University)

[MIS28-P09] Discovery of Original Material of Nakamura Nakazo's Account on the 1855 Ansei Edo Earthquake

*Ryoichi Nakamura[1], Motoko Ishise[1], Reiko Sugimori[2,3], Kenji Satake[1,3] (1.Earthquake Research Institute, The University of Tokyo, 2.Historiographical Institute, The University of Tokyo, 3.Collaborative Research Organization for Historical Materials on Earthquakes and Volcanoes)

[MIS28-P10] Comparison between interannual variation of snowfall frequency in Nagasaki and 20th century reanalysis data from 1836 to 1868

*Junpei Hirano[1], Takehiko Mikami[2], Masumi Zaiki[3], Mika Ichino[4] (1.Teikyo University, 2.Tokyo Metropolitan University, 3.Seikei University, 4.Center for Open Data in the Humanities)

[MIS28-P11] Attempt to restore the forest cover in China's planned economic period using declassified American and Soviet reconnaissance information: A case of Northern Shaanxi Loess Plateau

★Invited Papers

*Yuta Hara[1] (1.Komaba Organization for Educational Excellence, College of Arts and Sciences, The University of Tokyo)

[MIS28-P12] Philological and scientific assessment of aurora records in historical documents

*Hiroaki Isobe[1], kiyomi iwahashi[2], Harufumi Tamazawa[1] (1.Faculty of Fine Arts, Kyoto City University of Arts, 2.National Institute of Japanese Literature)

Recompilation of online data for historical earthquake studies

*Yasuyuki Kano[1]

1. Earthquake Research Institute, The University of Tokyo

Several databases publish text data of materials for historical earthquake studies. The coverage of databases is limited in time and space because the amount of materials are too large to compile and emend at one time or because of scope of each project. A cross-search system for the databases are useful to analyze earthquakes recorded in wide range of time and space. Many historical materials were collected and organized, and collections of earthquake records that compiled articles on earthquakes (some of which include volcanic eruptions and landslides) have been published. These collections amount to 35 volumes and 27,000 pages. This series of archived collection can be viewed in a PDF format currently at the special materials database by the Earthquake Research Institute Libary, University of Tokyo , and a part of the collection is also included in the digital collection of the National Diet Library . A "historical earthquake record search system" is also available to the public, where a visitor can search for a volume and pages of an article. There have been efforts to build full-text database of compiled articles on earthquakes.

We have developed database for intensity or macroseismic data for historical earthquakes occurred in and around Japan based on a report compiled by T. Usami. The database is published using “midop” software which is a tool for easily transforming macroseismic intensity data tables into interactive maps. We compiled several datasets for historical intensity data of Japan. We also trying to build dataset related to Japanese historical earthquake in the Linked Data format.

Keywords: Materials for Historical Earthquake Studies, Database, LOD

©2020. Japan Geoscience Union. All Right Reserved.

Estimation of the rice production in the early 20th century of China: its explanation and impact in both hydrological and historical ways

*CHANG LIU[1], Akiyuki KAWASAKI[1], Tomoko SHIROYAMA[2]

1. Department of Civil Engineering, The University of Tokyo, 2. Graduate School of Economics, The University of Tokyo

Because of the wide consumption and transportation, rice has played an essential role in the economic development of China in the early 20th century. However, despite of its importance, the rice production was uncertain in most regions at that time because of the confusing management and statistical mistakes of the state bureaucracy. Therefore, to give a reasonable estimation of the rice production, we proposed a new approach combining numerical models and historical documents. In this study, the Water and Energy Budget-based Distributed Hydrological Model (WEB-DHM) was applied to reconstruct the long-term hydrological condition in the early 20th century of China. Then an AquaCrop scheme was used to estimate the potential rice production. Finally, the result was validated according to the historical records of Jiangxi Province. This study showed a reasonable rice production change regarding the 1931 flood and 1934 drought and a possible impact on economic development afterwards. It also suggested a great potential of utilizing the same approach in other monsoon regions in Asia.

Keywords: rice production, historical hydrology, WEB-DHM, AquaCrop

©2020. Japan Geoscience Union. All Right Reserved.

Historical flood disaster in the southern area of Gunma Prefecture infered from the memorial monuments of flood

*Masafumi Aoyama[1]

1. Faculty of Education, Gunma University

Distribution of memorial monuments related to the flood damages and their description in the central and southern area of Gunma Prefecture were investigated. Many memorial monuments related to the debris flow and flood caused by the typhoon Kathleen 1947 are distributed in the southern and western foot area of Mt. Akagi. Karasu river, Kabura river and Kanna river confluence in the Karasu river lowland. This area is flood prone area, and many memorial monuments of past flood are also distributed. These memorial monuments in this area are related to the flood caused by heavy rain of 1846, 1910 and 1935.

Keywords: memorial monuments of flood, Flood caused by typhoon kathleen 1947, Great flood of 1910, Gunma Prefecture

©2020. Japan Geoscience Union. All Right Reserved.

Consideration on problems and classification methods of "Disaster Monument"

*Junzo Ohmura[1]

1. Earthquake Research Institute,The University of Tokyo

In recent years, research on monuments related to natural disasters has been actively conducted. The Geospatial Information Authority of Japan added the disaster monument to the map symbol. It is hoped that the monuments about disasters will tell the past disasters. However, the debate on how to organize and classify monuments is delayed. From the perspective of disaster prevention, it is important to convey past natural disasters, and they do not necessarily have to be stone monuments. For example, some trees and faults have the function of handing down disasters. If you stick to the shape too much, you may lose essence.
Unless the nature of the monument is clarified, it may not be possible to properly preserve and use it. The stele indicating the depth of the flood should not be moved easily. Steles about the dead must be treated with dignity. Therefore, appropriate classification needs to be performed.
In this study, we thought that it was necessary to set a higher-level concept to analyze the monument. Next, the monuments were classified into those that describe the disaster by text and those that do not use text. Some monuments that do not use text do not reveal the relationship to the disaster just by looking at them. In addition, there are potential monuments in which the relationship with the disaster has not been scientifically clarified. These are likely to be forgotten unless a connection with the disaster is proved or explanations are provided. The classification method shown here is a private idea. Many researchers' discussions are needed to solve various issues.

This research was conducted as part of the Research Grants for Young Researchers of the Association for Disaster Prevention Research.

Keywords: Disaster, Monument, Classification

©2020. Japan Geoscience Union. All Right Reserved.

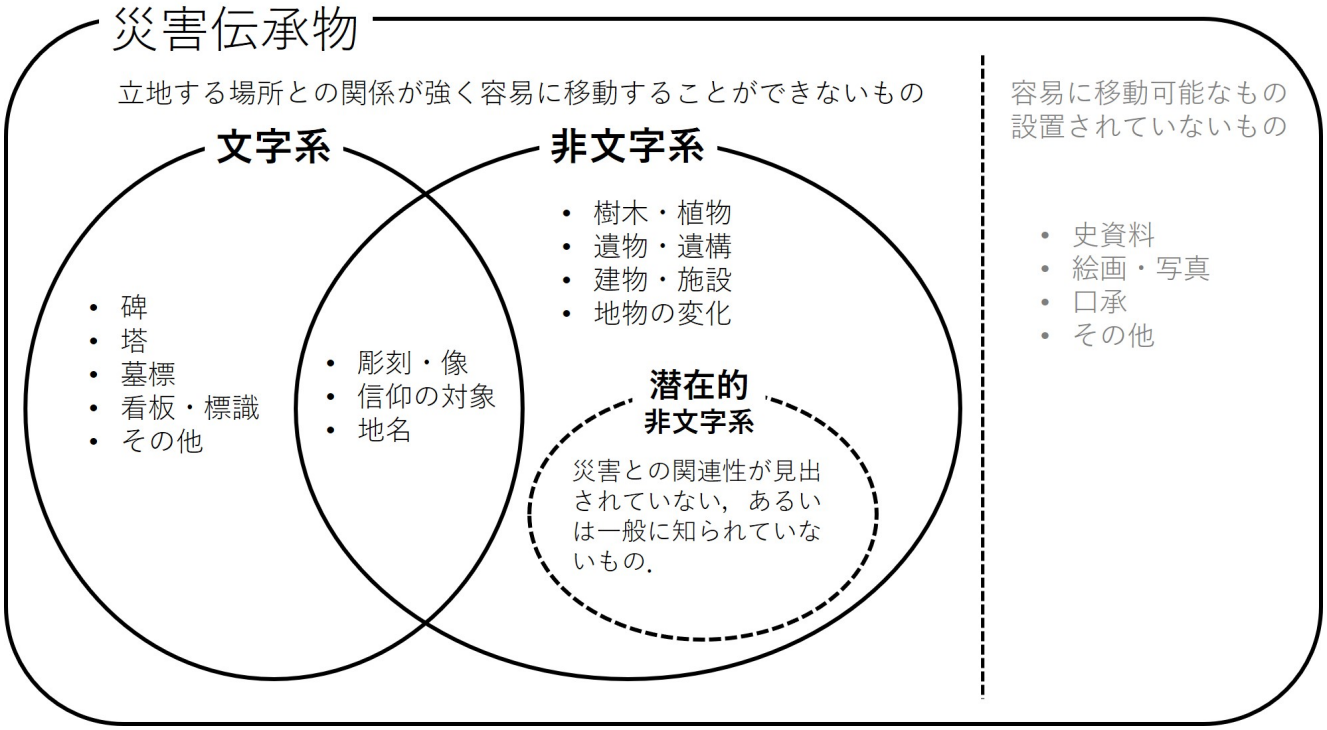

©2020. Japan Geoscience Union. All Right Reserved.

Atmospheric data assimilation which accomodates weather descriptions as observations of solar radiation: Evaluation of performance with a modern one-year case

*Kooiti Masuda[1], Panduka Neluwala[2], Kinya Toride[4,3], Kei Yoshimura[3], Hidenori Tanaka[5], Sho Miyazaki[5], Satoshi Nozawa[5], Mika Ichino[6], Yu Okubo[7,8], Junpei Hirano[7]

1. Department of Geography, Tokyo Metropolitan University, 2. Department of Civil Engineering, University of Peradeniya, 3. Institue of Industrial Science, University of Tokyo, 4. Department of Atmospheric Sciences, University of Washington, 5. Department of Earth Science, College of Science, Ibaraki University, 6. ROIS-DS Center for Open Data in the Humanities, 7. Department of History, Teikyo University, 8. Department of Geography, Senshu University

To acquire information about climate before the beginning of instrumental observations, we can use documentary records written by people in addition to natural objects such as tree rings. In particular, many diaries that contains descriptions of daily weather are available in Japan. On the other hand, data assimilation systems have so developed that they can incorporate such observed quantities that are not prognostic variables of the forecast model. Thus, we expect that we can know space-time distribution of meteorological elements of the times without instrumental observations by taking weather descriptions as input to atmospheric data assimilation systems.

In this study, we apply the method to a time period with instrumental observations, and examine how weather phenomena in the real world can be reproduced.

As the atmospheric model, the NCEP GSM (Global Spectral Model) of the version used for seasonal weather forecasts till 2004 is used. The spatial resolution is T62 (grid spacing ca. 250 km) and 28 layers. As for the assimilation scheme, LETKF (local ensemble transform Kalman filter) of Miyoshi (2011, Monthly Weather Review) is used. The sea surface temperature given as a boundary condition is based on monthly mean NOAA OISST, interpolated to daily time steps.

As present-day data which mimic weather descriptions in diaries, the general weather conditions ("tenki gaikyo") of Japan Meteorological Agency is used. 18 stations are chosen so that each station corresponds to one grid box of the GSM. We classify the daytime general weather condition of every day into three categories, "fine", "cloudy", and "rainy and snowy", and convert it into the daily amount of global solar radiation by the method of Ichino et al. (2001, "Tenki"; 2018, "Chigaku Zasshi"). Then we re-scale it into 6-hourly values and gave them to the assimilation system as observations of the downward shortwave radiative flux at the surface of the earth. In addition, we give zero as the observed amount of precipitation if and only if no rain or snow in daytime was documented in the general weather condition of the day. We call this the "weather assimilation experiment." As for comparison, we also conduct the "no-observation experiment" where no observations are given to the assimilation system.

The period of the experiments is one year of 1995, from 1 January to 31 December. The number of members of the ensemble of LETKF is 30.

Among the results of assimilation, we mainly look at the ensemble average analysis fields of sea level pressure, and additionally those of vorticity at 850 hPa and of precipitation. As for information on the real situation, we use JRA55 and surface weather charts.

©2020. Japan Geoscience Union. All Right Reserved.

When extra-tropical cyclones pass Japan in the actual situation, low pressure systems often appear in our "weather assimilation experiment" in positions similar to the real situation, over Japan as well as over oceans to the east of Japan. However, correspondence of their strengths are not always good. Since the position of troughs does not match the actual condition at all in our "no-observation experiment", we consider that assimilation of weather information is effective. Tropical storms are not well reproduced. We consider that this is partly because that the spatial resolution of our atmospheric model is insufficient, and partly because that the time span of overlapping between the course of a tropical storm and the spatial coverage of observations is short. The meteorological situations of the Baiu are not well reproduced, either. In terms of seasons, the performance of this technique seems good
in spring and autumn.

Keywords: climate in historical times, data assimilation, weather records in diaries, extratropical cyclones

©2020. Japan Geoscience Union. All Right Reserved.

Application of Observational Seismology to Historical Seismology (1) A pilot seismic observations in the suburbs to investigate regional variations in seismic intensity from the 1855 Ansei Edo-Earthquake

*Motoko Ishise[1], Ryoichi Nakamura[1], Tomoya Harada[1], Takashi Iidaka[1], Shigeki Nakagawa[1], Ayakia Saiki[1], Kazuhito Hikima[2], Shin'ichi Sakai[1]

1. Earthquake Reseach Institute, University of Tokyo, 2. Tokyo Electric Power Company Holdings, Inc.

A pilot program for seismic observation was implemented in the suburbs of Tokyo for two months from September 26 to December 5, 2019. The purpose of the observation is to evaluate the quality of historical documents and regional variations in seismic intensity.

Prior to the observation, following three analyses were performed: (1) judgement of seismic intensity of the historical description about seismic damage, (2) identification of the exact location of the damage described in the document and mapping of seismic intensity, (3) selection of observation points.

As an example of a study on the 1855 Ansei-Edo earthquake, the analyses and results for Narita city are as follows. (1) judgement of seismic intensity of the historical description about seismic damage: based on descriptions of several historical documents, 8 seismic intensities were judged according to Usami (1995), (2) identification of the exact location of the damage described in the document and mapping of seismic intensity: 4 locations were identified by using of old maps, (3) selection of observation points: 10 observation points were selected, including the 3 points identified in (2).

Analysis of several relatively large earthquakes showed that the magnitude relation of calculated seismic intensity among the seismic stations is similar to that of judged seismic intensity of the 1855 Ansei-Edo earthquake. The similarity suggests that the descriptions in the historical documents used in this analysis are reliable and also that the surface geology strongly influences seismic intensity.

Acknowledgements: This study was supported by the Tokyo Metropolitan resilience project.

Keywords: judgement of seismic intensity of histrical earthquakea, seismic observation, 1855 Ansei-Edo earthquake

©2020. Japan Geoscience Union. All Right Reserved.

Sunspot Observation before 1945 in Nagashima Aiseien

*Harufumi Tamazawa[1], Hiroaki Isobe[1]

1. Kyoto City University of Arts

At Nagashima Aiseien, a national Hansen's disease sanatorium, Issei Yamamoto, the first director of the Kwasan Observatory at Kyoto University, performed a comforting performance in 1941, and the observatory was established in the sanatorium. Astronomical and meteorological observation were done here. Sketches of sunspot observation was one of them. Yamamoto's materials have been deposited at the Kwasan Observatory, where the exchange between Yamamoto and Aiseien is described. Yamamoto is the person who created the foundation of amateur astronomy in Japan that continues to the present day. This is one of the suggestions for understanding how to be.

Keywords: Sunspot

©2020. Japan Geoscience Union. All Right Reserved.

A Linkage between climatic condition and market economy in the 19th century Japan
- Analysis of solar radiation from historical documents and rice price -

*Mika Ichino[1], Kooiti Masuda[2], Takehiko Mikami[2], Yasuo Takatsuki[3]

1. Center for Open Data in the Humanities, Joint Support-Center for Data Science Research, Research Organization of Information and Systems , 2. Tokyo Metropolitan University, 3. Research Institute for Economics and Business Administration, Kobe University

Japan has plenty of diaries in the 17th to 19th centuries, which include records of daily weather conditions ("fine", "cloudy", "rainy", etc.) It is well known that they have been used for reconstructing climate variation and events, although it provided qualitative data, not instrumental observations.

We estimate global solar radiation from weather conditions. Global solar radiation is an important factor for the energy balance of the Earth, and is also fundamental to the hydrological cycle and agricultural productivity. Our method is effective for all seasons and which could produce reconstruction with higher temporal resolution than other proxy data, for example tree rings.

Weather descriptions are classified into 3 categories and weather categories convert to solar radiation. The parameters of conversion are calculated by using JMA observations from 1995 to 1999.

We reconstructed monthly mean global solar radiation from 1821 to 1850 based on the weather records described in 11 historical diary documents. We focused on the years of Tempo Famine from 1833 to 1839.

In 1836, monthly solar radiation in summer in the east-west zone of Japan including Kanto, Kinki, and northern Kyushu was smaller than the provisional normal (average of 1821-1850). It was 10% or more smaller than the normal in July and August. However, it was not particularly small in Tohoku to the north of the zone and in southern Kyushu to the south of the zone. The characteristic of reconstruction in 1836 is that lower solar radiation prolonged from May to September in the central area of Japan. This suggests that climatic condition similar to Baiu was prolonged, and that it was cold in Tohoku. On the other hand, in 1833 and 1838, when famines also occurred, the reconstructed solar radiation was low in Tohoku.

We also checked the effect on market economy by observing the daily price of rice, the main crop at that time. For 1836, we can observe the sharp rise of the price in July. It suggests that the market had reacted to the bad climate condition before the harvest season. After this sharp rise, four times higher than usual, rice price reached a plateau then fell in September 1837.

While the rice price in 1833 and 1838 also rose up in summer, they were only two or three times higher than usual and, more importantly, they quickly bounced back.
Cross check between the reconstructed solar radiation and the rice price data support thus enables us to conclude that there existed a big difference even among the years recorded as “famine years” on the historical documents.

Keywords: documentary sources, historical climatic fluctuation, market economy, famine, global solar radiation, 19th century

©2020. Japan Geoscience Union. All Right Reserved.

©2020. Japan Geoscience Union. All Right Reserved.

Discovery of Original Material of Nakamura Nakazo’s Account on the 1855 Ansei Edo Earthquake

*Ryoichi Nakamura[1], Motoko Ishise[1], Reiko Sugimori[2,3], Kenji Satake[1,3]

1. Earthquake Research Institute, The University of Tokyo, 2. Historiographical Institute, The University of Tokyo, 3. Collaborative Research Organization for Historical Materials on Earthquakes and Volcanoes

1. Introduction

Estimated depth of the 1855 Ansei Edo Earthquake varies from deep in/on the Philippine Sea Plate (PHS) to very shallow in the crust. These estimates base on the seismic intensity distribution and/or the S-P time estimated from historical materials.

A famous kabuki actor, Nakamura Nakazo, left the following description that included P and S-wave arrivals. “The strong upward movement came from the ground. Almost all the women were surprised and screamed. I said, ‘calm down, it’s a big earthquake.’ Omitu said to me ‘you should stand up rather than sitting.’ I stood up and walked. Then the strong shaking started, and I could not walk normally.” Three studies investigated the hypocentral depth based the above description. Hagiwara(1990) estimated the S-P time as approximately 10 s and the hypocentral depth as ~100 km. Nakamura et al. (2003) estimated the S-P time as 5–10 s based on the above description and other documents, concluding that it was an intra-slab earthquake within the PHS. Usami (1983) estimated the S-P time as 3–5 s based on the above description, for which case the depth would be shallower.

Above description was based on the contents in "Japan Earthquake Historical Materials" (Musha,1951), called “the Musha book” hereafter. On the other hand, we discovered the original of Nakazo's own two handwriting books in the National Diet Library, hereafter called “the 9th Diet book” and "the 10th Diet book”.

2. Comparison between Nakamura Nakazo's articles

There are four versions on Nakamura Nakazo’s description: "the Musha book", "Kabuki Shimpo", "the 9th of the Diet book" and "the 10th of the Diet book".

The decoding of “the Diet books” has been performed by one of the authors, Sugimori. Table 1 shows the description of S-P time parts on “the 9th Diet book” and " the Musha book". The bold characters show the difference. At the first part, it can be seen that "movement" where the ground lifts is depicted in "the Musha book", whereas "rumble" is depicted in “the 9th Diet Book”. There are many historical materials reported rumble in the Ansei Edo Earthquake.

Descriptions for the first part in "The Musha book ", "the 10th Diet Book" and "the Kabuki Shimpo" are almost the same, but that in “the 9th Diet Book” is different. The article of "the Kabuki Shinpo" was written by Kyogen writer Kubota Hikosaku, based on the record of Nakazo's handwritings, as a prosthesis and was abbreviated.

©2020. Japan Geoscience Union. All Right Reserved.

Our analysis of indicates that “the 9th Diet Book” was written earlier than the other three historical materials, and is considered as a contemporary document. It is desirable to use it for future studies of this earthquake.

3. Effect on S-P time estimation

The first difference between the "the Musha Book" and “the 9th Diet Book” is sound (rumble) or movement (Table 1). However, it does not significantly affect the estimation of the arrival time of the P-wave if the ground motion of the P-wave is transmitted to the air. Regarding the S-wave main motion, the "the Musha Book" states that it began to sway after walking, while it began to sway when he stood up (before walking) in "the 9th Diet Book", indicating S-P time is slightly shorter. It is known for large earthquakes that a large rupture at the so-called strong ground motion generation area (SMGA) is delayed from the initial rupture at the epicenter. In this case, the amplitude of the initial S-wave is small and large shaking occur later. Therefore, the actual S-P time can become shorter.

4. Possible depth from S-P time

Using the JMA2001 travel time table, an S-P time of 5 seconds indicates the epicenter depth of 40 km for the epicentral distance of 20 km. However, in the Kanto region covered with thick sedimentary layers, the depth can be shallower. Fig. 2 shows the waveform, indicating S-P time of 5 seconds, from the 2015/12/26 earthquake (M3.4, depth=23 km) at the K-NET Sarue (TKY021) station (epicentral distance=20 km). This depth can be possible for the 1855 earthquake.

Keywords: the 1855 Ansei Edo Earthquake, Historical Material, S-P time

©2020. Japan Geoscience Union. All Right Reserved.

表 1　中村仲蔵記事の地震動の部分の記事

Table 1 Article on the seismic motion part of Nakamura Nakazo.

「日本地震史料」 The Musha Book	「国会本」第 9 冊（翻刻：杉森による） The 9th Diet Book
地よりドゝゝゝと持ち上る。皆々女の事ゆゑキャッといつて立騒ぐ。我れ之を鎮め騒ぐことはない、是は地震の大きいのだといふ時に、小みつは親方座つて居ずとマアお立ちでないかといはれ、成程座つて居るにも及ばぬと思つて**立て歩行き出すと揺れ出し**、足を取られて歩行自由ならず	其内**大地轟キ出ス**，女子供ハハットいって立騒く，我夫ヲ押へ，騒ぐニ及ばず，此ハ地震の大キイのだ，静まり候へと言ふ，坂東小三津と言ふ師匠，親方すわって居づ共，マア御立ナサイといふ，本ニそふだと**立上るとゆれ初メ**，ヒヨロヒヨロして歩行れず
The strong upward movement came from the ground. Almost all the women were surprised and screamed. I said, ‘calm down, it’s a big earthquake.’ Omitu said to me ‘you should stand up rather than sitting.’ **I stood up and walked. Then the strong shaking started,** and I could not walk normally.	**The strong rumble occurred.** The women and children were surprised and screamed. I said, ‘calm down, it’s a big earthquake.’ Omitu Bando said to me ‘you should stand up rather than sitting.’ **I stood up. Then the strong shaking started**, and I could not walk normally.

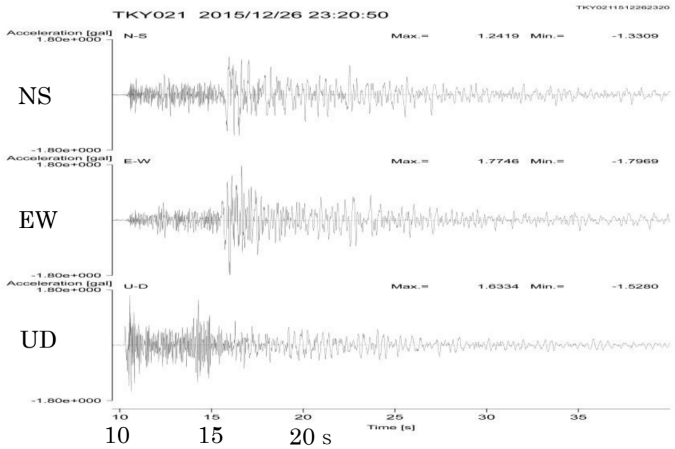

図 1 2015/12/26 23:20 の地震(M3.4, 深さ 23 km) K-NET 猿江(TKY0021)での加速度記録.
震央距離　20km　SMDA により描画・加筆.

Fig. 2 Acceleration wave form of the 2015/12/26 earthquake (M3.4, depth=23 km) at the K-NET Sarue (TKY021) station (epicentral distance=20 km).

©2020. Japan Geoscience Union. All Right Reserved.

Comparison between interannual variation of snowfall frequency in Nagasaki and 20th century reanalysis data from 1836 to 1868

*Junpei Hirano[1], Takehiko Mikami[2], Masumi Zaiki[3], Mika Ichino[4]

1. Teikyo University, 2. Tokyo Metropolitan University, 3. Seikei University, 4. Center for Open Data in the Humanities

In the present study, we compared interannual variation of snowfall frequency documented in old diary in Nagasaki and 20th century reanalysis data V.3 (Slivinski et al.,2019)for the years from 1836/37 to1867/68.As a result, we detected that interannual variation of snowfall frequency in Nagasaki is negatively correlated with variation of Aleutian low intensity. Interannual variation of snowfall frequency is also strongly correlated with development of East Asian trough and strength of westerly jet over East Asia. Moreover, interannual variation of snowfall frequency seems to relate to El Niño and Southern Oscillation (ENSO) over the tropical Pacific Ocean. All of these features were also detected for the present day(1970/71-2014/15). On the other hand, we could not find significant correlation between Siberian high intensity and interannual variation of snowfall frequency. Surface pressure data in Siberia was not used for data assimilation in 20th century reanalysis data. Lack of significant signal over Siberia is probably caused by few observed pressure data over this area.

Keywords: Hisrorical weather records, Snowfall frequency, Reanalysis data

©2020. Japan Geoscience Union. All Right Reserved.

Attempt to restore the forest cover in China's planned economic period using declassified American and Soviet reconnaissance information: A case of Northern Shaanxi Loess Plateau

*Yuta Hara[1]

1. Komaba Organization for Educational Excellence, College of Arts and Sciences, The University of Tokyo

Land degradation caused by agricultural activities is a major issue which further gives rise to the problems of poverty, inequality and environmental deterioration. This is the case in the Loess Plateau, which is a semi-arid rural region in central China. In the Loess Plateau, many measures have been taken over the past 100 years for the various problems caused by land degradation, and the Conversion of Cropland to Forest Program (CCFP) has been implemented as the culmination of these previous measures since 1999. During the past 20 years, after the CCFP, the terrestrial ecosystem in the Loess Plateau has been being monitored by the scientists of such as ecology, geography and remote sensing. However, the rural natural environment is unclear before the above afforestation program when the planned economic period of P. R. China (1950s-1970s). There are mainly three reasons for this. First is because the quantitative domestic statistic data and research results is limited due to the civil wars and social disturbances. Second is because information is often dramatized in the form of sensational revelation due to the propaganda. Thirds is because there are not the multispectral satellite images until 1972 when Landsat/MSS appeared. Thus, two evaluations for the landscape in the planned economic period coexist in the Loess Plateau. One is that agricultural development was taken precedence and ecosystem were more seriously injured than before. The other one is that greening for wasteland was promoted temporarily to mitigate land degradation from premodern period.
This study focuses on the location and the distribution changes of forest resources in the Loess Plateau during the China's planned economic period, using the declassified reconnaissance photographs and maps made by the US and Soviet Union. The target area is Huanglong and Ziwu mountains, where the valuable forest area in the northern Shaanxi Province. It is thought that the progress of this study will be able to provide important information for the present vegetation monitoring and management, as well as the vegetation reconstruction in premodern period.

Keywords: semi-arid climate, Land degradation , Soviet Military Topographic Maps, CORONA Satellite Photography, Modern history

©2020. Japan Geoscience Union. All Right Reserved.

Philological and scientific assessment of aurora records in historical documents

*Hiroaki Isobe[1], kiyomi iwahashi[2], Harufumi Tamazawa[1]

1. Faculty of Fine Arts, Kyoto City University of Arts, 2. National Institute of Japanese Literature

We discuss the methodology for the assessment of reliability of historical records of extraordinary natural phenomena by combining philological and scientific analyses. Records of natural phenomena in historical literature are important sources for earth and planetary sciences. Assessment of the reliability the information such as the date, place, scale of the phenomenon is the essential process to use such records as scientific data. In this presentation, we will introduce the process of examining the reliability of historical records by philological and scientific methods, taking the records of aurora display in Japanese Edo era as an example. We show that scientific and philological methods work together to improve the accuracy and reliability of the information extracted from the historical records. The results provide valuable insights for both natural sciences and history, enabling reciprocal and therefore sustainable collaborative research.

Keywords: historical documents, aurora

©2020. Japan Geoscience Union. All Right Reserved.

[J] Poster | M (Multidisciplinary and Interdisciplinary)：M-IS Intersection

[M-IS29] Mud volcano x Chemosynthetic communities

convener:Yusuke Miyajima(Geomicrobiology Research Group, Research Institute for Geo-Resources and Environment, Geological Survey of Japan, National Institute of Advanced Industrial Science and Technology), Tomohiro Toki(Faculty of Science, University of the Ryukyus), Robert Jenkins(School of Geosciences and Civil Engineering, College of Science and Engineering, Kanazawa University), Akira Ijiri(Japan Agency for Marine-Earth Science and Technology)

Mud volcanoes transport fluids and sediments from the deep subsurface to the Earth's surface and form topographic features. Mud volcanoes play a role in material cycling connecting the underground and surface, pipe of life in depth, emissions of methane leading to environmental change, and natural disasters. However, the formation mechanism, activity, and spatiotemporal distribution of mud volcanoes are not well-understood. On the summit of submarine mud volcanoes, chemosynthetic communities are sustained by energy produced from methane and hydrogen sulfide contained in the transported fluid. Chemosynthetic communities are distributed in extreme environments such as deep-sea hydrothermal vents, mud volcanoes, and/or cold seeps and have changed their taxonomic composition and spatial distribution through the Earth history. However, the causes and background of their evolution remain unclear.
This session aims to reveal interactions between geosphere and biosphere from the past to the present and in the future through investigations on mud volcanoes as "windows to subsurface environments" and chemosynthetic communities as "ecosystems sustained by geofluid". We welcome not only studies focusing on either fluid-flow systems including mud volcanoes, cold seeps, and hydrothermal vents, or biological communities depending on them, but also cross-cutting contributions combining biological, geochemical, geological, or geophysical methods. Talks and discussions in this session will be held in Japanese, though presentation slides may be prepared in English.

[MIS29-P01] Characteristics and origin of sediments collected from mud volcanos off Tanegashima

Ryoma Setoguchi[1], *Masafumi MURAYAMA[1], Akira Ijiri[2], Juichiro Ashi[3], Takeyasu Yamagata[4], Hiroyuki Matsuzaki[4] (1.Faculty of Agriculture and Marine Science, Kochi University, 2.Kochi Institute for Core Sample Research, JAMSTEC, 3.The Atmosphere and Ocean Research Institute, The University of Tokyo , 4.The University Museum,The University of Tokyo)

[MIS29-P02] An *in situ* rapid burial experiment of "*Calyptogena*" clams for decoding history of submarine mud volcano activities

*Takami Nobuhara[1] (1.Shizuoka Univ. (Fac. Educ.))

[MIS29-P03] Community compositions in Late Cretaceous methane-seeps in the Nakagawa area, Hokkaido

So Watanabe[2], *Robert Jenkins[1] (1.School of Geosciences and Civil Engineering, College of Science and Engineering, Kanazawa University, 2.Graduate School of Natural Science and Technology, Kanazawa University)

[MIS29-P04] Estimated and realized dispersal potentials in deep-sea chemosynthesis-based communities: the case of a Pacific galatheid crab

*Hiromi Kayama WATANABE[1], Satoshi Mitarai[2], Chen Chong[1], Hiroyuki Yamamoto[1] (1.Japan Agency for Marine-Earth Science and Technology (JAMSTEC), 2.Okinawa Institute of Science and Technology (OIST))

Characteristics and origin of sediments collected from mud volcanos off Tanegashima

Ryoma Setoguchi[1], *Masafumi MURAYAMA[1], Akira Ijiri[2], Juichiro Ashi[3], Takeyasu Yamagata[4], Hiroyuki Matsuzaki[4]

1. Faculty of Agriculture and Marine Science, Kochi University, 2. Kochi Institute for Core Sample Research, JAMSTEC, 3. The Atmosphere and Ocean Research Institute, The University of Tokyo , 4. The University Museum,The University of Tokyo

Mud volcanoes are found to be surface elevations where light-weight sediments supplied from underground reach the ground surface and form, or are found on land or on the sea floor. In the process, gases such as hydrocarbons and methane, and substances such as pore water move, and there are few examples of research in spite of being a special phenomenon in geoscience. In this study, we will use sediment cores collected during the KH19-5 cruise on mud volcanoes off Tanegashima along the Nankai Trough, and clarify their characteristics such as age, origin, physical properties, age, and origin. The purpose was to. During the KH-19-5 cruise on the scientific research vessel "Hakuho Maru", the Navigable Sampling System (Using NSS), core samples (approximately 4 m) were collected directly on top of the sediment core mud volcano, where MV # 2 and MV # 3 of the mud volcano group off Tanegashima were numbered. The core sediment core sample is obtained by observing internal structure using X-ray CT scan, measuring gamma ray transmittance and magnetic susceptibility using Multi-Sensor Core Logger, radioisotope using accelerator mass spectrometer We analyzed 10Be dating, 3D of the core using X-ray diffractometer, γ -ray transmittance, susceptibility, sediment age, and clay minerals. Radiometric dating using 10Be in sediments was performed for dating in accelerator mass spectrometry.
The sediment cores of MV # 2 and MV # 3, including the results of X-ray CT scan and MSCL measurement, showed that many gravels were seen from the top to the bottom of the whole core, and the number of gravels increased toward the top It was confirmed that there was no sediment covering. This indicates that pebbles are included in the sediments, which is a characteristic of mud volcanoes, and since no pelagic sediments are seen, both MV # 2 and MV # 3 are currently active mud volcanoes. It was confirmed that it was. In terms of dating by 10Be dating, MV # 2 shows an old age of around 7.0 to 11.1 Ma, and MV # 3 shows an old age of around 10.3 to 11.8 Ma, which clearly indicates that it originated from sediments of that era became. As for XRD clay minerals, both MV # 2 and MV # 3 have more illite and less smectite when compared to the mud volcano off Kumano. Therefore, the peak of the illite smectite mixed layer was not observed, the count of illite was large, and the smectite was low. Therefore, this deposit experienced a temperature of 160 ˚C. or more and was dehydrated. The result is a higher temperature than the mud volcano off Kumano, which shows the peak of the mixed layer of illite and smectite. Based on these results, two MV # 2 and MV # 3 off Tanegashima, MV # 2 and MV # 3, of mud volcanoes, light-weight sediments from deep underground rolled up gravel from new strata of various ages. MV # 2 and MV # 3 were found to have been derived from strata of the same origin.

Keywords: Mud Volcano, X-ray CT scan, 10Be, Off Tanegashima

©2020. Japan Geoscience Union. All Right Reserved.

An *in situ* rapid burial experiment of “*Calyptogena*" clams for decoding history of submarine mud volcano activities

*Takami Nobuhara[1]

1. Shizuoka Univ. (Fac. Educ.)

Vesicomyid bivalves are representative chemosynthetic animals using sulfide as an energy source and forming dominant communities in both seep and vent sites all over the world. They also often colonize in seep sites supported by submarine mud volcanism, but their taphonomy (fossilization processes) has not yet been fully studied enough to apply their modern analogues for decoding mud-volcano activities in fossil seep-sites and boring core records. This deep-sea *in situ* experimental study focuses on escape ability of vesicomyid clams from rapid burial events to provide constraints on thickness of the event sediments.

Artificial rapid burial experiment was conducted in the JAMSTEC cruise KR12-05, using ROV KAIKO 7000II (Dive#544) on 22nd Feb. 2012. A transparent acrylic enclosure (25 cm X 25 cm with 18 cm height) was set on outer margin of “*Calyptogena*” colony in the seep site, 1170 m in bathymetric depth off Hatsushima Island, central Japan. The acrylic enclosure imprisoned 16 individuals of “*Calyptogena*.” *In situ* mud sediments was shoveled up and covered on the imprisoned clams by Kumade-sampler using the ROV manipulator. The burial surface were tilted in the enclosure, and the burial condition ranged from 3 cm-thick powdered mud to 9 cm-thick mixture of powdered mud and viscous mud clasts.

After the rapid burial, several individuals of “*Calyptogena*” promptly jet water from their exhalant siphons and blow away the covering powdered mud. After about 10 minutes, “*Calyptogena*” clams exposed their siphons above the sediment surface in the 3 cm-thick burial area. After about 20 minutes, “*Calyptogena*” clams pushed up covering mud clasts in the 9 cm-thick burial area, and after about 1 hour, total six individuals of “*Calyptogena*” returned their original semi-infaunal position. Their effective and powerful escape activity is accomplished by the combination of siphon blow-away current and foot movement. These suggest that over 10 cm-thick burial is necessary to form a buried-alive fossil “*Calyptogena*” assemblage.

Keywords: mud volcano, chemosynthetic community, vesicomyid bivalve

©2020. Japan Geoscience Union. All Right Reserved.

Community compositions in Late Cretaceous methane-seeps in the Nakagawa area, Hokkaido

So Watanabe[2], *Robert Jenkins[1]

1. School of Geosciences and Civil Engineering, College of Science and Engineering, Kanazawa University, 2. Graduate School of Natural Science and Technology, Kanazawa University

Many Late Cretaceous seep deposits and associated chemosyntheic communities have been distributed in the Nakagawa Town, Hokkaido, Japan. Faunal composition of the communities can be categorized into several types, e.g. ?vestimentiferan-provannid community, and thyasirid-solemyid community. To reveal reason of the faunal differences, we have investigated four seep deposits, Omagari, Gakkonosawa, Yasukawa-E and Tannno-sawa, using comprehensive approaches, such as detailed lithological observations, carbon isotope analyses, and biomarker analyses. The Omagari and Gakkonosawa yield numerous ?vestimentiferans with seep restricted gastropods such as *Provanna* sp. and *Hikidea* sp., Yasukawa-Eyield *Acharax cretacea* and *Thyasira* sp., and Tannno-sawa seep, and Tannno-sawa seep yoled no obvious chemosynthetic taxa but background fauna such as inoceramid bivalves. Lithological observations indicate that the Omagari and Gakkonosawa seep carbonate were partially formed above the seafloor whereas the Yasukawa-E and Tannno-sawa seep carbonates were formed within sediments entirely. The carbon isotopic compositions of earlier precipitated carbonate minerals in each site ranges from -40 to -50 per mil (VPDB). The biomarker analysis detected following characteristic molecules; PMI, biomarker of anaerobic methane-oxidizing archaea and 8,14-secohexahydrobenzohopanes, biomarkers of aerobic methane-oxidizing bacteria, from all investigated sites. In addition, amounts of 8,14-secohexahydrobenzohopanes are higher in the Omagari and Gakkonosawa sites compared to Yasukawa-E and Tannno-sawa sites. These lines of evidence strongly suggested that the Omagari and Gakkonosawa sites had strong methane fluids (high methane concentrations) compared to Yasukawa-E and Tanno-sawa sites. This flux (or methane concentrations) differences caused the faunal differences as like in modern seeps.

Keywords: Methane seep

©2020. Japan Geoscience Union. All Right Reserved.

Estimated and realized dispersal potentials in deep-sea chemosynthesis-based communities: the case of a Pacific galatheid crab

*Hiromi Kayama WATANABE[1], Satoshi Mitarai[2], Chen Chong[1], Hiroyuki Yamamoto[1]

1. Japan Agency for Marine-Earth Science and Technology (JAMSTEC), 2. Okinawa Institute of Science and Technology (OIST)

Recognizing the distribution of animals provides a clue to reveal dynamics of marine ecosystems. In marine benthic animals the adult distribution is often the only distribution considered, despite their planktonic larval stages being key for their dispersal and therefore realized ranges. Population genetics, phylogeographic analyses, and physic-oceanographic modelling are powerful tools that help biologists estimate and understand the expected and realized larval dispersal potentials and connectivity among sites. The *Shinkaia crosnieri* galatheid crab is a widely distributed and iconic species in deep-sea chemosynthesis-based communities in the Indo-West Pacific, including hot vents and cold seeps. They harbor chemoautotrophic bacteria on their ventral surface which they feed on, and consequently they are specific to chemosynthesis-based ecosystems. Recent surveys on faunal distribution in such habitats has revealed some new distributions for the galatheid crab, revealing that its distributional pattern differs from other dominant species such as “*Bathymodiolus*” mussels. Here, we apply dispersal model estimation and phylogeographic analyses to the galatheid crab in order to compare its estimated and known realized larval dispersal ranges, and to discuss dynamics of plankton larvae from deep-sea vents and seeps. The results were mostly in agreement, but with some differences. Distribution patterns and the mechanisms underlying them are extremely important in making informed decisions on effectively managing upcoming deep-sea mining events and planning marine protected areas, and should be elucidated for the representative dominant species, at the very least.

Keywords: Chemosynthesis-based fauna, planktonic larvae, phylogeography

©2020. Japan Geoscience Union. All Right Reserved.

[J] Poster | M (Multidisciplinary and Interdisciplinary)：M-IS Intersection

[M-IS30] Ocean Plastics, an earth science perspective

convener:Atsuhiko Isobe(Research Institute for Applied Mechanics, Kyushu University), Kiichiro Kawamura(Yamaguchi University), Yusuke Okazaki(Department of Earth and Planetary Sciences, Graduate School of Science, Kyushu University), Masashi Tsuchiya(Research Institute for Global Change, Japan Agency for Marine-Earth Science and Technology)

Mismanaged plastic wastes accounting for 70% of marine debris remain persistently in the marine environment, even if they are degraded and fragmentized to tiny microplastics. To date, it has been unknown how this anthropogenic, buoyant, and persistent matter which was first appeared in the earth history, contaminates (or is incorporated into) the earth system. The ocean plastic study requires the insight and methodology of a variety of earth sciences such as the oceanography, geology, and palaeontology. Studies on the plastic circulation loaded from the land/atmosphere to upper oceans and bottom sediments, studies on microplastics as a proxy of the 'Anthropocene', and studies to establish procedures in monitoring and analyzing macro/microplastics are welcomed.

[MIS30-P01] A numerical approach to determining the behavior of microplastics and mesoplastics from the Changjiang River in the East Asian marginal seas

*Iwasaki Shinsuke[1] (1.Civil Engineering Research Institute for Cold Region of Public Works Research Institute)

[MIS30-P02] The horizontal distribution of pelagic microplastics around Japan

*Daisuke Ito[1], Atsuhiko Isobe[2] (1.Kyushu University, 2.Research Institute for Applied Mechanics, Kyushu University)

[MIS30-P03] Foraminiferal thamatocoenosis as a tracer of the sorting process in the coastal surf zone

*Hiroki Hayashi[1], Masashi Tsuchiya[2] (1.Interdisciplinary Faculty of Science and Engineering, Shimane University, 2.Japan Agency For Marine-Earth Science and Technology)

[MIS30-P04] Microplastics in the river bottom sediment in the urban river of Mongolia

*Masayuki Kawahigashi[1], Batdulam Battulga[1] (1.Tokyo Metropolitan University)

[MIS30-P05] Detection of microplastics less than 330 μm using μFTIR

*HARUKA NAKANO[1], Ridvan Kaan Gürses[1], Yuji Tanaka[1], Hisayuki Arakawa[1], Mao Kuroda[1], Keiichi Uchida[1], Tetsutaro Aikawa[1], Toshifumi Hayashi[1], Tadashi Tokai[1] (1.Tokyo University of Marine Science and Technology)

[MIS30-P06] Fundanmental parameters for detection of Microplastics based on hyperspectral imaging

*Chunmao Zhu[1], Yugo Kanaya[1], Ryota Nakajima[1], Masashi Tsuchiya[1], Hidetaka Nomaki[1], Tomo Kitahashi[1], Katsunori Fujikura[1] (1.Japan Agency for Marine-Earth Science and Technology)

[MIS30-P07] Time-course analysis of gene expression of a benthic protist during exposure to titanium dioxide nanoscale particles.

*Yoshiyuki Ishitani[1], Yurika Ujiie[2], Caterina Ciacci[3], Frontalini Fabrizio[3], Yuji Inagaki[1] (1.University of Tsukuba, 2.Center for Advanced Marine Core Research, Kochi University, 3.Urbino University)

[MIS30-P08] Spatial distribution of microplastics in Shimane Peninsula, Japan

*Akira Tsujimoto[1], Kana Yamaguchi[1] (1.Faculty of Education, Shimane University)

A numerical approach to determining the behavior of microplastics and mesoplastics from the Changjiang River in the East Asian marginal seas

*Iwasaki Shinsuke[1]

1. Civil Engineering Research Institute for Cold Region of Public Works Research Institute

In the environment, plastic debris gradually degrades into small plastic fragments that can be categorized by size as macroplastics (> a few centimeters in size), mesoplastics (>5 mm), microplastics (<5 mm), and nanoplastics (less than a few micrometers). The present study uses “small plastic fragments” to refer to all fragments smaller than mesoplastics. A number of studies have shown that small plastic fragments have spread to the world’s oceans. A recent study demonstrated that the output of small plastic fragments from the Changjiang River (or the Yangtze River), which flows into the East China Sea, is greater than that of such fragments from any other river in the world. The present study aims to clarify the transport processes of small plastic fragments from the Changjiang River to the East Asian marginal seas (the Yellow Sea, the East China Sea, the southwestern part of the Sea of Japan, and the northern part of the South China Sea) using a numerical model. Pelagic small plastic fragments consist mostly of polyethylene or polypropylene, which are less dense than seawater; thus, they move in the uppermost layer (depth < 5m) of the water column. Hence, previous studies suggested that small plastic fragments are carried partly by mass transport (Stokes drift) generated in the uppermost layer in response to wind waves, as well as by ocean currents that extend to deeper layers. The present study established a three-dimensional particle tracking model in which the modeled particles were carried by a combination of ocean currents, provided by ocean reanalysis data, and the Stokes drift, computed separately in a wave model driven by satellite-derived winds. Most of the microplastic fragments from the river were found to be carried by the northeastward Tsushima and Kuroshio currents to the Sea of Japan and the North Pacific. In contrast, some of the mesoplastic fragments were carried to the northern part of the South China Sea by the southwestward Stokes drift that prevails in winter. In addition, the northward Stokes drift that results from the Yellow Sea high in May carries mesoplastic fragments into the Yellow Sea, even though the Stokes drift is smaller in May than in winter. Thus, the Stokes drift plays a role in selectively decreasing the large mesosized plastics into the Sea of Japan by greatly reducing the number of mesoplastic fragments passing through the Tsushima Strait.

©2020. Japan Geoscience Union. All Right Reserved.

The horizontal distribution of pelagic microplastics around Japan

*Daisuke Ito[1], Atsuhiko Isobe[2]

1. Kyushu University, 2. Research Institute for Applied Mechanics, Kyushu University

Currently, microplastics (less than 5 mm plastic-debris pieces) are observed in the world’ s ocean, and are found to be ingested by various marine organisms. According to a previous study (Isobe et al., 2019) , pelagic microplastics were found from the Antarctic Ocean to the seas around Japan. It was revealed that the number of microplastics in the North Pacific become one order of magnitude larger than the South Pacific.
We here attempt to elucidate the horizontal distribution of pelagic microplastics and its causes around Japan. First, using the field surveys conducted since 2014, we confirmed that high concentrate areas were located off the Sanriku coast , off Akita coast , south of Sikoku and around Kyushu using observation data. These intense convergence of pelagic microplastics were inconsistent with the convergence of surface ocean currents. We now try to establish a back-trajectory experiment of microplastics using a modeled field with the ocean currents directed to the opposite directions, and will introduce its accomplishments in the session.

Keywords: microplastic, around Japan

©2020. Japan Geoscience Union. All Right Reserved.

Foraminiferal thamatocoenosis as a tracer of the sorting process in the coastal surf zone

*Hiroki Hayashi[1], Masashi Tsuchiya[2]

1. Interdisciplinary Faculty of Science and Engineering, Shimane University, 2. Japan Agency For Marine-Earth Science and Technology

Microplastic wastes (<5 mm in size) in marine environments might seriously affect on marine ecosystem. Recently, a noteworthy case has been reported that microplastic fragments were included in an agglutinated shell of foraminifera, a unicellular microorganism of Protista (Tsuchiya et al., 2019; Tsuchiya and Nomaki, 2019). This case arrises a serious fear of ecologic pollution because such microorganism shows generally high productivity and plays an important primary consumer of the ecologic system.
It has been suggested that secondary microplastic grains might be generated from macro-size plastic wastes by fragmentation process affected by both ultraviolet light and wave energies. However, the physical processes of fracturing, sorting and accumulating microplastics such as included in foraminiferal shells has been still unknown. The purpose of the present talk is to propose a model that braking wave at the surf zone of the pocket beach plays an important role for generating and sorting the microfragments of plastic wastes.
We have studied the bottom sediments of the well-known singing sand beach Kotogahama since 2013. According to the results, the distribution of singing sand corresponds to the surf zone (0--8 m in depth) owing to the repeated sorting process driven by braking wave. Focussing on the foraminiferal shells in the sand grain, the assemblage is dominated by rock-reef species transported from neighboring rocky areas. The foraminiferal content shows significant deviation pattern from coast to offshore areas. It clearly indicates that foraminiferal shell might be a good tracer for coastal sorting process of bottom sediments. In previous studies, fluorescent particles have been frequently used for such tracer of beach process. However, using fluorescent particles should not be desirable for future studies because the material might induce further microplastic contamination to the coastal region. We would like to clarify the detailed coastal process generating microplastic particles using foraminiferal shells as a tracer of coastal sorting process.

Keywords: microplastic wastes, foraminifera, surf zone

©2020. Japan Geoscience Union. All Right Reserved.

Microplastics in the river bottom sediment in the urban river of Mongolia

*Masayuki Kawahigashi[1], Batdulam Battulga[1]

1. Tokyo Metropolitan University

The urban river takes many anthropogenic influences including plastic solid waste disposal, resulting in microplastic pollution in marine environment through their fragmentation processes. During their transportation, reaction of plastic debris with suspended solids in the river affect properties of plastic debris in their sizes, surfaces and specific density. Even in light plastics can be settled in the river bottom sediments. This study evaluates the dynamics of plastic debris from the composition of plastics in the river bottom sediments.

The study area was set along the Tuul River in Ulaanbaatar, which is the capital city of Mongolia. The sampling points were distributed from the upstream with low population density to just the downstream of the waste water treatment plant (WWTP) through the drain canal of city center. Sediments were directly collected from the depth of 5cm using a stainless steel shovel. After air-drying, samples were separated into three size fractions for further analyses. Each sediment fraction was digested with the mixture of peroxide and iron catalyst. Using sodium polytungstate solution as a density fractionation media, microplastics were separated from sediments. The number of plastics in a unit weight of sediment was counted using a digital micro scope and morphotypes of microplastics were also counted under the digital microscopic views. The chemical structure of plastics were also evaluated using micro-FTIR to evaluate the composition of the sedimentary microplastics.

The major morphotype of plastic was fibrous plastics of synthetic fibers. Other morphotypes of films, fragments and foams were also detected. However, the size range of fiber microplastics was specifically different from other three types. That has a broad range of size in the sediment. The form type plastics, which was the dominant plastic debris in this river, were less amount probably due to their specific density with its porous structure. Distribution of microplastics in the sediment size fractions was different depending on the location. The downstream of WWTP was occupied by microplastics in the coarse sediments different from other points where fine sediments collected much amount of microplastics. The water management in the urban area influences the distribution of plastic debris in the river bottom sediments. Poly-styrene and poly-ethylene with lower specific density than water were commonly found in the bottom sediments, indicating that changes in their surface with suspended solids increase their density to settle to the sediments.

Keywords: river bottom sediment, urban river, plastic debris, sedimentation

©2020. Japan Geoscience Union. All Right Reserved.

Detection of microplastics less than 330 μm using μFTIR

*HARUKA NAKANO[1], Ridvan Kaan Gürses[1], Yuji Tanaka[1], Hisayuki Arakawa[1], Mao Kuroda[1], Keiichi Uchida[1], Tetsutaro Aikawa[1], Toshifumi Hayashi[1], Tadashi Tokai[1]

1. Tokyo University of Marine Science and Technology

A total of 150 million tons of plastic waste has accumulated in the oceans. Presently, eight million tons per year of plastic waste flow into the oceans as marine debris. However, the amount of identified plastic waste is below 1 % of the total plastic waste (e.g., 0.44 million tons) and the remaining 99% is undetected. Unidentified plastics referred to as missing plastics are not observed as they sink to the ocean bottom and/or break down into small pieces called microplastics (MPs) (e.g., MPs with maximum lengths less than 5 mm). MPs larger than 330 μm have been detected. However, no widespread observation methods or measurement protocols exist for MPs smaller than 330 μm that are considered to be more influential particles for ecosystems. Therefore, in this report, we introduce new protocols for detecting MPs having less than 330 μm.

The water samples were collected by T/V Shinyo-Maru of Tokyo University Marine Science and Technology in July 2019. We use two systems for sampling; 1) Multiple Opening/Closing Net and Environmental Sensing System (MOCNESS); and 2) large capacity pump. In the case of MOCNESS, we used a 64 μm mesh net, although a 330 μm mesh net is typically used. MOCNESS was opened and closed in each layer up to 1000 m depth, and filtered particles from seawater of several hundred m^3 from a volume of several tens. For the pump system, we collected 20 L of each layer (maximum is 50 m) in to a 7 μm mesh plankton net.

The collected net samples were extracted so that the volume after reduction was 0.1 m^3 because a few hundred m^3 of sea water was concentrated in the sample. For the pump samples, the number of smaller particles should be greater than the number of net samples, and we used a volume after the reduction of 0.01 m^3. After extracting the seawater, we added a 30 % H_2O_2 and 0.05M Fe (2) solution and the samples were then heated to 60 ˚C to eliminate the contaminants. After two weeks, density separation was conducted by adding NaI to the sample to adjust the specific gravity to 1.5. The candidate particles in the supernatant were collected by a PTFE filter using vacuum filtration. The filters were dried overnight. The infrared spectra of the candidates measured using micro Fourier transform infrared spectroscopy (IR/T-7200 of JASCO Inc., Japan). The measured spectra were compared with stored plastic spectra. A color image map of the correlation coefficients was converted into a bicolor figure to determine the particle sizes using the imaging software.

We focused on the polyethylene and polypropylene particles that were smaller than 330 μm. A sample collected by the pump system showed concentrations of a few million particles/m^3 at the surface and showed concentrations of a few thousand particles/m^3 at 50 m depth. These concentrations are several thousand times greater than those obtained in the surface layer using the Neuston net (330 μm); Previous observation and measurement protocols would underestimate the amount of MPs.

Keywords: microplastics, μFTIR

©2020. Japan Geoscience Union. All Right Reserved.

Fundanmental parameters for detection of Microplastics based on hyperspectral imaging

*Chunmao Zhu[1], Yugo Kanaya[1], Ryota Nakajima[1], Masashi Tsuchiya[1], Hidetaka Nomaki[1], Tomo Kitahashi[1], Katsunori Fujikura[1]

1. Japan Agency for Marine-Earth Science and Technology

Plastic has become one of the most common materials in daily applications of human life in the past decades. Ingestion of plastic particles and pieces were found in the marine ecosystem from micro-to-small lives such as plankton, corals, mussels to large animals such as turtles and cetaceans. It is preliminarily considered that many plastics will behave over geological timescales. Consequently, the accumulation of plastics in the ocean would become an inevitable issue. Microplastics are plastic particles < 5 mm in diameter. With their large surface area to volume ratio, adsorption of waterborne pollutants, such as aqueous metals, endocrine disrupting chemicals and persistent organic pollutants on microplastics added another threat to the food chain. Despite recent concerns by various levels of policy-makers, scientific communities and the public, one of the fundamental recognition, the current situation of microplastic pollution in the marine ecosystem, is still less understood. Aiming to characterize marine microplastics based on hyper-spectral imaging techniques, we examined the fundamental spectral features of microplastics over as much as wide range of 11 polymertypes in the wavelength range of 900 to 1700 nm. Toward the application of hyper-spectral imaging techniques to automatic detection of microplastics in seawater filtrations, we examined various membrane filters to propose appropriate candidates for filtration stage background. We also report the innovatively optimized hyper-spectral imaging system in which small microplastics down to the size range of 100 μm was able to detect by improving lighting and focal lengths.

Keywords: Microplastic, Hyperspectral imaging, Substrate filter

©2020. Japan Geoscience Union. All Right Reserved.

Time-course analysis of gene expression of a benthic protist during exposure to titanium dioxide nanoscale particles.

*Yoshiyuki Ishitani[1], Yurika Ujiie[2], Caterina Ciacci[3], Frontalini Fabrizio[3], Yuji Inagaki[1]

1. University of Tsukuba, 2. Center for Advanced Marine Core Research, Kochi University, 3. Urbino University

The engineered nanomaterials have caused serious environmental pollution in the ocean. Marine environmental pollution represents nowadays an international issue, because they potentially destruct the marine ecosystem. Especially along the coast, the inflow and sedimentation from rivers and the convection by tides concentrate such pollutants, leading lethal exposure to the benthic organisms. The accumulation of artificial materials has been reported from many marine vertebrates (fish, turtles, whales, etc.), however few from benthic organisms. Moreover, we have still not known the effect of those materials to life *in vitro*. Benthic foraminifers, a group of benthic protists play important roles for supporting food web and carbon cycles. They have three unique features: (1) wide distribution in marine and transitional marine environments including polluted area, (2) large-sized cell (> 200 μm), and (3) uptake of external materials into the cell through the pseudopodia. These characters provide us an excellent condition for exposure experiments to test physiological reactions (i.e., stress) of foraminifera to the engineered nanoparticles additive sea-water (Ciacci et al., 2019). This study presents “*in vitro*” exposure experiments in time-series with foraminiferal culture in titanium dioxide nanoscale particle (TNP) additive sea-water to understand molecular metabolisms against the pollutant. At each of 1, 6, and 24 hours, we observed the time change in biological response with confocal laser scanning microscopy and inspected the expressed gene differences, among the foraminiferal cells. Cell observation indicates high productions of lipids and reactive oxygen species (ROS) in the foraminiferal cell. Our time-course analysis of gene expression also suggests high activity of the biosynthesis of unsaturated fatty acid and ROS quenching. Both experiments show these processes as the key to survive in the polluted area.
Ciacci, C., et al., 2019. Scientific Reports 19(9),19441.

Keywords: Foraminifera, titanium dioxide nanoscale particle, gene expression

©2020. Japan Geoscience Union. All Right Reserved.

Spatial distribution of microplastics in Shimane Peninsula, Japan

*Akira Tsujimoto[1], Kana Yamaguchi[1]

1. Faculty of Education, Shimane University

Marine plastics and microplastics are becoming a global problem. Shimane peninsula is located along the Sea of Japan coast in the Chugoku Region, and has a problem of drifted wastes. We examined spatial distribution of microplastics in Shimane Peninsula. Surface sand samples were collected from four sandy beach in eastern part of Shimane Peninsula. We analyzed size fraction between 1 mm and 4.75 mm, and identified microplastics using Raman spectroscopy.
Foamed plastics were the most abundant in each beach. On the Mitsu coast, the number of foamed plastics and resin pellets decreases with increasing distance from the shoreline. This may be because the waves transport the foamed plastics near the shoreline. Foamed plastics accounted for 80.2% of all microplastics.
From the results of Raman Spectroscopy and morphological characteristics, polypropylene was 78.3% and polyethylene was 21.7% as the material for the drifted resin pellets on the Mitsu coast. Since resin pellets are an intermediate material for making plastics, they are considered to be related to the production volume of plastic products. However, the composition of resin pellets around the coast of Tokyo Bay is about 60% polyethylene and 40% polypropylene (Kuriyama et al., 2002), so it is considered that there is a regional difference in the origin.

Keywords: Shimane Peninsula, microplastics

©2020. Japan Geoscience Union. All Right Reserved.

[J] Poster | M (Multidisciplinary and Interdisciplinary)：M-IS Intersection

[M-IS31] Planetary Volcanology

convener:Rina Noguchi(Institute of Space and Astronautical Science, Japan Aerospace Exploration Agency), Tomokatsu Morota(Department of Earth and Planetary Science, The University of Tokyo), Nobuo Geshi(Geological Survey of Japan, The National Institute of Advanced Industrial Science and Technology)

Volcanoes exist on solid planetary surfaces across the solar system. They tell insight into the interior, and the surface environment when they were formed and subsequent evolution. Recent high-resolution remote sensing data on the extraterrestrial body allows us to analyze on outcrop scales. Now we are on the stage to share the research targets beyond fields of general volcanology and planetary science. Because some geomorphological and geological environments in other planets are similar to those on Earth, research on volcanic geomorphology and geology on Earth will provide good terrestrial analogs to understand planetary volcanology. The aim of this session is to discuss the formation history and mechanism of volcanoes across the solar system.

[MIS31-P01] Study of the lava flow under the Marius Hills Hole on the Moon by analogy on the Earth

*Tsutomu Honda[1] (1.Vulcano-speleological Society)

[MIS31-P02] Machine learning for grain images of volcanic ash based on grain shape and transparency

*Rina Noguchi[1], Takuya Itaki[2], Daigo Shoji[3], Shizuka Otsuki[4] (1.Institute of Space and Astronautical Science, Japan Aerospace Exploration Agency, 2.Geological Survey of Japan, AIST, 3.Earth-Life Science Institute, Tokyo Institute of Technology, 4.Nippon Steel Technology Co., Ltd.)

[MIS31-P03] Relation between volcanism on Jupiter moon Io and the atmosphere and plasma torus observed by ALMA and Hisaki

*Ryoichi Koga[1], Yasuhiro Hirahara[2], Tatsuya Suzuki[2], Fuminori Tsuchiya[1], Masato Kagitani[1], Takeshi Sakanoi[1], Tomoki Kimura[1], Ichiro Yoshikawa[3], Kazuo Yoshioka[3], Go Murakami[4], Atsushi Yamazaki[4] (1.Tohoku University, 2.Nagoya University, 3.The University of Tokyo, 4.ISAS/JAXA)

Study of the lava flow under the Marius Hills Hole on the Moon by analogy on the Earth

*Tsutomu Honda[1]

1. Vulcano-speleological Society

1.Introduction: The purpose of this study is to estimate the scenario and temperature at the lava tube formation assumed in the lava flow in the lava river (Rilles-A) in the Marius Hills on the Moon by comparing the lava flows related to lava tube formation on the Earth. In Newtonian fluids, the flow changes from laminar to turbulent flow when the Reynolds number(Re) exceeds about 2000, whether it is a flow in a circular pipe or an inclined surface gravity flow [1)]. Though,lava flow is considered to be a Bingham fluid. Bingham number(B) and Hedstrom number(He) indicate the degree of Bingham properties, and it is known that the transition Reynolds number from laminar to turbulent flow increases as He increases [1,2)]. Here, by focusing on Re, B, and He of lava flow, the scenario of lava tube[3)] formation assumed in the Rilles-A were estimated.

2.Examination of the earth's lava flow: Tables 1 (a), (b) and (c) show the in-situ measured values such as temperature, lava thickness, viscosity coefficient, yield strength, etc. are shown for Miharayama 1951 lava flow (SiO_2: 52-53 wt%) [4)], Mauna Loa 1984 lava flow (SiO_2: 52 wt%) [5)], Tolbatik 2013 lava flow (SiO_2: 52wt%) [6)] Each flow shows a low Reynolds number. In the Mauna Loa example, temperature and fluid properties including yield strength and estimated B, He are shown over long distances. As the temperature decreases along the flow, the fluid property value increases significantly. These flows are all in the laminar region from the outlet to the downstream by creating the lava tubes. The lava tube on the earth is formed in a laminar region.

3. Examination of lava flow in the lava river Rilles-A of Marius Hills on the Moon: To know B, He, and Re of the Rilles-A lava flow of Marius Hill, the lava flow thickness, viscosity coefficient, yield strength, gravity acceleration, lava density, lava flow velocity, and slope angle are required. The lava flow thickness is assumed as 17m which is tube height below Marius Hills Hole in the Rilles-A. The yield strength 131Pa[7)] was used as fixed value. Viscosity coefficient was assumed in the range from 5 Pa.s to 16000 Pa.s. The flow velocity was calculated by the formula [8)] of free surface gravity flow and parallel plate gravity flow with an inclination angle of 0.31 ˚as laminar flow. Tables 1 (d) and 1 (e) show B, Re, and He based on the obtained flow velocity. The free surface gravity flow is in the transition region with a viscosity coefficient of 100 Pa.s, and shows laminar flow at 3000 Pa.s, The parallel plate gravity flow shows laminar flow at 100 Pa.s. The temperature dependent viscosity coefficient of lunar lava is summarized in Chevrel et al (2014) [9)] for lava of various chemical compositions. Although the chemical composition of Marius Hill is unknown, 100Pa.s to 3000Pa.s for high-titanium lava (sample 15555) shown in Fig. 3 of Cukierman et al (1973) [10)] corresponds to lava temperature 1050-1000℃ as shown in Table 1 (d) (e). For a lava with a low titanium content (sample 68502), 100Pa.s to 3000Pa.s may correspond to a higher lava temperature of 1200-1100˚C. Since the lava tube is thought not to be formed by the turbulent mixing effect avoiding the tube ceiling formation, a scenario where the laminar lava flow forms a lava tube seems to be reasonable

4. Summary:A possible scenario of lava tube formation in the Rilles-A is assumed as follows;(1) the lava is in a turbulent state in the vicinity of the eruption point when the lava is hot (low viscosity coefficient, low yield strength), (2) the temperature decreases along the flow direction (viscosity coefficient and yield value increase), and the transition from turbulent to laminar flow occurs together with formation of lava tube. The estimated lava tube formation temperature may be around 1000-1200℃ depending on the lava chemical composition. Future study needs accumulation and examination of data base with synthetic sample experiment for viscosity coefficient,yield strength based on the chemical composition of lunar lava

©2020. Japan Geoscience Union. All Right Reserved.

as a function of temperature(Ishibashi[11])measured both for Fuji1707 lava).

References:see abstract of Japanese version

Keywords: lava tube, viscosity, yield strength, lava flow, lunar pit

表１．地球上の玄武岩溶岩流と月・マリウス丘のリルAの溶岩流の傾斜表面重力流の比較検討

(a)三原山1951年溶岩流測定の位置[4]	溶岩温度[4]	流速[4]	溶岩深さ[4]	降伏値	粘性係数[4]	密度	傾斜角度[4]	ビンガム数:B	レイノルズ数:Re	ヘドストロム数:He
I	1125℃	1.02±0.08 m/sec	0.31 m	-	560 Pa.s	(2500 Kg/m³)	35°	-	1.41	-
II	1108℃	0.35±0.04 m/sec	0.5 m	-	1800 Pa.s	(2500 Kg/m³)	27°	-	0.24	-
III	1083℃	0.15±0.03 m/sec	0.77 m	-	7100 Pa.s	(2500 Kg/m³)	16°	-	0.04	-
VI	1038℃	0.08±0.02 m/sec	1.3 m	-	23000 Pa.s	(2500 Kg/m³)	11°	-	0.01	-

(b)マウナウル1987年溶岩流測定の位置[5]	参考溶岩温度[5]	流速[5]	溶岩深さ[5]	降伏値[5]	粘性係数[5]	密度[5]	傾斜角度[5]	ビンガム数:B	レイノルズ数:Re	ヘドストロム数:He
火口から3km	1140±3℃(火口)	5.3 m/sec	4 m	150 Pa	1134 Pa.s	1000 Kg/m³	5.6°	0.099	18.7	1.86
火口から8km上段	1135±5℃(火口から10km)	1.6 m/sec	5 m	970 Pa	3014 Pa.s	1700 Kg/m³	3.75°	1.005	4.5	4.54
火口から8km下段	1135±5℃(火口から10km)	1 m/sec	6 m	891 Pa	2885 Pa.s	1700 Kg/m³	2°	1.853	3.5	6.55
火口から15km	1086-1126℃(火口から12km以上)	0.34 m/sec	9.3 m	3200 Pa	81110 Pa.s	2400 Kg/m³	3.3°	1.079	0.09	0.10

(c)トルバチク2013年溶岩流測定の位置[6]	溶岩温度[6]	流速[6]	溶岩深さ[6]	降伏値	粘性係数[6]	密度[6]	傾斜角度[6]	ビンガム数:B	レイノルズ数:Re	ヘドストロム数:He
火口から2.4km	1069℃～1082℃	0.008 m/sec	3.5 m	-	1800000 Pa.s	2500 Kg/m³	8°	-	3.89×10^{-4}	-

(d)月マリウス丘溶岩流(表面流れ)の位置	推定溶岩温度(試料15555から推定)	推定流速(層流として計算)	溶岩深さ[7]	設定降伏値[7]	推定粘性係数	密度	傾斜角度[7]	ビンガム数:B	レイノルズ数:Re	ヘドストロム数:He
縦孔下	不明(900℃)	0.08 m/sec	17m	131 Pa	16000 Pa.s	2500 Kg/m³	0.31°	1.68	0.22	0.37
縦孔下	不明(1000℃)	0.44 m/sec	17m	131 Pa	3000 Pa.s	2500 Kg/m³	0.31°	1.68	6.26	10.5
縦孔下	不明(1050℃)	13.3 m/sec	17m	131 Pa	100 Pa.s	2500 Kg/m³	0.31°	1.68	5634	9464
縦孔下	不明(1100℃)	44.2 m/sec	17m	131 Pa	30 Pa.s	2500 Kg/m³	0.31°	1.68	6.3×10^{4}	1.05×10^{5}
縦孔下	不明(1200℃)	265 m/sec	17m	131 Pa	5 Pa.s	2500 Kg/m³	0.31°	1.68	2.3×10^{6}	3.79×10^{6}

(e)月マリウス丘溶岩流(並行平板間)の位置	推定溶岩温度(試料15555から推定)	推定流速(層流として計算)	溶岩深さ[7]	設定降伏値[7]	推定粘性係数	密度	傾斜角度[7]	ビンガム数:B	レイノルズ数:Re	ヘドストロム数:He
縦孔下	不明(900℃)	0.02 m/sec	17m	131 Pa	16000 Pa.s	2500 Kg/m³	0.31°	6.72	0.06	0.37
縦孔下	不明(1000℃)	0.11 m/sec	17m	131 Pa	3000 Pa.s	2500 Kg/m³	0.31°	6.72	1.56	10.5
縦孔下	不明(1050℃)	3.31 m/sec	17m	131 Pa	100 Pa.s	2500 Kg/m³	0.31°	6.72	1408	9464
縦孔下	不明(1100℃)	11.1 m/sec	17m	131 Pa	30 Pa.s	2500 Kg/m³	0.31°	6.72	1.56×10^{4}	1.05×10^{5}
縦孔下	不明(1200℃)	66.3 m/sec	17m	131 Pa	5 Pa.s	2500 Kg/m³	0.31°	6.72	5.6×10^{5}	3.79×10^{6}

©2020. Japan Geoscience Union. All Right Reserved.

Machine learning for grain images of volcanic ash based on grain shape and transparency

*Rina Noguchi[1], Takuya Itaki[2], Daigo Shoji[3], Shizuka Otsuki[4]

1. Institute of Space and Astronautical Science, Japan Aerospace Exploration Agency, 2. Geological Survey of Japan, AIST, 3. Earth-Life Science Institute, Tokyo Institute of Technology, 4. Nippon Steel Technology Co., Ltd.

Volcanic ash consists of a variety of components such as juvenile and/or old magma fragments, minerals, and fragments of surroundings. The component of volcanic ash varies with magma composition, eruption style, fragmentation/transportation mechanism, and surrounding geological units. In other word, the component of volcanic ash would be a key to infer characteristics of volcanic activity, though its classification has no universally standardized criteria and is time consuming and complex even for professional people.
One of the most parametrizable information of volcanic ash grains is shape. Previous studies have tried to characterize and classify ash grains by statistical analysis using shape parameters such as circularity, aspect ratio, and shape factor (e.g., Maria and Carey, 2007; Liu et al., 2015). Miwa et al., 2015 used not only shape but also luminance consists of red, green, and blue tones to characterize properties of volcanic ash.
Image classification using machine learning techniques can be applied to volcanic ash. Calculating mixing ratio of four learned grain types using a convolutional neural network (CNN), Shoji et al., 2018 tried to classify and characterize volcanic ash samples which were generated in different eruption styles: magmatic, phreatomagmatic, and rootless (explosive and continuous lava-water interaction) eruptions.
In this study, we try to distinguish eruption style from the component of volcanic ash, which its grain images were automatically collected using an automatic grain analyzer and were classified by a commercial machine learning software. We used same volcanic ash samples with Shoji et al., 2018 which were produced by three types of eruption style, magmatic (scoria cones in Izu Peninsula and 1983 products in Miyakejima, Japan), phreatomagmatic (Nippana tuff ring, Miyakejima, Japan), and rootless (rootless cones in Myvatn, Iceland) eruptions. Images of volcanic ash grains of these samples were obtained by Morphologi G3S (Malvern Instruments) at the Geological Survey of Japan, AIST. In the machine learning performed by Shoji et al., 2018, the training data was prepared so that classify grain images by shape: blocky, vesicular, elongated, and rounded. To identify glass fragments and transparent crystals, we prepared eight types of training images based on not only shape but also whether transparent or not. The training data consists of typical basal grains, does not include ambiguous grains. To increase number of images, we rotated, flipped, and shifted images. We used Rapid Machine Learning Image Analysis software (NEC Advanced Analytics) while Shoji et al., 2018 used the Keras package to structure CNN. This software has been applied to identification of micro fossils (Hoshino et al., 2018). The training was performed under CNN structure with 30 epochs. Using the trained network, we automatically classified volcanic ash grains which also include ambiguous ash grains. This software calculates the probabilities for each of the eight grain type for every grain. Integrating this probabilities within each sample, we can obtain the component of volcanic ash automatically. In this presentation, we will show preliminary results of training and classification and discuss its relation with eruption styles. Such grain analysis method can be applied to various types of grains such as fluvial sediments and returned samples from extraterrestrial regions (e.g., Itokawa and Ryugu).

Keywords: Volcanic ash, grain image, machine learning

©2020. Japan Geoscience Union. All Right Reserved.

©2020. Japan Geoscience Union. All Right Reserved.

Relation between volcanism on Jupiter moon Io and the atmosphere and plasma torus observed by ALMA and Hisaki

*Ryoichi Koga[1], Yasuhiro Hirahara[2], Tatsuya Suzuki[2], Fuminori Tsuchiya[1], Masato Kagitani[1], Takeshi Sakanoi[1], Tomoki Kimura[1], Ichiro Yoshikawa[3], Kazuo Yoshioka[3], Go Murakami[4], Atsushi Yamazaki[4]

1. Tohoku University, 2. Nagoya University, 3. The University of Tokyo, 4. ISAS/JAXA

In this study, we try to find effects of volcanism to generate the Io’ s atmosphere. Io’ s atmosphere is thin (several nbar) and is dominated by SO_2 (~90%). Oxygen and sulfur atoms in the upper atmosphere are escaped and ionized, and then generate Io plasma torus around Io’ s orbit. Io’ s volcanism can be classified in two types. One is effusive eruption. Lava directly flows out of a volcano and onto the ground. The other is explosive eruption. Gases in the magma under volcanoes suddenly froth, and are ejected SO_2 -rich gas through the volcanic vent (called plume). In powerful volcanoes such as Loki and Pele, lava eruptions sometimes accompany with plume. It is still unknown which type of eruptions emit gasses enough to change the profile of Io’ s atmosphere and Io plasma torus.

We demonstrated the spatial and velocity distribution of Io’ s SO_2 atmosphere by analyzing the ALMA (Atacama Large Millimeter/Submillimeter Array) archive data (~332-346 GHz) observed on 20 March 2018. We found the presumed volcanically active areas in the east side and northern high latitude region (Volcano 1) and in the west side near the equator (Volcano 2). In Region 1, high and low velocity components are clearly identified in the velocity distribution before ingress. The Doppler shift of the high velocity component relative to the low velocity is ~0.6 km/s (red shift). The result suggests the significant volcanic plume generated atmospheric dynamics and supply SO_2 gases to the upper atmosphere. In Volcano 2, we could not detect the high velocity component of SO_2 gas. The rotational temperature of SO_2 is 311±41 K after ingress, much higher than temperature of sublimation atmosphere (~100-200 K). It might reflect the temperature of low velocity gases which are emitted from volcanoes or/and heated by a hot lava lake in Volcano 2.

We also observed the enhancement of Io plasma torus on the dusk side by Hisaki satellite with the ultraviolet spectrometer EXCEED in the same period of the ALMA observation. The result suggests the direct volcanic input of SO_2 gases may trigger the enhancement of Io plasma torus. We detected gases that may be emitted by effusive and explosive eruptions from the ALMA archive data simultaneously. However, we need further observation by Hisaki and ground-based telescope to clarify which type of eruptions contribute to enhance Io plasma torus.

Keywords: Planetary volcanism, Jupiter moon Io, Atmosphere, Io plasma torus

©2020. Japan Geoscience Union. All Right Reserved.

[J] Poster | M (Multidisciplinary and Interdisciplinary)：M-IS Intersection

[M-IS32] Gas hydrate in environmental-resource sciences

convener:Hitoshi Tomaru(Department of Earth Sciences, Chiba University), Akihiro Hachikubo(Kitami Institute of Technology), Shusaku Goto(Institute for Geo-Resources and Environment National Institute of Advanced Industrial Science and Technology), Atsushi Tani(Department of Human Environmental Science, Graduate School of Human Development and Environment, Kobe University)

An increasing number of researches focusing on natural gas hydrates has recently been conducted from the environmental, material, and resource scientific viewpoints. This session aims to share and discuss the latest research results associated with natural/experimental gas hydrates to understand and examine the nature and potential of gas hydrates in the past-present-future of the Earth and the development/application for our life. Because the researches on gas hydrates are interdisciplinary, broad topics from field and experimental researches, modeling, etc. will be presented in this session.

[MIS32-P01] Bacterial Clathrate-Binding Proteins Alter Gas Clathrate Morphology

*Jennifer B Glass[1], Abigail M. Johnson[1], Dustin J.E. Huard[1], Jongchan Kim[1], Priyam Raut[1], Anton S. Petrov[1], Loren Dean Williams[1], Sheng Dai[1], Raquel L. Lieberman[1] (1.Georgia Institute of Technology Main Campus)

[MIS32-P02] Gas hydrate survey at the gas seepage area off Rebun Island, Japan Sea

*Yunosuke Hase[1], Akihiro Hachikubo[1], Satoshi Yamashita[1], Hirotoshi Sakagami[1], Masaaki Konishi[1], Hirotsugu Minami[1], Kenji Nishina[2], Tadashi Misaka[3] (1.Kitami Institute of Technology, 2.Geological Survey of Hokkaido, Hokkaido Research Organization, 3.Wakkanai Fisheries Research Institute, Hokkaido Research Organization)

[MIS32-P03] Total organic carbon in subsurface sediment off Abashiri, the Sea of Okhotsk

*daisuke yahagi[1], Akihiro Hachikubo[1], Masaaki Konishi[1], Hirotoshi Sakagami[1], Hirotsugu Minami[1], Satoshi Yamashita[1], Kenji Nishina[2], Yasuhito Uchida[2], Kenji Sakaguchi[3] (1.kitami institute of technology, 2.Geological Survey of Hokkaido, Hokkaido Research Organization, 3.Kushiro Fisheries Research Institute, Hokkaido Research Organization)

[MIS32-P04] Characteristics of gas in shallow sediments from seepage field off Tokachi (the Pacific Ocean)

*Hiromi Kimura[1], Yunosuke Hase[1], Yuki Ikeura[1], Ryoya Kamata[1], Akihiro Hachikubo[1], Masaaki Konishi[1], Hirotoshi Sakagami[1], Hirotsugu Minami[1], Satoshi Yamashita[1] (1.Kitami Institute of Technology)

[MIS32-P05] Geochemistry of pore water and headspace gas in the Tatar Trough

*Musashi Yokoyama[1], Hitoshi Tomaru[1], Ryo Matsumoto[2], Glen Snyder[2], A.V. Yatsuk[3], Shvalov D.A.[3] (1.Chiba University, 2.Meiji University, 3.Gas Geochemistry Laboratory, V.I.Ilichev Pacific Oceanological Institude)

[MIS32-P06] Characteristics of methane hydrate fields in the southwestern margin of the Yamato Basin, southern Japan Sea

*Naoto Ishida[1], Hidefumi Fujioka[2], Hitoshi Tomaru[3], Takao Ebinuma[1], Ryo Matsumoto[4] (1.Social Systems and Civil Engineering, Graduate School of Engineering, Tottori University, 2.Tottori Prefectural Fisheries Experiment Station, 3.Department of Sciences, Chiba University, 4.Gas hydrate Labratory, Meiji University)

[MIS32-P07] Origin of methane in gas hydrate field, Hikurangi Subduction Margin: application of geochronological method using a long-lived radioisotope of iodine

*Satoko Owari[1], Hitoshi Tomaru[2] (1.Tokyo University of Marine Science and Technology, 2.Chiba University)

[MIS32-P08] Observation of hydrogen transfer reactions via radical species in chibaite

*Yuka Yokoyama[1], Shusuke Isogai[1], Kenta Kusuki[1], Hirotsugu Nishido[2], Atsushi Tani[1] (1.Graduate School of Human Development and Environment, Kobe University, 2.Faculty of Biosphere-Geosphere Science, Okayama University of Science)

[MIS32-P09] Investigation on thermal stability of radical species in chibaite

*Shusuke Isogai[1], Yuka Yokoyama[1], Kenta Kusuki[1], Hirotsugu Nishido[2], Atsushi Tani[1] (1.Graduate School of Human Development and Environment, Kobe University, 2.Faculty of Biosphere-Geosphere Science, Okayama University of Science)

[MIS32-P10] Experimental study on the phase equilibrium condition of carbon dioxide hydrate with sediments

*Tatsuki Iwamoto[1] (1.Chiba University)

[MIS32-P11] Formation of gas hydrates composed of methane and helium

*Hiromi Kimura[1], Shota Shirakura[1], Akihiro Hachikubo[1], Satoshi Takeya[2] (1.Kitami Institute of Technology, 2.National Institute of Advanced Industrial Science and Technology (AIST))

[MIS32-P12] Direct measurement of hydration number of gas hydrates

*RYOYA KAMATA[1], Hiromi Kimura[1], Emi Sugimori[1], Akihiro Hachikubo[1], Satoshi Takeya[2] (1.Kitami Institute Of Technology, 2.National Institute of Advanced Industrial Science and Technology (AIST))

[MIS32-P13] Effect of salinity on self-preservation effect of mixed gas hydrate

*Yunosuke Hase[1], Hiromi Kimura[1], Akihiro Hachikubo[1], Satoshi Takeya[2] (1.Kitami Institute of Technology, 2.National Institute of Advanced Industrial Science and Technology (AIST))

[MIS32-P14] Making of large scale ice block simulating shallow type methane hydrate for performance confirmation of submarine drilling rig

*yuya ono[1], Satoshi Yamashita[2], shunsuke Iwamoto[3], kouzi Mochiduki[3] (1.KITAMI Institute of Teclhnology, graduate school, 2.KITAMI Institute of Technology, 3.Mitsui E&S Shipbuilding Co., Ltd)

Bacterial Clathrate-Binding Proteins Alter Gas Clathrate Morphology

*Jennifer B Glass[1], Abigail M. Johnson[1], Dustin J.E. Huard[1], Jongchan Kim[1], Priyam Raut[1], Anton S. Petrov[1], Loren Dean Williams[1], Sheng Dai[1], Raquel L. Lieberman[1]

1. Georgia Institute of Technology Main Campus

Gas clathrates are found on Earth along continental margins and in permafrost and are extreme habitats due to low water activity, high salinity, low temperatures, and high pressures. Survival strategies used by gas clathrate-inhabiting microbes could provide clues for searching for life beyond Earth, such as Mars, Titan, and Pluto. Our hypothesis is that bacteria living in gas clathrates employ a strategy similar to that of cold-water fish that express ice-binding proteins (IBPs) to inhibit the growth of ice crystals. Antarctic fish IBPs have been successfully tested for their efficacy to inhibit gas clathrate formation. To test our hypothesis, we engineered a temperature-controlled chamber to synthesize tetrahydrofuran (THF) clathrate in the presence of recombinantly-expressed bacterial proteins. We chose eight protein sequences that were predicted to be IBPs from metagenomes sequenced from methane clathrate sediments from coastal Oregon, USA and coastal Japan. All assayed proteins have been confirmed to be clathrate-binding proteins (CBPs). We assayed CBPs 2-6 by testing their effect on morphology of THF-clathrate crystal structure, visualization of clathrate binding via fluorescence of tagged enhanced green fluorescent protein (eGFP), and protein quantification. Winter-flounder antifreeze protein was used as a positive control, which formed numerous small, platy crystals. Phosphate-buffered saline solution, cytochrome c, and eGFP were used as negative controls, which formed single, native-like crystals. In the presence of CBPs, THF-clathrate crystals formed nonnative-like morphologies. CBPs 2 and 3 formed small, platy crystals, similar to the positive control, whereas CBPs 4-6 formed larger, flat crystals. eGFP-tagged CBPs showed clear evidence of clathrate binding compared to eGFP alone. CBPs were more enriched in the clathrate compared to the negative controls. Taken together, these data support our hypothesis that CBPs are employed by microorganisms in clathrate-rich zones for survival. Future studies include directly assaying CBPs for activity toward methane hydrate.

Keywords: hydrate, clathrate, microbe

©2020. Japan Geoscience Union. All Right Reserved.

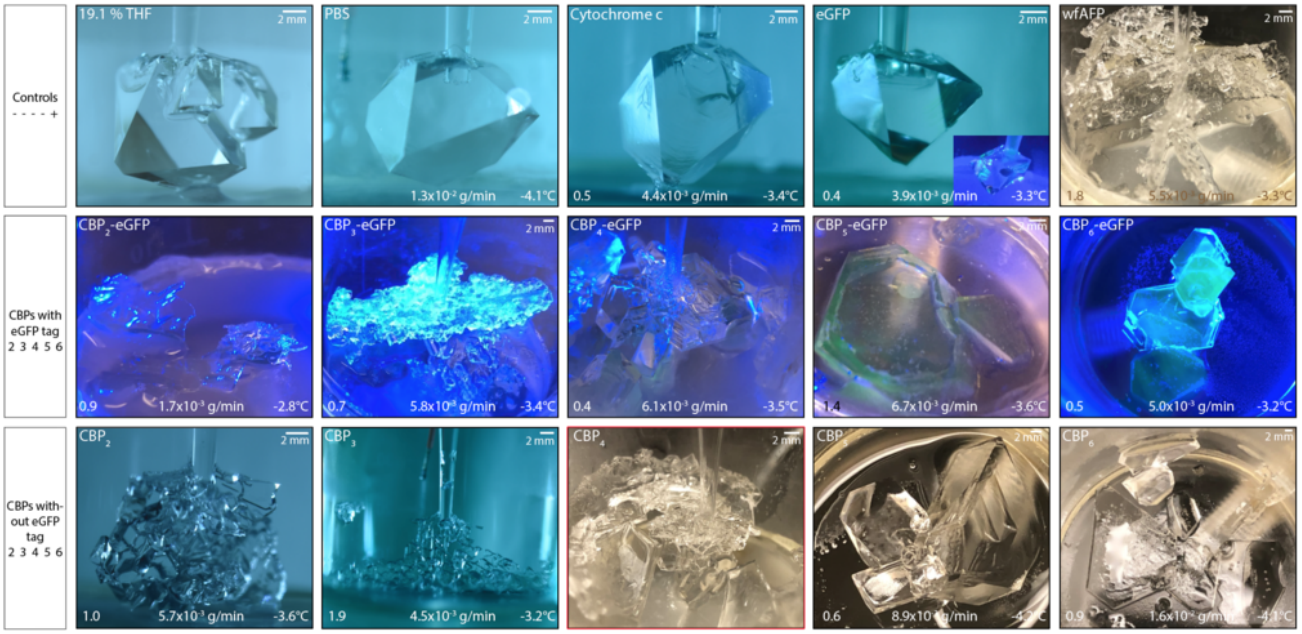

Figure 1. Representative images of each treatment. The top row includes the negative controls (19.1% THF with no additives, the phosphate buffered solution in which all proteins were suspended, cytochrome c, and enhanced green fluorescent protein) and the positive control (winter flounder antifreeze protein). The middle row contains CBPs 2-6 with eGFP tags. The bottom row contains CBPs 2-6 without eGFP tags. Each image is labeled with the treatment (top left), the scale (top right), the average protein concentration ratio in crystal : non-crystallized solution (bottom left), the crystal growth rate (bottom middle) and the nucleation temperature (bottom right).

©2020. Japan Geoscience Union. All Right Reserved.

Gas hydrate survey at the gas seepage area off Rebun Island, Japan Sea

*Yunosuke Hase[1], Akihiro Hachikubo[1], Satoshi Yamashita[1], Hirotoshi Sakagami[1], Masaaki Konishi[1], Hirotsugu Minami[1], Kenji Nishina[2], Tadashi Misaka[3]

1. Kitami Institute of Technology, 2. Geological Survey of Hokkaido, Hokkaido Research Organization, 3. Wakkanai Fisheries Research Institute, Hokkaido Research Organization

We investigated sea-floor sediments off Rebun Island (Japan Sea) to understand environment of near-surface gas hydrates, where gas plumes exist and ascend from the sea floor. HKY17, HKY18, and HKY19 cruses were conducted in 2017-2019 using RV Hokuyo-Maru (237 t) of the Wakkanai Fisheries Research Institute, in a framework of joint research between Kitami Institute of Technology and Hokkaido Research Organization. We observed gas plumes in this area and obtained 14 sediment cores during the three cruises using a gravity corer and hydrostatic corer. Their maximum length was around 140 cm, and some cores showed high concentration of methane (more than 0.1 mM), indicating high methane flux from the deep sediment layer. HKY1701 core showed heavy methane isotope (more than -50‰), however, it was not a proof of thermogenic gas because methane concentration was low (less than 0.002 mM). Methane $\delta^{13}C$ of sediment gases in other cores were around -80‰, suggesting their microbial origin. The relation between $\delta^{13}C$ of methane and carbon dioxide showed that the sediment gases were in the field of methane oxidation in the upper sediment layer. Methane-rich cores (HKY1804, HKY1805, HKY1901, and HKY1902) showed high concentration of hydrogen sulfide, generating by the process of anaerobic methane oxidation. Although hydrate-bound thermogenic gas were retrieved off Sakhalin Island and off Joetsu city (eastern margin of Japan Sea), it is concluded that microbial methane is dominant at the gas plume field off Rebun Island.

Keywords: gas hydrate, Japan Sea, gas origin

©2020. Japan Geoscience Union. All Right Reserved.

Total organic carbon in subsurface sediment off Abashiri, the Sea of Okhotsk

*daisuke yahagi[1], Akihiro Hachikubo[1], Masaaki Konishi[1], Hirotoshi Sakagami[1], Hirotsugu Minami[1], Satoshi Yamashita[1], Kenji Nishina[2], Yasuhito Uchida[2], Kenji Sakaguchi[3]

1. kitami institute of technology, 2. Geological Survey of Hokkaido, Hokkaido Research Organization, 3. Kushiro Fisheries Research Institute, Hokkaido Research Organization

Because ultimate origin of hydrate-bound hydrocarbon is organic matter deposited on the sea floor, total organic carbon in sediment relates to formation of natural gas hydrates. Waseda (1998) noted that content of total organic carbon is a key factor controlling formation of gas hydrates of microbial origin. In this study, we report total organic carbon and its $\delta^{13}C$ in subsurface sediment retrieved off Abashiri (the Sea of Okhotsk), where natural gas hydrate exists, and compared with those of other places off Hokkaido. Sediment samples were obtained off Abashiri (C032, 1KY17, HKS17, and HKS18), off Monbetsu (GA18 and GA19), and off Tokachi (C046, C061, and C080). 182 sediment samples were dried, homogenized, and about 5 mg of samples were put into silver foil capsules. They were decarbonized with 12N hydrochloric acid for 24 h, and then dried and analyzed their TOC with a Flash 2000 Elemental Analyzer connected to a Delta V isotope ratio mass spectrometer. These samples were wrapped in tin capsules and combusted in an oxygen atmosphere. The system was calibrated using a standard of JCAC-01 (L-alanine, -23.43‰ in V-PDB).

Natural gas hydrates were retrieved in the sediment cores of HKS1807 and HKS1808 using a hydrostatic corer, and 1KYPS1701-04 using a push corer with ROV. The content of total organic carbon was 1.3-1.6% in HKS1807 and HKS1808, 0.8-2.3% in 1KYPS1701-04, and generally less than 1% for other sediment cores off Abashiri. It is reasonable to say that hydrate-bound sediment cores are rich in organic matter. On the other hand, C061-GC1803 off Tokachi showed around 2% and cores of GA18 and GA19 partly exceeded 3%, suggesting that the content of organic matter is not a sufficient condition for gas hydrate formation. $\delta^{13}C$ of total organic carbon distributed around -25‰ for all samples, however, some samples of 1KY17 showed less than -30‰. Because sediment cores of 1KY17 (1KYPS1701-04) were short (up to 25 cm) and obtained from the gas seepage, the organic matter might be affected by oxidized methane.

Reference

Waseda A (1998) Organic carbon content, bacterial methanogenesis, and accumulation processes of gas hydrates in marine sediments. Geochem J 32: 143-157

Keywords: TOC, gas hydrate, methane

©2020. Japan Geoscience Union. All Right Reserved.

Characteristics of gas in shallow sediments from seepage field off Tokachi (the Pacific Ocean)

*Hiromi Kimura[1], Yunosuke Hase[1], Yuki Ikeura[1], Ryoya Kamata[1], Akihiro Hachikubo[1], Masaaki Konishi[1], Hirotoshi Sakagami[1], Hirotsugu Minami[1], Satoshi Yamashita[1]

1. Kitami Institute of Technology

In the framework of practical education of Kitami Institute of Technology (name of lecture: “Practical learning about the Okhotsk Region, its history and the natural environment”), we conducted research cruises off Tokachi from 2014 to 2019, where many gas seeps ascend from the sea floor and their height exceeded 700 m. During the cruises of C008, C046, C061, and C080 using TS Oshoro-maru of Hokkaido University, 11 sediment cores were retrieved from this area using a gravity and hydrostatic corers. In this report we summarize characteristics of sediment gas in this area. Sediment gas samples were obtained by a headspace gas method. We measured gas composition of the sediment gases onboard using a portable gas chromatograph (CP-4900, Varian), and after that we measured the molecular and isotopic compositions of the samples using another gas chromatograph (GC2014, Shimadzu) and CF-IRMS (Delta V, Thermo Fisher Scientific) in our laboratory. SMI (sulfate-methane interface) depths of C008-GC1403 and C080-GC1901 cores were around 50 cm, indicating active gas seepage. However, those of C008-GC1401 and C080-GC1902 cores were more than 2 m. C061-GC1802 core only contained carbonates. These coring points locate within 200 m, suggesting that gas seepage field is not uniform. Hydrogen sulfide was detected except two sediment cores, indicating that the process of anaerobic methane oxidation is active beneath the sea floor. $C_1 / (C_2 + C_3)$ showed minimum around the depths of SMI (sulfate-methane interface), because concentration of ethane simply increased with depth compared with methane. The above high methane flux points showed depletion in $\delta^{13}C$ of carbon dioxide, because light carbon dioxide was generated by oxidation of light methane.

Keywords: gas hydrate, methane, the Pacific Ocean

©2020. Japan Geoscience Union. All Right Reserved.

Geochemistry of pore water and headspace gas in the Tatar Trough

*Musashi Yokoyama[1], Hitoshi Tomaru[1], Ryo Matsumoto[2], Glen Snyder[2], A.V. Yatsuk[3], Shvalov D.A.[3]

1. Chiba University, 2. Meiji University, 3. Gas Geochemistry Laboratory, V.I.Ilichev Pacific Oceanological Institude

During the LV81 and LV85 expeditions, we have collected a number of sediment cores from various sites in the Tatar Trough where the gas chimney, indicative of methane-rich columnar sediment structure, pockmark, gas flare, carbonate nodules, and high methane flux had been reported. In methane-rich marine environment, geochemistry of pore water have been useful to estimate the methane flux using the depth of SMI (sulfate gradient) as well as the distribution of gas hydrate (low chloride anomaly). The headspace gas analysis also reflects the information of the origin of hydrocarbons as well as the methane-oxidation in the shallow sediments. In this research, we analyzed chemical composition of pore water and chemical/isotopic composition of headspace gas to characterize the biogeochemical processes associated with generation, migration, oxidation, and fixation of methane in the Tatar Trough.

The overall depths of SMI is significantly shallow in the northern area (SMI at 1-3 mbsf) compared those in the middle and southern areas (SMI mostly at >3-5 mbsf). In particular, the SMIs of gas hydrate-bearing core in the northern area at which low chloride anomalies due to gas hydrate dissolution were observed locate at <1.5 mbsf, corresponding to the highest values of all sites, high methane flux is essentially required for the accumulation of gas hydrate in shallow sediments. Within the northern area, the SMI depths are relatively shallow at the eastern slope sites, particularly at shallow sites, compared to those at trough floor sites. The SMI depth on the western slope is apparently deep, methane migration system is different between eastern and western slopes in the northern trough. The SMI depths in the middle research area are generally shallower than those in the southern area; higher methane fluxes are found from the gas chimney sites (SMI at <2 mbsf).

All the methane concentrations and C1/C2 ratios in headspace gases increase with depth due to the active upward methane flux although the methane is oxidized at the SMI. These values in the northern area are higher than those in the middle and southern areas. This probably indicates that the biogenic methane inputs are greater in the northern area, distribution and flux of gases reflect well the subsurface gas system in the Tatar Trough.

Keywords: pore water, headspace gas, AOM, SMI

©2020. Japan Geoscience Union. All Right Reserved.

Characteristics of methane hydrate fields in the southwestern margin of the Yamato Basin, southern Japan Sea

*Naoto Ishida[1], Hidefumi Fujioka[2], Hitoshi Tomaru[3], Takao Ebinuma[1], Ryo Matsumoto[4]

1. Social Systems and Civil Engineering, Graduate School of Engineering, Tottori University, 2. Tottori Prefectural Fisheries Experiment Station, 3. Department of Sciences, Chiba University, 4. Gas hydrate Labratory, Meiji University

The Yamato Basin is one of the methane hydrate fields located in the southern part of the Japan Sea. In the southwestern margin of the Yamato Basin, gas chimneys have been detected by the shallow-type methane hydrate survey conducted by METI. Subsequent researches by the Gas Hydrate Research Laboratory of the Meiji University and Tottori Prefecture revealed characteristics of the methane hydrate fields using sub-bottom profiling, piston and gravity coring, geothermal measuring, interstitial water analysis etc.

Geothermal gradient was measured at the southwestern slope of the basin as 71.33 mK/m and base of gas hydrate stability was estimated to be 138.6 mbsf. Several huge gas chimneys, hundreds of meters in width, were found in the northwestern slope of the Oki Ridge. Carbonate concretions just below the seafloor and shallow (<2.4 m) sulfate-methane interface (SMI) depths around the gas chimneys indicate high methane flux and strongly suggest large volumes of methane hydrate in the gas chimneys.

Keywords: shallow-type methane hydrate, Yamato Basin, Japan Sea

©2020. Japan Geoscience Union. All Right Reserved.

Origin of methane in gas hydrate field, Hikurangi Subduction Margin: application of geochronological method using a long-lived radioisotope of iodine

*Satoko Owari[1], Hitoshi Tomaru[2]

1. Tokyo University of Marine Science and Technology, 2. Chiba University

Organic materials such as marine algae are enriched in iodine because iodine is incorporated with the algae due to its strongly biophilic character. Iodine and methane are released into an interstitial water during the degradation of the organic materials and migrate together due to the similar diffusion coefficient in marine sediment. Iodine is concentrated in interstitial water relative to seawater (0.4 μM), the concentration therefore increases up to a few hundred μM. Iodine has one long-lived radio isotope (^{129}I, $t_{½}$= 15.7 Myr) and it has been used as a geochronological indicator. The ^{129}I geochronology has been applied to identify the depositional age of source organic materials, fluid migration pathway, and relative age of iodine/methane-rich fluid in gas hydrate field. This research aims at characterizing the source and potential age of organic materials for methane in the gas hydrate field related to the fracture-developed sediment in the Hikurangi Subduction Margin.
We collected interstitial water (down to ~1000 mbsf) at four sites across the trench axis in the Hikurangi margin during the IODP Exps. 372 and 375. The iodine and methane concentration at Site U1520, seaward of the trench axis, increased from seawater level to 200 μM and 10^5 ppmv, respectively, at 100 mbsf and decreased with depth. The $^{129}I/I$ ratios were almost constant at ~100×10^{-15}, corresponding to the potential iodine age ~50 Ma. The old iodine are derived from Cretaceous sediment underlying Site U1520. The seaward iodine and methane were, therefore, liberated through the degradation of iodine-rich organic matter and mixed with young/shallow iodine. Pore-filling gas hydrate layers were found by IR scanning at Sites U1517, U1518, and U1519, landward of the trench axis. The saturation and depths of gas hydrates were identified by low concentration anomaly of the chloride. The chloride data suggest the presence of gas hydrate occurrences between ~100 to 170 mbsf, with S_h values ranging between 1 to 70 % at the Site U1517 and between ~33 to 390 mbsf, with 2 to 46% of saturation at the site U1518. At the Site U1519, the low concentration of chloride were found between ~600 to 620 mbsf, however there is not a clearly defined background Cl concentration profile due to the coring gap, there is no saturation data at this site. Most gas hydrate layers were found in the relatively high permeability sediments such as sand or silt. The iodine concentrations at landward sites increased up to 700 μM with depth and the methane concentration increased rapidly to 10^3 to 10^4 ppmv at 50 mbsf. The $^{129}I/I$ ratios at landward site were constant around 100×10^{-15}, corresponding to the potential iodine age ~50 Ma. The iodine and methane landward sites are potentially derived from deep/old landward sediment such as deformed backstop at these sites. The distribution of methane is controlled by advection/migration of iodine-methane-rich fluid through fractured layers developed in accreted landward sediments. The landward sediments of the Hikurangi subduction margin are characterized by relatively old fluid with high methane concentration. The gas hydrate system is, therefore, developed typically within the landward sediment especially porous layers.

Keywords: Iodine geochronology, 129I, Interstitial water, Hikurangi Subduction margin, IODP, Gas hydrate

©2020. Japan Geoscience Union. All Right Reserved.

Observation of hydrogen transfer reactions via radical species in chibaite

*Yuka Yokoyama[1], Shusuke Isogai[1], Kenta Kusuki[1], Hirotsugu Nishido[2], Atsushi Tani[1]

1. Graduate School of Human Development and Environment, Kobe University, 2. Faculty of Biosphere-Geosphere Science, Okayama University of Science

In 2011, new mineral named “chibaite” was discovered in Chiba prefecture (Momma et al., 2011). Chibaite is one of the silica clathrate minerals and has a framework structure of silica with cage-like voids occupied by guest species. The structures of silica clathrates are very similar to those of clathrate hydrates. There are three types of structures which are called structure I, II, and H in clathrate hydrates, and chibaite is isostructural with structure II. Chibaite can include methane, ethane, propane, and iso-butane (2-methyl-propane) in the cages as guest species. This means that 6 organic radicals (methyl, ethyl, n-propyl, iso-propyl, iso-butyl, and tert-butyl radicals) could be formed in gamma-irradiated chibaite. The preliminary electron spin resonance (ESR) measurements of the gamma-irradiated chibaite at 110 K and 290 K showed that four radicals (methyl, iso-propyl, iso-butyl, and tert-butyl radicals) were observed at 110 K, whereas only two radicals (methyl and tert-butyl radicals) were observed at 290 K. Since the kinds and amounts of the observed radicals are different at the measurement temperatures between 110 K and 290 K, hydrogen picking process would occur in chibaite. The hydrogen picking process (atomic hydrogen transfer reaction) in this presentation is an intermolecular reaction where atomic hydrogen is transferred from guest organic species to radicals formed by gamma-ray irradiation. This process was observed in clathrate hydrates such as propane hydrate and iso-butane hydrate with structure II (e.g. Ohgaki et al., 2008). The activation energy of this process was evaluated and may be caused by the potential barrier through the shared hexagonal face between adjacent cages which is composed by hydrogen bonds. If activation energy of hydrogen picking process in chibaite is estimated, the properties of framework structure of silica and hydrate could be compared and discussed. In this study, we performed isochronal annealing experiments to investigate whether hydrogen picking process was observed in chibaite.

We gently crushed chibaite samples in a mortar into several pieces with about 1 mm in diameter and irradiated at 77 K by gamma-rays with 60-Co source. ESR signals of the gamma-irradiated samples were measured at 120 K after annealing the samples for 15 min at each temperature (120, 140, 170, 200, 230, 260, and 290 K). The ESR signals of 5 organic radicals were observed and the amount of these radicals showed the different thermal behavior; especially around 260 K, tert-butyl radical increased, whereas methyl radical decreased. This may indicate that hydrogen picking process also occurs in chibaite.

Keywords: silica clathrate, chibaite, hydrogen transfer reaction, radical species, electron spin resonance

©2020. Japan Geoscience Union. All Right Reserved.

Investigation on thermal stability of radical species in chibaite

*Shusuke Isogai[1], Yuka Yokoyama[1], Kenta Kusuki[1], Hirotsugu Nishido[2], Atsushi Tani[1]

1. Graduate School of Human Development and Environment, Kobe University, 2. Faculty of Biosphere-Geosphere Science, Okayama University of Science

Silica clathrates have a framework structure with cage-like voids occupied by guest species and are very similar to gas hydrates which are crystalline inclusion compounds composed of cage-like structures with water molecules. In 2011, chibaite was discovered in Chiba prefecture (Momma et al., 2011). Chibaite is isostructural with gas hydrate structure II and has larger cages than melanophlogite which is isostructural with gas hydrate structure I. This means that it includes propane and isobutane together with methane and ethane as guest molecules. Chibaite was found in marine sediments of Early Miocene age (Hota Group) at Arakawa, Minami-boso City, Chiba Prefecture, Japan. It occurs as quartz veins ranging from a few mm to 1 cm thick in tuffaceous sandstone and mudstone. Although chibaite is formed after the formation of marine sediments, it is not clear when it formed.
If organic radical species like methyl radicals in silica clathrates are thermally stable in geological time scale, electron spin resonance (ESR) dating could be applied to obtain the formation age. In ESR dating, the total radiation dose due to natural radiation is obtained in natural minerals and fossils by the additive dose method and the formation age is estimated by considering annual natural dose. In ESR, unpaired electrons such as point defects and radical species can be detected and the amount of the ESR signal is directly related to the age of the sample. To obtain a reliable ESR age, it is necessary to know the ESR signal response to the radiation dose and the thermal stability of the defects and radical species. In chibaite, propyl radicals and butyl radicals might be formed and stored in the sample because they are enclathrated in the large cages. In this study, we measure chibaite samples by ESR to investigate whether radical species are observed at the first stage, and then if observed in natural samples, how the ESR signals of the radicals respond to artificial irradiation and how stable they are.
We gently crushed chibaite samples in a mortar into several pieces with about 1 mm in diameter and measured ESR signal of each piece before irradiation. All samples were irradiated by gamma-rays with 60-Co source with different doses from 34.5 Gy to 1 kGy and measured by ESR again. Methyl and tert-butyl radicals were observed at room temperature in the natural samples before irradiation. It suggests that chibaite formation age could be dated by ESR using these organic radicals. In dose response experiments, the amount of methyl radicals was not changed or even decreased in 12 samples, though it was increased in 4 samples. The reason might be because the amount of the methyl radicals is already saturated by natural radiation. In contrast, the ESR signal of tert-butyl radicals was increased in artificial radiation dose. In this presentation, we will show the results of annealing experiments for investigation of the thermal stability of the radical species and discuss the possibility of ESR dating especially using tert-butyl radicals.

Keywords: silica clathrate, chibaite, electron spin resonance, radical species, thermal stability

©2020. Japan Geoscience Union. All Right Reserved.

Experimental study on the phase equilibrium condition of carbon dioxide hydrate with sediments

*Tatsuki Iwamoto[1]

1. Chiba University

Gas hydrate has been found in marine sediments around Japan and been attracting attention as an unconventional natural gas resource. It forms under the environment where enough amounts of gas-water coexist and temperature-pressure satisfy the stability condition, which may change easily in response to the surrounding physicochemical environment. A number of experimental studies have been conducted to examine the effects of sediments on the gas hydrate stability, little quantitative research has, however, reported the physicochemical effects of particle-scale phenomena. Detailed examinations of such fundamental effects lead to further understanding of the nature of gas hydrates. In this research, we carried out artificial gas hydrate experiment using carbon dioxide in order to discuss the formation/dissociation conditions under the presence of natural sediments.

Carbon dioxide hydrate was formed using a pressure vessel with sediment collected from the seafloor where shallow gas hydrate accumulated in the Japan Sea. The formation pressure of the hydrate with 10wt% sediment was higher than that without any sediments.This is probably due to the increased liquid-solid boundaryby fine sedimentsand to the adsorption of water molecules with structures similar to hydrate lattice on clay minerals, which may promote the nucleation of gas hydrate.The dissolution temperature of hydrate with sediment was lower than that for the sediment-free condition, which reduced the stability region slightly.This indicates that the depression of solidifying points due to the leached ions from the sediments, the influence of adsorption by clay minerals, and the increase of solid-liquid contact area due to the presence of clay minerals. These microscopic effects may constrain the stability of gas hydrate, which largely control the distribution and occurrence of natural gas hydrates.

©2020. Japan Geoscience Union. All Right Reserved.

Formation of gas hydrates composed of methane and helium

*Hiromi Kimura[1], Shota Shirakura[1], Akihiro Hachikubo[1], Satoshi Takeya[2]

1. Kitami Institute of Technology, 2. National Institute of Advanced Industrial Science and Technology (AIST)

Because helium is one of the components of natural gas, it is possible that helium molecules are enclathrated in natural gas hydrates. Actually, helium is detected in natural gas where gas hydrates exist. However, direct detection of helium in gas hydrates is not reported yet. Maekawa (2004) reported that equilibrium pressure of mixed-gas (methane + helium) hydrate increased with composition of helium. In this study, we we formed methane and helium mixed-gas hydrate and measured composition of helium in GH and residual gases. Fine ice powder was put into a pressure cell (42 mL) and pressurized methane and helium. Gas hydrate formed at around 273 K, and residual gas in the cell was sampled and the rest of residual gas was evacuated at the temperature of liquid nitrogen (77 K). After completion of evacuation, hydrate remained in the cell was dissociated at a room temperature. Molecular composition of GH and residual gases were measured using a portable gas chromatograph (CP-4900, Varian). Some hydrate samples were retrieved at 77 K and determined their crystallographic properties by a PXRD (powder X-ray diffraction) and Raman spectroscopy. The gas hydrate samples were close to be normal methane hydrate from the results by PXRD pattern and Raman spectra. Methane preferred to be encaged in hydrate phase rather than helium. The maximum concentration of helium in hydrate was about 6% (the rest 94% was methane) when the initial partial pressures of methane and helium were about 3 and 15 MPa, respectively. Concentration of helium in hydrate increased with the partial pressure of helium in the initial gas. Because helium cannot be trapped and is difficult to adsorb to sample surface at 77 K, We can conclude that helium molecules can be enclathrated slightly into hydrate cages.

Reference

Maekawa T (2003) Gas hydrate formation for mixtures of methane + helium and ethane + helium. J Chem Eng Data 48: 1283-1285, doi:10.1021/je0301592

Keywords: gas hydrate, helium, deep source gas

©2020. Japan Geoscience Union. All Right Reserved.

Direct measurement of hydration number of gas hydrates

*RYOYA KAMATA[1], Hiromi Kimura[1], Emi Sugimori[1], Akihiro Hachikubo[1], Satoshi Takeya[2]

1. Kitami Institute Of Technology, 2. National Institute of Advanced Industrial Science and Technology (AIST)

Hydration number of gas hydrates is an important parameter, and it decides quality of natural gas hydrates. In the case of full occupancy of methane, hydration number of the crystallographic structure I becomes 5.75, however, hydration number of methane hydrate has been reported as 6, indicating that empty cages exist. Hydration number depends on temperature and pressure at the formation process (Cady, 1981; 1983) as van der Waals & Platteeuw model predicts. In this study, we tried to obtain hydration number of gas hydrates directly by a gravimetric determination. We selected argon as a guest gas, forms the crystallographic structure II. Theoretical value of hydration number is 5.67 in the case of full occupancy. We put 5 g of fine ice powder into a pressure chamber (volume: 42 mL), and introduced pure argon (purity: 99.999%, Air Water Inc.). Temperature was controlled at around 273 K to form argon hydrate. After completion of formation, the residual gas was evacuated at 77 K without dissociation of hydrate. Then, we weighed the cell before and after degasification and calculated weights of gas and water. Purity of the argon hydrate sample was checked by PXRD and it is confirmed that contamination of ice was less than 1%. Besides this, argon hydrate was synthesized in another cell (volume: 30 mL) and measured its equilibrium pressure from 270 K to 276 K. Hydration number at the quadruple point was estimated using Clausius-Clapeyron equation. Hydration number of argon hydrate obtained by gravimetric determination decreased with increasing pressure at the formation process; 6.7 at 10.2 MPa and 5.8 at 18.7 MPa. Hydration number at the quadruple point (273.2 K and 8.27 MPa) was 6.9, agrees with the data by gravimetric determination.

References

Cady GH (1981) Composition of clathrate gas hydrates of $CHClF_2$, CCl_3F, Cl_2, ClO_3F, H_2S, and SF_6. J Phys Chem 85: 3225-3230

Cady GH (1983) Composition of Clathrate Gas Hydrates of H_2S, Xe, SO_2, Cl_2, CH_3Cl, CH_3Br, $CHClF_2$, CCl_2F_2, and C_3H_8. J Phys Chem 87: 4437-4441

Keywords: gas hydrate, hydration number, argon, methane

©2020. Japan Geoscience Union. All Right Reserved.

Effect of salinity on self-preservation effect of mixed gas hydrate

*Yunosuke Hase[1], Hiromi Kimura[1], Akihiro Hachikubo[1], Satoshi Takeya[2]

1. Kitami Institute of Technology, 2. National Institute of Advanced Industrial Science and Technology (AIST)

Self-preservation occurs at the dissociation process of methane hydrate and stores the crystal itself even in unstable P-T conditions. We reported in the last JpGU meeting that mixed-gas hydrate composed of methane and ethane showed complicated pattern of dissociation and speed of dissociation depended on both the composition of mixed-gas and the crystallographic structure (Hase *et al.*, 2019). In natural condition, gas hydrates exist mainly in sea-bottom sediments where salinity is abundant. Recently, Prasad and Kiran (2019) reported self-preservation of methane hydrate with NaCl; however, natural gas hydrates comprise not only methane, but also ethane, propane, butane, hydrogen sulfide, etc. In this study, we tried to check preservation effect of mixed-gas hydrate composed of methane and ethane in the presence of salinity.
Fine ice balls were formed from filtered sea water using a spray system and liquid nitrogen, and put 0.7 g into a pressure cell (volume: 30 mL). Then, mixed-gas of methane and ethane was introduced in the cell and their hydrate were formed at 273.2 K. The gas hydrate sample was degassed and recovered at the temperature of liquid nitrogen. We measured compositions of methane and ethane by a gas chromatograph (GC-2014, Shimadzu). Mixed-gas hydrate samples were placed on a temperature-controlled device and kept at 80 K. Raman spectra of hydrate samples were obtained using a Raman spectrometer (RMP-210, JASCO). We observed the Raman spectra of C-H stretching mode at 83 K, and then increased the sample temperature every 10 K until complete dissociation. We calculated the Raman peak area for C-H stretching mode of methane and ethane around 2900 cm^{-1} by a peak fitting method and obtained the survival rate of gas hydrate samples with temperature.
In the case of pure methane hydrate (composition of ethane: 0%), the survival rate rapidly decreased at around 253 K, agreed with the report by Prasad and Kiran (2019). Although ethane-rich gas hydrate of the structure I showed weak self-preservation at 253 K in the case of no salinity as we reported (Hase *et al.*, 2019), the survival rate also decreased with salinity, indicating that the existence of salt effected the dissociation process of mixed-gas hydrate.

References

Hase Y, Matsuda J, Hachikubo A, Takeya S (2019) Validation of self-preservation effect of methane and ethane mixed-gas hydrate by Raman spectroscopy. Japan Geoscience Union Meeting 2019, Makuhari Messe, Chiba, Japan.

Prasad PSR, Kiran BS (2019) Self-preservation and stability of methane hydrates in the presence of NaCl. Sci Rep 9: 5860, doi:10.1038/s41598-019-42336-1

Keywords: gas hydrate, self preservation effect, methane, ethane

©2020. Japan Geoscience Union. All Right Reserved.

Making of large scale ice block simulating shallow type methane hydrate for performance confirmation of submarine drilling rig

*yuya ono[1], Satoshi Yamashita[2], shunsuke Iwamoto[3], kouzi Mochiduki[3]

1. KITAMI Institute of Teclhnology, graduate school, 2. KITAMI Institute of Technology, 3. Mitsui E&S Shipbuilding Co., Ltd

Shallow type methane hydrates (MH), which are attracting attention as a future energy resource, exist as a massive solid beneath the seabed. In order to obtain the design data of the drill for excavating this shallow type MH, large ice blocks simulating the MH were prepared and the mechanical property of ice was evaluated. Large scale ice blocks were prepared outdoors in winter season at Kitami Institute of Technology. The dimensions of the water tank for preparing the ice block are 3 m square and 1 m high. Water cooled close to 0 degree was put into a water tank every 5, 10 or 20 cm and frozen. An ice block about 1 m in height could be manufactured in about two months.

Unconfined compression tests were performed for ice frozen in a water tank, commercial ice, and ice frozen under various conditions in laboratory. As a result, the similar compressive strength was obtained regardless of the frozen method. In addition, the strength of ice was similar or slightly higher than that of natural MH (Yoneda et. al., 2019). Furthermore, the stiffness of ice was higher than that of MH. Therefore, it was found that the performance confirmation test of the drilling rig was possible using the ice prepared by the method of this study.

Keywords: methane hydrate, ice, drilling rig

©2020. Japan Geoscience Union. All Right Reserved.

[J] Poster | M (Multidisciplinary and Interdisciplinary)：M-GI General Geosciences, Information Geosciences & Simulations

[M-GI39] Data-driven geosciences

convener:Tatsu Kuwatani(Japan Agency for Marine-Earth Science and Technology), Hiromichi Nagao(Earthquake Research Institute, The University of Tokyo), Kenta Ueki(Japan Agency for Marine-Earth Science and Technology), Shin-ichi Ito(The University of Tokyo)

It is important to extract essential processes and structures from observed data sets in order to understand and predict the dynamic behavior of the earth and planetary systems. Recently, many powerful methodologies have been proposed to extract useful information from high-dimensional data sets in mathematical and information sciences. This session aims to provide an opportunity to gather various geoscientists to have a productive discussion for interdisciplinary collaborations.

[MGI39-P01] Global Seismicity Dynamics – Synchronicity in Correlated Seismicity of Global Subduction and Ridge Zone

*mitsuhiro toriumi[1] (1.Japan agency of marine science and technology)

[MGI39-P02] Forward modeling and inversion analysis for geochemical-process extraction: an application to chemical compositions of surface soils in Ibaraki Prefecture, Japan

*Tatsu Kuwatani[1], Kengo Nakamura[2], Shotaro Akaho[3], Takeshi Komai[2] (1.Japan Agency for Marine-Earth Science and Technology (JAMSTEC), 2.Tohoku University, 3.National Institute of Advanced Industrial Science and Technology (AIST),)

[MGI39-P03] Geochemical characteristics of Japan Arc basements from the geochemical database, and origin of these characteristics

*Satoru Haraguchi[1], Kenta Ueki[2], Hikaru Iwamori[1] (1.Earthquake Research Institute, University of Tokyo, 2.Japan Agency for Marine-Earth Science and Technology)

[MGI39-P04] **Estimation of mass transfer and protolith composition for mafic metamorphic rocks using machine learning**

*Matsuno Satoshi[1], Masaoki Uno[1], Atsushi Okamoto[1], Noriyoshi Tsuchiya[1] (1.Tohoku University)

[MGI39-P05] Numerical Evaluation of geochemical discrimination of tsunami deposits by HCA(Hierarchical Clustering Analysis)

*Satoh Kenta[1], Noriyoshi Tsuchiya[1] (1.Graduate school of environmental studies)

[MGI39-P06] **Characterization of permeability based on topological data of fracture network**

*Anna Suzuki[1], Miyuki Miyazawa[1], James Minto[2], Takeshi Tsuji[3], Takatoshi Ito[1] (1.Tohoku Univ., 2.Univ. of Strathclyde, 3.Kyushu Univ.)

[MGI39-P07] Bayesian Data-driven Approach for Extracting Nonlinear Dynamics of Heterogeneous Reactions

*MASAKI ITO[1], Tatsu Kuwatani[2], Ryosuke Oyanagi[2], Toshiaki Omori[1] (1.Kobe University, 2.JAMSTEC)

[MGI39-P08] Super-resolution for seafloor topography using deep convolutoinal neural networks

*Mitsuko Hidaka[1], Daisuke Matsuoka[1], Tatsu Kuwatani[1], Yukari Kido[1], Junji Kaneko[1], Takafumi Kasaya[1], Eiichi Kikawa[1] (1.Japan Agency for Marine-Earth Science and Technology)

[MGI39-P09] Detection of hydrothermal alteration zones distribution by applying linear unmixing method to hyperspectral satellite imagery for densely vegetated geothermal area

*Hiroaki Gonnokami[1], Taiki Kubo[1], Arie Naftali Hawu Hede[2], Asep Saepuloh[2], Katsuaki Koike[1]
(1.Laboratory of Environmental Geosphere Engineering, Department of Urban Management, Graduate School of Engineering, Kyoto University, 2.Bandung Institute of Technology)

Global Seismicity Dynamics –Synchronicity in Correlated Seismicity of Global Subduction and Ridge Zone

*mitsuhiro toriumi[1]

1. Japan agency of marine science and technology

Global Seismicity Dynamics –Synchronicity in Correlated Seismicity of Global Subduction and Ridge Zone.

Mitsuhiro TORIUMI

JAMSTEC

The global seismic data in the USGS catalogue are transformed to the seismic density of unit volume divided along global subduction zone and oceanic ridges between magnitude 4 to 5 from 1990 to 2018. The large data matrixes made by logarithmic transformation are decomposed into coefficient matrixes and orthogonal basis matrix by means of the deterministic PCA (Toriumi 2009, Toriumi 2010, Okada et al., 2017) and probabilistic PCA with LASSO. The results are shown by time series of correlated seismicity rates z1 to z3 for both global subduction zone and oceanic ridge and by intensity spectra of coefficients contributing to the z1 to z3.

The time series of the correlated seismicity rate z1 of the global subduction zone display the step –like increase from 1990 to 2018 with somewhat lowering before and after Tohoku-Oki earthquake but that of the z2 does periodic secular trend having 20 years cycle with Gaussian noise. On the other hand, the time series of the correlated seismicity rate z1 of the global oceanic ridge also appears as step like increase with some degree of undulation. The z2 time series display the weak periodic spike clusters with large noise.

The relationship of z1 between the global subduction zone and the global oceanic ridge clearly shows three clusters and general increase of them with advancing time in their diagram. It seems that three clusters of correlated seismicity rates z1 and z2 of subduction and ridge zones should be due to three times of the globally rapid change of plate motion during recent 30 years. Furthermore, the general trend of these clusters indicates clearly synchronous motion of the subduction and spreading of the plate.

References

Toriumi, M., (2009), Jour. Disaster Res., 4,2,209-213.

Toriumi, M., (2011), COE Lecture Note vol.39, Kyushu Univ., 116-131.

Okada, A., Toriumi, M., and Kaneda, T., 2017, Int. Jour. Geol., 1, 11, 26-34.

Keywords: correlated seismicity, synchronicity, global subduction and ridge

©2020. Japan Geoscience Union. All Right Reserved.

©2020. Japan Geoscience Union. All Right Reserved.

Forward modeling and inversion analysis for geochemical-process extraction: an application to chemical compositions of surface soils in Ibaraki Prefecture, Japan

*Tatsu Kuwatani[1], Kengo Nakamura[2], Shotaro Akaho[3], Takeshi Komai[2]

1. Japan Agency for Marine-Earth Science and Technology (JAMSTEC), 2. Tohoku University, 3. National Institute of Advanced Industrial Science and Technology (AIST),

This study aims to propose a framework based on forward modeling and inversion analysis to extract geochemical processes using matrix decomposition. Matrix decomposition methods, such as principal component analysis (PCA) and independent component analysis (ICA), can be used to extract processes from geochemical datasets across a wide range of geoscientific fields. However, it has still been only a heuristic approach; moreover, it is not well-understood whether the extracted basis vectors correspond to geological processes. In this study, in order to verify the effectiveness of the inversion analysis using matrix decomposition, we conducted synthetic-data analyses using artificial soil composition data that were generated by a simple forward model that simulates geochemical weathering. We also conducted a real-data analysis using soil composition data of ground surface in Ibaraki Prefecture, Japan. In the presentation, we will discuss geochemical processes for extracted basis vectors and try to quantitatively interpret them.

Keywords: matrix decomposition, data-driven, soil

©2020. Japan Geoscience Union. All Right Reserved.

Geochemical characteristics of Japan Arc basements from the geochemical database, and origin of these characteristics

*Satoru Haraguchi[1], Kenta Ueki[2], Hikaru Iwamori[1]

1. Earthquake Research Institute, University of Tokyo, 2. Japan Agency for Marine-Earth Science and Technology

Various models have been proposed as a mechanism of the growth of the continental crust. Particularly, subduction processes (magmatism and accretion) are thought to be playing predominant role in the evolution of the continental crust. Detailed investigation on the lithological and compositional variations of arc crustal rocks allows us to discuss the development process of the island arc crust as well as the dynamics occurring the subduction zone. The Japan Arc is the suitable field for such study.
As the Japan Arc crust is formed through complicated evolution until Paleozoic, for example, acidic plutons such as Hida and Ryoke granitoids produced by multiple activities after Paleozoic are distributed, accretion prisms are observed in SW Japan and Hokkaido arc, and the addition of arc crust occurs at the Izu collision zone. As such, geochemical discussion based on regionality is required to discuss a growth process of the earth crust.
As a database to use for this study, the data of the lithofacies to be related to the Japan Arc crust (basement) is extracted from the DODAI database. DODAI (Haraguchi et al., 2018) is a geochemical database for the basement rocks of the Japanese islands including major and trace element concentrations, isotopic ratios and geographical coordinates (latitude, longitude, and altitude) of sampling points, and geological and lithological information. This dataset is sorted by lithofacies and locations, and geochemical variations between lithofacies and locations are compared. For locality, we subdivided our dataset to Northeast (NE) and Southwest (SW) Japan divided at the Itoigawa - Shizuoka tectonic line. For lithological classification, a definition in Takeuchi et al. (2019) is used. We construct compositional histogram of each major and trace elements of each group. Based on the histogram, we calculate various statistics, average, median, mode, variance, skewness and kurtosis, and compare these plots and parameters.
when comparing the same lithological type between NE and SW Japan, many elements show different characteristics. Rocks of SW Japan typically show more evolved characteristics. On the other hand, rocks of NE Japan show low K_2O, Rb and HREE, and high CaO and Sr. These statics also show more differentiated characteristics in SW Japan. In terms of statistical variables, rocks of SW Japan show larger variance and skewness, and lower kurtosis. In this report, we examine regionality of the compositional characteristics of Japan Arc crust from these data comparisons, and discuss a genetic process of the Japan arc.

References

Haraguchi et al. (2018) J. Geol. Soc. Japan 124, 1049-1054
Takeuchi et al. (2019) Phys. Earth Planet. Inter. 288, 37-57

Keywords: geochemical database, composition of Japanese arc crust, comparison between NE and SW Japan, statistics

©2020. Japan Geoscience Union. All Right Reserved.

Estimation of mass transfer and protolith composition for mafic metamorphic rocks using machine learning

*Matsuno Satoshi[1], Masaoki Uno[1], Atsushi Okamoto[1], Noriyoshi Tsuchiya[1]

1. Tohoku University

Geochemical compositional data obtained from rocks and soils are essentially multi-dimensional, and consist of a large number of element concentrations and isotope ratio compositions of several tens of dimensions. The “current” rock composition we can obtain is that of the protolith affected by the geochemical process. Therefore, in order to evaluate the geochemical process from the "current" rock composition, it is necessary to quantitatively estimate the composition of the protolith.

In previous studies on protolith estimation, the type of protolith was identified by discrimination diagrams, yet, quantitative estimation of the protolith composition was not performed. On the other hand, in recent years, the use of machine learning has been increasing in the geochemistry field due to technological advances in programming languages and machine learning (eg, Kuwatani et al., 2014; Harsterok et al., 2019). However, there has been no application of machine learning to the problem of quantitative estimation of geochemical composition data, and it is necessary to establish a new method.

In this study, we aimed to quantitatively evaluate geochemical processes by estimating the composition of basalt, which is the protolith of metamorphic rocks. Geochemical processes of metamorphic rocks include weathering and metamorphism. Elements transferred by these processes are Rb, Ba, Sr, Ce, etc., and elements are not transferred are Nb, La, P, Nd, Zr, Ti, Y, etc. (e.g., Ludden 1979; Uno et al., 2014; Kessel et al., 2005). Therefore, Rb, Ba, Sr, and Ce were defined as mobile elements, and Nb, La, P, Nd, Zr, Ti, and Y were defined as immobile elements.

The chemical composition of basalt, which is the protolith of metamorphic rocks, was used as the teaching data of the machine learning model. The chemical compositional data were compiled from PetDB. A machine learning model was constructed in which the input variable was the concentration of immobile elements and the output variable was the concentration of mobile elements. Since the concentration of immobile elements does not change between metamorphic rocks and protoliths, it is possible to estimate the "mobile element concentration of protoliths" by giving the "immobile element concentration of metamorphic rocks" as an input variable to the machine learning model. LightGBM, an ensemble of decision trees, was used as the machine learning algorithm.

As a result, it was possible to construct a model that estimates the Rb, Ba, Sr, and Ce concentrations of protolith within an error of 10% to 20%. When metamorphic rocks are actually applied to the model, a significant difference is derived between the “metamorphic rock composition” and the “estimated protolith composition”, and this significant difference is considered to be the amount of mass transfer by geochemical processes during metamorphism. Therefore, the machine learning model, constructed by decision trees with LightGBM algorisms, is effective for estimating the mobile element concentration from the immobile element concentration. Our model can quantitatively evaluate geochemical processes during metamorphism when applied to compositional data of metamorphic rocks.

Keywords: Machine Learning, Fluid rock interaction, Metamorphism, Mass transfer, Protolith estimation

©2020. Japan Geoscience Union. All Right Reserved.

©2020. Japan Geoscience Union. All Right Reserved.

Numerical Evaluation of geochemical discrimination of tsunami deposits by HCA(Hierarchical Clustering Analysis)

*Satoh Kenta[1], Noriyoshi Tsuchiya[1]

1. Graduate school of environmental studies

Several methods have been proposed for discriminating historical tsunami deposits, including methods using particle size distribution and the presence of marine microfossils, but most of them are for sand deposits. It is necessary to identify mud tsunami deposits for identification of more accurate inundation area, but the method of discrimination for mud tsunami deposits has not been established yet. On the other hand, there is a study that mud tsunami deposits have less temporal change of marine ions than sand tsunami deposits. Therefore, geochemical methods may be an effective method for judging mud tsunami deposits. As a previous study, there is a method of discrimination of mud tsunami deposits by machine learning, but it is difficult to define training data for non-tsunami deposits, and adaptation to unknown samples has not yet been performed. In this presentation, we examined the discrimination by applying unsupervised learning using the chemical composition (major component + trace component) of tsunami deposits without data of non-tsunami deposits. We also applied unknown samples and tried to discover unknown tsunami deposits. I verified the usefulness of this method for discriminating tsunami sediments by classifying tsunami deposits caused by the Great East Japan Earthquake and Pliocene marine sediments widely distributed in northeastern Japan(Tatsunokuchi Formation) using whole-rock chemical composition as feature values by hierarchical clustering analysis(HCA). To discuss the accuracy quantitatively, we classified the cluster results into clusters dominated by tsunami deposits and clusters dominated by non-tsunami deposits and calculated the accuracy rate. In addition, we attempted to extract unknown tsunami deposits by applying the same method to unknown samples collected in East-Matsushima City. As a result, tsunami deposits and non-tsunami deposits were correctly classified with an accuracy of 96.6%. In addition, as a result of applying this method to unknown samples collected in East-Matsushima City, the possibility of unknown tsunami deposits could be pointed out. Compared to the conventional discrimination method using machine learning, this method does not require teacher data of non-tsunami deposits, so there is a possibility that tsunami deposits can be discriminated more easily.

Keywords: Tsunami deposits, machine learning, Hierarchical Clustering Analysis

©2020. Japan Geoscience Union. All Right Reserved.

Characterization of permeability based on topological data of fracture network

*Anna Suzuki[1], Miyuki Miyazawa[1], James Minto[2], Takeshi Tsuji[3], Takatoshi Ito[1]

1. Tohoku Univ., 2. Univ. of Strathclyde, 3. Kyushu Univ.

Fracture structures controls fluid flow in rocks. The distributions of 3D fracture networks is difficult to be distinguished, and it is not possible to directly estimate the flow properties unless information related to flow (e.g., fracture apertures, connectivity) can be obtained. Persistent homology is a method for computing topological features of shapes and functions, which provides complex and multiscale geometric information in large datasets. This study applies persistent homology to analyzing fracture network patterns in order to understand the relationship between flow properties and fracture structures. We considered fracture aperture distributions and flow paths in fracture networks can be derived from the parameters of persistent homology, which can estimate the permeability of the fracture network. Synthetic 3D fracture network patterns were generated and used to validate the method to estimate permeability. Direct simulation of fluid flow was conducted by using the same fracture networks. The results show that opening aperture distributions of flow paths could be obtained by persistent homology analysis and that estimated permeability was almost the same order of magnitude as the permeability derived from the simulation. Persistent homology can contribute to characterize the relationship between structures and flow.

Keywords: 3D Fracture network, Permeability, Persistent homology, Image analysis, Direct simulation

©2020. Japan Geoscience Union. All Right Reserved.

Bayesian Data-driven Approach for Extracting Nonlinear Dynamics of Heterogeneous Reactions

*MASAKI ITO[1], Tatsu Kuwatani[2], Ryosuke Oyanagi[2], Toshiaki Omori[1]

1. Kobe University, 2. JAMSTEC

Heterogeneous reactions are chemical reactions with conjugation of multiple phases, and they have the intrinsic nonlinearity of their dynamics caused by the effect of surface area between different phases. In earth science, it is important to understand heterogeneous reactions in order to figure out the dynamics of rock formation near surface of the earth. We propose a Bayesian data-driven approach for estimating nonlinear dynamics of heterogeneous reactions from noisy observable data. We employ sequential Monte Carlo algorithm to partial observation problem, in order to extract hidden variables. Using our proposed method, we show that heterogeneous reactions can be estimated successfully from noisy observable data under conditions that the number of observed variables is less than that of hidden variables. Moreover, we show how our proposed method extracts substantial nonlinear dynamics of heterogeneous reactions under realistic environments.

Keywords: Heterogeneous Reactions, Data-driven Approach, Nonlinear Dynamics

©2020. Japan Geoscience Union. All Right Reserved.

Super-resolution for seafloor topography using deep convolutoinal neural networks

*Mitsuko Hidaka[1], Daisuke Matsuoka[1], Tatsu Kuwatani[1], Yukari Kido[1], Junji Kaneko[1], Takafumi Kasaya[1], Eiichi Kikawa[1]

1. Japan Agency for Marine-Earth Science and Technology

Understanding the detailed information on seafloor topography is required to deal with natural disaster prevention, assessing and mitigating environmental problems, biogeographic studies, mineral mining, and a range of other topics. JAMSTEC has launched the new research program "Mathematical Seafloor Geomorphology" to establish a method to provide high resolution seafloor topography from existing low resolution data, by using super-resolution techniques based on deep convolutional neural networks (DCNNs). We applied two different algorithms of DCNN, a Super-Resolution Convolutional Neural Network (SRCNN) and a Super-Resolution Generative Adversarial Network (SRGAN) to improve the resolution of the data obtained from the middle part of the Okinawa Trough (southwest Japan). Both SRCNN and SRGAN produced better high super-resolution performance for both root mean square error (RMSE) and peak signal-to-noise ratio (PSNR) compared with bicubic interpolation. We will present the results, and would also like to discuss the effects of training data selection on the super-resolution performance.

Keywords: seafloor topography, super-resolution , SRCNN , SRGAN

©2020. Japan Geoscience Union. All Right Reserved.

Detection of hydrothermal alteration zones distribution by applying linear unmixing method to hyperspectral satellite imagery for densely vegetated geothermal area

*Hiroaki Gonnokami[1], Taiki Kubo[1], Arie Naftali Hawu Hede[2], Asep Saepuloh[2], Katsuaki Koike[1]

1. Laboratory of Environmental Geosphere Engineering, Department of Urban Management, Graduate School of Engineering, Kyoto University, 2. Bandung Institute of Technology

For exploring geothermal resources in areas with surface manifestations, detection of alteration minerals by remote sensing technology is effective, because such minerals were generated by hydrothermal fluids (water and gas) that rose from geothermal reservoir in shallow depth to the ground surface. However, this detection is difficult in wide area by optical sensor remote sensing due to limited spatial resolution and mixture of several materials in an image pixel. Therefore, unmixing method that can separate correctly end members is indispensable. Band math method is traditional for mineral mapping using multispectral imagery. Accurate mineral mapping is expected to be possible by an application of hyperspectral imagery with high wavelength resolution.
Thus, a typical hyperspectral satellite imagery, Hyperion was used in this study by selecting the Wayang Windu geothermal field in West Java, Indonesia in which a large-scale geothermal power plant with 227 MW is operated. This field is covered by thick vegetation. To improve detection accuracy of hydrothermal alteration zone in such dense vegetation field, linear spectral unmixing was applied to the Hyperion data by focusing on the spectral reflection and absorption characteristics of alteration minerals. As the result, most pixels extracted as alteration mineral zones corresponded to known geothermal manifestations and fault traces and additionally, main minerals constituting the zones were identified. This research is supported by JST and JICA through a project of Science and Technology Research Partnership for Sustainable Development (SATREPS, Grant No. JPMJSA1401).

Keywords: remote sensing, Hyperion satellite imagery, geothermal manifestation, geothermal-resource exploration, Wayang Windu field (Indonesia)

©2020. Japan Geoscience Union. All Right Reserved.

[J] Poster | M (Multidisciplinary and Interdisciplinary)：M-GI General Geosciences, Information Geosciences & Simulations

[M-GI40] Development of computational sciences on planetary formation, evolution and surface environment

convener:Yoshi-Yuki Hayashi(Department of Planetology/CPS, Graduate School of Science, Kobe University), Masaki Ogawa(Division of General Systems Studies, Graduate School of Arts and Sciences, University of Tokyo), Shigeru Ida(Earth-Life Science Institute, Tokyo Institute of Technology), Kanya Kusano(Institute for Space-Earth Environmental Research, Nagoya University)

Computer simulations have been recognized as one of the fundamental tools in understanding planetary formation, evolution and diversity of surface environment. However, is may be notified that the continuous development of computational abilities in recent years does not seem to be well utilized in improving numerical simulations in those fields; computational efficiency has been improved by 6 orders of magnitude compared from the early 90's, many of our simulations do not seem to catch up qualitatively and quantitatively such improvement. We propose here in this session to ask those who are interested in computational sciences of various fields not only of planetary formation and evolution but also of earth and planetary sciences in general to join. The aim is to discuss various scientific and technical aspects of our numerical simulations to improve our skills to fully utilize those development of computational resources that has been realized as "K" or will be realized in near future as "Fugaku".

[MGI40-P01] A study on numerical accuracy of atmospheric dynamical cores necessary for large eddy simulations

*Yuta Kawai[1], Hirofumi Tomita[1] (1.RIKEN Center for Computational Science)

[MGI40-P02] Surface zonal flows induced by anelastic thermal convection in a rapidly rotating spherical shell

*Youhei SASAKI[1], Shin-ichi Takehiro[2], Keiichi Ishioka[3], Takeshi Enomoto[4] (1.Institute of Fundamental Sciences, Faculity of Science and Engineering, Setsunan University, 2.Research Institute for Mathematical Sciences, Kyoto University, 3.Department of Earth and Planetary Sciences, Kyoto University, 4.Disaster Prevention Research Institute, Kyoto University)

[MGI40-P03] Local node refinement using the Schmidt transform for RBF advection models

*Koji Ogasawara[1], Takeshi Enomoto[2] (1.Graduate School of Science, Kyoto University, 2.Disaster Prevention Research Institute, Kyoto University)

[MGI40-P04] Evolution of orbits of Trans Neptunian Objects in the Galactic Potential

*Yoko Funato[1] (1.University of Tokyo)

A study on numerical accuracy of atmospheric dynamical cores necessary for large eddy simulations

*Yuta Kawai[1], Hirofumi Tomita[1]

1. RIKEN Center for Computational Science

1. Introduction

As computational resources of supercomputers increase, spatial scale which global atmospheric models can resolve has been recently approaching that in large eddy simulations (LES). Then, the authors consider that one of issue is the accuracy of numerical schemes applied for the dynamical core of nonhydrostatic atmospheric models. Because it is possible that the numerical dissipation associated with advection schemes by low-order finite volume method dominates eddy mixing parametrized by the Smagorinsky-Lilly type turbulent model. We derive a criterion of numerical accuracy necessary for LES of atmospheric planetary boundary layer turbulence, based on the theory of 3-dimensional isotropic homogeneous turbulent flow, and check whether the criterion is reasonable in actual simulations.

2. Criterion for numerical accuracy necessary to LES

For the spatial scale, $l\Delta x$ (where l=1,2,.., and Δx is grid spacing), the ratio of e-folding time of decay due to eddy viscosity term to that due to numerical diffusion term with 2n differential operator is derived:

$$R= (m/\pi)^{4/3} * (2\pi Cs)^2 /(|U|\ \gamma_{adv}) * (l/\pi)^{2(n-1)} * (\Delta x)^{1/3}$$

where the magnitude of strain velocity tensor in eddy viscosity is related to Δx, following the theory of 3-dimensional isotropic homogeneous turbulent flow (note that we determine the value of η based on the results from numerical experiments), Cs is the Smagorinsky constant, m is the ration of spatial filter length to Δx and γ_{adv} is non-dimensional strength of numerical diffusion related to the background advective velocity, |U|. For upwind schemes, the numerical diffusion is implicitly determined proportional to wind velocity, while for central schemes it is explicitly added. In order for the numerical diffusion not to dominant the eddy viscosity, It is important that R>>1 in effective resolution. However, the R tends to reduce as spatial resolution increases. Next, we investigate the influence of numerical diffusion on calculations of typical atmospheric LES, and consider the range of R realized.

3. Investigation by numerical experiment

[Experimental setup]

We perform idealized numerical experiments same as ones in Nishizawa et al. (2015), in which we use both of central and upwind advection schemes with several spatial accuracy. A regional nonhydrostatic model, SCALE-RM, is used in this study. The size of computational domain is 9.6 x 9.6 x 3 km^3. As the initial condition, potential temperature disturbance is added to stably stratified atmosphere. The initial background horizontal wind is set to 5 m/s, and heat flux with 200 W/m^2 is continuously given at surface. As advection schemes, 3rd and 5th order upwind schemes (UD3, UD5), and 2nd, 4th and 6th order central schemes (CD2, CD4 and CD6) are used. For central schemes, numerical diffusion is explicitly added. The e-folding time is about 1 minute for 2-grid scale, and the number of differential operater (ND) is basically set to 2, 4 and 6 so that leading dispersive error terms are eliminated for CD2, CD4 and CD6, respectively. We also conduct a experiment with CD4ND8 as in Nishizawa et al. (2015). For all cases, the grid size is 10m, and the temporal integrations are performed over 4 hours.

©2020. Japan Geoscience Union. All Right Reserved.

[Result]
Figure (a) shows that, in irrespective of advection schemes, the energy spectra in inertial subrange are lower than that following -5/3 power law at wavelength shorter than 8-10 times grid spacing (referred to as “effective resolution” here). Furthermore, due to the implicit diffusion proportional to background wind speed, the fields for upwind schemes are more diffusive than that for central schemes. Over the wavelength shorter than effective resolution, the energy spectra for 3rd and 5th order upwind schemes are lower than 2nd and 4th order central schemes with weak numerical filter, respectively. Our examination suggests, if upwind scheme is used, it is desirable that the accuracy of spatial discretization for advection terms is 5th order or higher. Figure (b) shows the dependence of R on Δx and l, which is consistent to the result from numerical experiment mentioned above. It indicates that R we derived here provides a guide for numerical accuracy of advection schemes necessary for LES.

4. Future work

We will investigate the influence of temporal discretization, and will evaluate the effect of “perfectly” high-order discretization where all terms are spatially and temporally discretized with accuracy precisely higher than 2nd order. To do so, we will also explore suitable numerical schemes for dynamical cores.

Keywords: atmospheric planetary boundary layer turbulence, large eddy simulation, numerical accuracy of discretization for dynamical core

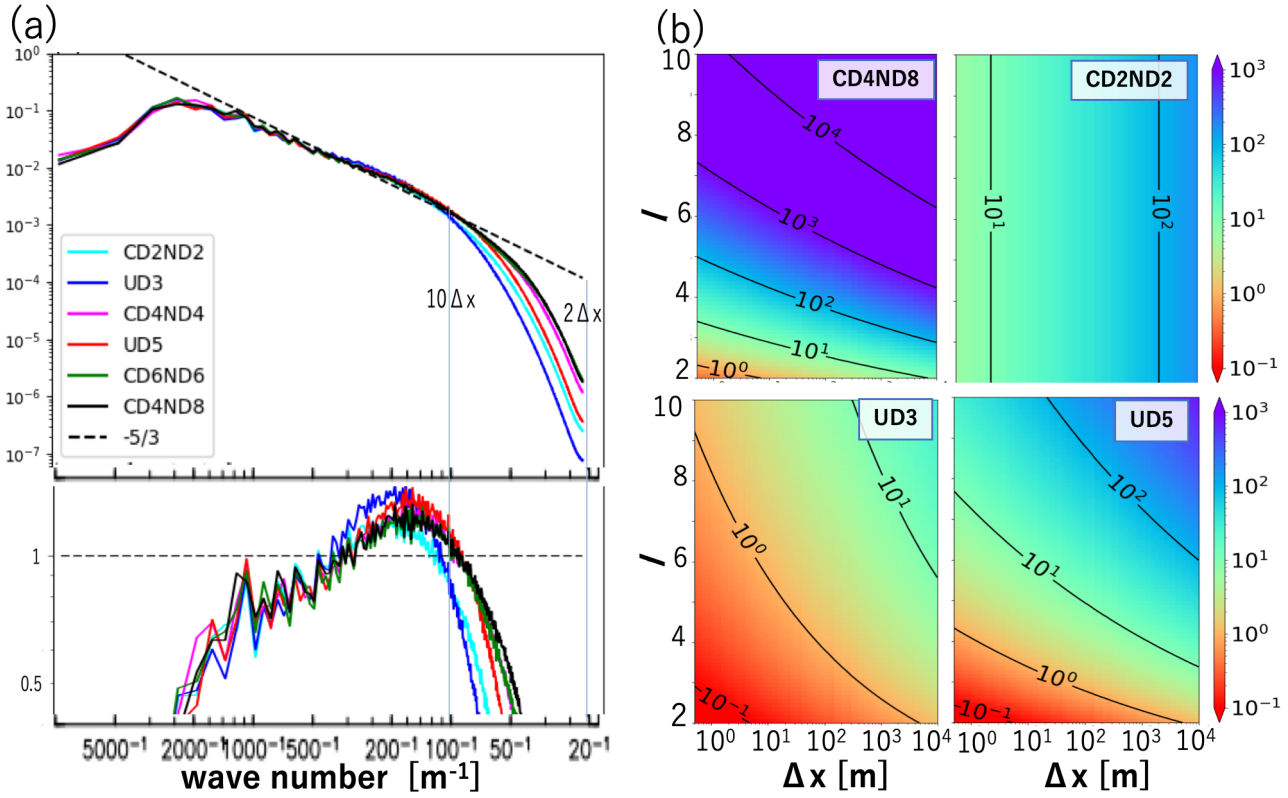

(a) (top) Energy spectra for 3-dimensional wind speed obtained by experiments with various advection schemes. (bottom) The ratios of energy spectra for each experiment to that denoted by dashed line in top figure. (b) R(Δx,l) for each experiment. It is calculated as |U|=5 m/s and η=0.01.

©2020. Japan Geoscience Union. All Right Reserved.

Surface zonal flows induced by anelastic thermal convection in a rapidly rotating spherical shell

*Youhei SASAKI[1], Shin-ichi Takehiro[2], Keiichi Ishioka[3], Takeshi Enomoto[4]

1. Institute of Fundamental Sciences, Faculity of Science and Engineering, Setsunan University, 2. Research Institute for Mathematical Sciences, Kyoto University, 3. Department of Earth and Planetary Sciences, Kyoto University, 4. Disaster Prevention Research Institute, Kyoto University

Banded structures and alternating zonal jets observed in the surface atmospheres of Jupiter and Saturn have attracted many researchers in planetary atmospheric sciences, however, satisfactory physical explanations and understandings are not yet obtained. In this study, we perform massive parallel numerical experiments treating both small scale convection and planetary scale flows simultaneously, solve fine structures of turbulent motions which have not yet been resolved by the previous numerical models so far, and try to illustrate dynamical origin of global scale structures of surface flows of Jovian planets.

For this purpose, we developed and parallelized an anelastic model of thermal convection in a rotating spherical shell considering basic radial density variation. The spectral transformation library used in this model was improved to introduce MPI parallelization not only in the latitude direction but also in the radial direction. As a result, we succeeded in increasing the number of parallel processes which had been limited by the number of latitudinal grid points, and more massive parallel numerical experiments became possible.

Followup and extended numerical experiments of Case 2 in Gastine al. (2014) were performed with the developed anelastic convection model. When the time integration is as short as viscous diffusion time, the latitudinal profile of induced surface zonal flow is consistent with that of Gastine et al. (2014). However, when time integration is further extended, prograde surface zonal flows in high latitudes start to develop, and become prominent. This result suggests that surface zonal flows obtained by the previous studies may not be statistically steady states.
We started to perform highly resolved numerical simulation of anelastic rotating spherical convection with full spherical domain. The numerical setup follows the case5 of Gastine eta al. (2014), which is one of the highest resolution and most rapid rotation cases performed so far, however, Gastine et al. do not treat full spherical domain but assumed eight-fold symmetry in the longitudinal direction. In the present stage, the broad and strong equatorial prograde jet emerges. The weak but alternating zonal jets are also generated in mid and high latitudes. However, kinetic energy does not steady but still increases, meaning that the system does not reach statistically steady state. It is necessary to continue the time integration and to observe the transition and characteristics of banded structures.

Keywords: Jovian planets, Anelastic system

©2020. Japan Geoscience Union. All Right Reserved.

Local node refinement using the Schmidt transform for RBF advection models

*Koji Ogasawara[1], Takeshi Enomoto[2]

1. Graduate School of Science, Kyoto University, 2. Disaster Prevention Research Institute, Kyoto University

Large-scale geophysical fluid motions are dominated by the advection process. Derivatives with rapid change using Eulerian advection require high resolution node. In this study, local node refinement was assessed in the test case in which two vortices roll-up on the sphere.

We approximated a spatial derivative operator with Radial Basis Functions (Flyer and Wright 2007)[1]. Radial Basis Functions (RBF) has the following useful characteristics. 1) RBF's are not linked to any coordinate systems because RBF's depend only on the distance between from node. For example, RBF's are free from the singularities of the derivative operators at the poles in spherical coordinates. 2) An RBF method is easy to perform calculation and does not increase complexity at higher dimensions. 3) The node placement is flexible to allow the use of more uniform nodes on the sphere.

Spectral accuracy can be achieved in advection on quasi uniform nodes. However, increase in the number of nodes make the condition number of interpolating matrix larger, therefore accurate calculation with high resolution nodes is not trivial. Thus, local refinement is attempted in this study.

Flyer and Lehto (2010)[2] constructed locally refined nodes near the vortex center from minimum energy nodes with electronic repulsion and showed that local refinement improves accuracy. However, the node generation with electronic repulsion that uses iterative numerical optimization may suffer from a convergence problem. Therefore, Schmidt transform that refines nodes deterministically is adopted. the test of vortex roll-up was conducted to investigate the relationship between the magnification parameter and accuracy, and improvement with the local node refinement. The shape parameter is varied by according to the minimum distance between nodes. Varying the shape parameter and improvement of the condition number with node refinement. However, excessive node clustering makes the maximum shape parameter too large. Consequently, excessive node clustering deteriorate approximation of derivative matrix. In the test case with local nodes refinement,

accuracy is improved by a factor of 7 approximately in normalized error l1 and l2.

Acknowledgements

This study was supported by JSPS KAKENHI JP19H05605.

Reference

[1] Flyer, N., G.B. Wright, J. Comput. Phys. 226 (2007) 1059–1084.

[2] Flyer, N. and E. Lehto, J. Comput. Phys 229 (2010) 1954–1969.

©2020. Japan Geoscience Union. All Right Reserved.

Keywords: geophysical fluid dynamics, advection scheme, radial basis function

©2020. Japan Geoscience Union. All Right Reserved.

Evolution of orbits of Trans Neptunian Objects in the Galactic Potential

*Yoko Funato[1]

1. University of Tokyo

Recently many distant Trans Neptunian Objects (TNOs) have been discovered. The range of their semi-major axes is in 100 AU to near 1000 AU.

Owing to the increasing number of the distant TNOs, the statistical properties of their orbits become clear. One of their characteristic properties is reported by Batygin and Brown (2016, AJ, 151). They reported a clustering of orbital elements of distant and eccentric TNOs. They found that the directions of periherions of TNOs with large semi-major axes and high eccentricities are clustering.

They argue that the clustering is explained by the 9th planet. But the 9th planet has not been discovered yet. There may be another reason for the clustering.

The Solar System is in the Galaxy. The Galactic gravitational field is rarely taken into account in the study of dynamical evolution of the Solar System. One of the reason may be its estimated weakness. It is weak if the Galaxy is regarded as a sphere. However the Galaxy is not a sphere. It is composed of a disk and a bar or spiral arms. If we consider such a structure, its gravitational field is not weak. And it is not known how it affects the orbital evolution of TNOs.

In this study, we numerically integrated the evolution of TNO's orbits in a galaxy model which mimics the potential field by the Galactic disk. We found that the Galactic potential causes large variations in orbital elements of TNOs. We also found that the direction of perihelion tends to turn towards the Galactic Center.

Our result suggests that the clustering of distant TNOs's orbits is caused by the Galactic Field.

It also suggests that the structure and dynamical evolution of the Galaxy has affected the orbital and dynamical evolution of planets and small objects in the Solar System and, therefore, the importance of the study of evolution of the Solar System in the more realistic Galaxy model.

Keywords: Trans Neptunian Object, Planet 9, The Galaxy

©2020. Japan Geoscience Union. All Right Reserved.

©2020. Japan Geoscience Union. All Right Reserved.

[J] Poster | M (Multidisciplinary and Interdisciplinary)：M-GI General Geosciences, Information Geosciences & Simulations

[M-GI41] Earth and planetary informatics with huge data management

convener:Ken T. Murata(National Institute of Information and Communications Technology), Rie Honda(Department of Science and Technology, System of Natual Science, Kochi University), Susumu Nonogaki(Geological Survey of Japan, National Institute of Advanced Industrial Science and Technology), Takeshi Horinouchi(Faculty of Environmental Earth Science, Hokkaido University)

Increasingly large and complex data are produced by observations and numerical simulations in earth and planetary sciences. The target of this session is to discuss a broad range of practices and new knowledge of informatics, international standard and modelling, including techniques for large-scale data processing and numerical simulation, data preservation and publication, data transfer and collection and other data technologies with a vision to advance an emerging data-intensive science, namely "geoplanetary informatics".

[MGI41-P01] Himawari Data Transfer to Asian Countries

*Praphan Pavarangkoon[1], Ken T. Murata[1], Kazunori Yamamoto[1], Atsushi Higuchi[2], Takamichi Mizuhara[3], Yuya Kagebayashi[3], Ayahiro Takaki[3], Kazuya Muranaga[4], Chalermpol Charnsripinyo[5], Bayani Benjamin R. Lara[6], Joel Joseph S. Marciano, Jr.[6], Eric Yen[7], Simon C. Lin[7], Keiichiro Fukazawa[8] (1.National Institute of Information and Communications Technology, Japan, 2.Center for Environmental Remote Sensing, Chiba University, Japan, 3.CLEALINK TECHNOLOGY Co., Ltd., Japan, 4.Systems Engineering Consultants Co., Ltd., Japan, 5.National Electronic and Computer Technology Center, Thailand, 6.Advanced Science and Technology Institute, Department of Science and Technology, Philippines, 7.Academia Sinica Grid Computing Centre, Taiwan, 8.Academic Center for Computing and Media Studies, Kyoto University, Japan)

[MGI41-P02] An Initial Report of StarBED for HpFP Development

*Praphan Pavarangkoon[1], Ken T. Murata[1], Tsubasa Yumura[1], Kazunori Yamamoto[1], Takamichi Mizuhara[2], Yuya Kagebayashi[2], Yasunori Kakizawa[2], Kazuya Muranaga[3] (1.National Institute of Information and Communications Technology, Tokyo, Japan, 2.CLEALINK TECHNOLOGY Co., Ltd., Kyoto, Japan, 3.Systems Engineering Consultants Co., Ltd., Tokyo, Japan)

[MGI41-P03] HpFP: development of high-speed data transfer applications (1)

Yasunori Kakizawa[1], Ayahiro Takaki[1], *Takamichi Mizuhara[1], Yuya Kagebayashi[1], Praphan Pavarangkoon[3], Kazuya Muranaga[2], Kazunori Yamamoto[3], Ken T. Murata[3] (1.CLEALINK TECHNOLOGY CO., LTD., 2.SEC CO., LTD., 3. National Institute of Information and Communications Technology)

[MGI41-P04] Programming Environment of Visual IoT Tools Working on Single-Board Computer (Raspberry Pi) (3)

Toshiki Aoki[1], *Takamichi Mizuhara[1], Ken T. Murata[2], Kazunori Yamamoto[2], Yakanari Yamasaki[2], Praphan Pavarangkoon[2], Kazuya Muranaga[3] (1.CLEALINK TECHNOLOGY CO., LTD., 2.National Institute of Information and Communications Technology, 3.SEC CO., LTD.)

[MGI41-P05] Investigation of Raspberry Pi and development of intelligent watch-dog

Mehdad Shirazi[1], *Takamichi Mizuhara[1], Toshiki Aoki[1], Ken T. Murata[2], Kazunori Yamamoto[2], Kazuya Muranaga[3], Praphan Pavarangkoon[2] (1.CLEALINK TECHNOLOGY CO., LTD., 2.National Institute of Information and Communications Technology, 3.SEC CO., LTD.)

[MGI41-P07] Communication Experiment of the Sensor Network in Chikuma City

*Kohei Mizuani[1], Takeshi Ken Murata[1], Kazunori Yamamoto[1], Praphan Pavarangkoon[1], Kazuya Muranaga[2], Takamichi Mizuhara[3] (1.National Institute of Information and Communications Technology, 2.Systems Engineering Consultants Co., LTD, 3.CLEALINKTECHNOLOGY Co.,Ltd.)

[MGI41-P08] **A Trial to Identify Problems in Multi-disciplinary Data Usage: Study of Environmental Influences on Economic Activities in 18th-19th Centuries including the Sunspot Dalton Minimum**

*Takashi Watanabe[1] (1.ICSU World Data System International Programme Office)

[MGI41-P09] Large-scale 4-D WebGIS applications to synchronize space and time (1)

Kazuya Muranaga[2], *Ken T. Murata[1], Kazunori Yamamoto[1], Praphan Pavarangkoon[1] (1.National Institute of Information and Communications Technology, 2.Systems Engineering Consultants Co., LTD.)

[MGI41-P10] **Improvement of database system of research vessel operation information and causal analysis of past cruise downtime**

*Yasuko Yamagishi[1], Ken Yatsu[1], Kazuhiko Kashiwase[1], Tetsuji Maki[1], Hide Sakaguchi[1] (1.Japan Agency for Marine-Earth Science and Technology)

Himawari Data Transfer to Asian Countries

*Praphan Pavarangkoon[1], Ken T. Murata[1], Kazunori Yamamoto[1], Atsushi Higuchi[2], Takamichi Mizuhara[3], Yuya Kagebayashi[3], Ayahiro Takaki[3], Kazuya Muranaga[4], Chalermpol Charnsripinyo[5], Bayani Benjamin R. Lara[6], Joel Joseph S. Marciano, Jr.[6], Eric Yen[7], Simon C. Lin[7], Keiichiro Fukazawa[8]

1. National Institute of Information and Communications Technology, Japan, 2. Center for Environmental Remote Sensing, Chiba University, Japan, 3. CLEALINK TECHNOLOGY Co., Ltd., Japan, 4. Systems Engineering Consultants Co., Ltd., Japan, 5. National Electronic and Computer Technology Center, Thailand, 6. Advanced Science and Technology Institute, Department of Science and Technology, Philippines, 7. Academia Sinica Grid Computing Centre, Taiwan, 8. Academic Center for Computing and Media Studies, Kyoto University, Japan

Quick dissemination of weather information to Asian countries in the risk region is of great significance from the viewpoint of weather disaster mitigation. Geostationary meteorological satellites play an important role to provide continuous atmospheric observations both for weather forecasting and for monitoring a wide range of environmental phenomena. The third-generation geostationary meteorological satellites equipped with highly improved imagers, e.g., Himawari-8/9 provide a huge amount of Earth observation data. In this research, we propose a high-speed data transmission system using a file transfer tool, called high-performance copy (HCP). The HCP is high-performance and flexible protocol 2 (HpFP2)-based and is a server-client command line tool, which works on several operating systems (OSs) such as Linux and Windows. It can push files to another server or pull files from another server. With the advantages of the HpFP2, the HCP is able to transfer files effectively under networks with high latency and packet loss, e.g., international networks. In addition, the HCP is a great way to synchronize files that a user can maintain on more than one system. In the proposed high-speed data transmission system, a set of tiled pyramid image files is generated every 10 minutes on the Himawari-8 real-time web in Japan, and then transferred to the mirror websites in Thailand, Philippines, and Taiwan. Moreover, we have a plan to provide the archive data to Asian countries in the near future. The results show that our system is effective and appropriate for real use. This suggests that the proposed high-speed data transmission system has a potential for deployment in other Asian countries.

Keywords: Himawari, Earth Observation, Data Transfer, HpFP

©2020. Japan Geoscience Union. All Right Reserved.

An Initial Report of StarBED for HpFP Development

*Praphan Pavarangkoon[1], Ken T. Murata[1], Tsubasa Yumura[1], Kazunori Yamamoto[1], Takamichi Mizuhara[2], Yuya Kagebayashi[2], Yasunori Kakizawa[2], Kazuya Muranaga[3]

1. National Institute of Information and Communications Technology, Tokyo, Japan, 2. CLEALINK TECHNOLOGY Co., Ltd., Kyoto, Japan, 3. Systems Engineering Consultants Co., Ltd., Tokyo, Japan

With the rapid development of big data and cloud computing technologies, Earth observation (EO) data generated by satellites and sensors are transferred to remote cloud data centers for analysis and storage. Real-time monitoring and tracking applications such as disaster management, military, agriculture, etc. utilize these EO data and play an important role in human life. However, it is hard to handle a large and growing amount of these EO data, and to achieve them in real time. We develop a novel transport protocol, named high-performance and flexible protocol (HpFP), to enhance the efficiency of data transfer of the EO data. The HpFP is designed on the top of user datagram protocol (UDP), but is a connection-oriented and reliable stream-type protocol. The original HpFP is designed first for specified networks and puts more emphasis on latency and packet loss tolerances than fairness and friendliness, while the HpFP2 is more suitable for real network environments. To accommodate different usage scenarios, we complete four operating modes of HpFP2: aggressive, fair, fast-start, and modest modes. StarBED is constructed and operated by National Institute of Information and Communications Technology (NICT), Japan as a large-scale, general-purpose Internet simulator connected by network switches to the 728 servers (nodes). In this research, we present an initial report of StarBED for HpFP development. We conduct to evaluate our HpFP2 under real-time situations with several QoS requirements using the StarBED. The details of setup and usage of the StarBED for HpFP development are presented. In addition, the experiment results are also presented and discussed.

Keywords: HpFP, Data Transfer, Earth Observation, Real-Time Monitoring

©2020. Japan Geoscience Union. All Right Reserved.

HpFP: development of high-speed data transfer applications (1)

Yasunori Kakizawa[1], Ayahiro Takaki[1], *Takamichi Mizuhara[1], Yuya Kagebayashi[1], Praphan Pavarangkoon[3], Kazuya Muranaga[2], Kazunori Yamamoto[3], Ken T. Murata[3]

1. CLEALINK TECHNOLOGY CO., LTD., 2. SEC CO., LTD., 3. National Institute of Information and Communications Technology

For LFNs (Long-Fat Networks) with 10 Gbps or more and satellite networks with large latency, a variety of TCP-based protocols have been proposed which show high performance on large latency network conditions. However, such TCP protocols are essentially unable to archive large bandwidth on high latency networks accompanied with packet-losses that are inevitable on practical LFNs or satellite networks. To overcome this issue, we designed a new data transfer protocol on TCP/IP transport layer built on top of UDP: High-performance and Flexible Protocol (HpFP). It constantly monitors latency (RTT) and packet losses, and conducts rate control and retransmission control based on them to enable higher bandwidth data transfer than 10 Gbps even on packet-loss conditions over LFNs. The basic concepts are addressed and protocol design of the HpFP are discussed. An applications to transfer many data files in small size (e.g., 1MB x 10000 files) with almost wire-rate bandwidth (10 Gbps) is also addressed. In this study we develop a tool to bind multiple connection of HpFP aiming at higher throughput on a broadband network faster than 100Gbps. In the near future, big data transfer with high speed is expected on LFNs such as SINET5.

Keywords: LFN, SINET, High-performance network

©2020. Japan Geoscience Union. All Right Reserved.

Programming Environment of Visual IoT Tools Working on Single-Board Computer (Raspberry Pi) (3)

Toshiki Aoki[1], *Takamichi Mizuhara[1], Ken T. Murata[2], Kazunori Yamamoto[2], Yakanari Yamasaki[2], Praphan Pavarangkoon[2], Kazuya Muranaga[3]

1. CLEALINK TECHNOLOGY CO., LTD., 2. National Institute of Information and Communications Technology, 3. SEC CO., LTD.

The recent emergence of low-cost single board computers such as Raspberry Pi and Arduino, which are used as sensing devices with connectivity to Internet gateways and cloud services, has led to Internet of Things (IoT) architectures in the real world. Visual IoT is one of the classes of IoT that poses crucial end-to end challenges due to the need for sensing and processing of visual data. One of the significant roles of the visual IoT is information extraction from images by using image recognition techniques. In this paper, we present a programming environment of visual IoT on Raspberry Pi, and develop a couple of applications. The first one is an application for real-time information extraction and the second one is an augmented reality (AR)-oriented application. The performance of both applications is examined in outdoor fields using 4G LTE mobile networks to prove that our environment has a potential for many types of visual IoT devices. Our presentation this year focuses on a remote operation function of PTZ-type IP camera (https://www.youtube.com/watch?v=cNCGVany0BQ).

Keywords: IoT, Programming, Visual IoT

©2020. Japan Geoscience Union. All Right Reserved.

Investigation of Raspberry Pi and development of intelligent watch-dog

Mehdad Shirazi[1], *Takamichi Mizuhara[1], Toshiki Aoki[1], Ken T. Murata[2], Kazunori Yamamoto[2], Kazuya Muranaga[3], Praphan Pavarangkoon[2]

1. CLEALINK TECHNOLOGY CO., LTD., 2. National Institute of Information and Communications Technology, 3. SEC CO., LTD.

Raspberry Pi is one of the single-board computers in low price. Raspberry Pi3 (RPi3) and Raspberry Pi zero (RPi zero) are now on sale. Recently Raspberry Pi4 (RPi4) shows up with higher specifications than RPi3. Since they cost less than 100 US dollars, there are many users of them for field sensors and measurements in Earth science domains. Instead of the cost effects, RPi is known as its vulnerability and instability. We performed a variety of instability test on RPi zero and RPi3 to find that RPi zero is more unstable than RPi3. Many of the instabilities are believed to be caused of heat effects on CPU. However, in our examinations, both of them did not show clear dependence of irregular stopping of system on CPU temperatures. In order to overcome this vulnerability issue, we designed and implemented a new watch-dog module for RPi. The watch-dog always monitors Rasbian OS on RPis, and also provide scheduling of periodic shutdown and wake-up as well.

Keywords: IoT, Raspberry Pi

©2020. Japan Geoscience Union. All Right Reserved.

Communication Experiment of the Sensor Network in Chikuma City

*Kohei Mizuani[1], Takeshi Ken Murata[1], Kazunori Yamamoto[1], Praphan Pavarangkoon[1], Kazuya Muranaga[2], Takamichi Mizuhara[3]

1. National Institute of Information and Communications Technology, 2. Systems Engineering Consultants Co., LTD, 3. CLEALINKTECHNOLOGY Co.,Ltd.

Internet of Things (IoT) where data of many kinds of sensors are collected through the Internet may become one of important social infrastructure technologies. Various sorts of data collection demonstration experiments through wireless technologies in many areas have been implemented to improve public services and solve problems in the community through use and application of the collected data. We are conducting data collection experiments using private LoRa (Long Range), which is one of the low-power wide area (LPWA) communication technologies, BLE and LTE in Chikuma city, Nagano prefecture, Japan. In this experiment, we set up LoRa relay stations at ten locations in the city like the governmental buildings. The LoRa relay stations have IoT Cameras and high-quality images are transferred. In addition, beacon transmitters were installed in the community buses and other cars. The location and time information were transferred from the cars to the NICT Science Cloud servers in real time through the relay stations. Weather stations are set near the all relay stations and data are transferred by these LoRa relay stations. A few tenths of small environment sensors are deployed in Togurakamiyamada Junior High School. These sensors are connected by BLE to LTE relay stations. Data are monitored in real time at WEB site. Many kinds of sensors could be connected through this sensor network and new applications are expected.

Keywords: IoT, Sensor network, LoRa

©2020. Japan Geoscience Union. All Right Reserved.

A Trial to Identify Problems in Multi-disciplinary Data Usage: Study of Environmental Influences on Economic Activities in 18th-19th Centuries including the Sunspot Dalton Minimum

*Takashi Watanabe[1]

1. ICSU World Data System International Programme Office

The promotion of data-led multi-disciplinary researches will be important in the Open Science era but there still exist problems in the provision and usage of data crossing disciplines. To identify problems in data usage to be encountered by out-of-the-discipline scientists, a trial of data-led study of environmental influences on economic activities in Europe in the 18th/19th century is performed because this interval is characterized by revolutionary socio-economic movements under a relatively cold environment in the last half of the Little Ice Age. The majority of environmental data in this interval came from research works of reconstructions basing on proxy records, but we saw inconsistency among datasets in some cases. Having “standardized data” is highly desired in wider data usage by nonprofessionals. In this provisional analysis, we discuss the environmental aspect of the apparent correlation seen between the sunspot number and the wheat price at the London Market shown in Figure 1. A decrease of the Summertime precipitation in the Dalton Minimum of the solar activity (1790-1830) is shown to be the principal reason for recorded poor harvesting and high market prices of wheat in England in the interval. Solar connection through the North Atlantic Oscillation is suggested although the effect of strong volcanic eruptions (e.g. Tambola in1815) should not be ignored. In conclusion, the period of the 18th/19th century will be pertinent to the collaborative data-led study of the basic influence of the natural environment on socio-economic activities in the period before the anthropological environmental changes became prominent.

Figure 1. Time series of yearly sunspot numbers (x 0.1) and the wheat price in England (shillings per bushel) in the interval of 1700-1910. The interval of small sunspot numbers in 1790 - 1830 is called as the "Dalton Minimum".

Keywords: Open Science, Solar Activity, Environmental Change, Economics

©2020. Japan Geoscience Union. All Right Reserved.

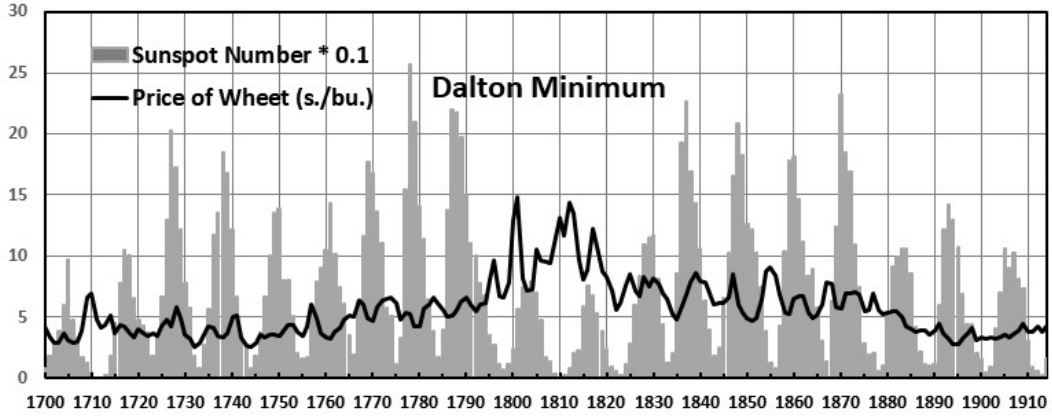

©2020. Japan Geoscience Union. All Right Reserved.

Large-scale 4-D WebGIS applications to synchronize space and time (1)

Kazuya Muranaga[2], *Ken T. Murata[1], Kazunori Yamamoto[1], Praphan Pavarangkoon[1]

1. National Institute of Information and Communications Technology, 2. Systems Engineering Consultants Co., LTD.

Various types of earth observation data, including meteorology and environment data, have become in large-scale, and Web applications for visualizing and analyzing them have become increasingly complex. On the other hand, cooperative visualization between data is essential from interdisciplinary viewpoints, thus WebGIS technologies that integrates and visualizes them are required. Authors have developed STARS (Spatially and Temporally Acquired Records Synchronizer), which is a technique to virtually link the time and space of each browser. WebGIS tools so far have been able to display space, but few of them provides functions of time management. We have developed and released “Timeline”, a jquery plugin for time management that is available with various WebGIS tools (http://k2go.jp/public/Timeline/). We present a method of synchronizing multiple WebGIS or graph applications using Timeline, and demonstrate examples of these synchronizations.

©2020. Japan Geoscience Union. All Right Reserved.

Improvement of database system of research vessel operation information and causal analysis of past cruise downtime

*Yasuko Yamagishi[1], Ken Yatsu[1], Kazuhiko Kashiwase[1], Tetsuji Maki[1], Hide Sakaguchi[1]

1. Japan Agency for Marine-Earth Science and Technology

Over the last 10 years, the ship time of JAMSTEC (Japan Agency for Marine-Earth Science and Technology) research vessels has been reduced drastically. It is simply due to a decrease in the number of vessels and the budget for research cruises. However under such situation, managing section of research cruise in JAMSTEC needs to plan the most optimal cruise to carry out the necessary oceanic observations. At present, JAMSTEC has to plan all research cruises for next fiscal year one year before. In order to provide useful information when planning future research cruise, we started to compile research vessel operation information of past cruises and to estimate downtime of them. Downtime is the period during which the observations and/or cruise are interrupted due to bad weather, troubles of observation equipments, or other causes, and is one of the important indicators to judge whether the cruise successfully carried out or not. Our project started in FY 2016, and we developed database system of research vessel operation information. This database can provide the downtime of the research cruises from FY 2008 to present. We have improved the database system to estimate more accurate downtime and to add needed new data, e.g., research sea area, kinds of observations, and so on for causal analysis of the downtime. In this study, we analyze the new downtime data of past research cruise. We will show the trend of the downtime and search the factors that have the most impact on the downtime. We think that this developed database system and the results of the causal analysis of the downtime of the past cruises enable to provide useful information for the planning of the future cruises. Acknowledgments: we are grateful to Mr. Morisaki and Ms. Sada for their supports to make data stored into the database system.

©2020. Japan Geoscience Union. All Right Reserved.

[J] Poster | M (Multidisciplinary and Interdisciplinary)：M-AG Applied Geosciences

[M-AG44] Dynamics of radionuclides emitted from Fukushima Dai-ichi Nuclear Power Plant in the environment

convener:Daisuke Tsumune(Central Research Institute of Electric Power Industry), Yoshio Takahashi(Department of Earth and Planetary Science, Graduate School of Science, The University of Tokyo), Yuichi Onda(Center for Research on Isotopes and Environmental Dynamics, University of Tsukuba), Kazuyuki Kita(Faculty of Science, Ibaraki University)

The Great East Japan Earthquake caused the severe accident in the TEPCO Fukushima Dai-ichi Nuclear Power Plant (FDNPP), leading to emission of huge amount of radionuclides to the environment. They have been transported and diffused by atmospheric motion, depositing them to soil and vegetation. Deposited radionuclides are dynamically shifted in the earth environment; atmosphere, soil, inland water, ocean, and ecosystem. To understand this dynamic shift in the environment and for the long-term prediction of the disaster by the radionuclides, investigation and discussion based on not only the earth sciences including ecology but also on the radiochemistry and other related sciences. This session focus on various efforts to understand the dynamic behavior of radionuclides emitted from FDNPP accident in the earth system as well as to predict their influences on the environment, furthermore, to develop as global migration studies by generalization, It is expected that this session will offer a good opportunity to discuss radionuclides in the earth environment from wide aspect and to exchange information in various research fields.

[MAG44-P01] The time-fractional diffusion equation as the governing equation of the concentraiton of Cs-137 in the environment

★Invited Papers

*Yuko Hatano[1], Eiichi Suetomi[1], Yukiko Okada[2], Naoto Hagura[2], Takafumi Uchiyama[2] (1.Graduate School of Systems and Information Engineering, University of Tsukuba, 2.Atomic Energy Research Laboratory, Tokyo City University)

[MAG44-P02] Atmospheric resuspension of insoluble Cs radioactive particles found in polluted area in Fukushima

Peng Tang[1], Kohtaro Hatanaka[1], *Kazuyuki Kita[1], Yukihiko Satou[2], Takeshi Kinase[3], Kouji Adachi[3], Yuji Zaizen[3], Kazuhiko Ninomiya[4], SHINOHARA ATSUSHI[4], Yasuhito Igarashi[5] (1.Faculty of Science, Ibaraki University, 2.JAEA, 3.MRI, 4.Osaka University, 5.Institute for Integrated Radiation and Nuclear Science, Kyoto University)

[MAG44-P03] Contribition of bioaerosols to the atmospheric resuspension of radioactive cesium in summer and autumn

*Kazuyuki Kita[1], Naho Hayashi[1], Koutaro Minami[1], Teruya Maki[2], Kentaro Hosaka[3], Yasuhito Igarashi[4] (1.Faculty of Science, Ibaraki University, 2.Kanazawa university, 3.National musium of nature and science, 4.Institute for Integrated Radiation and Nuclear Science, Kyoto University)

[MAG44-P04] Preferential infiltration of the Fukushima accident-derived radiocesium into soil in the vicinity of Japanese cedar trunk

*Hikaru Iida[1], Hiroaki Kato[1], Tomoki Shinozuka[1], Satoru Akaiwa[1], Tatsuya Yokoyama[1], Sean Hudson[1], Janice Hudson[1], Yuichi Onda[1] (1.Center for Research in Isotopes and Environmental Dynamics, University of Tsukuba)

[MAG44-P05] Variation of soil water content in litter and soil layer impacts radiocesium air dose in the forests of Yamakiya District, Fukushima Prefecture

*Janice Elaine Hudson[1], Momo Kurihara[2], Sean Andrew Hudson[1], Kato Hiroaki[1], Yuichi Onda[1] (1.University of Tsukuba, 2.National Institutes for Quantum and Radiological Science and Technology)

[MAG44-P06] Difference of ^{137}Cs concentration between Preferential flow and Matrix in forest soil in Fukushima Prefecture

*Ono Tetsuya[1], Junko Takahashi[2], Tetsuya Sasaki[2], Yuichi Onda[2] (1.Doctoral program in integrative environment and biomass science, Graduate school of life and environmental science, University of Tsukuba, 2.Center for reserch in isotopes and environmental dynamics, University of Tsukuba)

[MAG44-P07] Formation mechanism of radiocesium concentration in throughfall in a cedar forest

*Tomoki Shinozuka[1], Hiroaki Kato[2], Yuichi Onda[2], Satoru Akaiwa[1] (1.Doctoral Program in Integrative Environment and Biomass Sciences, Graduate School of Life and Environmental Sciences, University of Tsukuba, 2.Center for Research on Isotope and Environmental Dynamics, University of Tsukuba)

[MAG44-P08] Change in the elution behavior of dissolved radiocesium and physical property in the decay degree of litter of deciduous broad-leaved trees

*Yoshito Sasaki[1], Tadafumi Niizato[1], Satomi Ito[1], Takayoshi Watanabe[1] (1.Japan Atomic Energy Agency)

[MAG44-P09] Dynamics of radioactive cesium in forest-stream ecosystem in a mountainous watershed

*Yuiko Chino[1], Takashi Gomi[1], Yoshito Oyama[1] (1.Department of Agriculture, Tokyo University of Agriculture and Technology)

[MAG44-P10] Seasonal change and formation factors of dissolved radiocesium concentration in a headwater catchment after the Fukushima Dai-ichi Nuclear Power Plant accident

*Satoru Akaiwa[1], Hiroaki Kato[2], Yuichi Onda[2], Tomoki Shinozuka[1] (1.Doctoral Program in Integrative Environment and Biomass Sciences, University of Tsukuba, 2.Center for Research in Isotopes and Environmental Dynamics, University of Tsukuba)

[MAG44-P11] Change in the spatial distribution of the air dose rate in the riverside park affected by decontamination and floods

*Takuhei Yamasaki[1], Satoshi Suzuki[1] (1.Fukushima Prefectural Centre for environmental Creation)

[MAG44-P12] Accumulation and redistribution of ^{137}Cs on floodplains along the Abukuma River

★Invited Papers

*Yoshifumi Wakiyama[1], Alexei Konoplev[1], Valentin Golosov[2], Maxim Ivanov[2], Mikhail Komissarov[3] (1.Institute of Environmental Radioacitivity, Fukushima Universiy, 2.Faculty of Geography, M.V. Lomonosov Moscow State University, 3.Ufa Institute of Biology UFRC, Russian Academy of Science)

[MAG44-P13] Re-circulation of ^{137}Cs concentrations in surface seawater in the western North Pacific Ocean

★Invited Papers

*Yayoi Inomata[1], Michio Aoyama[2] (1.Kanazawa University, Institute of Nature and Environmental Technology, 2.Tsukuba University, Center for Research in isotopes and Environmental Dynamics)

[MAG44-P15] Distribution of dissolved and particulate radiocesium from the downstream of rivers to the costal waters off Fukushima.

*Hyoe Takata[1], Tatsuo Aono[2], Michio Aoyama[3], Hideki Kaeriyama[4], Mutsuo Inoue[5] (1.Fukushima Univ., 2.QST, 3.Tsukuba Univ., 4.FRA, 5.Kanazawa Univ.)

The time-fractional diffusion equation as the governing equation of the concentraiton of Cs-137 in the environment

*Yuko Hatano[1], Eiichi Suetomi[1], Yukiko Okada[2], Naoto Hagura[2], Takafumi Uchiyama[2]

1. Graduate School of Systems and Information Engineering, University of Tsukuba, 2. Atomic Energy Research Laboratory, Tokyo City University

After almost 10 years of the Fukushima accident, measurement data have been accumulated in various environment. We propose a new model on how the radioactive cesium decreases in the long time such as a decade, other than the box model. The box model, for Cs-137 in the lake water for example, assumes instantaneous, homogeneous mixing of solute and water, two or three boxes are connected with each other to reproduce the data of the Cs-137 concentration (IAEA-TECDOC-1143, 2000). Transfer coefficients, k, are used in the box model, that if the value of k's are constants, the exponential function exp(-kt) is intrinsic for the behavior of the concentration. In case of several boxes, the concentration should follow the sum of these exponential functions as A exp(-k1 t) + B exp(- k2 t) + ... There have been critics among several researchers that this model implies a "fatalist" attitude; it means that from the initial stage, each radionuclide is designated for its process to follow. In particular, we would meet the situation that the second exponential function appears after we have conducted a couple of years of measurement. This study is intended to improve such situations. We thus propose a new model with a time-fractional diffusion equation. Because the actual data decrease in time in such a manner that they decrease very rapidly with the exponential function at first; then, several years later, they decrease more slowly as the power function. This behavior is very similar characteristics of Mittag-Leffer function, which is the fundamental solution of the time-fractional diffusion equation (Cauchy problem). The significance of fractional time-derivative is that it can cope with the "memory" effect that every cesium particle has, the flux of cesium at a specific time at a specific location depends on the previous concentration of cesium as a power law of the time. We use the Mittag-Leffler function to reproduce actual measured concentration of Cs-137. We note that Bulgakov et al.(2002)'s study yields an semi-analytical solution of the lake concentration of Cs-137 in Bryansk, Russia as $\exp(-\lambda t)/\sqrt{t}$, which is a special case of the Mittag-Leffler function when its parameter alpha=1/2. It seems that the fractional derivatives have been used for other problems such as the geothermal energy productions (A. Suzuki et al.) and solute transport in porous media (B. Berkowitz et al.).

Keywords: diffusion; dispersion, fractional derivatives, long-term predictions

©2020. Japan Geoscience Union. All Right Reserved.

Atmospheric resuspension of insoluble Cs radioactive particles found in polluted area in Fukushima

Peng Tang[1], Kohtaro Hatanaka[1], *Kazuyuki Kita[1], Yukihiko Satou[2], Takeshi Kinase[3], Kouji Adachi[3], Yuji Zaizen[3], Kazuhiko Ninomiya[4], SHINOHARA ATSUSHI[4], Yasuhito Igarashi[5]

1. Faculty of Science, Ibaraki University, 2. JAEA, 3. MRI, 4. Osaka University, 5. Institute for Integrated Radiation and Nuclear Science, Kyoto University

By the TEPCO Fukushima Daiichi Nuclear Power Plant accident, a large amount of radio-cesium (Cs) was emitted into the environment, and was deposited on soil and vegetation. Significant part of the emitted Cs are included in so-called spherical caesium-bearing particles or caesium-rich microparticles (CsMP) . Sampling of atmospheric Cs was been conducted at a polluted area in Fukushima since 2012, and Cs bearing particles are tried to detect from the samples taken in 2015, 2016, 2018 and 2019. The particles were detected and isolated from the filter sample with micromanipulator and multi-step autoradiography with an Imaging Plate. Total 15 particles of approximate diameter between 1-2 μm were identified using Scanning Electron Microscope with both backscattered electron. They were characterized by their shape and energy dispersive spectroscopy (EDS) analysis and were categorized as so-called Type A particles. We will discuss seasonal and long-term trend of frequency of atmospheric resuspension of these Cs bearing particles, and will discuss of resuspension mechanisms.

Keywords: spherical caesium-bearing particles, atmospheric resuspension, Fukushima Daiichi Nuclear Power Plant accident

©2020. Japan Geoscience Union. All Right Reserved.

Contribition of bioaerosols to the atmospheric resuspension of radioactive cesium in summer and autumn

*Kazuyuki Kita[1], Naho Hayashi[1], Koutaro Minami[1], Teruya Maki[2], Kentaro Hosaka[3], Yasuhito Igarashi[4]

1. Faculty of Science, Ibaraki University, 2. Kanazawa university, 3. National musium of nature and science, 4. Institute for Integrated Radiation and Nuclear Science, Kyoto University

Radio-cesium emitted by the TEPCO FDNPP accident has been deposited on soil and vegetation after transpiration in the atmosphere. Re-suspension of the deposited radio cesium is increased atmospheric concentration of its radioactivity even now. Quantitative understanding of re-suspension processes of radio-cesium is essential for the modelling of radio-cesium transition from soil and vegetation via the atmosphere.
Our group showed the seasonal variation of atmospheric radio-cesium sampled in a polluted area in Fukushima (Kinase et al., 2018) and possibility that bioaerosols such as fungal spores bring radioactive cesium into the atmosphere especially in summer and autumn near forest area (Igarashi et al., 2019). In this study, quatitative estimation of contribution of bioaerosol to the atmospheric resuspenstion of atmospheric radio-cesium.
Atmospheric radio-cesium samples were obtained at a site in polluted area in Fukushima in september, 2017, on a quartz fiber filters using high volume air samplers. The radioactivty were measured with Ge-detercters, and number and volume of bioaerosols were estimeted using optical/fluorescence microscope. Radioactivity of cesium included in fungal spore was measured with fungi sampled around the observation sites. The atmospheric radio-cesium activity showed a good positive colleration with the nu,ber and volume of the bioarerosols.

Keywords: radioactive cesium, atmospheric resuspension, bioaerosols

©2020. Japan Geoscience Union. All Right Reserved.

Preferential infiltration of the Fukushima accident-derived radiocesium into soil in the vicinity of Japanese cedar trunk

*Hikaru Iida[1], Hiroaki Kato[1], Tomoki Shinozuka[1], Satoru Akaiwa[1], Tatsuya Yokoyama[1], Sean Hudson[1], Janice Hudson[1], Yuichi Onda[1]

1. Center for Research in Isotopes and Environmental Dynamics, University of Tsukuba

Stemflow takes important role on the hydrological and chemical cycling in the rhizosphere because it brings intensive rainwater input to forest soil and enhances downward infiltration of rainwater along tree root network to deep soil horizon. However, there are few studies about the effects of stemflow on rainwater infiltration mechanisms by collecting of soil water. In addition, the radiocesium derived from the Fukushima Dai-ichi Nuclear Power Plant accident is mostly intercepted by forest canopy, and transferred to forest soil by rainfall and stemflow. In particular, at the base of tree trunk, it is reported that the concentrations of radiocesium in soil increases due to contribution of stemflow with the high concentrations, and it is concerned that root uptake is promoted. However, there are studies limited to soil only, and few studies analyzed the concentrations of infiltration water that transports radiocesium.
In this study, stemflow from ceder tree, and soil water at the vicinity area of the tree roots (Rd : root downslope) and far from the trunk (Bt : between trees) are collected from a cedar forest in Namie Town, Fukushima Prefecture, Japan. Samples were collected from June 24 to December 11, 2019 with a total precipitation of 1100 mm during the period. Water volume and dissolved ^{137}Cs concentration drived from the Fukushima Dai-ichi Nuclear Power Plant accident were measured. As a result, stemflow flux per unit basal area was much larger than throughfall, and the average dissolved ^{137}Cs concentration weighted by volume was about 5.0 times larger than throughfall. Regarding to soil water, the Rd which is located in neighbor of the trunk showed greater water infiltration flux than that of the Bt, and the average amounts of infiltration water which were normalized for open rainfall depth during the whole sampling period were 1.4 times and 3.0 times larger at 5 cm and 20 cm depth for the Rd than the Bt. On the other hand, the average dissolved ^{137}Cs concentration weighted by depth was 1.6 times and 1.5 times larger at 5 cm and 20 cm depth for the Rd than the Bt, respectively. The average flux of dissolved ^{137}Cs into soil during the observation period was 1.15 kBq/m^2 and 0.73 kBq/m^2 at 5 cm depth, and 0.73 kBq/m^2 and 0.16 kBq/m^2 at 20 cm depth of Rd and Bt, respectively.
Therefore, this suggests that infiltration water flux can be increased due to contribution of stemflow input at the base of tree trunk. In particular, it was found that infiltration at the depth of 20 cm exceeded the depth of throughfall. Also, for dissolved ^{137}Cs, the concentration of soil infiltration water is higher at the base of tree trunk contributed by stemflow with the high concentration than between trees contributed by throughfall with the low concentration, and it was clarified that dissolved ^{137}Cs flux at the vicinity area of tree trunk was increased by the large amounts of infiltraion water. However, the observation data of this study alone cannot quantify the proportion of rainwater components derived from stemflow in infiltration water at the base of the trunk and the effect on radioactive cesium concentration of infiltration water. To determine the role of stemflow on rainwater infiltration flux and the concentration of dissolved elements in the rhizosphere, further analysis is required to clarify detailed infiltration mechanisms by using multiple tracer techniques such as stable isotopic composition of water and by collecting root oriented preferential flow.

Keywords: radioactive cesium, infiltration water, stemflow, forest soil, the Fukushima Dai-ichi Nuclear Power Plant accident

©2020. Japan Geoscience Union. All Right Reserved.

©2020. Japan Geoscience Union. All Right Reserved.

Variation of soil water content in litter and soil layer impacts radiocesium air dose in the forests of Yamakiya District, Fukushima Prefecture

*Janice Elaine Hudson[1], Momo Kurihara[2], Sean Andrew Hudson[1], Kato Hiroaki[1], Yuichi Onda[1]

1. University of Tsukuba, 2. National Institutes for Quantum and Radiological Science and Technology

The Fukushima Daiichi Nuclear Power Plant (NPP) accident in March of 2011 released over 1800 kbq/m2 of radiocesium over the forests of Fukushima Prefecture. Of the total deposition of radiocesium from the accident, forests in Fukushima accumulated nearly three quarters. As such, in addition to understanding the rates of stabilization in these forests, inquiries into the natural processes that may mitigate contamination to humans through air dose exposure has been of great importance in the years following the accident.
As atmospherically deposited radiocesium accumulates in the litterfall and upper soil layers of the forest, these compartments greatly contribute to the air dose rates near the forest floor. The litter layer and forest soil have high water retention capacities due to the presence of pore spaces, and the radiation dose derived from radioactive cesium on the forest floor may vary greatly depending on their moisture content. As these compartments retain moisture after rainfall events, and given water’ s properties as an absorber of gamma radiation, this pore water can have a shielding effect which may change over time as the water in soil pores drains, evaporates, and refills. Therefore, it was our goal to determine how the variation of water content in litter and soil layers impacts radiocesium air dose rates, and at which time-scale pore-water is most effective in shielding gamma radiation and reducing air dose rates within the forest. In this study, we measured the change over time of the moisture content of the litter layer and soil surface, and the change over time of the air dose rate at 40 cm and 1 m for three forest stands in the Yamakiya district in Fukushima Prefecture. Results indicate that there is a weak negative correlation between the antecedent precipitation index and air dose rate, and it appears that there are a seasonal trend and event-based periodicity to this relationship, especially within the broadleaf site. Long-term drainage processes associated with small pores seems to be the driving factor behind decreases in air dose associated with antecedent precipitation index, and the strength of the relationship between API and air dose increases when short and long-term drainage are combined.

Keywords: forest hydrology, 137Cs deposition, 137Cs inventory

©2020. Japan Geoscience Union. All Right Reserved.

Difference of ^{137}Cs concentration between Preferential flow and Matrix in forest soil in Fukushima Prefecture

*Ono Tetsuya[1], Junko Takahashi[2], Tetsuya Sasaki[2], Yuichi Onda[2]

1. Doctoral program in integrative environment and biomass science, Graduate school of life and environmental science, University of Tsukuba, 2. Center for reserch in isotopes and environmental dynamics, University of Tsukuba

On March 11, 2011, the Fukushima Daiichi Nuclear Power Plant (FDNPP) accident released large amounts of radionuclides into the environment. The environmental pollution caused by ^{137}Cs is considered to be a long-term problem. Clarifying the dynamics of ^{137}Cs in the environment will help revitalization of Fukushima Prefecture and provision of nuclear disasters in the future.

It is estimated that 70% of the ^{137}Cs released into land areas have been deposited in forested areas. In forests, radioactive cesium deposited on the canopy migrates to the land surface, and most of the radiocesium is now present in soil surface nine years after the accident. Radioactive cesium in soil surface deposited on land surface has gradually penetrated deeper soil layer over time. On the other hand, the mechanism of vertical migration of radioactive cesium in soil has not been elucidated exactly. Especially, infiltration by rainfall, biological disturbance, migration of soil particles, and preferential flow are regarded as important mechanism of downward migration.

The preferential flow is a flow of water that moves quickly downward through the macro pore in soil due to gravity. A study in swiss using dye tracer showed that ^{137}Cs concentration in stained soil (Preferential flow) are higher than in unstained soil (Matrix). However, although the method of this study can show the difference between only the concentration of radioactive cesium in the preferential flow and the matrix, it cannot show the total amount of radioactive cesium at each depth. The purpose of this study is to quantitatively clarify the influence of preferential flow on the vertical migration of radioactive cesium in soil.

The study was conducted on a plots of 1 m by 2 m situated in a cedar forest in the Akougi district of Namiemachi, Futabagun, Fukushima prefecture affected by the FDNPP accident. The soil is an acidic brown cambisol. To stain the preferential flow paths in the soil, we applied 10 L of deionized water containing 2 g L^{-1} rhodamine B with a portable sprinkling device. Two days after dye application, the scraper plate was firmly secure at two points near the tree and far away from the tree in the plot. The soil inside the fixed scraper plate was collected vertically downward at each depth. The sampling depth were set to 0-1 cm, 1-2 cm, 2-4 cm, 4-6 cm, 6-10 cm. At this time, the soil was collected separately into stained soil and unstained soil with spoons. By covering the area around the plot with a shading sheet and using blue light, the fluorescent dye was excited and the dyed soil was clearly visible. The collected samples was dried in a oven at 40 ℃ and sieved through a 2 mm sieve. Thereafter, the concentration of ^{137}Cs was measured using a Ge gamma ray detector.

As a result of the analysis, there was no significant difference between the two points near the tree and far away from the tree. The ^{137}Cs concentration of the preferential flow and the matrix decreased at each depth except for the depth of 0-1cm. The ^{137}Cs concentration of the preferential flow was higher than that of the matrix except for the depth of 0-1cm. Taking the ratio of ^{137}Cs concentration of preferential flow and matrix, in the plots near the trees, 0.57(0-1 cm), 1.07(1-2 cm), 1.27(2-4 cm), 1.62(4-6 cm), 3.02(6-10 cm). This indicated that as the depth increased, the preferential flow and strongly affected the ^{137}Cs

©2020. Japan Geoscience Union. All Right Reserved.

concentration.

These results suggested that ^{137}Cs may have been moved by preferential flow associated with rainfall. It is also considered that the preferential flow path is a stable environment even after more than 7 years from the accident. From these facts, it was shown that the influence of preferential flow is greatly observed in forest soil in Fukushima Prefecture.

Keywords: Preferential flow, 137Cs, FDNPP accident, Scraper plate

©2020. Japan Geoscience Union. All Right Reserved.

Formation mechanism of radiocesium concentration in throughfall in a cedar forest

*Tomoki Shinozuka[1], Hiroaki Kato[2], Yuichi Onda[2], Satoru Akaiwa[1]

1. Doctoral Program in Integrative Environment and Biomass Sciences, Graduate School of Life and Environmental Sciences, University of Tsukuba, 2. Center for Research on Isotope and Environmental Dynamics, University of Tsukuba

The Fukushima Daiichi nuclear accident (FDNPP) in 2011 released large amounts of radioactive material into the atmosphere. In particular, ^{137}Cs which has a long-half-life of 30.17 years will be a radiation source in the long term, thus it is necessary to clarify its dynamics in the environment. It was estimated that approximately 70% of radiocesium deposited on land is accumulated in forests. Therefore, it is important to understand the dynamics in forest environment. The most of radiocesium deposited on forests, especially evergreen conifer forest, was intercepted by the forest canopy. After that, it is known that the intercepted radiocesium will be transported from canopy to forest floor in association with rainfall leaching and litterfall.

The major pathway of radiocesium dynamic from canopy to forest floor peculiarly during the early the accident is throughfall, but the concentration of radiocesium in throughfall exponentially decreased with time. However, recently the trend that the reduction rate of the concentration of radiocesium in throughfall slowed down, it is necessary to monitor the radiocesium dynamics as a long-term input pathway to forest floor. In addition, it has been confirmed that the radiocesium concentration in throughfall varies greatly depending on the canopy cover and seasons and rainfall events. Therefore, it may be useful to clarify the elution mechanism of atmospheric deposit from forest canopy into rainwater. In this study, we investigated the formation mechanism of radiocesium concentration in throughfall of a cedar forest in Namie Town, Fukushima Prefecture. Using a rainwater sampler installed inside and outside the forest, rainfall over the canopy (12 locations) and rain outside the forest (3 locations) were collected, and the rainfall and radiocesium concentration were quantified. Based on these observations, we analyzed the spatial distribution characteristics of throughfall and the fluctuation factors of radiocesium concentration. It is considered that the fluctuation of radiocesium concentration is affected not only by the time since the accident but also by the difference between each rainfall event and the spatial variation.

The correlation between the canopy rainfall and the openness of the upper part of the sampler indicated that the canopy structure affected the rainfall distribution under the cedar canopy. In addition, the canopy passage rate of rainwater showed a tendency to increase with the event rainfall. Since the radiocesium concentration in the throughfall tends to decrease with increasing the amount of throughfall, it is highly possible that the effect of dilution with the increase in rainfall is working. The radiocesium migration flux showed a tendency to increase with increasing canopy rainfall per stand. However, observations with small transition flux have been obtained even when the event rainfall is relatively large. The formation of radiocesium is affected by the amount of rainfall, but the trend is changed by the difference of the interception process in canopy and spatial distribution of throughfall due to differences in rainfall characteristics, and it is suggested that it may affect the amount of radiocesium dynamics.

Keywords: Throughfall, Radiocesium, Interception by forest canopy, monitoring

©2020. Japan Geoscience Union. All Right Reserved.

Change in the elution behavior of dissolved radiocesium and physical property in the decay degree of litter of deciduous broad-leaved trees

*Yoshito Sasaki[1], Tadafumi Niizato[1], Satomi Ito[1], Takayoshi Watanabe[1]

1. Japan Atomic Energy Agency

Approximately 70% of radiocesium released to land area by the Fukushima Daiichi Nuclear Power Station of Tokyo Electric Power Company Holdings accident was deposited in the forest and would remain in the forest. Dissolved radiocesium would be easy to be incorporated into organisms. There are many unknown parts regarding the elution mechanism of the elution of dissolved radiocesium from organic matter such as litter, which would be a potential source of dissolved radiocesium. Here we report the results of the study on the difference in transfer behavior of dissolved radiocesium at the different degree of decomposition of organic matter of deciduous broad-leaved tree leaves. After making organic matter with different degree of decomposition (litter, leaf mold, humus) using litter collected in deciduous broad - leaved forest in Fukushima prefecture, elution rates of dissolved radiocesium eluted from these organic matters were compared. The highest elution rate was litter in organic matters with different degrees of decomposition. The elution rate of leaf mold and humus was about 1/10 of that of litter. Also, a correlation was observed between the elution rate and the cation exchange capacity. These results suggested that elution rate of dissolved radiocesium from organic matter in forest floor changed, due to changes in physical properties of organic matter accompanying the decomposition.

Keywords: radiocesium, deciduous broad-leaved tree, litter layer, Fukushima Dai-ichi Nuclear Power Plant accident

©2020. Japan Geoscience Union. All Right Reserved.

Dynamics of radioactive cesium in forest-stream ecosystem in a mountainous watershed

*Yuiko Chino[1], Takashi Gomi[1], Yoshito Oyama[1]

1. Department of Agriculture, Tokyo University of Agriculture and Technology

Nine years have passed since the nuclear power plant accident at Fukushima Daiichi Nuclear Power Plant accident, but much radioactive cesium (^{137}Cs) still remains in forests. Given that around 70% of the contaminated area is covered by forest, the fate of radioactive cesium in forest environments is an important topic because of the long half-life of ^{137}Cs and the complicated forest ecosystem. Especially in manufactured cedar forests, ^{137}Cs migrates within the linkage of the stream and riparian ecosystems via food web from cedar litter as the primary energy source to the highest consumer of fish. Whereas the ^{137}Cs contamination is strongly related to both of the stream and riparian ecosystems, most of the previous studies about ^{137}Cs contamination in forest ecosystems have focused on one ecosystem or some specific species. In this study, we examined the temporal change of ^{137}Cs concentration in a headwater stream-riparian ecosystem at Towa-region in Nihonmatsu-city, Fukushima, for four seasons during two sampling periods; 2012-2013 and 2016-2017. The ^{137}Cs concentration significantly decreased among the sampling periods for all the samples; cedar litter from riparian and stream, terrestrial and aquatic insects, and white-spotted char (*Salvelinus leucomaenis*). We also calculated ecological half-lives (T_{eco}), which are indicators of temporal contamination change, including various environmental processes and commonly applied to long-time assessments of environmental radioactive contamination. The calculated T_{ecos} were 1.6-3.9 years with the shortest of riparian litter and the longest of stream litter. These T_{ecos} were relatively short compared to the previous studies for Fukushima and other contaminated sites, suggesting that headwater ecosystems had faster contamination decrease because of the faster nutrient cycle. Also, the T_{ecos} in aquatic components were longer than terrestrial components. It was estimated that ^{137}Cs contamination in stream ecosystems decreased more slowly than riparian systems since newly supplied litter, less and less contaminated with time, was the only source of contamination in riparian systems. In contrast, fallen litter, as well as resuspension of sediment and POM, kept the contamination in stream ecosystems.

Keywords: radioactive cesium, temporal change, dynamics in the environment, forest ecosystem, watershed management

©2020. Japan Geoscience Union. All Right Reserved.

Seasonal change and formation factors of dissolved radiocesium concentration in a headwater catchment after the Fukushima Dai-ichi Nuclear Power Plant accident

*Satoru Akaiwa[1], Hiroaki Kato[2], Yuichi Onda[2], Tomoki Shinozuka[1]

1. Doctoral Program in Integrative Environment and Biomass Sciences, University of Tsukuba, 2. Center for Research in Isotopes and Environmental Dynamics, University of Tsukuba

Nine years after the Fukushima Daiichi Nuclear Power Plant accident, the presence of radioactive cesium is still a problem in forests and uncontaminated evacuation areas, and evaluating its behavior is an important issue in resident return and industrial rehabilitation. It has been reported that the radiocesium migration behavior changes with time, and that the cesium concentration of river water shows an exponential decreasing trend with time, but the mechanism has not been fully elucidated yet. Particularly in the forest basin at the headwater areas, the concentration of dissolved cesium in stream water may be maintained high due to leach from organic materials such as litter and mixing with soil water. In this study, we set up a test basin for a forest basin at the headwater catchment located in a high deposition area in Namie city, Fukushima Prefecture, Japan and investigated components that contribute to the formation of dissolved cesium concentration in stream water. The flow rates of spring water and stream water in the test basin were observed, and the concentrations of dissolved cesium-137 and various dissolved ions contained in spring water, stream water, and soil water were measured. A net and a suspended sediment sampler were installed downstream of the test basin to capture coarse organic matter, and the concentration of cesium-137 in the coarse organic matter and suspended sediment was measured. In addition, rainfall and temperature were observed, and research was conducted to elucidate the formation mechanism of radiocesium concentration in stream water based on those observation data. The survey period was approximately one year and six months from June 2018 to December 2019. The observation results showed that dissolved cesium-137 concentration in stream water increased with increasing temperature from June to July and decreased with increasing flow in August. In winter, a slight increase was observed. The concentration of soil water is higher than that of stream water by about 1-2 orders of magnitude, and the concentration of dissolved cesium-137 in the stream water and soil water showed a positive correlation. Furthermore, the concentration of dissolved 137Cs in the stream water tended to increase from the spring point toward the downstream. From the above results, the concentration of dissolved cesium-137 in stream water shows seasonal changes with changes in temperature and flow rate. Moreover, the dilution effect due to the increase in flow rate, the mixing with soil water in the process of stream water flow down, and the effect of leaching from the coarse organic matter deposited the forest floor and river channels was suggested.

Keywords: dissolved Cs-137, Fukushima Dai-ichi nuclaer power plant accident, stream water

©2020. Japan Geoscience Union. All Right Reserved.

Change in the spatial distribution of the air dose rate in the riverside park affected by decontamination and floods

*Takuhei Yamasaki[1], Satoshi Suzuki[1]

1. Fukushima Prefectural Centre for environmental Creation

Introduction

The accident at the TEPCO’ s Fukushima Dai-ichi nuclear power plant resulted in the release of a large amount of radionuclides in the environment. To assess the impact of the radiation dose to the human health, air dose rate has been measured widely in and around Fukushima prefecture. Air dose rate at the riverside park often decreases by the erosion/deposition of the sediments during floods as well as the decontamination work, radiocesium migration through soil, and physical decay. Moreover, topographic conditions such as elevation and undulations affect the change in the air dose rate.
Walking survey can easily get the spatial distribution of the air dose rate. However, each data by the walking survey has different acquisition positions due to the automatic records during measurement. To evaluate the temporal change in the air dose rate by the walking survey spatially, correction to match the comparison positions is needed. Kriging would be an effective tool for the interpolation of data having the spatial correlation such as air dose rate. The objective of our study is to evaluate the spatial patterns of the change in the air dose rate at the riverside park by using walking survey and kriging interpolation technique.

Methods

Study site was a riverside park facing the Niida River, located in Minami-Souma city, Fukushima prefecture. The radiocesium deposition by the accident was estimated to 300-600 kBq m-2. Remediation work against the radiation dose was conducted in 2016, and 3 typhoons (Etau in 2015, Lan in 2017, and Hagibis in 2019) attacked and river bank has been damaged by the typhoons in 2015 and 2019. We started walking survey measurement just before the attack of the typhoon Etau to January 2020. Gamma plotter H (Mimura et al., 2012) was used to measure the air dose rate at 1-m and 5-cm height. Time constant was set to 3 s, and measurement interval was 5 s.
Experimental semivariogram was calculated by using the Stanford Geostatistical Modeling Software. Lag separation and lag tolerance was set to 1 m and 0.2 m, respectively. Anisotropy was not considered. The spherical semivariogram model was fitted to the experimental one. Ordinary kriging was applied for the interpolation with ArcGIS ver. 10.5.1. Cell size of the grid was set to 2 m. Analysis area was limited to the inside of the riverside park.

Results and discussion

Among the semivariogram parameters, sill decreased with time, which reflects the temporal attenuation of the air dose rate. On the other hand, range did not changed with time. Range of 1-m measurement data was longer than that of 5-cm. This agrees with the fact that the air dose rate closer to the ground surface was affected by the radionuclides deposited on the narrower area.
The median value of the interpolated air dose rate always decreased with time faster than the rate by physical decay of radiocesiums. Especially, the typhoon events and the decontamination work accelerated the decrease in the air dose rate compared to the migration in soil due to the rainfall. The decrease in the air dose rate due to the floods was greater at the position near the river, while those by the decontamination occurred mainly in the west of the park with gardens or covered with grass.

©2020. Japan Geoscience Union. All Right Reserved.

Keywords: air dose rate, kriging, decontamination, flooding

©2020. Japan Geoscience Union. All Right Reserved.

Accumulation and redistribution of ^{137}Cs on floodplains along the Abukuma River

*Yoshifumi Wakiyama[1], Alexei Konoplev[1], Valentin Golosov[2], Maxim Ivanov[2], Mikhail Komissarov[3]

1. Institute of Environmental Radioacitivity, Fukushima Universiy, 2. Faculty of Geography, M.V. Lomonosov Moscow State University, 3. Ufa Institute of Biology UFRC, Russian Academy of Science

A portion of sediment-borne ^{137}Cs in river water accumulates on floodplains during high-flow events and becomes a source of secondary contaminations in subsequent events. This study aims to elucidate processes of ^{137}Cs accumulation / redistribution on floodplains and presents the ^{137}Cs inventory and depth distribution in deposited sediments. The sediment cores were taken in 2018 and 2019 at six floodplain cross-sections, located along the Abukuma River in Nihonmatsu (NIH), Fukushima (KUR), Date (FUS), Marumori (MAR), Kakuda (KAK), and river mouth area in Iwanuma (Mouth). The mean ^{137}Cs inventory obtained by sampling campaigns in October 2018 at NIH, KUR, FUS, MAR, KAK, and Mouth were 150 kBq m^{-2} (n = 2), 600 kBq m^{-2} (n = 3), 490 kBq m^{-2} (n = 2), 270 kBq m^{-2} (n = 2), 90 kBq m^{-2} (n = 2), and 40 kBq m^{-2} (n = 1), respectively. These values were 1.2-9.1 times higher than those estimated by 6th airborne survey at each point, suggesting secondary accumulation of ^{137}Cs. The ^{137}Cs inventory and maximum ^{137}Cs concentrations in sediment depth profile tended to be high at the sampling points, located on the highest floodplain level above the river channel within each floodplain cross-section. The mean ^{137}Cs inventory obtained by sampling campaigns in October and November 2019 at NIH, KUR, FUS, MAR, KAK, and Mouth were 180 kBq m^{-2} (n = 2), 540 kBq m^{-2} (n =2), 410 kBq m^{-2} (n = 1), 120 kBq m^{-2} (n = 2), 420 kBq m^{-2} (n = 3), and 46 kBq m^{-2} (n = 1), respectively. Although ^{137}Cs inventory on the floodplains are not so different, depth distributions of ^{137}Cs in the deposited sediment changed from those of 2018. These results suggest that an extreme flood triggered by Typhoon *Hagibis* in middle of October 2019 resulted in a substantial redistribution of ^{137}Cs at Abukuma fluvial system.

Keywords: Abukuma River, floodplains, sediment dynamics

©2020. Japan Geoscience Union. All Right Reserved.

Re-circulation of ^{137}Cs concentrations in surface seawater in the western North Pacific Ocean

*Yayoi Inomata[1], Michio Aoyama[2]

1. Kanazawa University, Institute of Nature and Environmental Technology, 2. Tsukuba University, Center for Research in isotopes and Environmental Dynamics

We investigated spatial and temporal variations in ^{137}Cs concentrations in the surface waters of the global ocean for the period from 1957 to 2018 by using HAM database global 2019 version. In order to study the distribution of ^{137}Cs concentrations in surface seawater, we divided the global ocean into 37 latitudinal boxes on the basis of known ocean current systems, latitudinal and longitudinal distributions of ^{137}Cs concentrations, the distribution of global fallout, locations of nuclear reprocessing plants, fallout from the Chernobyl accident, and release from Fukushima Nuclear Power Plant accident. The 0.5-y average value of ^{137}Cs concentrations in the surface water in each box were estimated.

In this study, we focus on temporal variation of ^{137}Cs concentrations in the western North Pacific Ocean (NPO) and its marginal sea. In the NPO where there was high fallout from atmospheric nuclear weapons tests, the rates of decrease in the ^{137}Cs concentrations changed over the five decades: the rate of decrease from the 1950s to the 1970s was much faster than that after the 1970s, and the ^{137}Cs concentrations were almost constant after the 1990s. The ^{137}Cs released into the western North Pacific Ocean by global fallout were transported eastward with the Kuroshio and North Pacific Currents and accumulated in the eastern NPO. Following then, global fallout-^{137}Cs were southward transport in the NPO and subducted into the subsurface layer (1). It was found that global fallout-^{137}Cs were westward transported into subtropical mode water and Central Mode Water in the NPO, suggesting the re-circulation of global fallout-^{137}Cs (2). The apparent half residence time (Tap) of ^{137}Cs in the surface sea water in the western NPO, Sea of Japan (SOJ), East China Sea (ECS) between 2000 and 2010 were 17.3yr, 23.5yr, and 18.0 yr, respectively. The longer Tap in SOJ and ECS suggests that ^{137}Cs derived from global fallout may be recirculated into the SOJ through ECS from wNPO. The recirculation of ^{137}Cs is also found by the intrusion of Fukushima Daiichi Nuclear Plant derived ^{137}Cs (FNPP1-^{137}Cs) after 2012 (3,4). Considering that the increase of FNPP1-^{137}Cs occurred within several years after the FNPP1 accident, the seawater transport route into the SOJ from the NPO with shorter time scale would be existed.

(Reference)
Inomata et al. (2012). J. Environ. Monit., 14, 3146. Aoyama et al. (2008) Geophys. Res. Lett. 35, L01604, doi:10.1029/2007GL031964. Aoyama et al. (2017) App. Radi. Isotopes, 126, 83-87. Inomata et al. (2018) Ocean Sci., 14, 813-826.

Keywords: radiocaesium, North Pacific Ocean , large scale nuclear weapons test, global fallout, Fukushima Dai-ichi Nuclear Power Plant accident, Apparent half-residence time

©2020. Japan Geoscience Union. All Right Reserved.

Distribution of dissolved and particulate radiocesium from the downstream of rivers to the costal waters off Fukushima.

*Hyoe Takata[1], Tatsuo Aono[2], Michio Aoyama[3], Hideki Kaeriyama[4], Mutsuo Inoue[5]

1. Fukushima Univ., 2. QST, 3. Tsukuba Univ., 4. FRA, 5. Kanazawa Univ.

Distribution of radiocesium in dissolved and particulate phases in the downstream of seven rivers (Tomioka, Kido, Asami, Natsui, Fujiwara, Same, and Binda Rivers), and adjacent shoreline and offshore has been studied in order to investigate the reasons why dissolved ^{137}Cs concentration in the shoreline was still high even eight years after the Fukushima Dai-ichi Nuclear Power Plant (FDNPP) accident (March 2011). Observations undertaken during the pre-typhoon period of June-September 2019 and the period of October 2019 immediately after the Typhoon Hagibis 2019 indicated that seawater with relatively high particulate and dissolved radiocesium concentrations in the shoreline, compared to rivers and offshore, was extending as long as about 60 km south of the FDNPP along the shoreline. This cannot be explained simply by the on-going release of highly contaminated water from the facility of the FDNPP, followed by the southward transport of the high radiocesium water along the shoreline. Desorption of radiocesium from riverine suspended particle while traversing of the particles on the shoreline could contribute to the heightening dissolved radiocesium concentration. This assumption is also supported by the evidence that steep reduction of the distribution coefficient, K_d (L/kg) from rivers to seawater in the shoreline. Our estimation showed that contribution of desorption to the dissolved radiocesium to shoreline waters increased after the typhoon. This study revealed that the distribution, especially the dynamics of the suspended particles bearing radiocesium along the shoreline, the importance of desorption process for the evaluation of the mass balance between run-off of radiocesium from land and its dispersion in the marine environment.

Keywords: Shoreline, Riverine suspended particle, Desorption

©2020. Japan Geoscience Union. All Right Reserved.

[J] Poster | M (Multidisciplinary and Interdisciplinary)：M-SD Space Development & Earth Observation from Space

[M-SD47] Future Missions of Satellite Earth Observation

convener:Yoshiaki HONDA(Center for Environmental Remote Sensing, Chiba University), Yukari Takayabu(Atmosphere and Ocean Research Institute, the University of Tokyo), Shinichi Sobue(Japan Aerospace Exploration Agency), Yuki Kaneko(Japan Aerospace Exploration Agency)

Satellite observation can be an effective tool in earth science and making human society apply to the rapid global environmental change. Monitoring for a long term, advancing new ideas and developing technologies to support them are needed. The Task Force on Future Space R&D System of the Subcommittee on Remote Sensing (TF) supported by 26 academic societies and affiliated organizations has formulated the ''Grand Design of Earth Observation'' from FY2017. From the academic point of view, it suggests earth observation missions that Japan should conduct within a decade. The TF calls for proposals of earth observation missions as a trial that aims to discover new ideas from the scientific and practical domains and refine those ideas through multidisciplinary discussion. The adopted proposals will be mentioned in the revised Grand Design, and the TF will work with the government on using it as a reference in updating the Implementation Plan of the Committee on National Space Policy. This session consists of oral presentations of the proposals that passed the preliminary examination of documents and active discussions to expand and deepen the study. We welcome attendees from various backgrounds who are interested in earth observation.

Introduction

[MSD47-P01] Realization of pseudo high-frequency high-resolution observation by combined observation of geostationary satellite and orbiting satellite

*Yoshiaki HONDA[1], Koji KAJIWARA[1], Ryota ISHIBASHI[1] (1.Center for Environmental Remote Sensing, Chiba University)

[MSD47-P02] Mission on monitoring and elucidating global environmental changes (global radiative forcing and ecosystem changes that affect global warming) (successor to GCOM-C)

*Yoshiaki HONDA[1], Teruo Aoki[2], Takashi Nakajima[3], Mitsuhiro Toratani[4], Koji KAJIWARA[1], Ryota Ishibashi[1] (1.Center for Environmental Remote Sensing, Chiba University, 2.Research Organization of Information and Systems, National Institute of Polar Research, 3.Tokai University Research & Information Center, 4.Tokai University Department of Optical and Imaging Science and Technology)

[MSD47-P03] Geostationary Satellite Ocean Color Mission

*Joji Ishizaka[1], Mitsuhiro Toratani[2], Toru Hirawake[3], Takafumi Hirata[4], Hiroshi Kobayashi[5], Yuji Sakuno[6], Hiroto Higa[7] (1.Institute for Space-Earth Environmental Research, Nagoya University, 2.School of Engineering, Tokai University, 3.Faculty of Fisheries Sciences, Hokkaido University, 4.Arctic Research Center, Hokkaido University, 5.Graduate School of Interdisciplinary Research, University of Yamanashi, 6.Graduate School of Engineering, Hiroshima University, 7.Faculty of Urban Innovation, Yokohama National University)

[MSD47-P04] Satellite Observation of the Whole Atmosphere - Superconducting Submillimeter-Wave Limb-Emission Sounder (SMILES-2)

*Masato Shiotani[1], Akinori Saito[1], Takatoshi Sakazaki[1], Satoshi Ochiai[2], Philippe Baron[2], Toshiyuki Nishibori[3], Makoto Suzuki[3], Takumi Abe[3], Hiroyuki Maezawa[4], Shin-ichiro Oyama[5,6] (1.Kyoto University, 2.National Institute of Information and Communications Technology, 3.Japan Aerospace Exploration Agency, 4.Osaka Prefecture University, 5.Nagoya University, 6.University of Oulu)

[MSD47-P05] FTS satellite observation mission for understanding chemical and dynamical processes in the upper atmosphere

*Nawo Eguchi[1], Kaley A. Walker[2], Naoko Saitoh[3], Yukio Yoshida[4], Kei Yoshimura[5], Kinya Toride[5], Masatomo Fujiwara[6], Yoshio Kawatani[7], Yousuke Eguchi Yamashita[7], Ray Nassar[8], Dylan Jones[2], David

Plummer[8], Kimberly Strong[2] (1.Kyushu University, 2.University of Toronto, 3.Chiba University, 4.National Institute for Environmental Studies, 5.University of Tokyo, 6.Hokkaido University, 7.JAMSTEC, 8.Environment and Climate Change Canada)

[MSD47-P06] Imaging spectrometer for km-class observation of SLCP

*YASUKO KASAI[1], Hiroshi Tanimoto[3], Yugo Kanaya[2], JPSAC Satellite group (1.NICT, 2.JAMSTEC, 3.NIES)

[MSD47-P07] **Global measurement system of wind using LIDAR and Imaging FTS**

*Okamoto Hajime[1], Toshiyoshi Kimura[2], Daisuke Sakaizawa[2], Shoken Ishii[3], Tomoaki Nishizawa[4] (1.Kyushu University, 2.Japan Aerospace Exploration Agency, 3.National Institute of Information and Communications Technology, 4.National Institute for Environmental Studies)

[MSD47-P08] Precipitation observation by small precipitation radar satellites

*Nobuhiro Takahashi[1], Kinji Furukawa[2], Takuji Kubota[2], Yamaji Moeka[2], Riko Oki[2] (1.Institute for Space-Earth Environmental Research, Nagoya University, 2.Japan Aerospace Exploration Agency)

[MSD47-P09] Technology demonstration mission for next generation precipitation observation radars

*Daisuke Jodoi[1], Kinji Furukawa[1], Riko Oki[1], Tomoo Ushio[2], Kenji Nakamura[3] (1.Japan Aerospace Exploration Agency, 2.Osaka University, 3.Dokkyo University)

[MSD47-P10] Monitoring and evaluation of near real-time water cycle fluctuations by microwave remote sensing

*Kazuyoshi Suzuki[1], Misako Kachi[2], Kazuyuki Saito[1], Hideki Kobayashi[1], Tetsuya Hiyama[3], Milija Zupanski[4] (1.Japan Agency for Marine-Earth Science and Technology, 2.JAXA, 3.ISEE, Nagoya University, 4.CIRA, Colorado State University)

[MSD47-P11] Development of new satellite to monitor SIF and PRI of terrestrial vegetation

*Hibiki M Noda[1], Kenji Omasa[2], Kouki Hikosaka[3], Kazuhito Ichii[4], Hideki Kobayashi[5], Tomomichi Kato[6], Hiroyuki Muraoka[7] (1.NIES National Institute of Environmental Studies, 2.Takasaki University of Health and Welfare, 3.Tohoku University, 4.Chiba University, 5.JAMSTEC, 6.Hokkaido University, 7.Gifu University)

Realization of pseudo high-frequency high-resolution observation by combined observation of geostationary satellite and orbiting satellite

*Yoshiaki HONDA[1], Koji KAJIWARA[1], Ryota ISHIBASHI[1]

1. Center for Environmental Remote Sensing, Chiba University

From both fields of earth science and practical use, higher frequency and higher resolution observation data is desired for the earth observation optical sensor data. However, high-frequency observation and high-resolution observation cannot be simultaneously realized with a single satellite, and a large number of microsatellite operations are being realized. However, microsatellites generally have problems such as a short design life and no calibration system. On the other hand, medium or larger satellites including geostationary satellites have a long design life and have a calibration system. However, in order to achieve high frequency and high resolution with a satellite of a medium or larger size, the budget is enormous and impractical to secure the number of satellites. This proposal is based on high-frequency observations of relatively low-resolution geostationary satellites and high-resolution but low-frequency orbiting satellite observations among satellites launched by Japan (assuming successors such as Himawari, GCOM-C, and ALOS) A framework for providing such high-quality, long-term provisions that aims to produce pseudo-high-frequency, high-resolution observation data through models that mutually adjust some of the sensor specifications of each satellite and adjust for differences in observation geometry To build. This aims to expand the use of satellite optical sensor data in earth science and practical applications, and to advance science and expand practical use. This framework is a step toward achieving greater results with the planned budget, and the expansion of practical applications will also contribute to ensuring the continuity of earth observation in Japan. Furthermore, by incorporating newly planned satellites from other countries into this framework, we aim to increase Japan's earth observation presence in the fields of earth science and practical use.

Keywords: Geostationary satellite, Orbiting satellite, Himawari, GCOM-C, ALOS

©2020. Japan Geoscience Union. All Right Reserved.

Mission on monitoring and elucidating global environmental changes (global radiative forcing and ecosystem changes that affect global warming) (successor to GCOM-C)

*Yoshiaki HONDA[1], Teruo Aoki[2], Takashi Nakajima[3], Mitsuhiro Toratani[4], Koji KAJIWARA[1], Ryota Ishibashi[1]

1. Center for Environmental Remote Sensing, Chiba University, 2. Research Organization of Information and Systems, National Institute of Polar Research, 3. Tokai University Research & Information Center, 4. Tokai University Department of Optical and Imaging Science and Technology

The purpose of this proposal is to monitor and clarify global environmental changes (global radiative forcing and ecosystem changes that affect global warming) through long-term and continuous quantitative monitoring. Optical (near-ultraviolet to thermal infrared) imager technology is a fundamental technology that can evolve into new optical sensors in the future and needs to be continued to maintain a global advantage.
By monitoring the optical imager, which is SGLI's genealogy, over a wide range of wavelengths, it is possible to monitor changes in the climate system that change with global warming, including changes not currently expected. In addition, by being able to accurately grasp the progress of climate change that has been predicted, it is possible to evaluate the effects of global warming control policies, formulate adaptation measures for the future, and make diagnostic corrections to the trajectories. . By having its own information source as its own sensor, it is possible to have Japan's own judgment material for grasping the situation of climate change, and to transmit it to the world as global standard information, and to implement international strategies on climate change. Can have. Furthermore, by using J-train type satellites for observations (meteorological research note No. 234, "Analysis of world trends related to future vision of earth observation", P16-18 In the next GCOM-C study at JAXA, the J-train concept was also included, and in cooperation with activities within JAXA, coordination and sharing with foreign activities such as MetOP and JPSS were examined. We are discussing how to enhance and prioritize the goals set out at GCOM-C.

Keywords: Global environmental change, GCOM-C, SGLI, J-train

©2020. Japan Geoscience Union. All Right Reserved.

Geostationary Satellite Ocean Color Mission

*Joji Ishizaka[1], Mitsuhiro Toratani[2], Toru Hirawake[3], Takafumi Hirata[4], Hiroshi Kobayashi[5], Yuji Sakuno[6], Hiroto Higa[7]

1. Institute for Space-Earth Environmental Research, Nagoya University, 2. School of Engineering, Tokai University, 3. Faculty of Fisheries Sciences, Hokkaido University, 4. Arctic Research Center, Hokkaido University, 5. Graduate School of Interdisciplinary Research, University of Yamanashi, 6. Graduate School of Engineering, Hiroshima University, 7. Faculty of Urban Innovation, Yokohama National University

Climate is changing, and seawater temperature and freshwater inflow is also changing significantly. The coastal marine ecosystem, which has been greatly affected by human influences, is considered to be changing further. Observation of ocean color is making it possible to continuously observe the coastal ecosystems, such as phytoplankton, suspended solids, salinity and seaweed beds. However, with the visible observations from single polar orbit satellite, sufficient data cannot be obtained in coastal areas where river water and tides tend to change in a short period of time, especially when there are many clouds. High-frequency observations of "Himawari" make it possible to observe both short-term fluctuations as well as data from even with frequent clouds area. On the other hand, the number of wavelengths and radiance resolution are insufficient to acquire accurate ocean color information. Therefore, we propose here the observation of ocean color with high frequency, high resolution and high radiance resolution by the geostationary satellite with additional ocean color band. This makes it possible to monitor phenomena affecting the coastal fisheries and aquaculture, such as red tide and river water, and to observe the material circulation along the coast. In addition, it is possible to contribute to understand the environment not only in Japan but also in the coastal areas of southeastern Asia, where it is influenced by relatively frequent clouds, by human activities, and by climate change. Furthermore, it is considered to be effective not only for observation of the ocean but also for observations of the atmosphere (aerosol) and land (vegetation and ice).

Keywords: Geostationary Satellite, Ocean Color, Ocean Environment, Coastal Environment, Phytoplankton

©2020. Japan Geoscience Union. All Right Reserved.

Satellite Observation of the Whole Atmosphere - Superconducting Submillimeter-Wave Limb-Emission Sounder (SMILES-2)

*Masato Shiotani[1], Akinori Saito[1], Takatoshi Sakazaki[1], Satoshi Ochiai[2], Philippe Baron[2], Toshiyuki Nishibori[3], Makoto Suzuki[3], Takumi Abe[3], Hiroyuki Maezawa[4], Shin-ichiro Oyama[5,6]

1. Kyoto University, 2. National Institute of Information and Communications Technology, 3. Japan Aerospace Exploration Agency, 4. Osaka Prefecture University, 5. Nagoya University, 6. University of Oulu

The Superconducting Submillimeter-Wave Limb-Emission Sounder (SMILES) was developed for deployment in the Japanese Experiment Module (JEM) on the International Space Station (ISS). SMILES conducted atmospheric observations for approximately six months, from October 2009 to April 2010, to measure concentrations of minor species in the stratosphere and mesosphere. Outstanding results have been achieved such as an identification of diurnal cycle of the stratospheric ozone, which had not been examined yet because of poor data quality in the previous satellite measurements. In addition, by comparing SMILES data with existing observation data and results from the chemistry climate models, it has been recognized that we need a reference data for temperature, wind, and minor species with high precision to constrain the models. After the launch there has been discussions about the possibility to derive wind information from the Doppler shift of observed lines, and the necessity to have temperature information from adequate line selection. Thus, we now recognize the potential of high-sensitivity observations about temperature and wind fields up to 150 km to cover the uncharted territory, the mesosphere and the lower thermosphere (MLT).

Based on the SMILES heritage, we propose a satellite mission to observe temperature and wind fields, and distributions of atmospheric minor species for the full diurnal cycle from the middle atmosphere (stratosphere and mesosphere) to the upper atmosphere (thermosphere and ionosphere) for a period of five years. SMILES-2 observations will enable us to obtain global information with unprecedented accuracy on the whole atmosphere including upper mesosphere and lower thermosphere where observation data have been lacking.

This mission has three specific science objectives.
(MO.1) To investigate the effects of lower atmosphere on the MLT via upward propagating atmospheric waves such as atmospheric tides
(MO.2) To understand atmospheric variations due to energy inputs from the magnetosphere (particle precipitation and magnetic storm)
(MO.3) To understand the solar-terrestrial system by providing benchmarks for whole atmosphere models

Using observation data from the middle atmosphere to the upper atmosphere as a whole, we will be able to grasp the 4-D dynamical structure of diurnal variations (atmospheric tides) which are one of the most essential variabilities in the earth’s atmosphere. For understanding climate change in view of chemical processes affecting the ozone layer, we will be able to utilize high-sensibility measurements of the atmospheric minor species in a quantitative manner. In the upper atmosphere, a transition layer between the atmosphere and the outer space, we will be able to clarify a role of energy inputs from the magnetosphere from the temperature and wind observations. The observation data will provide unprecedented benchmark data to comprehensive whole-atmosphere simulation models whose development is necessary for accurate seasonal weather forecasts, future climate projections, and space weather forecasts.

©2020. Japan Geoscience Union. All Right Reserved.

Keywords: middle atmosphere, upper atmosphere, satellite observations, temperature, wind

©2020. Japan Geoscience Union. All Right Reserved.

FTS satellite observation mission for understanding chemical and dynamical processes in the upper atmosphere

*Nawo Eguchi[1], Kaley A. Walker[2], Naoko Saitoh[3], Yukio Yoshida[4], Kei Yoshimura[5], Kinya Toride[5], Masatomo Fujiwara[6], Yoshio Kawatani[7], Yousuke Eguchi Yamashita[7], Ray Nassar[8], Dylan Jones[2], David Plummer[8], Kimberly Strong[2]

1. Kyushu University, 2. University of Toronto, 3. Chiba University, 4. National Institute for Environmental Studies, 5. University of Tokyo, 6. Hokkaido University, 7. JAMSTEC, 8. Environment and Climate Change Canada

Tropospheric warming/stratospheric cooling due to increasing anthropogenic greenhouse gas concentrations in the atmosphere and the recovery of the stratospheric ozone layer are ongoing concerns for our changing climate. To understand the current climate and to predict future climate change, continuing observations of atmospheric trace gases and clouds are required on a global scale.
In this mission, we will use a mid-infrared Fourier-Transform Spectrometer (FTS) to perform solar occultation observations (2 to 13 μm, resolution 0.02 cm^{-1}). With this method, it is possible to observe a large number of atmospheric trace gases (including isotopes) and clouds with high vertical resolution (1.5 km) from the upper troposphere to the lower thermosphere (6-100 km).
This mission is expected to refine our understanding of the chemical processes in the stratosphere and elucidate new mechanisms, and to improve the accuracy of forecasting using numerical models based on information on water vapor and its isotope (HDO) in the upper troposphere . Furthermore, by reproducing the chemical processes in the stratosphere in detail, it is possible to improve the reproducibility of the dynamics of the stratosphere and thereby more realistically reproduce the effects of atmospheric changes in the middle atmosphere on the troposphere, and to better predict impacts of climate change. It is expected to contribute to society and government policies through improving the performance of climate models.

Keywords: Fourier Transform Spectrometer, upper atmosphere, trace gases, isotope

©2020. Japan Geoscience Union. All Right Reserved.

Imaging spectrometer for km-class observation of SLCP

*YASUKO KASAI[1], Hiroshi Tanimoto[3], Yugo Kanaya[2], JPSAC Satellite group

1. NICT, 2. JAMSTEC, 3. NIES

Short-lived climate pollutants are powerful climate forcers that remain in the atmosphere for a much shorter period of time than carbon dioxide (CO_2), yet their potential to warm the atmosphere can be many times greater. Certain short-lived climate pollutants are also dangerous air pollutants that have harmful effects for people, ecosystems and agricultural productivity. In SLCP, since the emission source is local, observation with a spatial resolution of 1 km class is necessary to understand the actual situation. However, it has not existed so far due to technical difficulties. We propose the SLCP Imaging Spectrometer with geostationally satellite to observe Asian region with high-resolution horizontal resolution (target: horizontal resolution 1-2 km), 1-2 hours time resolution to obtain diurnal variation observations.

Keywords: Short-Lived Climate Pollutants: SLCPs, Satellite Observation

©2020. Japan Geoscience Union. All Right Reserved.

Global measurement system of wind using LIDAR and Imaging FTS

*Okamoto Hajime[1], Toshiyoshi Kimura[2], Daisuke Sakaizawa[2], Shoken Ishii[3], Tomoaki Nishizawa[4]

1. Kyushu University, 2. Japan Aerospace Exploration Agency, 3. National Institute of Information and Communications Technology, 4. National Institute for Environmental Studies

We present the concept of synergy space-borne- lidar and FTS system of observations of global wind velocity. Main aims of the observing system is to provide three dimensional wind with high vertical resolution and also to provide a unique data sets of three dimensional water vapor, temperature to study cloud generation mechanism and its interaction to convection.
We propose measurement system of wind, water vapor, temperature, clouds, and aerosols by using FTS on Geostationary satellites with Doppler lidars and radars. Wind as atmospheric circulation is the most important element in climate and weather studies. Air- and ship-traffic are also using wind information as most prioritized one to ensure their safe operation. Current systems cannot measure global distribution of winds. Recent progress of Doppler lidar technology made precise wind measurement possible in three-dimensional manner, limited to narrow swarth over its orbit. A wind lidar satellite was already launched by European Space Agency, and NASA is also planning to launch. In Japan, NICT and JAXA are studying wind LIDAR. Also, recent geostationary weather satellite made possible to distinguish wind distribution by altitude using water vapor band imagery. Measurement error is still considerably large. The basic concept is to combine wind lidar and FTS on Geostationary satellites to complement each other. To cover the globe using geostationary orbit, we need about four satellites at each region. Using current weather satellite network is the most demanded approach. For LIDAR satellites, NASA, ESA and JAXA/NICT can make a strong network to maintain LIDAR data to calibrate the results of retrieved wind from imaging FTS on Geostationary satellite. The temporal requirement for the system is 1km horizontal resolution, 300m height distribution, <1m/s windspeed accuracy and wind vector. Since the FTS will offer high resolution data of water vapor and temperature, it can provide a unique opportunity to study cloud formation in relation to convection when space-borne cloud radar and lidar will be available with FTS.

Keywords: Geostationary satellite, Doppler, lidar, FTS, cloud, wind

©2020. Japan Geoscience Union. All Right Reserved.

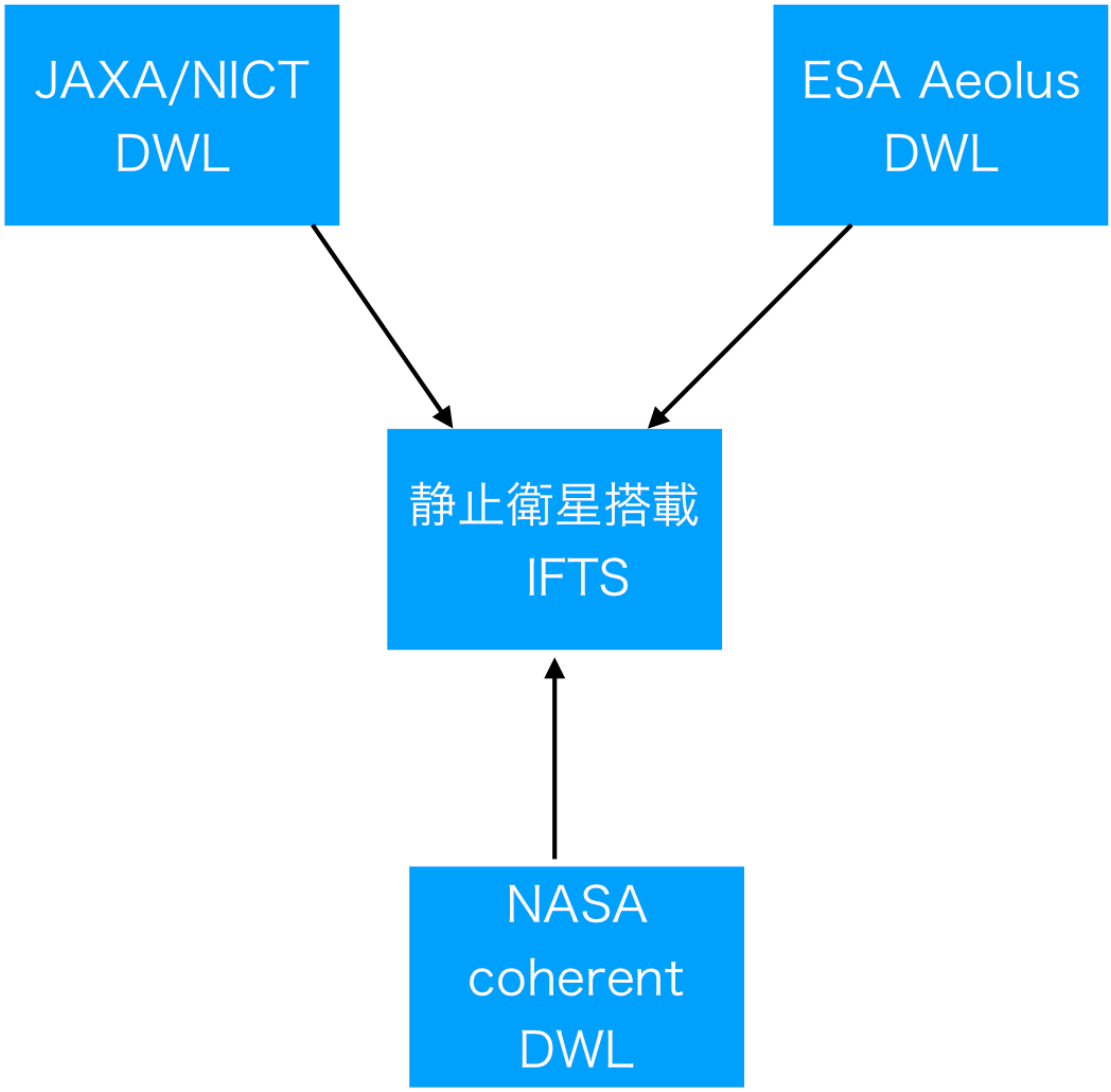

©2020. Japan Geoscience Union. All Right Reserved.

Precipitation observation by small precipitation radar satellites

*Nobuhiro Takahashi[1], Kinji Furukawa[2], Takuji Kubota[2], Yamaji Moeka[2], Riko Oki[2]

1. Institute for Space-Earth Environmental Research, Nagoya University, 2. Japan Aerospace Exploration Agency

Based on the heritages from TRMM/PR and GPM/DPR, a low-cost and wide swath precipitation radar constellation is proposed. With the proposed Small Precipitation Radar Constellation, it is possible to greatly improve the observation frequency of the same spot with respect to GPM/DPR. Although the number of satellites will increase, both the precipitation radar and the satellite bus will utilize already developed products and it will be mounted on relatively inexpensive small satellite to reduce the cost of the overall system. Assuming that both the precipitation radar and the satellite bus utilize already developed products, we aim to target the development cost of the first observatory to 10 billion yen or less (excluding ground equipment, launch, operation cost).
As the application of the small precipitation radar constellation, it is assumed that utilization in disaster prevention such as improving the accuracy of weather forecast, predicting the occurrence of flood caused by typhoon and severe rainfall. Scientifically, it is useful for the study of the diurnal change of precipitation by high frequency observation in tropical zone. Observation data of this precipitation radar can also be used in Southeast Asian countries (Indonesia, the Philippines, Vietnam, etc.), and it is assumed that a satellite constellation will be constructed by countries which are interested in development and launch (Realized by ODA). As a technical development, we aim increase the number of constellation satellite for further high frequent precipitation observation through further size down and cost reduction.

In addition, trade-off study against radar-equipped CubeSat satellite which can observe only nadir direction. The result indicates that the CubeSat type observation is required to have scanning capability to achieve low-cost observation with the comparable observation efficiency of GPM/DPR.

Keywords: Precipitation

©2020. Japan Geoscience Union. All Right Reserved.

Technology demonstration mission for next generation precipitation observation radars

*Daisuke Jodoi[1], Kinji Furukawa[1], Riko Oki[1], Tomoo Ushio[2], Kenji Nakamura[3]

1. Japan Aerospace Exploration Agency, 2. Osaka University, 3. Dokkyo University

We have studied doppler velocity measurement for precipitation particles using a precipitation observation radar in a low Earth orbit as a post-mission of Dual-frequency Precipitation Radar (DPR) on the Global Precipitation Measurement (GPM) core satellite. Also, we have studied Geostationary Precipitation Radar (GPR) which can observe precipitation continuously and flexibly from a geostationary orbit as a future mission. In this study, we have studied the method which can separate precipitation echoes from ground/sea clutters by the doppler velocities in order to observe high latitude areas. Therefore, we need to verify the feasibility of the doppler velocity measurement for precipitation particles. Additionally, we need to improve antenna performance drastically in order to observe precipitation from a geostationary orbit which is far away from a low Earth orbit. Therefore, we need to verify the feasibility of upsizing an antenna for the GPR.
Based on the above background, the purpose of the proposed mission is to demonstrate that it is possible to measure the doppler velocity of precipitation particles from an orbit by a pulse compression radar using a planar antenna and to operate antenna deployment and connection mechanisms normally in an orbit. Also, we aim to get data regarding antenna deployment behavior and structural characteristics.
We consider the value of the proposed mission as follows. Firstly, the value of the doppler velocity measurement demonstration is as follows.
1. This demonstration contributes to realize post-GPM/DPR mission. If the doppler velocity measurement becomes possible in the mission, it is expected to understand the mechanical structure of a precipitation system globally and to improve the accuracy of weather and flood forecasts.
2. This demonstration contributes to realize the GPR mission. If the GPR becomes possible, it is expected to identify the forming process of a typhoon and to improve the accuracy of weather and flood forecasts.
Next, the value of the antenna deployment and connection demonstration is as follows.
1. This demonstration contributes to improve the performance of satellite antennas for earth observation, communication, radio astronomy, disaster monitoring, national security, etc. because the deployment and connection mechanisms make it possible to enlarge planar antennas.
2. This demonstration contributes to realize innovative missions like the GPR because the deployment and connection mechanisms make it possible to construct a 30-m-class large planar antenna.
3. The deployment and connection mechanisms have the potential to construct super large space structures like Space Solar Power Systems (SSPS).
We consider the feasibility of the proposed mission as follows. When we assume that the size of a demonstration system is 1.2m x 2.2m x 0.7m in storage state and 1.2m x 2.2m x 4.4m in deployment state, we expect that the system meets the installation condition for HTV-X which has been developed as a post-KOUNOTORI (HTV) by JAXA. Also, as a result of thermal analysis for the system, we expect that the system meets the thermal condition for HTV-X. Furthermore, we demonstrated that it is possible to operate the half size deployment and connection mechanisms of the system normally by a ground experiment in FY2017 and we improved the function and performance of the mechanisms in FY2018.
As future works, we will study the feasibility of the doppler velocity measurement from the aspect of HTV-X attitude control performance.

©2020. Japan Geoscience Union. All Right Reserved.

Keywords: Precipitation observation radar, Technology demonstration, Doppler velocity, Deployable antenna

©2020. Japan Geoscience Union. All Right Reserved.

Monitoring and evaluation of near real-time water cycle fluctuations by microwave remote sensing

*Kazuyoshi Suzuki[1], Misako Kachi[2], Kazuyuki Saito[1], Hideki Kobayashi[1], Tetsuya Hiyama[3], Milija Zupanski[4]

1. Japan Agency for Marine-Earth Science and Technology, 2. JAXA, 3. ISEE, Nagoya University, 4. CIRA, Colorado State University

Changes in the water cycle associated with global warming have caused water-related problems in various parts of the world and have had a significant impact on local environments and ecosystems. It is essential to establish a water cycle monitoring system that integrates data from the atmosphere and land in order to facilitate a better understanding of the world's water issues and water resources. In this study, we will build a global water cycle monitoring system that integrates the atmospheric water cycle and the terrestrial water cycle. This monitoring system will allow a water cycle database to be published in near real-time. This database will be essential for the understanding of global water issues and water resources management. In this study, we focused on the amount of available global water storage, assessed by monitoring and evaluating the amount of precipitable air relative to the amount of terrestrial storage in light of global warming. We will build a water cycle reanalysis system that merges microwave remote sensing data and general meteorological data into a near-real-time coupled atmospheric and land surface database. We will obtain hydrometeorological observation data in Siberia, Alaska, and Mongolia, where water cycle fluctuations due to global warming are extreme, and compare and verify them with satellite data to evaluate the accuracy of the reanalysis database created. Based on this research, we hope to contribute to understanding the damage caused by global warming to the global water cycle, and perhaps help reverse this damage and route to resolving critical water resource problems.

Keywords: Strongly coupled data assimilation, Atmosphere-land interaction, Global hydrological cycle

©2020. Japan Geoscience Union. All Right Reserved.

Development of new satellite to monitor SIF and PRI of terrestrial vegetation

*Hibiki M Noda[1], Kenji Omasa[2], Kouki Hikosaka[3], Kazuhito Ichii[4], Hideki Kobayashi[5], Tomomichi Kato[6], Hiroyuki Muraoka[7]

1. NIES National Institute of Environmental Studies, 2. Takasaki University of Health and Welfare, 3. Tohoku University, 4. Chiba University, 5. JAMSTEC, 6. Hokkaido University, 7. Gifu University

To deal effectively with global warming by mitigation and adaptation, it is necessary to monitor emission and sequestration of greenhouse gases with their underlying mechanisms including biogeochemical processes. The Earth-observation satellite is powerful tool to observe temporal and spatial variations in structure and function on ecosystem in regional to global scale. It has been conducted to estimate GPP (gross primary production) by using satellite-measured optical properties of vegetation canopy such as NDVI (normalized vegetation index). Those vegetation indices are related to greenness of the canopy but not reflect the photosynthetic activity, that are quite sensitive to climatic conditions. Thus, there are still large uncertainty in the estimation of GPP.

In recent years, advent of the Earth-observation satellite with high wavelength-resolution sensors enable us to observe SIF (Solar-Induced chlorophyll Fluorescence) emitted from terrestrial vegetation. Since the chlorophyll fluorescence is emitted in photochemical reaction, which is a part of photosynthetic process, SIF would be good indicator of photosynthetic activity. In the photochemical reaction, xanthophyll cycle is also play important roll to release extra energy and it is able to monitor its condition by using PRI (Photochemical Reflectance Index). In the recent study in single-leaf scale, it has been shown that simultaneously measured SIF and PRI help us to estimate accurate photosynthetic rate based on ecophysiological model (Hikosaka and Noda 2019). Similarly, simultaneous measurement of SIF and PRI with the Earth-observation satellite would be helpful to estimate GPP and understand the in regional to global scale. However, there are no satellite to measure SIF and PRI simultaneously to date. FLEX, which will be launched in 2023 is the only satellite mission to measure them.

In this talk, we will propose development of new satellite or only optical sensor to observe SIF and PRI. If the sensor onboard with other optical sensor like GCOM-C SGLI, we could obtain SIF, PRI and other vegetation indices such as NDVI simultaneously. These satellite data would contribute accurate estimation of GPP and effective policy making against global warming.

Keywords: Vegetation remote sensing

©2020. Japan Geoscience Union. All Right Reserved.

[J] Poster | M (Multidisciplinary and Interdisciplinary)：M-TT Technology & Techniques

[M-TT51] Frontiers in Geochemistry

convener:Shogo Tachibana(UTokyo Organization for Planetary and Space Science, University of Tokyo), Yusuke Yokoyama(Atmosphere and Ocean Research Institute, University of Tokyo), Hiroyuki Kagi(Geochemical Research Center, Graduate School of Science, University of Tokyo)

In modern earth and planetary sciences, many new findings have been obtained by using state-of-the-art technique. These new findings include highly precise and accurate data, which is supported by recent developments of the new analytical methods. To use these data correctly and effectively, we need to deepen our knowledge on the methodology. This session aims at providing an opportunity for various geoscientists to get together and have a strategic discussion on frontiers in geochemistry and cosmochemistry. Especially, researchers, who would like to apply such innovative techniques, will have chances to discuss with those who work on devising new geochemical methods. We welcome a wide range of cutting-edge geochemical topics, including technical development, which have a potential for breakthrough of earth and planetary sciences. Any presentations related to the direction of geochemistry and cosmochemistry in future are also welcome. We expect wide-ranged and future-oriented discussion to develop geochemistry and cosmochemistry. We ntote that a presenter can choose his/her presentation language (English or Japanese) in this session.

[MTT51-P01] Measurement of helium isotope ratio using multi-turn time-of-flight mass spectrometer

*Yuki Hattori[1], Yoshihide Akiyama[1], Hirochika Sumino[1] (1.Department of Basic Science, Graduate School of Arts and Sciences, The University of Tokyo)

[MTT51-P02] **Ba stable isotopes in the East China Sea, Japan Sea, Gulf of Alaska, and the South Pacific**

*Keiji Horikawa[1], Yuuki Tezuka[2], Takashi Miyazaki[3], Shigeyuki Wakaki[4] (1.Graduate School of Engineer and Science for Research, University of Toyama, 2.Graduate School of Engineer and Science for Education, University of Toyama, 3.Department of Solid Earth Geochemistry, JAMSTEC, 4.Kochi Institute for Core Sample Research, JAMSTEC)

[MTT51-P03] Boron isotope as tracer for seawater pH reconstruction and submarine hydrothermal circulation

*Ryuichi Shinjo[1] (1.Department of Physics and Earth Sciences, University of the Ryukyus)

[MTT51-P04] **Effect of experimental, optical, and geometrical variables on the laser heating of inclusions during Raman spectroscopic analysis**

*Yuuki Hagiwara[1], Kenta Yoshida[2], Akira Yoneda[3], Junji Torimoto[2], Junji Yamamoto[1] (1.Hokkaido University, 2.Japan Agency for Marine-earth Science and Technology, 3.Osaka University)

[MTT51-P05] Pressure dependence of micro-Raman mass spectrometry for carbon isotopic composition of carbon dioxide fluid

*Lena Yokokura[1], Yuuki Hagiwara[1], Junji Yamamoto[2] (1.Hokkaido University, 2.Hokkaido University Museum)

Measurement of helium isotope ratio using multi-turn time-of-flight mass spectrometer

*Yuki Hattori[1], Yoshihide Akiyama[1], Hirochika Sumino[1]

1. Department of Basic Science, Graduate School of Arts and Sciences, The University of Tokyo

The helium isotope ratio ($^3He/^4He$ ratio) of volcanic gas has a great potential as a monitoring tool of volcanic activity. $^3He/^4He$ ratio shows different values in geochemical reservoirs such as the atmosphere, crust, and mantle, depending on the balance of primordial (relatively enriched in ^3He compared to the atmosphere) and radiogenic (predominantly ^4He) helium. The $^3He/^4He$ ratios of volcanic gases have values between magmatic (up to 1.1×10^{-5} or lower) and crustal (less than 1×10^{-7}) values. When magma becomes active, the $^3He/^4He$ ratio of volcanic gas may increase as the contribution of magmatic helium is expected to be higher. Such $^3He/^4He$ ratio increases preceding volcanic eruptions have been reported for El Hierro, Canary Islands[1], Mt. Etna, Italy[2], and Ontake, Japan[3].

Continuous analysis of volcanic gas is necessary to monitor volcanic activity; however, it is difficult for $^3He/^4He$ ratio because magnetic-sector mass spectrometer equipped with a massive electromagnet is currently used to analyze helium isotopes. Adequate mass resolution to distinguish $^3He^+$ from HD^+ and high sensitivity to detect trace amounts of ^3He are required to measure $^3He/^4He$ ratio. Furthermore, high-vacuum line is also needed to purify and separate helium from other gaseous species because helium concentration in volcanic gas is generally quite low. For these reasons, helium isotope analysis is limited to suitable laboratory, and on-site, real-time measurement of the $^3He/^4He$ ratio around volcano is almost impossible.

We have been developing a new technique of noble gas analysis using “infiTOF” (MSI TOKYO, Inc., Japan), which is a small and portable time-of-flight (TOF) mass spectrometer derived from the MULTUM-S II multi-turn TOF mass spectrometer[4, 5], in order to measure the $^3He/^4He$ ratio of volcanic gas on site and in real time. The high mass resolution achieved by infiTOF is more than enough to distinguish $^3He^+$ and $^{20}Ne^+$ from their interferences, HD^+ and $^{40}Ar^{++}$, respectively. However, sensitivity of a normal infiTOF was not high enough to analyze noble gases in volcanic gas because most of noble gas molecules admitted to the infiTOF were pumped out by vacuum pumps directly connected to the spectrometer before ionized by an electron ionization source. In order to realize static operation (*i.e.* the spectrometer is isolated from the vacuum pumps so that sample gas molecules are closed off within the spectrometer envelope and analyzed for a long time enough to accumulate signals), we installed valves between the spectrometer volume and the vacuum pumps. Getter pumps, which absorb active gases but not noble gases, were also installed to keep the pressure in the spectrometer low during the operation. In addition, we introduced the ion counting method for signal processing to detect weak signals of ^3He. As a result, significant number of ^3He in the helium standard gas (HESJ[6]) has been detected. Although as high sensitivity as that of the magnetic-sector mass spectrometer has not yet been achieved, accumulating number of ^3He signals with a longer time will increase statistical precision of $^3He/^4He$ ratio enough to distinguish the origin of helium in volcanic gas sample based on its isotope ratio.

[1] Padrón *et. al.*, *Geology* (2013). [2] Paonita *et. al.*, *Geology* (2016). [3] Sano *et. al.*, *Sci. Rep.* (2014). [4] Toyoda *et. al.*, *J. Mass Spectrom.* (2003). [5] Shimma *et. al.*, *Anal. Chem.* (2010). [6] Matsuda *et. al.*, *Geochem. J.* (2002).

©2020. Japan Geoscience Union. All Right Reserved.

Keywords: mass spectrometry, isotope ratio, helium isotope, noble gas, volcanic gas

©2020. Japan Geoscience Union. All Right Reserved.

Ba stable isotopes in the East China Sea, Japan Sea, Gulf of Alaska, and the South Pacific

*Keiji Horikawa[1], Yuuki Tezuka[2], Takashi Miyazaki[3], Shigeyuki Wakaki[4]

1. Graduate School of Engineer and Science for Research, University of Toyama, 2. Graduate School of Engineer and Science for Education, University of Toyama, 3. Department of Solid Earth Geochemistry, JAMSTEC, 4. Kochi Institute for Core Sample Research, JAMSTEC

Barium has been used as a geochemical tracer for alkalinity, productivity (barite), and riverine inputs to the ocean. Recently, to further constrain Ba oceanic cycle and to improve the utility as a geochemical tracer, Ba stable isotopes in seawaters in the Atlantic Ocean and the North Pacific, river waters, and marine sediments have been measured. These previous studies highlight that (1) riverine input is the dominant source of barium to coastal seas and Ba isotopes in the marginal sea show the binary mixing with riverine and offshore seawaters, (2) deep waters in the Atlantic Ocean are mixed with water masses of lower $\delta^{138/134}$Ba AABW (Antarctic Bottom Water) and higher $\delta^{138/134}$Ba NADW (North Atlantic Deep Water), and (3) barite dissolution in the water column and benthic sediments should be an additional important source for Ba oceanic cycle.

In this study, we measured Ba isotopic compositions ($\delta^{138/134}$Ba, relative to NIST3104a) of sea waters in the East China Sea, Kuroshio region, the Japan Sea, Gulf of Alaska, and the South Pacific. These seawater samples were obtained by multiple research cruises from 2013 to 2019. The $\delta^{138/134}$Ba showed the highest values of ~0.73‰ in the Kuroshio region (S=~34.7), and the lowest value of ~0.27‰ in the inner shelf of the ECS (S=~31). Our $\delta^{138/134}$Ba data in the ECS were significantly lower than the previously reported Ba isotopic compositions in the ECS (Cao et al., 2016), but consistent with other seawater data in the North Pacific (Geyman et al., 2019). Although our seawater samples only cover the range of salinity from 30 to 34.7 in the ECS, the $\delta^{138/134}$Ba and salinity data can be explained by the binary mixing with end-members of Kuroshio and Changjiang River waters. The surface water samples in the Japan Sea also plotted on this binary mixing line, suggesting that Changjiang River water accounts for ~5% to the Japan Sea. If [Ba] and its isotope supplied from the Changjiang River were not temporally fluctuated (i.e., repetitive adsorption-desorption of Ba to clay particles do not induce significantly temporal changes in [Ba] and its isotope), our binary mixing line can be used to estimate paleo-salinity from $\delta^{138/134}$Ba of planktonic foraminifer, bivalves, and corals.

Finally, we also found that the deep waters (>2000 m) in the North–South Pacific ranged from 0.18 to 0.32‰, indicatingrelatively lower values than the deep waters in the Atlantic (0.25–0.45‰) (Hsieh and Henderson, 2017). The distribution of $\delta^{138/134}$Ba in the Pacific deep water can be simply explained by two processes; the LCDW injection of ~0.3‰ from the south to north and an additional input of Ba with relatively lower $\delta^{138/134}$Ba, probably from sediments and sinking particulate barite.

Keywords: Barium stable isotope, seawater, barite, salinity, water mass tracer

©2020. Japan Geoscience Union. All Right Reserved.

Boron isotope as tracer for seawater pH reconstruction and submarine hydrothermal circulation

*Ryuichi Shinjo[1]

1. Department of Physics and Earth Sciences, University of the Ryukyus

Here I present case study by using boron isotope, to demonstrate potential of boron isotopic investigation.
1) Seawater pH reconstruction from coral record
Ocean acidification caused by anthropogenically elevated CO_2 concentration in the atmosphere can pose a critical threat to calcifying marine organisms and coral reef ecosystems. However, because of temporally and spatially limited instrumental pH records, little is known about the actual long-term trend and natural variability of seawater pH during the past century. We present an annually resolved time series of a pH proxy record for 1940–1999 using boron-isotope composition ($\delta^{11}B$) in a modern massive Porites coral from Guam Island (NW Pacific). When superimposed onto interannualvariability, the data show a slightly decreasing trend of ~0.39‰ (equivalent to ~0.05–0.08 pH units for surface water pH) in the northwestern tropical Pacific since the mid-20th century (Shinjo et al., 2013).
2) Submarine hydrothermal circulation: interstitial water B isotope profile
Many active hydrothermal venting fields have been discovered at the spreading axes of the Okinawa Trough, a nascent back-arc basin. In order to explore sub-seafloor extent of hydrothermal fluid circulation, boron isotopic compositions of interstitial water (IW) of drilled core sediments by the D/V CHIKYU were analyzed. While IW at the reference site have $\delta^{11}B$ similar to seawater ~70 m below sea floor (mbsf), IW from active venting site and site at 200 m far from venting site show depth profile lowering $\delta^{11}B$ at deeper than ~40 mbsf. Low $\delta^{11}B$ values are approaching to those of venting fluids on $\delta^{11}B$ vs $1/B$ diagram, implying hydrothermal fluid extension to far from the venting site. These results confirm that boron isotope of IW is a powerful tracer for exploration of hydrothermal activity at young rift or back-arc basin system (Ishibashi et al., 2017).

Keywords: boron isotope, ocean acidification, submarine hydrothermal ore deposits

©2020. Japan Geoscience Union. All Right Reserved.

Effect of experimental, optical, and geometrical variables on the laser heating of inclusions during Raman spectroscopic analysis

*Yuuki Hagiwara[1], Kenta Yoshida[2], Akira Yoneda[3], Junji Torimoto[2], Junji Yamamoto[1]

1. Hokkaido University, 2. Japan Agency for Marine-earth Science and Technology, 3. Osaka University

Raman spectroscopy for fluid, melt, and mineral inclusions provide direct insights into the physicochemical conditions of the environment surrounding the host mineral at the time of trapping. However, the obtained Raman spectral characteristics such as peak position are modified due to the local temperature enhancement of the inclusions by the excitation laser, which may lead to systematic errors and incorrect conclusions if the effect is not corrected. Despite the potentially non-negligible effect of laser heating, laser heating coefficient (*B*) (˚C/mW) of inclusions have remained unsolved. Here, we determined *B* by two independent experiments and heat transport simulation to evaluate how various parameters such as experimental conditions, mineral properties, and inclusion geometry affect *B* of inclusions. To determine the influential experimental parameters on laser heating, we measured *B* of a total of 21 CO_2-rich fluid inclusions hosted in olivine, orthopyroxene, clinopyroxene, Cr-spinel, and quartz. Our results revealed that the measured *B* of fluid inclusions in spinel show highest (approx. 6 ˚C/mW) and those in quartz is lowest (approx. 1×10^{-2} ˚C/mW), consistent with previous inferences and our simulation results that absorption coefficient of the host mineral (a_{spinel} = 20 and a_{quartz} = 0.02 cm^{-1}) is linearly correlated with *B* and is the most influential parameter when absorption coefficient of the host mineral (a_h) is larger than those of a inclusion (a_{inc}). Furthermore, our results show that both inclusion size and depth have little impact, whereas thickness and radius of host mineral have significant influence on *B*. This suggests that the differences in inclusion size and depth to be analyzed in a given sample do not cause any systematic errors in the Raman data due to laser heating, but the host radius and thickness, which can be adjusted to some extent at the time of sample preparation, can be the cause of systematic errors between samples.

Our results show that even with a laser power of 10 mW, which is typical for inclusion analysis, the inclusion temperature rises to tens to one-hundred of degrees during the analysis depending especially on the host mineral geometry and optical properties. Therefore, correction of the effect of heating will be necessary to obtain reliable data from the Raman spectroscopic analysis of inclusions. In this study, we propose some correction methods for the non-negligible effect of laser heating.

Keywords: Raman spectroscopy, Laser heating, Fluid inclusion, Mineral inclusion, Melt inclusion, Finite element method

©2020. Japan Geoscience Union. All Right Reserved.

Pressure dependence of micro-Raman mass spectrometry for carbon isotopic composition of carbon dioxide fluid

*Lena Yokokura[1], Yuuki Hagiwara[1], Junji Yamamoto[2]

1. Hokkaido University, 2. Hokkaido University Museum

Micro-Raman spectroscopy can find the carbon isotopic ratio of CO_2 fluid from the ratio of intensity or area of a $^{13}CO_2$ peak to that of a $^{12}CO_2$ peak. We exam- ined the precisions of carbon isotopic ratios (δ^{13} C) of CO_2 at constant room temperature and pressure of 10–150 MPa. Measurement of the intensity ratio has precision of 2.8–8.7‰, which is better than that of the area ratio of 4.5–14.7‰. We also investigated the pressure dependence of the Raman inten- sity ratios and area ratio by changing fluid pressure. When changing fluid pres- sure from 10 to 150 MPa, the ratios of intensity and area both show negative correlation with fluid pressure (CO_2 density). Pressures of two types affect the Raman spectrum of CO_2 peaks, affecting the peak position and peak shape. To evaluate effects on the peak position, we repeatedly measured the intensity ratio at constant CO_2 pressure (10 MPa) with movement of the grating center position, which is defined as the center value of the analyzed wave number range. Although we moved the grating center position from 1248.5 to 1251.5 cm^{-1}, no significant correlation was observed for either ratio of inten- sity or area. The pressure effect on the ratios can be corrected by ascertaining the CO2 pressure. Combination with the Raman spectroscopic barometry for CO_2 enables analyses of δ^{13}C of CO_2 respectively using the intensity ratio and the area ratio of CO_2 Raman peaks within 8.7 and 14.7‰.

Keywords: carbon isotope ratio, Micro-Raman spectroscopy, CO2 fluid, fluid inclusion

©2020. Japan Geoscience Union. All Right Reserved.

[J] Poster | M (Multidisciplinary and Interdisciplinary)：M-TT Technology & Techniques

[M-TT52] Brand-new scope of coupling geophysics being established by infrasound and associated waves

convener:Masa-yuki Yamamoto(Department of systems engineering, Kochi University of Technology), Nobuo Arai(Disaster Mitigation Research Center, Nagoya University), Mie Ichihara(Earthquake Research Institute, University of Tokyo), Takayuki Otsu(Japan Weather Association)

Infrasound and associated wave studies are recently focused on coupling waves with long-distant and vertical propagation characteristics. Such kinds of waves, having with coupling process between the atmosphere and the surface of ground and ocean, are linked with elastic waves in lithosphere and oceanic sphere, as well as to atmospheric regions up to the upper atmosphere, playing a role of generating many kinds of wavelike turbulence in thermosphere. Moreover, whole on the globe, these waves excited depending on the latitude regions, as well as on the environmental regions, such as snow ice, desert, rainforest, mountain, ocean, etc., have their own characteristics. These waves can be excited by large-scale geophysical events like volcanic eruptions, tsunami, thunderstorms, etc. as well as artificial explosions, propagating with long distance. In this session, we would like to discuss such "coupling geophysics" by using many new or well-known investigated data and simulations of infrasound and associated low frequency waves. It can combine multiple spheres in geophysics and bring a brand-new scope of geophysics. Your contributions from many regions are welcome!

[MTT52-P01] Establishment of Nationwide Infrasound Observation Consortium and Future Plan for Disaster Mitigation Application

*Masa-yuki Yamamoto[1,2], Nobuo Arai[2,3], Takayuki Otsu[2,4] (1.Department of systems engineering, Kochi University of Technology, 2.Nationwide Infrasound Observation Consortium, 3.Disaster Mitigation Research Center, Nagoya University, 4.Japan Weather Association)

[MTT52-P02] Infrasound signals propagated from volcanic eruption detected at long distances

*Makiko Iwakuni[1], Takayuki Otsu[1], Nobuo Arai[2], Mami Nogami[1], Masashi Motohashi[1], Takanari Fujii[1], RYOHEI EMURA[1], Takahiko Murayama[1] (1.JAPAN WEATHER ASSOCIATION, 2.Disaster Mitigation Research Center, Nagoya University)

[MTT52-P03] Volcanic atmospheric perturbation detected with barometer, broadband seismometer, and GNSS-TEC: comparison with ray-tracing calculation

*Yuki Nakashima[1], Kiwamu Nishida[1], Yosuke Aoki[1], Kosuke Heki[2] (1.ERI, Univ. Tokyo, 2.Space Geodesy Lab., Hokkaido Univ.)

[MTT52-P04] The 3 types of infrasound generated by "The 2018 Hokkaido Eastern Iburi Earthquake"

★Invited Papers

*Mami Nogami[1], Takahiko Murayama[1], Takayuki Otsu[1], Makiko Iwakuni[1] (1.Japan Weather Association)

[MTT52-P05] Development and test operation of small infrasound data loggers

*Yuichiro Inoue[1], Masa-yuki Yamamoto[1] (1.Kochi University of Technology)

[MTT52-P06] Infrasound measurement with MEMS sensors

★Invited Papers

*Ryouichi Nishimura[1] (1.National Institute of Information and Communications Technology)

Establishment of Nationwide Infrasound Observation Consortium and Future Plan for Disaster Mitigation Application

*Masa-yuki Yamamoto[1,2], Nobuo Arai[2,3], Takayuki Otsu[2,4]

1. Department of systems engineering, Kochi University of Technology, 2. Nationwide Infrasound Observation Consortium, 3. Disaster Mitigation Research Center, Nagoya University, 4. Japan Weather Association

Infrasound (low-frequency sound wave, Micro-pressure wave) is the wave generated by various geophysical phenomena and propagates long distance in Earth's atmosphere, and it is expected to be applied to disaster prevention/mitigation. A researcher group who have been continuously discussed with in this JpGU session is now establishing "Nationwide Infrasound Observation Consortium" (provisional) aiming at disaster-mitigation engineering application based on scientific production.
In this paper, we will introduce previously-accumulated validating insight for various geophysical events and artificial sound sources, as well as application examples in some model regions aiming at constructing nationwide remote-sensing facility for disaster prevention/mitigation with applying already existing 100 or more infrasound sensing facilities in Japan, then we expected it could be an opportunity to discuss about the near future vision to become.
We, on behalf of the consortium members, will wait and would like to be reviewed with giving opinions directly by, all of the researchers and developers who are interested in this theme, any fruitful ideas for our future plan as well as comments for collaborating activities are welcome.

Keywords: Infrasound, Nationwide consortium, Disaster prevention/mitigation application

©2020. Japan Geoscience Union. All Right Reserved.

Infrasound signals propagated from volcanic eruption detected at long distances

*Makiko Iwakuni[1], Takayuki Otsu[1], Nobuo Arai[2], Mami Nogami[1], Masashi Motohashi[1], Takanari Fujii[1], RYOHEI EMURA[1], Takahiko Murayama[1]

1. JAPAN WEATHER ASSOCIATION, 2. Disaster Mitigation Research Center, Nagoya University

The infrasound signals generated by the eruption of Showa Crater of Sakurajima Volcano on 5 February 2016 was observed at microbarograph array in Mie, Isumi and Ofunato. Mie is 640 kilometers to the northeast of Sakurajima Volcano, Isumi is 990km and Ofunato is 1,300km. This event was reported at JpGU2017. Another event of Sakurajima Volcano eruption was recorded at microbarographs in Mie and Isumi. According to the weather conditions of that day, these infrasound signals of both stations are presumed to propagate around the ground surface. Celerity were about 0.34km/s at both stations.

Keywords: Infrasound, Volcano eruption, Microbarograph

©2020. Japan Geoscience Union. All Right Reserved.

Volcanic atmospheric perturbation detected with barometer, broadband seismometer, and GNSS-TEC: comparison with ray-tracing calculation

*Yuki Nakashima[1], Kiwamu Nishida[1], Yosuke Aoki[1], Kosuke Heki[2]

1. ERI, Univ. Tokyo, 2. Space Geodesy Lab., Hokkaido Univ.

We investigate an atmospheric perturbation excited by the Kuchinoerabujima phreatomagmatic eruption that occurred at 0:59 UT on 25th May in 2015. It made an ionospheric perturbation, and we extracted the signal from GEONET 1 Hz sampling data by the GNSS-TEC method. The signal has a ~10 mHz N-shaped pulse and a ~5 Hz wave continuing about 15 min. These features are quite similar to ionospheric perturbation excited by the Asama volcano eruption in 2004 (Heki 2006; Chonan et al., 2017). We also found barometric disturbance in almost the same frequency band with barometers and broadband seismometers installed by NIED and AIST. We tried to explain all of the detected signals with ray-tracing calculation. In this presentation, we will introduce the results and discuss the features of the phenomena.

Acknowledgment
We thank the Geospatial Information Authority of Japan (GSI) for the GEONET RINEX data (ftp://terras.gsi.go.jp/), National Research Institute for Earth Science and Disaster Resilience (NIED) for F-net and V-net data, and National Institute of Advanced Industrial Science and Technology (AIST) for the barometers data.

Keywords: GPS, GNSS, Ionosphere, Volcanic eruption, GPS-TEC, GNSS-TEC

©2020. Japan Geoscience Union. All Right Reserved.

The 3 types of infrasound generated by "The 2018 Hokkaido Eastern Iburi Earthquake"

*Mami Nogami[1], Takahiko Murayama[1], Takayuki Otsu[1], Makiko Iwakuni[1]

1. Japan Weather Association

The 2018 Hokkaido Eastern Iburi Earthquake(M6.7, focal depth 37 km) occurred on 5th September, 2018, 18:07(UTC), recorded seismic intensity 7 around the epicenter. Large strong motions were recorded in most of Hokkaido, in mountains near the epicenter large-scale landslides happened subsequently. I30JP and I45RU deployed for the nuclear test monitoring regime of CTBT were observed the waveforms, these analyses are corresponded to the azimuth of the epicenter and these wave chains have about 20 minutes interval respectively.

The 3 types infrasound generated by large earthquakes is reported by past many studies. The 1st observations of infrasound from earthquakes are identified as infrasound from vertical ground motion associated with local Rayleigh waves in both microbarometer and co-located broad-band seismogram at the same time, which were recorded very correlated signals of about 20 periods at I45RU and USRK deployed for seismic monitoring regime of CTBT. The 2nd observations of infrasound are identified as infrasound generated by the sudden strong vertical motion near the epicenter, for the earthquake, these analyses from I30JP and I45RU are corresponded to the azimuth of the epicenter, the assumption of propagation between stratosphere and surface are not conflicted with the observed time. The 3rd observations of infrasound are identified as infrasound generated in regions far from the epicenter by the interaction of surface waves with topographic features, such as mountains, for the earthquake, azimuths of these analyses from I30JP and I45RU have variations (+-10 degrees) directed toward the whole Hokkaido island, and the assumption described before is not also conflicted with the observed time.
In the poster presentation, we present features of the observed waveform, dominant frequency, amplitude and observed interval for the infrasound and seismic records. Furthermore, we present the result of the analysis about azimuth, speed and observed time, in addition to sound origin specification and propagation transmission.

Keywords: infrasound, seismoacoustic, Rayleigh wave, CTBTO

©2020. Japan Geoscience Union. All Right Reserved.

Development and test operation of small infrasound data loggers

*Yuichiro Inoue[1], Masa-yuki Yamamoto[1]

1. Kochi University of Technology

Infrasound, which is a low-pressure micro-pressure wave with a frequency of 20 Hz or less, has a characteristic that it is less susceptible for attenuation when propagating in the air and easily propagates over long distances. In 2019, Our Laboratory in Kochi University of Technology succeeded in producing a low cost and compact infrasound sensor by joint development with companies. The purpose of this research is to develop an infrasound data logger that is smaller and consumes less power than the conventional type or a laptop PC, and to operate the logger for a long period of time. Another objective is to develop a logger can that easily be deployed for observations, taking advantage of its small size.
The developed logger saves the data observed by the small infrasound sensor (INF04LE) on the Raspberry Pi Zero, and has been in continuous operation in the laboratory since September 2019. In addition, we conducted a cold-area test in the Svalbard Islands, Norway for 15 days from November 24 to December 8, 2019 using the developed prototype loggers, and confirmed that data could be acquired normally.
In the near future, we plan to design loggers with fixed point installation type loggers and temporary observation type loggers with different functions. Since the small infrasound sensor is a late-generation sensor, it is necessary to perform the observations in parallel with existing reference sensors and compare observation data of the same events.Therefore, it is necessary to perform the analysis at the timing when some large geophysical event occurs.In addition, we plan to develop a logger alive management and data graph display system.For the temporary observation type logger, we will further reduce power consumption and simplify the operation, aiming to data a data logger that anyone can handle easily in weak power supply condition.
In this study, we developed a prototype data logger for a small infrasound sensor. To date, a prototype has been developed and actually observed in test field. Since there are points for improvements, we plan to continue development and conduct long-term stable operation tests. Since there are improvements, we will continue to develop. A long-term stable operation test is also planned.

Keywords: Infrasound, Data logger

©2020. Japan Geoscience Union. All Right Reserved.

Infrasound measurement with MEMS sensors

*Ryouichi Nishimura[1]

1. National Institute of Information and Communications Technology

MEMS sensors are small in size and low power consumption. Because of that, they are suitable for a sensor network which usually requires a large number of sensors as well as their distribution over a wide area. Recent smartphones are usually equipped with multiple MEMS sensors inside. Therefore, they could play a role of good sensor devices, However, we cannot expect that a single MEMS sensor alone achieves high precision. Evaluation of their ability in use for infrasound monitoring is necessary.

We conducted some experiments with different configurations. In an experiment, multiple MEMS pressure sensors are simultaneously used at one place to measure a sound signal. Variance of the observed signals and improvement in signal-to-noise ratio by averaging them are quantitatively discussed. Meanwhile, sound has been continuously recorded using different types of measurement devices, including a smartphone, in the field for a couple of months. The aim was to compare the infrasound signals obtained by different devices in a practical situation. Results of the experiments and some findings are presented.

In addition, an application of the infrasound measurement device using MEMS sensors to the estimation of sound localization for volcanic eruption is demonstrated.

Keywords: Smartphone, MEMS sensor, Localization

©2020. Japan Geoscience Union. All Right Reserved.

[J] Poster | M (Multidisciplinary and Interdisciplinary)：M-ZZ Others

[M-ZZ55] Culture geology

convener:Hisashi Suzuki(Otani University), Tohru Sakiyama(Institute of Geo History, Japan Geochronology Network), Naoki Takahashi(Natural History Museum and Institute, Chiba)

Culture geology is an interdisciplinary field that deals with the relationship between human and geology. We have developed following research themes on the culture geology. (1) geology as a raw material, (2) geochemical analyses of archaeological remains, (3) relationship between geology and regional cultures, (4) geoeducation with museum and geopark, (5) letters and music with geology, and (6) geology and religion. We invite presentations of research results on all geological themes concerning human being.

[MZZ55-P01] Did Mitsuhide AKECHI change the channel of the River Yura?

★Invited Papers

*Kotaki Atsuo[1] (1.Kyoto Prefectural University)

[MZZ55-P02] Consideration on quarrying history of Rokko Granites on the basis of historical booklets “Meisho-zue” .

*Tohru Sakiyama[1] (1.Institute of Geo History, Japan Geochronology Network)

[MZZ55-P03] Transition of the use of building stones through the age in Chiba Prefecture

*Naoki Takahashi[1], Takuya Akashi[2] (1.Natural History Museum and Institute, Chiba, 2.Hisui-no-kai)

[MZZ55-P04] Finding the context of culture geology by utilizing local stone: A case study of the "Shindosaki stone" of Oiso town, Kanagawa prefecture

*Kiminori Taguchi [1] (1.Kanagawa Prefectural Museum of Natural History)

[MZZ55-P05] **Geomorphology and geology of pilgrimage grottoes in mountain region, northern part of Oita Prefecture, Japan**

*Norihito Kawamura[1] (1.School of Regional Resource Management, Graduate School, University of Hyogo)

[MZZ55-P06] Progress of culture geology in Japan and other countries

*Hisashi Suzuki[1] (1.Otani University)

Did Mitsuhide AKECHI change the channel of the River Yura?

*Kotaki Atsuo[1]

1. Kyoto Prefectural University

Mitsuhide AKECHI, a commander in the period of civil war of medieval Japan, established the Fukuchiyama castle town in the northern region of Kyoto prefecture. Fukuchiyama people believe that Mitsuhide changed the flow channel of the River Yura that runs through Fukuchiyama city, when he constructed the Fukuchiyama castle town.
Is this story really fact? I have checked boring core data of the Fukuchiyama basin, especially around the castle town. As a result, at the fork of the old flow channel from the River Yura, more than 10 m thick pebbly sediments are distributed instead of such channel sediments as mud. The pebbly sediments are regarded as a natural levee, not artificial one. The evidence suggested that the Mitsuhide’ s story changing the flow channel seems not to be a fact, but he constructed the castle town on the sturdy pebbly mound of a natural levee.

Keywords: Mitsuhide AKECHI, Fukuchi castle, River Yura, natural levee

©2020. Japan Geoscience Union. All Right Reserved.

Consideration on quarrying history of Rokko Granites on the basis of historical booklets “Meisho-zue” .

*Tohru Sakiyama[1]

1. Institute of Geo History, Japan Geochronology Network

Medium to coarse-grained hornblende bearing biotite granites distributed in Rokko Mountains were quarried for building stones in ancient time. Measurement of magnetic susceptibility and observation of rock facies have revealed that many tombstones of 13th to 16th century made by Rokko Granites are widely distributed in coastal areas of western Japan. But main quarries have been moved to islands and coastal area of Inland Sea from Rokko Mountains after 17th century.

Quarrying history of Rokko Granites are shown by historical booklets so-called “Meisho-zue” in 18th century. Granitc stones from Rokko Mountains have been originally called Mikage-Ishi, because they were shipped off from Mikage in Kobe. Explanatory note of “Meisho-zue” indicates that quarrying area moved from seaside area to deep in mountains during Edo Period. Furthermore, another granitic stones from some area located far apart from the Rokko Mountains are included in item on Mikage-ishi in “Meisho-zue”. This fact indicates that Mikage-ishi is not only proper noun of the granitic stones in Rokko Mountains but common noun of granitic stones at least late 18th century.

Geological study shows that some granitic sones have been quarried in sediments by debris flow. On the other hand, debris flow frequently occurred throughout history at the foot area of Rokko Mountains.

Frequent debris flow brought large amount of granitic stones near seaside area, and such granite stones were shipped off and widely distributed in various places. As a result, Mikage-ishi changed from proper noun of Rokko Granite to common noun of granitic stones at 17th to 18th century.

Keywords: granite, magnetic susceptibility, building stone, booklet of historic sites, debris flow

©2020. Japan Geoscience Union. All Right Reserved.

Transition of the use of building stones through the age in Chiba Prefecture

*Naoki Takahashi[1], Takuya Akashi[2]

1. Natural History Museum and Institute, Chiba, 2. Hisui-no-kai

Cenozoic sedimentary strata are dominant in the Chiba Prefecture, so productions of hard rocks are poor in the area. But various kinds of rocks produce in and out of the area are used as tools, building stones, and stone cultural properties, and differences of the kinds of rocks through the age are recognized. They are reflected by the difference of the purpose of use, means of transport and technique of taking out from the ground. In the early modern period, rocks produced at the coast area of the Izu Peninsula such as andesites of the Hakone Volcano and tuffs of the Shirahama Group were used as tombstones and stone cultural properties by common peoples. They were transported by ships. In the modern age, rocks produced at the inland areas such as 'Oya-ishi' (green tuff), 'Ashino-ishi' (welded tuff), 'Inada-ishi' (granite) were transported by trains and trucks. After the Heisei era, rocks produced at the foreign countries are overwhelmingly dominant for economic reasons.

Keywords: building stones, Chiba Prefecture

©2020. Japan Geoscience Union. All Right Reserved.

Finding the context of culture geology by utilizing local stone: A case study of the "Shindosaki stone" of Oiso town, Kanagawa prefecture

*Kiminori Taguchi [1]

1. Kanagawa Prefectural Museum of Natural History

The local stones were once used as stone materials in people's lives and were familiar to them. Stones in such areas are likely to be an element of useful local resources in the context of culture geology, because local stone materials are closely related to the geographical and geological environment, regional history and people's lives in a given area. In addition to regional geology, regional resources related to a wide range of natural environments, living environments, regional culture, history and landscapes are factors for understanding area's contexts.
In this presentation, I introduce the "Sindosaki stone" in Oiso town, Kanagawa prefecture, as an example of interpretation of the cultural and geological context of local stone.
On the old stone walls in Oiso town, you can find two types of local stone called "Koma-ishi" and "Sindosaki stone". Judging from the state of their use, it is considered that the stones were used from the Meiji to Showa periods. Although there are many historical records on the quarrying and the use of Koma-ishi, there are few historical records on the quarrying and use of the Sindosaki stone. To determine the origin of the Sindosaki stone, observation of the stone itself and comparison of the stratum from which it originated are effective measures. Considering that the lithofacies of the Oiso Formation of the Miura Group on the Oiso coast correspond to the Sindosaki stone, the utilization of the Sindosaki stone in the area has been seen frequently.
On the other hand, it is also useful to check the quarries in the survey of regional stone. On the Oiso coast, rocks of the Oiso Formation are now widely exposed due to the erosion of gravels on the coast caused by the Typhoon 19 in 2019, and quarry traces that were previously difficult to see have been confirmed there. As a result, it became clear that various lithologies of the Oiso Formation had been cut out as stone materials.
Assuming that this quarrying is in the Meiji era, the altitude of the quarry needs to be subtracted from the uplift of the Kanto Earthquake. If we subtract a 1.8 m height from the present altitude, the quarry will be underwater at the intertidal level. It can be assumed that cut stones could be transported with the buoyancy in seawater.
When I take these issues into account in the regional context of culture geology, several keywords can be seen. One of them is "uplift" which is the geologic key factor of the Oiso region. The topography of Oiso Hills is related to the development of villas in the Meiji period and the establishment of swimming beaches on rocky shores. The location of the stone quarry on the Oiso coast, where terraces and shore platform are developed, can be related to the uplift.
Thus, geological materials can be made more attractive by finding area's contexts related to cultural matters such as local history and people's lives in accordance with local geologic/geographic phenomena. It is a interdisciplinal perspective of culture geology.

Keywords: local stone, regional resources, culture geology, area's context

©2020. Japan Geoscience Union. All Right Reserved.

Geomorphology and geology of pilgrimage grottoes in mountain region, northern part of Oita Prefecture, Japan

*Norihito Kawamura[1]

1. School of Regional Resource Management, Graduate School, University of Hyogo

In this study, geomorphological and geological field research is conducted for discovering the relations between natural environments and pilgrimage sites that are located in the mountainous region of the Kunisaki Peninsula, Oita Prefecture, southwest Japan. The research exhibits that pilgrimage sites that are located at the cliffs appear as volcanic breccia at the Pleistocene formation.

Keywords: religion, grotto, pyroclastic rocks

©2020. Japan Geoscience Union. All Right Reserved.

Progress of culture geology in Japan and other countries

*Hisashi Suzuki[1]

1. Otani University

The culture geology was proposed by Prof. Wolfgang Vetters in Salzburg University, Austria, in 2003. In Japan, the first session was held in the meeting of the Geological Society of Japan in 2014 (Kagoshima). After that, academic meetings on culture geology have been held in the Tokyo Geographical Society, the Association for the Geological Collaboration in Japan and so on. In 2018 the Society of Culture Geology was established in Kyoto, and a new journal "Geology and Culture" has been published.
As is developed in Japan, the culture geology in Austria was previously active. But now in Austria the activity of culture geology is not so energetic. Recently, the culture geology session was held in the XXI International Congress of the Carpathian Balkan Geological Association (CBGA) and total 25 oral and poster presentations were made (in Salzburg, 2018). Their contents were mostly chemical analyses of archaeological remains.
On the contrary to European trend, such humanistic contents as geoliterature, odd-shaped rocks, cliff Buddha etc. have been studied in Japan as well as stone materials for base of castles, modern buildings and so on. Humanistic contents concerning religion seem to come from animistic natural beliefs in Japan.
I now try to study the culture geology of Myanmar, which is a Buddhistic country like Japan. Myanmar people believe also a peculiar religion *Nat* as well as Buddhism. Remarkable is the geologic setting in Myanmar, which is situated in an active plate zone like Japan. In March 2021 the first international conference of culture geology will be held in Kyoto. I hope interdisciplinal geosciences will be advanced with international collaborations.

Keywords: culture geology, stone material, religion, Myanmar

©2020. Japan Geoscience Union. All Right Reserved.

[J] Poster | M (Multidisciplinary and Interdisciplinary)：M-ZZ Others

[M-ZZ56] Studies of Geoscience : historical, philosophical and STS studies

convener:Michiko Yajima(College of Humanity and Science, Nihon University), Toshihiro Yamada(Taisho University), Shigeyuki Aoki(Faculty of Letters, Chuo University), Shigeo Yoshida(Department of Earth and Planetary Sciences, Faculty of Sciences, Kyushu University)

Topics on history, philosophy and STS (science, technology and society)studies of geoscience will be discussed. Any related subject is welcome, such as history of mining, historical studies of geohazards, methodology of geoscience, sociology of natural hazards, politics of environmental issues, and risk theory.

[MZZ56-P01] **Inquiry of Origin**,
All Inquiries can not be achieved by **Induction** and **Deduction** alone;
Creative Inference using **Results (characteristics) of Evolution**,
called **Abduction** is a **Method of Evaluation** that transcends **Time** and **Space**.

*Akira Taneko[1] (1.SEED SCIENCE Lab.)

[MZZ56-P02] A study on recognition of indigenous knowledge in college students

*LU KE[1], CHENWEI CAI[1], HANQIU ZHANG[1], SHIXIAN LUO[1], JIAYING SHI[1], Damayanti Rosyi[1], Azuki Kiriyama[1], Mai Uemura[1], Katsunori Furuya[1] (1.Chiba University)

[MZZ56-P03] Harnessing the power of geoscience as a vehicle for interdisciplinary collaboration across borders

*Felix Kwabena Donkor[1] (1.University of South Africa)

[MZZ56-P04] An Archaeological Investigation inti the Use of Landscape for the Irrigation of Ancient Sri Lanka

*Chandana Rohana Withanachchi[1,2] (1.Sri Lanka Council of Archaeologists, 2.Rajarata University of Sri Lanka)

[MZZ56-P05] “The life and achievement of Sugi, Kenichi” Chikukagaku, 56, 35-39, by Miyashiro, Akiho, 1961

*Hidehisa Mashima[1] (1.Center for Obsidian and Lithic Studies, Meiji University)

Inquiry of Origin, All Inquiries can not be achieved by Induction and Deduction alone; *Creative Inference* using Results (characteristics) of Evolution, called Abduction is a Method of Evaluation that transcends Time and Space.

*Akira Taneko[1]

1. SEED SCIENCE Lab.

Inquiry of Origin,
All **Inquiries** can not be achieved by **Induction** and **Deduction** alone; **Creative Inference** using **Results (characteristics) of Evolution**, called **Abduction** is a **Method of Evaluation** that transcends **Time** and **Space.**

In **Induction** and **Deduction Methods**, it is Impossible to verify because **Reproducibility Experiment cannot be erformed** even if Initial state is assumed.
Even if only One Item can be confirmed by **Simulation**, it is ***necessary to explain*** **All Results of Evolution** ***in a unified manner.*** *If that is* ***Not Possible,*** it cannot **be Verified**.

On Other hand, in **Multi-Impact Hypothesis** [3], **Differentiated Mars-Sized Protoplanet CERRA** formed at Asteroid Belt Position is perturbed by Giant Mass Planet (Jupiter) formed thereafter. In about 600 million years, CERRA Orbit flattened to Near Point of Jupiter, and Tidal Rupture occurred at Point where Gravitational pull of Jupiter and Sun coincided, resulting in Multiple Train Mantle Asteroids and a Single Orbit around Same Elliptical Orbit. Because Core and Rest of Mantle were large in Mass, Peripheral Speed decreased due to Law of Equal Energy Distribution and moved to Inner Orbit to become Mercury.

By Comparison, Mercury's Core / Mantle ratio was shown to be about twice that of other terrestrial planets, and Origin of Same Component Ratio of Inner Planets was also easily shown; Of course, Feeding Zone could be explained. Was calculated from Theoretical Hypothesis that Inevitable Collision at Intersection with Earth's Orbit, Relative Angle of 36.45 degrees, and Relative Speed of 12.3 km /s were obtained.

Furthermore, Orbital Energy of Moon (60×Re) was also shown, and Collision of Earth Mantle with Mantle Fragment did not deform Earth core and could explain Eccentricity of Moon due to Ejection of Earth Mantle. Origin of Deep Ocean Floor (approximately 70% of Surface Area) with an average Depth of about 4 km and Origins of Pacific Rim-Arc, Back Arc Basin, and Arc Trench were also explained by Isostasy.

Collision causes Cracks in Mantle, lowers Viscosity of Upper Mantle and makes Plate easier to move. Unbalance of Moment of Inertia between Marine Plate and Land Plate and Couple due to Earth's Rotation cause Movement of Plate and Transformation Fault and Rring Oceanic Convex Plate began to dive beneath Pacific Back-Arc Concave Basin, giving rise to Plate Tectonics.

On Other Side of Collision of Giant Mantle Fragment, a **Shock Wave** is transmitted *at Same Time*, Forming a **Kimberlite Pipe** and a **Diamond Mine**. Collisions to High latitude (near **Drake Strait**) that formed Tethys Sea caused **Tilting of Earth Aaxis**, Origin of Mirunui Mine, and caused a **Sudden Change** in Direction of

©2020. Japan Geoscience Union. All Right Reserved.

Plate driving.
It cannot be explained by **Thermal Convection Driving Force**.

Since the Earth's mantle is as dense as the interior, the moon from the ejected mantle is eccentric (approximately 2 km). Even if the mantle near the molten crust is re-covered in a spherical shape, the dense basalt remains near the lunar surface and faces the surface When a meteorite collides with the surface, Black basalt inside melts and flows out, forming a Moon-Sea and Rabbit Pattern.

The eccentric moon rotates around the earth and the common center of gravity inside the earth, and the heavy part is located on the side of the center of gravity, causing it to always face the earth.

More Items that can explain Multiple Results of Evolution (Yuichi's experiment) in a unified manner, More True it is in Abduction.

Origin of Earth as well as **Origin of Moon** [3] and the solar system could be verified by **Abduction** using **Results** of **Evolution.** [3]**JpGU Sep.2014 P1-22 Akira Taneko**

Keywords: Search for All Origins cannot be achieved by Induction and Deduction alone., Creative reasoning using Results (Characteristics) of Evolution called Abduction, An Evaluation Method that transcends Time and Space, The example of transcending time: "Multi-Impact Hypothesis", Example of transcending space and time: "New stationary cosmology with quantum redshift", Induction and Ddeduction can verify only Periodic Phenomena

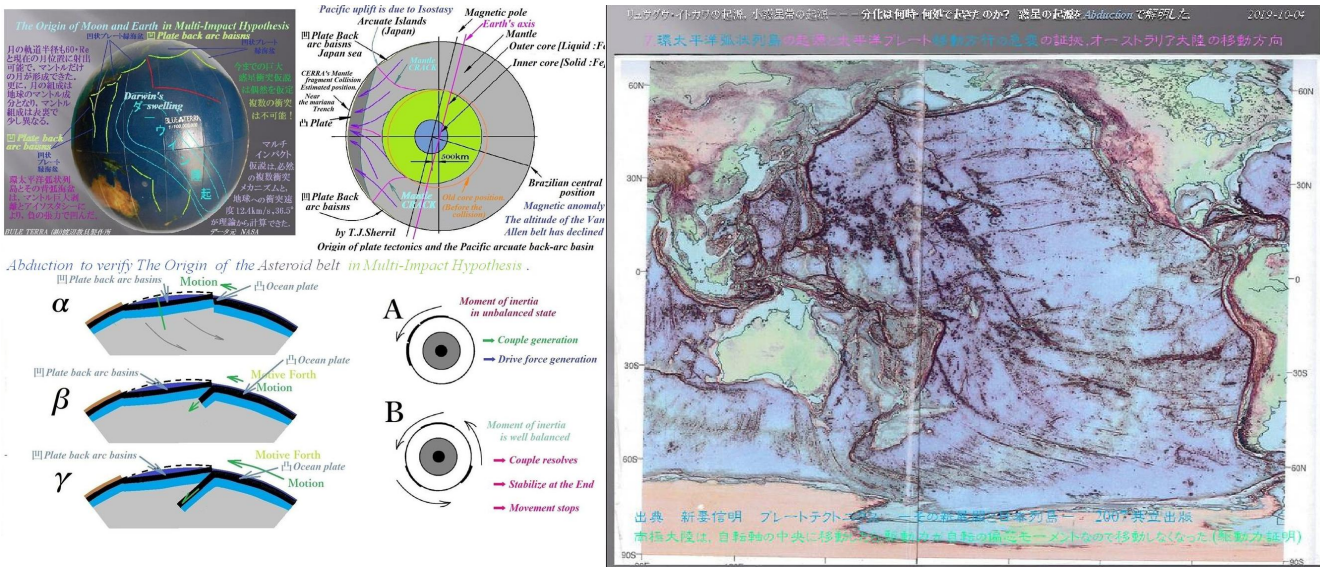

©2020. Japan Geoscience Union. All Right Reserved.

A study on recognition of indigenous knowledge in college students

*LU KE[1], CHENWEI CAI[1], HANQIU ZHANG[1], SHIXIAN LUO[1], JIAYING SHI[1], Damayanti Rosyi[1], Azuki Kiriyama[1], Mai Uemura[1], Katsunori Furuya[1]

1. Chiba University

Since the cognitive change of the boundary of scientific cognition, the concepts of Falsifiability and Adaptability have been applied to the related research of human and natural environment. As a kind of empirical knowledge, indigenous knowledge has been despised and ignored because it does not meet the standard of scientific knowledge, and has been placed on the opposite of scientific knowledge. However, it is undeniable that although the indigenous knowledge remains at the level of experience and skills, it is still used to serve the relationship between human and nature. Nowadays, more and more scientists are calling for the integration of indigenous knowledge and science. Also, at the same time, there are two sides in indigenous knowledge, such as subjective and objective, useful and useless, indigenous' science' and indigenous' beliefs'. This paper attempts to study how well-educated college students view indigenous knowledge and the relationship between indigenous knowledge and science. A total of 98 undergraduate students were investigated by paper questionnaire and online questionnaire. The research shows that regardless of gender, the vast majority of respondents show a neutral and positive attitude towards indigenous knowledge, and are in favor of the integration of indigenous knowledge and science. And with deeper understanding of scientific knowledge, the more positive the evaluation of indigenous knowledge and clearer the overall attitude to it will be.

Keywords: indigenous knowledge, scientific knowledge, Adaptability, Falsifiability, college students

©2020. Japan Geoscience Union. All Right Reserved.

Harnessing the power of geoscience as a vehicle for interdisciplinary collaboration across borders

*Felix Kwabena Donkor[1]

1. University of South Africa

A core theme in the Sustainable Development Goals (SDGs) is the need for knowledge co-creation to inform policy and fostering of partnerships that will safeguard sustainability development. Moreover, in our contemporary society characterised by knowledge economies challenged by wicked problems the importance of interdisciplinary collaborations cannot be overemphasised. The field of geoscience provides a unique platform for enhanced cross-disciplinary collaboration by researchers across the globe as well as fostering of crucial partnerships to address some of the pressing global challenges. This study uses the theory of team science to explore the opportunities and constraints of geoscience as a vehicle for international and cross disciplinary research towards sustainability.

Keywords: Geoscience, Sustainability, cross-disciplinary, Knowledge co-creation, Wicked problems

©2020. Japan Geoscience Union. All Right Reserved.

An Archaeological Investigation inti the Use of Landscape for the Irrigation of Ancient Sri Lanka

*Chandana Rohana Withanachchi[1,2]

1. Sri Lanka Council of Archaeologists, 2. Rajarata University of Sri Lanka

Water is one of the main factors that make human life more organized. Water was an essential part of all forms of life based on agriculture in civilization. As a result, the irrigation industry begins during the human civilization. It is clear that the ancestors' ability to identify suitable land for agriculture was based on experience gained from the surrounding environment over time. The main problem was the irrigation of the farm. The reason for this is that rain-free areas cover most areas of the world where soil deposits are suitable for agriculture. The ancestors accepted the challenge and built irrigation systems based on the natural location of the land. There is evidence that they started primary irrigation in the early stages of development, the proto- historical period, and gradually developed them. The nature of the land they have used for this purpose. There is living and archaeological evidence for this in the Dry Zone of Sri Lanka. This research paper focuses on the way land was used for ancient irrigation in Sri Lanka. The main objective of the research is to investigate how the ancestors used the landscape in the construction of irrigation in Sri Lanka. This research was carried out based on the data collected from field exploration and available archaeological evidence. In the Mesolithic period, where water meets in the lowlands of the plains used by their water use could be converted into tanks. By examining the contours of the Dry Zone plain, and by surveying the land, it is evident that these natural maps are made into tanks utilizing minimally fried short dams. The role of the human factor has been significant over a long period, and its correlation with spatial, cultural patterns has been remarkable. Particularly in the prehistoric period, people have assumed that agriculture was the primary means of storing water in the catchment. It is assumed that such small tanks could have been created in the area because of the location of the macro-land and the agriculture-friendly soil zone. In the study of the use of the landscape for irrigation, the evidence obtained from small rural tanks in the dry zone, which are recognized as the oldest irrigation works in the country, is vital. These tanks, which have already evolved into the cascade system, can also be referred to as the tanks. This is because the interconnected network of tanks has been created. The nature of the landscape is directly affected by this. The effective use of land for irrigation is evident from the fact that many small tanks have developed into small tanks, medium sized tanks and large tanks with the intervention of the state in the later stages. According to the available information, it is clear that the dry zone rural settlements were established using these small tanks. There is much archaeological evidence in the dry zone of Sri Lanka. It is clear from the above information that irrigation works have been established based on the people's understanding of the natural landscape. Many of the irrigation works that were built by the ancestors are now in operation because they are located in the right places. Accordingly, the Dry Zone landscape which is responsible for irrigation can be considered as our heritage.

Keywords: Cultural landscape, Irrigation, dry zone, Sri Lanka, Traditional Knowledge

©2020. Japan Geoscience Union. All Right Reserved.

©2020. Japan Geoscience Union. All Right Reserved.

“The life and achievement of Sugi, Kenichi” Chikukagaku, 56, 35-39, by Miyashiro, Akiho, 1961

*Hidehisa Mashima[1]

1. Center for Obsidian and Lithic Studies, Meiji University

Descriptions by Miyashiro, Akiho have been regarded as strong evidence for the negative exegesis for the history of Japanese geology. Any description, however, has some biases from the viewpoint of its author. In order to claim that Japanese geology before world war II was less-developed, we need to examine the adjectively of Miyashiro’s descriptions. Sugi Kenichi (1901 –1948) was one of the representative petrologists prior to world war II in Japan. Miyashiro (1961) published “Life and Achievements of Sugi, Kenichi.” The examination of Miyashiro (1961) is important to understand the characteristics of his descriptions about the history of Japanese geology. Sugi was also the supervisor of Gorai Masao and Kroda Yoshimasu, who debated with Miyashiro and his colleagues about the genesis of the Abukuma metamorphic rocks, which is called the Abukuma issue, in 1960 –70s. Miyashiro (1961) is one of the reasons why the Abukuma issue was so escalated between the Sugi’s students and Miyashiro. The examination of Miyashiro (1961) therefore is also important for us to understand the dynamics of Japanese geology after world war II. In this presentation, I examine Miyashiro (1961). Discerptions about Sugi in Miyashiro (1961) are natively biased. Some issues were described with an inadequate timeline, which leads readers to feel that Sugi would have been a backward researcher. There is no description about the contributions of Sugi to the foundation of the department of geology at Kyushu University, three posthumous articles in the science reports of Kyushu University, the special issue dedicated to the late Prof. Sugi, Kenichi in 1951, and the Sugi Library which is composed of his bibliotheca donated to Kyushu University by his bereaved family. These features of Miyashiro (1961) indicate that we would be misinformed by Miyashsiro’s descriptions that Japanese geology before than him was backward and sluggish.

Keywords: history of Japanese geology, Sugi Kenichi, Miyashiro Akiho

©2020. Japan Geoscience Union. All Right Reserved.

[J] Poster | M (Multidisciplinary and Interdisciplinary)：M-ZZ Others

[M-ZZ57] Marine Manganese Minerals: Science, Engineering and Application

convener:Akira Usui(Marine Core Research Center, Kochi University), Yoshio Takahashi(Department of Earth and Planetary Science, Graduate School of Science, The University of Tokyo), Katsuhiko Suzuki(Submarine Resources Research Center, Japan Agency for Marine-Earth Science and Technology), Takashi Ito(Faculty of Education, Ibaraki University)

Marine manganese deposits include nodules and crusts of massive iron-manganese oxide aggregates associated with useful metals. The deposits are known as potential resources of Co, Cu, Ni, REE, Pt and Te. However, the controlling parameters on the regional and temporal variations in chemical and mineralogical composition have not been clarified yet. In this session, various factors in the growth of manganese oxides, enrichment and circulation of metals, paleoenvironment, formation age of manganese deposits, and results of exploration and environmental impact studies will be discussed from viewpoints of geosciences, engineering, environmental sciences.

[MZZ57-P01] Sediment property in the exploration area for cobalt-rich crusts

*Kyoko Yamaoka[1], Atsushi Suzuki[1], Yuki Ota[1], Yuichiro Tanaka[1], Akifumi Shimamoto[2], Tatsuo Fukuhara[2], Junpei Minatoya[3], Shogo Kato[3], Yoshiaki Igarashi[3], Nobuyuki Okamoto[3] (1.Geological Survey of Japan, National Institute of Advanced Industrial Science and Technology, 2.KANSO Co.,Ltd., 3.Japan Oil, Gas and Metals National Corporation (JOGMEC))

[MZZ57-P02] GEOCHEMICAL AND MINERALOGICAL CHARACTERIZATION OF THE MOLANGO MN DEPOSITS: CONSTRAITS ON GENESIS

*Joseph Madondo[1], Carles Canet[2,1], Eduardo Gonzalez-Partida[4], Augusto Antonio Rodriguez-Diaz[1], Fernando Nuñez-Useche[3] (1.Institute of Geophysiscs (UNAM) , 2.Centre for Atmospheric Sciences (UNAM), 3.Institute of Geology (UNAM), 4.Centre for Geosciences (UNAM))

[MZZ57-P03] Relationship between isotope fractionation and valence of tellurium adsorbed on the Fe-Mn oxides from seawater

*Yusuke Fukami[1], Teruhiko Kashiwabara[2], Hiroshi Amakawa[3], Takazo Shibuya[2], Akira Usui[4], Katsuhiko Suzuki[2] (1.Gakushuin University, 2.Japan Agency for Marine-Earth Science and Technology, 3.Atmosphere and Ocean Research Institute The University of Tokyo, 4.Marine Core Research Center, Kochi University)

[MZZ57-P04] Formation process of different types of manganese nodules collected on seamounts in the Northeast Pacific

Wataru Katanoda[1], *Masafumi MURAYAMA[1], Akira Usui[2], Takeyasu Yamagata[3], Hiroyuki Matsuzaki[3] (1.Faculty of Agriculture and Marine Science, Kochi University, 2.Center for advanced Marine Core Research, Kochi University, 3.The University Museum,The University of Tokyo)

Sediment property in the exploration area for cobalt-rich crusts

*Kyoko Yamaoka[1], Atsushi Suzuki[1], Yuki Ota[1], Yuichiro Tanaka[1], Akifumi Shimamoto[2], Tatsuo Fukuhara[2], Junpei Minatoya[3], Shogo Kato[3], Yoshiaki Igarashi[3], Nobuyuki Okamoto[3]

1. Geological Survey of Japan, National Institute of Advanced Industrial Science and Technology, 2. KANSO Co.,Ltd., 3. Japan Oil, Gas and Metals National Corporation (JOGMEC)

Surface sediment cores were obtained from 5 seamounts (JA02, JA03, JA04, JA06, and JA17 Seamounts) as a part of the environment baseline survey in the exploration area for cobalt-rich crusts, and physical property and chemical composition of the sediments were investigated. In some of the sediment cores, DO, pH, and ORP of pore waters were measured using a microsensor. The flat-top sediments from all seamounts (1,300-1,500 m water depth) were calcareous ooze (CaCO3 content >90%), which is consistent with carbonate-dominant production and shallower depth than CCD. The flat-top sediments had similar density of 2.6-2.7 g/cm3 and water content of about 50%. In contrast, the flat-top sediments at JA02 and JA04 Seamounts showed larger median grain size (100-350 μm) than the other JA03, JA06, and JA17 Seamounts (10-60 μm). Chemical compositions of the flat-top sediments were characterized by low TOC (<0.15%), TN (<0.03%) and biogenic opal (<0.9%). The TOC, TN, and biogenic opal decreased with depth, corresponding to decrease of DO in the pore waters. Surface sediments in the base of seamounts (4,000-5,000 m water depth) were collected from JA03 and JA06 Seamounts. The base sediments consisted of pelagic clay except for one sediment core composed of siliceous ooze from JA06 Seamount. The physical properties of siliceous ooze were significantly deferent from pelagic clay, showing lower density, higher water content, and larger median size. TOC and TN in the base sediments were also low with the maximum values of 0.4% and 0.08%, respectively, reflecting oligotrophic condition in the area. and. C/N ratios decreased with depth, suggesting the preservations of inorganic ammonium and nitrogen-rich organic matter within clay minerals. Several large manganese nodules (2-5 cm in diameter) were observed on the surface of base sediments from JA03 Seamount, whereas small manganese nodules (~1 cm in diameter) were existed on the surface of one sediment core from JA06 Seamount. While the DO in pore waters was relatively constant in the base sediments from JA03 Seamount, the rapid decline of DO within 2 cm surface layer was observed in the base sediments from JA06 Seamount. Mn concentration of the base sediments from JA03 Seamount was 0.3-0.4% with no vertical variation. In contrast, Mn was concentrated up to 4.6% in the surface layer of the base sediments from JA06 Seamount and showed decrease trend with depth. Co, Ni, Cu, Zn, Cd concentrations also showed similar depth distribution patterns. The chemical compositions of manganese nodules from the base of JA03 Seamount indicated hydrogenetic origin, which is consistent with the observed oxic sedimentary environment. On the other hand, the base sediments from JA06 Seamount would represent suboxic conditions, favorable to the growth of diagenetic manganese nodules.

Keywords: seamount, sediment, redox

©2020. Japan Geoscience Union. All Right Reserved.

GEOCHEMICAL AND MINERALOGICAL CHARACTERIZATION OF THE MOLANGO MN DEPOSITS: CONSTRAITS ON GENESIS

*Joseph Madondo[1], Carles Canet[2,1], Eduardo Gonzalez-Partida[4], Augusto Antonio Rodriguez-Diaz[1], Fernando Nuñez-Useche[3]

1. Institute of Geophysiscs (UNAM) , 2. Centre for Atmospheric Sciences (UNAM), 3. Institute of Geology (UNAM), 4. Centre for Geosciences (UNAM)

The Molango deposits of eastern central Mexico are the largest Mn deposits in Northamerica. These deposits are hosted by late Jurassic (Kimmeridgian) black shales belonging to the Chipoco formation. Mineralogical, sedimentological, geochemical and isotopic methods were employed to investigate the genesis of the deposit. Mineralogical and geochemical results of the ore zone reveal a relationship between the host black shales and Mn enrichment. Carbon isotopic values and total organic carbon (TOC) indicate manganese carbonate (rhodochrosite) formation occurred by reduction of manganese oxides concurrent with organic matter oxidation. Sedimentological and microfacies analyses indicate formation under sub oxic conditions , characterized by absence of microfauna in the ore zone. Framboidal pyrite analysis is also consistent with formation under sub oxic to anoxic conditions (Wilkin, 1996). REE multiple-proxy analyses on the other hand indicate possible oxic conditions. Organic matter enrichment and anoxic conditions are a product of high productivity caused by nutrient-rich hydrothermal plumes released during the opening of the Gulf of Mexico. These plumes also acted as carriers of metals to the basin. Anoxic waters of the Huayacocotla basin concentrated Mn^{+2} before its transformation during early diagenesis to manganese carbonate. This process was likely mediated by manganese reducing bacteria. Close analogues of the Molango deposits are the Toarcian Urkut deposits of Hungary.

Keywords: Manganese, Sedimentary, Molango, Rhodochrosite, Black shales

©2020. Japan Geoscience Union. All Right Reserved.

Relationship between isotope fractionation and valence of tellurium adsorbed on the Fe-Mn oxides from seawater

*Yusuke Fukami[1], Teruhiko Kashiwabara[2], Hiroshi Amakawa[3], Takazo Shibuya[2], Akira Usui[4], Katsuhiko Suzuki[2]

1. Gakushuin University, 2. Japan Agency for Marine-Earth Science and Technology, 3. Atmosphere and Ocean Research Institute The University of Tokyo, 4. Marine Core Research Center, Kochi University

Marine ferromanganese crusts (Fe-Mn crusts) are Fe-Mn oxide deposits widely distributed on the seafloor, and are important materials for (paleo)oceanographic studies (e.g. Hein et al., 2014). Tellurium (Te) is one of the highly enriched elements in the Fe-Mn crusts by more than ten thousand times relative to that in the continental crusts (Hein et al., 2010). Variation of concentration and isotopic compositions of Te in the Fe-Mn crusts could be a potential indicator for changes in redox condition of seawater, because of the existence of two valences of Te in ocean environments (+4 and +6; Lee and Edmond, 1985). In this study, we performed the measurement for concentration and isotopic compositions of Te in the surface layer of the Fe-Mn crusts, which directly contacted with ambient seawater, to investigate the relationship between ambient water environments and the compositions of Fe-Mn oxide deposits, such as the concentration and isotopic compositions. The Fe-Mn crust samples were collected from two seamounts located in the Northwest Pacific, which possess different depth profile of the dissolved oxygen concentration in seawater. Furthermore, laboratory experiments were performed to investigate the isotope fractionation associated with Te adsorption on ferromanganese oxides.

The results show that the correlation between the Te concentration and isotopic compositions in the surface layer of the Fe-Mn crusts changes as the water depth increases. With increasing depth, the Te concentration decreases more drastically at shallower water depth than at deeper water depth, and changes in isotopic fractionation were also observed at similar water depths. Moreover, between two seamounts with different depth profile of dissolved oxygen in seawater, the water depth where the concentration gradient of Te in the Fe-Mn crusts changes is different. For laboratory experiments, it is revealed that when tetravalent Te is adsorbed on iron oxide, isotope composition of the liquid phase becomes lighter, and when hexavalent Te adsorbs it becomes heavier. These results suggest that Te isotope fractionation in ferromanganese oxide deposits in the ocean may correspond to the valence of tellurium in the ocean.

Keywords: tellurium, isotope fractionation, Fe-Mn oxides, ocean environment

©2020. Japan Geoscience Union. All Right Reserved.

Formation process of different types of manganese nodules collected on seamounts in the Northeast Pacific

Wataru Katanoda[1], *Masafumi MURAYAMA[1], Akira Usui[2], Takeyasu Yamagata[3], Hiroyuki Matsuzaki[3]

1. Faculty of Agriculture and Marine Science, Kochi University, 2. Center for advanced Marine Core Research, Kochi University, 3. The University Museum,The University of Tokyo

Manganese nodules are a low-grade large-scale deposit that are situated on the seabed, and future development is expected. However, the etiology is not well understood. The purpose of this study was to elucidate the formation process of three different types of manganese nodules collected from seamounts in the northeast Pacific, where there are few reported cases, based on the internal structure, element concentration, and age of formation. A sample with a thin coating on the surface of the seafloor, a sample buried in sediment, and a diameter of 8 cm, collected during the KH-17-03 cruise, Hakuho-Maru. The three types of samples were analyzed. Observation of the internal microstructure using μ-focus X-ray CT, elemental concentration distribution using an X-ray analysis microscope, and 10Be ages were obtained from accelerator mass spectrometry.
As a result, (1) In the sample with thin coating produced from the surface of the seafloor, the part formed in seawater from the buried surface of the sediment is thicker and layered, and the part formed in the sediment is thinner than seawater and sponge. And the layer thickness ratio was about 2: 1. (2) Correlation of element concentration was clear in the part formed in seawater, and that in sediment was unclear. (3) The growth rate was almost constant in seawater and not constant in sediments. From the above results, it was found that there is a difference between the element concentration distribution and the growth rate in seawater, which is an oxidative environment, and in sediment, which is a reductive environment. It was suggested that it affected the collection.

Keywords: Mn nodule, μ-focus X-ray CT, 10Be, Northeast Pacific

©2020. Japan Geoscience Union. All Right Reserved.